Editors' Suggestion | Featured in Physics

Averages of b-hadron, c-hadron, and τ-lepton properties as of 2021

Y. Amhis,[1] Sw. Banerjee,[2] E. Ben-Haim,[3] E. Bertholet,[4] F. U. Bernlochner,[5] M. Bona,[6] A. Bozek,[7] C. Bozzi,[8] J. Brodzicka,[7] V. Chobanova,[9] M. Chrzaszcz,[7] S. Duell,[5] U. Egede,[10] M. Gersabeck,[11] T. Gershon,[12] P. Goldenzweig,[13] K. Hayasaka,[14] D. Johnson,[15] M. Kenzie,[12] T. Kuhr,[16] O. Leroy,[17] A. Lusiani,[18,19] H.-L. Ma,[20] M. Margoni,[21] K. Miyabayashi,[22] R. Mizuk,[4] P. Naik,[23] T. Nanut Petrič,[24] A. Oyanguren,[25] A. Pompili,[26,27] M. T. Prim,[5] M. Roney,[28] M. Rotondo,[29] O. Schneider,[30] C. Schwanda,[31] A. J. Schwartz,[32] J. Serrano,[17] A. Soffer,[4] D. Tonelli,[33] P. Urquijo,[34] and J. Yelton[35]

(Heavy Flavor Averaging Group Collaboration)

[1]*Université Paris-Saclay, CNRS/IN2P3, IJCLab, Orsay, France*
[2]*University of Louisville, Louisville, Kentucky, USA*
[3]*LPNHE, Sorbonne Université, Paris Diderot Sorbonne Paris Cité, CNRS/IN2P3, Paris, France*
[4]*Tel Aviv University, Tel Aviv, Israel*
[5]*University of Bonn, Bonn, Germany*
[6]*Department of Physics and Astronomy, Queen Mary University of London, London, United Kingdom*
[7]*H. Niewodniczanski Institute of Nuclear Physics, Kraków, Poland*
[8]*INFN Sezione di Ferrara, Ferrara, Italy*
[9]*Instituto Galego de Física de Altas Enerxías (IGFAE), Universidade de Santiago de Compostela, Spain*
[10]*School of Physics and Astronomy, Monash University, Melbourne, Australia*
[11]*School of Physics and Astronomy, University of Manchester, Manchester, United Kingdom*
[12]*Department of Physics, University of Warwick, Coventry, United Kingdom*
[13]*Institut für Experimentelle Teilchenphysik, Karlsruher Institut für Technologie, Karlsruhe, Germany*
[14]*Niigata University, Niigata, Japan*
[15]*Massachusetts Institute of Technology, Cambridge, Massachusetts, USA*
[16]*Ludwig-Maximilians-University, Munich, Germany*
[17]*Aix Marseille Univ, CNRS/IN2P3, CPPM, Marseille, France*
[18]*Scuola Normale Superiore, Pisa, Italy*
[19]*INFN Sezione di Pisa, Pisa, Italy*
[20]*Institute of High Energy Physics, Beijing 100049, People's Republic of China*
[21]*Universita degli Studi di Padova, Universita e INFN, Padova, Italy*
[22]*Nara Women's University, Nara, Japan*
[23]*H.H. Wills Physics Laboratory, University of Bristol, Bristol, United Kingdom*
[24]*European Organization for Nuclear Research (CERN), Geneva, Switzerland*
[25]*Instituto de Fisica Corpuscular, Centro Mixto Universidad de Valencia—CSIC, Spain*
[26]*Università di Bari Aldo Moro, Bari, Italy*
[27]*INFN Sezione di Bari, Bari, Italy*
[28]*University of Victoria, Victoria, British Columbia, Canada*
[29]*Laboratori Nazionali dell'INFN di Frascati, Frascati, Italy*
[30]*Institute of Physics, Ecole Polytechnique Fédérale de Lausanne (EPFL), Lausanne, Switzerland*
[31]*Institute of High Energy Physics, Vienna, Austria*
[32]*University of Cincinnati, Cincinnati, Ohio, USA*
[33]*INFN Sezione di Trieste, Trieste, Italy*
[34]*School of Physics, University of Melbourne, Melbourne, Victoria, Australia*
[35]*University of Florida, Gainesville, Florida, USA*

(Received 25 June 2022; accepted 20 September 2022; published 23 March 2023)

This paper reports world averages of measurements of b-hadron, c-hadron, and τ-lepton properties obtained by the Heavy Flavor Averaging Group using results available before April 2021. In rare cases, significant results obtained several months later are also used. For the averaging, common input parameters

Published by the American Physical Society under the terms of the Creative Commons Attribution 4.0 International license. Further distribution of this work must maintain attribution to the author(s) and the published article's title, journal citation, and DOI. Funded by SCOAP³.

used in the various analyses are adjusted (rescaled) to common values, and known correlations are taken into account. The averages include branching fractions, lifetimes, neutral meson mixing parameters, CP violation parameters, parameters of semileptonic decays, and Cabibbo-Kobayashi-Maskawa matrix elements.

DOI: 10.1103/PhysRevD.107.052008

CONTENTS

I. EXECUTIVE SUMMARY 4
II. INTRODUCTION 7
III. AVERAGING METHODOLOGY 8
A. Treatment of correlated systematic uncertainties 9
B. Treatment of unknown correlations 11
C. Treatment of asymmetric uncertainties 11
D. Splitting uncertainty for an average into components 12
IV. b-HADRON PRODUCTION FRACTIONS 12
A. b-hadron production fractions in $\Upsilon(4S)$ decays 13
B. b-hadron production fractions at the $\Upsilon(5S)$ energy 14
C. b-hadron production fractions at high energy 15
V. LIFETIMES AND MIXING PARAMETERS OF b HADRONS 16
A. b-hadron lifetimes 16
1. Overview of lifetime measurements 17
2. B^0 and B^+ lifetimes and their ratio 19
3. B_s^0 lifetimes 20
4. B_c^+ lifetime 22
5. Λ_b^0 and other b-baryon lifetimes 23
6. Summary and comparison with theoretical predictions 24
B. Neutral B-meson mixing 25
1. B^0 mixing parameters $\Delta\Gamma_d$ and Δm_d 26
2. B_s^0 mixing parameters $\Delta\Gamma_s$ and Δm_s 28
3. CP violation in B^0 and B_s^0 mixing 32
4. Mixing-induced CP violation in B_s^0 decays 34
VI. MEASUREMENTS RELATED TO UNITARITY TRIANGLE ANGLES 38
A. Introduction 38
B. Notations 39
1. CP asymmetries 40
2. Time-dependent CP asymmetries in decays to CP eigenstates 40
3. Time-dependent distributions with nonzero decay width difference 41
4. Time-dependent CP asymmetries in decays to vector-vector final states 42
5. Time-dependent asymmetries: Self-conjugate multiparticle final states 42
a. $B^0 \to D^{(*)}h^0$ with $D \to K_S^0\pi^+\pi^-$ 43
b. $B^0 \to D^{*+}D^{*-}K_S^0$ 43
c. $B^0 \to J/\psi\pi^+\pi^-$ 43
d. $B^0 \to K^+K^-K^0$ 43
e. $B^0 \to \pi^+\pi^-K_S^0$ 44
f. $B^0 \to \pi^+\pi^-\pi^0$ 44
6. Time-dependent CP asymmetries in decays to non-CP eigenstates 45
a. $B^0 \to D^{*\pm}D^{\mp}$ 46
b. $B^0 \to \rho^{\pm}\pi^{\mp}$ 46
c. $B^0 \to D^{\mp}\pi^{\pm}, D^{*\mp}\pi^{\pm}, D^{\mp}\rho^{\pm}$ 46
d. $B_s^0 \to D_s^{\mp}K^{\pm}$ 47
e. Time-dependent asymmetries in radiative B decays 47
7. Asymmetries in $B \to D^{(*)}K^{(*)}$ decays 48
a. $B \to D^{(*)}K^{(*)}$ with $D \to CP$ eigenstate decays 49
b. $B \to D^{(*)}K^{(*)}$ with $D \to$ non-CP eigenstate two-body decays 49
c. $B \to D^{(*)}K^{(*)}$ with $D \to$ multibody final state decays 50
C. Common inputs and uncertainty treatment 51
D. Time-dependent asymmetries in $b \to c\bar{c}s$ transitions 51
1. Time-dependent CP asymmetries in $b \to c\bar{c}s$ decays to CP eigenstates 51
2. Constraints on $\beta \equiv \phi_1$ 53
3. Time-dependent transversity analysis of $B^0 \to J/\psi K^{*0}$ decays 54
4. Time-dependent CP asymmetries in $B^0 \to D^{*+}D^{*-}K_S^0$ decays 54
5. Time-dependent analysis of B_s^0 decays through the $b \to c\bar{c}s$ transition 55
E. Time-dependent CP asymmetries in color-suppressed $b \to c\bar{u}d$ transitions 55
1. Time-dependent CP asymmetries: $b \to c\bar{u}d$ decays to CP eigenstates 55
2. Time-dependent Dalitz-plot analyses of $b \to c\bar{u}d$ decays 55
3. Combined results from time-dependent analyses of $b \to c\bar{u}d$ decays 56
F. Time-dependent CP asymmetries in $b \to c\bar{c}d$ transitions 56
1. Time-dependent CP asymmetries in B_s^0 decays mediated by $b \to c\bar{c}d$ transitions 57
G. Time-dependent CP asymmetries in charmless $b \to q\bar{q}s$ transitions 60
1. Time-dependent CP asymmetries: $b \to q\bar{q}s$ decays to CP eigenstates 61
2. Time-dependent Dalitz plot analyses: $B^0 \to K^+K^-K^0$ and $B^0 \to \pi^+\pi^-K_S^0$ 63
3. Time-dependent analyses of $B^0 \to \phi K_S^0\pi^0$ 63
4. Time-dependent CP asymmetries in $B_s^0 \to K^+K^-$ 66
5. Time-dependent CP asymmetries in $B_s^0 \to \phi\phi$ 67

6. Time-dependent CP asymmetries in $B_s^0 \to K^{*0}\bar{K}^{*0}$ 67
H. Time-dependent CP asymmetries in $b \to q\bar{q}d$ transitions 68
I. Time-dependent asymmetries in $b \to s\gamma$ transitions 68
J. Time-dependent asymmetries in B_s^0 decays mediated by $b \to s\gamma$ transitions 70
K. Time-dependent asymmetries in $b \to d\gamma$ transitions 70
L. Time-dependent CP asymmetries in $b \to u\bar{u}d$ transitions 71
1. Constraints on $\alpha \equiv \phi_2$ 73
M. Time-dependent CP asymmetries in $b \to c\bar{u}d/u\bar{c}d$ transitions 77
N. Time-dependent CP asymmetries in $b \to c\bar{u}s/u\bar{c}s$ transitions 77
1. Time-dependent CP asymmetries in $B^0 \to D^{\mp}K_S^0\pi^{\pm}$ 77
2. Time-dependent CP asymmetries in $B_s^0 \to D_s^{\mp}K^{\pm}$ and similar modes 77
O. Rates and asymmetries in $B \to D^{(*)}K^{(*)}$ decays 78
1. D decays to CP eigenstates 79
2. D decays to quasi-CP eigenstates 81
3. D decays to suppressed final states 81
4. D decays to multiparticle self-conjugate final states (model-dependent analysis) 82
5. D decays to multiparticle self-conjugate final states (model-independent analysis) 86
6. D decays to multiparticle nonself-conjugate final states (model-independent analysis) 88
7. Combinations of results on rates and asymmetries in $B \to D^{(*)}K^{(*)}$ decays to obtain constraints on $\gamma \equiv \phi_3$ 90
P. Summary of the constraints on the angles of the unitarity triangle 94
VII. SEMILEPTONIC b HADRON DECAYS 94
A. Exclusive CKM-favored decays 96
1. $\bar{B} \to D^*\ell^-\bar{\nu}_\ell$ 96
2. $\bar{B} \to D\ell^-\bar{\nu}_\ell$ 99
3. $B_s^0 \to D_s^{(*)-}\mu^+\nu_\mu$ 101
4. $\bar{B} \to D^{(*)}\pi\ell^-\bar{\nu}_\ell$ 102
5. $\bar{B} \to D^{**}\ell^-\bar{\nu}_\ell$ 104
B. Inclusive CKM-favored decays 106
1. Global analysis of $\bar{B} \to X_c\ell^-\bar{\nu}_\ell$ 106
2. Analysis in the kinetic scheme 106
3. Analysis in the 1S scheme 107
C. Exclusive CKM-suppressed decays 108
1. $B \to \pi\ell\nu$ branching fraction and q^2 spectrum 109
2. $|V_{ub}|$ from $B \to \pi\ell\nu$ 110
3. $B \to \rho\ell\nu_\ell$ and $B \to \omega\ell\nu_\ell$ branching fraction and q^2 spectrum 112
4. Other exclusive charmless semileptonic B decays 114
5. Direct measurements of $|V_{ub}|/|V_{cb}|$ 114
D. Inclusive CKM-suppressed decays 115
1. BLNP 117
2. DGE 118
3. GGOU 118
4. ADFR 119
5. BLL 119
6. Summary 120
E. Combined extraction of $|V_{ub}|$ and $|V_{cb}|$ 120
F. $B \to D^{(*)}\tau\nu_\tau$ decays 121
VIII. DECAYS OF b-HADRONS INTO OPEN OR HIDDEN CHARM HADRONS 123
A. Decays of B^0 mesons 124
1. Decays to a single open charm meson 124
2. Decays to two open charm mesons 130
3. Decays to charmonium states 133
4. Decays to charm baryons 137
5. Decays to exotic states 139
B. Decays of B^+ mesons 140
1. Decays to a single open charm meson 140
2. Decays to two open charm mesons 144
3. Decays to charmonium states 146
4. Decays to charm baryons 150
5. Decays to exotic states 150
C. Decays of admixtures of B^0/B^+ mesons 152
1. Decays to two open charm mesons 152
2. Decays to charmonium states 153
3. Decays to exotic states 154
D. Decays of B_s^0 mesons 154
1. Decays to a single open charm meson 154
2. Decays to two open charm mesons 156
3. Decays to charmonium states 157
4. Decays to charm baryons 159
E. Decays of B_c^+ mesons 159
1. Decays to a single open charm meson 159
2. Decays to two open charm mesons 160
3. Decays to charmonium states 161
4. Decays to a B meson 161
F. Decays of b baryons 162
1. Decays to a single open charm meson 162
2. Decays to charmonium states 162
3. Decays to charm baryons 164
4. Decays to exotic states 165
IX. b-HADRON DECAYS TO CHARMLESS FINAL STATES 166
A. Mesonic decays of B^+ and B^0 mesons 168
B. Baryonic decays of B^+ and B^0 mesons 190
C. Decays of b baryons 194
D. Decays of B_s^0 mesons 199
E. Decays of B_c^+ mesons 206
F. Rare decays of B^0 and B^+ mesons with photons and/or leptons 206
G. Charge asymmetries in b-hadron decays 224
H. Polarization measurements in b-hadron decays 233
X. CHARM CP VIOLATION AND OSCILLATIONS 237
A. D^0-$\bar{D}^0$ mixing and CP violation 237
1. Introduction 237
2. Input observables 238
3. Fit results 242
4. Conclusions 242
B. CP asymmetries 245

C. T-odd asymmetries 254
D. Interplay between direct and indirect CP violation 256
XI. CHARM DECAYS 257
A. Semileptonic decays 257
1. Introduction 257
2. $D \to P\ell\nu_\ell$ decays 257
3. Form factor parametrizations 258
4. Simple pole 258
5. z expansion 259
6. Three-pole formalism 259
7. Experimental techniques and results 260
8. Combined results for the $D \to P\ell\nu_\ell$ channels 261
9. Form factors of other $D_{(s)} \to P\ell\nu_\ell$ decays 263
10. Determinations of $|V_{cs}|$ and $|V_{cd}|$ 264
11. Test of $e-\mu$ lepton flavor universality 264
12. $D \to V\ell\nu_\ell$ decays 265
13. Vector form factor measurements 266
14. $D \to S\ell\nu_\ell$ decays 268
15. $D \to A\ell\nu_\ell$ decays 268
B. Leptonic decays 268
1. $D^+ \to \ell^+\nu_\ell$ decays and $|V_{cd}|$ 269
2. $D_s^+ \to \ell^+\nu_\ell$ decays and $|V_{cs}|$ 270
3. Comparison with other determinations of $|V_{cd}|$ and $|V_{cs}|$ 271
4. Extraction of $D_{(s)}$ meson decay constants 272
C. Hadronic D^0 decays and final state radiation 273
1. Updates to the branching fractions 273
2. Average branching fractions for $D^0 \to K^-\pi^+$, $D^0 \to \pi^+\pi^-$ and $D^0 \to K^+K^-$ 275
3. Average branching fraction for $D^0 \to K^+\pi^-$ 277
4. Consideration of PHOTOS++ 278
D. Excited $D_{(s)}$ mesons 278
E. Excited charmed baryons 286
F. Rare and forbidden decays 289
XII. TAU LEPTON PROPERTIES 297
A. Branching fraction fit 298
1. Fit results 298
2. Changes with respect to the previous report 308
3. Differences between the HFLAV 2021 fit and the PDG 2021 fit 308
4. Branching fraction fit results and experimental inputs 309
5. Correlation coefficients between basis branching fractions uncertainties 309
6. Equality constraints 311
B. Tests of lepton universality 315
C. Universality-improved $\mathcal{B}(\tau \to e\nu\bar{\nu})$ and $R_{\rm had}$ 316
D. Measurements of $|V_{us}|$ 317
1. $|V_{us}|$ from $\mathcal{B}(\tau \to X_s\nu)$ 317
2. $|V_{us}|$ from $\mathcal{B}(\tau \to K\nu)/\mathcal{B}(\tau \to \pi\nu)$ 318
3. $|V_{us}|$ from $\mathcal{B}(\tau \to K\nu)$ 318
4. Summary of $|V_{us}|$ from τ decays 318
ACKNOWLEDGMENTS 319

I. EXECUTIVE SUMMARY

This paper provides updated world averages of measurements of b-hadron, c-hadron, and τ-lepton properties using results available by March 2021. In a few cases, important results that appeared later are included and are clearly labeled as such. While new measurements since the previous version of this paper [1] have been dominated by the LHCb and the BESIII experiments, there are new results from other experiments as well, and the older results from previous generations of experiments are still very important and contribute to the averages that we report. Significant results are expected in the near future, with the notable addition of measurements from the Belle II experiment which started taking data in 2019.

Since the previous version of the paper, the b-hadron lifetime and mixing averages have progressed only in the B_s^0 sector, but with significant improvements both in precision and in the averaging procedures. In total, new B_s^0 results from 9 publications (of which 1 from ATLAS, 2 from CMS and 6 from LHCb) have been incorporated in these averages. The lifetime hierarchy for the most abundant weakly decaying b-hadron species is well established, with a precision below 10 fs for all meson and Λ_b^0-baryon lifetimes, and compatible with the expectations from the heavy quark expansion. However, small sample sizes still limit the precision for b baryons heavier than Λ_b^0 (Ξ_b^-, Ξ_b^0, Ω_b, and all other yet-to-be-discovered b baryons). A sizable value of the decay width difference in the B_s^0–$\bar{B}_s^0$ system is measured with a relative precision of 6% and is well predicted by the Standard Model (SM). In contrast, the experimental results for the decay width difference in the B^0–$\bar{B}^0$ system are not yet precise enough to distinguish the small (expected) value from zero. The mass differences in both the B^0–$\bar{B}^0$ and B_s^0–$\bar{B}_s^0$ systems are known very accurately at the $\mathcal{O}(10^{-3})$ and $\mathcal{O}(10^{-4})$ level, respectively. On the other hand, CP violation in the mixing of either system has not been observed yet, with asymmetries known within a couple per mil but still consistent both with zero and their SM predictions. A similar conclusion holds for the CP violation induced by B_s^0 mixing in the $b \to c\bar{c}s$ transition, although in this case the experimental uncertainty on the corresponding weak phase is an order of magnitude larger, but now twice smaller than the SM central value. Many measurements are still dominated by statistical uncertainties and will improve once new results from the LHC Run 2 become available, and later from LHC Run 3 and Belle II.

The measurement of $\sin 2\beta \equiv \sin 2\phi_1$ from $b \to c\bar{c}s$ transitions such as $B^0 \to J/\psi K_S^0$ has reached better than 2.5% precision: $\sin 2\beta \equiv \sin 2\phi_1 = 0.699 \pm 0.017$. Measurements of the same parameter using different quark-level processes provide a consistency test of the SM and allow insight into possible beyond the Standard Model effects. All results among hadronic $b \to s$ penguin

dominated decays of B^0 mesons are currently consistent with the SM expectations. Measurements of CP violation parameters in $B_s^0 \to \phi\phi$ and $B_s^0 \to K^{*0}\bar{K}^{*0}$ enable similar comparisons to the value of $\phi_s^{c\bar{c}s}$, where results are again consistent with the small SM expectation. Among measurements related to the unitarity triangle angle $\alpha \equiv \phi_2$, results from B decays to $\pi\pi$, $\rho\pi$ and $\rho\rho$ are combined to obtain a world average value of $(85.2^{+4.8}_{-4.3})^\circ$. Knowledge of the third angle $\gamma \equiv \phi_3$ also continues to improve, with the current world average being $(66.2^{+3.4}_{-3.6})^\circ$. The world average for γ has changed significantly since the previous HFLAV report [1], due mainly to new LHCb measurements which also improve the overall consistency of the combination. The constraints on the angles of the unitarity triangle are summarized in Fig. 48.

In exclusive semileptonic b hadron decays, determinations of the CKM elements $|V_{cb}|$ and $|V_{ub}|$ are now available from the decays $B \to D^{(*)}\ell\nu$, $B_s \to D_s^{(*)}\mu\nu$, $B \to \pi\ell\nu$, $B_s \to K\mu\nu$ and $\Lambda_b \to p\mu\nu$. A global fit to all exclusive results yields $|V_{cb}| = (39.10 \pm 0.50) \times 10^{-3}$ and $|V_{ub}| = (3.51 \pm 0.12) \times 10^{-3}$. The tension with the determinations from inclusive B meson decays is thus 3.3σ for both $|V_{cb}|$ and $|V_{ub}|$. The numerical values of $\mathcal{R}(D^*)$ and $\mathcal{R}(D)$, characterizing semitauonic decays $B \to D^{(*)}\tau\nu_\tau$, have been stable since the last update. With respect to the most recent theory calculations, the combined tension with the SM expectation is 3.3σ.

The most important new measurements of rare b-hadron decays are coming from the LHC and new results are provided by Belle II. Precision measurements of B_s^0 decays are noteworthy, including several measurements of the longitudinal polarization fraction from LHCb. CMS and LHCb have updated their measurements of the branching fractions of $B_{(s)}^0 \to \mu^+\mu^-$ decays with additional data from Run II of the LHC, improving the sensitivity. There are more and more measurements of observables related to $b \to s\ell\ell$ transitions, and the so called "anomalies" previously observed persist with the new data. Global fits of Wilson coefficients performed with the measured observables yield inconsistencies at the typical level of 3 standard deviations from the standard model predictions. Improved measurements from LHCb and other experiments are keenly anticipated. The anomalies in tests of lepton flavor universality, for instance in the measurement of the ratio of branching fractions of $B^+ \to K^+\mu^+\mu^-$ and $B^+ \to K^+e^+e^-$ decays (R_K) from LHCb, with Run II data have also been confirmed. In the low squared dilepton mass region, it differs from the SM prediction by 3.1σ. In addition, more and more stringent limits on lepton flavor violating modes are being established. Among the CP violating observables in rare decays, the "$K\pi$ CP puzzle" persists, and important new results have appeared in two- and three-body decays. LHCb has produced many other results on a wide variety of decays, including b-baryon and B_c^+-meson decays. Among the first results from Belle II, it is worth mentioning the limit on the branching fraction of $B^+ \to K^+\nu\bar{\nu}$ ($<41 \times 10^{-6}$ at 90% confidence level). With a dataset of 63 fb^{-1} this limit is getting close to that obtained by the first-generation B factories, *BABAR* and Belle.

More than 800 b to charm results from *BABAR*, Belle, CDF, D0, LHCb, CMS, and ATLAS reported in approximately 300 papers are compiled in a list of about 500 averages. The large samples of b hadrons that are available in contemporary experiments allows measurements of decays to states with open or hidden charm content with unprecedented precision. In addition to improvements in precision for branching fractions of B^0 and B^+ mesons, many new decay modes have been discovered. In addition,

TABLE 1. Selected world averages. Where two uncertainties are given the first is statistical and the second is systematic.

b-hadron lifetimes	
$\tau(B^0)$	1.519 ± 0.004 ps
$\tau(B^+)$	1.638 ± 0.004 ps
$\tau(B_s^0) = 1/\Gamma_s$	1.520 ± 0.005 ps
$\tau(B_{\rm SL}^0)$	1.429 ± 0.007 ps
$\tau(B_{s\rm H}^0)$	1.624 ± 0.009 ps
$\tau(B_c^+)$	0.510 ± 0.009 ps
$\tau(\Lambda_b^0)$	1.471 ± 0.009 ps
$\tau(\Xi_b^-)$	1.572 ± 0.040 ps
$\tau(\Xi_b^0)$	1.480 ± 0.030 ps
$\tau(\Omega_b^-)$	$1.64^{+0.18}_{-0.17}$ ps
B^0 and B_s^0 mixing & CP violation	
Δm_d	0.5065 ± 0.0019 ps^{-1}
$\Delta\Gamma_d/\Gamma_d$	0.001 ± 0.010
$\lvert q_d/p_d\rvert$	1.0010 ± 0.0008
Δm_s	17.765 ± 0.006 ps^{-1}
$\Delta\Gamma_s$	$+0.084 \pm 0.005$ ps^{-1}
$\lvert q_s/p_s\rvert$	1.0003 ± 0.0014
$\phi_s^{c\bar{c}s}$	-0.049 ± 0.019 rad
Unitarity-triangle angle parameters	
$\sin 2\beta \equiv \sin 2\phi_1$	0.699 ± 0.017
$\beta \equiv \phi_1$	$(22.2 \pm 0.7)^\circ$
$-\eta S_{\phi K_S^0}$	$0.74^{+0.11}_{-0.13}$
$-\eta S_{\eta' K^0}$	0.63 ± 0.06
$-\eta S_{K_S^0 K_S^0 K_S^0}$	0.83 ± 0.17
$\phi_s(\phi\phi)$	$-0.073 \pm 0.115 \pm 0.027$ rad
$(S_{B_s^0\to K^+K^-}, C_{B_s^0\to K^+K^-})$	$(0.14 \pm 0.03, 0.17 \pm 0.03)$
$-\eta S_{J/\psi\pi^0}$	0.86 ± 0.14
$-\eta S_{D^+D^-}$	0.84 ± 0.12
$-\eta S_{J/\psi\rho^0}$	$0.66^{+0.12\ +0.03}_{-0.13\ -0.09}$
$S_{K^*\gamma}$	-0.16 ± 0.22
$(S_{\pi^+\pi^-}, C_{\pi^+\pi^-})$	$(-0.666 \pm 0.029, -0.311 \pm 0.030)$
$(S_{\rho^+\rho^-}, C_{\rho^+\rho^-})$	$(-0.14 \pm 0.13, 0.00 \pm 0.09)$
$\alpha \equiv \phi_2$	$(85.2^{+4.8}_{-4.3})^\circ$
$a(D^\mp\pi^\pm)$, $a(D^{*\mp}\pi^\pm)$	-0.038 ± 0.013, -0.039 ± 0.010
$A_{CP}(B^+ \to D_{CP+}K^+)$	0.139 ± 0.009
$A_{\rm ADS}(B^+ \to D_{K\pi}K^+)$	-0.453 ± 0.026
$\gamma \equiv \phi_3$	$(66.2^{+3.4}_{-3.6})^\circ$

TABLE 2. Selected world averages. Where two uncertainties are given the first is statistical and the second is systematic.

Semileptonic b-hadron decay parameters	
$\mathcal{B}(\bar{B}^0 \to D^{*+}\ell^-\bar{\nu}_\ell)$	$(4.97 \pm 0.12)\%$
$\mathcal{B}(B^- \to D^{*0}\ell^-\bar{\nu}_\ell)$	$(5.58 \pm 0.22)\%$
$\mathcal{B}(\bar{B}^0 \to D^{+}\ell^-\bar{\nu}_\ell)$	$(2.24 \pm 0.09)\%$
$\mathcal{B}(B^- \to D^{0}\ell^-\bar{\nu}_\ell)$	$(2.30 \pm 0.09)\%$
$\mathcal{B}(\bar{B}^0 \to \pi^{+}\ell^-\bar{\nu}_\ell)$	$(1.50 \pm 0.06) \times 10^{-4}$
$\lvert V_{cb}\rvert$ from exclusive B, B_s and Λ_b decays	$(39.10 \pm 0.50) \times 10^{-3}$
$\lvert V_{ub}\rvert$ from exclusive B, B_s and Λ_b decays	$(3.51 \pm 0.12) \times 10^{-3}$
$\mathcal{B}(\bar{B} \to X_c\ell^-\bar{\nu}_\ell)$	$(10.65 \pm 0.16)\%$
$\mathcal{B}(\bar{B} \to X\ell^-\bar{\nu}_\ell)$	$(10.84 \pm 0.16)\%$
$\lvert V_{cb}\rvert$ from inclusive B decays	$(42.19 \pm 0.78) \times 10^{-3}$
$\lvert V_{ub}\rvert$ from inclusive B decays	$(4.19 \pm 0.17) \times 10^{-3}$
$\mathcal{R}(D) = \mathcal{B}(B \to D\tau\nu_\tau)/\mathcal{B}(B \to D\ell\nu_\ell)$	0.339 ± 0.030
$\mathcal{R}(D^*) = \mathcal{B}(B \to D^*\tau\nu_\tau)/\mathcal{B}(B \to D^*\ell\nu_\ell)$	0.295 ± 0.014
b-hadron decays to charmed hadrons	
$\mathcal{B}(B^0 \to D^-\pi^+)$	$(2.56 \pm 0.13) \times 10^{-3}$
$\mathcal{B}(B^+ \to \bar{D}^0\pi^+)$	$(4.67 \pm 0.14) \times 10^{-3}$
$\mathcal{B}(B_s^0 \to D_s^-\pi^+)$	$(2.85 \pm 0.18) \times 10^{-3}$
$\mathcal{B}(\Lambda_b^0 \to \Lambda_c^+\pi^-)$	$(4.45 \pm 0.25) \times 10^{-3}$
$\mathcal{B}(B^0 \to J/\psi K^0)$	$(0.864 \pm 0.029) \times 10^{-3}$
$\mathcal{B}(B^+ \to J/\psi K^+)$	$(1.006 \pm 0.026) \times 10^{-3}$
$\mathcal{B}(B_s^0 \to J/\psi \phi)$	$(1.061 \pm 0.090) \times 10^{-3}$
$\mathcal{B}(\Lambda_b^0 \to J/\psi \Lambda^0)$	$(0.47 \pm 0.29) \times 10^{-3}$
$\mathcal{B}(B_c^+ \to J/\psi D_s^+)/\mathcal{B}(B_c^+ \to J/\psi \pi^+)$	3.09 ± 0.55
b-hadron decays to charmless final states	
$\mathcal{B}(B_s^0 \to \mu^+\mu^-)$	$(2.95 \pm 0.41) \times 10^{-9}$
$\mathcal{B}(B^0 \to \mu^+\mu^-)$	$<0.21 \times 10^{-9}$ (CL = 90%)
$\mathcal{B}(B^0 \to e^+e^-)$	$<2.5 \times 10^{-9}$ (CL = 90%)
$\mathcal{B}(B \to X_s\gamma)$ ($E_\gamma > 1.6$ GeV)	$(3.49 \pm 0.19) \times 10^{-4}$
$R_K = \mathcal{B}(B^+ \to K^+\mu^+\mu^-)/\mathcal{B}(B^+ \to K^+e^+e^-)$ in $1.1 < m^2_{\ell^+\ell^-} < 6.0$ GeV$^2/c^4$ (LHCb)	$0.846^{+0.042+0.013}_{-0.039-0.012}$
$R_{K^*} = \mathcal{B}(B^+ \to K^{*0}\mu^+\mu^-)/\mathcal{B}(B^+ \to K^{*0}e^+e^-)$ in $1.1 < m^2_{\ell^+\ell^-} < 6.0$ GeV$^2/c^4$	$0.72^{+0.12}_{-0.09}$
$A_{CP}(B^0 \to K^+\pi^-)$	-0.0836 ± 0.0032
$A_{CP}(B^+ \to K^+\pi^0)$	0.027 ± 0.013
$A_{CP}(B_s^0 \to K^-\pi^+)$	0.224 ± 0.012
$\mathcal{B}(B^0 \to \mu^+\tau^- + \text{c.c.})$	$<12 \times 10^{-6}$ (CL = 90%)
Observables in $B^0 \to K^{*0}\mu^+\mu^-$ decays in bins of $q^2 = m^2(\mu^+\mu^-)$	See Sec. IX F

the set of measurements available for B_s^0 and B_c^+ mesons as well as for b baryon decays is rapidly increasing. The averaging method is improved to take into account and determine correlations between averages.

In the charm sector, the main highlight is the LHCb observation of dispersive mixing, i.e., the mixing parameter $x \equiv \Delta M/\bar{\Gamma} \neq 0$. The statistical significance of this observation is 8.2σ, which is much greater than the previous significance of 3.1σ. The measurement of x, along with measurements of 48 other observables by the E791, FOCUS, Belle, *BABAR*, CLEO-c, BESIII, CDF, and LHCb experiments, is input into a global fit for 9–10 (depending on theoretical assumptions for subleading amplitudes) mixing and CP violation parameters. From this fit, the no-mixing hypothesis is excluded at a confidence level above 11.5σ. The precision on x is improved by a factor of two from that of previous HFLAV fits. The mixing parameter $y \equiv \Delta\Gamma/\bar{\Gamma} \neq 0$ with a statistical significance greater than 11.4σ. The world average value for the observable y_{CP} is positive, indicating that the CP-even state is shorter-lived, as in the K^0–$\bar{K}^0$ system. However, $x > 0$ and thus the CP-even state is the heavier one, which differs from the K^0–$\bar{K}^0$ system. The CP violation parameters $|q/p|$ and ϕ are compatible with CP symmetry at the level of 1.6σ; thus there is no evidence for *indirect CP* violation, i.e., that arising from mixing ($|q/p| \neq 1$) or from a phase difference between the mixing amplitude and a direct decay amplitude ($\phi \neq 0$). A separate fit to time-integrated

TABLE 3. Selected world averages. Where two uncertainties are given the first is statistical and the second is systematic.

D^0 mixing and CP violation	
x	$(0.41 \pm 0.05)\%$
y	$(0.62 \pm 0.06)\%$
$\delta_{K\pi}$	$(7.2^{+7.9}_{-9.2})^\circ$
A_D	$(-0.70 \pm 0.36)\%$
$\lvert q/p \rvert$	0.995 ± 0.016
ϕ	$(-2.5 \pm 1.2)^\circ$
x_{12} (no direct CP violation)	$(0.41 \pm 0.05)\%$
y_{12} (no direct CP violation)	$(0.60 \pm 0.06)\%$
ϕ_{12} (no direct CP violation)	$(0.58 \pm 0.91)^\circ$
$a_{CP}^{\rm ind}$	$(-0.010 \pm 0.012)\%$
$\Delta a_{CP}^{\rm dir}$	$(-0.161 \pm 0.028)\%$
Charm meson (semi)leptonic decays	
f_D	(205.1 ± 4.4) MeV
f_{D_s}	(252.2 ± 2.5) MeV
$\lvert V_{cd} \rvert$	0.2208 ± 0.0040
$\lvert V_{cs} \rvert$	0.9701 ± 0.0081
Charm meson hadronic decays	
$\mathcal{B}(D^0 \to K^-\pi^+)$	$(3.999 \pm 0.006 \pm 0.031 \pm 0.032_{\rm FSR})\%$
$\mathcal{B}(D^0 \to K^+\pi^-)/\mathcal{B}(D^0 \to K^-\pi^+)$	$(0.343 \pm 0.002)\%$
τ parameters, lepton universality, and $\lvert V_{us} \rvert$	
g_τ/g_μ	1.0009 ± 0.0014
g_τ/g_e	1.0027 ± 0.0014
g_μ/g_e	1.0019 ± 0.0014
$\mathcal{B}_e^{\rm uni}$	$(17.812 \pm 0.022)\%$
$R_{\rm had}$	3.6343 ± 0.0082
$\lvert V_{us} \rvert$ from $\mathcal{B}(\tau^- \to X_s\nu_\tau)$	0.2184 ± 0.0021
$\lvert V_{us}/V_{ud} \rvert$ from $\mathcal{B}(\tau^- \to X_s\nu_\tau)$	0.2243 ± 0.0022
$\lvert V_{us} \rvert$ from $\mathcal{B}(\tau^- \to K^-\nu_\tau)/\mathcal{B}(\tau^- \to \pi^-\nu_\tau)$	0.2229 ± 0.0019
$\lvert V_{us} \rvert/\lvert V_{ud} \rvert$ from $\mathcal{B}(\tau^- \to K^-\nu_\tau)/\mathcal{B}(\tau^- \to \pi^-\nu_\tau)$	0.2289 ± 0.0019
$\lvert V_{us} \rvert$ from $\mathcal{B}(\tau^- \to K^-\nu_\tau)$	0.2219 ± 0.0017
$\lvert V_{us} \rvert$ τ average	0.2207 ± 0.0014

measurements of $D^0 \to K^+K^-/\pi^+\pi^-$ decays gives $\Delta a_{CP}^{\rm dir} = (-0.161 \pm 0.028)\%$, which, like the previous HFLAV fit, establishes direct CP violation in singly Cabibbo-suppressed decays. The contribution of indirect CP violation in this fit is consistent with zero, as expected.

The world's most precise measurements of $\lvert V_{cd} \rvert$ and $\lvert V_{cs} \rvert$ are obtained from leptonic $D^+ \to \mu^+\nu$ and $D_s^+ \to \mu^+\nu/\tau^+\nu$ decays, respectively. These measurements have theoretical uncertainties arising from decay constants. However, calculations of decay constants within lattice QCD have improved such that the theory error is below ~20% of the experimental uncertainties of the measurements. Measurements of the branching fractions for hadronic decays such as $D^0 \to K^\mp\pi^\pm$ are at a precision where final state radiation must be treated correctly and consistently across the measurements for the accuracy of the averages to match the precision; the required informed averages are performed.

The τ branching fraction fit has become more similar to the PDG τ branching fraction fit (also produced by HFLAV) by abandoning some custom elaborations of experimental results that were used in the previous reports. For some lepton universality tests and some $\lvert V_{us} \rvert$ calculations this edition uses recent new estimations of the radiative corrections for the theory predictions of the τ branching fractions. The central values are close to the previous calculations and the uncertainties are larger but considerably more reliable. When updating the external inputs corresponding to the physical fundamental constants for the $\lvert V_{us} \rvert$ determination from the τ branching fractions, an accidental transcription error has been fixed, which caused in the previous report an incorrect shift of about $+0.5\sigma$ in $\lvert V_{us} \rvert$ computed from $\mathcal{B}(\tau \to K\nu)$. Recent updates on the radiative corrections used in the procedure to extract $\lvert V_{ud} \rvert$ from experimental data have shifted the $\lvert V_{ud} \rvert$ world average, resulting in a significant violation of the unitarity of the first row of the CKM matrix. Like the $\lvert V_{us} \rvert$ calculations that rely on kaon decay measurements, the $\lvert V_{us} \rvert$ measurements with τ decays (less precise than the ones obtained from kaon decays) are smaller than the $\lvert V_{us} \rvert$ value that would be required by unitarity and the measured $\lvert V_{ud} \rvert$ and $\lvert V_{ub} \rvert$ values.

A small selection of highlights of the results described in Secs. V–XII are given in Tables 1–3.

II. INTRODUCTION

Flavor dynamics plays an important role in elementary particle interactions. The accurate knowledge of properties of heavy flavor hadrons, especially b hadrons, plays an essential role in determination of the elements of the Cabibbo-Kobayashi-Maskawa (CKM) quark-mixing matrix [2,3]. The operation of the Belle and *BABAR* e^+e^- B factory experiments led to a large increase in the size of available B-meson, D-hadron and τ-lepton samples, enabling dramatic improvement in the accuracies of related measurements. The CDF and D0 experiments at the Fermilab Tevatron have also provided important results in heavy flavor physics, most notably in the B_s^0 sector. In the D-meson sector, the dedicated e^+e^- charm factory experiments CLEO-c and BESIII have made significant contributions. Run I and Run II of the CERN Large Hadron Collider delivered high luminosity, enabling the collection of even larger samples of b and c hadrons, and thus a further leap in precision in many areas, at the ATLAS, CMS, and (especially) LHCb experiments. With ongoing analyses of the LHC Run II data, further improvements are anticipated.

The Heavy Flavor Averaging Group (HFLAV)[1] was formed in 2002 to continue the activities of the LEP

[1]The group was originally known by the acronym "HFAG." Following feedback from the community, this was changed to HFLAV in 2017.

Heavy Flavor Steering Group [4], which was responsible for calculating averages of measurements of b-flavor related quantities. HFLAV has evolved since its inception and currently consists of seven subgroups:

(i) the "B lifetime and oscillations" subgroup provides averages for b-hadron lifetimes and various parameters governing B^0–$\bar{B}^0$ and B_s^0–$\bar{B}_s^0$ mixing and CP violation;
(ii) the "unitarity triangle angles" subgroup provides averages for parameters associated with time-dependent CP asymmetries and $B \to DK$ decays, and resulting determinations of the angles of the CKM unitarity triangle;
(iii) the "semileptonic B decays" subgroup provides averages for inclusive and exclusive measurements of B-decay branching fractions, and subsequent determinations of the CKM matrix element magnitudes $|V_{cb}|$ and $|V_{ub}|$;
(iv) the "B to charm decays" subgroup provides averages of branching fractions for b-hadron decays to final states involving open charm or charmonium mesons, as well as branching fractions for b-hadron production in $\Upsilon(4S)$ and $\Upsilon(5S)$ decays;
(v) the "rare b decays" subgroup provides averages of branching fractions, CP asymmetries and other observables for charmless, radiative, leptonic, and baryonic B-meson and b-baryon decays;
(vi) the "charm CP violation and oscillations" subgroup provides averages of mixing, CP-, and T-violation parameters in the D^0–$\bar{D}^0$ system;
(vii) the "charm decays" subgroup provides averages of charm-hadron branching fractions, properties of excited D^{**} and D_{sJ} mesons, properties of charm baryons, and the D^+ and D_s^+ decay constants f_D and f_{D_s};
(viii) the "tau physics" subgroup provides averages for τ branching fractions using a global fit, elaborates on the results to test lepton universality and to determine the CKM matrix element magnitude $|V_{us}|$, and lists and combines branching-fraction upper limits for τ lepton-flavor-violating decays.

Subgroups consist of representatives from experiments producing relevant results in that area, i.e., representatives from *BABAR*, Belle, Belle II, BESIII, CLEO(c), CDF, D0, LHCb, ATLAS, and CMS.

This article is an update of the last HFLAV publication, which used results available by September 2018 [1]. Here we report world averages using results available by March 2021. In some cases, important new results made available later are included where possible. In general, we use all publicly available results, including preliminary results that are supported by written documentation, such as conference proceedings or publicly available reports from the collaborations. However, we do not use preliminary results that remain unpublished for an extended period of time, or for which no publication is planned. Since HFLAV members are also members of the different collaborations, we exploit our close contact with analyzers to ensure that the results are prepared in a form suitable for combinations.

Section III describes the methodology used for calculating averages. In the averaging procedure, common input parameters used in the various analyses are adjusted (rescaled) to common values, and, where possible, known correlations are taken into account. Sections V–XII present world average values from each of the subgroups listed above. A complete listing of the averages and plots, including updates since this document was prepared, is available on the HFLAV web site [5].

III. AVERAGING METHODOLOGY

The main task of HFLAV is to combine independent but possibly correlated measurements of a parameter to obtain the world's best estimate of that parameter's value and uncertainty. These measurements are typically made by different experiments, or by the same experiment using different datasets, or by the same experiment using the same data but with different analysis methods. In this section, the general approach adopted by HFLAV is outlined. The software used to provide this is either the COMBOS package [6], the HFLAVAVERAGING package [7] or dedicated tools for some averages.

Our methodology focuses on the problem of combining measurements obtained with different assumptions about external (or "nuisance") parameters and with potentially correlated systematic uncertainties. Unless otherwise noted, we assume for our combinations that the quantities measured by experiments were performed in the asymptotic regime (large data samples), so that the measured estimates have a (one- or multidimensional) Gaussian likelihood function. We use $\boldsymbol{x}$ to represent a set of n parameters and $\boldsymbol{x}_i$ to denote the ith set of measurements of those parameters. The covariance matrix for the measurement is $\boldsymbol{V}_i$. In all fits, we ensure that $\boldsymbol{x}$ and $\boldsymbol{x}_i$ do not contain redundant information, i.e., they are vectors with n elements that represents exactly n parameters. A χ^2 statistic is constructed as

$$\chi^2(\boldsymbol{x}) = \sum_i^N (\boldsymbol{x}_i - \boldsymbol{x})^{\mathrm{T}} \boldsymbol{V}_i^{-1} (\boldsymbol{x}_i - \boldsymbol{x}), \tag{1}$$

where the sum is over the N independent determinations of the quantities $\boldsymbol{x}$, typically coming from different experiments. This is the best linear unbiased estimator with minimum variance [8] The results of the average are the central values $\hat{\boldsymbol{x}}$, which are the values of $\boldsymbol{x}$ at the minimum of $\chi^2(\boldsymbol{x})$, and their covariance matrix

$$\hat{\boldsymbol{V}}^{-1} = \sum_i^N \boldsymbol{V}_i^{-1}, \tag{2}$$

which is a generalization of the one-dimensional estimate $\sigma^{-2} = \sum_i \sigma_i^{-2}$.

The value of $\chi^2(\hat{\boldsymbol{x}})$ provides a measure of the consistency of the independent measurements of $\boldsymbol{x}$ after accounting for the number of degrees of freedom (dof), which is the difference $N - n$ between the number of measurements and the number of fitted parameters. The values of $\chi^2(\hat{\boldsymbol{x}})$ and dof are typically converted to a p-value and reported together with the averages. Unlike the Particle Data Group [9], when $\chi^2/\text{dof} > 1$ we do not by default scale the resulting uncertainty. Rather, we examine the systematic uncertainties of each measurement to better understand potential sources of the discrepancy.

In many cases, publications do not quote a direct measurement of a parameter of interest, but of a quantity that is a function of multiple parameters. An example is the measurement of a ratio of branching fractions, from which a branching fraction of interest is determined using previous (and usually more precise) knowledge of the branching fraction of a "normalization mode." This leads to a correlation between the determinations of the two branching fractions that appear in the ratio. In addition, if the same normalization mode is used for measurements of different branching fraction ratios, they too become correlated. These correlations can be evaluated by performing a simultaneous fit to all averages involved. This is done by generalizing Eq. (1) to the form

$$\chi^2(\boldsymbol{p}) = \sum_i^N (\boldsymbol{f}_i(\boldsymbol{p}) - \boldsymbol{x}_i)^{\mathrm{T}} \boldsymbol{V}_i^{-1} (\boldsymbol{f}_i(\boldsymbol{p}) - \boldsymbol{x}_i), \qquad (3)$$

where $\boldsymbol{p}$ are the fit parameters, including the quantities whose averages we want to determine, $\boldsymbol{x}_i$ is the set of ith measurements (e.g., of branching fractions and branching-fraction ratios), and $\boldsymbol{f}_i$ is the dependence of the measured quantities $\boldsymbol{x}_i$ on the parameters $\boldsymbol{p}$. This procedure is used for branching-fraction and related averages in Secs. VIII and IX. An alternative approach, used in Sec. XII A, is to construct the χ^2 as in Eq. (1) and minimize it subject to a list of constraints implemented with Lagrange multipliers. The two approaches are essentially identical, except that the covariance matrix is given in terms of $\boldsymbol{p}$ in the former and in terms of $\boldsymbol{x}_i$ in the latter.

If a special treatment is necessary in order to calculate an average, or if an approximation used in the calculation might not be sufficiently accurate (e.g., assuming Gaussian uncertainties when the likelihood function exhibits non-Gaussian behavior), we point this out. Further modifications to the averaging procedures for non-Gaussian situations are discussed in Sec. III C.

A. Treatment of correlated systematic uncertainties

Consider two hypothetical measurements of a parameter x, which can be summarized as

$$x_1 \pm \delta x_1 \pm \Delta x_{1,1} \pm \Delta x_{1,2} \ldots$$
$$x_2 \pm \delta x_2 \pm \Delta x_{2,1} \pm \Delta x_{2,2} \ldots,$$

where the δx_k are statistical uncertainties and the $\Delta x_{k,i}$ are contributions to the systematic uncertainty. The simplest approach is to combine statistical and systematic uncertainties in quadrature

$$x_1 \pm (\delta x_1 \oplus \Delta x_{1,1} \oplus \Delta x_{1,2} \oplus \ldots)$$
$$x_2 \pm (\delta x_2 \oplus \Delta x_{2,1} \oplus \Delta x_{2,2} \oplus \ldots),$$

and then perform a weighted average of x_1 and x_2 using their combined uncertainties, treating the measurements as independent. This approach suffers from two potential problems that we try to address. First, the values x_k may have been obtained using different assumptions for nuisance parameters; e.g., different values of the B^0 lifetime may have been used for different measurements of the oscillation frequency Δm_d. The second potential problem is that some systematic uncertainties may be correlated between measurements. For example, different measurements of Δm_d may depend on the same branching fraction used to model a common background.

The above two problems are related. We can represent the systematic uncertainties as a set of nuisance parameters y_i upon which x_k depends. The uncertainty Δy_i, which is the uncertainty on y_i coming from external measurements, contributes $\Delta x_{k,i}$ to the systematic uncertainty on x_i. We thus use the values of y_i and Δy_i assumed by each measurement in our averaging. To properly treat correlated systematic uncertainties among measurements, requires decomposing the overall systematic uncertainties into correlated and uncorrelated components. Correlated systematic uncertainties are those that depend on a shared nuisance parameter, e.g., a lifetime as mentioned above; uncorrelated systematic uncertainties do not share a nuisance parameter, e.g., the statistical uncertainty resulting from independent limited size simulations of background components. As different measurements often quote different types of systematic uncertainties, achieving consistent definitions in order to properly treat correlations requires close coordination between HFLAV and the experiments. In some cases, a group of systematic uncertainties must be combined into a coarser description in order to obtain an average that is consistent among measurements. Systematic uncertainties that are uncorrelated with any other source of uncertainty are combined together with the statistical uncertainty, so that the only systematic uncertainties treated explicitly are those that are correlated with at least one other measurement via a consistently defined external parameter y_i.

The fact that a measurement of x is sensitive to y_i indicates that, in principle, the data used to measure x could also be used for a simultaneous measurement of x and y_i.

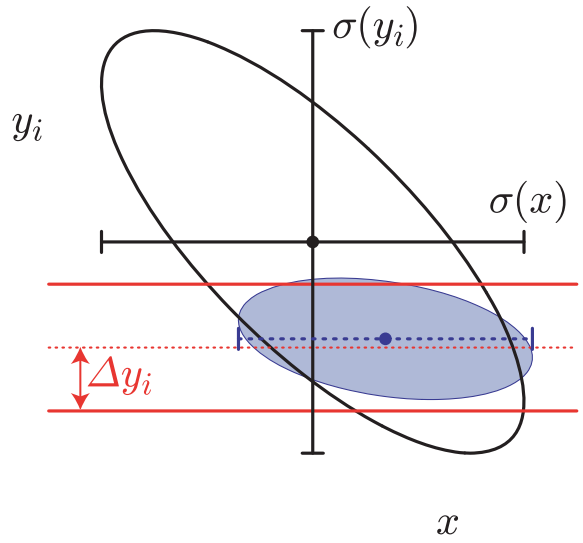

FIG. 1. Illustration of the possible dependence of a measured quantity x on a nuisance parameter y_i. The plot compares the 68% confidence level contours of a hypothetical measurement's unconstrained (large ellipse) and constrained (filled ellipse) likelihoods, using the Gaussian constraint on y_i represented by the horizontal band. The solid error bars represent the statistical uncertainties $\sigma(x)$ and $\sigma(y_i)$ of the unconstrained likelihood. The dashed error bar shows the statistical uncertainty on x from a constrained simultaneous fit to x and y_i.

This is illustrated by the large contour in Fig. 1. However, there often exists an external measurement of y_i with uncertainty Δy_i [represented by the horizontal band in Fig. 1(a)] that is more precise than the constraint $\sigma(y_i)$ from the x data alone. In this case, the results presented in a publication can be from a simultaneous fit to x and y_i, including the external measurement as a constraint, and obtain the filled (x, y) contour and dashed one-dimensional estimate of x shown in Fig. 1. We call the fit without the external measurement *unconstrained*, and the fit that include the external measurement is referred to as *constrained*.

To combine two or more measurements that share a systematic uncertainty due to the same external parameter(s) y_i, the optimal solution is to take the unconstrained results from the publications and perform a constrained simultaneous fit of all measurements to obtain values of x and y_i. Let us consider two statistically independent measurements, $x_1 \pm (\delta x_1 \oplus \Delta x_{1,i})$ and $x_2 \pm (\delta x_2 \oplus \Delta x_{2,i})$, of the quantity x as shown in Figs. 2(a) and 2(b). For simplicity we consider only one correlated systematic uncertainty for each external parameter y_i. Since the publications were made, our knowledge of y_i will often have improved, causing the measurements of x to shift to different central values and have different uncertainties.

If the unconstrained likelihoods $\mathcal{L}_k(x, y_1, y_2, \ldots)$ for each of the measurements are available, the exact method is to minimize the simultaneous likelihood

$$\mathcal{L}_{\text{comb}}(x, y_1, y_2, \ldots) \equiv \prod_k \mathcal{L}_k(x, y_1, y_2, \ldots) \prod_i \mathcal{L}_i(y_i), \tag{4}$$

with an independent Gaussian constraint

$$\mathcal{L}_i(y_i) = \exp\left[-\frac{1}{2}\left(\frac{y_i - y_i'}{\Delta y_i'}\right)^2\right] \tag{5}$$

for each y_i.

However, most publications do not include the full likelihood, in which case we use an approximate method instead. The first step of our procedure is to adjust the values of each measurement to reflect the current best knowledge of the external parameters y_i' and their ranges $\Delta y_i'$, as illustrated in Figs. 2(c) and 2(d). We adjust the central values x_k and correlated systematic uncertainties $\Delta x_{k,i}$ linearly for each measurement (indexed by k) and each external parameter (indexed by i):

$$x_k' = x_k + \sum_i \frac{\Delta x_{k,i}}{\Delta y_{k,i}}(y_i' - y_{k,i}) \tag{6}$$

$$\Delta x_{k,i}' = \Delta x_{k,i} \frac{\Delta y_i'}{\Delta y_{k,i}}. \tag{7}$$

This procedure is exact in the limit that the unconstrained likelihood of each measurement is Gaussian and the linear relationships in Eqs. (6)) and (7) are valid.

The second step is to combine the adjusted measurements, $x_k' \pm (\delta x_k \oplus \Delta x_{k,1}' \oplus \Delta x_{k,2}' \oplus \ldots)$ by constructing the goodness-of-fit statistic

$$\chi^2_{\text{comb}}(x, y_1, y_2, \ldots) \equiv \sum_k \frac{1}{\delta x_k^2}\left[x_k' - \left(x + \sum_i (y_i - y_i')\frac{\Delta x_{k,i}'}{\Delta y_i'}\right)\right]^2 + \sum_i \left(\frac{y_i - y_i'}{\Delta y_i'}\right)^2. \tag{8}$$

We minimize this χ^2 to obtain the best values of x and y_i and their uncertainties, as shown in Fig. 3. Although this method determines new values for the y_i, we typically do not report them as the $\Delta x_{i,k}$ reported by each experiment are generally not intended for this purpose (for example, they may represent a conservative upper limit rather than a true reflection of a 68% confidence level).

The results of the approximate method agree with the exact method when the $\mathcal{L}_k$ are Gaussian, $\Delta y_i' \ll \sigma(y_i)$ and the linear assumption for the approximate method is valid.

For averages where common sources of systematic uncertainty are important, central values and uncertainties are rescaled to a common set of input parameters following the prescription above. We use the most up-to-date values for common inputs, taking values for experimental constraints from within HFLAV or from the Particle Data

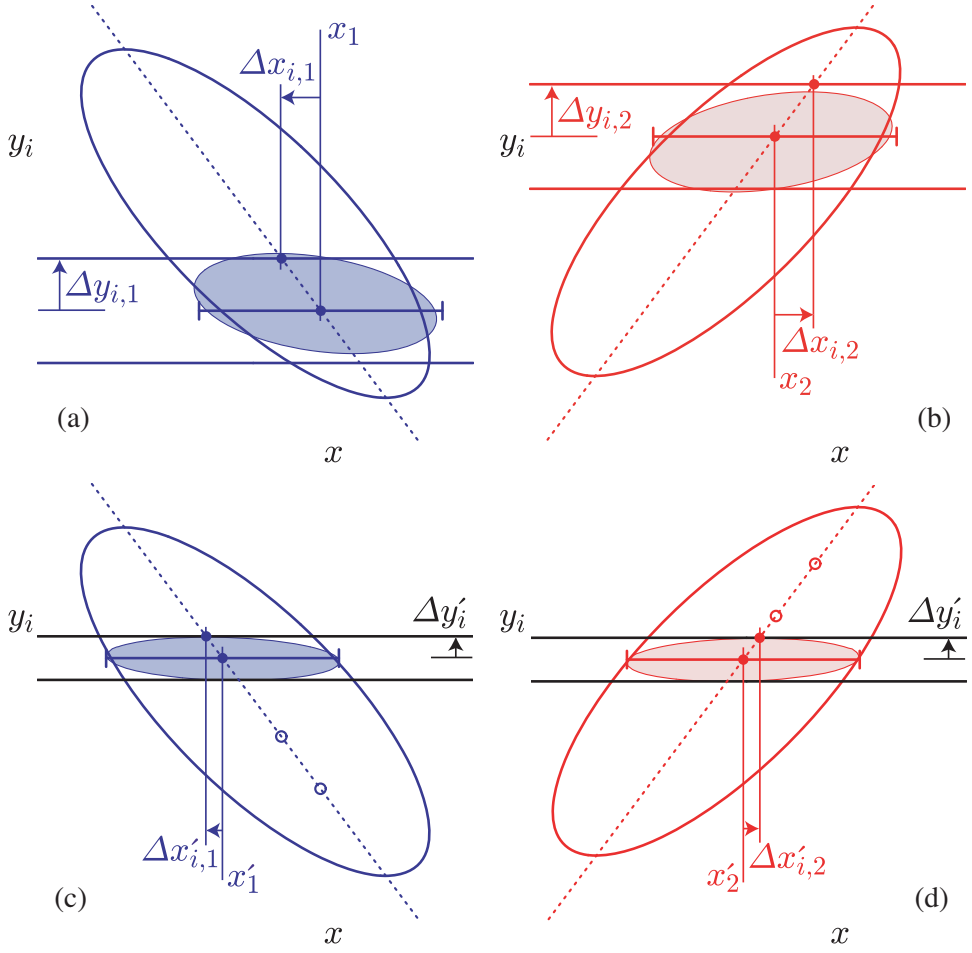

FIG. 2. Illustration of the HFLAV combination procedure for correlated systematic uncertainties. Upper plots (a) and (b) show examples of two individual measurements to be combined. The large (filled) ellipses represent their unconstrained (constrained) iso-likelihood contours, while horizontal bands indicate the different assumptions about the value and uncertainty of y_i used by each measurement. The error bars show the results of the method described in the text for obtaining x by performing fits with y_i fixed to different values. Lower plots (c) and (d) illustrate the adjustments to accommodate updated and consistent knowledge of y_i. Open circles mark the central values of the unadjusted fits to x with y fixed; these determine the dashed line used to obtain the adjusted values.

Group when possible, and updated values of theoretical parameters from their publications.

B. Treatment of unknown correlations

Another issue that needs careful treatment is that of unknown correlations among measurements, e.g., due to use of the same decay model for intermediate states to calculate acceptances. A common practice is to set the correlation coefficient to unity to indicate full correlation. However, this is not necessarily conservative and can result in an underestimated uncertainty on the average. The most conservative choice of correlation coefficient between two measurements i and j is that which maximizes the uncertainty on $\hat{x}$ due to the pair of measurements,

$$\sigma^2_{\hat{x}(i,j)} = \frac{\sigma_i^2\sigma_j^2(1-\rho_{ij}^2)}{\sigma_i^2+\sigma_j^2-2\rho_{ij}\sigma_i\sigma_j}, \tag{9}$$

with

$$\rho_{ij} = \min\left(\frac{\sigma_i}{\sigma_j}, \frac{\sigma_j}{\sigma_i}\right). \tag{10}$$

This corresponds to setting $\sigma^2_{\hat{x}(i,j)} = \min(\sigma_i^2, \sigma_j^2)$. Setting $\rho_{ij} = 1$ when $\sigma_i \neq \sigma_j$ can lead to a significant underestimate of the uncertainty on $\hat{x}$, as can be seen from Eq. (9). In the absence of better information on the correlation, we always use Eq. (9).

C. Treatment of asymmetric uncertainties

For measurements with no correlation between them and with Gaussian uncertainties, the usual estimator for the average of a set of measurements is obtained by minimizing

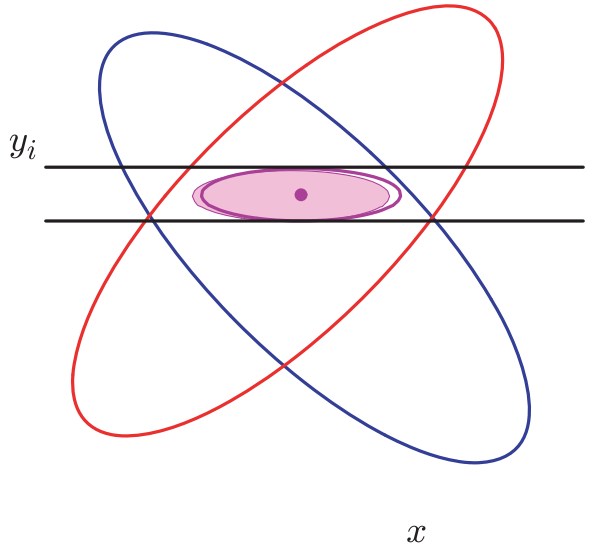

FIG. 3. Illustration of the combination of two hypothetical measurements of x using the method described in the text. The ellipses represent the unconstrained likelihoods of each measurement, and the horizontal band represents the latest knowledge about y_i that is used to adjust the individual measurements. The filled small ellipse shows the result of the exact method using $\mathcal{L}_{\text{comb}}$, and the hollow small ellipse and dot show the result of the approximate method using χ^2_{comb}.

$$\chi^2(x) = \sum_k^N \frac{(x_k - x)^2}{\sigma_k^2}, \tag{11}$$

where x_k is the kth measured value of x and σ_k^2 is the variance of the distribution from which x_k was drawn. The value $\hat{x}$ at minimum χ^2 is the estimate for the parameter x. The true σ_k are unknown but typically the uncertainty as assigned by the experiment σ_k^{raw} is used as an estimator for it. However, caution is advised when σ_k^{raw} depends on the measured value x_k. Examples of this are multiplicative systematic uncertainties such as those due to acceptance, or the $\sqrt{N}$ dependence of Poisson statistics for which $x_k \propto N$ and $\sigma_k \propto \sqrt{N}$. Failing to account for this type of dependence when averaging leads to a biased average. Such biases can be minimized

$$\chi^2(x) = \sum_k^N \frac{(x_k - x)^2}{\sigma_k^2(\hat{x})}, \tag{12}$$

where $\sigma_k(\hat{x})$ is the uncertainty on x_k that includes the dependence of the uncertainty on the value measured. As an example, consider the uncertainty due to detector acceptance, for which $\sigma_k(\hat{x}) = (\hat{x}/x_k) \times \sigma_k^{\text{raw}}$. Inserting this into Eq. (12) leads to the solution

$$\hat{x} = \frac{\sum_k^N x_k^3/(\sigma_k^{\text{raw}})^2}{\sum_k^N x_k^2/(\sigma_k^{\text{raw}})^2},$$

which is the correct behavior, i.e., every measurement is weighted by the inverse square of the fractional uncertainty $\sigma_k^{\text{raw}}/x_k$. When it is not possible to assess the dependence of σ_k^{raw} on $\hat{x}$ from the uncertainties quoted by the experiments, this dependence is ignored.

Another example of a non-Gaussian likelihood function is when a measurement is given with asymmetric uncertainties. In general we symmetrize them by taking their linear average, however for branching fractions and asymmetries, we take asymmetric uncertainties into account through the use of Eq. (1) with a variable value for the kth diagonal element V^{kk} of the covariance matrix for the measurement (dropping the measurement index i for simplicity). We take $V^{kk} = (\sigma_-^k)^2$ for $f^k(\boldsymbol{p}) - x^k < -\sigma_{k-}$ and $V^{kk} = (\sigma_+^k)^2$ for $f^k(\boldsymbol{p}) - x^k > \sigma_+^k$, where σ_-^k (σ_+^k) are the left- (right-side) uncertainty quoted on the measurement of x^k, and f^k is the kth element of $\boldsymbol{f}$. Between these regions, V^{kk} is interpolated linearly. While this will not fully recover the likelihood, it is the optimal solution when no further information is provided [10].

D. Splitting uncertainty for an average into components

We carefully consider the various uncertainties contributing to the overall uncertainty of an average. The covariance matrix describing the uncertainties of different measurements and their correlations is constructed, i.e., $\boldsymbol{V} = \boldsymbol{V}_{\text{stat}} + \boldsymbol{V}_{\text{sys}} + \boldsymbol{V}_{\text{theory}}$. If the measurements are from independent data samples, then $\boldsymbol{V}_{\text{stat}}$ is diagonal, but $\boldsymbol{V}_{\text{sys}}$ and $\boldsymbol{V}_{\text{theory}}$ may contain correlations. The variance on the average $\hat{x}$ can be written as

$$\sigma_{\hat{x}}^2 = \frac{1}{\sum_{i,j} \boldsymbol{V}_{ij}^{-1}} = \frac{\sum_{i,j} (\boldsymbol{V}^{-1}\boldsymbol{V}\boldsymbol{V}^{-1})_{ij}}{(\sum_{i,j} \boldsymbol{V}_{ij}^{-1})^2} \tag{13}$$

$$= \frac{\sum_{i,j} (\boldsymbol{V}^{-1}[\boldsymbol{V}_{\text{stat}} + \boldsymbol{V}_{\text{sys}} + \boldsymbol{V}_{\text{theory}}]\boldsymbol{V}^{-1})_{ij}}{(\sum_{i,j} \boldsymbol{V}_{ij}^{-1})^2}$$

$$= \sigma_{\text{stat}}^2 + \sigma_{\text{sys}}^2 + \sigma_{\text{th}}^2. \tag{14}$$

To calculate σ_{stat}^2 in the last step, the calculation is repeated without including $\boldsymbol{V}_{\text{stat}}$ in $\boldsymbol{V}$ and this is then subtracted from the total. The same is done for the other two components. This breakdown of uncertainties is provided in certain cases, but usually only a single, total uncertainty is quoted for an average.

IV. b-HADRON PRODUCTION FRACTIONS

We consider here the relative fractions of the different b-hadron species produced in a specific process. These fractions are needed for characterizing the signal

TABLE 4. Published measurements of the B^+/B^0 production ratio in $\Upsilon(4S)$ decays, together with their average (see text). Systematic uncertainties due to the imperfect knowledge of $\tau(B^+)/\tau(B^0)$ are included.

Experiment, year	References	Decay modes or method	Published value of $R^{+-/00} = f^{+-}/f^{00}$	Assumed value of $\tau(B^+)/\tau(B^0)$
CLEO, 2001	[11]	$J/\psi K^{(*)}$	$1.04 \pm 0.07 \pm 0.04$	1.066 ± 0.024
CLEO, 2002	[12]	$D^*\ell\nu$	$1.058 \pm 0.084 \pm 0.136$	1.074 ± 0.028
Belle, 2003	[13]	Dilepton events	$1.01 \pm 0.03 \pm 0.09$	1.083 ± 0.017
BABAR, 2005	[14]	$(c\bar{c})K^{(*)}$	$1.06 \pm 0.02 \pm 0.03$	1.086 ± 0.017
Average			1.059 ± 0.027 (tot)	1.076 ± 0.004

composition in inclusive b-hadron analyses, predicting the background composition in exclusive analyses, and converting observed event yields (or event yield ratios) into branching fraction (or branching fraction ratio) measurements. We distinguish here the following three b-hadron production processes: $\Upsilon(4S)$ decays, $\Upsilon(5S)$ decays, and high-energy collisions (including Z^0 decays).

A. b-hadron production fractions in $\Upsilon(4S)$ decays

Only the two lightest (charged and neutral) B-meson species can be pair-produced in $\Upsilon(4S)$ decays. Therefore, only the following two branching fractions must be considered:

$$f^{+-} = \frac{\Gamma(\Upsilon(4S) \to B^+B^-)}{\Gamma_{\text{tot}}(\Upsilon(4S))}, \tag{15}$$

$$f^{00} = \frac{\Gamma(\Upsilon(4S) \to B^0\bar{B}^0)}{\Gamma_{\text{tot}}(\Upsilon(4S))}. \tag{16}$$

In practice, most analyses measure their ratio

$$R^{+-/00} = \frac{f^{+-}}{f^{00}} = \frac{\Gamma(\Upsilon(4S) \to B^+B^-)}{\Gamma(\Upsilon(4S) \to B^0\bar{B}^0)}, \tag{17}$$

which is easier to access experimentally. An inclusive (but separate) reconstruction of B^+ and B^0 is difficult. Therefore, $R^{+-/00}$ is measured with exclusive decays $B^+ \to f^+$ and $B^0 \to f^0$ to specific final states f^+ and f^0 that are related by isospin symmetry. Under the assumption that $\Gamma(B^+ \to f^+) = \Gamma(B^0 \to f^0)$, i.e., that isospin invariance holds in relating these B decays, the ratio of the number of reconstructed $B^+ \to f^+$ and $B^0 \to f^0$ mesons, after correcting for efficiency, is equal to

$$\frac{f^{+-}\mathcal{B}(B^+ \to f^+)}{f^{00}\mathcal{B}(B^0 \to f^0)} = \frac{f^{+-}\Gamma(B^+ \to f^+)\tau(B^+)}{f^{00}\Gamma(B^0 \to f^0)\tau(B^0)} = \frac{f^{+-}}{f^{00}}\frac{\tau(B^+)}{\tau(B^0)}, \tag{18}$$

where $\tau(B^+)$ and $\tau(B^0)$ are the B^+ and B^0 lifetimes, respectively. Hence the primary quantity measured in these analyses is $R^{+-/00}\tau(B^+)/\tau(B^0)$, and the extraction of $R^{+-/00}$ with this method therefore requires the knowledge of the $\tau(B^+)/\tau(B^0)$ lifetime ratio.

The published measurements of $R^{+-/00}$ are listed[2] in Table 4 together with the corresponding values of $\tau(B^+)/\tau(B^0)$ assumed in each measurement. All measurements are based on the above-mentioned method, except the one from Belle, which is a by-product of the B^0 mixing frequency analysis using dilepton events (but note that it too assumes isospin invariance, namely $\Gamma(B^+ \to \ell^+\mathrm{X}) = \Gamma(B^0 \to \ell^+\mathrm{X})$). The latter is therefore treated in a slightly different manner in the following procedure used to combine these measurements:

(i) each published value of $R^{+-/00}$ from CLEO and *BABAR* is first converted back to the original measurement of $R^{+-/00}\tau(B^+)/\tau(B^0)$, using the value of the lifetime ratio assumed in the corresponding analysis;
(ii) a simple weighted average of these original measurements of $R^{+-/00}\tau(B^+)/\tau(B^0)$ from CLEO and *BABAR* is then computed, assuming no statistical or systematic correlations between them;
(iii) the weighted average of $R^{+-/00}\tau(B^+)/\tau(B^0)$ is converted into a value of $R^{+-/00}$, using the latest average of the lifetime ratios, $\tau(B^+)/\tau(B^0) = 1.076 \pm 0.004$ (see Sec. V A 2);
(iv) the Belle measurement of $R^{+-/00}$ is adjusted to the current values of $\tau(B^0) = 1.519 \pm 0.004$ ps and $\tau(B^+)/\tau(B^0) = 1.076 \pm 0.004$ (see Sec. V A 2), using the procedure described in Sec. III A;
(v) the combined value of $R^{+-/00}$ from CLEO and *BABAR* is averaged with the adjusted value of $R^{+-/00}$ from Belle, assuming a 100% correlation of the systematic uncertainty due to the limited knowledge on $\tau(B^+)/\tau(B^0)$; no other correlation is considered.

The resulting global average,

$$R^{+-/00} = \frac{f^{+-}}{f^{00}} = 1.059 \pm 0.027, \tag{19}$$

[2]An old and imprecise R measurement from CLEO [15] is included in neither Table 4 nor the average.

is consistent with equal production rate of charged and neutral B mesons, although only at the 2.2σ level.

On the other hand, the *BABAR* collaboration has performed a direct measurement of the f^{00} fraction using a method that neither relies on isospin symmetry nor requires knowledge of $\tau(B^+)/\tau(B^0)$. Rather, the method is based on comparing the number of events where a single $B^0 \to D^{*-}\ell^+\nu$ decay is reconstructed to the number of events where two such decays are reconstructed. The result of this measurement is [16]

$$f^{00} = 0.487 \pm 0.010(\text{stat}) \pm 0.008(\text{syst}). \quad (20)$$

The results of Eqs. (19) and (20) are obtained with very different methods and are completely independent of each other. Their product yields $f^{+-} = 0.516 \pm 0.019$, and combining them into the sum of the charged and neutral fractions gives $f^{+-} + f^{00} = 1.003 \pm 0.029$.

To improve the accuracy in f^{+-} and f^{00}, we use the relation $f^{+-} + f^{00} + f_{\not B} = 1$, where $f_{\not B}$ is the fraction of non-$B\bar{B}$ events. The non-$B\bar{B}$ events are primarily transitions to lower bottomonia with emission of light hadrons, while the contribution of decays to lepton pairs is negligibly small. *BABAR* and Belle have observed transitions to five final states: $\Upsilon(1S)\pi^+\pi^-$, $\Upsilon(1S)\eta$, $\Upsilon(1S)\eta'$, $h_b(1P)\eta$ and $\Upsilon(2S)\pi^+\pi^-$ [17–20]. Their total fraction is

$$f_{\not B} = 0.00264 \pm 0.00021, \quad (21)$$

where the channels with $\pi^0\pi^0$ are included using isospin relations. The rates of the above transitions are higher then expected for the bottomonium states; the enhancement could be due to a "molecular" admixture of the on-shell $B\bar{B}$ pairs in the $\Upsilon(4S)$ wave function (for a review see, for example, [21]). Quantitative understanding of the enhancement pattern has not been reached yet. In particular, it remains puzzling why the branching fraction of $\Upsilon(4S) \to h_b(1P)\eta$ is 10 times higher than that of any other decay to a bottomonium state. Since many transitions remain unexplored, we consider the $f_{\not B}$ value in Eq. (21) as a lower limit. We perform a fit to $R^{+-/00}$ in Eq. (19), f^{00} in Eq. (20) and $f_{\not B}$ in Eq. (21) with the constraint $f^{+-} + f^{00} + f_{\not B} = 1$. The positive error of $f_{\not B}$ is set to infinity. The results of the fit are

$$f^{00} = 0.485^{+0.006}_{-0.011}, \qquad f^{+-} = 0.512^{+0.006}_{-0.016},$$
$$f_{\not B} = 0.00264^{+0.025}_{-0.00021}, \qquad \frac{f^{+-}}{f^{00}} = 1.057^{+0.024}_{-0.025}. \quad (22)$$

The latter ratio differs from unity by 2.2σ.

B. b-hadron production fractions at the $\Upsilon(5S)$ energy

Hadronic events produced in e^+e^- collisions at the $\Upsilon(5S)$ [also known as $\Upsilon(10860)$] energy can be classified into three categories: light-quark (u, d, s, c) continuum events, $b\bar{b}$ continuum events (including $b\bar{b}\gamma$, etc., with initial-state-radiation photons), and $\Upsilon(5S)$ events. The latter two cannot be distinguished and are referred to as $b\bar{b}$ events in the following. These $b\bar{b}$ events can hadronize into different final states. We define $f_{u,d}^{\Upsilon(5S)}$ to be the fraction of $b\bar{b}$ events with a pair of nonstrange bottom mesons, namely, $B\bar{B}$, $B\bar{B}^*$, $B^*\bar{B}$, $B^*\bar{B}^*$, $B\bar{B}\pi$, $B\bar{B}^*\pi$, $B^*\bar{B}\pi$, $B^*\bar{B}^*\pi$, and $B\bar{B}\pi\pi$, where B denotes a B^0 or B^+ meson and $\bar{B}$ denotes a $\bar{B}^0$ or B^- meson. Similarly, we define $f_s^{\Upsilon(5S)}$ to be the fraction of $b\bar{b}$ events that hadronize into a pair of strange bottom mesons ($B_s^0\bar{B}_s^0$, $B_s^0\bar{B}_s^{*0}$, $B_s^{*0}\bar{B}_s^0$, and $B_s^{*0}\bar{B}_s^{*0}$). Note that the excited bottom-meson states decay via $B^* \to B\gamma$ and $B_s^{*0} \to B_s^0\gamma$. Lastly, $f_{\not B}^{\Upsilon(5S)}$ is defined to be the fraction of $b\bar{b}$ events without open-bottom mesons in the final state (which includes production of light bottomonium). By construction, these fractions satisfy

$$f_{u,d}^{\Upsilon(5S)} + f_s^{\Upsilon(5S)} + f_{\not B}^{\Upsilon(5S)} = 1. \quad (23)$$

The CLEO and Belle collaborations have published measurements of the inclusive $\Upsilon(5S)$ branching fractions $\mathcal{B}(\Upsilon(5S) \to D_sX)$, $\mathcal{B}(\Upsilon(5S) \to \phi X)$ and $\mathcal{B}(\Upsilon(5S) \to D^0X)$, from which they extracted the model-dependent estimates of $f_s^{\Upsilon(5S)}$ reported in Table 5. This extraction was performed under the implicit assumption $f_{\not B}^{\Upsilon(5S)} = 0$ in the relation

$$\begin{aligned}&\frac{1}{2}\mathcal{B}(\Upsilon(5S) \to D_sX)\\ &= f_s^{\Upsilon(5S)} \times \mathcal{B}(B_s^0 \to D_sX)\\ &\quad + (1 - f_s^{\Upsilon(5S)} - f_{\not B}^{\Upsilon(5S)}) \times \mathcal{B}(B \to D_sX), \end{aligned} \quad (24)$$

and similar relations for $\mathcal{B}(\Upsilon(5S) \to D^0X)$ and $\mathcal{B}(\Upsilon(5S) \to \phi X)$.

However, the assumption $f_{\not B}^{\Upsilon(5S)} = 0$ is known to be incorrect, given the observed production in e^+e^- collisions at the $\Upsilon(5S)$ energy of the final states $\Upsilon(1S,2S,3S)\pi^+\pi^-$, $\Upsilon(1S,2S,3S)\pi^0\pi^0$, $\Upsilon(1S)K^+K^-$, $h_b(1P,2P)\pi^+\pi^-$, $\chi_{b1,2}(1P)\pi^+\pi^-\pi^0$, $\Upsilon_J(1D)\eta$ and $\Upsilon(2S)\eta$ [26–30]. The sum of the visible (i.e., uncorrected for initial-state radiation) cross sections into these final states, plus those of the unmeasured final states $\Upsilon(1S)K^0\bar{K}^0$ and $h_b(1P,2P)\pi^0\pi^0$, which are obtained by assuming isospin conservation, amounts to

$$\sigma^{\text{vis}}(e^+e^- \to (b\bar{b})X) = 16.1 \pm 1.5 \text{ pb},$$

where $(b\bar{b}) = \Upsilon(1S,2S,3S)$, $\Upsilon_J(1D)$, $h_b(1P,2P)$, $\chi_{b1,2}$, and $X = \pi\pi$, $\pi^+\pi^-\pi^0$, KK, η. We divide this by the $b\bar{b}$ production cross section, $\sigma(e^+e^- \to b\bar{b}X) = 340 \pm 16$ pb [31], to obtain

TABLE 5. Published measurements of $f_s^{\Upsilon(5S)}$, obtained assuming $f_{\not B}^{\Upsilon(5S)} = 0$. The results are quoted as in the original publications, except for the 2010 Belle measurement, which is quoted as $1 - f_{u,d}^{\Upsilon(5S)}$ with $f_{u,d}^{\Upsilon(5S)}$ from Ref. [22].

Experiment, year, dataset	Decay mode or method	Value of $f_s^{\Upsilon(5S)}$
CLEO, 2006, 0.42 fb^{-1} [23]	$\Upsilon(5S) \to D_s X$	$0.168 \pm 0.026^{+0.067}_{-0.034}$
	$\Upsilon(5S) \to \phi X$	$0.246 \pm 0.029^{+0.110}_{-0.053}$
	$\Upsilon(5S) \to B\bar{B}X$	$0.411 \pm 0.100 \pm 0.092$
	CLEO average of above 3	$0.21^{+0.06}_{-0.03}$
Belle, 2006, 1.86 fb^{-1} [24]	$\Upsilon(5S) \to D_s X$	$0.179 \pm 0.014 \pm 0.041$
	$\Upsilon(5S) \to D^0 X$	$0.181 \pm 0.036 \pm 0.075$
	Belle average of above 2	$0.180 \pm 0.013 \pm 0.032$
Belle, 2010, 23.6 fb^{-1} [22]	$\Upsilon(5S) \to B\bar{B}X$	$0.263 \pm 0.032 \pm 0.051$

$$f_{(b\bar{b})X} = 0.0473 \pm 0.0048.$$

This should be taken as a lower bound for $f_{\not B}^{\Upsilon(5S)}$.

To simultaneously extract the fractions under the exact constraints of Eqs. (23) and (24) and the one-sided Gaussian constraint $f_{\not B}^{\Upsilon(5S)} \geq f_{(b\bar{b})X}$, we perform a simultaneous χ^2 fit to the measurements of Refs. [22–24] taking into account all known correlations. The details of the fit are described in Ref. [32]. The latest Belle measurement of $f_s^{\Upsilon(5S)}$ [31] lacks the information needed for the averaging, and is therefore not included. Taking the inputs of Table 6, the best fit values are

$$f_{u,d}^{\Upsilon(5S)} = 0.755^{+0.027}_{-0.038}, \tag{25}$$

$$f_s^{\Upsilon(5S)} = 0.198^{+0.030}_{-0.029}, \tag{26}$$

$$f_{\not B}^{\Upsilon(5S)} = 0.047^{+0.043}_{-0.005}, \tag{27}$$

where the strongly asymmetric uncertainty on $f_{\not B}^{\Upsilon(5S)}$ is due to the one-sided constraint from the observed $(b\bar{b})X$ decays. These results, together with their correlations, imply

$$f_s^{\Upsilon(5S)}/f_{u,d}^{\Upsilon(5S)} = 0.261^{+0.051}_{-0.043}. \tag{28}$$

This is in fair agreement with *BABAR* results [33], obtained as a function of center-of-mass energy and as a by-product of another measurement, and which are not used in our average due to insufficient information.

The production of B_s^0 mesons at the $\Upsilon(5S)$ is observed to be dominated by the $B_s^{*0}\bar{B}_s^{*0}$ channel, with $\sigma(e^+e^- \to B_s^{*0}\bar{B}_s^{*0})/\sigma(e^+e^- \to B_s^{(*)0}\bar{B}_s^{(*)0}) = (87.0 \pm 1.7)\%$ [34] measured as described in Ref. [35]. The proportions of the various production channels for nonstrange B mesons have also been measured [22].

C. b-hadron production fractions at high energy

At high energy, all species of weakly decaying b hadrons may be produced, either directly or in strong and electromagnetic decays of excited b hadrons. Before 2010, it was assumed that the fractions of different species in unbiased samples of high-p_T b-hadron jets where independent of whether they originated from Z decays, $p\bar{p}$ collisions at the Tevatron, or pp collisions at the LHC. This hypothesis was plausible under the condition $Q^2 \gg \Lambda^2_{\rm QCD}$, namely, that the square of the momentum transfer to the produced b quarks is large compared with the square of the hadronization energy scale. This hypothesis is correct in the limit

TABLE 6. External inputs on which the $f_s^{\Upsilon(5S)}$ averages are based.

Branching fraction	Value	Explanation and references
$\mathcal{B}(B \to D_s X) \times \mathcal{B}(D_s \to \phi\pi)$	0.00374 ± 0.00014	Derived from [9]
$\mathcal{B}(B_s^0 \to D_s X)$	0.92 ± 0.11	Model-dependent estimate [25]
$\mathcal{B}(D_s \to \phi\pi)$	0.045 ± 0.004	[9]
$\mathcal{B}(B \to D^0 X) \times \mathcal{B}(D^0 \to K\pi)$	0.02429 ± 0.00113	Derived from [9]
$\mathcal{B}(B_s^0 \to D^0 X)$	0.08 ± 0.07	Model-dependent estimate [24,25]
$\mathcal{B}(D^0 \to K\pi)$	0.03965 ± 0.00031	[9]
$\mathcal{B}(B \to \phi X)$	0.0343 ± 0.0012	[9]
$\mathcal{B}(B_s^0 \to \phi X)$	0.161 ± 0.024	Model-dependent estimate [23]

$p_T \to \infty$, in which the production mechanism of a b hadron is completely described by the fragmentation of the b quark. For finite p_T, however, there are interference effects of the production mechanism of the b quark and its hadronization. While formally suppressed by inverse powers of p_T, these effects may be sizable, especially when the fragmentation probabilities are small as, e.g., in the case of b baryons. In fact, the available data show that the fractions depend on the kinematics of the produced b hadron. Both CDF and LHCb reported a p_{T} dependence of the fractions, with the fraction of Λ_b^0 baryons observed at low p_{T} being enhanced with respect to that seen at LEP at higher p_{T}.

In our previous publication [1], we presented two sets of averages, one including only measurements performed at LEP, and another including only measurements performed by CDF at the Tevatron.[3] While the first set is well defined and is basically related to branching fractions of inclusive Z decays, the other set is somewhat ill defined, since it depends on the geometrical and kinematical acceptance of the experiments over which the measurements are integrated. With the ever increasing precision in heavy flavor measurements, the b-hadron fraction averages provided by HFLAV for high-energy hadron collisions are no longer of interest, since they are not directly transferable from one experiment to the other. We have therefore decided to no longer maintain these averages. The interested reader should refer to Sec. 4.1.3 of our previous publication [1].

The relative fractions of b-hadron types produced in Z decays are universal and therefore still of interest. Since the averages we have reported in Ref. [1] have remained stable over the last decade and new data are not expected until a future new electron-positron collider operates again at the Z pole, they are not reported here.

V. LIFETIMES AND MIXING PARAMETERS OF b HADRONS

Quantities such as b-hadron production fractions, b-hadron lifetimes, and neutral B-meson oscillation frequencies were studied in the 1990s at LEP and SLC, at DORIS II and CESR, as well as at the Tevatron. This was followed by precise measurements of the B^0 and B^+ mesons performed at the asymmetric B factories, KEKB and PEPII, as well as measurements related to the other b hadrons, in particular B_s^0, B_c^+ and Λ_b^0, performed at the upgraded Tevatron. Currently, the most precise measurements are coming from the ATLAS, CMS and LHCb experiments at the LHC.

In many cases, these basic quantities, in addition to being interesting by themselves, are necessary ingredients for more refined measurements, for example decay-time-dependent CP-violating asymmetries. Hence, some of the averages presented in this section are used as input for the results given in subsequent sections. In the past, many b-hadron lifetime and mixing measurements had a significant dependence on the b-hadron production fractions, which themselves depended on the lifetime and mixing measurements. This circular coupling had to be dealt with carefully whenever inclusive or semiexclusive measurements of b-hadron lifetime and mixing parameters were considered. In the past decade, this dependence has reduced to a negligible level, with increasingly precise exclusive measurements becoming available and dominating practically all averages.

In addition to lifetimes and oscillation frequencies, this section also deals with CP violation in the B^0 and B_s^0 mixing amplitudes, as well as the phase $\phi_s^{c\bar{c}s}$ that describes CP violation in the interference between B_s^0 mixing and decay in $b \to c\bar{c}s$ transitions. In the absence of new physics and subleading penguin contributions, this phase is equal to $-2\beta_s = -\arg[(V_{ts}V_{tb}^*)^2/(V_{cs}V_{cb}^*)^2]$. The angle β, which is the equivalent of β_s for the B^0 system, is discussed in Sec. VI.

Throughout this section, published results that have been superseded by subsequent publications are ignored (i.e., excluded from the averages) and are only referred to if necessary.

A. b-hadron lifetimes

Lifetime calculations are performed in the framework of the Heavy Quark Expansion (HQE) [36–38]. In these calculations, the total decay rate of a hadron H_b is expressed as a series of expectation values of operators of increasing dimension,

$$\Gamma_{H_b} = |\mathrm{CKM}|^2 \sum_{n,k} \frac{c_{nk}}{m_b^n} \langle H_b | O_{nk} | H_b \rangle, \tag{29}$$

where $|\mathrm{CKM}|^2$ is the relevant combination of CKM matrix elements. The coefficients c_{nk} are calculated perturbatively [39], i.e., as a series in $\alpha_s(m_b)$. The nonperturbative QCD effects are comprised in the matrix elements $\langle H_b | O_{nk} | H_b \rangle \propto \Lambda_{\mathrm{QCD}}^n$ of the operators O_{nk}. For a given dimension n, there are usually several operators, indicated by the index k. Hence the HQE predicts Γ_{H_b} in the form of an expansion in both $\Lambda_{\mathrm{QCD}}/m_b$ and $\alpha_s(m_b)$. The leading term in Eq. (29) corresponds to the weak decay of a free b quark. At this order all b-flavored hadrons have the same lifetime. The concept of the HQE and first calculations of valence quark effects emerged in 1986 [36]. In the early 1990s experiments became sensitive enough to detect lifetime differences among various H_b species. The possible existence of exponential contributions to Γ_{H_b}, referred to as *violation of quark-hadron duality*, is not captured by the power series of the HQE [40,41]. The sizes of such

[3]The LHC production fractions results were still incomplete, lacking measurements of the production of weakly decaying baryons heavier than Λ_b^0.

terms can only be determined experimentally, by confronting the HQE predictions with data. Possible violation of quark-hadron duality has been shown to be severely constrained by experimental results [42]. The matrix elements can be calculated using lattice QCD or QCD sum rules. In some cases they can also be related to those appearing in other observables by utilizing symmetries of QCD. One may reasonably expect that powers of $\Lambda_{\rm QCD}/m_b \sim 0.1$ provide enough suppression that only the first terms of the sum in Eq. (29) matter. Importantly, starting from the third power the coefficients are enhanced by a factor of $16\pi^2$. The dominant contribution to lifetime differences stems from these terms of order $16\pi^2(\Lambda_{\rm QCD}/m_b)^3$ [43]. State-of-the-art calculations of first-order corrections to these predictions exist in terms of both $\Lambda_{\rm QCD}/m_b$ [44,45] and $\alpha_s(m_b)$ [46–50], with all subsequent theory papers using these results.

Theoretical predictions are usually made for the ratios of the lifetimes (with $\tau(B^0)$ often chosen as the common denominator) rather than for the individual lifetimes, since this leads to cancellation of several uncertainties. The precision of the HQE calculations (see Refs. [47,48,51–54], and Refs. [55,56] for the latest updates) is in some instances already surpassed by the measurements, e.g., in the case of $\tau(B^+)/\tau(B^0)$. Improvement in the precision of calculations requires progress along two lines. First, better nonperturbative matrix elements are needed. One expects precise calculations, especially from lattice QCD where significant advances have been made in the past decade. Second, the coefficients c_{nk} must be calculated to higher orders of α_s. In particular, the α_s^2 and $\alpha_s\Lambda_{\rm QCD}/m_b$ contributions to the lifetime differences are needed to keep up with the experimental precision.

The following important conclusions, which are in agreement with experimental observation, can be drawn from the HQE, even in its present state:

(i) The larger the mass of the heavy quark, the smaller the variation in the lifetimes among different hadrons containing this quark. This is illustrated by the fact that lifetimes are rather similar in the b sector, while they differ by large factors in the charm sector.

(ii) First corrections to the spectator model occur at order $\Lambda_{\rm QCD}^2/m_b^2$, leading to lifetime differences around one percent.

(iii) The dominant contribution to the lifetime splittings is of order $16\pi^2(\Lambda_{\rm QCD}/m_b)^3$ and typically amounts to several percent.

1. Overview of lifetime measurements

This section gives an overview of the types of b-hadron lifetime measurements, with details given in subsequent sections. In most cases, the decay time of an H_b state is estimated by measuring its flight distance and dividing it by the relativistic factor $\beta\gamma c$. Methods of accessing lifetime information can roughly be divided into the following five categories:

(1) *Inclusive (flavor-blind) measurements*. Early, low-statistics measurements were aimed at extracting the lifetime from a mixture of b-hadron decays, without distinguishing the decaying species. Often, the exact H_b composition was ill defined and analysis-dependent. Monte Carlo simulation was used for estimating the $\beta\gamma$ factor, because the decaying hadrons were not fully reconstructed. In the 1990s, these were the largest-statistics b-hadron lifetime measurements accessible to a given experiment, and could therefore serve as an important performance benchmark. Nowadays, the average b-hadron lifetime, which is certainly less fundamental than the precisely measured lifetimes of the individual species, is of very little interest. As a result, we no longer review the inclusive b-hadron lifetime measurements, the latest of which was published in 2004 [57]. The interested reader can refer to our previous publication [1].

(2) *Measurements in semileptonic decays of a specific* $\boldsymbol{H_b}$. The virtual W boson from $b \to Wc$ produces a $\ell\nu_l$ pair ($\ell = e, \mu$) in about 21% of the cases. The electron or muon from such decays provides a clean and efficient trigger signature. The c quark and the H_b spectator quark(s) combine into a charm hadron H_c, which is reconstructed in one or more exclusive decay channels. Identification of the H_c species allows one to separate, at least statistically, different H_b species. The advantage of these measurements is in the sample size, which is usually larger than in the case of exclusively reconstructed hadronic H_b decays (described next). The main disadvantages are related to the difficulty of estimating the lepton + charm sample composition and to the reliance on Monte Carlo for the momentum (and hence $\beta\gamma$ factor) estimate.

(3) *Measurements in exclusively reconstructed hadronic decays*. These have the advantage of complete reconstruction of the decaying H_b state, which allows one to infer the decaying species, as well as to perform precise measurement of the $\beta\gamma$ factor. Both lead to generally smaller systematic uncertainties than in the above two categories. The downsides are smaller branching fractions and larger combinatorial backgrounds when the signal channel involves multihadron decays, such as $H_b \to H_c\pi(\pi\pi)$ with multibody H_c decays. This problem is often more serious in a hadron collider environment, which has many hadrons and a nontrivial underlying event. Decays of the type $H_b \to J/\psi H_s$ are often used, as they are relatively clean and easy to trigger on due to the $J/\psi \to \ell^+\ell^-$ signature.

(4) *Measurements at asymmetric B factories*. In the $\Upsilon(4S) \to B\bar{B}$ decay, the B mesons (B^+ or B^0) are

essentially at rest in the $\Upsilon(4S)$ frame. This makes direct lifetime measurements impossible in experiments at symmetric-energy colliders, which produce the $\Upsilon(4S)$ at rest. At asymmetric B factories the $\Upsilon(4S)$ meson is boosted, resulting in the B and $\bar{B}$ moving nearly parallel to each other with similar boosts. The decay time is inferred from the distance Δz separating the B and $\bar{B}$ decay vertices along the boost axis and from the $\Upsilon(4S)$ boost, which is known from the beam energies. This boost was $\beta\gamma \approx 0.55$ (0.43) in the *BABAR* (Belle) experiment, resulting in an average B decay length of approximately 250 (190) μm.

While one B^0 or B^+ meson is fully reconstructed in a semileptonic or hadronic decay mode, the other B in the event is typically not fully reconstructed, in order to avoid loss of efficiency. Rather, only the position of its decay vertex is determined from the remaining tracks in the event. These measurements benefit from large sample sizes, but suffer from poor proper time resolution, comparable to the B lifetime itself. The resolution is dominated by the uncertainty on the decay-vertex positions, which is typically 50 (100) μm for a fully (partially) reconstructed B meson. With much larger samples in the future, the resolution and purity could be improved (and hence the systematics reduced) by fully reconstructing both B mesons in the event. Finally, the better vertex precision of the Belle II experiment will also contribute to the resolution improvement.

(5) *Measurement of lifetime ratios*. This method, initially applied in the measurement of $\tau(B^+)/\tau(B^0)$, is now also used for other b-hadron species at the LHC.

TABLE 7. Measurements of the B^0 lifetime with exclusive (excl.) or inclusive (incl.) decays, B charge determination from the secondary vertex (sec. vtx), or partial reconstruction. See Sec. VA for a detailed explanation of the method.

Experiment	Method	Data set	$\tau(B^0)$ (ps)	References
ALEPH	$D^{(*)}\ell$	91–95	$1.518 \pm 0.053 \pm 0.034$	[58]
ALEPH	Exclusive	91–94	$1.25^{+0.15}_{-0.13} \pm 0.05$	[59]
ALEPH	Partial rec. $\pi^+\pi^-$	91–94	$1.49^{+0.17+0.08}_{-0.15-0.06}$	[59]
DELPHI	$D^{(*)}\ell$	91–93	$1.61^{+0.14}_{-0.13} \pm 0.08$	[60]
DELPHI	Charge sec. vtx	91–93	$1.63 \pm 0.14 \pm 0.13$	[61]
DELPHI	Inclusive $D^*\ell$	91–93	$1.532 \pm 0.041 \pm 0.040$	[62]
DELPHI	Charge sec. vtx	94–95	$1.531 \pm 0.021 \pm 0.031$	[57]
L3	Charge sec. vtx	94–95	$1.52 \pm 0.06 \pm 0.04$	[63]
OPAL	$D^{(*)}\ell$	91–93	$1.53 \pm 0.12 \pm 0.08$	[64]
OPAL	Charge sec. vtx	93–95	$1.523 \pm 0.057 \pm 0.053$	[65]
OPAL	Inclusive $D^*\ell$	91–00	$1.541 \pm 0.028 \pm 0.023$	[66]
SLD	Charge sec. vtx ℓ	93–95	$1.56^{+0.14}_{-0.13} \pm 0.10$	[67][a]
SLD	Charge sec. vtx	93–95	$1.66 \pm 0.08 \pm 0.08$	[67][a]
CDF1	$D^{(*)}\ell$	92–95	$1.474 \pm 0.039^{+0.052}_{-0.051}$	[68]
CDF1	Excl. $J/\psi K^{*0}$	92–95	$1.497 \pm 0.073 \pm 0.032$	[69]
CDF2	Excl. $J/\psi K^0_S$, $J/\psi K^{*0}$	02–09	$1.507 \pm 0.010 \pm 0.008$	[70]
D0	Excl. $J/\psi K^{*0}$	03–07	$1.414 \pm 0.018 \pm 0.034$	[71]
D0	Excl. $J/\psi K^0_S$	02–11	$1.508 \pm 0.025 \pm 0.043$	[72]
D0	Inclusive $D^-\mu^+$	02–11	$1.534 \pm 0.019 \pm 0.021$	[73]
BABAR	Exclusive	99–00	$1.546 \pm 0.032 \pm 0.022$	[74]
BABAR	Inclusive $D^*\ell$	99–01	$1.529 \pm 0.012 \pm 0.029$	[75]
BABAR	Exclusive $D^*\ell$	99–02	$1.523^{+0.024}_{-0.023} \pm 0.022$	[76]
BABAR	Incl. $D^*\pi$, $D^*\rho$	99–01	$1.533 \pm 0.034 \pm 0.038$	[77]
BABAR	Inclusive $D^*\ell$	99–04	$1.504 \pm 0.013^{+0.018}_{-0.013}$	[78]
Belle	Exclusive	00–03	$1.534 \pm 0.008 \pm 0.010$	[79]
ATLAS	Excl. $J/\psi K^0_S$	2011	$1.509 \pm 0.012 \pm 0.018$	[80]
CMS	Excl. $J/\psi K^{*0}$	2012	$1.511 \pm 0.005 \pm 0.006$	[81][b]
CMS	Excl. $J/\psi K^0_S$	2012	$1.527 \pm 0.009 \pm 0.009$	[81][b]
LHCb	Excl. $J/\psi K^{*0}$	2011	$1.524 \pm 0.006 \pm 0.004$	[82]
LHCb	Excl. $J/\psi K^0_S$	2011	$1.499 \pm 0.013 \pm 0.005$	[82]
LHCb	$K^+\pi^-$	2011	$1.524 \pm 0.011 \pm 0.004$	[83]
Average			± 0.004	

[a]The combined SLD result quoted in Ref. [67] is $1.64 \pm 0.08 \pm 0.08$ ps.
[b]The combined CMS result quoted in Ref. [81] is $1.515 \pm 0.005 \pm 0.006$ ps.

The ratio of the lifetimes is extracted from the proper-time dependence of the ratio of the observed yields of two different b-hadron species, both reconstructed in decay modes with similar topologies. The advantage of this method is that subtle efficiency effects and systematic uncertainties (partially) cancel in the ratio.

In some analyses, measurements of two [e.g., $\tau(B^+)$ and $\tau(B^+)/\tau(B^0)$] or three (e.g., $\tau(B^+)$, $\tau(B^+)/\tau(B^0)$, and Δm_d) quantities are combined. This introduces correlations among measurements. Another source of correlations among the measurements is systematic effects, which could be common to a number of measurements in the same experiment or to an analysis technique across different experiments. When calculating the averages presented below, such known correlations are taken into account.

2. B^0 and B^+ lifetimes and their ratio

After a number of years of dominating the B^0 and B^+ lifetime averages, the LEP experiments yielded the scene to the asymmetric B factories and the Tevatron experiments. The B factories have been very successful in utilizing their potential—in only a few years of running, *BABAR* and, to a greater extent, Belle, have struck a balance between the statistical and the systematic uncertainties, with both being close to (or even better than) an impressive 1% level. Meanwhile, CDF and D0 emerged as significant contributors to the field as the Tevatron Run II data flowed in. More recently, the LHC experiments came into play, matching the precision and, in case of LHCb and CMS, even improving it by a further factor of ∼2.

At the present time, we have three sets of measurements (from LEP/SLC, the B factories and Tevatron/LHC) performed in different environments, obtained using substantially different techniques, and precise enough for cross-checking and comparison.

The $\tau(B^+)$, $\tau(B^0)$ and $\tau(B^+)/\tau(B^0)$ measurements, and their averages, are summarized in Tables 7, 8, and 9. For the average of $\tau(B^+)/\tau(B^0)$ we use only direct measurements of this ratio and not separate measurements of $\tau(B^+)$ and $\tau(B^0)$. The following sources of systematic uncertainties that are correlated within each experiment/machine are considered in the averaging:

(i) for the SLC and LEP measurements—D^{**} branching fraction uncertainties [4], estimation of the momentum of b mesons produced in Z^0 decays (b-quark fragmentation parameter $\langle X_E \rangle = 0.702 \pm 0.008$ [4]), B_s^0 and b-baryon lifetimes (see Secs. V A 3 and V A 5), and b-hadron production fractions at high energy [1];
(ii) for the B-factory measurements—detector alignment and length scale, machine boost, and sample composition (where applicable);
(iii) for the Tevatron and LHC measurements—detector alignment, length scale and reconstruction effects.

The resultant averages are

$$\tau(B^0) = 1.519 \pm 0.004 \text{ ps}, \tag{30}$$

$$\tau(B^+) = 1.638 \pm 0.004 \text{ ps}, \tag{31}$$

$$\tau(B^+)/\tau(B^0) = 1.076 \pm 0.004. \tag{32}$$

TABLE 8. Measurements of the B^+ lifetime with exclusive (excl.) or inclusive (incl.) decays or with B charge determination from the secondary vertex (sec. vtx). See Sec. V A for a detailed explanation of the method.

Experiment	Method	Dataset	$\tau(B^+)$ (ps)	References
ALEPH	$D^{(*)}\ell$	91–95	$1.648 \pm 0.049 \pm 0.035$	[58]
ALEPH	Exclusive	91–94	$1.58^{+0.21+0.04}_{-0.18-0.03}$	[59]
DELPHI	$D^{(*)}\ell$	91–93	$1.61 \pm 0.16 \pm 0.12$	[60][a]
DELPHI	Charge sec. vtx	91–93	$1.72 \pm 0.08 \pm 0.06$	[61][a]
DELPHI	Charge sec. vtx	94–95	$1.624 \pm 0.014 \pm 0.018$	[57]
L3	Charge sec. vtx	94–95	$1.66 \pm 0.06 \pm 0.03$	[63]
OPAL	$D^{(*)}\ell$	91–93	$1.52 \pm 0.14 \pm 0.09$	[64]
OPAL	Charge sec. vtx	93–95	$1.643 \pm 0.037 \pm 0.025$	[65]
SLD	Charge sec. vtx ℓ	93–95	$1.61^{+0.13}_{-0.12} \pm 0.07$	[67][b]
SLD	Charge sec. vtx	93–95	$1.67 \pm 0.07 \pm 0.06$	[67][b]
CDF1	$D^{(*)}\ell$	92–95	$1.637 \pm 0.058^{+0.045}_{-0.043}$	[68]
CDF1	Excl. $J/\psi K$	92–95	$1.636 \pm 0.058 \pm 0.025$	[69]
CDF2	Excl. $J/\psi K$	02–09	$1.639 \pm 0.009 \pm 0.009$	[70]
CDF2	Excl. $D^0\pi$	02–06	$1.663 \pm 0.023 \pm 0.015$	[84]
BABAR	Exclusive	99–00	$1.673 \pm 0.032 \pm 0.023$	[74]
Belle	Exclusive	00–03	$1.635 \pm 0.011 \pm 0.011$	[79]
LHCb	Excl. $J/\psi K$	2011	$1.637 \pm 0.004 \pm 0.003$	[82]
Average			1.638 ± 0.004	

[a]The combined DELPHI result quoted in [61] is 1.70 ± 0.09 ps.
[b]The combined SLD result quoted in [67] is $1.66 \pm 0.06 \pm 0.05$ ps.

TABLE 9. Measurements of the ratio $\tau(B^+)/\tau(B^0)$ from exclusive (excl.) decays modes or with B charge determination from the secondary vertex (sec. vtx). See Sec. VA for a detailed explanation of the method.

Experiment	Method	Dataset	Ratio $\tau(B^+)/\tau(B^0)$	References
ALEPH	$D^{(*)}\ell$	91–95	$1.085 \pm 0.059 \pm 0.018$	[58]
ALEPH	Exclusive	91–94	$1.27^{+0.23+0.03}_{-0.19-0.02}$	[59]
DELPHI	$D^{(*)}\ell$	91–93	$1.00^{+0.17}_{-0.15} \pm 0.10$	[60]
DELPHI	Charge sec. vtx	91–93	$1.06^{+0.13}_{-0.11} \pm 0.10$	[61]
DELPHI	Charge sec. vtx	94–95	$1.060 \pm 0.021 \pm 0.024$	[57]
L3	Charge sec. vtx	94–95	$1.09 \pm 0.07 \pm 0.03$	[63]
OPAL	$D^{(*)}\ell$	91–93	$0.99 \pm 0.14^{+0.05}_{-0.04}$	[64]
OPAL	Charge sec. vtx	93–95	$1.079 \pm 0.064 \pm 0.041$	[65]
SLD	Charge sec. vtx ℓ	93–95	$1.03^{+0.16}_{-0.14} \pm 0.09$	[67][a]
SLD	Charge sec. vtx	93–95	$1.01^{+0.09}_{-0.08} \pm 0.05$	[67][a]
CDF1	$D^{(*)}\ell$	92–95	$1.110 \pm 0.056^{+0.033}_{-0.030}$	[68]
CDF1	Excl. $J/\psi K$	92–95	$1.093 \pm 0.066 \pm 0.028$	[69]
CDF2	Excl. $J/\psi K^{(*)}$	02–09	$1.088 \pm 0.009 \pm 0.004$	[70]
D0	$D^{*+}\mu D^0 \mu$ ratio	02–04	$1.080 \pm 0.016 \pm 0.014$	[85]
BABAR	Exclusive	99–00	$1.082 \pm 0.026 \pm 0.012$	[74]
Belle	Exclusive	00–03	$1.066 \pm 0.008 \pm 0.008$	[79]
LHCb	Excl. $J/\psi K^{(*)}$	2011	$1.074 \pm 0.005 \pm 0.003$	[82]
Average			1.076 ± 0.004	

[a]The combined SLD result quoted in [67] is $1.01 \pm 0.07 \pm 0.06$.

3. B_s^0 lifetimes

Like neutral kaons, neutral B mesons contain short- and long-lived components, since the light (L) and heavy (H) eigenstates differ not only in their masses but also in their total decay widths. While in the B^0 system the decay width difference $\Delta\Gamma_d$ can be neglected, the B_s^0 system exhibits a significant value of the width difference $\Delta\Gamma_s = \Gamma_{s\mathrm{L}} - \Gamma_{s\mathrm{H}}$, where $\Gamma_{s\mathrm{L}}$ and $\Gamma_{s\mathrm{H}}$ are the total decay widths of the light eigenstate $B_{s\mathrm{L}}^0$ and the heavy eigenstate $B_{s\mathrm{H}}^0$, respectively. The sign of $\Delta\Gamma_s$ is measured to be positive [86], i.e., $B_{s\mathrm{H}}^0$ has a longer lifetime than $B_{s\mathrm{L}}^0$. Specific measurements of $\Delta\Gamma_s$ and $\Gamma_s = (\Gamma_{s\mathrm{L}} + \Gamma_{s\mathrm{H}})/2$, which are more involved than simple lifetime measurements, are explained and averaged in Sec. V B 2, but the resulting averages for $1/\Gamma_{s\mathrm{L}} = 1/(\Gamma_s + \Delta\Gamma_s/2)$, $1/\Gamma_{s\mathrm{H}} = 1/(\Gamma_s - \Delta\Gamma_s/2)$ and the mean B_s^0 lifetime, defined as $\tau(B_s^0) = 1/\Gamma_s$ are also quoted at the end of this section. Neglecting CP violation in $B_s^0 - \bar{B}_s^0$ mixing, which is expected to be very small [42,49,50,87–89] (see also Sec. V B 3), the mass eigenstates are also CP eigenstates, with the short-lived (light) state being CP-even and the long-lived (heavy) state being CP-odd [86].

Many B_s^0 lifetime analyses, in particular the early ones performed before the nonzero value of $\Delta\Gamma_s$ was firmly established, ignore $\Delta\Gamma_s$ and fit the proper time distribution of a sample of B_s^0 candidates reconstructed in a certain final state f with a model containing a single exponential function for the signal. Such *effective lifetime* measurements, which we denote as $\tau_{\mathrm{single}}(B_s^0 \to f)$, are estimates of the expectation value $\int_0^\infty t\Gamma(B_s(t) \to f)dt / \int_0^\infty \Gamma(B_s(t) \to f)dt$ of the total untagged time-dependent decay rate $\Gamma(B_s(t) \to f)$ [90–92]. This expectation value may lie *a priori* anywhere between $1/\Gamma_{s\mathrm{L}}$ and $1/\Gamma_{s\mathrm{H}}$, depending on the proportion of $B_{s\mathrm{L}}^0$ and $B_{s\mathrm{H}}^0$ in the final state f. More recent determinations of effective lifetimes may be interpreted as measurements of the relative composition of $B_{s\mathrm{L}}^0$ and $B_{s\mathrm{H}}^0$ decaying to the final state f. Table 10 summarizes the effective lifetime measurements.

Averaging measurements of $\tau_{\mathrm{single}}(B_s^0 \to f)$ over several final states f would yield a result corresponding to an ill-defined observable when the proportions of $B_{s\mathrm{L}}^0$ and $B_{s\mathrm{H}}^0$ differ. Therefore, the effective B_s^0 lifetime measurements are broken down into the following categories and averaged separately.

(i) $\boldsymbol{B_s^0 \to D_s^{\mp} X}$ *decays* include mostly flavor-specific decays but also decays with an unknown mixture of light and heavy components. Measurements performed with such inclusive states are no longer used in our averages.

(ii) *Decays to flavor-specific final states*, i.e., decays to final states f with decay amplitudes satisfying $A(B_s^0 \to f) \neq 0$, $A(\bar{B}_s^0 \to \bar{f}) \neq 0$, $A(B_s^0 \to \bar{f}) = 0$ and $A(\bar{B}_s^0 \to f) = 0$. Since there are equal fractions of $B_{s\mathrm{L}}^0$ and $B_{s\mathrm{H}}^0$ at production time ($t = 0$), the corresponding effective lifetime, called the *flavor-specific lifetime*, is equal to [90]

$$\tau_{\mathrm{single}}(B_s^0 \to \text{flavor specific}) = \frac{1/\Gamma_{s\mathrm{L}}^2 + 1/\Gamma_{s\mathrm{H}}^2}{1/\Gamma_{s\mathrm{L}} + 1/\Gamma_{s\mathrm{H}}} = \frac{1}{\Gamma_s}\frac{1 + (\frac{\Delta\Gamma_s}{2\Gamma_s})^2}{1 - (\frac{\Delta\Gamma_s}{2\Gamma_s})^2}. \quad (33)$$

TABLE 10. Measurements of the effective B_s^0 lifetimes obtained from single exponential fits (except for the $J/\psi\pi^+\pi^-$ result of Ref. [93], obtained from a time-dependent amplitude analysis).

Experiment	Final state f		Dataset		$\tau_{\text{single}}(B_s^0 \to f)$ (ps)	References
ALEPH	$D_s h$	Ill-defined	91–95		$1.47 \pm 0.14 \pm 0.08$	[94]
DELPHI	$D_s h$	Ill-defined	91–95		$1.53^{+0.16}_{-0.15} \pm 0.07$	[95]
OPAL	D_s incl.	Ill-defined	90–95		$1.72^{+0.20+0.18}_{-0.19-0.17}$	[96]
ALEPH	$D_s^- \ell^+$	Flavor-specific	91–95		$1.54^{+0.14}_{-0.13} \pm 0.04$	[97]
CDF1	$D_s^- \ell^+$	Flavor-specific	92–96		$1.36 \pm 0.09^{+0.06}_{-0.05}$	[98]
DELPHI	$D_s^- \ell^+$	Flavor-specific	92–95		$1.42^{+0.14}_{-0.13} \pm 0.03$	[99]
OPAL	$D_s^- \ell^+$	Flavor-specific	90–95		$1.50^{+0.16}_{-0.15} \pm 0.04$	[100]
D0	$D_s^- \mu^+ X$	Flavor-specific	02–11	10.4 fb^{-1}	$1.479 \pm 0.010 \pm 0.021$	[73]
CDF2	$D_s^- \pi^+(X)$	Flavor-specific	02–06	1.3 fb^{-1}	$1.518 \pm 0.041 \pm 0.027$	[101]
LHCb	$D_s^- D^+$	Flavor-specific	11–12	3 fb^{-1}	$1.52 \pm 0.15 \pm 0.01$	[102]
LHCb	$D_s^- \pi^+$	Flavor-specific	2011	1 fb^{-1}	$1.535 \pm 0.015 \pm 0.014$	[103]
LHCb	$\pi^+ K^-$	Flavor-specific	2011	1.0 fb^{-1}	$1.60 \pm 0.06 \pm 0.01$	[83]
LHCb	$D_s^{(*)-} \mu^+ \nu_\mu$	Flavor-specific	11–12	3.0 fb^{-1}	$1.547 \pm 0.013 \pm 0.011$	[104]
Average of above 10 flavor-specific lifetime measurements					1.527 ± 0.011	
CDF1	$J/\psi\phi$	CP even + odd	92–95		$1.34^{+0.23}_{-0.19} \pm 0.05$	[105]
D0	$J/\psi\phi$	CP even + odd	02–04		$1.444^{+0.098}_{-0.090} \pm 0.02$	[106]
LHCb	$J/\psi\phi$	CP even + odd	2011	1 fb^{-1}	$1.480 \pm 0.011 \pm 0.005$	[82]
CMS	$J/\psi\phi$	CP even + odd	2012	19.7 fb^{-1}	$1.481 \pm 0.007 \pm 0.005$	[81]
Average of above 4 $J/\psi\phi$ lifetime measurements					1.480 ± 0.007	
LHCb	$\mu^+\mu^-$	CP even + odd	11–18	8.7 fb^{-1}	$2.07 \pm 0.29 \pm 0.03$	[107]
CMS	$\mu^+\mu^-$	CP even + odd	11–16	61 fb^{-1}	$1.70^{+0.61}_{-0.44}$	[108]
Average of above 2 $\mu^+\mu^-$ lifetime measurements					$2.00^{+0.27}_{-0.26}$	
ALEPH	$D_s^{(*)+} D_s^{(*)-}$	mostly CP even	91–95		$1.27 \pm 0.33 \pm 0.08$	[109]
LHCb	K^+K^-	CP-even	2010	0.037 fb^{-1}	$1.440 \pm 0.096 \pm 0.009$	[110]
LHCb	K^+K^-	CP-even	2011	1.0 fb^{-1}	$1.407 \pm 0.016 \pm 0.007$	[83]
Average of above 2 K^+K^- lifetime measurements					1.408 ± 0.017	
LHCb	$D_s^+ D_s^-$	CP-even	11–12	3 fb^{-1}	$1.379 \pm 0.026 \pm 0.017$	[102]
LHCb	$J/\psi\eta$	CP-even	11–12	3 fb^{-1}	$1.479 \pm 0.034 \pm 0.011$	[111]
Average of above 2 measurements of $1/\Gamma_{sL}$					1.422 ± 0.023	
LHCb	$J/\psi K_S^0$	CP-odd	2011	1.0 fb^{-1}	$1.75 \pm 0.12 \pm 0.07$	[112]
CDF2	$J/\psi f_0(980)$	CP-odd	02–08	3.8 fb^{-1}	$1.70^{+0.12}_{-0.11} \pm 0.03$	[113]
D0	$J/\psi f_0(980)$	CP-odd	02–11	10.4 fb^{-1}	$1.70 \pm 0.14 \pm 0.05$	[114]
LHCb	$J/\psi\pi^+\pi^-$	CP-odd	2011	1.0 fb^{-1}	$1.652 \pm 0.024 \pm 0.024$	[115]
CMS	$J/\psi\pi^+\pi^-$	CP-odd	2012	19.7 fb^{-1}	$1.677 \pm 0.034 \pm 0.011$	[81]
LHCb	$J/\psi\pi^+\pi^-$	CP-odd	15–16	1.9 fb^{-1}	$1.645 \pm 0.011 \pm 0.012$	[93]
Average of above 5 measurements of $1/\Gamma_{sH}$					1.650 ± 0.013	

Because of the fast $B_s^0 - \bar{B}_s^0$ oscillations, possible biases of the flavor-specific lifetime due to a combination of $B_s^0/\bar{B}_s^0$ production asymmetry, CP violation in the decay amplitudes ($|A(B_s^0 \to f)| \neq |A(\bar{B}_s^0 \to \bar{f})|$), and CP violation in $B_s^0 - \bar{B}_s^0$ mixing ($|q_s/p_s| \neq 1$, see Sec. V B) are strongly suppressed, by a factor $\sim x_s^2$ [where the definition of x_s is given in Eq. (48) and its value in Eq. (67)]. The $B_s^0/\bar{B}_s^0$ production asymmetry at LHCb and the CP asymmetry due to mixing have been measured to be compatible with zero with a precision below 3% [116] and 0.3% [see Eq. (75)], respectively. The corresponding effects on the flavor-specific lifetime, which therefore have a relative size of the order of 10^{-5} or smaller, can be neglected at the current level of experimental precision. Under the assumption of no production asymmetry and no CP violation in mixing, Eq. (33) is exact even for a flavor-specific

decay with CP violation in the decay amplitudes. Hence any flavor-specific decay mode can be used to measure the flavor-specific lifetime.

The average of all flavor-specific B_s^0 lifetime measurements [73,83,97–104] is

$$\tau_{\text{single}}(B_s^0 \to \text{flavor specific}) = 1.527 \pm 0.011 \text{ ps}. \tag{34}$$

(iii) *The* $\boldsymbol{B_s^0 \to J/\psi\phi}$ *decay* contains a well-measured mixture of CP-even and CP-odd states. The published $B_s^0 \to J/\psi\phi$ effective lifetime measurements [81,82,105,106] are combined into the average $\tau_{\text{single}}(B_s^0 \to J/\psi\phi) = 1.480 \pm 0.007$ ps. Analyses that separate the CP-even and CP-odd components in this decay through a full angular study, outlined in Sec. V B 2, provide directly precise measurements of $1/\Gamma_s$ and $\Delta\Gamma_s$ (see Table 21).

(iv) *The* $\boldsymbol{B_s^0 \to \mu^+\mu^-}$ *decay* is predicted to be CP-odd in the Standard Model, but the mixture of CP-even and CP-odd states has not been determined experimentally. Effective lifetime measurements have been published by LHCb [107] and CMS [108].

(v) *Decays to CP eigenstates* have also been measured. These include the CP-even modes $B_s^0 \to D_s^{(*)+}D_s^{(*)-}$ by ALEPH [109], $B_s^0 \to K^+K^-$ by LHCb [83,110], $B_s^0 \to D_s^+D_s^-$ by LHCb [102] and $B_s^0 \to J/\psi\eta$ by LHCb [111], as well as the CP-odd modes $B_s^0 \to J/\psi f_0(980)$ by CDF [113] and D0 [114], $B_s^0 \to J/\psi\pi^+\pi^-$ by LHCb[4] [93,115] and CMS [81], and $B_s^0 \to J/\psi K_S^0$ by LHCb [112]. If these decays are dominated by a single weak phase and if CP violation can be neglected, then $\tau_{\text{single}}(B_s^0 \to CP\text{-even}) = 1/\Gamma_{sL}$ and $\tau_{\text{single}}(B_s^0 \to CP\text{-odd}) = 1/\Gamma_{sH}$ (see Eqs. (62) and (63) for approximate relations in the presence of mixing-induced CP violation). However, not all these modes are pure CP eigenstates: a small CP-odd component is present in $B_s^0 \to J/\psi\pi^+\pi^-$ decays and most probably also in $B_s^0 \to D_s^{(*)+}D_s^{(*)-}$ decays. Furthermore, the decays $B_s^0 \to K^+K^-$ and $B_s^0 \to J/\psi K_S^0$ may suffer from direct CP violation due to interfering tree and loop amplitudes. The averages for the effective lifetimes obtained for decays to the (nearly) pure CP-even ($D_s^+D_s^-$, $J/\psi\eta$) and CP-odd ($J/\psi f_0(980)$, $J/\psi\pi^+\pi^-$) final states, where CP conservation can be assumed, are

$$\tau_{\text{single}}(B_s^0 \to CP\text{-even}) = 1.422 \pm 0.023 \text{ ps}, \tag{35}$$

$$\tau_{\text{single}}(B_s^0 \to CP\text{-odd}) = 1.650 \pm 0.013 \text{ ps}. \tag{36}$$

As described in Sec. V B 2, the effective lifetime averages of Eqs. (34), (35), and (36) are used as constraints to improve the determination of $1/\Gamma_s$ and $\Delta\Gamma_s$ obtained from the full angular analyses of $B_s^0 \to J/\psi\phi$, $B_s^0 \to \psi(2S)\phi$ and $B_s^0 \to J/\psi K^+K^-$ decays. The resulting world averages for the B_s^0 lifetimes are

$$\tau(B_{sL}^0) = \frac{1}{\Gamma_{sL}} = \frac{1}{\Gamma_s + \Delta\Gamma_s/2} = 1.429 \pm 0.007 \text{ ps}, \tag{37}$$

$$\tau(B_{sH}^0) = \frac{1}{\Gamma_{sH}} = \frac{1}{\Gamma_s - \Delta\Gamma_s/2} = 1.624 \pm 0.009 \text{ ps}, \tag{38}$$

$$\tau(B_s^0) = \frac{1}{\Gamma_s} = \frac{2}{\Gamma_{sL} + \Gamma_{sH}} = 1.520 \pm 0.005 \text{ ps}. \tag{39}$$

4. B_c^+ lifetime

Early measurements of the B_c^+ meson lifetime, from CDF [117,118] and D0 [119], use the semileptonic decay mode $B_c^+ \to J/\psi\ell^+\nu$ and are based on a simultaneous fit to the mass and lifetime using the vertex formed with the leptons from the decay of the J/ψ and the third lepton. Correction factors are used to estimate the boost, which cannot be measured directly due to the invisible neutrino. Systematic uncertainties that are correlated among the measurements include the impact of the uncertainty of the B_c^+ transverse-momentum spectrum on the correction factors, the level of feed-down from $\psi(2S)$ decays, Monte Carlo modeling of the decay (estimated by varying the decay model from phase space to the ISGW model), and uncertainties in the B_c^+ mass. With more statistics, CDF2 was able to perform the first B_c^+ lifetime based on fully reconstructed $B_c^+ \to J/\psi\pi^+$ decays [120], which does not suffer from a missing neutrino. More recent measurements at the LHC, both with $B_c^+ \to J/\psi\mu^+\nu$ decays from LHCb [121] and $B_c^+ \to J/\psi\pi^+$ decays from LHCb [122] and CMS [81], achieve the highest level of precision. Two of them [81,122] are made relative to the B^+ lifetime. Before averaging, they are scaled to our latest B^+ lifetime average, and the induced correlation is taken into account.

All the measurements are summarized in Table 11. The world average, dominated by the LHCb measurements, is determined to be

$$\tau(B_c^+) = 0.510 \pm 0.009 \text{ ps}. \tag{40}$$

[4]The result of Ref. [93] for the $B_s^0 \to J/\psi\pi^+\pi^-$ lifetime is not obtained through a single exponential fit of the lifetime distribution, but through a full time-dependent amplitude analysis, which concludes that the CP-odd fraction is greater than 97% at 95% C.L. and yields $\Gamma_{sH} - \Gamma_d = -0.050 \pm 0.004 \pm 0.004$ ps^{-1}, where $1/\Gamma_d$ is the B^0 lifetime. Before being averaged with other determinations of the $B_s^0 \to J/\psi\pi^+\pi^-$ effective lifetime, this result is converted to a measurement of $1/\Gamma_{sH}$ using the latest average of the B^0 lifetime.

TABLE 11. Measurements of the B_c^+ lifetime.

Experiment	Method	Dataset		$\tau(B_c^+)$ (ps)	References
CDF1	$J/\psi\ell$	92–95	0.11 fb^{-1}	$0.46^{+0.18}_{-0.16} \pm 0.03$	[117]
CDF2	$J/\psi e$	02–04	0.36 fb^{-1}	$0.463^{+0.073}_{-0.065} \pm 0.036$	[118]
D0	$J/\psi\mu$	02–06	1.3 fb^{-1}	$0.448^{+0.038}_{-0.036} \pm 0.032$	[119]
CDF2	$J/\psi\pi$		6.7 fb^{-1}	$0.452 \pm 0.048 \pm 0.027$	[120]
LHCb	$J/\psi\mu$	2012	2 fb^{-1}	$0.509 \pm 0.008 \pm 0.012$	[121]
LHCb	$J/\psi\pi$	11–12	3 fb^{-1}	$0.5134 \pm 0.0110 \pm 0.0057$	[122]
CMS	$J/\psi\pi$	2012	19.7 fb^{-1}	$0.541 \pm 0.026 \pm 0.014$	[81]
Average				0.510 ± 0.009	

5. Λ_b^0 and other b-baryon lifetimes

The first measurements of b-baryon lifetimes, performed at LEP, originate from two classes of partially reconstructed decays. In the first class, decays with a fully reconstructed Λ_c^+ baryon and a lepton of opposite charge are used. These products are likely to occur in the decay of Λ_b^0 baryons. In the second class, more inclusive final states with a baryon (p, $\bar{p}$, Λ, or $\bar{\Lambda}$) and a lepton have been used, and these final states can generally arise from any b baryon. With the large b-hadron samples available at the Tevatron and the LHC, the most precise measurements of b baryons now come from fully reconstructed exclusive decays.

The following sources of correlated systematic uncertainties have been accounted for when averaging these measurements: experimental time resolution within a given experiment, b-quark fragmentation distribution into weakly decaying b baryons, Λ_b^0 polarization, decay model, and evaluation of the b-baryon purity in the selected event samples. In computing the averages, the central values of the masses are scaled to $M(\Lambda_b^0) = 5619.60 \pm 0.17$ MeV$/c^2$ [9].

For measurements with partially reconstructed decays, the meaning of the decay model systematic uncertainties and the correlation of these uncertainties between measurements are not always clear. Uncertainties related to the decay model are dominated by assumptions on the fraction of n-body semileptonic decays. To be conservative, it is assumed that these are 100% correlated whenever given as an uncertainty. DELPHI varies the fraction of four-body decays from 0.0 to 0.3. In computing the average, the DELPHI result is scaled to a value of 0.2 ± 0.2 for this fraction. Furthermore, the semileptonic decay results from LEP are scaled to a Λ_b^0 polarization of $-0.45^{+0.19}_{-0.17}$ [4] and a b fragmentation parameter $\langle x_E \rangle_b = 0.702 \pm 0.008$ [123].

The list of all measurements are given in Table 12. We do not attempt to average measurements performed with $p\ell$ or $\Lambda\ell$ combinations, which select unknown mixtures of b baryons. Measurements performed with $\Lambda_c^+\ell$ or $\Lambda\ell^+\ell^-$ combinations can be assumed to correspond to semileptonic Λ_b^0 decays. Their average ($1.247^{+0.071}_{-0.069}$ ps) is significantly different from the average using only measurements performed with exclusively reconstructed hadronic Λ_b^0 decays (1.471 ± 0.009 ps). The latter is much more precise and less prone to potential biases than the former. The discrepancy between the two averages is at the level of 3.1σ and assumed to be due to a systematic effect in the semileptonic measurements, where the Λ_b^0 momentum is not determined directly, or to a rare statistical fluctuation. The best estimate of the Λ_b^0 lifetime is therefore taken as the average of the exclusive measurements only. The CDF $\Lambda_b^0 \to J/\psi\Lambda$ lifetime result [131] is larger than the average of all other exclusive measurements by 2.4σ. It is nonetheless kept in the average without adjustment of input uncertainties. The world average Λ_b^0 lifetime is then

$$\tau(\Lambda_b^0) = 1.471 \pm 0.009 \text{ ps}. \tag{41}$$

For the strange b baryons, we do not include the measurements based on inclusive $\Xi^\mp\ell^\mp$ final states, which consist of a mixture of Ξ_b^- and Ξ_b^0 baryons. Rather, we only average results obtained with fully reconstructed Ξ_b^-, Ξ_b^0 and Ω_b^- baryons, and obtain

$$\tau(\Xi_b^-) = 1.572 \pm 0.040 \text{ ps}, \tag{42}$$

$$\tau(\Xi_b^0) = 1.480 \pm 0.030 \text{ ps}, \tag{43}$$

$$\tau(\Omega_b^-) = 1.64^{+0.18}_{-0.17} \text{ ps}. \tag{44}$$

It should be noted that several b-baryon lifetime measurements from LHCb [133,138–140] were made with respect to the lifetime of another b hadron (i.e., the original measurement is that of a decay width difference). Before these measurements are included in the averages quoted above, we rescale them according to our latest lifetime average of that reference b hadron. This introduces correlations between our averages, in particular between the Ξ_b^- and Ξ_b^0 lifetimes. Taking this correlation into account leads to

$$\tau(\Xi_b^0)/\tau(\Xi_b^-) = 0.929 \pm 0.028. \tag{45}$$

TABLE 12. Measurements of the b-baryon lifetimes.

Experiment	Method	Dataset	Lifetime (ps)	References
ALEPH	$\Lambda\ell$	91–95	$1.20 \pm 0.08 \pm 0.06$	[124]
DELPHI	$\Lambda\ell\pi$ vtx	91–94	$1.16 \pm 0.20 \pm 0.08$	[125][b]
DELPHI	$\Lambda\mu$ i.p.	91–94	$1.10^{+0.19}_{-0.17} \pm 0.09$	[126][b]
DELPHI	$p\ell$	91–94	$1.19 \pm 0.14 \pm 0.07$	[125][b]
OPAL	$\Lambda\ell$ i.p.	90–94	$1.21^{+0.15}_{-0.13} \pm 0.10$	[127][c]
OPAL	$\Lambda\ell$ vtx	90–94	$1.15 \pm 0.12 \pm 0.06$	[127][c]
ALEPH	$\Lambda_c^+\ell$	91–95	$1.18^{+0.13}_{-0.12} \pm 0.03$	[124][a]
ALEPH	$\Lambda\ell^-\ell^+$	91–95	$1.30^{+0.26}_{-0.21} \pm 0.04$	[124][a]
DELPHI	$\Lambda_c^+\ell$	91–94	$1.11^{+0.19}_{-0.18} \pm 0.05$	[125][b]
OPAL	$\Lambda_c^+\ell$, $\Lambda\ell^-\ell^+$	90–95	$1.29^{+0.24}_{-0.22} \pm 0.06$	[100]
CDF1	$\Lambda_c^+\ell$	91–95	$1.32 \pm 0.15 \pm 0.07$	[128]
D0	$\Lambda_c^+\mu$	02–06	$1.290^{+0.119+0.087}_{-0.110-0.091}$	[129]
Average of above 6			$1.247^{+0.071}_{-0.069}$	
CDF2	$\Lambda_c^+\pi$	02–06	$1.401 \pm 0.046 \pm 0.035$	[130]
CDF2	$J/\psi\Lambda$	01–11	$1.565 \pm 0.035 \pm 0.020$	[131]
D0	$J/\psi\Lambda$	02–11	$1.303 \pm 0.075 \pm 0.035$	[72]
ATLAS	$J/\psi\Lambda$	2011	$1.449 \pm 0.036 \pm 0.017$	[80]
CMS	$J/\psi\Lambda$	2011	$1.503 \pm 0.052 \pm 0.031$	[132]
CMS	$J/\psi\Lambda$	2012	$1.477 \pm 0.027 \pm 0.009$	[81]
LHCb	$J/\psi\Lambda$	2011	$1.415 \pm 0.027 \pm 0.006$	[82]
LHCb	$J/\psi pK$ (w.r.t. B^0)	11–12	$1.479 \pm 0.009 \pm 0.010$	[133]
Average of above 8:	Λ_b^0 lifetime =		1.471 ± 0.009	
ALEPH	$\Xi^-\ell^-X$	90–95	$1.35^{+0.37+0.15}_{-0.28-0.17}$	[134]
DELPHI	$\Xi^-\ell^-X$	91–93	$1.5^{+0.7}_{-0.4} \pm 0.3$	[135][d]
DELPHI	$\Xi^-\ell^-X$	92–95	$1.45^{+0.55}_{-0.43} \pm 0.13$	[136][d]
CDF2	$J/\psi\Xi^-$	01–11	$1.32 \pm 0.14 \pm 0.02$	[131]
LHCb	$J/\psi\Xi^-$	11–12	$1.55^{+0.10}_{-0.09} \pm 0.03$	[137]
LHCb	$\Xi_c^0\pi^-$ (w.r.t. Λ_b^0)	11–12	$1.599 \pm 0.041 \pm 0.022$	[138]
Average of above 3:	Ξ_b^- lifetime =		1.572 ± 0.040	
LHCb	$\Xi_c^+\pi^-$ (w.r.t. Λ_b^0)	11–12	$1.477 \pm 0.026 \pm 0.019$	[139]
Average of above 1:	Ξ_b^0 lifetime =		1.480 ± 0.030	
CDF2	$J/\psi\Omega^-$	01–11	$1.66^{+0.53}_{-0.40} \pm 0.02$	[131]
LHCb	$J/\psi\Omega^-$	11–12	$1.54^{+0.26}_{-0.21} \pm 0.05$	[137]
LHCb	$\Omega_c^0\pi^-$ (w.r.t. Ξ_b^-)	11–12	$1.78 \pm 0.26 \pm 0.05 \pm 0.06$	[140]
Average of above 3:	Ω_b^- lifetime =		$1.64^{+0.18}_{-0.17}$	

[a]The combined ALEPH result quoted in [124] is 1.21 ± 0.11 ps.
[b]The combined DELPHI result quoted in [125] is $1.14 \pm 0.08 \pm 0.04$ ps.
[c]The combined OPAL result quoted in [127] is $1.16 \pm 0.11 \pm 0.06$ ps.
[d]The combined DELPHI result quoted in [136] is $1.48^{+0.40}_{-0.31} \pm 0.12$ ps.

6. Summary and comparison with theoretical predictions

Averages of lifetimes of specific b-hadron species are collected in Table 13. As described in the introduction to Sec. VA, the HQE can be employed to explain the hierarchy $\tau(B_c^+) \ll \tau(\Lambda_b^0) < \tau(B_s^0) \approx \tau(B^0) < \tau(B^+)$, and to predict the ratios between lifetimes. Recent predictions are compared to the measured lifetime ratios in Table 14, where the experimental values of $\tau(B_s^0)/\tau(B^0)$ and $\tau(\Lambda_b^0)/\tau(B^0)$ have been computed as the ratio of our averages of the individual lifetimes.

The predictions of the ratio between the B^+ and B^0 lifetimes, $1.082^{+0.022}_{-0.026}$ [56], is in good agreement with experiment.

The total widths of the B_s^0 and B^0 mesons are expected to be very close and to differ by at most 1% [44,54–56,141]. This prediction is consistent with the experimental ratio $\tau(B_s^0)/\tau(B^0)$, which is smaller than 1 by $(-0.1 \pm 0.4)\%$. The authors of Refs. [42,88] predict $\tau(B_s^0)/\tau(B^0) = 1.00050 \pm 0.00108 \pm 0.0225 \times \delta$, where δ quantifies a possible breaking of the quark-hadron duality. In this

TABLE 13. Summary of the lifetime averages for the different b-hadron species.

b-hadron species		Measured lifetime
B^+		1.638 ± 0.004 ps
B^0		1.519 ± 0.004 ps
B_s^0	$1/\Gamma_s =$	1.520 ± 0.005 ps
B_{sL}^0	$1/\Gamma_{sL} =$	1.429 ± 0.007 ps
B_{sH}^0	$1/\Gamma_{sH} =$	1.624 ± 0.009 ps
B_c^+		0.510 ± 0.009 ps
Λ_b^0		1.471 ± 0.009 ps
Ξ_b^-		1.572 ± 0.040 ps
Ξ_b^0		1.480 ± 0.030 ps
Ω_b^-		$1.64^{+0.18}_{-0.17}$ ps

TABLE 14. Experimental averages of b-hadron lifetime ratios and heavy-quark expansion (HQE) predictions.

Lifetime ratio	Experimental average	HQE prediction
$\tau(B^+)/\tau(B^0)$	1.076 ± 0.004	$1.082^{+0.022}_{-0.026}$ [56]
$\tau(B_s^0)/\tau(B^0)$	1.001 ± 0.004	1.0007 ± 0.0025 [56]
$\tau(\Lambda_b^0)/\tau(B^0)$	0.969 ± 0.006	0.935 ± 0.054 [55]
$\tau(\Xi_b^0)/\tau(\Xi_b^-)$	0.929 ± 0.028	0.95 ± 0.06 [55]

context, they propose to interpret any difference between theory and experiment as being due to either new physics or a sizable duality violation. The key message is that improved experimental precision on this ratio will be beneficial.

The ratio $\tau(\Lambda_b^0)/\tau(B^0)$ in particular has been the source of theoretical scrutiny, since earlier calculations using the HQE [36–38,43] predicted a value larger than 0.90, almost 2σ above the world average at the time. Many predictions cluster around a most likely central value of 0.94 [142]. Calculations of this ratio that include higher-order effects predict a smaller value [48] and reduced this difference. Since then, the experimental average has settled at a value significantly larger than initially, in agreement with the latest theoretical predictions. A review [55] concludes that the long-standing Λ_b^0 lifetime puzzle is resolved, with a nice agreement between the precise experimental determination of $\tau(\Lambda_b^0)/\tau(B^0)$ and the less precise HQE prediction, which needs new lattice calculations. There is also good agreement for the $\tau(\Xi_b^0)/\tau(\Xi_b^-)$ ratio, for which the prediction is based on the next-to-leading-order calculation of Ref. [47].

B. Neutral B-meson mixing

The $B^0 - \bar{B}^0$ and $B_s^0 - \bar{B}_s^0$ systems both exhibit the phenomenon of particle-antiparticle mixing. For each of them, there are two mass eigenstates which are linear combinations of the two flavor states, B_q^0 and $\bar{B}_q^0$,

$$|B_{qL}^0\rangle = p_q|B_q^0\rangle + q_q|\bar{B}_q^0\rangle, \tag{46}$$

$$|B_{qH}^0\rangle = p_q|B_q^0\rangle - q_q|\bar{B}_q^0\rangle, \tag{47}$$

where the subscript $q = d$ is used for the B_d^0 $(= B^0)$ meson and $q = s$ for the B_s^0 meson. The heavier (lighter) of these mass states is denoted B_{qH}^0 (B_{qL}^0), with mass m_{qH} (m_{qL}) and total decay width Γ_{qH} (Γ_{qL}). We define

$$\Delta m_q = m_{qH} - m_{qL}, \qquad x_q = \Delta m_q/\Gamma_q, \tag{48}$$

$$\Delta\Gamma_q = \Gamma_{qL} - \Gamma_{qH}, \qquad y_q = \Delta\Gamma_q/(2\Gamma_q), \tag{49}$$

where $\Gamma_q = (\Gamma_{qH} + \Gamma_{qL})/2 = 1/\bar{\tau}(B_q^0)$ is the average decay width. Δm_q is positive by definition, and $\Delta\Gamma_q$ is expected to be positive within the Standard Model.[5]

Four different time-dependent probabilities are needed to describe the evolution of a neutral B meson that is produced as a flavor state and decays without CP violation to a flavor-specific final state. If CPT is conserved (which will be assumed throughout), they can be written as

$$\begin{cases} \mathcal{P}(B_q^0 \to B_q^0) = \frac{1}{2}e^{-\Gamma_q t}\left[\cosh\left(\frac{1}{2}\Delta\Gamma_q t\right) + \cos\left(\Delta m_q t\right)\right] \\ \mathcal{P}(B_q^0 \to \bar{B}_q^0) = \frac{1}{2}e^{-\Gamma_q t}\left[\cosh\left(\frac{1}{2}\Delta\Gamma_q t\right) - \cos\left(\Delta m_q t\right)\right]|q_q/p_q|^2 \\ \mathcal{P}(\bar{B}_q^0 \to B_q^0) = \frac{1}{2}e^{-\Gamma_q t}\left[\cosh\left(\frac{1}{2}\Delta\Gamma_q t\right) - \cos\left(\Delta m_q t\right)\right]|p_q/q_q|^2 \\ \mathcal{P}(\bar{B}_q^0 \to \bar{B}_q^0) = \frac{1}{2}e^{-\Gamma_q t}\left[\cosh\left(\frac{1}{2}\Delta\Gamma_q t\right) + \cos\left(\Delta m_q t\right)\right] \end{cases}, \tag{50}$$

[5]For reasons of symmetry in Eqs. (48) and (49), $\Delta\Gamma$ is sometimes defined with the opposite sign. The definition adopted in Eq. (49) is the one used in most experimental papers and many phenomenology papers on B physics.

where t is the proper time of the system (i.e., the time interval between the production and the decay in the rest frame of the B meson). At the B factories, only the proper-time difference Δt between the decays of the two neutral B mesons from the $\Upsilon(4S)$ can be determined. However, since the two B mesons evolve coherently (keeping opposite flavors as long as neither of them has decayed), the above formulas remain valid if t is replaced with Δt and the production flavor is replaced by the flavor at the time of the decay of the accompanying B meson into a flavor-specific state. As can be seen in the above expressions, the mixing probabilities depend on three mixing observables: Δm_q, $\Delta\Gamma_q$, and $|q_q/p_q|^2$. In particular, CP violation in mixing exists if $|q_q/p_q|^2 \neq 1$. Another (nonindependent) observable often used to characterize CP violation in the mixing is the so-called semileptonic asymmetry, defined as

$$\mathcal{A}_{\mathrm{SL}}^q = \frac{|p_q/q_q|^2 - |q_q/p_q|^2}{|p_q/q_q|^2 + |q_q/p_q|^2}. \tag{51}$$

All mixing observables depend on two complex numbers, M_{12}^q and Γ_{12}^q, which are the off-diagonal elements of the 2×2 mass and decay matrices describing the evolution of the $B_q^0 - \bar{B}_q^0$ system. In the Standard Model the quantity $|\Gamma_{12}^q/M_{12}^q|$ is small, of the order of $(m_b/m_t)^2$, where m_b and m_t are the bottom and top quark masses. The following relations hold to first order in $|\Gamma_{12}^q/M_{12}^q|$:

$$\Delta m_q = 2|M_{12}^q|[1 + \mathcal{O}(|\Gamma_{12}^q/M_{12}^q|^2)], \tag{52}$$

$$\Delta\Gamma_q = 2|\Gamma_{12}^q|\cos\phi_{12}^q[1 + \mathcal{O}(|\Gamma_{12}^q/M_{12}^q|^2)], \tag{53}$$

$$\begin{aligned}\mathcal{A}_{\mathrm{SL}}^q &= \mathrm{Im}(\Gamma_{12}^q/M_{12}^q) + \mathcal{O}(|\Gamma_{12}^q/M_{12}^q|^2)\\ &= \frac{\Delta\Gamma_q}{\Delta m_q}\tan\phi_{12}^q + \mathcal{O}(|\Gamma_{12}^q/M_{12}^q|^2),\end{aligned} \tag{54}$$

where

$$\phi_{12}^q = \arg(-M_{12}^q/\Gamma_{12}^q) \tag{55}$$

is the observable phase difference between $-M_{12}^q$ and Γ_{12}^q (often called the mixing phase). It should be noted that the theoretical predictions for Γ_{12}^q are based on the same HQE as the lifetime predictions.

In the next sections we review in turn the experimental knowledge on the B^0 decay-width and mass differences, the B_s^0 decay-width and mass differences, CP violation in B^0 and B_s^0 mixing, and mixing-induced CP violation in B_s^0 decays.

1. B^0 mixing parameters $\Delta\Gamma_d$ and Δm_d

A large number of time-dependent B^0–$\bar{B}^0$ oscillation analyses have been performed in the past 20 years by the ALEPH, DELPHI, L3, OPAL, CDF, D0, *BABAR*, Belle, and LHCb collaborations. The corresponding measurements of Δm_d are summarized in Table 15. It is notable that the systematic uncertainties are comparable to the statistical uncertainties; they are often dominated by sample composition, mistag probability, or b-hadron lifetime contributions. Before being combined, the measurements are adjusted to a common set of input values, including the averages of the b-hadron fractions and lifetimes given in this report (see Secs. IV and V A). Some measurements are statistically correlated. Systematic correlations arise both from common physics sources (fractions, lifetimes, branching fractions of b hadrons), and from purely experimental or algorithmic effects (efficiency, resolution, flavor tagging, background description). Combining all published measurements listed in Table 15 and accounting for all identified correlations as described in Ref. [4] yields $\Delta m_d = 0.5065 \pm 0.0016 \pm 0.0011$ ps^{-1}.

In addition, ARGUS and CLEO have published measurements of the time-integrated mixing probability χ_d [162] [163,164], which average to $\chi_d = 0.182 \pm 0.015$. Following Ref. [164], the decay width difference $\Delta\Gamma_d$ could in principle be extracted from the measured value of $\Gamma_d = 1/\tau(B^0)$ and the above averages for Δm_d and χ_d (provided that $\Delta\Gamma_d$ has a negligible impact on the Δm_d and $\tau(B^0)$ analyses that have assumed $\Delta\Gamma_d = 0$), using the relation

$$\chi_d = \frac{x_d^2 + y_d^2}{2(x_d^2 + 1)}. \tag{56}$$

However, $\Delta\Gamma_d/\Gamma_d$ is too small and the knowledge of χ_d too imprecise to provide useful sensitivity on $\Delta\Gamma_d/\Gamma_d$. Direct time-dependent studies provide much stronger constraints: $|\Delta\Gamma_d|/\Gamma_d < 18\%$ at 95% CL from DELPHI [145], $-6.8\% < \mathrm{sign}(\mathrm{Re}\lambda_{CP})\Delta\Gamma_d/\Gamma_d < 8.4\%$ at 90% CL from *BABAR* [165], and $\mathrm{sign}(\mathrm{Re}\lambda_{CP})\Delta\Gamma_d/\Gamma_d = (1.7 \pm 1.8 \pm 1.1)\%$ [166] from Belle, where $\lambda_{CP} = (q_d/p_d)A(\bar{B}^0 \to f_{CP})/A(B^0 \to f_{CP})$ with A the denoting decays amplitudes to a CP-even final state. The sensitivity to the overall sign of $\mathrm{Re}\lambda_{CP}\Delta\Gamma_d/\Gamma_d$ comes from the use of B^0 decays to CP eigenstates. In addition, LHCb has obtained $\Delta\Gamma_d/\Gamma_d = (-4.4 \pm 2.5 \pm 1.1)\%$ [82] by comparing measurements of the lifetime for $B^0 \to J/\psi K^{*0}$ and $B^0 \to J/\psi K_S^0$ decays, following the method of Ref. [167]. Using a similar method, ATLAS and CMS have measured $\Delta\Gamma_d/\Gamma_d = (-0.1 \pm 1.1 \pm 0.9)\%$ [168] and $\Delta\Gamma_d/\Gamma_d = (+3.4 \pm 2.3 \pm 2.4)\%$ [81], respectively. Assuming $\mathrm{Re}\lambda_{CP} > 0$, as expected from the global fits of the unitarity triangle within the Standard Model [169], a combination of these six results (after adjusting the DELPHI and *BABAR* results to $1/\Gamma_d = \tau(B^0) = 0.001 \pm 0.004$ ps) yields

$$\Delta\Gamma_d/\Gamma_d = 0.001 \pm 0.010. \tag{57}$$

TABLE 15. Time-dependent measurements included in the Δm_d average. The results obtained from multidimensional fits involving also the B^0 (and B^+) lifetime(s) as free parameter(s) [76,78,79] have been converted into one-dimensional measurements of Δm_d. All measurements have then been adjusted to a common set of physics parameters before being combined.

	Method			
Experiment and references	rec.	tag	Δm_d in ps^{-1} before adjustment	Δm_d in ps^{-1} after adjustment
ALEPH [143]	ℓ	$Q_{\rm jet}$	$0.404 \pm 0.045 \pm 0.027$	
ALEPH [143]	ℓ	ℓ	$0.452 \pm 0.039 \pm 0.044$	
ALEPH [143]	Above two combined		$0.422 \pm 0.032 \pm 0.026$	$0.440 \pm 0.032\,^{+0.020}_{-0.019}$
ALEPH [143]	D^*	$\ell, Q_{\rm jet}$	$0.482 \pm 0.044 \pm 0.024$	$0.482 \pm 0.044 \pm 0.024$
DELPHI [144]	ℓ	$Q_{\rm jet}$	$0.493 \pm 0.042 \pm 0.027$	$0.499 \pm 0.042 \pm 0.024$
DELPHI [144]	$\pi^*\ell$	$Q_{\rm jet}$	$0.499 \pm 0.053 \pm 0.015$	$0.500 \pm 0.053 \pm 0.015$
DELPHI [144]	ℓ	ℓ	$0.480 \pm 0.040 \pm 0.051$	$0.495 \pm 0.040\,^{+0.042}_{-0.040}$
DELPHI [144]	D^*	$Q_{\rm jet}$	$0.523 \pm 0.072 \pm 0.043$	$0.518 \pm 0.072 \pm 0.043$
DELPHI [145]	vtx	comb	$0.531 \pm 0.025 \pm 0.007$	$0.525 \pm 0.025 \pm 0.006$
L3 [146]	ℓ	ℓ	$0.458 \pm 0.046 \pm 0.032$	$0.468 \pm 0.046 \pm 0.028$
L3 [146]	ℓ	$Q_{\rm jet}$	$0.427 \pm 0.044 \pm 0.044$	$0.439 \pm 0.044 \pm 0.042$
L3 [146]	ℓ	ℓ(IP)	$0.462 \pm 0.063 \pm 0.053$	$0.472 \pm 0.063 \pm 0.044$
OPAL [147]	ℓ	ℓ	$0.430 \pm 0.043\,^{+0.028}_{-0.030}$	$0.467 \pm 0.043\,^{+0.017}_{-0.016}$
OPAL [148]	ℓ	$Q_{\rm jet}$	$0.444 \pm 0.029\,^{+0.020}_{-0.017}$	$0.482 \pm 0.029 \pm 0.013$
OPAL [149]	$D^*\ell$	$Q_{\rm jet}$	$0.539 \pm 0.060 \pm 0.024$	$0.544 \pm 0.060 \pm 0.023$
OPAL [149]	D^*	ℓ	$0.567 \pm 0.089\,^{+0.029}_{-0.023}$	$0.572 \pm 0.089\,^{+0.028}_{-0.022}$
OPAL [66]	$\pi^*\ell$	$Q_{\rm jet}$	$0.497 \pm 0.024 \pm 0.025$	$0.496 \pm 0.024 \pm 0.025$
CDF1 [150]	$D\ell$	SST	$0.471\,^{+0.078\,+0.033}_{-0.068\,-0.034}$	$0.470\,^{+0.078\,+0.033}_{-0.068\,-0.034}$
CDF1 [151]	μ	μ	$0.503 \pm 0.064 \pm 0.071$	$0.514 \pm 0.064\,^{+0.070}_{-0.069}$
CDF1 [152]	ℓ	$\ell, Q_{\rm jet}$	$0.500 \pm 0.052 \pm 0.043$	$0.545 \pm 0.052 \pm 0.036$
CDF1 [153]	$D^*\ell$	ℓ	$0.516 \pm 0.099\,^{+0.029}_{-0.035}$	$0.523 \pm 0.099\,^{-0.035}_{+0.028}$
D0 [154]	$D^{(*)}\mu$	OST	$0.506 \pm 0.020 \pm 0.016$	$0.506 \pm 0.020 \pm 0.016$
BABAR [155]	B^0	ℓ, K, NN	$0.516 \pm 0.016 \pm 0.010$	$0.521 \pm 0.016 \pm 0.008$
BABAR [156]	ℓ	ℓ	$0.493 \pm 0.012 \pm 0.009$	$0.487 \pm 0.012 \pm 0.006$
BABAR [76]	$D^*\ell\nu$	ℓ, K, NN	$0.492 \pm 0.018 \pm 0.014$	$0.493 \pm 0.018 \pm 0.013$
BABAR [78]	$D^*\ell\nu$(part)	ℓ	$0.511 \pm 0.007 \pm 0.007$	$0.513 \pm 0.007 \pm 0.007$
Belle [79]	$B^0, D^*\ell\nu$	comb	$0.511 \pm 0.005 \pm 0.006$	$0.514 \pm 0.005 \pm 0.006$
Belle [157]	$D^*\pi$(part)	ℓ	$0.509 \pm 0.017 \pm 0.020$	$0.514 \pm 0.017 \pm 0.019$
Belle [13]	ℓ	ℓ	$0.503 \pm 0.008 \pm 0.010$	$0.506 \pm 0.008 \pm 0.008$
LHCb [158]	B^0	OST	$0.499 \pm 0.032 \pm 0.003$	$0.499 \pm 0.032 \pm 0.003$
LHCb [159]	B^0	OST,SST	$0.5156 \pm 0.0051 \pm 0.0033$	$0.5156 \pm 0.0051 \pm 0.0033$
LHCb [160]	$D\mu$	OST,SST	$0.503 \pm 0.011 \pm 0.013$	$0.503 \pm 0.011 \pm 0.013$
LHCb [161]	$D^{(*)}\mu$	OST	$0.5050 \pm 0.0021 \pm 0.0010$	$0.5050 \pm 0.0021 \pm 0.0010$
World average (all above measurements included):				$0.5065 \pm 0.0016 \pm 0.0011$
—ALEPH, DELPHI, L3 and OPAL only:				$0.494 \pm 0.011 \pm 0.009$
—CDF and D0 only:				$0.509 \pm 0.017 \pm 0.013$
—*BABAR* and Belle only:				$0.509 \pm 0.003 \pm 0.003$
—LHCb only:				$0.5063 \pm 0.0019 \pm 0.0010$

This average is consistent with zero and with the latest Standard Model prediction of $(3.97 \pm 0.90) \times 10^{-3}$ [88]. An independent result, $\Delta\Gamma_d/\Gamma_d = (0.50 \pm 1.38)\%$ [170], was obtained by the D0 collaboration from their measurements of the single muon and same-sign dimuon charge asymmetries, under the interpretation that the observed asymmetries are due to CP violation in neutral B-meson mixing and interference. This indirect determination was called into question [171] and is therefore not included in the above average, as explained in Sec. V B 3.

Assuming $\Delta\Gamma_d = 0$ and using $1/\Gamma_d = \tau(B^0) = 1.519 \pm 0.004$ ps, the Δm_d and χ_d results are combined through Eq. (56) to yield the world average

$$\Delta m_d = 0.5065 \pm 0.0019 \text{ ps}^{-1}, \tag{58}$$

or, equivalently,

$$x_d = 0.769 \pm 0.004 \quad \text{and} \quad \chi_d = 0.1858 \pm 0.0011. \tag{59}$$

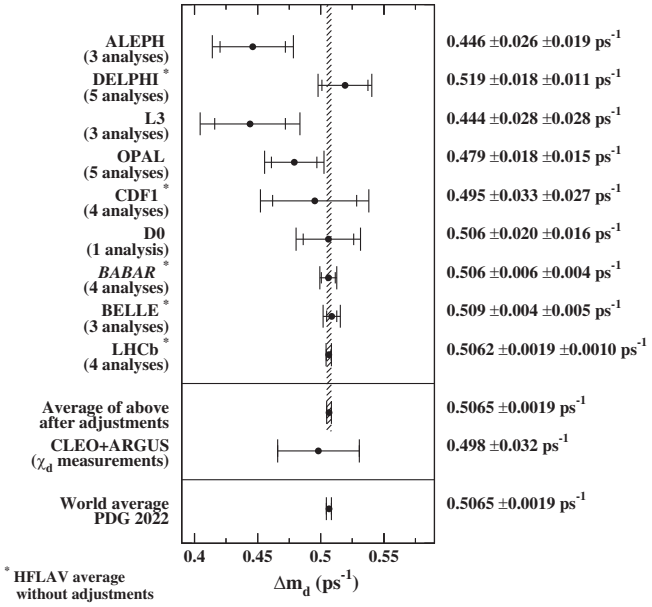

FIG. 4. The B^0–$\bar{B}^0$ oscillation frequency Δm_d as measured by the different experiments. The averages quoted for ALEPH, L3 and OPAL are taken from the original publications, while the ones for DELPHI, CDF, *BABAR*, Belle and LHCb are computed from the individual results listed in Table 15 without performing any adjustments. The time-integrated measurements of χ_d from the symmetric B factory experiments ARGUS and CLEO are converted to a Δm_d value using $\tau(B^0) = 1.519 \pm 0.004$ ps. The two global averages are obtained after adjustments of all the individual Δm_d results of Table 15 (see text).

Figure 4 compares the Δm_d values obtained by the different experiments.

The B^0 mixing averages given in Eqs. (58) and (59) and the b-hadron fractions of Ref. [1] have been obtained in a fully consistent way, taking into account the fact that the fractions are computed using the χ_d value of Eq. (59) and that many individual measurements of Δm_d at high energy depend on the assumed values for the b-hadron fractions. Furthermore, this set of averages is consistent with the lifetime averages of Sec. V A.

2. B_s^0 mixing parameters $\Delta\Gamma_s$ and Δm_s

The best sensitivity to $\Delta\Gamma_s$ is currently achieved by the recent time-dependent measurements of the $B_s^0 \to J/\psi\phi$ (or more generally $B_s^0 \to (c\bar{c})K^+K^-$) decay rates performed at CDF [172], D0 [173], ATLAS [174–176] CMS [177,178] and LHCb [179–183], where the CP-even and CP-odd amplitudes are statistically separated through a full angular analysis. These studies use both untagged and tagged B_s^0 candidates and are optimized for the measurement of the CP-violating phase $\phi_s^{c\bar{c}s}$, defined later in Sec. V B 4. The LHCb collaboration analyzed the $B_s^0 \to J/\psi K^+K^-$ decay, considering that the K^+K^- system can be in a P-wave or S-wave state, and measured the dependence of the strong phase difference between the P-wave and S-wave amplitudes as a function of the K^+K^- invariant mass [86]. This allowed, for the first time, the unambiguous determination of the sign of $\Delta\Gamma_s$, which was found to be positive at the 4.7σ level. The following

TABLE 16. Measurements of $\Delta\Gamma_s$ and Γ_s using $B_s^0 \to J/\psi\phi$, $B_s^0 \to J/\psi K^+K^-$ and $B_s^0 \to \psi(2S)\phi$ decays. Only the solution with $\Delta\Gamma_s > 0$ is shown, since the two-fold ambiguity has been resolved in Ref. [86]. The first error is due to statistics, the second one to systematics. The last line gives our average.

Experiment	Mode	Dataset	$\Delta\Gamma_s$ (ps^{-1})	Γ_s (ps^{-1})	References
CDF	$J/\psi\phi$	9.6 fb^{-1}	$+0.068 \pm 0.026 \pm 0.009$	$0.654 \pm 0.008 \pm 0.004$	[172]
D0	$J/\psi\phi$	8.0 fb^{-1}	$+0.163^{+0.065}_{-0.064}$	$0.693^{+0.018}_{-0.017}$	[173]
ATLAS	$J/\psi\phi$	4.9 fb^{-1}	$+0.053 \pm 0.021 \pm 0.010$	$0.677 \pm 0.007 \pm 0.004$	[174]
ATLAS	$J/\psi\phi$	14.3 fb^{-1}	$+0.101 \pm 0.013 \pm 0.007$	$0.676 \pm 0.004 \pm 0.004$	[175]
ATLAS	$J/\psi\phi$	80.5 fb^{-1}	$+0.0607 \pm 0.0047 \pm 0.0043$	$0.6687 \pm 0.0015 \pm 0.0022$	[176]
ATLAS	above 3 combined		$+0.0657 \pm 0.0043 \pm 0.0037$	$0.6703 \pm 0.0014 \pm 0.0018$	[176]
CMS	$J/\psi\phi$	19.7 fb^{-1}	$+0.095 \pm 0.013 \pm 0.007$	$0.6704 \pm 0.0043 \pm 0.0055$	[177]
CMS	$J/\psi\phi$	96.4 fb^{-1}	$+0.114 \pm 0.014 \pm 0.007$	$0.6531 \pm 0.0042 \pm 0.0026$	[178]
CMS	above 2 combined		$+0.1032 \pm 0.0095 \pm 0.0048$	$0.6590 \pm 0.0032 \pm 0.0023$	[178]
LHCb	$J/\psi K^+K^-$	3.0 fb^{-1}	$+0.0805 \pm 0.0091 \pm 0.0032$	$0.6603 \pm 0.0027 \pm 0.0015$	[179]
LHCb	$J/\psi K^+K^-$[a]	3.0 fb^{-1}	$+0.066 \pm 0.018 \pm 0.010$	$0.650 \pm 0.006 \pm 0.004$	[180]
LHCb	Above 2 combined		$+0.0813 \pm 0.0073 \pm 0.0036$	$0.6588 \pm 0.0022 \pm 0.0015$	[180]
LHCb	$J/\psi K^+K^-$	1.9 fb^{-1}	$+0.077 \pm 0.008 \pm 0.003$	$-0.0041 \pm 0.0024 \pm 0.0015$[b]	[183]
LHCb	$J/\psi K^+K^-$[c]	3.0 fb^{-1}	$+0.115 \pm 0.045 \pm 0.011$	$0.608 \pm 0.018 \pm 0.012$	[182]
LHCb	$\psi(2S)\phi$	3.0 fb^{-1}	$+0.066^{+0.041}_{-0.044} \pm 0.007$	$0.668 \pm 0.011 \pm 0.006$	[181]
All combined			$+0.074 \pm 0.006$	0.6627 ± 0.0036	

[a] $m(K^+K^-) > 1.05\,\text{GeV}/c^2$.
[b] $\Gamma_s - \Gamma_d$.
[c] $J/\psi \to e^+e^-$.

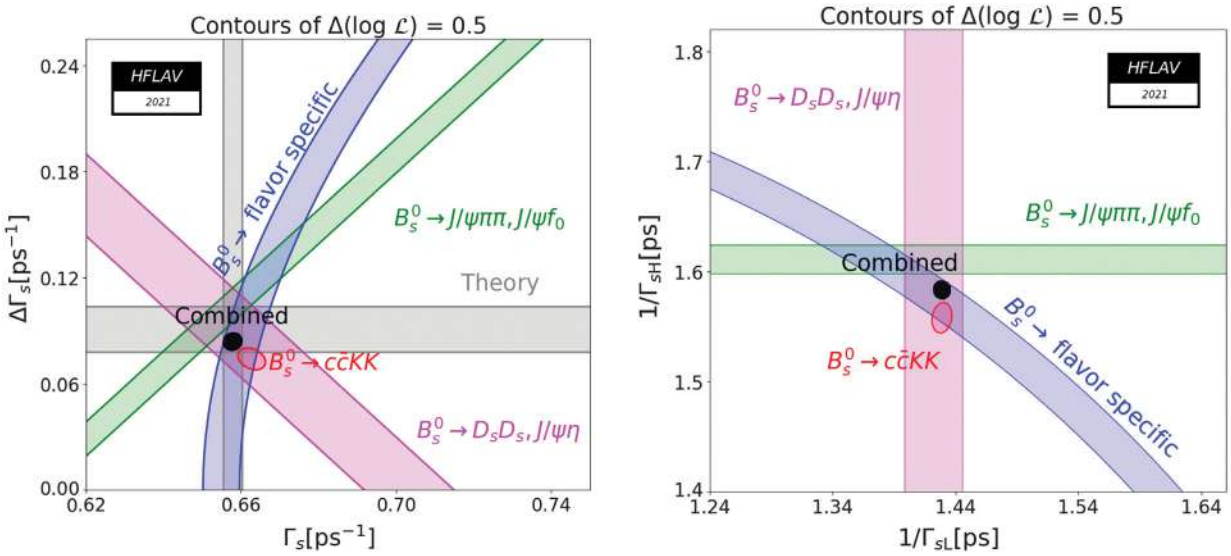

FIG. 5. Contours of $\Delta \ln L = 0.5$ (39% CL for the enclosed 2D regions, 68% CL for the bands) shown in the $(\Gamma_s, \Delta\Gamma_s)$ plane on the left and in the $(1/\Gamma_{sL}, 1/\Gamma_{sH})$ plane on the right. The average of all the $B_s^0 \to J/\psi\phi$, $B_s^0 \to J/\psi K^+K^-$ and $B_s^0 \to \psi(2S)\phi$ results is shown as the red contour, where Γ_s and $\Delta\Gamma_s$ are scaled by factors 2.56 and 1.72. The constraints given by the effective lifetime measurements of B_s^0 to flavor-specific, pure CP-odd and pure CP-even final states are shown as the blue, green and purple bands, respectively. The average taking all constraints into account is shown as the dark-filled contour. The light-gray bands are theory predictions. The horizontal band is $\Delta\Gamma_s = +0.091 \pm 0.013$ ps^{-1} [42,45,87,88] that assumes no new physics in B_s^0 mixing. The vertical Γ_s band is calculated from Ref. [56] assuming the experimental world average for the B^0 lifetime, 1.519 ± 0.004 ps.

averages present only the $\Delta\Gamma_s > 0$ solutions. Two degenerate solutions, differing in the values of two of the measured strong phases, $\delta_\perp$ and $\delta_\parallel$, were found in the ATLAS Run 2 analysis [176]. These show minor differences in the B_s^0 lifetime and mixing parameters, so for simplicity, the following averages only use solution (a) of Ref. [176].

The published results [172–183] are shown in Table 16. They are combined in a fit that includes all measured parameters and their correlations. These are $\phi_s^{c\bar{c}s}$, the direct CP violation parameter $|\lambda| = |(q_s/p_s)\bar{A}/A|$ ($\bar{A}$ and A being the $\bar{B}_s^0$ and B_s^0 decay amplitudes, respectively), Δm_s, polarization fractions and strong phases. As detailed further in Sec. V B 4, the $B_s^0 \to J/\psi\phi$ measurements of ATLAS [175,176], CMS [177,178] and LHCb [179,183] are in tension at the level of approximately 3σ, driven by the time and angular parameters. To address this, the total uncertainty for each parameter in each $B_s^0 \to J/\psi\phi$ set of results by ATLAS, CDF, D0, CMS and LHCb is scaled up in a way that results in an agreement of 1σ. For the parameters already in agreement (i.e., the ϕ_s and S-wave parameters), the uncertainties are not scaled. The covariance matrix is recomputed to preserve the correlations between the parameters. The resulting scale factors for Γ_s and $\Delta\Gamma_s$ are 2.56 and 1.72. The results, displayed as the red contours labeled "$B_s^0 \to (c\bar{c})KK$" in the plots of Fig. 5, are given in the first column of numbers of Table 17.

An alternative approach, which is directly sensitive to first order in $\Delta\Gamma_s/\Gamma_s$, is to determine the effective lifetime of untagged B_s^0 candidates decaying to pure CP eigenstates; we use here measurements with $B_s^0 \to D_s^+D_s^-$ [102], $B_s^0 \to J/\psi\eta$ [111], $B_s^0 \to J/\psi f_0(980)$ [113,114] and $B_s^0 \to J/\psi\pi^+\pi^-$ [93,115] decays. The precise extraction of $1/\Gamma_s$ and $\Delta\Gamma_s$ from such measurements, discussed in detail in Refs. [90–92], requires additional information in the form of theoretical assumptions or external inputs on weak phases and hadronic parameters. If f denotes a final state into which both B_s^0 and $\bar{B}_s^0$ can decay, the ratio of the effective $B_s^0 \to f$ lifetime τ_{single}, found by fitting the decay-time distribution to a single exponential, relative to the mean B_s^0 lifetime is [92][6]

$$\frac{\tau_{\mathrm{single}}(B_s^0 \to f)}{\tau(B_s^0)} = \frac{1}{1-y_s^2}\left[\frac{1 - 2A_f^{\Delta\Gamma}y_s + y_s^2}{1 - A_f^{\Delta\Gamma}y_s}\right], \quad (60)$$

where

$$A_f^{\Delta\Gamma} = -\frac{2\mathrm{Re}(\lambda_f)}{1+|\lambda_f|^2}. \quad (61)$$

To include the measurements of the effective $B_s^0 \to D_s^+D_s^-$ (CP-even), $B_s^0 \to J/\psi\eta$ (CP-even), $B_s^0 \to J/\psi f_0(980)$ (CP-odd) and $B_s^0 \to J/\psi\pi^+\pi^-$ (CP-odd) lifetimes as

[6]The definition of $A_f^{\Delta\Gamma}$ given in Eq. (61) has the sign opposite to that given in Ref. [92].

TABLE 17. Averages of $\Delta\Gamma_s$, Γ_s and related quantities, obtained from $B_s^0 \to J/\psi\phi$, $B_s^0 \to J/\psi K^+K^-$ and $B_s^0 \to \psi(2S)\phi$ alone (first column), adding the constraints from the effective lifetimes measured in pure CP modes $B_s^0 \to D_s^+D_s^-, J/\psi\eta$ and $B_s^0 \to J/\psi f_0(980), J/\psi\pi^+\pi^-$ (second column), and adding the constraint from the effective lifetime measured in flavor-specific modes $B_s^0 \to D_s^-\ell^+\nu X, D_s^-\pi^+, D_s^-D^+$ (third column, recommended world averages).

	$B_s^0 \to (c\bar{c})K^+K^-$ modes only (see Table 16)	$B_s^0 \to (c\bar{c})K^+K^-$ modes + pure CP modes	$B_s^0 \to (c\bar{c})K^+K^-$ modes + pure CP modes + flavor-specific modes
Γ_s	0.6627 ± 0.0036 ps^{-1}	0.6570 ± 0.0027 ps^{-1}	0.6578 ± 0.0024 ps^{-1}
$1/\Gamma_s$	1.509 ± 0.008 ps	1.522 ± 0.006 ps	1.520 ± 0.005 ps
$1/\Gamma_{s\mathrm{L}}$	1.429 ± 0.008 ps	1.430 ± 0.008 ps	1.429 ± 0.007 ps
$1/\Gamma_{s\mathrm{H}}$	1.598 ± 0.014 ps	1.626 ± 0.010 ps	1.624 ± 0.009 ps
$\Delta\Gamma_s$	$+0.074 \pm 0.006$ ps^{-1}	$+0.084 \pm 0.005$ ps^{-1}	$+0.084 \pm 0.005$ ps^{-1}
$\Delta\Gamma_s/\Gamma_s$	$+0.112 \pm 0.010$	$+0.128 \pm 0.008$	$+0.128 \pm 0.007$
$\rho(\Gamma_s, \Delta\Gamma_s)$	-0.30	0.00	$+0.09$

constraints in the $\Delta\Gamma_s$ fit,[7] we neglect subleading penguin contributions and possible direct CP violation. Explicitly, in Eq. (60), we set $A^{\Delta\Gamma}_{CP\text{-even}} = \cos\phi_s^{c\bar{c}s}$ and $A^{\Delta\Gamma}_{CP\text{-odd}} = -\cos\phi_s^{c\bar{c}s}$. Given the small value of $\phi_s^{c\bar{c}s}$, we have, to first order in y_s:

$$\tau_{\text{single}}(B_s^0 \to CP\text{-even}) \approx \frac{1}{\Gamma_{s\mathrm{L}}}\left(1 + \frac{(\phi_s^{c\bar{c}s})^2 y_s}{2}\right), \quad (62)$$

$$\tau_{\text{single}}(B_s^0 \to CP\text{-odd}) \approx \frac{1}{\Gamma_{s\mathrm{H}}}\left(1 - \frac{(\phi_s^{c\bar{c}s})^2 y_s}{2}\right). \quad (63)$$

The numerical inputs are taken from Eqs. (35) and (36), and the resulting averages, combined with the $B_s^0 \to J/\psi K^+K^-$ information, are indicated in the second column of numbers of Table 17.

Information on $\Delta\Gamma_s$ is also obtained from the study of the proper time distribution of untagged samples of flavor-specific B_s^0 decays [90], e.g., semileptonic B_s^0 decays, where the flavor (i.e., B_s^0 or $\bar{B}_s^0$) at the time of decay is determined by the decay products. Since there is an equal mix of the heavy and light mass eigenstates at production time ($t = 0$), the proper time distribution is a superposition of two exponential functions with decay constants $\Gamma_{s\mathrm{L}}$ and $\Gamma_{s\mathrm{H}}$. This provides sensitivity to both $1/\Gamma_s$ and $(\Delta\Gamma_s/\Gamma_s)^2$. Ignoring $\Delta\Gamma_s$ and fitting for a single exponential leads to an estimate of Γ_s with a relative bias proportional to $(\Delta\Gamma_s/\Gamma_s)^2$, as shown in Eq. (33). Including the constraint from the world-average flavor-specific B_s^0 lifetime, given in Eq. (34), leads to the results shown in the last column of Table 17. These world averages are displayed as the dark-filled contours labeled "Combined" in the plots of Fig. 5. They correspond to the lifetime averages $1/\Gamma_s = 1.520 \pm 0.005$ ps, $1/\Gamma_{s\mathrm{L}} = 1.429 \pm 0.007$ ps, $1/\Gamma_{s\mathrm{H}} = 1.624 \pm 0.009$ ps, and to the decay-width difference

$$\Delta\Gamma_s = +0.084 \pm 0.005 \text{ ps}^{-1} \quad \text{and}$$
$$\Delta\Gamma_s/\Gamma_s = +0.128 \pm 0.007. \quad (64)$$

The good agreement with the Standard Model prediction $\Delta\Gamma_s = +0.091 \pm 0.013$ ps^{-1} [42,45,87,88] excludes significant quark-hadron duality violation in the HQE [184]. Estimates of $\Delta\Gamma_s/\Gamma_s$ obtained from measurements of the $B_s^0 \to D_s^{(*)+}D_s^{(*)-}$ branching fraction [109,185–188] are not used in the average, since they are based on the questionable [45] assumption that these decays account for all CP-even final states. The results of early lifetime analyses that attempted to measure $\Delta\Gamma_s/\Gamma_s$ [63,95,99,105] are not used either.

The probability of B_s^0 mixing has been known to be large for more than 20 years. Indeed the time-integrated measurements of the flavor blind measurement $\bar{\chi} = f'_d\chi_d + f'_s\chi_s$, where f'_d and f'_s are the fractions of B^0 and B_s^0 hadrons in a sample of semileptonic b-hadron decays,[8] when compared to our knowledge of χ_d and the b-hadron fractions, indicated that χ_s should be close to its maximal possible value of $1/2$. Many searches of the time dependence of this mixing have been performed by ALEPH [189], DELPHI [95,99,145,190], OPAL [191,192], SLD [193,194], CDF (Run I) [195] and D0 [196] but did not have enough statistical power and proper time resolution to resolve the small period of the B_s^0 oscillations.

B_s^0 oscillations were observed for the first time in 2006 by the CDF collaboration [197], based on samples of flavor-tagged hadronic and semileptonic B_s^0 decays in flavor-specific final states, partially or fully reconstructed in 1 fb^{-1} of data collected during Tevatron's Run II. Since then, the LHCb collaboration obtained the most precise

[7]The effective lifetimes measured in $B_s^0 \to K^+K^-$ (mostly CP-even) and $B_s^0 \to J/\psi K_S^0$ (mostly CP-odd) are not used because we cannot quantify the penguin contributions in those modes.

[8]See Sec. IV. 1. 3 of our previous publication [1].

TABLE 18. Measurements of Δm_s.

Experiment	Method	Dataset		Δm_s (ps^{-1})	References
CDF2	$D_s^{(*)-}\ell^+\nu$, $D_s^{(*)-}\pi^+$, $D_s^-\rho^+$		1 fb^{-1}	$17.77 \pm 0.10 \pm 0.07$	[197]
LHCb	$D_s^-\pi^+$, $D_s^-\pi^+\pi^-\pi^+$	2010	0.036 fb^{-1}	$17.63 \pm 0.11 \pm 0.02$	[198]
LHCb	$D_s^-\mu^+X$	2011	1.0 fb^{-1}	$17.93 \pm 0.22 \pm 0.15$	[160]
LHCb	$D_s^-\pi^+$	2011	1.0 fb^{-1}	$17.768 \pm 0.023 \pm 0.006$	[199]
LHCb	$J/\psi K^+K^-$	2011–2012	3.0 fb^{-1}	$17.711\ ^{+0.055}_{-0.057} \pm 0.011$	[179]
LHCb	$J/\psi K^+K^-$	2015–2016	1.9 fb^{-1}	$17.703 \pm 0.059 \pm 0.018$	[183]
LHCb	above 2 combined	2011–2016	4.9 fb^{-1}	$17.694 \pm 0.041 \pm 0.011$	[183]
CMS	$J/\psi\phi$	2017–2018	96.4 fb^{-1}	$17.51\ ^{+0.10}_{-0.09} \pm 0.03$	[178]
LHCb	$D_s^-\pi^+\pi^-\pi^+$	2011–2018	9 fb^{-1}	$17.757 \pm 0.007 \pm 0.008$	[200]
LHCb	$D_s^-\pi^+$	2015–2018	6 fb^{-1}	$17.768 \pm 0.005 \pm 0.003$	[201]
Average				$17.765 \pm 0.004 \pm 0.004$	

results using fully reconstructed $B_s^0 \to D_s^-\pi^+$ and $B_s^0 \to D_s^-\pi^+\pi^-\pi^+$ decays [198–201]. LHCb has also observed B_s^0 oscillations with semileptonic $B_s^0 \to D_s^-\mu^+X$ decays [160]. In addition, measurements with nonflavor-specific final states have been performed by LHCb with $B_s^0 \to J/\psi K^+K^-$ decays [179,183] and CMS with $B_s^0 \to J/\psi\phi$ decays [178]. The measurements of Δm_s are summarized in Table 18.

An average of all the published CDF, LHCb and CMS results yields

$$\Delta m_s = 17.765 \pm 0.004 \pm 0.004 \text{ ps}^{-1} \tag{65}$$

and is illustrated in Fig. 6. The systematic uncertainties of the LHCb results due to the length scale (affecting all modes), the momentum scale ($B_s^0 \to D_s^-\pi^+$ Run 1 and Run 2, $B_s^0 \to D_s^-\pi^+\pi^-\pi^+$ Run 1 and $B_s^0 \to J/\psi K^+K^-$), the fit bias ($B_s^0 \to D_s^-\pi^+$ Run 1 and $B_s^0 \to D_s^-\pi^+\pi^-\pi^+$ Run 1) and the decay-time bias ($B_s^0 \to D_s^-\pi^+$ Run 1 and Run 2) are

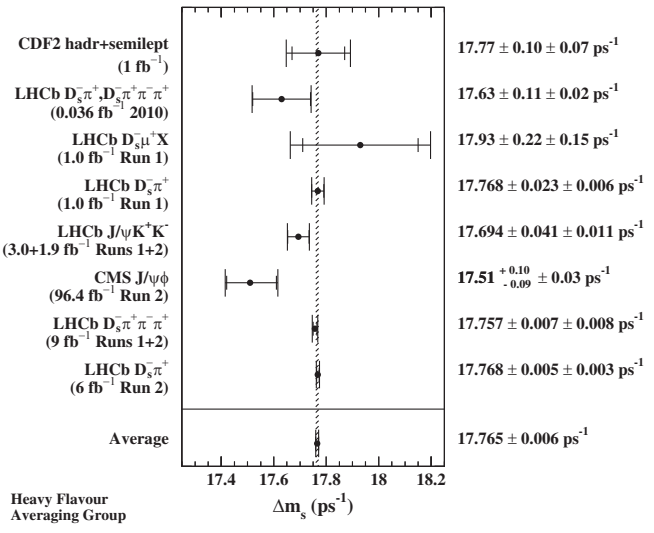

FIG. 6. Measurements of Δm_s, together with their average.

considered to be 100% correlated. Furthermore, the CMS and LHCb measurements of Δm_s in $B_s^0 \to J/\psi K^+K^-$ decays are averaged using the measured central values and uncertainties of the full set of observables determined in these studies (ϕ_s, $\Delta\Gamma_s$, Γ_s, $|\lambda|$, strong phases and polarization fractions) in order to account for their correlations with Δm_s.

The Standard Model prediction $\Delta m_s = 18.77 \pm 0.86$ ps^{-1} [87] is consistent with the experimental value, but has a much larger uncertainty, dominated by the uncertainty on the hadronic matrix elements recently determined in [56,202–207]. The ratio $\Delta\Gamma_s/\Delta m_s$ can be predicted more accurately to be 0.00482 ± 0.00065 [45,87,88,208], in good agreement with the experimental determination of

$$\Delta\Gamma_s/\Delta m_s = 0.00472 \pm 0.00028. \tag{66}$$

Multiplying the Δm_s result of Eq. (68) by the mean B_s^0 lifetime of Eq. (39), $1/\Gamma_s = 1.520 \pm 0.005$ ps, yields

$$x_s = 27.01 \pm 0.10. \tag{67}$$

With $2y_s = +0.128 \pm 0.007$ [see Eq. (64)] and under the assumption of no CP violation in B_s^0 mixing, this corresponds to

$$\chi_s = \frac{x_s^2 + y_s^2}{2(x_s^2+1)} = 0.499318 \pm 0.000005. \tag{68}$$

The ratio

$$\frac{\Delta m_d}{\Delta m_s} = 0.02851 \pm 0.00011, \tag{69}$$

of the B^0 and B_s^0 oscillation frequencies, obtained from Eqs. (58) and (65), can be used to extract the following magnitude of the ratio of CKM matrix elements,

$$\left|\frac{V_{td}}{V_{ts}}\right| = \xi\sqrt{\frac{\Delta m_d}{\Delta m_s}\frac{m(B_s^0)}{m(B^0)}} = \begin{cases} 0.2053 \pm 0.0004 \pm 0.0029\ (\text{lattice QCD}) \\ 0.2045 \pm 0.0004^{+0.0011}_{-0.0012}\ (\text{sum rules}) \end{cases}. \quad (70)$$

The first uncertainty is from experimental uncertainties (with the masses $m(B_s^0)$ and $m(B^0)$ taken from Ref. [9]). The second uncertainty arises from theoretical uncertainties in the estimation of the SU(3) flavor-symmetry breaking factor $\xi = 1.206 \pm 0.017$ [209], which is an average of three-flavor lattice QCD calculations dominated by the results of Ref. [203], or $\xi = 1.201^{+0.006}_{-0.007}$ [206] obtained from sum rules. Note that Eq. (70) assumes that Δm_s and Δm_d only receive Standard Model contributions.

3. *CP* violation in B^0 and B_s^0 mixing

Evidence for *CP* violation in B^0 mixing has been searched for, both with flavor-specific and inclusive B^0 decays, in samples where the initial flavor state is tagged. In the case of semileptonic (or other flavor-specific) decays, where the final state tag is also available, the asymmetry

$$\mathcal{A}_{\rm SL}^d = \frac{N(\bar{B}^0(t) \to \ell^+\nu_\ell X) - N(B^0(t) \to \ell^-\bar{\nu}_\ell X)}{N(\bar{B}^0(t) \to \ell^+\nu_\ell X) + N(B^0(t) \to \ell^-\bar{\nu}_\ell X)} \quad (71)$$

has been measured, either in decay-time-integrated analyses at CLEO [164,210], *BABAR* [211], CDF [212] and D0 [170], or in decay-time-dependent analyses at OPAL [148], ALEPH [213], *BABAR* [165,214,215] and Belle [216]. Note that the asymmetry of time-dependent decay rates in Eq. (71) is related to $|q_d/p_d|$ through Eq. (51) and is therefore time-independent. In the inclusive case, also investigated and published by ALEPH [213] and OPAL [65], no final state tag is used, and the asymmetry [217]

$$\frac{N(B^0(t) \to \text{all}) - N(\bar{B}^0(t) \to \text{all})}{N(B^0(t) \to \text{all}) + N(\bar{B}^0(t) \to \text{all})} \simeq \mathcal{A}_{\rm SL}^d\left[\frac{\Delta m_d}{2\Gamma_d}\sin(\Delta m_d t) - \sin^2\left(\frac{\Delta m_d t}{2}\right)\right] \quad (72)$$

must be measured as a function of the proper time to extract information on *CP* violation. Furthermore, D0 [218] and LHCb [219] have studied the time-dependence of the charge asymmetry of $B^0 \to D^{(*)-}\mu^+\nu_\mu X$ decays without tagging the initial state, which would be equal to

$$\frac{N(D^{(*)-}\mu^+\nu_\mu X) - N(D^{(*)+}\mu^-\bar{\nu}_\mu X)}{N(D^{(*)-}\mu^+\nu_\mu X) + N(D^{(*)+}\mu^-\bar{\nu}_\mu X)} = \mathcal{A}_{\rm SL}^d\frac{1 - \cos(\Delta m_d t)}{2} \quad (73)$$

TABLE 19. Measurements [9] of *CP* violation in B^0 mixing and their average in terms of both $\mathcal{A}_{\rm SL}^d$ and $|q_d/p_d|$. The individual results are listed as quoted in the original publications, or converted [11] to an $\mathcal{A}_{\rm SL}^d$ value. The ALEPH and OPAL results assume no *CP* violation in B_s^0 mixing.

Experiment and references	Method	Measured $\mathcal{A}_{\rm SL}^d$	Measured $\lvert q_d/p_d\rvert$
CLEO [164]	Partial hadronic rec.	$+0.017 \pm 0.070 \pm 0.014$	
CLEO [210]	Dileptons	$+0.013 \pm 0.050 \pm 0.005$	
CLEO [210]	Average of above two	$+0.014 \pm 0.041 \pm 0.006$	
BABAR [165]	Full hadronic rec.		$1.029 \pm 0.013 \pm 0.011$
BABAR [214]	Partial rec. $D^*X\ell\nu$	$+0.0006 \pm 0.0017^{+0.0038}_{-0.0032}$	$0.99971 \pm 0.00084 \pm 0.00175$
BABAR [211]	Dileptons	$-0.0039 \pm 0.0035 \pm 0.0019$	
Belle [216]	Dileptons	$-0.0011 \pm 0.0079 \pm 0.0085$	$1.0005 \pm 0.0040 \pm 0.0043$
Average of above 6 *B*-factory results		-0.0019 ± 0.0027 (tot)	1.0009 ± 0.0013 (tot)
D0 [218]	$B^0 \to D^{(*)-}\mu^+\nu X$	$+0.0068 \pm 0.0045 \pm 0.0014$	
LHCb [219]	$B^0 \to D^{(*)-}\mu^+\nu X$	$-0.0002 \pm 0.0019 \pm 0.0030$	
Average of above 8 pure B^0 results		$+0.0001 \pm 0.0020$ (tot)	1.0000 ± 0.0010 (tot)
D0 [170]	Muons and dimuons	-0.0062 ± 0.0043 (tot)	
Average of above 9 direct measurements		-0.0010 ± 0.0018 (tot)	1.0005 ± 0.0009 (tot)
OPAL [148]	Leptons	$+0.008 \pm 0.028 \pm 0.012$	
OPAL [65]	Inclusive [Eq. (72)]	$+0.005 \pm 0.055 \pm 0.013$	
ALEPH [213]	Leptons	$-0.037 \pm 0.032 \pm 0.007$	
ALEPH [213]	Inclusive [Eq. (72)]	$+0.016 \pm 0.034 \pm 0.009$	
ALEPH [213]	Average of above two	-0.013 ± 0.026 (tot)	
Average of above 13 results		-0.0010 ± 0.0018 (tot)	1.0005 ± 0.0009 (tot)
Best fit value from 2D combination of $\mathcal{A}_{\rm SL}^d$ and $\mathcal{A}_{\rm SL}^s$ results [see Eq. (74)]		-0.0021 ± 0.0017 (tot)	1.0010 ± 0.0008 (tot)

TABLE 20. Measurements of CP violation in B^0 and B_s^0 mixing, together with their correlations $\rho(\mathcal{A}_{\rm SL}^s, \mathcal{A}_{\rm SL}^d)$ and their two-dimensional average. Only total errors are quoted.

Experiment and references	Method	Measured $\mathcal{A}_{\rm SL}^d$	Measured $\mathcal{A}_{\rm SL}^s$	$\rho(\mathcal{A}_{\rm SL}^d, \mathcal{A}_{\rm SL}^s)$
B-factory average of Table 19		-0.0019 ± 0.0027		
D0 [218,222]	$B_{(s)}^0 \to D_{(s)}^{(*)-}\mu^+\nu X$	$+0.0068 \pm 0.0047$	-0.0112 ± 0.0076	$+0.$
LHCb [219,223]	$B_{(s)}^0 \to D_{(s)}^{(*)-}\mu^+\nu X$	-0.0002 ± 0.0036	$+0.0039 \pm 0.0033$	$+0.13$
Average of above		$+0.0000 \pm 0.0019$	$+0.0016 \pm 0.0030$	$+0.066$
D0 [170]	Muons and dimuons	-0.0062 ± 0.0043	-0.0082 ± 0.0099	-0.61
Average of all above		-0.0021 ± 0.0017	-0.0006 ± 0.0028	-0.054

in absence of detection and production asymmetries. Note that Eqs. (72) and (73) assume $\Delta\Gamma_d = 0$.

Table 19 summarizes the different measurements[9] of $\mathcal{A}_{\rm SL}^d$ and $|q_d/p_d|$. In all cases asymmetries compatible with zero have been found. A simple average of all measurements performed at the B factories [164,165,210,211,214,216] yields $\mathcal{A}_{\rm SL}^d = -0.0019 \pm 0.0027$. Adding also the D0 [218] and LHCb [219] measurements obtained with reconstructed semileptonic B^0 decays yields $\mathcal{A}_{\rm SL}^d = +0.0001 \pm 0.0020$. As discussed in more detail later in this section, the D0 analysis with single muons and like-sign dimuons [170] separates the B^0 and B_s^0 contributions by exploiting the dependence on the muon impact parameter cut; including this $\mathcal{A}_{\rm SL}^d$ result from D0 in the average yields $\mathcal{A}_{\rm SL}^d = -0.0010 \pm 0.0018$.

All the other B^0 analyses performed at high energy, either at LEP or at the Tevatron, did not separate the contributions from the B^0 and B_s^0 mesons. Under the assumption of no CP violation in B_s^0 mixing ($\mathcal{A}_{\rm SL}^s = 0$), a number of these early analyses [65,148,213,220] report a measurement of $\mathcal{A}_{\rm SL}^d$ or $|q_d/p_d|$ for the B^0 meson. However, although we include them in Table 19, these imprecise determinations no longer improve the world average of $\mathcal{A}_{\rm SL}^d$. Furthermore, the assumption makes sense within the Standard Model, since $\mathcal{A}_{\rm SL}^s$ is predicted to be about a factor 20 smaller than $\mathcal{A}_{\rm SL}^d$ [87], but may not be suitable in the presence of new physics.

The Tevatron experiments have measured linear combinations of $\mathcal{A}_{\rm SL}^d$ and $\mathcal{A}_{\rm SL}^s$ using inclusive semileptonic decays of b hadrons. CDF (Run I) finds $\mathcal{A}_{\rm SL}^b = +0.0015 \pm 0.0038({\rm stat}) \pm 0.0020({\rm syst})$ [212], and D0 obtains $\mathcal{A}_{\rm SL}^b = -0.00496 \pm 0.00153({\rm stat}) \pm 0.00072({\rm syst})$ [170]. While the imprecise CDF result is compatible with no CP violation, the D0 result, obtained by measuring the single muon and like-sign dimuon charge asymmetries, differs by 2.8 standard deviations from the Standard Model expectation of $\mathcal{A}_{\rm SL}^{b,{\rm SM}} = (-2.3 \pm 0.4) \times 10^{-4}$ [45,170]. With a more sophisticated analysis in bins of the muon impact parameters, D0 conclude that the overall deviation of their measurements from the SM is at the level of 3.6σ. Interpreting the observed asymmetries in bins of the muon impact parameters in terms of CP violation in B-meson mixing and in interference, and using the mixing parameters and the world-average b-hadron production fractions of Ref. [221], the D0 collaboration extracts [170] values for $\mathcal{A}_{\rm SL}^d$ and $\mathcal{A}_{\rm SL}^s$ and their correlation coefficient,[10] as shown in Table 20. However, the various contributions to the total quoted uncertainties from this analysis and from the external inputs are not given, so the adjustment of these results to different or more recent values of the external inputs cannot (easily) be done.

Finally, direct determinations of $\mathcal{A}_{\rm SL}^s$, also shown in Table 20, have been obtained by D0 [222] and LHCb [223] from the time-integrated charge asymmetry of untagged $B_s^0 \to D_s^-\mu^+\nu X$ decays.

Using a two-dimensional fit, all measurements of $\mathcal{A}_{\rm SL}^d$ and $\mathcal{A}_{\rm SL}^s$ obtained by D0 and LHCb are combined with the B-factory average of Table 19. Correlations are taken into account as shown in Table 20. The results, displayed graphically in Fig. 7, are

$$\mathcal{A}_{\rm SL}^d = -0.0021 \pm 0.0017 \Leftrightarrow |q_d/p_d| = 1.0010 \pm 0.0008, \tag{74}$$

[9] A low-statistics result published by CDF using the Run I data [212] is not included in our averages, nor in Table 19.

[10] In each impact parameter bin i the measured same-sign dimuon asymmetry is interpreted as $A_i = K_i^s \mathcal{A}_{\rm SL}^s + K_i^d \mathcal{A}_{\rm SL}^d + \lambda K_i^{\rm int} \Delta\Gamma_d/\Gamma_d$, where the factors K_i^s, K_i^d and $K_i^{\rm int}$ are obtained by D0 from Monte Carlo simulation. The D0 publication [170] assumes $\lambda = 1$, but it has been demonstrated subsequently that $\lambda \leq 0.49$ [171]. This particular point invalidates the $\Delta\Gamma_d/\Gamma_d$ result published by D0, but not the $\mathcal{A}_{\rm SL}^d$ and $\mathcal{A}_{\rm SL}^s$ results. As stated by D0, their $\mathcal{A}_{\rm SL}^d$ and $\mathcal{A}_{\rm SL}^s$ results assume the above expression for A_i, i.e., that the observed asymmetries are due to CP violation in B mixing. As long as this assumption is not shown to be wrong (or withdrawn by D0), we include the $\mathcal{A}_{\rm SL}^d$ and $\mathcal{A}_{\rm SL}^s$ results in our world average.

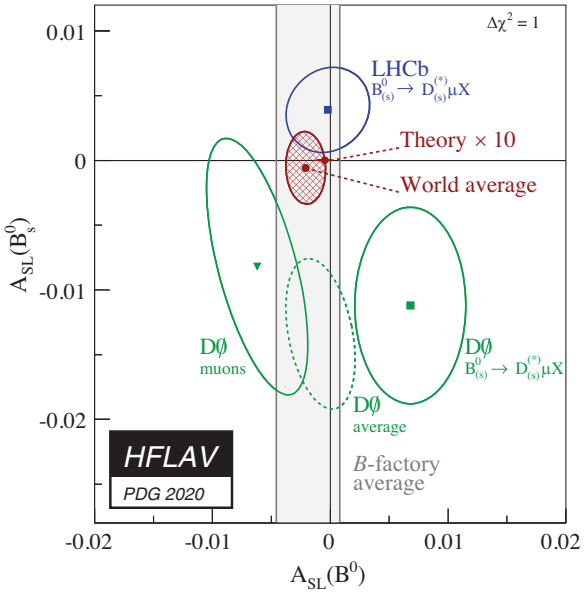

FIG. 7. Measurements of $\mathcal{A}^d_{\rm SL}$ and $\mathcal{A}^s_{\rm SL}$ listed in Table 20 (*B*-factory average as the gray band, D0 measurements as the green ellipses, LHCb measurements as the blue ellipse) together with their two-dimensional average (red hatched ellipse). The red point close to (0, 0) is the Standard Model prediction of Ref. [87] with error bars multiplied by 10. The prediction and the experimental world average deviate from each other by 0.5σ.

$$\mathcal{A}^s_{\rm SL} = -0.0006 \pm 0.0028 \Leftrightarrow |q_s/p_s| = 1.0003 \pm 0.0014, \tag{75}$$

$$\rho(\mathcal{A}^d_{\rm SL}, \mathcal{A}^s_{\rm SL}) = -0.054, \tag{76}$$

where $\rho(\mathcal{A}^d_{\rm SL}, \mathcal{A}^s_{\rm SL})$ is the correlation coefficient between the two measured parameters, and the relation between $\mathcal{A}^q_{\rm SL}$ and $|q_q/p_q|$ is given in Eq. (51).[11] However, the fit χ^2 probability is only 4.5%. This is mostly due to an overall discrepancy between the D0 and LHCb averages at the level of 2.2σ. Since the assumptions underlying the inclusion of the D0 muon results in the average [10] are somewhat controversial [224], we also provide in Table 20 an average excluding these results.

The above averages show no evidence of *CP* violation in B^0 or B^0_s mixing. They deviate by 0.5σ from the very small predictions of the Standard Model (SM), $\mathcal{A}^{d,\rm SM}_{\rm SL} = -(4.73 \pm 0.42) \times 10^{-4}$ and $\mathcal{A}^{s,\rm SM}_{\rm SL} = +(2.06 \pm 0.18) \times 10^{-5}$ [87]. Given the current experimental uncertainties, there is still significant room for a possible new physics contribution, in particular in the B^0_s system. In this respect, the deviation of the D0 dimuon asymmetry [170] from expectation has generated significant interest. However, the recent $\mathcal{A}^s_{\rm SL}$ and $\mathcal{A}^d_{\rm SL}$ results from LHCb are not precise enough yet to settle the issue. It has been pointed out [225] that the D0 dimuon result can be reconciled with the SM expectations of $\mathcal{A}^s_{\rm SL}$ and $\mathcal{A}^d_{\rm SL}$ if there are non-SM sources of *CP* violation in the semileptonic decays of the *b* and *c* quarks. A Run 1 ATLAS study [226] of charge asymmetries in muon + jets $t\bar{t}$ events, in which a *b*-hadron decays semileptonically to a soft muon, yields results with limited statistical precision, compatible both with the D0 dimuon asymmetry and with the SM predictions.

At the more fundamental level, *CP* violation in B^0_s mixing is caused by the weak phase difference ϕ^s_{12} defined in Eq. (55). The SM prediction for this phase is tiny [42,88],

$$\phi^{s,\rm SM}_{12} = 0.0046 \pm 0.0012. \tag{77}$$

However, new physics in B^0_s mixing could change the observed phase to

$$\phi^s_{12} = \phi^{s,\rm SM}_{12} + \phi^{s,\rm NP}_{12}. \tag{78}$$

Using Eq. (54), the current knowledge of $\mathcal{A}^s_{\rm SL}$, $\Delta\Gamma_s$ and Δm_s, given in Eqs. (75), (64), and (65) respectively, yields an experimental determination of ϕ^s_{12},

$$\tan\phi^s_{12} = \mathcal{A}^s_{\rm SL}\frac{\Delta m_s}{\Delta\Gamma_s} = -0.1 \pm 0.6, \tag{79}$$

which represents only a very weak constraint.

4. Mixing-induced CP violation in B^0_s decays

CP violation arising in the interference between $B^0_s - \bar{B}^0_s$ mixing and decay is a very active field in which large experimental progress has been achieved in the last decade. The main observable is the phase $\phi^{c\bar{c}s}_s$, which describes *CP* violation in the interference between B^0_s mixing and decay in $b \to c\bar{c}s$ transitions.

The golden mode for such studies is $B^0_s \to J/\psi\phi$, followed by $J/\psi \to \mu^+\mu^-$ and $\phi \to K^+K^-$, for which a full angular analysis of the decay products is performed to statistically separate the *CP*-even and *CP*-odd contributions in the final state. As already mentioned in Sec. V B 2, CDF [172], D0 [173], ATLAS [174–176], CMS [177,178] and LHCb [179–183] have used both untagged and tagged $B^0_s \to J/\psi\phi$ (and more generally $B^0_s \to (c\bar{c})K^+K^-$) decays for the measurement of $\phi^{c\bar{c}s}_s$. LHCb [93,227] has used $B^0_s \to J/\psi\pi^+\pi^-$ events, analyzed with a full amplitude model including several $\pi^+\pi^-$ resonances (e.g., $f_0(980)$), although the $J/\psi\pi^+\pi^-$ final state had already been shown to have a *CP*-odd fraction larger than 0.977 at 95% CL [228]. In addition, LHCb has used the $B^0_s \to D^+_s D^-_s$ channel [229] to measure $\phi^{c\bar{c}s}_s$.

[11] Early analyses and the PDG use the complex parameter $\epsilon_B = (p_q - q_q)/(p_q + q_q)$ for the B^0; if *CP* violation in the mixing is small, $\mathcal{A}^d_{\rm SL} \cong 4{\rm Re}(\epsilon_B)/(1 + |\epsilon_B|^2)$ and the average of Eq. (74) corresponds to ${\rm Re}(\epsilon_B)/(1 + |\epsilon_B|^2) = -0.0005 \pm 0.0004$.

TABLE 21. Direct experimental measurements of $\phi_s^{c\bar{c}s}$, $\Delta\Gamma_s$ and Γ_s using $B_s^0 \to J/\psi\phi$, $J/\psi K^+K^-$, $\psi(2S)\phi$, $J/\psi\pi^+\pi^-$ and $D_s^+D_s^-$ decays. The first error is due to statistics, the second one to systematics. The last (last but one) line gives our averages, where the $\Delta\Gamma_s$ uncertainties have been multiplied by 1.78 (1.72) to account for inconsistencies between the $B_s^0 \to J/\psi\phi$ measurements. Only solution (a) of Ref. [176] is used.

Experiment	Mode	Dataset	$\phi_s^{c\bar{c}s}$	$\Delta\Gamma_s$ (ps^{-1})	References
CDF	$J/\psi\phi$	9.6 fb^{-1}	$[-0.60, +0.12]$, 68% CL	$+0.068 \pm 0.026 \pm 0.009$	[172]
D0	$J/\psi\phi$	8.0 fb^{-1}	$-0.55^{+0.38}_{-0.36}$	$+0.163^{+0.065}_{-0.064}$	[173]
ATLAS	$J/\psi\phi$	4.9 fb^{-1}	$+0.12 \pm 0.25 \pm 0.05$	$+0.053 \pm 0.021 \pm 0.010$	[174]
ATLAS	$J/\psi\phi$	14.3 fb^{-1}	$-0.110 \pm 0.082 \pm 0.042$	$+0.101 \pm 0.013 \pm 0.007$	[175]
ATLAS	$J/\psi\phi$	80.5 fb^{-1}	$-0.081 \pm 0.041 \pm 0.022$	$+0.0607 \pm 0.0047 \pm 0.0043$	[176]
ATLAS	Above 3 combined		$-0.087 \pm 0.036 \pm 0.021$	$+0.0657 \pm 0.0043 \pm 0.0037$	[176]
CMS	$J/\psi\phi$	19.7 fb^{-1}	$-0.075 \pm 0.097 \pm 0.031$	$+0.095 \pm 0.013 \pm 0.007$	[177]
CMS	$J/\psi\phi$	96.4 fb^{-1}	$-0.011 \pm 0.050 \pm 0.010$	$+0.114 \pm 0.0014 \pm 0.0007$	[178]
CMS	Above 2 combined		$-0.021 \pm 0.044 \pm 0.010$	$+0.1032 \pm 0.0095 \pm 0.0048$	[178]
LHCb	$J/\psi\phi$	3.0 fb^{-1}	$-0.058 \pm 0.049 \pm 0.006$	$+0.0805 \pm 0.0091 \pm 0.0032$	[179]
LHCb	$J/\psi\pi^+\pi^-$	3.0 fb^{-1}	$+0.070 \pm 0.068 \pm 0.008$	…	[227]
LHCb	$J/\psi K^+K^-$[a]	3.0 fb^{-1}	$+0.119 \pm 0.107 \pm 0.034$	$+0.066 \pm 0.018 \pm 0.010$	[180]
LHCb	$\psi(2S)\phi$	3.0 fb^{-1}	$+0.23^{+0.29}_{-0.28} \pm 0.02$	$+0.066^{+0.41}_{-0.44} \pm 0.007$	[181]
LHCb	$D_s^+D_s^-$	3.0 fb^{-1}	$+0.02 \pm 0.17 \pm 0.02$	…	[229]
LHCb	$J/\psi\pi^+\pi^-$	1.9 fb^{-1}[b]	$-0.057 \pm 0.060 \pm 0.011$	…	[93]
LHCb	$J/\psi\phi$	1.9 fb^{-1}[b]	$-0.083 \pm 0.041 \pm 0.006$	$+0.077 \pm 0.008 \pm 0.003$	[183]
LHCb	Above 7 combined		-0.042 ± 0.025	$+0.0813 \pm 0.0048$	[183]
LHCb	$J/\psi\phi$[c]	3.0 fb^{-1}	$+0.00 \pm 0.28 \pm 0.07$	$+0.115 \pm 0.045 \pm 0.011$	[182]
$B_s^0 \to J/\psi\phi$ combined			-0.070 ± 0.022	$+0.074 \pm 0.006$	
All combined			-0.049 ± 0.019	$+0.077 \pm 0.006$	

[a] $m(K^+K^-) > 1.05$ GeV/c^2.
[b] Run 2.
[c] $J/\psi \to e^+e^-$.

All CDF, D0, ATLAS and CMS analyses provide two mirror solutions related by the transformation $(\Delta\Gamma_s, \phi_s^{c\bar{c}s}) \to (-\Delta\Gamma_s, \pi - \phi_s^{c\bar{c}s})$. However, the LHCb analysis of $B_s^0 \to J/\psi K^+K^-$ resolves this ambiguity and rules out the solution with negative $\Delta\Gamma_s$ [86], a result in agreement with the Standard Model expectation. Therefore, in what follows, we only consider the solution with $\Delta\Gamma_s > 0$.

In the $B_s^0 \to J/\psi\phi$ and $B_s^0 \to J/\psi K^+K^-$ analyses, $\phi_s^{c\bar{c}s}$ and $\Delta\Gamma_s$ come from a simultaneous fit that determines also the B_s^0 lifetime, the longitudinal and perpendicular ϕ polarization amplitudes $|A_0|^2$ and $|A_\perp|^2$, the S-wave amplitude $|A_S|^2$, and the strong phases. While the correlation between $\phi_s^{c\bar{c}s}$ and all other parameters is small, the correlations between $\Delta\Gamma_s$, Γ_s and the polarization amplitudes are sizeable. Therefore the full set of parameters provided by the measurements are combined in a multidimensional fit that considers the correlations between them. The combination uses the single-experiment averages provided by ATLAS [176], CMS [178] and LHCb [183].

As second-order loop processes could have different contributions to $\phi_s^{c\bar{c}s}$, we perform two combinations. In the first one, we perform a combination of all the CDF [172], D0 [173], ATLAS [174–176], CMS [177,178] and LHCb [93,179–183,227,229] results listed in Table 21. The second one uses only the $B_s^0 \to J/\psi\phi$ measurements [172–179,182,183].

ATLAS [176] measures two solutions for the strong phases $\delta_\perp$ and $\delta_\parallel$. Using one or the other only leads to minor differences in the main parameters of interest, $\phi_s^{c\bar{c}s}$, $\Delta\Gamma_s$ and Γ_s. For simplicity, in this average, only solution (a) is used. As some analyses fix or constrain Δm_s, in this average it is fixed to 17.757 ps^{-1} [1], which is the value used in most measurements. Furthermore, $|\lambda|$ is considered an independent observable in each decay mode, and is fixed to 1 for $B_s^0 \to J/\psi\phi$. As the different $B_s^0 \to J/\psi\phi$ analyses use different $m(K^+K^-)$ regions, the S-wave amplitude phases and fractions in the measurements that report them are mapped to the $m(K^+K^-)$ region used by CMS [177,178], by arbitrary choice. The mapping is introduced as a transformation of the S-wave fractions of ATLAS and LHCb, assuming that the S wave component is the f_0 resonance and the P wave component is the ϕ resonance. While the ϕ presence is very clear and its shape is well measured, the shape of the S wave is not known well. Therefore, the impact of the S-wave on the average of the parameters of interest, $\phi_s^{c\bar{c}s}$, Γ_s, $\Delta\Gamma_s$, is studied assuming different S-wave mass shapes, such as a constant, and with variations to the parameters of the P- and S-wave amplitudes. The effect is found to be negligible in all cases.

TABLE 22. Results of the averaging procedure, including the fit results and the scale factors of the individual parameters, for all $b \to c\bar{c}s$ modes (second and third column) and for $B_s^0 \to J/\psi\phi$ modes only (fourth and fifth column).

Parameter	All $b \to c\bar{c}s$		$B_s^0 \to J/\psi\phi$	
	Fit result	Scale factor	Fit result	Scale factor
$\lvert A_0\rvert^2$	0.520 ± 0.003	1.46	0.519 ± 0.003	1.46
$\lvert A_\perp\rvert^2$	0.253 ± 0.006	2.45	0.254 ± 0.006	2.37
$\lvert A_S\rvert^2$	0.030 ± 0.005	1.00	0.030 ± 0.005	1.00
$\delta_\parallel$	3.18 ± 0.06	1.46	3.18 ± 0.06	1.46
$\delta_\perp$	3.08 ± 0.12	2.04	3.08 ± 0.13	2.07
$\delta_S - \delta_\perp$	0.23 ± 0.05	1.00	0.23 ± 0.05	1.00
Γ_s	0.663 ± 0.004 ps^{-1}	2.60	0.664 ± 0.004 ps^{-1}	2.44
$\Delta\Gamma_s$	$+0.077 \pm 0.006$ ps^{-1}	1.78	$+0.074 \pm 0.006$ ps^{-1}	1.72
ϕ_s	-0.049 ± 0.019	1.00	-0.070 ± 0.022	1.00

In some decay channels, LHCb measures $\Gamma_s - \Gamma_d$ [180,181,183] instead of Γ_s. References [180,181] also quote Γ_s assuming a τ_{B^0} value of 1.520 ps. Therefore, in the combination the same τ_{B^0} value is assumed.

Using the same approach as discussed in Sec. V B 2 to address the tension between the $B_s^0 \to J/\psi\phi$ measurements of ATLAS [175,176], CMS [177,178] and LHCb [179,183], the total uncertainty for each parameter in each

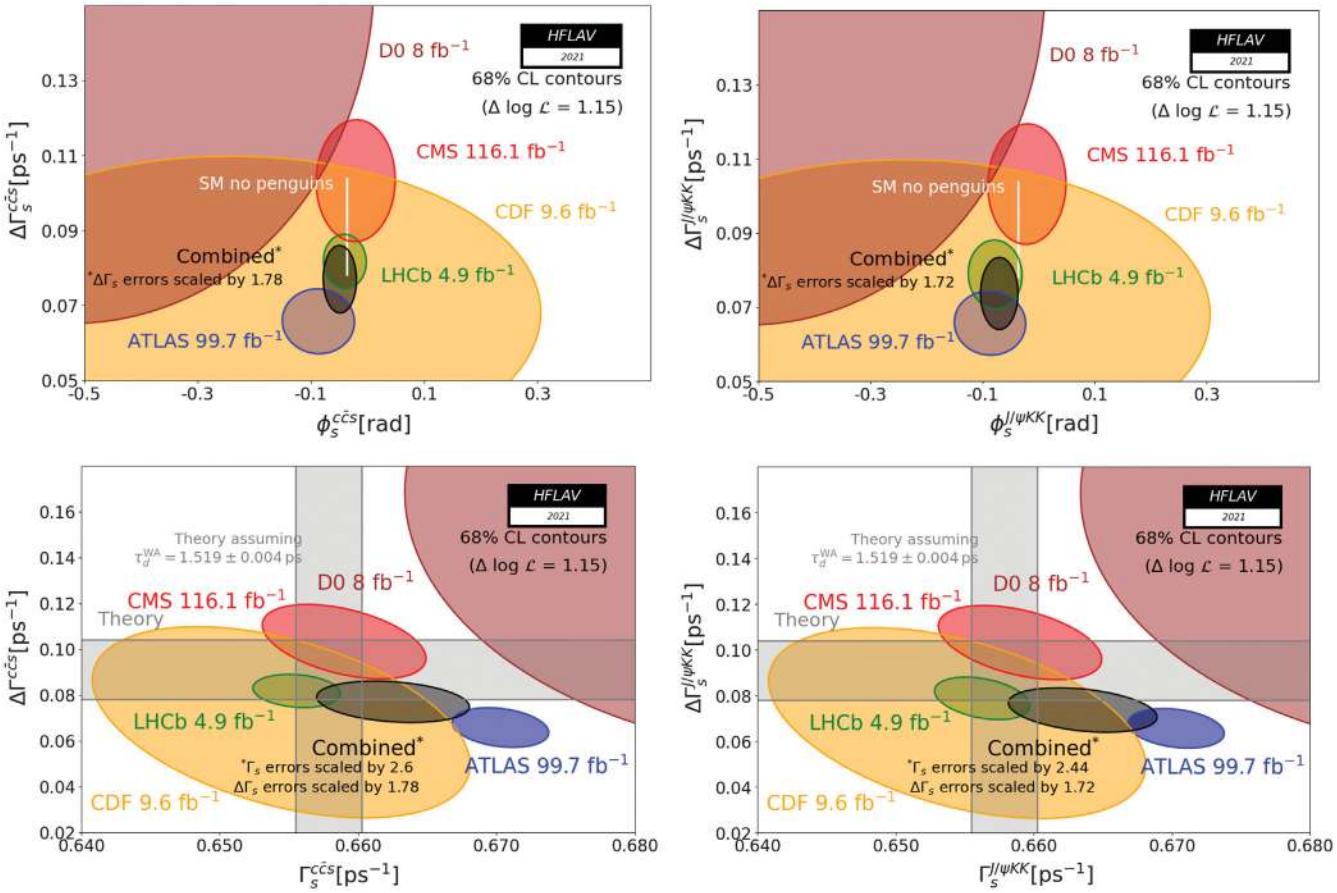

FIG. 8. 68% CL regions shown in the $(\phi_s^{c\bar{c}s}, \Delta\Gamma_s)$ plane on the top and in the $(\Gamma_s, \Delta\Gamma_s)$ plane on the bottom, for individual experiments and their combination. The left plots are obtained from all CDF [172], D0 [173], ATLAS [174–176], CMS [177,178] and LHCb [93,179–183,227,229] measurements of $B_s^0 \to J/\psi\phi$, $B_s^0 \to J/\psi K^+K^-$, $B_s^0 \to \psi(2S)\phi$, $B_s^0 \to J/\psi\pi^+\pi^-$ and $B_s^0 \to D_s^+D_s^-$ decays, while the right plots are obtained from $B_s^0 \to J/\psi\phi$ measurements only [172–179,182,183]. The expectation within the Standard Model neglecting penguin contributions [42,45,87,88,169] is shown as the white rectangle in the top plots. The Γ_s theory value in the bottom plots is calculated from Ref. [56] assuming the experimental world average for the B^0 lifetime, 1.519 ± 0.004 ps.

TABLE 23. Correlation tables of the averaged observables from the fit to all $b \to c\bar{c}s$ modes (top) and to the $B_s^0 \to J/\psi\phi$ modes only (bottom).

Parameter	$\lvert A_0\rvert^2$	$\lvert A_\perp\rvert^2$	$\lvert A_S\rvert^2$	$\delta_\parallel$	$\delta_\perp$	$\delta_S - \delta_\perp$	Γ_s	$\Delta\Gamma_s$	ϕ_s
$\lvert A_0\rvert^2$	1.00	−0.67	0.08	−0.03	−0.04	−0.05	−0.09	0.28	−0.01
$\lvert A_\perp\rvert^2$		1.00	−0.03	−0.03	0.01	0.04	0.15	−0.4	0.01
$\lvert A_S\rvert^2$			1.00	−0.02	−0.03	−0.10	0.03	0.00	0.00
$\delta_\parallel$				1.00	0.21	−0.01	−0.01	0.01	0.00
$\delta_\perp$					1.00	0.00	−0.02	−0.02	0.01
$\delta_S - \delta_\perp$						1.0	−0.02	−0.01	0.00
Γ_s							1.00	−0.24	−0.01
$\Delta\Gamma_s$								1.00	−0.02
ϕ_s									1.00

Parameter	$\lvert A_0\rvert^2$	$\lvert A_\perp\rvert^2$	$\lvert A_S\rvert^2$	$\delta_\parallel$	$\delta_\perp$	$\delta_S - \delta_\perp$	Γ_s	$\Delta\Gamma_s$	ϕ_s
$\lvert A_0\rvert^2$	1.00	−0.68	0.08	−0.03	−0.04	−0.05	−0.12	0.32	−0.01
$\lvert A_\perp\rvert^2$		1.00	−0.03	−0.03	0.00	0.04	0.19	−0.45	0.01
$\lvert A_S\rvert^2$			1.00	−0.03	−0.04	−0.09	0.03	0.01	0.0
$\delta_\parallel$				1.00	0.20	−0.01	−0.01	0.01	0.01
$\delta_\perp$					1.00	−0.01	−0.02	−0.02	0.03
$\delta_S - \delta_\perp$						1.0	−0.02	0.00	0.00
Γ_s							1.00	−0.32	−0.01
$\Delta\Gamma_s$								1.00	0.00
ϕ_s									1.00

$B_s^0 \to J/\psi\phi$ set of results by ATLAS, CDF, D0, CMS and LHCb is scaled up in a way that results in an agreement of 1σ. The resulting scale factors are summarized in Table 22.

Given the increasing experimental precision of the LHC results, we have stopped using the two-dimensional $\Delta\Gamma_s - \phi_s^{c\bar{c}s}$ histograms provided by the CDF and D0 collaborations, and are now approximating them with two-dimensional Gaussian likelihoods.

We obtain the individual and combined contours shown in Fig. 8. Maximizing the likelihood, we find, as summarized in Table 21,

$$\Delta\Gamma_s = +0.077 \pm 0.006\ \text{ps}^{-1}, \tag{80}$$

$$\phi_s^{c\bar{c}s} = -0.049 \pm 0.019. \tag{81}$$

This $\Delta\Gamma_s$ average is consistent but highly correlated with the average of Eq. (64). Our final recommended average for $\Delta\Gamma_s$ is the one of Eq. (64), which includes all available information on this quantity. The complete set of averaged parameters are listed in Table 22, and their correlations are in Table 23.

In the Standard Model and ignoring subleading penguin contributions, $\phi_s^{c\bar{c}s}$ is expected to be equal to $-2\beta_s$, where $\beta_s = \arg\left[-(V_{ts}V_{tb}^*)/(V_{cs}V_{cb}^*)\right]$ is a phase analogous to the angle β of the usual CKM unitarity triangle (aside from a sign change). An indirect determination via global fits to experimental data gives [169]

$$(\phi_s^{c\bar{c}s})^{\text{SM}} = -2\beta_s = -0.0368^{+0.0006}_{-0.0009}. \tag{82}$$

The average value of $\phi_s^{c\bar{c}s}$ from Eq. (81) is consistent with this Standard Model expectation. Penguin contributions to $\phi_s^{c\bar{c}s}$ from $B_s^0 \to J/\psi\phi$ are calculated to be smaller than 0.021 in magnitude [230–232] but may become relevant if future measurements reduce the error in Eq. (81). There are no reliable estimates of the penguin contribution to $B_s^0 \to J/\psi f_0$.

From its measurements of time-dependent CP violation in $B_s^0 \to K^+K^-$ decays, the LHCb collaboration has determined the B_s^0 mixing phase to be $-2\beta_s = -0.12^{+0.14}_{-0.12}$ [233], assuming a U-spin relation (with up to 50% breaking effects) between the decay amplitudes of $B_s^0 \to K^+K^-$ and $B^0 \to \pi^+\pi^-$, and a value of the CKM angle γ of $(70.1 \pm 7.1)°$. This determination is compatible with, and less precise than, the world average of $\phi_s^{c\bar{c}s}$ from Eq. (81).

New physics could contribute to $\phi_s^{c\bar{c}s}$. Assuming that new physics only enters in M_{12}^s (rather than in Γ_{12}^s), one can write [45]

$$\phi_s^{c\bar{c}s} = -2\beta_s + \phi_{12}^{s,\text{NP}}, \tag{83}$$

where the new physics phase $\phi_{12}^{s,\text{NP}}$ is the same as that appearing in Eq. (78). In this case

$$\phi_{12}^s = \phi_{12}^{s,\text{SM}} + 2\beta_s + \phi_s^{c\bar{c}s} = -0.008 \pm 0.019, \tag{84}$$

where the numerical estimation was performed with the values of Eqs. (77), (82), and (81). Keeping in mind the approximation and assumption mentioned above, this can serve as a reference value to which the measurement of Eq. (79) can be compared.

VI. MEASUREMENTS RELATED TO UNITARITY TRIANGLE ANGLES

We provide averages of measurements obtained from analyses of decay-time-dependent asymmetries and other quantities that are related to the angles of the unitarity triangle (UT). Straightforward interpretations of the averages are given, where possible. However, no attempt to extract the angles is made in cases where considerable theoretical input is required to do so.

In Sec. VI A a brief introduction to the relevant phenomenology is given. In Sec. VI B an attempt is made to clarify the various different notations in use. In Sec. VI C the common inputs to which experimental results are rescaled in the averaging procedure are listed. We also briefly introduce the treatment of experimental uncertainties. In the remainder of this section, the experimental results and their averages are given, divided into subsections based on the underlying quark-level decays. All the measurements reported are quantities determined from decay-time-dependent analyses, with the exception of several in Sec. VI O, which are related to the UT angle γ and are obtained from decay-time-integrated analyses. In the compilations of measurements, indications of the sizes of the data samples used by each experiment are given. For the e^+e^- B factory experiments, this is quoted in terms of the number of $B\bar{B}$ pairs in the data sample, while the integrated luminosity is given for experiments at hadron colliders.

A. Introduction

In the Standard Model, the Cabibbo-Kobayashi-Maskawa (CKM) quark-mixing matrix is a unitary matrix, conventionally written as the product of three (complex) rotation matrices [234]. The rotations are parametrized by the Euler mixing angles between the generations, θ_{12}, θ_{13} and θ_{23}, and one overall phase δ,

$$V = \begin{pmatrix} V_{ud} & V_{us} & V_{ub} \\ V_{cd} & V_{cs} & V_{cb} \\ V_{td} & V_{ts} & V_{tb} \end{pmatrix} = \begin{pmatrix} c_{12}c_{13} & s_{12}c_{13} & s_{13}e^{-i\delta} \\ -s_{12}c_{23} - c_{12}s_{23}s_{13}e^{i\delta} & c_{12}c_{23} - s_{12}s_{23}s_{13}e^{i\delta} & s_{23}c_{13} \\ s_{12}s_{23} - c_{12}c_{23}s_{13}e^{i\delta} & -c_{12}s_{23} - s_{12}c_{23}s_{13}e^{i\delta} & c_{23}c_{13} \end{pmatrix}, \tag{85}$$

where $c_{ij} = \cos\theta_{ij}$, $s_{ij} = \sin\theta_{ij}$ for $i < j = 1, 2, 3$.

The often used Wolfenstein parametrization [235] involves the replacements [236]

$$\begin{aligned} s_{12} &\equiv \lambda, \\ s_{23} &\equiv A\lambda^2, \\ s_{13}e^{-i\delta} &\equiv A\lambda^3(\rho - i\eta). \end{aligned} \tag{86}$$

The observed hierarchy among the CKM matrix elements is captured by the small value of λ, in which a Taylor expansion of V leads to the familiar approximation

$$V = \begin{pmatrix} 1-\lambda^2/2 & \lambda & A\lambda^3(\rho - i\eta) \\ -\lambda & 1-\lambda^2/2 & A\lambda^2 \\ A\lambda^3(1-\rho-i\eta) & -A\lambda^2 & 1 \end{pmatrix} + \mathcal{O}(\lambda^4). \tag{87}$$

At order λ^5, the CKM matrix in this parametrization is

$$V = \begin{pmatrix} 1 - \frac{1}{2}\lambda^2 - \frac{1}{8}\lambda^4 & \lambda & A\lambda^3(\rho - i\eta) \\ -\lambda + \frac{1}{2}A^2\lambda^5[1 - 2(\rho + i\eta)] & 1 - \frac{1}{2}\lambda^2 - \frac{1}{8}\lambda^4(1 + 4A^2) & A\lambda^2 \\ A\lambda^3[1 - (1 - \frac{1}{2}\lambda^2)(\rho + i\eta)] & -A\lambda^2 + \frac{1}{2}A\lambda^4[1 - 2(\rho + i\eta)] & 1 - \frac{1}{2}A^2\lambda^4 \end{pmatrix} + \mathcal{O}(\lambda^6). \tag{88}$$

A nonzero value of η implies that the CKM matrix is not purely real, and is the source of CP violation in the Standard Model. This is encapsulated in a parametrization-invariant way through the Jarlskog parameter $J = \mathrm{Im}(V_{us}V_{cb}V_{ub}^*V_{cs}^*)$ [237], which is nonzero if and only if CP violation exists.

The unitarity relation $V^\dagger V = 1$ results in a total of nine equations, which can be written as $\sum_{i=u,c,t} V_{ij}^* V_{ik} = \delta_{jk}$, where δ_{jk} is the Kronecker symbol. Of the off-diagonal expressions ($j \neq k$), three can be transformed into the other three (under $j \leftrightarrow k$, corresponding to complex conjugation). This leaves three relations in which three complex

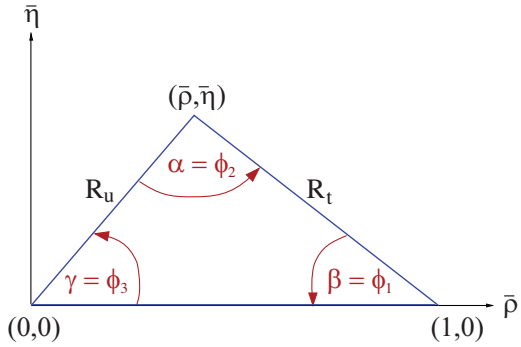

FIG. 9. The unitarity triangle.

numbers sum to zero, which therefore can be expressed as triangles in the complex plane. The diagonal terms yield three relations, in which the squares of the elements in each column of the CKM matrix sum to unity. Similar relations are obtained for the rows of the matrix from $VV^\dagger = 1$. Thus, there are in total six triangle relations and six sums to unity. More details about unitarity triangles can be found in Refs. [238–241].

One of the triangle relations,

$$V_{ud}V_{ub}^* + V_{cd}V_{cb}^* + V_{td}V_{tb}^* = 0, \tag{89}$$

is of particular importance to the B system, being specifically related to flavor-changing neutral-current $b \to d$ transitions, and since the three terms in Eq. (89) are of the same order, $\mathcal{O}(\lambda^3)$. This relation is commonly known as the unitarity triangle (UT). For presentational purposes, it is convenient to rescale the triangle by $(V_{cd}V_{cb}^*)^{-1}$, so that one of its sides becomes 1, as shown in Fig. 9.

Two popular naming conventions for the UT angles exist in the literature,

$$\begin{aligned}
\alpha \equiv \phi_2 &= \arg\left[-\frac{V_{td}V_{tb}^*}{V_{ud}V_{ub}^*}\right], \\
\beta \equiv \phi_1 &= \arg\left[-\frac{V_{cd}V_{cb}^*}{V_{td}V_{tb}^*}\right], \\
\gamma \equiv \phi_3 &= \arg\left[-\frac{V_{ud}V_{ub}^*}{V_{cd}V_{cb}^*}\right].
\end{aligned} \tag{90}$$

In this document the (α, β, γ) set is used predominantly. The sides R_u and R_t of the UT (see Fig. 9) are given by

$$\begin{aligned}
R_u &= \left|\frac{V_{ud}V_{ub}^*}{V_{cd}V_{cb}^*}\right| = \sqrt{\bar{\rho}^2 + \bar{\eta}^2}, \\
R_t &= \left|\frac{V_{td}V_{tb}^*}{V_{cd}V_{cb}^*}\right| = \sqrt{(1-\bar{\rho})^2 + \bar{\eta}^2}.
\end{aligned} \tag{91}$$

Determinations of R_u rely on measurements of semileptonic B decays and are discussed in Sec. VII, while R_t is constrained by measurements of B meson oscillation frequencies (Sec. V) and of rare decays (Sec. IX). The parameters $\bar{\rho}$ and $\bar{\eta}$ define the apex of the UT, and are given by [236]

$$\begin{aligned}
\bar{\rho} + i\bar{\eta} &\equiv -\frac{V_{ud}V_{ub}^*}{V_{cd}V_{cb}^*} \equiv 1 + \frac{V_{td}V_{tb}^*}{V_{cd}V_{cb}^*} \\
&= \frac{\sqrt{1-\lambda^2}(\rho + i\eta)}{\sqrt{1-A^2\lambda^4} + \sqrt{1-\lambda^2}A^2\lambda^4(\rho + i\eta)}.
\end{aligned} \tag{92}$$

The inverse relation between (ρ, η) and $(\bar{\rho}, \bar{\eta})$ is

$$\rho + i\eta = \frac{\sqrt{1-A^2\lambda^4}(\bar{\rho} + i\bar{\eta})}{\sqrt{1-\lambda^2}[1 - A^2\lambda^4(\bar{\rho} + i\bar{\eta})]}. \tag{93}$$

By expanding in powers of λ, several useful approximate expressions can be obtained, including

$$\begin{aligned}
\bar{\rho} &= \rho\left(1 - \frac{1}{2}\lambda^2\right) + \mathcal{O}(\lambda^4), \\
\bar{\eta} &= \eta\left(1 - \frac{1}{2}\lambda^2\right) + \mathcal{O}(\lambda^4), \\
V_{td} &= A\lambda^3(1 - \bar{\rho} - i\bar{\eta}) + \mathcal{O}(\lambda^6).
\end{aligned} \tag{94}$$

Recent world-average values for the Wolfenstein parameters, evaluated using many of the measurements reported in this document, are [242].

$$\begin{aligned}
A &= 0.8132^{+0.0119}_{-0.0060}, & \lambda &= 0.22500^{+0.00024}_{-0.00022}, \\
\bar{\rho} &= 0.1566^{+0.0085}_{-0.0048}, & \bar{\eta} &= 0.3475^{+0.0118}_{-0.0054}.
\end{aligned} \tag{95}$$

The relevant unitarity triangle for the $b \to s$ transition is obtained by replacing $d \leftrightarrow s$ in Eq. (89). Definitions of the set of angles $(\alpha_s, \beta_s, \gamma_s)$ can be obtained using equivalent relations to those of Eq. (90). However, this gives a value of β_s that is negative in the Standard Model, so that the sign is usually flipped in the literature; this convention, i.e. $\beta_s = \arg\left[-(V_{ts}V_{tb}^*)/(V_{cs}V_{cb}^*)\right]$, is also followed here and in Sec. V. Since the sides of the $b \to s$ unitarity triangle are not all of the same order in λ, the triangle is squashed, and $\beta_s \sim \lambda^2\eta$.

B. Notations

Several different notations for CP violation parameters are commonly used. This section reviews those found in the experimental literature, in the hope of reducing the potential for confusion, and to define the frame that is used for the averages.

In some cases, when B mesons decay into multibody final states via broad resonances (ρ, K^*, etc.), the experimental analyses ignore the effects of interference between

the overlapping structures. This is referred to as the quasi-two-body (Q2B) approximation in the following.

1. CP asymmetries

The CP asymmetry is defined as the difference between the rate of a decay involving a b quark and that involving a $\bar{b}$ quark, divided by the sum. For example, the partial rate asymmetry for a charged B decay would be given as

$$\mathcal{A}_f \equiv \frac{\Gamma(B^- \to f) - \Gamma(B^+ \to \bar{f})}{\Gamma(B^- \to f) + \Gamma(B^+ \to \bar{f})}, \tag{96}$$

where f and $\bar{f}$ are CP-conjugate final states.

2. Time-dependent CP asymmetries in decays to CP eigenstates

In the case of decays to a final state f, which is a CP eigenstate with eigenvalue η_f, the B^0 and $\bar{B}^0$ decay amplitudes can be written as A_f and $\bar{A}_f$, respectively. The time-dependent decay rates for neutral B mesons, with known (i.e., "tagged") flavor at time $\Delta t = 0$, are then given by

$$\Gamma_{\bar{B}^0 \to f}(\Delta t) = \frac{e^{-|\Delta t|/\tau(B^0)}}{4\tau(B^0)}\left[1 + \frac{2\mathrm{Im}(\lambda_f)}{1+|\lambda_f|^2}\sin(\Delta m \Delta t) - \frac{1-|\lambda_f|^2}{1+|\lambda_f|^2}\cos(\Delta m \Delta t)\right], \tag{97}$$

$$\Gamma_{B^0 \to f}(\Delta t) = \frac{e^{-|\Delta t|/\tau(B^0)}}{4\tau(B^0)}\left[1 - \frac{2\mathrm{Im}(\lambda_f)}{1+|\lambda_f|^2}\sin(\Delta m \Delta t) + \frac{1-|\lambda_f|^2}{1+|\lambda_f|^2}\cos(\Delta m \Delta t)\right]. \tag{98}$$

This formulation assumes CPT invariance and neglects a possible lifetime difference between the two physical states. The case where nonzero lifetime differences are taken into account, which must be considered for B^0_s decays, is discussed in Sec. VI B 3.

The notation and normalization used here are relevant for the e^+e^- B factory experiments. In this case, neutral B mesons are produced via the $e^+e^- \to \Upsilon(4S) \to B\bar{B}$ process, and the wave function of the produced $B\bar{B}$ pair evolves coherently until one meson decays. When one of the pair decays into a final state that tags its flavor, the flavor of the other at that instant is known. The evolution of the other neutral B meson is therefore described in terms of Δt, the difference between the decay times of the two mesons in the pair. At hadron collider experiments, t is usually used in place of Δt, since the flavor tagging is done at production ($t = 0$); due to the nature of the production in hadron colliders (incoherent $b\bar{b}$ quark pair production with many additional associated particles), very different methods are used for tagging compared to those in e^+e^- experiments. Moreover, since negative values of t are not possible, the normalization is such that $\int_0^{+\infty}(\Gamma_{\bar{B}^0 \to f}(t) + \Gamma_{B^0 \to f}(t))dt = 1$, rather than the $\int_{-\infty}^{+\infty}(\Gamma_{\bar{B}^0 \to f}(\Delta t) + \Gamma_{B^0 \to f}(\Delta t))d(\Delta t) = 1$ normalization in Eqs. (97) and (98).

The term

$$\lambda_f = \frac{q}{p}\frac{\bar{A}_f}{A_f} \tag{99}$$

contains factors related to the decay amplitudes and to B^0–$\bar{B}^0$ mixing, which originates from the fact that the Hamiltonian eigenstates with physical masses and lifetimes are $|B_\pm\rangle = p|B^0\rangle \pm q|\bar{B}^0\rangle$ (see Sec. V B, where the mass difference Δm is also defined). The definition of λ_f in Eq. (99) allows three different categories of CP violation to be distinguished, both in the B^0 and B^0_s systems.

(i) CP violation in mixing, where $|\frac{q}{p}| \neq 1$. The strongest constraints on the associated parameters are obtained using semileptonic decays, and are discussed in Sec. V. There is currently no evidence for CP violation in mixing in either of the B^0–$\bar{B}^0$ or B^0_s–$\bar{B}^0_s$ systems; therefore $|\frac{q}{p}| = 1$ is assumed throughout the discussion in this section.

(ii) CP violation in decay, where $|\frac{\bar{A}_f}{A_f}| \neq 1$. This is the only possible category of CP violation for charged B mesons and b baryons (see, for example, results reported in Sec. IX). Several parameters measured in time-dependent analyses are also sensitive to CP violation in decay, and are discussed in this section.

(iii) CP violation in the interference between mixing and decay, where $\mathrm{Im}(\lambda_f) \neq 0$. Results related to this category, also referred to as mixing-induced CP violation, are reported in this section.

The time-dependent CP asymmetry, again defined as the normalized difference between the decay rate involving a b quark and that involving a $\bar{b}$ quark, is then given by

$$\mathcal{A}_f(\Delta t) \equiv \frac{\Gamma_{\bar{B}^0 \to f}(\Delta t) - \Gamma_{B^0 \to f}(\Delta t)}{\Gamma_{\bar{B}^0 \to f}(\Delta t) + \Gamma_{B^0 \to f}(\Delta t)} = \frac{2\mathrm{Im}(\lambda_f)}{1+|\lambda_f|^2}\sin(\Delta m \Delta t) - \frac{1-|\lambda_f|^2}{1+|\lambda_f|^2}\cos(\Delta m \Delta t). \tag{100}$$

While the coefficient of the $\sin(\Delta m \Delta t)$ term in Eq. (100) is customarily[12] denoted S_f:

$$S_f \equiv \frac{2\,\mathrm{Im}(\lambda_f)}{1+|\lambda_f|^2}, \tag{101}$$

different notations are in use for the coefficient of the $\cos(\Delta m \Delta t)$ term:

[12]Occasionally one also finds Eq. (100) written as $\mathcal{A}_f(\Delta t) = \mathcal{A}_f^{\mathrm{mix}}\sin(\Delta m \Delta t) + \mathcal{A}_f^{\mathrm{dir}}\cos(\Delta m \Delta t)$, or similar.

$$C_f \equiv -A_f \equiv \frac{1-|\lambda_f|^2}{1+|\lambda_f|^2}. \quad (102)$$

The C notation has been used by the *BABAR* collaboration (see e.g., Ref. [243]), and subsequently by the LHCb collaboration (see e.g., Ref. [244]), and is also adopted in this document. The A notation has been used by the Belle collaboration (see e.g., Ref. [245]). For the case when the final state is a CP eigenstate, as is being considered here, the notation S_{CP} and C_{CP} is widely used, including in this document, instead of specifying the final state f. In addition, a subscript indicating which transition is under consideration is often added to the S, C notation, particularly when grouping together measurements with different final states mediated by the same quark-level transition.

Neglecting effects due to CP violation in mixing, if the decay amplitude contains terms with a single weak (i.e., CP-violating) phase then $|\lambda_f| = 1$, and one finds $S_f = -\eta_f \sin(\phi_{\rm mix} + \phi_{\rm dec})$, $C_f = 0$, where $\phi_{\rm mix} = \arg(q/p)$ and $\phi_{\rm dec} = \arg(\bar{A}_f/A_f)$. The B^0–$\bar{B}^0$ mixing phase $\phi_{\rm mix}$ is approximately equal to 2β in the Standard Model (in the usual phase convention) [246,247].

If amplitudes with different weak phases contribute to the decay, no clean interpretation of S_f in terms of UT angles is possible without further input. In this document, only the theoretically cleanest channels are interpreted as measurements of the weak phase (e.g., $b \to c\bar{c}s$ transitions for $\sin(2\beta)$), although even in these cases some care is necessary. In channels in which a second amplitude with a different weak phase to the leading amplitude contributes but is expected to be suppressed, the concept of an effective weak phase difference is sometimes used, e.g., $\sin(2\beta^{\rm eff})$ in $b \to q\bar{q}s$ transitions.

If, in addition to having a weak phase difference, two contributing decay amplitudes have different strong (i.e., CP-conserving) phases, then $|\lambda_f| \neq 1$, and the coefficient of the cosine term becomes nonzero, indicating CP violation in decay. Additional input is then required for interpretation of the results, which in some cases is possible through theoretical relations between different decay channels. In many other modes, however, it is not possible to make a theoretically clean interpretation of S_f and C_f measurements in terms of weak phases.

Due to the fact that $\sin(\Delta m \Delta t)$ and $\cos(\Delta m \Delta t)$ are, respectively, odd and even functions of Δt, only small correlations (that can be induced by backgrounds, for example) between S_f and C_f are expected at an e^+e^- B factory experiment, where the range of Δt is $-\infty < \Delta t < +\infty$. The situation is different for measurements at hadron collider experiments, where the range of the time variable is $0 < t < +\infty$, so that more sizable correlations can be expected. We include the correlations in the averages where available.

Frequently, we are interested in combining measurements governed by similar or identical short-distance physics, but with different final states (e.g., $B^0 \to J/\psi K^0_S$ and $B^0 \to J/\psi K^0_L$). In this case, we remove the dependence on the CP eigenvalue of the final state by quoting $-\eta S_f$. In cases where the final state is not a CP eigenstate but has an effective CP content (see Sec. VI B 4), the reported $-\eta S$ is corrected by the effective CP.

3. Time-dependent distributions with nonzero decay width difference

A complete analysis of the time-dependent decay rates of neutral B mesons must also take into account the difference between the widths of the Hamiltonian eigenstates, denoted $\Delta\Gamma$. This is particularly important in the B^0_s system, where a non-negligible value of $\Delta\Gamma_s$ has been established (see Sec. V B). The formalism given here is appropriate for measurements of B^0_s decays to a CP eigenstate f as studied at hadron colliders, but appropriate modifications for B^0 mesons or for the e^+e^- environment are straightforward to make.

Neglecting CP violation in mixing, the relevant replacements for Eqs. (97) and (98) are [91]

$$\Gamma_{\bar{B}^0_s \to f}(t) = \mathcal{N}\frac{e^{-t/\tau(B^0_s)}}{2\tau(B^0_s)}\left[\cosh\left(\frac{\Delta\Gamma_s t}{2}\right) + S_f \sin(\Delta m_s t) - C_f \cos(\Delta m_s t) + A_f^{\Delta\Gamma}\sinh\left(\frac{\Delta\Gamma_s t}{2}\right)\right] \quad (103)$$

and

$$\Gamma_{B^0_s \to f}(t) = \mathcal{N}\frac{e^{-t/\tau(B^0_s)}}{2\tau(B^0_s)}\left[\cosh\left(\frac{\Delta\Gamma_s t}{2}\right) - S_f \sin(\Delta m_s t) + C_f \cos(\Delta m_s t) + A_f^{\Delta\Gamma}\sinh\left(\frac{\Delta\Gamma_s t}{2}\right)\right], \quad (104)$$

where S_f and C_f are as defined in Eqs. (101) and (102), respectively, $\tau(B^0_s) = 1/\Gamma_s$ is defined in Sec. V A 3, and the coefficient of the sinh term is[13]

$$A_f^{\Delta\Gamma} = -\frac{2\,\mathrm{Re}(\lambda_f)}{1+|\lambda_f|^2}. \quad (105)$$

With the requirement $\int_0^{+\infty}[\Gamma_{\bar{B}^0_s \to f}(t) + \Gamma_{B^0_s \to f}(t)]dt = 1$, the normalization factor is fixed to $\mathcal{N} = (1 - (\frac{\Delta\Gamma_s}{2\Gamma_s})^2)/(1 + \frac{A_f^{\Delta\Gamma}\Delta\Gamma_s}{2\Gamma_s})$.[14]

[13] As ever, alternative and conflicting notations appear in the literature. One popular alternative notation for this parameter is $\mathcal{A}_{\Delta\Gamma}$. Particular care must be taken regarding the signs.

[14] The prefactor of $\mathcal{N}/2\tau(B^0_s)$ in Eqs. (101) and (102) has been chosen so that $\mathcal{N} = 1$ in the limit $\Delta\Gamma_s = 0$. In the e^+e^- environment, where the range is $-\infty < \Delta t < \infty$, the prefactor should be $\mathcal{N}/4\tau(B^0_s)$ and $\mathcal{N} = 1 - (\frac{\Delta\Gamma_s}{2\Gamma_s})^2$.

A time-dependent analysis of *CP* asymmetries in flavor-tagged B_s^0 decays to a *CP* eigenstate f can thus determine the parameters S_f, C_f and $A_f^{\Delta\Gamma}$. Note that, by definition,

$$(S_f)^2 + (C_f)^2 + (A_f^{\Delta\Gamma})^2 = 1, \tag{106}$$

and this constraint may or may not be imposed in the fits. Since these parameters have sensitivity to both $\mathrm{Im}(\lambda_f)$ and $\mathrm{Re}(\lambda_f)$, alternative choices of parametrization, including those directly involving *CP* violating phases (such as β_s), are possible. These can also be adopted for vector-vector final states (see Sec. VI B 4).

The *untagged* time-dependent decay rate is given by

$$\Gamma_{\bar{B}_s^0\to f}(t) + \Gamma_{B_s^0\to f}(t) = \mathcal{N}\frac{e^{-t/\tau(B_s^0)}}{\tau(B_s^0)}\left[\cosh\left(\frac{\Delta\Gamma_s t}{2}\right) + A_f^{\Delta\Gamma}\sinh\left(\frac{\Delta\Gamma_s t}{2}\right)\right]. \tag{107}$$

Thus, an untagged time-dependent analysis can probe λ_f, through the dependence of $A_f^{\Delta\Gamma}$ on $\mathrm{Re}(\lambda_f)$, given that $\Delta\Gamma_s \neq 0$. This is equivalent to determining the "*effective lifetime*" [92], as discussed in Sec. V A 3. The analysis of flavor-tagged B_s^0 mesons is, of course, more sensitive.

The discussion in this and the previous section is relevant for decays to *CP* eigenstates. In the remainder of Sec. VI B, various cases of time-dependent *CP* asymmetries in decays to non-*CP* eigenstates are considered. For brevity, equations will usually be given assuming that the decay width difference $\Delta\Gamma$ is negligible. Modifications similar to those described here can be made to take into account a nonzero decay width difference.

4. Time-dependent CP asymmetries in decays to vector-vector final states

Consider B decays to states consisting of two spin-1 particles, such as $J/\psi K^{*0}(\to K_S^0\pi^0)$, $J/\psi\phi$, $D^{*+}D^{*-}$ and $\rho^+\rho^-$, which are eigenstates of charge conjugation but not of parity.[15] For such a system, there are three possible final states. In the helicity basis, these are denoted h_{-1}, h_0, h_{+1}. The h_0 state is an eigenstate of parity, and hence of *CP*. By contrast, *CP* transforms $h_{+1} \leftrightarrow h_{-1}$ (up to an unobservable phase). These states are transformed into the transversity basis states $h_\parallel = (h_{+1} + h_{-1})/2$ and $h_\perp = (h_{+1} - h_{-1})/2$. In this basis all three states are *CP* eigenstates, and $h_\perp$ has the opposite *CP* to the others.

The amplitude for decays to the transversity basis states are usually given by $A_{0,\perp,\parallel}$, with normalization such that $|A_0|^2 + |A_\perp|^2 + |A_\parallel|^2 = 1$. Given the relation between the *CP* eigenvalues of the states, the effective *CP* content of the vector-vector state is known if $|A_\perp|^2$ is measured. An alternative strategy is to measure just the longitudinally polarized component, $|A_0|^2$ (sometimes denoted by f_{long}), which allows a limit to be set on the effective *CP* content, since $|A_\perp|^2 \leq |A_\perp|^2 + |A_\parallel|^2 = 1 - |A_0|^2$. The value of the effective *CP* content can be used to treat the decay with the same formalism as for *CP* eigenstates. The most complete treatment for neutral B decays to vector-vector final states is, however, time-dependent angular analysis (also known as time-dependent transversity analysis). In such an analysis, interference between *CP*-even and *CP*-odd states provides additional sensitivity to the weak and strong phases involved.

In most analyses of time-dependent *CP* asymmetries in decays to vector-vector final states carried out to date, an assumption has been made that each helicity (or transversity) amplitude has the same weak phase. This is a good approximation for decays that are dominated by amplitudes with a single weak phase, such $B^0 \to J/\psi K^{*0}$, and is a reasonable approximation in any mode for which only small sample sizes are available. However, for modes that have contributions from amplitudes with different weak phases, the relative size of these contributions can be different for each helicity (or transversity) amplitude, and therefore the time-dependent *CP* asymmetry parameters can also differ. The most generic analysis, suitable for analyses with sufficiently large samples, allows for this effect; such an analysis has been carried out by LHCb for the $B^0 \to J/\psi\rho^0$ decay [231]. An intermediate analysis can allow different parameters for the *CP*-even and *CP*-odd components; such an analysis has been carried out by *BABAR* for the decay $B^0 \to D^{*+}D^{*-}$ [248]. The independent treatment of each helicity (or transversity) amplitude, as in the study of $B_s^0 \to J/\psi\phi$ [179] (discussed in Sec. V), becomes increasingly important for high precision measurements.

5. Time-dependent asymmetries: Self-conjugate multiparticle final states

Amplitudes for neutral B decays into self-conjugate multiparticle final states such as $\pi^+\pi^-\pi^0$, $K^+K^-K_S^0$, $\pi^+\pi^-K_S^0$, $J/\psi\pi^+\pi^-$ or $D\pi^0$ with $D \to K_S^0\pi^+\pi^-$ may be written in terms of *CP*-even and *CP*-odd amplitudes. As above, the interference between these terms provides additional sensitivity to the weak and strong phases involved in the decay, and the time-dependence depends on both the sine and cosine of the weak phase difference. In order to perform unbinned maximum likelihood fits, and thereby extract as much information as possible from the distributions, it is necessary to choose a model for the multiparticle decay, and therefore the results acquire some model dependence. In certain cases, model-independent methods are also possible, but the resulting need to bin the Dalitz plot leads to some loss of statistical precision. The number of observables depends on the final state (and on

[15] This is not true for all vector-vector final states, e.g., $D^{*\pm}\rho^{\mp}$ is clearly not an eigenstate of charge conjugation.

the model used); the key feature is that as long as there are kinematic regions where both CP-even and CP-odd amplitudes contribute, the interference terms will be sensitive to the cosine of the weak phase difference. Therefore, these measurements allow distinction between multiple solutions for, e.g., the two values of 2β from the measurement of $\sin(2\beta)$.

In model-dependent analysis of multibody decays, the decay amplitude is typically described as a coherent sum of contributions that proceed via different intermediate resonances and through nonresonant interactions. It is therefore of interest to present results in terms of the CP violation parameters associated with each resonant amplitude, e.g., $\rho^0 K^0_S$ in the case of the $\pi^+\pi^- K^0_S$ final state. These are referred to as Q2B parameters, since in the limit that there was no other contribution to the multibody decay, the amplitude analysis and the Q2B analysis would give the same results.

We now consider the various notations that have been used in experimental studies of time-dependent asymmetries in decays to self-conjugate multiparticle final states.

a. $B^0 \to D^{(*)}h^0$ *with* $D \to K^0_S\pi^+\pi^-$.—The states $D\pi^0$, $D^*\pi^0$, $D\eta$, $D^*\eta$, $D\omega$ are collectively denoted $D^{(*)}h^0$. When the D decay model is fixed, fits to the time-dependent decay distributions can be performed to extract the weak phase difference. However, it is experimentally advantageous to use the sine and cosine of this phase as fit parameters, since these behave as essentially independent parameters, with low correlations and (potentially) rather different uncertainties. A parameter representing CP violation in the B decay can be simultaneously determined. For consistency with other analyses, this could be chosen to be C_f, but could equally well be $|\lambda_f|$, or other possibilities.

Belle performed an analysis of these channels with $\sin(2\beta)$ and $\cos(2\beta)$ as free parameters [249]. *BABAR* has performed an analysis in which $|\lambda_f|$ was also determined [250]. A joint analysis of the final *BABAR* and Belle data samples supersedes these earlier measurements, and uses $\sin(2\beta)$ and $\cos(2\beta)$ as free parameters [251,252]. Belle has in addition performed a model-independent analysis [253] using as input information about the average strong phase difference between symmetric bins of the Dalitz plot determined by CLEO-c [254].[16] The results of this analysis are measurements of $\sin(2\phi_1)$ and $\cos(2\phi_1)$.

b. $B^0 \to D^{*+}D^{*-}K^0_S$.—The hadronic structure of the $B^0 \to D^{*+}D^{*-}K^0_S$ decay is not sufficiently well understood to perform a full time-dependent Dalitz-plot analysis. Instead, following Ref. [255], *BABAR* [256] and Belle [257] divide the Dalitz plane into two regions: $m(D^{*+}K^0_S)^2 > m(D^{*-}K^0_S)^2$ (labeled $\eta_y = +1$) and $m(D^{*+}K^0_S)^2 < m(D^{*-}K^0_S)^2$ ($\eta_y = -1$); and then fit to a decay-time distribution with asymmetry given by

$$\mathcal{A}_f(\Delta t) = \eta_y \frac{J_c}{J_0}\cos(\Delta m \Delta t) - \left[\frac{2J_{s1}}{J_0}\sin(2\beta) + \eta_y \frac{2J_{s2}}{J_0}\cos(2\beta)\right]\sin(\Delta m \Delta t). \quad (108)$$

The fitted observables are $\frac{J_c}{J_0}$, $\frac{2J_{s1}}{J_0}\sin(2\beta)$ and $\frac{2J_{s2}}{J_0}\cos(2\beta)$, where the parameters J_0, J_c, J_{s1} and J_{s2} are the integrals over the half Dalitz plane $m(D^{*+}K^0_S)^2 < m(D^{*-}K^0_S)^2$ of the functions $|a|^2 + |\bar{a}|^2$, $|a|^2 - |\bar{a}|^2$, $\mathrm{Re}(\bar{a}a^*)$ and $\mathrm{Im}(\bar{a}a^*)$, respectively, where a and $\bar{a}$ are the decay amplitudes of $B^0 \to D^{*+}D^{*-}K^0_S$ and $\bar{B}^0 \to D^{*+}D^{*-}K^0_S$, respectively. The parameter J_{s2} (and hence J_{s2}/J_0) is predicted to be positive [255]; assuming this prediction to be correct, it is possible to determine the sign of $\cos(2\beta)$.

c. $B^0 \to J/\psi\pi^+\pi^-$.—Amplitude analyses of $B^0 \to J/\psi\pi^+\pi^-$ decays [231,258] show large contributions from the $\rho(770)^0$ and $f_0(500)$ states, together with smaller contributions from higher resonances. Since modeling the $f_0(500)$ structure is challenging [259], it is difficult to determine reliably its associated CP violation parameters. Corresponding parameters for the $J/\psi\rho^0$ decay can, however, be determined. In the LHCb analysis [231], the effective weak phase difference $2\beta^{\mathrm{eff}}$ is determined from the fit; results are then converted into values for S_{CP} and C_{CP} to allow comparison with other modes. Here, the notation S_{CP} and C_{CP} denotes parameters obtained for the $J/\psi\rho^0$ final state accounting for the composition of CP-even and CP-odd amplitudes (while assuming that all amplitudes involve the same phases), so that no dilution occurs. Possible CP violation effects in the other amplitudes contributing to the Dalitz plot are treated as a source of systematic uncertainty.

Amplitude analyses have also been done for the $B^0_s \to J/\psi\pi^+\pi^-$ decay, where the final state is dominated by scalar resonances, including the $f_0(980)$ [227,228]. Time-dependent analyses of this B^0_s decay allow a determination of $2\beta_s$, as discussed in Sec. V.

d. $B^0 \to K^+K^-K^0$.—Studies of $B^0 \to K^+K^-K^0$ [260–262] and of the related decay $B^+ \to K^+K^-K^+$ [262–264], show that the decay is dominated by a large nonresonant contribution with significant components from the intermediate K^+K^- resonances $\phi(1020)$, $f_0(980)$, and other higher resonances, as well as a contribution from χ_{c0}.

The full time-dependent Dalitz plot analysis allows the complex amplitudes of each contributing term to be

[16]The external input needed for this analysis is the same as in the model-independent analysis of $B^+ \to DK^+$ with $D \to K^0_S\pi^+\pi^-$, discussed in Sec. VI O 5.

determined from data, including CP violation effects (i.e., allowing the complex amplitude for the B^0 decay to be independent from that for $\bar{B}^0$ decay), although one amplitude must be fixed to serve as a reference. There are several choices for parametrization of the complex amplitudes (e.g., real and imaginary part, or magnitude and phase). Similarly, there are various approaches to the inclusion of CP violation effects. Note that the use of positive definite parameters such as magnitudes are disfavored in certain circumstances (it inevitably leads to biases for small values). In order to compare results between analyses, it is useful for each experiment to present results in terms of the parameters that can be measured in a Q2B analysis (such as $\mathcal{A}_f$, S_f, C_f, $\sin(2\beta^{\rm eff})$, $\cos(2\beta^{\rm eff})$, etc.)

In the *BABAR* analysis of the $B^0 \to K^+K^-K^0$ decay [262], the complex amplitude for each resonant contribution was written as

$$A_f = c_f(1+b_f)e^{i(\phi_f+\delta_f)}, \qquad \bar{A}_f = c_f(1-b_f)e^{i(\phi_f-\delta_f)}, \tag{109}$$

where b_f and δ_f parametrize CP violation in the magnitude and phase, respectively. Belle [261] used the same parametrization but with a different notation for the parameters.[17] The Q2B parameter of CP violation in decay is directly related to b_f,

$$\mathcal{A}_f = \frac{-2b_f}{1+b_f^2} \approx C_f, \tag{110}$$

and the mixing-induced CP violation parameter can be used to obtain $\sin(2\beta^{\rm eff})$,

$$-\eta_f S_f \approx \frac{1-b_f^2}{1+b_f^2}\,\sin(2\beta_f^{\rm eff}), \tag{111}$$

where the approximations are exact in the case that $|q/p| = 1$.

Both *BABAR* [262] and Belle [261] present results for c_f and ϕ_f, for each resonant contribution, and in addition present results for $\mathcal{A}_f$ and $\beta_f^{\rm eff}$ for $\phi(1020)K^0$, $f_0(980)K^0$ and for the remainder of the contributions to the $K^+K^-K^0$ Dalitz plot combined. *BABAR* also presents results for the Q2B parameter S_f for these channels. The models used to describe the resonant structure of the Dalitz plot differ, however. Both analyses suffer from symmetries in the likelihood that lead to multiple solutions, from which we select only one for averaging.

e. $B^0 \to \pi^+\pi^-K^0_S$.—Studies of $B^0 \to \pi^+\pi^-K^0_S$ [265,266] and of the related decay $B^+ \to \pi^+\pi^-K^+$ [263,267–269] show that the decay is dominated by components from intermediate resonances in the $K\pi$ ($K^*(892)$, $K_0^*(1430)$) and $\pi\pi$ ($\rho(770)$, $f_0(980)$, $f_2(1270)$) spectra, together with a poorly understood scalar structure that peaks near $m(\pi\pi) \sim 1300$ MeV/c^2 and is denoted f_X,[18] as well as a large nonresonant component. There is also a contribution from the χ_{c0} state.

The full time-dependent Dalitz plot analysis allows the complex amplitudes of each contributing term to be determined from data, including CP violation effects. In the *BABAR* analysis [265], the magnitude and phase of each component (for both B^0 and $\bar{B}^0$ decays) are measured relative to $B^0 \to f_0(980)K^0_S$, using the following parametrization:

$$A_f = |A_f|e^{i\,\arg(A_f)}, \qquad \bar{A}_f = |\bar{A}_f|e^{i\,\arg(\bar{A}_f)}. \tag{112}$$

In the Belle analysis [266], the $B^0 \to K^{*+}\pi^-$ amplitude is chosen as the reference, and the amplitudes are parametrized as

$$A_f = a_f(1+c_f)e^{i(b_f+d_f)}, \quad \bar{A}_f = a_f(1-c_f)e^{i(b_f-d_f)}. \tag{113}$$

In both cases, the results are translated into Q2B parameters such as $2\beta_f^{\rm eff}$, S_f, C_f for each CP eigenstate f, and parameters of CP violation in decay for each flavor-specific state. Relative phase differences between resonant terms are also extracted.

f. $B^0 \to \pi^+\pi^-\pi^0$.—The $B^0 \to \pi^+\pi^-\pi^0$ decay is dominated by intermediate ρ resonances. Although it is possible, as above, to directly determine the complex amplitudes for each component, an alternative approach [270,271] has been used by both *BABAR* [272,273] and Belle [274,275]. The amplitudes for B^0 and $\bar{B}^0$ decays to $\pi^+\pi^-\pi^0$ are written as

$$\begin{aligned} A_{3\pi} &= f_+A_+ + f_-A_- + f_0A_0, \\ \bar{A}_{3\pi} &= f_+\bar{A}_+ + f_-\bar{A}_- + f_0\bar{A}_0, \end{aligned} \tag{114}$$

respectively. The symbols A_+, A_- and A_0 represent the complex decay amplitudes for $B^0 \to \rho^+\pi^-$, $B^0 \to \rho^-\pi^+$ and $B^0 \to \rho^0\pi^0$ while $\bar{A}_+$, $\bar{A}_-$ and $\bar{A}_0$ represent those for $\bar{B}^0 \to \rho^+\pi^-$, $\bar{B}^0 \to \rho^-\pi^+$ and $\bar{B}^0 \to \rho^0\pi^0$, respectively. The terms f_+, f_- and f_0 incorporate kinematic and dynamical factors and depend on the Dalitz plot coordinates. The full decay-time-dependent distribution can then be written in terms of 27 free parameters, one for each coefficient of the form factor bilinears, as listed in Table 24. These parameters are sometimes referred to as "the Us and Is", and can

[17] $(c, b, \phi, \delta) \leftrightarrow (a, c, b, d)$. See Eq. (113).

[18] The f_X component may originate from either the $f_0(1370)$ or $f_0(1500)$ resonances, or from interference between those or other states and nonresonant amplitudes in this region.

TABLE 24. Definitions of the U and I coefficients. Adapted from Ref. [272].

Parameter	Description
U_+^+	Coefficient of $\lvert f_+\rvert^2$
U_0^+	Coefficient of $\lvert f_0\rvert^2$
U_-^+	Coefficient of $\lvert f_-\rvert^2$
U_0^-	Coefficient of $\lvert f_0\rvert^2\cos(\Delta m\Delta t)$
U_-^-	Coefficient of $\lvert f_-\rvert^2\cos(\Delta m\Delta t)$
U_+^-	Coefficient of $\lvert f_+\rvert^2\cos(\Delta m\Delta t)$
I_0	Coefficient of $\lvert f_0\rvert^2\sin(\Delta m\Delta t)$
I_-	Coefficient of $\lvert f_-\rvert^2\sin(\Delta m\Delta t)$
I_+	Coefficient of $\lvert f_+\rvert^2\sin(\Delta m\Delta t)$
$U_{+-}^{+,\mathrm{Im}}$	Coefficient of $\mathrm{Im}[f_+f_-^*]$
$U_{+-}^{+,\mathrm{Re}}$	Coefficient of $\mathrm{Re}[f_+f_-^*]$
$U_{+-}^{-,\mathrm{Im}}$	Coefficient of $\mathrm{Im}[f_+f_-^*]\cos(\Delta m\Delta t)$
$U_{+-}^{-,\mathrm{Re}}$	Coefficient of $\mathrm{Re}[f_+f_-^*]\cos(\Delta m\Delta t)$
I_{+-}^{Im}	Coefficient of $\mathrm{Im}[f_+f_-^*]\sin(\Delta m\Delta t)$
I_{+-}^{Re}	Coefficient of $\mathrm{Re}[f_+f_-^*]\sin(\Delta m\Delta t)$
$U_{+0}^{+,\mathrm{Im}}$	Coefficient of $\mathrm{Im}[f_+f_0^*]$
$U_{+0}^{+,\mathrm{Re}}$	Coefficient of $\mathrm{Re}[f_+f_0^*]$
$U_{+0}^{-,\mathrm{Im}}$	Coefficient of $\mathrm{Im}[f_+f_0^*]\cos(\Delta m\Delta t)$
$U_{+0}^{-,\mathrm{Re}}$	Coefficient of $\mathrm{Re}[f_+f_0^*]\cos(\Delta m\Delta t)$
I_{+0}^{Im}	Coefficient of $\mathrm{Im}[f_+f_0^*]\sin(\Delta m\Delta t)$
I_{+0}^{Re}	Coefficient of $\mathrm{Re}[f_+f_0^*]\sin(\Delta m\Delta t)$
$U_{-0}^{+,\mathrm{Im}}$	Coefficient of $\mathrm{Im}[f_-f_0^*]$
$U_{-0}^{+,\mathrm{Re}}$	Coefficient of $\mathrm{Re}[f_-f_0^*]$
$U_{-0}^{-,\mathrm{Im}}$	Coefficient of $\mathrm{Im}[f_-f_0^*]\cos(\Delta m\Delta t)$
$U_{-0}^{-,\mathrm{Re}}$	Coefficient of $\mathrm{Re}[f_-f_0^*]\cos(\Delta m\Delta t)$
I_{-0}^{Im}	Coefficient of $\mathrm{Im}[f_-f_0^*]\sin(\Delta m\Delta t)$
I_{-0}^{Re}	Coefficient of $\mathrm{Re}[f_-f_0^*]\sin(\Delta m\Delta t)$

be expressed in terms of A_+, A_-, A_0, $\bar{A}_+$, $\bar{A}_-$ and $\bar{A}_0$. If the full set of parameters is determined, together with their correlations, other parameters, such as weak and strong phases, parameters of CP violation in decay, etc., can be subsequently extracted. Note that one of the parameters (typically U_+^+, the coefficient of $|f_+|^2$) is often fixed to unity to provide a reference; this does not affect the analysis.

6. Time-dependent CP asymmetries in decays to non-CP eigenstates

Consider a non-CP eigenstate f, and its conjugate $\bar{f}$. For neutral B decays to these final states, there are four amplitudes to consider: those for B^0 to decay to f and $\bar{f}$ (A_f and $A_{\bar{f}}$, respectively), and the equivalents for $\bar{B}^0$ ($\bar{A}_f$ and $\bar{A}_{\bar{f}}$). If CP is conserved in the decay, then $A_f = \bar{A}_{\bar{f}}$ and $A_{\bar{f}} = \bar{A}_f$.

The decay-time-dependent distributions can be written in many different ways. Here, we follow Sec. VI B 2 and define $\lambda_f = \frac{q}{p}\frac{\bar{A}_f}{A_f}$ and $\lambda_{\bar{f}} = \frac{q}{p}\frac{\bar{A}_{\bar{f}}}{A_{\bar{f}}}$. The time-dependent CP asymmetries that are sensitive to mixing-induced CP violation effects then follow Eq. (100):

$$\mathcal{A}_f(\Delta t) \equiv \frac{\Gamma_{\bar{B}^0\to f}(\Delta t) - \Gamma_{B^0\to f}(\Delta t)}{\Gamma_{\bar{B}^0\to f}(\Delta t) + \Gamma_{B^0\to f}(\Delta t)} = S_f\,\sin(\Delta m\Delta t) - C_f\,\cos(\Delta m\Delta t), \quad (115)$$

$$\mathcal{A}_{\bar{f}}(\Delta t) \equiv \frac{\Gamma_{\bar{B}^0\to \bar{f}}(\Delta t) - \Gamma_{B^0\to \bar{f}}(\Delta t)}{\Gamma_{\bar{B}^0\to \bar{f}}(\Delta t) + \Gamma_{B^0\to \bar{f}}(\Delta t)} = S_{\bar{f}}\,\sin(\Delta m\Delta t) - C_{\bar{f}}\,\cos(\Delta m\Delta t), \quad (116)$$

with the definitions of the parameters C_f, S_f, $C_{\bar{f}}$ and $S_{\bar{f}}$, following Eqs. (101) and (102).

The time-dependent decay rates are given by

$$\Gamma_{\bar{B}^0\to f}(\Delta t) = \frac{e^{-|\Delta t|/\tau(B^0)}}{8\tau(B^0)}(1+\langle\mathcal{A}_{f\bar{f}}\rangle) \times [1 + S_f\sin(\Delta m\Delta t) - C_f\cos(\Delta m\Delta t)], \quad (117)$$

$$\Gamma_{B^0\to f}(\Delta t) = \frac{e^{-|\Delta t|/\tau(B^0)}}{8\tau(B^0)}(1+\langle\mathcal{A}_{f\bar{f}}\rangle) \times [1 - S_f\sin(\Delta m\Delta t) + C_f\cos(\Delta m\Delta t)], \quad (118)$$

$$\Gamma_{\bar{B}^0\to \bar{f}}(\Delta t) = \frac{e^{-|\Delta t|/\tau(B^0)}}{8\tau(B^0)}(1-\langle\mathcal{A}_{f\bar{f}}\rangle) \times [1 + S_{\bar{f}}\sin(\Delta m\Delta t) - C_{\bar{f}}\cos(\Delta m\Delta t)], \quad (119)$$

$$\Gamma_{B^0\to \bar{f}}(\Delta t) = \frac{e^{-|\Delta t|/\tau(B^0)}}{8\tau(B^0)}(1-\langle\mathcal{A}_{f\bar{f}}\rangle) \times [1 - S_{\bar{f}}\sin(\Delta m\Delta t) + C_{\bar{f}}\cos(\Delta m\Delta t)], \quad (120)$$

where the time-independent parameter $\langle\mathcal{A}_{f\bar{f}}\rangle$ represents an overall asymmetry in the production of the f and $\bar{f}$ final states in B^0 and $\bar{B}^0$ decays,[19]

$$\langle\mathcal{A}_{f\bar{f}}\rangle = \frac{(|A_f|^2 + |\bar{A}_f|^2) - (|A_{\bar{f}}|^2 + |\bar{A}_{\bar{f}}|^2)}{(|A_f|^2 + |\bar{A}_f|^2) + (|A_{\bar{f}}|^2 + |\bar{A}_{\bar{f}}|^2)}. \quad (121)$$

Assuming $|q/p| = 1$, i.e., absence of CP violation in mixing, the parameters C_f and $C_{\bar{f}}$ can also be written in terms of the decay amplitudes as

$$C_f = \frac{|A_f|^2 - |\bar{A}_f|^2}{|A_f|^2 + |\bar{A}_f|^2} \quad \text{and} \quad C_{\bar{f}} = \frac{|A_{\bar{f}}|^2 - |\bar{A}_{\bar{f}}|^2}{|A_{\bar{f}}|^2 + |\bar{A}_{\bar{f}}|^2}, \quad (122)$$

[19]This parameter is often denoted $\mathcal{A}_f$ (or $\mathcal{A}_{CP}$), but here we avoid this notation to prevent confusion with the time-dependent CP asymmetry.

giving rise to asymmetries in the decay amplitudes for the final states f and $\bar{f}$. In this notation, the conditions for the absence of CP violation in decay are $\langle \mathcal{A}_{f\bar{f}} \rangle = 0$ and $C_f = -C_{\bar{f}}$. Note that C_f and $C_{\bar{f}}$ are typically nonzero; e.g., for a flavor-specific final state where $\bar{A}_f = A_{\bar{f}} = 0$, they take the values $C_f = -C_{\bar{f}} = 1$.

The coefficients of the sine terms contain information about the weak phase. In the case that each decay amplitude contains only a single weak phase (i.e., no CP violation in decay as well as none in mixing), these terms can be written as

$$S_f = \frac{-2|A_f||\bar{A}_f| \sin(\phi_{\rm mix} + \phi_{\rm dec} - \delta_f)}{|A_f|^2 + |\bar{A}_f|^2} \quad \text{and}$$
$$S_{\bar{f}} = \frac{-2|A_{\bar{f}}||\bar{A}_{\bar{f}}| \sin(\phi_{\rm mix} + \phi_{\rm dec} + \delta_f)}{|A_{\bar{f}}|^2 + |\bar{A}_{\bar{f}}|^2}, \tag{123}$$

where δ_f is the strong phase difference between the decay amplitudes. If there is no CP violation, the condition $S_f = -S_{\bar{f}}$ holds. If decay amplitudes with different weak and strong phases contribute, no straightforward interpretation of S_f and $S_{\bar{f}}$ is possible.

The conditions for CP invariance $C_f = -C_{\bar{f}}$ and $S_f = -S_{\bar{f}}$ motivate a rotation of the parameters:

$$S_{f\bar{f}} = \frac{S_f + S_{\bar{f}}}{2}, \qquad \Delta S_{f\bar{f}} = \frac{S_f - S_{\bar{f}}}{2},$$
$$C_{f\bar{f}} = \frac{C_f + C_{\bar{f}}}{2}, \qquad \Delta C_{f\bar{f}} = \frac{C_f - C_{\bar{f}}}{2}. \tag{124}$$

With these parameters, the CP invariance conditions become $S_{f\bar{f}} = 0$ and $C_{f\bar{f}} = 0$. The parameter $\Delta C_{f\bar{f}}$ gives a measure of the "flavor-specificity" of the decay: $\Delta C_{f\bar{f}} = \pm 1$ corresponds to a completely flavor-specific decay, in which no interference between decays with and without mixing can occur, while $\Delta C_{f\bar{f}} = 0$ results in maximum sensitivity to mixing-induced CP violation. The parameter $\Delta S_{f\bar{f}}$ is related to the strong phase difference between the decay amplitudes of the B^0 meson to the f and to $\bar{f}$ final states. We note that the observables of Eq. (124) exhibit experimental correlations (typically of ∼20%, depending on the tagging purity, and other effects) between $S_{f\bar{f}}$ and $\Delta S_{f\bar{f}}$, and between $C_{f\bar{f}}$ and $\Delta C_{f\bar{f}}$. On the other hand, the final-state-specific observables of Eqs. (117)–(120) tend to have low correlations.

Alternatively, if we recall that the CP invariance conditions at the decay amplitude level are $A_f = \bar{A}_{\bar{f}}$ and $A_{\bar{f}} = \bar{A}_f$, we are led to consider the parameters [242]

$$\mathcal{A}_{f\bar{f}} = \frac{|\bar{A}_{\bar{f}}|^2 - |A_f|^2}{|\bar{A}_{\bar{f}}|^2 + |A_f|^2} \quad \text{and} \quad \mathcal{A}_{\bar{f}f} = \frac{|\bar{A}_f|^2 - |A_{\bar{f}}|^2}{|\bar{A}_f|^2 + |A_{\bar{f}}|^2}. \tag{125}$$

These are sometimes considered more physically intuitive parameters, since they characterize CP violation in decay in decays with particular topologies. For example, in the case of $B^0 \to \rho^\pm \pi^\mp$ (choosing $f = \rho^+\pi^-$ and $\bar{f} = \rho^-\pi^+$), $\mathcal{A}_{f\bar{f}}$ (also denoted $\mathcal{A}_{\rho\pi}^{+-}$) parametrizes CP violation in decays in which the produced ρ meson does not contain the spectator quark, while $\mathcal{A}_{\bar{f}f}$ (also denoted $\mathcal{A}_{\rho\pi}^{-+}$) parametrizes CP violation in decays in which it does. Note that we have again followed the sign convention that the asymmetry is the difference between the rate involving a b quark and that involving a $\bar{b}$ quark, cf. Eq. (96). Of course, these parameters are not independent of the other sets of parameters given above, and can be written as

$$\mathcal{A}_{f\bar{f}} = -\frac{\langle \mathcal{A}_{f\bar{f}} \rangle + C_{f\bar{f}} + \langle \mathcal{A}_{f\bar{f}} \rangle \Delta C_{f\bar{f}}}{1 + \Delta C_{f\bar{f}} + \langle \mathcal{A}_{f\bar{f}} \rangle C_{f\bar{f}}} \quad \text{and}$$
$$\mathcal{A}_{\bar{f}f} = \frac{-\langle \mathcal{A}_{f\bar{f}} \rangle + C_{f\bar{f}} + \langle \mathcal{A}_{f\bar{f}} \rangle \Delta C_{f\bar{f}}}{-1 + \Delta C_{f\bar{f}} + \langle \mathcal{A}_{f\bar{f}} \rangle C_{f\bar{f}}}. \tag{126}$$

They usually exhibit strong correlations.

We now consider the various notations used in experimental studies of time-dependent CP asymmetries in decays to non-CP eigenstates.

a. $B^0 \to D^{*\pm} D^\mp$.—The $(\langle \mathcal{A}_{f\bar{f}} \rangle, C_f, S_f, C_{\bar{f}}, S_{\bar{f}})$ set of parameters was used in early publications by both *BABAR* [276] and Belle [277] (albeit with slightly different notations), with $f = D^{*+}D^-$, $\bar{f} = D^{*-}D^+$. In a more recent paper on this topic, Belle [278] instead uses the parametrization $(A_{D^*D}, S_{D^*D}, \Delta S_{D^*D}, C_{D^*D}, \Delta C_{D^*D})$, while *BABAR* [248] gives results in both sets of parameters. We therefore use the $(A_{D^*D}, S_{D^*D}, \Delta S_{D^*D}, C_{D^*D}, \Delta C_{D^*D})$ set.

b. $B^0 \to \rho^\pm \pi^\mp$.—In the $\rho^\pm\pi^\mp$ system, the $(\langle \mathcal{A}_{f\bar{f}} \rangle, C_{f\bar{f}}, S_{f\bar{f}}, \Delta C_{f\bar{f}}, \Delta S_{f\bar{f}})$ set of parameters was originally used by *BABAR* [279] and Belle [280] in the Q2B approximation; the exact names[20] used in this case were $(\mathcal{A}_{CP}^{\rho\pi}, C_{\rho\pi}, S_{\rho\pi}, \Delta C_{\rho\pi}, \Delta S_{\rho\pi})$, and these names are also used in this document.

Since $\rho^\pm\pi^\mp$ is reconstructed in the final state $\pi^+\pi^-\pi^0$, the interference between the ρ resonances can provide additional information about the phases (see Sec. VI B 5). Both *BABAR* [272] and Belle [274,275] have performed time-dependent Dalitz-plot analyses, from which the weak phase α is directly extracted. In such an analysis, the measured Q2B parameters are also naturally corrected for interference effects.

c. $B^0 \to D^\mp \pi^\pm, D^{*\mp}\pi^\pm, D^\mp \rho^\pm$.—Time-dependent CP analyses have also been performed for the final states

[20] *BABAR* has used the notations $A_{CP}^{\rho\pi}$ [279] and $\mathcal{A}_{\rho\pi}$ [272] in place of $\mathcal{A}_{CP}^{\rho\pi}$.

$D^{\mp}\pi^{\pm}$, $D^{*\mp}\pi^{\pm}$ and $D^{\mp}\rho^{\pm}$. In these theoretically clean cases, no penguin contributions are possible, so there is no CP violation in decay. Furthermore, due to the smallness of the ratio of the magnitudes of the suppressed ($b \to u$) and favored ($b \to c$) amplitudes (denoted R_f), to a very good approximation, $C_f = -C_{\bar{f}} = 1$ (using $f = D^{(*)-}h^+$, $\bar{f} = D^{(*)+}h^-$, $h = \pi, \rho$), and the coefficients of the sine terms are given by

$$S_f = -2R_f \sin(\phi_{\rm mix} + \phi_{\rm dec} - \delta_f) \quad \text{and}$$
$$S_{\bar{f}} = -2R_f \sin(\phi_{\rm mix} + \phi_{\rm dec} + \delta_f). \tag{127}$$

Thus, weak phase information can be obtained from measurements of S_f and $S_{\bar{f}}$, although external information on at least one of R_f or δ_f is necessary, constituting a source of theoretical uncertainty. Note that $\phi_{\rm mix} + \phi_{\rm dec} = 2\beta + \gamma \equiv 2\phi_1 + \phi_3$ for all the decay modes in question, while R_f and δ_f depend on the decay mode.

Again, different notations have been used in the literature. *BABAR* [281,282] defines the time-dependent probability function by

$$f^{\pm}(\eta, \Delta t) = \frac{e^{-|\Delta t|/\tau}}{4\tau}[1 \mp S_\zeta \sin(\Delta m \Delta t) \mp \eta C_\zeta \cos(\Delta m \Delta t)], \tag{128}$$

where the upper (lower) sign corresponds to the tagging meson being a B^0 ($\bar{B}^0$). The parameter η takes the value $+1$ (-1) and ζ denotes $+$ ($-$) when the final state is, e.g., $D^-\pi^+$ ($D^+\pi^-$). However, in the fit, the substitutions $C_\zeta = 1$ and $S_\zeta = a \mp \eta b_i - \eta c_i$ are made, where the subscript i denotes the flavor tagging category. These are motivated by the possibility of CP violation on the tag side [283]. The parameter a is not affected by tag-side CP violation. The parameter b only depends on tag-side CP violation parameters and is not directly useful for determining UT angles. A clean interpretation of the c parameter is only possible for lepton-tagged events, which are not affected by tag-side CP violation effects, so the *BABAR* measurements report c measured with those events only. Neglecting b terms,

$$S_+ = a - c \quad \text{and} \quad S_- = a + c \Leftrightarrow a = (S_+ + S_-)/2 \quad \text{and}$$
$$c = (S_- - S_+)/2, \tag{129}$$

in analogy to the parameters of Eq. (124).

The parameters used by Belle in the analysis using partially reconstructed B decays [284], are similar to the S_ζ parameters defined above. However, in the Belle convention, a tagging B^0 corresponds to a $+$ sign in front of the sine coefficient; furthermore the correspondence between the super/subscript and the final state is opposite, so that $S_\pm$ (*BABAR*) $= -S^{\mp}$ (Belle). In this analysis, only lepton tags are used, so there is no effect from tag-side CP violation. In the Belle analysis that used fully reconstructed B decays [285], this effect is measured and taken into account using $D^*\ell\nu$ decays; in neither Belle analysis are the a, b and c parameters used. The parameters measured by Belle are $2R_{D^{(*)}\pi}\sin(2\phi_1 + \phi_3 \pm \delta_{D^{(*)}\pi})$; the definition is such that $S^{\pm}(\text{Belle}) = -2R_{D^*\pi}\sin(2\phi_1 + \phi_3 \pm \delta_{D^*\pi})$. This definition includes an angular momentum factor $(-1)^L$ [286], and so for the results in the $D\pi$ system, there is an additional factor of -1 in the conversion.

LHCb has also measured the parameters of $B^0 \to D^{\mp}\pi^{\pm}$ decays [287]. The convention used is essentially the same as Belle, but with the notation $(S_f, S_{\bar{f}}) = (S_-, S_+)$. For the averages in this document, we use the a and c parameters. Correlations are taken into account in the LHCb case, where significant correlations are reported. Explicitly, the conversion reads

$$a = -(S_+ + S_-)/2, \qquad c = -(S_+ - S_-)/2. \tag{130}$$

d. $B_s^0 \to D_s^{\mp}K^{\pm}$.—The phenomenology of $B_s^0 \to D_s^{\mp}K^{\pm}$ decays is similar to that of $B^0 \to D^{\mp}\pi^{\pm}$, with some important caveats. The two amplitudes for $b \to u$ and $b \to c$ transitions have the same level of Cabibbo-suppression (i.e., are of the same order in λ) though the former is suppressed by $\sqrt{\rho^2 + \eta^2}$. The large value of the ratio R of their magnitudes allows it to be determined from data, as the deviation of $|C_f|$ and $|C_{\bar{f}}|$ from unity can be observed. Moreover, the nonzero value of $\Delta\Gamma_s$ allows the determination of additional terms, $A_f^{\Delta\Gamma}$ and $A_{\bar{f}}^{\Delta\Gamma}$ (see Sec. VI B 3), that break ambiguities in the solutions for $\phi_{\rm mix} + \phi_{\rm dec}$, which for $B_s^0 \to D_s^{\mp}K^{\pm}$ decays is equal to $\gamma - 2\beta_s$.

LHCb [288,289] has performed such an analysis with $B_s^0 \to D_s^{\mp}K^{\pm}$ decays. The absence of CP violation in decay was assumed, and the parameters determined from the fit were labeled C, $A^{\Delta\Gamma}$, $\bar{A}^{\Delta\Gamma}$, S, $\bar{S}$. These are trivially related to the definitions used in this section.

e. Time-dependent asymmetries in radiative B decays.—As a special case of decays to non-CP eigenstates, let us consider radiative B decays. Here, the emitted photon has a distinct helicity, which is in principle observable, but in practice is not usually measured. Thus, the measured time-dependent decay rates for neutral B meson decays are given by sums of the expressions of Eqs. (117)–(120) for the final states with left-handed (γ_L) and right-handed (γ_R) photon helicity [290,291]

$$\Gamma_{\bar{B}^0 \to X\gamma}(\Delta t) = \Gamma_{\bar{B}^0 \to X\gamma_L}(\Delta t) + \Gamma_{\bar{B}^0 \to X\gamma_R}(\Delta t)$$
$$= \frac{e^{-|\Delta t|/\tau(B^0)}}{4\tau(B^0)}[1 + (S_L + S_R)\sin(\Delta m \Delta t)$$
$$- (C_L + C_R)\cos(\Delta m \Delta t)], \tag{131}$$

$$\Gamma_{B^0\to X_\gamma}(\Delta t) = \Gamma_{B^0\to X_{\gamma_L}}(\Delta t) + \Gamma_{B^0\to X_{\gamma_R}}(\Delta t)$$
$$= \frac{e^{-|\Delta t|/\tau(B^0)}}{4\tau(B^0)}[1 - (S_L + S_R)\,\sin(\Delta m \Delta t) + (C_L + C_R)\,\cos(\Delta m \Delta t)]. \quad (132)$$

Here, in place of the subscripts f and $\bar{f}$, we have used L and R to indicate the photon helicity. In order for interference between decays with and without B^0-$\bar{B}^0$ mixing to occur, the X system must not be flavor-specific, e.g., in the case of $B^0 \to K^{*0}\gamma$, the final state must be $K^0_S\pi^0\gamma$. The sign of the sine term depends on the C eigenvalue of the X system. At leading order, the photons from $b \to q\gamma$ ($\bar{b} \to \bar{q}\gamma$) are predominantly left (right) polarized, with corrections of order of m_q/m_b, and thus interference effects are suppressed. Higher-order effects can lead to corrections of order $\Lambda_{\rm QCD}/m_b$ [292,293], although explicit calculations indicate that such corrections may be small for exclusive final states [294,295]. The predicted smallness of the S terms in the Standard Model results in sensitivity to new physics contributions.

The formalism discussed above is valid for any radiative decay to a final state where the hadronic system is an eigenstate of C. In addition to $K^0_S\pi^0\gamma$, experiments have presented results using B^0 decays to $K^0_S\eta\gamma$, $K^0_S\rho^0\gamma$ and $K^0_S\phi\gamma$. For the case of the $K^0_S\rho^0\gamma$ final state, particular care is needed, as due to the non-negligible width of the ρ^0 meson, decays selected as $B^0 \to K^0_S\rho^0\gamma$ can include a significant contribution from $K^{*\pm}\pi^\mp\gamma$ decays, which are flavor-specific and do not have the same oscillation phenomenology. It is therefore necessary to correct the fitted asymmetry parameter for a "dilution factor".

In the case of radiative B^0_s decays, the time-dependent decay rates of Eqs. (131) and (132) must be modified, in a similar way to that discussed in Sec. VI B 3, to account for the nonzero value of $\Delta\Gamma_s$. Thus, for decays such as $B^0_s \to \phi\gamma$, there is an additional observable, $A^{\Delta\Gamma}_{\phi\gamma}$, which can be determined from an untagged effective lifetime measurement [296].

7. Asymmetries in $B \to D^{(*)}K^{(*)}$ decays

CP asymmetries in $B \to D^{(*)}K^{(*)}$ decays are sensitive to γ. The neutral $D^{(*)}$ meson produced is an admixture of $D^{(*)0}$ (produced by a $b \to c$ transition) and $\bar{D}^{(*)0}$ (produced by a color-suppressed $b \to u$ transition) states. If the final state is chosen so that both $D^{(*)0}$ and $\bar{D}^{(*)0}$ can contribute, the two amplitudes interfere, and the resulting observables are sensitive to γ, the relative weak phase between the two B decay amplitudes [297]. Various methods have been proposed to exploit this interference, including those where the neutral D meson is reconstructed as a CP eigenstate (GLW) [298,299], in a suppressed final state (ADS) [300,301], or in a self-conjugate three-body final state, such as $K^0_S\pi^+\pi^-$ (BPGGSZ or Dalitz) [302,303]. While each method differs in the choice of D decay, they are all sensitive to the same parameters of the B decay, and can be considered as variations of the same technique.

Consider the case of $B^\mp \to DK^\mp$, with D decaying to a final state f, which is accessible from both D^0 and $\bar{D}^0$. We can write the decay rates $\Gamma_\mp$ for B^- and B^+, the charge averaged rate $\Gamma = (\Gamma_- + \Gamma_+)/2$, and the charge asymmetry $A = (\Gamma_- - \Gamma_+)/(\Gamma_- + \Gamma_+)$ [see Eq. (96)] as

$$\Gamma_\mp \propto r_B^2 + r_D^2 + 2r_B r_D\,\cos(\delta_B + \delta_D \mp \gamma), \quad (133)$$

$$\Gamma \propto r_B^2 + r_D^2 + 2r_B r_D\,\cos(\delta_B + \delta_D)\,\cos(\gamma), \quad (134)$$

$$A = \frac{2r_B r_D\,\sin(\delta_B + \delta_D)\,\sin(\gamma)}{r_B^2 + r_D^2 + 2r_B r_D\,\cos(\delta_B + \delta_D)\,\cos(\gamma)}, \quad (135)$$

where the ratios of B decay amplitudes are written in terms of γ, r_B and δ_B,[21]

$$r_B e^{i(\delta_B - \gamma)} \equiv \frac{A(B^- \to \bar{D}^0 K^-)}{A(B^- \to D^0 K^-)} \quad \text{and}$$
$$r_B e^{i(\delta_B + \gamma)} \equiv \frac{A(B^+ \to D^0 K^+)}{A(B^+ \to \bar{D}^0 K^+)}, \quad (136)$$

such that r_B is less than one. The ratio of D decay amplitudes is correspondingly written, assuming CP conservation in D decay, in terms of r_D and δ_D,

$$r_D e^{-i\delta_D} \equiv \frac{A(D^0 \to f)}{A(\bar{D}^0 \to f)}. \quad (137)$$

The relation between B^- and B^+ amplitudes given in Eq. (136) is a result of there being only one weak phase contributing to each amplitude in the Standard Model, which is the source of the theoretical cleanliness of this approach for measuring γ [304]. The parameters δ_B and δ_D are the strong phase differences between the B and D decay amplitudes, respectively.[22] The values of r_D and δ_D depend on the final state f: for the GLW analysis, $r_D = 1$ and δ_D is trivial (either zero or π); for other modes, values of r_D and δ_D are not trivial, and for multibody final states they vary across the phase space. This can be quantified either by an explicit D decay amplitude model or by model-independent information. In the case that the multibody final state (or a subsample of it) is treated inclusively, the formalism is

[21]Note that here we use the notation r_B to denote the ratio of B decay amplitudes, whereas in Sec. VI. B. 6 we used, e.g., $R_{D\pi}$, for a rather similar quantity. The reason is that here we need to be concerned also with D decay amplitudes, and so it is convenient to use the subscript to denote the decaying particle. Hopefully, using r in place of R will reduce the potential for confusion.

[22]Note that the definition of δ_D in Eq. (137) differs by a shift of π from that used for $D^0 \to K^\pm\pi^\mp$ decays in Sec. X.

modified by the inclusion of a coherence factor, usually denoted κ, while r_D and δ_D become effective parameters corresponding to amplitude-weighted averages across the phase space.

Note that, for given values of r_B and r_D, the maximum size of A (at $\sin(\delta_B+\delta_D)=1$) is $2r_Br_D\sin(\gamma)/(r_B^2+r_D^2)$. Thus, even for D decay modes with small r_D, large asymmetries, and hence sensitivity to γ, may occur for B decay modes with similar values of r_B. For this reason, the ADS analysis of the decay $B^{\mp}\to D\pi^{\mp}$ is also of interest.

The expressions of Eq. (133)–(137) are for a specific point in phase space, and therefore are relevant where both B and D decays are to two-body final states. Additional coherence factors enter the expressions when the B decay is to a multibody final state (further discussion of multibody D decays can be found below). In particular, experiments have studied $B^+\to DK^*(892)^+$, $B^0\to DK^*(892)^0$ and $B^+\to DK^+\pi^+\pi^-$ decays. Considering, for concreteness, the $B\to DK^*(892)$ case, the non-negligible width of the $K^*(892)$ resonance implies that contributions from other $B\to DK\pi$ decays can pass the selection requirements. Their effect on the Q2B analysis can be accounted for with a coherence factor [305], usually denoted κ, which tends to unity in the limit that the $K^*(892)$ resonance is the only signal amplitude contributing in the selected region of phase space. In this case, the hadronic parameters r_B and δ_B become effectively weighted averages across the selected phase space of the magnitude ratio and relative strong phase between the CKM-suppressed and -favored amplitudes; these effective parameters are denoted $\bar{r}_B$ and $\bar{\delta}_B$ (the notations r_s, δ_s and r_S, δ_S are also found in the literature). An alternative, and in certain cases more advantageous, approach is a Dalitz plot analysis of the full $B\to DK\pi$ phase space [306–309].

We now consider the various notations used in experimental studies of CP asymmetries in $B\to D^{(*)}K^{(*)}$ decays. To simplify the notation the $B^+\to DK^+$ decay is considered; the extension to other modes mediated by the same quark-level transitions is straightforward.

a. $B\to D^{(*)}K^{(*)}$ with $D\to CP$ eigenstate decays.—In the GLW analysis, the measured quantities are the partial rate asymmetry

$$A_{CP}=\frac{\Gamma(B^-\to D_{CP}K^-)-\Gamma(B^+\to D_{CP}K^+)}{\Gamma(B^-\to D_{CP}K^-)+\Gamma(B^+\to D_{CP}K^+)} \tag{138}$$

and the charge-averaged rate

$$R_{CP}=\frac{2\Gamma(B^+\to D_{CP}K^+)}{\Gamma(B^+\to \bar{D}^0K^+)}, \tag{139}$$

which are measured for D decays to both CP-even and CP-odd final states. It is often experimentally convenient to measure R_{CP} using a double ratio,

$$R_{CP}\approx\frac{\Gamma(B^+\to D_{CP}K^+)/\Gamma(B^+\to \bar{D}^0K^+)}{\Gamma(B^+\to D_{CP}\pi^+)/\Gamma(B^+\to \bar{D}^0\pi^+)} \tag{140}$$

that is normalized both to the rate for the favored $\bar{D}^0\to K^+\pi^-$ decay, and to the equivalent quantities for $B^+\to D\pi^+$ decays [charge conjugate processes are implicitly included in Eqs. (139) and (140)]. In this way the constant of proportionality drops out of Eq. (134). Eq. (140) is exact in the limit that the contribution of the $b\to u$ decay amplitude to $B^+\to D\pi^+$ vanishes and when the flavor-specific rates $\Gamma(B^+\to\bar{D}^0h^+)$ ($h=\pi$, K) are determined using appropriately flavor-specific D decays. In reality, the Cabibbo-favored $D\to K\pi$ decay is used, which is not perfectly flavor-specific. This introduces a small bias, and corresponding systematic uncertainty, in measurements of R_{CP} using Eq. (140). The effect can however be fully accounted for when combining multiple measurements with sensitivity to γ, including results from $B\to D\pi$ decays (see Sec. VI O 7).

b. $B\to D^{(*)}K^{(*)}$ with $D\to$ non-CP eigenstate two-body decays.—For the ADS analysis, which is based on a suppressed $D\to f$ decay, the measured quantities are again the partial rate asymmetry and the charge-averaged rate. In this case it is sufficient to measure the rate in a single ratio (normalized to the favored $D\to\bar{f}$ decay) since potential systematic uncertainties related to detection cancel naturally; the observed charge-averaged rate is then

$$R_{\rm ADS}=\frac{\Gamma(B^-\to[f]_DK^-)+\Gamma(B^+\to[\bar{f}]_DK^+)}{\Gamma(B^-\to[\bar{f}]_DK^-)+\Gamma(B^+\to[f]_DK^+)}, \tag{141}$$

where the inclusion of charge-conjugate modes has been made explicit. The CP asymmetry is defined as

$$A_{\rm ADS}=\frac{\Gamma(B^-\to[f]_DK^-)-\Gamma(B^+\to[f]_DK^+)}{\Gamma(B^-\to[f]_DK^-)+\Gamma(B^+\to[f]_DK^+)}. \tag{142}$$

Since the uncertainty of $A_{\rm ADS}$ depends on the central value of $R_{\rm ADS}$, for some statistical treatments it is preferable to use an alternative pair of parameters [310]

$$R_-=\frac{\Gamma(B^-\to[f]_DK^-)}{\Gamma(B^-\to[\bar{f}]_DK^-)}\qquad R_+=\frac{\Gamma(B^+\to[\bar{f}]_DK^+)}{\Gamma(B^+\to[f]_DK^+)}, \tag{143}$$

where there is no implied inclusion of charge-conjugate processes. These parameters are statistically uncorrelated but may be affected by common sources of systematic uncertainty. We use the $(R_{\rm ADS},A_{\rm ADS})$ set in our compilation where available.

In the ADS analysis, there are two additional unknowns (r_D and δ_D) compared to the GLW case. Additional constraints are therefore required in order to obtain sensitivity to γ. Generally, one needs access to two different

TABLE 25. Summary of relations between measured and physical parameters in GLW, ADS and Dalitz analyses of $B \to D^{(*)}K^{(*)}$ decays.

GLW analysis	
$R_{CP\pm}$	$1 + r_B^2 \pm 2r_B \cos(\delta_B)\cos(\gamma)$
$A_{CP\pm}$	$\pm 2r_B \sin(\delta_B)\sin(\gamma)/R_{CP\pm}$
ADS analysis	
$R_{\rm ADS}$	$r_B^2 + r_D^2 + 2r_B r_D \cos(\delta_B + \delta_D)\cos(\gamma)$
$A_{\rm ADS}$	$2r_B r_D \sin(\delta_B + \delta_D)\sin(\gamma)/R_{\rm ADS}$
BPGGSZ Dalitz analysis ($D \to K^0_S\pi^+\pi^-$)	
$x_\pm$	$r_B \cos(\delta_B \pm \gamma)$
$y_\pm$	$r_B \sin(\delta_B \pm \gamma)$
Dalitz analysis ($D \to \pi^+\pi^-\pi^0$)	
$\rho^\pm$	$\lvert z_\pm - x_0\rvert$
$\theta^\pm$	$\tan^{-1}(\mathrm{Im}(z_\pm)/(\mathrm{Re}(z_\pm) - x_0))$

linear admixtures of D^0 and $\bar{D}^0$ states in order to determine the relative phase: one such sample can be flavor tagged D mesons, which are available in abundant quantities in many experiments; the other can be CP-tagged D mesons from $\psi(3770)$ decays, or a superposition of D^0 and $\bar{D}^0$ from D^0–$\bar{D}^0$ mixing or from production in $B \to DK$ decays. In fact, the most precise information on both r_D and δ_D for $D \to K\pi$ currently comes from global fits to charm mixing data, as discussed in Sec. X A.

The relation of $A_{\rm ADS}$ to the underlying parameters given in Eq. (135) and Table 25 is exact for a two-body D decay. For multibody decays, a similar formalism can be used with the introduction of a coherence factor [311]. This is most appropriate for doubly Cabibbo-suppressed decays to non-self-conjugate final states, but can also be modified for use with singly Cabibbo-suppressed decays [312]. For multibody self-conjugate final states, such as $K^0_S\pi^+\pi^-$, a Dalitz plot analysis (discussed below) is often more appropriate. However, in certain cases where the final state can be approximated as a CP eigenstate, a modified version of the GLW formalism can be used [313]. In such cases the observables are denoted $A_{\rm qGLW}$ and $R_{\rm qGLW}$ to indicate that the final state is not a pure CP eigenstate.

c. $B \to D^{(*)}K^{(*)}$ with $D \to$ multibody final state decays.— In the model-dependent Dalitz-plot (or BPGGSZ) analysis of D decays to multibody self-conjugate final states, the values of r_D and δ_D across the Dalitz plot are given by an amplitude model (with parameters typically obtained from data). A simultaneous fit to the B^+ and B^- samples can then be used to obtain γ, r_B and δ_B directly. The uncertainties on the phases depend approximately inversely on r_B, which is positive definite and therefore tends to be overestimated leading to an underestimation of the uncertainty on γ that must be corrected statistically (unless $\sigma(r_B) \ll r_B$). An alternative approach is to fit for the "Cartesian" variables

$$\begin{aligned}(x_\pm, y_\pm) &= (\mathrm{Re}(r_B e^{i(\delta_B \pm \gamma)}), \mathrm{Im}(r_B e^{i(\delta_B \pm \gamma)})) \\ &= (r_B\cos(\delta_B \pm \gamma), r_B\sin(\delta_B \pm \gamma)).\end{aligned} \quad (144)$$

These variables tend to be statistically well behaved, and are therefore appropriate for combination of results obtained from independent $B^\pm$ data samples.

The assumption of a model for the D decay leads to a non-negligible, and hard to quantify, source of uncertainty. To obviate this, it is possible to use instead a model-independent approach, in which the Dalitz plot (or, more generally, the phase space) is binned [302,314,315]. In this case, hadronic parameters describing the average strong phase difference in each bin between the interfering decay amplitudes enter the equations. These parameters can be determined from interference effects in decays of quantum-correlated $D\bar{D}$ pairs produced at the $\psi(3770)$ resonance. Measurements of such parameters have been made for several hadronic D decays by CLEO-c and BESIII.

When a multibody D decay is dominated by one CP state, additional sensitivity to γ is obtained from the relative widths of the $B^+ \to DK^+$ and $B^- \to DK^-$ decays. This can be taken into account in various ways. One possibility is to perform a GLW-like analysis, as mentioned above. An alternative approach proceeds by defining

$$\begin{aligned}z_\pm &= x_\pm + iy_\pm, \\ x_0 &= -\int \mathrm{Re}[f(s_1, s_2)f^*(s_2, s_1)]ds_1 ds_2,\end{aligned} \quad (145)$$

where s_1, s_2 are the coordinates of invariant mass squared that define the Dalitz plot and f is the complex amplitude for D decay as a function of the Dalitz plot coordinates.[23] The fitted parameters $(\rho^\pm, \theta^\pm)$ are then defined by

$$\rho^\pm e^{i\theta^\pm} = z_\pm - x_0. \quad (146)$$

Note that the yields of $B^\pm$ decays are proportional to $1 + (\rho^\pm)^2 - (x_0)^2$. This choice of variables has been used by *BABAR* in the analysis of $B^+ \to DK^+$ with $D \to \pi^+\pi^-\pi^0$ [317]; for this D decay, and with the assumed amplitude model, a value of $x_0 = 0.850$ is obtained.

The relations between the measured quantities and the underlying parameters are summarized in Table 25. It must be emphasized that the hadronic factors r_B and δ_B are different, in general, for each B decay mode.

[23]The x_0 parameter gives a model-dependent measure of the net CP content of the final state [313,316]. It is closely related to the c_i parameters of the model dependent Dalitz plot analysis [302,314,315], and the coherence factor of inclusive ADS-type analyses [311], integrated over the entire Dalitz plot.

TABLE 26. Common inputs used in calculating the averages.

$\tau(B^0)$	1.519 ± 0.004 ps
Δm_d	0.5065 ± 0.0019 ps^{-1}
$\Delta\Gamma_d/\Gamma_d$	0.001 ± 0.010
$\lvert A_\perp\rvert^2(J/\psi K^*)$	0.209 ± 0.006

C. Common inputs and uncertainty treatment

As described in Sec. III, where measurements combined in an average depend on external parameters, it can be important to rescale to the latest values of those parameters in order to obtain the most precise and accurate results. In practice, this is only necessary for modes with reasonably small statistical uncertainties, so that the systematic uncertainty associated with the knowledge of the external parameter is not negligible. Among the averages in this section, rescaling to common inputs is only done for $b \to c\bar{c}s$ transitions of B^0 mesons. Correlated sources of systematic uncertainty are also taken into account in these averages. For most other modes, the effects of common inputs and sources of systematic uncertainty are currently negligible, however similar considerations are applied when combining results to obtain constraints on $\alpha \equiv \phi_2$ and $\gamma \equiv \phi_3$ as discussed in Secs. VI L 1 and VI O 7, respectively.

The common inputs used for calculating the averages are listed in Table 26. The average values for the B^0 lifetime ($\tau(B^0)$), mixing parameter (Δm_d) and relative width difference ($\Delta\Gamma_d/\Gamma_d$) averages are discussed in Sec. V. The fraction of the perpendicularly polarized component ($|A_\perp|^2$) in $B \to J/\psi K^*(892)$ decays, which determines the CP composition in these decays, is averaged from results by *BABAR* [318], Belle [319], CDF [320], D0 [71] and LHCb [321] (see also Sec. VIII).

As explained in Sec. II, we do not apply a rescaling factor on the uncertainty of an average that has $\chi^2/\mathrm{dof} > 1$ (unlike the procedure currently used by the PDG [9]). We provide a confidence level of the fit so that one can know the consistency of the measurements included in the average, and attach comments in case some care needs to be taken in the interpretation. Note that, in general, results obtained from small data samples will exhibit some non-Gaussian behavior. We average measurements with asymmetric uncertainties using the PDG [9] prescription. In cases where several measurements are correlated (e.g., S_f and C_f in measurements of time-dependent CP violation in B decays to a particular CP eigenstate) we take these into account in the averaging procedure if the uncertainties are sufficiently Gaussian. For measurements where one uncertainty is given, it represents the total uncertainty, where statistical and systematic uncertainties have been added in quadrature. If two uncertainties are given, the first is statistical and the second systematic. If more than two uncertainties are given, the origin of the additional uncertainty will be explained in the text.

D. Time-dependent asymmetries in $b \to c\bar{c}s$ transitions

1. Time-dependent CP asymmetries in $b \to c\bar{c}s$ decays to CP eigenstates

In the Standard Model, the time-dependent parameters for B^0 decays governed by $b \to c\bar{c}s$ transitions are

TABLE 27. Results and averages for $S_{b\to c\bar{c}s}$ and $C_{b\to c\bar{c}s}$. The averages are given from a combination of the most precise results only, and also including less precise measurements.

Experiment		Sample size	$-\eta S_{b\to c\bar{c}s}$	$C_{b\to c\bar{c}s}$
		Most precise		
BABAR $b \to c\bar{c}s$	[324]	$N(B\bar{B}) = 465$M	$0.687 \pm 0.028 \pm 0.012$	$0.024 \pm 0.020 \pm 0.016$
Belle $b \to c\bar{c}s$	[325]	$N(B\bar{B}) = 772$M	$0.667 \pm 0.023 \pm 0.012$	$-0.006 \pm 0.016 \pm 0.012$
LHCb $J/\psi K^0_S$	[326,327]	$\int \mathcal{L}\,dt = 3$ fb^{-1}	0.75 ± 0.04	-0.014 ± 0.030
LHCb $\psi(2S)K^0_S$	[327]	$\int \mathcal{L}\,dt = 3$ fb^{-1}	$0.84 \pm 0.10 \pm 0.01$	$-0.05 \pm 0.10 \pm 0.01$
Average			0.698 ± 0.017	-0.005 ± 0.015
Confidence level			$0.09(1.7\sigma)$	$0.54(0.6\sigma)$
		Less precise		
BABAR $\chi_{c0}K^0_S$	[265]	$N(B\bar{B}) = 383$M	$0.69 \pm 0.52 \pm 0.04 \pm 0.07$	$-0.29^{+0.53}_{-0.44} \pm 0.03 \pm 0.05$
BABAR $J/\psi K^0_S$ [a]	[328]	$N(B\bar{B}) = 88$M	$1.56 \pm 0.42 \pm 0.21$	…
ALEPH	[329]	$N(Z \to \text{hadrons}) = 4$ M	$0.84^{+0.82}_{-1.04} \pm 0.16$	…
OPAL	[330]	$N(Z \to \text{hadrons}) = 4.4$M	$3.2^{+1.8}_{-2.0} \pm 0.5$	…
CDF	[331]	$\int \mathcal{L}\,dt = 110$ pb^{-1}	$0.79^{+0.41}_{-0.44}$	…
Belle $\Upsilon(5S)$	[332]	$\int \mathcal{L}\,dt = 121$ fb^{-1}	$0.57 \pm 0.58 \pm 0.06$	…
Average of all			0.699 ± 0.017	-0.005 ± 0.015

[a]This result uses "*hadronic and previously unused muonic decays of the* J/ψ". We neglect a small possible correlation of this result with the main *BABAR* result [324] that could be caused by reprocessing of the data.

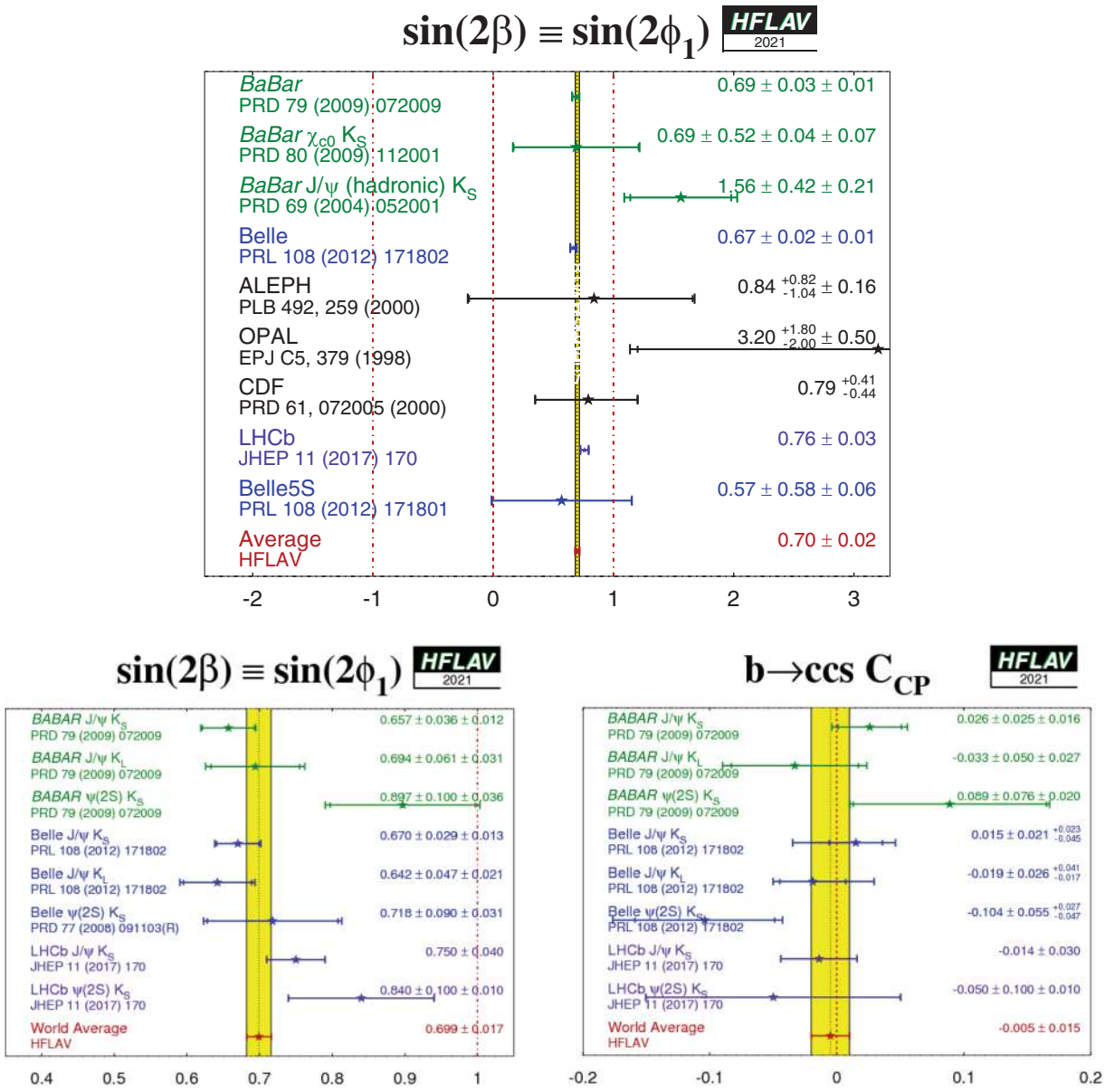

FIG. 10. Top: average of measurements of $S_{b\to c\bar{c}s}$, interpreted as $\sin(2\beta)$, with (bottom left) the same but excluding less precise measurements to allow inspection of the detail. Bottom right: more precise results and the world average for $C_{b\to c\bar{c}s}$.

predicted to be $S_{b\to c\bar{c}s} = -\eta \sin(2\beta)$ and $C_{b\to c\bar{c}s} = 0$ to very good accuracy. Deviations from this relation are currently limited to the level of $\lesssim 1°$ on 2β [230,322,323]. The averages for $-\eta S_{b\to c\bar{c}s}$ and $C_{b\to c\bar{c}s}$ are provided in Table 27 and shown in Fig. 10 In all such figures in this section, error bars cover 68% confidence regions, and the corresponding ranges accounting only for statistical uncertainties are also indicated (though sometimes not distinguishable from the total uncertainty).

Both *BABAR* and Belle have used the $\eta = -1$ modes $J/\psi K_S^0$, $\psi(2S)K_S^0$, $\chi_{c1}K_S^0$ and $\eta_c K_S^0$, as well as $J/\psi K_L^0$, which has $\eta = +1$ and $J/\psi K^{*0}(892)$, which is found to have η close to $+1$ based on the measurement of $|A_\perp|$ (see Sec. VI C). The most recent Belle result does not use $\eta_c K_S^0$ or $J/\psi K^{*0}(892)$ decays.[24] LHCb has used $J/\psi K_S^0$ (data with $J/\psi \to \mu^+\mu^-$ and e^+e^- are reported in different publications) and $\psi(2S)K_S^0$ decays. ALEPH, OPAL, and CDF have used only the $J/\psi K_S^0$ final state. *BABAR* has also determined the *CP* violation parameters of the $B^0 \to \chi_{c0}K_S^0$ decay from the time-dependent Dalitz-plot analysis of the $B^0 \to \pi^+\pi^- K_S^0$ mode (see Sec. VI G 2). In addition, Belle has performed a measurement with data accumulated at the $\Upsilon(5S)$ resonance, using the $J/\psi K_S^0$ final state—this

[24]Previous analyses from Belle did include these channels [79], but it is not possible to obtain separate results for those modes from the published information.

TABLE 28. Breakdown of results on $S_{b\to c\bar{c}s}$ and $C_{b\to c\bar{c}s}$.

Mode		Sample size	$-\eta S_{b\to c\bar{c}s}$	$C_{b\to c\bar{c}s}$
		BABAR		
$J/\psi K_S^0$	[324]	$N(B\bar{B}) = 465$M	$0.657 \pm 0.036 \pm 0.012$	$0.026 \pm 0.025 \pm 0.016$
$J/\psi K_L^0$	[324]	$N(B\bar{B}) = 465$M	$0.694 \pm 0.061 \pm 0.031$	$-0.033 \pm 0.050 \pm 0.027$
$\boldsymbol{J/\psi K^0}$	[324]	$N(B\bar{B}) = 465$M	$0.666 \pm 0.031 \pm 0.013$	$0.016 \pm 0.023 \pm 0.018$
$\psi(2S)K_S^0$	[324]	$N(B\bar{B}) = 465$ M	$0.897 \pm 0.100 \pm 0.036$	$0.089 \pm 0.076 \pm 0.020$
$\chi_{c1}K_S^0$	[324]	$N(B\bar{B}) = 465$M	$0.614 \pm 0.160 \pm 0.040$	$0.129 \pm 0.109 \pm 0.025$
$\eta_c K_S^0$	[324]	$N(B\bar{B}) = 465$M	$0.925 \pm 0.160 \pm 0.057$	$0.080 \pm 0.124 \pm 0.029$
$J/\psi K^{*0}(892)$	[324]	$N(B\bar{B}) = 465$M	$0.601 \pm 0.239 \pm 0.087$	$0.025 \pm 0.083 \pm 0.054$
All	[324]	$N(B\bar{B}) = 465$M	$0.687 \pm 0.028 \pm 0.012$	$0.024 \pm 0.020 \pm 0.016$
		Belle		
$J/\psi K_S^0$	[325]	$N(B\bar{B}) = 772$M	$0.670 \pm 0.029 \pm 0.013$	$0.015 \pm 0.021^{+0.023}_{-0.045}$
$J/\psi K_L^0$	[325]	$N(B\bar{B}) = 772$M	$0.642 \pm 0.047 \pm 0.021$	$-0.019 \pm 0.026^{+0.041}_{-0.017}$
$\psi(2S)K_S^0$	[325]	$N(B\bar{B}) = 772$M	$0.738 \pm 0.079 \pm 0.036$	$-0.104 \pm 0.055^{+0.027}_{-0.047}$
$\chi_{c1}K_S^0$	[325]	$N(B\bar{B}) = 772$M	$0.640 \pm 0.117 \pm 0.040$	$0.017 \pm 0.083^{+0.026}_{-0.046}$
All	[325]	$N(B\bar{B}) = 772$M	$0.667 \pm 0.023 \pm 0.012$	$-0.006 \pm 0.016 \pm 0.012$
		LHCb		
$J/\psi(\to \mu^+\mu^-)K_S^0$	[326]	$\int \mathcal{L}\,dt = 3$ fb^{-1}	$0.731 \pm 0.035 \pm 0.020$	$-0.038 \pm 0.032 \pm 0.005$
$J/\psi(\to e^+e^-)K_S^0$	[327]	$\int \mathcal{L}\,dt = 3$ fb^{-1}	$0.83 \pm 0.08 \pm 0.01$	$0.12 \pm 0.07 \pm 0.02$
$\psi(2S)K_S^0$	[327]	$\int \mathcal{L}\,dt = 3$ fb^{-1}	$0.84 \pm 0.10 \pm 0.01$	$-0.05 \pm 0.10 \pm 0.01$
		Averages		
$J/\psi K_S^0$ ([a])			0.695 ± 0.019	0.000 ± 0.020
$J/\psi K_L^0$			0.663 ± 0.041	-0.023 ± 0.030
$\psi(2S)K_S^0$			0.817 ± 0.056	-0.019 ± 0.048
$\chi_{c1}K_S^0$			0.632 ± 0.099	0.066 ± 0.074

[a]Belle II has presented a first result with $B^0 \to J/\psi K_S^0$, measuring $\sin(2\beta) = 0.55 \pm 0.21 \pm 0.04$, where the first uncertainty is statistical and the second is systematic [333]. We do not include this result in our averages as it is not planned to be published.

involves a different flavor tagging method compared to the measurements performed with data accumulated at the $\Upsilon(4S)$ resonance. A breakdown of results in each charmonium-kaon final state is given in Table 28.

While the uncertainty in the average for $-\eta S_{b\to c\bar{c}s}$ is limited by the statistical uncertainty, the precision for $C_{b\to c\bar{c}s}$ is close to being dominated by the systematic uncertainty, particularly for measurements from the e^+e^- B factory experiments. This occurs due to the possible effect of tag-side interference [283] on the $C_{b\to c\bar{c}s}$ measurement, an effect which is correlated between different $e^+e^- \to \Upsilon(4S) \to B\bar{B}$ experiments. Understanding of this effect may continue to improve in the future, allowing the uncertainty to reduce.

2. Constraints on $\beta \equiv \phi_1$

From the average for $-\eta S_{b\to c\bar{c}s}$ above, we obtain the following solutions for β (in $[0, \pi]$):

$$\beta = (22.2 \pm 0.7)^\circ \quad \text{or} \quad \beta = (67.8 \pm 0.7)^\circ. \qquad (147)$$

This result gives a precise constraint on the $(\bar{\rho}, \bar{\eta})$ plane, as shown in Fig. 11. The measurement is in remarkable

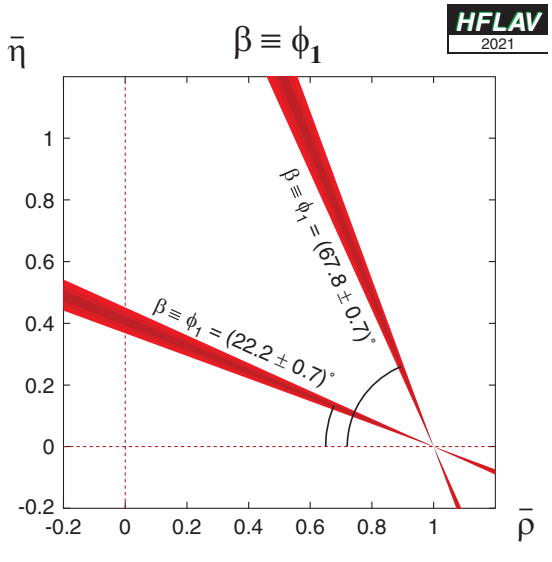

FIG. 11. Constraints on the $(\bar{\rho}, \bar{\eta})$ plane, obtained from the average of $-\eta S_{b\to c\bar{c}s}$ and Eq. (147). Note that the solution with the smaller (larger) value of β has $\cos(2\beta) > 0$ (<0).

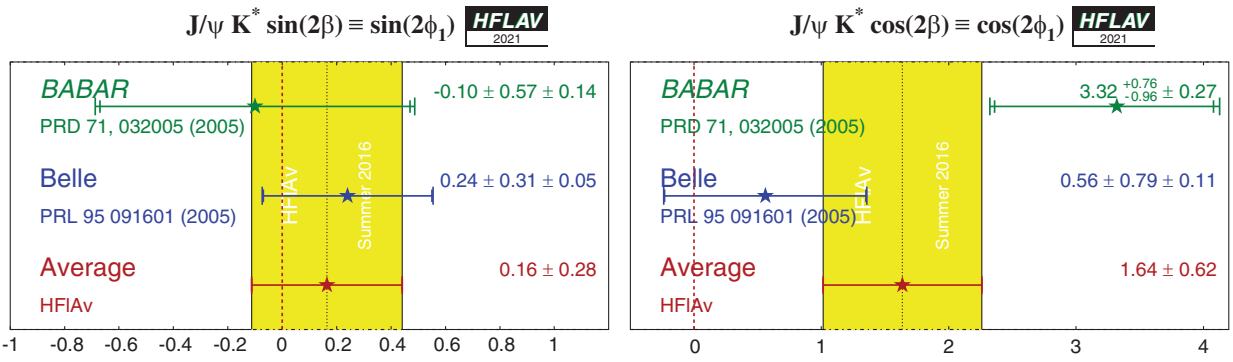

FIG. 12. Averages of (left) $\sin(2\beta) \equiv \sin(2\phi_1)$ and (right) $\cos(2\beta) \equiv \cos(2\phi_1)$ from time-dependent analyses of $B^0 \to J/\psi K^{*0}$ decays.

agreement with other constraints from CP-conserving quantities, and with CP violation in the kaon system, in the form of the parameter ϵ_K. Such comparisons have been performed by various phenomenological groups, such as CKMfitter [242] and UTFit [334] (see also Refs. [335,336]).

3. Time-dependent transversity analysis of $B^0 \to J/\psi K^{*0}$ decays

B meson decays to the vector-vector final state $J/\psi K^{*0}$ are also mediated by the $b \to c\bar{c}s$ transition. When a final state that is not flavor-specific ($K^{*0} \to K^0_S\pi^0$) is used, a time-dependent transversity analysis can be performed, yielding sensitivity to both $\sin(2\beta)$ and $\cos(2\beta)$ [337]. Such analyses have been performed by both B factory experiments. In principle, the strong phases between the transversity amplitudes are not uniquely determined by such an analysis, leading to a discrete ambiguity in the sign of $\cos(2\beta)$. The *BABAR* collaboration resolves this ambiguity using the known variation [338] of the P-wave phase (fast) relative to that of the S-wave phase (slow) with the invariant mass of the $K\pi$ system in the vicinity of the $K^*(892)$ resonance. The result is in agreement with the prediction from s-quark helicity conservation, and corresponds to Solution II defined by Suzuki [339]. We include only the solutions consistent with this phase variation in Table 29 and Fig. 12.

At present, the results are dominated by large and non-Gaussian statistical uncertainties, and exhibit significant correlations. We perform uncorrelated averages, which necessitates care in the interpretation of these averages. Nonetheless, it is clear that $\cos(2\beta) > 0$ is preferred by the experimental data in $J/\psi K^{*0}$ (for example, *BABAR* [340] finds a confidence level for $\cos(2\beta) > 0$ of 89%).

4. Time-dependent CP asymmetries in $B^0 \to D^{*+}D^{*-}K^0_S$ decays

Both *BABAR* [256] and Belle [257] have performed time-dependent analyses of the $B^0 \to D^{*+}D^{*-}K^0_S$ decay, to obtain information on the sign of $\cos(2\beta)$. More information can be found in Sec. VI. B. 5. The results are given in Table 30, and shown in Fig. 13. From their result and the

TABLE 29. Averages from $B^0 \to J/\psi K^{*0}$ transversity analyses.

Experiment		$N(B\bar{B})$	$\sin 2\beta$	$\cos 2\beta$	Correlation
BABAR	[340]	88M	$-0.10 \pm 0.57 \pm 0.14$	$3.32^{+0.76}_{-0.96} \pm 0.27$	-0.37
Belle	[319]	275M	$0.24 \pm 0.31 \pm 0.05$	$0.56 \pm 0.79 \pm 0.11$	0.22
Average			0.16 ± 0.28	1.64 ± 0.62	Uncorrelated averages
Confidence level			$0.61(0.5\sigma)$	$0.03(2.2\sigma)$	

TABLE 30. Results from time-dependent analysis of $B^0 \to D^{*+}D^{*-}K^0_S$.

Experiment		$N(B\bar{B})$	$\frac{J_c}{J_0}$	$\frac{2J_{s1}}{J_0}\sin(2\beta)$	$\frac{2J_{s2}}{J_0}\cos(2\beta)$
BABAR	[256]	230M	$0.76 \pm 0.18 \pm 0.07$	$0.10 \pm 0.24 \pm 0.06$	$0.38 \pm 0.24 \pm 0.05$
Belle	[257]	449M	$0.60^{+0.25}_{-0.28} \pm 0.08$	$-0.17 \pm 0.42 \pm 0.09$	$-0.23^{+0.43}_{-0.41} \pm 0.13$
Average			0.71 ± 0.16	0.03 ± 0.21	0.24 ± 0.22
Confidence level			$0.63(0.5\sigma)$	$0.59(0.5\sigma)$	$0.23(1.2\sigma)$

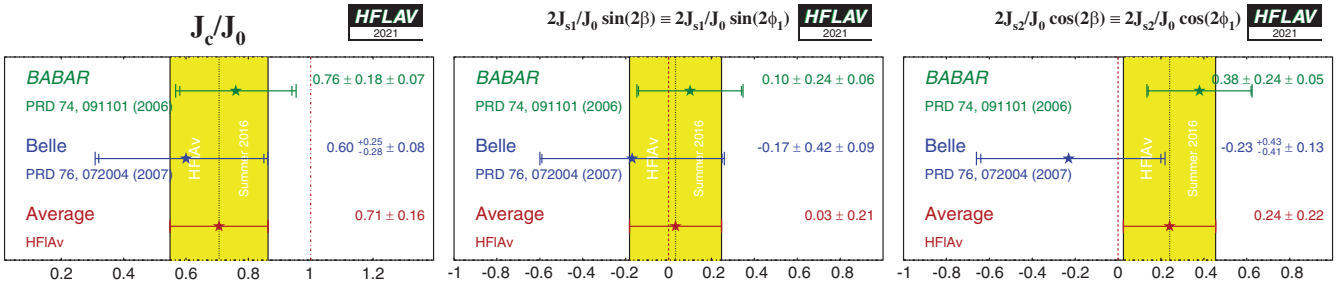

FIG. 13. Averages of (left) (J_c/J_0), (middle) $(2J_{s1}/J_0)\sin(2\beta)$ and (right) $(2J_{s2}/J_0)\cos(2\beta)$ from time-dependent analyses of $B^0 \to D^{*+}D^{*-}K^0_S$ decays.

assumption that $J_{s2} > 0$, *BABAR* infers that $\cos(2\beta) > 0$ at the 94% confidence level [256].

5. Time-dependent analysis of B^0_s decays through the $b \to c\bar{c}s$ transition

As described in Sec. VI B 3, time-dependent analysis of decays such as $B^0_s \to J/\psi\phi$ probes the CP violating phase of B^0_s–$\bar{B}^0_s$ oscillations, ϕ_s.[25] The combination of results on $B^0_s \to J/\psi\phi$ decays, including also results from channels such a $B^0_s \to J/\psi\pi^+\pi^-$ and $B^0_s \to D^+_s D^-_s$ decays, is discussed in Sec. V.

E. Time-dependent CP asymmetries in color-suppressed $b \to c\bar{u}d$ transitions

1. Time-dependent CP asymmetries: $b \to c\bar{u}d$ decays to CP eigenstates

Decays of B mesons to final states such as $D\pi^0$ are governed by $b \to c\bar{u}d$ transitions. If the final state is a CP eigenstate, e.g. $D_{CP}\pi^0$, the usual time-dependent formulas are recovered, with the sine coefficient sensitive to $\sin(2\beta)$. Since there is no penguin contribution to these decays, there is even less associated theoretical uncertainty than for $b \to c\bar{c}s$ decays such as $B \to J/\psi K^0_S$. Such measurements therefore allow to test the Standard Model prediction that the CP violation parameters in $b \to c\bar{u}d$ transitions are the same as those in $b \to c\bar{c}s$ [341]. Although there is an additional contribution from CKM suppressed $b \to u\bar{c}d$ amplitudes, which have a different weak phase compared to the leading $b \to c\bar{u}d$ transition, the effect is small and can be taken into account in the analysis [342,343].

Results are available from a joint analysis of *BABAR* and Belle data [344]. The following CP-even final states are included: $D\pi^0$ and $D\eta$ with $D \to K^0_S\pi^0$ and $D \to K^0_S\omega$; $D\omega$ with $D \to K^0_S\pi^0$; $D^*\pi^0$ and $D^*\eta$ with $D^* \to D\pi^0$ and $D \to K^+K^-$. The following CP-odd final states are included: $D\pi^0$, $D\eta$ and $D\omega$ with $D \to K^+K^-$, $D^*\pi^0$ and $D^*\eta$ with $D^* \to D\pi^0$ and $D \to K^0_S\pi^0$. All $B^0 \to D^{(*)}h^0$ decays are analyzed together, taking into account the different CP factors (denoted $D^{(*)}_{CP}h^0$). The results are summarized in Table 31.

2. Time-dependent Dalitz-plot analyses of $b \to c\bar{u}d$ decays

When multibody D decays, such as $D \to K^0_S\pi^+\pi^-$ are used, a time-dependent analysis of the Dalitz plot of the neutral D decay allows for a direct determination of the weak phase 2β or, equivalently, of both $\sin(2\beta)$ and $\cos(2\beta)$. This information can be used to resolve the ambiguity in the measurement of 2β from $\sin(2\beta)$ [345].

Results are available from a joint analysis of *BABAR* and Belle data [251,252]. The decays $B \to D\pi^0$, $B \to D\eta$, $B \to D\omega$, $B \to D^*\pi^0$ and $B \to D^*\eta$ are used. (This collection of states is denoted by $D^{(*)}h^0$.) The daughter decays are $D^* \to D\pi^0$ and $D \to K^0_S\pi^+\pi^-$. These results supersede those from previous analyses done separately by Belle [249] and *BABAR* [250] and are given in Table 32. Treating β as a free parameter in the fit, the result $\beta = (22.5 \pm 4.4 \pm 1.2 \pm 0.6)°$ is obtained. This corresponds to an observation of CP violation ($\beta \neq 0$) at 5.1σ significance, and evidence for $\cos(2\beta) > 0$ at 3.7σ. The solution with $\cos(2\beta) < 0$, corresponding to the ambiguous solution for $\sin(2\beta)$ from $b \to c\bar{c}s$ transitions, is ruled out at 7.3σ.

A model-independent time-dependent analysis of $B^0 \to D^{(*)}h^0$ decays, with $D \to K^0_S\pi^+\pi^-$, has been performed by Belle [253]. The decays $B^0 \to D\pi^0$, $B^0 \to D\eta$, $B^0 \to D\eta'$, $B^0 \to D\omega$, $B^0 \to D^*\pi^0$ and $B^0 \to D^*\eta$ are used. The results are also included in Table 32. From these results, Belle disfavors the $\cos(2\phi_1) < 0$ solution that corresponds to the $\sin(2\phi_1)$ results from $b \to c\bar{c}s$ transitions at 5.1σ significance. The solution with $\cos(2\phi_1) > 0$ is consistent with the data at the level of 1.3σ. Note that due to the strong statistical and systematic correlations, model-dependent results and model-independent results from the same experiment cannot be combined.

[25] We use ϕ_s here to denote the same quantity labeled $\phi_s^{c\bar{c}s}$ in Sec. V. It should not be confused with the parameter $\phi_{12} \equiv \arg[-M_{12}/\Gamma_{12}]$, which historically was also often referred to as ϕ_s.

TABLE 31. Results from analyses of $B^0 \to D^{(*)}h^0$, $D \to CP$ eigenstates decays.

Experiment	$N(B\bar{B})$	S_{CP}	C_{CP}	Correlation
BABAR and Belle [344]	1243M	$0.66 \pm 0.10 \pm 0.06$	$-0.02 \pm 0.07 \pm 0.03$	-0.05

TABLE 32. Averages from $B^0 \to D^{(*)}h^0$, $D \to K^0_S\pi^+\pi^-$ analyses.

Experiment		$N(B\bar{B})$	$\sin 2\beta$	$\cos 2\beta$
		Model-dependent		
BABAR and Belle	[251,252]	1240M	$0.80 \pm 0.14 \pm 0.06 \pm 0.03$	$0.91 \pm 0.22 \pm 0.09 \pm 0.07$
		Model-independent		
Belle	[253]	772M	$0.43 \pm 0.27 \pm 0.08$	$1.06 \pm 0.33^{+0.21}_{-0.15}$

3. *Combined results from time-dependent analyses of $b \to c\bar{u}d$ decays*

A comparison of the results for $\sin(2\beta)$ from $B^0 \to D^{(*)}h^0$ decays, with D decays to CP eigenstates or to $D \to K^0_S\pi^+\pi^-$, is shown in Fig. 14. Averaging these results gives $\sin(2\beta) = 0.71 \pm 0.09$, which is consistent with, but not as precise as, the value from $b \to c\bar{c}s$ transitions.

F. Time-dependent *CP* asymmetries in $b \to c\bar{c}d$ transitions

The transition $b \to c\bar{c}d$ can occur via either a $b \to c$ tree or a $b \to d$ penguin amplitude. The flavor changing neutral current $b \to d$ penguin can be mediated by any up-type quark in the loop, and hence the amplitude can be written as

$$\begin{aligned} A_{b\to d} &= F_u V_{ub}V^*_{ud} + F_c V_{cb}V^*_{cd} + F_t V_{tb}V^*_{td} \\ &= (F_u - F_c)V_{ub}V^*_{ud} + (F_t - F_c)V_{tb}V^*_{td}, \end{aligned} \quad (148)$$

where $F_{u,c,t}$ describe all factors, except CKM suppression, in each quark loop diagram. In the last line, both terms are $\mathcal{O}(\lambda^3)$, exposing that the $b \to d$ penguin amplitude contains terms with different weak phases at the same order of CKM suppression.

In Eq. (148), we have chosen to eliminate the F_c term using unitarity. However, we could equally well write

$$\begin{aligned} A_{b\to d} &= (F_u - F_t)V_{ub}V^*_{ud} + (F_c - F_t)V_{cb}V^*_{cd} \\ &= (F_c - F_u)V_{cb}V^*_{cd} + (F_t - F_u)V_{tb}V^*_{td}. \end{aligned} \quad (149)$$

Since the $b \to c\bar{c}d$ tree amplitude has the weak phase of $V_{cb}V^*_{cd}$, either of the above expressions allows the penguin amplitude to be decomposed into a part with the same weak phase as the tree amplitude and a part with another weak phase, which can be chosen to be either β or γ. The choice of parametrization cannot, of course, affect the physics [346]. In any case, if the tree amplitude dominates, there is little sensitivity to any phase other than that from B^0–$\bar{B}^0$ mixing.

The $b \to c\bar{c}d$ transitions can be investigated with studies of various final states. Results are available from both *BABAR* and Belle using the final states $J/\psi\pi^0$, D^+D^-, $D^{*+}D^{*-}$ and $D^{*\pm}D^{\mp}$, and from LHCb using the final states $J/\psi\rho^0$, D^+D^- and $D^{*\pm}D^{\mp}$; the averages of these results are given in Tables 33 and 34. The results using the CP-even modes $J/\psi\pi^0$ and D^+D^- are shown in Fig. 15 and Fig. 16 respectively, with two-dimensional constraints shown in Fig. 17. In all figures showing two-dimensional constraints in this section, the contours contain 39.3% confidence regions, corresponding to a $\Delta\chi^2$ or change in twice the

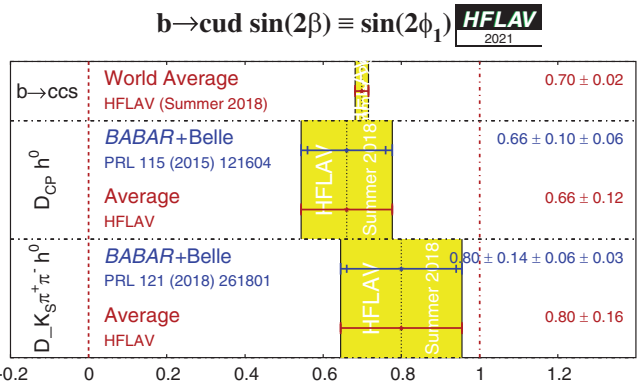

FIG. 14. Averages of $\sin(2\beta)$ measured in color-suppressed $b \to c\bar{u}d$ transitions.

TABLE 33. Averages for the $b \to c\bar{c}d$ modes, $B^0 \to J/\psi\pi^0$ and D^+D^-.

Experiment		Sample size	S_{CP}	C_{CP}	Correlation
			$J/\psi\pi^0$		
BABAR	[347]	$N(B\bar{B}) = 466$M	$-1.23 \pm 0.21 \pm 0.04$	$-0.20 \pm 0.19 \pm 0.03$	0.20
Belle	[348]	$N(B\bar{B}) = 772$M	$-0.59 \pm 0.19 \pm 0.03$	$0.15 \pm 0.14^{+0.03}_{-0.04}$	0.01
Average			-0.86 ± 0.14	0.04 ± 0.12	0.08
Confidence level			$0.04(2.0\sigma)$		
			D^+D^-		
BABAR	[248]	$N(B\bar{B}) = 467$M	$-0.65 \pm 0.36 \pm 0.05$	$-0.07 \pm 0.23 \pm 0.03$	-0.01
Belle	[278]	$N(B\bar{B}) = 772$M	$-1.06^{+0.21}_{-0.14} \pm 0.08$	$-0.43 \pm 0.16 \pm 0.05$	-0.12
LHCb	[349]	$\int \mathcal{L}\, dt = 3$ fb^{-1}	$-0.54^{+0.17}_{-0.16} \pm 0.05$	$0.26^{+0.18}_{-0.17} \pm 0.02$	0.48
Average			-0.84 ± 0.12	-0.13 ± 0.10	0.18
Confidence level			$0.027(2.2\sigma)$		

negative log-likelihood of one unit. The corresponding regions accounting only for statistical uncertainties are also indicated (though sometimes not distinguishable from the total uncertainty).

Results for the vector-vector mode $J/\psi\rho^0$ are obtained from a full time-dependent amplitude analysis of $B^0 \to J/\psi\pi^+\pi^-$ decays. LHCb [231] finds a $J/\psi\rho^0$ fit fraction of $65.6 \pm 1.9\%$ and a longitudinal polarization fraction of $56.7 \pm 1.8\%$ (uncertainties are statistical only; both results are consistent with those from a time-integrated amplitude analysis [258] where systematic uncertainties were also evaluated). Fits are performed to obtain $2\beta^{\text{eff}}$ in the cases that all transversity amplitudes are assumed to have the same CP violation parameter. A separate fit is performed allowing different parameters. The results in the former case are presented in terms of S_{CP} and C_{CP} in Table 34.

The vector-vector mode $D^{*+}D^{*-}$ is found to be dominated by the CP-even, longitudinally polarized component. *BABAR* measures a CP-odd fraction of $0.158 \pm 0.028 \pm 0.006$ [248], and Belle measures $0.138 \pm 0.024 \pm 0.006$ [351]. These values are listed as $R_\perp$ in Table 34, and are included in the averages so that correlations are taken into account.[26] *BABAR* has also performed an additional fit in which the CP-even and CP-odd components have independent pairs of CP violation parameters S and C. These results are included in Table 34. Results using $D^{*+}D^{*-}$ are shown in Fig. 18.

As discussed in Sec. VI B 6, the most recent papers on the non-CP eigenstate mode $D^{*\pm}D^{\mp}$ use the (A, S, ΔS, C, ΔC) set of parameters. Therefore, we perform the averages with this choice, with results presented in Table 34.

[26]Note that the *BABAR* value given in Table 34 differs from the value quoted here, since that in the table is not corrected for efficiency.

In the absence of the penguin contribution (so-called tree dominance), the time-dependent parameters are given by $S_{b\to c\bar{c}d} = -\eta \sin(2\beta)$, $C_{b\to c\bar{c}d} = 0$, $S_{+-} = \sin(2\beta + \delta)$, $S_{-+} = \sin(2\beta - \delta)$, $C_{+-} = -C_{-+}$ and $\mathcal{A} = 0$, where δ is the strong phase difference between the $D^{*+}D^-$ and $D^{*-}D^+$ decay amplitudes. In the presence of the penguin contribution, there is no straightforward interpretation in terms of CKM parameters; however, CP violation in decay may be observed through any of $C_{b\to c\bar{c}d} \neq 0$, $C_{+-} \neq -C_{-+}$ or $A_{+-} \neq 0$.

The averages for the $b \to c\bar{c}d$ modes are shown in Figs. 19 and 20. Results are consistent with tree dominance and with the Standard Model, although the Belle results in $B^0 \to D^+D^-$ [353] show an indication of CP violation in decay, and hence a nonzero penguin contribution. The average of $S_{b\to c\bar{c}d}$ in each of the $J/\psi\pi^0$, D^+D^- and $D^{*+}D^{*-}$ final states is more than 5σ away from zero, corresponding to observations of CP violation in these decay channels. Possible non-Gaussian effects due to some of the input measurements being outside the physical region ($S_{CP}^2 + C_{CP}^2 \leq 1$) should, however, be borne in mind.

1. Time-dependent CP asymmetries in B_s^0 decays mediated by $b \to c\bar{c}d$ transitions

Time-dependent CP asymmetries in B_s^0 decays mediated by $b \to c\bar{c}d$ transitions provide a determination of $2\beta_s^{\text{eff}}$, where possible effects from penguin amplitudes may cause a shift from the value of $2\beta_s$ seen in $b \to c\bar{c}s$ transitions. Results in the $b \to c\bar{c}d$ case, with larger penguin effects, can be used together with flavor symmetries to derive limits on the possible size of penguin effects in the $b \to c\bar{c}s$ transitions [354,355].

The parameters have been measured in $B_s^0 \to J/\psi K_S^0$ decays by LHCb, as summarized in Table 35. The results supersede an earlier measurement of the effective lifetime, which is directly related to $A^{\Delta\Gamma}$, in the same mode [112].

TABLE 34. Averages for the $b \to c\bar{c}d$ modes, $J/\psi\rho^0$, $D^{*+}D^{*-}$ and $D^{*\pm}D^{\mp}$.

Experiment		$N(B\bar{B})$	S_{CP}	C_{CP}	$R_\perp$
			$J/\psi\rho^0$		
LHCb	[231]	3 fb^{-1}	$-0.66^{+0.13\,+0.09}_{-0.12\,-0.03}$	$-0.06 \pm 0.06^{+0.02}_{-0.01}$	0.198 ± 0.017
			$D^{*+}D^{*-}$		
BABAR	[248]	467M	$-0.70 \pm 0.16 \pm 0.03$	$0.05 \pm 0.09 \pm 0.02$	0.17 ± 0.03
BABAR part. rec.	[350]	471M	$-0.49 \pm 0.18 \pm 0.07 \pm 0.04$	$0.15 \pm 0.09 \pm 0.04$	...
Belle	[351]	772M	$-0.79 \pm 0.13 \pm 0.03$	$-0.15 \pm 0.08 \pm 0.02$	$0.14 \pm 0.02 \pm 0.01$
Average			-0.71 ± 0.09	-0.01 ± 0.05	0.15 ± 0.02
Confidence level				$0.72(0.4\sigma)$	

Experiment		$N(B\bar{B})$	S_{CP+}	C_{CP+}	S_{CP-}	C_{CP-}	$R_\perp$
				$D^{*+}D^{*-}$			
BABAR	[248]	467M	$-0.76 \pm 0.16 \pm 0.04$	$0.02 \pm 0.12 \pm 0.02$	$-1.81 \pm 0.71 \pm 0.16$	$0.41 \pm 0.50 \pm 0.08$	0.15 ± 0.03

Experiment		$N(B\bar{B})$	S	C	ΔS	ΔC	$\mathcal{A}$
				$D^{*\pm}D^{\mp}$			
BABAR	[248]	467M	$-0.68 \pm 0.15 \pm 0.04$	$0.04 \pm 0.12 \pm 0.03$	$0.05 \pm 0.15 \pm 0.02$	$0.04 \pm 0.12 \pm 0.03$	$0.01 \pm 0.05 \pm 0.01$
Belle	[278]	772M	$-0.78 \pm 0.15 \pm 0.05$	$-0.01 \pm 0.11 \pm 0.04$	$-0.13 \pm 0.15 \pm 0.04$	$0.12 \pm 0.11 \pm 0.03$	$0.06 \pm 0.05 \pm 0.02$
LHCb	[352]	$\int \mathcal{L}dt = 9$ fb^{-1}	$-0.86 \pm 0.08 \pm 0.02$	$-0.06 \pm 0.09 \pm 0.02$	$0.02 \pm 0.07 \pm 0.01$	$-0.03 \pm 0.09 \pm 0.02$	$0.01 \pm 0.01 \pm 0.01$
Average			-0.81 ± 0.06	-0.01 ± 0.06	0.02 ± 0.06	0.03 ± 0.06	0.01 ± 0.01
Confidence level					$0.93(0.1\sigma)$		

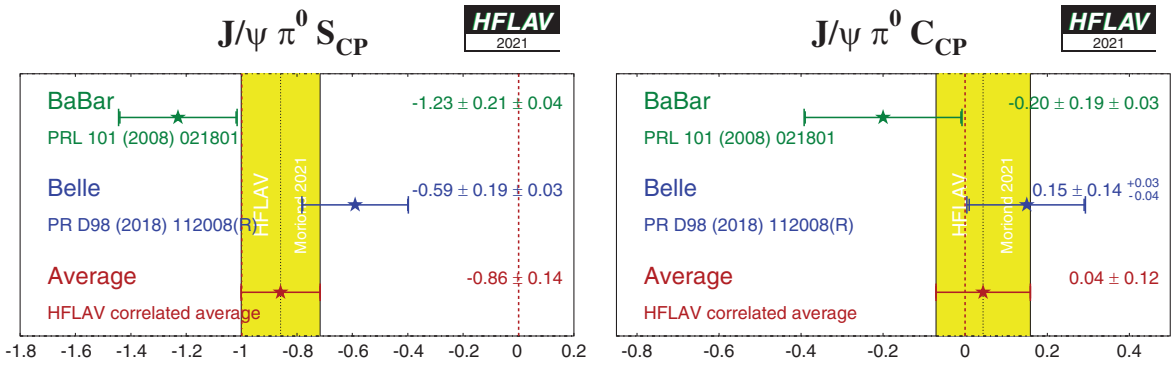

FIG. 15. Averages of (left) $S_{b\to c\bar{c}d}$ and (right) $C_{b\to c\bar{c}d}$ for the mode $B^0 \to J/\psi\pi^0$.

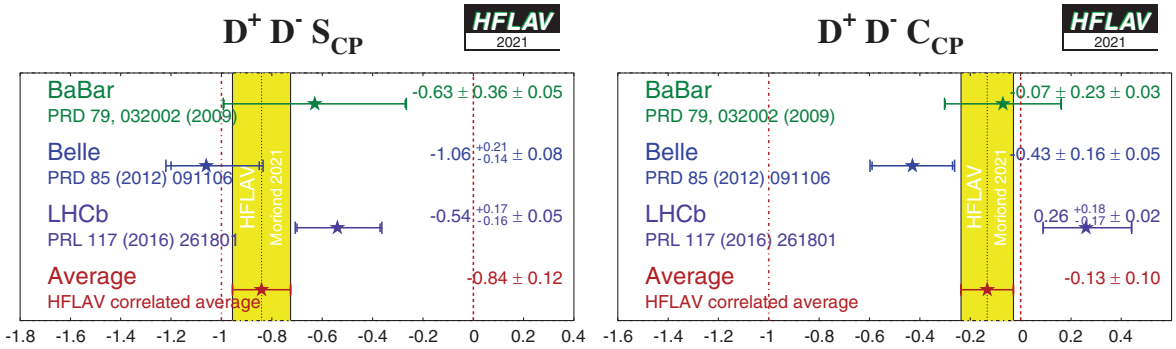

FIG. 16. Averages of (left) $S_{b\to c\bar{c}d}$ and (right) $C_{b\to c\bar{c}d}$ for the mode $B^0 \to D^+D^-$.

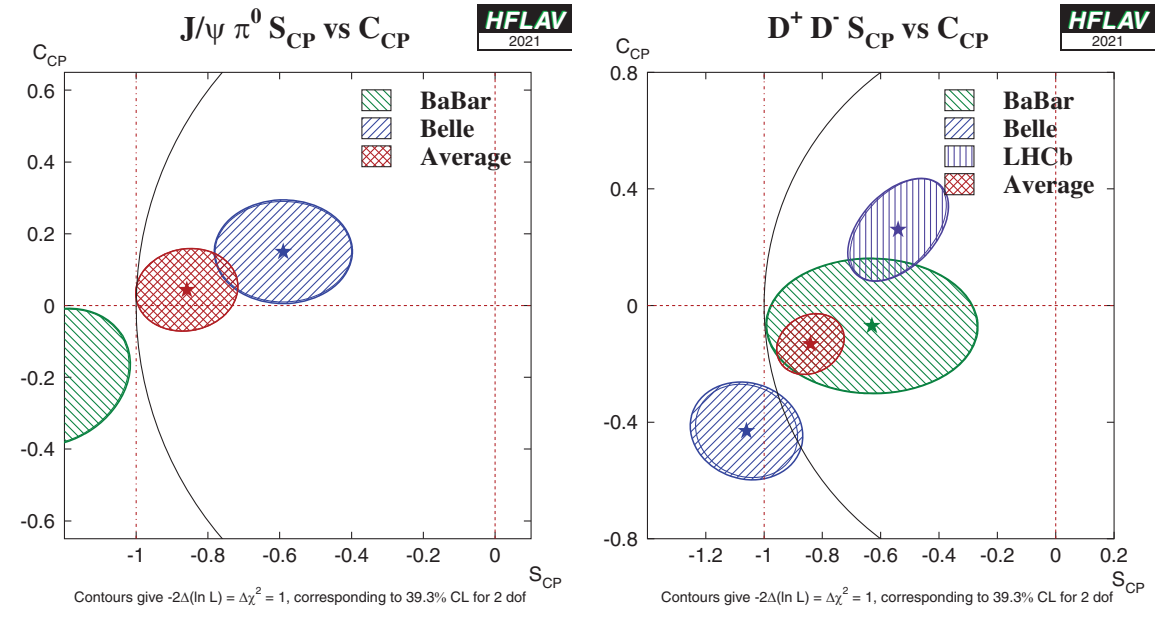

FIG. 17. Averages of two $b \to c\bar{c}d$ dominated channels, for which correlated averages are performed, in the S_{CP} vs. C_{CP} plane. Contours at $S_{CP}^2 + C_{CP}^2 = 1$ represent the physical boundary for the parameters. (Left) $B^0 \to J/\psi\pi^0$ and (right) $B^0 \to D^+D^-$.

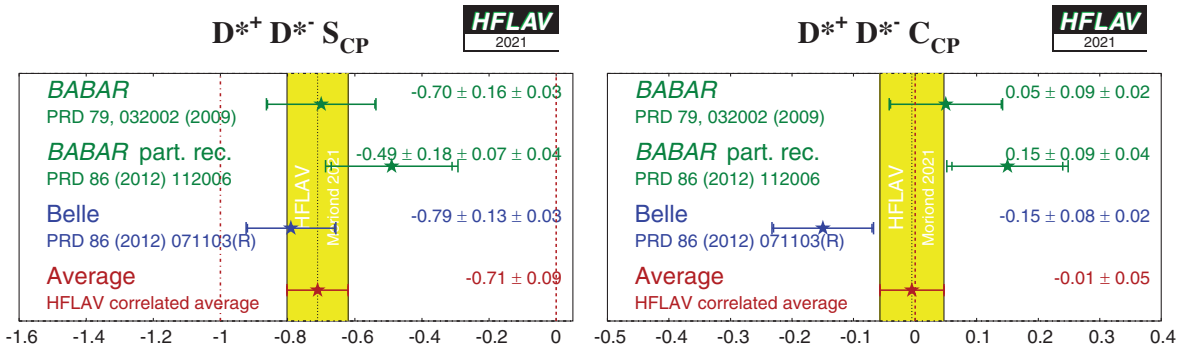

FIG. 18. Averages of (left) $S_{b\to c\bar{c}d}$ and (right) $C_{b\to c\bar{c}d}$ for the mode $B^0 \to D^{*+}D^{*-}$.

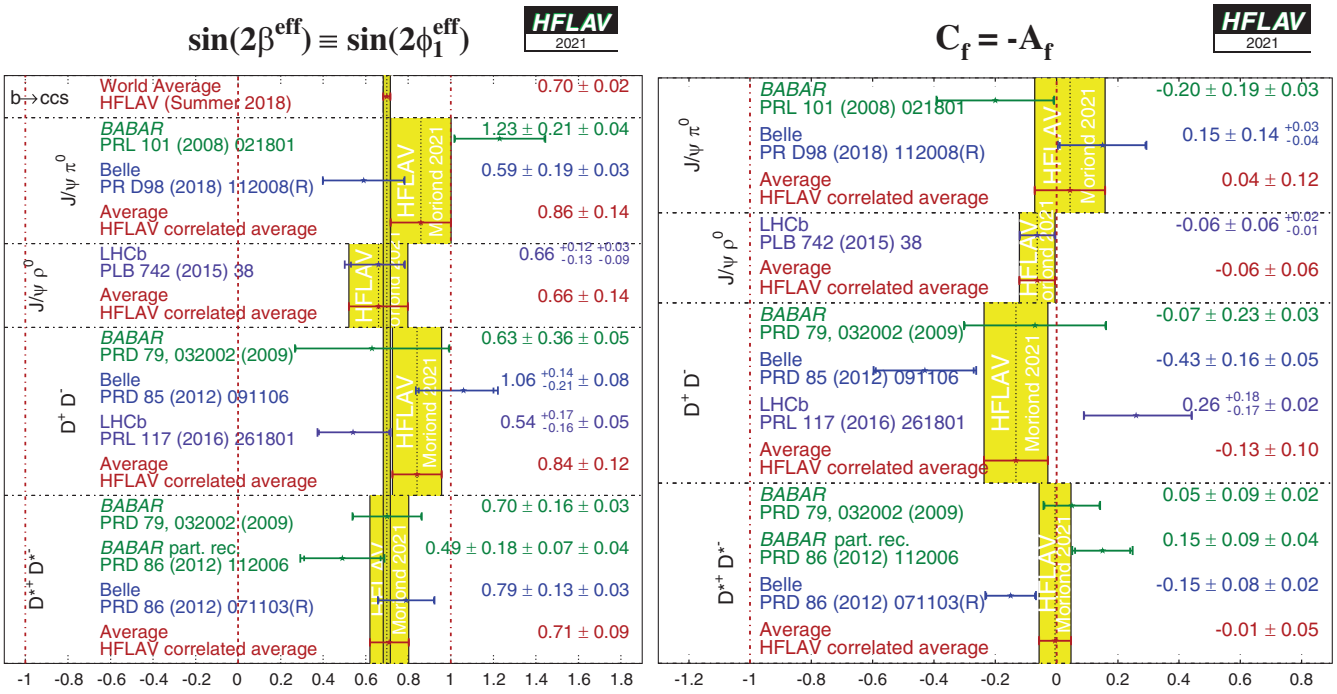

FIG. 19. Averages of (left) $-\eta S_{b\to c\bar{c}d}$ interpreted as $\sin(2\beta^{\rm eff})$ and (right) $C_{b\to c\bar{c}d}$. The $-\eta S_{b\to c\bar{c}d}$ figure compares the results to the world average for $-\eta S_{b\to c\bar{c}s}$ (see Sec. VI D 1).

G. Time-dependent *CP* asymmetries in charmless $b \to q\bar{q}s$ transitions

Similarly to Eq. (148), the $b \to s$ penguin amplitude can be written as

$$A_{b\to s} = F_u V_{ub} V_{us}^* + F_c V_{cb} V_{cs}^* + F_t V_{tb} V_{ts}^* = (F_u - F_c) V_{ub} V_{us}^* + (F_t - F_c) V_{tb} V_{ts}^*, \quad (150)$$

using the unitarity of the CKM matrix to eliminate the F_c term. In this case, the first term in the last line is $\mathcal{O}(\lambda^4)$ while the second is $\mathcal{O}(\lambda^2)$. Therefore, in the Standard Model, this amplitude is dominated by $V_{tb}V_{ts}^*$, and to within a few degrees ($|\delta\beta^{\rm eff}| \equiv |\beta^{\rm eff} - \beta| \lesssim 2°$ for $\beta \approx 20°$) the time-dependent parameters can be written as[27] $S_{b\to q\bar{q}s} \approx -\eta \sin(2\beta)$, $C_{b\to q\bar{q}s} \approx 0$, assuming $b \to s$ penguin contributions only ($q = u, d, s$).

Due to the suppression of the Standard Model amplitude, contributions of additional diagrams from physics beyond the Standard Model, with heavy virtual particles in the penguin loops, may have observable effects. In general, these contributions will affect the values of $S_{b\to q\bar{q}s}$ and

[27]The presence of a small ($\mathcal{O}(\lambda^2)$) weak phase in the dominant amplitude of the s penguin decays introduces a phase shift given by $S_{b\to q\bar{q}s} = -\eta \sin(2\beta)(1 + \Delta)$. Using the CKMfitter results for the Wolfenstein parameters [242], one finds $\Delta \simeq 0.033$, which corresponds to a shift of 2β of $+2.1°$. Nonperturbative contributions can alter this result.

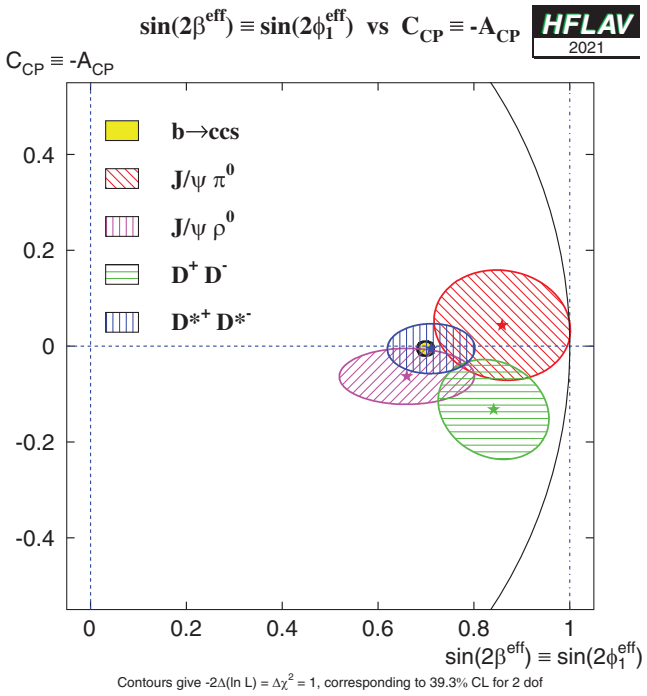

FIG. 20. Compilation of constraints in the $-\eta S_{b\to c\bar{c}d}$, interpreted as $\sin(2\beta^{\rm eff})$, vs $C_{b\to c\bar{c}d}$ plane. The contours at $\sin(2\beta^{\rm eff})^2 + C^2_{b\to c\bar{c}d} = 1$ represents the physical boundary for the parameters.

$C_{b\to q\bar{q}s}$. A discrepancy between the values of $S_{b\to c\bar{c}s}$ and $S_{b\to q\bar{q}s}$ can therefore provide a solid indication of non-Standard Model physics [341,357–359].

However, there is an additional consideration to take into account. The above argument assumes that only the $b\to s$ penguin contributes to the $b\to q\bar{q}s$ transition. For $q=s$ this is a good assumption, which neglects only rescattering effects. However, for $q=u$ there is a color-suppressed $b\to u$ tree diagram (of order $\mathcal{O}(\lambda^4)$), which has a different weak (and possibly strong) phase. In the case $q=d$, any light neutral meson that is formed from $d\bar{d}$ also has a $u\bar{u}$ component, and so again there is "tree pollution." The B^0 decays to $\pi^0K^0_S$, $\rho^0K^0_S$ and ωK^0_S belong to this category. The mesons ϕ, f_0 and η' are expected to have predominant $s\bar{s}$ composition, which reduces the relative size of the possible tree pollution. If the inclusive decay $B^0\to K^+K^-K^0$ (excluding ϕK^0) is dominated by a nonresonant three-body transition, an Okubo-Zweig-Iizuka-suppressed [360–362] tree-level diagram can occur through insertion of an $s\bar{s}$ pair. The corresponding penguin-type transition proceeds via insertion of a $u\bar{u}$ pair, which is expected to be favored over the $s\bar{s}$ insertion by fragmentation models. Neglecting rescattering, the final state $K^0\bar{K}^0K^0$ (reconstructed as $K^0_SK^0_SK^0_S$) has no tree pollution [363]. Various estimates, using different theoretical approaches, of the values of $\Delta S = S_{b\to q\bar{q}s} - S_{b\to c\bar{c}s}$ exist in the literature [364–377]. In general, there is agreement that the modes ϕK^0, $\eta' K^0$ and $K^0\bar{K}^0K^0$ are the cleanest, with values of $|\Delta S|$ at or below the few percent level, with ΔS usually predicted to be positive. Nonetheless, the uncertainty is sufficient that interpretation is given here in terms of $\sin(2\beta^{\rm eff})$.

1. Time-dependent CP asymmetries: $b\to q\bar{q}s$ decays to CP eigenstates

The averages for $-\eta S_{b\to q\bar{q}s}$ and $C_{b\to q\bar{q}s}$ can be found in Tables 36 and 37, and are shown in Figs. 21, 22 and 23. Results from both *BABAR* and Belle are averaged for the modes $\eta' K^0$ (K^0 indicates that both K^0_S and K^0_L are used) $K^0_SK^0_SK^0_S$, $\pi^0K^0_S$ and ωK^0_S.[28] Results on ϕK^0_S and $K^+K^-K^0_S$ (implicitly excluding ϕK^0_S and $f_0K^0_S$) are taken from time-dependent Dalitz plot analyses of $K^+K^-K^0_S$; results on $\rho^0K^0_S$, $f_2K^0_S$, $f_XK^0_S$ and $\pi^+\pi^-K^0_S$ nonresonant are taken from time-dependent Dalitz-plot analyses of $\pi^+\pi^-K^0_S$ (see Sec. VI G 2).[29] The results on $f_0K^0_S$ are from combinations of both Dalitz plot analyses. *BABAR* has also presented results with the final states $\pi^0\pi^0K^0_S$ and $\phi K^0_S\pi^0$.

Of these final states, ϕK^0_S, $\eta' K^0_S$, $\pi^0K^0_S$, $\rho^0K^0_S$, ωK^0_S and $f_0K^0_L$ have CP eigenvalue $\eta=-1$, while ϕK^0_L, $\eta' K^0_L$, $K^0_SK^0_SK^0_S$, $f_0K^0_S$, $f_2K^0_S$, $f_XK^0_S$, $\pi^0\pi^0K^0_S$ and $\pi^+\pi^-K^0_S$ nonresonant have $\eta=+1$. The final state $K^+K^-K^0_S$ (with ϕK^0_S and $f_0K^0_S$ implicitly excluded) is not a CP eigenstate, but the CP content can be absorbed in the amplitude analysis to allow the determination of a single effective S parameter. (In earlier analyses of the $K^+K^-K^0$ final state, its CP composition was determined using an isospin argument [379] and a moments analysis [380]).

The final state $\phi K^0_S\pi^0$ is also not a CP eigenstate but its CP-composition can be determined from an angular analysis. Since the parameters are common to the $B^0\to\phi K^0_S\pi^0$ and $B^0\to\phi K^+\pi^-$ decays (because only $K\pi$ resonances contribute), *BABAR* performed a simultaneous analysis of the two final states [388] (see Sec. VI G 3).

It must be noted that Q2B parameters extracted from Dalitz-plot analyses are constrained to lie within the physical boundary ($S^2_{CP}+C^2_{CP}<1$). Consequently, the obtained uncertainties are highly non-Gaussian when the central value is close to the boundary. This is

[28]Belle [378] includes the $\pi^0K^0_L$ final state together with $\pi^0K^0_S$ in order to improve the constraint on the parameter of CP violation in decay; these events cannot be used for time-dependent analysis.

[29]Throughout this section, $f_0\equiv f_0(980)$ and $f_2\equiv f_2(1270)$. Details of the assumed lineshapes of these states, and of the f_X (which is taken to have even spin), can be found in the relevant experimental papers [261,262,265,266].

TABLE 35. Measurements of CP violation parameters from $B_s^0 \to J/\psi K_S^0$.

Experiment		$\int \mathcal{L}\, dt$	S_{CP}	C_{CP}	$A^{\Delta\Gamma}$
LHCb	[356]	3 fb^{-1}	$0.49^{+0.77}_{-0.65} \pm 0.06$	$-0.28 \pm 0.41 \pm 0.08$	$-0.08 \pm 0.40 \pm 0.08$

TABLE 36. Averages of $-\eta S_{b\to q\bar{q}s}$ and $C_{b\to q\bar{q}s}$. Where a third source of uncertainty is given, it is due to model uncertainties arising in Dalitz plot analyses.

Experiment		$N(B\bar{B})$	$-\eta S_{b\to q\bar{q}s}$	$C_{b\to q\bar{q}s}$	Correlation
			ϕK^0		
BABAR	[262]	470M	$0.66 \pm 0.17 \pm 0.07$	$0.05 \pm 0.18 \pm 0.05$	···
Belle	[261]	657M	$0.90^{+0.09}_{-0.19}$	$-0.04 \pm 0.20 \pm 0.10 \pm 0.02$	···
Average			$0.74^{+0.11}_{-0.13}$	0.01 ± 0.14	Uncorrelated averages
			$\eta' K^0$		
BABAR	[381]	467M	$0.57 \pm 0.08 \pm 0.02$	$-0.08 \pm 0.06 \pm 0.02$	0.03
Belle	[382]	772M	$0.68 \pm 0.07 \pm 0.03$	$-0.03 \pm 0.05 \pm 0.03$	0.03
Average			0.63 ± 0.06	-0.05 ± 0.04	0.02
Confidence level			$0.53(0.6\sigma)$		
			$K_S^0 K_S^0 K_S^0$		
BABAR	[383]	468M	$0.94^{+0.21}_{-0.24} \pm 0.06$	$-0.17 \pm 0.18 \pm 0.04$	0.16
Belle	[384]	722M	$0.71 \pm 0.23 \pm 0.05$	$-0.12 \pm 0.16 \pm 0.05$	···
Average			0.83 ± 0.17	-0.15 ± 0.12	0.07
Confidence level			$0.76(0.3\sigma)$		
			$\pi^0 K^0$		
BABAR	[381]	467M	$0.55 \pm 0.20 \pm 0.03$	$0.13 \pm 0.13 \pm 0.03$	0.06
Belle	[378]	657M	$0.67 \pm 0.31 \pm 0.08$	$-0.14 \pm 0.13 \pm 0.06$	−0.04
Average			0.57 ± 0.17	0.01 ± 0.10	0.02
Confidence level			$0.37(0.9\sigma)$		
			$\rho^0 K_S^0$		
BABAR	[265]	383M	$0.35^{+0.26}_{-0.31} \pm 0.06 \pm 0.03$	$-0.05 \pm 0.26 \pm 0.10 \pm 0.03$	···
Belle	[266]	657M	$0.64^{+0.19}_{-0.25} \pm 0.09 \pm 0.10$	$-0.03^{+0.24}_{-0.23} \pm 0.11 \pm 0.10$	···
Average			$0.54^{+0.18}_{-0.21}$	-0.06 ± 0.20	Uncorrelated averages
			ωK_S^0		
BABAR	[381]	467M	$0.55^{+0.26}_{-0.29} \pm 0.02$	$-0.52^{+0.22}_{-0.20} \pm 0.03$	0.03
Belle	[385]	772M	$0.91 \pm 0.32 \pm 0.05$	$0.36 \pm 0.19 \pm 0.05$	−0.00
Average			0.71 ± 0.21	-0.04 ± 0.14	0.01
Confidence level			$0.007(2.7\sigma)$		
			$f_0 K^0$		
BABAR	[262,265]	···	$0.74^{+0.12}_{-0.15}$	0.15 ± 0.16	···
Belle	[261,266]	···	$0.63^{+0.16}_{-0.19}$	0.13 ± 0.17	···
Average			$0.69^{+0.10}_{-0.12}$	0.14 ± 0.12	Uncorrelated averages
			$f_2 K_S^0$		
BABAR	[265]	383M	$0.48 \pm 0.52 \pm 0.06 \pm 0.10$	$0.28^{+0.35}_{-0.40} \pm 0.08 \pm 0.07$	···
			$f_X K_S^0$		
BABAR	[265]	383M	$0.20 \pm 0.52 \pm 0.07 \pm 0.07$	$0.13^{+0.33}_{-0.35} \pm 0.04 \pm 0.09$	···

particularly evident in the *BABAR* results for $B^0 \to f_0 K^0$ with $f_0 \to \pi^+\pi^-$ [265]. These results must be treated with caution.

As explained above, each of the modes listed in Tables 36 and 37 has potentially different subleading contributions within the Standard Model, and thus each

TABLE 37. Averages of $-\eta S_{b\to q\bar{q}s}$ and $C_{b\to q\bar{q}s}$ (cont.). Where a third source of uncertainty is given, it is due to model uncertainties arising in Dalitz plot analyses.

Experiment		$N(B\bar{B})$	$-\eta S_{b\to q\bar{q}s}$	$C_{b\to q\bar{q}s}$	Correlation
			$\pi^0\pi^0 K^0_S$		
BABAR	[386]	227M	$-0.72 \pm 0.71 \pm 0.08$	$0.23 \pm 0.52 \pm 0.13$	-0.02
Belle	[387]	772M	$0.92^{+0.27}_{-0.31} \pm 0.11$	$-0.28 \pm 0.21 \pm 0.04$	0.00
Average			0.66 ± 0.28	-0.21 ± 0.20	0.00
Confidence level			$0.08(1.8\sigma)$		
			$\phi K^0_S \pi^0$		
BABAR	[388]	465M	$0.97^{+0.03}_{-0.52}$	$-0.20 \pm 0.14 \pm 0.06$	…
			$\pi^+\pi^- K^0_S$ nonresonant		
BABAR	[265]	383M	$0.01 \pm 0.31 \pm 0.05 \pm 0.09$	$0.01 \pm 0.25 \pm 0.06 \pm 0.05$	…
			$K^+K^-K^0$		
BABAR	[262]	470M	$0.65 \pm 0.12 \pm 0.03$	$0.02 \pm 0.09 \pm 0.03$	…
Belle	[261]	657M	$0.76^{+0.14}_{-0.18}$	$0.14 \pm 0.11 \pm 0.08 \pm 0.03$	…
Average			$0.68^{+0.09}_{-0.10}$	0.06 ± 0.08	Uncorrelated averages

may have a different value of $-\eta S_{b\to q\bar{q}s}$. Therefore, there is no strong motivation to make a combined average over the different modes. We refer to such an average as a "naïve s-penguin average." It is naïve not only because the theoretical uncertainties are neglected, but also since possible correlations of systematic effects between different modes are not included. In spite of these caveats, there remains interest in the value of this quantity and therefore it is given here: $\langle -\eta S_{b\to q\bar{q}s}\rangle = 0.648 \pm 0.038$, with confidence level $0.63(0.5\sigma)$. This value is in agreement with the average $-\eta S_{b\to c\bar{c}s}$ given in Sec. VI D 1. The average for $C_{b\to q\bar{q}s}$ is $\langle C_{b\to q\bar{q}s}\rangle = -0.003 \pm 0.029$ with a confidence level of $0.43(0.8\sigma)$.

From Table 36 it may be noted that the averages for $-\eta S_{b\to q\bar{q}s}$ in ϕK^0_S, $\eta' K^0$, $f_0 K^0_S$ and $K^+K^-K^0_S$ are all now more than 5σ away from zero, so that CP violation in these modes can be considered well established. There is no evidence (above 2σ) for CP violation in decay in any of these $b \to q\bar{q}s$ transitions.

2. Time-dependent Dalitz plot analyses: $B^0 \to K^+K^-K^0$ and $B^0 \to \pi^+\pi^- K^0_S$

As mentioned in Sec. VI. B. 5 and above, both *BABAR* and Belle have performed time-dependent Dalitz plot analyses of $B^0 \to K^+K^-K^0$ and $B^0 \to \pi^+\pi^- K^0_S$ decays. The results are summarized in Tables 38 and 39. Averages for the $B^0 \to f_0 K^0_S$ decay, which contributes to both Dalitz plots, are shown in Fig. 24. Results are presented in terms of the effective weak phase (from mixing and decay) difference $\beta^{\rm eff}$ and the parameter of CP violation in decay $\mathcal{A}$ ($\mathcal{A} = -C$) for each of the resonant contributions. Note that Dalitz-plot analyses, including all those included in these averages, often suffer from ambiguous solutions—we quote the results corresponding to those presented as "solution 1" in all cases. Results on flavor-specific amplitudes that may contribute to these Dalitz plots (such as $K^{*+}\pi^-$) are given in Sec. IX.

For the $B^0 \to K^+K^-K^0$ decay, both *BABAR* and Belle measure the CP violation parameters for the ϕK^0, $f_0 K^0$ and "other $K^+K^-K^0$" amplitudes, where the latter includes all remaining resonant and nonresonant contributions to the charmless three-body decay. For the $B^0 \to \pi^+\pi^- K^0_S$ decay, *BABAR* reports CP violation parameters for all of the CP eigenstate components in the Dalitz plot model ($\rho^0 K^0_S$, $f_0 K^0_S$, $f_2 K^0_S$, $f_X K^0_S$ and nonresonant decays; see Sec. VI. B. 5), while Belle reports the CP violation parameters for only the $\rho^0 K^0_S$ and $f_0 K^0_S$ amplitudes, although the Dalitz-plot models used by the two collaborations are rather similar.

3. Time-dependent analyses of $B^0 \to \phi K^0_S \pi^0$

The final state in the decay $B^0 \to \phi K^0_S \pi^0$ is a mixture of CP-even and CP-odd amplitudes. However, since only ϕK^{*0} resonant states contribute (in particular, $\phi K^{*0}(892)$, $\phi K^{*0}_0(1430)$ and $\phi K^{*0}_2(1430)$ are seen), the composition can be determined from the analysis of $B \to \phi K^+\pi^-$ decays, assuming only that the ratio of branching fractions $\mathcal{B}(K^{*0} \to K^0_S\pi^0)/\mathcal{B}(K^{*0} \to K^+\pi^-)$ is the same for each excited kaon state.

BABAR [388] has performed a simultaneous analysis of $B^0 \to \phi K^0_S \pi^0$ and $B^0 \to \phi K^+\pi^-$ decays that is time-dependent for the former mode and time-integrated for the latter. Such an analysis allows, in principle, all parameters of the $B^0 \to \phi K^{*0}$ system to be determined, including mixing-induced CP violation effects. The latter is determined to be $\Delta\phi_{00} = 0.28 \pm 0.42 \pm 0.04$, where $\Delta\phi_{00}$ is half the weak phase difference between B^0 and $\bar{B}^0$ decays to the $\phi K^{*0}_0(1430)$ final state. As discussed above, this can

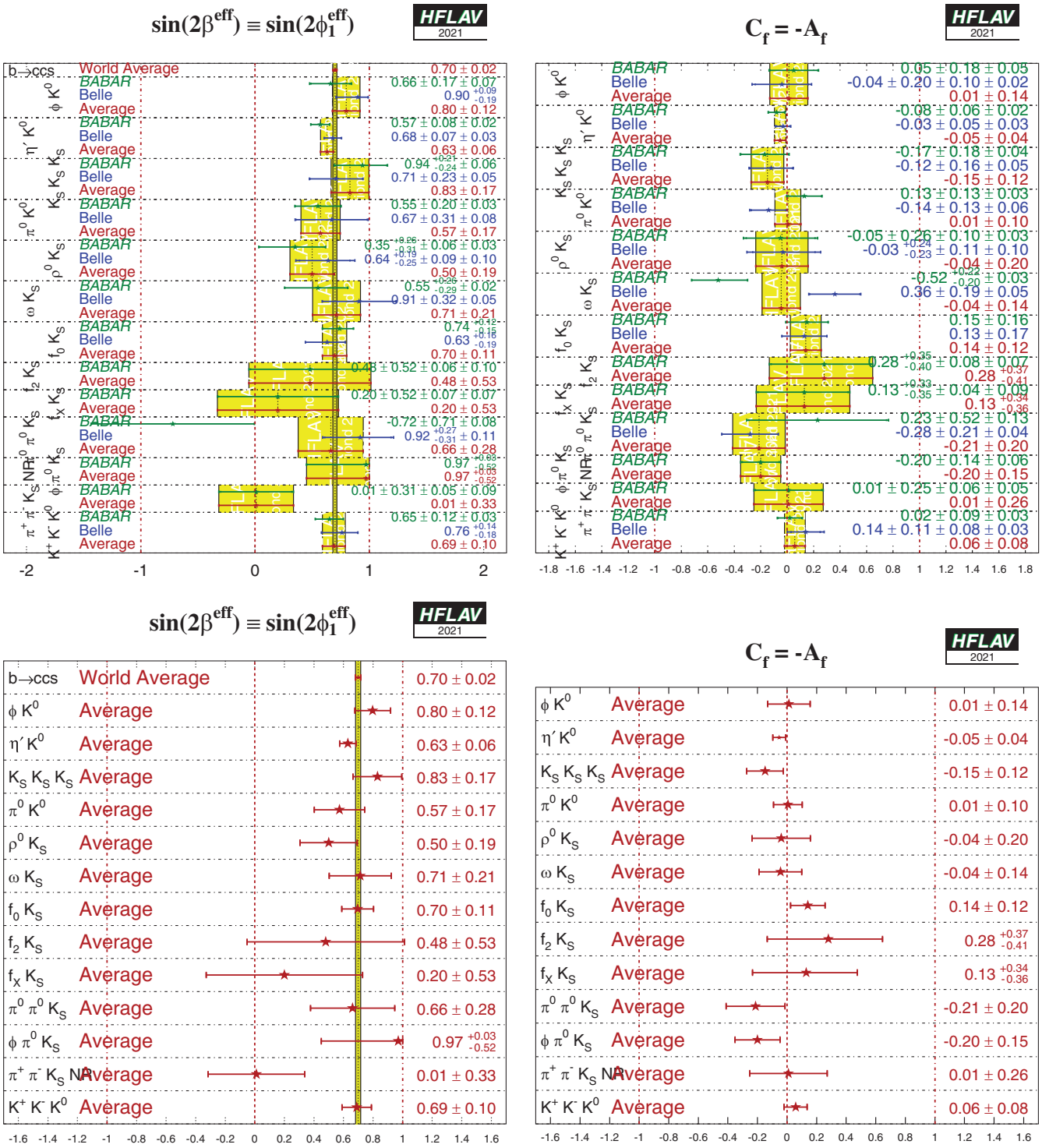

FIG. 21. Top: averages of (left) $-\eta S_{b\to q\bar{q}s}$, interpreted as $\sin(2\beta^{\rm eff}$ and (right) $C_{b\to q\bar{q}s}$. The $-\eta S_{b\to q\bar{q}s}$ figure compares the results to the world average for $-\eta S_{b\to c\bar{c}s}$ (see Sec. VI D 1). Bottom: same, but only averages for each mode are shown. More figures are available from the HFLAV web pages.

also be presented in terms of the Q2B parameter $\sin(2\beta^{\rm eff}_{00}) = \sin(2\beta + 2\Delta\phi_{00}) = 0.97^{+0.03}_{-0.52}$. The highly asymmetric uncertainty arises due to the conversion from the phase to the sine of the phase, and the proximity of the physical boundary.

Similar $\sin(2\beta^{\rm eff})$ parameters can be defined for each of the helicity amplitudes for both $\phi K^{*0}(892)$ and $\phi K_2^{*0}(1430)$. However, the relative phases between these decays are constrained due to the nature of the simultaneous analysis of $B^0 \to \phi K_S^0 \pi^0$ and $B^0 \to \phi K^+ \pi^-$, decays

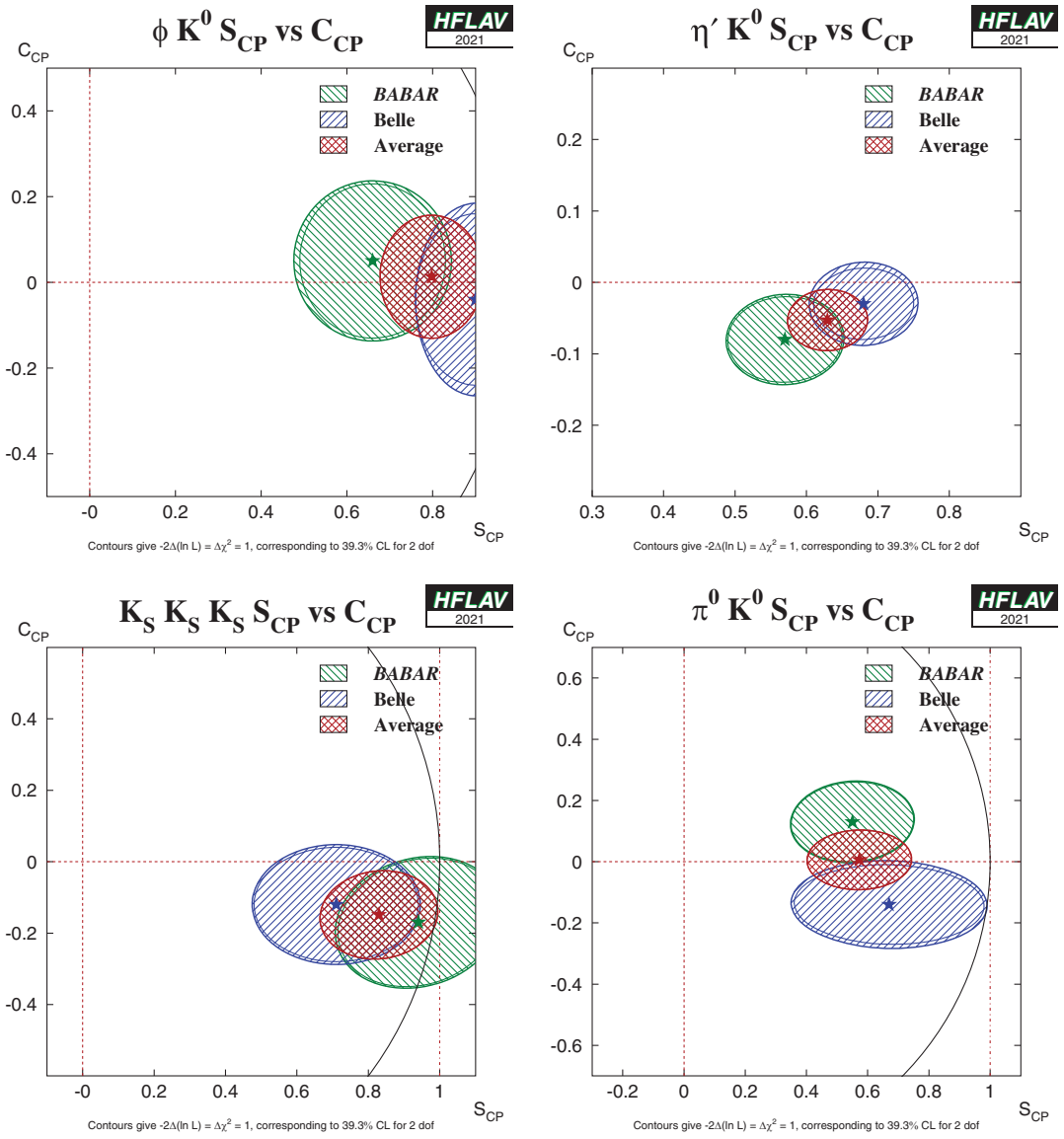

FIG. 22. Averages of four $b \to q\bar{q}s$ dominated channels, for which correlated averages are performed, in the S_{CP} *vs*. C_{CP} plane, where S_{CP} has been corrected by the CP eigenvalue to give $\sin(2\beta^{\rm eff})$. Contours at $S_{CP}^2 + C_{CP}^2 = 1$ represent the physical boundary for the parameters. Top left: $B^0 \to \phi K^0$, (top right) $B^0 \to \eta' K^0$, (bottom left) $B^0 \to K_S^0 K_S^0 K_S^0$, (bottom right) $B^0 \to \pi^0 K_S^0$. More figures are available from the HFLAV web pages.

and therefore these measurements are highly correlated. Instead of quoting all these results, *BABAR* provides an illustration of the measurements with the following differences:

$$\sin(2\beta - 2\Delta\delta_{01}) - \sin(2\beta) = -0.42^{+0.26}_{-0.34}, \quad (151)$$

$$\sin(2\beta - 2\Delta\phi_{\|1}) - \sin(2\beta) = -0.32^{+0.22}_{-0.30}, \quad (152)$$

$$\sin(2\beta - 2\Delta\phi_{\perp 1}) - \sin(2\beta) = -0.30^{+0.23}_{-0.32}, \quad (153)$$

$$\sin(2\beta - 2\Delta\phi_{\perp 1}) - \sin(2\beta - 2\Delta\phi_{\|1}) = 0.02 \pm 0.23, \quad (154)$$

$$\sin(2\beta - 2\Delta\delta_{02}) - \sin(2\beta) = -0.10^{+0.18}_{-0.29}, \quad (155)$$

where the first subscript indicates the helicity amplitude and the second indicates the spin of the kaon resonance. For the complete definitions of the $\Delta\delta$ and $\Delta\phi$ parameters, refer to the *BABAR* paper [388].

Parameters of CP violation in decay for each of the contributing helicity amplitudes can also be measured. Again, these are determined from a simultaneous fit of $B^0 \to \phi K_S^0 \pi^0$ and $B^0 \to \phi K^+ \pi^-$ decays, with the precision being dominated by the statistics of the latter mode.

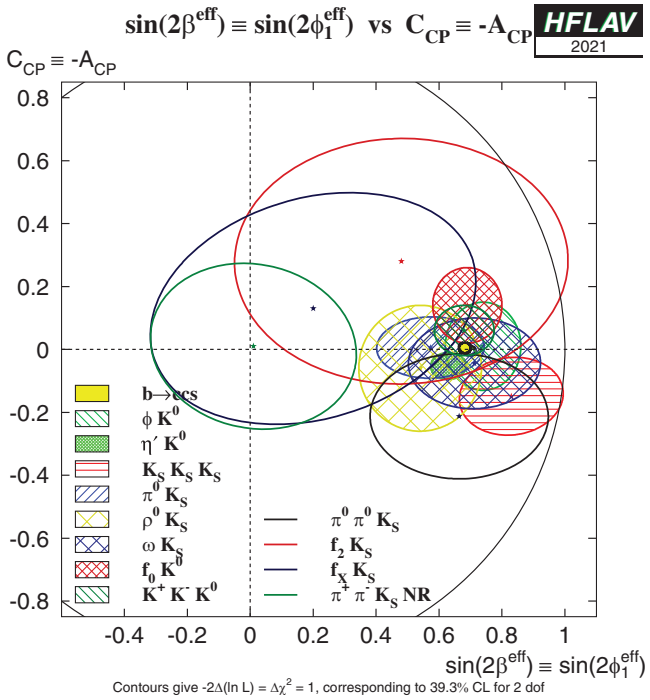

FIG. 23. Compilation of constraints in the $-\eta S_{b\to q\bar{q}s}$, interpreted as $\sin(2\beta^{\rm eff})$, vs $C_{b\to q\bar{q}s}$ plane. The contours at $\sin(2\beta^{\rm eff})^2 + C^2_{b\to q\bar{q}s} = 1$ represents the physical boundary for the parameters.

Measurements of *CP* violation in decay, obtained from decay-time-integrated analyses, are tabulated in Sec. IX.

4. Time-dependent CP asymmetries in $B^0_s \to K^+K^-$

The decay $B^0_s \to K^+K^-$ involves a $b \to u\bar{u}s$ transition, and hence has both penguin and tree contributions. Both mixing-induced and *CP* violation in decay effects may arise, and additional input is needed to disentangle the contributions and determine γ and $\beta^{\rm eff}_s$. For example, the observables in $B^0 \to \pi^+\pi^-$ can be related using U-spin, as proposed in Refs. [389,390].

The observables are S_{CP}, C_{CP}, and $A_{\Delta\Gamma}$. They are related by $S^2_{CP} + C^2_{CP} + A^2_{\Delta\Gamma} = 1$, but are usually treated as independent (albeit correlated) free parameters in experimental analyses, since this approach yields results with better statistical behavior. Note that the untagged decay distribution, from which an "effective lifetime" can be measured, retains sensitivity to $A_{\Delta\Gamma}$; measurements of the $B^0_s \to K^+K^-$ effective lifetime have been made by LHCb [83,110]. Compilations and averages of effective lifetimes are given in Sec. V.

The observables in $B^0_s \to K^+K^-$ have been measured by LHCb [391,392]. The results are shown in Table 40, and correspond to an observation of time-dependent *CP* violation in B^0_s decays. Note that in Ref. [392] the results of Ref. [391] are updated, when making a combined result, to

TABLE 38. Results from time-dependent Dalitz plot analyses of the $B^0 \to K^+K^-K^0$ decay. Correlations (not shown) are taken into account in the average.

Experiment	$N(B\bar{B})$	$\beta^{\rm eff}(\phi K^0_S)(^\circ)$	$\mathcal{A}(\phi K^0_S)$	$\beta^{\rm eff}(f_0 K^0_S)(^\circ)$	$\mathcal{A}(f_0 K^0_S)$	$\beta^{\rm eff}(K^+K^-K^0_S)(^\circ)$	$\mathcal{A}(K^+K^-K^0_S)$
BABAR [262]	470M	$21 \pm 6 \pm 2$	$-0.05 \pm 0.18 \pm 0.05$	$18 \pm 6 \pm 4$	$-0.28 \pm 0.24 \pm 0.09$	$20.3 \pm 4.3 \pm 1.2$	$-0.02 \pm 0.09 \pm 0.03$
Belle [261]	657M	32.2 ± 9.0 $\pm 2.6 \pm 1.4$	0.04 ± 0.20 $\pm 0.10 \pm 0.02$	31.3 ± 9.0 $\pm 3.4 \pm 4.0$	-0.30 ± 0.29 $\pm 0.11 \pm 0.09$	24.9 ± 6.4 $\pm 2.1 \pm 2.5$	-0.14 ± 0.11 $\pm 0.08 \pm 0.03$
Average		24 ± 5	-0.01 ± 0.14	22 ± 6	-0.29 ± 0.20	21.6 ± 3.7	-0.06 ± 0.08
Confidence level					$0.93(0.1\sigma)$		

TABLE 39. Results from time-dependent Dalitz plot analysis of the $B^0 \to \pi^+\pi^-K^0_S$ decay. Correlations (not shown) are taken into account in the average.

Experiment	$N(B\bar{B})$	$\beta^{\rm eff}(\rho^0 K^0_S)(^\circ)$	$\mathcal{A}(\rho^0 K^0_S)$	$\beta^{\rm eff}(f_0 K^0_S)(^\circ)$	$\mathcal{A}(f_0 K^0_S)$
BABAR [265]	383M	$10.2 \pm 8.9 \pm 3.0 \pm 1.9$	$0.05 \pm 0.26 \pm 0.10 \pm 0.03$	$36.0 \pm 9.8 \pm 2.1 \pm 2.1$	$-0.08 \pm 0.19 \pm 0.03 \pm 0.04$
Belle [266]	657M	$20.0^{+8.6}_{-8.5} \pm 3.2 \pm 3.5$	$0.03^{+0.23}_{-0.24} \pm 0.11 \pm 0.10$	$12.7^{+6.9}_{-6.5} \pm 2.8 \pm 3.3$	$-0.06 \pm 0.17 \pm 0.07 \pm 0.09$
Average		16.4 ± 6.8	0.06 ± 0.20	20.6 ± 6.2	-0.07 ± 0.14
Confidence level				$0.39(0.9\sigma)$	

Experiment	$N(B\bar{B})$	$\beta^{\rm eff}(f_2 K^0_S)(^\circ)$	$\mathcal{A}(f_2 K^0_S)$	$\beta^{\rm eff}(f_X K^0_S)(^\circ)$	$\mathcal{A}(f_X K^0_S)$
BABAR [265]	383M	$14.9 \pm 17.9 \pm 3.1 \pm 5.2$	$-0.28^{+0.40}_{-0.35} \pm 0.08 \pm 0.07$	$5.8 \pm 15.2 \pm 2.2 \pm 2.3$	$-0.13^{+0.35}_{-0.33} \pm 0.04 \pm 0.09$

Experiment	$N(B\bar{B})$	$\beta^{\rm eff}(\pi^+\pi^-K^0_S{\rm NR})(^\circ)$	$\mathcal{A}(\pi^+\pi^-K^0_S{\rm NR})$	$\beta^{\rm eff}(\chi_{c0}K^0_S)(^\circ)$	$\mathcal{A}(\chi_{c0}K^0_S)$
BABAR [265]	383M	$0.4 \pm 8.8 \pm 1.9 \pm 3.8$	$-0.01 \pm 0.25 \pm 0.06 \pm 0.05$	$23.2 \pm 22.4 \pm 2.3 \pm 4.2$	$0.29^{+0.44}_{-0.53} \pm 0.03 \pm 0.05$

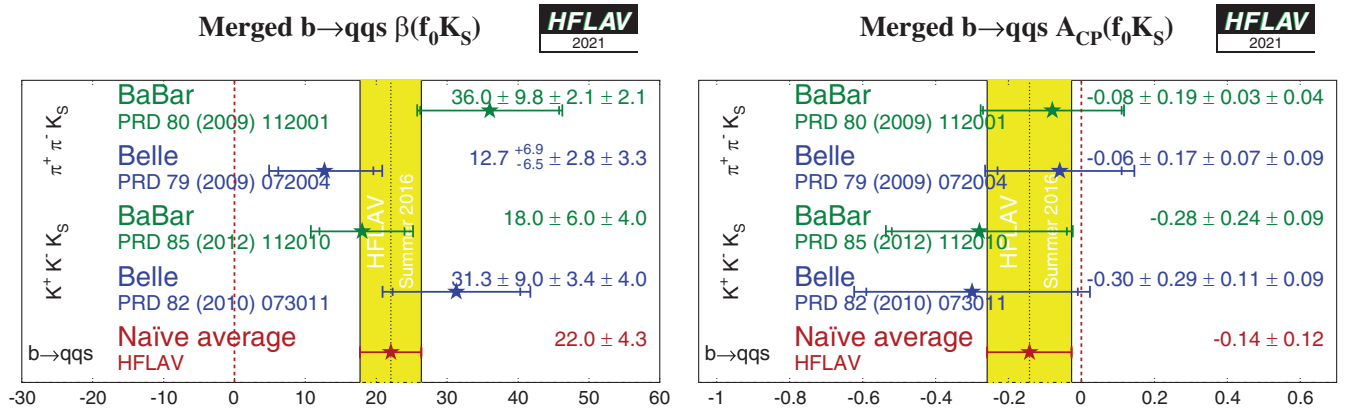

FIG. 24. Averages of (left) $\beta^{\rm eff} \equiv \phi_1^{\rm eff}$ and (right) A_{CP} for the $B^0 \to f_0 K_S^0$ decay including measurements from Dalitz plot analyses of both $B^0 \to K^+K^-K_S^0$ and $B^0 \to \pi^+\pi^-K_S^0$.

account for improved knowledge of Γ_s and $\Delta\Gamma_s$. The central value of $A_{\Delta\Gamma}$ changes to -0.97 ± 0.07, which is expected due to a shift in Γ_s with which it is strongly correlated.

Interpretations of an earlier set of results [393], in terms of constraints on γ and $2\beta_s$, have been separately published by LHCb [233].

5. Time-dependent CP asymmetries in $B_s^0 \to \phi\phi$

The decay $B_s^0 \to \phi\phi$ involves a $b \to s\bar{s}s$ transition, and hence is a "pure penguin" mode (in the limit that the ϕ meson is considered a pure $s\bar{s}$ state). Since the mixing phase and the decay phase are expected to cancel in the Standard Model, the phase from the interference of mixing and decay is predicted to be $\phi_s(\phi\phi) = 0$ with low uncertainty [394]. Due to the vector-vector nature of the final state, angular analysis is needed to separate the CP-even and CP-odd contributions. Such an analysis also makes it possible to fit directly for $\phi_s(\phi\phi)$.

A constraint on $\phi_s(\phi\phi)$ has been obtained by LHCb using 5 fb^{-1} [395]. The result is $\phi_s(\phi\phi) = -0.073 \pm 0.115 \pm 0.027$ rad, where the first uncertainty is statistical and the second is systematic.

6. Time-dependent CP asymmetries in $B_s^0 \to K^{*0}\bar{K}^{*0}$

The decay $B_s^0 \to K^{*0}\bar{K}^{*0}$ involves a $b \to d\bar{d}s$ transition, and similarly is a "pure penguin" mode. In this case, a U-spin analysis with the B^0 decay mode to the same final state can be used to make clean tests of the Standard Model [396–398].

A significant complication arises due to the width of the $K^*(892)^0$ meson. This has been addressed by LHCb, through a full analysis of the $B_s^0 \to (K^+\pi^-)(K^-\pi^+)$ decay, using a $K\pi$ mass window from 750 to 1600 MeV/c^2. In addition to the vector $K^*(892)$ resonance, contributions from $K\pi$ S-wave and from the tensor $K_2^*(1430)$ states are included. Assuming all amplitudes have contributions only from the same weak phase, a value of

TABLE 40. Results from time-dependent analysis of the $B_s^0 \to K^+K^-$ decay.

Experiment		Sample size	S_{CP}	C_{CP}	$A_{\Delta\Gamma}$
LHCb Run 1	[391]	$\int \mathcal{L}\,dt = 3.0$ fb^{-1}	$0.18 \pm 0.06 \pm 0.02$	$0.20 \pm 0.06 \pm 0.02$	$-0.79 \pm 0.07 \pm 0.10$
LHCb Run 2	[392]	$\int \mathcal{L}\,dt = 1.9$ fb^{-1}	$0.12 \pm 0.03 \pm 0.01$	$0.16 \pm 0.03 \pm 0.01$	$-0.83 \pm 0.05 \pm 0.09$
LHCb Average	[392]		0.14 ± 0.03	0.17 ± 0.03	-0.90 ± 0.09

TABLE 41. Results for $B^0 \to K_S^0K_S^0$.

Experiment		$N(B\bar{B})$	S_{CP}	C_{CP}	Correlation
BABAR	[400]	350M	$-1.28^{+0.80+0.11}_{-0.73-0.16}$	$-0.40 \pm 0.41 \pm 0.06$	-0.32
Belle	[401]	657M	$-0.38^{+0.69}_{-0.77} \pm 0.09$	$0.38 \pm 0.38 \pm 0.05$	0.48
Average			-1.08 ± 0.49	-0.06 ± 0.26	0.14
Confidence level			$0.29(1.1\sigma)$		

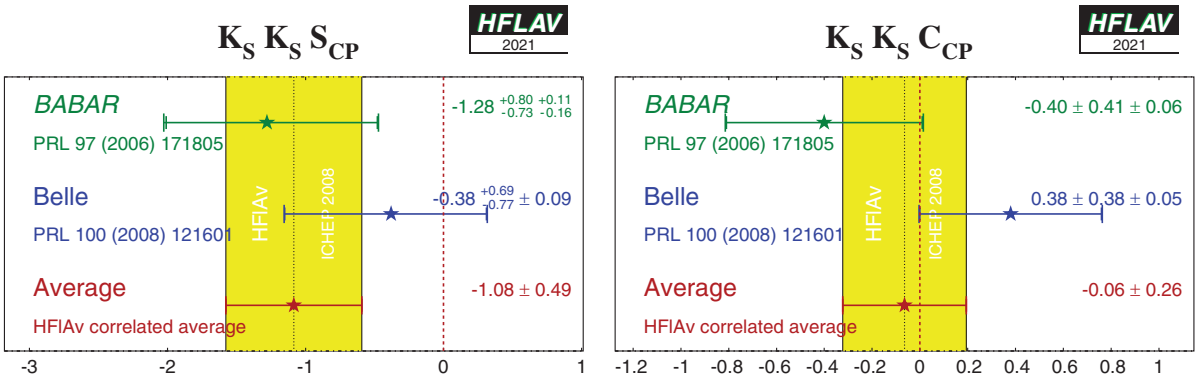

FIG. 25. Averages of (left) S_{CP} and (right) C_{CP} for the mode $B^0 \to K^0_S K^0_S$.

$\phi_s((K^+\pi^-)(K^-\pi^+)) = -0.10 \pm 0.13 \pm 0.14$ rad is measured, where the first uncertainty is statistical and the second is systematic, from a data sample of $\int \mathcal{L}\, dt = 3.0\ \text{fb}^{-1}$ [399].

H. Time-dependent *CP* asymmetries in $b \to q\bar{q}d$ transitions

Decays such as $B^0 \to K^0_S K^0_S$ are pure $b \to q\bar{q}d$ penguin transitions. As shown in Eq. (148), this diagram has different contributing weak phases, and therefore the observables are sensitive to their difference (which can be chosen to be either β or γ). Note that if the contribution with the top quark in the loop dominates, the weak phase from the decay amplitudes should cancel that from mixing, so that no *CP* violation (neither mixing-induced nor in decay) occurs. Nonzero contributions from loops with intermediate up and charm quarks can result in both types of effect (as usual, a strong phase difference is required for *CP* violation in decay to occur).

Both *BABAR* [400] and Belle [401] have performed time-dependent analyses of $B^0 \to K^0_S K^0_S$ decays. The results are given in Table 41 and shown in Fig. 25.

I. Time-dependent asymmetries in $b \to s\gamma$ transitions

The radiative decays $b \to s\gamma$ produce photons that are highly polarized in the Standard Model. The decays $B^0 \to F\gamma$ and $\bar{B}^0 \to F\gamma$, where F is a strange hadronic system, produce photons with opposite helicities, and since the polarization is, in principle, observable, these final states cannot interfere. The finite mass of the s quark introduces small corrections to the limit of maximum polarization, but any large mixing-induced *CP* violation would be a signal for new physics. Since a single weak phase dominates the $b \to s\gamma$ transition in the Standard Model, the cosine term is also expected to be small.

Atwood *et al.* [291] have shown that an inclusive analysis of $K^0_S\pi^0\gamma$ can be performed, since the properties of the decay amplitudes are independent of the angular momentum of the $K^0_S\pi^0$ system. However, if nondipole operators contribute significantly to the amplitudes, then the Standard Model mixing-induced *CP* violation could be larger than the naïve expectation $S \simeq -2(m_s/m_b)\sin(2\beta)$ [292,293]. In this case, the *CP* parameters may vary over the $K^0_S\pi^0\gamma$ Dalitz plot, for example, as a function of the $K^0_S\pi^0$ invariant mass.

With the above in mind, we quote two averages: one for the final state $K^*(892)\gamma$ only, and one for the inclusive $K^0_S\pi^0\gamma$ final state (including $K^*(892)\gamma$). If the Standard Model dipole operator is dominant, both should give the same *CP*-violation parameters (the latter, naturally, with smaller statistical uncertainties). If not, care needs to be taken in interpretation of the inclusive parameters, while the results on the $K^*(892)$ resonance remain relatively clean. Results from *BABAR* and Belle are used for both averages; both experiments use the invariant-mass range $0.60 < M_{K^0_S\pi^0} < 1.80\ \text{GeV}/c^2$ in the inclusive analysis.

In addition to the $K^0_S\pi^0\gamma$ decay, both *BABAR* and Belle have presented results using the $K^0_S\rho\gamma$ mode, while *BABAR* (Belle) has in addition presented results using the $K^0_S\eta\gamma$ ($K^0_S\phi\gamma$) channel. For the $K^0_S\rho\gamma$ case, due to the non-negligible width of the ρ^0 meson, decays selected as $B^0 \to K^0_S\rho^0\gamma$ can include a significant contribution from $K^{*\pm}\pi^{\mp}\gamma$ decays, which are flavor-specific and do not have the same oscillation phenomenology. Both *BABAR* and Belle measure S_{eff} for all B decay candidates with the ρ^0 selection being $0.6 < m(\pi^+\pi^-) < 0.9\ \text{GeV}/c^2$, obtaining $0.14 \pm 0.25^{+0.04}_{-0.03}$ (*BABAR*) and $0.09 \pm 0.27^{+0.04}_{-0.07}$ (Belle). These values are then corrected for a "dilution factor" [402], that is evaluated with different methods in the two experiments: *BABAR* [403,404] obtains a dilution factor of $-0.78^{+0.19}_{-0.17}$, while Belle [405] obtains $+0.83^{+0.19}_{-0.03}$. Until the discrepancy between these values is understood, the average of the results should be treated with caution.

The results are given in Table 42, and shown in Figs. 26 and 27. No significant *CP* violation is seen; the results are consistent with the Standard Model and with other measurements in the $b \to s\gamma$ system (see Sec. IX).

TABLE 42. Averages for $b \to s\gamma$ modes.

Experiment		$N(B\bar{B})$	$S_{CP}(b \to s\gamma)$	$C_{CP}(b \to s\gamma)$	Correlation
			$K^*(892)\gamma$		
BABAR	[406]	467M	$-0.03 \pm 0.29 \pm 0.03$	$-0.14 \pm 0.16 \pm 0.03$	0.05
Belle	[407]	535M	$-0.32^{+0.36}_{-0.33} \pm 0.05$	$0.20 \pm 0.24 \pm 0.05$	0.08
Average			-0.16 ± 0.22	-0.04 ± 0.14	0.06
Confidence level			$0.40(0.9\sigma)$		
			$K^0_S\pi^0\gamma$ (including $K^*(892)\gamma$)		
BABAR	[406]	467M	$-0.17 \pm 0.26 \pm 0.03$	$-0.19 \pm 0.14 \pm 0.03$	0.04
Belle	[407]	535M	$-0.10 \pm 0.31 \pm 0.07$	$0.20 \pm 0.20 \pm 0.06$	0.08
Average			-0.15 ± 0.20	-0.07 ± 0.12	0.05
Confidence level			$0.30(1.0\sigma)$		
			$K^0_S\eta\gamma$		
BABAR	[408]	465M	$-0.18^{+0.49}_{-0.46} \pm 0.12$	$-0.32^{+0.40}_{-0.39} \pm 0.07$	−0.17
Belle	[409]	772M	$-1.32 \pm 0.77 \pm 0.36$	$0.48 \pm 0.41 \pm 0.07$	−0.15
Average			-0.49 ± 0.42	0.06 ± 0.29	−0.15
Confidence level			$0.24(1.2\sigma)$		
			$K^0_S\rho^0\gamma$		
BABAR	[404]	471M	$-0.18 \pm 0.32^{+0.06}_{-0.05}$	$-0.39 \pm 0.20^{+0.03}_{-0.02}$	−0.09
Belle	[405]	657M	$0.11 \pm 0.33^{+0.05}_{-0.09}$	$-0.05 \pm 0.18 \pm 0.06$	0.04
Average			-0.06 ± 0.23	-0.22 ± 0.14	−0.02
Confidence level			$0.38(0.9\sigma)$		
			$K^0_S\phi\gamma$		
Belle	[410]	772M	$0.74^{+0.72+0.10}_{-1.05-0.24}$	$-0.35 \pm 0.58^{+0.10}_{-0.23}$	–

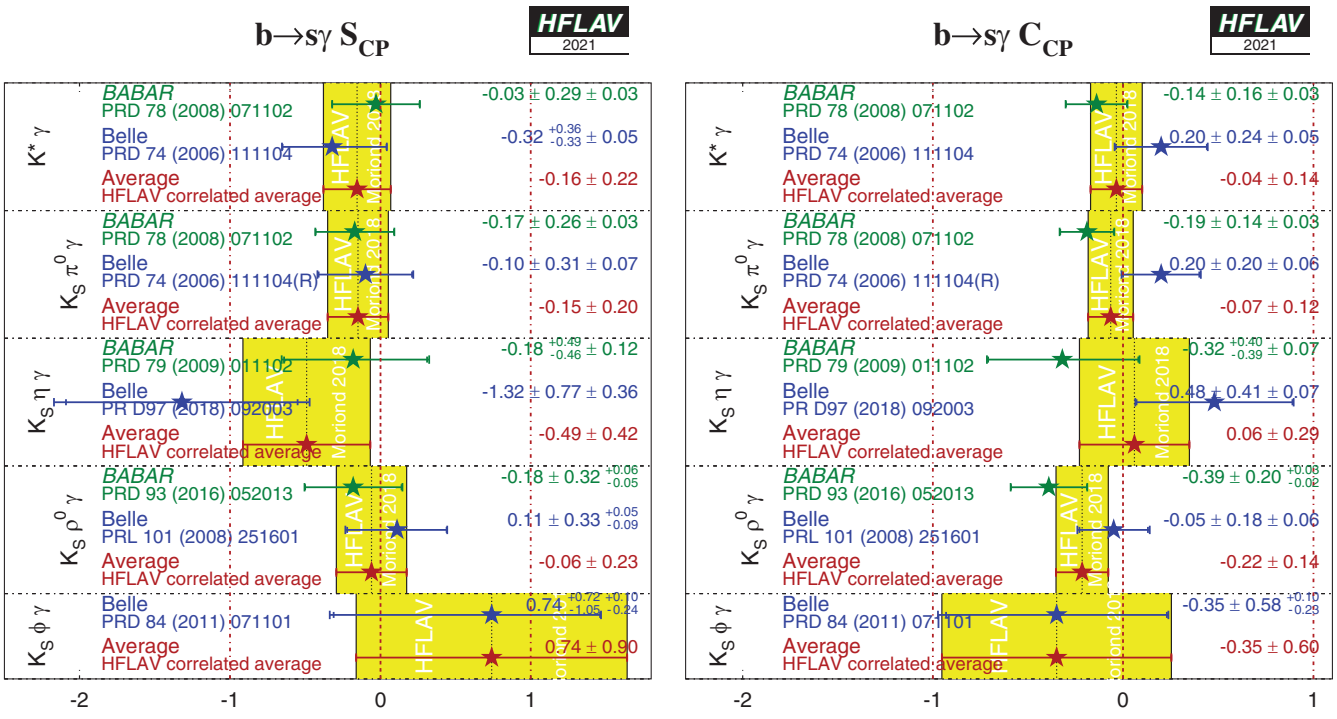

FIG. 26. Averages of (left) $S_{b\to s\gamma}$ and (right) $C_{b\to s\gamma}$. Recall that the data for $K^*\gamma$ is a subset of that for $K^0_S\pi^0\gamma$.

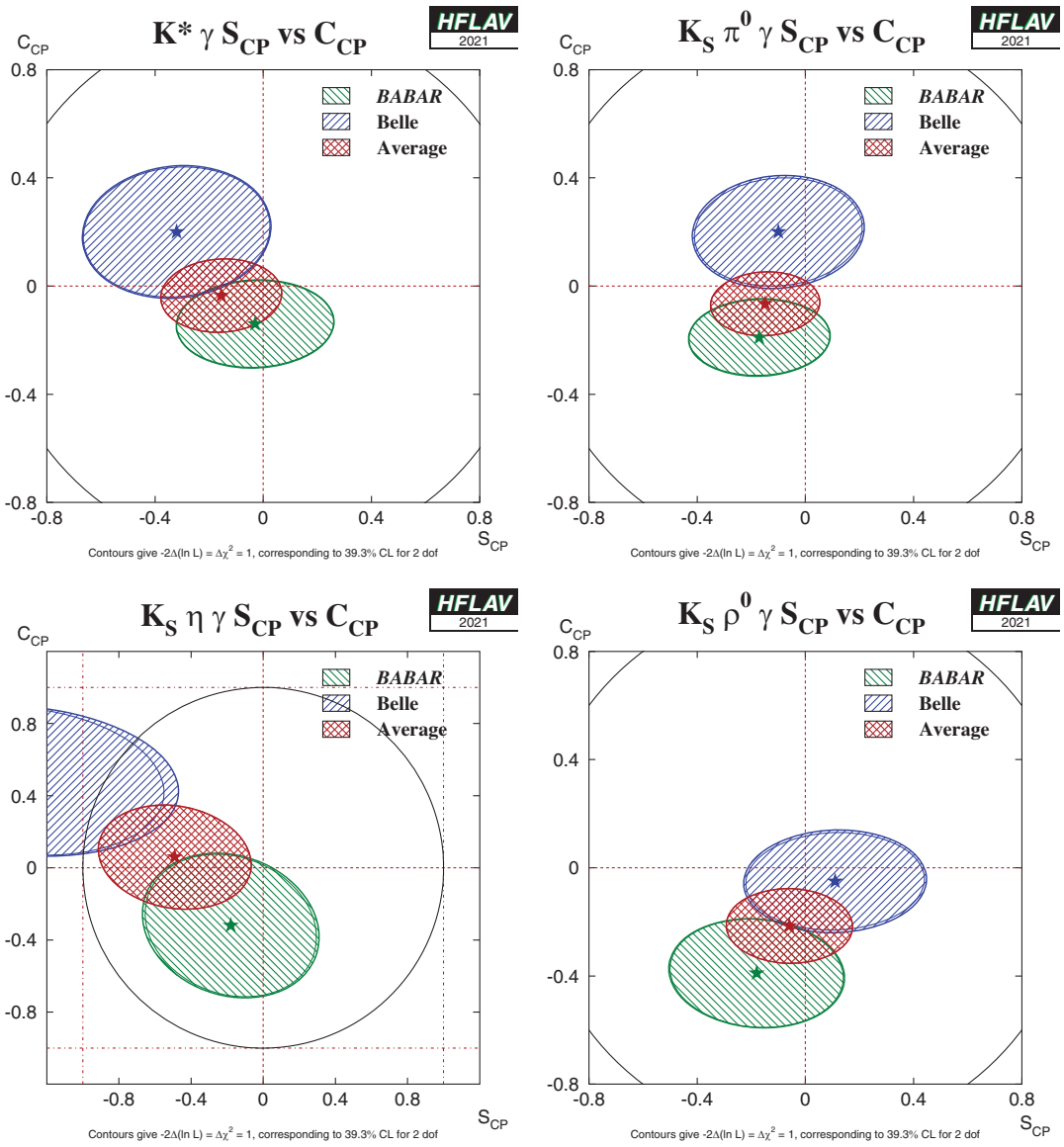

FIG. 27. Averages of four $b \to s\gamma$ dominated channels in the S_{CP} vs C_{CP} plane. Contours at $S_{CP}^2 + C_{CP}^2 = 1$ represent the physical boundary for the parameters. (Top left) $B^0 \to K^*\gamma$, (top right) $B^0 \to K_S^0\pi^0\gamma$ (including $K^*\gamma$), (bottom left) $B^0 \to K_S^0\eta\gamma$, (bottom right) $B^0 \to K_S^0\rho^0\gamma$.

J. Time-dependent asymmetries in B_s^0 decays mediated by $b \to s\gamma$ transitions

A similar analysis can be performed for radiative B_s^0 decays to, for example, the $\phi\gamma$ final state. As for other observables determined with self-conjugate final states produced in B_s^0 decays the effective lifetime, or equivalently the parameter $A^{\Delta\Gamma}$ also provides sensitivity to the underlying amplitudes. The LHCb collaboration has determined the relevant parameters in $B_s^0 \to \phi\gamma$ decays [411] as shown in Table 43.

K. Time-dependent asymmetries in $b \to d\gamma$ transitions

The formalism for the radiative decays $b \to d\gamma$ is much the same as that for $b \to s\gamma$ discussed above. In the limit

TABLE 43. Results from time-dependent analysis of the $B_s^0 \to \phi\gamma$ decay.

Experiment		Sample size	S_{CP}	C_{CP}	$A^{\Delta\Gamma}$
LHCb	[411]	$\int \mathcal{L}\,dt = 3.0$ fb^{-1}	$0.43 \pm 0.30 \pm 0.11$	$0.11 \pm 0.29 \pm 0.11$	$-0.67^{+0.37}_{-0.41} \pm 0.17$

TABLE 44. Averages for $B^0 \to \rho^0\gamma$.

Experiment		$N(B\bar{B})$	S_{CP}	C_{CP}	Correlation
Belle	[412]	657M	$-0.83 \pm 0.65 \pm 0.18$	$0.44 \pm 0.49 \pm 0.14$	-0.08

that the top quark contribution dominates the loop amplitude, the weak phase in decay should cancel with that from mixing making the mixing-induced CP violation parameter $S_{b\to d\gamma}$ very small. Corrections due to the finite light-quark mass are smaller compared to $b \to s\gamma$, since $m_d < m_s$, but QCD corrections of $\mathcal{O}(\Lambda_{\rm QCD}/m_b)$ may be sizable [292]. Significantly nonzero values of $S_{b\to d\gamma}$ and $C_{b\to d\gamma}$ can also arise if the up and charm quark contributions to the loop amplitude are not negligible.

Results using the mode $B^0 \to \rho^0\gamma$ are available from Belle and are given in Table 44.

L. Time-dependent CP asymmetries in $b \to u\bar{u}d$ transitions

The $b \to u\bar{u}d$ transition can be mediated by either a $b \to u$ tree amplitude or a $b \to d$ penguin amplitude. These transitions can be investigated using the time dependence of B^0 decays to final states containing light mesons. Results are available from both *BABAR* and Belle for the CP eigenstate ($\eta = +1$) $\pi^+\pi^-$ final state and for the vector-vector final state $\rho^+\rho^-$, which is found to be dominated by the CP-even longitudinally polarized component (*BABAR* measures $f_{\rm long} = 0.992 \pm 0.024^{+0.026}_{-0.013}$ [413], and Belle measures $f_{\rm long} = 0.988 \pm 0.012 \pm 0.023$ [414]). *BABAR* has also performed a time-dependent analysis of the vector-vector final state $\rho^0\rho^0$ [415], in which $f_{\rm long} = 0.70 \pm 0.14 \pm 0.05$ is determined; Belle measures a smaller branching fraction than *BABAR* for $B^0 \to \rho^0\rho^0$ [416] with corresponding signal yields too small to perform a time-dependent analysis, and finds $f_{\rm long} = 0.21^{+0.18}_{-0.22} \pm 0.13$ for the longitudinal polarization. LHCb has measured the branching fraction and longitudinal polarization for $B^0 \to \rho^0\rho^0$, and for the latter finds $f_{\rm long} = 0.745^{+0.048}_{-0.058} \pm 0.034$ [417], but has not yet performed a time-dependent analysis of this decay. The Belle measurement for $f_{\rm long}$ is thus in some tension with the other results. Both *BABAR* and Belle have furthermore performed time-dependent analyses of the $B^0 \to a_1^\pm\pi^\mp$ decay [418,419]; *BABAR* in addition has reported further experimental input for the extraction of α from this channel in a later publication [420].

Results and averages of time-dependent CP violation parameters in $b \to u\bar{u}d$ transitions are listed in Table 45. The averages for $\pi^+\pi^-$ are shown in Fig. 28, and those for $\rho^+\rho^-$ are shown in Fig. 29, with the averages in the S_{CP} *vs.* C_{CP} plane shown in Fig. 30, and averages of CP violation parameters in $B^0 \to a_1^\pm\pi^\mp$ decay shown in Fig. 31.

If the penguin contribution is negligible, the time-dependent parameters for $B^0 \to \pi^+\pi^-$ and $B^0 \to \rho^+\rho^-$ are given by $S_{b\to u\bar{u}d} = \eta\sin(2\alpha)$ and $C_{b\to u\bar{u}d} = 0$. In the presence of the penguin contribution, CP violation in decay may arise, and there is no straightforward interpretation of $S_{b\to u\bar{u}d}$ and $C_{b\to u\bar{u}d}$. An isospin analysis [423] can be used to disentangle the contributions and extract α, as discussed further in Sec. VI L 1.

For the non-CP eigenstate $\rho^\pm\pi^\mp$, both *BABAR* [272] and Belle [274,275] have performed time-dependent Dalitz-plot analyses of the $\pi^+\pi^-\pi^0$ final state [270]; such analyses allow direct measurements of the phases. Both experiments have measured the U and I parameters discussed in Sec. VI. B. 5 and defined in Table 24. We have performed a full correlated average of these parameters, the results of which are summarized in Fig. 32.

Both experiments have also extracted the Q2B parameters for the $\rho\pi$ channels. We have performed a full correlated average of these parameters, which is equivalent to determining the values from the averaged U and I parameters. The results are given in Table 46.[30] Averages of the $B^0 \to \rho^0\pi^0$ Q2B parameters are shown in Figs. 33 and 34.

With the notation described in Sec. VI B [Eq. (124)], the time-dependent parameters for the Q2B $B^0 \to \rho^\pm\pi^\mp$ analysis are, in the limit of negligible penguin contributions, given by

$$S_{\rho\pi} = \sqrt{1 - \left(\frac{\Delta C}{2}\right)^2}\,\sin(2\alpha)\,\cos(\delta),$$
$$\Delta S_{\rho\pi} = \sqrt{1 - \left(\frac{\Delta C}{2}\right)^2}\,\cos(2\alpha)\,\sin(\delta) \qquad (156)$$

and $C_{\rho\pi} = \mathcal{A}_{CP}^{\rho\pi} = 0$, where $\delta = \arg(A_{-+}A_{+-}^*)$ is the strong phase difference between the $\rho^-\pi^+$ and $\rho^+\pi^-$ decay amplitudes. In the presence of penguin contributions, there is no straightforward interpretation of the Q2B observables in the $B^0 \to \rho^\pm\pi^\mp$ system in terms of CKM parameters. However, CP violation in decay may arise, resulting in either or both of $C_{\rho\pi} \neq 0$ and $\mathcal{A}_{CP}^{\rho\pi} \neq 0$. Equivalently, CP violation in decay may be detected via a deviation from

[30]The $B^0 \to \rho^\pm\pi^\mp$ Q2B parameters are comparable to the parameters used for $B^0 \to a_1^\pm\pi^\mp$ decays, reported in Table 45. For the $B^0 \to a_1^\pm\pi^\mp$ case there has not yet been a full amplitude analysis of $B^0 \to \pi^+\pi^-\pi^+\pi^-$ and therefore only the Q2B parameters are available.

TABLE 45. Averages for $b \to u\bar{u}d$ modes.

Experiment		Sample size	S_{CP}	C_{CP}	Correlation
			$\pi^+\pi^-$		
BABAR	[421]	$N(B\bar{B}) = 467$M	$-0.68 \pm 0.10 \pm 0.03$	$-0.25 \pm 0.08 \pm 0.02$	-0.06
Belle	[422]	$N(B\bar{B}) = 772$M	$-0.64 \pm 0.08 \pm 0.03$	$-0.33 \pm 0.06 \pm 0.03$	-0.10
LHCb Run 1	[391]	$\int \mathcal{L}\,dt = 3.0$ fb^{-1}	$-0.63 \pm 0.05 \pm 0.01$	$-0.34 \pm 0.06 \pm 0.01$	0.45
LHCb Run 2	[392]	$\int \mathcal{L}\,dt = 1.9$ fb^{-1}	$-0.706 \pm 0.042 \pm 0.013$	$-0.311 \pm 0.045 \pm 0.015$	0.394(stat), 0.306(syst)
LHCb Average [392]			-0.672 ± 0.034	-0.320 ± 0.038	0.405
Average			-0.666 ± 0.029	-0.311 ± 0.030	0.288
Confidence level				$0.94(0.1\sigma)$	
			$\rho^+\rho^-$		
BABAR	[413]	$N(B\bar{B}) = 387$M	$-0.17 \pm 0.20^{+0.05}_{-0.06}$	$0.01 \pm 0.15 \pm 0.06$	-0.04
Belle	[414]	$N(B\bar{B}) = 772$M	$-0.13 \pm 0.15 \pm 0.05$	$0.00 \pm 0.10 \pm 0.06$	-0.02
Average			-0.14 ± 0.13	0.00 ± 0.09	-0.02
Confidence level				$0.99(0.02\sigma)$	
			$\rho^0\rho^0$		
BABAR	[415]	$N(B\bar{B}) = 465$M	$0.3 \pm 0.7 \pm 0.2$	$0.2 \pm 0.8 \pm 0.3$	-0.04

Experiment		$N(B\bar{B})$	$A_{CP}^{a_1\pi}$	$C_{a_1\pi}$	$S_{a_1\pi}$	$\Delta C_{a_1\pi}$	$\Delta S_{a_1\pi}$
				$a_1^\pm\pi^\mp$			
BABAR	[418]	384M	$-0.07 \pm 0.07 \pm 0.02$	$-0.10 \pm 0.15 \pm 0.09$	$0.37 \pm 0.21 \pm 0.07$	$0.26 \pm 0.15 \pm 0.07$	$-0.14 \pm 0.21 \pm 0.06$
Belle	[419]	772M	$-0.06 \pm 0.05 \pm 0.07$	$-0.01 \pm 0.11 \pm 0.09$	$-0.51 \pm 0.14 \pm 0.08$	$0.54 \pm 0.11 \pm 0.07$	$-0.09 \pm 0.14 \pm 0.06$
Average			-0.06 ± 0.06	-0.05 ± 0.11	-0.20 ± 0.13	0.43 ± 0.10	-0.10 ± 0.12
Confidence level					$0.03(2.1\sigma)$		

Experiment		$N(B\bar{B})$	$\mathcal{A}_{a_1\pi}^{-+}$	$\mathcal{A}_{a_1\pi}^{+-}$	Correlation
BABAR	[418]	384M	$0.07 \pm 0.21 \pm 0.15$	$0.15 \pm 0.15 \pm 0.07$	0.63
Belle	[419]	772M	$-0.04 \pm 0.26 \pm 0.19$	$0.07 \pm 0.08 \pm 0.10$	0.61
Average			0.02 ± 0.20	0.10 ± 0.10	0.38
Confidence level				$0.92(0.1\sigma)$	

zero of either of the decay-type-specific observables $\mathcal{A}_{\rho\pi}^{+-}$ and $\mathcal{A}_{\rho\pi}^{-+}$, defined in Eq. (125). Results and averages for these parameters are also given in Table 46. Averages of CP violation parameters in $B^0 \to \rho^\pm\pi^\mp$ decays are shown in Fig. 35, both in $\mathcal{A}_{CP}^{\rho\pi}$ vs $C_{\rho\pi}$ space and in $\mathcal{A}_{\rho\pi}^{-+}$ vs $\mathcal{A}_{\rho\pi}^{+-}$ space.

The averages for $S_{b\to u\bar{u}d}$ and $C_{b\to u\bar{u}d}$ in $B^0 \to \pi^+\pi^-$ decays are both more than 5σ away from zero, suggesting

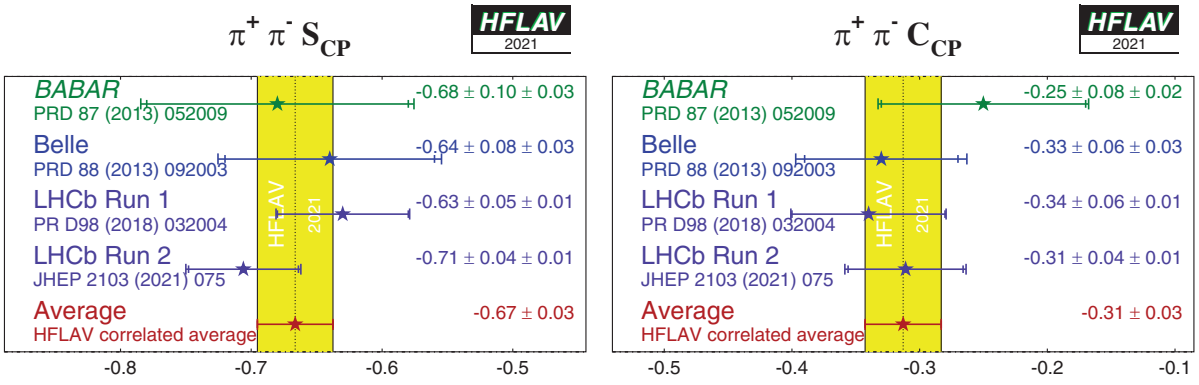

FIG. 28. Averages of (left) S_{CP} and (right) C_{CP} for the mode $B^0 \to \pi^+\pi^-$.

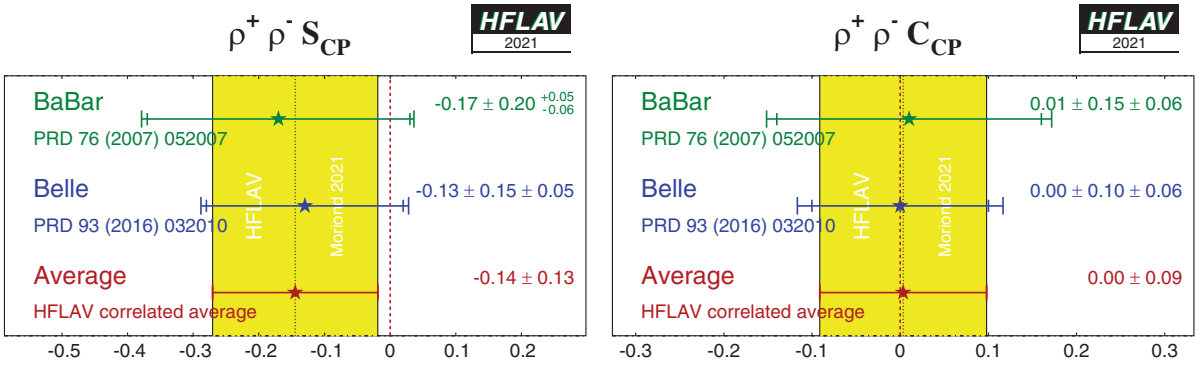

FIG. 29. Averages of (left) S_{CP} and (right) C_{CP} for the mode $B^0 \to \rho^+\rho^-$.

that both mixing-induced and CP violation in decay are well established in this channel. The discrepancy between results from *BABAR* and Belle that used to exist in this channel (see, for example, Ref. [424]) is no longer apparent, and the results from LHCb are also fully consistent with other measurements. Some difference is, however, seen between the *BABAR* and Belle measurements in the $a_1^{\pm}\pi^{\mp}$ system. The confidence level of the five-dimensional average is 0.03, which corresponds to a 2.1σ discrepancy. As seen in Table 45, this discrepancy is primarily in the values of $S_{a_1\pi}$, and is not evident in the $\mathcal{A}^{-+}_{a_1\pi}$ vs $\mathcal{A}^{+-}_{a_1\pi}$ projection shown in Fig. 31. Since there is no evidence of underestimation of uncertainties in either analysis, we do not rescale the uncertainties of the averages.

In $B^0 \to \rho^{\pm}\pi^{\mp}$ decays, both experiments see an indication of CP violation in the $\mathcal{A}_{CP}^{\rho\pi}$ parameter (as seen in Fig. 35). The average is more than 3σ from zero, providing evidence of CP violation in decay in this channel. In $B^0 \to \rho^+\rho^-$ decays there is no evidence for CP violation, neither mixing-induced nor in decay. The absence of evidence of penguin contributions in this mode leads to strong constraints on $\alpha \equiv \phi_2$.

1. Constraints on $\alpha \equiv \phi_2$

The precision of the measured CP violation parameters in $b \to u\bar{u}d$ transitions allows constraints to be set on the UT angle $\alpha \equiv \phi_2$. Constraints have been obtained with various methods:

(i) Both *BABAR* [421] and Belle [422] have performed isospin analyses in the $\pi\pi$ system. Belle excludes $23.8° < \phi_2 < 66.8°$ at 68% CL while *BABAR* gives a confidence level interpretation for α, and constrain $\alpha \in [71°, 109°]$ at 68% CL Values in the range

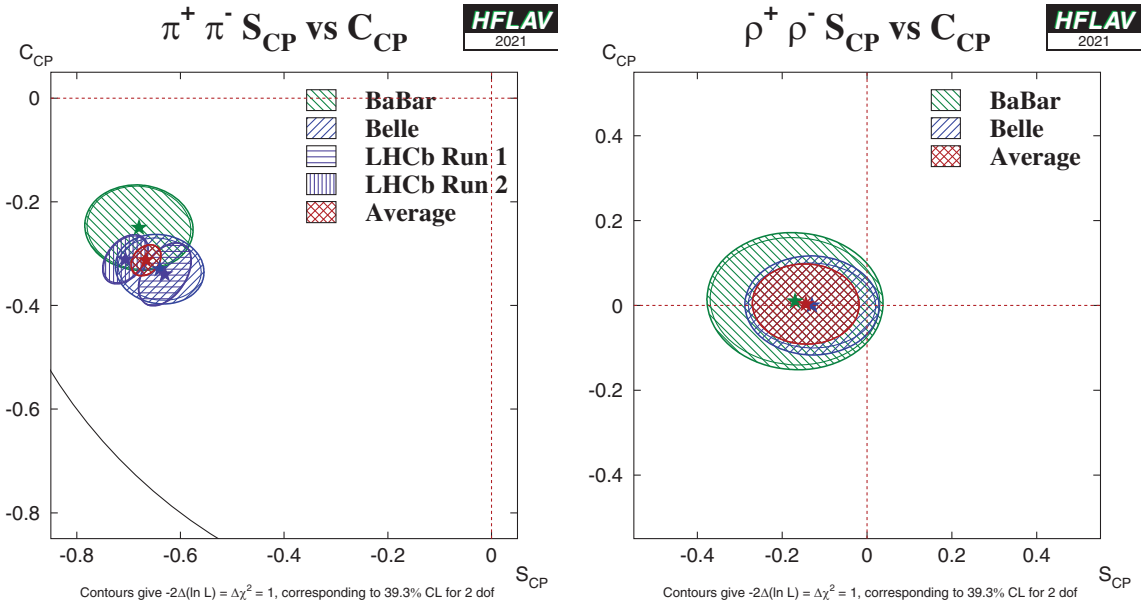

FIG. 30. Averages of $b \to u\bar{u}d$ dominated channels, for which correlated averages are performed, in the S_{CP} vs C_{CP} plane. Contours at $S_{CP}^2 + C_{CP}^2 = 1$ represent the physical boundary for the parameters. Left: $B^0 \to \pi^+\pi^-$ and (right) $B^0 \to \rho^+\rho^-$.

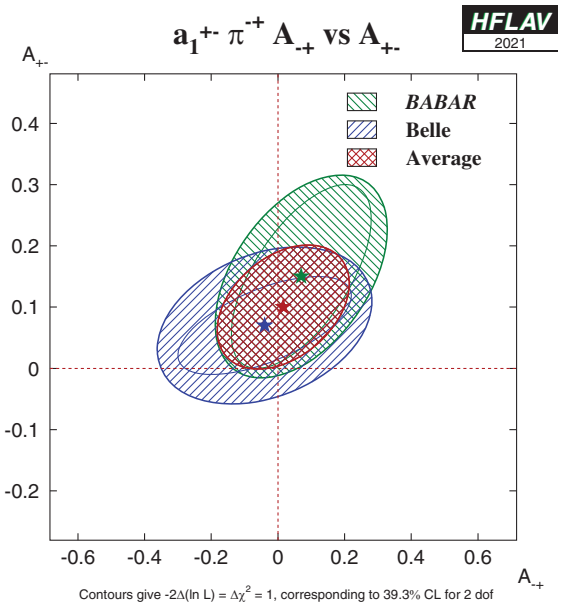

FIG. 31. Averages of CP violation parameters in $B^0 \to a_1^{\pm}\pi^{\mp}$ in $\mathcal{A}_{a_1\pi}^{-+}$ vs $\mathcal{A}_{a_1\pi}^{+-}$ space.

$[23°, 67°]$ are excluded at 90% CL In both cases, only solutions in 0°–180° are quoted.

(ii) Both experiments have also performed isospin analyses in the $\rho\rho$ system. The most recent result from *BABAR* is given in an update of the measurements of the $B^+ \to \rho^+\rho^0$ decay [425], and sets the constraint $\alpha = (92.4^{+6.0}_{-6.5})°$. The most recent result from Belle is given in their paper on time-dependent CP violation parameters in $B^0 \to \rho^+\rho^-$ decays, and sets the constraint $\phi_2 = (93.7 \pm 10.6)°$ [414].

(iii) The time-dependent Dalitz-plot analysis of the $B^0 \to \pi^+\pi^-\pi^0$ decay allows a determination of α without input from any other channels. *BABAR* [273] presents a scan, but not an interval, for α, since their studies indicate that the scan is not statistically robust and cannot be interpreted in terms of 1-CL. Belle [274,275] has obtained a constraint on α using additional information from SU(2) relations between $B \to \rho\pi$ decay amplitudes, which can be used to constrain α via an isospin pentagon relation [426]. With this analysis, Belle obtains the constraint $\phi_2 = (83^{+12}_{-23})°$.

(iv) The results from *BABAR* on $B^0 \to a_1^{\pm}\pi^{\mp}$ [418] can be combined with results from modes related by flavor symmetries ($a_1 K$ and $K_1\pi$) [427]. This has been done by *BABAR* [420], resulting in the constraint $\alpha = (79 \pm 7 \pm 11)°$, where the first uncertainty is from the analysis of $B^0 \to a_1^{\pm}\pi^{\mp}$ that obtains α^{eff}, and the second is due to the constraint on $|\alpha^{\text{eff}} - \alpha|$. This approach gives a result with several ambiguous solutions; only the one that is consistent with other determinations of α and with

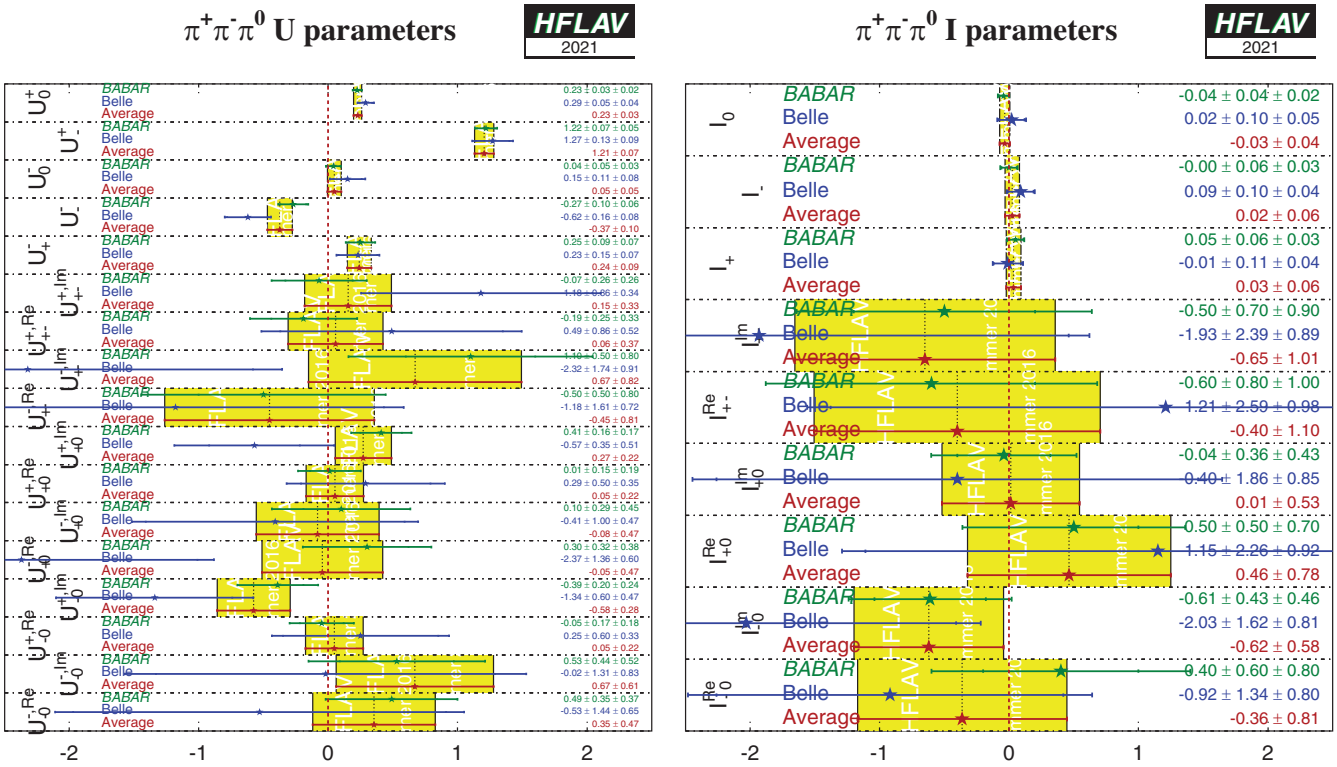

FIG. 32. Summary of the U and I parameters measured in the time-dependent $B^0 \to \pi^+\pi^-\pi^0$ Dalitz plot analysis.

TABLE 46. Averages of quasi-two-body parameters extracted from time-dependent Dalitz plot analysis of $B^0 \to \pi^+\pi^-\pi^0$.

Experiment	$N(B\bar{B})$	$\mathcal{A}_{CP}^{\rho\pi}$	$C_{\rho\pi}$	$S_{\rho\pi}$	$\Delta C_{\rho\pi}$	$\Delta S_{\rho\pi}$
BABAR [273]	471M	$-0.10 \pm 0.03 \pm 0.02$	$0.02 \pm 0.06 \pm 0.04$	$0.05 \pm 0.08 \pm 0.03$	$0.23 \pm 0.06 \pm 0.05$	$0.05 \pm 0.08 \pm 0.04$
Belle [274,275]	449M	$-0.12 \pm 0.05 \pm 0.04$	$-0.13 \pm 0.09 \pm 0.05$	$0.06 \pm 0.13 \pm 0.05$	$0.36 \pm 0.10 \pm 0.05$	$-0.08 \pm 0.13 \pm 0.05$
Average		-0.11 ± 0.03	-0.03 ± 0.06	0.06 ± 0.07	0.27 ± 0.06	0.01 ± 0.08
Confidence level				$0.63(0.5\sigma)$		

Experiment		$N(B\bar{B})$	$\mathcal{A}_{\rho\pi}^{-+}$	$\mathcal{A}_{\rho\pi}^{+-}$	Correlation
BABAR	[273]	471M	$-0.12 \pm 0.08^{+0.04}_{-0.05}$	$0.09^{+0.05}_{-0.06} \pm 0.04$	0.55
Belle	[274,275]	449M	$0.08 \pm 0.16 \pm 0.11$	$0.21 \pm 0.08 \pm 0.04$	0.47
Average			-0.08 ± 0.08	0.13 ± 0.05	0.37
Confidence level			$0.47(0.7\sigma)$		

Experiment		$N(B\bar{B})$	$C_{\rho^0\pi^0}$	$S_{\rho^0\pi^0}$	Correlation
BABAR	[273]	471M	$0.19 \pm 0.23 \pm 0.15$	$-0.37 \pm 0.34 \pm 0.20$	0.00
Belle	[274,275]	449M	$0.49 \pm 0.36 \pm 0.28$	$0.17 \pm 0.57 \pm 0.35$	0.08
Average			0.27 ± 0.24	-0.23 ± 0.34	0.02
Confidence level			$0.68(0.4\sigma)$		

global fits to the CKM matrix parameters is quoted here.

(v) The CKMfitter [242] and UTFit [334] groups use the measurements from Belle and *BABAR* given above with other branching fractions and CP asymmetries in $B \to \pi\pi$, $\pi\pi\pi^0$ and $\rho\rho$ modes to perform isospin analyses for each system, and to obtain combined constraints on α.

(vi) The *BABAR* and Belle collaborations have combined their results on $B \to \pi\pi$, $\pi\pi\pi^0$ and $\rho\rho$ decays to obtain [428]

$$\alpha \equiv \phi_2 = (88 \pm 5)^\circ. \tag{157}$$

The above solution is that consistent with the Standard Model (there exists an ambiguous solution, shifted by 180°). The strongest constraint currently comes from the $B \to \rho\rho$ system. The inclusion of results from $B^0 \to a_1^\pm \pi^\mp$ does not significantly affect the average.

(vii) All results for $\alpha \equiv \phi_2$ based on isospin symmetry have a theoretical uncertainty due to possible isospin-breaking effects. This is expected to be small, $\lesssim 1^\circ$ [429–431], but is hard to quantify reliably and is usually not included in the quoted uncertainty.

Note that methods based on isospin symmetry make extensive use of measurements of branching fractions and CP asymmetries, for which averages are reported in Sec. IX. Note also that each method suffers from discrete ambiguities in the solutions. The model assumption in the $B^0 \to \pi^+\pi^-\pi^0$ analysis helps resolve some of the multiple solutions, and results in a single preferred value for α in $[0, \pi]$. All the above measurements correspond to the choice that is in agreement with the global CKM fit.

Independently from the constraints on $\alpha \equiv \phi_2$ obtained by the experiments, the results summarized in Sec. VI L are statistically combined to produce world average constraints on $\alpha \equiv \phi_2$. The combination is performed with the GAMMACOMBO framework [432] and follows a frequentist

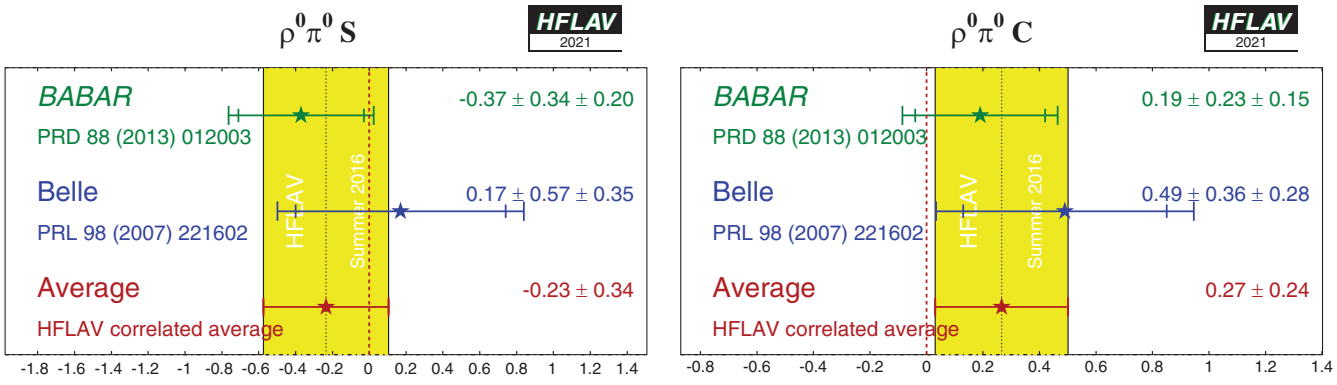

FIG. 33. Averages of (left) $S_{b\to u\bar{u}d}$ and (right) $C_{b\to u\bar{u}d}$ for the mode $B^0 \to \rho^0\pi^0$.

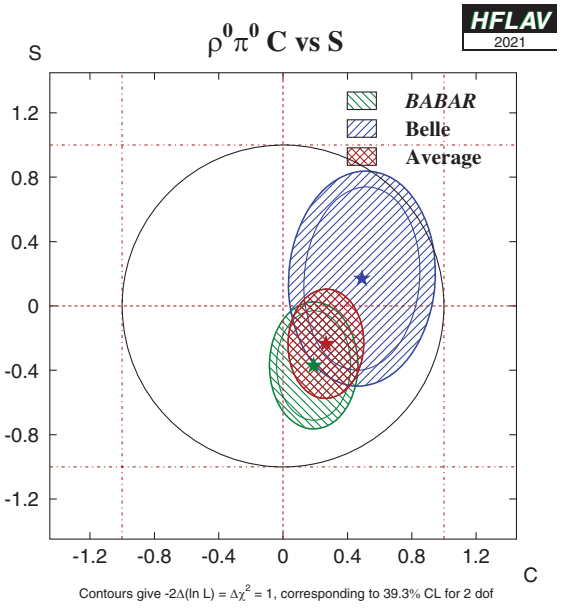

FIG. 34. Averages of $b \to u\bar{u}d$ dominated channels, for the mode $B^0 \to \rho^0\pi^0$ in the S_{CP} vs C_{CP} plane. The contour at $S_{CP}^2 + C_{CP}^2 = 1$ represents the physical boundary for the parameters.

procedure, similar to that used by *BABAR* and Belle [428], and described in detail in Ref. [431].

The input measurements used in the combination are those listed above and are summarized in Table 47. Additional inputs, summarized in Table 48, for the branching fractions and (for $\rho\rho$) polarization fractions, for the relevant modes and their isospin partners are taken from Sec. IX, while the ratio of B^+ to B^0 lifetimes is taken from Sec. V. Individual measurements are used as inputs, rather than the HFLAV averages, in order to facilitate cross-checks and to ensure the most appropriate treatment of correlations. A combination based on HFLAV averages gives consistent results. Results on $B^0 \to a_1^{\pm}\pi^{\mp}$ decays are not included, as to do so requires additional theoretical assumptions, but as shown in Ref. [428] this does not significantly affect the average.

The fit has a χ^2 of 16.6 with 51 observables and 24 parameters. Using the χ^2 distribution, this corresponds to a p-value of 94.1% (or 0.1σ). A coverage check with pseudoexperiments gives a p-value of $(91.9 \pm 0.3)\%$.

TABLE 47. List of measurements used in the α combination. Results are obtained from either time-dependent (TD) *CP* asymmetries of decays to *CP* eigenstates or vector-vector final states, or time-integrated *CP* asymmetry measurements (*CP*). Results from time-dependent asymmetries in decays to self-conjugate three-body final states (TD-Dalitz) are also used in the form of the U and I parameters defined in Table 24.

B decay	Method	Parameters	Experiment	References
$B^0 \to \pi^+\pi^-$	TD	S_{CP}, C_{CP}	*BABAR* Belle LHCb	[421] [422] [392]
$B^0 \to \pi^0\pi^0$	CP	C_{CP}	*BABAR* Belle	[421] [433]
$B^0 \to \rho^+\rho^-$	TD	S_{CP}, C_{CP}	*BABAR* Belle	[413] [414]
$B^0 \to \rho^0\rho^0$	TD	S_{CP}, C_{CP}	*BABAR*	[415]
$B^0 \to \pi^+\pi^-\pi^0$	TD-Dalitz	$\{U, I\}$	*BABAR* Belle	[273] [274]

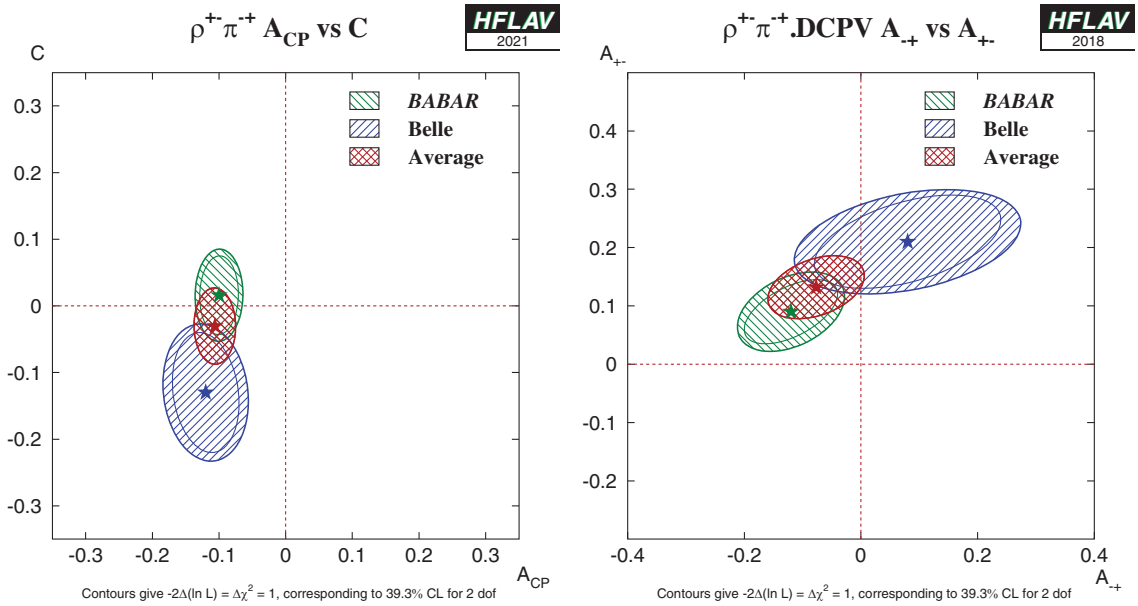

FIG. 35. *CP* violation in $B^0 \to \rho^{\pm}\pi^{\mp}$ decays. Left: $\mathcal{A}_{CP}^{\rho\pi}$ vs $C_{\rho\pi}$ space, (right) $\mathcal{A}_{\rho\pi}^{-+}$ *vs.* $\mathcal{A}_{\rho\pi}^{+-}$ space.

TABLE 48. List of the auxiliary inputs used in the α combination.

Particle/decay	Parameters	Source	References
B^+/B^0	$\tau(B^+)/\tau(B^0)$	HFLAV	Sec. V
$B^0 \to \pi^+\pi^-$	BR	HFLAV	Sec. IX
$B^0 \to \pi^0\pi^0$	BR	HFLAV	Sec. IX
$B^\pm \to \pi^\pm\pi^0$	BR	HFLAV	Sec. IX
$B^0 \to \rho^+\rho^-$	BR, f_L	HFLAV	Sec. IX
$B^0 \to \rho^0\rho^0$	BR, f_L	HFLAV	Sec. IX
$B^\pm \to \rho^\pm\rho^0$	BR, f_L	HFLAV	Sec. IX

TABLE 49. Averages of $\alpha \equiv \phi_2$ split by B meson decay mode. Only solutions consistent with the obtained world average are shown.

Decay mode	Value
$B \to \pi\pi$	$(84.8^{+22.1}_{-5.6})^\circ$
	$(99.6^{+7.3}_{-20.4})^\circ$
$B \to \rho\rho$	$(91.0 \pm 5.5)^\circ$
$B^0 \to (\rho\pi)^0$	$(53.4^{+8.3}_{-11.1})^\circ$

The obtained world average for the unitarity triangle angle $\alpha \equiv \phi_2$ is

$$\alpha \equiv \phi_2 = (85.2^{+4.8}_{-4.3})^\circ. \quad (158)$$

An ambiguous solution also exists at $\alpha \equiv \phi_2 \Leftrightarrow \alpha + \pi \equiv \phi_2 + \pi$. The quoted uncertainty does not include effects due to isospin-breaking. A secondary minimum close to zero is disfavored, as discussed in Ref. [431]. Results split by decay mode are shown in Table 49 and Fig. 36.

M. Time-dependent CP asymmetries in $b \to c\bar{u}d/u\bar{c}d$ transitions

Non-CP eigenstates such as $D^\mp\pi^\pm$, $D^{*\mp}\pi^\pm$ and $D^\mp\rho^\pm$ can be produced in decays of B^0 mesons either via Cabibbo-favored ($b \to c$) or doubly Cabibbo-suppressed ($b \to u$) tree amplitudes. Since no penguin contribution is possible, these modes are theoretically clean. The ratio of the magnitudes of the suppressed and favored amplitudes, R, is sufficiently small (predicted to be about 0.02), that $\mathcal{O}(R^2)$ terms can be neglected, and the sine terms give sensitivity to the combination of UT angles $2\beta + \gamma$.

As described in Sec. VI. B. 6, the averages are given in terms of the parameters a and c of Eq. (129). CP violation would appear as $a \neq 0$. Results for the $D^\mp\pi^\pm$ mode are available from *BABAR*, Belle and LHCb, while for $D^{*\mp}\pi^\pm$ *BABAR* and Belle have results with both full and partial reconstruction techniques. Results are also available from *BABAR* using $D^\mp\rho^\pm$. These results, and their averages, are listed in Table 50 and shown in Fig. 37. It is notable that the average value of a from $D^*\pi$ is more than 3σ from zero, providing evidence of CP violation in this channel.

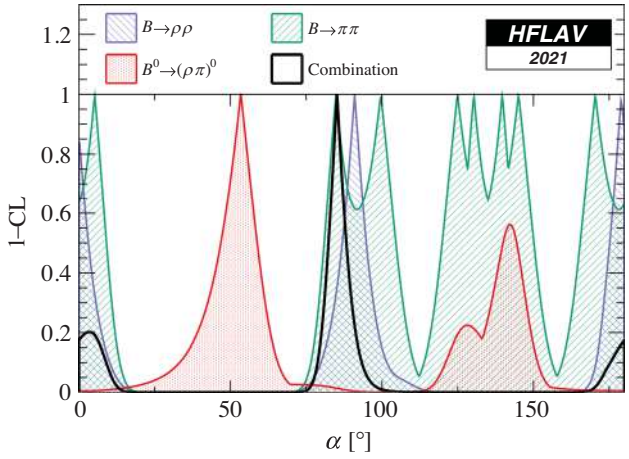

FIG. 36. World average of $\alpha \equiv \phi_2$, in terms of 1−CL, split by decay mode.

For each mode, $D\pi$, $D^*\pi$ and $D\rho$, there are two measurements (a and c, or S^+ and S^-) that depend on three unknowns (R, δ and $2\beta + \gamma$), of which two are different for each decay mode. Therefore, there is not enough information to solve directly for $2\beta + \gamma$. Constraints can be obtained if one is willing to use theoretical input on the values of R and/or δ. One popular choice is the use of SU(3) symmetry to obtain R by relating the suppressed decay mode to B decays involving D_s mesons. More details can be found in Refs. [286,434–437].

N. Time-dependent CP asymmetries in $b \to c\bar{u}s/u\bar{c}s$ transitions

1. Time-dependent CP asymmetries in $B^0 \to D^\mp K^0_S\pi^\pm$

Time-dependent analyses of transitions such as $B^0 \to D^\mp K^0_S\pi^\pm$ can be used to probe $\sin(2\beta + \gamma)$ in a similar way to that discussed above (Sec. VI M). Since the final state contains three particles, a Dalitz-plot analysis is necessary to maximize the sensitivity. *BABAR* [438] has carried out such an analysis, finding $2\beta + \gamma = (83 \pm 53 \pm 20)^\circ$ (with an ambiguity $2\beta + \gamma \leftrightarrow 2\beta + \gamma + \pi$) assuming the ratio of the $b \to u$ and $b \to c$ amplitude to be constant across the Dalitz plot at 0.3.

2. Time-dependent CP asymmetries in $B^0_s \to D^\mp_s K^\pm$ and similar modes

Time-dependent analysis of $B^0_s \to D^\mp_s K^\pm$ decays can be used to determine $\gamma - 2\beta_s$ [439,440]. Compared to the situation for $B^0 \to D^{(*)\mp}\pi^\pm$ decays discussed in Sec. VI M, the larger value of the ratio R of the magnitudes of the suppressed and favored amplitudes allows it to be determined from the data. Moreover, the nonzero value of $\Delta\Gamma_s$

TABLE 50. Averages for $b \to c\bar{u}d/u\bar{c}d$ modes.

Experiment		Sample size	a	c	Correlation
			$D^{\mp}\pi^{\pm}$		
BABAR (full rec.)	[281]	$N(B\bar{B}) = 232$M	$-0.010 \pm 0.023 \pm 0.007$	$-0.033 \pm 0.042 \pm 0.012$	⋯
Belle (full rec.)	[285]	$N(B\bar{B}) = 386$M	$-0.050 \pm 0.021 \pm 0.012$	$0.019 \pm 0.021 \pm 0.012$	⋯
LHCb	[287]	$\int \mathcal{L}dt = 3.0$ fb^{-1}	$-0.048 \pm 0.018 \pm 0.005$	$0.010 \pm 0.009 \pm 0.008$	-0.46 (syst)
Average			-0.038 ± 0.013	0.009 ± 0.010	-0.05
Confidence level			$0.56(0.6\sigma)$		
			$D^{*\mp}\pi^{\pm}$		
BABAR (full rec.)	[281]	$N(B\bar{B}) = 232$M	$-0.040 \pm 0.023 \pm 0.010$	$0.049 \pm 0.042 \pm 0.015$	
BABAR (partial rec.)	[282]	$N(B\bar{B}) = 232$M	$-0.034 \pm 0.014 \pm 0.009$	$-0.019 \pm 0.022 \pm 0.013$	
Belle (full rec.)	[285]	$N(B\bar{B}) = 386$M	$-0.039 \pm 0.020 \pm 0.013$	$-0.011 \pm 0.020 \pm 0.013$	
Belle (partial rec.)	[284]	$N(B\bar{B}) = 657$M	$-0.046 \pm 0.013 \pm 0.015$	$-0.015 \pm 0.013 \pm 0.015$	
Average			-0.039 ± 0.010	-0.010 ± 0.013	
Confidence level			$0.97(0.03\sigma)$	$0.59(0.6\sigma)$	
			$D^{\mp}\rho^{\pm}$		
BABAR (full rec.)	[281]	$N(B\bar{B}) = 232$M	$-0.024 \pm 0.031 \pm 0.009$	$-0.098 \pm 0.055 \pm 0.018$	

allows the determination of additional terms, labeled $A^{\Delta\Gamma}$ and $\bar{A}^{\Delta\Gamma}$, that break ambiguities in the solutions for $\gamma - 2\beta_s$.

A similar analysis can also be done with $B_s^0 \to D_s^{\mp}K^{\pm}\pi^+\pi^-$ decays. In this case the quasi-two-body parameters are effective parameters, integrated over the phase space of the decay.

LHCb [289] has measured the time-dependent CP violation parameters in $B_s^0 \to D_s^{\mp}K^{\pm}$ decays, using 3.0 fb^{-1} of data. The results are given in Table 51, and correspond to 3.8σ evidence for CP violation in the interference between mixing and $B_s^0 \to D_s^{\mp}K^{\pm}$ decays. From these results, and the world average constraint on $2\beta_s$ [441], LHCb determine $\gamma = (128^{+17}_{-22})°$, $\delta_{D_sK} = (358^{+13}_{-14})°$ and $R_{D_sK} = 0.37^{+0.10}_{-0.09}$.

LHCb [200] has also measured the time-dependent CP violation parameters in $B_s^0 \to D_s^{\mp}K^{\pm}\pi^+\pi^-$ decays. Both model-dependent and -independent analysis have been performed; results for the latter are quoted in Table 51. From these results, LHCb determine $\gamma = (44 \pm 12)°$.

O. Rates and asymmetries in $B \to D^{(*)}K^{(*)}$ decays

As explained in Sec. VI B 7, rates and asymmetries in $B^+ \to D^{(*)}K^{(*)+}$ decays are sensitive to γ, and have

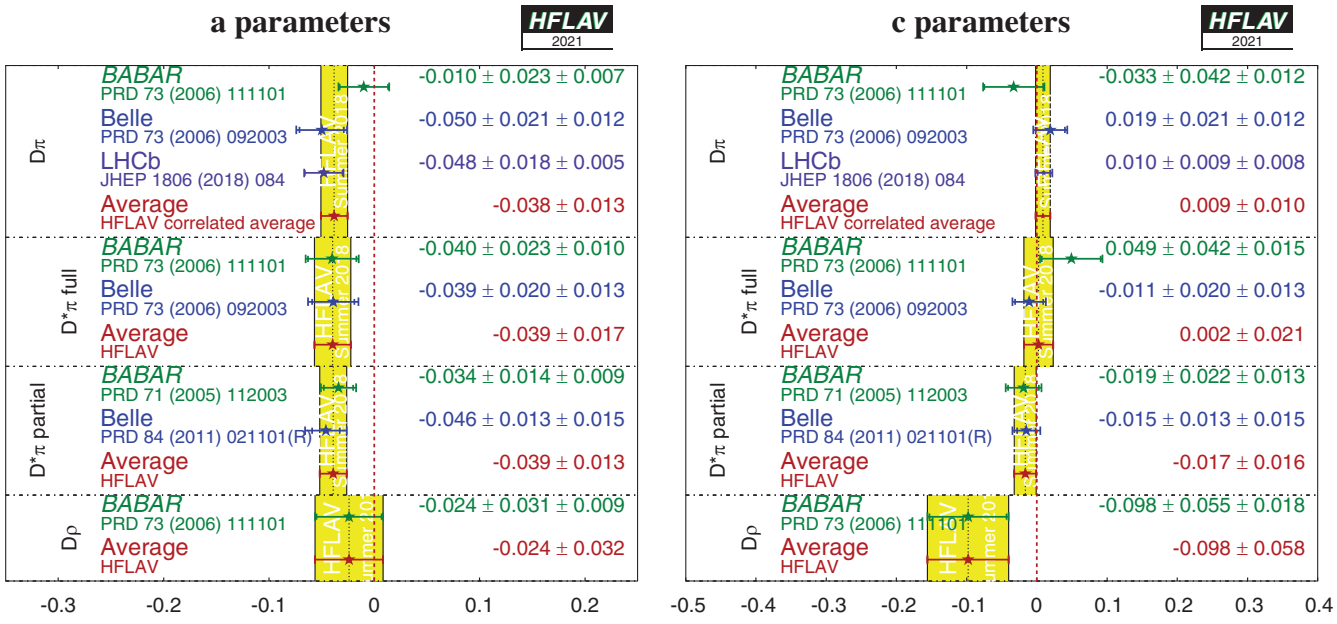

FIG. 37. Averages for $b \to c\bar{u}d/u\bar{c}d$ modes.

TABLE 51. Results for $B_s^0 \to D_s^{\mp} K^{\pm}$ and $D_s^{\mp} K^{\pm}\pi^+\pi^-$.

Experiment		$\int \mathcal{L}\,dt$	C	$A^{\Delta\Gamma}$	$\bar{A}^{\Delta\Gamma}$	S	$\bar{S}$
				$B_s^0 \to D_s^{\mp} K^{\pm}$			
LHCb	[289]	3 fb^{-1}	$0.73 \pm 0.14 \pm 0.05$	$0.39 \pm 0.28 \pm 0.15$	$0.31 \pm 0.28 \pm 0.15$	$-0.52 \pm 0.20 \pm 0.07$	$-0.49 \pm 0.20 \pm 0.07$
				$B_s^0 \to D_s^{\mp} K^{\pm}\pi^+\pi^-$			
LHCb	[200]	9 fb^{-1}	$0.631 \pm 0.096 \pm 0.032$	$-0.334 \pm 0.232 \pm 0.097$	$-0.695 \pm 0.215 \pm 0.081$	$-0.424 \pm 0.135 \pm 0.033$	$-0.463 \pm 0.134 \pm 0.031$

TABLE 52. Averages from GLW analyses of $b \to c\bar{u}s/u\bar{c}s$ modes. The sample size is given in terms of number of $B\bar{B}$ pairs, $N(B\bar{B})$, for the e^+e^- B factory experiments *BABAR* and Belle, and in terms of integrated luminosity, $\int \mathcal{L}\,dt$, for the hadron collider experiments CDF and LHCb.

Experiment		Sample size $N(B\bar{B})$ or $\int \mathcal{L}dt$	A_{CP+}	A_{CP-}	R_{CP+}	R_{CP-}
				$B^+ \to D_{CP}K^+$		
BABAR	[443]	467M	$0.25 \pm 0.06 \pm 0.02$	$-0.09 \pm 0.07 \pm 0.02$	$1.18 \pm 0.09 \pm 0.05$	$1.07 \pm 0.08 \pm 0.04$
Belle	[444]	275M	$0.06 \pm 0.14 \pm 0.05$	$-0.12 \pm 0.14 \pm 0.05$	$1.13 \pm 0.16 \pm 0.08$	$1.17 \pm 0.14 \pm 0.14$
CDF	[445]	1 fb^{-1}	$0.39 \pm 0.17 \pm 0.04$	…	$1.30 \pm 0.24 \pm 0.12$	…
LHCb	[446]	8.7 fb^{-1}	$0.136 \pm 0.009 \pm 0.001$	…	$0.950 \pm 0.009 \pm 0.010$	…
Average			0.139 ± 0.009	-0.096 ± 0.065	0.956 ± 0.013	1.087 ± 0.082
Confidence level			$0.14(1.5\sigma)$	$0.86(0.2\sigma)$	$0.06(1.9\sigma)$	$0.65(0.5\sigma)$
				$B^+ \to D^*_{CP}K^+$		
BABAR	[447]	383M	$-0.11 \pm 0.09 \pm 0.01$	$0.06 \pm 0.10 \pm 0.02$	$1.31 \pm 0.13 \pm 0.03$	$1.09 \pm 0.12 \pm 0.04$
Belle	[444]	275M	$-0.20 \pm 0.22 \pm 0.04$	$0.13 \pm 0.30 \pm 0.08$	$1.41 \pm 0.25 \pm 0.06$	$1.15 \pm 0.31 \pm 0.12$
LHCb	[446]	8.7 fb^{-1}	$-0.115 \pm 0.019 \pm 0.009$	$0.123 \pm 0.054 \pm 0.031$	$1.051 \pm 0.022 \pm 0.028$	$0.952 \pm 0.062 \pm 0.065$
Average			-0.109 ± 0.019	0.096 ± 0.052	1.077 ± 0.034	1.011 ± 0.071
Confidence level				$0.59(0.5\sigma)$		
				$B^+ \to D_{CP}K^{*+}$		
BABAR	[448]	379M	$0.09 \pm 0.13 \pm 0.06$	$-0.23 \pm 0.21 \pm 0.07$	$2.17 \pm 0.35 \pm 0.09$	$1.03 \pm 0.27 \pm 0.13$
LHCb KK	[449]	4.8 fb^{-1}	$0.06 \pm 0.07 \pm 0.01$	…	$1.22 \pm 0.09 \pm 0.01$	…
LHCb $\pi\pi$	[449]	4.8 fb^{-1}	$0.15 \pm 0.13 \pm 0.02$	…	$1.08 \pm 0.14 \pm 0.03$	…
LHCb average	[449]	4.8 fb^{-1}	$0.08 \pm 0.06 \pm 0.01$	…	$1.18 \pm 0.08 \pm 0.02$	…
Average			0.08 ± 0.06	-0.23 ± 0.22	1.22 ± 0.07	1.03 ± 0.30
Confidence level			$0.83(0.2\sigma)$		$0.02(2.3\sigma)$	
				$B^+ \to D_{CP}K^+\pi^+\pi^-$		
LHCb KK	[450]	3 fb^{-1}	$-0.045 \pm 0.064 \pm 0.011$	…	$1.043 \pm 0.069 \pm 0.034$	…
LHCb $\pi\pi$	[450]	3 fb^{-1}	$-0.054 \pm 0.101 \pm 0.011$	…	$1.035 \pm 0.108 \pm 0.038$	…
LHCb average	[450]	3 fb^{-1}	-0.048 ± 0.055	…	1.040 ± 0.064	…
				$B^0 \to D_{CP}K^{*0}$		
LHCb KK	[451]	4.8 fb^{-1}	$-0.05 \pm 0.10 \pm 0.01$	…	$0.92 \pm 0.10 \pm 0.02$	…
LHCb $\pi\pi$	[451]	4.8 fb^{-1}	$-0.18 \pm 0.14 \pm 0.01$	…	$1.32 \pm 0.19 \pm 0.03$	…

negligible theoretical uncertainty [304]. Various methods using different $D^{(*)}$ final states have been used.

1. D decays to CP eigenstates

Results are available from *BABAR*, Belle, CDF and LHCb on GLW analyses in the decay mode $B^+ \to DK^+$. All experiments use the CP-even D decay final states K^+K^- and $\pi^+\pi^-$; *BABAR* and Belle in addition use the CP-odd decay modes $K^0_S\pi^0$, $K^0_S\omega$ and $K^0_S\phi$, though care is taken to avoid statistical overlap with the $K^0_SK^+K^-$ sample used for Dalitz plot analyses (see Sec. VI O 4). *BABAR* and Belle also have results in the decay mode $B^+ \to D^*K^+$, using both the $D^* \to D\pi^0$ decay, for which $CP(D^*) = CP(D)$, and the $D^* \to D\gamma$ decay, for which $CP(D^*) = -CP(D)$. LHCb also has results in the $B^+ \to D^*K^+$ decay mode, exploiting a partial reconstruction technique in which the π^0 or γ produced in the D^* decay is not explicitly reconstructed. Results obtained with this technique have significant correlations, and therefore a correlated average is performed for the $B^+ \to D^*K^+$ observables. In addition, *BABAR* and LHCb have results in the decay mode $B^+ \to DK^{*+}$, and LHCb has results in the decay mode $B^+ \to DK^+\pi^+\pi^-$. In many cases LHCb presents results

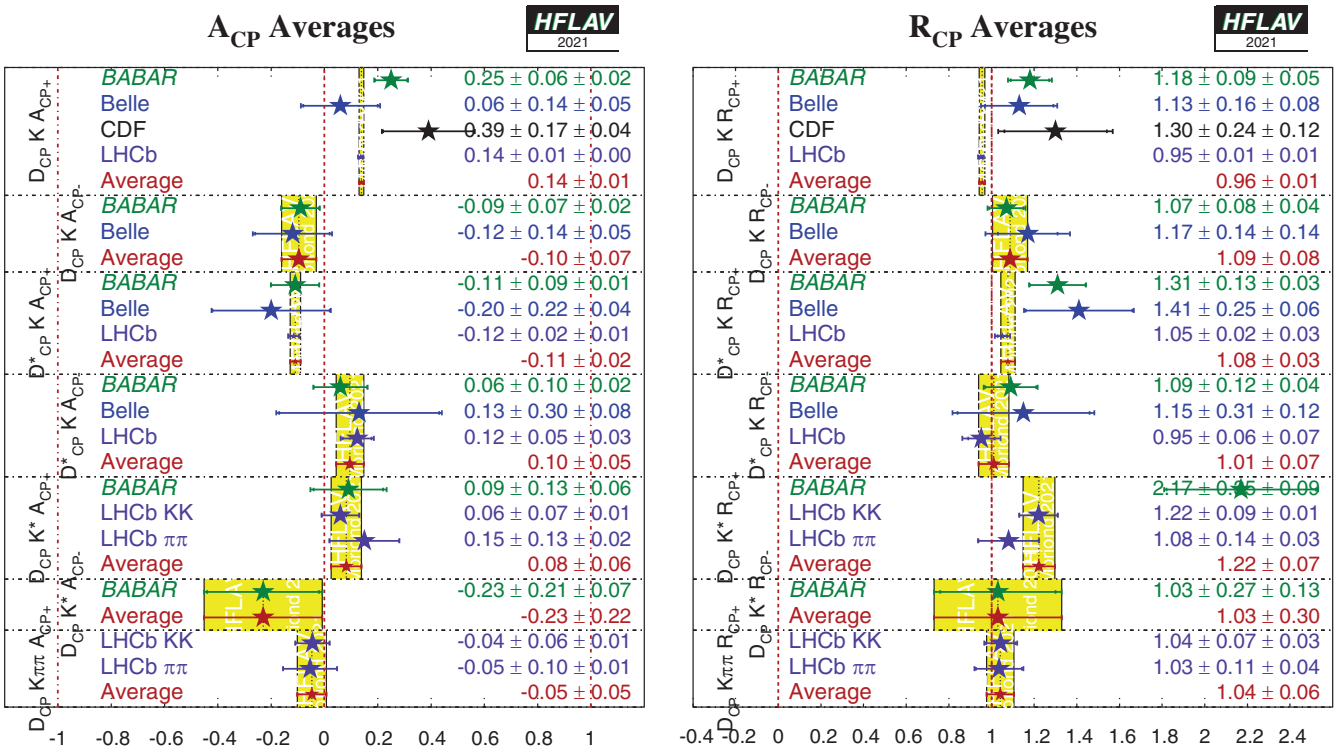

FIG. 38. Averages of A_{CP} and R_{CP} from GLW analyses.

separately for the cases of D decay to K^+K^- and $\pi^+\pi^-$ to allow for possible effects related to D^0–$\bar{D}^0$ mixing and CP violation in charm decays [442], which, however, are known to be small and are neglected in our averages. These separate results are presented together with their combination, as provided in the LHCb publications, where possible. The results and averages are given in Table 52 and shown in Fig. 38. LHCb has performed a GLW analysis using the $B^0 \to DK^{*0}$ decay with the CP-even $D \to K^+K^-$ and $D \to \pi^+\pi^-$ channels, which are also included in Table 52.

As pointed out in Refs. [307,308], a Dalitz plot analysis of $B^0 \to DK^+\pi^-$ decays provides more sensitivity to $\gamma \equiv \phi_3$ than the Q2B DK^{*0} approach. The analysis provides direct sensitivity to the hadronic parameters r_B and δ_B associated with the $B^0 \to DK^{*0}$ decay amplitudes, rather than effective hadronic parameters averaged over the K^{*0} selection window as in the Q2B case.

Such an analysis has been performed by LHCb. A simultaneous fit is performed to the $B^0 \to DK^+\pi^-$ Dalitz plots with the neutral D meson reconstructed in the $K^+\pi^-$, K^+K^- and $\pi^+\pi^-$ final states. The reported results in Table 53 are for the Cartesian parameters, defined in Eq. (144) associated with the $B^0 \to DK^*(892)^0$ decay. Note that, since the measurements use overlapping data samples, these results cannot be combined with the LHCb results for GLW observables in $B^0 \to DK^*(892)^0$ decays reported in Table 52.

LHCb uses the results of the $B^0 \to DK^+\pi^-$ Dalitz analysis to obtain confidence levels for γ, $r_B(DK^{*0})$ and $\delta_B(DK^{*0})$. In addition, results are reported for the hadronic parameters needed to relate these results to Q2B measurements of $B^0 \to DK^*(892)^0$ decays, where a selection window of $m(K^+\pi^-)$ within 50 MeV/c^2 of the pole mass and helicity angle satisfying $|\cos(\theta_{K^{*0}})| > 0.4$ is assumed. These parameters are the coherence factor κ, the ratio of Q2B and amplitude level r_B values, $\bar{R}_B = \bar{r}_B/r_B$, and the difference between Q2B and amplitude level δ_B values, $\Delta\bar{\delta}_B = \bar{\delta}_B - \delta_B$. LHCb [452] obtains

$$\kappa = 0.958^{+0.005+0.002}_{-0.010-0.045}, \qquad \bar{R}_B = 1.02^{+0.03}_{-0.01} \pm 0.06,$$
$$\Delta\bar{\delta}_B = 0.02^{+0.03}_{-0.02} \pm 0.11. \tag{159}$$

TABLE 53. Results from Dalitz plot analysis of $B^0 \to DK^+\pi^-$ decays with $D \to K^+K^-$ and $\pi^+\pi^-$.

Experiment	$\int \mathcal{L}\,dt$	x_+	y_+	x_-	y_-
LHCb [452]	3 fb^{-1}	$0.04 \pm 0.16 \pm 0.11$	$-0.47 \pm 0.28 \pm 0.22$	$-0.02 \pm 0.13 \pm 0.14$	$-0.35 \pm 0.26 \pm 0.41$

TABLE 54. Averages from GLW-like analyses of $b \to c\bar{u}s/u\bar{c}s$ modes.

Experiment		Sample size	$A_{\rm qGLW}$	$R_{\rm qGLW}$
		$D_{\pi^+\pi^-\pi^0}K^+$		
LHCb	[454]	$\int \mathcal{L}\,dt = 3$ fb^{-1}	$0.05 \pm 0.09 \pm 0.01$	$0.98 \pm 0.11 \pm 0.05$
BABAR	[317]	$N(B\bar{B}) = 324$M	$-0.02 \pm 0.15 \pm 0.03$	⋯
Average			0.03 ± 0.08	0.98 ± 0.12
Confidence level			$0.68(0.4\sigma)$	⋯
		$D_{K^+K^-\pi^0}K^+$		
LHCb	[454]	$\int \mathcal{L}\,dt = 3$ fb^{-1}	$0.30 \pm 0.20 \pm 0.02$	$0.95 \pm 0.22 \pm 0.04$
		$D_{\pi^+\pi^-\pi^+\pi^-}K^+$		
LHCb	[455]	$\int \mathcal{L}\,dt = 3$ fb^{-1}	$0.10 \pm 0.03 \pm 0.02$	$0.97 \pm 0.04 \pm 0.02$
		$D_{\pi^+\pi^-\pi^+\pi^-}K^{*+}$		
LHCb	[449]	$\int \mathcal{L}\,dt = 4.8$ fb^{-1}	$0.02 \pm 0.11 \pm 0.01$	$1.08 \pm 0.13 \pm 0.03$
		$D_{\pi^+\pi^-\pi^+\pi^-}K^{*0}$		
LHCb	[451]	$\int \mathcal{L}\,dt = 1.8$ fb^{-1}	$-0.03 \pm 0.15 \pm 0.01$	$1.01 \pm 0.16 \pm 0.04$

2. D decays to quasi-CP eigenstates

As discussed in Sec. VI B 7, if a multibody neutral D meson decay can be shown to be dominated by one CP eigenstate, it can be used in a "GLW-like" (sometimes called "quasi-GLW") analysis [313]. The same observables R_{CP}, A_{CP} as for the GLW case are measured, but an additional factor of $(2F_+ - 1)$, where F_+ is the fractional CP-even content, enters the expressions relating these observables to $\gamma \equiv \phi_3$. The F_+ factors have been measured using CLEO-c data to be $F_+(\pi^+\pi^-\pi^0) = 0.973 \pm 0.017$, $F_+(K^+K^-\pi^0) = 0.732 \pm 0.055$, $F_+(\pi^+\pi^-\pi^+\pi^-) = 0.737 \pm 0.028$ [453].

The GLW-like observables for $B^+ \to DK^+$ with $D \to \pi^+\pi^-\pi^0$, $K^+K^-\pi^0$ and $D \to \pi^+\pi^-\pi^+\pi^-$ have been measured by LHCb. The $A_{\rm qGLW}$ observable for $B^+ \to DK^+$ with $D \to \pi^+\pi^-\pi^0$ was measured in an earlier analysis by *BABAR*, from which additional observables, discussed in Sec. VI B 7 and reported in Table 58 below, were reported. The observables for $B^+ \to DK^{*+}$ and $B^0 \to DK^{*0}$ with $D \to \pi^+\pi^-\pi^+\pi^-$ have also been measured by LHCb. The results are given in Table 54.

3. D decays to suppressed final states

For ADS analyses, all of *BABAR*, Belle, CDF and LHCb have studied the modes $B^+ \to DK^+$ and $B^+ \to D\pi^+$. *BABAR* has also analyzed the $B^+ \to D^*K^+$ mode with full reconstruction of the D^* decay, while LHCb have studied the same B^+ decay with a partial reconstruction technique. There is an effective shift of π in the strong phase difference between the cases that the D^* is reconstructed as $D\pi^0$ and $D\gamma$ [310], therefore these modes are studied separately. In addition, both *BABAR* and LHCb have studied the $B^+ \to DK^{*+}$ mode, where K^{*+} is reconstructed as $K^0_S\pi^+$, and LHCb has studied the $B^+ \to DK^+\pi^+\pi^-$ mode. In all the above cases the suppressed decay $D \to K^-\pi^+$ has been used. *BABAR*, Belle and LHCb also have results using $B^+ \to DK^+$ with $D \to K^-\pi^+\pi^0$, while LHCb has results using $B^+ \to DK^+$ with $D \to K^-\pi^+\pi^+\pi^-$. The results and averages are given in Table 55 and shown in Fig. 39.

Similar phenomenology as for $B \to DK$ decays holds for $B \to D\pi$ decays, although in this case the interference is between $b \to c\bar{u}d$ and $b \to u\bar{c}d$ transitions, and the ratio of suppressed to favored amplitudes is expected to be much smaller, $\mathcal{O}(1\%)$. For most D meson final states this implies that the interference effect is too small to be of interest, but in the case of the ADS analysis it is possible that effects due to γ may be observable. Accordingly, the experiments now measure the corresponding observables in the $D\pi$ final states. The results and averages are given in Table 56 and shown in Fig. 40.

BABAR, Belle and LHCb have also presented results from a similar analysis method with self-tagging neutral B decays: $B^0 \to DK^{*0}$ with $D \to K^-\pi^+$ (all), $D \to K^-\pi^+\pi^0$ (*BABAR* only) and $D \to K^-\pi^+\pi^+\pi^-$ (*BABAR* and LHCb). All these results are obtained with the $K^{*0} \to K^+\pi^-$ decay. Effects due to the natural width of the K^{*0} are handled using the parametrization suggested by Gronau [305].

The following 95% CL limits are set by *BABAR* [461]:

$$R_{\rm ADS}(K\pi) < 0.244 \qquad R_{\rm ADS}(K\pi\pi^0) < 0.181$$
$$R_{\rm ADS}(K\pi\pi\pi) < 0.391, \tag{160}$$

while Belle [462] obtains

$$R_{\rm ADS}(K\pi) < 0.16. \tag{161}$$

The results from LHCb, which are presented in terms of the parameters R_+ and R_- instead of $R_{\rm ADS}$ and $A_{\rm ADS}$, are given in Table 57.

TABLE 55. Averages from ADS analyses of $b \to c\bar{u}s/u\bar{c}s$ modes.

Experiment		Sample size $N(B\bar{B})$ or $\int \mathcal{L}dt$	$A_{\rm ADS}$	$R_{\rm ADS}$
		DK^+, $D \to K^-\pi^+$		
BABAR	[456]	467M	$-0.86 \pm 0.47^{+0.12}_{-0.16}$	$0.011 \pm 0.006 \pm 0.002$
Belle	[457]	772M	$-0.39^{+0.26\,+0.04}_{-0.28\,-0.03}$	$0.0163^{+0.0044\,+0.0007}_{-0.0041\,-0.0013}$
CDF	[458]	7 fb^{-1}	$-0.82 \pm 0.44 \pm 0.09$	$0.0220 \pm 0.0086 \pm 0.0026$
LHCb	[446]	8.7 fb^{-1}	-0.451 ± 0.026	0.0173 ± 0.0006
Average			-0.453 ± 0.026	0.0172 ± 0.0006
Confidence level			$0.70(0.4\sigma)$	$0.73(0.4\sigma)$
		DK^+, $D \to K^-\pi^+\pi^0$		
BABAR	[459]	474M	–	$0.0091^{+0.0082\,+0.0014}_{-0.0076\,-0.0037}$
Belle	[460]	772M	$0.41 \pm 0.30 \pm 0.05$	$0.0198 \pm 0.0062 \pm 0.0024$
LHCb	[454]	3 fb^{-1}	$-0.20 \pm 0.27 \pm 0.03$	$0.0140 \pm 0.0047 \pm 0.0019$
Average			0.07 ± 0.20	0.0148 ± 0.0036
Confidence level			$0.13(1.5\sigma)$	$0.59(0.5\sigma)$
		DK^+, $D \to K^-\pi^+\pi^+\pi^-$		
LHCb	[455]	3 fb^{-1}	$-0.313 \pm 0.102 \pm 0.038$	$0.0140 \pm 0.0015 \pm 0.0006$
		D^*K^+, $D^* \to D\pi^0$, $D \to K^-\pi^+$		
BABAR	[456]	467M	$0.77 \pm 0.35 \pm 0.12$	$0.018 \pm 0.009 \pm 0.004$
LHCb	[446]	8.7 fb^{-1}	0.717 ± 0.286	0.0118 ± 0.0034
Average			0.74 ± 0.23	0.0125 ± 0.0032
Confidence level			$0.91(0.1\sigma)$	$0.55(0.6\sigma)$
		D^*K^+, $D^* \to D\gamma$, $D \to K^-\pi^+$		
BABAR	[456]	467M	$0.36 \pm 0.94^{+0.25}_{-0.41}$	$0.013 \pm 0.014 \pm 0.008$
LHCb	[446]	8.7 fb^{-1}	-0.558 ± 1.349	0.0163 ± 0.0373
Average			0.03 ± 0.81	0.0135 ± 0.0148
Confidence level			$0.59(0.6\sigma)$	$0.94(0.1\sigma)$
		DK^{*+}, $D \to K^-\pi^+$, $K^{*+} \to K^0_S\pi^+$		
BABAR	[448]	379M	$-0.34 \pm 0.43 \pm 0.16$	$0.066 \pm 0.031 \pm 0.010$
LHCb	[449]	4.8 fb^{-1}	$-0.81 \pm 0.17 \pm 0.04$	$0.011 \pm 0.004 \pm 0.001$
Average			-0.75 ± 0.16	0.012 ± 0.004
Confidence level			$0.34(1.0\sigma)$	$0.09(1.7\sigma)$
		DK^{*+}, $D \to K^-\pi^+\pi^+\pi^-$, $K^{*+} \to K^0_S\pi^+$		
LHCb	[449]	4.8 fb^{-1}	$-0.45 \pm 0.21 \pm 0.14$	$0.011 \pm 0.005 \pm 0.003$
		$DK^+\pi^+\pi^-$, $D \to K^-\pi^+$		
LHCb	[450]	3 fb^{-1}	$-0.32^{+0.27}_{-0.34}$	$0.0082^{+0.0038}_{-0.0030}$

Combining the results and using additional input from CLEO [463,464] a limit on the ratio between the $b \to u$ and $b \to c$ amplitudes of $\bar{r}_B(DK^{*0}) \in [0.07, 0.41]$ at 95% CL limit is set by *BABAR*. Belle sets a limit of $\bar{r}_B < 0.4$ at 95% CL LHCb, combining all results on $B^0 \to DK^{*0}$ decays, obtains $\bar{r}_B = 0.265 \pm 0.023$.

4. D decays to multiparticle self-conjugate final states (model-dependent analysis)

For the model-dependent Dalitz plot analysis, both *BABAR* and Belle have studied the modes $B^+ \to DK^+$, $B^+ \to D^*K^+$ and $B^+ \to DK^{*+}$. For $B^+ \to D^*K^+$, both experiments have used both D^* decay modes, $D^* \to D\pi^0$ and $D^* \to D\gamma$, taking the effective shift in the strong phase difference into account.[31] In all cases the decay $D \to K^0_S\pi^+\pi^-$ has been used. *BABAR* also used the decay $D \to K^0_SK^+K^-$. LHCb has also studied $B^+ \to DK^+$ decays with $D \to K^0_S\pi^+\pi^-$. *BABAR* has also performed an analysis of $B^+ \to DK^+$ with $D \to \pi^+\pi^-\pi^0$. Results and averages

[31]Belle [465] quotes separate results for $B^+ \to D^*K^+$ with $D^* \to D\pi^0$ and $D^* \to D\gamma$. The results presented in Table 58 are from our average, performed using the statistical correlations provided, and neglecting all systematic correlations; model uncertainties are not included. The first uncertainty on the given results is combined statistical and systematic, the second is the model error (taken from the Belle results on $B^+ \to D^*K^+$ with $D^* \to D\pi^0$).

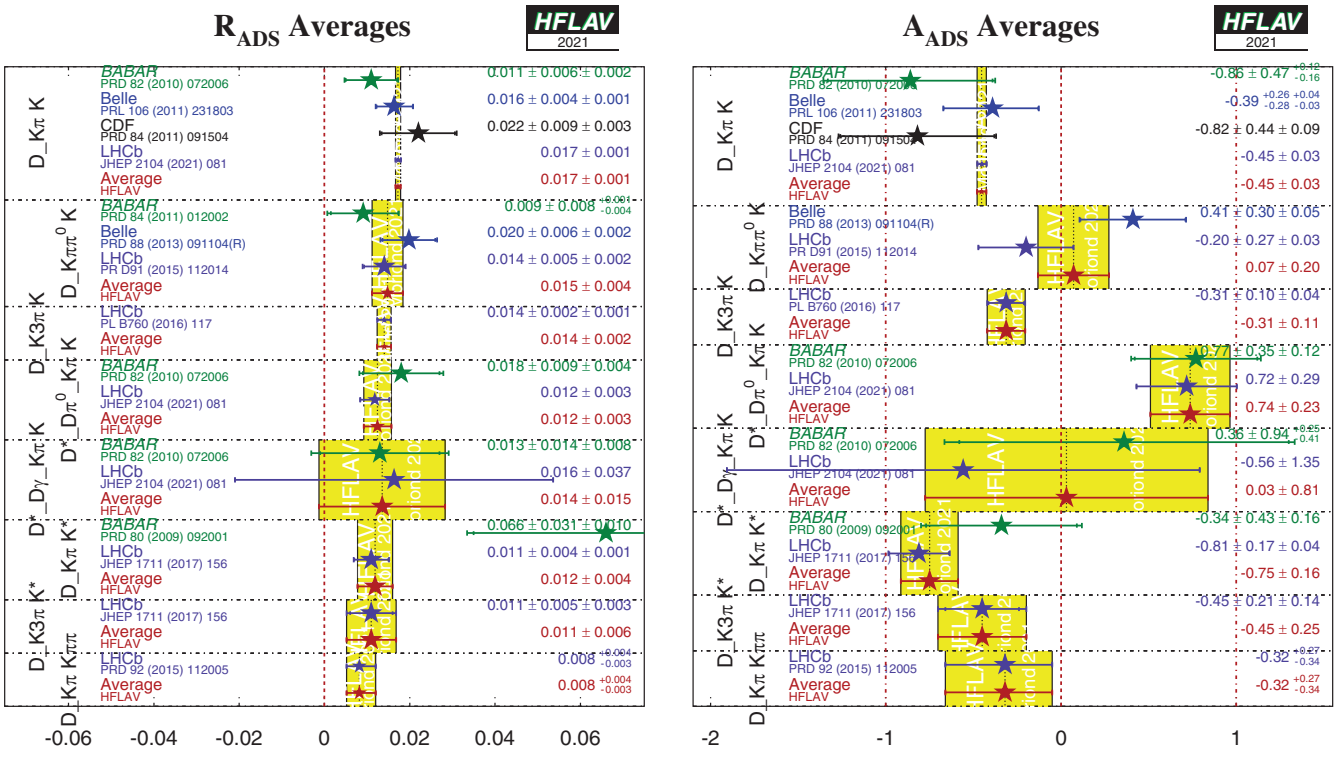

FIG. 39. Averages of $R_{\rm ADS}$ and $A_{\rm ADS}$ for $B \to D^{(*)}K^{(*)}$ decays.

TABLE 56. Averages from ADS analyses of $b \to c\bar{u}d/u\bar{c}d$ modes.

Experiment		Sample size $N(B\bar{B})$ or $\int \mathcal{L}\,dt$	$A_{\rm ADS}$	$R_{\rm ADS}$
		$D\pi^+$, $D \to K^-\pi^+$		
BABAR	[456]	467M	$0.03 \pm 0.17 \pm 0.04$	$0.0033 \pm 0.0006 \pm 0.0004$
Belle	[457]	772M	$-0.04 \pm 0.11^{+0.02}_{-0.01}$	$0.00328^{+0.00038\ +0.00012}_{-0.00036\ -0.00018}$
CDF	[458]	7 fb^{-1}	$0.13 \pm 0.25 \pm 0.02$	$0.0028 \pm 0.0007 \pm 0.0004$
LHCb	[446]	8.7 fb^{-1}	0.129 ± 0.014	0.00368 ± 0.00007
Average			0.126 ± 0.014	0.00366 ± 0.00007
Confidence level			$0.47(0.7\sigma)$	$0.50(0.7\sigma)$
		$D\pi^+$, $D \to K^-\pi^+\pi^0$		
Belle	[460]	772M	$0.16 \pm 0.27^{+0.03}_{-0.04}$	$0.00189 \pm 0.00054^{+0.00022}_{-0.00025}$
LHCb	[454]	3 fb^{-1}	$0.44 \pm 0.19 \pm 0.01$	$0.00235 \pm 0.00049 \pm 0.00004$
Average			0.35 ± 0.16	0.00216 ± 0.00038
Confidence level			$0.40(0.8\sigma)$	$0.55(0.6\sigma)$
		$D\pi^+$, $D \to K^-\pi^+\pi^+\pi^-$		
LHCb	[455]	3 fb^{-1}	$0.023 \pm 0.048 \pm 0.005$	$0.00377 \pm 0.00018 \pm 0.00006$
		$D^*\pi^+$, $D^* \to D\pi^0$, $D \to K^-\pi^+$		
BABAR	[456]	467M	$-0.09 \pm 0.27 \pm 0.05$	$0.0032 \pm 0.0009 \pm 0.0008$
LHCb	[446]	8.7 fb^{-1}	-0.140 ± 0.059	0.00471 ± 0.00077
Average			-0.138 ± 0.058	0.00427 ± 0.00065
Confidence level			$0.86(0.2\sigma)$	$0.29(1.1\sigma)$
		$D^*\pi^+$, $D^* \to D\gamma$, $D \to K^-\pi^+$		
BABAR	[456]	467M	$-0.65 \pm 0.55 \pm 0.22$	$0.0027 \pm 0.0014 \pm 0.0022$
LHCb	[446]	8.7 fb^{-1}	0.079 ± 0.128	0.00420 ± 0.00138
Average			0.046 ± 0.125	0.00387 ± 0.00122
Confidence level			$0.23(1.2\sigma)$	$0.61(0.5\sigma)$
		$D\pi^+\pi^+\pi^-$, $D \to K^-\pi^+$		
LHCb	[450]	3 fb^{-1}	-0.003 ± 0.090	0.00427 ± 0.00043

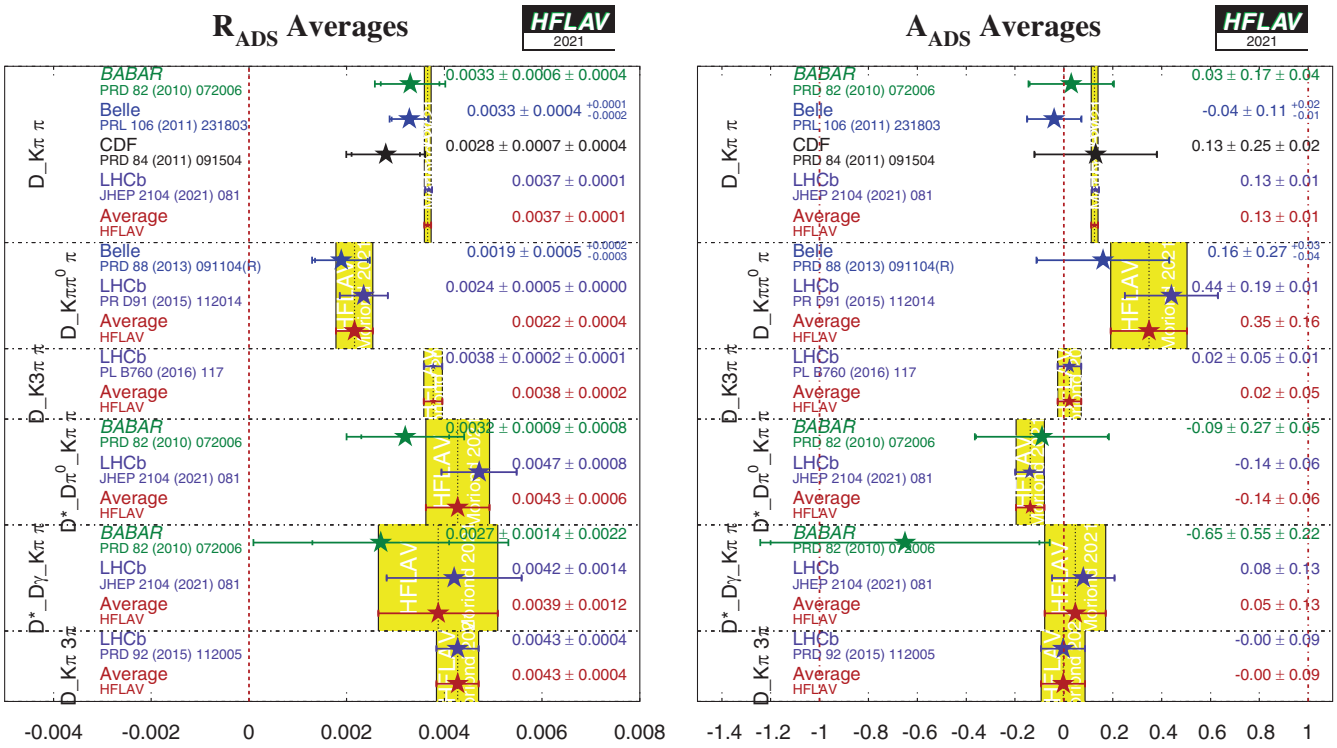

FIG. 40. Averages of $R_{\rm ADS}$ and $A_{\rm ADS}$ for $B \to D^{(*)}\pi$ decays.

are given in Table 58, and shown in Figs. 41 and 42. The third error on each measurement is due to D decay model uncertainty.

The parameters measured in the analyses are explained in Sec. VI B 7. All experiments measure the Cartesian variables, defined in Eq. (144), and perform frequentist statistical procedures, to convert these into measurements of γ, r_B and δ_B. In the $B^+ \to DK^+$ with $D \to \pi^+\pi^-\pi^0$ analysis, the parameters $(\rho^{\pm}, \theta^{\pm})$ are used instead.

In the $B^+ \to DK^{*+}$ analysis both *BABAR* and Belle experiments reconstruct K^{*+} as $K^0_S\pi^+$, but the treatment of possible nonresonant $K^0_S\pi^+$ differs: Belle assigns an additional model uncertainty, while *BABAR* uses a parametrization suggested by Gronau [305] in which the parameters r_B and δ_B are replaced with effective parameters $\kappa\bar{r}_B$ and $\bar{\delta}_B$. In this case no attempt is made to extract the true hadronic parameters of the $B^+ \to DK^{*+}$ decay.

We perform averages using the following procedure, which is based on a set of reasonable, though imperfect, assumptions.

(i) It is assumed that effects due to differences in the D decay models used by the two experiments are negligible. Therefore, we do not rescale the results to a common model.

(ii) It is further assumed that the D decay model uncertainty is 100% correlated between experiments. (This approximation is compromised by the fact that the *BABAR* results include $D \to K^0_S K^+ K^-$ decays in addition to $D \to K^0_S\pi^+\pi^-$.) Other than the D decay model, we do not consider common sources of systematic uncertainty.

(iii) We include in the average the effect of correlations within each experiment's set of measurements.

(iv) At present it is unclear how to assign a model uncertainty to the average. We have not attempted to do so. An unknown amount of model uncertainty should be added to the final uncertainty.

(v) We follow the suggestion of Gronau [305] in making the DK^* averages. Explicitly, we assume that the selection of $K^{*+} \to K^0_S\pi^+$ is the same across

TABLE 57. Results from ADS analysis of $B^0 \to DK^{*0}$.

Experiment		Sample size	R_+	R_-
		$D \to K^-\pi^+$		
LHCb	[451]	$\int \mathcal{L}\,dt = 4.8$ fb^{-1}	$0.064 \pm 0.021 \pm 0.002$	$0.095 \pm 0.021 \pm 0.003$
		$D \to K^-\pi^+\pi^+\pi^-$		
LHCb	[451]	$\int \mathcal{L}\,dt = 4.8$ fb^{-1}	$0.074 \pm 0.026 \pm 0.002$	$0.072 \pm 0.025 \pm 0.003$

TABLE 58. Averages from model-dependent Dalitz plot analyses of $b \to c\bar{u}s/u\bar{c}s$ modes. Note that the uncertainities assigned to the averages do not include model errors.

Experiment		Sample size	x_+	y_+	x_-	y_-
			DK^+, $D \to K^0_S\pi^+\pi^-$			
BABAR	[466]	$N(B\bar{B}) = 468$M	$-0.103 \pm 0.037 \pm 0.006 \pm 0.007$	$-0.021 \pm 0.048 \pm 0.004 \pm 0.009$	$0.060 \pm 0.039 \pm 0.007 \pm 0.006$	$0.062 \pm 0.045 \pm 0.004 \pm 0.006$
Belle	[465]	$N(B\bar{B}) = 657$M	$-0.107 \pm 0.043 \pm 0.011 \pm 0.055$	$-0.067 \pm 0.059 \pm 0.018 \pm 0.063$	$0.105 \pm 0.047 \pm 0.011 \pm 0.064$	$0.177 \pm 0.060 \pm 0.018 \pm 0.054$
LHCb	[467]	$\int \mathcal{L}\,dt = 1$ fb^{-1}	$-0.084 \pm 0.045 \pm 0.009 \pm 0.005$	$-0.032 \pm 0.048^{+0.010}_{-0.009} \pm 0.008$	$0.027 \pm 0.044^{+0.010}_{-0.008} \pm 0.001$	$0.013 \pm 0.048^{+0.009}_{-0.007} \pm 0.003$
Average			-0.098 ± 0.024	-0.036 ± 0.030	0.070 ± 0.025	0.075 ± 0.029
Confidence level				$0.52(0.7\sigma)$		
			D^*K^+, $D^* \to D\pi^0$ or $D\gamma$, $D \to K^0_S\pi^+\pi^-$			
BABAR	[466]	$N(B\bar{B}) = 468$M	$0.147 \pm 0.053 \pm 0.017 \pm 0.003$	$-0.032 \pm 0.077 \pm 0.008 \pm 0.006$	$-0.104 \pm 0.051 \pm 0.019 \pm 0.002$	$-0.052 \pm 0.063 \pm 0.009 \pm 0.007$
Belle	[465]	$N(B\bar{B}) = 657$M	$0.100 \pm 0.074 \pm 0.081$	$0.155 \pm 0.101 \pm 0.063$	$-0.023 \pm 0.112 \pm 0.090$	$-0.252 \pm 0.112 \pm 0.049$
Average			0.132 ± 0.044	0.037 ± 0.061	-0.081 ± 0.049	-0.107 ± 0.055
Confidence level				$0.22(1.2\sigma)$		
			DK^{*+}, $D \to K^0_S\pi^+\pi^-$			
BABAR	[466]	$N(B\bar{B}) = 468$M	$-0.151 \pm 0.083 \pm 0.029 \pm 0.006$	$0.045 \pm 0.106 \pm 0.036 \pm 0.008$	$0.075 \pm 0.096 \pm 0.029 \pm 0.007$	$0.127 \pm 0.095 \pm 0.027 \pm 0.006$
Belle	[468]	$N(B\bar{B}) = 386$M	$-0.105^{+0.177}_{-0.167} \pm 0.006 \pm 0.088$	$-0.004^{+0.164}_{-0.156} \pm 0.013 \pm 0.095$	$-0.784^{+0.249}_{-0.295} \pm 0.029 \pm 0.097$	$-0.281^{+0.440}_{-0.335} \pm 0.046 \pm 0.086$
Average			-0.152 ± 0.077	0.024 ± 0.091	-0.043 ± 0.094	0.091 ± 0.096
Confidence level				$0.011(2.5\sigma)$		
			DK^{*0}, $D \to K^0_S\pi^+\pi^-$, $K^{*0} \to K^+\pi^-$			
LHCb	[469]	$\int \mathcal{L}\,dt = 3$ fb^{-1}	$0.05 \pm 0.24 \pm 0.04 \pm 0.01$	$-0.65^{+0.24}_{-0.23} \pm 0.08 \pm 0.01$	$-0.15 \pm 0.14 \pm 0.03 \pm 0.01$	$0.25 \pm 0.15 \pm 0.06 \pm 0.01$
Experiment		$N(B\bar{B})$	ρ^+	θ^+	ρ^-	θ^-
			DK^+, $D \to \pi^+\pi^-\pi^0$			
BABAR	[317]	324M	$0.75 \pm 0.11 \pm 0.04$	$147 \pm 23 \pm 1$	$0.72 \pm 0.11 \pm 0.04$	$173 \pm 42 \pm 2$

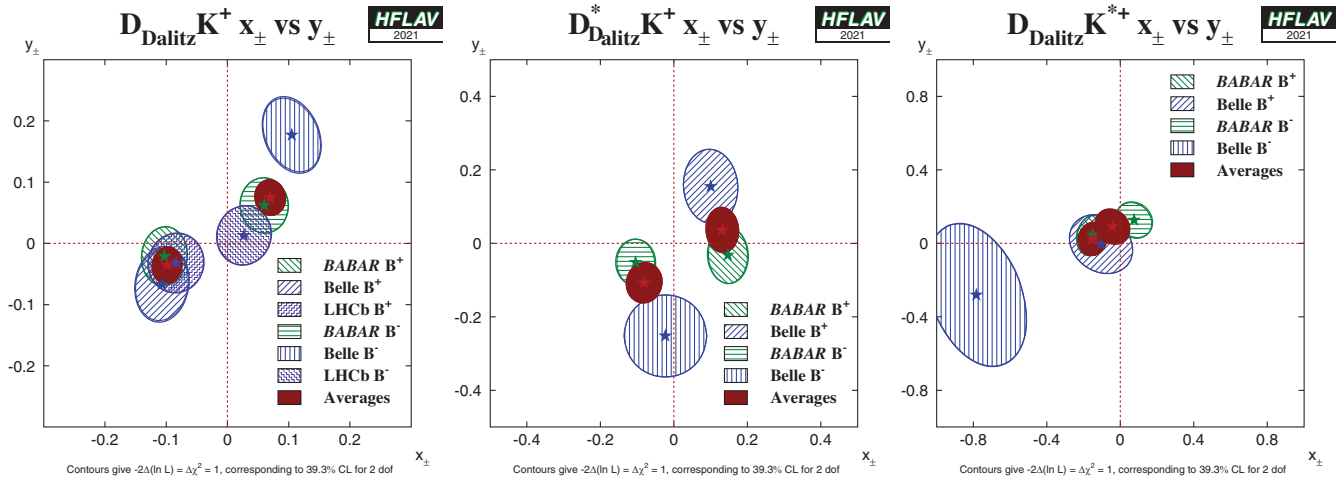

FIG. 41. Contours in the $(x_\pm, y_\pm)$ from model-dependent analysis of $B^+ \to D^{(*)}K^{(*)+}$, $D \to K^0_S h^+ h^-$ ($h = \pi, K$). Left: $B^+ \to DK^+$, (middle) $B^+ \to D^*K^+$, (right) $B^+ \to DK^{*+}$. Note that the uncertainties assigned to the averages given in these plots do not include model uncertainties.

experiments (so that κ, $\bar{r}_B$ and $\bar{\delta}_B$ are the same), and drop the additional source of model uncertainty assigned by Belle due to possible nonresonant decays.

Constraints on $\gamma \equiv \phi_3$

The measurements of $(x_\pm, y_\pm)$ can be used to obtain constraints on $\gamma \equiv \phi_3$, as well as the hadronic parameters r_B and δ_B. *BABAR* [466], Belle [465,468] and LHCb [467] have all done so using a frequentist procedure, with some differences in the details of the techniques used.

(i) *BABAR* obtains $\gamma = (68^{+15}_{-14} \pm 4 \pm 3)°$ from DK^+, D^*K^+ and DK^{*+}.
(ii) Belle obtains $\phi_3 = (78^{+11}_{-12} \pm 4 \pm 9)°$ from DK^+ and D^*K^+.
(iii) LHCb obtains $\gamma = (84^{+49}_{-42})°$ from DK^+ using 1 fb^{-1} of data (a more precise result using 9 fb^{-1} and the model-independent method is reported below).
(iv) The experiments also obtain values for the hadronic parameters as detailed in Table 59.
(v) In the *BABAR* analysis of $B^+ \to DK^+$ with $D \to \pi^+\pi^-\pi^0$ decays [317], a constraint of $-30° < \gamma < 76°$ is obtained at the 68% confidence level.
(vi) The results discussed here are included in the HFLAV combination to obtain a world average value for $\gamma \equiv \phi_3$, as discussed in Sec. VI O 7.

BABAR and LHCb have performed a similar analysis using the self-tagging neutral B decay $B^0 \to DK^{*0}$ (with $K^{*0} \to K^+\pi^-$). Effects due to the natural width of the K^{*0} are handled using the parametrization suggested by Gronau [305]. LHCb [469] gives results in terms of the Cartesian parameters, as shown in Table 58. *BABAR* [470] presents results only in terms of γ and the hadronic parameters. The obtained constraints are:

(i) *BABAR* obtains $\gamma = (162 \pm 56)°$;
(ii) LHCb obtains $\gamma = (80^{+21}_{-22})°$;
(iii) Values for the hadronic parameters are given in Table 59.

5. *D decays to multiparticle self-conjugate final states (model-independent analysis)*

A model-independent approach to the analysis of $B^+ \to D^{(*)}K^+$ with multibody D decays was proposed by Giri, Grossman, Soffer and Zupan [302], and further developed by Bondar and Poluektov [314,315]. The method relies on information on the average strong phase difference between D^0 and $\bar{D}^0$ decays in bins of Dalitz plot position that can be obtained from quantum-correlated $\psi(3770) \to D^0\bar{D}^0$ events. This information is measured in the form of parameters c_i and s_i that are the weighted averages of the cosine and sine of the strong phase difference in a Dalitz plot bin labeled by i, respectively. These quantities have been obtained for $D \to K^0_S\pi^+\pi^-$ (and $D \to K^0_S K^+K^-$) decays by CLEO [254,471] and BES-III [472–474].

Belle [475] and LHCb [476] have performed model-independent BPGGSZ analyses of the $B^+ \to DK^+$ decay with subsequent $D \to K^0_S\pi^+\pi^-$ and $D \to K^0_S K^+K^-$ decays. In the LHCb analysis the $B^+ \to D\pi^+$ mode, with the same D decays, is also fitted simultaneously. This allows for better control of some sources of systematic uncertainty, and also allows additional parameters, denoted x_ξ and y_ξ following the proposal in Ref. [477], to be determined from the data. Since these additional parameters do not have significant sensitivity to $\gamma \equiv \phi_3$, we do not list them here and do not include them in our global combination. However, this parametrization does mean that the small amount of sensitivity to γ from the $B^+ \to D\pi^+$ modes is included in the $x_\pm$ and $y_\pm$ observables measured in this analysis.

Both Belle [478] and LHCb [479] have also used the model-independent Dalitz-analysis approach to study

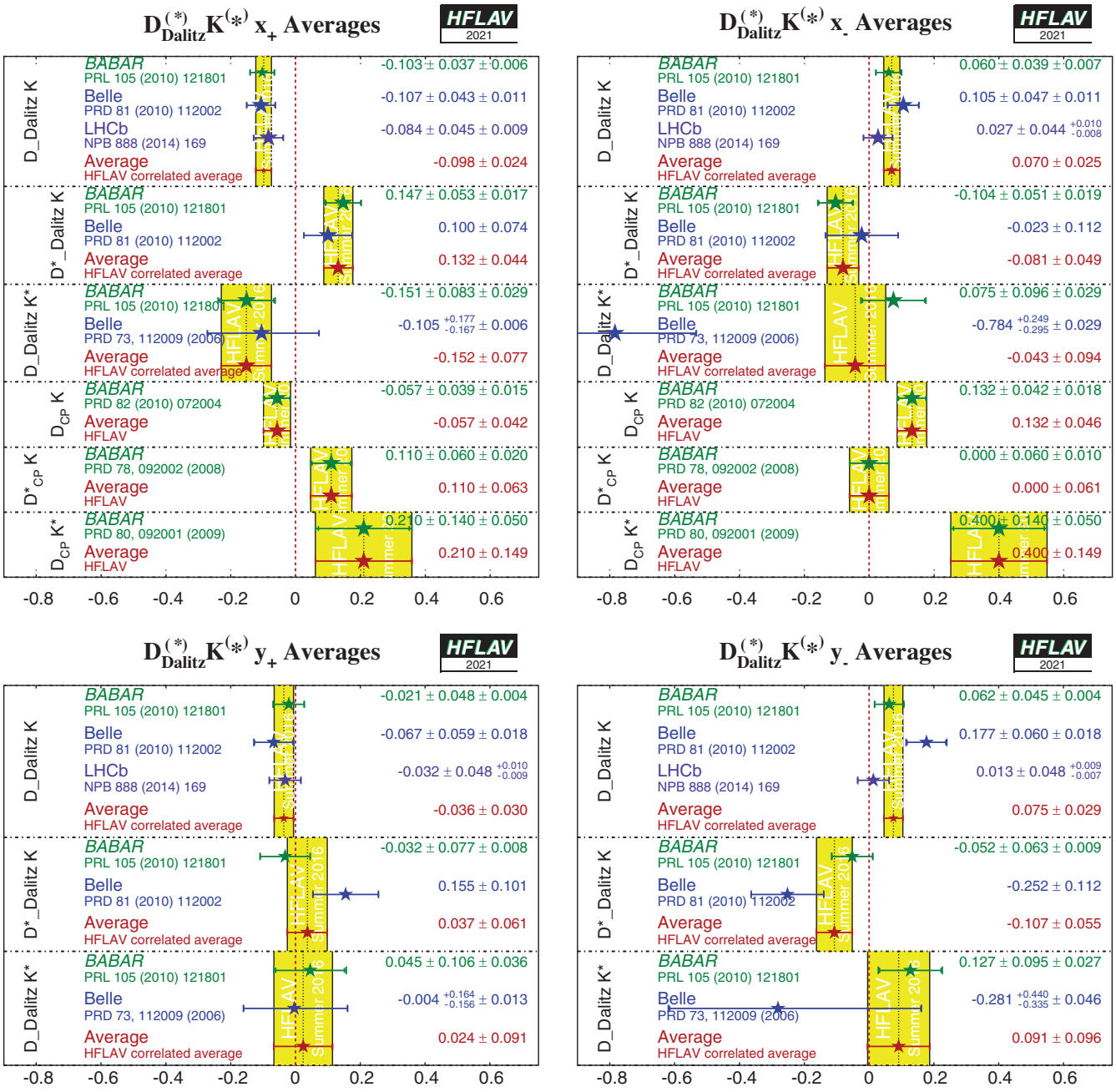

FIG. 42. Averages of $(x_\pm, y_\pm)$ from model-dependent analyses of $B^+ \to D^{(*)}K^{(*)+}$ with $D \to K^0_S h^+ h^-$ ($h = \pi, K$). Top left: x_+, (top right) x_-, (bottom left) y_+, (bottom right) y_-. The top plots include constraints on $x_\pm$ obtained from GLW analyses (see Sec. VI O 1). Note that the uncertainties assigned to the averages given in these plots do not include model uncertainties.

$B^0 \to DK^*(892)^0$ decays. In both cases, the experiments use $D \to K^0_S\pi^+\pi^-$ decays, and LHCb has also included the $D \to K^0_S K^+ K^-$ decay. Belle [480] have in addition carried out a model-independent analysis of $B^+ \to DK^+$, $D \to K^0_S\pi^+\pi^-\pi^0$ decays. The Cartesian variables $(x_\pm, y_\pm)$, defined in Eq. (144), were determined from the data. Note that due to the strong statistical and systematic correlations with the model-dependent results given in Sec. VI O 4, these sets of results cannot be combined.

The results and averages are given in Table 60, and shown in Fig. 43. Most results have three sets of uncertainties, which are, respectively, statistical, systematic, and the uncertainty coming from the knowledge of c_i and s_i. To perform the average, we remove the last uncertainty. If identical c_i and s_i inputs are used in different experiments, one might expect this uncertainty to be 100% correlated between the measurements. The size of the uncertainty from c_i and s_i is, however, found to depend on the size of the $B \to DK$ data sample, and so we assign the LHCb

TABLE 59. Summary of constraints on hadronic parameters from model-dependent analyses of $B^+ \to D^{(*)}K^{(*)+}$ and $B^0 \to DK^{*0}$ decays. Note the alternative parametrization of the hadronic parameters used by *BABAR* in the DK^{*+} mode.

Experiment		Sample size	r_B	δ_B
			In DK^+	
BABAR	[466]	$N(B\bar{B}) = 468\text{M}$	$0.096 \pm 0.029 \pm 0.005 \pm 0.004$	$(119^{+19}_{-20} \pm 3 \pm 3)°$
Belle	[465]	$N(B\bar{B}) = 657\text{M}$	$0.160^{+0.040}_{-0.038} \pm 0.011^{+0.05}_{-0.010}$	$(138^{+13}_{-16} \pm 4 \pm 23)°$
LHCb	[467]	$\int \mathcal{L}\,dt = 1\ \text{fb}^{-1}$	0.06 ± 0.04	$(115^{+41}_{-51})°$
			In D^*K^+	
BABAR	[466]	$N(B\bar{B}) = 468\text{M}$	$0.133^{+0.042}_{-0.039} \pm 0.014 \pm 0.003$	$(-82 \pm 21 \pm 5 \pm 3)°$
Belle	[465]	$N(B\bar{B}) = 657\text{M}$	$0.196^{+0.072}_{-0.069} \pm 0.012^{+0.062}_{-0.012}$	$(342^{+19}_{-21} \pm 3 \pm 23)°$
			$\bar{r}_B$	$\bar{\delta}_B$
			In DK^{*+}	
BABAR	[466]	$N(B\bar{B}) = 468\text{M}$	$\kappa\bar{r}_B = 0.149^{+0.066}_{-0.062} \pm 0.026 \pm 0.006$	$(111 \pm 32 \pm 11 \pm 3)°$
Belle	[468]	$N(B\bar{B}) = 386\text{M}$	$0.56^{+0.22}_{-0.16} \pm 0.04 \pm 0.08$	$(243^{+20}_{-23} \pm 3 \pm 50)°$
			In DK^{*0}	
BABAR	[470]	$N(B\bar{B}) = 371\text{M}$	<0.55 at 95% probability	$(62 \pm 57)°$
LHCb	[469]	$\int \mathcal{L}\,dt = 3\ \text{fb}^{-1}$	0.39 ± 0.13	$(197^{+24}_{-20})°$

uncertainties (which are mostly the smaller of the Belle and LHCb values) to the averaged result. This procedure should be conservative. In the LHCb $B^0 \to DK^*(892)^0$ results [479], the values of c_i and s_i are constrained to their measured values within uncertainties in the fit to data, and hence the systematic uncertainties associated with the knowledge of these parameters is absorbed in their statistical uncertainties. The $B^0 \to DK^*(892)^0$ average is performed neglecting the model uncertainties on the Belle results.

Constraints on $\gamma \equiv \phi_3$

The measurements of $(x_\pm, y_\pm)$ can be used to obtain constraints on γ, as well as the hadronic parameters r_B and δ_B. The experiments have done so using frequentist procedures, with some differences in the details of the techniques used.

(i) From $B^+ \to DK^+$, Belle [475] obtains $\phi_3 = (77.3^{+15.1}_{-14.9} \pm 4.1 \pm 4.3)°$.
(ii) From $B^+ \to DK^+$, LHCb [476] obtains $\gamma = (68.7^{+5.2}_{-5.1})°$.
(iii) From $B^0 \to DK^*(892)^0$, LHCb [479] obtains $\gamma = (71 \pm 20)°$.
(iv) The experiments also obtain values for the hadronic parameters as detailed in Table 62.
(v) The results discussed here are included in the HFLAV combination to obtain a world average value for $\gamma \equiv \phi_3$, as discussed in Sec. VI O 7.

6. D decays to multiparticle nonself-conjugate final states (model-independent analysis)

Following the original suggestion of Grossman, Ligeti and Soffer [312], decays of D mesons to $K^0_S K^\pm \pi^\mp$ can be used in a similar approach to that discussed above to determine $\gamma \equiv \phi_3$. Since these decays are less abundant, the event samples available to date have not been sufficient for a fine binning of the Dalitz plots, but the analysis can be performed using only an overall coherence factor and related strong phase difference for the decay. These quantities have been determined by CLEO [482] both for the full Dalitz plots and in a restricted region $\pm 100\ \text{MeV}/c^2$ around the peak of the $K^*(892)^\pm$ resonance.

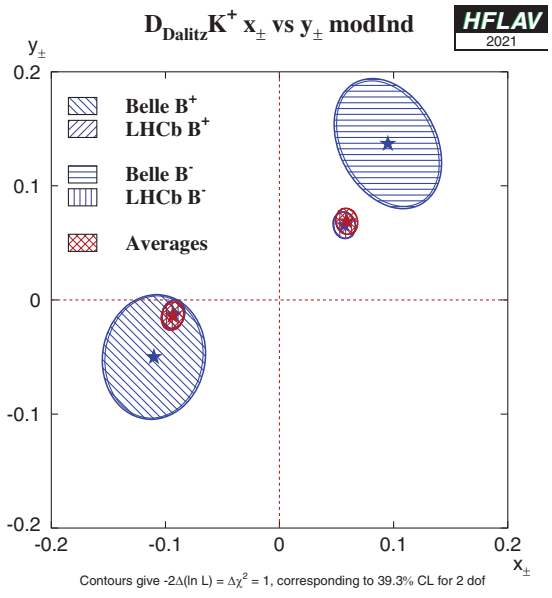

FIG. 43. Contours in the $(x_\pm, y_\pm)$ plane from model-independent analysis of $B^+ \to DK^+$ with $D \to K^0_S h^+ h^-$ $(h = \pi, K)$.

TABLE 60. Averages from model-independent Dalitz plot analyses of $b \to c\bar{u}s/u\bar{c}s$ modes.

Experiment		Sample size	x_+	y_+	x_-	y_-
			DK^+, $D \to K^0_S\pi^+\pi^-$ and $D \to K^0_S K^+K^-$			
Belle	[475]	$N(B\bar{B}) = 772$M	$-0.110 \pm 0.043 \pm 0.014 \pm 0.007$	$-0.050^{+0.052}_{-0.055} \pm 0.011 \pm 0.007$	$0.095 \pm 0.045 \pm 0.014 \pm 0.010$	$0.137^{+0.053}_{-0.057} \pm 0.015 \pm 0.023$
LHCb	[476]	$\int \mathcal{L}\,dt = 9$ fb^{-1}	$-0.093 \pm 0.010 \pm 0.002 \pm 0.002$	$-0.013 \pm 0.012 \pm 0.003 \pm 0.003$	$0.057 \pm 0.010 \pm 0.002 \pm 0.002$	$0.066 \pm 0.011 \pm 0.003 \pm 0.004$
Average			$-0.094 \pm 0.010 \pm 0.002$	$-0.014 \pm 0.012 \pm 0.003$	$0.059 \pm 0.010 \pm 0.002$	$0.069 \pm 0.011 \pm 0.004$
Confidence level				$0.48(0.7\sigma)$		
			DK^+, $D \to K^0_S\pi^+\pi^-\pi^0$			
Belle	[480]	$N(B\bar{B}) = 772$M	$-0.030 \pm 0.121^{+0.017+0.019}_{-0.018-0.018}$	$0.220^{+0.182}_{-0.541} \pm 0.032^{+0.072}_{-0.071}$	$0.095 \pm 0.121^{+0.017+0.023}_{-0.016-0.025}$	$0.354^{+0.144+0.015+0.032}_{-0.197-0.021-0.049}$
			DK^{*0}, $D \to K^0_S\pi^+\pi^-$ and $D \to K^0_S K^+K^-$			
Belle	[478]	$N(B\bar{B}) = 772$M	$0.1^{+0.7+0.0}_{-0.4-0.1} \pm 0.1$	$0.3^{+0.5+0.0}_{-0.8-0.1} \pm 0.1$	$0.4^{+1.0+0.0}_{-0.6-0.1} \pm 0.0$	$-0.6^{+0.8+0.1}_{-1.0-0.0} \pm 0.1$
LHCb	[479]	$\int \mathcal{L}\,dt = 3$ fb^{-1}	$0.05 \pm 0.35 \pm 0.02$	$-0.81 \pm 0.28 \pm 0.06$	$-0.31 \pm 0.20 \pm 0.04$	$0.31 \pm 0.21 \pm 0.05$
Average			0.10 ± 0.30	-0.63 ± 0.26	-0.27 ± 0.20	0.27 ± 0.21
Confidence level				$0.38(0.9\sigma)$		

TABLE 61. Results from model-independent Dalitz plot analysis of $B^+ \to DK^+$, $D \to K^0_S K^\pm\pi^\mp$.

Experiment		$\int \mathcal{L}\,dt$	$A_{\mathrm{SS},D\pi}$	$A_{\mathrm{OS},D\pi}$	$A_{\mathrm{SS},DK}$	$A_{\mathrm{OS},DK}$	R_{SS}	R_{OS}
			$D \to K^*(892)^\pm K^\mp$					
LHCb	[481]	9 fb^{-1}	$-0.020 \pm 0.011 \pm 0.003$	$0.007 \pm 0.017 \pm 0.003$	$0.084 \pm 0.049 \pm 0.008$	$0.021 \pm 0.094 \pm 0.017$	$0.079 \pm 0.004 \pm 0.002$	$0.062 \pm 0.006 \pm 0.003$
			$D \to K^0_S K^\pm\pi^\mp$ (non-$K^*(892)$ region)					
LHCb	[481]	9 fb^{-1}	$-0.034 \pm 0.020 \pm 0.003$	$0.003 \pm 0.015 \pm 0.003$	$0.095 \pm 0.089 \pm 0.018$	$-0.038 \pm 0.075 \pm 0.011$	$0.081 \pm 0.008 \pm 0.004$	$0.073 \pm 0.006 \pm 0.002$

LHCb [481] has reported results of an analysis of $B^+ \to DK^+$ and $B^+ \to D\pi^+$ decays with $D \to K^0_S K^\pm \pi^\mp$. The decays with different final states of the D meson are distinguished by the charge of the kaon from the decay of the D meson relative to the charge of the B meson, and are labeled "same sign" (SS) and "opposite sign" (OS). Six observables potentially sensitive to $\gamma \equiv \phi_3$ are measured: two ratios of rates for DK and $D\pi$ decays (one each for SS and OS) and four asymmetries (for DK and $D\pi$, SS and OS). This is done both for $K^*(892)^\pm$-dominated region (with the same boundaries as used by CLEO-c) and the remainder of the D decay Dalitz plot. The results, shown in Table 61, do not yet have sufficient precision to set significant constraints on $\gamma \equiv \phi_3$ independently of other results.

7. Combinations of results on rates and asymmetries in $B \to D^{(*)}K^{(*)}$ decays to obtain constraints on $\gamma \equiv \phi_3$

BABAR and LHCb have both produced constraints on $\gamma \equiv \phi_3$ from combinations of their results on $B^+ \to DK^+$ and related processes. The experiments use a frequentist procedure, with some differences in the details of the techniques used.

(i) *BABAR* [483] uses results from DK, D^*K and DK^* modes with GLW, ADS and BPGGSZ analyses, to obtain $\gamma = (69^{+17}_{-16})°$.

(ii) LHCb [484,485] uses results from the DK^+ mode with GLW, GLW-like, ADS, BPGGSZ ($K^0_S h^+ h^-$) and GLS ($K^0_S K^\pm \pi^\mp$) analyses, as well as DK^{*0} with GLW, ADS and BPGGSZ analyses, $DK^+\pi^-\pi^+$ with GLW and ADS analyses and $B^0_s \to D^\mp_s K^\pm (\pi^+\pi^-)$ decays. The LHCb combination also includes inputs from $B^+ \to D\pi^+$ decays. The LHCb combination takes into account subleading effects due to charm mixing [442], which are important for hadron collider experiments since selection requirements result in the acceptance varying with D decay time. The result is $\gamma = (65.4^{+3.8}_{-4.2})°$.

(iii) All of the combinations use inputs determined from $\psi(3770) \to D^0\bar{D}^0$ data samples (and/or from the HFLAV global fits on charm mixing parameters; see Sec. X A) to constrain the hadronic parameters in the charm system. The LHCb combination simultaneously fits charm mixing data in order to obtain the best constraint on $\delta_{K\pi}$, thereby improving knowledge on both charm mixing parameters and γ.

(iv) Constraints are also obtained on the hadronic parameters involved in the decays. A summary of these is given in Table 63.

(v) The CKMfitter [242] and UTFit [334] groups perform similar combinations of all available results to obtain combined constraints on $\gamma \equiv \phi_3$.

Independently from the constraints on $\gamma \equiv \phi_3$ obtained by the experiments, the results summarized in Sec. VI O are statistically combined to produce world average constraints on $\gamma \equiv \phi_3$ and the hadronic parameters involved. The combination is performed with the GAMMACOMBO framework [432] and follows a frequentist procedure, identical to that used in Ref. [486].

The input measurements used in the combination are listed in Table 64. Individual measurements are used as inputs, rather than the averages presented in Sec. VI O, in order to facilitate cross-checks and to ensure the most appropriate treatment of correlations. A combination based on our averages for each of the quantities measured by experiments gives consistent results.

All results from GLW and GLW-like analyses of $B^+ \to D^{(*)}K^{(*)+}$ modes, as listed in Tables 52 and 54, are used. All results from ADS analyses of $B^+ \to D^{(*)}K^{(*)+}$ as listed in Table 55 are also used. Regarding $B^0 \to DK^{*0}$ decays, the results of the LHCb GLW/ADS analysis of $B^0 \to DK^{*0}$ (Tables 52 and 57) are included. Concerning results of BPGGSZ analyses of $B^+ \to D^{(*)}K^{(*)+}$ with $D \to K^0_S h^+ h^-$, the model-dependent results, as listed in Table 58, are used for the *BABAR* and Belle experiments, while the model-independent results, as listed in Table 60, are used for LHCb. This choice is made in order to maintain consistency of the approach across experiments while maximizing the size of the samples used to obtain inputs for the combination. For BPGGSZ analyses of $B^0 \to DK^{*0}$ with $D \to K^0_S h^+ h^-$, the model-independent result from LHCb (given in Table 60) is used for consistency with the treatment of the LHCb $B^+ \to DK^+$ BPGGSZ result; the model-independent result by Belle is also included. The result of the GLS analysis of $B^+ \to DK^+$ with $D \to K^{*\pm}K^\mp$ from LHCb (Table 61) are used. Finally, results from the time-dependent analyses of $B^0_s \to D^\mp_s K^\pm$ and $B^0_s \to D^\mp_s K^\pm \pi^+\pi^-$ from LHCb (Table 51) are used.

Several results with sensitivity to γ are not included in the combination. Results from time-dependent analyses of $B^0 \to D^{(*)\mp}\pi^\pm$ and $D^\mp \rho^\pm$ (Table 50) are not used, as there are insufficient constraints on the associated hadronic parameters. Similarly, results from $B^0 \to D^\mp K^0_S \pi^\pm$ (Sec. VI N 1) are not used. Results from the LHCb $B^0 \to DK^+\pi^-$ GLW-Dalitz analysis (Table 53) are not used because of the statistical overlap with the GLW DK^{*0} analysis, which is used instead. Limits on ADS parameters reported in Sec. VI O 3 are not used. Results on $B^+ \to D\pi^+$ decays, given in Table 56, are not used, since the small value of $r_B(D\pi^+)$ means that these channels have less sensitivity to γ and are more vulnerable to biases from subleading effects [487]. Results from the *BABAR* Dalitz plot analysis of $B^+ \to DK^+$ with $D \to \pi^+\pi^-\pi^0$ (given in Table 58) are not included due to their limited sensitivity. Results from the $B^+ \to DK^+$, $D \to K^0_S \pi^+\pi^-$ BPGGSZ model-dependent analysis by LHCb (given in Table 58), and of the model-independent analysis of the same decay

TABLE 62. Summary of constraints on hadronic parameters from model-independent analyses of $B^+ \to DK^+$ and $B^0 \to DK^{*0}$, $D \to K^0_S h^+ h^-$ ($h = \pi$, K) decays.

Experiment		Sample size	$r_B(DK^+)$	$\delta_B(DK^+)$
Belle	[475]	$N(B\bar{B}) = 772$M	$0.145 \pm 0.030 \pm 0.010 \pm 0.011$	$(129.9 \pm 15.0 \pm 3.8 \pm 4.7)°$
LHCb	[476]	$\int \mathcal{L}\,dt = 9$ fb^{-1}	$0.0904^{+0.0077}_{-0.0075}$	$(118.3^{+5.5}_{-5.6})°$
			$\bar{r}_B(DK^{*0})$	$\bar{\delta}_B(DK^{*0})$
Belle	[478]	$N(B\bar{B}) = 772$M	<0.87 at 68% confidence level	
LHCb	[479]	$\int \mathcal{L}\,dt = 3$ fb^{-1}	0.56 ± 0.17	$(204^{+21}_{-20})°$

TABLE 63. Summary of constraints on hadronic parameters obtained from global combinations of results in $B^+ \to D^{(*)}K^{(*)+}$ and $B^0 \to DK^{*0}$ decays. Results for parameters associated with the other decay modes discussed in this section are less precise and are not included in this summary.

Experiment		$r_B(DK^+)$	$\delta_B(DK^+)$	$r_B(D^*K^+)$	$\delta_B(D^*K^+)$
BABAR	[483]	$0.092^{+0.013}_{-0.012}$	$(105^{+16}_{-17})°$	$0.106^{+0.019}_{-0.036}$	$(294^{+21}_{-31})°$
LHCb	[484,485]	$0.0984^{+0.0027}_{-0.0026}$	$(127.6^{+4.0}_{-4.2})°$	$0.099^{+0.016}_{-0.019}$	$(310^{+12}_{-23})°$

TABLE 64. List of measurements used in the γ combination.

B decay	D decay	Method	Experiment	References
$B^+ \to DK^+$	$D \to K^+K^-$, $D \to \pi^+\pi^-$, $D \to K^0_S\pi^0$, $D \to K^0_S\omega$, $D \to K^0_S\phi$	GLW	*BABAR*	[443]
$B^+ \to DK^+$	$D \to K^+K^-$, $D \to \pi^+\pi^-$, $D \to K^0_S\pi^0$, $D \to K^0_S\omega$, $D \to K^0_S\phi$	GLW	Belle	[444]
$B^+ \to DK^+$	$D \to K^+K^-$, $D \to \pi^+\pi^-$	GLW	CDF	[445]
$B^+ \to DK^+$	$D \to K^+K^-$, $D \to \pi^+\pi^-$	GLW	LHCb	[446]
$B^+ \to D^*K^+$, $D^* \to D\gamma(\pi^0)$	$D \to K^+K^-$, $D \to \pi^+\pi^-$, $D \to K^0_S\pi^0$, $D \to K^0_S\omega$, $D \to K^0_S\phi$	GLW	*BABAR*	[447]
$B^+ \to D^*K^+$, $D^* \to D\gamma(\pi^0)$	$D \to K^+K^-$, $D \to \pi^+\pi^-$, $D \to K^0_S\pi^0$, $D \to K^0_S\omega$, $D \to K^0_S\phi$	GLW	Belle	[444]
$B^+ \to D^*K^+$, $D^* \to D\gamma(\pi^0)$	$D \to K^+K^-$, $D \to \pi^+\pi^-$	GLW	LHCb	[446]
$B^+ \to DK^{*+}$	$D \to K^+K^-$, $D \to \pi^+\pi^-$, $D \to K^0_S\pi^0$, $D \to K^0_S\omega$, $D \to K^0_S\phi$	GLW	*BABAR*	[448]
$B^+ \to DK^{*+}$	$D \to K^+K^-$, $D \to \pi^+\pi^-$	GLW	LHCb	[449]
$B^+ \to DK^+\pi^+\pi^-$	$D \to K^+K^-$, $D \to \pi^+\pi^-$	GLW	LHCb	[450]
$B^0 \to DK^{*0}$	$D \to K^+K^-$, $D \to \pi^+\pi^-$	GLW	LHCb	[451]
$B^+ \to DK^+$	$D \to \pi^+\pi^-\pi^0$	GLW-like	*BABAR*	[317]
$B^+ \to DK^+$	$D \to K^+K^-\pi^0$, $D \to \pi^+\pi^-\pi^0$	GLW-like	LHCb	[454]
$B^+ \to DK^+$	$D \to \pi^+\pi^-\pi^+\pi^-$	GLW-like	LHCb	[455]
$B^+ \to DK^{*+}$	$D \to \pi^+\pi^-\pi^+\pi^-$	GLW-like	LHCb	[449]
$B^+ \to DK^+$	$D \to K^\pm\pi^\mp$	ADS	*BABAR*	[456]
$B^+ \to DK^+$	$D \to K^\pm\pi^\mp$	ADS	Belle	[457]
$B^+ \to DK^+$	$D \to K^\pm\pi^\mp$	ADS	CDF	[458]
$B^+ \to DK^+$	$D \to K^\pm\pi^\mp$	ADS	LHCb	[446]

(Table continued)

TABLE 64. *(Continued)*

B decay	D decay	Method	Experiment	References
$B^+ \to DK^+$	$D \to K^\pm\pi^\mp\pi^0$	ADS	*BABAR*	[459]
$B^+ \to DK^+$	$D \to K^\pm\pi^\mp\pi^0$	ADS	Belle	[460]
$B^+ \to DK^+$	$D \to K^\pm\pi^\mp\pi^0$	ADS	LHCb	[454]
$B^+ \to DK^+$	$D \to K^\pm\pi^\mp\pi^+\pi^-$	ADS	LHCb	[455]
$B^+ \to D^*K^+$ $D^* \to D\gamma(\pi^0)$	$D \to K^\pm\pi^\mp$	ADS	*BABAR*	[456]
$B^+ \to D^*K^+$ $D^* \to D\gamma(\pi^0)$	$D \to K^\pm\pi^\mp$	ADS	LHCb	[446]
$B^+ \to DK^{*+}$	$D \to K^\pm\pi^\mp$	ADS	*BABAR*	[448]
$B^+ \to DK^{*+}$	$D \to K^\pm\pi^\mp$	ADS	LHCb	[449]
$B^+ \to DK^{*+}$	$D \to K^\pm\pi^\mp\pi^+\pi^-$	ADS	LHCb	[449]
$B^0 \to DK^{*0}$	$D \to K^\pm\pi^\mp$	ADS	LHCb	[451]
$B^0 \to DK^{*0}$	$D \to K^\pm\pi^\mp\pi^+\pi^-$	ADS	LHCb	[451]
$B^+ \to DK^+\pi^+\pi^-$	$D \to K^\pm\pi^\mp$	ADS	LHCb	[450]
$B^+ \to DK^+$	$D \to K^0_S\pi^+\pi^-$	BPGGSZ MD	*BABAR*	[466]
$B^+ \to DK^+$	$D \to K^0_S\pi^+\pi^-$	BPGGSZ MD	Belle	[465]
$B^+ \to DK^+$	$D \to K^0_S\pi^+\pi^-$, $D \to K^0_SK^+K^-$	BPGGSZ MI	LHCb	[476]
$B^+ \to D^*K^+$ $D^* \to D\gamma(\pi^0)$	$D \to K^0_S\pi^+\pi^-$	BPGGSZ MD	*BABAR*	[466]
$B^+ \to D^*K^+$ $D^* \to D\gamma(\pi^0)$	$D \to K^0_S\pi^+\pi^-$	BPGGSZ MD	Belle	[465]
$B^+ \to DK^{*+}$	$D \to K^0_S\pi^+\pi^-$	BPGGSZ MD	*BABAR*	[466]
$B^+ \to DK^{*+}$	$D \to K^0_S\pi^+\pi^-$	BPGGSZ MD	Belle	[468]
$B^0 \to DK^{*0}$	$D \to K^0_S\pi^+\pi^-$	BPGGSZ MI	Belle	[478]
$B^0 \to DK^{*0}$	$D \to K^0_S\pi^+\pi^-$, $D \to K^0_SK^+K^-$	BPGGSZ MI	LHCb	[479]
$B^+ \to DK^+$	$D \to K^0_SK^\pm\pi^\mp$	GLS	LHCb	[481]
$B^0_s \to D^\mp_sK^\pm$	$D^+_s \to h^+h^-\pi^+$	TD	LHCb	[289]
$B^0_s \to D^\mp_sK^\pm\pi^+\pi^-$	$D^+_s \to h^+h^-\pi^+$	TD	LHCb	[200]

by Belle (given in Table 60) are not included due to the statistical overlap with results from model-(in)dependent analyses of the same data.

Auxiliary inputs are used in the combination in order to constrain the D system parameters and subsequently improve the determination of $\gamma \equiv \phi_3$. These include the ratio of suppressed to favored decay amplitudes and the strong phase difference for $D \to K^\pm\pi^\mp$ decays, taken from the charm global fits (see Sec. X). The amplitude ratios, strong phase differences and coherence factors of $D \to K^\pm\pi^\mp\pi^0$, $D \to K^\pm\pi^\mp\pi^+\pi^-$ and $D \to K^0_SK^\pm\pi^\pm$ decays are taken from a combination of BES-III, CLEO-c and LHCb measurements [482,488–491]. The fraction of CP-even content for the GLW-like $D \to \pi^+\pi^-\pi^+\pi^-$, $D \to K^+K^-\pi^0$ and $D \to \pi^+\pi^-\pi^0$ decays are taken from CLEO-c measurements [453]. Finally, the value of $-2\beta_s$ is taken from the HFLAV averages (see Sec. V); this is required to obtain sensitivity to $\gamma \equiv \phi_3$ from the time-dependent analysis of $B^0_s \to D^\mp_sK^\pm(\pi^+\pi^-)$ decays. A summary of the auxiliary constraints is given in Table 65.

The following reasonable, although imperfect, assumptions are made when performing the averages.

(i) CP violation in $D \to K^+K^-$ and $D \to \pi^+\pi^-$ decays is assumed to be zero. The results of Sec. X anyhow suggest such effects to be negligible.

(ii) The combination is potentially sensitive to subleading effects from D^0–$\bar{D}^0$ mixing [442,492,493] which are not accounted for. The effect is expected to be small given that $r_B \geq 0.1$ (for all modes) while $r_D \sim 0.05$.

(iii) All $B^+ \to DK^{*+}$ modes are treated as two-body decays. In other words any dilution caused by non-K^{*+} contributions in the selected regions of the $DK^0_S\pi^+$ or $DK^+\pi^0$ Dalitz plots is assumed to be

TABLE 65. List of the auxiliary inputs used in the combinations.

Decay	Parameters	Source	Ref.
$D \to K^{\pm}\pi^{\mp}$	$r_D^{K\pi}$, $\delta_D^{K\pi}$	HFLAV	Sec. X
$D \to K^{\pm}\pi^{\mp}\pi^{+}\pi^{-}$	$\delta_D^{K3\pi}$, $\kappa_D^{K3\pi}$, $r_D^{K3\pi}$	BESIII + CLEO + LHCb	[488]
$D \to \pi^{+}\pi^{-}\pi^{+}\pi^{-}$	$F_+(\pi^+\pi^-\pi^+\pi^-)$	CLEO	[453]
$D \to K^{\pm}\pi^{\mp}\pi^{0}$	$\delta_D^{K2\pi}$, $\kappa_D^{K2\pi}$, $r_D^{K2\pi}$	BESIII + CLEO + LHCb	[489]
$D \to h^{+}h^{-}\pi^{0}$	$F_+(\pi^+\pi^-\pi^0)$, $F_+(K^+K^-\pi^0)$	CLEO	[453]
$D \to K^0_S K^{\pm}\pi^{\mp}$	$\delta_D^{K_SK\pi}$, $\kappa_D^{K_SK\pi}$, $r_D^{K_SK\pi}$	CLEO	[482]
	$r_D^{K_SK\pi}$	LHCb	[490]
$B^0 \to DK^{*0}$	$\kappa_B^{DK^{*0}}$	LHCb	[452]
$B_s^0 \to D_s^{\mp}K^{\pm}$	ϕ_s	HFLAV	Sec. V

negligible. As a check of this assumption, it was found that including a coherence factor for $B^+ \to DK^{*+}$ modes, $\kappa_B(DK^{*+}) = 0.9$, had negligible impact on the results.

(iv) Each individual set of input measurements listed in Table 38 is assumed to be completely uncorrelated, although correlations between observables in a set are used if provided by the experiment. While this assumption is true for the statistical uncertainties, it is not necessarily the case for systematic uncertainties. In particular, the model uncertainties for different model-dependent BPGGSZ analyses are fully correlated (when the same model is used). Similarly, the model-independent BPGGSZ analyses have correlated systematic uncertainties originating from the measurement of the strong phase variation across the Dalitz plot. The effect of including these correlations is estimated to be $<1°$.

In total, there are 154 observables and 35 free parameters. The combination has a χ^2 value of 122.3, which corresponds to a global p-value of 0.398 (or 0.8σ). A coverage check with pseudoexperiments gives a p-value of $(36.8 \pm 0.5)\%$. The obtained world average for the unitarity triangle angle $\gamma \equiv \phi_3$ is

$$\gamma \equiv \phi_3 = (66.2^{+3.4}_{-3.6})°. \tag{162}$$

An ambiguous solution at $\gamma \equiv \phi_3 \to \gamma \equiv \phi_3 + \pi$ also exists. The results for the hadronic parameters are listed in Table 66. Results for input analyses split by B meson decay mode are shown in Table 67 and Fig. 44. Results for input analyses split by the method are shown in Table 68 and Fig. 45. Results for the hadronic ratios, r_B, are shown

TABLE 66. Averages values obtained for the hadronic parameters in $B \to D^{(*)}K^{(*)}$ decays.

Parameter	Value
$r_B(DK^+)$	0.0996 ± 0.0026
$r_B(D^*K^+)$	$0.104^{+0.013}_{-0.014}$
$r_B(DK^{*+})$	$0.101^{+0.016}_{-0.037}$
$r_B(DK^{*0})$	$0.257^{+0.021}_{-0.022}$
$\delta_B(DK^+)$	$(128.0^{+3.8}_{-4.0})°$
$\delta_B(D^*K^+)$	$(314.9^{+7.8}_{-10.0})°$
$\delta_B(DK^{*+})$	$(49^{+61}_{-16})°$
$\delta_B(DK^{*0})$	$(194^{+9.5}_{-8.8})°$

TABLE 67. Averages of $\gamma \equiv \phi_3$ split by B meson decay mode.

Decay mode	Value
$B^+ \to DK^+$	$(64.0^{+4.0}_{-4.1})°$
$B^+ \to D^*K^+$	$(67^{+12}_{-23})°$
$B^+ \to DK^{*+}$	$(45^{+13}_{-11})°$
$B^0 \to DK^{*0}$	$(81.4^{+9}_{-9.6})°$
$B_s^0 \to D_s^{\mp}K^{\pm}$	$(130^{+17}_{-23})°$
$B_s^0 \to D_s^{\mp}K^{\pm}\pi^{+}\pi^{-}$	$(45^{+20}_{-13})°$

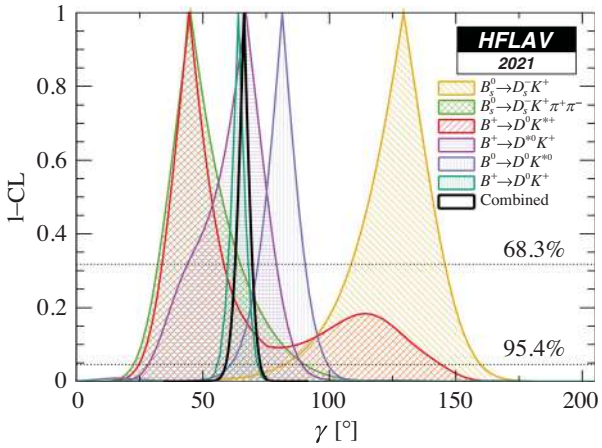

FIG. 44. World average of $\gamma \equiv \phi_3$, in terms of 1−CL, split by decay mode.

TABLE 68. Averages of $\gamma \equiv \phi_3$ split by method. For GLW method only the solution nearest the combined average is shown.

Method	Value
GLW	$(74.0^{+5.5}_{-47.6})°$
ADS	$(71^{+15}_{-33})°$
BPGGSZ	$(68.8^{+4.5}_{-4.6})°$

in Fig. 46. A demonstration of how the various analyses contribute to the combination is shown in Fig. 47. There are two overlapping solutions for the $B^+ \to DK^{*+}$ modes which is why their uncertainties are so asymmetric. It should be noted that the global combination for γ has moved substantially since the previous combination [1], which found $\gamma = (71.1^{+4.6}_{-5.3})°$. This is mainly driven by updates of LHCb measurements to the full 9 fb^{-1} dataset of $B^+ \to DK^+$ decays with GLW/ADS and BPGGSZ analyses which have both moved to lower values of γ and are now in very close agreement. The changes and consistency of these measurements can be seen by inspecting the two-dimensional confidence interval contours shown in Fig. 47. While the change in central value to γ alone looks substantial, a proper comparison should be made in the multidimensional space including the relevant r_B and δ_B parameters as well, which suggests a much better compatibility between the current and previous combinations.

P. Summary of the constraints on the angles of the unitarity triangle

World averages for the angles of the unitarity triangle $\beta \equiv \phi_1$, $\alpha \equiv \phi_2$ and $\gamma \equiv \phi_3$ are given in Sec. VI D 2, Sec. VI L 1 and Sec. VI O 7, respectively. These constraints are summarized in Fig. 48 in terms of the CKM parameters $\bar{\rho}$ and $\bar{\eta}$ defined in Eq. (92) using the relations, $\tan\gamma = \bar{\eta}/\bar{\rho}$,

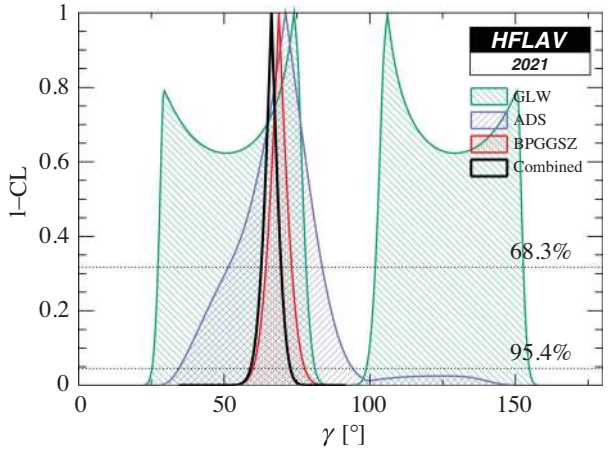

FIG. 45. World average of $\gamma \equiv \phi_3$, in terms of 1−CL, split by analysis method.

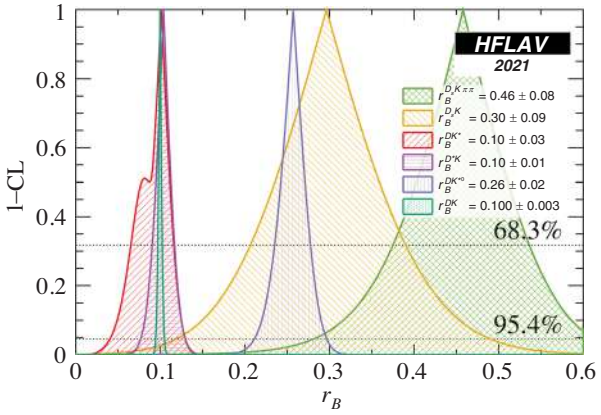

FIG. 46. World averages for the hadronic parameters r_B in the different decay modes, in terms of 1−CL.

$\tan\beta = \bar{\eta}/(1-\bar{\rho})$, $\alpha = \tan^{-1}(\bar{\rho}/\bar{\eta}) + \tan^{-1}((1-\bar{\rho})/\bar{\eta})$. The overlap of the constraints demonstrates agreement with the unitarity of the CKM matrix as predicted in the Standard Model. The obtained values of $\bar{\rho}$ and $\bar{\eta}$ from this angles only combination are

$$\bar{\rho} = 0.140 \pm 0.018, \qquad \bar{\eta} = 0.353 \pm 0.012, \qquad (163)$$

with a correlation of −0.287.

VII. SEMILEPTONIC *b* HADRON DECAYS

In this section we present averages for semileptonic b hadron decays, i.e. decays of the type $B \to X\ell\nu_\ell$, where X refers to one or more hadrons, ℓ to a charged lepton and ν_ℓ to its associated neutrino. Unless otherwise stated, ℓ stands for an electron or a muon, lepton universality is assumed, and both charge conjugate states are combined. Some averages assume isospin symmetry which is explicitly mentioned at every instance.

Averages are presented separately for CKM favored $b \to c$ quark transitions and CKM suppressed $b \to u$ transitions. We further distinguish *exclusive* decays involving a specific meson ($X = D, D^*, \pi, \rho, \ldots$) from *inclusive* decay modes, i.e. the sum over all possible hadronic states. Semileptonic decays proceed via first order weak interactions and are well described in the framework of the SM. Their decay rates are sensitive to the magnitude squared of the CKM elements V_{cb} and V_{ub}, the determination of which is one of the primary goals for the study of these decays. Semileptonic decays involving the τ lepton might be more sensitive to beyond-SM processes, because the high τ mass can result in enhanced couplings to hypothetical new particles such as a charged Higgs boson or leptoquarks.

The technique for obtaining the averages follows the general HFLAV procedure (see Sec. III) unless otherwise stated. More information on the averages, in particular on the common input parameters, is available on the HFLAV

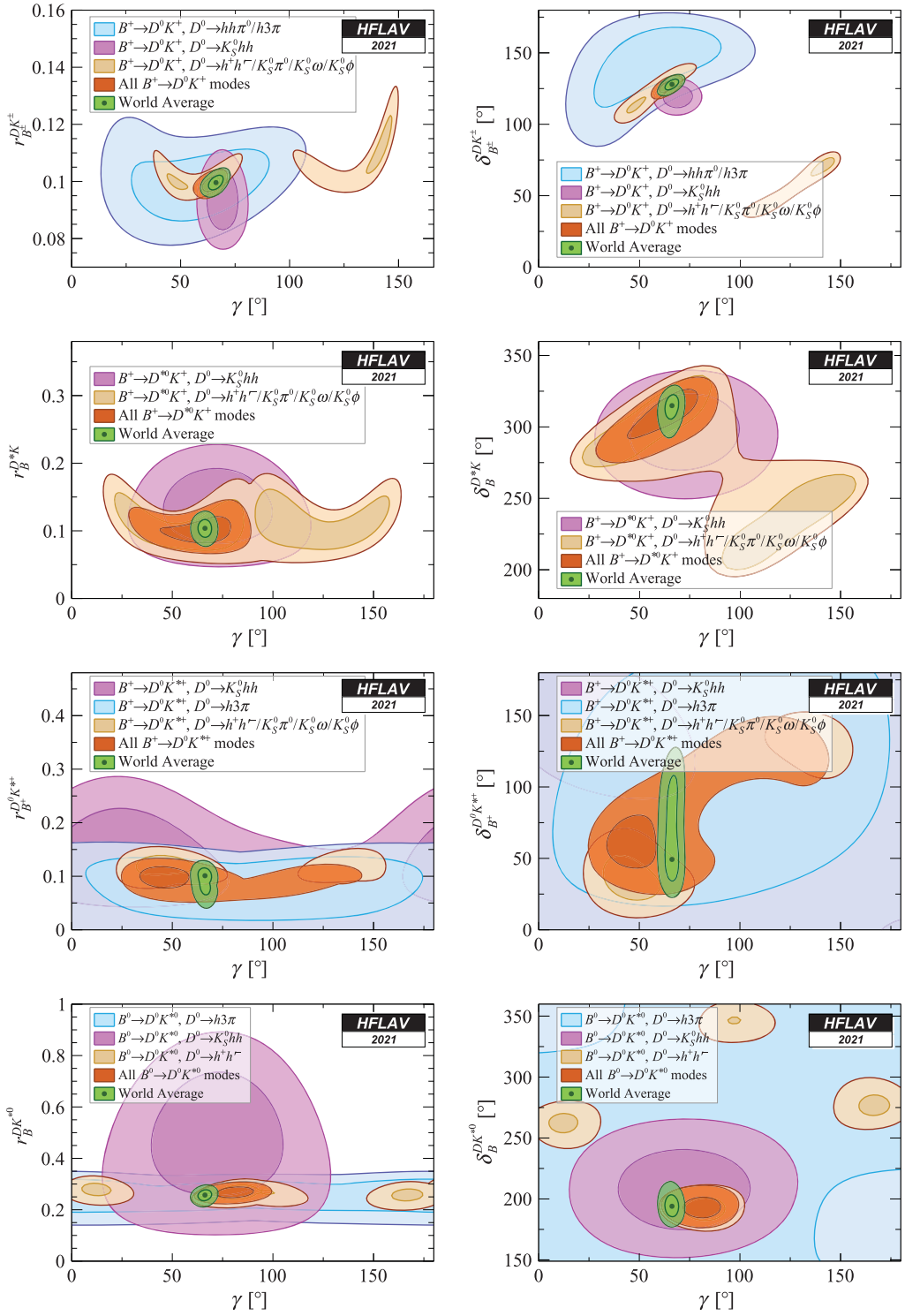

FIG. 47. Contributions to the combination from different input measurements, shown in the plane of the relevant r_B (left) or δ_B (right) parameter *vs.* $\gamma \equiv \phi_3$. From top to bottom: $B^+ \to DK^+$, $B^+ \to D^*K^+$, $B^+ \to DK^{*+}$ and $B^0 \to DK^{*0}$. Contours show the two-dimensional 68% and 95% CL regions.

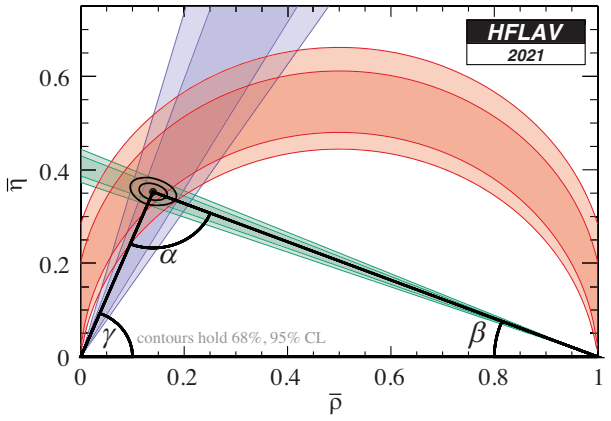

FIG. 48. Summary of the constraints on the angles of the unitarity triangle.

semileptonic webpage. In general, averages in this section use experimental results available through spring 2021.

A. Exclusive CKM-favored decays

1. $\bar{B} \to D^* \ell^- \bar{\nu}_\ell$

$\bar{B} \to D^* \ell^- \bar{\nu}_\ell$ decays are described in terms of the recoil variable $w = v_B \cdot v_{D^{(*)}}$, the product of the four-velocities of the initial and final state mesons. The differential decay rate for massless fermions as a function of w is given by (see, e.g., [494])

$$\frac{d\Gamma(\bar{B} \to D^* \ell^- \bar{\nu}_\ell)}{dw} = \frac{G_F^2 m_{D^*}^3}{48\pi^3}(m_B - m_{D^*})^2 \times \chi(w)\eta_{EW}^2 \mathcal{F}^2(w)|V_{cb}|^2, \quad (164)$$

where G_F is Fermi's constant, m_B and m_{D^*} are the B and D^* meson masses, $\chi(w)$ is a known phase-space factor, and η_{EW} is a small electroweak correction [495]. Some authors also include a long-distance EM radiation effect (Coulomb correction) in this factor. The form factor $\mathcal{F}(w)$ for the $\bar{B} \to D^* \ell^- \bar{\nu}_\ell$ decay contains three independent functions, $h_{A_1}(w)$, $R_1(w)$ and $R_2(w)$,

$$\chi(w)\mathcal{F}^2(w) = h_{A_1}^2(w)\sqrt{w^2-1}(w+1)^2\left\{2\left[\frac{1-2wr+r^2}{(1-r)^2}\right] \times \left[1 + R_1^2(w)\frac{w-1}{w+1}\right] + \left[1 + (1-R_2(w))\frac{w-1}{1-r}\right]^2\right\}, \quad (165)$$

where $r = m_{D^*}/m_B$.

Branching fraction.—First, we perform separate one-dimensional averages of the $\bar{B}^0 \to D^{*+}\ell^-\bar{\nu}_\ell$ and $B^- \to D^{*0}\ell^-\bar{\nu}_\ell$ branching fractions. In the fit to the measurements listed in Tables 69 and 70, external parameters (such as the branching fractions of charmed mesons) are constrained to their latest values and the following results are obtained

$$\mathcal{B}(\bar{B}^0 \to D^{*+}\ell^-\bar{\nu}_\ell) = (4.97 \pm 0.02 \pm 0.12)\%, \quad (166)$$

$$\mathcal{B}(B^- \to D^{*0}\ell^-\bar{\nu}_\ell) = (5.58 \pm 0.07 \pm 0.21)\%, \quad (167)$$

where the first uncertainty is statistical and the second one is systematic. The results of these two fits are also shown in Fig. 49.

Extraction of $|V_{cb}|$ based on the CLN form factor.—To extract $|V_{cb}|$, we consider the parametrizations of the form factor functions $h_{A_1}(w)$, $R_1(w)$ and $R_2(w)$ by Caprini, Lellouch and Neubert (CLN) [507],

TABLE 69. Average of the $\bar{B}^0 \to D^{*+}\ell^-\bar{\nu}_\ell$ branching fraction measurements.

Experiment	$\mathcal{B}(\bar{B}^0 \to D^{*+}\ell^-\bar{\nu}_\ell)$ [%] (rescaled)	$\mathcal{B}(\bar{B}^0 \to D^{*+}\ell^-\bar{\nu}_\ell)$ [%] (published)
ALEPH [496]	$5.45 \pm 0.26_{\text{stat}} \pm 0.33_{\text{syst}}$	$5.53 \pm 0.26_{\text{stat}} \pm 0.52_{\text{syst}}$
OPAL incl [497]	$6.13 \pm 0.28_{\text{stat}} \pm 0.57_{\text{syst}}$	$5.92 \pm 0.27_{\text{stat}} \pm 0.68_{\text{syst}}$
OPAL excl [497]	$5.12 \pm 0.20_{\text{stat}} \pm 0.36_{\text{syst}}$	$5.11 \pm 0.19_{\text{stat}} \pm 0.49_{\text{syst}}$
DELPHI incl [498]	$4.95 \pm 0.14_{\text{stat}} \pm 0.35_{\text{syst}}$	$4.70 \pm 0.13_{\text{stat}}\,^{+0.36}_{-0.31\,\text{syst}}$
DELPHI excl [499]	$5.08 \pm 0.20_{\text{stat}} \pm 0.42_{\text{syst}}$	$5.90 \pm 0.22_{\text{stat}} \pm 0.50_{\text{syst}}$
CLEO [500]	$6.08 \pm 0.19_{\text{stat}} \pm 0.37_{\text{syst}}$	$6.09 \pm 0.19_{\text{stat}} \pm 0.40_{\text{syst}}$
Belle untagged [501]	$4.83 \pm 0.02_{\text{stat}} \pm 0.15_{\text{syst}}$	$4.90 \pm 0.02_{\text{stat}} \pm 0.16_{\text{syst}}$
BABAR untagged [502]	$4.41 \pm 0.04_{\text{stat}} \pm 0.32_{\text{syst}}$	$4.69 \pm 0.04_{\text{stat}} \pm 0.34_{\text{syst}}$
BABAR tagged [503]	$5.17 \pm 0.16_{\text{stat}} \pm 0.31_{\text{syst}}$	$5.49 \pm 0.16_{\text{stat}} \pm 0.25_{\text{syst}}$
Belle II untagged [504]	$4.60 \pm 0.05_{\text{stat}} \pm 0.48_{\text{syst}}$	$4.60 \pm 0.05_{\text{stat}} \pm 0.48_{\text{syst}}$
Belle II tagged [505]	$4.51 \pm 0.41_{\text{stat}} \pm 0.52_{\text{syst}}$	$4.51 \pm 0.41_{\text{stat}} \pm 0.52_{\text{syst}}$
Average	$\mathbf{4.97 \pm 0.02_{stat} \pm 0.12_{syst}}$	$\boldsymbol{\chi^2/\text{dof} = 16.4/10}$ **(C.L.=8.85%)**

TABLE 70. Average of the $B^- \to D^{*0}\ell^-\bar{\nu}_\ell$ branching fraction measurements.

Experiment	$\mathcal{B}(B^- \to D^{*0}\ell^-\bar{\nu}_\ell)$ [%] (rescaled)	$\mathcal{B}(B^- \to D^{*0}\ell^-\bar{\nu}_\ell)$ [%] (published)
CLEO [500]	$6.20 \pm 0.20_{\text{stat}} \pm 0.26_{\text{syst}}$	$6.50 \pm 0.20_{\text{stat}} \pm 0.43_{\text{syst}}$
BABAR tagged [503]	$5.30 \pm 0.15_{\text{stat}} \pm 0.33_{\text{syst}}$	$5.83 \pm 0.15_{\text{stat}} \pm 0.30_{\text{syst}}$
BABAR untagged [506]	$5.00 \pm 0.08_{\text{stat}} \pm 0.31_{\text{syst}}$	$5.56 \pm 0.08_{\text{stat}} \pm 0.41_{\text{syst}}$
Average	$\mathbf{5.58 \pm 0.07_{stat} \pm 0.21_{syst}}$	$\boldsymbol{\chi^2/\text{dof} = 7.36/2}$ **(C.L.=2.52%)**

$$h_{A_1}(w) = h_{A_1}(1)[1 - 8\rho^2 z + (53\rho^2 - 15)z^2 - (231\rho^2 - 91)z^3], \quad (168)$$

$$R_1(w) = R_1(1) - 0.12(w-1) + 0.05(w-1)^2, \quad (169)$$

$$R_2(w) = R_2(1) + 0.11(w-1) - 0.06(w-1)^2, \quad (170)$$

where $z = (\sqrt{w+1} - \sqrt{2})/(\sqrt{w+1} + \sqrt{2})$. The form factor $\mathcal{F}(w)$ in Eq. (164) is thus described by the slope ρ^2 and the ratios $R_1(1)$ and $R_2(1)$.

Experiments have measured these three CLN parameters and extrapolated the rate to zero recoil $w = 1$ to determine $\eta_{\text{EW}}\mathcal{F}(1)|V_{cb}|$. At this kinematic point, the form factor normalization $\mathcal{F}(1)$ can be obtained from theory with high precision to measure $|V_{cb}|$. We perform a four-dimensional fit of $\eta_{\text{EW}}\mathcal{F}(1)|V_{cb}|$, ρ^2, $R_1(1)$ and $R_2(1)$ to the measurements shown in Table 71 taking into account correlated statistical and systematic uncertainties. A side product of the fit are best fit values of the original measurements, which we refer to a rescaled measurements. Most of the measurements in Table 71 are based on the decay $\bar{B}^0 \to D^{*+}\ell^-\bar{\nu}_\ell$. Some measurements [500,508] are sensitive also to $B^- \to D^{*0}\ell^-\bar{\nu}_\ell$, and one measurement [506] is based on the decay $B^- \to D^{*0}e^-\bar{\nu}_\ell$. Isospin symmetry is assumed in this average. We note that the earlier results from the LEP experiments and CLEO required significant rescaling and have significantly larger uncertainties than the recent measurements by Belle and *BABAR*. Only two measurements constrain all four parameters [501,502], and the remaining measurements determine only the normalization $\eta_{\text{EW}}\mathcal{F}(1)|V_{cb}|$ and the slope ρ^2.

The result of the fit is

$$\eta_{\text{EW}}\mathcal{F}(1)|V_{cb}| = (35.00 \pm 0.36) \times 10^{-3}, \quad (171)$$

$$\rho^2 = 1.121 \pm 0.024, \quad (172)$$

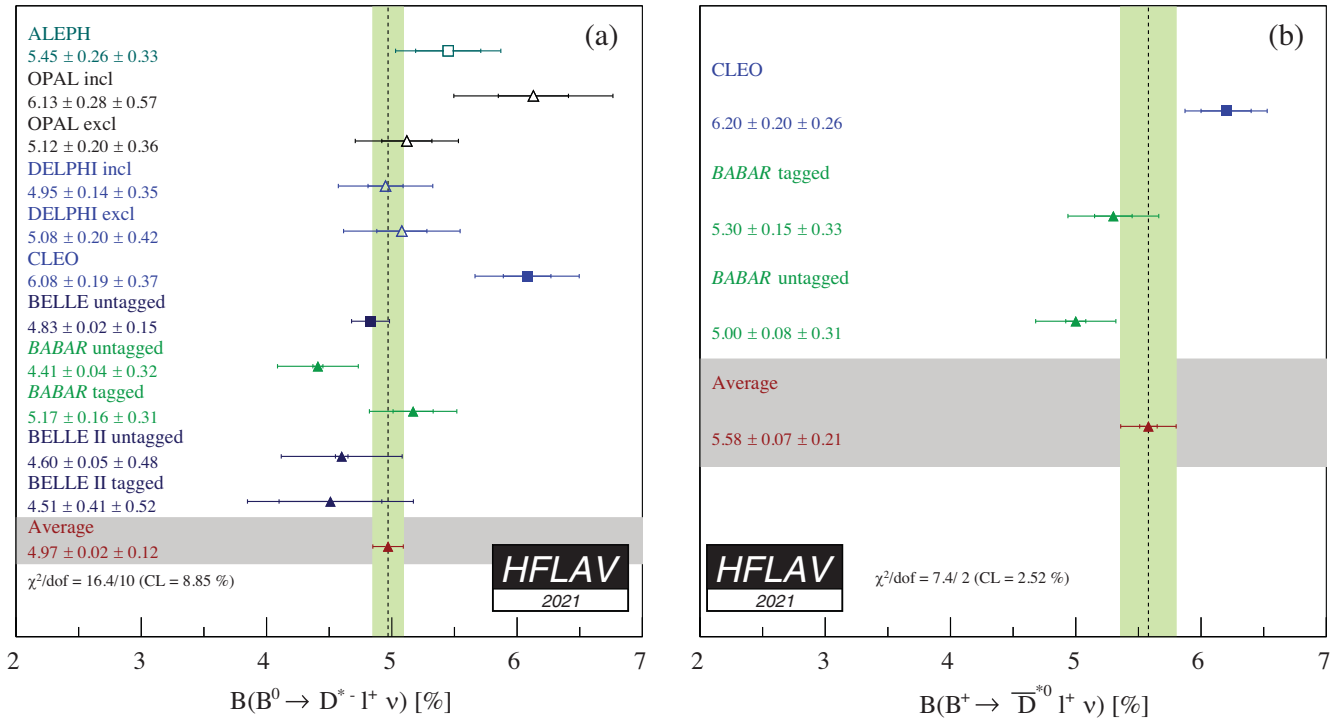

FIG. 49. Branching fractions of exclusive semileptonic B decays: (a) $\bar{B}^0 \to D^{*+}\ell^-\bar{\nu}_\ell$ (Table 69) and (b) $B^- \to D^{*0}\ell^-\bar{\nu}_\ell$ (Table 70).

TABLE 71. Measurements of the Caprini, Lellouch and Neubert (CLN) [507] form factor parameters in $\bar{B} \to D^* \ell^- \bar{\nu}_\ell$ before and after rescaling. Most analyses (except [502]) measure only $\eta_{\rm EW}\mathcal{F}(1)|V_{cb}|$, and ρ^2, so only these two parameters are shown here.

Experiment	$\eta_{\rm EW}\mathcal{F}(1)\lvert V_{cb}\rvert[10^{-3}]$ (rescaled) $\eta_{\rm EW}\mathcal{F}(1)\lvert V_{cb}\rvert[10^{-3}]$ (published)	ρ^2 (rescaled) ρ^2 (published)
ALEPH [496]	$31.38 \pm 1.80_{\rm stat} \pm 1.24_{\rm syst}$ $31.9 \pm 1.8_{\rm stat} \pm 1.9_{\rm syst}$	$0.488 \pm 0.226_{\rm stat} \pm 0.146_{\rm syst}$ $0.37 \pm 0.26_{\rm stat} \pm 0.14_{\rm syst}$
CLEO [500]	$40.16 \pm 1.24_{\rm stat} \pm 1.54_{\rm syst}$ $43.1 \pm 1.3_{\rm stat} \pm 1.8_{\rm syst}$	$1.363 \pm 0.084_{\rm stat} \pm 0.087_{\rm syst}$ $1.61 \pm 0.09_{\rm stat} \pm 0.21_{\rm syst}$
OPAL excl [497]	$36.20 \pm 1.58_{\rm stat} \pm 1.47_{\rm syst}$ $36.8 \pm 1.6_{\rm stat} \pm 2.0_{\rm syst}$	$1.198 \pm 0.206_{\rm stat} \pm 0.153_{\rm syst}$ $1.31 \pm 0.21_{\rm stat} \pm 0.16_{\rm syst}$
OPAL partial reco [497]	$37.44 \pm 1.20_{\rm stat} \pm 2.32_{\rm syst}$ $37.5 \pm 1.2_{\rm stat} \pm 2.5_{\rm syst}$	$1.090 \pm 0.137_{\rm stat} \pm 0.297_{\rm syst}$ $1.12 \pm 0.14_{\rm stat} \pm 0.29_{\rm syst}$
DELPHI partial reco [498]	$35.52 \pm 1.41_{\rm stat} \pm 2.29_{\rm syst}$ $35.5 \pm 1.4_{\rm stat}\,^{+2.3}_{-2.4\,\rm syst}$	$1.139 \pm 0.123_{\rm stat} \pm 0.382_{\rm syst}$ $1.34 \pm 0.14_{\rm stat}\,^{+0.24}_{-0.22\,\rm syst}$
DELPHI excl [499]	$35.87 \pm 1.69_{\rm stat} \pm 1.95_{\rm syst}$ $39.2 \pm 1.8_{\rm stat} \pm 2.3_{\rm syst}$	$1.070 \pm 0.141_{\rm stat} \pm 0.153_{\rm syst}$ $1.32 \pm 0.15_{\rm stat} \pm 0.33_{\rm syst}$
Belle [501]	$34.82 \pm 0.15_{\rm stat} \pm 0.55_{\rm syst}$ $35.06 \pm 0.15_{\rm stat} \pm 0.56_{\rm syst}$	$1.106 \pm 0.031_{\rm stat} \pm 0.008_{\rm syst}$ $1.106 \pm 0.031_{\rm stat} \pm 0.007_{\rm syst}$
BABAR excl [502]	$33.37 \pm 0.29_{\rm stat} \pm 0.97_{\rm syst}$ $34.7 \pm 0.3_{\rm stat} \pm 1.1_{\rm syst}$	$1.182 \pm 0.048_{\rm stat} \pm 0.029_{\rm syst}$ $1.18 \pm 0.05_{\rm stat} \pm 0.03_{\rm syst}$
BABAR D^{*0} [506]	$34.55 \pm 0.58_{\rm stat} \pm 1.06_{\rm syst}$ $35.9 \pm 0.6_{\rm stat} \pm 1.4_{\rm syst}$	$1.124 \pm 0.058_{\rm stat} \pm 0.053_{\rm syst}$ $1.16 \pm 0.06_{\rm stat} \pm 0.08_{\rm syst}$
BABAR global fit [508]	$35.45 \pm 0.20_{\rm stat} \pm 1.08_{\rm syst}$ $35.7 \pm 0.2_{\rm stat} \pm 1.2_{\rm syst}$	$1.171 \pm 0.019_{\rm stat} \pm 0.060_{\rm syst}$ $1.21 \pm 0.02_{\rm stat} \pm 0.07_{\rm syst}$
Average	$\mathbf{35.00 \pm 0.11_{stat} \pm 0.34_{syst}}$	$\mathbf{1.121 \pm 0.014_{stat} \pm 0.019_{syst}}$

$$R_1(1) = 1.269 \pm 0.026, \tag{173}$$

$$R_2(1) = 0.853 \pm 0.017, \tag{174}$$

and the correlation coefficients are

$$\rho_{\eta_{\rm EW}\mathcal{F}(1)|V_{cb}|,\rho^2} = 0.337, \tag{175}$$

$$\rho_{\eta_{\rm EW}\mathcal{F}(1)|V_{cb}|,R_1(1)} = -0.097, \tag{176}$$

$$\rho_{\eta_{\rm EW}\mathcal{F}(1)|V_{cb}|,R_2(1)} = -0.085, \tag{177}$$

$$\rho_{\rho^2,R_1(1)} = 0.565, \tag{178}$$

$$\rho_{\rho^2,R_2(1)} = -0.824, \tag{179}$$

$$\rho_{R_1(1),R_2(1)} = -0.714. \tag{180}$$

The uncertainties and correlations quoted here include both statistical and systematic contributions. The χ^2 of the fit is 42.2 for 23 degrees of freedom, which corresponds to a confidence level of 0.9%. The largest contribution to the χ^2 of the average is due to the ALEPH and CLEO measurements [496,500]. An illustration of this fit result is given in Fig. 50.

To convert this result into $|V_{cb}|$, theory input for the form factor normalization is required. We use the result of the FLAG 2021 average [509], with LQCD results from Refs. [510,511],

$$\eta_{\rm EW}\mathcal{F}(1) = 0.910 \pm 0.013, \tag{181}$$

where $\eta_{\rm EW} = 1.0066 \pm 0.0050$ has been used. The central value of the latter corresponds to the electroweak correction only. The uncertainty has been increased to accommodate the Coulomb effect [510,512]. With Eq. (171), this gives

$$|V_{cb}| = (38.46 \pm 0.40_{\rm exp} \pm 0.55_{\rm th}) \times 10^{-3}, \tag{182}$$

where the first uncertainty combines the statistical and systematic uncertainties from the experimental measurement and the second is theoretical (lattice QCD calculation and electroweak correction).

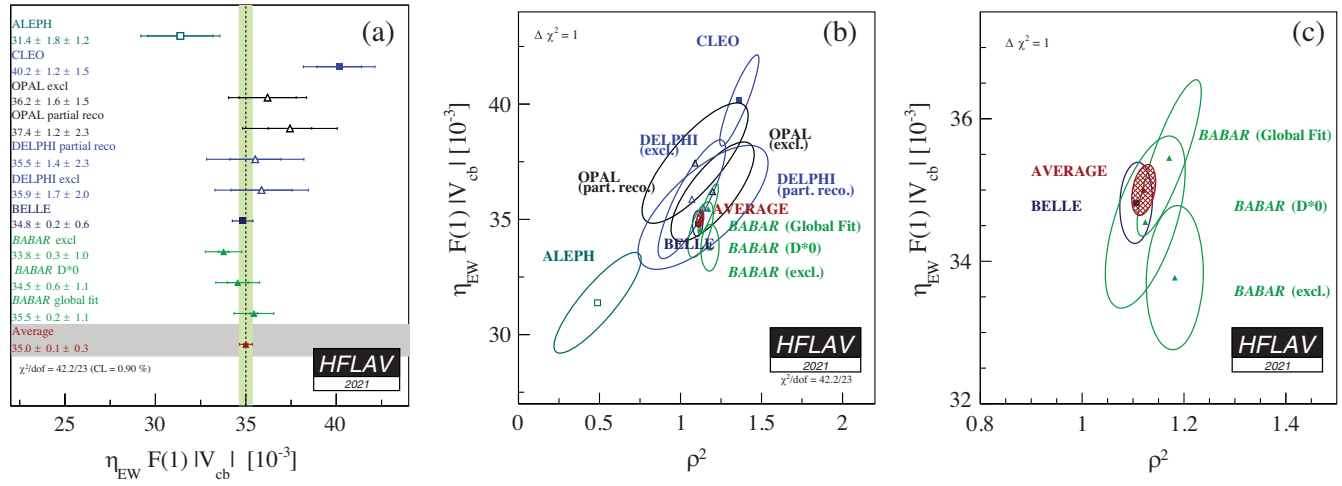

FIG. 50. Illustration of (a) the average and (b) the dependence of $\eta_{\rm EW}\mathcal{F}(1)|V_{cb}|$ on ρ^2. The error ellipses correspond to $\Delta\chi^2 = 1$ (CL = 39%). Figure (c) is a zoomed in view of the Belle and *BABAR* measurements.

Extraction of $|V_{cb}|$ based on the BGL form factor.—A more general parametrization of the $\bar{B} \to D^*\ell^-\bar{\nu}_\ell$ form factor is provided by Boyd, Grinstein and Lebed(BGL) [513–515]. Both Belle [501] and *BABAR* [516] have recently published analyses of $\bar{B} \to D^*\ell^-\bar{\nu}_\ell$ using the BGL form factor parametrization: While Belle performs an extraction of $|V_{cb}|$ using BGL, the *BABAR* analysis only fits the BGL form factor parameters but not the normalization. Due to the limited set of input measurements we do not perform a combination of the BGL form factor parameters or $|V_{cb}|$ obtained with the BGL form factor at this point. We simply note that $|V_{cb}|$ obtained in Refs. [501,517] using BGL is consistent with our average in Eq. (182).

2. $\bar{B} \to D\ell^-\bar{\nu}_\ell$

The differential decay rate for massless fermions as a function of w (introduced in the previous section) is given by (see, e.g., [494])

$$\frac{\bar{B} \to D\ell^-\bar{\nu}_\ell}{dw} = \frac{G_{\rm F}^2 m_D^3}{48\pi^3}(m_B + m_D)^2(w^2-1)^{3/2}\eta_{\rm EW}^2 \times \mathcal{G}^2(w)|V_{cb}|^2, \quad (183)$$

where $G_{\rm F}$ is Fermi's constant, and m_B and m_D are the B and D meson masses. Again, $\eta_{\rm EW}$ is the electroweak correction. In contrast to $\bar{B} \to D^*\ell^-\bar{\nu}_\ell$, $\mathcal{G}(w)$ contains a single form-factor function $f_+(w)$,

$$\mathcal{G}^2(w) = \frac{4r}{(1+r)^2} f_+^2(w), \quad (184)$$

where $r = m_D/m_B$.

Branching fraction.—Separate one-dimensional averages of the $\bar{B}^0 \to D^+\ell^-\bar{\nu}_\ell$ and $B^- \to D^0\ell^-\bar{\nu}_\ell$ branching fractions are shown in Tables 72 and 73. We obtain

$$\mathcal{B}(\bar{B}^0 \to D^+\ell^-\bar{\nu}_\ell) = (2.24 \pm 0.04 \pm 0.08)\%, \quad (185)$$

$$\mathcal{B}(B^- \to D^0\ell^-\bar{\nu}_\ell) = (2.30 \pm 0.03 \pm 0.08)\%, \quad (186)$$

where the first uncertainty is statistical and the second one is systematic. These fits are also shown in Fig. 51.

Extraction of $|V_{cb}|$ based on the CLN form factor.—As for $\bar{B} \to D^*\ell^-\bar{\nu}_\ell$ decays, we again adopt the prescription by Caprini, Lellouch and Neubert [507], which describes the shape and normalization of the measured decay distributions in terms of two parameters: the normalization $\mathcal{G}(1)$ and the slope ρ^2,

TABLE 72. Average of $\bar{B}^0 \to D^+\ell^-\bar{\nu}_\ell$ branching fraction measurements.

Experiment	$\mathcal{B}(\bar{B}^0 \to D^+\ell^-\bar{\nu}_\ell)$ [%] (rescaled)	$\mathcal{B}(\bar{B}^0 \to D^+\ell^-\bar{\nu}_\ell)$ [%] (published)
ALEPH [496]	$2.17 \pm 0.18_{\rm stat} \pm 0.35_{\rm syst}$	$2.35 \pm 0.20_{\rm stat} \pm 0.44_{\rm syst}$
CLEO [518]	$2.10 \pm 0.13_{\rm stat} \pm 0.15_{\rm syst}$	$2.20 \pm 0.16_{\rm stat} \pm 0.19_{\rm syst}$
BABAR [519]	$2.15 \pm 0.11_{\rm stat} \pm 0.14_{\rm syst}$	$2.23 \pm 0.11_{\rm stat} \pm 0.11_{\rm syst}$
Belle [520]	$2.33 \pm 0.04_{\rm stat} \pm 0.11_{\rm syst}$	$2.39 \pm 0.04_{\rm stat} \pm 0.11_{\rm syst}$
Average	$\mathbf{2.24 \pm 0.04_{stat} \pm 0.08_{syst}}$	$\mathbf{\chi^2/dof = 1.41/3}$ **(C.L.=70.2%)**

TABLE 73. Average of $B^- \to D^0 \ell^- \bar{\nu}_\ell$ branching fraction measurements.

Experiment	$\mathcal{B}(B^- \to D^0 \ell^- \bar{\nu}_\ell)$ [%] (rescaled)	$\mathcal{B}(B^- \to D^0 \ell^- \bar{\nu}_\ell)$ [%] (published)
CLEO [518]	$2.14 \pm 0.13_{\text{stat}} \pm 0.17_{\text{syst}}$	$2.32 \pm 0.17_{\text{stat}} \pm 0.20_{\text{syst}}$
BABAR [519]	$2.16 \pm 0.08_{\text{stat}} \pm 0.12_{\text{syst}}$	$2.31 \pm 0.08_{\text{stat}} \pm 0.09_{\text{syst}}$
Belle [520]	$2.46 \pm 0.04_{\text{stat}} \pm 0.12_{\text{syst}}$	$2.54 \pm 0.04_{\text{stat}} \pm 0.13_{\text{syst}}$
Average	$\mathbf{2.30 \pm 0.03_{stat} \pm 0.08_{syst}}$	$\boldsymbol{\chi^2/\text{dof} = 3.04/2}$ **(C.L.=21.8%)**

$$\mathcal{G}(w) = \mathcal{G}(1)[1 - 8\rho^2 z + (51\rho^2 - 10)z^2 - (252\rho^2 - 84)z^3], \tag{187}$$

where $z = (\sqrt{w+1} - \sqrt{2})/(\sqrt{w+1} + \sqrt{2})$.

Table 74 shows experimental measurements of the two CLN parameters, which are corrected to match the latest values of the input parameters. Both measurements of $\bar{B}^0 \to D^+ \ell^- \bar{\nu}_\ell$ and $B^- \to D^0 \ell^- \bar{\nu}_\ell$ are used and isospin symmetry is assumed in the analysis.

The form factor parameters are extracted by a two-parameter fit to the rescaled measurements of $\eta_{\text{EW}} \mathcal{G}(1)|V_{cb}|$ and ρ^2 taking into account correlated statistical and systematic uncertainties. The result of the fit is

$$\eta_{\text{EW}} \mathcal{G}(1)|V_{cb}| = (41.53 \pm 0.98) \times 10^{-3}, \tag{188}$$

$$\rho^2 = 1.129 \pm 0.033, \tag{189}$$

with a correlation of

$$\rho_{\eta_{\text{EW}} \mathcal{G}(1)|V_{cb}|, \rho^2} = 0.758. \tag{190}$$

The uncertainties and the correlation coefficient include both statistical and systematic contributions. The χ^2 of the fit is 4.6 for 8 degrees of freedom, which corresponds to a probability of 80.0%. An illustration of this fit result is given in Fig. 52.

The most recent lattice QCD result obtained for the form factor normalization is [512]

$$\mathcal{G}(1) = 1.0541 \pm 0.0083. \tag{191}$$

Using again $\eta_{\text{EW}} = 1.0066 \pm 0.0050$, we determine $|V_{cb}|$ from Eq. (188),

$$|V_{cb}| = (39.14 \pm 0.92_{\text{exp}} \pm 0.36_{\text{th}}) \times 10^{-3}, \tag{192}$$

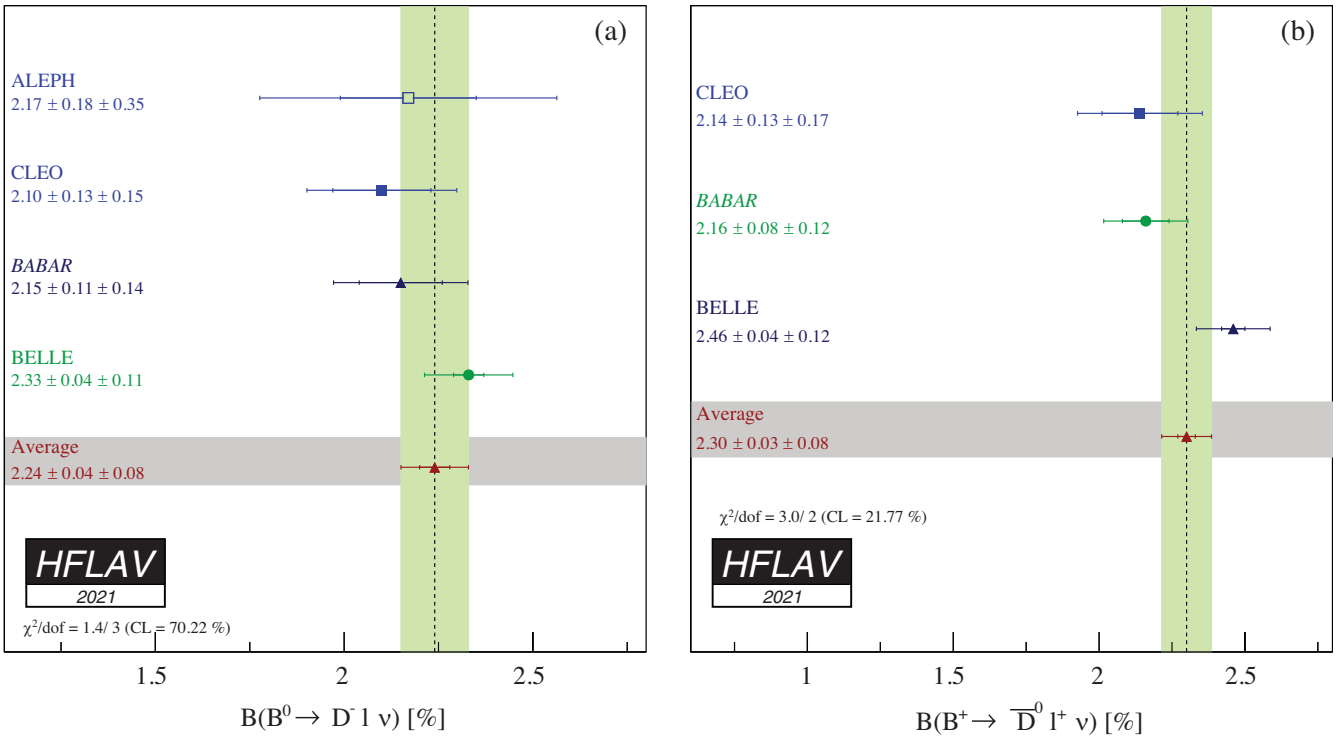

FIG. 51. Branching fractions of exclusive semileptonic B decays: (a) $\bar{B}^0 \to D^+ \ell^- \bar{\nu}_\ell$ (Table 72) and (b) $B^- \to D^0 \ell^- \bar{\nu}_\ell$ (Table 73).

TABLE 74. Measurements of the Caprini, Lellouch and Neubert (CLN) [507] form factor parameters in $\bar{B} \to D\ell^-\bar{\nu}_\ell$ before and after rescaling.

Experiment	$\eta_{\rm EW}\mathcal{G}(1)\lvert V_{cb}\rvert$ $[10^{-3}]$ (rescaled) $\eta_{\rm EW}\mathcal{G}(1)\lvert V_{cb}\rvert$ $[10^{-3}]$ (published)	ρ^2 (rescaled) ρ^2 (published)
ALEPH [496]	$36.19 \pm 9.38_{\rm stat} \pm 6.83_{\rm syst}$ $31.1 \pm 9.9_{\rm stat} \pm 8.6_{\rm syst}$	$0.814 \pm 0.821_{\rm stat} \pm 0.419_{\rm syst}$ $0.70 \pm 0.98_{\rm stat} \pm 0.50_{\rm syst}$
CLEO [518]	$44.17 \pm 5.68_{\rm stat} \pm 3.46_{\rm syst}$ $44.8 \pm 6.1_{\rm stat} \pm 3.7_{\rm syst}$	$1.270 \pm 0.214_{\rm stat} \pm 0.121_{\rm syst}$ $1.30 \pm 0.27_{\rm stat} \pm 0.14_{\rm syst}$
Belle [520]	$41.83 \pm 0.60_{\rm stat} \pm 1.20_{\rm syst}$ 42.29 ± 1.37	$1.090 \pm 0.036_{\rm stat} \pm 0.019_{\rm syst}$ 1.09 ± 0.05
BABAR global fit [508]	$42.55 \pm 0.71_{\rm stat} \pm 2.06_{\rm syst}$ $43.1 \pm 0.8_{\rm stat} \pm 2.3_{\rm syst}$	$1.194 \pm 0.034_{\rm stat} \pm 0.060_{\rm syst}$ $1.20 \pm 0.04_{\rm stat} \pm 0.07_{\rm syst}$
BABAR tagged [519]	$42.54 \pm 1.71_{\rm stat} \pm 1.26_{\rm syst}$ $42.3 \pm 1.9_{\rm stat} \pm 1.0_{\rm syst}$	$1.200 \pm 0.088_{\rm stat} \pm 0.043_{\rm syst}$ $1.20 \pm 0.09_{\rm stat} \pm 0.04_{\rm syst}$
Average	$\mathbf{41.53 \pm 0.44_{stat} \pm 0.88_{syst}}$	$\mathbf{1.129 \pm 0.024_{stat} \pm 0.023_{syst}}$

where the first error combines the statistical and systematic uncertainties from the experimental measurement and the second is theoretical. This number is in excellent agreement with $|V_{cb}|$ obtained from $\bar{B} \to D^*\ell^-\bar{\nu}_\ell$ decays given in Eq. (182).

Extraction of $|V_{cb}|$ based on the BGL form factor.—A more general expression for the $\bar{B} \to D\ell^-\bar{\nu}_\ell$ form factor is again BGL. If experimental data on the w spectrum is available, a BGL fit allows to include available lattice QCD data at nonzero recoil $w > 1$ [512,521] to improve the extrapolation to the zero recoil point $w = 1$. A w spectrum of $\bar{B} \to D\ell^-\bar{\nu}_\ell$ has been published by *BABAR* [519] and Belle [520]. As the *BABAR* result does not include the full error matrix of the w spectrum, we refrain from performing a combined BGL fit at this point. In Ref. [520] the values of $|V_{cb}|$ obtained by the CLN and BGL fits are consistent.

3. $B_s^0 \to D_s^{(*)-}\mu^+\nu_\mu$

LHCb has recently extracted $|V_{cb}|$ from semileptonic B_s^0 decays for the first time [522]. The measurement uses both $B_s^0 \to D_s^-\mu^+\nu_\mu$ and $B_s^0 \to D_s^{*-}\mu^+\nu_\mu$ decays using 3 fb^{-1} collected in 2011 and 2012. The value of $|V_{cb}|$ is determined from the observed yields of B_s^0 decays normalized to those of B^0 decays after correcting for the relative reconstruction and selection efficiencies, and considering the known relative B_s^0 and B^0 fragmentation fractions, f_s/f_d, in the LHCb acceptance.

The normalization channels are $B^0 \to D^-\mu^+\nu_\mu$ and $B^0 \to D^{*-}\mu^+\nu_\mu$ decays. One of the key features of the

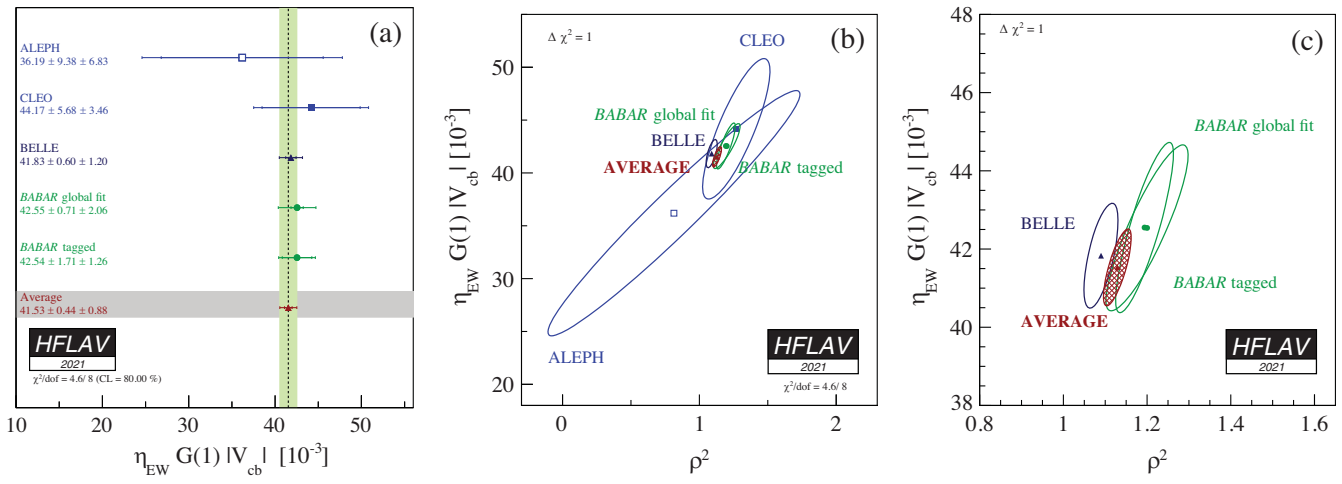

FIG. 52. Illustration of (a) the average and (b) dependence of $\eta_{\rm EW}\mathcal{G}(w)|V_{cb}|$ on ρ^2. The error ellipses correspond to $\Delta\chi^2 = 1$ (CL = 39%). Figure (c) is a zoomed in view of the Belle and *BABAR* measurements.

analysis is that the D^- is reconstructed with the same decay mode of the D_s ($D^-_{(s)} \to [K^+K^-]_\phi \pi^-$). With this choice the signal and the reference channels have the same particles in the final state and this minimizes the systematic uncertainties.

The shape of the form factors are extracted as well, exploiting the kinematic variable $p_\perp(D_s)$, which is the component of the D_s^- momentum perpendicular to the B_s^0 flight direction. This variable is highly correlated with q^2 and also slightly correlated with the helicity angles in the $B_s^0 \to D_s^{*-}\mu^+\nu_\mu$ decay. The D_s^{*-} is not explicitly reconstructed, but its contribution is disentangled kinematically from the D_s.

For the $B_s^0 \to D_s^-\mu^+\nu_\mu$ decay, $|V_{cb}|$ is connected with the measured ratio of signal yields, $N_{\rm sig}$, and the normalization channel yields, $N_{\rm ref}$, through the relation

$$\frac{N_{\rm sig}}{N_{\rm ref}} = \mathcal{K}\tau_s \int \frac{d\Gamma(B_s^0 \to D_s^-\mu^+\nu_\mu)}{dw} dw$$

where τ_s is the B_s^0 lifetime, and the constant $\mathcal{K}$ depends on the external inputs as

$$\mathcal{K} = \xi \frac{f_s}{f_d} \frac{\mathcal{B}(D_s^- \to K^+K^-\pi^-)}{\mathcal{B}(D^- \to K^+K^-\pi^-)} \frac{1}{\mathcal{B}(B^0 \to D^-\mu^+\nu_\mu)}$$

where ξ is the efficiency ratio between the signal and the normalization. In the analogous expression for the $B_s^0 \to D_s^{*-}\mu^+\nu_\mu$ decay, the integral of the decay width is done on the variables $(w, \cos\theta_\ell, \cos\theta_V, \chi)$, and there is an explicit dependence on the branching fraction of the $D^{*-} \to D^-\pi^0$ decay. The analysis takes advantage of the recent results from lattice on the $B_s^0 \to D_s^-$ and $B_s^0 \to D_s^{*-}$ form factor calculations. In particular, for the $B_s^0 \to D_s^{*-}$ only the calculation at zero recoil, $h_{A1}^{B_s}(1)$ from Ref. [523] is used. For the $B_s^0 \to D_s^-\mu^+\nu_\mu$ decay, the very recent calculation of the $B_s^0 \to D_s^-$ form factors performed in the full w-range [524] are used.

In this analysis both the CLN parametrization and a 5-parameter version of BGL have been used. The results of the form factors are affected by large statistical uncertainty, but are consistent with the results from the B decays. The result for $|V_{cb}|$, updated with the most recent determination of f_s/f_d and $\mathcal{B}(D_s^- \to K^+K^-\pi^-)$ from Ref. [525], are

$$\begin{aligned} |V_{cb}|_{\rm CLN} &= (40.8 \pm 0.6 \pm 0.9 \pm 1.1) \times 10^{-3}, \\ |V_{cb}|_{\rm BGL} &= (41.7 \pm 0.8 \pm 0.9 \pm 1.1) \times 10^{-3}, \end{aligned} \quad (193)$$

where the first uncertainty is statistical, the second systematic and the third due to the limited knowledge of the external inputs, in particular the constant $f_s/f_d \times \mathcal{B}(D_s^- \to K^+K^-\pi^-)$. The results obtained are in agreement with the exclusive determinations of $|V_{cb}|$ using the B^0 and B^+ decays.

4. $\bar{B} \to D^{(*)}\pi\ell^-\bar{\nu}_\ell$

The average inclusive branching fractions for $\bar{B} \to D^{(*)}\pi\ell^-\bar{\nu}_\ell$ decays, where no constraint is applied to the

TABLE 75. Averages of the $B \to D^{(*)}\pi^-\ell^-\bar{\nu}_\ell$ branching fractions and individual results.

Experiment	$\mathcal{B}(B^- \to D^+\pi^-\ell^-\bar{\nu}_\ell)$ [%] (rescaled)	$\mathcal{B}(B^- \to D^+\pi^-\ell^-\bar{\nu}_\ell)$ [%] (published)
Belle [526]	$0.455 \pm 0.027_{\rm stat} \pm 0.035_{\rm syst}$	$0.455 \pm 0.027_{\rm stat} \pm 0.039_{\rm syst}$
BABAR [503]	$0.405 \pm 0.060_{\rm stat} \pm 0.031_{\rm syst}$	$0.42 \pm 0.06_{\rm stat} \pm 0.03_{\rm syst}$
Average	**0.440±0.025±0.027**	**χ^2/dof=0.387 (C.L.=53.4%)**
Experiment	$\mathcal{B}(B^- \to D^{*+}\pi^-\ell^-\bar{\nu}_\ell)$ [%] (rescaled)	$\mathcal{B}(B^- \to D^{*+}\pi^-\ell^-\bar{\nu}_\ell)$ [%] (published)
Belle [526]	$0.603 \pm 0.043_{\rm stat} \pm 0.039_{\rm syst}$	$0.604 \pm 0.043_{\rm stat} \pm 0.038_{\rm syst}$
BABAR [503]	$0.567 \pm 0.050_{\rm stat} \pm 0.045_{\rm syst}$	$0.59 \pm 0.05_{\rm stat} \pm 0.04_{\rm syst}$
Average	**0.587±0.033±0.029**	**χ^2/dof=0.171 (C.L.=67.9%)**
Experiment	$\mathcal{B}(\bar{B}^0 \to D^0\pi^+\ell^-\bar{\nu}_\ell)$ [%] (rescaled)	$\mathcal{B}(\bar{B}^0 \to D^0\pi^+\ell^-\bar{\nu}_\ell)$ [%] (published)
Belle [526]	$0.405 \pm 0.036_{\rm stat} \pm 0.043_{\rm syst}$	$0.405 \pm 0.036_{\rm stat} \pm 0.041_{\rm syst}$
BABAR [503]	$0.406 \pm 0.080_{\rm stat} \pm 0.035_{\rm syst}$	$0.43 \pm 0.08_{\rm stat} \pm 0.03_{\rm syst}$
Average	**0.405±0.033±0.034**	**χ^2/dof=0.0002 (C.L.=99.0%)**
Experiment	$\mathcal{B}(\bar{B}^0 \to D^{*0}\pi^+\ell^-\bar{\nu}_\ell)$ [%] (rescaled)	$\mathcal{B}(\bar{B}^0 \to D^{*0}\pi^+\ell^-\bar{\nu}_\ell)$ [%] (published)
Belle [526]	$0.646 \pm 0.053_{\rm stat} \pm 0.062_{\rm syst}$	$0.646 \pm 0.053_{\rm stat} \pm 0.052_{\rm syst}$
BABAR [503]	$0.461 \pm 0.081_{\rm stat} \pm 0.044_{\rm syst}$	$0.48 \pm 0.08_{\rm stat} \pm 0.04_{\rm syst}$
Average	**0.564±0.044±0.042**	**χ^2/dof=2.28 (C.L.=13.1%)**

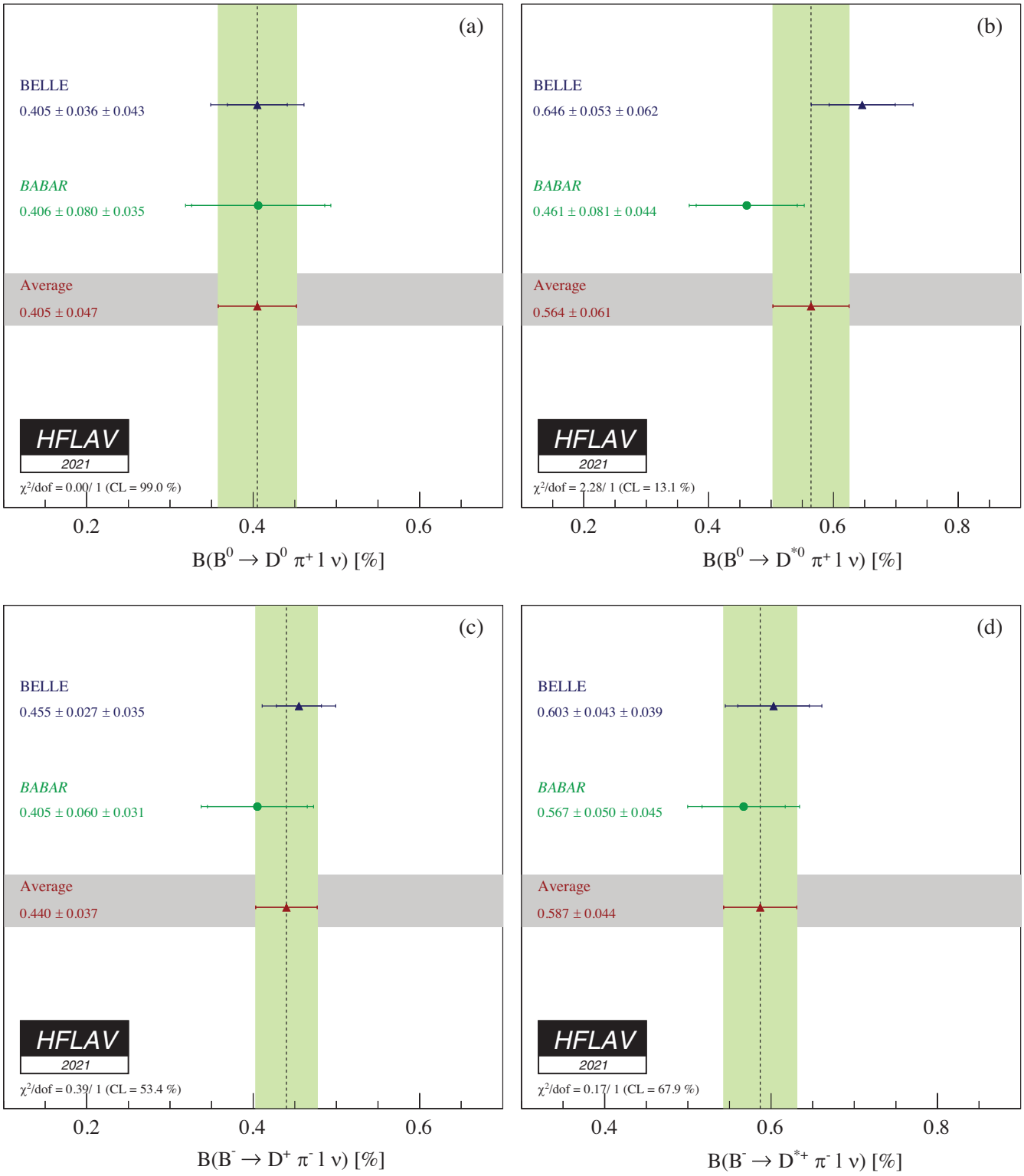

FIG. 53. Average branching fraction of exclusive semileptonic B decays (a) $\bar{B}^0 \to D^0\pi^+\ell^-\bar{\nu}_\ell$, (b) $\bar{B}^0 \to D^{*0}\pi^+\ell^-\bar{\nu}_\ell$, (c) $B^- \to D^+\pi^-\ell^-\bar{\nu}_\ell$, and (d) $B^- \to D^{*+}\pi^-\ell^-\bar{\nu}_\ell$. The corresponding individual results are also shown.

mass of the $D^{(*)}\pi$ system, are determined by the combination of the results provided in Table 75 for $\bar{B}^0 \to D^0\pi^+\ell^-\bar{\nu}_\ell$, $\bar{B}^0 \to D^{*0}\pi^+\ell^-\bar{\nu}_\ell$, $B^- \to D^+\pi^-\ell^-\bar{\nu}_\ell$, and $B^- \to D^{*+}\pi^-\ell^-\bar{\nu}_\ell$ decays. For the $\bar{B}^0 \to D^0\pi^+\ell^-\bar{\nu}_\ell$ decays a veto to reject the $D^{*+} \to D^0\pi^+$ decays is applied. The measurements included in the average are scaled to a consistent set of input parameters and their uncertainties. For both the *BABAR* and Belle results, the B semileptonic

TABLE 76. Published and rescaled individual measurements and their averages for the branching fraction $\mathcal{B}(B^- \to D_1^0 \ell^- \bar{\nu}_\ell) \times \mathcal{B}(D_1^0 \to D^{*+}\pi^-)$.

Experiment	$\mathcal{B}(B^- \to D_1^0(D^{*+}\pi^-)\ell^-\bar{\nu}_\ell)$ [%] (rescaled)	$\mathcal{B}(B^- \to D_1^0(D^{*+}\pi^-)\ell^-\bar{\nu}_\ell)$ [%] (published)
ALEPH [531]	$0.436 \pm 0.098_{\text{stat}} \pm 0.067_{\text{syst}}$	$0.47 \pm 0.10_{\text{stat}} \pm 0.07_{\text{syst}}$
OPAL [532]	$0.553 \pm 0.210_{\text{stat}} \pm 0.100_{\text{syst}}$	$0.70 \pm 0.21_{\text{stat}} \pm 0.10_{\text{syst}}$
CLEO [533]	$0.345 \pm 0.085_{\text{stat}} \pm 0.056_{\text{syst}}$	$0.373 \pm 0.085_{\text{stat}} \pm 0.057_{\text{syst}}$
D0 [534]	$0.214 \pm 0.018_{\text{stat}} \pm 0.035_{\text{syst}}$	$0.219 \pm 0.018_{\text{stat}} \pm 0.035_{\text{syst}}$
Belle Tagged B^- [529]	$0.430 \pm 0.070_{\text{stat}} \pm 0.059_{\text{syst}}$	$0.42 \pm 0.07_{\text{stat}} \pm 0.07_{\text{syst}}$
Belle Tagged B^0 [529]	$0.593 \pm 0.200_{\text{stat}} \pm 0.076_{\text{syst}}$	$0.42 \pm 0.07_{\text{stat}} \pm 0.07_{\text{syst}}$
BABAR Tagged [528]	$0.273 \pm 0.030_{\text{stat}} \pm 0.029_{\text{syst}}$	$0.29 \pm 0.03_{\text{stat}} \pm 0.03_{\text{syst}}$
BABAR Untagged B^- [535]	$0.289 \pm 0.017_{\text{stat}} \pm 0.016_{\text{syst}}$	$0.30 \pm 0.02_{\text{stat}} \pm 0.02_{\text{syst}}$
BABAR Untagged B^0 [535]	$0.277 \pm 0.026_{\text{stat}} \pm 0.023_{\text{syst}}$	$0.30 \pm 0.02_{\text{stat}} \pm 0.02_{\text{syst}}$
Average	**$0.277 \pm 0.010 \pm 0.015$**	**χ^2/dof=11.9/8 (C.L.=15.5%)**

TABLE 77. Published and rescaled individual measurements and their averages for $\mathcal{B}(B^- \to D_2^0 \ell^- \bar{\nu}_\ell) \times \mathcal{B}(D_2^0 \to D^{*+}\pi^-)$.

Experiment	$\mathcal{B}(B^- \to D_2^0(D^{*+}\pi^-)\ell^-\bar{\nu}_\ell)$ [%] (rescaled)	$\mathcal{B}(B^- \to D_2^0(D^{*+}\pi^-)\ell^-\bar{\nu}_\ell)$ [%] (published)
CLEO [533]	$0.055 \pm 0.066_{\text{stat}} \pm 0.011_{\text{syst}}$	$0.059 \pm 0.066_{\text{stat}} \pm 0.011_{\text{syst}}$
D0 [534]	$0.086 \pm 0.018_{\text{stat}} \pm 0.020_{\text{syst}}$	$0.088 \pm 0.018_{\text{stat}} \pm 0.020_{\text{syst}}$
Belle tagged [529]	$0.184 \pm 0.060_{\text{stat}} \pm 0.025_{\text{syst}}$	$0.18 \pm 0.06_{\text{stat}} \pm 0.03_{\text{syst}}$
BABAR tagged [528]	$0.076 \pm 0.013_{\text{stat}} \pm 0.009_{\text{syst}}$	$0.078 \pm 0.013_{\text{stat}} \pm 0.010_{\text{syst}}$
BABAR untagged B^- [535]	$0.087 \pm 0.009_{\text{stat}} \pm 0.007_{\text{syst}}$	$0.087 \pm 0.013_{\text{stat}} \pm 0.007_{\text{syst}}$
BABAR untagged B^0 [535]	$0.065 \pm 0.010_{\text{stat}} \pm 0.004_{\text{syst}}$	$0.087 \pm 0.013_{\text{stat}} \pm 0.007_{\text{syst}}$
Average	**$0.077 \pm 0.006 \pm 0.004$**	**χ^2/dof=5.34/5 (C.L.=37.6%)**

signal yields are extracted from a fit to the missing mass squared distribution for a sample of fully reconstructed $B\bar{B}$ events. Figure 53 shows the measurements and the resulting average for the four decay modes.

5. $\bar{B} \to D^{**}\ell^-\bar{\nu}_\ell$

In this section we report results on $\bar{B} \to D^{**}\ell^-\bar{\nu}_\ell$ decays, where D^{**} here denotes the lightest excited charm mesons above the D and D^* states. According to heavy quark symmetry (HQS) [527], the D^* mesons with a charm and antiquark with relative angular momentum $L = 1$, form one doublet of states with angular momentum $j \equiv s_q + L = 3/2$ $[D_1(2420), D_2^*(2460)]$ and another doublet with $j = 1/2$ $[D_0^*(2400), D_1'(2430)]$, where s_q is the light quark spin.[32] Parity and angular momentum conservation constrain the decays allowed for each state. The D_1 and D_2^* states decay predominantly via D-wave to $D^*\pi$ and $D^{(*)}\pi$, respectively, and have small decay widths, while the D_0^* and D_1' states decay via S-wave to $D\pi$ and $D^*\pi$ and are very broad. For the narrow states, the averages are determined by the combination of the results provided in Table 76 and 77 for $\mathcal{B}(B^- \to D_1^0 \ell^- \bar{\nu}_\ell) \times \mathcal{B}(D_1^0 \to D^{*+}\pi^-)$ and $\mathcal{B}(B^- \to D_2^0 \ell^- \bar{\nu}_\ell) \times \mathcal{B}(D_2^0 \to D^{*+}\pi^-)$. For the broad states, the averages are determined by the combination of the results provided in Table 78 and 79 for $\mathcal{B}(B^- \to D_1'^0 \ell^- \bar{\nu}_\ell) \times \mathcal{B}(D_1'^0 \to D^{*+}\pi^-)$ and $\mathcal{B}(B^- \to D_0^{*0} \ell^- \bar{\nu}_\ell) \times \mathcal{B}(D_0^{*0} \to D^+\pi^-)$. The measurements are scaled to a consistent set of input parameters and their uncertainties. The results are reported for B^-, and when measurements for both B^0 and B^- are available, the combination assumes the isospin symmetry. It is worth noticing that, while the results for the narrow resonances and the D_0^* are consistent between the various experiments, the available measurements for $B^- \to D_1'^0 \ell^- \bar{\nu}_\ell$ obtained by *BABAR* [528], Belle [529] and DELPHI [530], are not compatible. In particular Belle did not observed a significant $B^- \to D_1'^0 \ell^- \bar{\nu}_\ell$ contribution and put an upper limit on the presence of the $D_1'^0$ state.

For both the B-factory and the LEP and Tevatron results, the B semileptonic signal yields are extracted

[32] At present only these $L = 1$ orbital excited states have been observed in the semileptonic B meson decays, but in principle also radial $2S$ excitation and states with $L = 2$, 3, observed in fully hadronic B decays, could contribute to semileptonic decays.

TABLE 78. Published and rescaled individual measurements and their averages for $\mathcal{B}(B^- \to D_1'^0 \ell^- \bar{\nu}_\ell) \times \mathcal{B}(D_1'^0 \to D^{*+}\pi^-)$.

Experiment	$\mathcal{B}(B^- \to D_1'^0(D^{*+}\pi^-)\ell^-\bar{\nu}_\ell)$ [%] (rescaled)	$\mathcal{B}(B^- \to D_1'^0(D^{*+}\pi^-)\ell^-\bar{\nu}_\ell)$ [%] (published)
DELPHI [530]	$0.69 \pm 0.17_{\text{stat}} \pm 0.18_{\text{syst}}$	$0.83 \pm 0.17_{\text{stat}} \pm 0.18_{\text{syst}}$
Belle [529]	$-0.03 \pm 0.06_{\text{stat}} \pm 0.07_{\text{syst}}$	$-0.03 \pm 0.06_{\text{stat}} \pm 0.07_{\text{syst}}$
BABAR [528]	$0.25 \pm 0.04_{\text{stat}} \pm 0.05_{\text{syst}}$	$0.27 \pm 0.04_{\text{stat}} \pm 0.05_{\text{syst}}$
Average	**0.19±0.03±0.04**	**χ^2/dof=11.1/2 (C.L.=0.38%)**

TABLE 79. Published and rescaled individual measurements and their averages for $\mathcal{B}(B^- \to D_0^{*0} \ell^- \bar{\nu}_\ell) \times \mathcal{B}(D_0^{*0} \to D^+\pi^-)$.

Experiment	$\mathcal{B}(B^- \to D_0^{*0}(D^+\pi^-)\ell^-\bar{\nu}_\ell)$ [%] (rescaled)	$\mathcal{B}(B^- \to D_0^{*0}(D^+\pi^-)\ell^-\bar{\nu}_\ell)$ [%] (published)
Belle Tagged B^- [529]	$0.25 \pm 0.04_{\text{stat}} \pm 0.06_{\text{syst}}$	$0.24 \pm 0.04_{\text{stat}} \pm 0.06_{\text{syst}}$
Belle Tagged B^0 [529]	$0.23 \pm 0.08_{\text{stat}} \pm 0.06_{\text{syst}}$	$0.24 \pm 0.04_{\text{stat}} \pm 0.06_{\text{syst}}$
BABAR Tagged [528]	$0.31 \pm 0.04_{\text{stat}} \pm 0.05_{\text{syst}}$	$0.26 \pm 0.05_{\text{stat}} \pm 0.04_{\text{syst}}$
Average	**0.28±0.03±0.04**	**χ^2/dof=0.65/2 (C.L.=72.0%)**

from a fit to the invariant mass distribution of the $D^{(*)+}\pi^-$ system. The LEP and Tevatron measurements are for the inclusive decays $\bar{B} \to D^{**}(D^*\pi^-)X\ell^-\bar{\nu}_\ell$. In the average with the results from the B-factories, we use these measurements assuming that no particles are left in the X system. The *BABAR* tagged analysis of $\bar{B} \to D_2^*\ell^-\bar{\nu}_\ell$ was performed selecting $D_2^* \to D\pi$ decays. The *BABAR* result reported in Table 77 is translated in a branching fraction for the $D_2^* \to D^*\pi$ decay mode assuming $\mathcal{B}(D_2^* \to D\pi)/\mathcal{B}(D_2^* \to D^*\pi) = 1.52 \pm 0.14$ [9]. Figure 54 and 55 show the measurements and the resulting averages.

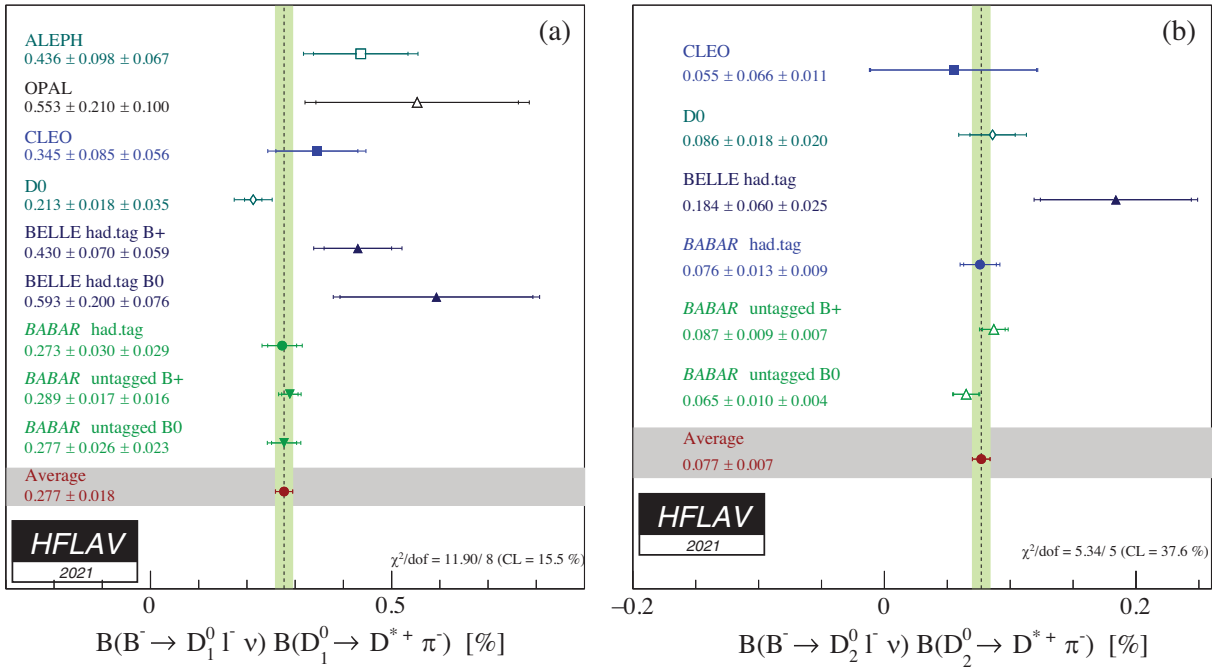

FIG. 54. Rescaled individual measurements and their averages for (a) $\mathcal{B}(B^- \to D_1^0\ell^-\bar{\nu}_\ell) \times \mathcal{B}(D_1^0 \to D^{*+}\pi^-)$ and (b) $\mathcal{B}(B^- \to D_2^0\ell^-\bar{\nu}_\ell) \times \mathcal{B}(D_2^0 \to D^{*+}\pi^-)$.

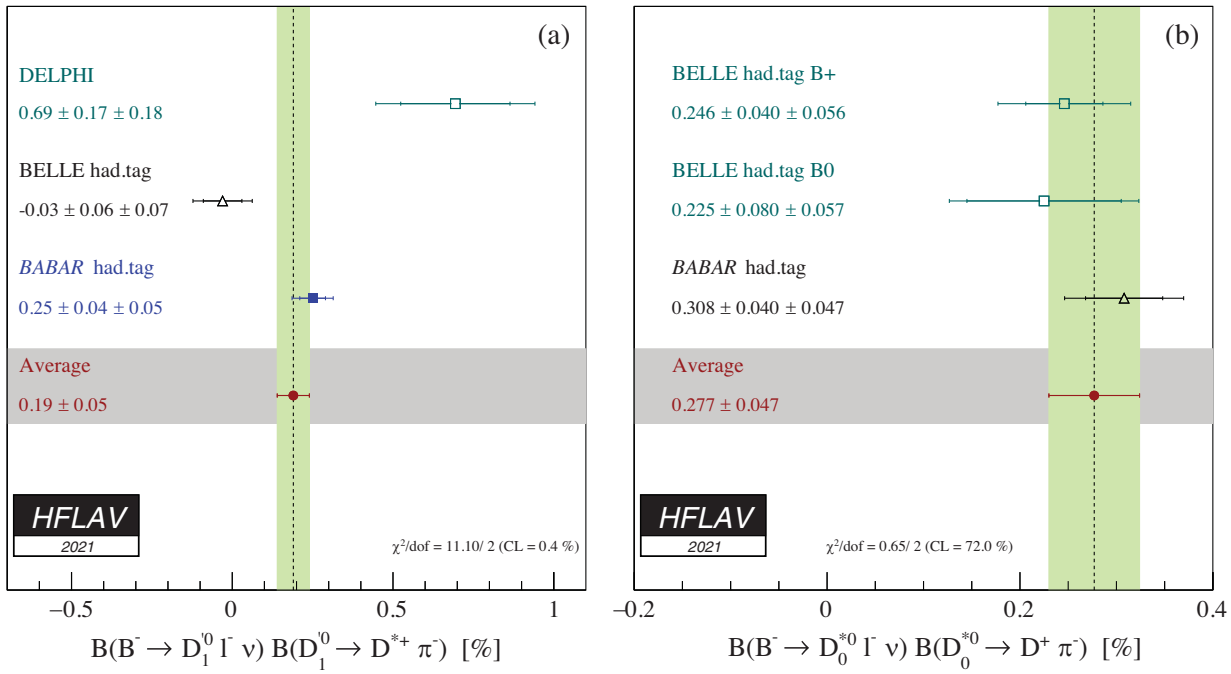

FIG. 55. Rescaled individual measurements and their averages for (a) $\mathcal{B}(B^- \to D_1'^0 \ell^- \bar{\nu}_\ell) \times \mathcal{B}(D_1'^0 \to D^{*+}\pi^-)$ and (b) $\mathcal{B}(B^- \to D_0^{*0} \ell^- \bar{\nu}_\ell) \times \mathcal{B}(D_0^{*0} \to D^+\pi^-)$.

B. Inclusive CKM-favored decays

1. Global analysis of $\bar{B} \to X_c \ell^- \bar{\nu}_\ell$

The semileptonic decay width $\Gamma(\bar{B} \to X_c \ell^- \bar{\nu}_\ell)$ has been calculated in the framework of the operator production expansion (OPE) [36–38]. The result is a double-expansion in $\Lambda_{\rm QCD}/m_b$ and α_s, which depends on a number of nonperturbative parameters. These parameters describe the dynamics of the b-quark inside the B hadron and can be measured using observables in $\bar{B} \to X_c \ell^- \bar{\nu}_\ell$ decays, such as the moments of the lepton energy and the hadronic mass spectrum.

Two renormalization schemes are commonly used to define the b-quark mass and other theoretical quantities: the kinetic [536–539] and the 1S [540] schemes. Independent sets of theoretical expressions are available for each, with several nonperturbative parameters. The nonperturbative parameters in the kinetic scheme are: the quark masses m_b and m_c, μ_π^2 and μ_G^2 at $O(1/m_b^2)$, and ρ_D^3 and ρ_{LS}^3 at $O(1/m_b^3)$. In the 1S scheme, the parameters are: m_b, λ_1 at $O(1/m_b^2)$, and ρ_1, τ_1, τ_2 and τ_3 at $O(1/m_b^3)$. Note that the numerical values of the kinetic and 1S b-quark masses cannot be compared without converting them to the same renormalization scheme.

We use two sets of inclusive observables in $\bar{B} \to X_c \ell^- \bar{\nu}_\ell$ decays to constrain OPE parameters: the moments of the hadronic system effective mass $\langle M_X^n \rangle$ of order $n = 2, 4, 6$, and the moments of the charged lepton momentum $\langle E_\ell^n \rangle$ of order $n = 0, 1, 2, 3$. Moments are determined for different values of $E_{\rm cut}$, the lower limit on the lepton momentum. Moments derived from the same spectrum with different value of $E_{\rm cut}$ are highly correlated. The list of measurements used in our analysis is given in Table 80. The only external input is the average lifetime τ_B of neutral and charged B mesons, taken to be (1.579 ± 0.004) ps (see Sec. V).

In the kinetic and 1S schemes, the moments in $\bar{B} \to X_c \ell^- \bar{\nu}_\ell$ are not sufficient to determine the b-quark mass precisely. In the kinetic scheme analysis, only a combination of m_b and m_c is well determined and we constrain the c-quark mass (defined in the $\overline{\rm MS}$ scheme) to the value of Ref. [547],

$$m_c^{\overline{\rm MS}}(3\ {\rm GeV}) = 0.986 \pm 0.013\ {\rm GeV} \qquad (194)$$

to pinpoint m_b. In the 1S scheme analysis, the b-quark mass is constrained by measurements of the photon energy moments in $B \to X_s\gamma$ [548–551].

2. Analysis in the kinetic scheme

We obtain $|V_{cb}|$ and the six nonperturbative parameters mentioned above with a fit that follows closely the procedure described in Ref. [552] and relies on the calculations of the lepton energy and hadronic mass moments in $\bar{B} \to X_c \ell^- \bar{\nu}_\ell$ decays described in Refs. [538,539]. The detailed fit result and the matrix of the correlation coefficients is given in Table 81. Projections of the fit onto the lepton energy and hadronic mass moments are shown in Figs. 56 and 57, respectively. The result in terms of the main parameters is

TABLE 80. Experimental inputs used in the global analysis of $\bar{B} \to X_c \ell^- \bar{\nu}_\ell$. n is the order of the moment, c is the threshold value of the lepton momentum in GeV. In total, there are 23 measurements from *BABAR*, 15 measurements from Belle and 12 from other experiments.

Experiment	Hadron moments $\langle M_X^n \rangle$	Lepton moments $\langle E_\ell^n \rangle$
BABAR	$n = 2$, $c = 0.9$, 1.1, 1.3, 1.5 $n = 4$, $c = 0.8$, 1.0, 1.2, 1.4 $n = 6$, $c = 0.9$, 1.3 [541]	$n = 0$, $c = 0.6$, 1.2, 1.5 $n = 1$, $c = 0.6$, 0.8, 1.0, 1.2, 1.5 $n = 2$, $c = 0.6$, 1.0, 1.5 $n = 3$, $c = 0.8$, 1.2 [541,542]
Belle	$n = 2$, $c = 0.7$, 1.1, 1.3, 1.5 $n = 4$, $c = 0.7$, 0.9, 1.3 [543]	$n = 0$, $c = 0.6$, 1.4 $n = 1$, $c = 1.0$, 1.4 $n = 2$, $c = 0.6$, 1.4 $n = 3$, $c = 0.8$, 1.2 [544]
CDF	$n = 2$, $c = 0.7$ $n = 4$, $c = 0.7$ [545]	
CLEO	$n = 2$, $c = 1.0$, 1.5 $n = 4$, $c = 1.0$, 1.5 [546]	
DELPHI	$n = 2$, $c = 0.0$ $n = 4$, $c = 0.0$ $n = 6$, $c = 0.0$ [530]	$n = 1$, $c = 0.0$ $n = 2$, $c = 0.0$ $n = 3$, $c = 0.0$ [530]

$$|V_{cb}| = (42.19 \pm 0.78) \times 10^{-3}, \tag{195}$$

$$m_b^{\rm kin} = 4.554 \pm 0.018 \text{ GeV}, \tag{196}$$

$$\mu_\pi^2 = 0.464 \pm 0.076 \text{ GeV}^2, \tag{197}$$

with a χ^2 of 15.6 for 43 degrees of freedom. The scale μ of the quantities in the kinetic scheme is 1 GeV.

The inclusive $\bar{B} \to X_c \ell^- \bar{\nu}_\ell$ branching fraction determined by this analysis is

$$\mathcal{B}(\bar{B} \to X_c \ell^- \bar{\nu}_\ell) = (10.65 \pm 0.16)\%. \tag{198}$$

Including the branching fraction of charmless semileptonic decays (Sec. VII D), $\mathcal{B}(\bar{B} \to X_u \ell^- \bar{\nu}_\ell) = (1.91 \pm 0.27) \times 10^{-3}$, we obtain the semileptonic branching fraction,

$$\mathcal{B}(\bar{B} \to X \ell^- \bar{\nu}_\ell) = (10.84 \pm 0.16)\%. \tag{199}$$

3. Analysis in the 1S scheme

The fit relies on the same set of moment measurements and the calculations of the spectral moments described in Ref. [540]. The theoretical uncertainties are estimated as explained in Ref. [553]. No theory error correlations between different moments are assumed (except between

TABLE 81. Fit result in the kinetic scheme, using a precise c-quark mass constraint. The error matrix of the fit contains experimental and theoretical contributions. In the lower part of the table, the correlation matrix of the parameters is given. The scale μ of the quantities in the kinematic scheme is 1 GeV.

	$\lvert V_{cb}\rvert$ [10^{-3}]	$m_b^{\rm kin}$ [GeV]	$m_c^{\overline{\rm MS}}$ [GeV]	μ_π^2 [GeV^2]	ρ_D^3 [GeV^3]	μ_G^2 [GeV^2]	ρ_{LS}^3 [GeV^3]
Value	42.19	4.554	0.987	0.464	0.169	0.333	−0.153
Error	0.78	0.018	0.015	0.076	0.043	0.053	0.096
$\lvert V_{cb}\rvert$	1.000	−0.257	−0.078	0.354	0.289	−0.080	−0.051
$m_b^{\rm kin}$		1.000	0.769	−0.054	0.097	0.360	−0.087
$m_c^{\overline{\rm MS}}$			1.000	−0.021	0.027	0.059	−0.013
μ_π^2				1.000	0.732	0.012	0.020
ρ_D^3					1.000	−0.173	−0.123
μ_G^2						1.000	0.066
ρ_{LS}^3							1.000

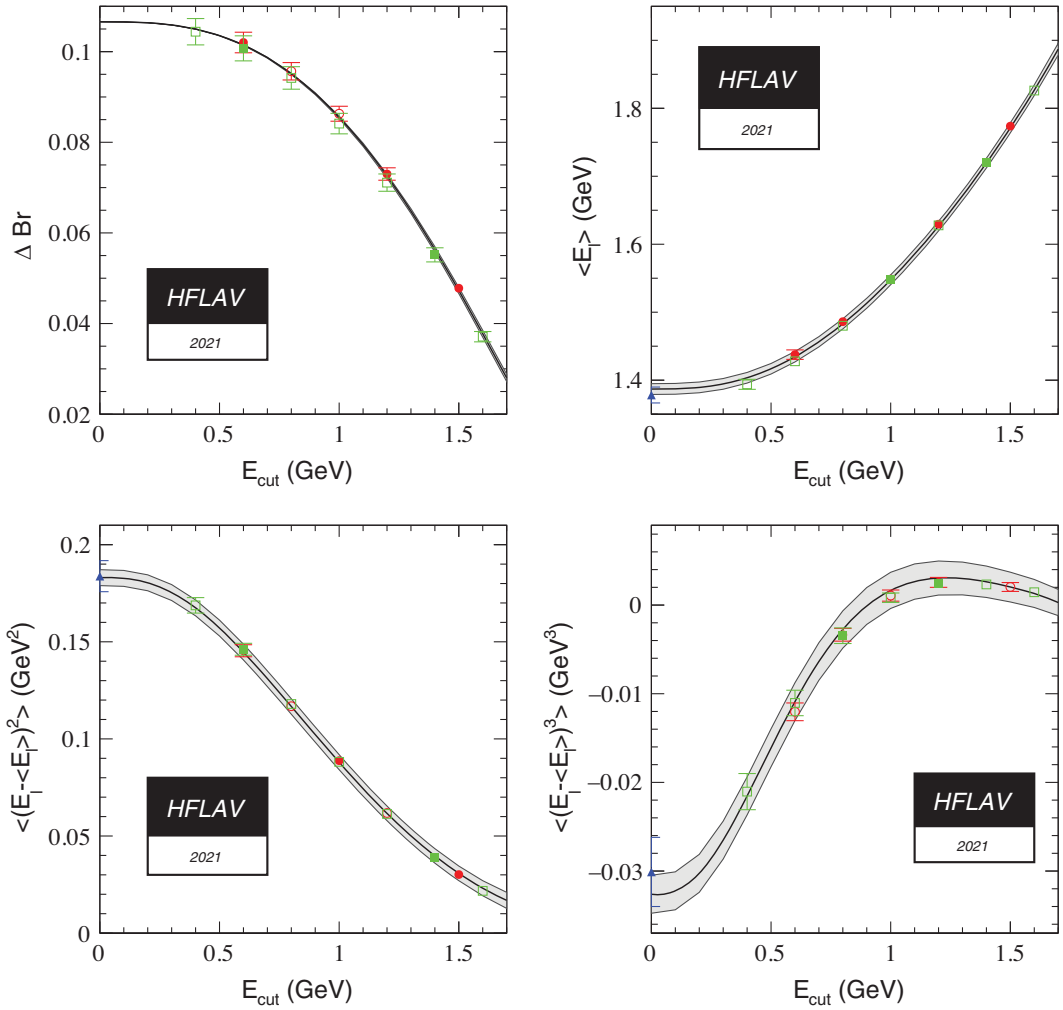

FIG. 56. Fit to the inclusive partial semileptonic branching fractions and to the lepton energy moments in the kinetic mass scheme. In all plots, the gray band is the theory prediction with total theory error. *BABAR* data are shown by circles, Belle by squares and other experiments (DELPHI, CDF, CLEO) by triangles. Filled symbols mean that the point was used in the fit. Open symbols are measurements that were not used in the fit.

identical moments, i.e., moments with same values of n and c). The detailed result of the fit using the $B \to X_s\gamma$ constraint is given in Table 82. The result in terms of the main parameters is

$$|V_{cb}| = (41.98 \pm 0.45) \times 10^{-3}, \tag{200}$$

$$m_b^{1S} = 4.691 \pm 0.037 \text{ GeV}, \tag{201}$$

$$\lambda_1 = -0.362 \pm 0.067 \text{GeV}^2, \tag{202}$$

with a χ^2 of 23.0 for 59 degrees of freedom. We find a good agreement in the central values of $|V_{cb}|$ between the kinetic and 1S scheme analyses. No conclusion should, however, be drawn regarding the uncertainties in $|V_{cb}|$, as the two approaches are not equivalent in the number of higher-order corrections that are included.

C. Exclusive CKM-suppressed decays

In this section, we give results on exclusive charmless semileptonic branching fractions and the determination of $|V_{ub}|$ based on $B \to \pi\ell\nu$ decays. The measurements are based on two different event selections: tagged events, in which the second B meson in the event is fully (or partially) reconstructed, and untagged events, for which the momentum of the undetected neutrino is inferred from measurements of the total momentum sum of the detected particles and the knowledge of the initial state.

The LHCb experiment has reported a direct measurement of $|V_{ub}|/|V_{cb}|$ [554], reconstructing the $\Lambda_b^0 \to p\mu\nu$ decays and normalizing the branching fraction to the $\Lambda_b^0 \to \Lambda_c^+(\to pK\pi)\mu\nu$ decays. Recently LHCb reported also a measurement of $|V_{ub}|/|V_{cb}|$ [555] using $B_s \to K\mu\nu$ decays normalized to $B_s \to D_s\mu\nu$ in two separate bins of q^2. We show a combination of $|V_{ub}|$ and $|V_{cb}|$ using the LHCb constraints on $|V_{ub}|/|V_{cb}|$, the exclusive determination of

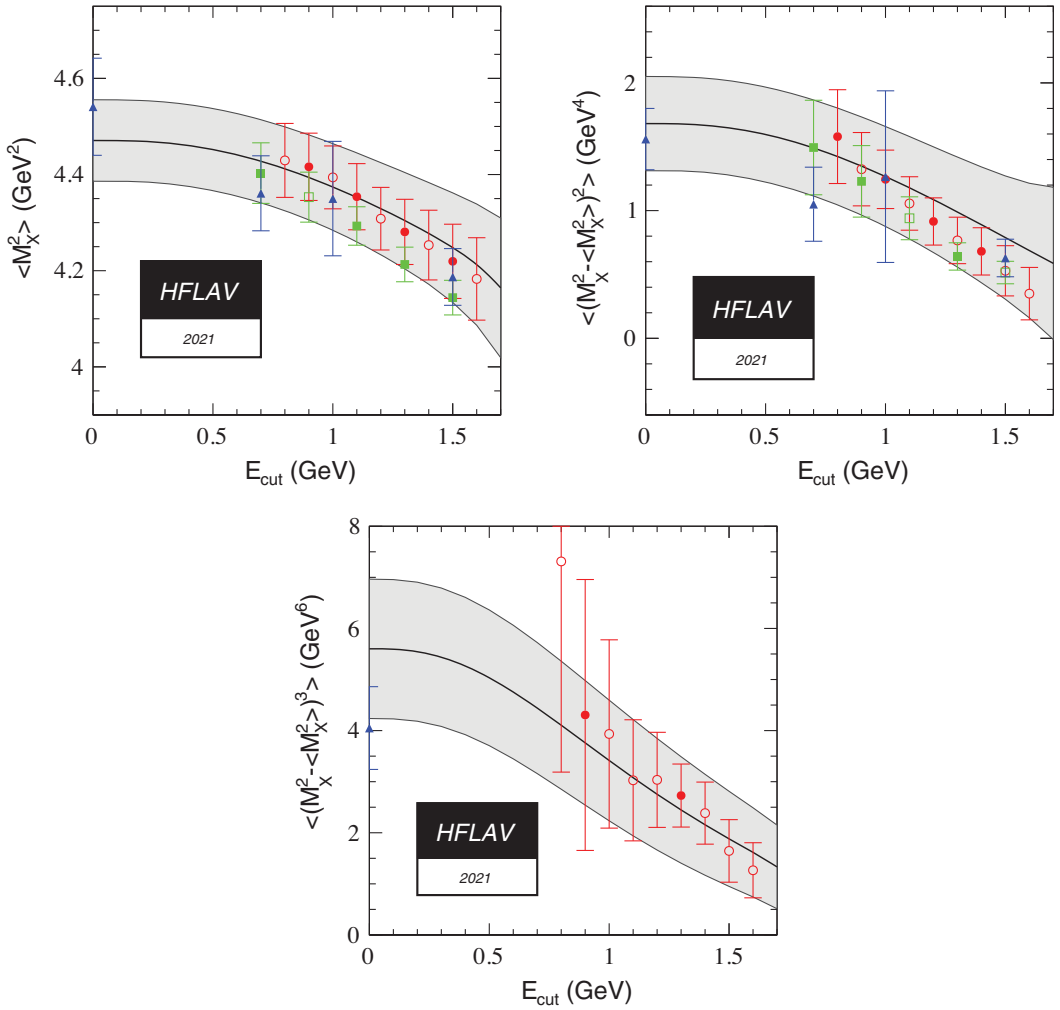

FIG. 57. Same as Fig. 56 for the fit to the hadronic mass moments in the kinetic mass scheme.

$|V_{ub}|$ from $B \to \pi\ell\nu$, and $|V_{cb}|$ from $B \to D^*\ell\nu$, $B \to D\ell\nu$ and $B \to D_s\mu\nu$.

We also present branching fraction averages for $B^0 \to \rho\ell^+\nu$, $B^+ \to \omega\ell^+\nu$, $B^+ \to \eta\ell^+\nu$ and $B^+ \to \eta'\ell^+\nu$. Using the available measurements of the partial branching fractions of $B^0 \to \rho\ell^+\nu$, $B^+ \to \omega\ell^+\nu$ decays, we also present for the first time the combined q^2 spectrum for these two decays.

1. $B \to \pi\ell\nu$ branching fraction and q^2 spectrum

We use the four most precise measurements of the differential $B \to \pi\ell\nu$ decay rate as a function of the four-momentum transfer squared, q^2, from *BABAR* and Belle [556–559] to obtain an average q^2 spectrum and an average for the total branching fraction. The measurements are presented in Fig. 58. From the two untagged *BABAR* analyses [558,559], the combined results for $B^0 \to \pi^-\ell^+\nu$ and $B^+ \to \pi^0\ell^+\nu$ decays based on isospin symmetry are used. The hadronic-tag analysis by Belle [557] provides results for $B^0 \to \pi^-\ell^+\nu$ and $B^+ \to \pi^0\ell^+\nu$ separately, but not for the combination of both channels. In the untagged analysis by Belle [556], only $B^0 \to \pi^-\ell^+\nu$ decays were measured. The experimental measurements use different binnings in q^2, but have matching bin edges, which allows them to be easily combined.

To arrive at an average q^2 spectrum, a binned maximum-likelihood fit to determine the average partial branching fraction in each q^2 interval is performed, differentiating between common and individual uncertainties and correlations for the various measurements. Shared sources of systematic uncertainty of all measurements are included in the likelihood as nuisance parameters constrained assuming Gaussian distributions. The most important shared sources of uncertainty are due to continuum subtraction, the number of B-meson pairs (only correlated among measurement by the same experiment), tracking efficiency (only correlated among measurements by the same experiment), uncertainties from modeling the $b \to u\ell\bar{\nu}_\ell$ contamination, modeling of final state radiation, and contamination from $b \to c\ell\bar{\nu}_\ell$ decays.

TABLE 82. Fit result in the 1S scheme, using $B \to X_s\gamma$ moments as a constraint. In the lower part of the table, the correlation matrix of the parameters is given.

	m_b^{1S} [GeV]	λ_1 [GeV^2]	ρ_1 [GeV^3]	τ_1 [GeV^3]	τ_2 [GeV^3]	τ_3 [GeV^3]	$\lvert V_{cb}\rvert$ [10^{-3}]
Value	4.691	−0.362	0.043	0.161	−0.017	0.213	41.98
Error	0.037	0.067	0.048	0.122	0.062	0.102	0.45
m_b^{1S}	1.000	0.434	0.213	−0.058	−0.629	−0.019	−0.215
λ_1		1.000	−0.467	−0.602	−0.239	−0.547	−0.403
ρ_1			1.000	0.129	−0.624	0.494	0.286
τ_1				1.000	0.062	−0.148	0.194
τ_2					1.000	−0.009	−0.145
τ_3						1.000	0.376
$\lvert V_{cb}\rvert$							1.000

The averaged q^2 spectrum is shown in Fig. 58. The probability of the average is computed as the χ^2 probability quantifying the agreement between the input spectra and the averaged spectrum and amounts to 6%. The partial branching fractions and the full covariance matrix obtained from the likelihood fit are given in Tables 83 and 84. The average for the total $B^0 \to \pi^-\ell^+\nu_\ell$ branching fraction is obtained by summing up the partial branching fractions:

$$\mathcal{B}(B^0 \to \pi^-\ell^+\nu_\ell) = (1.50 \pm 0.02_{\text{stat}} \pm 0.06_{\text{syst}}) \times 10^{-4}. \tag{203}$$

2. $|V_{ub}|$ from $B \to \pi\ell\nu$

The $|V_{ub}|$ average can be determined from the averaged q^2 spectrum in combination with a prediction for the normalization of the $B \to \pi$ form factor. The differential decay rate for light leptons (e, μ) is given by

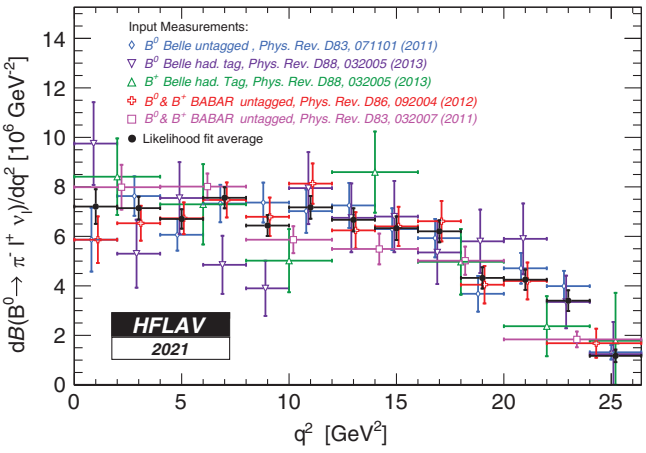

FIG. 58. The $B \to \pi\ell\nu q^2$ spectrum measurements and the average spectrum obtained from the likelihood combination (shown in black).

$$\Delta\Gamma = \Delta\Gamma(q^2_{\text{low}}, q^2_{\text{high}}) = \int_{q^2_{\text{low}}}^{q^2_{\text{high}}} \mathrm{d}q^2 \left[\frac{8|\vec{p}_\pi|}{3}\frac{G_F^2|V_{ub}|^2 q^2}{256\pi^3 m_B^2} H_0^2(q^2)\right], \tag{204}$$

where G_F is Fermi's constant, $|\vec{p}_\pi|$ is the magnitude of the three-momentum of the final state π (a function of q^2), m_B the B^0-meson mass, and $H_0(q^2)$ the only nonzero helicity amplitude. The helicity amplitude is a function of the form factor f_+,

$$H_0 = \frac{2m_B|\vec{p}_\pi|}{\sqrt{q^2}} f_+(q^2). \tag{205}$$

The form factor f_+ can be calculated with nonperturbative methods, but its general form can be constrained by the differential $B \to \pi\ell\nu$ spectrum. Here, we parametrize the form factor using the BCL parametrization [560].

The decay rate is proportional to $|V_{ub}|^2|f_+(q^2)|^2$. Thus to extract $|V_{ub}|$ one needs to determine $f_+(q^2)$ (at least at one value of q^2). In order to enhance the precision, a binned χ^2 fit is performed using a χ^2 function of the form

$$\chi^2 = (\vec{\mathcal{B}} - \Delta\vec{\Gamma}\tau)^T C^{-1} (\vec{\mathcal{B}} - \Delta\vec{\Gamma}\tau) + \chi^2_{\text{LQCD}} + \chi^2_{\text{LCSR}} \tag{206}$$

where C denotes the covariance matrix given in Table 84, $\vec{\mathcal{B}}$ is the vector of averaged partial branching fractions, and $\Delta\vec{\Gamma}\tau$ is the product of the vector of theoretical predictions of the partial decay rates and the B^0-meson lifetime. The form factor normalization is included in the fit by the two extra terms in Eq. (206): χ_{LQCD} uses the latest FLAG lattice average [509] from two state-of-the-art unquenched lattice QCD calculations [561,562]. The resulting constraints are quoted directly in terms of the coefficients b_j of the BCL parametrization and enter Eq. (206) as

$$\chi^2_{\text{LQCD}} = (\vec{b} - \vec{b}_{\text{LQCD}})^T C^{-1}_{\text{LQCD}} (\vec{b} - \vec{b}_{\text{LQCD}}), \tag{207}$$

TABLE 83. Partial $B^0 \to \pi^- \ell^+ \nu_\ell$ branching fractions per GeV^2 for the input measurements and the average obtained from the likelihood fit. The uncertainties are the combined statistical and systematic uncertainties.

	$\Delta\mathcal{B}(B^0 \to \pi^- \ell^+ \nu_\ell)/\Delta q^2$ [10^{-7}]					
	Belle untagged	Belle tagged	Belle tagged	*BABAR* untagged	*BABAR* untagged	
Δq^2 [GeV^2]	(B^0)	(B^0)	(B^+)	($B^{0,+}$, 12 bins)	($B^{0,+}$, 6 bins)	Average
0–2	58.7 ± 12.9	97.5 ± 16.7	84.1 ± 15.5	58.7 ± 9.4	79.9 ± 9.1	72.0 ± 7.0
2–4	76.3 ± 8.0	53.0 ± 13.8		65.3 ± 7.1		71.4 ± 4.6
4–6	60.6 ± 6.4	75.5 ± 14.5	73.0 ± 16.2	67.3 ± 6.4	80.1 ± 5.3	67.0 ± 3.9
6–8	73.3 ± 7.6	48.5 ± 11.8		74.7 ± 7.1		75.6 ± 4.3
8–10	73.7 ± 8.1	39.0 ± 11.2	50.2 ± 12.8	67.9 ± 7.8	58.7 ± 5.5	64.4 ± 4.3
10–12	70.2 ± 8.8	79.5 ± 14.6		81.3 ± 8.2		71.7 ± 4.6
12–14	72.5 ± 9.1	67.5 ± 13.9	86.0 ± 16.4	62.4 ± 7.4	54.9 ± 6.2	66.7 ± 4.7
14–16	63.0 ± 8.4	68.0 ± 14.4		64.0 ± 7.9		63.3 ± 4.8
16–18	59.3 ± 7.8	53.5 ± 12.8	49.7 ± 13.3	66.1 ± 8.2	50.2 ± 5.7	62.0 ± 4.4
18–20	36.8 ± 7.2	58.0 ± 12.8		40.5 ± 7.6		43.2 ± 4.3
20–22	47.1 ± 6.2	59.0 ± 14.3	23.7 ± 12.1	42.0 ± 7.5	18.4 ± 3.2	42.5 ± 4.1
22–24	39.9 ± 6.2	33.5 ± 10.6		16.8 ± 5.9		34.0 ± 4.2
24–26.4	13.2 ± 2.9	12.4 ± 13.0	17.8 ± 19.4			11.7 ± 2.6

TABLE 84. Covariance matrix of the averaged partial branching fractions per GeV^2 in units of 10^{-14}.

Δq^2 [GeV^2]	0–2	2–4	4–6	6–8	8–10	10–12	12–14	14–16	16–18	18–20	20–22	22–24	24–26.4
0–2	49.091	1.164	8.461	7.996	7.755	9.484	7.604	9.680	8.868	7.677	7.374	7.717	2.877
2–4		21.487	−0.0971	7.155	4.411	5.413	4.531	4.768	4.410	3.442	3.597	3.388	1.430
4–6			15.489	−0.563	5.818	4.449	4.392	4.157	4.024	3.185	3.169	3.013	1.343
6–8				18.2	2.377	7.889	6.014	5.938	5.429	4.096	3.781	3.863	1.428
8–10					18.124	1.540	7.496	5.224	5.441	4.197	3.848	4.094	1.673
10–12						21.340	4.213	7.696	6.493	5.170	4.686	4.888	1.950
12–14							21.875	0.719	6.144	3.846	3.939	3.922	1.500
14–16								23.040	5.219	6.123	4.045	4.681	1.807
16–18									19.798	1.662	4.362	4.140	1.690
18–20										18.0629	2.621	3.957	1.438
20–22											16.990	1.670	1.127
22–24												17.774	−0.293
24–26.4													6.516

with $\vec{b}$ the vector containing the free parameters of the χ^2 fit constraining the form factor, $\vec{b}_{\rm LQCD}$ the averaged values from Ref. [509], and $C_{\rm LQCD}$ their covariance matrix. Additional information about the form factor can be obtained from light-cone sum rule (LCSR) calculations. The state-of-the-art calculation includes up to two-loop contributions [563]. It is included in Eq. (206) via

$$\chi^2_{\rm LQCR} = (f_+^{\rm LCSR} - f_+(q^2 = 0; \vec{b}))^2 / \sigma^2_{f_+^{\rm LCSR}}. \tag{208}$$

The $|V_{ub}|$ average is obtained for two versions: the first combines the data with the LQCD constraints and the second additionally includes the information from the LCSR calculation. The resulting values for $|V_{ub}|$ are

$$|V_{ub}| = (3.70 \pm 0.10_{\rm exp} \pm 0.12_{\rm theo}) \times 10^{-3} ({\rm data + LCQD}), \tag{209}$$

$$|V_{ub}| = (3.67 \pm 0.09_{\rm exp} \pm 0.12_{\rm theo}) \times 10^{-3} ({\rm data + LCQD + LCSR}), \tag{210}$$

for the first and second fit version, respectively. The result of the fit including both LQCD and LCSR is shown in Fig. 59. The χ^2 probability of the fit is 47%. We quote the result of the fit including both LQCD and LCSR calculations as our average for $|V_{ub}|$. The best fit values for $|V_{ub}|$ and the BCL parameters and their correlation matrix are given in Tables 85 and 86.

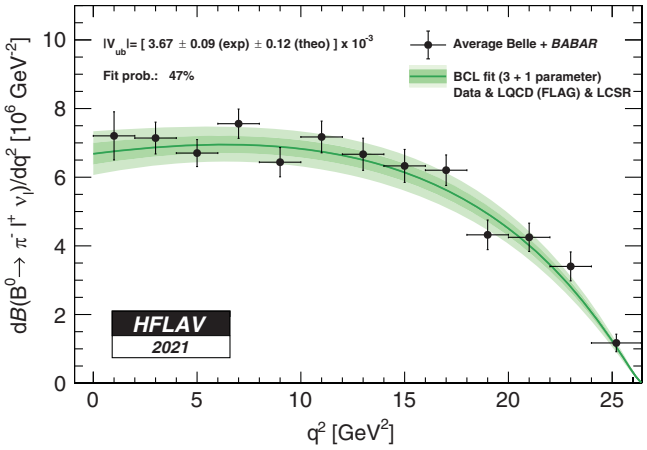

FIG. 59. Fit of the BCL parametrization to the averaged q^2 spectrum from *BABAR* and Belle and the LQCD and LCSR calculations. The error bands represent the 1σ (dark green) and 2σ (light green) uncertainties of the fitted spectrum.

3. $B \to \rho \ell \nu_\ell$ and $B \to \omega \ell \nu_\ell$ branching fraction and q^2 spectrum

We report the branching fraction averages for $B \to V \ell \nu_\ell$, $V = \rho$, ω. The measurements and their averages are listed in Tables 87, 88, and presented in Fig. 60.

In the $B^+ \to \rho^0 \ell^+ \nu$ average, both the $B^0 \to \rho^- \ell^+ \nu$ and $B^+ \to \rho^0 \ell^+ \nu$ decays are used, where the $B^0 \to \rho^- \ell^+ \nu$ are rescaled by $0.5\tau_{B^+}/\tau_{B^0}$ assuming the isospin symmetry. The $B^+ \to \rho^0 \ell^+ \nu$ results show significant differences, in particular the *BABAR* untagged analysis gives a branching fraction significantly lower (by about 3σ) than the Belle measurement based on the hadronic-tag. The difference is about 2σ for the $B^+ \to \rho^0 \ell^+ \nu$ decay modes.

We use the most precise measurements of the differential $B \to V \ell \nu_\ell$, $V = \rho$, ω decay rates as a function of the four-momentum transfer q^2 published by *BABAR* [558,568] and Belle [557]. To obtain an averaged q^2 spectrum and averaged branching fractions, we perform a χ^2 of the form

$$\chi^2(\vec{x}) = \sum_{m \in \{\text{Belle}, BABAR\}} \Delta\vec{y}_m^T C_m^{-1} \Delta\vec{y}_m,$$

$$\Delta\vec{y}_m = \begin{pmatrix} \vdots \\ x_i^m - \sum_{j>N_{i-1}}^{N_i} \bar{x}_j \\ \vdots \end{pmatrix}, \tag{211}$$

where C_m is the covariance of the measurement and x_i^m is the measured differential rate in bin i multiplied by the corresponding bin width. Further, $\bar{\boldsymbol{x}}$ denotes the averaged spectrum and $(N_{i-1}, N_i]$ the range of averaged bins used to map to the ith measured bin. The binning of the averaged spectrum is chosen to match the most granular experimental binning.

For the average of the $B \to \omega \ell \bar{\nu}$ measurements from Belle and *BABAR* we again chose the binning of the most granular spectrum, in this case *BABAR*'s. However the experimental spectra do not have a compatible binning in terms of matching bin boundaries. In order to incorporate the Belle data and create an averaged spectrum, the LCSR fit results [570] are used to create a model with which to split the second and fifth bin of the chosen binning, shown

TABLE 85. Best fit values and uncertainties for the combined fit to data, LQCD and LCSR results.

Parameter	Value
$\lvert V_{ub}\rvert$	$(3.67 \pm 0.15) \times 10^{-3}$
b_0	0.418 ± 0.012
b_1	-0.399 ± 0.033
b_2	-0.578 ± 0.130

TABLE 86. Correlation matrix for the combined fit to data, LQCD and LCSR results.

Parameter	$\lvert V_{ub}\rvert$	b_0	b_1	b_2
$\lvert V_{ub}\rvert$	1.000	−0.780	−0.404	0.401
b_0	−0.780	1.000	2.110	−0.587
b_1	−0.404	2.110	1.000	−0.686
b_2	0.401	−0.587	−0.686	1.000

TABLE 87. Summary of exclusive determinations of $B^+ \to \rho^0 \ell^+ \nu$. The errors quoted correspond to statistical and systematic uncertainties, respectively.

	$\mathcal{B}[10^{-4}]$
CLEO (Untagged) ρ^+ [564]	$1.49 \pm 0.22 \pm 0.28$
CLEO (Untagged) ρ^+ [565]	$1.58 \pm 0.20 \pm 0.20$
Belle (Hadronic tag) ρ^+ [557]	$1.73 \pm 0.15 \pm 0.13$
Belle (Hadronic tag) ρ^0 [557]	$1.82 \pm 0.10 \pm 0.10$
Belle (Semileptonic tag) ρ^+ [566]	$1.21 \pm 0.29 \pm 0.17$
Belle (Semileptonic tag) ρ^0 [566]	$1.35 \pm 0.23 \pm 0.18$
BABAR (Untagged) ρ^+ [558]	$1.05 \pm 0.11 \pm 0.21$
BABAR (Untagged) ρ^0 [558]	$1.00 \pm 0.10 \pm 0.21$
Average	$\mathbf{1.58 \pm 0.11}$

TABLE 88. Summary of exclusive determinations of $B^+ \to \omega \ell^+ \nu$. The errors quoted correspond to statistical and systematic uncertainties, respectively.

	$\mathcal{B}[10^{-4}]$
Belle (Untagged) [567]	$1.30 \pm 0.40 \pm 0.36$
BABAR (Loose ν reco.) [559]	$1.19 \pm 0.16 \pm 0.09$
BABAR (Untagged) [568]	$1.21 \pm 0.14 \pm 0.08$
Belle (Hadronic tag) [557]	$1.07 \pm 0.16 \pm 0.07$
BABAR (Semileptonic tag) [569]	$1.35 \pm 0.21 \pm 0.11$
Average	$\mathbf{1.19 \pm 0.10}$

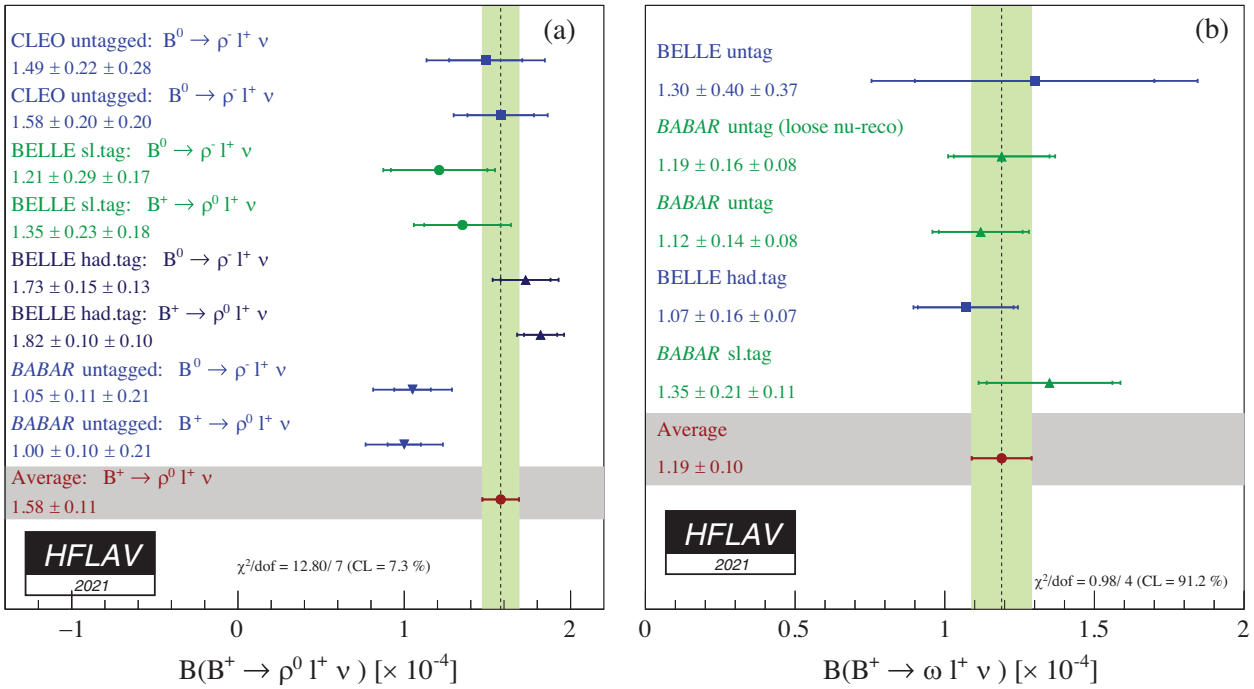

FIG. 60. (a) Summary of exclusive determinations of $\mathcal{B}(B^+ \to \rho^0 \ell^+ \nu)$ and their average. Measurements of $B^0 \to \rho^- \ell^+ \nu$ branching fractions have been scaled by $0.5\tau_{B^+}/\tau_{B^0}$ in accordance with isospin symmetry. (b) Summary of exclusive determinations of $B^+ \to \omega \ell^+ \nu$ and their average.

in black in Fig. 61. To match the average bin onto a measurement without matching bin edges, the average bin $\bar{x}_i$, $i = 2$ or 5, is split into two parts delimited by the lower bin edge, the q^2 value where the bin is split, and the upper bin edge. We label the two parts of the split bin as "left" and "right," respectively, in the following and define:

$$\begin{aligned} \bar{\boldsymbol{x}}_{i,\text{left}} &= I_{i,\text{left}}/I_i(1+\theta_i\varepsilon_{i,\text{left}}), \\ \bar{\boldsymbol{x}}_{i,\text{right}} &= I_{i,\text{right}}/I_i(1-\theta_i\varepsilon_{i,\text{right}}), \end{aligned} \tag{212}$$

where $I_{i,\text{left}}$ ($I_{i,\text{right}}$) is the integral of the model function on the support of the left (right) part of the split bin, the sum $I_i = I_{i,\text{left}} + I_{i,\text{right}}$ is the integral over the entire bin, $\varepsilon_{i,\text{left}}$ ($\varepsilon_{i,\text{right}}$) the uncertainty of the integration given by the model uncertainty, and θ_i the nuisance parameter for the model dependence. We point out that the averaged spectrum does not depend on $|V_{ub}|$, as $|V_{ub}|$ cancels in the ratios $I_{i,\text{left}}/I_i$ ($I_{i,\text{right}}/I_i$).

The averaged spectra are shown in black in Fig. 61 and tabulated in Table 89.

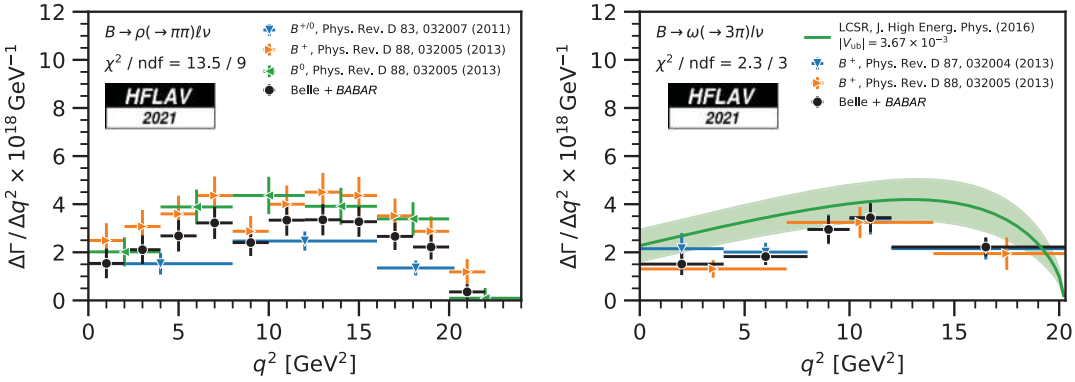

FIG. 61. The averaged q^2 spectrum of the measurements listed in the text for the ρ (left) and ω (right) final state on top of the latest Belle and *BABAR* measurements. The isospin transformation is applied to the $B^0 \to \rho^- \ell^+ \nu$ measurements. In the right figure we also show the model (green band) which was used to split the bins in the averaging procedure.

TABLE 89. Averaged spectra. For the corresponding correlation matrices see Tables 90 and 91.

$B \to \rho \ell \bar{\nu}$	
q^2 bin	$\Delta\Gamma/\Delta q^2 \times 10^6$
[0, 2]	1.54 ± 0.62
[2, 4]	2.11 ± 0.60
[4, 6]	2.68 ± 0.65
[6, 8]	3.22 ± 0.67
[8, 10]	2.40 ± 0.56
[10, 12]	3.34 ± 0.65
[12, 14]	3.35 ± 0.65
[14, 16]	3.27 ± 0.63
[16, 18]	2.66 ± 0.57
[18, 20]	2.22 ± 0.52
[20, 22]	0.35 ± 0.32
$B \to \omega \ell \bar{\nu}$	
q^2 bin	$\Delta\Gamma/\Delta q^2 \times 10^6$
[0, 4]	1.51 ± 0.46
[4, 8]	1.82 ± 0.35
[8, 10]	2.95 ± 0.56
[10, 12]	3.44 ± 0.59
[12, 21]	2.22 ± 0.40
Nuisance parameters	
θ_2	-0.01 ± 1.00
θ_5	0.00 ± 1.00

4. Other exclusive charmless semileptonic B decays

We report the branching fraction averages for $B^+ \to \eta \ell^+ \nu$ and $B^+ \to \eta' \ell^+ \nu$. The measurements and their averages are listed in Tables 92 and 93, and presented in Fig. 62. For $B^+ \to \eta \ell^+ \nu$ decays, the agreement between the different measurements is good, while $B^+ \to \eta' \ell^+ \nu$ shows a significant discrepancy between the old CLEO measurement and the *BABAR* untagged analysis.

5. Direct measurements of $|V_{ub}|/|V_{cb}|$

The LHCb experiment reported the first observation of the CKM suppressed decay $\Lambda_b^0 \to p\mu\nu$ [554] and the measurement of the ratio of partial branching fractions at high q^2 for $\Lambda_b^0 \to p\mu\nu$ and $\Lambda_b^0 \to \Lambda_c^+(\to pK\pi)\mu\nu$ decays,

$$R = \frac{\mathcal{B}(\Lambda_b^0 \to p\mu\nu)_{q^2>15\,\mathrm{GeV}^2}}{\mathcal{B}(\Lambda_b^0 \to \Lambda_c^+\mu\nu)_{q^2>7\,\mathrm{GeV}^2}} = (1.00 \pm 0.04 \pm 0.08) \times 10^{-2}. \tag{213}$$

The ratio R is proportional to $(|V_{ub}|/|V_{cb}|)^2$ and sensitive to the form factors of $\Lambda_b^0 \to p$ and $\Lambda_b^0 \to \Lambda_c^+$ transitions that have to be computed with nonperturbative methods, such as lattice QCD. The uncertainty on $\mathcal{B}(\Lambda_c^+ \to pK\pi)$ is the largest source of systematic uncertainties on R. Using the recent average of $\mathcal{B}(\Lambda_c^+ \to pK\pi) = (6.28 \pm 0.32)\%$ [9], the rescaled value for R is

$$R = (0.92 \pm 0.04 \pm 0.07) \times 10^{-2}. \tag{214}$$

Using the precise lattice QCD prediction [576] of the form factors in the experimentally interesting q^2 region considered, we obtain

$$\frac{|V_{ub}|}{|V_{cb}|} = 0.079 \pm 0.004_{\mathrm{exp}} \pm 0.004_{\mathrm{FF}} \tag{215}$$

where the first uncertainty is the total experimental uncertainty, and the second one is due to the knowledge of the form factors.

The LHCb experiment also reported the first observation of the decay $B_s^0 \to K^-\mu^+\nu_\mu$ and the measurements of its branching fraction normalized to the $B_s^0 \to D_s^-\mu^+\nu_\mu$ decays [555]. The measurement has been performed in two bins of q^2. The results of the partial branching fractions has been translated in measurements of $|V_{ub}|/|V_{cb}|$ using form factor calculation from LCSR for $q^2 < 7$ GeV^2 [577],

TABLE 90. Correlation matrix of the averaged $B \to \rho \ell \nu_\ell$ spectrum.

	[0, 2]	[2, 4]	[4, 6]	[6, 8]	[8, 10]	[10, 12]	[12, 14]	[14, 16]	[16, 18]	[18, 20]	[20, 22]
[0, 2]	1.00	−0.30	0.03	0.01	0.09	0.09	0.09	0.09	0.08	0.08	0.02
[2, 4]	−0.30	1.00	−0.03	0.09	0.11	0.12	0.12	0.12	0.11	0.10	0.02
[4, 6]	0.03	−0.03	1.00	−0.18	0.13	0.13	0.15	0.14	0.13	0.12	0.03
[6, 8]	0.01	0.09	−0.18	1.00	0.06	0.18	0.18	0.18	0.16	0.14	0.04
[8, 10]	0.09	0.11	0.13	0.06	1.00	−0.21	0.05	0.04	0.12	0.10	0.03
[10, 12]	0.09	0.12	0.13	0.18	−0.21	1.00	−0.00	0.07	0.15	0.13	0.04
[12, 14]	0.09	0.12	0.15	0.18	0.05	−0.00	1.00	−0.16	0.14	0.12	0.04
[14, 16]	0.09	0.12	0.14	0.18	0.04	0.07	−0.16	1.00	0.10	0.14	0.05
[16, 18]	0.08	0.11	0.13	0.16	0.12	0.15	0.14	0.10	1.00	−0.27	−0.11
[18, 20]	0.08	0.10	0.12	0.14	0.10	0.13	0.12	0.14	−0.27	1.00	−0.13
[20, 22]	0.02	0.02	0.03	0.04	0.03	0.04	0.04	0.05	−0.11	−0.13	1.00

TABLE 91. Correlation matrix of the averaged $B \to \omega \ell \nu_\ell$ spectrum.

	[0, 4]	[4, 8]	[8, 10]	[10, 12]	[12, 21]	θ_2	θ_5
[0, 4]	1.00	−0.15	0.08	0.04	0.06	−0.01	0.00
[4, 8]	−0.15	1.00	0.09	0.09	0.15	−0.01	−0.00
[8, 10]	0.08	0.09	1.00	−0.01	0.12	−0.00	−0.00
[10, 12]	0.04	0.09	−0.01	1.00	0.15	0.00	−0.00
[12, 21]	0.06	0.15	0.12	0.15	1.00	−0.00	−0.00
θ_2	−0.01	−0.01	−0.00	0.00	−0.00	1.00	0.00
θ_5	0.00	−0.00	−0.00	−0.00	−0.00	0.00	1.00

TABLE 92. Summary of exclusive determinations of $B^+ \to \eta \ell^+ \nu$. The errors quoted correspond to statistical and systematic uncertainties, respectively.

	$\mathcal{B}[10^{-4}]$
CLEO [571]	$0.45 \pm 0.23 \pm 0.11$
BABAR (Untagged) [572]	$0.31 \pm 0.06 \pm 0.08$
BABAR (Semileptonic Tag) [573]	$0.64 \pm 0.20 \pm 0.04$
BABAR (Loose ν-reco.) [559]	$0.38 \pm 0.05 \pm 0.05$
Belle (Hadronic Tag) [574]	$0.42 \pm 0.11 \pm 0.09$
Belle (Untagged) [575]	$0.283 \pm 0.055 \pm 0.034$
Average	$\mathbf{0.344 \pm 0.043}$

TABLE 93. Summary of exclusive determinations of $B^+ \to \eta' \ell^+ \nu$. The errors quoted correspond to statistical and systematic uncertainties, respectively.

	$\mathcal{B}[10^{-4}]$
CLEO [571]	$2.71 \pm 0.80 \pm 0.56$
BABAR (Semileptonic Tag) [573]	$0.04 \pm 0.22 \pm 0.04$, (<0.47@90%CL)
BABAR (Untagged) [559]	$0.24 \pm 0.08 \pm 0.03$
Belle (Hadronic Tag) [574]	$0.36 \pm 0.27 \pm 0.04$
Belle (Untagged) [575]	$0.279 \pm 0.129 \pm 0.030$
Average	$\mathbf{0.249 \pm 0.067 \pm 0.03}$

and recent Lattice calculation for $q^2 > 7$ GeV^2 [578]. The results are

$$\frac{|V_{ub}|}{|V_{cb}|} = 0.0607 \pm 0.0021_{\rm exp} \pm 0.0030_{\rm FF}, \quad q^2 < 7\,{\rm GeV}^2, \tag{216}$$

$$\frac{|V_{ub}|}{|V_{cb}|} = 0.0946 \pm 0.0041_{\rm exp} \pm 0.0068_{\rm FF}, \quad q^2 > 7\,{\rm GeV}^2, \tag{217}$$

where the experimental uncertainties include also the uncertainties on the external inputs, and the last errors are due to the form factor calculations for both $B \to K$ and $B_s \to D_s$ decays. The discrepancy between the values of $|V_{ub}|/|V_{cb}|$ for the low and high q^2, requires further investigations.

D. Inclusive CKM-suppressed decays

Measurements of $B \to X_u \ell^+ \nu$ decays are very challenging because of background from the Cabibbo-favored $B \to X_c \ell^+ \nu$ decays, whose branching fraction is about 50 times larger than that of the signal. Cuts designed to suppress this dominant background severely complicate the perturbative QCD calculations required to extract $|V_{ub}|$. Tight cuts necessitate parametrization of the so-called shape functions in order to describe the unmeasured regions of phase space. We use several theoretical calculations to extract $|V_{ub}|$ and do not advocate the use of one method over another. The authors of the different calculations have provided codes to compute the partial rates in limited regions of phase space covered by the measurements. Belle [579] and *BABAR* [580] produced measurements that explore large portions of phase space and thus reduce theoretical uncertainties.

In the averages, the systematic uncertainties associated with the modeling of $B \to X_c \ell^+ \nu_\ell$ and $B \to X_u \ell^+ \nu_\ell$ decays and the theoretical uncertainties are taken as fully correlated among all measurements. Reconstruction-related uncertainties are taken as fully correlated within a given experiment. Measurements of partial branching fractions for $B \to X_u \ell^+ \nu_\ell$ transitions from $\Upsilon(4S)$ decays, together with the corresponding selected region, are given in Table 94. We use all results published by *BABAR* in Ref. [580], since the statistical correlations are given. To make use of the theoretical calculations of Ref. [581], we restrict the kinematic range of the invariant mass of the hadronic system, M_X, and the square of the invariant mass of the lepton pair, q^2. This reduces the size of the data sample significantly, but also the theoretical uncertainty, as stated by the authors [581]. The dependence of the quoted error on the measured value for each source of uncertainty is taken into account in the calculation of the averages.

It was first suggested by Neubert [582] and later detailed by Leibovich, Low, and Rothstein (LLR) [583] and Lange, Neubert and Paz (LNP) [584], that the uncertainty of the leading shape functions can be eliminated by comparing

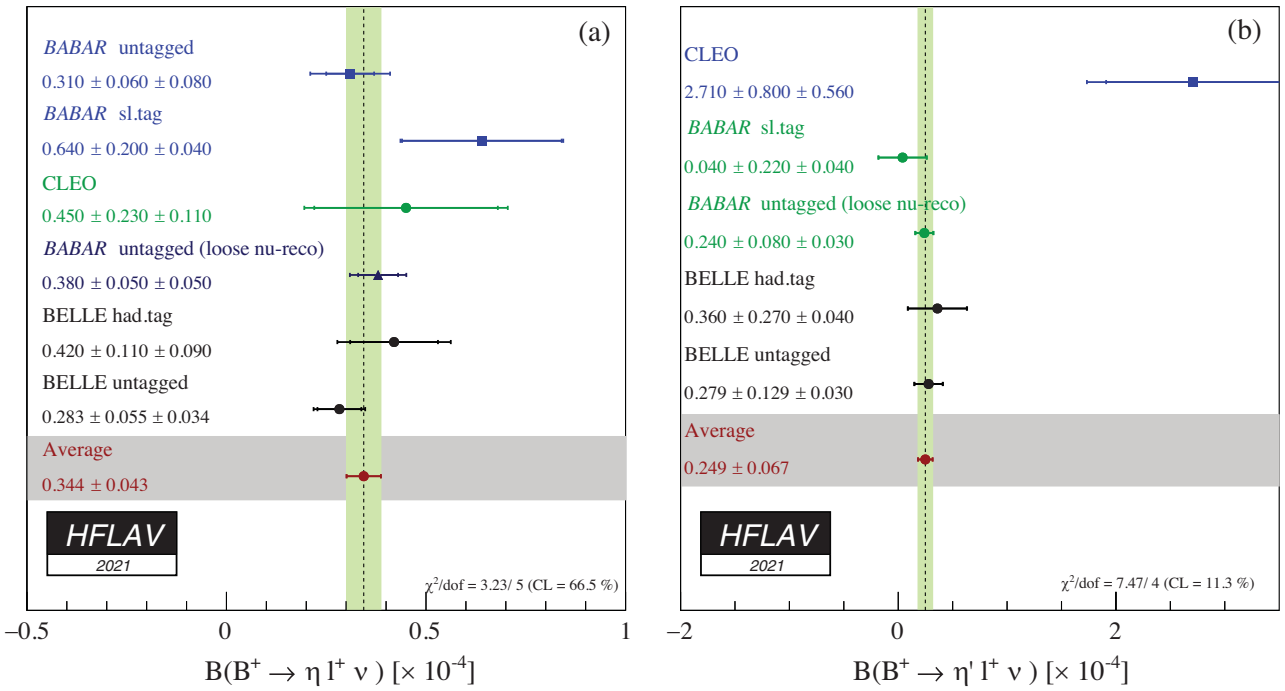

FIG. 62. (a) Summary of exclusive determinations of $\mathcal{B}(B^+ \to \eta \ell^+ \nu)$ and their average. (b) Summary of exclusive determinations of $\mathcal{B}(B^+ \to \eta' \ell^+ \nu)$ and their average.

inclusive rates for $B \to X_u \ell^+ \nu_\ell$ decays with the inclusive photon spectrum in $B \to X_s \gamma$, based on the assumption that the shape functions for transitions to light quarks, u or s, are the same to first order. However, shape function uncertainties are only eliminated at the leading order and they still enter via the signal models used for the determination of efficiency.

In a paper by *BABAR* [585], detailed studies are performed to assess the impact of various theoretical predictions, on the measurements of the electron spectrum, the branching fraction, and the extraction of $|V_{ub}|$, where the lower limit on the electron momentum is varied from 0.8 GeV/c to the kinematic endpoint. An important difference of this paper with respect to the other ones is that the dependency on the theoretical models enters primarily through the partial branching fractions, as the fit is sensitive to signal decays only in regions with good signal-to-noise such as the endpoint region. All other measurements instead determine a partial branching fraction by using a single model, and this partial branching fraction is then

TABLE 94. Summary of measurements of partial branching fractions for $B \to X_u \ell^+ \nu_\ell$ decays. The errors quoted on $\Delta\mathcal{B}$ correspond to statistical and systematic uncertainties. E_e is the electron energy in the B rest frame, p^* the lepton momentum in the B frame and m_X is the invariant mass of the hadronic system. The light-cone momentum P_+ is defined in the B rest frame as $P_+ = E_X - |\vec{p}_X|$. The $s_{\rm h}^{\rm max}$ variable is described in Refs. [587,588].

Measurement	Accepted region	$\Delta\mathcal{B}[10^{-4}]$	Notes
CLEO [589]	$E_e > 2.1$ GeV	$3.3 \pm 0.2 \pm 0.7$	
BABAR [588]	$E_e > 2.0$ GeV, $s_{\rm h}^{\rm max} < 3.5$ GeV^2	$4.4 \pm 0.4 \pm 0.4$	
BABAR [585]	$E_e > 0.8$ GeV	$1.55 \pm 0.08 \pm 0.09$	Using the GGOU model
Belle [590]	$E_e > 1.9$ GeV	$8.5 \pm 0.4 \pm 1.5$	
BABAR [580]	$M_X < 1.7$ GeV/c^2, $q^2 > 8$ GeV$^2/c^4$	$6.9 \pm 0.6 \pm 0.4$	
Belle [591]	$M_X < 1.7$ GeV/c^2, $q^2 > 8$ GeV$^2/c^4$	$7.4 \pm 0.9 \pm 1.3$	
Belle [592]	$M_X < 1.7$ GeV/c^2, $q^2 > 8$ GeV$^2/c^4$	$8.5 \pm 0.9 \pm 1.0$	Used only in BLL average
BABAR [580]	$P_+ < 0.66$ GeV	$9.9 \pm 0.9 \pm 0.8$	
BABAR [580]	$M_X < 1.7$ GeV/c^2	$11.6 \pm 1.0 \pm 0.8$	
BABAR [580]	$M_X < 1.55$ GeV/c^2	$10.9 \pm 0.8 \pm 0.6$	
Belle [593]	$M_X < 1.7$ GeV/c^2, $q^2 > 8$ GeV$^2/c^4$	$15.9 \pm 0.9 \pm 1.6$	
BABAR [580]	(M_X, q^2) fit, $p_\ell^* > 1$ GeV/c	$18.2 \pm 1.3 \pm 1.5$	
BABAR [580]	$p_\ell^* > 1.3$ GeV/c	$15.5 \pm 1.3 \pm 1.4$	

converted into a $|V_{ub}|$ measurement by taking the corresponding partial rate predicted by the theory calculations. Due to this difference, the $|V_{ub}|$ results obtained in this paper, with a lower limit of 0.8 GeV/c on the electron momentum, are directly used as input to the averages based on the theoretical framework provided by Bosh, Lange, Neubert, and Paz (BLNP) [594–597], Andersen and Gardi (DGE) [600] and Gambino, Giordano, Ossola and Uralsev (GGOU) [604] averages. These determinations supersede the previous *BABAR* endpoint measurement [586]. The partial branching ratio quoted in Table 94 for Ref. [585] is taken as that obtained with the GGOU calculation.

A new measurement of partial branching fractions in three phase-space regions, covering about 31% to 86% of the accessible phase space, was performed by Belle [593], where machine learning techniques and hadronic tagging were used to reduce backgrounds. The measurement of the partial branching fraction obtained in the $E_\ell^B > 1$ GeV region, the most precise one, is used to obtain $|V_{ub}|$. This measurement supersedes the one of Ref. [579], based on similar techniques.

In the following, the different theoretical methods and the resulting averages are described.

1. BLNP

Bosch, Lange, Neubert and Paz (BLNP) [594–597] provide theoretical expressions for the triple differential decay rate for $B \to X_u \ell^+ \nu_\ell$ events, incorporating all known contributions, while smoothly interpolating between the "shape-function region" of large hadronic energy and small invariant mass, and the "OPE region" in which all hadronic kinematical variables scale with the b-quark mass. BLNP assign uncertainties to the b-quark mass, which enters through the leading shape function, to subleading shape function forms, to possible weak annihilation contribution, and to matching scales. The BLNP calculation uses the shape function renormalization scheme; the heavy quark parameters determined from the global fit in the kinetic scheme, described in Sec. VII B 2, were therefore translated into the shape function scheme by using a prescription by Neubert [598,599]. The resulting parameters are $m_b(\mathrm{SF}) = (4.582 \pm 0.023 \pm 0.018)$ GeV, $\mu_\pi^2(\mathrm{SF}) = (0.202 \pm 0.089^{+0.020}_{-0.040})$ GeV/c^2, where the second uncertainty is due to the scheme translation. The extracted values of $|V_{ub}|$ for each measurement along with their average are given in Table 95 and illustrated in Fig. 63(a). The total uncertainty is $^{+5.6}_{-5.7}\%$ and is due to: statistics ($^{+1.5}_{-1.6}\%$), detector effects ($^{+1.7}_{-1.7}\%$), $B \to X_c \ell^+ \nu_\ell$ model ($^{+0.9}_{-1.0}\%$), $B \to X_u \ell^+ \nu_\ell$ model ($^{+1.8}_{-1.8}\%$), heavy quark parameters ($^{+2.7}_{-2.8}\%$), SF functional form ($^{+0.1}_{-0.3}\%$), subleading shape functions ($^{+0.8}_{-0.8}\%$), matching scales in BLNP μ, μ_i, μ_h ($^{+3.8}_{-3.8}\%$), and weak annihilation ($^{+0.0}_{-0.7}\%$). The error assigned to the matching scales is the source of the largest uncertainty, while the uncertainty due to HQE parameters (b-quark mass

TABLE 95. Summary of input parameters used by the different theory calculations, corresponding inclusive determinations of $|V_{ub}|$ and their average. The errors quoted on $|V_{ub}|$ correspond to experimental and theoretical uncertainties, respectively.

	BLNP	DGE	GGOU	ADFR	BLL
			Input parameters		
Scheme	SF	$\overline{\mathrm{MS}}$	Kinetic	$\overline{\mathrm{MS}}$	1S
References	[598,599]	Ref. [600]	see Sec. VII B 2	Ref. [601]	Ref. [581]
m_b (GeV)	4.582 ± 0.026	4.188 ± 0.043	4.554 ± 0.018	4.188 ± 0.043	4.704 ± 0.029
μ_π^2 (GeV^2)	$0.202\ ^{+0.091}_{-0.098}$	…	0.464 ± 0.076	…	…
References			$\lvert V_{ub}\rvert$ values $[10^{-3}]$		
CLEO E_e [589]	$4.22 \pm 0.49^{+0.29}_{-0.34}$	$3.86 \pm 0.45^{+0.25}_{-0.27}$	$4.23 \pm 0.49^{+0.22}_{-0.31}$	$3.42 \pm 0.40^{+0.17}_{-0.17}$	…
Belle M_X, q^2 [591]	$4.51 \pm 0.47^{+0.27}_{-0.29}$	$4.43 \pm 0.47^{+0.19}_{-0.21}$	$4.52 \pm 0.48^{+0.25}_{-0.28}$	$3.93 \pm 0.41^{+0.18}_{-0.17}$	$4.68 \pm 0.49^{+0.30}_{-0.30}$
Belle E_e [590]	$4.93 \pm 0.46^{+0.26}_{-0.29}$	$4.82 \pm 0.45^{+0.23}_{-0.23}$	$4.95 \pm 0.46^{+0.16}_{-0.21}$	$4.48 \pm 0.42^{+0.20}_{-0.20}$	…
BABAR E_e [585]	$4.41 \pm 0.12^{+0.27}_{-0.27}$	$3.85 \pm 0.11^{+0.08}_{-0.07}$	$3.96 \pm 0.10^{+0.17}_{-0.17}$	…	…
BABAR $E_e, s_{\mathrm{h}}^{\max}$ [588]	$4.71 \pm 0.32^{+0.33}_{-0.38}$	$4.35 \pm 0.29^{+0.28}_{-0.30}$	…	$3.81 \pm 0.19^{+0.19}_{-0.18}$	
Belle E_ℓ^B, (M_X, q^2) fit [593]	$4.05 \pm 0.23^{+0.18}_{-0.20}$	$4.16 \pm 0.24^{+0.12}_{-0.11}$	$4.15 \pm 0.24^{+0.08}_{-0.09}$	$4.05 \pm 0.23^{+0.18}_{-0.18}$	…
BABAR M_X [580]	$4.24 \pm 0.19^{+0.25}_{-0.25}$	$4.47 \pm 0.20^{+0.19}_{-0.24}$	$4.30 \pm 0.20^{+0.20}_{-0.21}$	$3.83 \pm 0.18^{+0.20}_{-0.19}$	…
BABAR M_X [580]	$4.03 \pm 0.22^{+0.22}_{-0.22}$	$4.22 \pm 0.23^{+0.21}_{-0.27}$	$4.10 \pm 0.23^{+0.16}_{-0.17}$	$3.75 \pm 0.21^{+0.18}_{-0.18}$	…
BABAR M_X, q^2 [580]	$4.32 \pm 0.23^{+0.26}_{-0.28}$	$4.24 \pm 0.22^{+0.18}_{-0.21}$	$4.33 \pm 0.23^{+0.24}_{-0.27}$	$3.75 \pm 0.20^{+0.17}_{-0.17}$	$4.50 \pm 0.24^{+0.29}_{-0.29}$
BABAR P_+ [580]	$4.09 \pm 0.25^{+0.25}_{-0.25}$	$4.17 \pm 0.25^{+0.28}_{-0.37}$	$4.25 \pm 0.26^{+0.26}_{-0.27}$	$3.57 \pm 0.22^{+0.19}_{-0.18}$	…
BABAR p_ℓ^*, (M_X, q^2) fit [580]	$4.33 \pm 0.24^{+0.19}_{-0.21}$	$4.45 \pm 0.24^{+0.12}_{-0.13}$	$4.44 \pm 0.24^{+0.09}_{-0.10}$	$4.33 \pm 0.24^{+0.19}_{-0.19}$	…
BABAR p_ℓ^* [580]	$4.34 \pm 0.27^{+0.20}_{-0.21}$	$4.43 \pm 0.27^{+0.13}_{-0.13}$	$4.43 \pm 0.27^{+0.09}_{-0.11}$	$4.28 \pm 0.27^{+0.19}_{-0.19}$	…
Belle M_X, q^2 [592]	…	…	…	…	$5.01 \pm 0.39^{+0.32}_{-0.32}$
Average	$4.28 \pm 0.13^{+0.20}_{-0.21}$	$3.93 \pm 0.10^{+0.09}_{-0.10}$	$4.19 \pm 0.12^{+0.11}_{-0.12}$	$3.92 \pm 0.12^{+0.18}_{-0.12}$	$4.62 \pm 0.20^{+0.29}_{-0.29}$

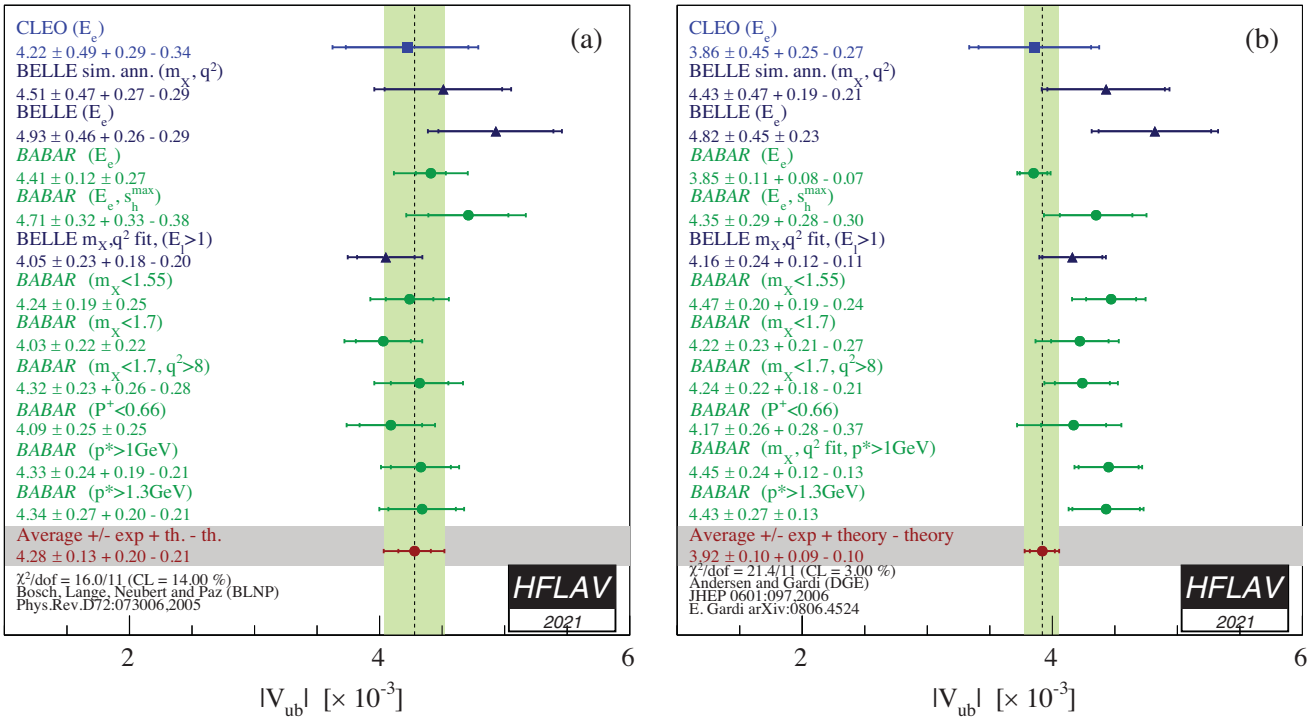

FIG. 63. Measurements of $|V_{ub}|$ from inclusive semileptonic decays and their average based on the BLNP (a) and DGE (b) prescription. The labels indicate the variables and selections used to define the signal regions in the different analyses.

and $\mu_\pi^2(\mathrm{SF})$) is second. The uncertainty due to weak annihilation is assumed to be asymmetric, i.e. it only tends to decrease $|V_{ub}|$.

2. DGE

Andersen and Gardi (dressed gluon exponentiation, DGE) [600] provide a framework where the on-shell b-quark calculation, converted into hadronic variables, is directly used as an approximation to the meson decay spectrum without the use of a leading-power nonperturbative function (or, in other words, a shape function). The DGE calculation uses the $\overline{MS}$ renormalization scheme. The heavy quark parameters determined from the global fit in the kinetic scheme, described in Sec. VII B 2, were therefore translated into the $\overline{MS}$ scheme by using code provided by Einan Gardi (based on Refs. [602,603]), giving $m_b(\overline{MS}) = (4.188 \pm 0.043)$ GeV. The extracted values of $|V_{ub}|$ for each measurement along with their average are given in Table 95 and illustrated in Fig. 63(b). The total error is $^{+3.3}_{-3.2}\%$, whose breakdown is: statistics ($^{+1.5}_{-1.5}\%$), detector effects ($^{+1.7}_{-1.7}\%$), $B \to X_c \ell^+ \nu_\ell$ model ($^{+0.3}_{-0.4}\%$), $B \to X_u \ell^+ \nu_\ell$ model ($^{+0.7}_{-0.7}\%$), strong coupling α_s ($^{+0.3}_{-0.3}\%$), m_b ($^{+2.2}_{-2.1}\%$), weak annihilation ($^{+0.0}_{-1.1}\%$), matching scales in DGE ($^{+0.4}_{-0.5}\%$). The largest contribution to the total error is due to the effect of the uncertainty on m_b. The uncertainty due to weak annihilation has been assumed to be asymmetric, i.e. it only tends to decrease $|V_{ub}|$.

3. GGOU

Gambino, Giordano, Ossola and Uraltsev (GGOU) [604] compute the triple differential decay rates of $B \to X_u \ell^+ \nu_\ell$, including all perturbative and nonperturbative effects through $O(\alpha_s^2 \beta_0)$ and $O(1/m_b^3)$. The Fermi motion is parametrized in terms of a single light cone function for each structure function and for any value of q^2, accounting for all subleading effects. The calculations are performed in the kinetic scheme, a framework characterized by a Wilsonian treatment with a hard cutoff $\mu \sim 1$ GeV. GGOU have not included calculations for the "$(E_e, s_h^{\max})$" analysis [588]. The heavy quark parameters determined from the global fit in the kinetic scheme, described in Sec. VII B 2, are used as inputs: $m_b^{\mathrm{kin}} = (4.554 \pm 0.018)$ GeV, $\mu_\pi^2 = (0.464 \pm 0.076)\mathrm{GeV}/c^2$. The extracted values of $|V_{ub}|$ for each measurement along with their average are given in Table 95 and illustrated in Fig. 64(a). The total error is $^{+3.9}_{-3.9}\%$ whose breakdown is: statistics ($^{+1.3}_{-1.3}\%$), detector effects ($^{+1.6}_{-1.6}\%$), $B \to X_c \ell^+ \nu_\ell$ model ($^{+0.9}_{-0.9}\%$), $B \to X_u \ell^+ \nu_\ell$ model ($^{+1.7}_{-1.7}\%$), α_s, m_b and other nonperturbative parameters ($^{+1.8}_{-1.8}\%$), higher order perturbative and nonperturbative corrections ($^{+1.5}_{-1.5}\%$), modeling of the q^2 tail ($^{+1.3}_{-1.3}\%$), weak annihilations matrix element ($^{+0.0}_{-1.1}\%$), functional form of the distribution functions ($^{+0.1}_{-0.1}\%$). The leading uncertainties on $|V_{ub}|$ are both from theory, and are due to perturbative and nonperturbative parameters and the modeling of the q^2 tail. The uncertainty due to weak annihilation

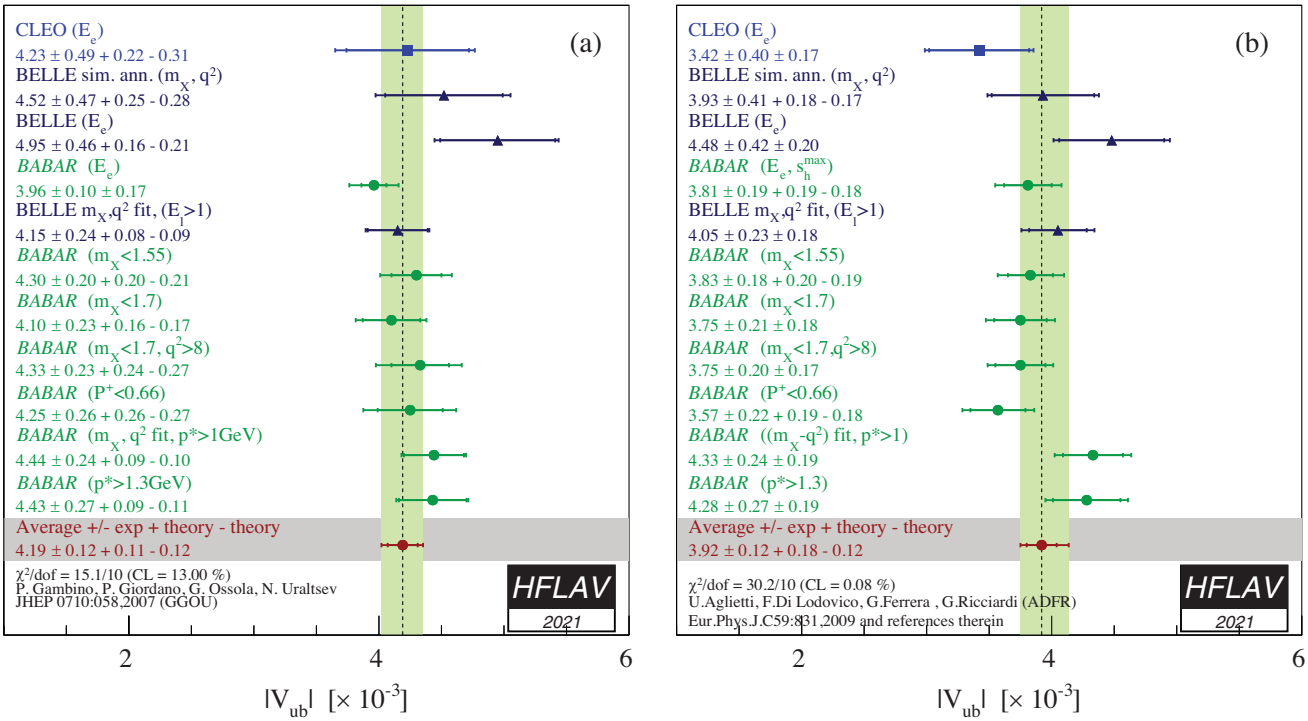

FIG. 64. Measurements of $|V_{ub}|$ from inclusive semileptonic decays and their average based on the GGOU (a) and ADFR (b) prescription. The labels indicate the variables and selections used to define the signal regions in the different analyses.

has been assumed to be asymmetric, i.e. it only tends to decrease $|V_{ub}|$.

4. ADFR

Aglietti, Di Lodovico, Ferrera and Ricciardi (ADFR) [605] use an approach to extract $|V_{ub}|$, that makes use of the ratio of the $B \to X_c \ell^+ \nu_\ell$ and $B \to X_u \ell^+ \nu_\ell$ widths. The normalized triple differential decay rate for $B \to X_u \ell^+ \nu_\ell$ [601,606–608] is calculated with a model based on (i) soft–gluon resummation to next-to-next-leading order and (ii) an effective QCD coupling without a Landau pole. This coupling is constructed by means of an extrapolation to low energy of the high–energy behavior of the standard coupling. More technically, an analyticity principle is used. The lower cut on the electron energy for the endpoint analyses is 2.3 GeV [601]. The ADFR calculation uses the $\overline{\text{MS}}$ renormalization scheme; the heavy quark parameters determined from the global fit in the kinetic scheme, described in Sec. VII B 2, were therefore translated into the $\overline{\text{MS}}$ scheme by using code provided by Einan Gardi (based on Refs. [602,603]), giving $m_b(\overline{\text{MS}}) = (4.188 \pm 0.043)$ GeV. The extracted values of $|V_{ub}|$ for each measurement along with their average are given in Table 95 and illustrated in Fig. 64(b). The total error is $^{+5.5}_{-5.5}\%$ whose breakdown is: statistics ($^{+1.6}_{-1.6}\%$), detector effects ($^{+1.7}_{-1.7}\%$), $B \to X_c \ell^+ \nu_\ell$ model ($^{+1.3}_{-1.3}\%$), $B \to X_u \ell^+ \nu_\ell$ model ($^{+1.6}_{-1.5}\%$), α_s ($^{+1.1}_{-1.1}\%$), $|V_{cb}|$ ($^{+1.9}_{-1.9}\%$), m_b ($^{+0.7}_{-0.7}\%$), m_c ($^{+1.3}_{-1.3}\%$), semileptonic branching fraction ($^{+0.8}_{-0.7}\%$), theory model ($^{+3.6}_{-3.6}\%$). The leading uncertainty is due to the theory model.

5. BLL

Bauer, Ligeti, and Luke (BLL) [581] give a HQET-based prescription that advocates combined cuts on the dilepton invariant mass, q^2, and hadronic mass, m_X, to minimize the overall uncertainty on $|V_{ub}|$. In their reckoning a cut on m_X only, although most efficient at preserving phase space (~80%), makes the calculation of the partial rate untenable due to uncalculable corrections to the b-quark distribution function or shape function. These corrections are suppressed if events in the low q^2 region are removed. The cut combination used in measurements is $M_x < 1.7$ GeV/c^2 and $q^2 > 8$ GeV$^2/c^4$. The extracted values of $|V_{ub}|$ for each measurement along with their average are given in Table 95 and illustrated in Fig. 65. The total error is $^{+7.7}_{-7.7}\%$ whose breakdown is: statistics ($^{+3.3}_{-3.3}\%$), detector effects ($^{+3.0}_{-3.0}\%$), $B \to X_c \ell^+ \nu_\ell$ model ($^{+1.6}_{-1.6}\%$), $B \to X_u \ell^+ \nu_\ell$ model ($^{+1.1}_{-1.1}\%$), spectral fraction (m_b) ($^{+3.0}_{-3.0}\%$), perturbative approach: strong coupling α_s ($^{+3.0}_{-3.0}\%$), residual shape function ($^{+2.5}_{-2.5}\%$), third order terms in the OPE ($^{+4.0}_{-4.0}\%$). The leading uncertainties, both from theory, are due to residual shape function effects and third order terms in the OPE expansion. The leading experimental uncertainty is due to statistics.

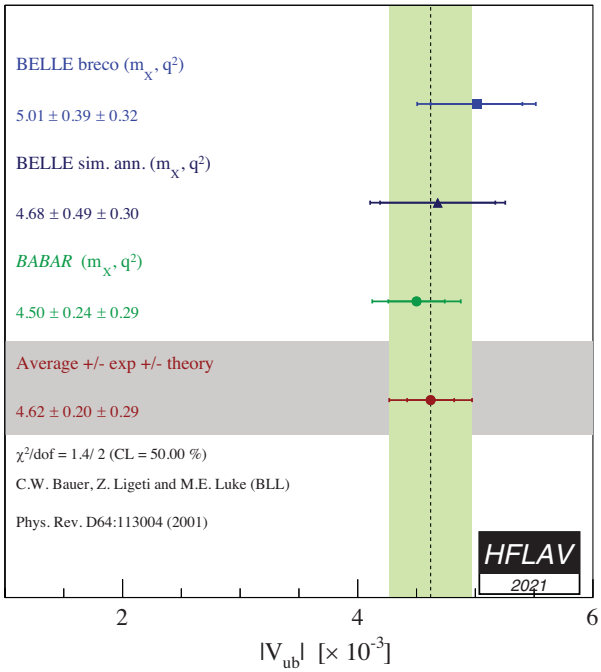

FIG. 65. Measurements of $|V_{ub}|$ from inclusive semileptonic decays and their average in the BLL prescription.

6. Summary

The averages presented in several different frameworks are presented in Table 96. In summary, we recognize that the experimental and theoretical uncertainties play out differently between the schemes and the theoretical assumptions for the theory calculations are different. Therefore, it is difficult to perform an average between the various determinations of $|V_{ub}|$. Since the methodology is similar to that used to determine the inclusive $|V_{cb}|$ average, we choose to quote as reference value the average determined by the GGOU calculation, which gives $|V_{ub}| = (4.19 \pm 0.12^{+0.11}_{-0.12}) \times 10^{-3}$.

E. Combined extraction of $|V_{ub}|$ and $|V_{cb}|$

In this section we report the result of a combined fit for $|V_{ub}|$ and $|V_{cb}|$ that includes the constraint from the averaged $|V_{ub}|/|V_{cb}|$, and the determination of $|V_{ub}|$ and $|V_{cb}|$ from exclusive B meson decays.

The average of the $|V_{ub}|/|V_{cb}|$ measurements from $\Lambda_b \to p\mu\nu$ and $B_s \to K\mu\nu$, using only results at high q^2 (based on Lattice-QCD), assuming the uncertainties due to trigger selection and tracking efficiency are fully correlated, is

$$\frac{|V_{ub}|}{|V_{cb}|} = 0.0838 \pm 0.0046 \tag{218}$$

where the reported uncertainty includes both experimental and theoretical contributions. The average of the $|V_{cb}|$ results from $B \to D\ell\nu$, $B \to D^*\ell\nu$ and $B_s \to D_s^{(*)}\mu\nu$, is

$$|V_{cb}| = (38.90 \pm 0.53) \times 10^{-3}, \tag{219}$$

where the uncertainty also in this case includes both experimental and theoretical contributions. The $P(\chi^2)$ of the average is 30%.

The combined fit for $|V_{ub}|$ and $|V_{cb}|$ results in

$$|V_{ub}| = (3.51 \pm 0.12) \times 10^{-3} \tag{220}$$

$$|V_{cb}| = (39.10 \pm 0.50) \times 10^{-3} \tag{221}$$

$$\rho(|V_{ub}|, |V_{cb}|) = 0.175, \tag{222}$$

where the uncertainties in the inputs are considered uncorrelated. The fit result is shown in Fig. 66, where

TABLE 96. Summary of inclusive determinations of $|V_{ub}|$. The errors quoted on $|V_{ub}|$ correspond to experimental and theoretical uncertainties.

Framework	$\lvert V_{ub}\rvert[10^{-3}]$
BLNP	$4.28 \pm 0.13^{+0.20}_{-0.21}$
DGE	$3.93 \pm 0.10^{+0.09}_{-0.10}$
GGOU	$4.19 \pm 0.12^{+0.11}_{-0.12}$
ADFR	$3.92 \pm 0.1^{+0.18}_{-0.12}$
BLL (m_X/q^2 only)	$4.62 \pm 0.20 \pm 0.29$

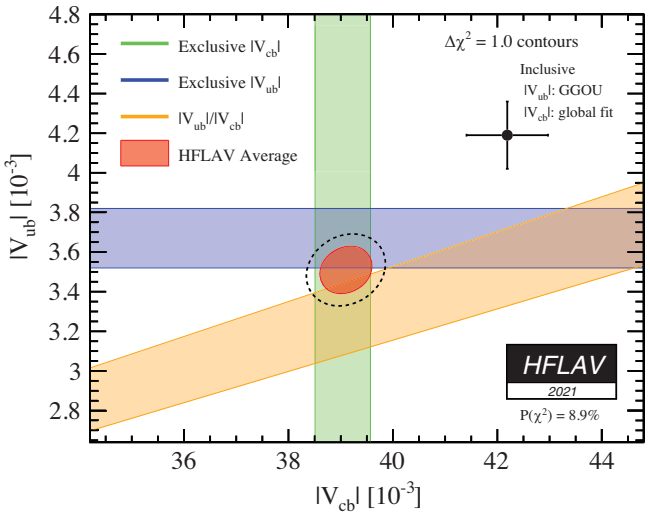

FIG. 66. Combined average on $|V_{ub}|$ and $|V_{cb}|$ including the LHCb measurement of $|V_{ub}|/|V_{cb}|$, the exclusive $|V_{ub}|$ measurement from $B \to \pi\ell\nu$, and the $|V_{cb}|$ average from $B \to D\ell\nu$, $B \to D^*\ell\nu$ and $B_s \to D_s^{(*)}\mu\nu$ measurements. The dashed ellipse corresponds to a 1σ two-dimensional contour (68% of CL). The point with the error bars corresponds to the inclusive $|V_{cb}|$ from the kinetic scheme (Sec. VII B 2), and the inclusive $|V_{ub}|$ from GGOU calculation (Sec. VII D 3).

both the $\Delta\chi^2 = 1$ and the two-dimensional 68% C.L. contours are indicated. The average value of $|V_{cb}|$ differs from the inclusive one, by about 3.3σ. The difference of $|V_{ub}|$ from the GGOU inclusive result taken as reference is also 3.3σ.

F. $B \to D^{(*)}\tau\nu_\tau$ decays

In the SM, the semileptonic decays are tree level processes which proceed via the coupling to the $W^\pm$ boson. These couplings are assumed to be universal for all leptons and are well understood theoretically, (see Section V. A and V. B). This universality has been tested in purely leptonic and semileptonic B meson decays involving a τ lepton, which might be sensitive to a hypothetical charged Higgs boson or other non-SM processes.

Compared to $B^+ \to \tau\nu_\tau$, the $B \to D^{(*)}\tau\nu_\tau$ decay has advantages: the branching fraction is relatively high, because it is not Cabibbo-suppressed, and it is a three-body decay allowing access to many observables besides the branching fraction, such as $D^{(*)}$ momentum, q^2 distributions, and measurements of the D^* and τ polarizations (see Ref. [609] and references therein for recent calculations).

Experiments have measured two ratios of branching fractions defined as

$$\mathcal{R}(D) = \frac{\mathcal{B}(B \to D\tau\nu_\tau)}{\mathcal{B}(B \to D\ell\nu_\ell)}, \tag{223}$$

$$\mathcal{R}(D^*) = \frac{\mathcal{B}(B \to D^*\tau\nu_\tau)}{\mathcal{B}(B \to D^*\ell\nu_\ell)} \tag{224}$$

where ℓ refers either to electron or μ. These ratios are independent of $|V_{cb}|$ and to a large extent, also of the $B \to D^{(*)}$ form factors. As a consequence, the SM predictions for these ratios are quite precise:

(i) $\mathcal{R}(D) = 0.298 \pm 0.004$: where the central value and the uncertainty are obtained from an arithmetic average of the predictions from Refs. [610–614]. The Refs. [610–612,614] are based on recent lattice calculations [512,521] and results on the $B \to D\ell\nu$ form factor measurements from *BABAR* and Belle. The prediction in Ref. [613] used here is based only on theoretical inputs.

(ii) $\mathcal{R}(D^*) = 0.254 \pm 0.005$: where the central value and the uncertainty are obtained from an arithmetic average of the predictions from Refs. [517,611–613,615]. These calculations are in good agreement between each other, and consistent with older predictions. The authors of Ref. [615] use as inputs the most recent Belle results of $B \to D^*\ell\nu$ form factors [501]. The authors of Ref. [613] obtain predictions with and without using experimental inputs. Compared with other calculations, their predictions on $R(D^*)$ are slightly shifted toward a lower value, resulting in $R(D^*) = 0.250 \pm 0.003$ and $R(D^*) = 0.247 \pm 0.006$ using and not using the experimental results, respectively. In this average we use the latter result. The calculation in Ref. [517] is the result of the full angular analysis of $B \to D^*\ell\nu$ decay by *BABAR*, and gives an independent prediction of $\mathcal{R}(D^*) = 0.253 \pm 0.005$, which is compatible with the predictions above.

The first unquenched lattice-QCD calculation of the $B \to D^*\ell\nu$ at nonzero recoil in Ref. [616], predicts a value of $R(D^*) = 0.265 \pm 0.013$, which reduces the tension, even if the larger uncertainty alleviates its significance. A combined analysis of $B \to D\ell\nu$ and $B \to D^*\ell\nu$ that includes both lattice calculations and experimental inputs would be desirable.

On the experimental side, in the case of the leptonic τ decay, the ratios $\mathcal{R}(D^{(*)})$ can be directly measured, and many systematic uncertainties cancel in the measurement. The $B^0 \to D^{*+}\tau\nu_\tau$ decay was first observed by Belle [617] performing an "inclusive" reconstruction, which is based on the reconstruction of the $B_{\rm tag}$ from all the particles of the events, other than the $D^{(*)}$ and the lepton candidate, without looking for any specific $B_{\rm tag}$ decay chain. Since then, both *BABAR* and Belle have published improved measurements and have observed the $B \to D\tau\nu_\tau$ decays [618,619].

The most powerful way to study these decays at the B-factories exploits the hadronic or semileptonic $B_{\rm tag}$. Using the full dataset and an improved hadronic $B_{\rm tag}$ selection, *BABAR* measured [620]:

$$\begin{aligned}\mathcal{R}(D) &= 0.440 \pm 0.058 \pm 0.042,\\ \mathcal{R}(D^*) &= 0.332 \pm 0.024 \pm 0.018\end{aligned} \tag{225}$$

where decays to both $e^\pm$ and $\mu^\pm$ were summed, and results for B^0 and B^- decays were combined in an isospin-constrained fit. The fact that the *BABAR* result exceeded SM predictions by 3.4σ raised considerable interest.

Belle, exploiting the full dataset, published measurements using both the hadronic [621] and the semileptonic tag [622]. Belle also performed a combined measurement of $\mathcal{R}(D^*)$ and τ polarization by reconstructing the τ in the hadronic $\tau \to \pi\nu$ and $\tau \to \rho\nu$ decay modes [623]. LHCb measurements of $R(D^*)$ use both the muonic τ decay [624], and the three-prong hadronic $\tau \to 3\pi(\pi^0)\nu$ decays [625]. The latter is a direct measurement of the ratio $\mathcal{B}(B^0 \to D^{*-}\tau^+\nu_\tau)/\mathcal{B}(B^0 \to D^{*-}\pi^+\pi^-\pi^+)$, and is translated into a measurement of $R(D^*)$ using the independently measured branching fractions $\mathcal{B}(B^0 \to D^{*-}\pi^+\pi^-\pi^+)$ and $\mathcal{B}(B^0 \to D^{*-}\mu^+\nu_\mu)$.

The most important source of systematic uncertainties that are correlated among the different measurement is the $B \to D^{**}$ background components, which are difficult to disentangle from the signal. In our average, the systematic

TABLE 97. Measurements of $\mathcal{R}(D^*)$ and $\mathcal{R}(D)$, their correlations and the combined average.

Experiment	$\mathcal{R}(D^*)$	$\mathcal{R}(D)$	ρ
BABAR [620,630]	$0.332 \pm 0.024_{\text{stat}} \pm 0.018_{\text{syst}}$	$0.440 \pm 0.058_{\text{stat}} \pm 0.042_{\text{syst}}$	−0.27
Belle [621]	$0.293 \pm 0.038_{\text{stat}} \pm 0.015_{\text{syst}}$	$0.375 \pm 0.064_{\text{stat}} \pm 0.026_{\text{syst}}$	−0.49
LHCb [624]	$0.336 \pm 0.027_{\text{stat}} \pm 0.030_{\text{syst}}$		
Belle [623]	$0.270 \pm 0.035_{\text{stat}}\,^{+0.028}_{-0.025\,\text{syst}}$		
LHCb [625,631]	$0.283 \pm 0.019_{\text{stat}} \pm 0.029_{\text{syst}}$		
Belle [622]	$0.283 \pm 0.018_{\text{stat}} \pm 0.014_{\text{syst}}$	$0.307 \pm 0.037_{\text{stat}} \pm 0.016_{\text{syst}}$	−0.51
Average	$\mathbf{0.295 \pm 0.010 \pm 0.010}$	$\mathbf{0.339 \pm 0.026 \pm 0.014}$	−0.38

uncertainties due to the $B \to D^{**}$ composition and kinematics are considered fully correlated among the measurements.

The results of the individual measurements, their averages and correlations are presented in Table 97 and Fig. 67. The combined results, projected separately on $\mathcal{R}(D)$ and $\mathcal{R}(D^*)$, are reported in Fig. 68(a) and Fig. 68(b) respectively.

The averaged $\mathcal{R}(D)$ and $\mathcal{R}(D^*)$ exceed the SM prediction given above, by 1.4σ and 2.8σ, respectively. Considering the $\mathcal{R}(D)$ and $\mathcal{R}(D^*)$ total correlation of −0.38, the difference with respect to the SM is about 3.3σ, and the combined $\chi^2 = 13.97$ for 2 degrees of freedom corresponds to a p-value of 0.92×10^{-3}, assuming Gaussian error distributions.

An analogous measurement using $B_c \to J/\psi \ell \nu$ decays has been performed by LHCb, leading to $R(J\psi) = 0.71 \pm 0.17_{\text{stat}} \pm 0.18_{\text{syst}}$ [626], which lies 1.8σ above the most recent SM prediction obtained by HPQCD collaboration [627]. Recently LHCb reported the first observation of the $\Lambda_b^0 \to \Lambda_c^+ \tau^- \bar{\nu}_\tau$ decay [628], exploiting the three-prong hadronic τ^- decays. The resulting ratio of semileptonic branching fractions is $\mathcal{R}(\Lambda_c) = 0.242 \pm 0.026_{\text{stat}} \pm 0.040_{\text{syst}} \pm 0.059_{\text{ext}}$, where the last term is due to the uncertainties on the external branching fractions measurement, in particular for the $\Lambda_b^0 \to \Lambda_c^+ \mu^- \bar{\nu}_\mu$ decay. This result is in agreement with the prediction of 0.324 ± 0.004 from Ref. [629].

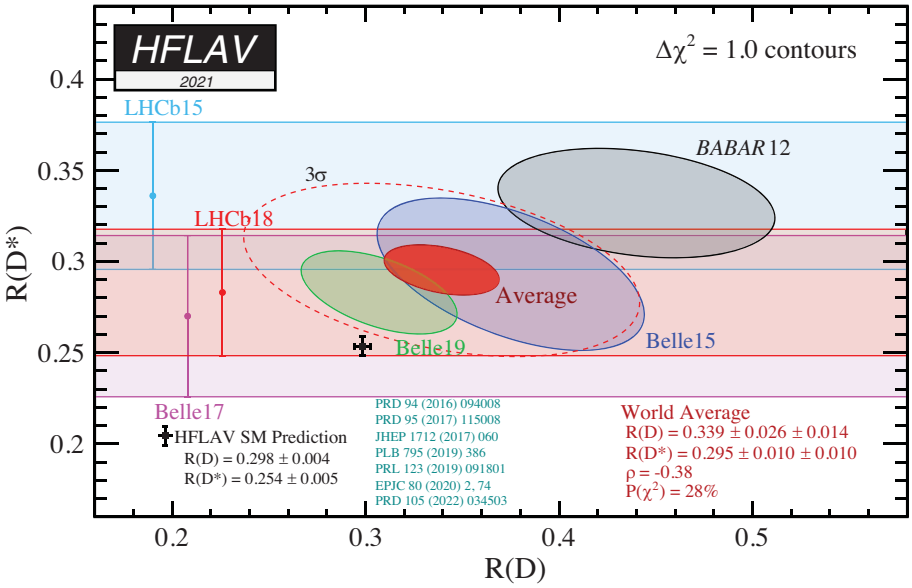

FIG. 67. Measurements of $\mathcal{R}(D)$ and $\mathcal{R}(D^*)$ listed in Table 97 and their two-dimensional average. Contours correspond to $\Delta\chi^2 = 1$, i.e., 68% CL for the bands and 39% CL for the ellipses. The black and blue points with error bars, are two recent SM prediction for $\mathcal{R}(D^*)$ and $\mathcal{R}(D)$. The SM predictions reported are based on results from Refs. [610,613,615]. More information is given in the text. An average of these predictions and the experimental average deviate from each other by about 3.3σ. The dashed ellipse correspond to a 3σ contour (99.73% CL).

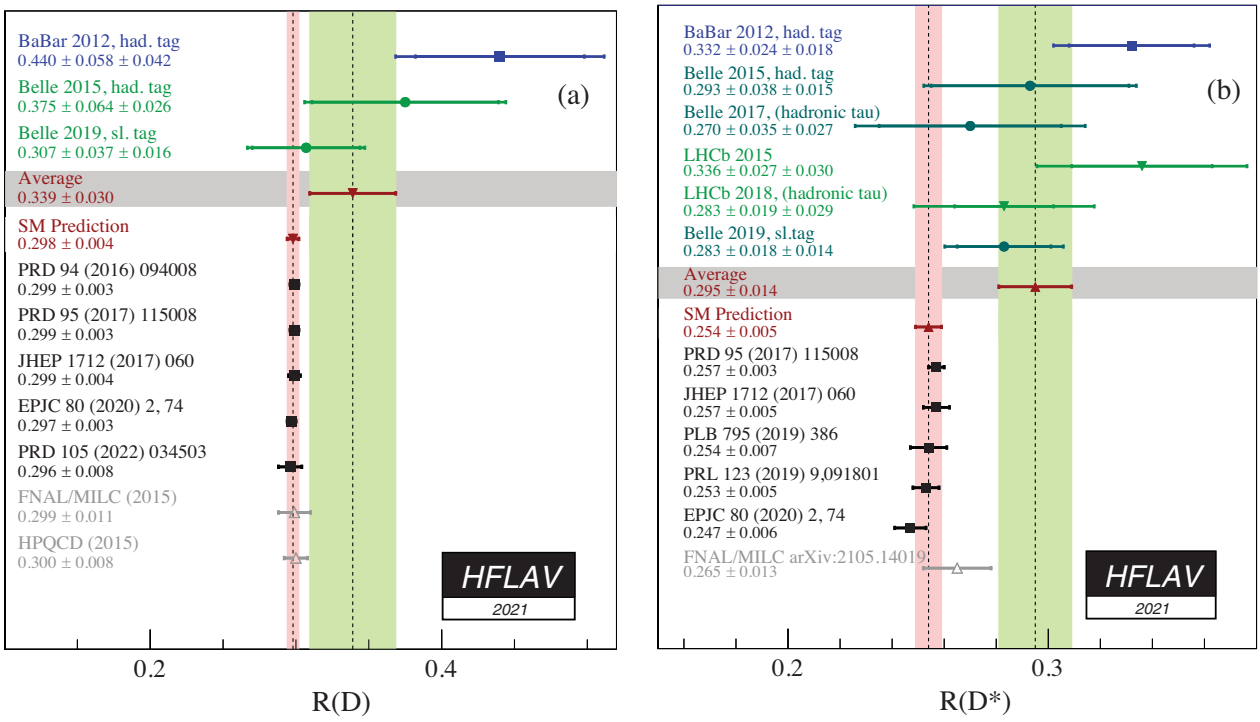

FIG. 68. (a) Measurements of $\mathcal{R}(D)$ and (b) $\mathcal{R}(D^*)$. The green bands are the averages obtained from the combined fit. The red bands are the averages of the theoretical predictions obtained as explained in the text.

VIII. DECAYS OF b-HADRONS INTO OPEN OR HIDDEN CHARM HADRONS

Ground-state B mesons and b baryons dominantly decay to particles containing a charm quark via the $b \to c$ quark transition. In this section, measurements of such decays to hadronic final states are summarized. The use of such decays for studying fundamental properties of the bottom hadrons and for obtaining parameters of the CKM matrix is discussed in Secs. V and VI, respectively.

Since hadronic $b \to c$ decays dominate the b-hadron widths, they are an important part of the experimental programme in heavy-flavor physics. Understanding the rate of charm production in b-hadron decays is crucial for validation of the heavy-quark expansion (HQE) that underpins much of the theoretical framework for b physics (see, for example, Ref. [632] for a review). Moreover, such decays are often used, in particular at hadron colliders, as normalization modes for measurements of rarer decays. At B-factories, hadronic $b \to c$ decays are used for the tagging of B mesons and a detailed knowledge is crucial for the optimization and calibration of the tagger performance. In addition, they are the dominant background in many analyses. To accurately model such backgrounds with simulated data, it is essential to have precise knowledge of the contributing decay modes. In particular, with the expected increase in the data samples at LHCb and Belle II, the enhanced statistical sensitivity has to be matched by low systematic uncertainties that arise from the limited understanding of the dominant b-hadron decay modes. For multibody decays, knowledge of the distribution of decays across the phase-space (e.g., the Dalitz plot density for three-body decays or the polarization amplitudes for vector-vector final states) is required in addition to the total branching fraction.

The large branching fractions of $b \to c$ decays make them ideal for studying the spectroscopy of both open and hidden charm hadrons. In particular, they have been used to both discover and measure the properties of exotic particles, such as the $X(3872)$ [633,634], $Z(4430)^+$ [635,636] and $P_c(4450)^+$ [637] states. Similarly, $b \to c$ transitions are very useful for studying charmed baryons.

In addition to the dominant $b \to c$ decays, there are several decays in this category that are expected to be highly suppressed in the Standard Model. These are of interest for probing particular decay amplitudes (e.g., the annihilation diagram, which dominates the $B^- \to D_s^- \phi$ decay) used to constrain effects in other hadronic decays, or for searching for new physics. There are also open charm production modes that involve $b \to u$ transitions, such as $\bar{B}^0 \to D_s^- \pi^+$, which are mediated by the W emission involving the $|V_{ub}|$ CKM matrix element. Finally, $b \to c$ decays involving lepton flavor or number violation are extremely suppressed in the Standard Model, and therefore provide highly sensitive tests of new physics.

In this section, we give an exhaustive list of measured branching ratios of decay modes to hadrons containing charm quarks. The averaging procedure follows the

methodology described in Sec. III. We perform fits of the full likelihood function and do not use the approximation described in Sec. III A. For the cases where more than one measurement is available, in total 81 fits are performed, with on average (maximally) 3.6 (128) parameters and 6.3 (221) measurements per fit. Systematic uncertainties are taken as quoted without the scaling of multiplicative uncertainties discussed in Sec. III C. Where available, correlations between measurements are taken into account. We consider correlations not only between measurements of the same parameter, as done in our previous publication Ref. [1], but also among parameters. The correlations among parameters are given on the HFLAV web page on hadronic B decays into open or hidden charm hadrons [638]. If an insignificant measurement and a limit for the same parameter are provided in the same paper, the former is quoted, so that it can be included in averages. We also provide averages of the polarization amplitudes of B meson decays to vector-vector states. We do not currently provide detailed averages of quantities obtained from Dalitz plot analyses, due to the complications arising from the dependence on the model used.

The results are presented in subsections organized according to the type of decaying bottom hadron: B^0 (Sec. VIII A), B^+ (Sec. VIII B), B^0/B^+ admixture (Sec. VIII C), B_s^0 (Sec. VIII D), B_c^+ (Sec. VIII E), b baryons (Sec. VIII F). For each subsection, the parameters $\boldsymbol{p}$ are arranged according to the final state into the following groups: a single charmed meson, two charmed mesons, a charmonium state, a charm baryon, or other states, e.g., $X(3872)$. In our tables, the individual measurements and average of each parameter p_j are shown in one row. We quote numerical values of all direct measurements of a parameter p_j. We also show numerical values derived from measurements of branching-fraction ratios p_j/p_k, performed with respect to the branching fraction p_k of a normalization mode, as well as measurements of products $p_j p_k$ of the branching fraction of interest with those of daughter-particle decays. In these cases, the quoted value and uncertainty of the measurement are determined with the fitted value of p_k, and the uncertainty of p_k is included in the systematic uncertainty. A footnote "Using p_k" is added in these cases. Note that the fit uses p_j/p_k or $p_j p_k$ directly and not the p_j value that is quoted in the table. The p_j value is quoted to give a sense of the contribution of the measurement to the average. When the measurement depends on p_j in some other way, it is also included in our fit for p_j, but in the tables no derived value is shown. Instead, the measured function f of parameters is given in a footnote "measurement of f used in the fit."

In most of the tables of this section the averages are compared to those from the Particle Data Group's 2020 Review of Particle Physics (PDG 2020) [9] and 2021 update. When this is done, the "Average" column quotes the PDG averages in green only if they differ from ours. In general, such differences are due to different input parameters and measurements, differences in the averaging methods and different rounding conventions. The fit p-value is quoted if it is below 1%. Input values that appear in red are not included in the PDG average. They are either new results published after the closing of PDG and before the closing of this report, May 2021, or results that do not quote a direct measurement of the parameter of interest and are therefore not considered in the PDG average. Input values in blue are unpublished results (that are never included in the PDG averages). Quoted upper limits are at 90% confidence level (CL), unless mentioned otherwise.

The symbol $\mathcal{B}$ is used for branching ratios, and f_X for the production fraction of quark or hadron X (see Sec. IV C). The decay amplitudes for longitudinal, parallel, and perpendicular transverse polarization in pseudoscalar to vector-vector decays are denoted $\mathcal{A}_0$, $\mathcal{A}_\parallel$, and $\mathcal{A}_\perp$, respectively, and the definitions $\delta_\parallel = \arg(\mathcal{A}_\parallel/\mathcal{A}_0)$ and $\delta_\perp = \arg(\mathcal{A}_\perp/\mathcal{A}_0)$ are used for their relative phases. For normalized P-wave amplitudes we use the notation $f_i = |\mathcal{A}_i|^2/(|\mathcal{A}_0|^2 + |\mathcal{A}_\parallel|^2 + |\mathcal{A}_\perp|^2)$. The inclusion of charge conjugate modes is always implied.

Following the approach used by the PDG [9], for decays that involve neutral kaons we mainly quote results in terms of final states including either a K^0 or $\bar{K}^0$ meson (instead of a K_S^0 or K_L^0), although the flavor of the neutral kaon is never determined experimentally. The specification as K^0 or $\bar{K}^0$ simply follows the quark model expectation for the dominant decay and the inclusion of the conjugate final state neutral kaon is implied. The exception is B_s^0 decays to CP eigenstates, where the width difference between the mass eigenstates (see Sec. V) means that the measured branching fraction, integrated over decay time, is specific to the final state [639]. In such cases it is appropriate to quote the branching fraction for, e.g., $\bar{B}_s^0 \to J/\psi K_S^0$ instead of $\bar{B}_s^0 \to J/\psi \bar{K}^0$.

Most B-meson branching-fraction measurements assume $\Gamma(\Upsilon(4S) \to B^+B^-) = \Gamma(\Upsilon(4S) \to B^0\bar{B}^0)$. While there is no evidence for isospin violation in $\Upsilon(4S)$ decays, deviations from this assumption can be of the order of a few percent, see Sec. IV A and Ref. [640]. As the effect is negligible for many averages, we take the quoted values without applying a correction or additional systematic uncertainty. However, we note that this can be relevant for averages with percent-level uncertainty.

A. Decays of B^0 mesons

Measurements of B^0 decays to charmed hadrons are summarized in Secs. VIII A 1 to VIII A 5.

1. Decays to a single open charm meson

Averages of B^0 decays to a single open charm meson are shown in Tables 98–106.

TABLE 98. Branching fractions for decays to a $D^{(*)}$ meson and one or more pions, I.

Parameter [10^{-3}]	Measurements		Average HFLAV PDG
$\mathcal{B}(B^0 \to D^-\pi^+)$	*BABAR* [641]	$2.55 \pm 0.05 \pm 0.16$	2.56 ± 0.13
	BABAR [642]	$3.03 \pm 0.23 \pm 0.23$	2.52 ± 0.13
	Belle [643][a]		
	CDF [644][b], [645][c], [646][d]		
	LHCb [647][e], [648][a]		
$\mathcal{B}(B^0 \to D^-\pi^+\pi^+\pi^-)$	LHCb [647]	$6.10 \pm 0.28^{+0.63\,f}_{-0.62}$	$5.95^{+0.66}_{-0.62}$
	CDF [645][g,h]		6.02 ± 0.67
	LHCb [647][i], [649][j]		
$\mathcal{B}(B^0 \to D^*(2010)^-\pi^+)$	Belle [650]	$2.22 \pm 0.04 \pm 0.19$	2.63 ± 0.10
	BABAR [641]	$2.79 \pm 0.08 \pm 0.17$	2.74 ± 0.13
	BABAR [642]	$2.99 \pm 0.23 \pm 0.24$	
	BABAR [651][k]		
	Belle [643][k]		
	LHCb [652][l]		
$\mathcal{B}(B^0 \to D^*(2010)^-\pi^+\pi^+\pi^-)$	LHCb [652]	$6.94 \pm 0.11 \pm 0.43^{m}$	7.08 ± 0.26
	BABAR [653]	$7.26 \pm 0.11 \pm 0.31$	7.21 ± 0.29
	Belle [654]	$6.81 \pm 0.23 \pm 0.72$	
	LHCb [652][n,o]		
$\mathcal{B}(B^0 \to \bar{D}^*(2007)^0\pi^+\pi^+\pi^-\pi^-)$	Belle [654]	$2.6 \pm 0.5 \pm 0.4$	2.60 ± 0.60
			2.72 ± 0.50
$\mathcal{B}(B^0 \to D^*(2010)^-\pi^+\pi^+\pi^+\pi^-\pi^-)$	Belle [654]	$4.72 \pm 0.59 \pm 0.71$	4.72 ± 0.92
$\mathcal{B}(B^0 \to D^*(2010)^-\omega(782)\pi^+)$	Belle [655]	$2.31 \pm 0.11 \pm 0.14$	2.41 ± 0.16
	BABAR [656]	$2.88 \pm 0.21 \pm 0.31$	2.46 ± 0.18

[a]Measurement of $\mathcal{B}(B^0 \to D^-K^+)/\mathcal{B}(B^0 \to D^-\pi^+)$ used in our fit.
[b]Measurement of $\mathcal{B}(B^+ \to \bar{D}^0\pi^+)/\mathcal{B}(B^0 \to D^-\pi^+)$ used in our fit.
[c]Measurement of $\mathcal{B}(B_s^0 \to D_s^-\pi^+)/\mathcal{B}(B^0 \to D^-\pi^+)$ used in our fit.
[d]Measurement of $\mathcal{B}(\Lambda_b^0 \to \Lambda_c^+\pi^-)/\mathcal{B}(B^0 \to D^-\pi^+)$ used in our fit.
[e]Measurement of $\mathcal{B}(B^0 \to D^-\pi^+\pi^+\pi^-)/\mathcal{B}(B^0 \to D^-\pi^+)$ used in our fit.
[f]Using $\mathcal{B}(B^0 \to D^-\pi^+)$.
[g]Using $f_s/f_d = 0.259 \pm 0.038$ from PDG 2006.
[h]Measurement of $\mathcal{B}(B_s^0 \to D_s^-\pi^+\pi^+\pi^-)/\mathcal{B}(B^0 \to D^-\pi^+\pi^+\pi^-)$ used in our fit.
[i]Measurement of $\mathcal{B}(B^0 \to D_1(2420)^-\pi^+) \times \mathcal{B}(D_1(2420)^+ \to D^+\pi^+\pi^-)/\mathcal{B}(B^0 \to D^-\pi^+\pi^+\pi^-)$ used in our fit.
[j]Measurement of $\mathcal{B}(B^0 \to D^-K^+\pi^+\pi^-)/\mathcal{B}(B^0 \to D^-\pi^+\pi^+\pi^-)$ used in our fit.
[k]Measurement of $\mathcal{B}(B^0 \to D^*(2010)^-K^+)/\mathcal{B}(B^0 \to D^*(2010)^-\pi^+)$ used in our fit.
[l]Measurement of $\mathcal{B}(B^0 \to D^*(2010)^-\pi^+\pi^+\pi^-)/\mathcal{B}(B^0 \to D^*(2010)^-\pi^+)$ used in our fit.
[m]Using $\mathcal{B}(B^0 \to D^*(2010)^-\pi^+)$.
[n]Measurement of $\mathcal{B}(B^0 \to D^*(2010)^-K^+\pi^+\pi^-)/\mathcal{B}(B^0 \to D^*(2010)^-\pi^+\pi^+\pi^-)$ used in our fit.
[o]Measurement of $\mathcal{B}(B^0 \to \bar{D}_1(2420)^0\pi^+\pi^-) \times \mathcal{B}(D_1(2420)^0 \to D^*(2010)^+\pi^-)/\mathcal{B}(B^0 \to D^*(2010)^-\pi^+\pi^+\pi^-)$ used in our fit.

TABLE 99. Branching fractions for decays to a $D^{(*)}$ meson and one or more pions, II.

Parameter [10^{-4}]	Measurements		Average HFLAV PDG
$\mathcal{B}(B^0 \to \bar{D}^0\pi^0)$	*BABAR* [657]	$2.69 \pm 0.09 \pm 0.13$	2.62 ± 0.15
	Belle [658]	$2.25 \pm 0.14 \pm 0.35$	2.63 ± 0.14
$\mathcal{B}(B^0 \to \bar{D}^*(2007)^0\pi^0)$	*BABAR* [657]	$3.05 \pm 0.14 \pm 0.28$	2.23 ± 0.22
	Belle [658]	$1.39 \pm 0.18 \pm 0.26$	p = 0.2‰
			2.23 ± 0.57
$\mathcal{B}(B^0 \to \bar{D}^0\pi^+\pi^-)$	LHCb [659]	$8.46 \pm 0.14 \pm 0.49$[a]	
	Belle [650]	$8.4 \pm 0.4 \pm 0.8$	8.45 ± 0.39
	LHCb [660][b,c], [661][d,e,f], [662][g,h]		8.80 ± 0.46
$\mathcal{B}(B^0 \to \bar{D}^*(2007)^0\pi^+\pi^-)$	Belle [663]	$6.2 \pm 1.2 \pm 1.8$	6.2 ± 2.2

[a]In phase space region $M(\bar{D}^0\pi^+) > 2.1$ GeV/c^2.
[b]Measurement of $\mathcal{B}(B_s^0 \to \bar{D}^0K^-\pi^+)/\mathcal{B}(B^0 \to \bar{D}^0\pi^+\pi^-)$ used in our fit.
[c]Measurement of $\mathcal{B}(B^0 \to \bar{D}^0K^+\pi^-)/\mathcal{B}(B^0 \to \bar{D}^0\pi^+\pi^-)$ used in our fit.
[d]Measurement of $\mathcal{B}(B_s^0 \to \bar{D}^0\phi(1020))/\mathcal{B}(B^0 \to \bar{D}^0\pi^+\pi^-)$ used in our fit.
[e]Measurement of $\mathcal{B}(B_s^0 \to \bar{D}^*(2007)^0\phi(1020))/\mathcal{B}(B^0 \to \bar{D}^0\pi^+\pi^-)$ used in our fit.
[f]Measurement of $\mathcal{B}(B^0 \to \bar{D}^0\phi(1020))/\mathcal{B}(B^0 \to \bar{D}^0\pi^+\pi^-)$ used in our fit.
[g]Measurement of $\mathcal{B}(B^0 \to \bar{D}^0K^+K^-)/\mathcal{B}(B^0 \to \bar{D}^0\pi^+\pi^-)$ used in our fit.
[h]Measurement of $\mathcal{B}(B_s^0 \to \bar{D}^0K^+K^-)/\mathcal{B}(B^0 \to \bar{D}^0\pi^+\pi^-)$ used in our fit.

TABLE 100. Branching fractions for decays to a $D^{(*)0}$ meson and a light meson.

Parameter [10^{-4}]	Measurements		Average HFLAV PDG
$\mathcal{B}(B^0 \to \bar{D}^0\rho^0(770))$	Belle [650]	$3.19 \pm 0.20 \pm 0.45$	
	Belle [663]	$4.1 \pm 2.0 \pm 0.2$[a]	3.07 ± 0.46
	LHCb [664][b]		3.21 ± 0.21
$\mathcal{B}(B^0 \to \bar{D}^*(2007)^0\rho^0(770))$	Belle [663]	<5.1	<5.1
$\mathcal{B}(B^0 \to \bar{D}^0\eta)$	*BABAR* [657]	$2.53 \pm 0.09 \pm 0.11$	2.36 ± 0.13
	Belle [658]	$1.77 \pm 0.16 \pm 0.21$	2.36 ± 0.32
$\mathcal{B}(B^0 \to \bar{D}^*(2007)^0\eta)$	*BABAR* [657]	$2.69 \pm 0.14 \pm 0.23$	2.26 ± 0.22
	Belle [658]	$1.4 \pm 0.3 \pm 0.3$	p = 5.8‰
			2.26 ± 0.61
$\mathcal{B}(B^0 \to \bar{D}^0\eta')$	*BABAR* [657]	$1.48 \pm 0.13 \pm 0.07$	1.38 ± 0.12
	Belle [665]	$1.14 \pm 0.20^{+0.10}_{-0.13}$	1.38 ± 0.16
$\mathcal{B}(B^0 \to \bar{D}^*(2007)^0\eta')$	*BABAR* [657]	$1.48 \pm 0.22 \pm 0.13$	1.40 ± 0.22
	Belle [665]	$1.21 \pm 0.34 \pm 0.22$	
$\mathcal{B}(B^0 \to \bar{D}^0\omega(782))$	*BABAR* [657]	$2.57 \pm 0.11 \pm 0.14$	
	Belle [658]	$2.37 \pm 0.23 \pm 0.28$	
	LHCb [659]	$2.81 \pm 0.72 \pm 0.18$	2.54 ± 0.16
	Belle [663][c]		
$\mathcal{B}(B^0 \to \bar{D}^*(2007)^0\omega(782))$	*BABAR* [657]	$4.55 \pm 0.24 \pm 0.39$	3.64 ± 0.35
	Belle [658]	$2.29 \pm 0.39 \pm 0.40$	p = 1.8‰
			3.64 ± 1.11
$\mathcal{B}(B^0 \to \bar{D}^0f_2(1270))$	LHCb [659]	$1.61 \pm 0.11 \pm 0.17$	1.54 ± 0.18
	Belle [650]	$1.2 \pm 0.2 \pm 0.4$	1.56 ± 0.21

[a]Using $\mathcal{B}(B^0 \to \bar{D}^0\omega(782))$.
[b]Measurement of $\mathcal{B}(B_s^0 \to \bar{D}^0\bar{K}^*(892)^0)/\mathcal{B}(B^0 \to \bar{D}^0\rho^0(770))$ used in our fit.
[c]Measurement of $\mathcal{B}(B^0 \to \bar{D}^0\rho^0(770))/\mathcal{B}(B^0 \to \bar{D}^0\omega(782))$ used in our fit.

TABLE 101. Branching fractions for decays to a $D^{(*)+}$ meson and one or more kaons.

Parameter [10^{-4}]	Measurements		Average HFLAV PDG
$\mathcal{B}(B^0 \to D^- K^+)$	LHCb [648]	$2.108 \pm 0.028^{+0.127}_{-0.124}$ [a]	2.10 ± 0.13
	Belle [643]	$1.74 \pm 0.38 \pm 0.20$ [a]	1.86 ± 0.20
$\mathcal{B}(B^0 \to D^*(2010)^- K^+)$	*BABAR* [651]	$2.040 \pm 0.089 \pm 0.109$ [b]	2.03 ± 0.14
	Belle [643]	$1.95 \pm 0.39 \pm 0.17$ [b]	$2.12^{+0.16}_{-0.15}$
$\mathcal{B}(B^0 \to D^- K^*(892)^+)$	*BABAR* [666]	$4.6 \pm 0.6 \pm 0.5$	4.60 ± 0.78
			4.46 ± 0.72
$\mathcal{B}(B^0 \to D^*(2010)^- K^*(892)^+)$	*BABAR* [666]	$3.2 \pm 0.6 \pm 0.3$	3.20 ± 0.67
			3.30 ± 0.61
$\mathcal{B}(B^0 \to D^- K^0 \pi^+)$	*BABAR* [666]	$4.9 \pm 0.7 \pm 0.5$	4.90 ± 0.86
$\mathcal{B}(B^0 \to D^*(2010)^- K^0 \pi^+)$	*BABAR* [666]	$3.0 \pm 0.7 \pm 0.3$	3.00 ± 0.76
$\mathcal{B}(B^0 \to D^- K^+ \bar{K}^0)$	Belle [667]	<3.1	<3.1
$\mathcal{B}(B^0 \to D^*(2010)^- K^+ \bar{K}^0)$	Belle [667]	<4.7	<4.7
$\mathcal{B}(B^0 \to D^- \bar{K}^*(892)^0 K^+)$	Belle [667]	$8.8 \pm 1.1 \pm 1.5$	8.8 ± 1.9
$\mathcal{B}(B^0 \to D^*(2010)^- \bar{K}^*(892)^0 K^+)$	Belle [667]	$12.9 \pm 2.2 \pm 2.5$	12.9 ± 3.3
$\mathcal{B}(B^0 \to D^- K^+ \pi^+ \pi^-)$	LHCb [649]	$3.51 \pm 0.65^{+0.49}_{-0.47}$ [c]	$3.51^{+0.85}_{-0.78}$
			3.55 ± 0.83
$\mathcal{B}(B^0 \to D^*(2010)^- K^+ \pi^+ \pi^-)$	LHCb [652]	$4.583 \pm 0.262 \pm 0.299$ [d]	4.58 ± 0.40
			4.66 ± 0.41

[a]Using $\mathcal{B}(B^0 \to D^- \pi^+)$.
[b]Using $\mathcal{B}(B^0 \to D^*(2010)^- \pi^+)$.
[c]Using $\mathcal{B}(B^0 \to D^- \pi^+ \pi^+ \pi^-)$.
[d]Using $\mathcal{B}(B^0 \to D^*(2010)^- \pi^+ \pi^+ \pi^-)$.

TABLE 102. Branching fractions for decays to a $D^{(*)0}$ meson and one or more kaons or a ϕ.

Parameter [10^{-5}]	Measurements		Average HFLAV PDG
$\mathcal{B}(B^0 \to \bar{D}^0 K^0)$	*BABAR* [668]	$5.3 \pm 0.7 \pm 0.3$	5.23 ± 0.67
	Belle [669]	$5.0^{+1.3}_{-1.2} \pm 0.6$	$5.23^{+0.67}_{-0.66}$
$\mathcal{B}(B^0 \to \bar{D}^*(2007)^0 K^0)$	*BABAR* [668]	$3.6 \pm 1.2 \pm 0.3$	3.6 ± 1.2
	Belle [669]	<6.6	
$\mathcal{B}(B^0 \to \bar{D}^0 K^+ \pi^-)$	LHCb [660]	$8.95 \pm 0.59 \pm 0.79$ [a]	8.92 ± 0.86
	BABAR [651]	$8.8 \pm 1.5 \pm 0.9$ [b]	8.80 ± 1.75
$\mathcal{B}(B^0 \to \bar{D}^0 K^*(892)^0)$	*BABAR* [651]	$3.8 \pm 0.6 \pm 0.4$ [c]	4.32 ± 0.42
	BABAR [668]	$4.0 \pm 0.7 \pm 0.3$	
	Belle [669]	$4.8^{+1.1}_{-1.0} \pm 0.5$	none
	LHCb [670] [d]		
$\mathcal{B}(B^0 \to \bar{D}^*(2007)^0 K^*(892)^0)$	Belle [669]	<6.9	<6.9
$\mathcal{B}(B^0 \to D^*(2007)^0 K^*(892)^0)$	Belle [669]	<4.0	<4.0
$\mathcal{B}(B^0 \to D^0 K^+ \pi^-)$	*BABAR* [651]	<1.9	<1.9
			0.5 ± 0.3
$\mathcal{B}(B^0 \to D^0 K^*(892)^0)$	Belle [669]	<1.8	0.00 ± 0.58
	BABAR [668]	$0.0 \pm 0.5 \pm 0.3$	$0.22^{+0.09}_{-0.10}$
$\mathcal{B}(B^0 \to \bar{D}^0 K^+ K^-)$	LHCb [662]	$5.83 \pm 0.34 \pm 0.37$ [a]	5.92 ± 0.39
	LHCb [662]	$6.1 \pm 0.4 \pm 0.4$	5.93 ± 0.52

(Table continued)

TABLE 102. *(Continued)*

Parameter [10^{-5}]	Measurements		Average HFLAV PDG
$\mathcal{B}(B^0 \to \bar{D}^0\phi(1020))$	LHCb [661]	$0.101 \pm 0.059 \pm 0.026$[a]	0.101 ± 0.064
	LHCb [661]	<0.20	<0.230

[a]Using $\mathcal{B}(B^0 \to \bar{D}^0\pi^+\pi^-)$.
[b]Excluding $D^*(2010)^+K^-$.
[c]Using $\mathcal{B}(K^*(892)^0 \to K^+\pi^-)$.
[d]Measurement of $\mathcal{B}(B_s^0 \to \bar{D}^0\bar{K}^*(892)^0)/\mathcal{B}(B^0 \to \bar{D}^0K^*(892)^0)$ used in our fit.

TABLE 103. Branching fractions for decays to a $D_s^{(*)}$ meson.

Parameter [10^{-4}]	Measurements		Average HFLAV PDG
$\mathcal{B}(B^0 \to D_s^+\pi^-)$	Belle [671]	$0.199 \pm 0.026 \pm 0.018$	0.216 ± 0.026
	BABAR [672]	$0.25 \pm 0.04 \pm 0.02$	
$\mathcal{B}(B^0 \to D_s^{*+}\pi^-)$	Belle [673]	$0.175 \pm 0.034 \pm 0.020$	0.212 ± 0.030
	BABAR [672]	$0.26^{+0.05}_{-0.04} \pm 0.02$	$0.212^{+0.045}_{-0.042}$
$\mathcal{B}(B^0 \to D_s^+\rho^-(770))$	*BABAR* [672]	$0.11^{+0.09}_{-0.08} \pm 0.03$	$0.110^{+0.095}_{-0.085}$
			<0.240
$\mathcal{B}(B^0 \to D_s^{*+}\rho^-(770))$	*BABAR* [672]	$0.41^{+0.13}_{-0.12} \pm 0.04$	0.41 ± 0.13
			$0.41^{+0.14}_{-0.13}$
$\mathcal{B}(B^0 \to D_s^+a_0(980)^-)$	*BABAR* [674]	$0.06^{+0.14}_{-0.11} \pm 0.01$[a]	$0.06^{+0.14}_{-0.11}$
			<0.19
$\mathcal{B}(B^0 \to D_s^{*+}a_0(980)^-)$	*BABAR* [674]	$0.14^{+0.21}_{-0.16} \pm 0.03$[a]	$0.14^{+0.21}_{-0.16}$
			<0.36
$\mathcal{B}(B^0 \to D_s^+a_2(1320)^-)$	*BABAR* [674]	$0.64^{+1.04}_{-0.57} \pm 0.15$[a]	$0.6^{+1.0}_{-0.6}$
			<1.9
$\mathcal{B}(B^0 \to D_s^{*+}a_2(1320)^-)$	*BABAR* [674]	<2.00	<2.0
$\mathcal{B}(B^0 \to D_s^-\pi^+)$	LHCb [675][b]		$17.1^{+2.4}_{-2.2}$
			none
$\mathcal{B}(B^0 \to D_s^-K^+)$	LHCb [675]	$0.221 \pm 0.009^{+0.034}_{-0.031}$[c]	
	Belle [671]	$0.191 \pm 0.024 \pm 0.017$	0.221 ± 0.024
	BABAR [672]	$0.29 \pm 0.04 \pm 0.02$	0.275 ± 0.049
$\mathcal{B}(B^0 \to D_s^{*-}K^+)$	Belle [673]	$0.202 \pm 0.033 \pm 0.022$	0.219 ± 0.030
	BABAR [672]	$0.24 \pm 0.04 \pm 0.02$	
$\mathcal{B}(B^0 \to D_s^-K^*(892)^+)$	*BABAR* [672]	$0.35^{+0.10}_{-0.09} \pm 0.04$	0.35 ± 0.10
			$0.35^{+0.11}_{-0.10}$
$\mathcal{B}(B^0 \to D_s^{*-}K^*(892)^+)$	*BABAR* [672]	$0.32^{+0.14}_{-0.12} \pm 0.04$	$0.32^{+0.15}_{-0.13}$
$\mathcal{B}(B^0 \to D_s^-K_S^0\pi^+)$	*BABAR* [676]	$0.55 \pm 0.13 \pm 0.10$	0.55 ± 0.17
			0.97 ± 0.14
$\mathcal{B}(B^0 \to D_s^{*-}K^0\pi^+)$	*BABAR* [676]	<0.55	<0.55
			<1.10
$\mathcal{B}(B^0 \to D_s^-K^+\pi^+\pi^-)$	LHCb [677]	$1.67 \pm 0.22^{+0.42}_{-0.38}$[d]	$1.66^{+0.50}_{-0.41}$
			1.73 ± 0.47

[a]Using *BABAR* result for $\mathcal{B}(D_s^+ \to \phi\pi^+)$ [678].
[b]Measurement of $\mathcal{B}(B^0 \to D_s^-K^+)/\mathcal{B}(B^0 \to D_s^-\pi^+)$ used in our fit.
[c]Using $\mathcal{B}(B^0 \to D_s^-\pi^+)$.
[d]Using $\mathcal{B}(B_s^0 \to D_s^-K^+\pi^+\pi^-)$.

TABLE 104. Branching fractions for decays to excited D mesons.

Parameter [10^{-3}]	Measurements		Average HFLAV PDG
$\mathcal{B}(B^0 \to D^{**-}\pi^+)$[a]	*BABAR* [642]	$2.34 \pm 0.65 \pm 0.88$	2.3 ± 1.1 1.9 ± 0.9

[a]D^{**} refers to the sum of all the nonstrange charm meson states with masses in the range 2.2–2.8 GeV/c^2.

TABLE 105. Branching fractions for decays to excited $D_{(s)}$ mesons.

Parameter [10^{-5}]	Measurements		Average HFLAV PDG
$\mathcal{B}(B^0 \to \bar{D}_1(2420)^0\pi^+\pi^-) \times \mathcal{B}(D_1(2420)^0 \to D^*(2010)^+\pi^-)$			
	LHCb [652]	$14.45 \pm 2.97 \pm 1.65$[a]	14.4 ± 3.4 14.7 ± 3.5
$\mathcal{B}(B^0 \to D_1(2420)^-\pi^+) \times \mathcal{B}(D_1(2420)^+ \to D^+\pi^+\pi^-)$			
	Belle [679]	$8.9 \pm 1.5^{+1.7}_{-3.1}$	$9.8^{+1.9}_{-2.3}$
	LHCb [647]	$12.5 \pm 3.0^{+2.3}_{-3.3}$[b]	$9.9^{+2.0}_{-2.5}$
$\mathcal{B}(B^0 \to \bar{D}_1(2430)^0\omega(782)) \times \mathcal{B}(D_1(2430)^0 \to D^*(2010)^+\pi^-)$			
	BABAR [656]	$41 \pm 12 \pm 11$	41 ± 16 27^{+8}_{-4}
$\mathcal{B}(B^0 \to D_0^*(2300)^-\pi^+) \times \mathcal{B}(D_0^*(2300)^+ \to \bar{D}^0\pi^+)$			
	Belle [650]	$6 \pm 1 \pm 3$	6.0 ± 3.0 none
$\mathcal{B}(B^0 \to D_2^*(2460)^-\pi^+) \times \mathcal{B}(D_2^*(2460)^+ \to \bar{D}^0\pi^+)$			
	Belle [650]	$21.5 \pm 1.7 \pm 3.1$	21.5 ± 3.6 23.8 ± 1.6
$\mathcal{B}(B^0 \to D_1(2420)^-\pi^+) \times \mathcal{B}(D_1(2420)^+ \to D^*(2010)^+\pi^+\pi^-)$			
	Belle [679]	<3.3	<3.3
$\mathcal{B}(B^0 \to D_2^*(2460)^-\pi^+) \times \mathcal{B}(D_2^*(2460)^+ \to D^*(2010)^+\pi^+\pi^-)$			
	Belle [679]	<2.4	<2.4
$\mathcal{B}(B^0 \to D_2^*(2460)^-K^+) \times \mathcal{B}(D_2^*(2460)^+ \to D^0\pi^+)$			
	BABAR [651]	$1.83 \pm 0.40 \pm 0.31$	1.83 ± 0.51 none
$\mathcal{B}(B^0 \to D_{s1}(2460)^-\pi^+)$	Belle [680]	<2.2[c]	<2.2 none
$\mathcal{B}(B^0 \to D_{s1}(2460)^-K^+)$	Belle [680]	<5.12[c]	<5.1 none
$\mathcal{B}(B^0 \to D_{s0}^*(2317)^-\pi^+)$	Belle [680]	<2.5[d]	<2.5 <0.4
$\mathcal{B}(B^0 \to D_{s0}^*(2317)^-K^+)$	Belle [680]	$5.3^{+1.5\ +1.6}_{-1.3\ -1.9}$[d]	$5.3^{+2.3}_{-2.0}$ none

[a]Using $\mathcal{B}(B^0 \to D^*(2010)^-\pi^+\pi^+\pi^-)$.
[b]Using $\mathcal{B}(B^0 \to D^-\pi^+\pi^+\pi^-)$.
[c]Using $\mathcal{B}(D_{s1}(2460)^+ \to D_s^+\gamma)$.
[d]Using $\mathcal{B}(D_{s0}^*(2317)^+ \to D_s^+\pi^0)$.

TABLE 106. Branching fractions for decays to baryons.

Parameter [10^{-4}]	Measurements		Average HFLAV PDG
$\mathcal{B}(B^0 \to D^- p\bar{p}\pi^+)$	*BABAR* [681]	$3.32 \pm 0.10 \pm 0.29$	3.32 ± 0.31
$\mathcal{B}(B^0 \to D^*(2010)^- p\bar{p}\pi^+)$	*BABAR* [681]	$4.55 \pm 0.16 \pm 0.39$	4.55 ± 0.42 4.68 ± 0.49
$\mathcal{B}(B^0 \to \bar{D}^0 p\bar{p}\pi^+\pi^-)$	*BABAR* [681]	$2.99 \pm 0.21 \pm 0.45$	2.99 ± 0.50
$\mathcal{B}(B^0 \to \bar{D}^*(2007)^0 p\bar{p}\pi^+\pi^-)$	*BABAR* [681]	$1.91 \pm 0.36 \pm 0.29$	1.91 ± 0.46
$\mathcal{B}(B^0 \to \bar{D}^0 p\bar{p})$	*BABAR* [681] Belle [682]	$1.02 \pm 0.04 \pm 0.06$ $1.18 \pm 0.15 \pm 0.16$	1.036 ± 0.069
$\mathcal{B}(B^0 \to \bar{D}^*(2007)^0 p\bar{p})$	*BABAR* [681] Belle [682]	$0.97 \pm 0.07 \pm 0.09$ $1.2 \pm 0.3 \pm 0.2$	0.99 ± 0.11
$\mathcal{B}(B^0 \to D_s^- \bar{\Lambda}^0 p)$	Belle [683]	$0.29 \pm 0.07 \pm 0.06$	$0.298^{+0.092}_{-0.093}$ 0.284 ± 0.088
$\mathcal{B}(B^0 \to \bar{D}^0 \Lambda^0 \bar{\Lambda}^0)$	*BABAR* [684] Belle [685]	$0.098^{+0.029}_{-0.026} \pm 0.019$ $0.105^{+0.057}_{-0.044} \pm 0.014$	0.100 ± 0.028 $0.100^{+0.030}_{-0.026}$
$\mathcal{B}(B^0 \to \bar{D}^0 \bar{\Sigma}^0 \Lambda^0 + \text{c.c.})$	*BABAR* [684]	$0.150^{+0.090}_{-0.080} \pm 0.030$	$0.150^{+0.095}_{-0.085}$ <0.310
$\mathcal{B}(B^0 \to D^- \bar{\Lambda}^0 p)$	Belle [686]	$0.336 \pm 0.063 \pm 0.044$	0.336 ± 0.077 0.251 ± 0.044
$\mathcal{B}(B^0 \to D^*(2010)^- \bar{\Lambda}^0 p)$	Belle [686]	$0.251 \pm 0.026 \pm 0.035$	0.251 ± 0.044 0.336 ± 0.077

2. Decays to two open charm mesons

Averages of B^0 decays to two open charm mesons are shown in Tables 107–111.

TABLE 107. Branching fractions for decays to $D^{(*)}\bar{D}^{(*)}$.

Parameter [10^{-4}]	Measurements		Average HFLAV PDG
$\mathcal{B}(B^0 \to D^+ D^-)$	Belle [278] *BABAR* [687] LHCb [688][a]	$2.12 \pm 0.16 \pm 0.18$ $2.8 \pm 0.4 \pm 0.5$	2.20 ± 0.23 2.11 ± 0.18
$\mathcal{B}(B^0 \to D^*(2010)^+ D^-)$	Belle [278] *BABAR* [687]	$6.14 \pm 0.29 \pm 0.50$ $5.7 \pm 0.7 \pm 0.7$[b]	6.03 ± 0.50 6.14 ± 0.58
$\mathcal{B}(B^0 \to D^*(2010)^+ D^*(2010)^-)$	Belle [351] *BABAR* [687]	$7.82 \pm 0.38 \pm 0.60$ $8.1 \pm 0.6 \pm 1.0$	7.90 ± 0.61 none
$\mathcal{B}(B^0 \to D^0 \bar{D}^0)$	LHCb [688] Belle [689] *BABAR* [687]	$0.134 \pm 0.057^{+0.024}_{-0.023}$[c] <0.43 <0.6	$0.134^{+0.064}_{-0.061}$ 0.140 ± 0.067
$\mathcal{B}(B^0 \to D^*(2007)^0 \bar{D}^0)$	*BABAR* [687]	<2.9	<2.9
$\mathcal{B}(B^0 \to D^*(2007)^0 \bar{D}^*(2007)^0)$	*BABAR* [687]	<0.9	<0.90

[a]Measurement of $\mathcal{B}(B_s^0 \to D^+ D^-)/\mathcal{B}(B^0 \to D^+ D^-)$ used in our fit.
[b]Including the charge-conjugate final state.
[c]Using $\mathcal{B}(B^+ \to D_s^+ \bar{D}^0)$.

TABLE 108. Branching fractions for decays to two D mesons and a kaon.

Parameter [10^{-3}]	Measurements		Average HFLAV PDG
$\mathcal{B}(B^0 \to D^*(2010)^- D^+ K^0)$	*BABAR* [690]	$6.41 \pm 0.36 \pm 0.39$	6.41 ± 0.53
$\mathcal{B}(B^0 \to D^*(2010)^+ D^*(2010)^- K^0)$	*BABAR* [690] *BABAR* [256][a,b] Belle [257][a]	$8.26 \pm 0.43 \pm 0.67$	8.33 ± 0.64 8.11 ± 0.65
$\mathcal{B}(B^0 \to D^*(2010)^- D^0 K^+)$	*BABAR* [690]	$2.47 \pm 0.10 \pm 0.18$	2.47 ± 0.21
$\mathcal{B}(B^0 \to D^*(2007)^0 D^- K^+)$	*BABAR* [690]	$3.46 \pm 0.18 \pm 0.37$	3.46 ± 0.41
$\mathcal{B}(B^0 \to D_s^- D^*(2007)^0 K^+)$	*BABAR* [690]	$10.6 \pm 0.3 \pm 0.9$	10.60 ± 0.92 none
$\mathcal{B}(B^0 \to D^*(2007)^0 \bar{D}^0 K^0)$	*BABAR* [690]	$1.08 \pm 0.32 \pm 0.36$	1.08 ± 0.48
$\mathcal{B}(B^0 \to D^*(2007)^0 \bar{D}^*(2007)^0 K^0)$	*BABAR* [690]	$2.4 \pm 0.6 \pm 0.7$	2.40 ± 0.87
$\mathcal{B}(B^0 \to D^+ D^- K^0)$	*BABAR* [690]	$0.75 \pm 0.12 \pm 0.12$	0.75 ± 0.17
$\mathcal{B}(B^0 \to D^- D^0 K^+)$	*BABAR* [690]	$1.07 \pm 0.07 \pm 0.09$	1.07 ± 0.11
$\mathcal{B}(B^0 \to D^0 \bar{D}^0 K^0)$	*BABAR* [690]	$0.27 \pm 0.10 \pm 0.05$	0.27 ± 0.11
$\mathcal{B}(B^0 \to D^0 \bar{D}^0 K^0 \pi^0)$	Belle [691]	$0.173 \pm 0.070^{+0.031}_{-0.053}$	$0.173^{+0.077}_{-0.088}$ none

[a]Measurement of $\mathcal{B}(B^0 \to D^*(2010)^+ D^*(2010)^- K^0)/2$ used in our fit.
[b]Measurement of $\mathcal{B}(B^0 \to D_{s1}(2536)^+ D^*(2010)^-)/\mathcal{B}(B^0 \to D^*(2010)^+ D^*(2010)^- K^0)2$ used in our fit.

TABLE 109. Branching fractions for decays to $D_s^{(*)-} D^{(*)+}$.

Parameter [10^{-3}]	Measurements		Average HFLAV PDG
$\mathcal{B}(B^0 \to D_s^+ D^-)$	Belle [692]	$7.5 \pm 0.2 \pm 1.1$	7.82 ± 0.72 7.24 ± 0.77
	BABAR [693]	$6.00 \pm 1.37^{+1.15}_{-1.14}$[a]	
	BABAR [693]	$9 \pm 2 \pm 1$	
	LHCb [688][b,c,d], [694][e,f]		
$\mathcal{B}(B^0 \to D_s^+ D^*(2010)^-)$	*BABAR* [695]	$10.3 \pm 1.4 \pm 2.9$	8.1 ± 1.4 8.0 ± 1.1
	BABAR [693]	$5.7 \pm 1.6 \pm 0.9$	
	BABAR [693]	$11.47 \pm 2.11^{+1.83}_{-1.82}$[a]	
$\mathcal{B}(B^0 \to D_s^{*+} D^*(2010)^-)$	*BABAR* [678]	$18.8 \pm 0.9 \pm 1.7$	18.7 ± 1.5 17.7 ± 1.4
	BABAR [695]	$19.7 \pm 1.5 \pm 5.7$	
	BABAR [693]	$16.5 \pm 2.3 \pm 1.9$	
	BABAR [693]	$27.4 \pm 4.9 \pm 5.3$[a]	
$\mathcal{B}(B^0 \to D_s^{*+} D^-)$	*BABAR* [693]	$6.7 \pm 2.0 \pm 1.1$	7.5 ± 1.9 7.4 ± 1.6
	BABAR [693]	$9.30 \pm 2.67 \pm 2.22$[a]	

[a]Using $\mathcal{B}(D_s^+ \to \phi(1020)\pi^+)$.
[b]Measurement of $\mathcal{B}(B_s^0 \to D_s^- D^+)/\mathcal{B}(B^0 \to D_s^+ D^-)$ used in our fit.
[c]Measurement of $\mathcal{B}(B_s^0 \to D_s^+ D_s^-)/\mathcal{B}(B^0 \to D_s^+ D^-)$ used in our fit.
[d]Measurement of $\mathcal{B}(B^+ \to D_s^+ \bar{D}^0)/\mathcal{B}(B^0 \to D_s^+ D^-)$ used in our fit.
[e]At CL = 95%.
[f]Measurement of $\mathcal{B}(B^0 \to \Lambda_c^+ \bar{\Lambda}_c^-)/\mathcal{B}(B^0 \to D_s^+ D^-)$ used in our fit.

TABLE 110. Branching fractions for decays to $D_s^{(*)+}D_s^{(*)-}$.

Parameter [10^{-4}]	Measurements		Average HFLAV PDG
$\mathcal{B}(B^0 \to D_s^+ D_s^-)$	Belle [692]	<0.36	<0.36
	BABAR [696]	<1.0	
$\mathcal{B}(B^0 \to D_s^{*-} D_s^+)$	*BABAR* [696]	<1.3	<1.3
$\mathcal{B}(B^0 \to D_s^{*+} D_s^{*-})$	*BABAR* [696]	<2.4	<2.4

TABLE 111. Branching fractions for decays to excited D_s mesons.

Parameter [10^{-3}]	Measurements		Average HFLAV PDG
$\mathcal{B}(B^0 \to D_{s0}^*(2317)^+ D^-)$	Belle [697]	$1.02^{+0.13\ +0.11}_{-0.12\ -0.23}$ [a]	$1.07^{+0.30}_{-0.16}$
	BABAR [698]	$1.8 \pm 0.4^{+0.7}_{-0.6}$ [a]	<0.95
$\mathcal{B}(B^0 \to D_{s0}^*(2317)^+ D^*(2010)^-)$	*BABAR* [698]	$1.5 \pm 0.4 \pm 0.5$ [a]	$1.50^{+0.70}_{-0.54}$
			$1.50^{+0.64}_{-0.57}$
$\mathcal{B}(B^0 \to D_{s1}(2460)^+ D^-)$	*BABAR* [698]	$4.4 \pm 1.1^{+1.8}_{-1.4}$ [b]	
	Belle [699]	$4.47^{+1.20}_{-1.04} \pm 1.53$ [b]	
	Belle [699]	$4.25^{+1.37}_{-1.16} \pm 1.43$ [c]	4.07 ± 0.86
	BABAR [698]	$5.2 \pm 1.5^{+2.2}_{-1.7}$ [c]	$3.55^{+1.14}_{-1.07}$
	BABAR [693]	$2.6 \pm 1.5 \pm 0.7$	
	Belle [699]	<2.2 [d]	
$\mathcal{B}(B^0 \to D_{s1}(2460)^+ D^*(2010)^-)$	*BABAR* [698]	$12.5 \pm 1.6^{+5.0}_{-3.7}$ [b]	
	BABAR [693]	$8.8 \pm 2.0 \pm 1.4$	10.0 ± 1.8
	BABAR [698]	$10.3 \pm 2.2^{+4.3}_{-3.3}$ [c]	$9.3^{+2.3}_{-2.2}$
$\mathcal{B}(B^0 \to D_{s1}(2536)^+ D^-)$	*BABAR* [700]	$0.358 \pm 0.101 \pm 0.083$ [e]	0.39 ± 0.11
	BABAR [700]	$0.464 \pm 0.183 \pm 0.077$ [f]	0.28 ± 0.07
$\mathcal{B}(B^0 \to D_{s1}(2536)^+ D^*(2010)^-)$	*BABAR* [700]	$0.696 \pm 0.184 \pm 0.167$ [e]	
	BABAR [256]	$0.766 \pm 0.200 \pm 0.059$ [g]	0.473 ± 0.094
	BABAR [700]	$0.89 \pm 0.27 \pm 0.16$ [f]	none
$\mathcal{B}(B^0 \to D_{s1}(2536)^- D^+)$	Belle [701] [h]		0.264 ± 0.073
			none
$\mathcal{B}(B^0 \to D_{s1}(2536)^- D^*(2010)^+)$	Belle [701] [i], [257] [j]		0.48 ± 0.14
			0.50 ± 0.14

[a] Using $\mathcal{B}(D_{s0}^*(2317)^+ \to D_s^+ \pi^0)$.
[b] Using $\mathcal{B}(D_{s1}(2460)^+ \to D_s^+ \gamma)$.
[c] Using $\mathcal{B}(D_{s1}(2460)^+ \to D_s^{*+} \pi^0)$.
[d] Using $\mathcal{B}(D_{s1}(2460)^+ \to D_s^+ \pi^+ \pi^-)$.
[e] Using $\mathcal{B}(D_{s1}(2536)^+ \to D^*(2007)^0 K^+)$.
[f] Using $\mathcal{B}(D_{s1}(2536)^+ \to D^*(2010)^+ K^0)$.
[g] Using $\mathcal{B}(B^0 \to D^*(2010)^+ D^*(2010)^- K^0)$.
[h] Measurement of $\mathcal{B}(B^0 \to D_{s1}(2536)^- D^+)(\mathcal{B}(D_{s1}(2536)^+ \to D^*(2007)^0 K^+) + \mathcal{B}(D_{s1}(2536)^+ \to D^*(2010)^+ K^0))$ used in our fit.
[i] Measurement of $\mathcal{B}(B^0 \to D_{s1}(2536)^- D^*(2010)^+)(\mathcal{B}(D_{s1}(2536)^+ \to D^*(2007)^0 K^+) + \mathcal{B}(D_{s1}(2536)^+ \to D^*(2010)^+ K^0))$ used in our fit.
[j] Measurement of $\mathcal{B}(B^0 \to D_{s1}(2536)^- D^*(2010)^+) BR_D s1(2536) *_D * +_K 0S$ used in our fit.

3. Decays to charmonium states

Averages of B^0 decays to charmonium states are shown in Tables 112–118.

TABLE 112. Branching fractions for decays to J/ψ and one kaon.

Parameter $[10^{-4}]$	Measurements		Average HFLAV PDG
$\mathcal{B}(B^0 \to J/\psi K^0)$	*BABAR* [14]	$8.69 \pm 0.22 \pm 0.30$	$8.64^{+0.29}_{-0.28}$
	Belle [702]	$7.9 \pm 0.4 \pm 0.9$	8.91 ± 0.21
	CDF [703]	$11.5 \pm 2.3 \pm 1.7$	
	BABAR [704][a], [14][b]		
	CDF [705][b]		
	LHCb [706][c], [707][d,e]		
$\mathcal{B}(B^0 \to J/\psi K^+\pi^-)$	Belle [708]	$11.5 \pm 0.1 \pm 0.5$	11.76 ± 0.49
	LHCb [709][f]		11.50 ± 0.51
$\mathcal{B}(B^0 \to J/\psi K^*(892)^0)$	Belle [708]	$11.9 \pm 0.1 \pm 0.8$	12.69 ± 0.45
	BABAR [14]	$13.09 \pm 0.26 \pm 0.77$	12.65 ± 0.46
	BABAR [14]	$13.05 \pm 0.43^{+0.82}_{-0.81}$[g]	
	CDF [710]	$17.4 \pm 2.0 \pm 1.8$	
	CDF [705]	$12.01 \pm 3.11 \pm 0.95$[g]	
	LHCb [711][h]		
$\mathcal{B}(B^0 \to J/\psi K^0\pi^+\pi^-)$	LHCb [707]	$4.261 \pm 0.294^{+0.273}_{-0.272}$[g]	4.32 ± 0.31
	LHCb [707]	$4.30 \pm 0.30 \pm 0.37$	4.46 ± 0.40
	CDF [712]	$10.3 \pm 3.3 \pm 1.5$	
	LHCb [707][i]		
$\mathcal{B}(B^0 \to J/\psi K^0\rho^0(770))$	CDF [712]	$5.4 \pm 2.9 \pm 0.9$	5.4 ± 3.0
$\mathcal{B}(B^0 \to J/\psi K^*(892)^+\pi^-)$	CDF [712]	$7.7 \pm 4.1 \pm 1.3$	7.7 ± 4.3
$\mathcal{B}(B^0 \to J/\psi\omega(782)K^0)$	*BABAR* [713]	$2.3 \pm 0.3 \pm 0.3$	2.28 ± 0.34
	BABAR [713]	$2.3 \pm 0.3^{+0.5}_{-0.4}$[j]	2.30 ± 0.42
$\mathcal{B}(B^0 \to J/\psi\phi(1020)K^0)$	*BABAR* [714]	$1.02 \pm 0.38 \pm 0.10$	1.02 ± 0.39
			0.49 ± 0.10
$\mathcal{B}(B^0 \to J/\psi K_1(1270)^0)$	Belle [715]	$13 \pm 3 \pm 3$[k]	13.1 ± 4.4
			13.0 ± 4.7
$\mathcal{B}(B^0 \to J/\psi\eta K_S^0)$	Belle [716]	$0.522 \pm 0.078 \pm 0.049$	0.540 ± 0.089
	BABAR [717]	$0.84 \pm 0.26 \pm 0.27$	
$\mathcal{B}(B^0 \to J/\psi K^*(892)^0\pi^+\pi^-)$	CDF [712]	$6.6 \pm 1.9 \pm 1.1$	6.6 ± 2.2
	LHCb [707][l]		

[a]Measurement of $\mathcal{B}(B^0 \to \eta_c K^0)/\mathcal{B}(B^0 \to J/\psi K^0)$ used in our fit.
[b]Measurement of $\mathcal{B}(B^0 \to J/\psi K^*(892)^0)/\mathcal{B}(B^0 \to J/\psi K^0)$ used in our fit.
[c]Measurement of $2\mathcal{B}(B_s^0 \to J/\psi K_S^0)/\mathcal{B}(B^0 \to J/\psi K^0)$ used in our fit.
[d]Measurement of $\mathcal{B}(B^0 \to J/\psi K^0\pi^+\pi^-)/\mathcal{B}(B^0 \to J/\psi K^0)$ used in our fit.
[e]Measurement of $\mathcal{B}(B^0 \to \psi(2S)K^0)\mathcal{B}(\psi(2S) \to J/\psi\pi^+\pi^-)/\mathcal{B}(B^0 \to J/\psi K^0)$ used in our fit.
[f]Measurement of $\mathcal{B}(B^0 \to \eta_c K^+\pi^-)/\mathcal{B}(B^0 \to J/\psi K^+\pi^-)$ used in our fit.
[g]Using $\mathcal{B}(B^0 \to J/\psi K^0)$.
[h]Measurement of $\mathcal{B}(B^0 \to \psi(2S)K^*(892)^0)/\mathcal{B}(B^0 \to J/\psi K^*(892)^0)$ used in our fit.
[i]Measurement of $\mathcal{B}(B_s^0 \to J/\psi K^0 K^-\pi^+ + \text{c.c.})/\mathcal{B}(B^0 \to J/\psi K^0\pi^+\pi^-)$ used in our fit.
[j]Using $\mathcal{B}(B^+ \to J/\psi\omega(782)K^+)$.
[k]Using $\mathcal{B}(B^+ \to J/\psi K^+)$.
[l]Measurement of $\mathcal{B}(B^0 \to J/\psi K^*(892)^0 K^+K^-)/\mathcal{B}(B^0 \to J/\psi K^*(892)^0\pi^+\pi^-)$ used in our fit.

TABLE 113. Branching fractions for decays to charmonium other than J/ψ and one kaon.

Parameter $[10^{-4}]$	Measurements		Average HFLAV PDG
$\mathcal{B}(B^0 \to \psi(2S)K^0)$	*BABAR* [14]	$6.46 \pm 0.65 \pm 0.51$	5.68 ± 0.38
	LHCb [707]	$4.7 \pm 0.7 \pm 0.7$	5.85 ± 0.46
	Belle [702]	6.7 ± 1.1	
	Belle [718]	$6.8 \pm 1.0 \pm 0.7$	
	Belle [718]	$4.7 \pm 1.6 \pm 0.8$	
	BABAR [14][a]		
	LHCb [707][b]		
$\mathcal{B}(B^0 \to \psi(2S)K^*(892)^0)$	LHCb [711]	$6.04 \pm 0.18 \pm 0.29$[c]	6.05 ± 0.28
	Belle [719]	$5.52^{+0.35\ +0.53}_{-0.32\ -0.58}$	$5.94^{+0.41}_{-0.45}$
	BABAR [14]	$6.49 \pm 0.59 \pm 0.97$	
	BABAR [14]	$5.7 \pm 0.8 \pm 0.6$[d]	
	CDF [710]	$9.0 \pm 2.2 \pm 0.9$	
	LHCb [720][e]		
$\mathcal{B}(B^0 \to \eta_c K^0)$	*BABAR* [704]	$9.1 \pm 1.4 \pm 0.9$[f]	8.5 ± 1.1
	BABAR [704]	$11.4 \pm 1.5 \pm 3.4$	8.0 ± 1.1
	BABAR [704]	$11.58 \pm 1.64 \pm 3.49$[g]	
	BABAR [721]	$6.4^{+2.2}_{-2.0} \pm 2.8$[h]	
	Belle [722]	$12.3 \pm 2.3^{+4.0}_{-4.1}$	
	Belle [722][i]		
$\mathcal{B}(B^0 \to \eta_c K^*(892)^0)$	*BABAR* [723]	$5.7 \pm 0.6 \pm 0.9$	6.55 ± 0.69
	BABAR [723]	$6.5 \pm 0.6 \pm 0.7$[f]	$5.21^{+0.78}_{-0.87}$
	BABAR [721]	$8 \pm 2 \pm 4$[h]	
	Belle [722]	$11.30 \pm 3.06^{+2.54}_{-3.18}$[j]	
	Belle [722]	$16.2 \pm 3.2^{+5.5}_{-6.0}$	
$\mathcal{B}(B^0 \to \eta_c K^+\pi^-)$	LHCb [709]	$4.20 \pm 0.18 \pm 0.20$[k]	4.31 ± 0.26
	LHCb [709]	$5.73 \pm 0.24 \pm 0.67$	0.62 ± 0.13
$\mathcal{B}(B^0 \to \eta_c(2S)K^*(892)^0)$	*BABAR* [723]	<3.9	<3.9
$\mathcal{B}(B^0 \to h_c K^*(892)^0)$	*BABAR* [723]	<4.3[l]	<4.3
	BABAR [723][m]		<4.0
$\mathcal{B}(B^0 \to \psi(3770)K^0)$	*BABAR* [700]	<2.35[n]	<2.3
	BABAR [700]	<4.64[o]	none

[a]Measurement of $\mathcal{B}(B^0 \to \psi(2S)K^*(892)^0)/\mathcal{B}(B^0 \to \psi(2S)K^0)$ used in our fit.
[b]Measurement of $\mathcal{B}(B^0 \to \psi(2S)K^0)\mathcal{B}(\psi(2S) \to J/\psi\pi^+\pi^-)/\mathcal{B}(B^0 \to J/\psi K^0)$ used in our fit.
[c]Using $\mathcal{B}(B^0 \to J/\psi K^*(892)^0)$.
[d]Using $\mathcal{B}(B^0 \to \psi(2S)K^0)$.
[e]Measurement of $\mathcal{B}(B_s^0 \to \psi(2S)\bar{K}^*(892)^0)/\mathcal{B}(B^0 \to \psi(2S)K^*(892)^0)$ used in our fit.
[f]Using $\mathcal{B}(B^+ \to \eta_c K^+)$.
[g]Using $\mathcal{B}(B^0 \to J/\psi K^0)$.
[h]Calculated using $\mathcal{B}(\eta_c \to p\bar{p})$.
[i]Measurement of $\mathcal{B}(B^0 \to \eta_c K^*(892)^0)/\mathcal{B}(B^0 \to \eta_c K^0)$ used in our fit.
[j]Using $\mathcal{B}(B^0 \to \eta_c K^0)$.
[k]Using $\mathcal{B}(B^0 \to J/\psi K^+\pi^-)$.
[l]Using $\mathcal{B}(h_c \to \eta_c\gamma)$.
[m]Measurement of $\mathcal{B}(B^0 \to h_c K^*(892)^0)\mathcal{B}(h_c \to \eta_c\gamma)/\mathcal{B}(B^+ \to \eta_c K^+)$ used in our fit.
[n]Using $\mathcal{B}(\psi(3770) \to D^0\bar{D}^0)$.
[o]Using $\mathcal{B}(\psi(3770) \to D^+D^-)$.

TABLE 114. Branching fractions for decays to χ_c and one kaon.

Parameter [10^{-4}]	Measurements		Average HFLAV / PDG
$\mathcal{B}(B^0 \to \chi_{c0} K^0)$	*BABAR* [724]	<12.4	<12 2 ± 0
$\mathcal{B}(B^0 \to \chi_{c0} K^*(892)^0)$	*BABAR* [725] *BABAR* [724]	$1.7 \pm 0.3 \pm 0.2$ <7.7	1.70 ± 0.36
$\mathcal{B}(B^0 \to \chi_{c1} K^0)$	Belle [726] *BABAR* [727] *BABAR* [14][a]	$3.78^{+0.17}_{-0.16} \pm 0.33$ $4.2 \pm 0.3 \pm 0.3$	3.93 ± 0.27 3.95 ± 0.27
$\mathcal{B}(B^0 \to \chi_{c1} K^+ \pi^-)$	Belle [728] *BABAR* [729]	$4.97 \pm 0.12 \pm 0.28$ $5.11 \pm 0.14 \pm 0.58$	5.00 ± 0.27 4.97 ± 0.30
$\mathcal{B}(B^0 \to \chi_{c1} K^*(892)^0)$	*BABAR* [727] Belle [730] *BABAR* [14]	$2.5 \pm 0.2 \pm 0.2$ $3.1 \pm 0.3 \pm 0.7$ $2.83 \pm 0.43 \pm 0.51$[b]	2.61 ± 0.25 $2.38^{+0.20}_{-0.19}$
$\mathcal{B}(B^0 \to \chi_{c1} K^+ \pi^- \pi^0)$	Belle [728]	$3.52 \pm 0.52 \pm 0.24$	3.52 ± 0.57
$\mathcal{B}(B^0 \to \chi_{c1} K^0 \pi^+ \pi^-)$	Belle [728]	$3.16 \pm 0.35 \pm 0.32$	3.16 ± 0.47
$\mathcal{B}(B^0 \to \chi_{c2} K^0)$	*BABAR* [727] Belle [726]	$0.15 \pm 0.09 \pm 0.03$ <0.15	0.150 ± 0.095 <0.150
$\mathcal{B}(B^0 \to \chi_{c2} K^*(892)^0)$	*BABAR* [727]	$0.66 \pm 0.18 \pm 0.05$	0.66 ± 0.19 0.49 ± 0.12
$\mathcal{B}(B^0 \to \chi_{c2} K^+ \pi^-)$	Belle [728]	$0.72 \pm 0.09 \pm 0.05$	0.72 ± 0.10

[a]Measurement of $\mathcal{B}(B^0 \to \chi_{c1} K^*(892)^0)/\mathcal{B}(B^0 \to \chi_{c1} K^0)$ used in our fit.
[b]Using $\mathcal{B}(B^0 \to \chi_{c1} K^0)$.

TABLE 115. Branching fractions for decays to charmonium and light mesons.

Parameter [10^{-5}]	Measurements		Average HFLAV / PDG
$\mathcal{B}(B^0 \to J/\psi \pi^0)$	*BABAR* [347] Belle [702]	$1.69 \pm 0.14 \pm 0.07$ $2.3 \pm 0.5 \pm 0.2$	1.74 ± 0.15 1.66 ± 0.10
$\mathcal{B}(B^0 \to J/\psi \pi^+ \pi^-)$	*BABAR* [731] LHCb [732][a]	$4.6 \pm 0.7 \pm 0.6$	4.60 ± 0.92 4.00 ± 0.15
$\mathcal{B}(B^0 \to J/\psi \pi^+ \pi^-(\mathrm{NR}))$	*BABAR* [733]	<1.2[b]	<1.2
$\mathcal{B}(B^0 \to J/\psi \rho^0(770))$	*BABAR* [733] LHCb [734][c], [734][d], [734][e]	$2.7 \pm 0.3 \pm 0.2$	2.96 ± 0.28 $2.55^{+0.18}_{-0.16}$
$\mathcal{B}(B^0 \to J/\psi \eta)$	Belle [735] LHCb [736] *BABAR* [714]	$1.23^{+0.18}_{-0.17} \pm 0.07$ $0.848 \pm 0.280^{+0.123\,\mathrm{f}}_{-0.114}$ <2.7	1.12 ± 0.16 $1.08^{+0.24}_{-0.23}$
$\mathcal{B}(B^0 \to J/\psi \eta')$	LHCb [736] Belle [735] *BABAR* [714]	$0.855 \pm 0.244^{+0.134\,\mathrm{g}}_{-0.124}$ <0.74 <6.3	0.86 ± 0.28 $0.76^{+0.24}_{-0.25}$
$\mathcal{B}(B^0 \to J/\psi \omega(782))$	LHCb [734]	$2.63 \pm 0.56^{+0.33\,\mathrm{h}}_{-0.46}$	2.63 ± 0.69 $1.76^{+0.70}_{-0.53}$

(Table continued)

TABLE 115. *(Continued)*

Parameter $[10^{-5}]$	Measurements		Average HFLAV PDG
$\mathcal{B}(B^0 \to J/\psi f_0(980))$	LHCb [737][i]		<0.11
$\mathcal{B}(B^0 \to J/\psi f_1(1285))$	LHCb [738]	$0.8450 \pm 0.1963 \pm 0.0752$[j]	0.84 ± 0.21
$\mathcal{B}(B^0 \to J/\psi f_2(1270))$	*BABAR* [733]	<0.46	<0.46 $0.33^{+0.05}_{-0.06}$
$\mathcal{B}(B^0 \to J/\psi K^0 K^+ \pi^- + \text{c.c.})$	LHCb [707]	<2.10	<2.1
$\mathcal{B}(B^0 \to J/\psi K^0 K^+ K^-)$	LHCb [707]	$2.02 \pm 0.43 \pm 0.19$	2.02 ± 0.47 2.49 ± 0.69
$\mathcal{B}(B^0 \to J/\psi K^*(892)^0 K^+ K^-)$	LHCb [707]	$3.10 \pm 0.66 \pm 1.07$[k]	$3.1^{+1.4}_{-1.2}$ none
$\mathcal{B}(B^0 \to J/\psi a_0(980)^0) \times \mathcal{B}(a_0(980)^0 \to K^+ K^-)$	LHCb [739]	<0.090	<0.090 0.047 ± 0.034
$\mathcal{B}(B^0 \to J/\psi K^+ K^-)$	LHCb [739]	$0.253 \pm 0.031 \pm 0.019$	0.253 ± 0.036 0.254 ± 0.035
$\mathcal{B}(B^0 \to J/\psi \phi(1020))$	LHCb [739] Belle [740] *BABAR* [714]	<0.019 <0.094 <0.9	<0.9
$\mathcal{B}(B^0 \to \psi(2S)\pi^+\pi^-)$	LHCb [732]	$2.58 \pm 0.32 \pm 0.57$[l]	$2.59^{+0.69}_{-0.62}$ 2.24 ± 0.35
$\mathcal{B}(B^0 \to \chi_{c1}\pi^0)$	Belle [741]	$1.12 \pm 0.25 \pm 0.12$	1.12 ± 0.28

[a]Measurement of $\mathcal{B}(B^0 \to \psi(2S)\pi^+\pi^-)/\mathcal{B}(B^0 \to J/\psi\pi^+\pi^-)$ used in our fit.
[b]Non resonant only: K^0_S, ρ and f_2 contributions have been subtracted out.
[c]Measurement of $\mathcal{B}(B^0 \to J/\psi\omega(782))/\mathcal{B}(B^0 \to J/\psi\rho^0(770))$ used in our fit.
[d]Measurement of $\mathcal{B}(B^0_s \to J/\psi\eta)/\mathcal{B}(B^0 \to J/\psi\rho^0(770))$ used in our fit.
[e]Measurement of $\mathcal{B}(B^0_s \to J/\psi\eta')/\mathcal{B}(B^0 \to J/\psi\rho^0(770))$ used in our fit.
[f]Using $\mathcal{B}(B^0_s \to J/\psi\eta)$.
[g]Using $\mathcal{B}(B^0_s \to J/\psi\eta')$.
[h]Using $\mathcal{B}(B^0 \to J/\psi\rho^0(770))$.
[i]Measurement of $\mathcal{B}(B^0 \to J/\psi f_0(980))BR_f 0_p i +_p i-$ used in our fit.
[j]Using $\mathcal{B}(f_1(1285) \to \pi^+\pi^+\pi^-\pi^-)$.
[k]Using $\mathcal{B}(B^0 \to J/\psi K^*(892)^0\pi^+\pi^-)$.
[l]Using $\mathcal{B}(B^0 \to J/\psi\pi^+\pi^-)$.

TABLE 116. Branching fractions for decays to J/ψ and photons, baryons, or heavy mesons.

Parameter $[10^{-6}]$	Measurements		Average HFLAV PDG
$\mathcal{B}(B^0 \to J/\psi\gamma)$	LHCb [742] *BABAR* [743]	<1.5 <1.6	<1.5
$\mathcal{B}(B^0 \to J/\psi p\bar{p})$	LHCb [744] LHCb [745] Belle [746] *BABAR* [747]	$0.451 \pm 0.040 \pm 0.044$ <0.52 <0.83 <1.9	0.451 ± 0.059
$\mathcal{B}(B^0 \to J/\psi\bar{D}^0)$	*BABAR* [748] Belle [749]	<13 <20	<13

TABLE 117. Branching fraction ratios.

Parameter [10^{-2}]	Measurements		Average
$\frac{\mathcal{B}(B^0\to J/\psi K^0_S K^+\pi^-+\text{c.c.})}{\mathcal{B}(B^0\to J/\psi K^0_S\pi^+\pi^-)}$	LHCb [707]	<4.8	<4.8

TABLE 118. Polarization fractions.

Parameter	Measurements		Average
$\frac{A_0(B^0\to J/\psi \bar{K}^*(892)^0)}{A_0(\bar{B}^0\to J/\psi \bar{K}^*(892)^0)}$	*BABAR* [750]	<0.32	<0.32
$\frac{A_\perp(\bar{B}^0\to J/\psi K^*(892)^0)}{A_\perp(B^0\to J/\psi K^*(892)^0)}$	*BABAR* [750]	<0.26	<0.26

4. Decays to charm baryons

Averages of B^0 decays to charm baryons are shown in Tables 119,120.

TABLE 119. Branching fractions, I.

Parameter [10^{-4}]	Measurements		Average HFLAV PDG
$\mathcal{B}(B^0\to\bar{\Lambda}_c^- p\pi^0)$	*BABAR* [751]	$1.94\pm0.17\pm0.52$	1.94 ± 0.55 1.55 ± 0.19
$\mathcal{B}(B^0\to\bar{\Lambda}_c^- p\pi^+\pi^-)$	*BABAR* [752] Belle [753]	$12.30\pm0.50\pm3.28$ $11.0\pm1.2\pm3.5$	11.7 ± 2.5 10.2 ± 1.4
$\mathcal{B}(B^0\to\bar{\Lambda}_c^- p\pi^+\pi^-(\text{NR}))$	*BABAR* [752]	$7.90\pm0.40\pm2.04$	7.9 ± 2.1 5.5 ± 1.0
$\mathcal{B}(B^0\to\bar{\Sigma}_c(2455)^0 p\pi^-)$	*BABAR* [752] Belle [754]	$0.91\pm0.07\pm0.24$ $1.4\pm0.2\pm0.4$	1.01 ± 0.22 1.08 ± 0.16
$\mathcal{B}(B^0\to\bar{\Sigma}_c(2455)^{--} p\pi^+)$	*BABAR* [752] Belle [754]	$2.13\pm0.10\pm0.56$ $2.1\pm0.2\pm0.6$	2.12 ± 0.42 1.83 ± 0.24
$\mathcal{B}(B^0\to\bar{\Sigma}_c(2520)^{--} p\pi^+)$	*BABAR* [752] Belle [754]	$1.15\pm0.10\pm0.30$ $1.2\pm0.1\pm0.4$	1.17 ± 0.24 1.02 ± 0.18
$\mathcal{B}(B^0\to\Lambda_c^+\bar{\Lambda}_c^-)$	LHCb [694] Belle [755]	$<0.16^{a,b}$ <0.57	<0.16
$\mathcal{B}(B^0\to\Lambda_c^+\bar{\Lambda}_c^- K^0)$	Belle [756] *BABAR* [757]	$7.9^{+2.9}_{-2.3}\pm4.3$ $3.8\pm3.1\pm2.1$	5.3 ± 2.9 4.0 ± 0.9
$\mathcal{B}(B^0\to\bar{\Xi}_c^-\Lambda_c^+)$	*BABAR* [757] Belle [758]	$5.2\pm3.7\pm2.8^c$ $32.0^{+12.7}_{-9.6}\pm17.9^c$	$7.1^{+7.7}_{-4.1}$ 11.6 ± 8.1

[a]At CL = 95%.
[b]Using $\mathcal{B}(B^0\to D_s^+ D^-)$.
[c]Using $\mathcal{B}(\Xi_c^+\to\Xi^-\pi^+\pi^+)$.

TABLE 120. Branching fractions, II.

Parameter $[10^{-5}]$	Measurements		Average HFLAV PDG
$\mathcal{B}(B^0 \to \bar{\Lambda}_c^- p K^+ K^-)$	*BABAR* [759]	$2.5 \pm 0.4 \pm 0.6$	2.50 ± 0.75 1.99 ± 0.37
$\mathcal{B}(B^0 \to \bar{\Lambda}_c^- p \phi(1020))$	*BABAR* [759]	<1.2	<1.2 <1.0
$\mathcal{B}(B^0 \to \bar{\Lambda}_c^- p)$	*BABAR* [760] Belle [761] *BABAR* [760][a]	$1.89 \pm 0.21 \pm 0.49$ $2.19^{+0.56}_{-0.49} \pm 0.65$	1.80 ± 0.31 1.54 ± 0.18
$\mathcal{B}(B^0 \to \bar{\Lambda}_c^- p K^*(892)^0)$	*BABAR* [762]	$1.6 \pm 0.6 \pm 0.4$	1.60 ± 0.75 <2.42
$\mathcal{B}(B^0 \to \bar{\Lambda}_c^- \Lambda^0 K^+)$	*BABAR* [763]	$3.8 \pm 0.8 \pm 1.0$	3.8 ± 1.3 4.8 ± 1.1
$\mathcal{B}(B^0 \to \bar{\Lambda}_c^- p K^+ \pi^-)$	*BABAR* [762]	$4.33 \pm 0.82 \pm 1.18$	4.3 ± 1.4 3.4 ± 0.7
$\mathcal{B}(B^0 \to \bar{\Sigma}_c(2455)^- p)$	*BABAR* [751]	<2.4[b]	<2.4
$\mathcal{B}(B^0 \to \bar{\Sigma}_c(2455)^{--} p K^+)$	*BABAR* [762]	$1.11 \pm 0.30 \pm 0.30$	1.11 ± 0.43 0.88 ± 0.25
$\mathcal{B}(B^0 \to \bar{\Sigma}_c(2520)^0 p \pi^-)$	*BABAR* [752] Belle [754]	$2.2 \pm 0.7 \pm 0.6$ <3.3	2.20 ± 0.93 <3.10
$\mathcal{B}(B^0 \to \bar{\Lambda}_c^- p p \bar{p})$	*BABAR* [764]	<0.22[b]	<0.22 <0.28

[a]Measurement of $\mathcal{B}(B^+ \to \bar{\Lambda}_c^- p \pi^+)/\mathcal{B}(B^0 \to \bar{\Lambda}_c^- p)$ used in our fit.
[b]Using $\mathcal{B}(\Lambda_c^+ \to p K^- \pi^+)$.

5. Decays to exotic states

Averages of B^0 decays to exotic states are shown in Tables 121–124.

TABLE 121. Branching fractions for decays to $X(3872)$.

Parameter [10^{-5}]	Measurements		Average HFLAV PDG
$\mathcal{B}(B^0 \to X(3872)K^0)$	Belle [726]	$12.87^{+2.53\ +3.89}_{-2.72\ -3.34}$ [a]	$11.9^{+3.6}_{-2.8}$
	Belle [765]	$10.3 \pm 2.9^{+3.2}_{-2.6}$ [b]	$11.1^{+4.2}_{-4.1}$
	BABAR [766]	$8.5 \pm 5.0^{+2.7}_{-2.3}$ [b]	
	BABAR [766]	$10.0 \pm 5.4 \pm 3.2$ [c]	
	BABAR [713]	$13 \pm 7 \pm 5$ [d]	
	BABAR [727]	$22.2 \pm 10.7^{+6.6}_{-5.6}$ [a]	
	Belle [726]	$25^{+13}_{-14} \pm 12$ [e]	
	BABAR [713]	$21^{+17}_{-12} \pm 6$ [b]	
	BABAR [727]	$27 \pm 19 \pm 10$ [e]	
	BABAR [700]	<118.1 [f]	
$\mathcal{B}(B^0 \to X(3872)K^*(892)^0)$	*BABAR* [727]	$-2.5 \pm 6.0^{+0.9}_{-0.8}$ [a]	-1.1 ± 5.6
	BABAR [727]	$7 \pm 14 \pm 3$ [e]	10.4 ± 5.2
$\mathcal{B}(B^0 \to X(3872)K^+\pi^-)$	Belle [767]	$22.6 \pm 3.7 \pm 6.9$ [c]	23^{+10}_{-6}
			21 ± 8
$\mathcal{B}(B^0 \to X(3872)K^0) \times \mathcal{B}(X(3872) \to \chi_{c1}\gamma)$			
	Belle [718]	<0.96	<0.96
			none
$\mathcal{B}(B^0 \to X(3872)K^0) \times \mathcal{B}(X(3872) \to \chi_{c2}\gamma)$			
	Belle [718]	<1.22	<1.2
			none

[a]Using $\mathcal{B}(X(3872) \to \psi(2S)\gamma)$.
[b]Using $\mathcal{B}(B^+ \to X(3872)K^+)$.
[c]Using $\mathcal{B}(X(3872) \to J/\psi\pi^+\pi^-)$.
[d]Using $\mathcal{B}(X(3872) \to J/\psi\omega(782))$.
[e]Using $\mathcal{B}(X(3872) \to J/\psi\gamma)$.
[f]Using $\mathcal{B}(X(3872) \to \bar{D}^*(2007)^0 D^0)$.

TABLE 122. Branching fractions for decays to neutral states other than $X(3872)$.

Parameter [10^{-5}]	Measurements		Average HFLAV PDG
$\mathcal{B}(B^0 \to \psi_2(3823)K^0) \times \mathcal{B}(\psi_2(3823) \to \chi_{c1}\gamma)$			
	Belle [718]	<0.99	<0.99
			none
$\mathcal{B}(B^0 \to \psi_2(3823)K^0) \times \mathcal{B}(\psi_2(3823) \to \chi_{c2}\gamma)$			
	Belle [718]	<2.28	<2.3
			none
$\mathcal{B}(B^0 \to Y(3940)K^0) \times \mathcal{B}(Y(3940) \to J/\psi\omega(782))$			
	BABAR [713]	$2.1 \pm 0.9 \pm 0.3$	2.10 ± 0.95
			none
$\mathcal{B}(B^0 \to X(4050)^+K^+) \times \mathcal{B}(X(4050)^+ \to \chi_{c1}\pi^+)$			
	Belle [768]	$3.0^{+1.5\ +3.7}_{-0.8\ -1.6}$	$3.0^{+4.0}_{-1.8}$
	BABAR [729]	<1.8	
$\mathcal{B}(B^0 \to X(4250)^-K^+) \times \mathcal{B}(X(4250)^+ \to \chi_{c1}\pi^+)$			
	Belle [768]	$4.0^{+2.3\ +19.7}_{-0.9\ -0.5}$	4^{+20}_{-1}
	BABAR [729]	<4.7	

TABLE 123. Branching fractions for decays to charged states.

Parameter [10^{-5}]	Measurements		Average HFLAV PDG
$\mathcal{B}(B^0 \to X(3872)^- K^+)$	*BABAR* [769]	<50	<50
$\mathcal{B}(B^0 \to X(3872)^- K^+) \times \mathcal{B}(X(3872)^+ \to J/\psi\pi^+\pi^0)$			
	BABAR [770]	<0.54	<0.54 none
$\mathcal{B}(B^0 \to Z_c(4430)^- K^+) \times \mathcal{B}(Z_c(4430)^+ \to J/\psi\pi^+)$			
	Belle [708]	$0.54^{+0.40\ +0.11}_{-0.10\ -0.09}$	$0.54^{+0.41}_{-0.13}$
	BABAR [771]	<0.4	$0.54^{+0.41}_{-0.12}$
$\mathcal{B}(B^0 \to Z_c(4430)^- K^+) \times \mathcal{B}(Z_c(4430)^+ \to \psi(2S)\pi^+)$			
	LHCb [636]	$3.4 \pm 0.5^{+0.9\,a}_{-1.9}$	
	Belle [719]	$3.2^{+1.8\ +5.3}_{-0.9\ -1.6}$	$3.4^{+1.1}_{-1.5}$
	BABAR [771]	<3.1	$6.0^{+3.0}_{-2.4}$
$\mathcal{B}(B^0 \to Z_c(3900)^- K^+) \times \mathcal{B}(Z_c(3900)^+ \to J/\psi\pi^+)$			
	Belle [708]	<0.090	<0.090
$\mathcal{B}(B^0 \to Z_c(4200)^- K^+) \times \mathcal{B}(Z_c(4200)^+ \to J/\psi\pi^+)$			
	Belle [708]	$2.2^{+0.7\ +1.1}_{-0.5\ -0.6}$	$2.2^{+1.3}_{-0.8}$

[a]The quoted amplitude fraction is multiplied by $\mathcal{B}(B^0 \to \psi(2S)K^+\pi^-) = (5.80 \pm 0.39) \times 10^{-4}$

TABLE 124. Branching fraction ratios.

Parameter	Measurements	Average
$\frac{\mathcal{B}(B^0 \to Y(3940)K^0)}{\mathcal{B}(B^+ \to Y(3940)K^+)}$	*BABAR* [713]	$0.7^{+0.4}_{-0.3} \pm 0.1$

B. Decays of B^+ mesons

Measurements of B^+ decays to charmed hadrons are summarized in Secs. VIII B 1 to VIII B 5.

1. Decays to a single open charm meson

Averages of B^+ decays to a single open charm meson are shown in Tables 125–132.

TABLE 125. Branching fractions for decays to a $\bar{D}^{(*)}$ meson and one or more pions.

Parameter [10^{-3}]	Measurements		Average HFLAV PDG
$\mathcal{B}(B^+ \to \bar{D}^0\pi^+)$	*BABAR* [641]	$4.90 \pm 0.07 \pm 0.22$	
	Belle [772]	$4.34 \pm 0.10 \pm 0.25$	
	BABAR [642]	$4.49 \pm 0.21 \pm 0.23$	
	CDF [644]	$5.05 \pm 0.26 \pm 0.60$[a]	4.67 ± 0.14
	BABAR [773][b,c]		4.68 ± 0.13
	Belle [774][c], [775][c]		
	LHCb [647][d], [455][c], [446][c]		
$\mathcal{B}(B^+ \to \bar{D}^*(2007)^0\pi^+)$	LHCb [776]	$4.664 \pm 0.029 \pm 0.268$	
	Belle [772]	$4.82 \pm 0.12 \pm 0.35$	
	BABAR [641]	$5.52 \pm 0.17 \pm 0.42$	
	BABAR [642]	$5.13 \pm 0.22 \pm 0.28$	4.84 ± 0.16
	BABAR [777][b,e]		4.90 ± 0.17
	Belle [643][e]		
	LHCb [446][e]		
$\mathcal{B}(B^+ \to \bar{D}^*(2007)^0\pi^+\pi^+\pi^-)$	Belle [654]	$10.55 \pm 0.47 \pm 1.29$	10.6 ± 1.4 10.3 ± 1.2

(Table continued)

TABLE 125. *(Continued)*

Parameter [10^{-3}]	Measurements		Average HFLAV PDG
$\mathcal{B}(B^+ \to \bar{D}^*(2007)^0\pi^+\pi^+\pi^+\pi^-\pi^-)$	Belle [654]	$5.67 \pm 0.91 \pm 0.85$	5.7 ± 1.2
$\mathcal{B}(B^+ \to D^-\pi^+\pi^+)$	*BABAR* [778] Belle [779]	$1.08 \pm 0.03 \pm 0.05$ $1.02 \pm 0.04 \pm 0.15$	1.073 ± 0.055
$\mathcal{B}(B^+ \to D^*(2010)^-\pi^+\pi^+)$	*BABAR* [780] Belle [779] LHCb [781][f]	$1.22 \pm 0.05 \pm 0.18$ $1.25 \pm 0.08 \pm 0.22$	1.23 ± 0.15 1.35 ± 0.22
$\mathcal{B}(B^+ \to D^*(2010)^-\pi^+\pi^+\pi^+\pi^-)$	Belle [654]	$2.56 \pm 0.26 \pm 0.33$	2.56 ± 0.42

[a]Using $\mathcal{B}(B^0 \to D^-\pi^+)$.
[b]Using non-CP modes for the D^0.
[c]Measurement of $\mathcal{B}(B^+ \to \bar{D}^0K^+)/\mathcal{B}(B^+ \to \bar{D}^0\pi^+)$ used in our fit.
[d]Measurement of $\mathcal{B}(B^+ \to \bar{D}^0\pi^+\pi^+\pi^-)/\mathcal{B}(B^+ \to \bar{D}^0\pi^+)$ used in our fit.
[e]Measurement of $\mathcal{B}(B^+ \to \bar{D}^*(2007)^0K^+)/\mathcal{B}(B^+ \to \bar{D}^*(2007)^0\pi^+)$ used in our fit.
[f]Measurement of $\mathcal{B}(B^+ \to D^*(2010)^-K^+\pi^+)/\mathcal{B}(B^+ \to D^*(2010)^-\pi^+\pi^+)$ used in our fit.

TABLE 126. Branching fractions for decays to a $\bar{D}^{(*)}$ meson and one or more kaons.

Parameter [10^{-4}]	Measurements		Average HFLAV PDG
$\mathcal{B}(B^+ \to \bar{D}^0K^+)$	LHCb [446] LHCb [455] Belle [774] *BABAR* [773] Belle [775] Belle [774][c] LHCb [776][d,e]	$3.716 \pm 0.014^{+0.127\,a}_{-0.125}$ $3.637 \pm 0.028^{+0.141\,a}_{-0.139}$ $3.160 \pm 0.107^{+0.169\,a}_{-0.168}$ $3.879 \pm 0.163^{+0.150\,b,a}_{-0.148}$ $3.59 \pm 0.23 \pm 0.30$[a]	3.67 ± 0.12 3.63 ± 0.12
$\mathcal{B}(B^+ \to \bar{D}^0K^*(892)^+)$	*BABAR* [782]	$5.29 \pm 0.30 \pm 0.34$	5.29 ± 0.45 5.32 ± 0.45
$\mathcal{B}(B^+ \to \bar{D}^0K^+\pi^+\pi^-)$	LHCb [649]	$5.02 \pm 0.69^{+0.72\,f}_{-0.71}$	5.0 ± 1.0 5.2 ± 2.1
$\mathcal{B}(B^+ \to \bar{D}^0K^+\bar{K}^0)$ $\mathcal{B}(B^+ \to \bar{D}^0\bar{K}^*(892)^0K^+)$	Belle [667] Belle [667]	$5.5 \pm 1.4 \pm 0.8$ $7.5 \pm 1.3 \pm 1.1$	5.5 ± 1.6 7.5 ± 1.7
$\mathcal{B}(B^+ \to \bar{D}^*(2007)^0K^+)$	LHCb [446] *BABAR* [777] LHCb [776] Belle [643]	$4.123 \pm 0.058 \pm 0.270$[g] $3.939 \pm 0.194^{+0.242\,b,g}_{-0.199}$ $3.642 \pm 0.283^{+0.118\,d,h}_{-0.114}$ $3.78 \pm 0.92 \pm 0.45$[g]	3.92 ± 0.18 none
$\mathcal{B}(B^+ \to \bar{D}^*(2007)^0K^*(892)^+)$	*BABAR* [783]	$8.3 \pm 1.1 \pm 1.0$	8.3 ± 1.5 4.0 ± 0.3
$\mathcal{B}(B^+ \to \bar{D}^*(2007)^0K^+\bar{K}^0)$	Belle [667]	<10.6	<11
$\mathcal{B}(B^+ \to \bar{D}^*(2007)^0\bar{K}^*(892)^0K^+)$	Belle [667]	$15.3 \pm 3.1 \pm 2.9$	15.3 ± 4.2
$\mathcal{B}(B^+ \to D^-K^+\pi^+)$	LHCb [784]	$0.731 \pm 0.019 \pm 0.045$	0.731 ± 0.049 0.772 ± 0.050
$\mathcal{B}(B^+ \to D^*(2010)^-K^+\pi^+)$	LHCb [781]	$0.787 \pm 0.033 \pm 0.110$[i]	0.79 ± 0.12 0.82 ± 0.14

[a]Using $\mathcal{B}(B^+ \to \bar{D}^0\pi^+)$.
[b]Using non-CP modes for the D^0.
[c]Measurement of $\mathcal{B}(B^+ \to D^0K^+)/\mathcal{B}(B^+ \to \bar{D}^0K^+)$ used in our fit.
[d]Statistical and systematic uncertainties are combined.
[e]Measurement of $\mathcal{B}(B^+ \to \bar{D}^*(2007)^0K^+)/\mathcal{B}(B^+ \to \bar{D}^0K^+)$ used in our fit.
[f]Using $\mathcal{B}(B^+ \to \bar{D}^0\pi^+\pi^+\pi^-)$.
[g]Using $\mathcal{B}(B^+ \to \bar{D}^*(2007)^0\pi^+)$.
[h]Using $\mathcal{B}(B^+ \to \bar{D}^0K^+)$.
[i]Using $\mathcal{B}(B^+ \to D^*(2010)^-\pi^+\pi^+)$.

TABLE 127. Branching fractions for decays to a $D^{(*)}$ meson.

Parameter [10^{-6}]	Measurements		Average HFLAV PDG
$\mathcal{B}(B^+ \to D^0 K^+)$	Belle [774]	<70[a]	<70 4 ± 0
$\mathcal{B}(B^+ \to D^+ K^0)$	*BABAR* [785]	$-3.8^{+2.2\ +1.2}_{-1.8\ -1.6}$	-3.8 ± 2.5 <2.9
$\mathcal{B}(B^+ \to D^+ K^*(892)^0)$	*BABAR* [785]	$-5.3^{+2.3\ +1.4}_{-2.0\ -1.8}$	-5.3 ± 2.7 <0.5
$\mathcal{B}(B^+ \to D^+ K^+ \pi^-)$	LHCb [786]	$5.31 \pm 0.90 \pm 0.59$	5.3 ± 1.1 5.6 ± 1.1
$\mathcal{B}(B^+ \to D^*(2010)^+ K^0)$	*BABAR* [787]	<9.0	<9.0
$\mathcal{B}(B^+ \to D^*(2010)^+ \pi^0)$	Belle [788]	<3.6	<3.6

[a]Using $\mathcal{B}(B^+ \to \bar{D}^0 K^+)$.

TABLE 128. Branching fractions for decays to excited D mesons.

Parameter [10^{-4}]	Measurements		Average HFLAV PDG
$\mathcal{B}(B^+ \to \bar{D}^{**0} \pi^+)$[a]	*BABAR* [642]	$55 \pm 5 \pm 10$	55 ± 12 57 ± 12
$\mathcal{B}(B^+ \to \bar{D}_0^*(2300)^0 \pi^+) \times \mathcal{B}(D_0^*(2300)^0 \to D^+ \pi^-)$			
	BABAR [778]	$6.8 \pm 0.3 \pm 2.0$	6.4 ± 1.4
	Belle [779]	$6.1 \pm 0.6 \pm 1.8$	
$\mathcal{B}(B^+ \to \bar{D}_1(2420)^0 \pi^+) \times \mathcal{B}(D_1(2420)^0 \to D^*(2010)^+ \pi^-)$			
	BABAR [780]	$5.9 \pm 0.3 \pm 1.1$	6.23 ± 0.91
	Belle [779]	$6.8 \pm 0.7 \pm 1.3$	7.43 ± 0.99
$\mathcal{B}(B^+ \to \bar{D}_1(2420)^0 \pi^+) \times \mathcal{B}(D_1(2420)^0 \to D^0 \pi^+ \pi^-)$			
	Belle [679]	$1.85 \pm 0.29^{+0.35}_{-0.58}$	$2.55^{+0.41}_{-0.42}$
	LHCb [647]	$5.50 \pm 0.80^{+0.76}_{-0.74}$[b]	$2.54^{+1.61}_{-1.43}$
$\mathcal{B}(B^+ \to \bar{D}_1(2420)^0 \pi^+) \times \mathcal{B}(D_1(2420)^0 \to D^0 \pi^+ \pi^-(\mathrm{NR}))$			
	LHCb [647]	$2.14 \pm 0.37 \pm 0.35$[c,b]	2.14 ± 0.52 $2.23^{+0.96}_{-0.95}$
$\mathcal{B}(B^+ \to \bar{D}_1(2420)^0 \pi^+) \times \mathcal{B}(D_1(2420)^0 \to D^*(2007)^0 \pi^+ \pi^-)$			
	Belle [679]	<0.06	<0.060
$\mathcal{B}(B^+ \to \bar{D}_1(2430)^0 \pi^+) \times \mathcal{B}(D_1(2430)^0 \to D^*(2010)^+ \pi^-)$			
	Belle [779]	$5.0 \pm 0.4 \pm 1.1$	4.98 ± 0.81
	LHCb [647]	$4.97 \pm 0.85^{+0.72}_{-0.70}$[b]	3.51 ± 0.61
$\mathcal{B}(B^+ \to \bar{D}_2^*(2460)^0 \pi^+) \times \mathcal{B}(D_2^*(2460)^0 \to D^+ \pi^-)$			
	BABAR [778]	$3.5 \pm 0.2 \pm 0.4$	3.47 ± 0.42
	Belle [779]	$3.4 \pm 0.3 \pm 0.7$	3.56 ± 0.24
$\mathcal{B}(B^+ \to \bar{D}_2^*(2460)^0 \pi^+) \times \mathcal{B}(D_2^*(2460)^0 \to D^*(2010)^+ \pi^-)$			
	BABAR [780]	$1.8 \pm 0.3 \pm 0.5$	
	Belle [779]	$1.8 \pm 0.3 \pm 0.4$	1.86 ± 0.33
	LHCb [647]	$2.08 \pm 0.64^{+0.31}_{-0.30}$[b]	1.98 ± 0.30
$\mathcal{B}(B^+ \to \bar{D}_2^*(2460)^0 \pi^+) \times \mathcal{B}(D_2^*(2460)^0 \to D^0 \pi^+ \pi^-)$			
	LHCb [647]	$0.75 \pm 0.32 \pm 0.13$[c,b]	1.10 ± 0.32
	LHCb [647]	$2.14 \pm 0.53 \pm 0.31$[b]	$2.23^{+1.03}_{-1.02}$
$\mathcal{B}(B^+ \to \bar{D}_2^*(2460)^0 \pi^+) \times \mathcal{B}(D_2^*(2460)^0 \to D^*(2007)^0 \pi^+ \pi^-)$			
	Belle [679]	<0.22	<0.22

[a]D^{**} refers to the sum of all the nonstrange charm meson states with masses in the range 2.2–2.8 GeV/c^2
[b]Using $\mathcal{B}(B^+ \to \bar{D}^0 \pi^+ \pi^+ \pi^-)$.
[c]Non-D^*

TABLE 129. Branching fraction ratios to excited D mesons.

Parameter	Measurements		Average
$\frac{\mathcal{B}(B^+\to\bar{D}_2^*(2460)^0\pi^+)}{\mathcal{B}(B^+\to\bar{D}_1(2420)^0\pi^+)}$	*BABAR* [780]	$0.8 \pm 0.1 \pm 0.2$	0.80 ± 0.17

TABLE 130. Branching fractions for decays to $D_s^{(*)}$ mesons.

Parameter [10^{-5}]	Measurements		Average HFLAV PDG
$\mathcal{B}(B^+ \to D_s^- K^+\pi^+)$	Belle [789]	$19.4^{+0.9}_{-0.8} \pm 2.6$	19.7 ± 2.3
	BABAR [676]	$20.2 \pm 1.3 \pm 3.8$	18.0 ± 2.2
$\mathcal{B}(B^+ \to D_s^- K^+K^+)$	*BABAR* [676]	$1.1 \pm 0.4 \pm 0.2$	1.10 ± 0.45
			0.97 ± 0.21
$\mathcal{B}(B^+ \to D_s^{*-} K^+\pi^+)$	Belle [789]	$14.7^{+1.5}_{-1.4} \pm 2.3$	15.4 ± 2.2
	BABAR [676]	$16.7 \pm 1.6 \pm 3.5$	14.5 ± 2.4
$\mathcal{B}(B^+ \to D_s^{*-} K^+K^+)$	*BABAR* [676]	<1.5	<1.5
$\mathcal{B}(B^+ \to D_s^+\pi^0)$	*BABAR* [790]	$1.5^{+0.5}_{-0.4} \pm 0.2$	$1.50^{+0.55}_{-0.46}$
			$1.56^{+0.57}_{-0.52}$
$\mathcal{B}(B^+ \to D_s^+ K^+K^-)$	LHCb [791][a]		$0.77^{+0.12}_{-0.11}$
			0.72 ± 0.11
$\mathcal{B}(B^+ \to D_s^+\phi(1020))$	LHCb [791]	$0.012^{+0.016}_{-0.014} \pm 0.008$	$0.012^{+0.018}_{-0.016}$
	BABAR [792]	<0.19	<0.042
$\mathcal{B}(B^+ \to D_s^{*+}\phi(1020))$	*BABAR* [792]	<1.2	<1.2

[a]Measurement of $\mathcal{B}(B^+ \to D_s^+ K^+K^-)/(\mathcal{B}(B^+ \to D_s^+\bar{D}^0)\mathcal{B}(D^0 \to K^+K^-))$ used in our fit.

TABLE 131. Branching fractions for decays to baryons.

Parameter [10^{-4}]	Measurements		Average HFLAV PDG
$\mathcal{B}(B^+ \to \bar{D}^0 p\bar{p}\pi^+)$	*BABAR* [681]	$3.72 \pm 0.11 \pm 0.25$	3.72 ± 0.27
$\mathcal{B}(B^+ \to \bar{D}^0\bar{\Lambda}^0 p)$	Belle [793]	$0.143^{+0.028}_{-0.025} \pm 0.018$	0.143 ± 0.032
			$0.143^{+0.033}_{-0.031}$
$\mathcal{B}(B^+ \to \bar{D}^*(2007)^0 p\bar{p}\pi^+)$	*BABAR* [681]	$3.73 \pm 0.17 \pm 0.27$	3.73 ± 0.32
$\mathcal{B}(B^+ \to \bar{D}^*(2007)^0\bar{\Lambda}^0 p)$	Belle [793]	<0.48	<0.48
			<0.50
$\mathcal{B}(B^+ \to D^- p\bar{p}\pi^+\pi^+)$	*BABAR* [681]	$1.66 \pm 0.13 \pm 0.27$	1.66 ± 0.30
$\mathcal{B}(B^+ \to D^*(2010)^- p\bar{p}\pi^+\pi^+)$	*BABAR* [681]	$1.86 \pm 0.16 \pm 0.19$	1.86 ± 0.25
$\mathcal{B}(B^+ \to D^+ p\bar{p})$	Belle [682]	<0.15	<0.15
$\mathcal{B}(B^+ \to D^*(2010)^+ p\bar{p})$	Belle [682]	<0.15	<0.15

TABLE 132. Branching fractions of lepton number violating decays.

Parameter [10^{-6}]	Measurements		Average HFLAV PDG
$\mathcal{B}(B^+ \to D^- e^+ e^+)$	Belle [794]	<2.6	<2.6
$\mathcal{B}(B^+ \to D^- \mu^+ e^+)$	Belle [794]	<1.8	<1.8
$\mathcal{B}(B^+ \to D^- \mu^+ \mu^+)$	Belle [794]	<1.0	<1.0 <0.7

2. Decays to two open charm mesons

Averages of B^+ decays to two open charm mesons are shown in Tables 136–136.

TABLE 133. Branching fractions for decays to $D^{(*)-}D^{(*)0}$.

Parameter [10^{-4}]	Measurements		Average HFLAV PDG
$\mathcal{B}(B^+ \to D^+ \bar{D}^0)$	Belle [689] *BABAR* [687] LHCb [795][a,b,c,d,e,f]	$3.85 \pm 0.31 \pm 0.38$ $3.8 \pm 0.6 \pm 0.5$	3.84 ± 0.42
$\mathcal{B}(B^+ \to \bar{D}^*(2007)^0 D^+)$	*BABAR* [687]	$6.3 \pm 1.4 \pm 1.0$	6.3 ± 1.7
$\mathcal{B}(B^+ \to D^*(2010)^+ \bar{D}^0)$	*BABAR* [687] Belle [796]	$3.6 \pm 0.5 \pm 0.4$ $4.59 \pm 0.72 \pm 0.56$	3.93 ± 0.52 3.92 ± 0.52
$\mathcal{B}(B^+ \to D^*(2010)^+ \bar{D}^*(2007)^0)$	*BABAR* [687]	$8.1 \pm 1.2 \pm 1.2$	8.1 ± 1.7

[a]Measurement of $f_c \times \mathcal{B}(B_c^+ \to D^+ \bar{D}^0)/(f_u \mathcal{B}(B^+ \to D^+ \bar{D}^0))$ used in our fit.
[b]Measurement of $f_c \times \mathcal{B}(B_c^+ \to D^+ D^0)/(f_u \mathcal{B}(B^+ \to D^+ \bar{D}^0))$ used in our fit.
[c]Measurement of $f_c \times (\mathcal{B}(B_c^- \to D^{*-} D^0) \times \mathcal{B}(D^{*-} \to D^-(\pi^0, \gamma)) + \mathcal{B}(B_c^- \to D^- D^{*0}))/(f_u \mathcal{B}(B^+ \to D^+ \bar{D}^0))$ used in our fit.
[d]Measurement of $f_c \times (\mathcal{B}(B_c^- \to D^{*-} \bar{D}^0) \times \mathcal{B}(D^{*-} \to D^-(\pi^0, \gamma)) + \mathcal{B}(B_c^- \to D^- \bar{D}^{*0}))/(f_u \mathcal{B}(B^+ \to D^+ \bar{D}^0))$ used in our fit.
[e]Measurement of $f_c \times \mathcal{B}(B_c^+ \to D^*(2010)^+ \bar{D}^*(2007)^0)/(f_u \mathcal{B}(B^+ \to D^+ \bar{D}^0))$ used in our fit.
[f]Measurement of $f_c \times \mathcal{B}(B_c^+ \to D^*(2010)^+ D^*(2007)^0)/(f_u \mathcal{B}(B^+ \to D^+ \bar{D}^0))$ used in our fit.

TABLE 134. Branching fractions for decays to two D mesons and a kaon.

Parameter [10^{-3}]	Measurements		Average HFLAV PDG
$\mathcal{B}(B^+ \to \bar{D}^*(2007)^0 D^0 K^+)$	*BABAR* [690]	$2.26 \pm 0.16 \pm 0.17$	2.26 ± 0.23
$\mathcal{B}(B^+ \to D^*(2007)^0 \bar{D}^0 K^+)$	*BABAR* [690]	$6.32 \pm 0.19 \pm 0.45$	6.32 ± 0.49
$\mathcal{B}(B^+ \to D^*(2007)^0 \bar{D}^*(2007)^0 K^+)$	*BABAR* [690]	$11.23 \pm 0.36 \pm 1.26$	11.2 ± 1.3
$\mathcal{B}(B^+ \to \bar{D}^*(2007)^0 D^+ K^0)$	*BABAR* [690]	$2.06 \pm 0.38 \pm 0.30$	2.06 ± 0.48
$\mathcal{B}(B^+ \to D^*(2010)^+ \bar{D}^0 K^0)$	*BABAR* [690]	$3.81 \pm 0.31 \pm 0.23$	3.81 ± 0.39
$\mathcal{B}(B^+ \to D^*(2010)^+ \bar{D}^*(2007)^0 K^0)$	*BABAR* [690]	$9.17 \pm 0.83 \pm 0.90$	9.2 ± 1.2
$\mathcal{B}(B^+ \to D^0 \bar{D}^0 K^+)$	*BABAR* [690] Belle [797]	$1.31 \pm 0.07 \pm 0.12$ $2.22 \pm 0.22^{+0.26}_{-0.24}$	1.45 ± 0.13 1.45 ± 0.33
$\mathcal{B}(B^+ \to D^0 \bar{D}^0 K^+ \pi^0)$	Belle [691]	$0.107 \pm 0.031^{+0.019}_{-0.033}$	$0.107^{+0.036}_{-0.045}$ none
$\mathcal{B}(B^+ \to D^+ D^- K^+)$	*BABAR* [690] Belle [798]	$0.22 \pm 0.05 \pm 0.05$ <0.9	0.220 ± 0.071
$\mathcal{B}(B^+ \to D^*(2010)^- D^+ K^+)$	*BABAR* [690]	$0.6 \pm 0.1 \pm 0.1$	0.60 ± 0.13
$\mathcal{B}(B^+ \to D^*(2010)^+ D^- K^+)$	*BABAR* [690]	$0.63 \pm 0.09 \pm 0.06$	0.63 ± 0.11
$\mathcal{B}(B^+ \to D^*(2010)^+ D^*(2010)^- K^+)$	*BABAR* [690]	$1.32 \pm 0.13 \pm 0.12$	1.32 ± 0.18
$\mathcal{B}(B^+ \to D^+ \bar{D}^0 K^0)$	*BABAR* [690]	$1.55 \pm 0.17 \pm 0.13$	1.55 ± 0.21

TABLE 135. Branching fractions for decays to $D_s^{(*)-}D^{(*)+}$.

Parameter [10^{-3}]	Measurements		Average HFLAV PDG
$\mathcal{B}(B^+ \to D_s^+ \bar{D}^0)$	LHCb [688]	$9.54 \pm 0.16^{+1.03\,a}_{-1.04}$	$9.58^{+0.99}_{-0.97}$
	BABAR [693]	$9.0 \pm 1.4 \pm 1.5^{b}$	9.01 ± 0.94
	BABAR [693]	$13.3 \pm 1.8 \pm 3.2$	
	LHCb [688][c,d], [795][e,f,g,h,i,j], [791][k]		
$\mathcal{B}(B^+ \to D_s^+ \bar{D}^*(2007)^0)$	*BABAR* [693]	$6.62 \pm 1.46^{+0.95\,b}_{-0.94}$	$7.9^{+1.6}_{-1.5}$
	BABAR [693]	$12.1 \pm 2.3 \pm 2.0$	8.2 ± 1.7
$\mathcal{B}(B^+ \to D_s^{*+} \bar{D}^0)$	*BABAR* [693]	$9.3 \pm 1.8 \pm 1.9$	8.3 ± 2.0
	BABAR [693]	$7.03 \pm 2.67 \pm 1.40^{b}$	7.6 ± 1.6
$\mathcal{B}(B^+ \to D_s^{*+} \bar{D}^*(2007)^0)$	*BABAR* [693]	$17 \pm 3 \pm 2$	17.9 ± 2.7
	BABAR [693]	$19.24 \pm 3.32^{+2.90\,b}_{-2.88}$	17.1 ± 2.4

[a]Using $\mathcal{B}(B^0 \to D_s^+ D^-)$.
[b]Using $\mathcal{B}(D_s^+ \to \phi(1020)\pi^+)$.
[c]Measurement of $\mathcal{B}(B_s^0 \to D^0\bar{D}^0)/\mathcal{B}(B^+ \to D_s^+\bar{D}^0)$ used in our fit.
[d]Measurement of $\mathcal{B}(B^0 \to D^0\bar{D}^0)/\mathcal{B}(B^+ \to D_s^+\bar{D}^0)$ used in our fit.
[e]Measurement of $f_c \times \mathcal{B}(B_c^+ \to D_s^+\bar{D}^0)/(f_u\mathcal{B}(B^+ \to D_s^+\bar{D}^0))$ used in our fit.
[f]Measurement of $f_c \times \mathcal{B}(B_c^+ \to D_s^+D^0)/(f_u\mathcal{B}(B^+ \to D_s^+\bar{D}^0))$ used in our fit.
[g]Measurement of $f_c \times \mathcal{B}(B_c^+ \to D_s^{*+}\bar{D}^0 + D_s^+\bar{D}^*(2007)^0)/(f_u\mathcal{B}(B^+ \to D_s^+\bar{D}^0))$ used in our fit.
[h]Measurement of $f_c \times \mathcal{B}(B_c^+ \to D_s^{*+}D^0 + D_s^+D^*(2007)^0)/(f_u\mathcal{B}(B^+ \to D_s^+\bar{D}^0))$ used in our fit.
[i]Measurement of $f_c \times \mathcal{B}(B_c^+ \to D_s^{*+}\bar{D}^*(2007)^0)/(f_u\mathcal{B}(B^+ \to D_s^+\bar{D}^0))$ used in our fit.
[j]Measurement of $f_c \times \mathcal{B}(B_c^+ \to D_s^{*+}D^*(2007)^0)/(f_u\mathcal{B}(B^+ \to D_s^+\bar{D}^0))$ used in our fit.
[k]Measurement of $\mathcal{B}(B^+ \to D_s^+K^+K^-)/(\mathcal{B}(B^+ \to D_s^+\bar{D}^0)\mathcal{B}(D^0 \to K^+K^-))$ used in our fit.

TABLE 136. Branching fractions for decays to excited D_s mesons.

Parameter [10^{-3}]	Measurements		Average HFLAV PDG
$\mathcal{B}(B^+ \to D_{s0}^*(2317)^+\bar{D}^0)$	Belle [697]	$0.80^{+0.13\ +0.12\,a}_{-0.12\ -0.20}$	$0.83^{+0.25}_{-0.15}$
	BABAR [698]	$1.0 \pm 0.3^{+0.4\,a}_{-0.3}$	$0.80^{+0.16}_{-0.13}$
$\mathcal{B}(B^+ \to D_{s0}^*(2317)^+\bar{D}^*(2007)^0)$	*BABAR* [698]	$0.9 \pm 0.6^{+0.4\,a}_{-0.3}$	0.90 ± 0.68 none
$\mathcal{B}(B^+ \to D_{s1}(2460)^+\bar{D}^0)$	Belle [699]	$3.05^{+0.87}_{-0.82} \pm 1.04^{b}$	3.28 ± 0.78 $3.09^{+0.97}_{-0.87}$
	Belle [699]	$2.23^{+1.14}_{-0.92} \pm 0.76^{c}$	
	BABAR [698]	$3.3 \pm 1.1^{+1.3\,b}_{-0.9}$	
	BABAR [698]	$5.1 \pm 1.3^{+2.1\,c}_{-1.7}$	
	BABAR [693]	$4.3 \pm 1.6 \pm 1.3$	
	Belle [699]	$<2.4^{d}$	
$\mathcal{B}(B^+ \to D_{s1}(2460)^+\bar{D}^*(2007)^0)$	*BABAR* [698]	$7.6 \pm 2.2^{+3.4\,b}_{-2.6}$	$10.5 \pm 2.412.0^{+3.1}_{-3.0}$
	BABAR [693]	$11.2 \pm 2.6 \pm 2.0$	
	BABAR [698]	$14.2 \pm 3.2^{+6.3\,c}_{-5.0}$	
$\mathcal{B}(B^+ \to D_{s1}(2536)^+\bar{D}^0)$	*BABAR* [700]	$0.453 \pm 0.109 \pm 0.112^{e}$	0.405 ± 0.084 none
	BABAR [700]	$0.41 \pm 0.17 \pm 0.09^{f}$	
	Belle [701][g]		
$\mathcal{B}(B^+ \to D_{s1}(2536)^+\bar{D}^*(2007)^0)$	*BABAR* [700]	$1.144 \pm 0.245 \pm 0.267^{e}$	$1.14^{+0.39}_{-0.34}$ none
	BABAR [700]	$<1.900^{f}$	

[a]Using $\mathcal{B}(D_{s0}^*(2317)^+ \to D_s^+\pi^0)$.
[b]Using $\mathcal{B}(D_{s1}(2460)^+ \to D_s^+\gamma)$.
[c]Using $\mathcal{B}(D_{s1}(2460)^+ \to D_s^{*+}\pi^0)$.
[d]Using $\mathcal{B}(D_{s1}(2460)^+ \to D_s^+\pi^+\pi^-)$.
[e]Using $\mathcal{B}(D_{s1}(2536)^+ \to D^*(2007)^0K^+)$.
[f]Using $\mathcal{B}(D_{s1}(2536)^+ \to D^*(2010)^+K^0)$.
[g]Measurement of $\mathcal{B}(B^+ \to D_{s1}(2536)^+\bar{D}^0)(\mathcal{B}(D_{s1}(2536)^+ \to D^*(2007)^0K^+) + \mathcal{B}(D_{s1}(2536)^+ \to D^*(2010)^+K^0))$ used in our fit.

3. Decays to charmonium states

Averages of B^+ decays to charmonium states are shown in Tables 137–143.

TABLE 137. Branching fractions for decays to J/ψ and one kaon.

Parameter [10^{-4}]	Measurements		Average HFLAV PDG
$\mathcal{B}(B^+ \to J/\psi K^+)$	*BABAR* [14]	$10.61 \pm 0.15 \pm 0.48$	10.06 ± 0.26 10.20 ± 0.19
	Belle [702]	$10.1 \pm 0.2 \pm 0.7$	
	Belle [772]	$8.9 \pm 0.6 \pm 0.5$	
	Belle [799]	$10.37 \pm 0.61 \pm 0.49$[a]	
	BABAR [800]	$10.3 \pm 0.9 \pm 0.5$[a]	
	BABAR [769]	$8.1 \pm 1.3 \pm 0.7$	
	Belle [799]	$10.6^{+1.8}_{-1.5} \pm 1.9$[b]	
	BABAR [704][c], [801][d], [14][e], [769][c]		
	Belle [802][f], [715][g,h]		
	CDF [705][e], [803][d], [804][d]		
	CMS [805][i]		
	D0 [806][j]		
	LHCb [807][k,i], [711][j], [808][l], [809][m,i]		
$\mathcal{B}(B^+ \to J/\psi K^*(892)^+)$	*BABAR* [14]	$13.8 \pm 0.5 \pm 0.9$[n]	13.64 ± 0.83 14.30 ± 0.81
	Belle [810]	$12.8 \pm 0.7 \pm 1.4$	
	CDF [703]	$15.8 \pm 4.7 \pm 2.7$	
	CDF [705]	$19.3 \pm 6.0 \pm 1.8$[n]	
$\mathcal{B}(B^+ \to J/\psi K_1(1270)^+)$	Belle [715]	$18 \pm 3 \pm 3$[n]	18.1 ± 4.8 18.0 ± 5.2
	Belle [715][o]		
$\mathcal{B}(B^+ \to J/\psi K_1(1400)^+)$	Belle [715]	<5[p]	<5.4 <5.0
$\mathcal{B}(B^+ \to J/\psi K^+\pi^+\pi^-)$	Belle [811]	$7.16 \pm 0.10 \pm 0.60$	8.07 ± 0.52 p = 2.3‰ 8.11 ± 1.28
	BABAR [812]	$11.6 \pm 0.7 \pm 0.9$	
	CDF [813]	$6.9 \pm 1.8 \pm 1.2$	
$\mathcal{B}(B^+ \to J/\psi \eta K^+)$	Belle [716]	$1.27 \pm 0.11 \pm 0.11$	1.24 ± 0.14
	BABAR [717]	$1.08 \pm 0.23 \pm 0.24$	
$\mathcal{B}(B^+ \to J/\psi \omega(782) K^+)$	*BABAR* [713]	$3.2 \pm 0.1^{+0.6}_{-0.3}$	$3.22^{+0.51}_{-0.31}$ $3.20^{+0.61}_{-0.32}$
	BABAR [713][q]		
$\mathcal{B}(B^+ \to J/\psi \phi(1020) K^+)$	*BABAR* [714]	$0.44 \pm 0.14 \pm 0.05$	0.44 ± 0.15 0.50 ± 0.04
	D0 [814][r]		
	LHCb [815][s,r], [815][st]		

[a]Using $\mathcal{B}(J/\psi \to p\bar{p})$.
[b]Using $\mathcal{B}(J/\psi \to \Lambda^0\bar{\Lambda}^0)$.
[c]Measurement of $\mathcal{B}(B^+ \to \eta_c K^+)/\mathcal{B}(B^+ \to J/\psi K^+)$ used in our fit.
[d]Measurement of $\mathcal{B}(B^+ \to J/\psi \pi^+)/\mathcal{B}(B^+ \to J/\psi K^+)$ used in our fit.
[e]Measurement of $\mathcal{B}(B^+ \to J/\psi K^*(892)^+)/\mathcal{B}(B^+ \to J/\psi K^+)$ used in our fit.
[f]Measurement of $\mathcal{B}(B^+ \to \chi_{c0} K^+)/\mathcal{B}(B^+ \to J/\psi K^+)$ used in our fit.
[g]Measurement of $\mathcal{B}(B^+ \to J/\psi K_1(1270)^+)/\mathcal{B}(B^+ \to J/\psi K^+)$ used in our fit.
[h]Measurement of $\mathcal{B}(B^0 \to J/\psi K_1(1270)^0)/\mathcal{B}(B^+ \to J/\psi K^+)$ used in our fit.
[i]Measurement of $f_c \times \mathcal{B}(B_c^+ \to J/\psi \pi^+)/(f_u \mathcal{B}(B^+ \to J/\psi K^+))$ used in our fit.
[j]Measurement of $\mathcal{B}(B^+ \to \psi(2S) K^+)/\mathcal{B}(B^+ \to J/\psi K^+)$ used in our fit.
[k]$\sqrt{s} = 7$ TeV, $p_T > 4$ GeV and $2.5 < y < 4.5$.
[l]Measurement of $(\mathcal{B}(B^+ \to \eta_c K^+)\mathcal{B}(\eta_c \to p\bar{p}))/(\mathcal{B}(B^+ \to J/\psi K^+)\mathcal{B}(J/\psi \to p\bar{p}))$ used in our fit.
[m]$\sqrt{s} = 8$ TeV, $0 < p_T < 20$ GeV and $2.0 < y < 4.5$.
[n]Using $\mathcal{B}(B^+ \to J/\psi K^+)$.
[o]Measurement of $\mathcal{B}(B^+ \to J/\psi K_1(1400)^+)/\mathcal{B}(B^+ \to J/\psi K_1(1270)^+)$ used in our fit.
[p]Using $\mathcal{B}(B^+ \to J/\psi K_1(1270)^+)$.
[q]Measurement of $\mathcal{B}(B^0 \to J/\psi \omega(782) K^0)/\mathcal{B}(B^+ \to J/\psi \omega(782) K^+)$ used in our fit.
[r]Measurement of $\mathcal{B}(B^+ \to \chi_{c1}(4140) K^+) \times \mathcal{B}(\chi_{c1}(4140) \to J/\psi \phi(1020))/\mathcal{B}(B^+ \to J/\psi \phi(1020) K^+)$ used in our fit.
[s]The quoted value is a fit fraction from a Dalitz plot fit.
[t]Measurement of $\mathcal{B}(B^+ \to \chi_{c1}(4274) K^+) \times \mathcal{B}(\chi_{c1}(4274) \to J/\psi \phi(1020))/\mathcal{B}(B^+ \to J/\psi \phi(1020) K^+)$ used in our fit.

TABLE 138. Branching fractions for decays to charmonium other than J/ψ and one kaon.

Parameter $[10^{-4}]$	Measurements		Average HFLAV / PDG
$\mathcal{B}(B^+ \to \psi(2S)K^+)$	LHCb [711]	$5.98 \pm 0.06 \pm 0.27$[a]	6.12 ± 0.21 6.24 ± 0.20
	BABAR [14]	$6.17 \pm 0.32 \pm 0.44$	
	D0 [806]	$6.5 \pm 0.4 \pm 0.8$[a]	
	Belle [702]	6.9 ± 0.6	
	Belle [718]	$7.7 \pm 0.8 \pm 0.9$	
	Belle [718]	$6.3 \pm 0.9 \pm 0.6$	
	Belle [772]	$6.4 \pm 1.0 \pm 0.4$	
	CDF [710]	$5.5 \pm 1.0 \pm 0.6$	
	BABAR [769]	$4.9 \pm 1.6 \pm 0.4$	
	BABAR [14][b]		
$\mathcal{B}(B^+ \to \psi(2S)K^*(892)^+)$	*BABAR* [14]	$5.88 \pm 0.92 \pm 0.59$[c]	5.9 ± 1.1 6.7 ± 1.4
$\mathcal{B}(B^+ \to \psi(2S)K^+\pi^+\pi^-)$	Belle [811]	$4.31 \pm 0.20 \pm 0.50$	4.31 ± 0.54 4.34 ± 0.54
$\mathcal{B}(B^+ \to \psi(2S)\phi(1020)K^+)$	CMS [816]	$0.040 \pm 0.004 \pm 0.006$	0.0400 ± 0.0075 0.0400 ± 0.0072
$\mathcal{B}(B^+ \to \psi(3770)K^+)$	*BABAR* [700]	$2.69 \pm 0.57^{+0.46}_{-0.48}$[d]	2.51 ± 0.49 4.34 ± 1.10
	BABAR [700]	$2.07 \pm 0.79 \pm 0.56$[e]	
	Belle [798]	$4.8 \pm 1.1 \pm 0.7$[f]	
	Belle [772]	$-0.2 \pm 1.4 \pm -0.0$	
	BABAR [769]	$3.5 \pm 2.5 \pm 0.3$	
$\mathcal{B}(B^+ \to \eta_c K^+)$	Belle [817]	$3.65 \pm 0.19^{+0.80}_{-0.78}$[g]	$10.45^{+0.69}_{-0.68}$ $10.86^{+0.77}_{-0.75}$
	Belle [772]	$12.0 \pm 0.8 \pm 0.7$	
	Belle [799]	$10.89 \pm 0.84^{+1.48}_{-1.73}$[h]	
	BABAR [704]	$12.9 \pm 0.9 \pm 3.8$	
	BABAR [704]	$12.9 \pm 1.0 \pm 3.8$[a]	
	Belle [722]	$12.5 \pm 1.4^{+3.9}_{-4.0}$	
	BABAR [800]	$13.8^{+2.3}_{-1.5}{}^{+1.9}_{-1.8}$[h]	
	BABAR [769]	$10.7 \pm 2.3 \pm 0.5$[a]	
	Belle [799]	$9.6^{+2.5}_{-2.2}{}^{+1.9}_{-2.0}$[i]	
	BABAR [704][j], [723][k,l,m]		
	LHCb [808][n]		
$\mathcal{B}(B^+ \to \eta_c K^*(892)^+)$	*BABAR* [721]	$12.1^{+4.3}_{-3.5}{}^{+6.4}_{-6.1}$[o]	$12.3^{+6.0}_{-5.2}$ $10.9^{+5.1}_{-4.2}$
$\mathcal{B}(B^+ \to \eta_c(2S)K^+)$	Belle [817]	$1.63^{+1.05}_{-0.72}{}^{+0.75}_{-0.64}$[p]	4.47 ± 0.93 4.42 ± 0.96
	Belle [772]	$4.8 \pm 1.1 \pm 0.3$	
	BABAR [769]	$3.4 \pm 1.8 \pm 0.3$	
$\mathcal{B}(B^+ \to h_c K^+)$	Belle [818]	<0.038	<0.038 $0.370^{+0.128}_{-0.120}$
	BABAR [723][m]		

[a]Using $\mathcal{B}(B^+ \to J/\psi K^+)$.
[b]Measurement of $\mathcal{B}(B^+ \to \psi(2S)K^*(892)^+)/\mathcal{B}(B^+ \to \psi(2S)K^+)$ used in our fit.
[c]Using $\mathcal{B}(B^+ \to \psi(2S)K^+)$.
[d]Using $\mathcal{B}(\psi(3770) \to D^0\bar{D}^0)$.
[e]Using $\mathcal{B}(\psi(3770) \to D^+D^-)$.
[f]Assumed $\mathcal{B}(\psi(3770) \to D^+D^-) + \mathcal{B}(\psi(3770) \to D^0\bar{D}^0) = 1$.
[g]Using $\mathcal{B}(\eta_c \to K\bar{K}\pi)$.
[h]Using $\mathcal{B}(\eta_c \to p\bar{p})$.
[i]Using $\mathcal{B}(\eta_c \to \Lambda^0\bar{\Lambda}^0)$.
[j]Measurement of $\mathcal{B}(B^0 \to \eta_c K^0)/\mathcal{B}(B^+ \to \eta_c K^+)$ used in our fit.
[k]Measurement of $\mathcal{B}(B^0 \to \eta_c K^*(892)^0)/\mathcal{B}(B^+ \to \eta_c K^+)$ used in our fit.
[l]Measurement of $\mathcal{B}(B^0 \to h_c K^*(892)^0)\mathcal{B}(h_c \to \eta_c\gamma)/\mathcal{B}(B^+ \to \eta_c K^+)$ used in our fit.
[m]Measurement of $\mathcal{B}(B^+ \to h_c K^+)\mathcal{B}(h_c \to \eta_c\gamma)/\mathcal{B}(B^+ \to \eta_c K^+)$ used in our fit.
[n]Measurement of $(\mathcal{B}(B^+ \to \eta_c K^+)\mathcal{B}(\eta_c \to p\bar{p}))/(\mathcal{B}(B^+ \to J/\psi K^+)\mathcal{B}(J/\psi \to p\bar{p}))$ used in our fit.
[o]Calculated using $\mathcal{B}(\eta_c \to p\bar{p})$.
[p]Using $\mathcal{B}(\eta_c(2S)) \to K\bar{K}\pi$.

TABLE 139. Branching fractions for decays to χ_c and one kaon.

Parameter [10^{-4}]	Measurements		Average HFLAV PDG
$\mathcal{B}(B^+ \to \chi_{c0}K^+)$	*BABAR* [264]	$1.84 \pm 0.32 \pm 0.31$	2.16 ± 0.38 $1.51^{+0.15}_{-0.13}$
	Belle [772]	$2.0 \pm 0.9 \pm 0.1$	
	Belle [802]	$6.0^{+2.1}_{-1.8} \pm 1.1$	
	Belle [802]	$6 \pm 2 \pm 1$[a]	
	BABAR [769]	<1.8	
$\mathcal{B}(B^+ \to \chi_{c0}K^*(892)^+)$	*BABAR* [725]	$1.4 \pm 0.5 \pm 0.2$	1.40 ± 0.54 <2.10
	BABAR [724]	<28.6	
$\mathcal{B}(B^+ \to \chi_{c1}K^+)$	*BABAR* [727]	$4.5 \pm 0.1 \pm 0.3$	4.85 ± 0.22 4.74 ± 0.22
	Belle [726]	$4.94 \pm 0.11 \pm 0.33$	
	Belle [772]	$5.8 \pm 0.9 \pm 0.5$	
	BABAR [769]	$8.0 \pm 1.4 \pm 0.7$	
	CDF [813]	$15.5 \pm 5.4 \pm 2.0$	
	BABAR [14][b]		
	Belle [819][c]		
$\mathcal{B}(B^+ \to \chi_{c1}K^*(892)^+)$	*BABAR* [727]	$2.6 \pm 0.5 \pm 0.4$	2.89 ± 0.50 2.96 ± 0.63
	Belle [730]	$4.1 \pm 0.6 \pm 0.9$	
	BABAR [14]	$2.48 \pm 0.83 \pm 0.78$[d]	
$\mathcal{B}(B^+ \to \chi_{c1}K^+\pi^0)$	Belle [728]	$3.29 \pm 0.29 \pm 0.19$	3.29 ± 0.35
$\mathcal{B}(B^+ \to \chi_{c1}K^0\pi^+)$	*BABAR* [729]	$5.52 \pm 0.26 \pm 0.61$	5.69 ± 0.35 5.75 ± 0.41
	Belle [728]	$5.75 \pm 0.26 \pm 0.32$	
$\mathcal{B}(B^+ \to \chi_{c1}K^+\pi^+\pi^-)$	Belle [728]	$3.74 \pm 0.18 \pm 0.24$	3.74 ± 0.30
$\mathcal{B}(B^+ \to \chi_{c2}K^+)$	Belle [726]	$0.111^{+0.036}_{-0.034} \pm 0.009$	0.108 ± 0.031 $0.111^{+0.037}_{-0.035}$
	BABAR [727]	$0.10 \pm 0.06 \pm 0.01$	
$\mathcal{B}(B^+ \to \chi_{c2}K^*(892)^+)$	*BABAR* [727]	$0.11 \pm 0.43 \pm 0.55$	0.11 ± 0.70 <1.20
$\mathcal{B}(B^+ \to \chi_{c2}K^0\pi^+)$	Belle [728]	$1.16 \pm 0.22 \pm 0.12$	1.16 ± 0.25
$\mathcal{B}(B^+ \to \chi_{c2}K^+\pi^+\pi^-)$	Belle [728]	$1.34 \pm 0.17 \pm 0.09$	1.34 ± 0.19

[a]Using $\mathcal{B}(B^+ \to J/\psi K^+)$.
[b]Measurement of $\mathcal{B}(B^+ \to \chi_{c1}K^*(892)^+)/\mathcal{B}(B^+ \to \chi_{c1}K^+)$ used in our fit.
[c]Measurement of $\mathcal{B}(B^+ \to \chi_{c1}\pi^+)/\mathcal{B}(B^+ \to \chi_{c1}K^+)$ used in our fit.
[d]Using $\mathcal{B}(B^+ \to \chi_{c1}K^+)$.

TABLE 140. Branching fractions for decays to charmonium and light mesons.

Parameter [10^{-5}]	Measurements		Average HFLAV PDG
$\mathcal{B}(B^+ \to J/\psi\pi^+)$	LHCb [820]	$3.88 \pm 0.11 \pm 0.15$	4.11 ± 0.16 3.92 ± 0.08
	BABAR [801]	$5.40 \pm 0.45 \pm 0.18$[a]	
	Belle [702]	$3.8 \pm 0.6 \pm 0.3$	
	CDF [804]	$4.89 \pm 0.82 \pm 0.20$[a]	
	CDF [803]	$5 \pm 2 \pm 0$[a]	
$\mathcal{B}(B^+ \to J/\psi\pi^+\pi^0)$	*BABAR* [733]	<0.73[b]	<0.73
$\mathcal{B}(B^+ \to J/\psi\rho^+(770))$	LHCb [821]	$3.81^{+0.25}_{-0.24} \pm 0.35$	4.10 ± 0.38 $4.10^{+0.51}_{-0.50}$
	BABAR [733]	$5.0 \pm 0.7 \pm 0.3$	
$\mathcal{B}(B^+ \to \psi(2S)\pi^+)$	LHCb [820]	$2.52 \pm 0.26 \pm 0.15$	2.52 ± 0.30 2.44 ± 0.30

(Table continued)

TABLE 140. *(Continued)*

Parameter [10^{-5}]	Measurements		Average HFLAV PDG
$\mathcal{B}(B^+ \to \chi_{c0}\pi^+)$	*BABAR* [822]	<6.1[c]	<6.1 <0.0
$\mathcal{B}(B^+ \to \chi_{c1}\pi^+)$	Belle [819] Belle [819]	$2.09 \pm 0.39 \pm 0.17$[d] $2.2 \pm 0.4 \pm 0.3$	2.13 ± 0.32 2.20 ± 0.50

[a]Using $\mathcal{B}(B^+ \to J/\psi K^+)$.
[b]Nonresonant only.
[c]Computed using PDG2004 value of $\mathcal{B}(\chi_{c0} \to \pi\pi)$.
[d]Using $\mathcal{B}(B^+ \to \chi_{c1}K^+)$.

TABLE 141. Branching fractions for decays to J/ψ and a heavy mesons.

Parameter [10^{-4}]	Measurements		Average HFLAV PDG
$\mathcal{B}(B^+ \to J/\psi D^+)$	*BABAR* [748]	<1.2	<1.2
$\mathcal{B}(B^+ \to J/\psi \bar{D}^0\pi^+)$	Belle [749] *BABAR* [812]	<0.25 <0.52	<0.25

TABLE 142. Branching fractions for decays to J/ψ and baryons.

Parameter [10^{-6}]	Measurements		Average HFLAV PDG
$\mathcal{B}(B^+ \to J/\psi \bar{\Lambda}^0 p)$	Belle [746] *BABAR* [747]	$11.6 \pm 2.8^{+1.8}_{-2.3}$ $11.6^{+7.4\ +4.2}_{-5.3\ -1.8}$	11.6 ± 3.1 14.6 ± 1.2
$\mathcal{B}(B^+ \to J/\psi \bar{\Sigma}^0 p)$	Belle [746]	<11	<11
$\mathcal{B}(B^+ \to J/\psi p \bar{p}\pi^+)$	LHCb [745]	<0.50	<0.50

TABLE 143. Direct CP violation parameters.

Parameter	Measurements		Average
$A_{CP}(B^+ \to J/\psi K^+)$	D0 [823]	$0.0059 \pm 0.0036 \pm 0.0007$	0.0059 ± 0.0037
$A_{CP}(B^+ \to J/\psi \pi^+)$	D0 [823]	$-0.042 \pm 0.044 \pm 0.009$	-0.042 ± 0.045
$A_{CP}(B^+ \to J/\psi \rho^+(770))$	LHCb [821] *BABAR* [733]	$-0.045^{+0.056}_{-0.057} \pm 0.008$ $-0.11 \pm 0.12 \pm 0.08$	-0.054 ± 0.053

4. Decays to charm baryons

Averages of B^+ decays to charm baryons are shown in Table 144.

TABLE 144. Branching fractions.

Parameter [10^{-4}]	Measurements		Average HFLAV / PDG
$\mathcal{B}(B^+ \to \bar{\Lambda}_c^- p\pi^+)$	*BABAR* [760]	$3.38 \pm 0.12 \pm 0.89$	2.71 ± 0.43
	BABAR [760]	$2.77 \pm 0.32 \pm 0.48$[a]	$2.25^{+0.37}_{-0.38}$
	Belle [753]	$1.87^{+0.43}_{-0.40} \pm 0.56$	
	BABAR [760][b,c]		
$\mathcal{B}(B^+ \to \Lambda_c^+ \bar{\Lambda}_c^- K^+)$	Belle [824]	$4.8 \pm 0.4 \pm 0.6$	4.89 ± 0.73
	BABAR [757]	$11.4 \pm 1.5 \pm 6.2$	4.91 ± 0.73
$\mathcal{B}(B^+ \to \bar{\Xi}_c^0 \Lambda_c^+)$	*BABAR* [757]	$14.54 \pm 4.54 \pm 5.40$[d]	$18.1^{+8.2}_{-6.2}$
	Belle [758]	$33.6^{+7.0}_{-6.3} \pm 13.7$[d]	9.5 ± 2.3
$\mathcal{B}(B^+ \to \bar{\Xi}_c(2930)^+ \Lambda_c^+)$	Belle [824]	$3.46 \pm 0.90 \pm 3.49$[e]	3.5 ± 3.9
			none
$\mathcal{B}(B^+ \to \bar{\Sigma}_c(2455)^0 p)$	*BABAR* [760]	$0.333 \pm 0.032 \pm 0.057$[f]	0.336 ± 0.065
	Belle [753]	$0.45^{+0.26}_{-0.19} \pm 0.14$	0.295 ± 0.066
$\mathcal{B}(B^+ \to \bar{\Sigma}_c(2520)^0 p)$	Belle [753]	<0.46	<0.46
			<0.03
$\mathcal{B}(B^+ \to \bar{\Sigma}_c(2455)^{--} p\pi^+\pi^+)$	*BABAR* [825]	$2.98 \pm 0.16 \pm 0.78$	2.98 ± 0.80
			2.37 ± 0.20
$\mathcal{B}(B^+ \to \bar{\Sigma}_c(2800)^0 p)$	*BABAR* [760]	$0.317 \pm 0.062 \pm 0.082$[f]	$0.32^{+0.11}_{-0.10}$
			0.26 ± 0.09

[a]Using $\mathcal{B}(B^0 \to \bar{\Lambda}_c^- p)$.
[b]Measurement of $\mathcal{B}(B^+ \to \bar{\Sigma}_c(2455)^0 p)/\mathcal{B}(B^+ \to \bar{\Lambda}_c^- p\pi^+)$ used in our fit.
[c]Measurement of $\mathcal{B}(B^+ \to \bar{\Sigma}_c(2800)^0 p)/\mathcal{B}(B^+ \to \bar{\Lambda}_c^- p\pi^+)$ used in our fit.
[d]Using $\mathcal{B}(\Xi_c^0 \to \Xi^- \pi^+)$.
[e]Using $\mathcal{B}(\Xi_c(2930)^+ \to \Lambda_c^+ K^-)$.
[f]Using $\mathcal{B}(B^+ \to \bar{\Lambda}_c^- p\pi^+)$.

5. Decays to exotic states

Averages of B^+ decays to exotic states are shown in Tables 145–148.

TABLE 145. Branching fractions.

Parameter [10^{-4}]	Measurements		Average HFLAV / PDG
$\mathcal{B}(B^+ \to X(3872)K^+)$	*BABAR* [727]	$1.85 \pm 0.52^{+0.54}_{-0.45}$[a]	$2.06^{+0.61}_{-0.49}$
	Belle [772]	$1.2 \pm 1.1 \pm 0.1$	2.10 ± 0.68
	Belle [726]	<0.671[a]	
	BABAR [769]	<3.2	
	BABAR [766][b], [713][b]		
	Belle [765][b]		
$\mathcal{B}(B^+ \to X(3872)K^*(892)^+)$	*BABAR* [727]	$1.24 \pm 1.91^{+1.90}_{-1.89}$[a]	$1.2^{+2.9}_{-2.7}$
			<6.0
$\mathcal{B}(B^+ \to X(3872)K^0\pi^+)$	Belle [767]	$3.03 \pm 0.86 \pm 0.94$[c]	$3.0^{+1.6}_{-1.1}$
			2.8 ± 1.2
$\mathcal{B}(B^+ \to X(3915)K^+)$	Belle [772]	$0.4 \pm 1.6 \pm -0.0$	0.4 ± 1.6
			<2.8

[a]Using $\mathcal{B}(X(3872) \to \psi(2S)\gamma)$.
[b]Measurement of $\mathcal{B}(B^0 \to X(3872)K^0)/\mathcal{B}(B^+ \to X(3872)K^+)$ used in our fit.
[c]Using $\mathcal{B}(X(3872) \to J/\psi\pi^+\pi^-)$.

TABLE 146. Product branching fractions to $X(3872)$.

Parameter $[10^{-5}]$	Measurements		Average HFLAV PDG
$\mathcal{B}(B^+ \to X(3872)K^+) \times \mathcal{B}(X(3872) \to D^*(2007)^0\bar{D}^0)$			
	BABAR [700]	$16.7 \pm 3.6 \pm 4.7$	16.7 ± 5.9 8.5 ± 2.6
$\mathcal{B}(B^+ \to X(3872)K^+) \times \mathcal{B}(X(3872) \to D^0\bar{D}^0\pi^0)$			
	Belle [798]	<6.0	<6.0 $10.2^{+3.7}_{-4.2}$
$\mathcal{B}(B^+ \to X(3872)K^+) \times \mathcal{B}(X(3872) \to D^0\bar{D}^0)$			
	Belle [798]	<6.0	<6.0
$\mathcal{B}(B^+ \to X(3872)K^+) \times \mathcal{B}(X(3872) \to D^+D^-)$			
	Belle [798]	<4.0	<4.0
$\mathcal{B}(B^+ \to X(3872)K^+) \times \mathcal{B}(X(3872) \to J/\psi\pi^+\pi^-)$			
	Belle [765]	$0.861 \pm 0.062 \pm 0.052$	0.857 ± 0.073
	BABAR [766]	$0.84 \pm 0.15 \pm 0.07$	0.857 ± 0.084
$\mathcal{B}(B^+ \to X(3872)K^+) \times \mathcal{B}(X(3872) \to J/\psi\omega(782))$			
	BABAR [713]	$0.6 \pm 0.2 \pm 0.1$	0.60 ± 0.22
$\mathcal{B}(B^+ \to X(3872)K^+) \times \mathcal{B}(X(3872) \to J/\psi\eta)$			
	BABAR [717]	<0.77	<0.77
$\mathcal{B}(B^+ \to X(3872)K^+) \times \mathcal{B}(X(3872) \to J/\psi\gamma)$			
	Belle [726]	$0.178^{+0.048}_{-0.044} \pm 0.012$	0.206 ± 0.043
	BABAR [727]	$0.28 \pm 0.08 \pm 0.01$	$0.205^{+0.046}_{-0.043}$
$\mathcal{B}(B^+ \to X(3872)K^*(892)^+) \times \mathcal{B}(X(3872) \to J/\psi\gamma)$			
	BABAR [727]	$0.07 \pm 0.26 \pm 0.01$	0.07 ± 0.26 <0.48
$\mathcal{B}(B^+ \to X(3872)K^+) \times \mathcal{B}(X(3872) \to \chi_{c1}\gamma)$			
	Belle [718]	<0.19	<0.19 none
$\mathcal{B}(B^+ \to X(3872)K^+) \times \mathcal{B}(X(3872) \to \chi_{c2}\gamma)$			
	Belle [718]	<0.67	<0.67 none

TABLE 147. Product branching fractions to neutral states other than $X(3872)$.

Parameter $[10^{-5}]$	Measurements		Average HFLAV PDG
$\mathcal{B}(B^+ \to \psi_2(3823)K^+) \times \mathcal{B}(\psi_2(3823) \to \chi_{c1}\gamma)$			
	Belle [718]	$0.97 \pm 0.28 \pm 0.11$	0.97 ± 0.30 none
$\mathcal{B}(B^+ \to \psi_2(3823)K^+) \times \mathcal{B}(\psi_2(3823) \to \chi_{c2}\gamma)$			
	Belle [718]	<0.36	<0.36 none
$\mathcal{B}(B^+ \to Y(3940)K^+) \times \mathcal{B}(Y(3940) \to J/\psi\gamma)$			
	BABAR [826]	<1.4	<1.4 none
$\mathcal{B}(B^+ \to Y(3940)K^+) \times \mathcal{B}(Y(3940) \to J/\psi\omega(782))$			
	BABAR [713]	$3.0^{+0.7+0.5}_{-0.6-0.3}$	$3.00^{+0.86}_{-0.67}$ none

(Table continued)

TABLE 147. *(Continued)*

Parameter [10^{-5}]	Measurements		Average HFLAV PDG
$\mathcal{B}(B^+ \to \psi(4260)K^+) \times \mathcal{B}(\psi(4260) \to J/\psi\pi^+\pi^-)$			
	BABAR [827]	$2.0 \pm 0.7 \pm 0.2$	2.00 ± 0.73 <1.56
$\mathcal{B}(B^+ \to \psi(4660)K^+) \times \mathcal{B}(\psi(4660) \to \Lambda_c^+\bar{\Lambda}_c^-)$			
	Belle [824]	<12	<12 none
$\mathcal{B}(B^+ \to Y_\eta K^+) \times \mathcal{B}(Y_\eta \to \Lambda_c^+\bar{\Lambda}_c^-)$			
	Belle [824]	<20	<20 none
$\mathcal{B}(B^+ \to \chi_{c1}(4140)K^+) \times \mathcal{B}(\chi_{c1}(4140) \to J/\psi\phi(1020))$			
	LHCb [815]	$0.57 \pm 0.14^{+0.28}_{-0.21}$ [a,b]	$0.66^{+0.37}_{-0.27}$
	D0 [814]	$0.922 \pm 0.351 \pm 0.358$ [b]	none
$\mathcal{B}(B^+ \to \chi_{c1}(4274)K^+) \times \mathcal{B}(\chi_{c1}(4274) \to J/\psi\phi(1020))$			
	LHCb [815]	$0.312 \pm 0.110^{+0.186}_{-0.149}$ [a,b]	$0.31^{+0.24}_{-0.16}$ $0.36^{+0.22}_{-0.18}$

[a]The quoted value is a fit fraction from a Dalitz plot fit.
[b]Using $\mathcal{B}(B^+ \to J/\psi\phi(1020)K^+)$.

TABLE 148. Product branching fractions to charged states.

Parameter [10^{-5}]	Measurements		Average HFLAV PDG
$\mathcal{B}(B^+ \to X(3872)^+K^0) \times \mathcal{B}(X(3872)^+ \to J/\psi\pi^+\pi^0)$			
	BABAR [770]	<2.2	<2.2 <0.6
$\mathcal{B}(B^+ \to Z_c(4430)^+K^0) \times \mathcal{B}(Z_c(4430)^+ \to J/\psi\pi^+)$			
	BABAR [771]	<1.5	<1.5
$\mathcal{B}(B^+ \to Z_c(4430)^+K^0) \times \mathcal{B}(Z_c(4430)^+ \to \psi(2S)\pi^+)$			
	BABAR [771]	<4.7	<4.7

C. Decays of admixtures of B^0/B^+ mesons

Measurements of B^0/B^+ decays to charmed hadrons are summarized in Secs. VIII C 1 to VIII C 3.

1. Decays to two open charm mesons

Averages of B^0/B^+ decays to two open charm mesons are shown in Table 149.

TABLE 149. Branching fractions for decays to double charm.

Parameter [10^{-4}]	Measurements		Average
$\mathcal{B}(B \to D^0\bar{D}^0K\pi^0)$	Belle [691]	$1.27 \pm 0.31^{+0.22}_{-0.39}$	$1.27^{+0.38}_{-0.50}$

2. Decays to charmonium states

Averages of B^0/B^+ decays to charmonium states are shown in Tables 150–154.

TABLE 150. Decay amplitudes for parallel transverse polarization.

Parameter	Measurements		Average
$A_\parallel(B \to J/\psi K^*)$	LHCb [321]	$0.227 \pm 0.004 \pm 0.011$	0.2219 ± 0.0072
	BABAR [318]	$0.211 \pm 0.010 \pm 0.006$	
	Belle [319]	$0.231 \pm 0.012 \pm 0.008$	
$A_\parallel(B \to \chi_{c1} K^*)$	*BABAR* [318]	$0.2 \pm 0.1 \pm 0.0$	0.200 ± 0.081
$A_\parallel(B \to \psi(2S) K^*)$	*BABAR* [318]	$0.22 \pm 0.06 \pm 0.02$	0.220 ± 0.063

TABLE 151. Decay amplitudes for perpendicular transverse polarization.

Parameter	Measurements		Average
$A_\perp(B \to J/\psi K^*)$	LHCb [321]	$0.201 \pm 0.004 \pm 0.008$	0.2100 ± 0.0063
	BABAR [318]	$0.233 \pm 0.010 \pm 0.005$	
	Belle [319]	$0.195 \pm 0.012 \pm 0.008$	
$A_\perp(B \to \chi_{c1} K^*)$	*BABAR* [318]	$0.03 \pm 0.04 \pm 0.02$	0.030 ± 0.045
$A_\perp(B \to \psi(2S) K^*)$	*BABAR* [318]	$0.3 \pm 0.1 \pm 0.0$	0.300 ± 0.063

TABLE 152. Decay amplitudes for longitudinal polarization.

Parameter	Measurements		Average
$A_0(B \to J/\psi K^*)$	*BABAR* [318]	$0.556 \pm 0.009 \pm 0.010$	0.564 ± 0.010
	Belle [319]	$0.574 \pm 0.012 \pm 0.009$	
$A_0(B \to \chi_{c1} K^*)$	*BABAR* [318]	$0.77 \pm 0.07 \pm 0.04$	0.770 ± 0.081
$A_0(B \to \psi(2S) K^*)$	*BABAR* [318]	$0.48 \pm 0.05 \pm 0.02$	0.480 ± 0.054

TABLE 153. Relative phases of parallel transverse polarization decay amplitudes.

Parameter	Measurements		Average
$\delta_\parallel(B \to J/\psi K^*)$	LHCb [321]	$-2.94 \pm 0.02 \pm 0.03$	-2.932 ± 0.031
	BABAR [318]	$-2.93 \pm 0.08 \pm 0.04$	
	Belle [319]	$-2.887 \pm 0.090 \pm 0.008$	
$\delta_\parallel(B \to \chi_{c1} K^*)$	*BABAR* [318]	$0.0 \pm 0.3 \pm 0.1$	0.00 ± 0.32
$\delta_\parallel(B \to \psi(2S) K^*)$	*BABAR* [318]	$-2.8 \pm 0.4 \pm 0.1$	-2.80 ± 0.41

TABLE 154. Relative phases of perpendicular transverse polarization decay amplitudes.

Parameter	Measurements		Average
$\delta_\perp(B \to J/\psi K^*)$	LHCb [321]	$2.94 \pm 0.02 \pm 0.02$	2.935 ± 0.024
	BABAR [318]	$2.91 \pm 0.05 \pm 0.03$	
	Belle [319]	$2.938 \pm 0.064 \pm 0.010$	
$\delta_\perp(B \to \psi(2S) K^*)$	*BABAR* [318]	$2.8 \pm 0.3 \pm 0.1$	2.80 ± 0.32

3. Decays to exotic states

Averages of B^0/B^+ decays to exotic states are shown in Table 155.

TABLE 155. Branching fractions for decays to X/Y states.

Parameter [10^{-4}]	Measurements		Average HFLAV PDG
$\mathcal{B}(B \to X(3872)K)$	Belle [828]	$2.2 \pm 0.5 \pm 0.6$[a]	$2.16^{+0.97}_{-0.70}$ $2.27^{+0.67}_{-0.70}$
$\mathcal{B}(B \to Y(3940)K) \times \mathcal{B}(Y(3940) \to D^*(2007)^0\bar{D}^*(2007)^0)$	Belle [828]	<0.67	<0.67
$\mathcal{B}(B \to Y(3940)K) \times \mathcal{B}(Y(3940) \to J/\psi\omega(782))$	Belle [829]	$0.71 \pm 0.13 \pm 0.31$	0.71 ± 0.34

[a]Using $\mathcal{B}(X(3872) \to \bar{D}^*(2007)^0 D^0)$.

D. Decays of B_s^0 mesons

Measurements of B_s^0 decays to charmed hadrons are summarized in Secs. VIII D 1 to VIII D 4.

1. Decays to a single open charm meson

Averages of B_s^0 decays to a single open charm meson are shown in Tables 156–159.

TABLE 156. Branching fractions for decays to a $D_s^{(*)}$.

Parameter [10^{-3}]	Measurements		Average HFLAV PDG
$\mathcal{B}(B_s^0 \to D_s^- \pi^+)$	LHCb [830] CDF [645] Belle [35] CDF [831][b] LHCb [647][c], [675][b]	$2.95 \pm 0.05^{+0.25}_{-0.28}$ $2.90 \pm 0.21 \pm 0.43$[a] $3.67^{+0.35}_{-0.33} \pm 0.65$	2.85 ± 0.18 $3.00^{+0.22}_{-0.24}$
$\mathcal{B}(B_s^0 \to D_s^{*-} \pi^+)$	Belle [832] LHCb [833][d]	$2.4^{+0.5}_{-0.4} \pm 0.4$	$2.21^{+0.61}_{-0.54}$ $1.95^{+0.52}_{-0.47}$
$\mathcal{B}(B_s^0 \to D_s^- \rho^+(770))$	Belle [832]	$8.5^{+1.3}_{-1.2} \pm 1.7$	$7.7^{+1.9}_{-1.8}$ 6.9 ± 1.4
$\mathcal{B}(B_s^0 \to D_s^{*-} \rho^+(770))$	Belle [832]	$11.8^{+2.2}_{-2.0} \pm 2.5$	$10.6^{+3.0}_{-2.9}$ $9.6^{+2.1}_{-2.2}$
$\mathcal{B}(B_s^0 \to D_s^- \pi^+ \pi^+ \pi^-)$	CDF [645] LHCb [647] LHCb [677][h,i]	$6.25 \pm 0.60^{+1.48\,e,f}_{-1.46}$ $5.72 \pm 1.05^{+0.67\,g}_{-0.68}$	5.9 ± 1.0 6.1 ± 1.0
$\mathcal{B}(B_s^0 \to D_s^{\mp} K^{\pm})$	LHCb [675] LHCb [830] CDF [831] Belle [35]	$0.2142 \pm 0.0043^{+0.0144\,g}_{-0.0147}$ $0.19 \pm 0.01 \pm 0.02$ $0.276 \pm 0.051 \pm 0.031$[g] $0.24^{+0.12}_{-0.10} \pm 0.04$	0.213 ± 0.014 $0.227^{+0.018}_{-0.019}$
$\mathcal{B}(B_s^0 \to D_s^{*\mp} K^{\pm})$	LHCb [833]	$0.150 \pm 0.011^{+0.042\,j}_{-0.037}$	$0.150^{+0.044}_{-0.038}$ $0.133^{+0.037}_{-0.034}$

(Table continued)

TABLE 156. *(Continued)*

Parameter [10^{-3}]	Measurements		Average HFLAV PDG
$\mathcal{B}(B_s^0 \to D_s^- K^+\pi^+\pi^-)$	LHCb [677]	$0.309 \pm 0.030^{+0.056\,k}_{-0.053}$	$0.308^{+0.066}_{-0.058}$
	LHCb [677][l]		0.319 ± 0.065

[a]Using $\mathcal{B}(B^0 \to D^-\pi^+)$.
[b]Measurement of $\mathcal{B}(B_s^0 \to D_s^{\mp} K^{\pm})/\mathcal{B}(B_s^0 \to D_s^-\pi^+)$ used in our fit.
[c]Measurement of $\mathcal{B}(B_s^0 \to D_s^-\pi^+\pi^+\pi^-)/\mathcal{B}(B_s^0 \to D_s^-\pi^+)$ used in our fit.
[d]Measurement of $\mathcal{B}(B_s^0 \to D_s^{*\mp} K^{\pm})/\mathcal{B}(B_s^0 \to D_s^{*-}\pi^+)$ used in our fit.
[e]Using $f_s/f_d = 0.259 \pm 0.038$ from PDG 2006.
[f]Using $\mathcal{B}(B^0 \to D^-\pi^+\pi^+\pi^-)$.
[g]Using $\mathcal{B}(B_s^0 \to D_s^-\pi^+)$.
[h]Measurement of $\mathcal{B}(B_s^0 \to D_s^- K^+\pi^+\pi^-)/\mathcal{B}(B_s^0 \to D_s^-\pi^+\pi^+\pi^-)$ used in our fit.
[i]Measurement of $\mathcal{B}(B_s^0 \to D_{s1}(2536)^-\pi^+) \times \mathcal{B}(D_{s1}(2536)^+ \to D_s^+\pi^+\pi^-)/\mathcal{B}(B_s^0 \to D_s^-\pi^+\pi^+\pi^-)$ used in our fit.
[j]Using $\mathcal{B}(B_s^0 \to D_s^{*-}\pi^+)$.
[k]Using $\mathcal{B}(B_s^0 \to D_s^-\pi^+\pi^+\pi^-)$.
[l]Measurement of $\mathcal{B}(B^0 \to D_s^- K^+\pi^+\pi^-)/\mathcal{B}(B_s^0 \to D_s^- K^+\pi^+\pi^-)$ used in our fit.

TABLE 157. Branching fractions for decays to a $D^{(*)}$.

Parameter [10^{-4}]	Measurements		Average HFLAV PDG
$\mathcal{B}(B_s^0 \to \bar{D}^0\bar{K}^0)$	LHCb [834]	$4.3 \pm 0.5 \pm 0.5$	4.30 ± 0.71
			4.30 ± 0.86
$\mathcal{B}(B_s^0 \to \bar{D}^*(2007)^0\bar{K}^0)$	LHCb [834]	$2.8 \pm 1.0 \pm 0.4$	2.8 ± 1.1
$\mathcal{B}(B_s^0 \to \bar{D}^0\bar{K}^*(892)^0)$	LHCb [670]	$3.37 \pm 0.30 \pm 0.44$[a]	
	LHCb [664]	$4.54 \pm 1.04 \pm 0.90$[b]	3.61 ± 0.44
	LHCb [670][c]		4.38 ± 0.58
$\mathcal{B}(B_s^0 \to \bar{D}^0\phi(1020))$	LHCb [661]	$0.287 \pm 0.034 \pm 0.022$[d]	
	LHCb [670]	$0.249 \pm 0.047 \pm 0.039$[e]	0.277 ± 0.031
	LHCb [661][f]		0.299 ± 0.047
$\mathcal{B}(B_s^0 \to \bar{D}^*(2007)^0\phi(1020))$	LHCb [661]	$0.355 \pm 0.042 \pm 0.038$[d]	0.348 ± 0.046
	LHCb [661]	$0.341 \pm 0.055 \pm 0.042$[g]	0.370 ± 0.060
$\mathcal{B}(B_s^0 \to D^{*\mp}\pi^{\pm})$	LHCb [835]	<0.061	<0.061
$\mathcal{B}(B_s^0 \to \bar{D}^0 f_0(980))$	LHCb [836]	<0.031	<0.031
$\mathcal{B}(B_s^0 \to \bar{D}^0 K^+K^-)$	LHCb [662]	$7.855 \pm 0.752 \pm 0.688$[d]	7.9 ± 1.0
			0.6 ± 0.1
$\mathcal{B}(B_s^0 \to \bar{D}^0 K^-\pi^+)$	LHCb [660]	$9.97 \pm 0.42 \pm 1.11$[d]	10.0 ± 1.2
			10.4 ± 1.3

[a]Using $\mathcal{B}(B^0 \to \bar{D}^0 K^*(892)^0)$.
[b]Using $\mathcal{B}(B^0 \to \bar{D}^0\rho^0(770))$.
[c]Measurement of $\mathcal{B}(B_s^0 \to \bar{D}^0\phi(1020))/\mathcal{B}(B_s^0 \to \bar{D}^0\bar{K}^*(892)^0)$ used in our fit.
[d]Using $\mathcal{B}(B^0 \to \bar{D}^0\pi^+\pi^-)$.
[e]Using $\mathcal{B}(B_s^0 \to \bar{D}^0\bar{K}^*(892)^0)$.
[f]Measurement of $\mathcal{B}(B_s^0 \to \bar{D}^*(2007)^0\phi(1020))/\mathcal{B}(B_s^0 \to \bar{D}^0\phi(1020))$ used in our fit.
[g]Using $\mathcal{B}(B_s^0 \to \bar{D}^0\phi(1020))$.

TABLE 158. Branching fractions for decays to excited D_s mesons.

Parameter [10^{-5}]	Measurements		Average HFLAV PDG
$\mathcal{B}(B_s^0 \to D_{s1}(2536)^-\pi^+) \times \mathcal{B}(D_{s1}(2536)^+ \to D_s^+\pi^+\pi^-)$			
	LHCb [677]	$2.37 \pm 0.59^{+0.47\,a}_{-0.45}$	$2.37^{+0.81}_{-0.70}$
			2.46 ± 0.78

[a]Using $\mathcal{B}(B_s^0 \to D_s^-\pi^+\pi^+\pi^-)$.

TABLE 159. Longitudinal polarization fraction.

Parameter	Measurements		Average
$f_L(B_s^0 \to \bar{D}^*(2007)^0\phi(1020))$	LHCb [661]	$0.730 \pm 0.150 \pm 0.030$	0.73 ± 0.15

2. Decays to two open charm mesons

Averages of B_s^0 decays to two open charm mesons are shown in Table 160.

TABLE 160. Branching fractions.

Parameter $[10^{-4}]$	Measurements		Average HFLAV / PDG
$\mathcal{B}(B_s^0 \to D_s^+ D_s^-)$	LHCb [688]	$43.8 \pm 2.3 \pm 5.1$[a]	$45.0^{+5.1}_{-5.0}$
	CDF [188]	$49 \pm 6 \pm 9$[b]	44.0 ± 4.8
	Belle [31]	$58^{+11}_{-9} \pm 13$	
	D0 [186][c]		
	LHCb [837][c]		
$\mathcal{B}(B_s^0 \to D_s^{*+} D_s^- + D_s^{*-} D_s^+)$	LHCb [837]	$135 \pm 6 \pm 17$	131 ± 13
	CDF [188]	$113 \pm 12 \pm 21$[b]	139 ± 17
	Belle [31]	$176^{+23}_{-22} \pm 40$	
	D0 [186][c]		
	LHCb [837][c]		
$\mathcal{B}(B_s^0 \to D_s^{*+} D_s^{*-})$	LHCb [837]	$127 \pm 8 \pm 17$	140 ± 15
	CDF [188]	$175 \pm 19 \pm 34$[b]	144 ± 21
	Belle [31]	198^{+33+51}_{-31-50}	
	D0 [186][c]		
	LHCb [837][c]		
$\mathcal{B}(B_s^0 \to D_s^- D^+)$	LHCb [688]	$3.9 \pm 0.6 \pm 0.5$[a]	$3.91^{+0.81}_{-0.76}$
	LHCb [694][d,e]		2.75 ± 0.46
$\mathcal{B}(B_s^0 \to D^+ D^-)$	LHCb [688]	$2.38 \pm 0.44 \pm 0.33$[f]	2.38 ± 0.55
			2.20 ± 0.57
$\mathcal{B}(B_s^0 \to D^0 \bar{D}^0)$	LHCb [688]	$1.82 \pm 0.29 \pm 0.34$[g]	$1.82^{+0.46}_{-0.43}$
			1.90 ± 0.50

[a]Using $\mathcal{B}(B^0 \to D_s^+ D^-)$.
[b]Using $f_s/f_d = 0.269 \pm 0.033$ and $\mathcal{B}(B^0 \to D_s^+ D^-) = (7.2 \pm 0.8) \times 10^{-3}$.
[c]Measurement of $\mathcal{B}(B_s^0 \to D_s^+ D_s^-) + \mathcal{B}(B_s^0 \to D_s^{*+} D_s^- + D_s^{*-} D_s^+) + \mathcal{B}(B_s^0 \to D_s^{*+} D_s^{*-})$ used in our fit.
[d]At CL = 95%.
[e]Measurement of $\mathcal{B}(B_s^0 \to \Lambda_c^+ \bar{\Lambda}_c^-)/\mathcal{B}(B_s^0 \to D_s^- D^+)$ used in our fit.
[f]Using $\mathcal{B}(B^0 \to D^+ D^-)$.
[g]Using $\mathcal{B}(B^+ \to D_s^+ \bar{D}^0)$.

3. Decays to charmonium states

Averages of B_s^0 decays to charmonium states are shown in Tables 161–165.

TABLE 161. Branching fractions for decays to J/ψ, I.

Parameter [10^{-4}]	Measurements		Average HFLAV PDG
$\mathcal{B}(B_s^0 \to J/\psi\phi(1020))$	LHCb [838] Belle [839] CDF [705] CDF [113][a], [840][b] CMS [841][a] D0 [806][b], [842][a], [843][c] LHCb [844][d], [845][a], [845][e,f], [711][b], [846][g]	$10.5 \pm 0.1 \pm 1.0$ $12.5 \pm 0.7 \pm 2.3$ $9.3 \pm 2.8 \pm 1.7$	10.61 ± 0.90 10.78 ± 0.85
$\mathcal{B}(B_s^0 \to J/\psi K^0 K^- \pi^+ + \text{c.c.})$	LHCb [707]	$9.15 \pm 0.65 \pm 0.95$[h]	$9.2^{+1.2}_{-1.1}$ 9.5 ± 1.3
$\mathcal{B}(B_s^0 \to J/\psi\eta)$	LHCb [734] Belle [847] LHCb [736][j]	$4.14 \pm 0.35^{+0.61}_{-0.66}$[i] $5.1 \pm 0.5^{+1.2}_{-0.8}$	$4.58^{+0.56}_{-0.51}$ 3.95 ± 0.70
$\mathcal{B}(B_s^0 \to J/\psi\eta')$	LHCb [734] Belle [847] LHCb [736][k]	$3.76 \pm 0.33^{+0.49}_{-0.45}$[i] $3.71 \pm 0.61^{+0.85}_{-0.60}$	$3.75^{+0.52}_{-0.47}$ $3.34^{+0.42}_{-0.45}$
$\mathcal{B}(B_s^0 \to J/\psi\phi(1020)\phi(1020))$	LHCb [846]	$0.122 \pm 0.013^{+0.012}_{-0.014}$[l]	0.122 ± 0.018 $0.124^{+0.017}_{-0.019}$
$\mathcal{B}(B_s^0 \to J/\psi K_S^0)$	CDF [848][m,n] LHCb [706][o]		0.180 ± 0.023 0.192 ± 0.014
$\mathcal{B}(B_s^0 \to J/\psi \bar{K}^*(892)^0)$	LHCb [232] CDF [848]	$0.417 \pm 0.018 \pm 0.035$ $0.83 \pm 0.12 \pm 0.35$[m]	0.422 ± 0.039 0.414 ± 0.039
$\mathcal{B}(B_s^0 \to J/\psi \bar{K}^0 \pi^+ \pi^-)$	LHCb [707]	<0.44	<0.44
$\mathcal{B}(B_s^0 \to J/\psi \bar{K}^0 K^+ K^-)$	LHCb [707]	<0.120	<0.12

[a]Measurement of $\mathcal{B}(B_s^0 \to J/\psi f_0(980)) \times \mathcal{B}(f_0(980) \to \pi^+\pi^-)/\mathcal{B}(B_s^0 \to J/\psi\phi(1020))/\mathcal{B}(\phi(1020) \to K^+K^-)$ used in our fit.
[b]Measurement of $\mathcal{B}(B_s^0 \to \psi(2S)\phi(1020))/\mathcal{B}(B_s^0 \to J/\psi\phi(1020))$ used in our fit.
[c]Measurement of $\mathcal{B}(B_s^0 \to J/\psi f_2'(1525))\mathcal{B}(f_2'(1525) \to K^+K^-)/\mathcal{B}(B_s^0 \to J/\psi\phi(1020))/\mathcal{B}(\phi(1020) \to K^+K^-)$ used in our fit.
[d]Measurement of $\mathcal{B}(B_s^0 \to J/\psi f_2'(1525))/\mathcal{B}(B_s^0 \to J/\psi\phi(1020))$ used in our fit.
[e]$|m(\pi^+\pi^-) - 980| < 90$ MeV.
[f]Measurement of $\mathcal{B}(B_s^0 \to J/\psi\pi^+\pi^-)/\mathcal{B}(B_s^0 \to J/\psi\phi(1020))/\mathcal{B}(\phi(1020) \to K^+K^-)$ used in our fit.
[g]Measurement of $\mathcal{B}(B_s^0 \to J/\psi\phi(1020)\phi(1020))/\mathcal{B}(B_s^0 \to J/\psi\phi(1020))$ used in our fit.
[h]Using $\mathcal{B}(B^0 \to J/\psi K^0\pi^+\pi^-)$.
[i]Using $\mathcal{B}(B^0 \to J/\psi\rho^0(770))$.
[j]Measurement of $\mathcal{B}(B^0 \to J/\psi\eta)/\mathcal{B}(B_s^0 \to J/\psi\eta)$ used in our fit.
[k]Measurement of $\mathcal{B}(B^0 \to J/\psi\eta')/\mathcal{B}(B_s^0 \to J/\psi\eta')$ used in our fit.
[l]Using $\mathcal{B}(B_s^0 \to J/\psi\phi(1020))$.
[m]Using $f_s/f_d = 0.269 \pm 0.033$.
[n]Measurement of $2\mathcal{B}(B_s^0 \to J/\psi K_S^0)$ used in our fit.
[o]Measurement of $2\mathcal{B}(B_s^0 \to J/\psi K_S^0)/\mathcal{B}(B^0 \to J/\psi K^0)$ used in our fit.

TABLE 162. Branching fractions for decays to J/ψ, II.

Parameter [10^{-5}]	Measurements		Average HFLAV PDG
$\mathcal{B}(B_s^0 \to J/\psi\pi^+\pi^-)$	LHCb [845][a,b], [732][c]		$8.5^{+1.6}_{-1.5}$ 20.9 ± 2.3
$\mathcal{B}(B_s^0 \to J/\psi f_0(980)) \times \mathcal{B}(f_0(980) \to \pi^+\pi^-)$			
	Belle [34]	$11.6^{+3.1+3.0}_{-1.9-3.1}$	
	CDF [113][d]		
	CMS [841][d]		10.8 ± 1.2
	D0 [842][d]		$12.8^{+1.8}_{-1.9}$
	LHCb [845][d], [849][e]		
$\mathcal{B}(B_s^0 \to J/\psi f_0(1370)) \times \mathcal{B}(f_0(1370) \to \pi^+\pi^-)$			
	Belle [34]	$3.4^{+1.1+0.9}_{-1.4-0.8}$	$2.9^{+1.3}_{-1.5}$ $4.5^{+0.7}_{-4.1}$
$\mathcal{B}(B_s^0 \to J/\psi f_1(1285))$	LHCb [738]	$7.202 \pm 1.000^{+0.906\text{f}}_{-1.009}$	7.2 ± 1.4
$\mathcal{B}(B_s^0 \to J/\psi f_2'(1525))$	LHCb [844]	$28.0 \pm 2.9 \pm 3.5$[g]	26.9 ± 4.2
	D0 [843][h]		$26.1^{+5.9}_{-5.4}$
$\mathcal{B}(B_s^0 \to J/\psi f_0(500)) \times \mathcal{B}(f_0(500) \to \pi^+\pi^-)$			
	LHCb [849]	<0.37[i]	<0.37 <0.40
$\mathcal{B}(B_s^0 \to J/\psi p\bar{p})$	LHCb [744]	$0.358 \pm 0.019 \pm 0.033$	0.358 ± 0.038
	LHCb [745]	<0.48	0.358 ± 0.043
$\mathcal{B}(B_s^0 \to J/\psi\gamma)$	LHCb [742]	<0.73	<0.73

[a] $|m(\pi^+\pi^-) - 980| < 90$ MeV.
[b] Measurement of $\mathcal{B}(B_s^0 \to J/\psi\pi^+\pi^-)/\mathcal{B}(B_s^0 \to J/\psi\phi(1020))/\mathcal{B}(\phi(1020) \to K^+K^-)$ used in our fit.
[c] Measurement of $\mathcal{B}(B_s^0 \to \psi(2S)\pi^+\pi^-)/\mathcal{B}(B_s^0 \to J/\psi\pi^+\pi^-)$ used in our fit.
[d] Measurement of $\mathcal{B}(B_s^0 \to J/\psi f_0(980)) \times \mathcal{B}(f_0(980) \to \pi^+\pi^-)/\mathcal{B}(B_s^0 \to J/\psi\phi(1020))/\mathcal{B}(\phi(1020) \to K^+K^-)$ used in our fit.
[e] Measurement of $\mathcal{B}(B_s^0 \to J/\psi f_0(500)) \times \mathcal{B}(f_0(500) \to \pi^+\pi^-)/\mathcal{B}(B_s^0 \to J/\psi f_0(980)) \times \mathcal{B}(f_0(980) \to \pi^+\pi^-)$ used in our fit.
[f] Using $\mathcal{B}(f_1(1285) \to \pi^+\pi^+\pi^-\pi^-)$.
[g] Using $\mathcal{B}(B_s^0 \to J/\psi\phi(1020))$.
[h] Measurement of $\mathcal{B}(B_s^0 \to J/\psi f_2'(1525))\mathcal{B}(f_2'(1525) \to K^+K^-)/\mathcal{B}(B_s^0 \to J/\psi\phi(1020))/\mathcal{B}(\phi(1020) \to K^+K^-)$ used in our fit.
[i] Using $\mathcal{B}(B_s^0 \to J/\psi f_0(980)) \times \mathcal{B}(f_0(980) \to \pi^+\pi^-)$.

TABLE 163. Branching fractions for decays to charmonium other than J/ψ.

Parameter [10^{-4}]	Measurements		Average HFLAV PDG
$\mathcal{B}(B_s^0 \to \psi(2S)\phi(1020))$	LHCb [711]	$5.19 \pm 0.28 \pm 0.51$[a]	
	D0 [806]	$5.8 \pm 1.2 \pm 1.1$[a]	5.28 ± 0.57
	CDF [840]	$5.5 \pm 1.4 \pm 0.9$[a]	5.42 ± 0.56
$\mathcal{B}(B_s^0 \to \psi(2S)K^-\pi^+)$	LHCb [720]	$0.3120 \pm 0.0209 \pm 0.0304$[b]	0.312 ± 0.037
$\mathcal{B}(B_s^0 \to \psi(2S)\bar{K}^*(892)^0)$	LHCb [720]	$0.3255 \pm 0.0345^{+0.0346\text{c}}_{-0.0344}$	$0.326^{+0.049}_{-0.048}$ $0.331^{+0.051}_{-0.052}$
$\mathcal{B}(B_s^0 \to \psi(2S)\pi^+\pi^-)$	LHCb [732]	$0.288 \pm 0.034^{+0.062\text{d}}_{-0.059}$	$0.291^{+0.075}_{-0.065}$ 0.711 ± 0.130

[a] Using $\mathcal{B}(B_s^0 \to J/\psi\phi(1020))$.
[b] Using $\mathcal{B}(B^0 \to \psi(2S)K^+\pi^-)$.
[c] Using $\mathcal{B}(B^0 \to \psi(2S)K^*(892)^0)$.
[d] Using $\mathcal{B}(B_s^0 \to J/\psi\pi^+\pi^-)$.

TABLE 164. Branching fraction ratios.

Parameter	Measurements		Average
$\frac{\mathcal{B}(B_s^0\to\chi_{c2}K^+K^-)}{\mathcal{B}(B_s^0\to\chi_{c1}K^+K^-)}$	LHCb [850]	$0.171 \pm 0.031 \pm 0.010$	0.171 ± 0.033

TABLE 165. Decay amplitudes and relative phases.

Parameter	Measurements		Average
$f_0(B_s^0 \to J/\psi \bar{K}^*(892)^0)$	LHCb [232]	$0.497 \pm 0.025 \pm 0.025$	0.497 ± 0.035
$f_\parallel(B_s^0 \to J/\psi \bar{K}^*(892)^0)$	LHCb [232]	$0.179 \pm 0.027 \pm 0.013$	0.179 ± 0.030
$\delta_\parallel(B_s^0 \to J/\psi \bar{K}^*(892)^0)$	LHCb [232]	$-2.7 \pm 0.2 \pm 0.2$	-2.70 ± 0.25
$\delta_\perp(B_s^0 \to J/\psi \bar{K}^*(892)^0)$	LHCb [232]	$0.01 \pm 0.11^{+0.12}_{-0.13}$	0.01 ± 0.17

4. Decays to charm baryons

Averages of B_s^0 decays to charm baryons are shown in Tables 166,167.

TABLE 166. Branching fractions for decays to one charm baryon.

Parameter [10^{-4}]	Measurements		Average HFLAV / PDG
$\mathcal{B}(B_s^0 \to \bar{\Lambda}_c^- \Lambda^0 \pi^+)$	Belle [851]	$3.6 \pm 1.1^{+0.9}_{-1.0}$	3.6 ± 1.5 3.6 ± 1.6

TABLE 167. Branching fractions for decays to two charm baryons.

Parameter [10^{-4}]	Measurements		Average HFLAV / PDG
$\mathcal{B}(B_s^0 \to \Lambda_c^+ \bar{\Lambda}_c^-)$	LHCb [694]	<1.2[a,b]	<1.2 <0.8

[a]At CL = 95%.
[b]Using $\mathcal{B}(B_s^0 \to D_s^- D^+)$.

E. Decays of B_c^+ mesons

Measurements of B_c^+ decays to charmed hadrons are summarized in Secs. VIII E 1 to VIII E 4.

1. Decays to a single open charm meson

Averages of B_c^+ decays to a single open charm meson are shown in Table 168.

TABLE 168. Branching fractions for decays to one charm meson.

Parameter [10^{-7}]	Measurements		Average
$f_c \times \mathcal{B}(B_c^+ \to D^0 K^+)$	LHCb [852]	$3.79^{+1.14}_{-1.02} \pm 0.25$[a]	$3.8^{+1.2}_{-1.0}$

[a]Using f_u.

2. Decays to two open charm mesons

Averages of B_c^+ decays to two open charm mesons are shown in Table 169.

TABLE 169. Branching fractions for decays to two D mesons.

Parameter $[10^{-6}]$	Measurements	Average
$f_c \times \mathcal{B}(B_c^+ \to D_s^+ \bar{D}^0)$	LHCb [795][a]	$1.2^{+1.5}_{-1.4}$
$f_c \times \mathcal{B}(B_c^+ \to D_s^+ D^0)$	LHCb [795][b]	-1.5 ± 1.0
$f_c \times \mathcal{B}(B_c^+ \to D^+ \bar{D}^0)$	LHCb [795][c]	1.3 ± 1.2
$f_c \times \mathcal{B}(B_c^+ \to D^+ D^0)$	LHCb [795][d]	0.45 ± 0.83
$f_c \times \mathcal{B}(B_c^+ \to D_s^{*+} \bar{D}^0 + D_s^+ \bar{D}^*(2007)^0)$	LHCb [795][e]	-0.4 ± 5.9
$f_c \times \mathcal{B}(B_c^+ \to D_s^{*+} D^0 + D_s^+ D^*(2007)^0)$	LHCb [795][f]	-1.2 ± 7.5
$f_c \times \mathcal{B}(B_c^+ \to D_s^{*+} \bar{D}^*(2007)^0)$	LHCb [795][g]	13 ± 17
$f_c \times \mathcal{B}(B_c^+ \to D_s^{*+} D^*(2007)^0)$	LHCb [795][h]	27 ± 36
$f_c \times (\mathcal{B}(B_c^- \to D^{*-} D^0) \times \mathcal{B}(D^{*-} \to D^-(\pi^0, \gamma)) + \mathcal{B}(B_c^- \to D^- D^{*0}))$	LHCb [795][i]	0.3 ± 5.0
$f_c \times (\mathcal{B}(B_c^- \to D^{*-} \bar{D}^0) \times \mathcal{B}(D^{*-} \to D^-(\pi^0, \gamma)) + \mathcal{B}(B_c^- \to D^- \bar{D}^{*0}))$	LHCb [795][j]	-2.3 ± 2.7
$f_c \times \mathcal{B}(B_c^+ \to D^*(2010)^+ D^*(2007)^0)$	LHCb [795][k]	-6 ± 14
$f_c \times \mathcal{B}(B_c^+ \to D^*(2010)^+ \bar{D}^*(2007)^0)$	LHCb [795][l]	53 ± 36

[a]Measurement of $f_c \times \mathcal{B}(B_c^+ \to D_s^+ \bar{D}^0)/(f_u \mathcal{B}(B^+ \to D_s^+ \bar{D}^0))$ used in our fit.
[b]Measurement of $f_c \times \mathcal{B}(B_c^+ \to D_s^+ D^0)/(f_u \mathcal{B}(B^+ \to D_s^+ \bar{D}^0))$ used in our fit.
[c]Measurement of $f_c \times \mathcal{B}(B_c^+ \to D^+ \bar{D}^0)/(f_u \mathcal{B}(B^+ \to D^+ \bar{D}^0))$ used in our fit.
[d]Measurement of $f_c \times \mathcal{B}(B_c^+ \to D^+ D^0)/(f_u \mathcal{B}(B^+ \to D^+ \bar{D}^0))$ used in our fit.
[e]Measurement of $f_c \times \mathcal{B}(B_c^+ \to D_s^{*+} \bar{D}^0 + D_s^+ \bar{D}^*(2007)^0)/(f_u \mathcal{B}(B^+ \to D_s^+ \bar{D}^0))$ used in our fit.
[f]Measurement of $f_c \times \mathcal{B}(B_c^+ \to D_s^{*+} D^0 + D_s^+ D^*(2007)^0)/(f_u \mathcal{B}(B^+ \to D_s^+ \bar{D}^0))$ used in our fit.
[g]Measurement of $f_c \times \mathcal{B}(B_c^+ \to D_s^{*+} \bar{D}^*(2007)^0)/(f_u \mathcal{B}(B^+ \to D_s^+ \bar{D}^0))$ used in our fit.
[h]Measurement of $f_c \times \mathcal{B}(B_c^+ \to D_s^{*+} D^*(2007)^0)/(f_u \mathcal{B}(B^+ \to D_s^+ \bar{D}^0))$ used in our fit.
[i]Measurement of $f_c \times (\mathcal{B}(B_c^- \to D^{*-} D^0) \times \mathcal{B}(D^{*-} \to D^-(\pi^0, \gamma)) + \mathcal{B}(B_c^- \to D^- D^{*0}))/(f_u \mathcal{B}(B^+ \to D^+ \bar{D}^0))$ used in our fit.
[j]Measurement of $f_c \times (\mathcal{B}(B_c^- \to D^{*-} \bar{D}^0) \times \mathcal{B}(D^{*-} \to D^-(\pi^0, \gamma)) + \mathcal{B}(B_c^- \to D^- \bar{D}^{*0}))/(f_u \mathcal{B}(B^+ \to D^+ \bar{D}^0))$ used in our fit.
[k]Measurement of $f_c \times \mathcal{B}(B_c^+ \to D^*(2010)^+ D^*(2007)^0)/(f_u \mathcal{B}(B^+ \to D^+ \bar{D}^0))$ used in our fit.
[l]Measurement of $f_c \times \mathcal{B}(B_c^+ \to D^*(2010)^+ \bar{D}^*(2007)^0)/(f_u \mathcal{B}(B^+ \to D^+ \bar{D}^0))$ used in our fit.

3. Decays to charmonium states

Averages of B_c^+ decays to charmonium states are shown in Tables 170–171.

TABLE 170. Branching fractions for decays to charmonium.

Parameter [10^{-6}]	Measurements		Average
$f_c \times \mathcal{B}(B_c^+ \to J/\psi\pi^+)$	CMS [805][a] LHCb [807][b,a], [809][c,a]		2.76 ± 0.12
$f_c \times \mathcal{B}(B_c^+ \to \chi_{c0}\pi^+)$	LHCb [853]	$4.00^{+1.39}_{-1.22} \pm 0.33$[d]	$4.0^{+1.4}_{-1.3}$

[a]Measurement of $f_c \times \mathcal{B}(B_c^+ \to J/\psi\pi^+)/(f_u \mathcal{B}(B^+ \to J/\psi K^+))$ used in our fit.
[b]$\sqrt{s} = 7$ TeV, $p_T > 4$ GeV and $2.5 < y < 4.5$.
[c]$\sqrt{s} = 8$ TeV, $0 < p_T < 20$ GeV and $2.0 < y < 4.5$.
[d]Using f_u.

TABLE 171. Branching fraction ratios.

Parameter	Measurements		Average
$\frac{\mathcal{B}(B_c^+ \to J/\psi D_s^+)}{\mathcal{B}(B_c^+ \to J/\psi\pi^+)}$	LHCb [854] ATLAS [855]	$2.9 \pm 0.6 \pm 0.2$ $3.8 \pm 1.1 \pm 0.4$	3.09 ± 0.55
$\frac{\mathcal{B}(B_c^+ \to J/\psi D_s^{*+})}{\mathcal{B}(B_c^+ \to J/\psi D_s^+)}$	ATLAS [855]	$2.8^{+1.2}_{-0.8} \pm 0.3$	$2.8^{+1.2}_{-0.9}$
$\frac{\mathcal{B}(B_c^+ \to J/\psi D_s^{*+})}{\mathcal{B}(B_c^+ \to J/\psi\pi^+)}$	ATLAS [855]	$10.4 \pm 3.1 \pm 1.6$	10.4 ± 3.5
$\frac{\mathcal{B}(B_c^+ \to J/\psi\pi^+\pi^+\pi^-)}{\mathcal{B}(B_c^+ \to J/\psi\pi^+)}$	LHCb [856] CMS [805]	$2.41 \pm 0.30 \pm 0.33$ $2.55 \pm 0.80 \pm 0.33$	2.45 ± 0.40
$\frac{\mathcal{B}(B_c^+ \to J/\psi D^*(2007)^0 K^+)}{\mathcal{B}(B_c^+ \to J/\psi D^0 K^+)}$	LHCb [857]	$5.1 \pm 1.8 \pm 0.4$	5.1 ± 1.8
$\frac{\mathcal{B}(B_c^+ \to J/\psi D^*(2010)^+ K^*(892)^0)}{\mathcal{B}(B_c^+ \to J/\psi D^0 K^+)}$	LHCb [857]	$2.1 \pm 1.1 \pm 0.3$	2.1 ± 1.1
$\frac{\mathcal{B}(B_c^+ \to J/\psi K^+)}{\mathcal{B}(B_c^+ \to J/\psi\pi^+)}$	LHCb [858]	$0.069 \pm 0.019 \pm 0.005$	0.069 ± 0.020
$\frac{\mathcal{B}(B_c^+ \to J/\psi K^+ K^-\pi^+)}{\mathcal{B}(B_c^+ \to J/\psi\pi^+)}$	LHCb [859]	$0.53 \pm 0.10 \pm 0.05$	0.53 ± 0.11
$\frac{\mathcal{B}(B_c^+ \to \psi(2S)\pi^+)}{\mathcal{B}(B_c^+ \to J/\psi\pi^+)}$	LHCb [860]	$0.268 \pm 0.032 \pm 0.009$	0.270 ± 0.033
$\frac{\mathcal{B}(B_c^+ \to J/\psi D^0 K^+)}{\mathcal{B}(B_c^+ \to J/\psi\pi^+)}$	LHCb [857]	$0.432 \pm 0.136 \pm 0.028$	0.43 ± 0.14
$\frac{\mathcal{B}(B_c^+ \to J/\psi D^+ K^*(892)^0)}{\mathcal{B}(B_c^+ \to J/\psi D^0 K^+)}$	LHCb [857]	$0.63 \pm 0.39 \pm 0.08$	0.63 ± 0.40

4. Decays to a B meson

Averages of B_c^+ decays to a B meson are shown in Table 172.

TABLE 172. Branching fractions for decays to B_s^0 meson.

Parameter [10^{-4}]	Measurements		Average
$f_c \times \mathcal{B}(B_c^+ \to B_s^0\pi^+)$	LHCb [861]	$2.323 \pm 0.304^{+0.291}_{-0.271}$[a]	$2.32^{+0.43}_{-0.39}$

[a]Using f_s.

F. Decays of b baryons

Measurements of b baryon decays to charmed hadrons are summarized in Secs. VIII F 1 to VIII F 4.

1. Decays to a single open charm meson

Averages of b baryon decays to a single open charm meson are shown in Table 173.

TABLE 173. Branching fractions for decays to D^0 mesons.

Parameter [10^{-5}]	Measurements		Average HFLAV / PDG
$\mathcal{B}(\Lambda_b^0 \to D^0 p K^-)$	LHCb [862] LHCb [862][b]	$4.28 \pm 0.47^{+0.44}_{-0.48}$[a]	$4.28^{+0.67}_{-0.65}$ $4.60^{+0.77}_{-0.80}$
$\frac{f_{\Xi_b^0}}{f_{\Lambda_b^0}} \times \mathcal{B}(\Xi_b^0 \to D^0 p K^-)$	LHCb [862]	$1.88 \pm 0.39^{+0.39}_{-0.38}$[c]	$1.88^{+0.58}_{-0.51}$ 0.17 ± 0.06

[a]Using $\mathcal{B}(\Lambda_b^0 \to D^0 p\pi^-)$.

[b]Measurement of $\frac{f_{\Xi_b^0}}{f_{\Lambda_b^0}} \times \mathcal{B}(\Xi_b^0 \to D^0 p K^-)/\mathcal{B}(\Lambda_b^0 \to D^0 p K^-)$ used in our fit.

[c]Using $\mathcal{B}(\Lambda_b^0 \to D^0 p K^-)$.

2. Decays to charmonium states

Averages of b baryon decays to charmonium states are shown in Tables 174–177.

TABLE 174. Λ_b^0 branching fractions to charmonium.

Parameter [10^{-4}]	Measurements		Average HFLAV / PDG
$\mathcal{B}(\Lambda_b^0 \to J/\psi p K^-)$	LHCb [863] LHCb [864][a], [865][b,c], [866][d,e,f], [867][g,h]	$3.17 \pm 0.04 \pm 0.08$	3.171 ± 0.088 $3.170^{+0.571}_{-0.452}$
$\mathcal{B}(\Lambda_b^0 \to J/\psi p K^- \pi^+ \pi^-)$	LHCb [865]	$0.6614 \pm 0.0304 \pm 0.0462$[i]	0.661 ± 0.055 $0.661^{+0.130}_{-0.108}$
$\mathcal{B}(\Lambda_b^0 \to J/\psi p \pi^-)$	LHCb [864]	$0.2613 \pm 0.0079 \pm 0.0151$[i]	0.261 ± 0.017 $0.261^{+0.050}_{-0.040}$
$\mathcal{B}(\Lambda_b^0 \to J/\psi \Lambda^0)$	CDF [868] ATLAS [869][j] CDF [870][k] LHCb [871][j]	$4.7 \pm 2.1 \pm 1.9$	$4.7^{+2.8}_{-2.9}$ none
$f_{\Lambda_b^0} \times \mathcal{B}(\Lambda_b^0 \to J/\psi \Lambda^0)$	D0 [872] CDF [870][l]	$0.601 \pm 0.060 \pm 0.064$	0.601 ± 0.088 0.585 ± 0.083
$\mathcal{B}(\Lambda_b^0 \to \psi(2S) p K^-)$	LHCb [865]	$0.656 \pm 0.024 \pm 0.026$[i]	0.656 ± 0.035 $0.075^{+0.016}_{-0.014}$
$\mathcal{B}(\Lambda_b^0 \to \psi(2S) \Lambda^0)$	LHCb [871] ATLAS [869]	$2.421 \pm 0.109^{+1.446}_{-1.466}$[m] $2.365 \pm 0.156^{+1.412}_{-1.432}$[m]	$2.4^{+1.4}_{-1.5}$ none

(Table continued)

TABLE 174. *(Continued)*

Parameter [10^{-4}]	Measurements		Average HFLAV PDG
$\mathcal{B}(\Lambda_b^0 \to \chi_{c1} p K^-)$	LHCb [867]	$0.767 \pm 0.044 \pm 0.054$[i]	0.768 ± 0.060
	LHCb [867][n]		$0.759^{+0.151}_{-0.126}$
$\mathcal{B}(\Lambda_b^0 \to \chi_{c2} p K^-)$	LHCb [867]	$0.786 \pm 0.063 \pm 0.057$[i]	0.785 ± 0.077
	LHCb [867]	$0.784 \pm 0.077 \pm 0.074$[o]	$0.793^{+0.165}_{-0.140}$

[a]Measurement of $\mathcal{B}(\Lambda_b^0 \to J/\psi p\pi^-)/\mathcal{B}(\Lambda_b^0 \to J/\psi p K^-)$ used in our fit.
[b]Measurement of $\mathcal{B}(\Lambda_b^0 \to \psi(2S) p K^-)/\mathcal{B}(\Lambda_b^0 \to J/\psi p K^-)$ used in our fit.
[c]Measurement of $\mathcal{B}(\Lambda_b^0 \to J/\psi p K^- \pi^+ \pi^-)/\mathcal{B}(\Lambda_b^0 \to J/\psi p K^-)$ used in our fit.
[d]Measurement of $\mathcal{B}(\Lambda_b^0 \to P_c(4380)^+ \pi^-)/\mathcal{B}(\Lambda_b^0 \to J/\psi p K^-)$ used in our fit.
[e]Measurement of $\mathcal{B}(\Lambda_b^0 \to P_c(4457)^+ \pi^-)/\mathcal{B}(\Lambda_b^0 \to J/\psi p K^-)$ used in our fit.
[f]Measurement of $\mathcal{B}(\Lambda_b^0 \to Z_c(4200)^- p)/\mathcal{B}(\Lambda_b^0 \to J/\psi p K^-)$ used in our fit.
[g]Measurement of $\mathcal{B}(\Lambda_b^0 \to \chi_{c1} p K^-)/\mathcal{B}(\Lambda_b^0 \to J/\psi p K^-)$ used in our fit.
[h]Measurement of $\mathcal{B}(\Lambda_b^0 \to \chi_{c2} p K^-)/\mathcal{B}(\Lambda_b^0 \to J/\psi p K^-)$ used in our fit.
[i]Using $\mathcal{B}(\Lambda_b^0 \to J/\psi p K^-)$.
[j]Measurement of $\mathcal{B}(\Lambda_b^0 \to \psi(2S)\Lambda^0)/\mathcal{B}(\Lambda_b^0 \to J/\psi \Lambda^0)$ used in our fit.
[k]Measurement of $\frac{f_{\Xi_b^-}}{f_{\Lambda_b^0}} \times \mathcal{B}(\Xi_b^- \to J/\psi \Xi^-)/\mathcal{B}(\Lambda_b^0 \to J/\psi \Lambda^0)$ used in our fit.
[l]Measurement of $f_{\Omega_b^-} \times \mathcal{B}(\Omega_b^- \to J/\psi \Omega^-)/f_{\Lambda_b^0} \times \mathcal{B}(\Lambda_b^0 \to J/\psi \Lambda^0)$ used in our fit.
[m]Using $\mathcal{B}(\Lambda_b^0 \to J/\psi \Lambda^0)$.
[n]Measurement of $\mathcal{B}(\Lambda_b^0 \to \chi_{c2} p K^-)/\mathcal{B}(\Lambda_b^0 \to \chi_{c1} p K^-)$ used in our fit.
[o]Using $\mathcal{B}(\Lambda_b^0 \to \chi_{c1} p K^-)$.

TABLE 175. Ξ_b^- and Ω_b^- branching fractions to charmonium.

Parameter [10^{-5}]	Measurements		Average HFLAV PDG
$\frac{f_{\Xi_b^-}}{f_{\Lambda_b^0}} \times \mathcal{B}(\Xi_b^- \to J/\psi \Xi^-)$	CDF [870]	$7.88^{+1.75+4.73}_{-1.18-4.80}$[a]	$7.9^{+5.3}_{-4.8}$
			$1.0^{+0.3}_{-0.2}$
$f_{\Omega_b^-} \times \mathcal{B}(\Omega_b^- \to J/\psi \Omega^-)$	CDF [870]	$0.270^{+0.102}_{-0.072} \pm 0.046$[b]	$0.27^{+0.12}_{-0.08}$
			$0.29^{+0.11}_{-0.08}$

[a]Using $\mathcal{B}(\Lambda_b^0 \to J/\psi \Lambda^0)$.
[b]Using $f_{\Lambda_b^0} \times \mathcal{B}(\Lambda_b^0 \to J/\psi \Lambda^0)$.

TABLE 176. Parity-violating asymmetry in Λ_b^0 decays to charmonium.

Parameter	Measurements		Average HFLAV PDG
$\alpha(\Lambda_b^0 \to J/\psi \Lambda^0)$	CMS [873]	$-0.14 \pm 0.14 \pm 0.10$	0.07 ± 0.10
	ATLAS [874]	$0.3 \pm 0.2 \pm 0.1$	
	LHCb [875]	$0.050 \pm 0.170 \pm 0.070$	none

TABLE 177. Transverse polarization of Λ_b^0 produced in pp collisions.

Parameter	Measurements		Average HFLAV PDG
$P(\Lambda_b^0 \to J/\psi \Lambda^0)$	LHCb [875]	$0.060 \pm 0.070 \pm 0.020$	0.035 ± 0.055
	CMS [873]	$0.0 \pm 0.1 \pm 0.1$	none

3. Decays to charm baryons

Averages of b baryon decays to charm baryons are shown in Tables 178–181.

TABLE 178. Λ_b branching fractions.

Parameter [10^{-3}]	Measurements		Average HFLAV PDG
$\mathcal{B}(\Lambda_b^0 \to \Lambda_c^+ \pi^-)$	LHCb [876]	$4.3 \pm 0.0 \pm 0.3$	4.45 ± 0.25
	CDF [646]	$8.5 \pm 0.8 \pm 3.0$[a]	4.91 ± 0.39
	CDF [877][b]		
	LHCb [647][b], [862][c,d], [878][e]		
$\mathcal{B}(\Lambda_b^0 \to \Lambda_c^+ \pi^+ \pi^- \pi^-)$	LHCb [647]	$6.36 \pm 0.71 \pm 0.68$[f]	7.15 ± 0.96
	CDF [877]	$13.53 \pm 1.47^{+3.21}_{-2.57}$[f]	7.68 ± 1.13
	CDF [877]	$26.8 \pm 2.9^{+11.5}_{-10.9}$	
	LHCb [647][g,h,i,j]		
$\mathcal{B}(\Lambda_b^0 \to \Lambda_c^+ K^-)$	LHCb [862]	$0.3253 \pm 0.0071 \pm 0.0198$[f]	0.325 ± 0.021
			0.359 ± 0.030
$\mathcal{B}(\Lambda_b^0 \to \Lambda_c^+ p \bar{p} \pi^-)$	LHCb [878]	$0.24031 \pm 0.01024 \pm 0.01975$[f]	$0.240^{+0.023}_{-0.022}$
	LHCb [878][k,l]		0.265 ± 0.029

[a]Using $\mathcal{B}(B^0 \to D^- \pi^+)$.
[b]Measurement of $\mathcal{B}(\Lambda_b^0 \to \Lambda_c^+ \pi^+ \pi^- \pi^-)/\mathcal{B}(\Lambda_b^0 \to \Lambda_c^+ \pi^-)$ used in our fit.
[c]Measurement of $\mathcal{B}(\Lambda_b^0 \to \Lambda_c^+ K^-)/\mathcal{B}(\Lambda_b^0 \to \Lambda_c^+ \pi^-)$ used in our fit.
[d]Measurement of $\mathcal{B}(\Lambda_b^0 \to D^0 p \pi^-)\mathcal{B}(D^0 \to K^- \pi^+)/(\mathcal{B}(\Lambda_b^0 \to \Lambda_c^+ \pi^-)\mathcal{B}(\Lambda_c^+ \to p K^- \pi^+))$ used in our fit.
[e]Measurement of $\mathcal{B}(\Lambda_b^0 \to \Lambda_c^+ p \bar{p} \pi^-)/\mathcal{B}(\Lambda_b^0 \to \Lambda_c^+ \pi^-)$ used in our fit.
[f]Using $\mathcal{B}(\Lambda_b^0 \to \Lambda_c^+ \pi^-)$.
[g]Measurement of $\mathcal{B}(\Lambda_b^0 \to \Sigma_c(2455)^0 \pi^+ \pi^-) \times \mathcal{B}(\Sigma_c(2455)^0 \to \Lambda_c^+ \pi^-)/\mathcal{B}(\Lambda_b^0 \to \Lambda_c^+ \pi^+ \pi^- \pi^-)$ used in our fit.
[h]Measurement of $\mathcal{B}(\Lambda_b^0 \to \Sigma_c(2455)^{++} \pi^- \pi^-) \times \mathcal{B}(\Sigma_c(2455)^{++} \to \Lambda_c^+ \pi^+)/\mathcal{B}(\Lambda_b^0 \to \Lambda_c^+ \pi^+ \pi^- \pi^-)$ used in our fit.
[i]Measurement of $\mathcal{B}(\Lambda_b^0 \to \Lambda_c(2595)^+ \pi^-) \times \mathcal{B}(\Lambda_c(2595)^+ \to \Lambda_c^+ \pi^+ \pi^-)/\mathcal{B}(\Lambda_b^0 \to \Lambda_c^+ \pi^+ \pi^- \pi^-)$ used in our fit.
[j]Measurement of $\mathcal{B}(\Lambda_b^0 \to \Lambda_c(2625)^+ \pi^-) \times \mathcal{B}(\Lambda_c(2625)^+ \to \Lambda_c^+ \pi^+ \pi^-)/\mathcal{B}(\Lambda_b^0 \to \Lambda_c^+ \pi^+ \pi^- \pi^-)$ used in our fit.
[k]Measurement of $\mathcal{B}(\Lambda_b^0 \to \Sigma_c(2455)^0 p \bar{p}) \times \mathcal{B}(\Sigma_c(2455)^0 \to \Lambda_c^+ \pi^-)/\mathcal{B}(\Lambda_b^0 \to \Lambda_c^+ p \bar{p} \pi^-)$ used in our fit.
[l]Measurement of $\mathcal{B}(\Lambda_b^0 \to \Sigma_c(2520)^0 p \bar{p}) \times \mathcal{B}(\Sigma_c(2520)^0 \to \Lambda_c^+ \pi^-)/\mathcal{B}(\Lambda_b^0 \to \Lambda_c^+ p \bar{p} \pi^-)$ used in our fit.

TABLE 179. Ξ_b branching fractions.

Parameter [10^{-4}]	Measurements		Average HFLAV PDG
$\frac{f_{\Xi_b^-}}{f_{\Lambda_b^0}} \times \mathcal{B}(\Xi_b^- \to \Lambda_b^0 \pi^-)$	LHCb [879]	$5.7 \pm 1.8^{+0.8}_{-0.9}$	5.7 ± 2.0

TABLE 180. Branching fraction ratios.

Parameter	Measurements		Average HFLAV PDG
$\frac{\mathcal{B}(\Lambda_b^0 \to \Lambda_c^+ D^-)}{\mathcal{B}(\Lambda_b^0 \to \Lambda_c^+ D_s^-)}$	LHCb [694]	$0.042 \pm 0.003 \pm 0.003$	0.0420 ± 0.0042
			0.0005 ± 0.0001
$\frac{\mathcal{B}(\Lambda_b^0 \to \Lambda_c(2860)^+ \pi^-) \times \mathcal{B}(\Lambda_c(2860)^+ \to D^0 p)}{\mathcal{B}(\Lambda_b^0 \to \Lambda_c(2880)^+ \pi^-) \times \mathcal{B}(\Lambda_c(2880)^+ \to D^0 p)}$	LHCb [880]	$4.51^{+0.51+0.21}_{-0.39-0.45}$	4.51 ± 0.57
			none

(Table continued)

TABLE 180. *(Continued)*

Parameter	Measurements		Average HFLAV PDG
$\frac{\mathcal{B}(\Lambda_b^0 \to \Lambda_c(2940)^+\pi^-) \times \mathcal{B}(\Lambda_c(2940)^+ \to D^0 p)}{\mathcal{B}(\Lambda_b^0 \to \Lambda_c(2880)^+\pi^-) \times \mathcal{B}(\Lambda_c(2880)^+ \to D^0 p)}$	LHCb [880]	$0.83^{+0.31\,+0.18}_{-0.10\,-0.43}$	$0.83^{+0.36}_{-0.45}$ none
$\frac{\mathcal{B}(\Xi_b^0 \to \Lambda_c^+ K^-)}{\mathcal{B}(\Xi_b^0 \to D^0 p K^-)}$	LHCb [862][a]		0.35 ± 0.19 0.00 ± 0.00

[a]Measurement of $\frac{\mathcal{B}(\Xi_b^0 \to \Lambda_c^+ K^-)}{\mathcal{B}(\Xi_b^0 \to D^0 p K^-)} \mathcal{B}(\Lambda_c^+ \to pK^-\pi^+)/\mathcal{B}(D^0 \to K^-\pi^+)$ used in our fit.

TABLE 181. Product branching fractions.

Parameter $[10^{-4}]$	Measurements		Average HFLAV PDG
$\mathcal{B}(\Lambda_b^0 \to \Sigma_c(2455)^0 p\bar{p}) \times \mathcal{B}(\Sigma_c(2455)^0 \to \Lambda_c^+\pi^-)$			
	LHCb [878]	$0.2138 \pm 0.0360^{+0.0251\,a}_{-0.0242}$	$0.214^{+0.045}_{-0.042}$ 0.236 ± 0.050
$\mathcal{B}(\Lambda_b^0 \to \Sigma_c(2520)^0 p\bar{p}) \times \mathcal{B}(\Sigma_c(2520)^0 \to \Lambda_c^+\pi^-)$			
	LHCb [878]	$0.2859 \pm 0.0481^{+0.0434\,a}_{-0.0425}$	$0.286^{+0.067}_{-0.062}$ 0.316 ± 0.073
$\mathcal{B}(\Lambda_b^0 \to \Lambda_c(2595)^+\pi^-) \times \mathcal{B}(\Lambda_c(2595)^+ \to \Lambda_c^+\pi^+\pi^-)$			
	LHCb [647]	$3.15 \pm 1.22^{+0.60\,b}_{-0.51}$	$3.1^{+1.4}_{-1.3}$ $3.4^{+1.5}_{-1.4}$
$\mathcal{B}(\Lambda_b^0 \to \Lambda_c(2625)^+\pi^-) \times \mathcal{B}(\Lambda_c(2625)^+ \to \Lambda_c^+\pi^+\pi^-)$			
	LHCb [647]	$3.08 \pm 1.07 \pm 0.50^{b}$	$3.1^{+1.2}_{-1.1}$ 3.3 ± 1.3
$\mathcal{B}(\Lambda_b^0 \to \Sigma_c(2455)^0\pi^+\pi^-) \times \mathcal{B}(\Sigma_c(2455)^0 \to \Lambda_c^+\pi^-)$			
	LHCb [647]	$5.29 \pm 1.72 \pm 1.11^{b}$	5.3 ± 2.1 5.7 ± 2.2
$\mathcal{B}(\Lambda_b^0 \to \Sigma_c(2455)^{++}\pi^-\pi^-) \times \mathcal{B}(\Sigma_c(2455)^{++} \to \Lambda_c^+\pi^+)$			
	LHCb [647]	$3.00 \pm 1.29 \pm 0.64^{b}$	3.0 ± 1.4 3.2 ± 1.6

[a]Using $\mathcal{B}(\Lambda_b^0 \to \Lambda_c^+ p\bar{p}\pi^-)$.
[b]Using $\mathcal{B}(\Lambda_b^0 \to \Lambda_c^+\pi^+\pi^-\pi^-)$.

4. Decays to exotic states

Averages of b baryon decays to $XYZP$ states are shown in Table 182.

TABLE 182. Branching fractions for decays to pentaquarks.

Parameter $[10^{-4}]$	Measurements		Average HFLAV PDG
$\mathcal{B}(\Lambda_b^0 \to P_c(4380)^+\pi^-)$	LHCb [866]	$0.162 \pm 0.048^{+0.083\,a}_{-0.051}$	$0.162^{+0.095}_{-0.070}$
	LHCb [866]	$0.161 \pm 0.052^{+0.386\,b}_{-0.131}$	none
$\mathcal{B}(\Lambda_b^0 \to P_c(4380)^+K^-)$	LHCb [866][c]		$3.2^{+7.4}_{-1.8}$ 0.3 ± 0.1
$\mathcal{B}(\Lambda_b^0 \to P_c(4457)^+\pi^-)$	LHCb [866]	$0.051^{+0.025\,+0.019\,a}_{-0.019\,-0.016}$	$0.051^{+0.032}_{-0.025}$

(Table continued)

TABLE 182. *(Continued)*

Parameter [10^{-4}]	Measurements		Average HFLAV PDG
	LHCb [866]	$0.051^{+0.025\,+0.088\,\mathrm{d}}_{-0.022\,-0.035}$	none
$\mathcal{B}(\Lambda_b^0 \to P_c(4457)^+ K^-)$	LHCb [866][e]		$1.5^{+2.6}_{-0.9}$ 0.1 ± 0.0
$\mathcal{B}(\Lambda_b^0 \to Z_c(4200)^- p)$	LHCb [866]	$0.244 \pm 0.089^{+0.108\,\mathrm{a}}_{-0.127}$	$0.24^{+0.14}_{-0.15}$ none

[a]Using $\mathcal{B}(\Lambda_b^0 \to J/\psi p K^-)$.
[b]Using $\mathcal{B}(\Lambda_b^0 \to P_c(4380)^+ K^-)$.
[c]Measurement of $\mathcal{B}(\Lambda_b^0 \to P_c(4380)^+ \pi^-)/\mathcal{B}(\Lambda_b^0 \to P_c(4380)^+ K^-)$ used in our fit.
[d]Using $\mathcal{B}(\Lambda_b^0 \to P_c(4457)^+ K^-)$.
[e]Measurement of $\mathcal{B}(\Lambda_b^0 \to P_c(4457)^+ \pi^-)/\mathcal{B}(\Lambda_b^0 \to P_c(4457)^+ K^-)$ used in our fit.

IX. *b*-HADRON DECAYS TO CHARMLESS FINAL STATES

This section provides branching fractions (BF), polarization fractions, partial rate asymmetries (A_{CP}) and other observables of b-hadron decays to final states that do not contain charm hadrons or charmonium mesons,[33] except for a few lepton-flavor- and lepton-number-violating decays reported in Sec. IX F. Four categories of B^0 and B^+ decays are reported: mesonic (i.e., final states containing only mesons), baryonic (hadronic final states with baryon-antibaryon pairs), radiative (including a photon or a lepton-antilepton pair) and semileptonic/leptonic (including/only leptons). We also report measurements of B_s^0, B_c^+ and b-baryon decays, and measurements of final-state polarization in b-hadron decays. Results of CKM-matrix parameters obtained from A_{CP} measurements are listed and described in Sec. VI. As discussed in Sec. II, measurements included in our averages are those supported with public notes, including journal papers, conference contributed papers, preprints or conference proceedings, except when a result has not led to a journal publication after an extended period of time.

The largest improvements since our last report [1] have come from a variety of new measurements from the LHC, especially LHCb. Also, the first results from Belle II are included.

The averaging procedure follows the methodology described in Sec. III. We perform fits of the full likelihood function and do not use the approximation described in Sec. III A. For the cases where more than one measurement is available, in total 235 fits are performed, with on average (maximally) 1.3 (20) parameters and 2.9 (23) measurements per fit. Systematic uncertainties are taken as quoted without the scaling of multiplicative uncertainties discussed in Sec. III C. In our tables, the individual measurements and average of each parameter p_j are shown in one row. We quote numerical values of all direct measurements of a parameter p_j. We also show numerical values derived from measurements of branching-fraction ratios p_j/p_k, performed with respect to the branching fraction p_k of a normalization mode, as well as measurements of products $p_j p_k$ of the branching fraction of interest with that of a daughter decay. In these cases, the quoted value and uncertainty of the measurement are determined with the fitted value of p_k, and the uncertainty of p_k is included in the systematic uncertainty. A footnote "Using p_k" is added in these cases. Note that the fit uses p_j/p_k or $p_j p_k$ directly and not the derived value of p_j, which is quoted in our table in order to give a sense of the contribution of the measurement to the average. When the measurement depends on p_j in some other way, it is also included in our fit for p_j, but in the tables no derived value is shown. Instead, the measured function f of parameters is given in a footnote "Measurement of f used in our fit." Where available, correlations between measurements are taken into account. We consider correlations not only between measurements of the same parameter, as done in our previous publication [1], but also among parameters. The correlation coefficients among parameters are quoted in our web page [881].

If one or more experiments report a BF measurement with a significance of more than three standard deviations (σ), all available central values for that BF are used in our average. For BFs that do not satisfy this criterion, the most stringent limit is used. Quoted upper limits are at 90% confidence level (CL), unless mentioned otherwise. For observables that are not BFs, such as A_{CP} or polarization fractions, we include in our averages all the available results, regardless of their significance. Most of the branching fractions from *BABAR* and Belle assume equal production of charged and neutral B-meson pairs. The best measurements to date show that this is still a reasonable approximation (see Sec. IV), and we make no correction for

[33]The treatment of intermediate charm or charmonium states differs between observables and sometimes among results for the same observable. In the latter case, when these results are averaged, we indicate the differences by footnotes.

it. At the end of some of the sections we list results that were not included in the tables. Typical cases are measurements of distributions, such as differential branching fractions or longitudinal polarizations, which are measured in different binning schemes by the different collaborations, and thus cannot be directly used to obtain averages.

Observables obtained by Dalitz-plot analyses are marked by footnotes. In these analyses, different experimental collaborations often use different models, in particular for the nonresonant component. When it applies we detail the model used for the nonresonant component in a footnote. In addition to this, Dalitz-plot analyses often yield multiple solutions. In this case, we take the results corresponding to the global minimum and follow the conclusions of the papers.

The order of entries in the tables of this section corresponds in most cases to that in the 2021 Review of Particle Physics (PDG 2021) [9]. In most of the tables the averages are compared to those from PDG 2021. When this is done, the "Average" column quotes the PDG averages (in green) only if they differ from ours. In general, this is due to different input parameters, differences in the averaging methods and different rounding conventions. Unlike the PDG, no error scaling is applied in our averages when the fit χ^2 is greater than 1. On the other hand, the fit p-value is quoted if it is below 1%. Input values that appear in red are not included in the PDG 2021 average. They are new results published since the closing of PDG 2021 and before the closing of this report in June 2021. Input values in blue are results that were unpublished at the closing of this report (unpublished results are never included in the PDG averages).

Sections IX A and IX B provide compilations of branching fractions of B^0 and B^+ to mesonic and baryonic charmless final states, respectively. Sections IX C and IX D give branching fractions of b-baryon and B_s^0-meson charmless decays, respectively. In Sec. IX F observables of interest are given for radiative decays and FCNC decays with leptons of B^0 and B^+ mesons, including limits from searches for lepton-flavor/number-violating decays. Sections IX G and IX H give CP asymmetries and results of polarization measurements, respectively, in various b-hadron charmless decays. Finally, Sec. IX E gives branching fractions of B_c^+ meson decays to charmless final states.

TABLE 183. Branching fractions of charmless mesonic B^+ decays with strange mesons (part 1).

Parameter [10^{-6}]	Measurements		Average HFLAV / PDG
$\mathcal{B}(B^+ \to K^0\pi^+)$[a]	Belle [882]	$23.97 \pm 0.53 \pm 0.71$	23.5±0.7 23.7±0.8
	BABAR [400]	$23.9 \pm 1.1 \pm 1.0$	
	Belle II [883]	$21.4^{+2.3}_{-2.2} \pm 1.6$	
	CLEO [884]	$18.8^{+3.7+2.1}_{-3.3-1.8}$	
	LHCb [885][b]		
$\mathcal{B}(B^+ \to K^+\pi^0)$	Belle [882]	$12.62 \pm 0.31 \pm 0.56$	12.9 ± 0.5
	BABAR [886]	$13.6 \pm 0.6 \pm 0.7$	
	Belle II [887]	$11.9^{+1.1}_{-1.0} \pm 1.6$	
	CLEO [884]	$12.9^{+2.4+1.2}_{-2.2-1.1}$	
$\mathcal{B}(B^+ \to \eta' K^+)$	*BABAR* [888]	$71.5 \pm 1.3 \pm 3.2$	68.9±2.3 70.4±2.5
	Belle [889]	$69.2 \pm 2.2 \pm 3.7$	
	Belle II [890]	$63.4^{+3.4}_{-3.3} \pm 3.4$	
	Belle [891]	$61^{+10}_{-8} \pm 1$	
	CLEO [892]	$80^{+10}_{-9} \pm 7$	
	LHCb [893][c]		
$\mathcal{B}(B^+ \to \eta' K^*(892)^+)$	*BABAR* [894]	$4.8^{+1.6}_{-1.4} \pm 0.8$	$4.8^{+1.8}_{-1.6}$
	Belle [895]	<2.9	
$\mathcal{B}(B^+ \to \eta'(K\pi)_0^{*+})$	*BABAR* [894]	$6.0^{+2.2}_{-2.0} \pm 0.9$	6.0 ± 2.3 none
$\mathcal{B}(B^+ \to \eta' K_0^*(1430)^+)$	*BABAR* [894]	$5.2 \pm 1.9 \pm 1.0$[d]	5.2 ± 2.1
$\mathcal{B}(B^+ \to \eta' K_2^*(1430)^+)$	*BABAR* [894]	$28.0^{+4.6}_{-4.3} \pm 2.6$	28.0 ± 5.2 $28.0^{+5.3}_{-5.0}$

[a]The PDG average is a result of a fit including input from other measurements.
[b]Measurement of $\mathcal{B}(B^+ \to K^+\bar{K}^0)/\mathcal{B}(B^+ \to K^0\pi^+)$ used in our fit.
[c]Measurement of $\mathcal{B}(B_s^0 \to \eta'\eta')/\mathcal{B}(B^+ \to \eta' K^+)$ used in our fit.
[d]Multiple systematic uncertainties are added in quadrature.

A. Mesonic decays of B^+ and B^0 mesons

This section provides branching fractions of charmless mesonic decays. Tables 183–192 to are for B^+ and Tables 193–206 to are for B^0 mesons. For both, decay modes with and without strange mesons in the final state appear in different tables. Finally, Tables 207 and 208 detail several relative branching fractions of B^+ and B^0 decays, respectively. Figure 69 gives a graphic representation of a selection of high-precision branching fractions given in this section.

TABLE 184. Branching fractions of charmless mesonic B^+ decays with strange mesons (part 2).

Parameter [10^{-6}]	Measurements		Average HFLAV PDG
$\mathcal{B}(B^+ \to \eta K^+)$[a]	Belle [896]	$2.12 \pm 0.23 \pm 0.11$	2.36 ± 0.21
	BABAR [888]	$2.94^{+0.39}_{-0.34} \pm 0.21$	$2.36^{+0.38}_{-0.37}$
	CLEO [892]	$2.2^{+2.8}_{-2.2}$	
$\mathcal{B}(B^+ \to \eta K^*(892)^+)$	*BABAR* [897]	$18.9 \pm 1.8 \pm 1.3$	19.3 ± 1.6
	Belle [898]	$19.3^{+2.0}_{-1.9} \pm 1.5$	
	CLEO [892]	$26.4^{+9.6}_{-8.2} \pm 3.3$	
$\mathcal{B}(B^+ \to \eta (K\pi)_0^{*+})$	*BABAR* [897]	$18.2 \pm 2.6 \pm 2.6$	18.2 ± 3.7 none
$\mathcal{B}(B^+ \to \eta K_0^*(1430)^+)$[b]	*BABAR* [897]	$12.9 \pm 1.8 \pm 1.8$[c]	12.9 ± 2.5 18.2 ± 3.7
$\mathcal{B}(B^+ \to \eta K_2^*(1430)^+)$	*BABAR* [897]	$9.1 \pm 2.7 \pm 1.4$	9.1 ± 3.0
$\mathcal{B}(B^+ \to \eta(1295)K^+) \times \mathcal{B}(\eta(1295) \to \eta\pi\pi)$	*BABAR* [899]	$2.9^{+0.8}_{-0.7} \pm 0.2$	$2.9^{+0.8}_{-0.7}$
$\mathcal{B}(B^+ \to \eta(1405)K^+) \times \mathcal{B}(\eta(1405) \to \eta\pi\pi)$	*BABAR* [899]	<1.3	<1.3
$\mathcal{B}(B^+ \to \eta(1405)K^+) \times \mathcal{B}(\eta(1405) \to K^*K)$	*BABAR* [899]	<1.2	<1.2
$\mathcal{B}(B^+ \to \eta(1475)K^+) \times \mathcal{B}(\eta(1475) \to K^*K)$	*BABAR* [899]	$13.8^{+1.8+1.0}_{-1.7-0.6}$	$13.8^{+2.1}_{-1.8}$
$\mathcal{B}(B^+ \to f_1(1285)K^+) \times \mathcal{B}(f_1(1285) \to \eta\pi\pi)$	*BABAR* [899]	<0.8	<0.80 none
$\mathcal{B}(B^+ \to f_1(1420)K^+) \times \mathcal{B}(f_1(1420) \to \eta\pi\pi)$	*BABAR* [899]	<2.9	<2.9
$\mathcal{B}(B^+ \to f_1(1420)K^+) \times \mathcal{B}(f_1(1420) \to K^*K)$	*BABAR* [899]	<4.1	<4.1
$\mathcal{B}(B^+ \to \phi(1680)K^+) \times \mathcal{B}(\phi(1680) \to K^*K)$	*BABAR* [899]	<3.4	<3.4
$\mathcal{B}(B^+ \to f_0(1500)K^+)$	*BABAR* [262]	$17 \pm 4 \pm 12$[d]	17 ± 12
	BABAR [262]	$20 \pm 10 \pm 27$[e]	4 ± 2
$\mathcal{B}(B^+ \to \omega(782)K^+)$[f]	Belle [385]	$6.8 \pm 0.4 \pm 0.4$	6.47 ± 0.40
	BABAR [900]	$6.3 \pm 0.5 \pm 0.3$	
	CLEO [901]	$3.2^{+2.4}_{-1.9} \pm 0.8$	
$\mathcal{B}(B^+ \to \omega(782)K^*(892)^+)$	*BABAR* [902]	<7.4	<7.4
$\mathcal{B}(B^+ \to \omega(782)(K\pi)_0^{*+})$	*BABAR* [902]	$27.5 \pm 3.0 \pm 2.6$	27.5 ± 4.0
$\mathcal{B}(B^+ \to \omega(782)K_0^*(1430)^+)$	*BABAR* [902]	$24.0 \pm 2.6 \pm 4.4$	24.0 ± 5.1
$\mathcal{B}(B^+ \to \omega(782)K_2^*(1430)^+)$	*BABAR* [902]	$21.5 \pm 3.6 \pm 2.4$	21.5 ± 4.3
$\mathcal{B}(B^+ \to a_0(980)^+K^0) \times \mathcal{B}(a_0(980)^+ \to \eta\pi^+)$	*BABAR* [903]	<3.9	<3.9
$\mathcal{B}(B^+ \to a_0(980)^0K^+) \times \mathcal{B}(a_0(980)^0 \to \eta\pi^0)$	*BABAR* [903]	<2.5	<2.5

[a]The PDG uncertainty includes a scale factor.
[b]The PDG entry corresponds to $\mathcal{B}(B^+ \to \eta(K\pi)_0^{*+})$.
[c]Multiple systematic uncertainties are added in quadrature.
[d]Result extracted from Dalitz-plot analysis of $B^+ \to K^+K^+K^-$ decays.
[e]Result extracted from Dalitz-plot analysis of $B^+ \to K_S^0K_S^0K^+$ decays.
[f]The measurement from the Dalitz-plot analysis of $B^+ \to K^+\pi^+\pi^-$ decays [269] was not included in this average. It is quoted as a separate entry.

TABLE 185. Branching fractions of charmless mesonic B^+ decays with strange mesons (part 3).

Parameter [10^{-6}]	Measurements		Average HFLAV PDG
$\mathcal{B}(B^+ \to K^*(892)^0\pi^+)$	*BABAR* [269]	$10.8 \pm 0.6^{+1.2}_{-1.4}$ [a]	10.4 ± 0.8
	Belle [267]	$9.67 \pm 0.64^{+0.81}_{-0.89}$ [a]	10.1 ± 0.8
	BABAR [904]	$14.6 \pm 2.4^{+1.4}_{-1.5}$ [b,c]	
$\mathcal{B}(B^+ \to K^*(892)^+\pi^0)$	*BABAR* [904]	$9.2 \pm 1.3^{+0.7}_{-0.8}$ [b,c]	8.8 ± 1.2
	BABAR [905]	$8.2 \pm 1.5 \pm 1.1$	6.8 ± 0.9
	CLEO [901]	$7.1^{+11.4}_{-7.1} \pm 1.0$	
$\mathcal{B}(B^+ \to K^+\pi^+\pi^-)$	LHCb [906]	$56.05 \pm 0.36 \pm 1.51$ [d]	55.7 ± 1.4
	BABAR [269]	$54.4 \pm 1.1 \pm 4.6$ [a]	51.0 ± 2.9
	Belle [267]	$48.8 \pm 1.1 \pm 3.6$ [a]	
$\mathcal{B}(B^+ \to K^+\pi^+\pi^-(\mathrm{NR}))$	*BABAR* [269]	$9.3 \pm 1.0^{+6.9}_{-1.7}$ [a,e]	$16.3^{+2.0}_{-1.8}$
	Belle [267]	$16.9 \pm 1.3^{+1.7}_{-1.6}$ [a] $16.3^{+2.1}_{-1.5}$	$16.3^{+2.1}_{-1.5}$
$\mathcal{B}(B^+ \to \omega(782)K^+(K^+\pi^+\pi^-))$ [f]	*BABAR* [269]	$5.9^{+8.8}_{-9.0}{}^{+0.5}_{-0.4}$ [a]	5.9 ± 8.9
			$5.9^{+8.8}_{-9.0}$
$\mathcal{B}(B^+ \to f_0(980)K^+) \times \mathcal{B}(f_0(980) \to \pi^+\pi^-)$	*BABAR* [269]	$10.3 \pm 0.5^{+2.0}_{-1.4}$ [a]	$9.40^{+0.84}_{-0.92}$
	Belle [267]	$8.78 \pm 0.82^{+0.85}_{-1.76}$ [a]	$9.40^{+1.02}_{-1.18}$
$\mathcal{B}(B^+ \to f_2(1270)K^+)$	Belle [267]	$1.33 \pm 0.30^{+0.23}_{-0.34}$ [a]	1.07 ± 0.31
	BABAR [269]	$0.89^{+0.38}_{-0.33}{}^{+0.01}_{-0.03}$ [a]	1.07 ± 0.27
$\mathcal{B}(B^+ \to f_0(1370)K^+) \times \mathcal{B}(f_0(1370) \to \pi^+\pi^-)$	*BABAR* [268]	<10.7 [a]	<11
$\mathcal{B}(B^+ \to \rho(1450)^0K^+) \times \mathcal{B}(\rho(1450)^0 \to \pi^+\pi^-)$	*BABAR* [268]	<11.7 [a]	<12
$\mathcal{B}(B^+ \to f_2'(1525)K^+) \times \mathcal{B}(f_2'(1525) \to \pi^+\pi^-)$	*BABAR* [268]	<3.4 [a]	<3.4
$\mathcal{B}(B^+ \to \rho^0(770)K^+)$	*BABAR* [269]	$3.56 \pm 0.45^{+0.57}_{-0.46}$ [a]	3.74 ± 0.47
	Belle [267]	$3.89 \pm 0.47^{+0.43}_{-0.41}$ [a]	$3.74^{+0.48}_{-0.45}$
$\mathcal{B}(B^+ \to K_0^*(1430)^0\pi^+)$ [g]	*BABAR* [269]	$32.0 \pm 1.2^{+10.8}_{-6.0}$ [a]	46.9 ± 5.0
	Belle [267]	$51.6 \pm 1.7^{+7.0}_{-7.5}$ [a]	$39.0^{+5.7}_{-5.0}$
	BABAR [904]	$50.0 \pm 4.8^{+6.7}_{-6.6}$ [b,c]	
$\mathcal{B}(B^+ \to K_2^*(1430)^0\pi^+)$	*BABAR* [269]	$5.6 \pm 1.2^{+1.8}_{-0.8}$ [a]	$5.6^{+2.2}_{-1.4}$
	Belle [263]	<6.9 [a]	$5.6^{+2.2}_{-1.5}$
$\mathcal{B}(B^+ \to K^*(1410)^0\pi^+)$	Belle [263]	<45.0 [a]	<45
$\mathcal{B}(B^+ \to K^*(1680)^0\pi^+)$	Belle [263]	<12.0 [a]	<12
	BABAR [268]	<15.0 [a]	

[a]Result extracted from Dalitz-plot analysis of $B^+ \to K^+\pi^+\pi^-$ decays.
[b]Result extracted from Dalitz-plot analysis of $B^+ \to K^0_S\pi^+\pi^0$ decays.
[c]Multiple systematic uncertainties are added in quadrature.
[d]Using $\mathcal{B}(B^+ \to K^+K^+K^-)$.
[e]The total nonresonant contribution is obtained by combining an exponential nonresonant component with the effective-range part of the LASS lineshape.
[f]This result was not included in the main entry of $\mathcal{B}(B^+ \to \omega(782)K^+)$.
[g]The PDG uncertainty includes a scale factor.

TABLE 186. Branching fractions of charmless mesonic B^+ decays with strange mesons (part 4).

Parameter [10^{-6}]	Measurements		Average $^{\text{HFLAV}}_{\text{PDG}}$
$\mathcal{B}(B^+ \to K^+\pi^0\pi^0)$	*BABAR* [905]	$16.2 \pm 1.2 \pm 1.5$	16.2 ± 1.9
$\mathcal{B}(B^+ \to f_0(980)K^+) \times \mathcal{B}(f_0(980) \to \pi^0\pi^0)$			
	BABAR [905]	$2.8 \pm 0.6 \pm 0.5$	$2.8 \pm 0.6 \pm 0.5$
$\mathcal{B}(B^+ \to K^-\pi^+\pi^+)$	LHCb [907]	<0.046	<0.046
	BABAR [908]	<0.95	
	Belle [909]	<4.5	
$\mathcal{B}(B^+ \to K^-\pi^+\pi^+(\text{NR}))$	CLEO [910]	<56	<56
$\mathcal{B}(B^+ \to K_1(1270)^0\pi^+)$	*BABAR* [420]	<40	<40
$\mathcal{B}(B^+ \to K_1(1400)^0\pi^+)$	*BABAR* [420]	<39	<39
$\mathcal{B}(B^+ \to K^0\pi^+\pi^0)$	CLEO [911]	<66.0	<66
$\mathcal{B}(B^+ \to K_0^*(1430)^+\pi^0)$	*BABAR* [904]	$17.2 \pm 2.4^{+1.5\,\text{a,b}}_{-3.0}$	$17.2^{+2.8}_{-3.8}$ $11.9^{+2.0}_{-2.3}$
$\mathcal{B}(B^+ \to \rho^+(770)K^0)$	*BABAR* [904]	$9.4 \pm 1.6^{+1.1\,\text{a,b}}_{-2.8}$	$9.4^{+1.9}_{-3.2}$ $7.3^{+1.0}_{-1.2}$
$\mathcal{B}(B^+ \to K^*(892)^+\pi^+\pi^-)$	*BABAR* [912]	$75.3 \pm 6.0 \pm 8.1$	75 ± 10
$\mathcal{B}(B^+ \to K^*(892)^+\rho^0(770))$	*BABAR* [913]	$4.6 \pm 1.0 \pm 0.4$	4.6 ± 1.1
$\mathcal{B}(B^+ \to f_0(980)K^*(892)^+) \times \mathcal{B}(f_0(980) \to \pi^+\pi^-)$			
	BABAR [913]	$4.2 \pm 0.6 \pm 0.3$	4.2 ± 0.7
$\mathcal{B}(B^+ \to a_1(1260)^+K^0)$	*BABAR* [914]	$34.9 \pm 5.0 \pm 4.4$	34.9 ± 6.7
$\mathcal{B}(B^+ \to b_1(1235)^+K^0) \times \mathcal{B}(b_1(1235)^0 \to \omega(782)\pi^+)$			
	BABAR [918]	$9.6 \pm 1.7 \pm 0.9$	9.6 ± 1.9
$\mathcal{B}(B^+ \to K^*(892)^0\rho^+(770))$	*BABAR* [915]	$9.6 \pm 1.7 \pm 1.5$	9.2 ± 1.5
	Belle [916]	$8.9 \pm 1.7 \pm 1.2^{\text{c}}$	
$\mathcal{B}(B^+ \to K_1(1400)^+\rho^0(770))$	ARGUS [917]	<780	<780
$\mathcal{B}(B^+ \to K_2^*(1430)^+\rho^0(770))$	ARGUS [917]	<1500	<1500
$\mathcal{B}(B^+ \to b_1(1235)^0K^+) \times \mathcal{B}(b_1(1235)^0 \to \omega(782)\pi^0)$			
	BABAR [919]	$9.1 \pm 1.7 \pm 1.0$	9.1 ± 2.0
$\mathcal{B}(B^+ \to b_1(1235)^+K^*(892)^0) \times \mathcal{B}(b_1(1235)^+ \to \omega(782)\pi^+)$			
	BABAR [920]	<5.9	<5.9
$\mathcal{B}(B^+ \to b_1(1235)^0K^*(892)^+) \times \mathcal{B}(b_1(1235)^0 \to \omega(782)\pi^0)$			
	BABAR [920]	<6.7	<6.7

[a]Result extracted from Dalitz-plot analysis of $B^+ \to K_S^0\pi^+\pi^0$ decays.
[b]Multiple systematic uncertainties are added in quadrature.
[c]See also Ref. [921].

TABLE 187. Branching fractions of charmless mesonic B^+ decays with strange mesons (part 5).

Parameter [10^{-6}]	Measurements		Average HFLAV / PDG
$\mathcal{B}(B^+ \to K^+\bar{K}^0)$[a]	Belle [882]	$1.11 \pm 0.19 \pm 0.05$	1.31 ± 0.14
	LHCb [885]	$1.51 \pm 0.21 \pm 0.10$[b]	1.31 ± 0.17
	BABAR [400]	$1.61 \pm 0.44 \pm 0.09$	
$\mathcal{B}(B^+ \to \bar{K}^0 K^+ \pi^0)$	CLEO [911]	<24.0	<24
$\mathcal{B}(B^+ \to K^+ K_S^0 K_S^0)$[c]	Belle [922]	$10.42 \pm 0.43 \pm 0.22$	10.29 ± 0.37
	BABAR [262]	$10.1 \pm 0.5 \pm 0.3$[d,e]	10.49 ± 0.37
$\mathcal{B}(B^+ \to f_0(980)K^+) \times \mathcal{B}(f_0(980) \to K_S^0 K_S^0)$			
	BABAR [262]	$14.7 \pm 2.8 \pm 1.8$[d]	14.7 ± 3.3
$\mathcal{B}(B^+ \to f_0(1710)K^+) \times \mathcal{B}(f_0(1710) \to K_S^0 K_S^0)$			
	BABAR [262]	$0.48^{+0.40}_{-0.24} \pm 0.11$[d]	$0.48^{+0.41}_{-0.26}$
$\mathcal{B}(B^+ \to K^+ K_S^0 K_S^0(\mathrm{NR}))$	*BABAR* [262]	$19.8 \pm 3.7 \pm 2.5$[f]	19.8 ± 4.5
$\mathcal{B}(B^+ \to K_S^0 K_S^0 \pi^+)$	*BABAR* [923]	<0.51	<0.51
	Belle [922]	<0.87	
$\mathcal{B}(B^+ \to K^+ K^- \pi^+)$	LHCb [906]	$4.97 \pm 0.13 \pm 0.29$[g]	5.06 ± 0.26
	Belle [924]	$5.38 \pm 0.40 \pm 0.35$[h]	5.24 ± 0.42
	BABAR [925]	$5.0 \pm 0.5 \pm 0.5$	
$\mathcal{B}(B^+ \to K^+ K^- \pi^+(\mathrm{NR}))$	LHCb [926]	$1.625 \pm 0.075 \pm 0.221$[i,j]	$1.62^{+0.24}_{-0.23}$ 1.68 ± 0.26
$\mathcal{B}(B^+ \to \bar{K}^*(892)^0 K^+)$	*BABAR* [927]	<1.1	$0.57^{+0.07}_{-0.06}$
	LHCb [926][k,l]		0.59 ± 0.08
$\mathcal{B}(B^+ \to \bar{K}_0^*(1430)^0 K^+)$	*BABAR* [927]	<2.2	$0.37^{+0.13}_{-0.12}$
	LHCb [926][k,m]		0.38 ± 0.13

[a]The PDG average is a result of a fit including input from other measurements.
[b]Using $\mathcal{B}(B^+ \to K^0\pi^+)$.
[c]PDG uses the *BABAR* result including the χ_{c0} intermediate state.
[d]Result extracted from Dalitz-plot analysis of $B^+ \to K_S^0 K_S^0 K^+$ decays.
[e]All charmonium resonances are vetoed. The analysis also reports $\mathcal{B}(B^+ \to K_S^0 K_S^0 K^+) = (10.6 \pm 0.5 \pm 0.3) \times 10^{-6}$ including the χ_{c0} intermediate state.
[f]The nonresonant amplitude is modeled using a polynomial function of order 2.
[g]Using $\mathcal{B}(B^+ \to K^+K^+K^-)$.
[h]Also measured in bins of $m_{K^+K^-}$.
[i]LHCb uses a model of nonresonant obtained from a phenomenological description of the partonic interaction that produces the final state. This contribution is called single pole in the paper, see Ref. [926] for details.
[j]Using $\mathcal{B}(B^+ \to K^+K^-\pi^+)$.
[k]Result extracted from Dalitz-plot analysis of $B^+ \to K^+K^-\pi^+$ decays.
[l]Measurement of $(\mathcal{B}(B^+ \to \bar{K}^*(892)^0K^+)\mathcal{B}(K^*(892)^0 \to K\pi)2/3)/\mathcal{B}(B^+ \to K^+K^-\pi^+)$ used in our fit.
[m]Measurement of $(\mathcal{B}(B^+ \to \overline{K}_0^*(1430)^0K^+)\mathcal{B}(K^*(1430) \to K\pi)2/3)/\mathcal{B}(B^+ \to K^+K^-\pi^+)$ used in our fit.

TABLE 188. Branching fractions of charmless mesonic B^+ decays with strange mesons (part 6).

Parameter [10^{-6}]	Measurements		Average HFLAV PDG
$\mathcal{B}(B^+ \to K^+K^-\pi^+)\pi\pi \leftrightarrow KK$ rescattering	LHCb [926]	$0.825 \pm 0.040 \pm 0.065$[a,b]	$0.825^{+0.078}_{-0.075}$ 0.853 ± 0.094
$\mathcal{B}(B^+ \to K^+K^+\pi^-)$	LHCb [907] *BABAR* [908] Belle [909]	<0.011 <0.16 <2.4	<0.011
$\mathcal{B}(B^+ \to f_2'(1525)K^+)$[c]	*BABAR* [262] *BABAR* [262] Belle [263]	$1.56 \pm 0.36 \pm 0.30$[d] $2.8 \pm 0.9^{+0.5}_{-0.4}$[e] <8.0[d]	1.79 ± 0.42 1.79 ± 0.48
$\mathcal{B}(B^+ \to f_J(2220)K^+) \times \mathcal{B}(f_J(2220) \to p\bar{p})$	Belle [928]	<0.41	<0.41
$\mathcal{B}(B^+ \to K^*(892)^+\pi^+K^-)$	*BABAR* [912]	<11.8	<12
$\mathcal{B}(B^+ \to K^*(892)^+\bar{K}^*(892)^0)$	Belle [929] *BABAR* [930]	$0.77^{+0.35}_{-0.30} \pm 0.12$ $1.2 \pm 0.5 \pm 0.1$	0.91 ± 0.30 $0.91^{+0.30}_{-0.27}$
$\mathcal{B}(B^+ \to K^*(892)^+K^+\pi^-)$	*BABAR* [912]	<6.1	<6.1
$\mathcal{B}(B^+ \to K^+K^+K^-)$[c,f]	*BABAR* [262] Belle [263] Belle II [931] LHCb [906][i,j,k]	$34.6 \pm 0.6 \pm 0.9$[d,g] $30.6 \pm 1.2 \pm 2.3$[d] $32.0 \pm 2.2 \pm 1.4$	32.9 ± 0.8 34.0 ± 1.4
$\mathcal{B}(B^+ \to \phi(1020)K^+)$[c]	*BABAR* [262] Belle [263] Belle II [932] CDF [933] CLEO [934]	$9.2 \pm 0.4^{+0.7}_{-0.5}$[d] $9.60 \pm 0.92^{+1.05}_{-0.85}$[d] $6.7 \pm 1.1 \pm 0.5$ $7.6 \pm 1.3 \pm 0.6$ $5.5^{+2.1}_{-1.8} \pm 0.6$	8.53 ± 0.47 $8.83^{+0.67}_{-0.57}$
$\mathcal{B}(B^+ \to f_0(980)K^+) \times \mathcal{B}(f_0(980) \to K^+K^-)$	*BABAR* [262]	$9.4 \pm 1.6 \pm 2.8$[d]	9.4 ± 3.2
$\mathcal{B}(B^+ \to a_2(1320)^0K^+) \times \mathcal{B}(a_2(1320)^0 \to K^+K^-)$	Belle [263]	<1.1[d]	<1.1
$\mathcal{B}(B^+ \to \phi(1680)K^+) \times \mathcal{B}(\phi(1680) \to K^+K^-)$	Belle [263]	<0.8[d]	<0.8
$\mathcal{B}(B^+ \to f_0(1710)K^+) \times \mathcal{B}(f_0(1710) \to K^+K^-)$	*BABAR* [262]	$1.12 \pm 0.25 \pm 0.50$[d]	1.12 ± 0.56
$\mathcal{B}(B^+ \to K^+K^+K^-(\mathrm{NR}))$	Belle [263] *BABAR* [262]	$24.0 \pm 1.5^{+2.6}_{-6.0}$[d] $22.8 \pm 2.7 \pm 7.6$[k]	$23.7^{+3.0}_{-4.9}$ $23.8^{+2.8}_{-4.9}$

[a]LHCb uses a dedicated lineshape to take into account $\pi\pi \leftrightarrow KK$ rescattering, which is particularly significant in the region $1 < m_{KK} < 1.5$ GeV/c^2. See Ref. [926] for details.
[b]Using $\mathcal{B}(B^+ \to K^+K^-\pi^+)$.
[c]The PDG uncertainty includes a scale factor.
[d]Result extracted from Dalitz-plot analysis of $B^+ \to K^+K^+K^-$ decays.
[e]Result extracted from Dalitz-plot analysis of $B^+ \to K^0_S K^0_S K^+$ decays.
[f]Treatment of charmonium intermediate components differs between the results.
[g]All charmonium resonances are vetoed, except for χ_{c0}. The analysis also reports $\mathcal{B}(B^+ \to K^+K^+K^-) = (33.4 \pm 0.5 \pm 0.9) \times 10^{-6}$ excluding χ_{c0}.
[h]Measurement of $\mathcal{B}(B^+ \to K^+K^-\pi^+)/\mathcal{B}(B^+ \to K^+K^+K^-)$ used in our fit.
[i]Measurement of $\mathcal{B}(B^+ \to K^+\pi^+\pi^-)/\mathcal{B}(B^+ \to K^+K^+K^-)$ used in our fit.
[j]Measurement of $\mathcal{B}(B^+ \to \pi^+\pi^+\pi^-)/\mathcal{B}(B^+ \to K^+K^+K^-)$ used in our fit.
[k]The nonresonant amplitude is modeled using a polynomial function including S-wave and P-wave terms.

TABLE 189. Branching fractions of charmless mesonic B^+ decays with strange mesons (part 7).

Parameter [10^{-6}]	Measurements		Average HFLAV PDG
$\mathcal{B}(B^+ \to K^*(892)^+K^+K^-)$	*BABAR* [912]	$36.2 \pm 3.3 \pm 3.6$	36.2 ± 4.9
$\mathcal{B}(B^+ \to \phi(1020)K^*(892)^+)$[a]	*BABAR* [935]	$11.2 \pm 1.0 \pm 0.9$[b]	10.6 ± 1.1
	Belle [936]	$6.7^{+2.1+0.7}_{-1.9-1.0}$	
	Belle II [932]	$21.7 \pm 4.6 \pm 1.9$	10.0 ± 2.0
	CLEO [934]	$10.6^{+6.4+1.8}_{-4.9-1.6}$	
$\mathcal{B}(B^+ \to \phi(1020)(K\pi)_0^{*+})$	*BABAR* [937]	$8.3 \pm 1.4 \pm 0.8$	8.3 ± 1.6
$\mathcal{B}(B^+ \to K_1(1270)^+\phi(1020))$	*BABAR* [937]	$6.1 \pm 1.6 \pm 1.1$	6.1 ± 1.9
$\mathcal{B}(B^+ \to K_1(1400)^+\phi(1020))$	*BABAR* [937]	<3.2	<3.2
$\mathcal{B}(B^+ \to K^*(1410)^+\phi(1020))$	*BABAR* [937]	<4.3	<4.3
$\mathcal{B}(B^+ \to K_0^*(1430)^+\phi(1020))$	*BABAR* [937]	$7.0 \pm 1.3 \pm 0.9$	7.0 ± 1.6
$\mathcal{B}(B^+ \to K_2^*(1430)^+\phi(1020))$	*BABAR* [937]	$8.4 \pm 1.8 \pm 1.0$	8.4 ± 2.1
$\mathcal{B}(B^+ \to K_2(1770)^+\phi(1020))$	*BABAR* [937]	<15.0	<15
$\mathcal{B}(B^+ \to \phi(1020)K_2(1820)^+)$	*BABAR* [937]	<16.3	<16
$\mathcal{B}(B^+ \to a_1(1260)^+K^*(892)^0)$	*BABAR* [938]	<3.6	<3.6
$\mathcal{B}(B^+ \to \phi(1020)\phi(1020)K^+)$[a]	*BABAR* [939]	$5.6 \pm 0.5 \pm 0.3$[c]	4.98 ± 0.52
	Belle [940]	$2.6^{+1.1}_{-0.9} \pm 0.3$[c]	$4.98^{+1.22}_{-1.16}$
$\mathcal{B}(B^+ \to \eta'\eta'K^+)$	*BABAR* [941]	<25.0	<25
$\mathcal{B}(B^+ \to \phi(1020)\omega(782)K^+)$	Belle [942]	<1.9	<1.9
$\mathcal{B}(B^+ \to X(1812)K^+) \times \mathcal{B}(X(1812) \to \phi(1020)\omega(782))$	Belle [942]	<0.32	<0.32
$\mathcal{B}(B^+ \to h^+X^0(\text{Familon}))$[d]	CLEO [943]	<49	<49

[a]The PDG uncertainty includes a scale factor.
[b]Combination of two final states of the $K^*(892)^\pm$, $K^0_S\pi^\pm$ and $K^\pm\pi^0$. In addition to the combined results, the paper reports separately the results for each individual final state.
[c]Measured in the $\phi\phi$ invariant mass range below the η_c resonance ($M_{\phi\phi} < 2.85$ GeV/c^2).
[d]$h = \pi$, K.

TABLE 190. Branching fractions of charmless mesonic B^+ decays without strange mesons (part 1).

Parameter [10^{-6}]	Measurements		Average HFLAV PDG
$\mathcal{B}(B^+ \to \pi^+\pi^0)$[a]	Belle [882]	$5.86 \pm 0.26 \pm 0.38$	5.48 ± 0.33
	BABAR [886]	$5.02 \pm 0.46 \pm 0.29$	
	Belle II [887]	$5.5^{+1.0}_{-0.9} \pm 0.7$	5.48 ± 0.41
	CLEO [884]	$4.6^{+1.8+0.6}_{-1.6-0.7}$	
$\mathcal{B}(B^+ \to \pi^+\pi^+\pi^-)$	LHCb [906]	$16.06 \pm 0.16 \pm 0.48$[b]	16.01 ± 0.49
	BABAR [944]	$15.2 \pm 0.6^{+1.3\text{c,d,e}}_{-1.2}$	$15.20^{+1.43}_{-1.34}$
$\mathcal{B}(B^+ \to \rho^0(770)\pi^+)$	LHCb [945]	$8.82 \pm 0.10 \pm 0.50$[c,f,e,g]	8.76 ± 0.47
	BABAR [944]	$8.1 \pm 0.7^{+1.3\text{c,e}}_{-1.6}$	
	Belle [946]	$8.0^{+2.3}_{-2.0} \pm 0.7$	$8.29^{+1.20}_{-1.28}$
	CLEO [901]	$10.4^{+3.3}_{-3.4} \pm 2.1$	
$\mathcal{B}(B^+ \to f_0(980)\pi^+) \times \mathcal{B}(f_0(980) \to \pi^+\pi^-)$	*BABAR* [944]	<1.5[c]	<1.5
$\mathcal{B}(B^+ \to f_2(1270)\pi^+) \times \mathcal{B}(f_2(1270) \to \pi^+\pi^-)$	LHCb [945]	$1.43 \pm 0.05 \pm 0.27$[c,f,e,g]	$1.27^{+0.20}_{-0.23}$

(Table continued)

TABLE 190. *(Continued)*

Parameter [10^{-6}]	Measurements		Average HFLAV PDG
	BABAR [944]	$0.9 \pm 0.2^{+0.3\,c,e}_{-0.1}$	none
$\mathcal{B}(B^+ \to f_2(1270)\pi^+) \times \mathcal{B}(f_2(1270) \to K^+K^-)$			
	LHCb [926]	$0.377 \pm 0.040 \pm 0.040^{h,i}$	$0.377^{+0.058}_{-0.056}$ none
$\mathcal{B}(B^+ \to \rho(1450)^0\pi^+) \times \mathcal{B}(\rho(1450)^0 \to \pi^+\pi^-)$			
	LHCb [945]	$0.83 \pm 0.05 \pm 0.89^{c,f,e,g}$	$1.14^{+0.59}_{-0.67}$
	BABAR [944]	$1.4 \pm 0.4^{+0.5\,c,e}_{-0.8}$	$1.40^{+0.64}_{-0.89}$
$\mathcal{B}(B^+ \to \rho(1450)^0\pi^+) \times \mathcal{B}(\rho(1450)^0 \to K^+K^-)$			
	LHCb [926]	$1.544 \pm 0.060 \pm 0.089^{h,i}$	1.54 ± 0.11 1.60 ± 0.14
$\mathcal{B}(B^+ \to \rho_3(1690)^0\pi^+) \times \mathcal{B}(\rho_3(1690)^0 \to \pi^+\pi^-)$			
	LHCb [945]	$0.08 \pm 0.02 \pm 0.16^{c,f,e,g}$	0.08 ± 0.16 none
$\mathcal{B}(B^+ \to \pi^+\pi^+\pi^-)S$–wave	LHCb [945]	$4.04 \pm 0.08 \pm 0.64^{j,e,g}$	4.04 ± 0.64 none
$\mathcal{B}(B^+ \to f_0(1370)\pi^+) \times \mathcal{B}(f_0(1370) \to \pi^+\pi^-)$	*BABAR* [944]	$<4.0^{c}$	<4.0
$\mathcal{B}(B^+ \to \pi^+\pi^-\pi^+(\mathrm{NR}))$	*BABAR* [944]	$5.3 \pm 0.7^{+1.3\,k,e}_{-0.8}$	$5.3^{+1.4}_{-1.0}$ $5.3^{+1.5}_{-1.1}$

[a]The PDG uncertainty includes a scale factor.
[b]Using $\mathcal{B}(B^+ \to K^+K^+K^-)$.
[c]Result extracted from Dalitz-plot analysis of $B^+ \to \pi^+\pi^+\pi^-$ decays.
[d]Charm and charmonium contributions are subtracted.
[e]Multiple systematic uncertainties are added in quadrature.
[f]This analysis uses three different approaches: isobar, K-matrix and quasi-model-independent, to describe the S-wave component. The results are taken from the isobar model with an additional error accounting for the different S-wave methods as reported in Appendix D of Ref. [947].
[g]Using $\mathcal{B}(B^+ \to \pi^+\pi^+\pi^-)$.
[h]Result extracted from Dalitz-plot analysis of $B^+ \to K^+K^-\pi^+$ decays.
[i]Using $\mathcal{B}(B^+ \to K^+K^-\pi^+)$.
[j]LHCb accounts the S-wave component using a model that comprises the coherent sum of a σ pole. See Ref. [945] for details.
[k]The nonresonant amplitude is modeled using a sum of exponential functions.

TABLE 191. Branching fractions of charmless mesonic B^+ decays without strange mesons (part 2).

Parameter [10^{-6}]	Measurements		Average HFLAV PDG
$\mathcal{B}(B^+ \to \pi^+\pi^0\pi^0)$	ARGUS [948]	<890	<890
$\mathcal{B}(B^+ \to \rho^+(770)\pi^0)$	*BABAR* [949]	$10.2 \pm 1.4 \pm 0.9$	10.9 ± 1.5
	Belle [950]	$13.2 \pm 2.3^{+1.4}_{-1.9}$	$10.9^{+1.4}_{-1.5}$
$\mathcal{B}(B^+ \to \pi^+\pi^+\pi^-\pi^0)$	ARGUS [948]	<4000	<4000
$\mathcal{B}(B^+ \to \rho^+(770)\rho^0(770))$	*BABAR* [425]	$23.7 \pm 1.4 \pm 1.4$	24.0 ± 1.9
	Belle [951]	$31.7 \pm 7.1^{+3.8}_{-6.7}$	
$\mathcal{B}(B^+ \to f_0(980)\rho^+(770)) \times \mathcal{B}(f_0(980) \to \pi^+\pi^-)$	*BABAR* [425]	<2.0	<2.0
$\mathcal{B}(B^+ \to a_1(1260)^+\pi^0)$	*BABAR* [952]	$26.4 \pm 5.4 \pm 4.1$	26.4 ± 6.8

(Table continued)

TABLE 191. *(Continued)*

Parameter [10^{-6}]	Measurements		Average HFLAV PDG
$\mathcal{B}(B^+ \to a_1(1260)^0\pi^+)$	*BABAR* [952]	$20.4 \pm 4.7 \pm 3.4$	20.4 ± 5.8
$\mathcal{B}(B^+ \to \omega(782)\pi^+)$	*BABAR* [900]	$6.7 \pm 0.5 \pm 0.4$	$6.60^{+0.46}_{-0.45}$
	Belle [953]	$6.9 \pm 0.6 \pm 0.5$	6.88 ± 0.49
	CLEO [901]	$11.3^{+3.3}_{-2.9} \pm 1.4$	
	LHCb [945][a,b,c,d]		
$\mathcal{B}(B^+ \to \omega(782)\rho^+(770))$	*BABAR* [902]	$15.9 \pm 1.6 \pm 1.4$	15.9 ± 2.1
$\mathcal{B}(B^+ \to \eta\pi^+)$	Belle [896]	$4.07 \pm 0.26 \pm 0.21$	4.02 ± 0.27
	BABAR [888]	$4.00 \pm 0.40 \pm 0.24$	$4.02^{+0.27}_{-0.26}$
	CLEO [892]	$1.2^{+2.8}_{-1.2}$	
$\mathcal{B}(B^+ \to \eta\rho^+(770))$[e]	*BABAR* [954]	$9.9 \pm 1.2 \pm 0.8$	6.9 ± 1.0
	Belle [898]	$4.1^{+1.4}_{-1.3} \pm 0.4$	$7.0^{+2.9}_{-2.8}$
	CLEO [892]	$4.8^{+5.2}_{-3.8}$	
$\mathcal{B}(B^+ \to \eta'\pi^+)$[e]	*BABAR* [888]	$3.5 \pm 0.6 \pm 0.2$	2.68 ± 0.46
	Belle [889]	$1.76^{+0.67+0.15}_{-0.62-0.14}$	$2.70^{+0.87}_{-0.84}$
	CLEO [892]	$1.0^{+5.8}_{-1.0}$	
$\mathcal{B}(B^+ \to \eta'\rho^+(770))$	*BABAR* [894]	$9.7^{+1.9}_{-1.8} \pm 1.1$	9.8 ± 2.1
	CLEO [892]	$11.2^{+11.9}_{-7.0}$	$9.7^{+2.2}_{-2.1}$
	Belle [895]	<5.8	

[a]Result extracted from Dalitz-plot analysis of $B^+ \to \pi^+\pi^+\pi^-$ decays.
[b]This analysis uses three different approaches: isobar, K-matrix and quasi-model-independent, to describe the S-wave component. The results are taken from the isobar model with an additional error accounting for the different S-wave methods as reported in Appendix D of Ref. [947].
[c]Multiple systematic uncertainties are added in quadrature.
[d]Measurement of $(\mathcal{B}(B^+ \to \omega(782)\pi^+)\mathcal{B}(\omega(782) \to \pi^+\pi^-))/\mathcal{B}(B^+ \to \pi^+\pi^+\pi^-)$ used in our fit.
[e]The PDG uncertainty includes a scale factor.

TABLE 192. Branching fractions of charmless mesonic B^+ decays without strange mesons (part 3).

Parameter [10^{-6}]	Measurements		Average HFLAV PDG
$\mathcal{B}(B^+ \to \phi(1020)\pi^+)$	*BABAR* [955]	<0.24	$0.031^{+0.015}_{-0.014}$
	Belle [956]	<0.33	0.032 ± 0.015
	LHCb [926][a,b]		
$\mathcal{B}(B^+ \to \phi(1020)\rho^+(770))$	*BABAR* [957]	<3.0	<3.0
$\mathcal{B}(B^+ \to a_0(980)^0\pi^+) \times \mathcal{B}(a_0(980)^0 \to \eta\pi^0)$	*BABAR* [903]	<5.8	<5.8
$\mathcal{B}(B^+ \to \pi^+\pi^+\pi^+\pi^-\pi^-)$	ARGUS [948]	<860	<860
$\mathcal{B}(B^+ \to a_1(1260)^+\rho^0(770))$	CLEO [958]	<620.0[c]	<620
$\mathcal{B}(B^+ \to a_2(1320)^+\rho^0(770))$	CLEO [958]	<720.0[c]	<720
$\mathcal{B}(B^+ \to b_1(1235)^0\pi^+) \times \mathcal{B}(b_1(1235)^0 \to \omega(782)\pi^0)$	*BABAR* [919]	$6.7 \pm 1.7 \pm 1.0$	6.7 ± 2.0
$\mathcal{B}(B^+ \to b_1^+\pi^0)$	*BABAR* [918]	<3.3	<3.3
$\mathcal{B}(B^+ \to \pi^+\pi^+\pi^+\pi^-\pi^-\pi^0)$	ARGUS [948]	<6300	<6300
$\mathcal{B}(B^+ \to b_1(1235)^+\rho^0(770)) \times \mathcal{B}(b_1(1235)^0 \to \omega(782)\pi^+)$	*BABAR* [920]	<5.2	<5.2
$\mathcal{B}(B^+ \to a_1(1260)^+a_1(1260)^0)$	ARGUS [948]	<13000	<13000

(Table continued)

TABLE 192. *(Continued)*

Parameter [10^{-6}]	Measurements		Average HFLAV PDG
$\mathcal{B}(B^+ \to b_1(1235)^0\rho^+(770)) \times \mathcal{B}(b_1(1235)^0 \to \omega(782)\pi^0)$			
	BABAR [920]	<3.3	<3.3

[a]Result extracted from Dalitz-plot analysis of $B^+ \to K^+K^-\pi^+$ decays.
[b]Measurement of $(\mathcal{B}(B^+ \to \phi(1020)\pi^+)\mathcal{B}(\phi(1020) \to K^+K^-))/\mathcal{B}(B^+ \to K^+K^-\pi^+)$ used in our fit.
[c]CLEO assumes $\mathcal{B}(\Upsilon(4S) \to B^0\bar{B}^0) = 0.43$. The result has been modified to account for a branching fraction of 0.50.

TABLE 193. Branching fractions of charmless mesonic B^0 decays with strange mesons (part 1).

Parameter [10^{-6}]	Measurements		Average HFLAV PDG
$\mathcal{B}(B^0 \to K^+\pi^-)$	Belle [882]	$20.00 \pm 0.34 \pm 0.60$	19.5 ± 0.5
	BABAR [959]	$19.1 \pm 0.6 \pm 0.6$	19.6 ± 0.5
	Belle II [883]	$18.0 \pm 0.9 \pm 0.9$	
	CLEO [884]	$18.0^{+2.3+1.2}_{-2.1-0.9}$	
	CDF [960][a,b], [961][c,d], [962][e,f]		
	LHCb [963][e,f,a], [964][c,d]		
$\mathcal{B}(B^0 \to K^0\pi^0)$	Belle [882]	$9.68 \pm 0.46 \pm 0.50$	9.96 ± 0.48
	BABAR [421]	$10.1 \pm 0.6 \pm 0.4$	9.93 ± 0.49
	Belle II [931]	$10.9^{+2.9}_{-2.6} \pm 1.6$	
	CLEO [884]	$12.8^{+4.0+1.7}_{-3.3-1.4}$	
$\mathcal{B}(B^0 \to \eta' K^0)$[g]	*BABAR* [888]	$68.5 \pm 2.2 \pm 3.1$	65.0 ± 2.8
	Belle [889]	$58.9^{+3.6}_{-3.5} \pm 4.3$	$66.1^{+4.5}_{-4.4}$
	Belle II [890]	$59.9^{+5.8}_{-5.5} \pm 2.7$	
	CLEO [892]	$89.0^{+18.0}_{-16.0} \pm 9.0$	
	LHCb [965][h,i]		
$\mathcal{B}(B^0 \to \eta' K^*(892)^0)$	Belle [966]	$2.6 \pm 0.7 \pm 0.2$	2.8 ± 0.6
	BABAR [894]	$3.1^{+0.9}_{-0.8} \pm 0.3$	
$\mathcal{B}(B^0 \to \eta' K_0^*(1430)^0)$	*BABAR* [894]	$6.3 \pm 1.3 \pm 0.9$[j]	6.3 ± 1.6
$\mathcal{B}(B^0 \to \eta'(K\pi)_0^{*0})$	*BABAR* [894]	$7.4^{+1.5}_{-1.4} \pm 0.6$	7.4 ± 1.6 none
$\mathcal{B}(B^0 \to \eta' K_2^*(1430)^0)$	*BABAR* [894]	$13.7^{+3.0}_{-2.9} \pm 1.2$	13.7 ± 3.2 $13.7^{+3.2}_{-3.1}$

[a]Measurement of $(\mathcal{B}(B_s^0 \to K^-\pi^+)/\mathcal{B}(B^0 \to K^+\pi^-))\frac{f_s}{f_d}$ used in our fit.
[b]Measurement of $(\mathcal{B}(\Lambda_b^0 \to p\pi^-)/\mathcal{B}(B^0 \to K^+\pi^-))(f_{\Lambda_b^0}/f_d)$ used in our fit.
[c]Measurement of $\mathcal{B}(B^0 \to K^+K^-)/\mathcal{B}(B^0 \to K^+\pi^-)$ used in our fit.
[d]Measurement of $(\mathcal{B}(B_s^0 \to \pi^+\pi^-)/\mathcal{B}(B^0 \to K^+\pi^-))\frac{f_s}{f_d}$ used in our fit.
[e]Measurement of $\mathcal{B}(B^0 \to \pi^+\pi^-)/\mathcal{B}(B^0 \to K^+\pi^-)$ used in our fit.
[f]Measurement of $(\mathcal{B}(B_s^0 \to K^+K^-)/\mathcal{B}(B^0 \to K^+\pi^-))\frac{f_s}{f_d}$ used in our fit.
[g]The PDG uncertainty includes a scale factor.
[h]Measurement of $\mathcal{B}(\Lambda_b^0 \to \Lambda^0\eta)/\mathcal{B}(B^0 \to \eta' K^0)$ used in our fit.
[i]Measurement of $\mathcal{B}(\Lambda_b^0 \to \Lambda^0\eta')/\mathcal{B}(B^0 \to \eta' K^0)$ used in our fit.
[j]Multiple systematic uncertainties are added in quadrature.

TABLE 194. Branching fractions of charmless mesonic B^0 decays with strange mesons (part 2).

Parameter $[10^{-6}]$	Measurements		Average HFLAV / PDG
$\mathcal{B}(B^0 \to \eta K^0)$	Belle [896]	$1.27^{+0.33}_{-0.29} \pm 0.08$	1.23 ± 0.25
	BABAR [888]	$1.15^{+0.43}_{-0.38} \pm 0.09$	$1.23^{+0.27}_{-0.24}$
$\mathcal{B}(B^0 \to \eta K^*(892)^0)$	*BABAR* [897]	$16.5 \pm 1.1 \pm 0.8$	15.9 ± 1.0
	Belle [898]	$15.2 \pm 1.2 \pm 1.0$	
	CLEO [892]	$13.8^{+5.5}_{-4.6} \pm 1.6$	
$\mathcal{B}(B^0 \to \eta(K\pi)_0^{*0})$	*BABAR* [897]	$11.0 \pm 1.6 \pm 1.5$	11.0 ± 2.2 none
$\mathcal{B}(B^0 \to \eta K_0^*(1430)^0)$	*BABAR* [897]	$7.8 \pm 1.1 \pm 1.1$[a]	7.8 ± 1.5 11.0 ± 2.2
$\mathcal{B}(B^0 \to \eta K_2^*(1430)^0)$	*BABAR* [897]	$9.6 \pm 1.8 \pm 1.1$	9.6 ± 2.1
$\mathcal{B}(B^0 \to \omega(782)K^0)$	Belle [385]	$4.5 \pm 0.4 \pm 0.3$	4.78 ± 0.43
	BABAR [900]	$5.4 \pm 0.8 \pm 0.3$	
	CLEO [901]	$10.0^{+5.4}_{-4.2} \pm 1.4$	
$\mathcal{B}(B^0 \to a_0(980)^0 K^0) \times \mathcal{B}(a_0(980)^0 \to \eta\pi^0)$	*BABAR* [903]	<7.8	<7.8
$\mathcal{B}(B^0 \to b_1(1235)^0 K^0) \times \mathcal{B}(b_1(1235)^0 \to \omega(782)\pi^0)$	*BABAR* [918]	<7.8	<7.8
$\mathcal{B}(B^0 \to a_0(980)^- K^+) \times \mathcal{B}(a_0(980)^- \to \eta\pi^-)$	*BABAR* [968]	<1.9	<1.9
$\mathcal{B}(B^0 \to b_1(1235)^- K^+) \times \mathcal{B}(b_1(1235)^- \to \omega(782)\pi^-)$	*BABAR* [919]	$7.4 \pm 1.0 \pm 1.0$	7.4 ± 1.4
$\mathcal{B}(B^0 \to b_1(1235)^0 K^*(892)^0) \times \mathcal{B}(b_1(1235)^0 \to \omega(782)\pi^0)$	*BABAR* [920]	<8.0	<8.0
$\mathcal{B}(B^0 \to b_1(1235)^- K^*(892)^+) \times \mathcal{B}(b_1(1235)^- \to \omega(782)\pi^-)$	*BABAR* [920]	<5.0	<5.0
$\mathcal{B}(B^0 \to a_0(1450)^- K^+) \times \mathcal{B}(a_0(1450)^- \to \eta\pi^-)$	*BABAR* [968]	<3.1	<3.1
$\mathcal{B}(B^0 \to K_S^0 X^0(\text{Familon}))$	CLEO [943]	<53	<53
$\mathcal{B}(B^0 \to \omega(782)K^*(892)^0)$	*BABAR* [902]	$2.2 \pm 0.6 \pm 0.2$	2.04 ± 0.49
	Belle [967]	$1.8 \pm 0.7 \pm 0.3$	
$\mathcal{B}(B^0 \to \omega(782)(K\pi)_0^{*0})$	*BABAR* [902]	$18.4 \pm 1.8 \pm 1.7$	18.4 ± 2.5
$\mathcal{B}(B^0 \to \omega(782)K_0^*(1430)^0)$	*BABAR* [902]	$16.0 \pm 1.6 \pm 3.0$	16.0 ± 3.4
$\mathcal{B}(B^0 \to \omega(782)K_2^*(1430)^0)$	*BABAR* [902]	$10.1 \pm 2.0 \pm 1.1$	10.1 ± 2.3
$\mathcal{B}(B^0 \to \omega(782)K^+\pi^-(\text{NR}))$	Belle [967]	$5.1 \pm 0.7 \pm 0.7$[b]	5.1 ± 1.0

[a]Multiple systematic uncertainties are added in quadrature.
[b]$0.755 < M_{K\pi} < 1.250$ GeV/c^2.

TABLE 195. Branching fractions of charmless mesonic B^0 decays with strange mesons (part 3).

Parameter [10^{-6}]	Measurements		Average HFLAV PDG
$\mathcal{B}(B^0 \to K^+\pi^-\pi^0)$	*BABAR* [969]	$38.5 \pm 1.0 \pm 3.9$[a]	37.8 ± 3.2
	Belle [970]	$36.6^{+4.2}_{-4.1} \pm 3.0$	
$\mathcal{B}(B^0 \to \rho^-(770)K^+)$	*BABAR* [969]	$6.6 \pm 0.5 \pm 0.8$[a]	7.01 ± 0.92
	Belle [970]	$15.1^{+3.4+2.4}_{-3.3-2.6}$[b]	
$\mathcal{B}(B^0 \to \rho(1450)^-K^+)$	*BABAR* [969]	$2.4 \pm 1.0 \pm 0.6$[a]	2.4 ± 1.2
$\mathcal{B}(B^0 \to \rho(1700)^-K^+)$	*BABAR* [969]	$0.6 \pm 0.6 \pm 0.4$[a]	0.6 ± 0.7
$\mathcal{B}(B^0 \to K^+\pi^-\pi^0(\mathrm{NR}))$	*BABAR* [969]	$2.8 \pm 0.5 \pm 0.4$[c]	2.8 ± 0.6
	Belle [970]	<9.4	
$\mathcal{B}(B^0 \to (K\pi)_0^{*+}\pi^-) \times \mathcal{B}((K\pi)_0^{*+} \to K^+\pi^0)$	*BABAR* [969]	$34.2 \pm 2.4 \pm 4.1$[a]	34.2 ± 4.8
$\mathcal{B}(B^0 \to (K\pi)_0^{*0}\pi^0) \times \mathcal{B}((K\pi)_0^{*0} \to K^+\pi^-)$	*BABAR* [969]	$8.6 \pm 1.1 \pm 1.3$[a]	8.6 ± 1.7
$\mathcal{B}(B^0 \to K_2^*(1430)^0\pi^0)$	*BABAR* [971]	<4.0[a]	<4.0
$\mathcal{B}(B^0 \to K^*(1680)^0\pi^0)$	*BABAR* [971]	<7.5[a]	<7.5
$\mathcal{B}(B^0 \to K_x^{*0}\pi^0)$	Belle [970]	$6.1^{+1.6+0.5}_{-1.5-0.6}$[d]	6.1 ± 1.6
			$6.1^{+1.7}_{-1.6}$

[a]Result extracted from Dalitz-plot analysis of $B^0 \to K^+\pi^-\pi^0$ decays.
[b]Multiple systematic uncertainties are added in quadrature.
[c]The nonresonant amplitude is taken to be constant across the Dalitz plane.
[d]$1.1 < m_{K\pi} < 1.6$ GeV/c^2.

TABLE 196. Branching fractions of charmless mesonic B^0 decays with strange mesons (part 4).

Parameter [10^{-6}]	Measurements		Average HFLAV PDG
$\mathcal{B}(B^0 \to K^0\pi^+\pi^-)$[a,b]	*BABAR* [265]	$50.15 \pm 1.47 \pm 1.76$[c,d]	49.7 ± 1.8
	Belle [972]	$47.5 \pm 2.4 \pm 3.7$[c]	
	CLEO [911]	$50.0^{+10.0}_{-9.0} \pm 7.0$	
	LHCb [973][d,e,f,g,h], [974][i], [975][j,k], [975][j,l], [975][j,m], [975][j,n], [975][j,o]		
$\mathcal{B}(B^0 \to K^0\pi^+\pi^-(\mathrm{NR}))$[p]	LHCb [976]	$12.60 \pm 0.67 \pm 3.05$[c,q,d,r]	14.0 ± 1.7
	BABAR [265]	$11.07^{+2.51}_{-0.99} \pm 0.90$[c,s,d]	$\mathrm{p} = 1.6\%_o$
	Belle [972]	$19.9 \pm 2.5^{+1.7}_{-2.0}$[c,t]	$13.9^{+2.6}_{-1.8}$

(Table continued)

TABLE 196. *(Continued)*

Parameter [10^{-6}]	Measurements		Average HFLAV PDG
$\mathcal{B}(B^0 \to \rho^0(770)K^0)$[p]	*BABAR* [265]	$4.36^{+0.71}_{-0.62} \pm 0.31$[c,d]	3.45 ± 0.48
	LHCb [976]	$1.97^{+0.57}_{-0.83} \pm 0.42$[c,d,r]	p = 1.6‰
	Belle [972]	$6.1 \pm 1.0^{+1.1}_{-1.2}$[c]	$3.41^{+1.08}_{-1.14}$

[a]The PDG average is a result of a fit including input from other measurements.
[b]Treatment of charmonium intermediate components differs between the results.
[c]Result extracted from Dalitz-plot analysis of $B^0 \to K^0_S\pi^+\pi^-$ decays.
[d]Multiple systematic uncertainties are added in quadrature.
[e]Measurement of $\mathcal{B}(\Lambda^0_b \to p\bar{K}^0\pi^-)/\mathcal{B}(B^0 \to K^0\pi^+\pi^-)$ used in our fit.
[f]Measurement of $\mathcal{B}(\Lambda^0_b \to pK^0K^-)/\mathcal{B}(B^0 \to K^0\pi^+\pi^-)$ used in our fit.
[g]Measurement of $\frac{f_{\Xi^0_b}}{f_d}\mathcal{B}(\Xi^0_b \to p\bar{K}^0\pi^-)/\mathcal{B}(B^0 \to K^0\pi^+\pi^-)$ used in our fit.
[h]Measurement of $\frac{f_{\Xi^0_b}}{f_d}\mathcal{B}(\Xi^0_b \to p\bar{K}^0K^-)/\mathcal{B}(B^0 \to K^0\pi^+\pi^-)$ used in our fit.
[i]Measurement of $\mathcal{B}(B^0 \to K^*(892)^0\bar{K}^0 + \text{c.c.})/\mathcal{B}(B^0 \to K^0\pi^+\pi^-)$ used in our fit.
[j]Regions corresponding to D, Λ_c^+ and charmonium resonances are vetoed in this analysis.>
[k]Measurement of $\mathcal{B}(B^0 \to K^0K^+\pi^- + \text{c.c.})/\mathcal{B}(B^0 \to K^0\pi^+\pi^-)$ used in our fit.
[l]Measurement of $\mathcal{B}(B^0 \to K^0K^+K^-)/\mathcal{B}(B^0 \to K^0\pi^+\pi^-)$ used in our fit.
[m]Measurement of $\mathcal{B}(B^0_s \to K^0\pi^+\pi^-)/\mathcal{B}(B^0 \to K^0\pi^+\pi^-)$ used in our fit.
[n]Measurement of $\mathcal{B}(B^0_s \to K^0K^+\pi^- + \text{c.c.})/\mathcal{B}(B^0 \to K^0\pi^+\pi^-)$ used in our fit.
[o]Measurement of $\mathcal{B}(B^0_s \to K^0K^+K^-)/\mathcal{B}(B^0 \to K^0\pi^+\pi^-)$ used in our fit.
[p]The PDG uncertainty includes a scale factor.
[q]The nonresonant component is modeled as a flat contribution over the Dalitz plane.
[r]Using $\mathcal{B}(B^0 \to K^0\pi^+\pi^-)$.
[s]This value includes the flat NR component and the effective range of the LASS lineshape. The value corresponding to the flat component alone is also given in the article.
[t]The nonresonant component is modeled using a sum of two exponential functions.

TABLE 197. Branching fractions of charmless mesonic B^0 decays with strange mesons (part 5).

Parameter [10^{-6}]	Measurements		Average HFLAV PDG
$\mathcal{B}(B^0 \to K^*(892)^+\pi^-)$	*BABAR* [265]	$8.29^{+0.92}_{-0.81} \pm 0.82$[a,b]	7.64 ± 0.44
	BABAR [969]	$8.0 \pm 1.1 \pm 0.8$[c]	p = 1.6‰
	Belle [972]	$8.4 \pm 1.1^{+1.0}_{-0.9}$[a]	7.50 ± 0.44
	CLEO [911]	$16.0^{+6.0}_{-5.0} \pm 2.0$	
	LHCb [977][d,e], [976][a,b,f]		
$\mathcal{B}(B^0 \to K^*_0(1430)^+\pi^-)$[g]	*BABAR* [265]	$29.9^{+2.3}_{-1.7} \pm 3.6$[a,b]	$33.6^{+3.8}_{-4.0}$
	Belle [972]	$49.7 \pm 3.8^{+6.8}_{-8.2}$[a]	$33.5^{+7.4}_{-7.2}$
$\mathcal{B}(B^0 \to K^{*+}_x\pi^-)$	Belle [970]	$5.1 \pm 1.5^{+0.6}_{-0.7}$[h]	5.1 ± 1.6
			$5.1^{+1.6}_{-1.7}$
$\mathcal{B}(B^0 \to K^*(1410)^+\pi^-) \times \mathcal{B}(K^*(1410)^+ \to K^0\pi^+)$			
	Belle [972]	<3.8[a]	<3.8
$\mathcal{B}(B^0 \to (K\pi)^{*+}_0\pi^-) \times \mathcal{B}((K\pi)^{*+}_0 \to K^0\pi^+)$			
	LHCb [976]	$16.95 \pm 0.73 \pm 1.12$[a,b,i]	18.6 ± 1.1
	BABAR [265]	$22.7^{+1.7}_{-1.3} \pm 1.3$[a,b]	p = 1.6‰
			16.2 ± 1.3
$\mathcal{B}(B^0 \to f_0(980)K^0) \times \mathcal{B}(f_0(980) \to \pi^+\pi^-)$[g]			
	LHCb [976]	$9.64 \pm 0.41 \pm 0.79$[a,b,i]	8.38 ± 0.61
	BABAR [265]	$6.92 \pm 0.77 \pm 0.56$[a,b]	p = 1.6‰
	Belle [972]	$7.6 \pm 1.7^{+0.9}_{-1.3}$[a]	$8.15^{+0.78}_{-0.79}$

(Table continued)

TABLE 197. *(Continued)*

Parameter [10^{-6}]	Measurements		Average HFLAV PDG
$\mathcal{B}(B^0 \to f_0(500)K^0)$	LHCb [976]	$0.166^{+0.207}_{-0.041} \pm 0.155^{a,b,i}$	$0.17^{+0.26}_{-0.16}$ p = 1.6‰ $0.16^{+0.25}_{-0.16}$
$\mathcal{B}(B^0 \to f_0(1500)K^0) \times \mathcal{B}(f_0(1500) \to \pi^+\pi^-)$			
	LHCb [976]	$1.348 \pm 0.280 \pm 0.734^{a,b,i}$	1.35 ± 0.79 p = 1.6‰ 1.29 ± 0.75
$\mathcal{B}(B^0 \to f_2(1270)K^0)$	*BABAR* [265]	$2.71^{+0.99}_{-0.83} \pm 0.87^{a,b}$	2.7 ± 1.3
	Belle [972]	$<2.5^{a,j}$	$2.7^{+1.3}_{-1.2}$
$\mathcal{B}(B^0 \to f_x(1300)^0K^0) \times \mathcal{B}(f_x(1300)^0 \to \pi^+\pi^-)$	*BABAR* [265]	$1.81^{+0.55}_{-0.45} \pm 0.48_{a,b}$	$1.81^{+0.73}_{-0.66}$

[a]Result extracted from Dalitz-plot analysis of $B^0 \to K^0_S\pi^+\pi^-$ decays.
[b]Multiple systematic uncertainties are added in quadrature.
[c]Result extracted from Dalitz-plot analysis of $B^0 \to K^+\pi^-\pi^0$ decays.
[d]Measurement of $\mathcal{B}(B^0_s \to K^*(892)^-\pi^+)/\mathcal{B}(B^0 \to K^*(892)^+\pi^-)$ used in our fit.
[e]Measurement of $\mathcal{B}(B^0 \to K^*(892)^-K^+ + \text{c.c.})/\mathcal{B}(B^0 \to K^*(892)^+\pi^-)$ used in our fit.
[f]Measurement of $(\mathcal{B}(B^0 \to K^*(892)^+\pi^-)2/3)/\mathcal{B}(B^0 \to K^0\pi^+\pi^-)$ used in our fit.
[g]The PDG uncertainty includes a scale factor.
[h]$1.1 < m_{K\pi} < 1.6$ GeV/c^2.
[i]Using $\mathcal{B}(B^0 \to K^0\pi^+\pi^-)$.
[j]Using $\mathcal{B}(f_2(1270) \to \pi^+\pi^-)$.

TABLE 198. Branching fractions of charmless mesonic B^0 decays with strange mesons (part 6).

Parameter [10^{-6}]	Measurements		Average HFLAV PDG
$\mathcal{B}(B^0 \to K^*(892)^0\pi^0)$	*BABAR* [969]	$3.3 \pm 0.5 \pm 0.4^a$	3.3 ± 0.6
	Belle [970]	<3.5	
$\mathcal{B}(B^0 \to K^*_2(1430)^+\pi^-)$	Belle [972]	$<6.3^b$	3.82 ± 0.36
	BABAR [971]	$<16.2^a$	p = 1.6‰
	LHCb [976]^{b,c,d}		$3.65^{+0.34}_{-0.33}$
$\mathcal{B}(B^0 \to K^*(1680)^+\pi^-)$	Belle [972]	$<10.1^b$	$14.7^{+1.5}_{-1.3}$
	BABAR [971]	$<25.0^a$	p = 1.6‰
	LHCb [976]^{b,c,e}		14.1 ± 1.0
$\mathcal{B}(B^0 \to K^+\pi^-\pi^+\pi^-)$	DELPHI [978]	<230	<230
$\mathcal{B}(B^0 \to \rho^0(770)K^+\pi^-)$	Belle [979]	$2.8 \pm 0.5 \pm 0.5^f$	2.8 ± 0.7
$\mathcal{B}(B^0 \to f_0(980)K^+\pi^-) \times \mathcal{B}(f_0(980) \to \pi\pi)$			
	Belle [979]	$1.4 \pm 0.4^{+0.3\,f}_{-0.4}$	$1.4^{+0.5}_{-0.6}$
$\mathcal{B}(B^0 \to K^+\pi^-\pi^+\pi^-(\text{NR}))$	Belle [979]	$<2.1^{f,g}$	<2.1
$\mathcal{B}(B^0 \to K^*(892)^0\pi^+\pi^-)$	*BABAR* [980]	$54.5 \pm 2.9 \pm 4.3$	54.5 ± 5.2
$\mathcal{B}(B^0 \to K^*(892)^0\rho^0(770))^h$	*BABAR* [981]	$5.1 \pm 0.6^{+0.6}_{-0.8}$	3.88 ± 0.77
	Belle [979]	$2.1^{+0.8+0.9}_{-0.7-0.5}$	$3.88^{+1.33}_{-1.25}$
$\mathcal{B}(B^0 \to f_0(980)K^*_0(892)^0) \times \mathcal{B}(f_0(980) \to \pi\pi)^h$			

(Table continued)

TABLE 198. *(Continued)*

Parameter [10^{-6}]	Measurements		Average HFLAV PDG
	Belle [979]	$1.4^{+0.6+0.6}_{-0.5-0.4}$	3.90 ± 0.55
	BABAR [981]	$5.7 \pm 0.6 \pm 0.4$	p = 0.1‰
			$3.90^{+2.12}_{-1.85}$

[a]Result extracted from Dalitz-plot analysis of $B^0 \to K^+\pi^-\pi^0$ decays.
[b]Result extracted from Dalitz-plot analysis of $B^0 \to K^0_S\pi^+\pi^-$ decays.
[c]Multiple systematic uncertainties are added in quadrature.
[d]Measurement of $(\mathcal{B}(B^0 \to K^*_2(1430)^+\pi^-)\mathcal{B}(K^*_2(1430)^+ \to K\pi)2/3)/\mathcal{B}(B^0 \to K^0\pi^+\pi^-)$ used in our fit.
[e]Measurement of $(\mathcal{B}(B^0 \to K^*(1680)^+\pi^-)\mathcal{B}(K^*(1680)^+ \to K\pi)2/3)/\mathcal{B}(B^0 \to K^0\pi^+\pi^-)$ used in our fit.
[f]$0.75 < M(K\pi) < 1.20$ GeV/c^2.
[g]$0.55 < M(\pi\pi) < 1.20$ GeV/c^2.
[h]The PDG uncertainty includes a scale factor.

TABLE 199. Branching fractions of charmless mesonic B^0 decays with strange mesons (part 7).

Parameter [10^{-6}]	Measurements		Average HFLAV PDG
$\mathcal{B}(B^0 \to K_1(1270)^+\pi^-)$	*BABAR* [420]	<30	<30
$\mathcal{B}(B^0 \to K_1(1400)^+\pi^-)$	*BABAR* [420]	<27	<27
$\mathcal{B}(B^0 \to a_1(1260)^-K^+)$	*BABAR* [914]	$16.3 \pm 2.9 \pm 2.3$	16.3 ± 3.7
$\mathcal{B}(B^0 \to K^*(892)^+\rho^-(770))$	*BABAR* [981]	$10.3 \pm 2.3 \pm 1.3$	10.3 ± 2.6
$\mathcal{B}(B^0 \to (K\pi)^{*+}_0\rho^-(770)) \times \mathcal{B}((K\pi)^*_0 \to K\pi)$	*BABAR* [981]	<48	<48 none
$\mathcal{B}(B^0 \to K^*_0(1430)^+\rho^-(770))$	*BABAR* [981]	$28 \pm 10 \pm 6$[a]	28 ± 12
$\mathcal{B}(B^0 \to K_1(1400)^0\rho^0(770))$	ARGUS [917]	<3000	<3000
$\mathcal{B}(B^0 \to (K\pi)^{*0}_0\rho^0(770)) \times \mathcal{B}((K\pi)^*_0 \to K\pi)$	*BABAR* [981]	$31 \pm 4 \pm 3$	31.0 ± 5.0 none
$\mathcal{B}(B^0 \to K^*_0(1430)^0\rho^0(770))$	*BABAR* [981]	$27 \pm 4 \pm 4$[a]	27.0 ± 5.4 27.0 ± 5.7
$\mathcal{B}(B^0 \to (K\pi)^{*0}_0 f_0(980)) \times \mathcal{B}(f_0(980) \to \pi\pi) \times \mathcal{B}((K\pi)^*_0 \to K\pi)$	*BABAR* [981]	$3.1 \pm 0.8 \pm 0.7$	3.1 ± 1.1 none
$\mathcal{B}(B^0 \to K^*_0(1430)^0 f_0(980)) \times \mathcal{B}(f_0(980) \to \pi\pi)$	*BABAR* [981]	$2.7 \pm 0.7 \pm 0.6$[a]	2.7 ± 0.9
$\mathcal{B}(B^0 \to K^*_2(1430)^0 f_0(980)) \times \mathcal{B}(f_0(980) \to \pi\pi)$	*BABAR* [981]	$8.6 \pm 1.7 \pm 1.0$	8.6 ± 2.0
$\mathcal{B}(B^0 \to K^+K^-)$	LHCb [964] Belle [882] CDF [961] *BABAR* [959]	$0.0774 \pm 0.0126 \pm 0.0084$[b] $0.10 \pm 0.08 \pm 0.04$ $0.23 \pm 0.10 \pm 0.10$[b] <0.5	0.080 ± 0.015 0.078 ± 0.015
$\mathcal{B}(B^0 \to K^0\bar{K}^0)$	Belle [882] *BABAR* [400]	$1.26 \pm 0.19 \pm 0.05$ $1.08 \pm 0.28 \pm 0.11$	1.21 ± 0.16
$\mathcal{B}(B^0 \to K^0K^+\pi^- + \text{c.c.})$	LHCb [975] Belle [982] *BABAR* [983]	$6.11 \pm 0.45 \pm 0.78$[c,d] $7.20 \pm 0.66 \pm 0.30$ $6.4 \pm 1.0 \pm 0.6$	6.7 ± 0.5
$\mathcal{B}(B^0 \to K^*(892)^-K^+ + \text{c.c.})$	LHCb [977]	<0.38[e]	<0.4

(Table continued)

TABLE 199. *(Continued)*

Parameter [10^{-6}]	Measurements		Average HFLAV PDG
$\mathcal{B}(B^0 \to K^*(892)^0\bar{K}^0 + \text{c.c.})$[f]	LHCb [974]	<1.0[d]	<0.99
	BABAR [984]	<1.9	

[a]Multiple systematic uncertainties are added in quadrature.
[b]Using $\mathcal{B}(B^0 \to K^+\pi^-)$.
[c]Regions corresponding to D, Λ_c^+ and charmonium resonances are vetoed in this analysis.
[d]Using $\mathcal{B}(B^0 \to K^0\pi^+\pi^-)$.
[e]Using $\mathcal{B}(B^0 \to K^*(892)^+\pi^-)$.
[f]$0.75 < M(K\pi) < 1.20$ GeV/c^2.

TABLE 200. Branching fractions of charmless mesonic B^0 decays with strange mesons (part 8).

Parameter [10^{-6}]	Measurements		Average HFLAV PDG
$\mathcal{B}(B^0 \to K^+K^-\pi^0)$	Belle [985]	$2.17 \pm 0.60 \pm 0.24$	2.17 ± 0.65
$\mathcal{B}(B^0 \to K^0_S K^0_S \pi^0)$	*BABAR* [986]	<0.9	<0.9
$\mathcal{B}(B^0 \to K^0_S K^0_S \eta)$	*BABAR* [986]	<1.0	<1.0
$\mathcal{B}(B^0 \to K^0_S K^0_S \eta')$	*BABAR* [986]	<2.0	<2.0
$\mathcal{B}(B^0 \to K^0K^+K^-)$	LHCb [975]	$27.29 \pm 0.89 \pm 1.90$[a,b]	26.8 ± 1.0
	BABAR [262]	$26.5 \pm 0.9 \pm 0.8$[c,d]	
	Belle [909]	$28.3 \pm 3.3 \pm 4.0$	26.8 ± 1.1
$\mathcal{B}(B^0 \to \phi(1020)K^0)$	*BABAR* [262]	$7.1 \pm 0.6^{+0.4c}_{-0.3}$	7.25 ± 0.60
	Belle II [932]	$5.9 \pm 1.8 \pm 0.7$	
	Belle [936]	$9.0^{+2.2}_{-1.8} \pm 0.7$	$7.32^{+0.69}_{-0.63}$
	LHCb [987][e], [988][f,g]		
$\mathcal{B}(B^0 \to f_0(980)K^0) \times \mathcal{B}(f_0(980) \to K^+K^-)$	*BABAR* [262]	$7.0^{+2.6}_{-1.8} \pm 2.4$[c]	$7.0^{+3.5}_{-3.0}$
$\mathcal{B}(B^0 \to f_0(1500)K^0)$	*BABAR* [262]	$13.3^{+5.8}_{-4.4} \pm 3.2$[c]	$13.3^{+6.6}_{-5.4}$
$\mathcal{B}(B^0 \to f'_2(1525)K^0)$	*BABAR* [262]	$0.29^{+0.27}_{-0.18} \pm 0.36$[c]	$0.29^{+0.45}_{-0.40}$
$\mathcal{B}(B^0 \to f_0(1710)K^0) \times \mathcal{B}(f_0(1710) \to K^+K^-)$	*BABAR* [262]	$4.4 \pm 0.7 \pm 0.5$[c]	4.4 ± 0.9
$\mathcal{B}(B^0 \to K^0K^+K^-(\text{NR}))$	*BABAR* [262]	$33 \pm 5 \pm 9$[h]	33 ± 10

[a]Regions corresponding to D, Λ_c^+ and charmonium resonances are vetoed in this analysis.
[b]Using $\mathcal{B}(B^0 \to K^0\pi^+\pi^-)$.
[c]Result extracted from Dalitz-plot analysis of $B^0 \to K^0_S K^+K^-$ decays.
[d]All charmonium resonances are vetoed, except for χ_{c0}. The analysis also reports $\mathcal{B}(B^0 \to K^0K^+K^-) = (25.4 \pm 0.9 \pm 0.8) \times 10^{-6}$ excluding χ_{c0}.
[e]Measurement of $(\mathcal{B}(\Lambda_b^0 \to \Lambda^0\phi(1020))/\mathcal{B}(B^0 \to \phi(1020)K^0))(f_{\Lambda_b^0}/f_d)2$ used in our fit.
[f]Multiple systematic uncertainties are added in quadrature.
[g]Measurement of $\mathcal{B}(B_s^0 \to K^0\bar{K}^0)/\mathcal{B}(B^0 \to \phi(1020)K^0)$ used in our fit.
[h]The nonresonant amplitude is modeled using a polynomial function including S-wave and P-wave terms.

TABLE 201. Branching fractions of charmless mesonic B^0 decays with strange mesons (part 9).

Parameter [10^{-6}]	Measurements		Average HFLAV PDG
$\mathcal{B}(B^0 \to K^0_S K^0_S K^0_S)$[a]	*BABAR* [383]	$6.19 \pm 0.48 \pm 0.19$[b,c]	6.04 ± 0.50
	Belle [909]	$4.2^{+1.6}_{-1.3} \pm 0.8$	$6.04^{+0.53}_{-0.52}$
$\mathcal{B}(B^0 \to f_0(980)K^0_S) \times \mathcal{B}(f_0(980) \to K^0_S K^0_S)$			
	BABAR [383]	$2.7^{+1.3}_{-1.2} \pm 1.3$[b,c]	2.7 ± 1.8
$\mathcal{B}(B^0 \to f_0(1710)K^0_S) \times \mathcal{B}(f_0(1710) \to K^0_S K^0_S)$			
	BABAR [383]	$0.50^{+0.46}_{-0.24} \pm 0.11$[b,c]	$0.50^{+0.47}_{-0.26}$
$\mathcal{B}(B^0 \to f_2(2010)K^0_S) \times \mathcal{B}(f_2(2010) \to K^0_S K^0_S)$			
	BABAR [383]	$0.54^{+0.21}_{-0.20} \pm 0.52$[b,c]	0.54 ± 0.56
$\mathcal{B}(B^0 \to K^0_S K^0_S K^0_S(\mathrm{NR}))$	*BABAR* [383]	$13.3^{+2.2}_{-2.3} \pm 0.6$[d,c]	13.3 ± 2.3
			$13.3^{+3.1}_{-3.2}$
$\mathcal{B}(B^0 \to K^0_S K^0_S K^0_L)$	*BABAR* [989]	<16[e]	<16
$\mathcal{B}(B^0 \to K^*(892)^0 K^+ K^-)$	*BABAR* [980]	$27.5 \pm 1.3 \pm 2.2$	27.5 ± 2.6
$\mathcal{B}(B^0 \to \phi(1020)K^*(892)^0)$	*BABAR* [388]	$9.7 \pm 0.5 \pm 0.5$	10.11 ± 0.48
	Belle [990]	$10.4 \pm 0.5 \pm 0.6$	10.04 ± 0.52
	Belle II [932]	$11.0 \pm 2.1 \pm 1.1$	
	CLEO [934]	$11.5^{+4.5+1.8}_{-3.7-1.7}$	
	LHCb [991][c,f], [992][c,g], [993][c,h], [417][i]		
$\mathcal{B}(B^0 \to K^+\pi^-\pi^+K^-(\mathrm{NR}))$	Belle [994]	<71.7[j]	<72
$\mathcal{B}(B^0 \to K^*(892)^0\pi^+K^-)$	*BABAR* [980]	$4.6 \pm 1.1 \pm 0.8$	4.5 ± 1.3
	Belle [994]	$2.11^{+5.63+4.85\mathrm{j}}_{-5.26-4.75}$	
$\mathcal{B}(B^0 \to K^*(892)^0\bar{K}^*(892)^0)$[a]	LHCb [995]	$0.834 \pm 0.063 \pm 0.158$[c,k]	0.83 ± 0.16
	Belle [994]	$0.26^{+0.33+0.10}_{-0.29-0.08}$	$0.83^{+0.25}_{-0.23}$
	BABAR [996]	$1.28^{+0.35}_{-0.30} \pm 0.11$	

[a]The PDG uncertainty includes a scale factor.
[b]Result extracted from Dalitz-plot analysis of $B^0 \to K^0_S K^0_S K^0_S$ decays.
[c]Multiple systematic uncertainties are added in quadrature.
[d]The nonresonant amplitude is modeled using an exponential function.
[e]$0.75 < M(K\pi) < 1.20$ GeV/c^2.
[f]Measurement of $\mathcal{B}(B^0_s \to \phi(1020)\bar{K}^*(892)^0)/\mathcal{B}(B^0 \to \phi(1020)K^*(892)^0)$ used in our fit.
[g]Measurement of $\mathcal{B}(B^0_s \to \phi(1020)\phi(1020))/\mathcal{B}(B^0 \to \phi(1020)K^*(892)^0)$ used in our fit.
[h]Measurement of $\mathcal{B}(B^0_s \to K^*(892)^0\bar{K}^*(892)^0)/\mathcal{B}(B^0 \to \phi(1020)K^*(892)^0)$ used in our fit.
[i]Measurement of $\mathcal{B}(B^0 \to \rho^0(770)\rho^0(770))/\mathcal{B}(B^0 \to \phi(1020)K^*(892)^0)$ used in our fit.
[j]$0.70 < M(K\pi) < 1.70$ GeV/c^2.
[k]Using $\mathcal{B}(B^0_s \to K^*(892)^0\bar{K}^*(892)^0)$.

TABLE 202. Branching fractions of charmless mesonic B^0 decays with strange mesons (part 10).

Parameter [10^{-6}]	Measurements		Average HFLAV PDG
$\mathcal{B}(B^0 \to K^+\pi^-K^+\pi^-(\mathrm{NR}))$	Belle [994]	<6.0[a]	<6.0
$\mathcal{B}(B^0 \to K^*(892)^0K^+\pi^-)$	*BABAR* [980]	<2.2	<2.2
	Belle [994]	<7.6[a]	
$\mathcal{B}(B^0 \to K^*(892)^0K^*(892)^0)$	Belle [994]	<0.20	<0.2
	BABAR [996]	<0.41	
$\mathcal{B}(B^0 \to K^*(892)^+K^*(892)^-)$	*BABAR* [997]	<2.0	<2.0
$\mathcal{B}(B^0 \to K_1(1400)^0\phi(1020))$	ARGUS [917]	<5000	<5000

(Table continued)

TABLE 202. *(Continued)*

Parameter [10^{-6}]	Measurements		Average HFLAV PDG
$\mathcal{B}(B^0 \to (K\pi)_0^{*0}\phi(1020))$	Belle [990]	$4.3 \pm 0.4 \pm 0.4$	4.30 ± 0.45
	BABAR [388]	$4.3 \pm 0.6 \pm 0.4$	
$\mathcal{B}(B^0 \to (K\pi)_0^{*0}\phi)$, $1.60 < M_{K\pi} < 2.15\text{GeV}/c^2$.			
	BABAR [998]	<1.7	<1.7
$\mathcal{B}(B^0 \to K_0^*(1430)^0\pi^+K^-)$	Belle [994]	<31.8[a]	<32
$\mathcal{B}(B^0 \to K_0^*(1430)^0\bar{K}^*(892)^0)$	Belle [994]	<3.3	<3.3
$\mathcal{B}(B^0 \to K_0^*(1430)^0\bar{K}_0^*(1430)^0)$	Belle [994]	<8.4	<8.4
$\mathcal{B}(B^0 \to \phi(1020)K_0^*(1430)^0)$	*BABAR* [388]	$3.9 \pm 0.5 \pm 0.6$	3.90 ± 0.78
$\mathcal{B}(B^0 \to K_0^*(1430)^0K^*(892)^0)$	Belle [994]	<1.7	<1.7
$\mathcal{B}(B^0 \to K_0^*(1430)^0K_0^*(1430)^0)$	Belle [994]	<4.7	<4.7
$\mathcal{B}(B^0 \to \phi(1020)K^*(1680)^0)$	*BABAR* [998]	<3.5	<3.5
$\mathcal{B}(B^0 \to \phi(1020)K_3^*(1780)^0)$	*BABAR* [998]	<2.7	<2.7
$\mathcal{B}(B^0 \to \phi(1020)K_4^*(2045)^0)$	*BABAR* [998]	<15.3	<15
$\mathcal{B}(B^0 \to \rho^0(770)K_2^*(1430)^0)$	ARGUS [917]	<1100	<1100
$\mathcal{B}(B^0 \to \phi(1020)K_2^*(1430)^0)$[b]	Belle [990]	$5.5^{+0.9}_{-0.7} \pm 1.0$	6.8 ± 0.8
	BABAR [388]	$7.5 \pm 0.9 \pm 0.5$	$6.8^{+1.0}_{-0.9}$
$\mathcal{B}(B^0 \to \phi(1020)\phi(1020)K^0)$	*BABAR* [939]	$4.5 \pm 0.8 \pm 0.3$[c]	4.5 ± 0.9
$\mathcal{B}(B^0 \to \eta'\eta'K^0)$	*BABAR* [941]	<31.0	<31

[a] $0.70 < M(K\pi) < 1.70$ GeV/c^2.
[b] The PDG uncertainty includes a scale factor.
[c] Measured in the $\phi\phi$ invariant mass range below the η_c resonance ($M_{\phi\phi} < 2.85$ GeV/c^2).

TABLE 203. Branching fractions of charmless mesonic B^0 decays without strange mesons (part 1).

Parameter [10^{-6}]	Measurements		Average HFLAV PDG
$\mathcal{B}(B^0 \to \pi^+\pi^-)$	LHCb [963]	$5.10 \pm 0.18 \pm 0.35$[a]	5.15 ± 0.19
	Belle [882]	$5.04 \pm 0.21 \pm 0.18$	5.12 ± 0.19
	CDF [962]	$5.04 \pm 0.33 \pm 0.33$[a]	
	BABAR [959]	$5.5 \pm 0.4 \pm 0.3$	
	Belle II [883]	$5.8 \pm 0.7 \pm 0.3$	
	CLEO [884]	$4.5^{+1.4+0.5}_{-1.2-0.4}$	
$\mathcal{B}(B^0 \to \pi^0\pi^0)$[b]	Belle [433]	$1.31 \pm 0.19 \pm 0.19$	1.59 ± 0.18
	BABAR [421]	$1.83 \pm 0.21 \pm 0.13$	1.59 ± 0.26
$\mathcal{B}(B^0 \to \eta\pi^0)$	Belle [999]	$0.41^{+0.17+0.05}_{-0.15-0.07}$	0.41 ± 0.17
	BABAR [954]	<1.5	$0.41^{+0.18}_{-0.17}$
	CLEO [892]	<2.9	
$\mathcal{B}(B^0 \to \eta\eta)$	*BABAR* [888]	<1.0	<1.0
$\mathcal{B}(B^0 \to \eta'\pi^0)$[b]	*BABAR* [954]	$0.9 \pm 0.4 \pm 0.1$	1.2 ± 0.4
	Belle [889]	$2.79^{+1.02+0.25}_{-0.96-0.34}$	1.2 ± 0.6

(Table continued)

TABLE 203. *(Continued)*

Parameter [10^{-6}]	Measurements		Average HFLAV PDG
$\mathcal{B}(B^0 \to \eta'\eta')$	*BABAR* [888]	<1.7	<1.7
	Belle [895]	<6.5	
$\mathcal{B}(B^0 \to \eta'\eta)$	*BABAR* [954]	<1.2	<1.2
	Belle [895]	<4.5	
$\mathcal{B}(B^0 \to \eta'\rho^0(770))$	Belle [895]	<1.3	<1.3
	BABAR [894]	<2.8	
$\mathcal{B}(B^0 \to f_0(980)\eta') \times \mathcal{B}(f_0(980) \to \pi^+\pi^-)$	*BABAR* [894]	<0.9	<0.9
$\mathcal{B}(B^0 \to \eta\rho^0(770))$	*BABAR* [968]	<1.5	<1.5
	Belle [898]	<1.9	
$\mathcal{B}(B^0 \to f_0(980)\eta) \times \mathcal{B}(f_0(980) \to \pi^+\pi^-)$	*BABAR* [968]	<0.4	<0.4
$\mathcal{B}(B^0 \to \omega(782)\eta)$	*BABAR* [888]	$0.94^{+0.35}_{-0.30} \pm 0.09$	$0.94^{+0.36}_{-0.31}$

[a]Using $\mathcal{B}(B^0 \to K^+\pi^-)$.
[b]The PDG uncertainty includes a scale factor.

TABLE 204. Branching fractions of charmless mesonic B^0 decays without strange mesons (part 2).

Parameter [10^{-6}]	Measurements		Average HFLAV PDG
$\mathcal{B}(B^0 \to \omega(782)\eta')$	*BABAR* [888]	$1.01^{+0.46}_{-0.38} \pm 0.09$	$1.01^{+0.47}_{-0.39}$
	Belle [895]	<2.2	
$\mathcal{B}(B^0 \to \omega(782)\rho^0(770))$	*BABAR* [902]	<1.6	<1.6
$\mathcal{B}(B^0 \to f_0(980)\omega(782)) \times \mathcal{B}(f_0(980) \to \pi^+\pi^-)$	*BABAR* [902]	<1.5	<1.5
$\mathcal{B}(B^0 \to \omega(782)\omega(782))$	*BABAR* [1000]	$1.2 \pm 0.3^{+0.3}_{-0.2}$	1.2 ± 0.4
$\mathcal{B}(B^0 \to \phi(1020)\pi^0)$	Belle [956]	<0.15	<0.15
	BABAR [955]	<0.28	
$\mathcal{B}(B^0 \to \phi(1020)\eta)$	*BABAR* [888]	<0.5	<0.5
$\mathcal{B}(B^0 \to \phi(1020)\eta')$	Belle [895]	<0.5	<0.5
	BABAR [888]	<1.1	
$\mathcal{B}(B^0 \to \phi(1020)\pi^+\pi^-)$	LHCb [1001]	$0.182 \pm 0.025 \pm 0.043$[a,b]	0.182 ± 0.050
$\mathcal{B}(B^0 \to \phi(1020)\rho^0(770))$	*BABAR* [957]	<0.33	<0.33
$\mathcal{B}(B^0 \to f_0(980)\phi(1020)) \times \mathcal{B}(f_0(980) \to \pi^+\pi^-)$	*BABAR* [957]	<0.38	<0.38
$\mathcal{B}(B^0 \to \omega(782)\phi(1020))$	*BABAR* [1000]	<0.7	<0.7
$\mathcal{B}(B^0 \to \phi(1020)\phi(1020))$	LHCb [1002]	<0.027	<0.027
	BABAR [957]	<0.2	
$\mathcal{B}(B^0 \to a_0(980)^+\pi^- + \text{c.c.}) \times \mathcal{B}(a_0(980)^+ \to \eta\pi^+)$	*BABAR* [968]	<3.1	<3.1
$\mathcal{B}(B^0 \to a_0(1450)^+\pi^- + \text{c.c.}) \times \mathcal{B}(a_0(1450)^+ \to \eta\pi^+)$	*BABAR* [968]	<2.3	<2.3
$\mathcal{B}(B^0 \to \pi^+\pi^-\pi^0)$	ARGUS [948]	<720	<720

(Table continued)

TABLE 204. *(Continued)*

Parameter [10^{-6}]	Measurements		Average HFLAV PDG
$\mathcal{B}(B^0 \to \rho^0(770)\pi^0)$	Belle [275]	$3.0 \pm 0.5 \pm 0.7$[c]	2.0 ± 0.5
	BABAR [1003]	$1.4 \pm 0.6 \pm 0.3$	
	CLEO [901]	$1.6^{+2.0}_{-1.4} \pm 0.8$	
$\mathcal{B}(B^0 \to \rho^+(770)\pi^- + \text{c.c.})$	Belle [275]	$22.6 \pm 1.1 \pm 4.4$[c]	23.0 ± 2.3
	BABAR [279]	$22.6 \pm 1.8 \pm 2.2$	
	CLEO [901]	$27.6^{+8.4}_{-7.4} \pm 4.2$	
$\mathcal{B}(B^0 \to \pi^+\pi^-\pi^+\pi^-)$	Belle [416]	<11.2[d]	<11
	BABAR [415]	<23.1[e]	

[a] $400 < M(\pi^+\pi^-) < 1600$ MeV/c^2.
[b] Multiple systematic uncertainties are added in quadrature.
[c] Result extracted from Dalitz-plot analysis of $B^0 \to \pi^+\pi^-\pi^0$ decays.
[d] $0.52 < m_{\pi^+\pi^-} < 1.15$ GeV/c^2.
[e] $0.55 < m_{\pi^+\pi^-} < 1.050$ GeV/c^2.

TABLE 205. Branching fractions of charmless mesonic B^0 decays without strange mesons (part 3).

Parameter [10^{-6}]	Measurements		Average HFLAV PDG
$\mathcal{B}(B^0 \to \rho^0(770)\pi^+\pi^-)$	*BABAR* [415]	<8.8[a]	<8.8
	Belle [416]	<12.0[b]	
$\mathcal{B}(B^0 \to \rho^0(770)\rho^0(770))$	LHCb [417]	$0.95 \pm 0.17 \pm 0.10$[c]	0.96 ± 0.15
	Belle [416]	$1.02 \pm 0.30 \pm 0.15$	
	BABAR [415]	$0.92 \pm 0.32 \pm 0.14$	
$\mathcal{B}(B^0 \to f_0(980)\pi^+\pi^-) \times \mathcal{B}(f_0(980) \to \pi^+\pi^-)$	Belle [416]	<3.0[b]	<3.0
$\mathcal{B}(B^0 \to f_0(980)\rho^0(770)) \times \mathcal{B}(f_0(980) \to \pi^+\pi^-)$	Belle [416]	$0.78 \pm 0.22 \pm 0.11$	0.78 ± 0.25
	BABAR [415]	<0.40	
$\mathcal{B}(B^0 \to f_0(980)f_0(980)) \times \mathcal{B}(f_0(980) \to \pi^+\pi^-) \times \mathcal{B}(f_0(980) \to \pi^+\pi^-)$	*BABAR* [415]	<0.19	<0.19
	Belle [416]	<0.2	
$\mathcal{B}(B^0 \to f_0(980)f_0(980)) \times \mathcal{B}(f_0(980) \to \pi^+\pi^-) \times \mathcal{B}(f_0(980) \to K^+K^-)$	*BABAR* [957]	<0.23	<0.23
$\mathcal{B}(B^0 \to a_1(1260)^+\pi^- + \text{c.c.})$[d]	Belle [419]	$22.2 \pm 2.0 \pm 2.8$	25.9 ± 2.8
	BABAR [1004]	$33.2 \pm 3.8 \pm 3.0$	25.9 ± 5.2
$\mathcal{B}(B^0 \to a_2(1320)^+\pi^- + \text{c.c.})$	Belle [419]	<6.3	<6.3
$\mathcal{B}(B^0 \to \pi^+\pi^-\pi^0\pi^0)$	ARGUS [948]	<3100	<3100
$\mathcal{B}(B^0 \to \rho^+(770)\rho^-(770))$	Belle [414]	$28.3 \pm 1.5 \pm 1.5$	27.7 ± 1.9
	BABAR [413]	$25.5 \pm 2.1^{+3.6}_{-3.9}$	
$\mathcal{B}(B^0 \to a_1(1260)^0\pi^0)$	ARGUS [948]	<1100	<1100

(Table continued)

TABLE 205. *(Continued)*

Parameter [10^{-6}]	Measurements		Average HFLAV PDG
$\mathcal{B}(B^0 \to \omega(782)\pi^0)$	*BABAR* [954]	<0.5	<0.5
	Belle [953]	<2.0	
$\mathcal{B}(B^0 \to \pi^+\pi^+\pi^-\pi^-\pi^0)$	ARGUS [948]	<9000	<9000
$\mathcal{B}(B^0 \to a_1(1260)^+\rho^-(770) + \text{c.c.})$	*BABAR* [1005]	<61.0	<61
$\mathcal{B}(B^0 \to a_1(1260)^0\rho^0(770))$	ARGUS [948]	<2400	<2400

[a]$0.55 < m_{\pi^+\pi^-} < 1.050$ GeV/c^2.
[b]$0.52 < m_{\pi^+\pi^-} < 1.15$ GeV/c^2.
[c]Using $\mathcal{B}(B^0 \to \phi(1020)K^*(892)^0)$.
[d]The PDG uncertainty includes a scale factor.

TABLE 206. Branching fractions of charmless mesonic B^0 decays without strange mesons (part 4).

Parameter [10^{-6}]	Measurements		Average HFLAV PDG
$\mathcal{B}(B^0 \to b_1(1235)^+\pi^- + \text{c.c.}) \times \mathcal{B}(b_1(1235)^+ \to \omega(782)\pi^+)$			
	BABAR [919]	$10.9 \pm 1.2 \pm 0.9$	10.9 ± 1.5
$\mathcal{B}(B^0 \to b_1(1235)^0\pi^0) \times \mathcal{B}(b_1(1235)^0 \to \omega(782)\pi^0)$			
	BABAR [918]	<1.9	<1.9
$\mathcal{B}(B^0 \to b_1(1235)^-\rho^+(770)) \times \mathcal{B}(b_1(1235)^- \to \omega(782)\pi^-)$			
	BABAR [920]	<1.4	<1.4
$\mathcal{B}(B^0 \to b_1(1235)^0\rho^0(770)) \times \mathcal{B}(b_1(1235)^0 \to \omega(782)\pi^0)$			
	BABAR [920]	<3.4	<3.4
$\mathcal{B}(B^0 \to \pi^+\pi^+\pi^+\pi^-\pi^-\pi^-)$	ARGUS [948]	<3000	<3000
$\mathcal{B}(B^0 \to a_1(1260)^+a_1(1260)^-) \times \mathcal{B}(a_1(1260)^+ \to \pi^+\pi^+\pi^-) \times \mathcal{B}(a_1(1260)^- \to \pi^-\pi^-\pi^+)$			
	BABAR [1006]	$11.8 \pm 2.6 \pm 1.6$	11.8 ± 3.1
$\mathcal{B}(B^0 \to \pi^+\pi^+\pi^+\pi^-\pi^-\pi^-\pi^0)$	ARGUS [948]	<11000	<11000

TABLE 207. Relative branching fractions of charmless mesonic B^+ decays.

Parameter	Measurements		Average
$\frac{\mathcal{B}(B^+ \to K^+K^-\pi^+)}{\mathcal{B}(B^+ \to K^+K^+K^-)}$	LHCb [906]	$0.151 \pm 0.004 \pm 0.008$	0.151 ± 0.009
$\frac{\mathcal{B}(B^+ \to K^+\pi^+\pi^-)}{\mathcal{B}(B^+ \to K^+K^+K^-)}$	LHCb [906]	$1.703 \pm 0.011 \pm 0.022$	1.703 ± 0.025
$\frac{\mathcal{B}(B^+ \to \pi^+\pi^+\pi^-)}{\mathcal{B}(B^+ \to K^+K^+K^-)}$	LHCb [906]	$0.488 \pm 0.005 \pm 0.009$	0.488 ± 0.010

TABLE 208. Relative branching fractions of charmless mesonic B^0 decays.

Parameter	Measurements		Average
$\frac{\mathcal{B}(B^0\to K^+K^-)}{\mathcal{B}(B^0\to K^+\pi^-)}$ $[10^{-3}]$	LHCb [964] CDF [961]	$3.98 \pm 0.65 \pm 0.42$ $12 \pm 5 \pm 5$	4.07 ± 0.77
$\frac{\mathcal{B}(B^0\to K^*(892)^+K^-+\text{c.c.})}{\mathcal{B}(B^0\to K^*(892)^+\pi^-)}$ $[10^{-2}]$	LHCb [977]	<5	<5.0
$\frac{\mathcal{B}(B^0\to K^0_S K^*(892)^0+\text{c.c.})}{\mathcal{B}(B^0\to K^0_S\pi^+\pi^-)}$ $[10^{-2}]$	LHCb [974]	<2	<2.0
$\frac{\mathcal{B}(B^0\to\pi^+\pi^-)}{\mathcal{B}(B^0\to K^+\pi^-)}$	LHCb [963] CDF [962]	$0.262 \pm 0.009 \pm 0.017$ $0.259 \pm 0.017 \pm 0.016$	0.261 ± 0.015
$\frac{\mathcal{B}(B^0\to K^0K^+\pi^-+\text{c.c.})}{\mathcal{B}(B^0\to K^0\pi^+\pi^-)}$	LHCb [975]	$0.123 \pm 0.009 \pm 0.015$[a]	0.123 ± 0.017
$\frac{\mathcal{B}(B^0\to K^0K^+K^-)}{\mathcal{B}(B^0\to K^0\pi^+\pi^-)}$	LHCb [975]	$0.549 \pm 0.018 \pm 0.033$[a]	0.549 ± 0.038
$\frac{\mathcal{B}(B^0\to K^*(892)^0\bar{K}^*(892)^0)}{\mathcal{B}(B^0_s\to K^*(892)^0\bar{K}^*(892)^0)}$ $[10^{-2}]$	LHCb [995]	$7.58 \pm 0.57 \pm 0.30$[b]	7.58 ± 0.64
$\frac{f_s}{f_d}\frac{\mathcal{B}(B^0\to K^+K^-)}{\mathcal{B}(B^0_s\to K^+K^-)}$ $[10^{-2}]$	LHCb [963]	$1.8^{+0.8}_{-0.7} \pm 0.9$	1.8 ± 1.2
$\frac{\mathcal{B}(B^0\to\rho^0(770)\rho^0(770))}{\mathcal{B}(B^0\to\phi(1020)K^*(892)^0)}$ $[10^{-2}]$	LHCb [417]	$9.4 \pm 1.7 \pm 0.9$	9.4 ± 1.9
$\frac{\mathcal{B}(B^0\to K^0\bar{K}^0)}{\mathcal{B}(B^0_s\to K^0\bar{K}^0)}$ $[10^{-2}]$	LHCb [988]	$7.5 \pm 3.1 \pm 0.6$[b]	7.5 ± 3.2
$\frac{\mathcal{B}(B^0\to K^0\bar{K}^0)}{\mathcal{B}(B^0\to\phi(1020)K^0)}$	LHCb [988]	$0.17 \pm 0.08 \pm 0.02$	0.17 ± 0.08
$\frac{\mathcal{B}(B^0\to\pi^+\pi^-\mu^+\mu^-)}{\mathcal{B}(B^0\to J/\psi K^{*0})\times\mathcal{B}(J/\psi\to\mu^+\mu^-)\times\mathcal{B}(K^{*0}\to K^+\pi^-)}$ $[10^{-4}]$	LHCb [1007]	$4.1 \pm 1.0 \pm 0.3$[c,d]	4.1 ± 1.0

[a]Regions corresponding to D, Λ_c^+ and charmonium resonances are vetoed in this analysis.
[b]Multiple systematic uncertainties are added in quadrature.
[c]The mass windows corresponding to ϕ and charmonium resonances decaying to $\mu\mu$ are vetoed.
[d]$0.5 < m_{\pi^+\pi^-} < 1.3$ GeV/c^2.

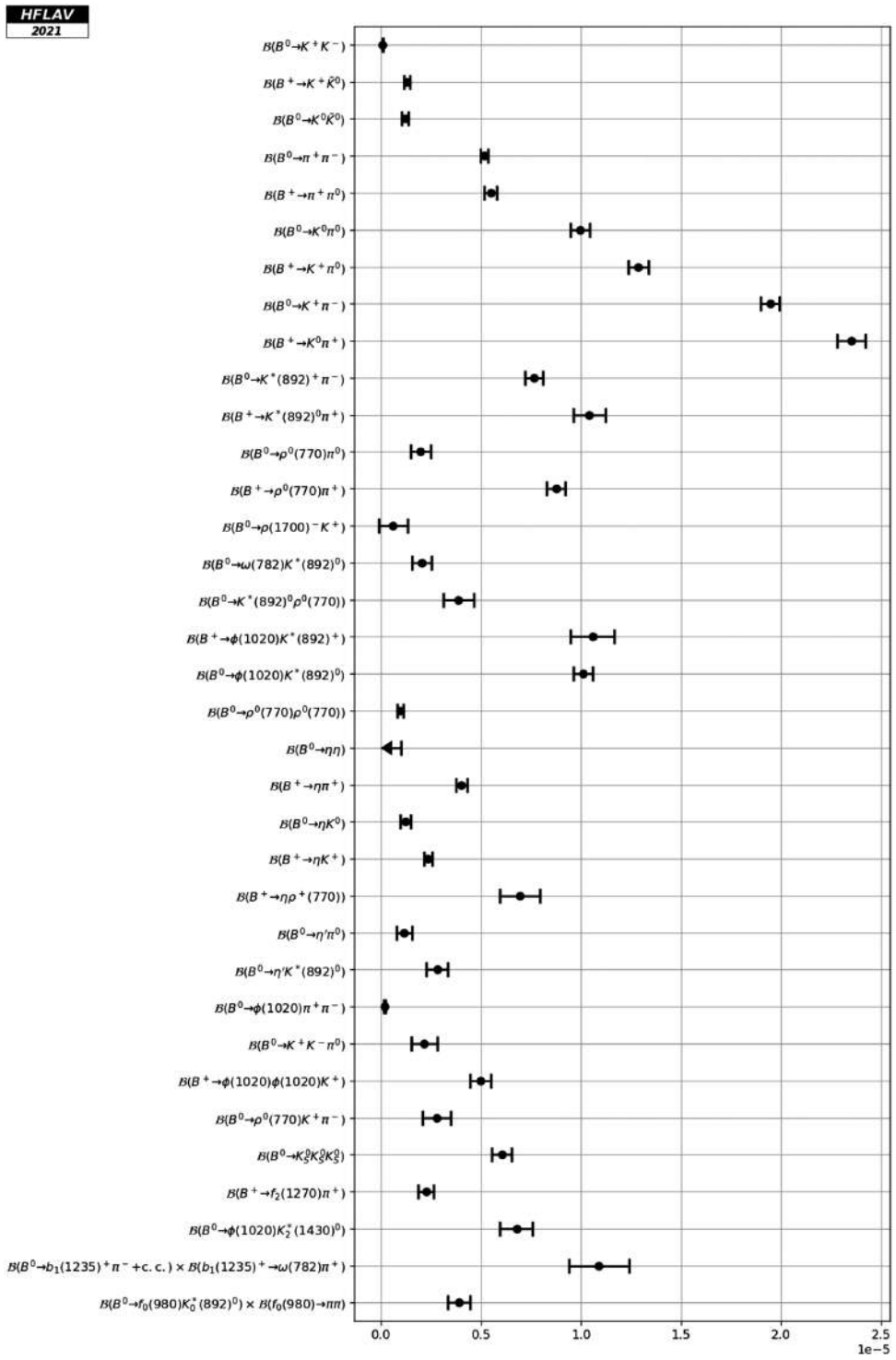

FIG. 69. A selection of high-precision charmless mesonic B meson branching fraction measurements.

B. Baryonic decays of B^+ and B^0 mesons

This section provides branching fractions of charmless baryonic decays of B^+ and B^0 mesons in Tables 209,210 and 211,212, respectively. Relative branching fractions are given in Table 213. Figures 70 and 71 show graphic representations of a selection of results given in this section.

TABLE 209. Branching fractions of charmless baryonic B^+ decays (part 1).

Parameter [10^{-6}]	Measurements		Average $^{\text{HFLAV}}_{\text{PDG}}$
$\mathcal{B}(B^+ \to p\bar{p}\pi^+)$	Belle [1008]	$1.60^{+0.22}_{-0.19} \pm 0.12$[a]	1.62 ± 0.21
	BABAR [721]	$1.69 \pm 0.29 \pm 0.26$[b]	$1.62^{+0.21}_{-0.19}$
$\mathcal{B}(B^+ \to p\bar{p}\pi^+), m_{p\bar{p}} < 2.85$ GeV/c^2	LHCb [1009][c]		1.00 ± 0.11 none
$\mathcal{B}(B^+ \to p\bar{p}\pi^+(\text{NR}))$	CLEO [910]	<53	<53
$\mathcal{B}(B^+ \to p\bar{p}\pi^+\pi^0)$	Belle [1010]	$4.58 \pm 1.17 \pm 0.67$[d]	4.6 ± 1.3
$\mathcal{B}(B^+ \to p\bar{p}\pi^+\pi^+\pi^-)$	ARGUS [1011]	<520	<520
$\mathcal{B}(B^+ \to p\bar{p}K^+)$[e]	Belle [1008]	$5.54^{+0.27}_{-0.25} \pm 0.36$[a]	5.9 ± 0.4
	BABAR [800]	$6.7 \pm 0.5 \pm 0.4$[b]	5.9 ± 0.5
$\mathcal{B}(B^+ \to p\bar{p}K^+), m_{p\bar{p}} < 2.85$ GeV/c^2	LHCb [808][f]		$4.37^{+0.30}_{-0.29}$ none
$\mathcal{B}(B^+ \to \Theta^{++}(1710)\bar{p}) \times \mathcal{B}(\Theta^{++}(1710) \to pK^+)$[g]	Belle [928]	<0.091	<0.091
$\mathcal{B}(B^+ \to f_J(2220)K^+) \times \mathcal{B}(f_J(2220) \to p\bar{p})$	Belle [928]	<0.41	<0.41
$\mathcal{B}(B^+ \to p\bar{\Lambda}(1520))$	*BABAR* [800]	<1.5	$0.305^{+0.084}_{-0.081}$
	LHCb [1009][h]		0.315 ± 0.055
$\mathcal{B}(B^+ \to p\bar{p}K^+(\text{NR}))$	CLEO [910]	<89	<89

[a]The charmonium mass regions are vetoed.
[b]Charmonium decays to $p\bar{p}$ have been statistically subtracted.
[c]Measurement of $\mathcal{B}(B^+ \to p\bar{p}\pi^+), m_{p\bar{p}} < 2.85$ GeV/c^2/$(\mathcal{B}(B^+ \to J/\psi\pi^+)\mathcal{B}(J/\psi \to p\bar{p}))$ used in our fit.
[d]$m_{\pi^+\pi^0} < 1.3$ GeV/c^2.
[e]The PDG uncertainty includes a scale factor.
[f]Measurement of $\mathcal{B}(B^+ \to p\bar{p}K^+), m_{p\bar{p}} < 2.85$ GeV/c^2/$(\mathcal{B}(\text{B}^+ \to \text{J}/\psi\text{K}^+)\mathcal{B}(\text{J}/\psi \to \text{p}\bar{\text{p}}))$ used in our fit.
[g]Pentaquark candidate.
[h]Measurement of $(\mathcal{B}(B^+ \to p\bar{\Lambda}(1520))\mathcal{B}(\overline{\Lambda(1520)} \to K^+p))/(\mathcal{B}(B^+ \to J/\psi K^+)\mathcal{B}(J/\psi \to p\bar{p}))$ used in our fit.

TABLE 210. Branching fractions of charmless baryonic B^+ decays (part 2).

Parameter [10^{-6}]	Measurements		Average HFLAV PDG
$\mathcal{B}(B^+ \to p\bar{p}K^*(892)^+)$	Belle [1012]	$3.38^{+0.73}_{-0.60} \pm 0.39$[a]	$3.6^{+0.8}_{-0.7}$
	BABAR [721]	$5.3 \pm 1.5 \pm 1.3$[b]	
$\mathcal{B}(B^+ \to f_J(2220)K^*(892)^+) \times \mathcal{B}(f_J(2220) \to p\bar{p})$			
	BABAR [721]	<0.77	<0.77
$\mathcal{B}(B^+ \to p\bar{\Lambda}^0)$	LHCb [1013]	$0.24^{+0.10}_{-0.08} \pm 0.03$	$0.24^{+0.10}_{-0.09}$
	Belle [1014]	<0.32	
$\mathcal{B}(B^+ \to p\bar{\Lambda}^0\pi^0)$	Belle [1015]	$3.00^{+0.61}_{-0.53} \pm 0.33$	$3.00^{+0.69}_{-0.62}$
$\mathcal{B}(B^+ \to p\bar{\Sigma}(1385)^0)$	Belle [1015]	<0.47	<0.47
$\mathcal{B}(B^+ \to \Delta(1232)^+\bar{\Lambda}^0)$	Belle [1015]	<0.82	<0.82
$\mathcal{B}(B^+ \to p\bar{\Lambda}^0\pi^+\pi^-)$	Belle [1016]	$11.28^{+0.91}_{-0.72} \pm 1.03$	11.3 ± 1.3 $11.3^{+1.4}_{-1.3}$
$\mathcal{B}(B^+ \to p\bar{\Lambda}^0\pi^+\pi^-(\mathrm{NR}))$	Belle [1016]	$5.92^{+0.88}_{-0.84} \pm 0.69$	5.9 ± 1.1
$\mathcal{B}(B^+ \to p\bar{\Lambda}^0\rho^0(770)) \times \mathcal{B}(\rho^0(770) \to \pi^+\pi^-)$			
	Belle [1016]	$4.78^{+0.67}_{-0.64} \pm 0.60$	4.8 ± 0.9
$\mathcal{B}(B^+ \to p\bar{\Lambda}^0 f_2(1270)) \times \mathcal{B}(f_2(1270) \to \pi^+\pi^-)$			
	Belle [1016]	$2.03^{+0.77}_{-0.72} \pm 0.27$	2.0 ± 0.8
$\mathcal{B}(B^+ \to p\bar{\Lambda}^0K^+K^-)$	Belle [1017]	$4.10^{+0.45}_{-0.43} \pm 0.50$	4.1 ± 0.7
$\mathcal{B}(B^+ \to p\bar{\Lambda}^0\phi(1020))$	Belle [1017]	$0.795 \pm 0.209 \pm 0.077$	0.80 ± 0.22
$\mathcal{B}(B^+ \to \bar{p}\Lambda^0K^+K^-)$	Belle [1017]	$3.70^{+0.39}_{-0.37} \pm 0.44$	3.7 ± 0.6
$\mathcal{B}(B^+ \to \Lambda^0\bar{\Lambda}^0\pi^+)$	Belle [685]	<0.94[c,d]	<0.94
$\mathcal{B}(B^+ \to \Lambda^0\bar{\Lambda}^0K^+)$	Belle [685]	$3.38^{+0.41}_{-0.36} \pm 0.41$[c]	3.4 ± 0.6 $3.4^{+0.6}_{-0.5}$
$\mathcal{B}(B^+ \to \Lambda^0\bar{\Lambda}^0K^*(892)^+)$	Belle [685]	$2.19^{+1.13}_{-0.88} \pm 0.33$[c,d]	$2.2^{+1.2}_{-0.9}$
$\mathcal{B}(B^+ \to \Lambda(1520)\bar{\Lambda}^0K^+)$	Belle [1017]	$2.23 \pm 0.63 \pm 0.25$	2.2 ± 0.7
$\mathcal{B}(B^+ \to \bar{\Lambda}(1520)\Lambda^0K^+)$	Belle [1017]	<2.08	<2.1
$\mathcal{B}(B^+ \to \bar{\Delta}(1232)^0p)$	Belle [1008]	<1.38	<1.4
$\mathcal{B}(B^+ \to \Delta^{++}\bar{p})$	Belle [1008]	<0.14	<0.14

[a]The charmonium mass region has been vetoed.
[b]Charmonium decays to $p\bar{p}$ have been statistically subtracted.
[c]The charmonium mass regions are vetoed.
[d]$M_{\Lambda^0\overline{\Lambda^0}} < 2.85\ \mathrm{GeV}/c^2$.

TABLE 211. Branching fractions of charmless baryonic B^0 decays (part 1).

Parameter [10^{-6}]	Measurements		Average HFLAV PDG
$\mathcal{B}(B^0 \to p\bar{p})$	LHCb [1018]	$0.0125 \pm 0.0027 \pm 0.0018$	0.0125 ± 0.0032
	Belle [1014]	<0.11	
	BABAR [1019]	<0.27	
$\mathcal{B}(B^0 \to p\bar{p}\pi^+\pi^-)$	LHCb [1020]	$2.7 \pm 0.1 \pm 0.2$[a,b]	2.7 ± 0.2 2.9 ± 0.2
$\mathcal{B}(B^0 \to p\bar{p}\pi^+\pi^-), m_{\pi^+\pi^-} < 1.22$ GeV/c^2	Belle [1010]	$0.83 \pm 0.17 \pm 0.17$[c]	0.83 ± 0.24 none
$\mathcal{B}(B^0 \to p\bar{p}K^+\pi^-)$	LHCb [1020]	$5.9 \pm 0.3 \pm 0.5$[a,b]	5.9 ± 0.6 6.3 ± 0.5
$\mathcal{B}(B^0 \to p\bar{p}K^0)$	Belle [1012]	$2.51^{+0.35}_{-0.29} \pm 0.21$[d]	2.7 ± 0.3
	BABAR [721]	$3.0 \pm 0.5 \pm 0.3$[e]	
$\mathcal{B}(B^0 \to \Theta(1540)^+\bar{p}) \times \mathcal{B}(\Theta(1540)^+ \to pK^0_S)$[f]	*BABAR* [721]	<0.05	<0.05
	Belle [928]	<0.23	
$\mathcal{B}(B^0 \to f_J(2220)K^0) \times \mathcal{B}(f_J(2220) \to p\bar{p})$	*BABAR* [721]	<0.45	<0.45
$\mathcal{B}(B^0 \to p\bar{p}K^*(892)^0)$	Belle [1012]	$1.18^{+0.29}_{-0.25} \pm 0.11$[d]	1.24 ± 0.27 $1.24^{+0.28}_{-0.25}$
	BABAR [721]	$1.47 \pm 0.45 \pm 0.40$[e]	
$\mathcal{B}(B^0 \to f_J(2220)K^*(892)^0) \times \mathcal{B}(f_J(2220) \to p\bar{p})$	*BABAR* [721]	<0.15	<0.15

[a] $m_{p\bar{p}} < 2.85$ GeV/c^2.
[b] Multiple systematic uncertainties are added in quadrature.
[c] $0.46 < m_{\pi^+\pi^-} < 0.53$ GeV/c^2 invariant mass region has been excluded.
[d] The charmonium mass region has been vetoed.
[e] Charmonium decays to $p\bar{p}$ have been statistically subtracted.
[f] Pentaquark candidate.

TABLE 212. Branching fractions of charmless baryonic B^0 decays (part 2).

Parameter [10^{-6}]	Measurements		Average HFLAV PDG
$\mathcal{B}(B^0 \to p\bar{p}K^+K^-)$	LHCb [1020]	$0.113 \pm 0.028 \pm 0.014$[a,b]	0.113 ± 0.031 0.121 ± 0.032
$\mathcal{B}(B^0 \to p\bar{p}\pi^0)$	Belle [1021]	$0.50 \pm 0.18 \pm 0.06$	0.50 ± 0.19
$\mathcal{B}(B^0 \to pp\bar{p}\,\bar{p})$	*BABAR* [1022]	<0.2	<0.2
$\mathcal{B}(B^0 \to p\bar{\Lambda}^0\pi^-)$	*BABAR* [1023]	$3.07 \pm 0.31 \pm 0.23$	3.14 ± 0.28 $3.14^{+0.29}_{-0.28}$
	Belle [1015]	$3.23^{+0.33}_{-0.29} \pm 0.29$	
$\mathcal{B}(B^0 \to p\bar{\Sigma}(1385)^-)$	Belle [1015]	<0.26	<0.26
$\mathcal{B}(B^0 \to \Delta(1232)^+\bar{p} + \text{c.c.})$	Belle [1021]	<1.6	<1.6
$\mathcal{B}(B^0 \to \Delta(1232)^0\bar{\Lambda}^0)$	Belle [1015]	<0.93	<0.93
$\mathcal{B}(B^0 \to p\bar{\Lambda}^0K^-)$	Belle [1024]	<0.82	<0.82
$\mathcal{B}(B^0 \to \bar{\Lambda}^0\Lambda^0)$	Belle [1014]	<0.32	<0.32
$\mathcal{B}(B^0 \to \bar{\Lambda}^0\Lambda^0K^0)$	Belle [685]	$4.76^{+0.84}_{-0.68} \pm 0.61$[c]	$4.8^{+1.0}_{-0.9}$

(Table continued)

TABLE 212. *(Continued)*

Parameter [10^{-6}]	Measurements		Average HFLAV PDG
$\mathcal{B}(B^0 \to \Lambda^0 \bar{\Lambda}^0 K^*(892)^0)$	Belle [685]	$2.46^{+0.87}_{-0.72} \pm 0.34$[c]	$2.46^{+0.93}_{-0.80}$
$\mathcal{B}(B^0 \to \Delta(1232)^0 \bar{\Delta}(1232)^0)$	CLEO [958]	<1500[d]	<1500
$\mathcal{B}(B^0 \to \Delta^{++}\bar{\Delta}^{--})$	CLEO [958]	<110[d]	<110

[a] $m_{p\bar{p}} < 2.85$ GeV/c^2.
[b] Multiple systematic uncertainties are added in quadrature.
[c] The charmonium mass regions are vetoed.
[d] CLEO assumes $\mathcal{B}(\Upsilon(4S) \to B^0\bar{B}^0) = 0.43$. The result has been modified to account for a branching fraction of 0.50.

TABLE 213. Baryonic relative branching fractions.

Parameter	Measurements		Average
$\frac{\mathcal{B}(B^+ \to p\bar{p}\pi^+, m_{p\bar{p}}<2.85\ \mathrm{GeV/c^2})}{\mathcal{B}(B^+ \to J/\psi\pi^+)\times\mathcal{B}(J/\psi \to p\bar{p})}$	LHCb [1009]	$12.0 \pm 1.2 \pm 0.3$	12.0 ± 1.2
$\frac{\mathcal{B}(B^+ \to p\bar{p}K^+)}{\mathcal{B}(B^+ \to J/\psi K^+)\times\mathcal{B}(J/\psi \to p\bar{p})}$	LHCb [808]	$4.91 \pm 0.19 \pm 0.14$[a]	4.91 ± 0.24
$\frac{\mathcal{B}(B^+ \to p\bar{p}K^+, m_{p\bar{p}}<2.85\ \mathrm{GeV/c^2})}{\mathcal{B}(B^+ \to J/\psi\pi^+)\times\mathcal{B}(J/\psi \to p\bar{p})}$	LHCb [808]	$2.02 \pm 0.10 \pm 0.08$	2.02 ± 0.13
$\frac{\mathcal{B}(B^+ \to \bar{\Lambda}(1520)p)\times\mathcal{B}(\bar{\Lambda}(1520) \to K^+\bar{p}))}{\mathcal{B}(B^+ \to J/\psi\pi^+)\times\mathcal{B}(J/\psi \to p\bar{p})}$	LHCb [1009]	$0.033 \pm 0.005 \pm 0.007$	0.033 ± 0.009
$\frac{\mathcal{B}(B^0 \to p\bar{p}K^+K^-)}{\mathcal{B}(B^0 \to p\bar{p}K^+\pi^-)}$	LHCb [1020]	$0.019 \pm 0.005 \pm 0.002$[b]	0.019 ± 0.005
$\frac{\mathcal{B}(B^0 \to p\bar{p}\pi^+\pi^-)}{\mathcal{B}(B^0 \to p\bar{p}K^+\pi^-)}$	LHCb [1020]	$0.46 \pm 0.02 \pm 0.02$[b]	0.46 ± 0.03

[a] Includes contribution where $p\bar{p}$ is produced in charmonium decays.
[b] $m_{p\bar{p}} < 2.85$ GeV/c^2.

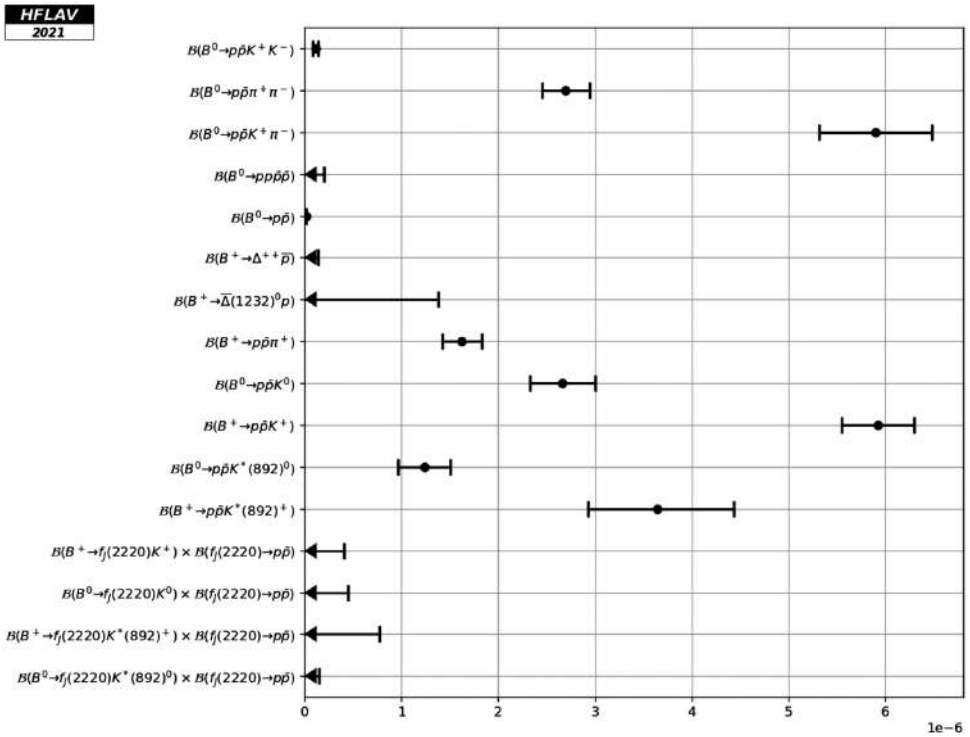

FIG. 70. Branching fractions of charmless baryonic B^+ and B^0 decays into nonstrange baryons.

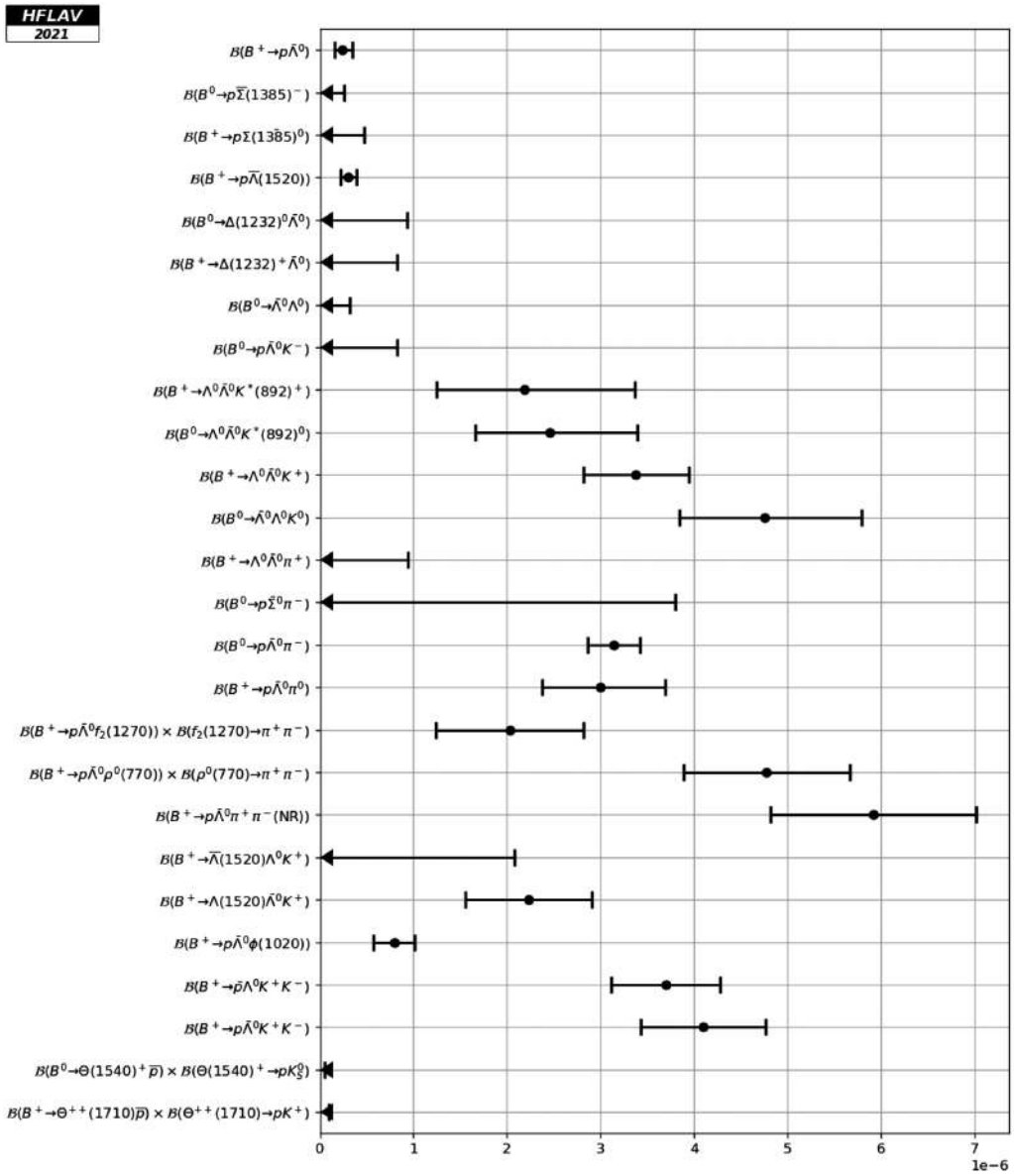

FIG. 71. Branching fractions of charmless baryonic B^+ and B^0 decays into strange baryons.

C. Decays of *b* baryons

A compilation of branching fractions of Λ_b^0 baryon decays is given in Tables 214 and 215. Table 216 provides the partial branching fractions of $\Lambda_b^0 \to \Lambda\mu^+\mu^-$ decays in intervals of $q^2 = m^2(\mu^+\mu^-)$. Compilations of branching fractions of Ξ_b^0, Ξ_b^- and Ω_b^- baryon decays are given in Tables 217, 218, and 219, respectively. Finally, ratios of branching fractions of Λ_b^0, Ξ_b^0 and Ω_b^- baryon decays are detailed in Tables 220, 221 and 222, respectively. Figure 72 shows a graphic representation of branching fractions of Λ_b^0 decays.

Measurements that are not included in the tables:

(i) In Ref. [1034], LHCb measures angular observables of the decay $\Lambda_b^0 \to \Lambda\mu^+\mu^-$, including the lepton-side, hadron-side and combined forward-backward asymmetries of the decay in the low recoil region $15 < m^2(\ell\ell) < 20\ \mathrm{GeV}^2/c^4$.

(ii) In Ref. [1035], LHCb performs a search for baryon-number-violating Ξ_b^0 oscillations and set an upper limit of $\omega < 0.08\ \mathrm{ps}^{-1}$ on the oscillation rate.

TABLE 214. Branching fractions of charmless Λ_b^0 decays (part 1).

Parameter [10^{-6}]	Measurements		Average HFLAV PDG
$\mathcal{B}(\Lambda_b^0 \to p\bar{K}^0\pi^-)$	LHCb [973]	$12.4 \pm 2.0 \pm 3.6$[a,b]	12.4 ± 4.2 12.6 ± 4.1
$\mathcal{B}(\Lambda_b^0 \to pK^0K^-)$	LHCb [973]	<3.5[b]	<3.5
$\mathcal{B}(\Lambda_b^0 \to p\pi^-)$[c]	LHCb [963] CDF [960][e]	$4.68 \pm 0.44 \pm 0.95$[d]	$4.5^{+0.9}_{-0.8}$ 4.5 ± 0.8
$\mathcal{B}(\Lambda_b^0 \to pK^-)$[c]	CDF [960] LHCb [963][f]	$6.3 \pm 1.2 \pm 0.8$	5.4 ± 1.1 5.4 ± 1.0
$\mathcal{B}(\Lambda_b^0 \to \Lambda^0\mu^+\mu^-)$	LHCb [1025] CDF [1026]	$0.955 \pm 0.186 \pm 0.249$[a,g] $1.520 \pm 0.366 \pm 0.387$[g]	$1.09^{+0.34}_{-0.29}$ 1.08 ± 0.28
$\mathcal{B}(\Lambda_b^0 \to p\pi^-\mu^+\mu^-)$	LHCb [1027][h]		$0.069^{+0.027}_{-0.023}$ $0.069^{+0.025}_{-0.024}$
$\mathcal{B}(\Lambda_b^0 \to pK^-e^+e^-)$	LHCb [1028]	$0.311^{+0.044\,+0.061}_{-0.041\,-0.051}$[i,j]	$0.31^{+0.08}_{-0.06}$ $0.31^{+0.07}_{-0.06}$
$\mathcal{B}(\Lambda_b^0 \to pK^-\mu^+\mu^-)$	LHCb [1028]	$0.266 \pm 0.013^{+0.050}_{-0.040}$[i,j]	$0.266^{+0.052}_{-0.041}$ $0.265^{+0.051}_{-0.041}$

[a]Multiple systematic uncertainties are added in quadrature.
[b]Using $\mathcal{B}(B^0 \to K^0\pi^+\pi^-)$.
[c]The PDG average is a result of a fit including input from other measurements.
[d]Using $\mathcal{B}(\Lambda_b^0 \to pK^-)$.
[e]Measurement of $(\mathcal{B}(\Lambda_b^0 \to p\pi^-)/\mathcal{B}(B^0 \to K^+\pi^-))(f_{\Lambda_b^0}/f_d)$ used in our fit.
[f]Measurement of $\mathcal{B}(\Lambda_b^0 \to p\pi^-)/\mathcal{B}(\Lambda_b^0 \to pK^-)$ used in our fit.
[g]Using $\mathcal{B}(\Lambda_b^0 \to J/\psi\Lambda^0)$.
[h]Measurement of $\mathcal{B}(\Lambda_b^0 \to p\pi^-\mu^+\mu^-)/(\mathcal{B}(\Lambda_b^0 \to J/\psi p\pi^-)\mathcal{B}(J/\psi \to \mu^+\mu^-))$ used in our fit.
[i]measured in the $m^2_{\ell^+\ell^-}$ bin $[0.1, 6.0]$ GeV^2/c^4 and for $m_{pK} < 2.6$ GeV/c^2.
[j]Using $\mathcal{B}(\Lambda_b^0 \to J/\psi pK^-)$.

TABLE 215. Branching fractions of charmless Λ_b^0 decays (part 2).

Parameter [10^{-6}]	Measurements		Average HFLAV PDG
$\mathcal{B}(\Lambda_b^0 \to \Lambda^0\gamma)$	LHCb [1029][a]		6.9 ± 1.5 7.1 ± 1.7
$\mathcal{B}(\Lambda_b^0 \to \Lambda^0\eta)$	LHCb [965]	$9.23^{+7.15}_{-5.20} \pm 0.40$[b]	$9.2^{+7.2}_{-5.2}$ $9.4^{+7.3}_{-5.3}$
$\mathcal{B}(\Lambda_b^0 \to \Lambda^0\eta')$	LHCb [965]	<3.05[b]	<3.1
$\mathcal{B}(\Lambda_b^0 \to \Lambda^0\pi^+\pi^-)$	LHCb [1030][c]		$4.7^{+2.0}_{-1.9}$ 4.7 ± 1.9
$\mathcal{B}(\Lambda_b^0 \to \Lambda^0K^+\pi^-)$	LHCb [1030][d]		$5.7^{+1.3}_{-1.2}$ 5.7 ± 1.3
$\mathcal{B}(\Lambda_b^0 \to \Lambda^0K^+K^-)$	LHCb [1030][e]		$16.1^{+2.4}_{-2.2}$ 16.2 ± 2.3
$\mathcal{B}(\Lambda_b^0 \to \Lambda^0\phi(1020))$	LHCb [987][f]		$10.1^{+2.9}_{-2.5}$ 9.8 ± 2.6

(Table continued)

TABLE 215. *(Continued)*

Parameter [10^{-6}]	Measurements	Average HFLAV PDG
$\mathcal{B}(\Lambda_b^0 \to p\pi^+\pi^-\pi^-)$	LHCb [1031][g,h,i]	$21.1^{+2.4}_{-2.3}$ 21.1 ± 2.3
$\mathcal{B}(\Lambda_b^0 \to pK^-K^+\pi^-)$	LHCb [1031][h,j]	$4.06^{+0.66}_{-0.61}$ 4.07 ± 0.63
$\mathcal{B}(\Lambda_b^0 \to pK^-\pi^+\pi^-)$	LHCb [1031][h,k]	$50.5^{+5.6}_{-5.3}$ 50.6 ± 5.4
$\mathcal{B}(\Lambda_b^0 \to pK^-K^+K^-)$	LHCb [1031][h,l]	$12.6^{+1.5}_{-1.4}$ 12.7 ± 1.4

[a]Measurement of $(\mathcal{B}(\Lambda_b^0 \to \Lambda^0\gamma)/\mathcal{B}(B^0 \to K^*(892)^0\gamma))\frac{f_{\Lambda_b^0}}{f_d}$ used in our fit.
[b]Using $\mathcal{B}(B^0 \to \eta' K^0)$.
[c]Measurement of $\mathcal{B}(\Lambda_b^0 \to \Lambda^0\pi^+\pi^-)/(\mathcal{B}(\Lambda_b^0 \to \Lambda_c^+\pi^-)\mathcal{B}(\Lambda_c^+ \to \Lambda^0\pi^+))$ used in our fit.
[d]Measurement of $\mathcal{B}(\Lambda_b^0 \to \Lambda^0K^+\pi^-)/(\mathcal{B}(\Lambda_b^0 \to \Lambda_c^+\pi^-)\mathcal{B}(\Lambda_c^+ \to \Lambda^0\pi^+))$ used in our fit.
[e]Measurement of $\mathcal{B}(\Lambda_b^0 \to \Lambda^0K^+K^-)/(\mathcal{B}(\Lambda_b^0 \to \Lambda_c^+\pi^-)\mathcal{B}(\Lambda_c^+ \to \Lambda^0\pi^+))$ used in our fit.
[f]Measurement of $(\mathcal{B}(\Lambda_b^0 \to \Lambda^0\phi(1020))/\mathcal{B}(B^0 \to \phi(1020)K^0))(f_{\Lambda_b^0}/f_d)2$ used in our fit.
[g]Vetoes on charm and charmonium resonances are applied.
[h]Multiple systematic uncertainties are added in quadrature.
[i]Measurement of $\mathcal{B}(\Lambda_b^0 \to p\pi^+\pi^-\pi^-)/(\mathcal{B}(\Lambda_b^0 \to \Lambda_c^+\pi^-)\mathcal{B}(\Lambda_c^+ \to pK^-\pi^+))$ used in our fit.
[j]Measurement of $\mathcal{B}(\Lambda_b^0 \to pK^-K^+\pi^-)/(\mathcal{B}(\Lambda_b^0 \to \Lambda_c^+\pi^-)\mathcal{B}(\Lambda_c^+ \to pK^-\pi^+))$ used in our fit.
[k]Measurement of $\mathcal{B}(\Lambda_b^0 \to pK^-\pi^+\pi^-)/(\mathcal{B}(\Lambda_b^0 \to \Lambda_c^+\pi^-)\mathcal{B}(\Lambda_c^+ \to pK^-\pi^+))$ used in our fit.
[l]Measurement of $\mathcal{B}(\Lambda_b^0 \to pK^-K^+K^-)/(\mathcal{B}(\Lambda_b^0 \to \Lambda_c^+\pi^-)\mathcal{B}(\Lambda_c^+ \to pK^-\pi^+))$ used in our fit.

TABLE 216. Partial branching fractions of $\Lambda_b^0 \to \Lambda\mu^+\mu^-$ decays in intervals of $m^2_{\mu^+\mu^-}$.

Parameter [10^{-7}]	Measurements		Average HFLAV PDG
$m^2_{\mu^+\mu^-} < 2.0$ GeV$^2/c^4$			
	LHCb [1032]	$0.72^{+0.24}_{-0.22} \pm 0.14$	0.7 ± 0.3
	CDF [1026]	$0.15 \pm 2.01 \pm 0.05$	
$2.0 < m^2_{\mu^+\mu^-} < 4.3$ GeV$^2/c^4$			
	LHCb [1032]	$0.253^{+0.276}_{-0.207} \pm 0.046$	$0.3^{+0.3}_{-0.2}$
	CDF [1026]	$1.84 \pm 1.66 \pm 0.59$	
$4.3 < m^2_{\mu^+\mu^-} < 8.68$ GeV$^2/c^4$			
	LHCb [1025]	$0.66 \pm 0.72 \pm 0.16$	0.5 ± 0.7
	CDF [1026]	$-0.20 \pm 1.64 \pm 0.08$	
$10.09 < m^2_{\mu^+\mu^-} < 12.86$ GeV$^2/c^4$			
	LHCb [1032]	$2.08^{+0.42}_{-0.39} \pm 0.42$	2.2 ± 0.6
	CDF [1026]	$2.97 \pm 1.47 \pm 0.95$	
$14.18 < m^2_{\mu^+\mu^-} < 16.00$ GeV$^2/c^4$			
	LHCb [1032]	$2.04^{+0.35}_{-0.33} \pm 0.42$	1.7 ± 0.4
	CDF [1026]	$0.96 \pm 0.73 \pm 0.31$	1.7 ± 0.5
$m^2_{\mu^+\mu^-} > 16.00$ GeV$^2/c^4$			
	CDF [1026]	$6.97 \pm 1.88 \pm 2.23$	7.0 ± 2.9

TABLE 217. Branching fractions of charmless Ξ_b^0 decays.

Parameter $[10^{-6}]$	Measurements		Average HFLAV PDG
$\frac{f_{\Xi_b^0}}{f_d}\mathcal{B}(\Xi_b^0 \to p\bar{K}^0\pi^-)$	LHCb [973]	<1.5[a]	<1.5 <1.6
$\frac{f_{\Xi_b^0}}{f_d}\mathcal{B}(\Xi_b^0 \to p\bar{K}^0K^-)$	LHCb [973]	<1.0[a]	<0.99 <1.10
$\frac{f_{\Xi_b^0}}{f_{\Lambda_b^0}}\mathcal{B}(\Xi_b^0 \to \Lambda\pi^+\pi^-)$	LHCb [1030]	<1.7	<1.7
$\frac{f_{\Xi_b^0}}{f_{\Lambda_b^0}}\mathcal{B}(\Xi_b^0 \to \Lambda K^-\pi^+)$	LHCb [1030]	<0.8	<0.8
$\frac{f_{\Xi_b^0}}{f_{\Lambda_b^0}}\mathcal{B}(\Xi_b^0 \to \Lambda K^+K^-)$	LHCb [1030]	<0.3	<0.3
$\frac{f_{\Xi_b^0}}{f_{\Lambda_b^0}}\mathcal{B}(\Xi_b^0 \to pK^-\pi^+\pi^-)$	LHCb [1031][b,c]		$1.91^{+0.41}_{-0.38}$ 1.91 ± 0.40
$\frac{f_{\Xi_b^0}}{f_{\Lambda_b^0}}\mathcal{B}(\Xi_b^0 \to pK^-K^-\pi^+)$	LHCb [1031][b,d]		$1.72^{+0.33}_{-0.30}$ 1.73 ± 0.32
$\frac{f_{\Xi_b^0}}{f_{\Lambda_b^0}}\mathcal{B}(\Xi_b^0 \to pK^+K^-K^-)$	LHCb [1031][b,e]		0.18 ± 0.10

[a]Using $\mathcal{B}(B^0 \to K^0\pi^+\pi^-)$.
[b]Multiple systematic uncertainties are added in quadrature.
[c]Measurement of $\frac{f_{\Xi_b^0}}{f_{\Lambda_b^0}}\mathcal{B}(\Xi_b^0 \to pK^-\pi^+\pi^-)/(\mathcal{B}(\Lambda_b^0 \to \Lambda_c^+\pi^-)\mathcal{B}(\Lambda_c^+ \to pK^-\pi^+))$ used in our fit.
[d]Measurement of $\frac{f_{\Xi_b^0}}{f_{\Lambda_b^0}}\mathcal{B}(\Xi_b^0 \to pK^-K^-\pi^+)/(\mathcal{B}(\Lambda_b^0 \to \Lambda_c^+\pi^-)\mathcal{B}(\Lambda_c^+ \to pK^-\pi^+))$ used in our fit.
[e]Measurement of $\frac{f_{\Xi_b^0}}{f_{\Lambda_b^0}}\mathcal{B}(\Xi_b^0 \to pK^+K^-K^-)/(\mathcal{B}(\Lambda_b^0 \to \Lambda_c^+\pi^-)\mathcal{B}(\Lambda_c^+ \to pK^-\pi^+))$ used in our fit.

TABLE 218. Relative branching fractions of charmless Ξ_b^- decays.

Parameter $[10^{-2}]$	Measurements		Average
$\frac{f_{\Xi_b^-}}{f_u}\frac{\mathcal{B}(\Xi_b^- \to pK^-K^-)}{\mathcal{B}(B^- \to K^+K^-K^-)}$	LHCb [1033]	$0.2650 \pm 0.0350 \pm 0.0470$	0.265 ± 0.059
$\frac{f_{\Xi_b^-}}{f_u}\frac{\mathcal{B}(\Xi_b^- \to p\pi^-\pi^-)}{\mathcal{B}(B^- \to K^+K^-K^-)}$	LHCb [1033]	<0.1470	<0.15
$\frac{f_{\Xi_b^-}}{f_u}\frac{\mathcal{B}(\Xi_b^- \to pK^-\pi^-)}{\mathcal{B}(B^- \to K^+K^-K^-)}$	LHCb [1033]	$0.2590 \pm 0.0640 \pm 0.0490$	0.259 ± 0.081
$\frac{\mathcal{B}(\Xi_b^- \to p\pi^-\pi^-)}{\mathcal{B}(\Xi_b^- \to pK^-K^-)}$	LHCb [1033]	<56	<56
$\frac{\mathcal{B}(\Xi_b^- \to pK^-\pi^-)}{\mathcal{B}(\Xi_b^- \to pK^-K^-)}$	LHCb [1033]	$98 \pm 27 \pm 9$	98 ± 28

TABLE 219. Branching fractions of charmless Ω_b^- decays.

Parameter $[10^{-8}]$	Measurements		Average
$\frac{f_{\Omega_b^-}}{f_u} \times \mathcal{B}(\Omega_b^- \to pK^-K^-)$	LHCb [1033]	<0.59[a]	<0.59
$\frac{f_{\Omega_b^-}}{f_u} \times \mathcal{B}(\Omega_b^- \to pK^-\pi^-)$	LHCb [1033]	<1.68[a]	<1.7
$\frac{f_{\Omega_b^-}}{f_u} \times \mathcal{B}(\Omega_b^- \to p\pi^-\pi^-)$	LHCb [1033]	<3.59[a]	<3.6

[a]Using $\mathcal{B}(B^+ \to K^+K^+K^-)$.

TABLE 220. Relative branching fractions of charmless Λ_b^0 decays.

Parameter	Measurements		Average
$\frac{\mathcal{B}(\Lambda_b^0\to p\pi^-)}{\mathcal{B}(\Lambda_b^0\to pK^-)}$	LHCb [963]	$0.86 \pm 0.08 \pm 0.05$	0.86 ± 0.09
$\frac{\mathcal{B}(\Lambda_b^0\to \Lambda^0\eta)}{\mathcal{B}(B^0\to\eta' K^0)}$	LHCb [965]	$0.142^{+0.110}_{-0.080}$	$0.14^{+0.11}_{-0.08}$
$\frac{f_{\Lambda_b^0}}{f_d}\frac{\mathcal{B}(\Lambda_b^0\to p\pi^-)}{\mathcal{B}(B^0\to K^+\pi^-)}$	CDF [960]	$0.042 \pm 0.007 \pm 0.006$	0.042 ± 0.009
$\frac{f_{\Lambda_b^0}}{f_d}\frac{\mathcal{B}(\Lambda_b^0\to pK^-)}{\mathcal{B}(B^0\to K^+\pi^-)}$	CDF [960]	$0.066 \pm 0.009 \pm 0.008$	0.066 ± 0.012
$\frac{f_{\Lambda_b^0}}{f_d}\frac{\mathcal{B}(\Lambda_b^0\to \Lambda^0\phi)}{\mathcal{B}(B^0\to K_S^0\phi)}$	LHCb [987]	$0.55 \pm 0.11 \pm 0.04$	0.55 ± 0.12
$\frac{\mathcal{B}(\Lambda_b^0\to p\pi^-\mu^+\mu^-)}{\mathcal{B}(\Lambda_b^0\to J/\psi p\pi^-)\times\mathcal{B}(J/\psi\to\mu^+\mu^-)}$	LHCb [1027]	$0.044 \pm 0.012 \pm 0.007$	0.044 ± 0.014
$\frac{\mathcal{B}(\Lambda_b^0\to \Lambda^0\pi^+\pi^-)}{\mathcal{B}(\Lambda_b^0\to\Lambda_c^+\pi^-)\times\mathcal{B}(\Lambda_c^+\to\Lambda^0\pi^+)}$	LHCb [1030]	$0.073 \pm 0.019 \pm 0.022$	0.073 ± 0.029
$\frac{\mathcal{B}(\Lambda_b^0\to \Lambda^0 K^+\pi^-)}{\mathcal{B}(\Lambda_b^0\to\Lambda_c^+\pi^-)\times\mathcal{B}(\Lambda_c^+\to\Lambda^0\pi^+)}$	LHCb [1030]	$0.089 \pm 0.012 \pm 0.013$	0.089 ± 0.018
$\frac{\mathcal{B}(\Lambda_b^0\to \Lambda^0 K^+K^-)}{\mathcal{B}(\Lambda_b^0\to\Lambda_c^+\pi^-)\times\mathcal{B}(\Lambda_c^+\to\Lambda^0\pi^+)}$	LHCb [1030]	$0.253 \pm 0.019 \pm 0.019$	0.253 ± 0.027
$\frac{\mathcal{B}(\Lambda_b^0\to p\pi^-\pi^+\pi^-)}{\mathcal{B}(\Lambda_b^0\to\Lambda_c^+\pi^-)\times\mathcal{B}(\Lambda_c^+\to pK^-\pi^+)}$	LHCb [1031]	$0.0685 \pm 0.0019 \pm 0.0033$[a]	0.0685 ± 0.0038
$\frac{\mathcal{B}(\Lambda_b^0\to pK^-\pi^+\pi^-)}{\mathcal{B}(\Lambda_b^0\to\Lambda_c^+\pi^-)\times\mathcal{B}(\Lambda_c^+\to pK^-\pi^+)}$	LHCb [1031]	$0.164 \pm 0.003 \pm 0.007$[a]	0.164 ± 0.008
$\frac{\mathcal{B}(\Lambda_b^0\to pK^-K^+\pi^-)}{\mathcal{B}(\Lambda_b^0\to\Lambda_c^+\pi^-)\times\mathcal{B}(\Lambda_c^+\to pK^-\pi^+)}$	LHCb [1031]	$0.0132 \pm 0.0009 \pm 0.0013$[a]	0.0132 ± 0.0016
$\frac{\mathcal{B}(\Lambda_b^0\to pK^-K^+K^-)}{\mathcal{B}(\Lambda_b^0\to\Lambda_c^+\pi^-)\times\mathcal{B}(\Lambda_c^+\to pK^-\pi^+)}$	LHCb [1031]	$0.0411 \pm 0.0012 \pm 0.0020$[a]	0.0411 ± 0.0023
$\frac{\mathcal{B}(\Lambda_b^0\to p\bar{K}^0\pi^-)}{\mathcal{B}(B^0\to K^0\pi^+\pi^-)}$	LHCb [973]	$0.25 \pm 0.04 \pm 0.07$[a]	0.25 ± 0.08
$\frac{\mathcal{B}(\Lambda_b^0\to p\bar{K}^0 K^-)}{\mathcal{B}(B^0\to K^0\pi^+\pi^-)}$	LHCb [973]	<0.07	<0.07
$\frac{\mathcal{B}(\Lambda_b^0\to \Lambda^0\mu^+\mu^-)}{\mathcal{B}(\Lambda_b^0\to J/\psi\Lambda^0)}$	LHCb [1025]	$0.00154 \pm 0.00030 \pm 0.00020$[a]	0.00154 ± 0.00036

[a]Multiple systematic uncertainties are added in quadrature.

TABLE 221. Relative branching fractions of charmless Ξ_b^0 decays.

Parameter $[10^{-2}]$	Measurements		Average
$\frac{f_{\Xi_b^0}}{f_d}\times\frac{\mathcal{B}(\Xi_b^0\to p\overline{K^0}\pi^-)}{\mathcal{B}(B^0\to K^0\pi^+\pi^-)}$	LHCb [973]	<3	<3.0
$\frac{f_{\Xi_b^0}}{f_d}\times\frac{\mathcal{B}(\Xi_b^0\to p\overline{K^0}K^-)}{\mathcal{B}(B^0\to K^0\pi^+\pi^-)}$	LHCb [973]	<2	<2.0
$\frac{f_{\Xi_b^0}}{f_{\Lambda_b^0}}\times\frac{\mathcal{B}(\Xi_b^0\to pK^-K^+K^-)}{\mathcal{B}(\Lambda_b^0\to\Lambda_c^+\pi^-)\times\mathcal{B}(\Lambda_c^+\to pK^-\pi^+)}$	LHCb [1031]	$0.057 \pm 0.028 \pm 0.013$[a]	0.057 ± 0.031
$\frac{f_{\Xi_b^0}}{f_{\Lambda_b^0}}\times\frac{\mathcal{B}(\Xi_b^0\to pK^-\pi^+\pi^-)}{\mathcal{B}(\Lambda_b^0\to\Lambda_c^+\pi^-)\times\mathcal{B}(\Lambda_c^+\to pK^-\pi^+)}$	LHCb [1031]	$0.62 \pm 0.08 \pm 0.08$[a]	0.62 ± 0.11
$\frac{f_{\Xi_b^0}}{f_{\Lambda_b^0}}\times\frac{\mathcal{B}(\Xi_b^0\to pK^-\pi^+K^-)}{\mathcal{B}(\Lambda_b^0\to\Lambda_c^+\pi^-)\times\mathcal{B}(\Lambda_c^+\to pK^-\pi^+)}$	LHCb [1031]	$0.56 \pm 0.06 \pm 0.06$[a]	0.560 ± 0.088

[a]Multiple systematic uncertainties are added in quadrature.

TABLE 222. Relative branching fractions of charmless Ω_b^- decays.

Parameter $[10^{-3}]$	Measurements		Average
$\frac{f_{\Omega_b^-}}{f_u}\frac{\mathcal{B}(\Omega_b^-\to pK^-K^-)}{\mathcal{B}(B^-\to K^+K^-K^-)}$	LHCb [1033]	<0.180	<0.18
$\frac{f_{\Omega_b^-}}{f_u}\frac{\mathcal{B}(\Omega_b^-\to p\pi^-\pi^-)}{\mathcal{B}(B^-\to K^+K^-K^-)}$	LHCb [1033]	<1.090	<1.1
$\frac{f_{\Omega_b^-}}{f_u}\frac{\mathcal{B}(\Omega_b^-\to pK^-\pi^-)}{\mathcal{B}(B^-\to K^+K^-K^-)}$	LHCb [1033]	<0.510	<0.51

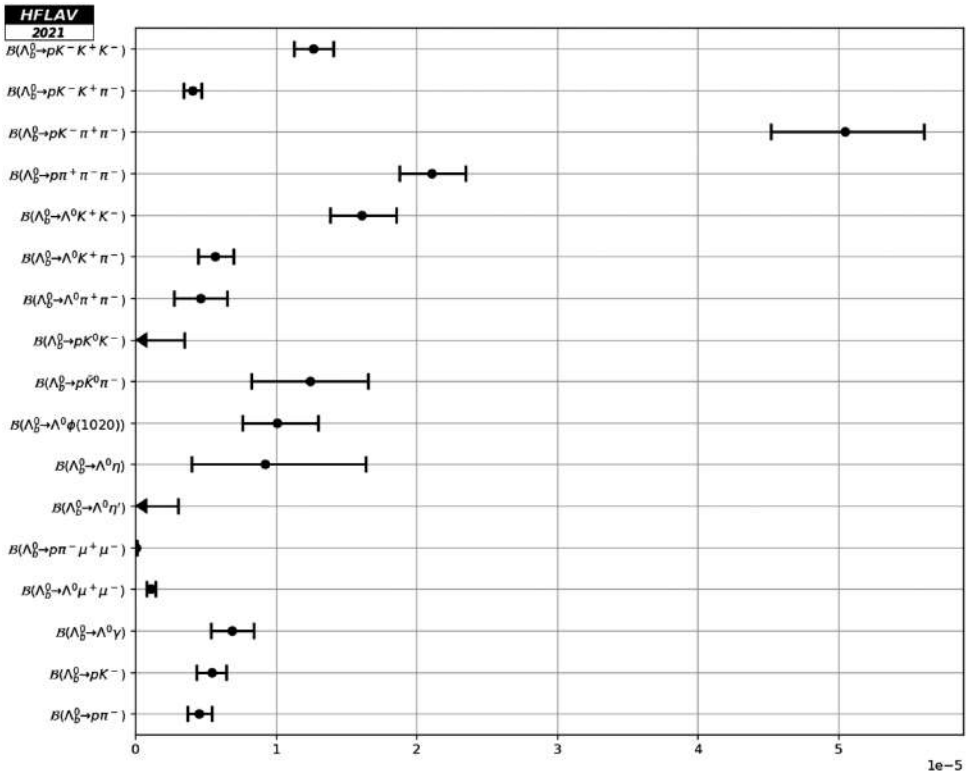

FIG. 72. Branching fractions of charmless Λ_b^0 decays.

D. Decays of B_s^0 mesons

Tables 223–226 and 227,228 detail branching fractions and relative branching fractions of B_s^0 meson decays, respectively. Figures 73 and 74 show graphic representations of a selection of results given in this section.

Measurements that are not included in the tables (the definitions of observables can be found in the corresponding experimental papers):

(i) In Ref. [1053], LHCb reports the differential $B_s^0 \to \phi\mu^+\mu^-$ branching fraction in bins of $m^2(\mu^+\mu^-)$.
(ii) In Ref. [1060], LHCb performs an angular analysis of $B_s^0 \to \phi\mu^+\mu^-$ decays and reports the differential branching fractions, F_L, S_3, S_4, S_7, A_5, A_6, A_8 and A_9 in bins of $m^2(\mu^+\mu^-)$.
(iii) In Ref. [1061], LHCb reports the photon polarization in $B_s^0 \to \phi\gamma$ decays.

TABLE 223. Branching fractions of charmless B_s^0 decays (part 1).

Parameter $[10^{-6}]$	Measurements		Average HFLAV PDG
$\mathcal{B}(B_s^0 \to \pi^+\pi^-)$	CDF [961][a] LHCb [964][a]		$0.70^{+0.11}_{-0.10}$ 0.70 ± 0.10
$\mathcal{B}(B_s^0 \to \pi^0\pi^0)$	L3 [1036]	<210	<210
$\mathcal{B}(B_s^0 \to \eta\pi^0)$	L3 [1036]	<1000	<1000
$\mathcal{B}(B_s^0 \to \eta\eta)$	L3 [1036]	<1500	<1500
$\mathcal{B}(B_s^0 \to \rho^0(770)\rho^0(770))$	SLD [1037]	<320	<320
$\mathcal{B}(B_s^0 \to \eta'\eta')$	LHCb [893]	$32.4 \pm 6.2 \pm 3.0$[b]	32 ± 7 33 ± 7
$\mathcal{B}(B_s^0 \to \eta'\phi(1020))$	LHCb [1038]	<0.82	<0.82

(Table continued)

TABLE 223. *(Continued)*

Parameter [10^{-6}]	Measurements		Average HFLAV PDG
$\mathcal{B}(B_s^0 \to \phi(1020) f_0(980)) \times \mathcal{B}(f_0(980) \to \pi^+\pi^-)$			
	LHCb [1001]	$1.12 \pm 0.16 \pm 0.14^{c}$	1.12 ± 0.21
$\mathcal{B}(B_s^0 \to f_2(1270)\phi(1020)) \times \mathcal{B}(f_2(1270) \to \pi^+\pi^-)$			
	LHCb [1001]	$0.61 \pm 0.13^{+0.13c}_{-0.08}$	$0.61^{+0.19}_{-0.15}$ $0.61^{+0.18}_{-0.15}$
$\mathcal{B}(B_s^0 \to \phi(1020)\rho^0(770))$	LHCb [1001]	$0.27 \pm 0.07 \pm 0.03^{c}$	0.27 ± 0.08
$\mathcal{B}(B_s^0 \to \phi(1020)\pi^+\pi^-)$	LHCb [1001]	$3.48 \pm 0.23 \pm 0.39^{d,c}$	3.48 ± 0.45
$\mathcal{B}(B_s^0 \to \phi(1020)\phi(1020))$	LHCb [992]	$18.6 \pm 0.5 \pm 1.6^{c,e}$	18.7 ± 1.5
	CDF [1039]	$19.1 \pm 1.5 \pm 2.5^{f}$	
$\mathcal{B}(B_s^0 \to K^-\pi^+)$	LHCb [963]	$5.9 \pm 0.7 \pm 0.6$	5.8 ± 0.7
	CDF [960]	$5.7 \pm 1.0 \pm 0.5$	
$\mathcal{B}(B_s^0 \to K^+K^-)$	LHCb [963]	$25.2 \pm 1.8 \pm 2.4$	26.7 ± 2.2 26.6 ± 2.2
	CDF [962]	$27.6 \pm 2.4 \pm 2.6$	
	Belle [1040]	$38^{+10}_{-9} \pm 7^{c}$	
$\mathcal{B}(B_s^0 \to K^0\bar{K}^0)$	LHCb [988]	$16.7 \pm 2.9 \pm 2.1^{c,g}$	17.4 ± 3.1 $17.6^{+3.2}_{-3.1}$
	Belle [1041]	$19.6^{+5.8}_{-5.1} \pm 2.2^{c}$	

[a]Measurement of $(\mathcal{B}(B_s^0 \to \pi^+\pi^-)/\mathcal{B}(B^0 \to K^+\pi^-))\frac{f_s}{f_d}$ used in our fit.
[b]Using $\mathcal{B}(B^+ \to \eta' K^+)$.
[c]Multiple systematic uncertainties are added in quadrature.
[d]$400 < M(\pi^+\pi^-) < 1600$ MeV/c^2.
[e]Using $\mathcal{B}(B^0 \to \phi(1020)K^*(892)^0)$.
[f]Using $\mathcal{B}(B_s^0 \to J/\psi\phi(1020))$.
[g]Using $\mathcal{B}(B^0 \to \phi(1020)K^0)$.

TABLE 224. Branching fractions of charmless B_s^0 decays (part 2).

Parameter [10^{-6}]	Measurements		Average HFLAV PDG
$\mathcal{B}(B_s^0 \to K^0\pi^+\pi^-)$	LHCb [975]	$9.50 \pm 1.34 \pm 1.67^{a}$	9.5 ± 2.1
$\mathcal{B}(B_s^0 \to K^0K^+\pi^- + \text{c.c.})$	LHCb [975]	$84.5 \pm 3.5 \pm 8.0^{a}$	84.5 ± 8.7 84.5 ± 8.8
$\mathcal{B}(B_s^0 \to K^*(892)^-\pi^+)$	LHCb [977]	$2.93 \pm 0.98 \pm 0.41^{b}$	2.9 ± 1.1
$\mathcal{B}(B_s^0 \to K^*(892)^+K^- + \text{c.c.})$	LHCb [1042]	$18.6 \pm 1.2 \pm 4.5^{c,d}$	18.6 ± 4.7
$\mathcal{B}(B_s^0 \to K_0^*(1430)^+K^- + \text{c.c.})$	LHCb [1042]	$31.3 \pm 2.3 \pm 25.3^{c,d}$	31 ± 25
$\mathcal{B}(B_s^0 \to K_2^*(1430)^+K^- + \text{c.c.})$	LHCb [1042]	$10.3 \pm 2.5 \pm 16.4^{c,d}$	10 ± 17
$\mathcal{B}(B_s^0 \to K^*(892)^0\bar{K}^0 + \text{c.c.})$	LHCb [1042]	$19.8 \pm 2.8 \pm 5.0^{c,d}$	19.8 ± 5.7
$\mathcal{B}(B_s^0 \to K_0^*(1430)^0\bar{K}^0 + \text{c.c.})$	LHCb [1042]	$33.0 \pm 2.5 \pm 9.8^{c,d}$	33 ± 10
$\mathcal{B}(B_s^0 \to K_2^*(1430)^0\bar{K}^0 + \text{c.c.})$	LHCb [1042]	$16.8 \pm 4.5 \pm 21.3^{c,d}$	17 ± 22
$\mathcal{B}(B_s^0 \to K_S^0K^*(892)^0)$	LHCb [974]	$16.7 \pm 3.5 \pm 2.3^{d,e}$	16.7 ± 4.2 16.4 ± 4.1
$\mathcal{B}(B_s^0 \to K^0K^+K^-)$	LHCb [975]	$1.29 \pm 0.55 \pm 0.36^{a}$	1.29 ± 0.66 1.29 ± 0.65
$\mathcal{B}(B_s^0 \to \bar{K}^*(892)^0\rho^0(770))$	SLD [1037]	<767	<767

(Table continued)

TABLE 224. *(Continued)*

Parameter [10^{-6}]	Measurements		Average HFLAV PDG
$\mathcal{B}(B_s^0 \to K^*(892)^0 \bar{K}^*(892)^0)$	LHCb [993]	$11.2 \pm 2.2 \pm 1.5^{d,f}$	11.2 ± 2.7 11.1 ± 2.7
$\mathcal{B}(B_s^0 \to \phi(1020)\bar{K}^*(892)^0)$	LHCb [991]	$1.14 \pm 0.24 \pm 0.17^{d,f}$	1.14 ± 0.30
$\mathcal{B}(B_s^0 \to p\bar{p})$	LHCb [1018]	<0.015	<0.015
$\mathcal{B}(B_s^0 \to p\bar{p}K^+K^-)$	LHCb [1020]	$4.2 \pm 0.3 \pm 0.4^{d}$	4.2 ± 0.5 4.5 ± 0.5
$\mathcal{B}(B_s^0 \to p\bar{p}K^+\pi^-)$	LHCb [1020]	$1.3 \pm 0.2 \pm 0.2^{d}$	1.3 ± 0.3 1.4 ± 0.3
$\mathcal{B}(B_s^0 \to p\bar{p}\pi^+\pi^-)$	LHCb [1020]	<0.66	<0.66 0.43 ± 0.20
$\mathcal{B}(B_s^0 \to p\bar{\Lambda}^0 K^- + \text{c.c.})$	LHCb [1043]	$5.46 \pm 0.61 \pm 0.82^{d}$	5.5 ± 1.0

[a]Using $\mathcal{B}(B^0 \to K^0\pi^+\pi^-)$.
[b]Using $\mathcal{B}(B^0 \to K^*(892)^+\pi^-)$.
[c]Result extracted from Dalitz plot analysis of $B_s^0 \to K_S^0 K^+\pi^-$ decays.
[d]Multiple systematic uncertainties are added in quadrature.
[e]Using $\mathcal{B}(B^0 \to K^0\pi^+\pi^-)$.
[f]Using $\mathcal{B}(B^0 \to \phi(1020)K^*(892)^0)$.

TABLE 225. Branching fractions of charmless B_s^0 decays (part 3).

Parameter [10^{-6}]	Measurements		Average HFLAV PDG
$\mathcal{B}(B_s^0 \to \gamma\gamma)$	Belle [1044]	<3.1	<3.1
$\mathcal{B}(B_s^0 \to \phi(1020)\gamma)$	LHCb [1045] Belle [1044]	$33.9 \pm 1.7 \pm 3.1^{a}$ $36.0 \pm 5.0 \pm 7.0$	34.1 ± 3.2 34.2 ± 3.6
$\mathcal{B}(B_s^0 \to \mu^+\mu^-)^{b}$	ATLAS [1046] LHCb [1047] CMS [108] CDF [1048]	$0.0028^{+0.0008}_{-0.0007}$ $0.0030 \pm 0.0006^{+0.0003}_{-0.0002}$ $0.0029 \pm 0.0007 \pm 0.0002$ $0.013^{+0.009}_{-0.007}$	0.00295 ± 0.00041 $0.00294^{+0.00042}_{-0.00039}$
$\mathcal{B}(B_s^0 \to e^+e^-)$	LHCb [1049] CDF [1050]	<0.0094 <0.28	<0.0094
$\mathcal{B}(B_s^0 \to \tau^+\tau^-)^{c}$	LHCb [1051]	<5200.0	<5200 <6800
$\mathcal{B}(B_s^0 \to \mu^+\mu^-\mu^+\mu^-)$	LHCb [1052]	$<0.0025^{d}$	<0.0025
$\mathcal{B}(B_s^0 \to \phi(1020)\mu^+\mu^-)^{e}$	LHCb [1053] CDF [1026]	$0.859 \pm 0.023 \pm 0.061^{f,g}$ $1.21 \pm 0.20 \pm 0.11^{g}$	0.865 ± 0.065 $0.823^{+0.119}_{-0.116}$
$\mathcal{B}(B_s^0 \to \bar{K}^*(892)^0\mu^+\mu^-)$	LHCb [1054]	$0.029 \pm 0.010 \pm 0.004^{f}$	0.029 ± 0.011
$\mathcal{B}(B_s^0 \to \pi^+\pi^-\mu^+\mu^-)$	LHCb [1007][h,i]		0.084 ± 0.016 0.084 ± 0.017
$\mathcal{B}(B_s^0 \to \phi(1020)\nu\bar{\nu})$	DELPHI [978]	<5400	<5400
$\mathcal{B}(B_s^0 \to e^+\mu^- + \text{c.c.})$	LHCb [1055] CDF [1050]	<0.0054 <0.2	<0.0054
$\mathcal{B}(B_s^0 \to \tau^+\mu^- + \text{c.c.})^{c}$	LHCb [1056]	<34.0	<34 <42

(Table continued)

TABLE 225. *(Continued)*

Parameter $[10^{-6}]$	Measurements		Average HFLAV PDG
$\mathcal{B}(B_s^0 \to \eta'\eta)$	Belle [1057]	<65	<65 none
$\mathcal{B}(B_s^0 \to f_2'(1525)\mu^+\mu^-)$	LHCb [1053]	$0.166 \pm 0.020 \pm 0.015$[f,g]	0.166 ± 0.025 none

[a]Using $\mathcal{B}(B^0 \to K^*(892)^0\gamma)$.
[b]The ATLAS measurement is correlated with $\mathcal{B}(B^0 \to \mu^+\mu^-)$. This correlation is not taken into account in our average. For more information see Ref. [1058].
[c]PDG shows the result obtained at 95% CL
[d]At CL = 95%.
[e]The PDG uncertainty includes a scale factor.
[f]Multiple systematic uncertainties are added in quadrature.
[g]Using $\mathcal{B}(B_s^0 \to J/\psi\phi(1020))$.
[h]Muon pairs do not originate from resonances and $0.5 < m_{\pi^+\pi^-} < 1.3$ GeV/c^2.
[i]Measurement of $\mathcal{B}(B_s^0 \to \pi^+\pi^-\mu^+\mu^-)/(\mathcal{B}(B^0 \to J/\psi K^*(892)^0)\mathcal{B}(J/\psi \to \mu^+\mu^-)\mathcal{B}(K^*(892)^0 \to K\pi)2/3)$ used in our fit.

TABLE 226. Branching fractions of charmless B_s^0 decays (part 4).

Parameter $[10^{-6}]$	Measurements		Average HFLAV PDG
$\mathcal{B}(B_s^0 \to \gamma\gamma)$	Belle [1044]	<3.1	<3.1
$\mathcal{B}(B_s^0 \to \phi(1020)\gamma)$	LHCb [1045] Belle [1044]	$33.9 \pm 1.7 \pm 3.1$[a] $36.0 \pm 5.0 \pm 7.0$	34.1 ± 3.2 34.2 ± 3.6
$\mathcal{B}(B_s^0 \to \mu^+\mu^-)$[b]	ATLAS [1046] LHCb [1047] CMS [108] CDF [1048]	$0.0028^{+0.0008}_{-0.0007}$ $0.0030 \pm 0.0006^{+0.0003}_{-0.0002}$ $0.0029 \pm 0.0007 \pm 0.0002$ $0.013^{+0.009}_{-0.007}$	0.00295 ± 0.00041 $0.00294^{+0.00042}_{-0.00039}$
$\mathcal{B}(B_s^0 \to e^+e^-)$	LHCb [1049] CDF [1050]	<0.0094 <0.28	<0.0094
$\mathcal{B}(B_s^0 \to \tau^+\tau^-)$[c]	LHCb [1051]	<5200.0	<5200 <6800
$\mathcal{B}(B_s^0 \to \mu^+\mu^-\mu^+\mu^-)$	LHCb [1052]	<0.0025[d]	<0.0025
$\mathcal{B}(B_s^0 \to \phi(1020)\mu^+\mu^-)$[e,f]	LHCb [1053] CDF [1026]	$0.859 \pm 0.023 \pm 0.061$[g,h] $1.21 \pm 0.20 \pm 0.11$[h]	$0.865^{+0.066}_{-0.064}$ $0.823^{+0.119}_{-0.116}$
$\mathcal{B}(B_s^0 \to \bar{K}^*(892)^0\mu^+\mu^-)$	LHCb [1054]	$0.029 \pm 0.010 \pm 0.004$[g]	0.029 ± 0.011
$\mathcal{B}(B_s^0 \to \pi^+\pi^-\mu^+\mu^-)$	LHCb [1007][i,j]		0.084 ± 0.016 0.084 ± 0.017
$\mathcal{B}(B_s^0 \to \phi(1020)\nu\bar{\nu})$	DELPHI [978]	<5400	<5400
$\mathcal{B}(B_s^0 \to e^+\mu^- + \text{c.c.})$	LHCb [1055] CDF [1050]	<0.0054 <0.2	<0.0054
$\mathcal{B}(B_s^0 \to \tau^+\mu^- + \text{c.c.})$[c]	LHCb [1056]	<34.0	<34 <42
$\mathcal{B}(B_s^0 \to \eta'\eta)$	Belle [1057]	<65	<65 none

(Table continued)

TABLE 226. *(Continued)*

Parameter [10^{-6}]	Measurements		Average HFLAV PDG
$\mathcal{B}(B_s^0 \to f_2'(1525)\mu^+\mu^-)$	LHCb [1053]	$0.166 \pm 0.020 \pm 0.015$[g,h]	$0.166^{+0.026}_{-0.024}$ none

[a]Using $\mathcal{B}(B^0 \to K^*(892)^0\gamma)$.
[b]The ATLAS measurement is correlated with $\mathcal{B}(B^0 \to \mu^+\mu^-)$. This correlation is not taken into account in our average. For more information see Ref. [1058].
[c]PDG shows the result obtained at 95% CL
[d]At CL = 95%.
[e]The PDG uncertainty includes a scale factor.
[f]Treatment of charmonium intermediate components differs between the results.
[g]Multiple systematic uncertainties are added in quadrature.
[h]Using $\mathcal{B}(B_s^0 \to J/\psi\phi(1020))$.
[i]$0.5 < m_{\pi^+\pi^-} < 1.3$ GeV/c^2.
[j]Measurement of $\mathcal{B}(B_s^0 \to \pi^+\pi^-\mu^+\mu^-)/(\mathcal{B}(B^0 \to J/\psi K^*(892)^0)\mathcal{B}(J/\psi \to \mu^+\mu^-)\mathcal{B}(K^*(892)^0 \to K\pi)2/3)$ used in our fit.

TABLE 227. Relative branching fractions of charmless B_s^0 decays (part 1).

Parameter [10^{-2}]	Measurements		Average
$\frac{f_s}{f_d}\frac{\mathcal{B}(B_s^0\to\pi^+\pi^-)}{\mathcal{B}(B^0\to K^+\pi^-)}$	LHCb [964] CDF [961]	$0.915 \pm 0.071 \pm 0.083$ $0.8 \pm 0.2 \pm 0.1$	0.893 ± 0.098
$\frac{f_s}{f_d}\frac{\mathcal{B}(B_s^0\to\pi^+\pi^-)}{\mathcal{B}(B^0\to\pi^+\pi^-)}$	LHCb [963]	$5.0^{+1.1}_{-0.9} \pm 0.4$	$5.0^{+1.2}_{-1.0}$
$\frac{\mathcal{B}(B_s^0\to\phi(1020)\phi(1020))}{\mathcal{B}(B_s^0\to J/\psi\phi(1020))}$[a]	CDF [1039]	$1.78 \pm 0.14 \pm 0.20$	1.78 ± 0.24
$\frac{\mathcal{B}(B_s^0\to\phi(1020)\phi(1020))}{\mathcal{B}(B^0\to\phi(1020)K^*(892)^0)}$	LHCb [992]	$184 \pm 5 \pm 13$[b]	184 ± 14
$\frac{f_s}{f_d}\frac{\mathcal{B}(B_s^0\to K^+\pi^-)}{\mathcal{B}(B_d^0\to K^+\pi^-)}$	LHCb [963] CDF [960]	$7.4 \pm 0.6 \pm 0.6$ $7.1 \pm 1.0 \pm 0.7$	7.30 ± 0.70
$\frac{f_s}{f_d}\frac{\mathcal{B}(B_s^0\to K^+K^-)}{\mathcal{B}(B_d^0\to K^+\pi^-)}$	LHCb [963] CDF [962]	$31.6 \pm 0.9 \pm 1.9$ $34.7 \pm 2.0 \pm 2.1$	32.7 ± 1.7
$\frac{\mathcal{B}(B_s^0\to K^0\pi^+\pi^-)}{\mathcal{B}(B^0\to K^0\pi^+\pi^-)}$	LHCb [975]	$19.1 \pm 2.7 \pm 3.3$[b]	19.1 ± 4.3
$\frac{\mathcal{B}(B_s^0\to K^0K^+\pi^-+\text{c.c.})}{\mathcal{B}(B^0\to K^0\pi^+\pi^-)}$	LHCb [975]	$170 \pm 7 \pm 15$[b]	170 ± 16
$\frac{\mathcal{B}(B_s^0\to K^0K^+K^-)}{\mathcal{B}(B^0\to K^0\pi^+\pi^-)}$	LHCb [975]	<5.1	<5.1
$\frac{\mathcal{B}(B_s^0\to K^*(892)^-\pi^+)}{\mathcal{B}(B^0\to K^*(892)^+\pi^-)}$	LHCb [977]	$39 \pm 13 \pm 5$	39 ± 14
$\frac{\mathcal{B}(B_s^0\to K^*(892)^0\bar{K}^*(892)^0)}{\mathcal{B}(B^0\to\phi(1020)K^*(892)^0)}$	LHCb [993]	$111 \pm 22 \pm 13$[b]	111 ± 26
$\frac{\mathcal{B}(B_s^0\to\phi(1020)\bar{K}^*(892)^0)}{\mathcal{B}(B^0\to\phi(1020)K^*(892)^0)}$	LHCb [991]	$11.3 \pm 2.4 \pm 1.6$[b]	11.3 ± 2.9
$\frac{\mathcal{B}(B_s^0\to\phi(1020)\mu^+\mu^-)}{\mathcal{B}(B_s^0\to J/\psi\phi(1020))}$[c]	LHCb [1053] CDF [1026]	$0.0800 \pm 0.0021 \pm 0.0016$[b] $0.113 \pm 0.019 \pm 0.007$	0.0806 ± 0.0026

[a]The PDG average is a result of a fit including input from other measurements.
[b]Multiple systematic uncertainties are added in quadrature.
[c]The PDG uncertainty includes a scale factor.

TABLE 228. Relative branching fractions of charmless B_s^0 decays (part 2).

Parameter $[10^{-2}]$	Measurements		Average
$\frac{\mathcal{B}(B_s^0\to p\bar{p}K^+\pi^-)}{\mathcal{B}(B^0\to p\bar{p}K^+\pi^-)}$	LHCb [1020]	$22 \pm 4 \pm 2^{a}$	22 ± 5
$\frac{\mathcal{B}(B_s^0\to p\bar{p}K^+\pi^-)}{\mathcal{B}(B_s^0\to p\bar{p}K^+K^-)}$	LHCb [1020]	$31 \pm 5 \pm 2$	31 ± 5
$\frac{\mathcal{B}(B_s^0\to \bar{K}^*(892)^0\mu^+\mu^-)}{\mathcal{B}(B_s^0\to J/\psi\bar{K}^*(892)^0)\times\mathcal{B}(J/\psi\to\mu^+\mu^-)}$	LHCb [1054]	$1.4 \pm 0.4 \pm 0.1^{a}$	1.4 ± 0.4
$\frac{\mathcal{B}(B_s^0\to \bar{K}^*(892)^0\mu^+\mu^-)}{\mathcal{B}(B^0\to \bar{K}^*(892)^0\mu^+\mu^-)}$	LHCb [1054]	$3.3 \pm 1.1 \pm 0.4^{a}$	3.3 ± 1.2
$\frac{\mathcal{B}(B_s^0\to \phi(1020)\phi(1020)\phi(1020))}{\mathcal{B}(B_s^0\to \phi(1020)\phi(1020))}$	LHCb [1059]	$11.7 \pm 3.0 \pm 1.5$	11.7 ± 3.4
$\frac{\mathcal{B}(B_s^0\to K^0\bar{K}^0)}{\mathcal{B}(B^0\to \phi(1020)K^0)}$	LHCb [988]	$230 \pm 40 \pm 22^{a}$	230 ± 46
$\frac{\mathcal{B}(B_s^0\to K_S^0K^*(892)^0)}{\mathcal{B}(B^0\to K_S^0\pi^+\pi^-)}$	LHCb [974]	$33 \pm 7 \pm 4^{a}$	33 ± 8
$\frac{\mathcal{B}(B_s^0\to f_2'(1525)\mu^+\mu^-)}{\mathcal{B}(B_s^0\to J/\psi\phi(1020))}$	LHCb [1053]	$0.0155 \pm 0.0019 \pm 0.0008^{a}$	0.0155 ± 0.0021
$\frac{\mathcal{B}(B_s^0\to \pi^+\pi^-\mu^+\mu^-)}{\mathcal{B}(B^0\to J/\psi K^{*0})\times\mathcal{B}(J/\psi\to\mu^+\mu^-)\times\mathcal{B}(K^{*0}\to K^+\pi^-)}$	LHCb [1007]	$0.167 \pm 0.029 \pm 0.013^{b}$	0.167 ± 0.032

[a]Multiple systematic uncertainties are added in quadrature.
[b]Muon pairs do not originate from resonances and $0.5 < m_{\pi^+\pi^-} < 1.3$ GeV$/c^2$.

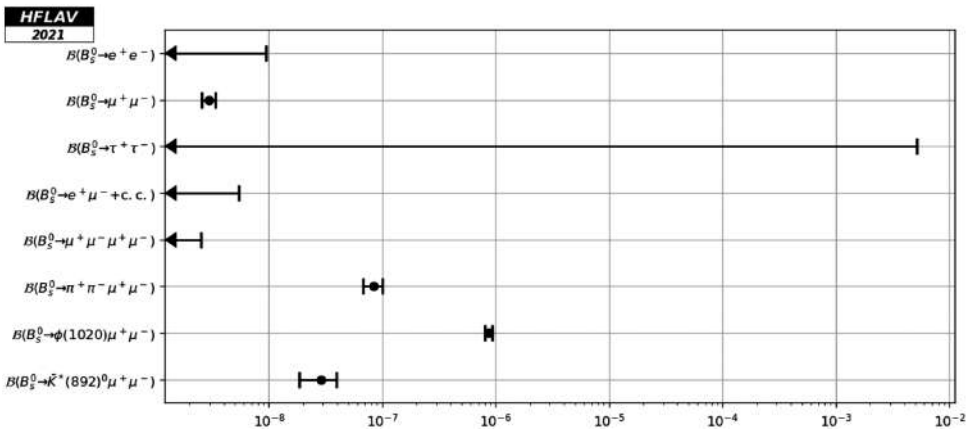

FIG. 73. Branching fractions of charmless leptonic B_s^0 decays.

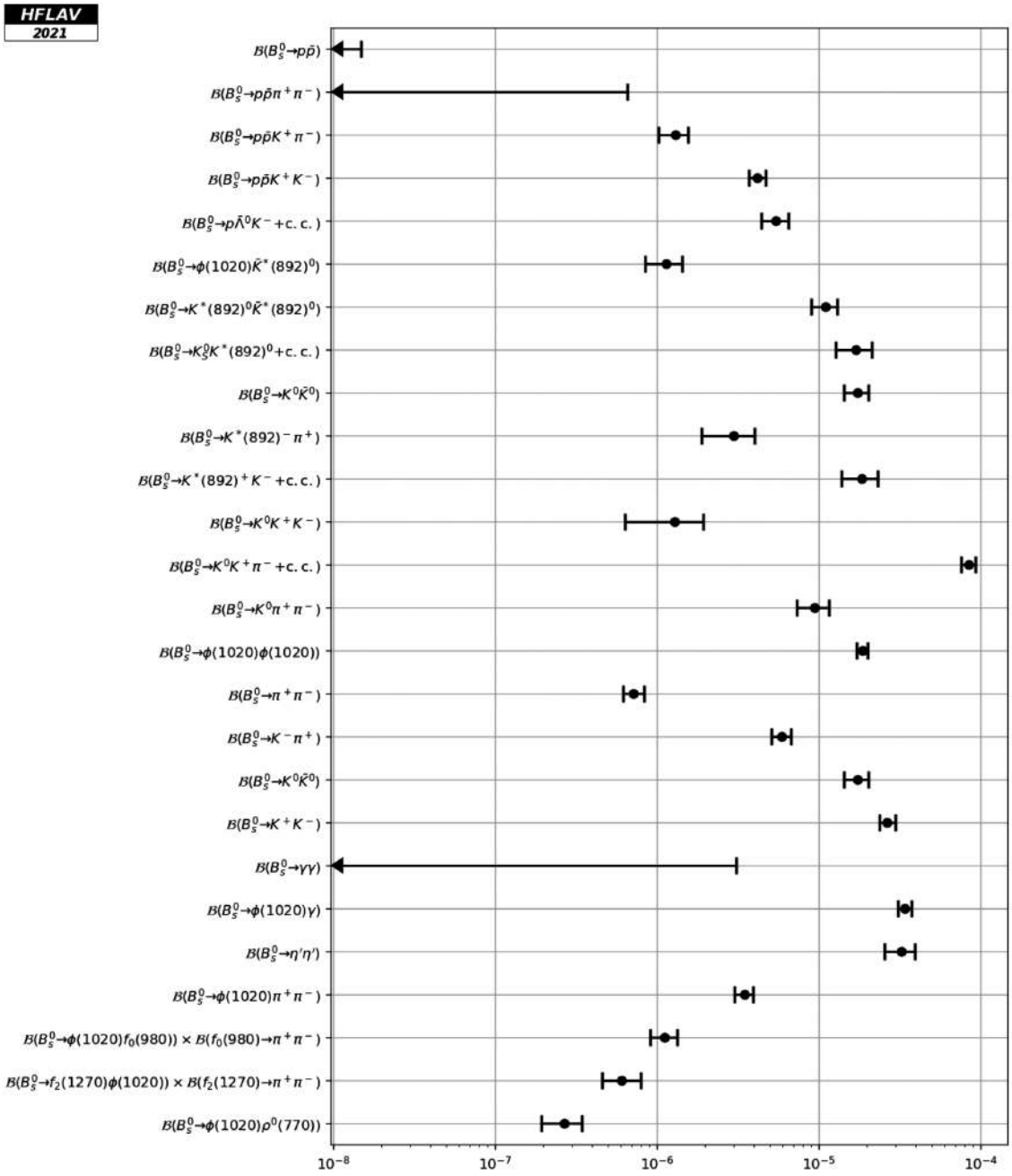

FIG. 74. Branching fractions of charmless nonleptonic B_s^0 decays.

TABLE 229. Branching fractions and relative branching fractions of B_c^+ decays.

Parameter	Measurements		Average
$\mathcal{B}(B_c^+ \to p\bar{p}\pi^+) \times \frac{f_c}{f_u}$ $[10^{-8}]$	LHCb [1062]	<2.8[a]	<2.8
$\frac{\mathcal{B}(B_c^+ \to K^+ K_S^0)}{\mathcal{B}(B^+ \to K_S^0 \pi^+)} \times \frac{f_c}{f_u}$ $[10^{-2}]$	LHCb [885]	<5.8	<5.8
$\mathcal{B}(B_c^+ \to K^+ \bar{K}^0)$[b] $[10^{-4}]$	LHCb [885]	<4.6	<4.6
$\mathcal{B}(B_c^+ \to K^+ K^- \pi^+) \times \frac{f_c}{f_u}$ $[10^{-7}]$	LHCb [853]	<1.50[c]	<1.5
$\mathcal{B}(B_c^+ \to B_s^0 \pi^+) \times \frac{f_c}{f_s}$ $[10^{-3}]$	LHCb [861]	$2.37 \pm 0.31^{+0.20}_{-0.17}$[d,e]	2.37 ± 0.36

[a]Measured in the region $m(p\bar{p}) < 2.85$ GeV/c^2, $p_T(B) < 20$ GeV/c and $2.0 < y(B) < 4.5$.
[b]Derived from the ratio in the previous entry using $\mathcal{B}(B^+ \to K^0\pi^+) = (23.97 \pm 0.53 \pm 0.71) \times 10^{-6}$, $f_u = 0.33$ and $f_c = 0.001$.
[c]Measured in the annihilation region $m_{K^+\pi^+} < 1.834$ GeV/c^2, and in the fiducial region $p_T(B) < 20$ GeV/c and $2.0 < y(B) < 4.5$
[d]In the pseudorapidity range $2 < \eta(B) < 5$.
[e]Multiple systematic uncertainties are added in quadrature.

E. Decays of B_c^+ mesons

Table 229 details branching fractions and ratios of branching fractions of B_c^+ meson decays to charmless hadronic final states.

F. Rare decays of B^0 and B^+ mesons with photons and/or leptons

This section reports different observables for radiative decays, lepton-flavor/number-violating (LFV/LNV) decays and flavor-changing-neutral-current (FCNC) decays with leptons of B^0 and B^+ mesons. In all decays listed in this section, charmonium intermediate states are vetoed. Tables 230–232, 233–236 and 237–239 provide compilations of branching fractions of radiative and FCNC decays with leptons of B^+ mesons, B^0 mesons and their admixture, respectively. Tables 236 and 239 also include LFV/LNV decays. Tables 240 and 241 contain branching fractions of leptonic and radiative-leptonic B^+ and B^0 decays. These are followed by Tables 242 and 243, which give relative branching fractions of B^+ and B^0 decays, then Table 244, which gives a compilation of inclusive decays. In the modes listed in Table 244, the radiated particle is a gluon, which is an exception in this section. Table 245 contains isospin asymmetry measurements. Finally, Tables 246 to 247 and 248 provide compilations of branching fractions of B^+ and B^0 mesons to lepton-flavor/number-violating final states, respectively. Figures 75–80 show graphic representations of a selection of results given in this section.

Measurements that are not included in the tables (the definitions of observables can be found in the corresponding experimental papers):

(i) In Ref. [1149], LHCb reports the up-down asymmetries in bins of the $K\pi\pi\gamma$ mass of the $B^+ \to K^+\pi^-\pi^+\gamma$ decay.

(ii) For the $B \to K\ell^-\ell^+$ channel, LHCb measures F_H and $A_{\rm FB}$ in 17 (5) bins of $m^2(\ell^+\ell^-)$ for the K^+ (K_S^0) final state [1150]. Belle measures F_L and $A_{\rm FB}$ in 6 $m^2(\ell^+\ell^-)$ [1089].

(iii) For the $B \to K^*\ell^-\ell^+$ analyses, partial branching fractions and angular observables in bins of $m^2(\ell^+\ell^-)$ are also available:
$B^0 \to K^{*0}e^-e^+$: LHCb reports F_L, $A_T^{(2)}$, $A_T^{\rm Im}$, $A_T^{\rm Re}$ in the $[0.0008, 0.257]$ GeV$^2/c^4$ bin of $m^2(\ell^+\ell^-)$ putting constraints on the $B \to K^{*0}\gamma$ photon polarization [1151]. In Ref. [1152], LHCb determines the branching fraction in the dilepton mass region $[0.0009, 1.0]$ GeV$^2/c^4$.
$B \to K^*\ell^-\ell^+$: Belle measures F_L, $A_{\rm FB}$, isospin asymmetry in 6 $m^2(\ell^+\ell^-)$ bins [1089] and P_4', P_5', P_6', P_8' in 4 $m^2(\ell^+\ell^-)$ bins [1153]. In a more recent paper [1154], they report measurements of P_4' and P_5', separately for $\ell = \mu$ or e, in 4 $m^2(\ell^+\ell^-)$ bins and in the region $[1,6]$ GeV$^2/c^4$. The measurements use both B^0 and B^+ decays. They also measure the LFU observables $Q_i = P_i^\mu - P_i^e$, for $i = 4, 5$. *BABAR* reports F_L, $A_{\rm FB}$, P_2 in 5 $m^2(\ell^+\ell^-)$ bins [1155].
$B^0 \to K^{*0}\mu^-\mu^+$: LHCb measures F_L, $A_{\rm FB}$, $S_3 - S_9$, $A_3 - A_9$, $P_1 - P_3$, $P_4' - P_8'$ in $8 m^2(\ell^+\ell^-)$ bins [1156]. An updated measurement of the CP-averaged observables is presented in Ref. [1157]. CMS measures F_L and $A_{\rm FB}$ in 7 $m^2(\ell^+\ell^-)$ bins [1158], as well as P_1, P_5' [1159]. ATLAS measures F_L, $S_{3,4,5,7,8}$ and $P'_{1,4,5,6,8}$ in 6 $m^2(\ell^+\ell^-)$ bins [1160].
$B^+ \to K^{*+}\mu^-\mu^+$: LHCb reports the full set of CP-averaged angular observables in 8 $m^2(\ell^+\ell^-)$ bins [1161]. CMS measures F_L and $A_{\rm FB}$ in 3 $m^2(\ell^+\ell^-)$ bins [1162].

(iv) $B \to X_s\ell^-\ell^+$ (where X_s is a hadronic system with an s quark): Belle measures $A_{\rm FB}$ in bins of $m^2(\ell^+\ell^-)$ with a sum of 10 exclusive final states [1163].

(v) $B^0 \to K^+\pi^-\mu^+\mu^-$, with $1330 < m(K^+\pi^-) < 1530$ GeV/c^2: LHCb measures the partial

TABLE 230. Branching fractions of charmless radiative and FCNC decays with leptons of B^+ mesons (part 1).

Parameter [10^{-6}]	Measurements		Average HFLAV / PDG
$\mathcal{B}(B^+ \to K^*(892)^+\gamma)$[a]	Belle [1063]	$37.6 \pm 1.0 \pm 1.2$	39.2 ± 1.2
	BABAR [1064]	$42.2 \pm 1.4 \pm 1.6$	39.2 ± 2.2
	CLEO [1065]	$37.6^{+8.9}_{-8.3} \pm 2.8$	
$\mathcal{B}(B^+ \to K_1(1270)^+\gamma)$	*BABAR* [404]	$44.1^{+6.3}_{-4.4} \pm 5.8$[b]	$43.8^{+7.0}_{-6.3}$
	Belle [1066]	$43.0 \pm 9.0 \pm 9.0$[c]	$43.8^{+7.1}_{-6.3}$
$\mathcal{B}(B^+ \to \eta K^+\gamma)$	*BABAR* [408]	$7.7 \pm 1.0 \pm 0.4$[d]	7.89 ± 0.92
	Belle [1067]	$8.4 \pm 1.5^{+1.2}_{-0.9}$[e]	$7.88^{+0.94}_{-0.92}$
$\mathcal{B}(B^+ \to \eta' K^+\gamma)$	Belle [1068]	$3.6 \pm 1.2 \pm 0.4$[f]	2.9 ± 1.0
	BABAR [1069]	$1.9^{+1.5}_{-1.2} \pm 0.1$[d]	$2.9^{+1.0}_{-0.9}$
$\mathcal{B}(B^+ \to \phi(1020) K^+\gamma)$[a]	Belle [410]	$2.48 \pm 0.30 \pm 0.24$	2.71 ± 0.34
	BABAR [1070]	$3.5 \pm 0.6 \pm 0.4$[g]	2.71 ± 0.42
$\mathcal{B}(B^+ \to K^+\pi^-\pi^+\gamma)$[a]	*BABAR* [404]	$24.5 \pm 0.9 \pm 1.2$[h]	24.6 ± 1.3
	Belle [1066]	$25.0 \pm 1.8 \pm 2.2$[c]	25.8 ± 1.5
$\mathcal{B}(B^+ \to K^*(892)^0\pi^+\gamma)$	*BABAR* [404]	$23.4 \pm 0.9^{+0.8}_{-0.7}$[h]	23.3 ± 1.2
	Belle [1071]	$20.0^{+7.0}_{-6.0} \pm 2.0$[i]	$23.3^{+1.2}_{-1.1}$
$\mathcal{B}(B^+ \to K^+\rho^0(770)\gamma)$	*BABAR* [404]	$8.2 \pm 0.4 \pm 0.8$[h]	8.2 ± 0.9
	Belle [1071]	<20.0[i]	
$\mathcal{B}(B^+ \to (K\pi)_0^{*0}\pi^+\gamma) \times \mathcal{B}((K\pi)_0^{*0} \to K^+\pi^-)$[j]			
	BABAR [404]	$10.3^{+0.7+1.5}_{-0.8-2.0}$[h]	$10.3^{+1.7}_{-2.2}$
			none
$\mathcal{B}(B^+ \to K^+\pi^-\pi^+\gamma(\mathrm{NR}))$	*BABAR* [404]	$9.9 \pm 0.7^{+1.5}_{-1.9}$[h,k]	$9.9^{+1.7}_{-2.0}$
	Belle [1071]	<9.2[l]	

[a]The PDG uncertainty includes a scale factor.
[b]Multiple systematic uncertainties are added in quadrature.
[c]$1 < M_{K\pi\pi} < 2$ GeV/c^2.
[d]$M_{K\eta^{(\prime)}} < 3.25$ GeV/c^2.
[e]$M_{K\eta} < 2.4$ GeV/c^2.
[f]$M_{K\eta'} < 3.4$ GeV/c^2
[g]$M_{\phi K} < 3.0$ GeV/c^2.
[h]$M_{K\pi\pi} < 1.8$ GeV/c^2.
[i]$M_{K\pi\pi} < 2.4$ GeV/c^2.
[j]This corresponds to the $(K\pi)$ S-wave obtained with LASS parametrization [338].
[k]$M_{K\pi} < 1.6$ GeV/c^2.
[l]$1.25 < M_{K\pi} < 1.6$ GeV/c^2 and $M_{K\pi\pi} < 2.4$ GeV/c^2.

branching fraction in bins of $m^2(\mu^+\mu^-)$ in the range $[0.1, 8.0]$ GeV$^2/c^4$, and reports angular moments [1164].

(vi) In Ref. [1165], LHCb measures the phase difference between the short- and long-distance contributions to the $B^+ \to K^+\mu^+\mu^-$ decay. The measurement is based on the analysis of the dimuon mass distribution in the regions of the J/ψ and $\psi(2S)$ resonances and far from their poles, to probe long and short distance effects, respectively.

(vii) In Ref. [1166], CMS performs the study of the angular distribution of the $B^+ \to K^+\mu^+\mu^-$ channel and measures, in 7 $m^2(\mu^+\mu^-)$ bins, A_{FB} and the contribution F_{H} from the pseudoscalar, scalar and tensor amplitudes to the decay.

(viii) In Ref. [1167], LHCb performs a search for a hidden-sector boson χ decaying into two muons in $B^0 \to K^{*0}\mu^+\mu^-$ decays. Results are given as function of mass and lifetime in the range $214 < m(\chi) < 4350$ MeV/c^2 and $0 < \tau(\chi) < 1000$ ps.

(ix) In Ref. [1168], LHCb performs a search for a hypothetical new scalar particle χ, assumed to have a narrow width, through the decay $B^+ \to K^+\chi(\mu^+\mu^-)$ in the ranges of mass $250 < m(\chi) < 4700$ MeV/c^2 and lifetime $0.1 < \tau(\chi) < 1000$ ps. Upper limits are given as a function of $m(\chi)$ and $\tau(\chi)$.

TABLE 231. Branching fractions of charmless radiative and FCNC decays with leptons of B^+ mesons (part 2).

Parameter $[10^{-6}]$	Measurements		Average HFLAV PDG
$\mathcal{B}(B^+ \to K^0\pi^+\pi^0\gamma)$	*BABAR* [1072]	$45.6 \pm 4.2 \pm 3.1$[a]	45.6 ± 5.2
$\mathcal{B}(B^+ \to K_1(1400)^+\gamma)$	*BABAR* [404] Belle [1066]	$9.7^{+4.6+2.9}_{-2.9-2.4}$[a,b] <15.0	$9.7^{+5.4}_{-3.8}$
$\mathcal{B}(B^+ \to K^*(1410)^+\gamma)$	*BABAR* [404]	$27.1^{+5.4+5.9}_{-4.8-3.7}$[a,b]	$27.1^{+8.0}_{-6.1}$
$\mathcal{B}(B^+ \to K_0^*(1430)^0\pi^+\gamma)$	*BABAR* [404]	$1.32^{+0.09+0.24}_{-0.10-0.30}$[a,b]	$1.32^{+0.26}_{-0.31}$ $1.32^{+0.26}_{-0.32}$
$\mathcal{B}(B^+ \to K_2^*(1430)^+\gamma)$	*BABAR* [1073] *BABAR* [404]	$14.5 \pm 4.0 \pm 1.5$ $8.7^{+7.0+8.7}_{-5.3-10.4}$[a,b]	13.8 ± 4.0
$\mathcal{B}(B^+ \to K^*(1680)^+\gamma)$	*BABAR* [404]	$66.7^{+9.3+14.4}_{-7.8-11.4}$[a,b]	67^{+17}_{-14}
$\mathcal{B}(B^+ \to K_3^*(1780)^+\gamma)$	Belle [1067]	<9.7	<9.7 <39.0
$\mathcal{B}(B^+ \to K_4^*(2045)^+\gamma)$	ARGUS [1074]	<9900	<9900
$\mathcal{B}(B^+ \to \rho^+(770)\gamma)$	Belle [1075] *BABAR* [1076]	$0.87^{+0.29+0.09}_{-0.27-0.11}$ $1.2 \pm 0.4 \pm 0.2$	0.98 ± 0.24 $0.98^{+0.25}_{-0.24}$
$\mathcal{B}(B^+ \to p\bar{\Lambda}^0\gamma)$	Belle [1015]	$2.45^{+0.44}_{-0.38} \pm 0.22$	$2.45^{+0.49}_{-0.44}$
$\mathcal{B}(B^+ \to p\bar{\Sigma}^0\gamma)$	Belle [1077]	<4.6	<4.6
$\mathcal{B}(B^+ \to \pi^+\ell^+\ell^-)$[c]	Belle [1078] *BABAR* [1079]	<0.049 <0.066	<0.049
$\mathcal{B}(B^+ \to \pi^+e^+e^-)$[c]	Belle [1078] *BABAR* [1079]	<0.08 <0.125	<0.08
$\mathcal{B}(B^+ \to \pi^+\mu^+\mu^-)$[c]	*BABAR* [1079] Belle [1078] LHCb [1080][d,e]	<0.055 <0.069	0.0178 ± 0.0023
$\mathcal{B}(B^+ \to \pi^+\nu\bar{\nu})$	Belle [1081] *BABAR* [1082]	<14.0 <100.0	<14

[a] $M_{K\pi\pi} < 1.8$ GeV$/c^2$.
[b] Multiple systematic uncertainties are added in quadrature.
[c] Treatment of charmonium intermediate components differs between the results.
[d] LHCb also reports the branching fraction in bins of $m^2_{\ell^+\ell^-}$.
[e] Measurement of $\mathcal{B}(B^+ \to \pi^+\mu^+\mu^-)/(\mathcal{B}(B^+ \to J/\psi K^+)\mathcal{B}(J/\psi \to \mu^+\mu^-))$ used in our fit.

TABLE 232. Branching fractions of charmless radiative and FCNC decays with leptons of B^+ mesons (part 3).

Parameter [10^{-6}]	Measurements		Average $^{\text{HFLAV}}_{\text{PDG}}$
$\mathcal{B}(B^+ \to K^+\ell^+\ell^-)$[a]	LHCb [1083]	$0.429 \pm 0.007 \pm 0.021$[b]	0.463 ± 0.019
	Belle [1084]	$0.599^{+0.045}_{-0.043} \pm 0.014$	p = 3.3%o
	BABAR [1085]	$0.476^{+0.092}_{-0.086} \pm 0.022$	0.471 ± 0.046
$\mathcal{B}(B^+ \to K^+e^+e^-)$[a]	Belle [1084]	$0.575^{+0.064}_{-0.061} \pm 0.015$	0.561 ± 0.056
	BABAR [1085]	$0.51^{+0.12}_{-0.11} \pm 0.02$	$0.560^{+0.058}_{-0.055}$
$\mathcal{B}(B^+ \to K^+\mu^+\mu^-)$[c,a]	LHCb [1083]	$0.429 \pm 0.007 \pm 0.021$	
	Belle [1084]	$0.624^{+0.065}_{-0.061} \pm 0.016$	0.450 ± 0.021
	BABAR [1085]	$0.41^{+0.16}_{-0.15} \pm 0.02$	0.453 ± 0.035
$\mathcal{B}(B^+ \to K^+\tau^+\tau^-)$	*BABAR* [1086]	<2250.0	<2250
$\mathcal{B}(B^+ \to K^+\nu\bar{\nu})$	*BABAR* [1087]	<16.0	
	Belle [1081]	<19.0	<16
	Belle II [1088]	<41.0	
$\mathcal{B}(B^+ \to \rho^+(770)\nu\bar{\nu})$	Belle [1081]	<30.0	<30
$\mathcal{B}(B^+ \to K^*(892)^+\ell^+\ell^-)$[c,a]	LHCb [1083]	$0.924 \pm 0.093 \pm 0.067$[b]	
	Belle [1089]	$1.24^{+0.23}_{-0.21} \pm 0.13$	1.010 ± 0.099
	BABAR [1085]	$1.40^{+0.40}_{-0.37} \pm 0.09$	$1.009^{+0.113}_{-0.112}$
$\mathcal{B}(B^+ \to K^*(892)^+e^+e^-)$[a]	*BABAR* [1085]	$1.38^{+0.47}_{-0.42} \pm 0.08$	1.55 ± 0.33
	Belle [1089]	$1.73^{+0.50}_{-0.42} \pm 0.20$	$1.55^{+0.36}_{-0.31}$
$\mathcal{B}(B^+ \to K^*(892)^+\mu^+\mu^-)$[a]	LHCb [1083]	$0.924 \pm 0.093 \pm 0.067$	
	Belle [1089]	$1.11^{+0.32}_{-0.27} \pm 0.10$	0.96 ± 0.10
	BABAR [1085]	$1.46^{+0.79}_{-0.75} \pm 0.12$	
$\mathcal{B}(B^+ \to K^*(892)^+\nu\bar{\nu})$	Belle [1090]	<40.0	
	Belle [1081]	<61.0	<40
	BABAR [1087]	<64.0	
$\mathcal{B}(B^+ \to K^+\pi^+\pi^-\mu^+\mu^-)$	LHCb [1091]	$0.4337^{+0.0287}_{-0.0268} \pm 0.0254$[d]	0.434 ± 0.038
			$0.433^{+0.038}_{-0.037}$
$\mathcal{B}(B^+ \to \phi(1020)K^+\mu^+\mu^-)$	LHCb [1091]	$0.0790^{+0.0180+0.0114}_{-0.0160-0.0072}$[e]	$0.079^{+0.022}_{-0.017}$
			$0.079^{+0.021}_{-0.017}$
$\mathcal{B}(B^+ \to \bar{\Lambda}^0 p\nu\bar{\nu})$	*BABAR* [1092]	<30.0	<30

[a]Treatment of charmonium intermediate components differs between the results.
[b]Only muons are used.
[c]The PDG uncertainty includes a scale factor.
[d]Using $\mathcal{B}(B^+ \to \psi(2S)K^+)$.
[e]Using $\mathcal{B}(B^+ \to J/\psi\phi(1020)K^+)$.

TABLE 233. Branching fractions of charmless radiative and FCNC decays with leptons of B^0 mesons (part 1).

Parameter $[10^{-6}]$	Measurements		Average HFLAV PDG
$\mathcal{B}(B^0 \to \eta K^0 \gamma)$	*BABAR* [408]	$7.1^{+2.1}_{-2.0} \pm 0.4^{a}$	7.6 ± 1.8
	Belle [1067]	$8.7^{+3.1+1.9b}_{-2.7-1.6}$	$7.6^{+1.8}_{-1.7}$
$\mathcal{B}(B^0 \to \eta' K^0 \gamma)$	Belle [1068]	$<6.4^{c}$	<6.4
	BABAR [1069]	$<6.6^{a}$	
$\mathcal{B}(B^0 \to \phi(1020) K^0 \gamma)$	Belle [410]	$2.74 \pm 0.60 \pm 0.32$	2.74 ± 0.68
	BABAR [1070]	$<27^{d}$	
$\mathcal{B}(B^0 \to K^+ \pi^- \gamma)$	Belle [1071]	$4.6^{+1.3+0.5e}_{-1.2-0.7}$	4.6 ± 1.4
$\mathcal{B}(B^0 \to K^*(892)^0 \gamma)^{f}$	Belle [1063]	$39.6 \pm 0.7 \pm 1.4$	41.8 ± 1.2
	BABAR [1064]	$44.7 \pm 1.0 \pm 1.6$	41.8 ± 2.5
	CLEO [1065]	$45.5^{+7.2}_{-6.8} \pm 3.4$	
	LHCb [1045][g], [1029][h]		
$\mathcal{B}(B^0 \to K^*(1410)^0 \gamma)$	Belle [1071]	$<130.0^{e}$	<130
$\mathcal{B}(B^0 \to K^+ \pi^- \gamma(\mathrm{NR}))$	Belle [1071]	$<2.6^{e}$	<2.6
$\mathcal{B}(K^{*0} X(214)) \times \mathcal{B}(X(214) \to \mu^+ \mu^-)$	Belle [1093]	$<0.0226^{i}$	<0.023
$\mathcal{B}(B^0 \to K^0 \pi^+ \pi^- \gamma)$	*BABAR* [404]	$20.5 \pm 2.0^{+2.6j}_{-2.2}$	19.9 ± 1.8
	BABAR [1072]	$18.5 \pm 2.1 \pm 1.2^{j}$	
	Belle [1066]	$24.0 \pm 4.0 \pm 3.0^{k}$	
$\mathcal{B}(B^0 \to K^+ \pi^- \pi^0 \gamma)$	*BABAR* [1072]	$40.7 \pm 2.2 \pm 3.1^{j}$	40.7 ± 3.8
$\mathcal{B}(B^0 \to K_1(1270)^0 \gamma)$	Belle [1066]	<58.0	<58

[a] $M_{K\eta^{(\prime)}} < 3.25\ \mathrm{GeV}/c^2$.
[b] $M_{K\eta} < 2.4\ \mathrm{GeV}/c^2$.
[c] $M_{K\eta'} < 3.4\ \mathrm{GeV}/c^2$
[d] $M_{\phi K} < 3.0\ \mathrm{GeV}/c^2$.
[e] $1.25 < M_{K\pi} < 1.6\ \mathrm{GeV}/c^2$.
[f] The PDG uncertainty includes a scale factor.
[g] Measurement of $\mathcal{B}(B_s^0 \to \phi(1020)\gamma)/\mathcal{B}(B^0 \to K^*(892)^0_{f_{K0}}\gamma)$ used in our fit.
[h] Measurement of $(\mathcal{B}(\Lambda_b^0 \to \Lambda^0 \gamma)/\mathcal{B}(B^0 \to K^*(892)^0\gamma))\frac{f_b}{f_\phi}$ used in our fit.
[i] $X(214)$ is searched in the mass range $[212, 300]\ \mathrm{MeV}/c^2$.
[j] $M_{K\pi\pi} < 1.8\ \mathrm{GeV}/c^2$.
[k] $1 < M_{K\pi\pi} < 2\ \mathrm{GeV}/c^2$.

TABLE 234. Branching fractions of charmless radiative and FCNC decays with leptons of B^0 mesons (part 2).

Parameter $[10^{-6}]$	Measurements		Average HFLAV PDG
$\mathcal{B}(B^0 \to K_1(1400)^0 \gamma)$	Belle [1066]	<12.0	<12
$\mathcal{B}(B^0 \to K_2^*(1430)^0 \gamma)$	*BABAR* [1073]	$12.2 \pm 2.5 \pm 1.0$	12.4 ± 2.4
	Belle [1071]	$13.0 \pm 5.0 \pm 1.0$	
$\mathcal{B}(B^0 \to K_3^*(1780)^0 \gamma)$	Belle [1067]	<21	<21
			<83
$\mathcal{B}(B^0 \to \rho^0(770)\gamma)$	Belle [1075]	$0.78^{+0.17+0.09}_{-0.16-0.10}$	0.86 ± 0.15
	BABAR [1076]	$0.97^{+0.24}_{-0.22} \pm 0.06$	
$\mathcal{B}(\rho^0 X(214)) \times \mathcal{B}(X(214) \to \mu^+ \mu^-)$	Belle [1093]	$<0.0173^{a}$	<0.017

(Table continued)

TABLE 234. *(Continued)*

Parameter $[10^{-6}]$	Measurements		Average HFLAV PDG
$\mathcal{B}(B^0 \to \omega(782)\gamma)$	Belle [1075]	$0.40^{+0.19}_{-0.17} \pm 0.13$	0.44 ± 0.17
	BABAR [1076]	$0.50^{+0.27}_{-0.23} \pm 0.09$	$0.44^{+0.18}_{-0.16}$
$\mathcal{B}(B^0 \to \phi(1020)\gamma)$	Belle [1094]	<0.1	<0.1
	BABAR [1095]	<0.85	
$\mathcal{B}(B^0 \to p\bar{\Lambda}^0\pi^-\gamma)$	Belle [1096]	<0.65	<0.65
$\mathcal{B}(B^0 \to \pi^0\ell^+\ell^-)$[b]	*BABAR* [1079]	<0.053	<0.053
	Belle [1078]	<0.154	
$\mathcal{B}(B^0 \to \pi^0 e^+e^-)$[b]	*BABAR* [1079]	<0.084	<0.084
	Belle [1078]	<0.227	
$\mathcal{B}(B^0 \to \pi^0\mu^+\mu^-)$[b]	*BABAR* [1079]	<0.069	<0.069
	Belle [1078]	<0.184	

[a]$X(214)$ is searched in the mass range $[212, 300]$ MeV$/c^2$.
[b]Treatment of charmonium intermediate components differs between the results.

TABLE 235. Branching fractions of charmless radiative and FCNC decays with leptons of B^0 mesons (part 3).

Parameter $[10^{-6}]$	Measurements		Average HFLAV PDG
$\mathcal{B}(B^0 \to \eta\ell^+\ell^-)$	*BABAR* [1079]	<0.064	<0.064
$\mathcal{B}(B^0 \to \eta e^+e^-)$	*BABAR* [1079]	<0.108	<0.11
$\mathcal{B}(B^0 \to \eta\mu^+\mu^-)$	*BABAR* [1079]	<0.112	<0.11
$\mathcal{B}(B^0 \to \pi^0\nu\bar{\nu})$	Belle [1081]	<9.0	<9.0
$\mathcal{B}(B^0 \to K^0\ell^+\ell^-)$[a]	LHCb [1083]	$0.327 \pm 0.034 \pm 0.017$[b]	0.328 ± 0.032
	Belle [1084]	$0.351^{+0.069}_{-0.060} \pm 0.010$	$0.329^{+0.063}_{-0.055}$
	BABAR [1085]	$0.21^{+0.15}_{-0.13} \pm 0.02$	
$\mathcal{B}(B^0 \to K^0 e^+e^-)$[a]	Belle [1084]	$0.306^{+0.098}_{-0.086} \pm 0.008$	0.249 ± 0.072
	BABAR [1085]	$0.08^{+0.15}_{-0.12} \pm 0.01$	$0.247^{+0.109}_{-0.094}$
$\mathcal{B}(B^0 \to K^0\mu^+\mu^-)$[a]	LHCb [1083]	$0.327 \pm 0.034 \pm 0.017$	0.341 ± 0.034
	Belle [1084]	$0.394^{+0.096}_{-0.084} \pm 0.012$	0.339 ± 0.035
	BABAR [1085]	$0.49^{+0.29}_{-0.25} \pm 0.03$	
$\mathcal{B}(B^0 \to K^0\nu\bar{\nu})$	Belle [1081]	<26.0	<26
	BABAR [1087]	<49.0	
$\mathcal{B}(B^0 \to \rho^0(770)\nu\bar{\nu})$	Belle [1081]	<40.0	<40
$\mathcal{B}(B^0 \to K^*(892)^0\ell^+\ell^-)$[a]	Belle [1089]	$0.97^{+0.13}_{-0.11} \pm 0.07$	0.99 ± 0.12
	BABAR [1085]	$1.03^{+0.22}_{-0.21} \pm 0.07$	$0.99^{+0.12}_{-0.11}$
$\mathcal{B}(B^0 \to K^*(892)^0 e^+e^-)$[a]	Belle [1089]	$1.18^{+0.27}_{-0.22} \pm 0.09$	1.04 ± 0.17
	BABAR [1085]	$0.86^{+0.26}_{-0.24} \pm 0.05$	$1.03^{+0.19}_{-0.17}$
$\mathcal{B}(B^0 \to K^*(892)^0\mu^+\mu^-)$[a]	LHCb [1097]	$0.904^{+0.016}_{-0.015} \pm 0.062$[c]	0.94 ± 0.06
	Belle [1089]	$1.06^{+0.19}_{-0.14} \pm 0.07$	0.94 ± 0.05
	BABAR [1085]	$1.35^{+0.40}_{-0.37} \pm 0.10$	

[a]Treatment of charmonium intermediate components differs between the results.
[b]Only muons are used.
[c]Multiple systematic uncertainties are added in quadrature.

TABLE 236. Branching fractions of charmless radiative and FCNC decays with leptons of B^0 mesons (part 4).

Parameter [10^{-6}]	Measurements		Average HFLAV PDG
$\mathcal{B}(B^0 \to \pi^+\pi^-\mu^+\mu^-)$	LHCb [1007][a,b,c]		0.021 ± 0.005
$\mathcal{B}(B^0 \to K^*(892)^0\nu\bar{\nu})$	Belle [1081] Belle [1090] *BABAR* [1087]	<18.0 <55.0 <120.0	<18
$\mathcal{B}(B^0 \to \phi(1020)\nu\bar{\nu})$	Belle [1090]	<127.0	<127
$\mathcal{B}(B^0 \to \pi^0 e^+\mu^- + \text{c.c.})$	*BABAR* [1098]	<0.14	<0.14
$\mathcal{B}(B^0 \to K^0 e^+\mu^- + \text{c.c.})$	Belle [1084] *BABAR* [1099]	<0.038 <0.27	<0.038
$\mathcal{B}(B^0 \to K^*(892)^0 e^+\mu^-)$	Belle [1100] *BABAR* [1099]	<0.16 <0.53	<0.16
$\mathcal{B}(B^0 \to K^*(892)^0 e^+\mu^-)$	Belle [1100] *BABAR* [1099]	<0.12 <0.34	<0.12
$\mathcal{B}(B^0 \to K^*(892)^0 e^+\mu^- + \text{c.c.})$	Belle [1100] *BABAR* [1099]	<0.18 <0.58	<0.18
$\mathcal{B}(B^0 \to \Lambda_c^+\mu^-)$	*BABAR* [1101]	<1.4	<1.4
$\mathcal{B}(B^0 \to \Lambda_c^+ e^-)$	*BABAR* [1101]	<4.0	<4.0

[a]The mass windows corresponding to ϕ and charmonium resonances decaying to $\mu\mu$ are vetoed.
[b]$0.5 < m_{\pi^+\pi^-} < 1.3$ GeV/c^2.
[c]Measurement of $\mathcal{B}(B^0 \to \pi^+\pi^-\mu^+\mu^-)/(\mathcal{B}(B^0 \to J/\psi K^*(892)^0)\mathcal{B}(J/\psi \to \mu^+\mu^-)\mathcal{B}(K^*(892)^0 \to K\pi)2/3)$ used in our fit.

TABLE 237. Branching fractions of charmless radiative, FCNC decays with leptons and LFV/LNV decays of $B^\pm/B^0$ admixture (part 1).

Parameter [10^{-6}]	Measurements		Average HFLAV PDG
$\mathcal{B}(B \to K\eta\gamma)$	Belle [1067]	$8.5 \pm 1.3^{+1.2}_{-0.9}$[a]	$8.5^{+1.8}_{-1.6}$
$\mathcal{B}(B \to K_1(1400)\gamma)$	CLEO [1065]	<127	<127
$\mathcal{B}(B \to K_2^*(1430)\gamma)$	CLEO [1065]	$16.6^{+5.9}_{-5.3} \pm 1.3$	$16.6^{+6.0}_{-5.5}$
$\mathcal{B}(B \to K_3^*(1780)\gamma)$	Belle [1067]	<9.3	<9.3 <37.0
$\mathcal{B}(B \to X_s\gamma)$	Belle [550] *BABAR* [1102] Belle [1103] *BABAR* [1104] CLEO [551] *BABAR* [1105]	$347 \pm 15 \pm 40$[b] $332 \pm 16 \pm 31$[b] $375 \pm 18 \pm 35$[b] $352 \pm 20 \pm 51$[b] $329 \pm 44 \pm 29$[b] $390 \pm 91 \pm 64$[b]	349 ± 19
$\mathcal{B}(B \to X_d\gamma)$	*BABAR* [1106]	$9.2 \pm 2.0 \pm 2.3$	9.2 ± 3.0
$\mathcal{B}(B \to \rho\gamma)$[c]	Belle [1075] *BABAR* [1076]	$1.21^{+0.24}_{-0.22} \pm 0.12$ $1.73^{+0.34}_{-0.32} \pm 0.17$	1.40 ± 0.22 $1.39^{+0.25}_{-0.24}$
$\mathcal{B}(B \to \rho/\omega\gamma)$[c]	Belle [1075] *BABAR* [1076]	$1.14 \pm 0.20^{+0.10}_{-0.12}$ $1.63^{+0.30}_{-0.28} \pm 0.16$	1.30 ± 0.18 $1.30^{+0.23}_{-0.24}$

(Table continued)

TABLE 237. *(Continued)*

Parameter $[10^{-6}]$	Measurements		Average HFLAV PDG
$\mathcal{B}(B \to X_s e^+ e^-)$[c,d,e]	*BABAR* [1107]	$7.69^{+0.82+0.71\,\mathrm{f}}_{-0.77-0.60}$	6.67 ± 0.83
	Belle [1108]	$4.04 \pm 1.30^{+0.87}_{-0.83}$	$6.67^{+1.76}_{-1.63}$
$\mathcal{B}(B \to X_s \mu^+ \mu^-)$[d,e]	Belle [1108]	$4.13 \pm 1.05^{+0.85}_{-0.81}$	4.27 ± 0.95
	BABAR [1107]	$4.41^{+1.31+0.63\,\mathrm{f}}_{-1.17-0.50}$	$4.27^{+0.99}_{-0.92}$
$\mathcal{B}(B \to X_s \ell^+ \ell^-)$[d,c,e]	*BABAR* [1107]	$6.73^{+0.70+0.60\,\mathrm{f}}_{-0.64-0.56}$	5.84 ± 0.69
	Belle [1108]	$4.11 \pm 0.83^{+0.85}_{-0.81}$	$5.84^{+1.31}_{-1.23}$

[a] $M_{K\eta} < 2.4$ GeV/c^2.
[b] Measurement extrapolated to $E_\gamma > 1.6$ GeV using the method from Ref. [1109].
[c] The PDG uncertainty includes a scale factor.
[d] Belle uses $m_{\ell^+\ell^-} > 0.2$ GeV/c^2, *BABAR* uses $m_{\ell^+\ell^-} > 0.1$ GeV/c^2.
[e] Treatment of charmonium intermediate components differs between the results.
[f] Multiple systematic uncertainties are added in quadrature.

TABLE 238. Branching fractions of charmless radiative, FCNC decays with leptons and LFV/LNV decays of $B^\pm/B^0$ admixture (part 2).

Parameter $[10^{-6}]$	Measurements		Average HFLAV PDG
$\mathcal{B}(B \to \pi \ell^+ \ell^-)$[a]	*BABAR* [1079]	<0.059	<0.059
	Belle [1078]	<0.062	
$\mathcal{B}(B \to \pi e^+ e^-)$	*BABAR* [1079]	<0.11	<0.11
$\mathcal{B}(B \to \pi \mu^+ \mu^-)$	*BABAR* [1079]	<0.05	<0.05
$\mathcal{B}(B \to K e^+ e^-)$[a]	Belle [1089]	$0.48^{+0.08}_{-0.07} \pm 0.03$	0.44 ± 0.06
	BABAR [1085]	$0.388^{+0.090}_{-0.083} \pm 0.020$	
$\mathcal{B}(B \to K^* e^+ e^-)$[b,a]	Belle [1089]	$1.39^{+0.23}_{-0.20} \pm 0.12$	1.20 ± 0.16
	BABAR [1085]	$0.99^{+0.23}_{-0.21} \pm 0.06$	$1.19^{+0.21}_{-0.19}$
$\mathcal{B}(B \to K \mu^+ \mu^-)$[a]	CDF [1026]	$0.42 \pm 0.04 \pm 0.02$	0.442 ± 0.036
	Belle [1089]	$0.50 \pm 0.06 \pm 0.03$	
	BABAR [1085]	$0.41^{+0.13}_{-0.12} \pm 0.02$	
$\mathcal{B}(B \to K^* \mu^+ \mu^-)$[a]	CDF [1026]	$1.01 \pm 0.10 \pm 0.05$	1.06 ± 0.09
	Belle [1089]	$1.10^{+0.16}_{-0.14} \pm 0.08$	
	BABAR [1085]	$1.35^{+0.35}_{-0.33} \pm 0.10$	
$\mathcal{B}(B \to K \ell^+ \ell^-)$[a]	Belle [1089]	$0.48^{+0.05}_{-0.04} \pm 0.03$	0.48 ± 0.04
	BABAR [1110]	$0.47 \pm 0.06 \pm 0.02$	
$\mathcal{B}(B \to K^* \ell^+ \ell^-)$[a]	Belle [1089]	$1.07^{+0.11}_{-0.10} \pm 0.09$	1.05 ± 0.10
	BABAR [1110]	$1.02^{+0.14}_{-0.13} \pm 0.05$	

[a] Treatment of charmonium intermediate components differs between the results.
[b] The PDG uncertainty includes a scale factor.

TABLE 239. Branching fractions of charmless radiative, FCNC decays with leptons and LFV/LNV decays of $B^{\pm}/B^{0}$ admixture (part 3).

Parameter $[10^{-6}]$	Measurements		Average HFLAV PDG
$\mathcal{B}(B \to K\nu\bar{\nu})$	Belle [1081]	<16.0	<16
	BABAR [1087]	<17.0	
$\mathcal{B}(B \to K^{*}\nu\bar{\nu})$	Belle [1081]	<27.0	<27
	BABAR [1087]	<76.0	
$\mathcal{B}(B \to \pi\nu\bar{\nu})$	Belle [1081]	<8.0	<8.0
$\mathcal{B}(B \to \rho\nu\bar{\nu})$	Belle [1081]	<28.0	<28
$\mathcal{B}(B \to \pi e^{\pm}\mu^{\mp})$	*BABAR* [1098]	<0.092	<0.092
$\mathcal{B}(B \to \rho e^{\pm}\mu^{\mp})$	CLEO [1111]	<3.2	<3.2
$\mathcal{B}(B \to K e^{\pm}\mu^{\mp})$	*BABAR* [1099]	<0.038	<0.038
$\mathcal{B}(B \to K^{*} e^{\pm}\mu^{\mp})$	*BABAR* [1099]	<0.51	<0.51

TABLE 240. Branching fractions of charmless leptonic and radiative-leptonic B^{+} and B^{0} decays (part 1).

Parameter $[10^{-7}]$	Measurements		Average HFLAV PDG
$\mathcal{B}(B^{+} \to e^{+}\nu_{e})$	Belle [1112]	<9.8	<9.8
	BABAR [1113]	<19	
$\mathcal{B}(B^{+} \to \mu^{+}\nu_{\mu})$	Belle [1114]	<8.6	<8.6
	BABAR [1113]	<10	
	Belle [1115]	<10.7	
$\mathcal{B}(B^{+} \to \tau^{+}\nu_{\tau})$[a]	Belle [1116]	$720^{+270}_{-250} \pm 110$	1094 ± 208
	Belle [1117]	$1250 \pm 280 \pm 270$	1094^{+247}_{-236}
	BABAR [1118]	$1830^{+530}_{-490} \pm 240$	
	BABAR [1119]	$1700 \pm 800 \pm 200$	
$\mathcal{B}(B^{+} \to \ell^{+}\nu_{\ell}\gamma)$	Belle [1120]	<30[b]	<30
	BABAR [1121]	<156	
$\mathcal{B}(B^{+} \to e^{+}\nu_{e}\gamma)$	Belle [1120]	<43[b]	<43
	BABAR [1121]	<170	
$\mathcal{B}(B^{+} \to \mu^{+}\nu_{\mu}\gamma)$	Belle [1120]	<34[b]	<34
	BABAR [1121]	<260	
$\mathcal{B}(B^{0} \to \gamma\gamma)$	*BABAR* [1122]	<3.3	<3.3
	Belle [1123]	<6.2	<3.2
$\mathcal{B}(B^{0} \to e^{+}e^{-})$	LHCb [1049]	<0.025	<0.025
	CDF [1050]	<0.83	
	BABAR [1124]	<1.13	
	Belle [1125]	<1.9	
$\mathcal{B}(B^{0} \to e^{+}e^{-}\gamma)$	*BABAR* [1126]	<1.2	<1.2
$\mathcal{B}(B^{0} \to \mu^{+}\mu^{-})$	ATLAS [1046]	<0.0021[c]	<0.0021
	LHCb [1047]	<0.0034[c]	$0.0005^{+0.0017}_{-0.0015}$
	CMS [108]	<0.0036[c]	
	CDF [1048]	<0.038	
	BABAR [1124]	<0.52	
	Belle [1125]	<1.6	

[a]The PDG uncertainty includes a scale factor.
[b]$E_{\gamma} > 1$ GeV.
[c]At CL = 95%.

TABLE 241. Branching fractions of charmless leptonic and radiative-leptonic B^+ and B^0 decays (part 2).

Parameter [10^{-7}]	Measurements		Average HFLAV PDG
$\mathcal{B}(B^0 \to \mu^+\mu^-\gamma)$	*BABAR* [1126]	<1.5	<1.5 <1.6
$\mathcal{B}(B^0 \to \mu^+\mu^-\mu^+\mu^-)$	LHCb [1052]	<0.0069[a,b]	<0.0069
$\mathcal{B}(B^0 \to SP) \times \mathcal{B}(S \to \mu^+\mu^-) \times \mathcal{B}(P \to \mu^+\mu^-)$	LHCb [1052]	<0.006[a,b]	<0.0060
$\mathcal{B}(B^0 \to \tau^+\tau^-)$	LHCb [1051] *BABAR* [1127]	<21000[b] <41000	<21000
$\mathcal{B}(B^0 \to \nu\bar{\nu})$	*BABAR* [1128] Belle [1129]	<240 <780	<240
$\mathcal{B}(B^0 \to \nu\bar{\nu}\gamma)$	Belle [1129] *BABAR* [1128]	<160[c] <170[d]	<160
$\mathcal{B}(B^+ \to \mu^+\mu^-\mu^+\nu_\mu)$	LHCb [1130]	<0.16[b]	<0.16

[a]The mass windows corresponding to ϕ and charmonium resonances decaying to $\mu\mu$ are vetoed.
[b]At CL = 95%.
[c]$E_\gamma > 0.5$ GeV.
[d]$E_\gamma > 1.2$ GeV.

TABLE 242. Relative branching fractions of charmless radiative and FCNC decays with leptons of B^+ and B^0 mesons (part 1).

Parameter	Measurements		Average
$\frac{\mathcal{B}(B^+\to\pi^+\mu^+\mu^-)}{\mathcal{B}(B^+\to K^+\mu^+\mu^-)}$, $1.0 < m^2_{\ell^+\ell^-} < 6.0$ GeV^2/c^4	LHCb [1080]	$0.038 \pm 0.009 \pm 0.001$	0.038 ± 0.009
$\frac{\mathcal{B}(B^+\to K^+\mu^+\mu^-)}{\mathcal{B}(B^+\to K^+e^+e^-)}$, Full $m^2_{\ell^+\ell^-}$ range	Belle [1084]	$1.08^{+0.16}_{-0.15} \pm 0.02$	1.08 ± 0.16
$\frac{\mathcal{B}(B^+\to K^+\mu^+\mu^-)}{\mathcal{B}(B^+\to K^+e^+e^-)}$, $1.1 < m^2_{\ell^+\ell^-} < 6.0$ GeV^2/c^4	LHCb [1131]	$0.846^{+0.042+0.013}_{-0.039-0.012}$[a]	0.846 ± 0.042
$\frac{\mathcal{B}(B^+\to K^+\mu^+\mu^-)}{\mathcal{B}(B^+\to K^+e^+e^-)}$, $0.10 < m^2_{\ell^+\ell^-} < 8.12$ GeV^2/c^4 and $m^2_{\ell^+\ell^-} > 10.11$ GeV^2/c^4	*BABAR* [1110]	$1.00^{+0.31}_{-0.25} \pm 0.07$	$1.00^{+0.32}_{-0.26}$
$\frac{\mathcal{B}(B^+\to K^+\mu^+\mu^-)}{\mathcal{B}(B^+\to K^+e^+e^-)}$, $1.0 < m^2_{\ell^+\ell^-} < 6.0$ GeV^2/c^4[b]	Belle [1084]	$1.39^{+0.36}_{-0.33} \pm 0.02$	1.39 ± 0.35
$\frac{\mathcal{B}(B^0\to K^0_S\mu^+\mu^-)}{\mathcal{B}(B^0\to K^0_S e^+e^-)}$, Full $m^2_{\ell^+\ell^-}$ range	Belle [1084]	$1.29^{+0.52}_{-0.45} \pm 0.01$	$1.29^{+0.52}_{-0.45}$
$\frac{\mathcal{B}(B^0\to K^0_S\mu^+\mu^-)}{\mathcal{B}(B^0\to K^0_S e^+e^-)}$, $1.0 < m^2_{\ell^+\ell^-} < 6.0$ GeV^2/c^4[b]	Belle [1084]	$0.55^{+0.46}_{-0.34} \pm 0.01$	$0.55^{+0.46}_{-0.34}$
$\frac{\mathcal{B}(B\to K\mu^+\mu^-)}{\mathcal{B}(B\to Ke^+e^-)}$, Full $m^2_{\ell^+\ell^-}$ range	Belle [1084]	$1.10^{+0.16}_{-0.15} \pm 0.02$	1.10 ± 0.16
$\frac{\mathcal{B}(B\to K\mu^+\mu^-)}{\mathcal{B}(B\to Ke^+e^-)}$, $1.0 < m^2_{\ell^+\ell^-} < 6.0$ GeV^2/c^4[b]	Belle [1084]	$1.03^{+0.28}_{-0.24} \pm 0.01$	$1.03^{+0.28}_{-0.24}$

[a]LHCb has also measured the branching fraction of $B^+ \to K^+e^+e^-$ in the $m^2_{\ell^+\ell^-}$ bin $[1.1, 6.0]$ GeV^2/c^4.
[b]For the other bins see the text.

TABLE 243. Relative branching fractions of charmless radiative and FCNC decays with leptons of B^+ and B^0 mesons (part 2).

Parameter	Measurements		Average
$\frac{\mathcal{B}(B\to K^*\mu^+\mu^-)}{\mathcal{B}(B\to K^*e^+e^-)}$, Full $m^2_{\ell^+\ell^-}$ range	Belle [1089]	$0.83 \pm 0.17 \pm 0.08$	0.83 ± 0.19
$\frac{\mathcal{B}(B\to K^*\mu^+\mu^-)}{\mathcal{B}(B\to K^*e^+e^-)}$, $0.10 < m^2_{\ell^+\ell^-} < 8.12$ GeV^2/c^4 and $m^2_{\ell^+\ell^-} > 10.11$ GeV^2/c^4	*BABAR* [1110]	$1.13^{+0.34}_{-0.26} \pm 0.10$	$1.13^{+0.35}_{-0.28}$
$\frac{\mathcal{B}(B\to K^*\mu^+\mu^-)}{\mathcal{B}(B\to K^*e^+e^-)}$, $0.045 < m^2_{\ell^+\ell^-} < 1.1$ GeV^2/c^4	Belle [1132]	$0.52^{+0.36}_{-0.26} \pm 0.06$	$0.52^{+0.36}_{-0.27}$
$\frac{\mathcal{B}(B\to K^*\mu^+\mu^-)}{\mathcal{B}(B\to K^*e^+e^-)}$, $1.1 < m^2_{\ell^+\ell^-} < 6.0$ GeV^2/c^4	Belle [1132]	$0.96^{+0.45}_{-0.29} \pm 0.11$	$0.96^{+0.46}_{-0.31}$
$\frac{\mathcal{B}(B\to K^*\mu^+\mu^-)}{\mathcal{B}(B\to K^*e^+e^-)}$, $15 < m^2_{\ell^+\ell^-} < 19$ GeV^2/c^4	Belle [1132]	$1.18^{+0.52}_{-0.32} \pm 0.11$	$1.18^{+0.53}_{-0.34}$
$\frac{\mathcal{B}(B^0\to K^*(892)^0\mu^+\mu^-)}{\mathcal{B}(B^0\to K^*(892)^0e^+e^-)}$, $0.045 < m^2_{\ell^+\ell^-} < 1.1$ GeV^2/c^4	LHCb [1133] Belle [1132]	$0.66^{+0.11}_{-0.07} \pm 0.03$ $0.46^{+0.55}_{-0.27} \pm 0.13$	$0.65^{+0.11}_{-0.07}$
$\frac{\mathcal{B}(B^0\to K^*(892)^0\mu^+\mu^-)}{\mathcal{B}(B^0\to K^*(892)^0e^+e^-)}$, $1.1 < m^2_{\ell^+\ell^-} < 6.0$ GeV^2/c^4	LHCb [1133] Belle [1132]	$0.69^{+0.11}_{-0.07} \pm 0.05$ $1.06^{+0.63}_{-0.38} \pm 0.14$	$0.72^{+0.12}_{-0.09}$
$\frac{\mathcal{B}(B^0\to K^*(892)^0\mu^+\mu^-)}{\mathcal{B}(B^0\to K^*(892)^0e^+e^-)}$, $15 < m^2_{\ell^+\ell^-} < 19$ GeV^2/c^4	Belle [1132]	$1.12^{+0.61}_{-0.36} \pm 0.10$	$1.12^{+0.62}_{-0.37}$
$\frac{\mathcal{B}(B^+\to K^*(892)^+\mu^+\mu^-)}{\mathcal{B}(B^+\to K^*(892)^+e^+e^-)}$, $0.045 < m^2_{\ell^+\ell^-} < 1.1$ GeV^2/c^4	Belle [1132]	$0.62^{+0.60}_{-0.36} \pm 0.09$	$0.62^{+0.61}_{-0.37}$
$\frac{\mathcal{B}(B^+\to K^*(892)^+\mu^+\mu^-)}{\mathcal{B}(B^+\to K^*(892)^+e^+e^-)}$, $1.1 < m^2_{\ell^+\ell^-} < 6.0$ GeV^2/c^4	Belle [1132]	$0.72^{+0.99}_{-0.44} \pm 0.15$	$0.7^{+1.0}_{-0.5}$
$\frac{\mathcal{B}(B^+\to K^*(892)^+\mu^+\mu^-)}{\mathcal{B}(B^+\to K^*(892)^+e^+e^-)}$, $15 < m^2_{\ell^+\ell^-} < 19$ GeV^2/c^4	Belle [1132]	$1.40^{+1.99}_{-0.68} \pm 0.12$	$1.4^{+2.0}_{-0.7}$
$\frac{\mathcal{B}(B^0\to K^*(892)^0\gamma)}{\mathcal{B}(B_s^0\to\phi(1020)\gamma)}$	LHCb [1045] Belle [1063]	$1.23 \pm 0.06 \pm 0.11$[a] $1.10 \pm 0.16 \pm 0.20$[a]	1.21 ± 0.11

[a]Multiple systematic uncertainties are added in quadrature.

TABLE 244. Branching fractions of $B^+/B^0 \to \bar{q}$ gluon decays.

Parameter [10^{-4}]	Measurements		Average HFLAV PDG
$\mathcal{B}(B \to \eta X)$	Belle [1134]	$2.610 \pm 0.300^{+0.440}_{-0.740}$ [a]	$2.61^{+0.53}_{-0.80}$
	CLEO [1135]	<4.400 [b]	
$\mathcal{B}(B \to \eta' X)$	*BABAR* [1136]	$3.90 \pm 0.80 \pm 0.90$ [c]	4.24 ± 0.87
	CLEO [1137]	$4.60 \pm 1.10 \pm 0.60$ [c]	
$\mathcal{B}(B \to K^+ X)$	*BABAR* [1138]	<1.87 [d]	<1.9
$\mathcal{B}(B \to K^0 X)$	*BABAR* [1138]	$1.95^{+0.51}_{-0.45} \pm 0.50$ [d]	1.95 ± 0.69 $1.95^{+0.71}_{-0.67}$
$\mathcal{B}(B \to \pi^+ X)$	*BABAR* [1138]	$3.72^{+0.50}_{-0.47} \pm 0.59$ [e]	3.72 ± 0.76 $3.72^{+0.77}_{-0.75}$

[a] $0.4 < m_X < 2.6$ GeV/c^2.
[b] $2.1 < p_\eta < 2.7$ GeV/c.
[c] $2.0 < p^*(\eta') < 2.7$ GeV/c.
[d] $p^*(K) < 2.34$ GeV/c.
[e] $p^*(\pi^+) < 2.36$ GeV/c.

TABLE 245. Isospin asymmetry in radiative and FCNC decays with leptons of B mesons. In some of the B-factory results it is assumed that $\mathcal{B}(\Upsilon(4S) \to B^+B^-) = \mathcal{B}(\Upsilon(4S) \to B^0\bar{B}^0)$, and in others a measured value of the ratio of branching fractions is used. See original papers for details. The averages quoted here are computed naively and should be treated with caution.

Parameter	Measurements		Average HFLAV PDG
$\Delta_{0^-}(B \to X_s\gamma)$	Belle [1139]	$-0.0048 \pm 0.0149 \pm 0.0150$ [a,b]	-0.005 ± 0.020
	BABAR [548]	$-0.006 \pm 0.058 \pm 0.026$ [a,b]	
$\Delta_{0^-}(B \to X_{s+d}\gamma)$	*BABAR* [1105]	$-0.06 \pm 0.15 \pm 0.07$ [c]	-0.06 ± 0.17
$\Delta_{0^+}(B \to K^*\gamma)$	Belle [1063]	$0.062 \pm 0.015 \pm 0.013$ [b]	0.063 ± 0.017
	BABAR [1064]	$0.066 \pm 0.021 \pm 0.022$	
$\frac{\Gamma(B^+\to\rho^+\gamma)}{2\Gamma(B^0\to\rho^0\gamma)} - 1$	Belle [1075]	$-0.48^{+0.21+0.08}_{-0.19-0.09}$	-0.46 ± 0.17
	BABAR [1076]	$-0.43^{+0.25}_{-0.22} \pm 0.10$	
$\Delta_{0-}(B \to K\ell^+\ell^-)$ [d]	LHCb [1083]	$-0.10^{+0.08}_{-0.09} \pm 0.02$ [e]	$-0.191^{+0.073}_{-0.071}$ -0.150 ± 0.060
	Belle [1084]	$-0.31^{+0.13}_{-0.11} \pm 0.01$ [f]	
	BABAR [1110]	$-0.41 \pm 0.25 \pm 0.01$ [f]	
$\Delta_{0-}(B \to K^*\ell^+\ell^-)$ [d]	*BABAR* [1110]	$-0.20^{+0.30}_{-0.23} \pm 0.03$ [f]	$-0.01^{+0.11}_{-0.09}$ $-0.03^{+0.08}_{-0.07}$
	Belle [1089]	$0.33^{+0.37}_{-0.43} \pm 0.08$ [f]	
	LHCb [1083]	$0.00^{+0.12}_{-0.10} \pm 0.02$ [e]	
$\Delta_{0^-}(B \to K^{(*)}\ell^+\ell^-)$ [d]	Belle [1089]	$-0.30^{+0.12}_{-0.11} \pm 0.08$ [g]	-0.45 ± 0.10 -0.45 ± 0.17
	BABAR [1085]	$-0.64^{+0.15}_{-0.14} \pm 0.03$ [h]	

[a] $M_{X_s} < 2.8$ GeV/c^2.
[b] Multiple systematic uncertainties are added in quadrature.
[c] $E_\gamma > 2.2$ GeV.
[d] The PDG uncertainty includes a scale factor.
[e] Only muons are used, $1.1 < m^2_{\ell^+\ell^-} < 6.0$ GeV^2/c^4.
[f] $1.0 < m^2_{\ell^+\ell^-} < 6.0$ GeV^2/c^4.
[g] $m^2_{\ell^+\ell^-} < 8.68$ GeV^2/c^4.
[h] $0.1 < m^2_{\ell^+\ell^-} < 7.02$ GeV^2/c^4.

TABLE 246. Branching fractions of charmless semileptonic B^+ decays to LFV and LNV final states (part 1).

Parameter [10^{-6}]	Measurements		Average HFLAV PDG
$\mathcal{B}(B^+ \to \pi^+ e^+ \mu^- + \text{c.c.})$	*BABAR* [1098]	<0.17	<0.17
$\mathcal{B}(B^+ \to \pi^+ e^+ \tau^-)$	*BABAR* [1140]	<74.0	<74
$\mathcal{B}(B^+ \to \pi^+ e^- \tau^+)$	*BABAR* [1140]	<20.0	<20
$\mathcal{B}(B^+ \to \pi^+ e^+ \tau^- + \text{c.c.})$	*BABAR* [1140]	<75.0	<75
$\mathcal{B}(B^+ \to \pi^+ \mu^+ \tau^-)$	*BABAR* [1140]	<62.0	<62
$\mathcal{B}(B^+ \to \pi^+ \mu^- \tau^+)$	*BABAR* [1140]	<45.0	<45
$\mathcal{B}(B^+ \to \pi^+ \mu^+ \tau^- + \text{c.c.})$	*BABAR* [1140]	<72.0	<72
$\mathcal{B}(B^+ \to K^+ e^+ \mu^-)$	LHCb [1141] Belle [1084] *BABAR* [1099]	<0.0070 <0.03 <0.091	<0.007
$\mathcal{B}(B^+ \to K^+ e^- \mu^+)$	LHCb [1141] Belle [1084] *BABAR* [1099]	<0.0064 <0.085 <0.13	<0.0064
$\mathcal{B}(B^+ \to K^+ e^+ \mu^- + \text{c.c.})$	*BABAR* [1099]	<0.091	<0.091
$\mathcal{B}(B^+ \to K^+ e^+ \tau^-)$	*BABAR* [1140]	<43.0	<43
$\mathcal{B}(B^+ \to K^+ e^- \tau^+)$	*BABAR* [1140]	<15.0	<15
$\mathcal{B}(B^+ \to K^+ e^+ \tau^- + \text{c.c.})$	*BABAR* [1140]	<30.0	<30
$\mathcal{B}(B^+ \to K^+ \mu^+ \tau^-)$	*BABAR* [1140]	<45.0	<45
$\mathcal{B}(B^+ \to K^+ \mu^- \tau^+)$	*BABAR* [1140] LHCb [1142]	<28.0 <39.0	<28
$\mathcal{B}(B^+ \to K^+ \mu^+ \tau^- + \text{c.c.})$	*BABAR* [1140]	<48.0	<48
$\mathcal{B}(B^+ \to K^*(892)^+ e^+ \mu^-)$	*BABAR* [1099]	<1.30	<1.3
$\mathcal{B}(B^+ \to K^*(892)^+ e^- \mu^+)$	*BABAR* [1099]	<0.99	<0.99
$\mathcal{B}(B^+ \to K^*(892)^+ e^+ \mu^- + \text{c.c.})$	*BABAR* [1099]	<1.40	<1.4
$\mathcal{B}(B^+ \to \pi^- e^+ e^+)$	*BABAR* [1143]	<0.023	<0.023
$\mathcal{B}(B^+ \to \pi^- \mu^+ \mu^+)$	LHCb [1144] *BABAR* [1143]	<0.0040[a] <0.107	<0.004
$\mathcal{B}(B^+ \to \pi^- e^+ \mu^+)$	*BABAR* [1145]	<0.15	<0.15
$\mathcal{B}(B^+ \to \rho^-(770) e^+ e^+)$	*BABAR* [1145]	<0.17	<0.17
$\mathcal{B}(B^+ \to \rho^-(770) \mu^+ \mu^+)$	*BABAR* [1145]	<0.42	<0.42
$\mathcal{B}(B^+ \to \rho^-(770) e^+ \mu^+)$	*BABAR* [1145]	<0.47	<0.47

[a]At CL = 95%.

TABLE 247. Branching fractions of charmless semileptonic B^+ decays to LFV and LNV final states (part 2).

Parameter [10^{-6}]	Measurements		Average HFLAV PDG
$\mathcal{B}(B^+ \to K^- e^+ e^+)$	*BABAR* [1143]	<0.030	<0.030
$\mathcal{B}(B^+ \to K^- \mu^+ \mu^+)$	LHCb [1146] *BABAR* [1143]	<0.041 <0.067	<0.041
$\mathcal{B}(B^+ \to K^- e^+ \mu^+)$	*BABAR* [1145]	<0.16	<0.16
$\mathcal{B}(B^+ \to K^*(892)^- e^+ e^+)$	*BABAR* [1145]	<0.40	<0.40
$\mathcal{B}(B^+ \to K^*(892)^- \mu^+ \mu^+)$	*BABAR* [1145]	<0.59	<0.59
$\mathcal{B}(B^+ \to K^*(892)^- e^+ \mu^+)$	*BABAR* [1145]	<0.30	<0.30
$\mathcal{B}(B^+ \to D^- e^+ e^+)$	*BABAR* [1145] BELLE [794]	<2.6 <2.6	<2.6
$\mathcal{B}(B^+ \to D^- e^+ \mu^+)$	BELLE [794] *BABAR* [1145]	<1.8 <2.1	<1.8
$\mathcal{B}(B^+ \to D^- \mu^+ \mu^+)$	LHCb [1147] BELLE [794] *BABAR* [1145]	<0.69[a] <1.0 <1.7	<0.69
$\mathcal{B}(B^+ \to D^*(2010)^- \mu^+ \mu^+)$	LHCb [1147]	<2.4[a]	<2.4
$\mathcal{B}(B^+ \to D_s^- \mu^+ \mu^+)$	LHCb [1147]	<0.58[a]	<0.58
$\mathcal{B}(B^+ \to \bar{D}^0 \pi^- \mu^+ \mu^+)$	LHCb [1147]	<1.5[a]	<1.5
$\mathcal{B}(B^+ \to \Lambda^0 \mu^+)$	*BABAR* [1101]	<0.061	<0.061 <0.060
$\mathcal{B}(B^+ \to \Lambda^0 e^+)$	*BABAR* [1101]	<0.032	<0.032
$\mathcal{B}(B^+ \to \bar{\Lambda}^0 \mu^+)$	*BABAR* [1101]	<0.062	<0.062 <0.060
$\mathcal{B}(B^+ \to \bar{\Lambda}^0 e^+)$	*BABAR* [1101]	<0.081	<0.081 <0.080

[a]At CL = 95%.

TABLE 248. Branching fractions of charmless semileptonic B^0 decays to LFV and LNV final states.

Parameter [10^{-6}]	Measurements		Average HFLAV PDG
$\mathcal{B}(B^0 \to K^*(892)^0 e^- \mu^+)$	Belle [1100] *BABAR* [1099]	<0.12 <0.34	<0.12
$\mathcal{B}(B^0 \to K^*(892)^0 e^+ \mu^-)$	Belle [1100] *BABAR* [1099]	<0.16 <0.53	<0.16
$\mathcal{B}(B^0 \to K^0 e^+ \mu^- + \text{c.c.})$	Belle [1084] *BABAR* [1099]	<0.038 <0.27	<0.038
$\mathcal{B}(B^0 \to \pi^0 e^+ \mu^- + \text{c.c.})$	*BABAR* [1098]	<0.14	<0.14
$\mathcal{B}(B^0 \to e^+ \mu^- + \text{c.c.})$	LHCb [1055] CDF [1050] *BABAR* [1124] Belle [1125]	<0.0010 <0.064 <0.092 <0.17	<0.001
$\mathcal{B}(B^0 \to e^+ \tau^- + \text{c.c.})$	*BABAR* [1148]	<28.0	<28
$\mathcal{B}(B^0 \to \mu^+ \tau^- + \text{c.c.})$	LHCb [1056] *BABAR* [1148]	<12.0 <22.0	<12 <14

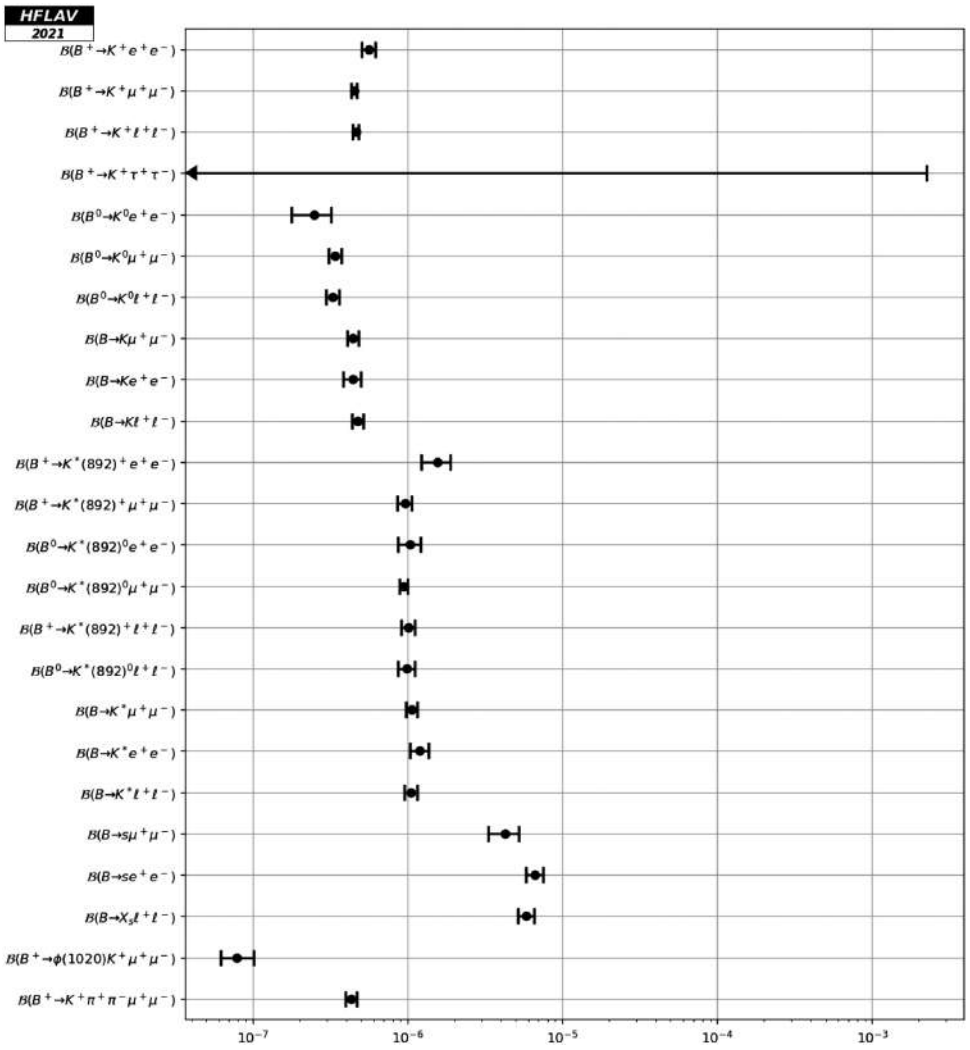

FIG. 75. Branching fractions of B^+ and B^0 decays of the type $b \to s\ell^+\ell^-$.

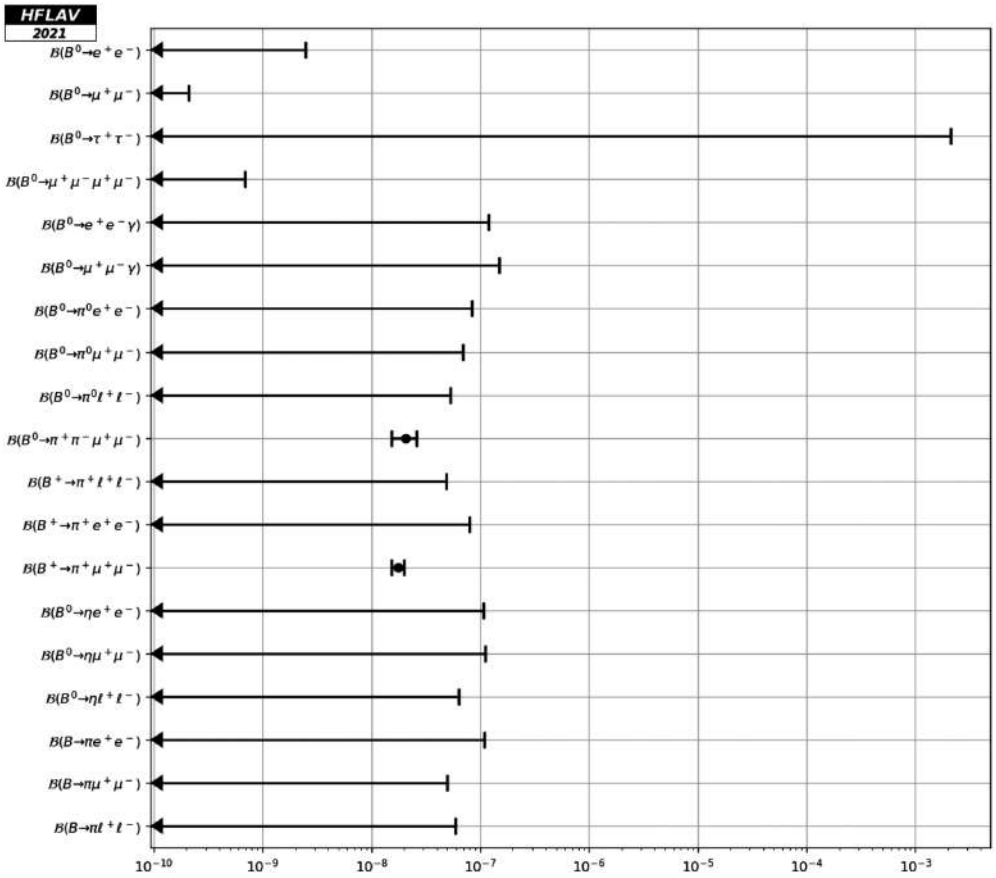

FIG. 76. Branching fractions of B^+ and B^0 decays of the type $b \to u\ell^+\ell^-$, purely leptonic and leptonic radiative.

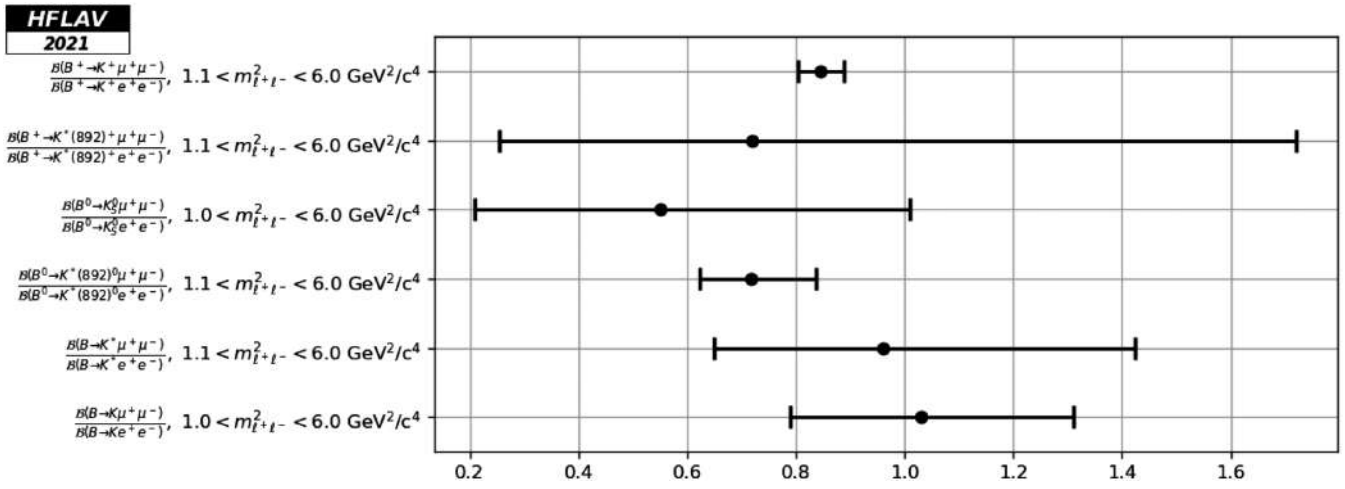

FIG. 77. Compilation of $R_K^{(*)}$ ratios in the low dilepton invariant-mass region. These are ratios between branching fractions of B-meson decays to $K^{(*)}\mu^+\mu^-$ and $K^{(*)}e^+e^-$, which provide information on lepton universality.

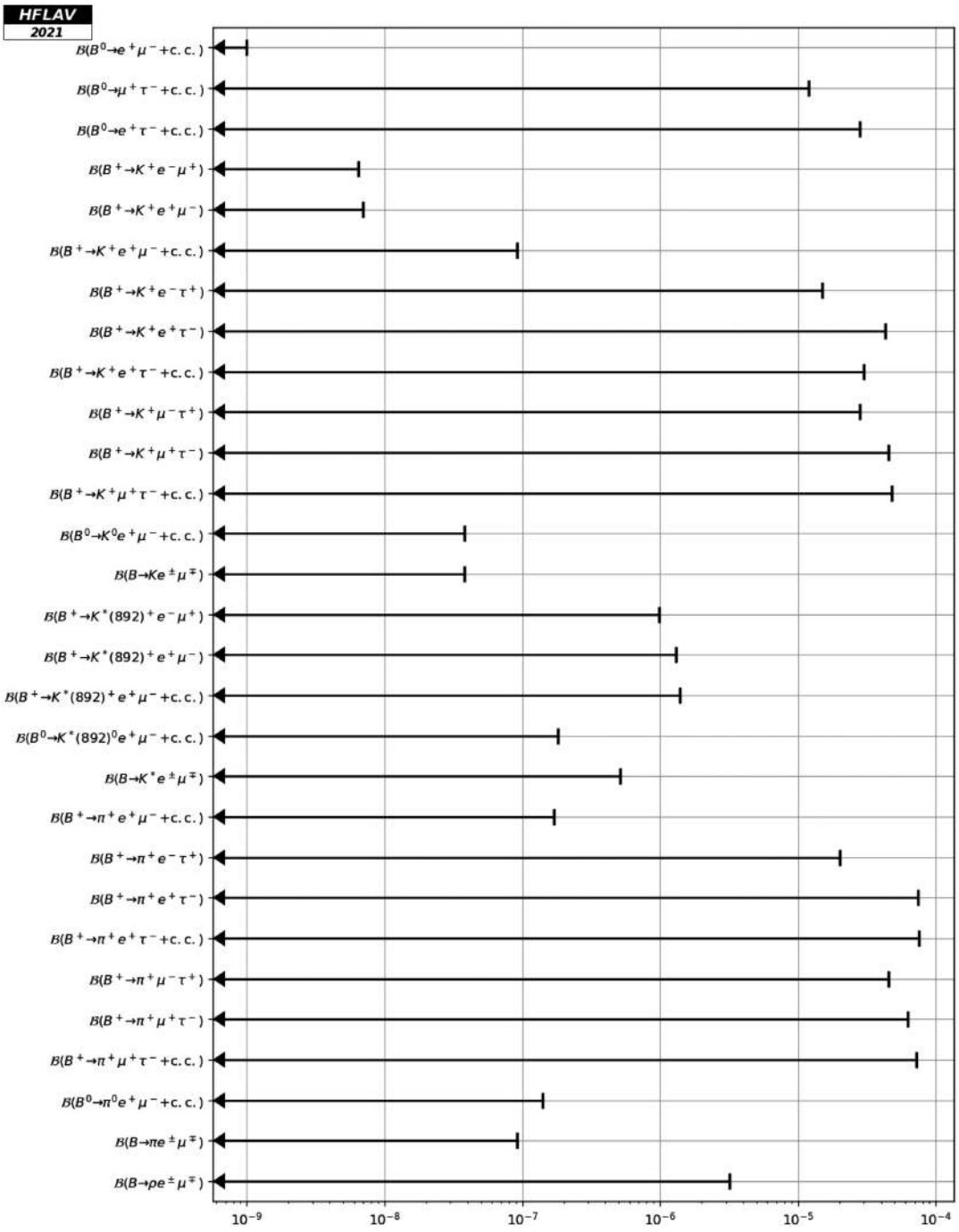

FIG. 78. Limits on branching fractions of lepton-flavor-violating B^+ and B^0 decays.

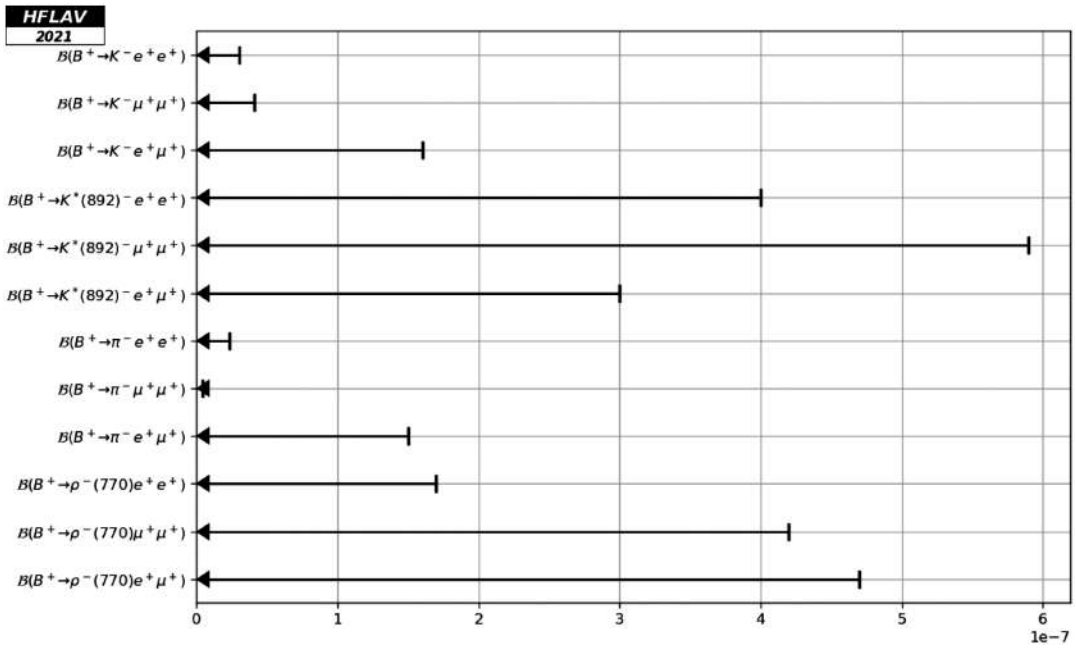

FIG. 79. Limits on branching fractions of lepton-number-violating B^+ and B^0 decays.

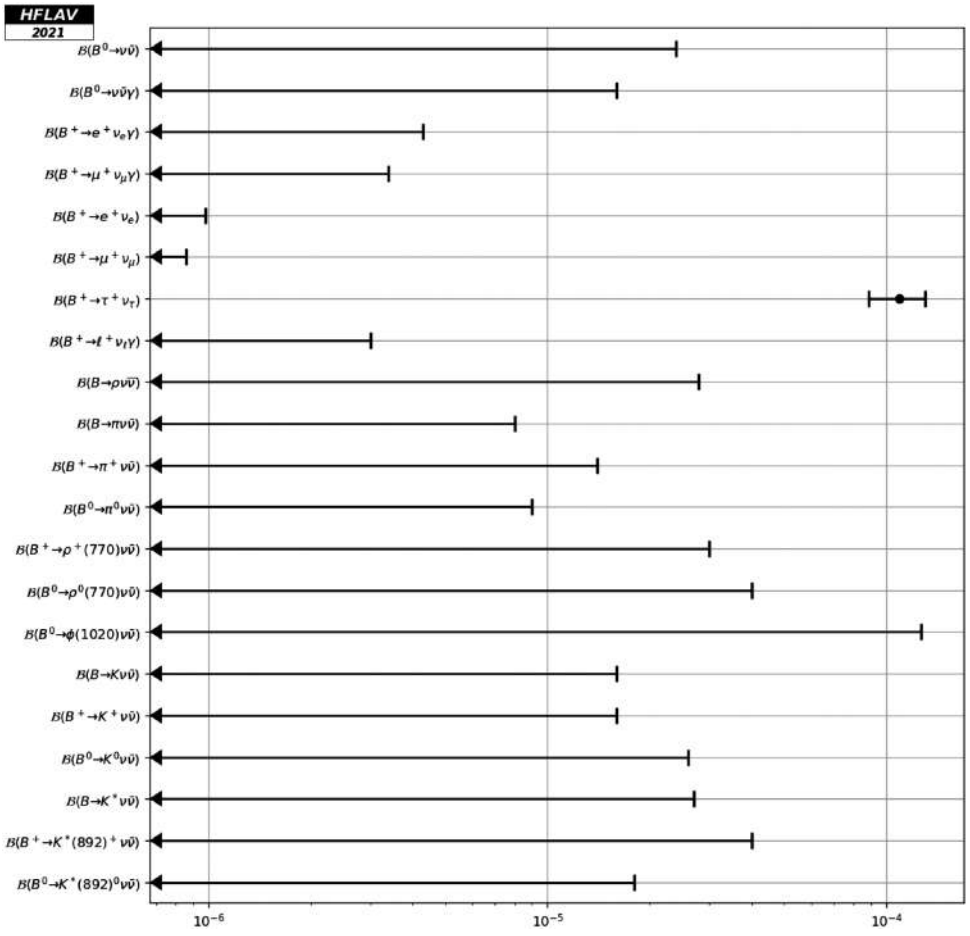

FIG. 80. Branching fractions of charmless B decays with neutrinos.

G. Charge asymmetries in *b*-hadron decays

This section contains, in Tables 249–260, compilations of *CP* asymmetries in decays of various *b*-hadrons: B^+, B^0 mesons, $B^\pm/B^0$ admixtures, B_s^0 mesons and finally Λ_b^0 baryons. The *CP* asymmetry is defined as

$$A_{CP} = \frac{N_b - N_{\bar{b}}}{N_b + N_{\bar{b}}}, \tag{226}$$

where N_b ($N_{\bar{b}}$) is the number of hadrons containing a b ($\bar{B}^0$) quark decaying into a specific final state (the *CP*-conjugate state). This definition is consistent with that of Eq. (96) in Sec. VI B 1. Measurements of time-dependent *CP* asymmetries are not listed here but are discussed in Sec. VI. Figure 81 shows a graphic representation of a selection of results given in this section.

TABLE 249. *CP* asymmetries of charmless hadronic B^+ decays (part 1).

Parameter	Measurements		Average
$A_{CP}(B^+ \to K_S^0\pi^+)$	Belle [882]	$-0.011 \pm 0.021 \pm 0.006$	-0.016 ± 0.015
	LHCb [885]	$-0.022 \pm 0.025 \pm 0.010$	
	BABAR [400]	$-0.029 \pm 0.039 \pm 0.010$	
	Belle II [883]	$-0.01 \pm 0.08 \pm 0.05$	
	CLEO [1169]	$0.18 \pm 0.24 \pm 0.02$	
$A_{CP}(B^+ \to K^+\pi^0)$	LHCb [1170]	$0.025 \pm 0.015 \pm 0.007$[a]	0.027 ± 0.013
	Belle [882]	$0.043 \pm 0.024 \pm 0.002$	
	BABAR [886]	$0.030 \pm 0.039 \pm 0.010$	
	Belle II [887]	$-0.09 \pm 0.09 \pm 0.03$	
	CLEO [1169]	$-0.29 \pm 0.23 \pm 0.02$	
$A_{CP}(B^+ \to \eta' K^+)$	LHCb [893]	$-0.002 \pm 0.012 \pm 0.006$[a]	0.004 ± 0.011
	BABAR [888]	$0.008^{+0.017}_{-0.018} \pm 0.009$	
	Belle [889]	$0.028 \pm 0.028 \pm 0.021$	
	CLEO [1169]	$0.03 \pm 0.12 \pm 0.02$	
$A_{CP}(B^+ \to \eta' K^*(892)^+)$	*BABAR* [894]	$-0.26 \pm 0.27 \pm 0.02$	-0.26 ± 0.27
$A_{CP}(B^+ \to \eta'(K\pi)_0^{*+})$	*BABAR* [894]	$0.06 \pm 0.20 \pm 0.02$	0.06 ± 0.20
$A_{CP}(B^+ \to \eta' K_2^*(1430)^+)$	*BABAR* [894]	$0.15 \pm 0.13 \pm 0.02$	0.15 ± 0.13
$A_{CP}(B^+ \to \eta K^+)$	*BABAR* [888]	$-0.36 \pm 0.11 \pm 0.03$	-0.37 ± 0.08
	Belle [896]	$-0.38 \pm 0.11 \pm 0.01$	
$A_{CP}(B^+ \to \eta K^*(892)^+)$	*BABAR* [897]	$0.01 \pm 0.08 \pm 0.02$	0.02 ± 0.06
	Belle [898]	$0.03 \pm 0.10 \pm 0.01$	
$A_{CP}(B^+ \to \eta(K\pi)_0^{*+})$	*BABAR* [897]	$0.05 \pm 0.13 \pm 0.02$	0.05 ± 0.13
$A_{CP}(B^+ \to \eta K_2^*(1430)^+)$	*BABAR* [897]	$-0.45 \pm 0.30 \pm 0.02$	-0.45 ± 0.30
$A_{CP}(B^+ \to \omega(782)K^+)$	Belle [385]	$-0.03 \pm 0.04 \pm 0.01$	-0.025 ± 0.036
	BABAR [900]	$-0.01 \pm 0.07 \pm 0.01$	
$A_{CP}(B^+ \to \omega(782)K^*(892)^+)$	*BABAR* [902]	$0.29 \pm 0.35 \pm 0.02$	0.29 ± 0.35
$A_{CP}(B^+ \to \omega(782)(K\pi)_0^{*+})$	*BABAR* [902]	$-0.10 \pm 0.09 \pm 0.02$	-0.10 ± 0.09
$A_{CP}(B^+ \to \omega(782)K_2^*(1430)^+)$	*BABAR* [902]	$0.14 \pm 0.15 \pm 0.02$	0.14 ± 0.15
$A_{CP}(B^+ \to K^*(892)^0\pi^+)$	*BABAR* [269]	$0.032 \pm 0.052^{+0.016}_{-0.013}$[b,a]	-0.04 ± 0.04
	Belle [267]	$-0.149 \pm 0.064 \pm 0.022$[b,a]	
	BABAR [904]	$-0.12 \pm 0.21^{+0.08}_{-0.14}$[c,a]	
$A_{CP}(B^+ \to K^*(892)^+\pi^0)$	*BABAR* [904]	$-0.52 \pm 0.14^{+0.06}_{-0.04}$[c,a]	-0.39 ± 0.13
	BABAR [905]	$-0.06 \pm 0.24 \pm 0.04$	

[a]Multiple systematic uncertainties are added in quadrature.
[b]Result extracted from Dalitz-plot analysis of $B^+ \to K^+\pi^+\pi^-$ decays.
[c]Result extracted from Dalitz-plot analysis of $B^+ \to K_S^0\pi^+\pi^0$ decays.

TABLE 250. CP asymmetries of charmless hadronic B^+ decays (part 2).

Parameter	Measurements		Average
$A_{CP}(B^+ \to K^+\pi^+\pi^-)$[a]	LHCb [1171]	$0.025 \pm 0.004 \pm 0.008$[b]	0.0268 ± 0.0084
	BABAR [269]	$0.028 \pm 0.020 \pm 0.023$[c,b]	
	Belle [267]	$0.049 \pm 0.026 \pm 0.020$[c]	
$A_{CP}(B^+ \to K^+K^+K^-(\mathrm{NR}))$	*BABAR* [262]	$0.060 \pm 0.044 \pm 0.019$[d]	0.06 ± 0.05
$A_{CP}(B^+ \to f_0(980)K^+)$	*BABAR* [269]	$-0.106 \pm 0.050^{+0.036}_{-0.015}$[c,b]	-0.08 ± 0.04
	Belle [267]	$-0.077 \pm 0.065^{+0.046}_{-0.026}$[c,b]	
	BABAR [262]	$-0.08 \pm 0.08 \pm 0.04$[e]	
	BABAR [905]	$0.18 \pm 0.18 \pm 0.04$	
$A_{CP}(B^+ \to f_2(1270)K^+)$	*BABAR* [269]	$-0.85 \pm 0.22^{+0.26}_{-0.13}$[c,b]	-0.67 ± 0.19
	Belle [267]	$-0.59 \pm 0.22 \pm 0.04$[c,b]	
$A_{CP}(B^+ \to f_2'(1525)K^+)$	*BABAR* [262]	$0.14 \pm 0.10 \pm 0.04$[e]	0.14 ± 0.11
$A_{CP}(B^+ \to \rho^0(770)K^+)$	*BABAR* [269]	$0.44 \pm 0.10^{+0.06}_{-0.14}$[c,b]	0.37 ± 0.12
	Belle [267]	$0.30 \pm 0.11^{+0.11}_{-0.04}$[c,b]	
$A_{CP}(B^+ \to K^0\pi^+\pi^0)$	*BABAR* [904]	$0.07 \pm 0.05 \pm 0.04$[f,b]	0.07 ± 0.06
$A_{CP}(B^+ \to K_0^*(1430)^0\pi^+)$	Belle [267]	$0.076 \pm 0.038^{+0.028}_{-0.022}$[c,b]	0.084 ± 0.043
	BABAR [904]	$0.14 \pm 0.10^{+0.14}_{-0.06}$[f,b]	
$A_{CP}(B^+ \to (K\pi)_0^{*0}\pi^+)$	*BABAR* [269]	$0.032 \pm 0.035^{+0.034}_{-0.028}$[c,b]	0.032 ± 0.046
$A_{CP}(B^+ \to K_0^*(1430)^+\pi^0)$	*BABAR* [904]	$0.26 \pm 0.02^{+0.14}_{-0.08}$[f,b]	$0.26^{+0.19}_{-0.14}$
$A_{CP}(B^+ \to K_2^*(1430)^+\pi^0)$	*BABAR* [269]	$0.05 \pm 0.23^{+0.18}_{-0.08}$[c,b]	$0.05^{+0.29}_{-0.24}$
$A_{CP}(B^+ \to K^+\pi^0\pi^0)$	*BABAR* [905]	$-0.06 \pm 0.06 \pm 0.04$	-0.06 ± 0.07
$A_{CP}(B^+ \to \rho^+(770)K^0)$	*BABAR* [904]	$0.21 \pm 0.19^{+0.24}_{-0.20}$[f,b]	$0.21^{+0.31}_{-0.28}$
$A_{CP}(B^+ \to K^*(892)^+\pi^+\pi^-)$	*BABAR* [912]	$0.07 \pm 0.07 \pm 0.04$	0.07 ± 0.08
$A_{CP}(B^+ \to K^*(892)^+\rho^0(770))$	*BABAR* [913]	$0.31 \pm 0.13 \pm 0.03$	0.31 ± 0.13
$A_{CP}(B^+ \to f_0(980)K^*(892)^+)$	*BABAR* [913]	$-0.15 \pm 0.12 \pm 0.03$	-0.15 ± 0.12
$A_{CP}(B^+ \to a_1(1260)^+K^0)$	*BABAR* [914]	$0.12 \pm 0.11 \pm 0.02$	0.12 ± 0.11
$A_{CP}(B^+ \to b_1(1235)^+K^0)$	*BABAR* [918]	$-0.03 \pm 0.15 \pm 0.02$	-0.03 ± 0.15
$A_{CP}(B^+ \to K^*(892)^0\rho^+(770))$	*BABAR* [915]	$-0.01 \pm 0.16 \pm 0.02$	-0.01 ± 0.16
$A_{CP}(B^+ \to b_1(1235)^0K^+)$	*BABAR* [919]	$-0.46 \pm 0.20 \pm 0.02$	-0.46 ± 0.20

[a]Treatment of charmonium intermediate components differs between the results.
[b]Multiple systematic uncertainties are added in quadrature.
[c]Result extracted from Dalitz-plot analysis of $B^+ \to K^+\pi^+\pi^-$ decays.
[d]The nonresonant amplitude is modeled using a polynomial function including S-wave and P-wave terms.
[e]Result extracted from Dalitz-plot analysis of $B^+ \to K^+K^+K^-$ decays.
[f]Result extracted from Dalitz-plot analysis of $B^+ \to K_S^0\pi^+\pi^0$ decays.

TABLE 251. CP asymmetries of charmless hadronic B^+ decays (part 3).

Parameter	Measurements		Average
$A_{CP}(B^+ \to K^+K_S^0)$	LHCb [885]	$-0.21 \pm 0.14 \pm 0.01$	-0.086 ± 0.100
	Belle [882]	$0.014 \pm 0.168 \pm 0.002$	
	BABAR [400]	$0.10 \pm 0.26 \pm 0.03$	
$A_{CP}(B^+ \to K^+K_S^0K_S^0)$[a]	Belle [922]	$0.016 \pm 0.039 \pm 0.009$[b]	0.025 ± 0.032
	BABAR [262]	$0.04^{+0.04}_{-0.05} \pm 0.02$[c]	

(Table continued)

TABLE 251. *(Continued)*

Parameter	Measurements		Average
$A_{CP}(B^+ \to K^+K^-\pi^+)$[a]	LHCb [1171]	$-0.123 \pm 0.017 \pm 0.014$[d]	-0.122 ± 0.021
	Belle [924]	$-0.170 \pm 0.073 \pm 0.017$[e]	
	BABAR [925]	$0.00 \pm 0.10 \pm 0.03$	
$A_{CP}(B^+ \to K^+K^-\pi^+(\mathrm{NR}))$	LHCb [926]	$-0.107 \pm 0.053 \pm 0.035$[f]	-0.107 ± 0.064
$A_{CP}(B^+ \to \bar{K}^*(892)^0K^+)$	LHCb [926]	$0.123 \pm 0.087 \pm 0.045$[g]	0.123 ± 0.098
$A_{CP}(B^+ \to \bar{K}_0^*(1430)^0K^+)$	LHCb [926]	$0.104 \pm 0.149 \pm 0.088$[g]	0.10 ± 0.17
$A_{CP}(B^+ \to \phi(1020)\pi^+)$	LHCb [926]	$0.098 \pm 0.436 \pm 0.266$[g]	0.10 ± 0.51
$A_{CP}(B^+ \to K^+K^-\pi^+)\pi\pi \leftrightarrow KK$ rescattering			
	LHCb [926]	$-0.664 \pm 0.038 \pm 0.019$[g]	-0.664 ± 0.042
$A_{CP}(B^+ \to K^+K^+K^-)$	LHCb [1171]	$-0.036 \pm 0.004 \pm 0.007$[d]	-0.033 ± 0.007
	BABAR [262]	$-0.017^{+0.019}_{-0.014} \pm 0.014$[h]	
	Belle II [931]	$-0.049 \pm 0.063 \pm 0.022$	
$A_{CP}(B^+ \to \phi(1020)K^+)$	LHCb [893]	$0.017 \pm 0.011 \pm 0.006$[d]	0.024 ± 0.012
	BABAR [262]	$0.128 \pm 0.044 \pm 0.013$[h]	
	Belle [936]	$0.01 \pm 0.12 \pm 0.05$	
	CDF [933]	$-0.07 \pm 0.17^{+0.03}_{-0.02}$	

[a]Treatment of charmonium intermediate components differs between the results.
[b]A_{CP} is also measured in bins of $m_{K^0_SK^0_S}$
[c]Result extracted from Dalitz-plot analysis of $B^0 \to K^0_SK^+K^-$ decays.
[d]Multiple systematic uncertainties are added in quadrature.
[e]Also measured in bins of $m_{K^+K^-}$.
[f]LHCb uses a model of nonresonant obtained from a phenomenological description of the partonic interaction that produces the final state. This contribution is called single pole in the paper, see Ref. [926] for details.
[g]Result extracted from Dalitz-plot analysis of $B^+ \to K^+K^-\pi^+$ decays.
[h]Result extracted from Dalitz-plot analysis of $B^+ \to K^+K^+K^-$ decays.

TABLE 252. *CP* asymmetries of charmless hadronic B^+ decays (part 4).

Parameter	Measurements		Average
$A_{CP}(B^+ \to K^*(892)^+K^+K^-)$	*BABAR* [912]	$0.11 \pm 0.08 \pm 0.03$	0.11 ± 0.09
$A_{CP}(B^+ \to \phi(1020)K^*(892)^+)$	Belle [1172]	$-0.02 \pm 0.14 \pm 0.03$	-0.01 ± 0.08
	BABAR [935]	$0.00 \pm 0.09 \pm 0.04$[a]	
$A_{CP}(B^+ \to (K\pi)_0^{*+}\phi(1020))$	*BABAR* [937]	$0.04 \pm 0.15 \pm 0.04$	0.04 ± 0.16
$A_{CP}(B^+ \to K_1(1270)^+\phi(1020))$	*BABAR* [937]	$0.15 \pm 0.19 \pm 0.05$	0.15 ± 0.20
$A_{CP}(B^+ \to K_2^*(1430)^+\phi(1020))$	*BABAR* [937]	$-0.23 \pm 0.19 \pm 0.06$	-0.23 ± 0.20
$A_{CP}(B^+ \to \phi(1020)\phi(1020)K^+)$	*BABAR* [939]	$-0.10 \pm 0.08 \pm 0.02$[b]	-0.10 ± 0.08
$A_{CP}(B^+ \to K^*(892)^+\gamma)$	Belle [1063]	$0.011 \pm 0.023 \pm 0.003$	0.014 ± 0.018
	BABAR [1064]	$0.018 \pm 0.028 \pm 0.007$	
$A_{CP}(B^+ \to X_s\gamma)$	Belle [1139]	$0.0275 \pm 0.0184 \pm 0.0032$[c]	0.028 ± 0.019
$A_{CP}(B^+ \to \eta K^+\gamma)$	Belle [1067]	$-0.16 \pm 0.09 \pm 0.06$[d]	-0.12 ± 0.07
	BABAR [408]	$-0.090^{+0.104}_{-0.098} \pm 0.014$[e]	
$A_{CP}(B^+ \to \phi(1020)K^+\gamma)$	Belle [410]	$-0.03 \pm 0.11 \pm 0.08$[f]	-0.13 ± 0.10
	BABAR [1070]	$-0.26 \pm 0.14 \pm 0.05$[g]	

(Table continued)

TABLE 252. *(Continued)*

Parameter	Measurements		Average
$A_{CP}(B^+ \to \rho^+(770)\gamma)$	Belle [1075]	$-0.11 \pm 0.32 \pm 0.09$	-0.11 ± 0.33

[a]Combination of two final states of the $K^*(892)^\pm$, $K^0_S\pi^\pm$ and $K^\pm\pi^0$. In addition to the combined results, the paper reports separately the results for each individual final state.
[b]Measured in the $\phi\phi$ invariant mass range below the η_c resonance ($M_{\phi\phi} < 2.85$ GeV/c^2).
[c]$M_{X_s} < 2.8$ GeV/c^2.
[d]$M_{K\eta} < 2.4$ GeV/c^2.
[e]$M_{K\eta^{(\prime)}} < 3.25$ GeV/c^2.
[f]$1.4 \le E^*_\gamma \le 3.4$ GeV/c^2, where E^*_γ is the photon energy in the center-of-mass frame.
[g]$M_{\phi K} < 3.0$ GeV/c^2.

TABLE 253. CP asymmetries of charmless hadronic B^+ decays (part 5).

Parameter	Measurements		Average
$A_{CP}(B^+ \to \pi^+\pi^0)$	Belle [882]	$0.025 \pm 0.043 \pm 0.007$	0.02 ± 0.04
	BABAR [886]	$0.03 \pm 0.08 \pm 0.01$	
	Belle II [887]	$-0.04 \pm 0.17 \pm 0.06$	
$A_{CP}(B^+ \to \pi^+\pi^+\pi^-)$[a]	LHCb [1171]	$0.058 \pm 0.008 \pm 0.011$[b]	0.057 ± 0.014
	BABAR [944]	$0.032 \pm 0.044^{+0.040}_{-0.037}$[c,b]	
$A_{CP}(B^+ \to \rho^0(770)\pi^+)$	LHCb [945]	$0.007 \pm 0.011 \pm 0.040$[c,d,b]	$0.016^{+0.041}_{-0.039}$
	BABAR [944]	$0.18 \pm 0.07^{+0.05}_{-0.15}$[c,b]	
$A_{CP}(B^+ \to f_2(1270)\pi^+)$	LHCb [945]	$0.468 \pm 0.061 \pm 0.103$[c,d,b]	0.365 ± 0.079
	LHCb [926]	$0.267 \pm 0.102 \pm 0.048$[e]	
	BABAR [944]	$0.41 \pm 0.25^{+0.18}_{-0.15}$[c,b]	
$A_{CP}(B^+ \to \rho(1450)^0\pi^+)$	LHCb [945]	$-0.129 \pm 0.033 \pm 0.421$[c,d,b]	-0.109 ± 0.049
	LHCb [926]	$-0.109 \pm 0.044 \pm 0.024$[e]	
	BABAR [944]	$-0.06 \pm 0.28^{+0.23}_{-0.40}$[c,b]	
$A_{CP}(B^+ \to \rho_3(1690)^0\pi^+)$	LHCb [945]	$-0.801 \pm 0.114 \pm 0.511$[c,d,b]	-0.80 ± 0.52
$A_{CP}(B^+ \to f_0(1370)\pi^+)$	*BABAR* [944]	$0.72 \pm 0.15 \pm 0.16$[c,b]	0.72 ± 0.22
$A_{CP}(B^+ \to \pi^+\pi^+\pi^-)$, S-wave	LHCb [945]	$0.144 \pm 0.018 \pm 0.026$[c,d,b]	0.144 ± 0.032
$A_{CP}(B^+ \to \pi^+\pi^+\pi^-(\mathrm{NR}))$	*BABAR* [944]	$-0.14 \pm 0.14^{+0.18}_{-0.08}$[f,b]	$-0.14^{+0.23}_{-0.16}$
$A_{CP}(B^+ \to \rho^+(770)\pi^0)$	*BABAR* [949]	$-0.01 \pm 0.13 \pm 0.02$	0.01 ± 0.11
	Belle [950]	$0.06 \pm 0.19^{+0.04}_{-0.06}$	
$A_{CP}(B^+ \to \rho^+(770)\rho^0(770))$	*BABAR* [425]	$-0.054 \pm 0.055 \pm 0.010$	-0.051 ± 0.054
	Belle [951]	$0.00 \pm 0.22 \pm 0.03$	
$A_{CP}(B^+ \to \omega(782)\pi^+)$	LHCb [945]	$-0.048 \pm 0.065 \pm 0.049$[c,d,b]	-0.041 ± 0.048
	BABAR [900]	$-0.02 \pm 0.08 \pm 0.01$	
	Belle [953]	$-0.02 \pm 0.09 \pm 0.01$	
	CLEO [1169]	$-0.34 \pm 0.25 \pm 0.02$	
$A_{CP}(B^+ \to \omega(782)\rho^+(770))$	*BABAR* [902]	$-0.20 \pm 0.09 \pm 0.02$	-0.20 ± 0.09

[a]Treatment of charmonium intermediate components differs between the results.
[b]Multiple systematic uncertainties are added in quadrature.
[c]Result extracted from Dalitz-plot analysis of $B^+ \to \pi^+\pi^+\pi^-$ decays.
[d]This analysis uses three different approaches: isobar, K-matrix and quasi-model-independent, to describe the S-wave component. The A_{CP} results are taken from the isobar model with an additional error accounting for the different S-wave methods as reported in Appendix D of Ref. [947].
[e]Result extracted from Dalitz-plot analysis of $B^+ \to K^+K^-\pi^+$ decays.
[f]The nonresonant amplitude is modeled using a sum of exponential functions.

TABLE 254. *CP* asymmetries of charmless hadronic B^+ decays (part 6).

Parameter	Measurements		Average
$A_{CP}(B^+ \to \eta\pi^+)$	Belle [896]	$-0.19 \pm 0.06 \pm 0.01$	-0.14 ± 0.05
	BABAR [888]	$-0.03 \pm 0.09 \pm 0.03$	
$A_{CP}(B^+ \to \eta\rho^+(770))$	*BABAR* [954]	$0.13 \pm 0.11 \pm 0.02$	0.11 ± 0.11
	Belle [898]	$-0.04^{+0.34}_{-0.32} \pm 0.01$	
$A_{CP}(B^+ \to \eta'\pi^+)$	*BABAR* [888]	$0.03 \pm 0.17 \pm 0.02$	0.06 ± 0.15
	Belle [889]	$0.20^{+0.37}_{-0.36} \pm 0.04$	
$A_{CP}(B^+ \to \eta'\rho^+(770))$	*BABAR* [894]	$0.26 \pm 0.17 \pm 0.02$	0.26 ± 0.17
$A_{CP}(B^+ \to b_1(1235)^0\pi^+)$	*BABAR* [919]	$0.05 \pm 0.16 \pm 0.02$	0.05 ± 0.16
$A_{CP}(B^+ \to p\bar{p}\pi^+)$	*BABAR* [721]	$0.04 \pm 0.07 \pm 0.04$	0.04 ± 0.08
$A_{CP}(B^+ \to p\bar{p}\pi^+), m_{p\bar{p}} < 2.85$ GeV/c^2			
	LHCb [1009]	$-0.041 \pm 0.039 \pm 0.005$	-0.058 ± 0.037
	Belle [1008]	$-0.17 \pm 0.10 \pm 0.02$	
$A_{CP}(B^+ \to p\bar{p}K^+), m_{p\bar{p}} < 2.85$ GeV/c^2			
	LHCb [1009]	$0.021 \pm 0.020 \pm 0.004$	
	Belle [1008]	$-0.02 \pm 0.05 \pm 0.02$	0.007 ± 0.019
	BABAR [800]	$-0.16^{+0.07}_{-0.08} \pm 0.04$	
$A_{CP}(B^+ \to p\bar{p}K^*(892)^+)$[a]	*BABAR* [721]	$0.32 \pm 0.13 \pm 0.05$	0.21 ± 0.11
	Belle [1012]	$-0.01 \pm 0.19 \pm 0.02$	
$A_{CP}(B^+ \to p\bar{\Lambda}^0\gamma)$	Belle [1015]	$0.17 \pm 0.16 \pm 0.05$	0.17 ± 0.17
$A_{CP}(B^+ \to p\bar{\Lambda}^0\pi^0)$	Belle [1015]	$0.01 \pm 0.17 \pm 0.04$	0.01 ± 0.17
$A_{CP}(B^+ \to K^+\ell^+\ell^-)$	Belle [1089]	$0.04 \pm 0.10 \pm 0.02$	0.02 ± 0.08
	BABAR [1110]	$-0.03 \pm 0.14 \pm 0.01$	
$A_{CP}(B^+ \to K^+e^+e^-)$	Belle [1089]	$0.14 \pm 0.14 \pm 0.03$	0.14 ± 0.14
$A_{CP}(B^+ \to K^+\mu^+\mu^-)$	LHCb [1173]	$0.012 \pm 0.017 \pm 0.001$[b,c]	0.011 ± 0.017
	Belle [1089]	$-0.05 \pm 0.13 \pm 0.03$[d]	
$A_{CP}(B^+ \to \pi^+\mu^+\mu^-)$	LHCb [1080]	$-0.11 \pm 0.12 \pm 0.01$	-0.11 ± 0.12
$A_{CP}(B^+ \to K^*(892)^+\ell^+\ell^-)$	Belle [1089]	$-0.13^{+0.17}_{-0.16} \pm 0.01$	-0.09 ± 0.14
	BABAR [1085]	$0.01^{+0.26}_{-0.24} \pm 0.02$	
$A_{CP}(B^+ \to K^*(892)^+e^+e^-)$	Belle [1089]	$-0.14^{+0.23}_{-0.22} \pm 0.02$	-0.14 ± 0.23
$A_{CP}(B^+ \to K^*(892)^+\mu^+\mu^-)$	Belle [1089]	$-0.12 \pm 0.24 \pm 0.02$	-0.12 ± 0.24

[a]Treatment of charmonium intermediate components differs between the results.
[b]A_{CP} is also measured in bins of $m_{\mu^+\mu^-}$
[c]Mass regions corresponding to ϕ, J/ψ and $\psi(2S)$ are vetoed.
[d]Mass regions corresponding to J/ψ and $\psi(2S)$ are vetoed.

TABLE 255. *CP* asymmetries of charmless hadronic B^0 decays (part 1).

Parameter	Measurements		Average
$A_{CP}(B^0 \to K^+\pi^-)$	LHCb [1174]	-0.0831 ± 0.0034[a]	-0.0836 ± 0.0032
	CDF [1175]	$-0.083 \pm 0.013 \pm 0.004$	
	Belle [882]	$-0.069 \pm 0.014 \pm 0.007$	
	BABAR [421]	$-0.107 \pm 0.016^{+0.006}_{-0.004}$	
	Belle II [883]	$-0.16 \pm 0.05 \pm 0.01$	

(Table continued)

TABLE 255. *(Continued)*

Parameter	Measurements		Average
$A_{CP}(B^0 \to \eta' K^*(892)^0)$	*BABAR* [894]	$0.02 \pm 0.23 \pm 0.02$	-0.07 ± 0.18
	Belle [966]	$-0.22 \pm 0.29 \pm 0.07$	
$A_{CP}(B^0 \to \eta'(K\pi)_0^{*0})$	*BABAR* [894]	$-0.19 \pm 0.17 \pm 0.02$	-0.19 ± 0.17
$A_{CP}(B^0 \to \eta' K_2^*(1430)^0)$	*BABAR* [894]	$0.14 \pm 0.18 \pm 0.02$	0.14 ± 0.18
$A_{CP}(B^0 \to \eta K^*(892)^0)$	*BABAR* [897]	$0.21 \pm 0.06 \pm 0.02$	0.19 ± 0.05
	Belle [898]	$0.17 \pm 0.08 \pm 0.01$	
$A_{CP}(B^0 \to \eta(K\pi)_0^{*0})$	*BABAR* [897]	$0.06 \pm 0.13 \pm 0.02$	0.06 ± 0.13
$A_{CP}(B^0 \to \eta K_2^*(1430)^0)$	*BABAR* [897]	$-0.07 \pm 0.19 \pm 0.02$	-0.07 ± 0.19
$A_{CP}(B^0 \to b_1(1235)^- K^+)$	*BABAR* [919]	$-0.07 \pm 0.12 \pm 0.02$	-0.07 ± 0.12
$A_{CP}(B^0 \to \omega(782) K^*(892)^0)$	*BABAR* [902]	$0.45 \pm 0.25 \pm 0.02$	0.45 ± 0.25
$A_{CP}(B^0 \to \omega(782)(K\pi)_0^{*0})$	*BABAR* [902]	$-0.07 \pm 0.09 \pm 0.02$	-0.07 ± 0.09
$A_{CP}(B^0 \to \omega(782) K_2^*(1430)^0)$	*BABAR* [902]	$-0.37 \pm 0.17 \pm 0.02$	-0.37 ± 0.17
$A_{CP}(B^0 \to K^+\pi^-\pi^0)$	*BABAR* [971]	$-0.030^{+0.045}_{-0.051} \pm 0.055$[b]	-0.00 ± 0.06
	Belle [970]	$0.07 \pm 0.11 \pm 0.01$	
$A_{CP}(B^0 \to \rho^-(770) K^+)$	*BABAR* [969]	$0.20 \pm 0.09 \pm 0.08$[b]	0.20 ± 0.11
	Belle [970]	$0.22^{+0.22\,+0.06}_{-0.23\,-0.02}$	
$A_{CP}(B^0 \to \rho(1450)^- K^+)$	*BABAR* [969]	$-0.10 \pm 0.32 \pm 0.09$[b]	-0.10 ± 0.33
$A_{CP}(B^0 \to \rho(1700)^- K^+)$	*BABAR* [969]	$-0.36 \pm 0.57 \pm 0.23$[b]	-0.36 ± 0.61
$A_{CP}(B^0 \to K^+\pi^-\pi^0(\mathrm{NR}))$	*BABAR* [969]	$0.10 \pm 0.16 \pm 0.08$[c]	0.10 ± 0.18
$A_{CP}(B^0 \to K^0\pi^+\pi^-)$	*BABAR* [265]	$-0.01 \pm 0.05 \pm 0.01$[d]	-0.01 ± 0.05
$A_{CP}(B^0 \to K^*(892)^+\pi^-)$	LHCb [976]	$-0.308 \pm 0.060 \pm 0.016$[d,e]	-0.274 ± 0.045
	BABAR [265]	$-0.21 \pm 0.10 \pm 0.02$[d,e]	
	BABAR [969]	$-0.29 \pm 0.11 \pm 0.02$[b]	
	Belle [266]	$-0.21 \pm 0.11 \pm 0.07$[d]	

[a]LHCb combines results of the 1.9 fb^{-1} run 2 data analysis with those based on Run 1 dataset [1176]. The full statistical and systematic covariance matrices are used in the combination.
[b]Result extracted from Dalitz-plot analysis of $B^0 \to K^+\pi^-\pi^0$ decays.
[c]The nonresonant amplitude is taken to be constant across the Dalitz plane.
[d]Result extracted from Dalitz-plot analysis of $B^0 \to K^0_S\pi^+\pi^-$ decays.
[e]Multiple systematic uncertainties are added in quadrature.

TABLE 256. CP asymmetries of charmless hadronic B^0 decays (part 2).

Parameter	Measurements		Average
$A_{CP}(B^0 \to (K\pi)_0^{*+}\pi^-)$	LHCb [976]	$-0.032 \pm 0.047 \pm 0.031$[a,b]	0.017 ± 0.043
	BABAR [265]	$0.09 \pm 0.07 \pm 0.03$[a,b]	
	BABAR [969]	$0.07 \pm 0.14 \pm 0.01$[c]	
$A_{CP}(B^0 \to K_2^*(1430)^+\pi^-)$	LHCb [976]	$-0.29 \pm 0.22 \pm 0.09$[a,b]	-0.29 ± 0.24
$A_{CP}(B^0 \to K^*(1680)^+\pi^-)$	LHCb [976]	$-0.07 \pm 0.13 \pm 0.04$[a,b]	-0.07 ± 0.13
$A_{CP}(B^0 \to f_0(980) K^0_S)$	LHCb [976]	$0.28 \pm 0.27 \pm 0.15$[a,b]	0.28 ± 0.31
$A_{CP}(B^0 \to (K\pi)_0^{*0}\pi^0)$	*BABAR* [969]	$-0.15 \pm 0.10 \pm 0.04$[c]	-0.15 ± 0.11
$A_{CP}(B^0 \to K^*(892)^0\pi^0)$	*BABAR* [969]	$-0.15 \pm 0.12 \pm 0.04$[c]	-0.15 ± 0.13

(Table continued)

TABLE 256. *(Continued)*

Parameter	Measurements		Average
$A_{CP}(B^0 \to K^*(892)^0\pi^+\pi^-)$	*BABAR* [980]	$0.07 \pm 0.04 \pm 0.03$	0.07 ± 0.05
$A_{CP}(B^0 \to K^*(892)^0\rho^0(770))$	*BABAR* [981]	$-0.06 \pm 0.09 \pm 0.02$	-0.06 ± 0.09
$A_{CP}(B^0 \to f_0(980)K^*(892)^0)$	*BABAR* [981]	$0.07 \pm 0.10 \pm 0.02$	0.07 ± 0.10
$A_{CP}(B^0 \to K^*(892)^+\rho^-(770))$	*BABAR* [981]	$0.21 \pm 0.15 \pm 0.02$	0.21 ± 0.15
$A_{CP}(B^0 \to K^*(892)^0K^+K^-)$	*BABAR* [980]	$0.01 \pm 0.05 \pm 0.02$	0.01 ± 0.05
$A_{CP}(B^0 \to a_1(1260)^-K^+)$	*BABAR* [914]	$-0.16 \pm 0.12 \pm 0.01$	-0.16 ± 0.12
$A_{CP}(B^0 \to K^0\bar{K}^0)$	Belle [1177]	$-0.58^{+0.73}_{-0.66} \pm 0.04$[d]	$-0.58^{+0.73}_{-0.66}$
$A_{CP}(B^0 \to \phi(1020)K^*(892)^0)$	Belle [990] *BABAR* [388]	$-0.007 \pm 0.048 \pm 0.021$ $0.01 \pm 0.06 \pm 0.03$	-0.001 ± 0.041
$A_{CP}(B^0 \to K^*(892)^0\pi^+K^-)$	*BABAR* [980]	$0.22 \pm 0.33 \pm 0.20$	0.22 ± 0.39
$A_{CP}(B^0 \to (K\pi)_0^{*0}\phi(1020))$	Belle [990] *BABAR* [388]	$0.093 \pm 0.094 \pm 0.017$ $0.20 \pm 0.14 \pm 0.06$	0.123 ± 0.081
$A_{CP}(B^0 \to K_2^*(1430)^0\phi(1020))$	*BABAR* [388] Belle [990]	$-0.08 \pm 0.12 \pm 0.05$ $-0.155^{+0.152}_{-0.133} \pm 0.033$	-0.112 ± 0.099
$A_{CP}(B^0 \to K^*(892)^0\gamma)$	LHCb [1045] Belle [1063] *BABAR* [1064]	$0.008 \pm 0.017 \pm 0.009$ $-0.013 \pm 0.017 \pm 0.004$ $-0.016 \pm 0.022 \pm 0.007$	-0.006 ± 0.011
$A_{CP}(B^0 \to K_2^*(1430)^0\gamma)$	*BABAR* [1073]	$-0.08 \pm 0.15 \pm 0.01$	-0.08 ± 0.15
$A_{CP}(B^0 \to X_s\gamma)$	Belle [1139]	$-0.0094 \pm 0.0174 \pm 0.0047$[e]	-0.009 ± 0.018

[a]Result extracted from Dalitz-plot analysis of $B^0 \to K^0_S\pi^+\pi^-$ decays.
[b]Multiple systematic uncertainties are added in quadrature.
[c]Result extracted from Dalitz-plot analysis of $B^0 \to K^+\pi^-\pi^0$ decays.
[d]Result extracted from a time-dependent analysis.
[e]$M_{X_s} < 2.8$ GeV/c^2.

TABLE 257. *CP* asymmetries of charmless hadronic B^0 decays (part 3).

Parameter	Measurements		Average
$A_{CP}(B^0 \to \rho^+(770)\pi^-)$	*BABAR* [273] Belle [274]	$0.09^{+0.05}_{-0.06} \pm 0.04$[a] $0.21 \pm 0.08 \pm 0.04$[a]	0.13 ± 0.05
$A_{CP}(B^0 \to \rho^-(770)\pi^+)$	*BABAR* [273] Belle [274]	$-0.12 \pm 0.08^{+0.04}_{-0.05}$[a] $0.08 \pm 0.16 \pm 0.11$[a]	-0.08 ± 0.08
$A_{CP}(B^0 \to a_1(1260)^+\pi^- + \text{c.c.})$	Belle [419] *BABAR* [418]	$0.01 \pm 0.11 \pm 0.09$[b] $0.10 \pm 0.15 \pm 0.09$[b]	0.05 ± 0.11
$A_{CP}(B^0 \to b_1(1235)^+\pi^- + \text{c.c.})$	*BABAR* [919]	$-0.05 \pm 0.10 \pm 0.02$	-0.05 ± 0.10
$A_{CP}(B^0 \to p\bar{p}K^*(892)^0)$[c]	*BABAR* [721] Belle [1012]	$0.11 \pm 0.13 \pm 0.06$ $-0.08 \pm 0.20 \pm 0.02$	0.05 ± 0.12
$A_{CP}(B^0 \to p\bar{\Lambda}^0\pi^-)$	*BABAR* [1023] Belle [1015]	$-0.10 \pm 0.10 \pm 0.02$ $-0.02 \pm 0.10 \pm 0.03$	-0.06 ± 0.07
$A_{CP}(B^0 \to K^*(892)^0\ell^+\ell^-)$	Belle [1089] *BABAR* [1085]	$-0.08 \pm 0.12 \pm 0.02$ $0.02 \pm 0.20 \pm 0.02$	-0.05 ± 0.10
$A_{CP}(B^0 \to K^*(892)^0e^+e^-)$	Belle [1089]	$-0.21 \pm 0.19 \pm 0.02$	-0.21 ± 0.19

(Table continued)

TABLE 257. *(Continued)*

Parameter	Measurements		Average
$A_{CP}(B^0 \to K^*(892)^0\mu^+\mu^-)$	LHCP [1173]	$-0.035 \pm 0.024 \pm 0.003$[d,e]	-0.034 ± 0.024
	Belle [1089]	$0.00 \pm 0.15 \pm 0.03$[f]	

[a]Result extracted from Dalitz-plot analysis of $B^0 \to \pi^+\pi^-\pi^0$ decays.
[b]Result extracted from a time-dependent analysis.
[c]Treatment of charmonium intermediate components differs between the results.
[d]A_{CP} is also measured in bins of $m_{\mu^+\mu^-}$
[e]Mass regions corresponding to ϕ, J/ψ and $\psi(2S)$ are vetoed.
[f]Mass regions corresponding to J/ψ and $\psi(2S)$ are vetoed.

TABLE 258. CP asymmetries of charmless hadronic decays of $B^\pm/B^0$ admixture.

Parameter	Measurements		Average
$A_{CP}(B \to K^*\gamma)$	Belle [1063]	$-0.004 \pm 0.014 \pm 0.003$	-0.004 ± 0.011
	BABAR [1064]	$-0.003 \pm 0.017 \pm 0.007$	
$A_{CP}(B \to X_s\gamma)$	Belle [1139]	$0.0144 \pm 0.0128 \pm 0.0011$[a]	0.015 ± 0.011
	BABAR [1178]	$0.017 \pm 0.019 \pm 0.010$[b]	
$A_{CP}(B \to X_{s+d}\gamma)$	Belle [1179]	$0.022 \pm 0.039 \pm 0.009$[c]	0.032 ± 0.034
	BABAR [1102]	$0.057 \pm 0.060 \pm 0.018$[d]	
$A_{CP}(B \to X_s\ell^+\ell^-)$	*BABAR* [1107]	$0.04 \pm 0.11 \pm 0.01$	0.04 ± 0.11
$A_{CP}(B \to K^*e^+e^-)$	Belle [1089]	$-0.18 \pm 0.15 \pm 0.01$	-0.18 ± 0.15
$A_{CP}(B \to K^*\mu^+\mu^-)$	Belle [1089]	$-0.03 \pm 0.13 \pm 0.02$	-0.03 ± 0.13
$A_{CP}(B \to K^*\ell^+\ell^-)$	Belle [1089]	$-0.10 \pm 0.10 \pm 0.01$	-0.05 ± 0.08
	BABAR [1110]	$0.03 \pm 0.13 \pm 0.01$	
$A_{CP}(B \to X_s\eta)$	Belle [1134]	$-0.13 \pm 0.04^{+0.02e}_{-0.03}$	$-0.13^{+0.04}_{-0.05}$
$A_{CP}(B \to K\ell^+\ell^-)$	*BABAR* [1110]	$-0.03 \pm 0.14 \pm 0.01$	-0.03 ± 0.14

[a]$M_{X_s} < 2.8$ GeV/c^2.
[b]$0.6 < M_{X_s} < 2.0$ GeV/c^2.
[c]$E^*_\gamma \geq 2.1$ GeV where E^*_γ is the photon energy in the center-of-mass frame.
[d]$2.1 < E^*_\gamma < 2.8$ GeV where E^*_γ is the photon energy in the center-of-mass frame.
[e]$0.4 < m_X < 2.6$ GeV/c^2.

TABLE 259. CP asymmetries of charmless hadronic B^0_s decays.

Parameter	Measurements		Average
$A_{CP}(B^0_s \to \pi^+K^-)$	LHCb [1174]	0.225 ± 0.012[a]	0.225 ± 0.012
	CDF [1175]	$0.22 \pm 0.07 \pm 0.02$	

[a]LHCb combines results of the 1.9 fb^{-1} run 2 data analysis with those based on Run 1 dataset [1176]. The full statistical and systematic covariance matrices are used in the combination.

TABLE 260. CP asymmetries of charmless hadronic Λ^0_b decays.

Parameter	Measurements		Average
$A_{CP}(\Lambda^0_b \to p\pi^-)$	LHCb [1180]	$-0.035 \pm 0.017 \pm 0.020$	-0.025 ± 0.025
	CDF [1175]	$0.06 \pm 0.07 \pm 0.03$	
$A_{CP}(\Lambda^0_b \to pK^-)$	LHCb [1180]	$-0.020 \pm 0.013 \pm 0.019$	-0.025 ± 0.022
	CDF [1175]	$-0.10 \pm 0.08 \pm 0.04$	

(Table continued)

TABLE 260. *(Continued)*

Parameter	Measurements		Average
$A_{CP}(\Lambda_b^0 \to p\bar{K}^0\pi^-)$	LHCb [973]	$0.22 \pm 0.13 \pm 0.03$	0.22 ± 0.13
$A_{CP}(\Lambda_b^0 \to \Lambda^0 K^+\pi^-)$	LHCb [1030]	$-0.53 \pm 0.23 \pm 0.11$	-0.53 ± 0.25
$A_{CP}(\Lambda_b^0 \to \Lambda^0 K^+K^-)$	LHCb [1030]	$-0.28 \pm 0.10 \pm 0.07$	-0.28 ± 0.12

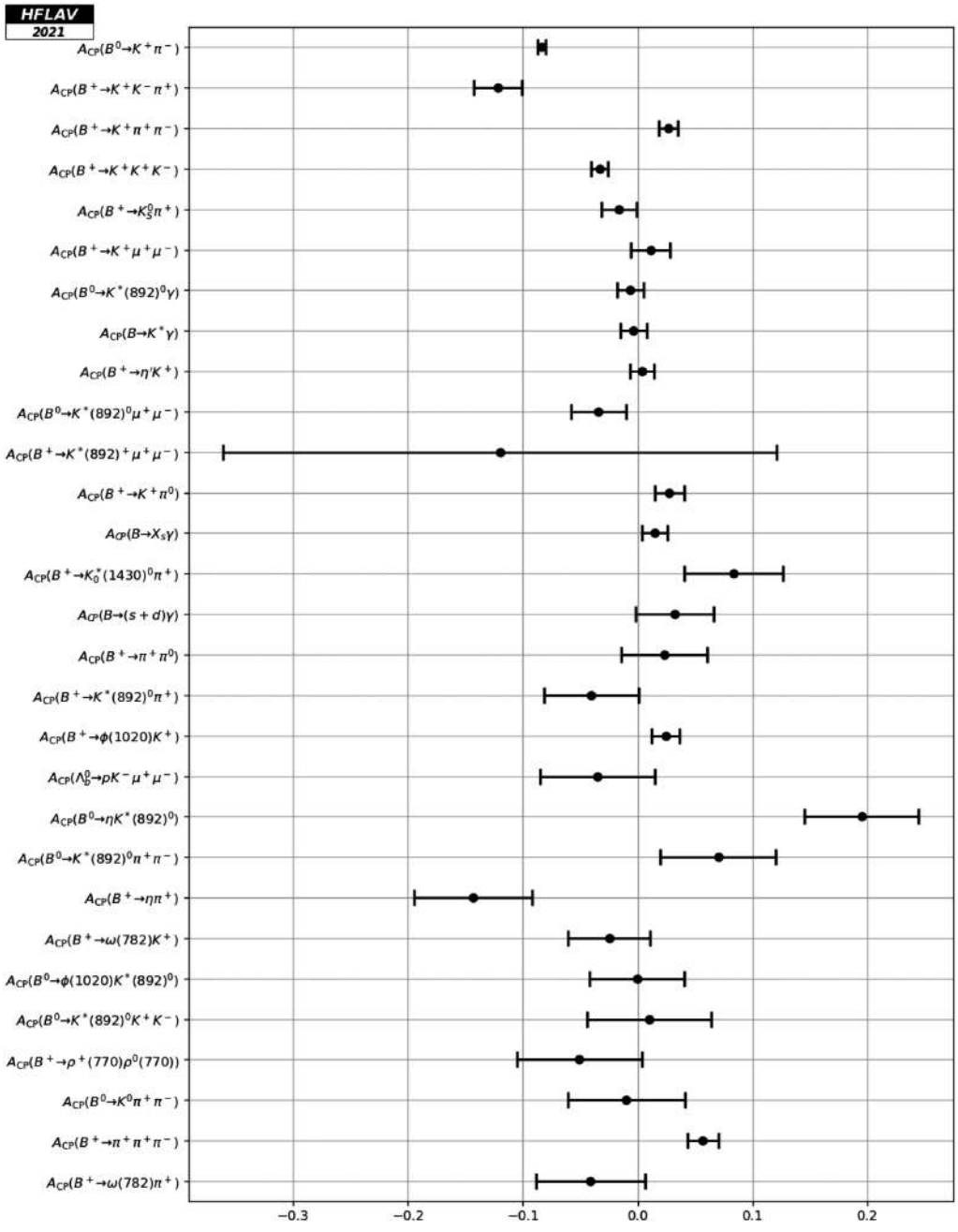

FIG. 81. A selection among the most precise direct *CP* asymmetries (A_{CP}) measured in charmless B^+ and B^0 decay modes.

Measurements that are not included in the tables (the definitions of observables can be found in the corresponding experimental papers):

(i) In Ref. [1181], LHCb reports the triple-product asymmetries ($a_{CP}^{\hat{T}-\text{odd}}$, $a_{P}^{\hat{T}-\text{odd}}$) for the decays $\Lambda_b^0 \to p\pi^-\pi^+\pi^-$ and $\Lambda_b^0 \to p\pi^-K^+K^-$.

(ii) In Ref. [1182], LHCb reports $a_{CP}^{\hat{T}-\text{odd}}$, $a_{P}^{\hat{T}-\text{odd}}$ and $\Delta(A_{CP}) = A_{CP}(\Lambda_b^0 \to pK^-\mu^+\mu^-) - A_{CP}(\Lambda_b^0 \to pK^-J/\psi)$.

(iii) In Ref. [1183], LHCb reports $a_{CP}^{\hat{T}-\text{odd}}$ and $a_{P}^{\hat{T}-\text{odd}}$ for the decays $\Lambda_b^0 \to pK^-\pi^+\pi^-$, $\Lambda_b^0 \to pK^-K^+K^-$ and $\Xi_b^0 \to pK^-K^-\pi^+$.

(iv) In Ref. [1184] LHCb measures differences of CP asymmetries between Λ_b^0 and Ξ_b^0 charmless decays into a proton and three charged mesons and the decays to the same final states with an intermediate charmed baryon.

H. Polarization measurements in b-hadron decays

In this section, compilations of polarization measurements in b-hadron decays are given. Tables 261, 262, and 263 detail measurements of the longitudinal fraction, f_L, in B^+, B^0, and B_s^0 decays, respectively. They are followed by Tables 264, 265 and 266, which list polarization fractions and CP parameters measured in full angular analyses of B^+, B^0 and B_s^0 decays. Figures 82 and 83 show graphic representations of a selection of results shown in this section.

Most of the final states considered in the tables are pairs of vector mesons and thus, we detail below the corresponding definitions. For specific definitions, for example regarding vector-tensor final states or vector recoiling against dispin-half states, please refer to the articles. In the decay of a pseudoscalar meson into two vector mesons, momentum conservation allows for three helicity configurations: $H_0, H_{\pm 1}$. They can be expressed in terms of longitudinal polarization amplitudes, $A_0 = H_0$, and transverse polarization amplitudes, $A_\perp = (H_{+1} - H_{-1})/\sqrt{2}$ and $A_\parallel = (H_{+1} + H_{-1})/\sqrt{2}$ and their charge conjugates: $\overline{A_0}$, $\overline{A_\parallel}$, and $\overline{A_\perp}$. Using the definitions:

$$F_{k=0,\parallel,\perp} = \frac{|A_k|^2}{|A_0|^2 + |A_\perp|^2 + |A_\parallel|^2},$$
$$\bar{F}_{k=0,\parallel,\perp} = \frac{|\overline{A_k}|^2}{|\overline{A_0}|^2 + |\overline{A_\perp}|^2 + |\overline{A_\parallel}|^2}, \tag{227}$$

the following CP conserving and CP violating observables, which are used in our tables, are defined:

$$f_{k=0,\parallel,\perp} = \frac{1}{2}(F_k + \overline{F_k}), \qquad A_{CP}^{k=0,\perp} = \frac{F_k - \overline{F_k}}{F_k + \overline{F_k}}. \tag{228}$$

Note that, in the literature, f_0 and f_L are used interchangeably to denote the longitudinal polarization fraction.

TABLE 261. Longitudinal polarization fraction, f_L, in B^+ decays.

Parameter	Measurements		Average HFLAV PDG
$f_L(B^+ \to \omega(782)K^*(892)^+)$	*BABAR* [902]	$0.41 \pm 0.18 \pm 0.05$	0.41 ± 0.19
$f_L(B^+ \to \omega(782)K_2^*(1430)^+)$	*BABAR* [902]	$0.56 \pm 0.10 \pm 0.04$	0.56 ± 0.11
$f_L(B^+ \to K^*(892)^+\bar{K}^*(892)^0)$	*BABAR* [930]	$0.75^{+0.16}_{-0.26} \pm 0.03$	$0.82^{+0.13}_{-0.17}$
	Belle [929]	$1.06 \pm 0.30 \pm 0.14$	$0.82^{+0.15}_{-0.21}$
$f_L(B^+ \to \phi(1020)K^*(892)^+)$	*BABAR* [935]	$0.49 \pm 0.05 \pm 0.03$[a]	0.50 ± 0.05
	Belle [1172]	$0.52 \pm 0.08 \pm 0.03$	
	Belle II [932]	$0.58 \pm 0.23 \pm 0.02$	
$f_L(B^+ \to \phi(1020)K_1(1270)^+)$	*BABAR* [937]	$0.46^{+0.12+0.06}_{-0.13-0.07}$	0.46 ± 0.14
$f_L(B^+ \to \phi(1020)K_2^*(1430)^+)$	*BABAR* [937]	$0.80^{+0.09}_{-0.10} \pm 0.03$	0.80 ± 0.10
$f_L(B^+ \to K^*(892)^+\rho^0(770))$	*BABAR* [913]	$0.78 \pm 0.12 \pm 0.03$	0.78 ± 0.12
$f_L(B^+ \to K^*(892)^0\rho^+(770))$	*BABAR* [915]	$0.52 \pm 0.10 \pm 0.04$	0.48 ± 0.08
	Belle [916]	$0.43 \pm 0.11^{+0.05}_{-0.02}$[b]	
$f_L(B^+ \to \rho^+(770)\rho^0(770))$	*BABAR* [425]	$0.950 \pm 0.015 \pm 0.006$	0.950 ± 0.016
	Belle [951]	$0.948 \pm 0.106 \pm 0.021$	
$f_L(B^+ \to \omega(782)\rho^+(770))$	*BABAR* [902]	$0.90 \pm 0.05 \pm 0.03$	0.90 ± 0.06
$f_L(B^+ \to p\bar{p}K^*(892)^+)$	Belle [1012]	$0.32 \pm 0.17 \pm 0.09$	0.32 ± 0.19

[a]Combination of two final states of the $K^*(892)^\pm$, $K_S^0\pi^\pm$ and $K^\pm\pi^0$. In addition to the combined results, the paper reports separately the results for each individual final state.
[b]See also Ref. [921].

TABLE 262. Longitudinal polarization fraction, f_L, in B^0 decays.

Parameter	Measurements		Average HFLAV PDG
$f_L(B^0 \to \omega(782)K^*(892)^0)$	*BABAR* [902]	$0.72 \pm 0.14 \pm 0.02$	0.69 ± 0.11
	LHCb [1185]	$0.68 \pm 0.17 \pm 0.16$	
	Belle [967]	$0.56 \pm 0.29^{+0.18}_{-0.08}$	
$f_L(B^0 \to \omega(782)K_2^*(1430)^0)$	*BABAR* [902]	$0.45 \pm 0.12 \pm 0.02$	0.45 ± 0.12
$f_L(B^0 \to K^*(892)^0\bar{K}^*(892)^0)$	LHCb [995]	$0.724 \pm 0.051 \pm 0.016$	0.73 ± 0.05
	BABAR [996]	$0.80^{+0.10}_{-0.12} \pm 0.06$	0.74 ± 0.05
$f_L(B^0 \to \phi(1020)K^*(892)^0)$	LHCb [1186]	$0.497 \pm 0.019 \pm 0.015$	0.497 ± 0.017
	Belle [990]	$0.499 \pm 0.030 \pm 0.018$	
	BABAR [388]	$0.494 \pm 0.034 \pm 0.013$	
	Belle II [932]	$0.57 \pm 0.20 \pm 0.04$	
$f_L(B^0 \to \phi(1020)K_2^*(1430)^0)$	Belle [990]	$0.918^{+0.029}_{-0.060} \pm 0.012$	$0.912^{+0.032}_{-0.046}$
	BABAR [388]	$0.901^{+0.046}_{-0.058} \pm 0.037$	$0.913^{+0.028}_{-0.050}$
$f_L(B^0 \to K^*(892)^0\rho^0(770))$	LHCb [1185]	$0.164 \pm 0.015 \pm 0.022$	0.173 ± 0.026
	BABAR [981]	$0.40 \pm 0.08 \pm 0.11$	
$f_L(B^0 \to K^*(892)^+\rho^-(770))$	*BABAR* [981]	$0.38 \pm 0.13 \pm 0.03$	0.38 ± 0.13
$f_L(B^0 \to \rho^+(770)\rho^-(770))$	Belle [414]	$0.988 \pm 0.012 \pm 0.023$	0.990 ± 0.020
	BABAR [413]	$0.992 \pm 0.024^{+0.026}_{-0.013}$	$0.990^{+0.021}_{-0.019}$
$f_L(B^0 \to \rho^0(770)\rho^0(770))$[a]	LHCb [417]	$0.745^{+0.048}_{-0.058} \pm 0.034$	0.71 ± 0.06
	BABAR [415]	$0.75^{+0.11}_{-0.14} \pm 0.04$	$0.71^{+0.08}_{-0.09}$
	Belle [416]	$0.21^{+0.18}_{-0.22} \pm 0.15$	
$f_L(B^0 \to a_1(1260)^+a_1(1260)^-)$	*BABAR* [1006]	$0.31 \pm 0.22 \pm 0.10$	0.31 ± 0.24
$f_L(B^0 \to p\bar{p}K^*(892)^0)$	Belle [1012]	$1.01 \pm 0.13 \pm 0.03$	1.01 ± 0.13
$f_L(B^0 \to \Lambda^0\bar{\Lambda}^0K^*(892)^0)$	Belle [685]	$0.60 \pm 0.22 \pm 0.08$[b,c]	0.60 ± 0.23
$f_L(B^0 \to K^{*0}\mu^+\mu^-), 0.04 < q^2 < 6.0\ \mathrm{GeV}^2/c^4$	ATLAS [1160]	$0.50 \pm 0.06 \pm 0.04$	0.50 ± 0.07
$f_L(B^0 \to K^{*0}e^+e^-), 0.002 < q^2 < 1.120\ \mathrm{GeV}^2/c^4$	LHCb [1187]	$0.16 \pm 0.06 \pm 0.03$	0.16 ± 0.07

[a]The PDG uncertainty includes a scale factor.
[b]The charmonium mass regions are vetoed.
[c]$M_{\Lambda^0\bar{\Lambda}^0} < 2.85\ \mathrm{GeV}/c^2$.

TABLE 263. Longitudinal polarization fraction, f_L, in B_s^0 decays.

Parameter	Measurements		Average HFLAV PDG
$f_L(B_s^0 \to \phi(1020)\phi(1020))$	LHCb [1002]	$0.381 \pm 0.007 \pm 0.012$	0.378 ± 0.013
	CDF [1039]	$0.348 \pm 0.041 \pm 0.021$	
$f_L(B_s^0 \to K^*(892)^0\bar{K}^*(892)^0)$	LHCb [995]	$0.240 \pm 0.031 \pm 0.025$	0.24 ± 0.04
$f_L(B_s^0 \to \phi(1020)\bar{K}^*(892)^0)$	LHCb [991]	$0.51 \pm 0.15 \pm 0.07$	0.51 ± 0.17
$f_L(B_s^0 \to \bar{K}_2^*(1430)^0K^*(892)^0)$	LHCb [399]	$0.911 \pm 0.020 \pm 0.165$	0.91 ± 0.17
$f_L(B_s^0 \to K_2^*(1430)^0\bar{K}^*(892)^0)$	LHCb [399]	$0.62 \pm 0.16 \pm 0.25$	0.62 ± 0.30
$f_L(B_s^0 \to K_2^*(1430)^0\bar{K}_2^*(1430)^0)$	LHCb [399]	$0.25 \pm 0.14 \pm 0.18$	0.25 ± 0.23

TABLE 264. Results of full angular analyses of B^+ decays.

Parameter	Measurements		Average HFLAV PDG
$f_\perp(B^+ \to \phi(1020)K^*(892)^+)$	*BABAR* [935]	$0.21 \pm 0.05 \pm 0.02$[a]	0.20 ± 0.05
	Belle [1172]	$0.19 \pm 0.08 \pm 0.02$	
$A^0_{CP}(B^+ \to \phi(1020)K^*(892)^+)$	*BABAR* [935]	$0.17 \pm 0.11 \pm 0.02$[a]	0.17 ± 0.11
$A^\perp_{CP}(B^+ \to \phi(1020)K^*(892)^+)$	*BABAR* [935]	$0.22 \pm 0.24 \pm 0.08$[a]	0.22 ± 0.25

[a]Combination of two final states of the $K^*(892)^\pm$, $K^0_S\pi^\pm$ and $K^\pm\pi^0$. In addition to the combined results, the paper reports separately the results for each individual final state.

TABLE 265. Results of full angular analyses of B^0 decays.

Parameter	Measurements		Average HFLAV PDG
$f_\perp(B^0 \to \phi(1020)K^*(892)^0)$	LHCb [1186]	$0.221 \pm 0.016 \pm 0.013$	0.224 ± 0.015
	Belle [990]	$0.238 \pm 0.026 \pm 0.008$	
	BABAR [388]	$0.212 \pm 0.032 \pm 0.013$	
$A^0_{CP}(B^0 \to \phi(1020)K^*(892)^0)$	LHCb [1186]	$-0.003 \pm 0.038 \pm 0.005$	-0.007 ± 0.030
	Belle [990]	$-0.030 \pm 0.061 \pm 0.007$	
	BABAR [388]	$0.01 \pm 0.07 \pm 0.02$	
$A^\perp_{CP}(B^0 \to \phi(1020)K^*(892)^0)$	LHCb [1186]	$0.047 \pm 0.074 \pm 0.009$	-0.02 ± 0.06
	Belle [990]	$-0.14 \pm 0.11 \pm 0.01$	
	BABAR [388]	$-0.04 \pm 0.15 \pm 0.06$	
$f_\perp(B^0 \to \phi(1020)K^*_2(1430)^0)$[a]	*BABAR* [388]	$0.002^{+0.018}_{-0.002} \pm 0.031$	$0.029^{+0.024}_{-0.026}$
	Belle [990]	$0.056^{+0.050}_{-0.035} \pm 0.009$	$0.027^{+0.031}_{-0.025}$
$A^0_{CP}(B^0 \to \phi(1020)K^*_2(1430)^0)$	Belle [990]	$-0.016^{+0.066}_{-0.051} \pm 0.031$	-0.031 ± 0.04
	BABAR [388]	$-0.05 \pm 0.06 \pm 0.01$	
$A^\perp_{CP}(B^0 \to \phi(1020)K^*_2(1430)^0)$	Belle [990]	$-0.01^{+0.85}_{-0.67} \pm 0.09$	$-0.01^{+0.85}_{-0.68}$

[a]The PDG uncertainty includes a scale factor.

TABLE 266. Results of full angular analyses of B^0_s decays.

Parameter	Measurements		Average HFLAV PDG
$f_\perp(B^0_s \to \phi(1020)\phi(1020))$	LHCb [1002]	$0.290 \pm 0.008 \pm 0.007$	0.293 ± 0.010
	CDF [1039]	$0.365 \pm 0.044 \pm 0.027$	0.292 ± 0.009
$f_\parallel(B^0_s \to \phi(1020)\bar{K}^*(892)^0)$	LHCb [991]	$0.21 \pm 0.11 \pm 0.02$	0.21 ± 0.11
$f_\perp(B^0_s \to K^*(892)^0\bar{K}^*(892)^0)$	LHCb [995]	$0.526 \pm 0.032 \pm 0.019$	0.526 ± 0.037
			0.380 ± 0.120
$f_\parallel(B^0_s \to K^*(892)^0\bar{K}^*(892)^0)$	LHCb [995]	$0.234 \pm 0.025 \pm 0.010$	0.23 ± 0.03
			0.30 ± 0.05

Measurements that are not included in the tables (the definitions of observables can be found in the corresponding experimental papers):

(i) In the angular analysis of $B^0 \to \phi K^*(892)^0$ decays [1186], in addition to the results quoted in Table 265, LHCb reports observables related to the S-wave component contributing the final state $K^+K^-K^+\pi^-$: $f_S(K\pi)$, $f_S(KK)$, $\delta_s(K\pi)$, $\delta_s(KK)$, $\mathcal{A}_S(K\pi)^{CP}$, $\mathcal{A}_S(KK)^{CP}$, $\delta_S(K\pi)^{CP}$, $\delta_S(KK)^{CP}$.

(ii) In the amplitude analysis of $B^0_s \to \phi\phi$ decays, in addition to the results quoted in Table 266, LHCb, in Ref. [395], extracts the CP-violating phase $\phi_s^{s\bar{s}ss}$ and the CP-violating parameter $|\lambda|$ from a decay-time-dependent and polarization independent fit. The CP-violating phases $\phi_{s,\parallel}$ and $\phi_{s,\perp}$ are obtained in a polarization-dependent fit. A time-integrated fit is performed to extract the triple-product asymmetries A_U and A_V. CDF, in

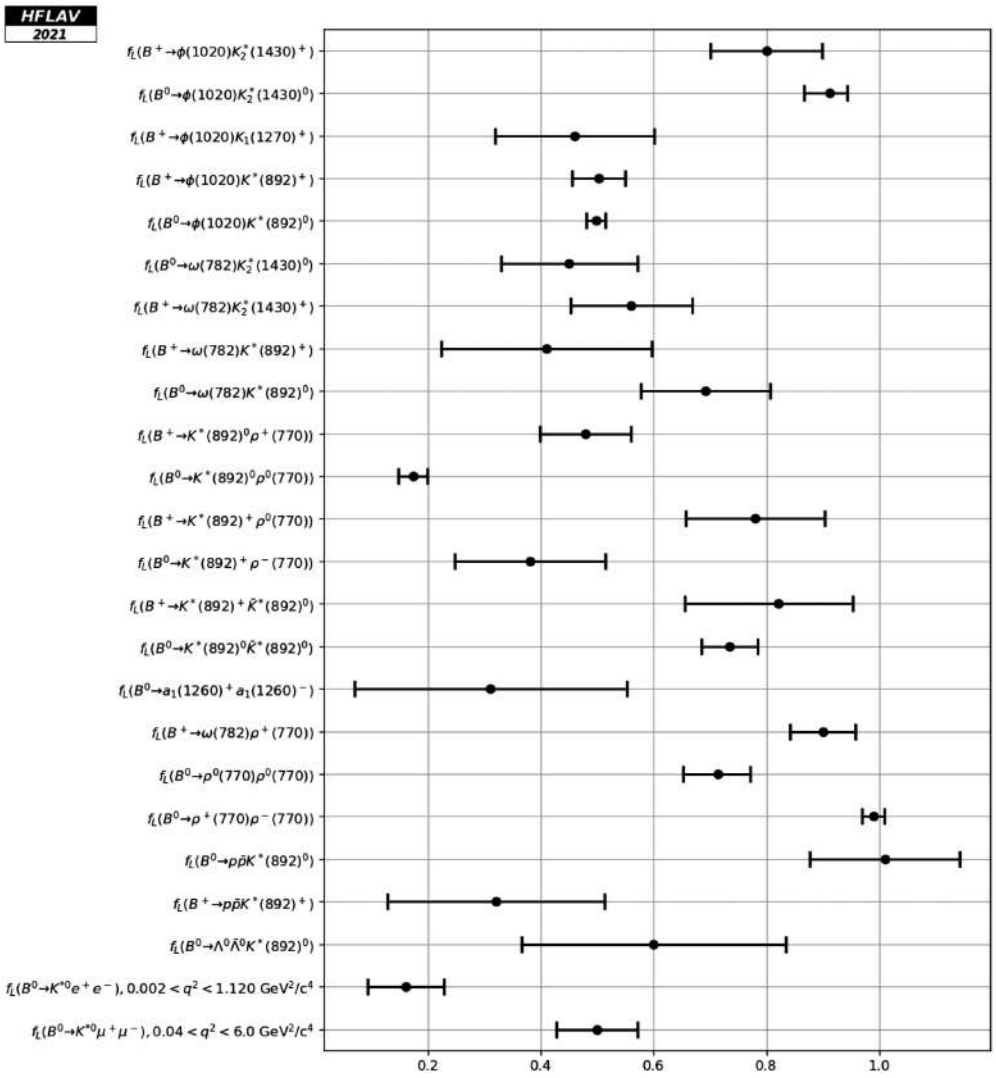

FIG. 82. Longitudinal polarization fraction in charmless B decays.

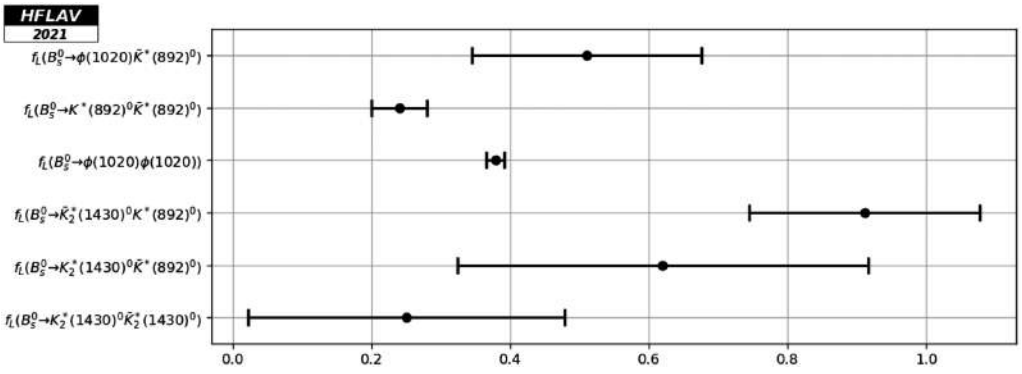

FIG. 83. Longitudinal polarization fraction in charmless B_s^0 decays.

Ref. [1039] also reports the triple-product asymmetries A_U and A_V.

(iii) In Ref. [399], LHCb presents a flavor-tagged, decay-time-dependent amplitude analysis of $B_s^0 \to (K^+\pi^-)(K^-\pi^+)$ decays in the $K^\pm\pi^\mp$ mass range from 750 to 1600 MeV/c^2. The paper includes measurements of 19 CP-averaged amplitude parameters corresponding to scalar, vector and tensor final states as well as the first measurement of the CP-violating phase $\phi_s^{d\bar{d}}$.

(iv) Reference [1185] presents an amplitude analysis of $B^0 \to \rho K^*(892)^0$ realized by LHCb. Scalar (S) and vector (V) contributions to the final state $(\pi^+\pi^+)(K^+\pi^-)$ are considered through partial waves sharing the same angular dependence (VV, SS, SV, VS) and the corresponding amplitudes are extracted for each case. Triple product asymmetries are also reported.

X. CHARM CP VIOLATION AND OSCILLATIONS

A. D^0-$\bar{D}^0$ mixing and CP violation

1. Introduction

The first evidence for D^0-$\bar{D}^0$ oscillations, or mixing, was obtained in 2007 by Belle [1188] and *BABAR* [1189]. These results were confirmed by CDF [1190] and, in 2013 with high statistics, by LHCb [1191]. There are now numerous measurements of D^0-$\bar{D}^0$ mixing with various levels of sensitivity. In 2019, LHCb used all its available data (8.9 fb^{-1}) to observe CP violation in D decays for the first time [1192]. Recently, LHCb measured the mixing parameters x and y (see below) with much higher precision [1193] than that of previous measurements. All these measurements, plus others, are input into a global fit performed by HFLAV to determine world average values for mixing parameters, CP violation (CPV) parameters, and strong phase differences.

Our notation is as follows. We use the phase convention $CP|D^0\rangle = -|\bar{D}^0\rangle$ and $CP|\bar{D}^0\rangle = -|D^0\rangle$ [1194] and denote the mass eigenstates as

$$D_1 = p|D^0\rangle - q|\bar{D}^0\rangle \tag{229}$$

$$D_2 = p|D^0\rangle + q|\bar{D}^0\rangle. \tag{230}$$

With this phase convention, in the absence of CP violation ($p = q$), D_1 is CP-even and D_2 is CP-odd. The mixing parameters are defined as $x \equiv (m_1 - m_2)/\Gamma$ and $y \equiv (\Gamma_1 - \Gamma_2)/(2\Gamma)$, where m_1, m_2 and Γ_1, Γ_2 are the masses and decay widths, respectively, of the mass eigenstates, and $\Gamma \equiv (\Gamma_1 + \Gamma_2)/2$. The global fit determines central values and uncertainties for ten underlying parameters. These parameters, in addition to x and y, consist of the following:

(i) CPV parameters $|q/p|$ and $\mathrm{Arg}(q/p) \equiv \phi$, which give rise to indirect CPV (see Sec. X B for a discussion of indirect and direct CPV). Here we assume indirect CPV is "universal," i.e., independent of the final state in $D^0 \to f$ decays.

(ii) direct CPV asymmetries

$$A_D \equiv \frac{\Gamma(D^0 \to K^+\pi^-) - \Gamma(\bar{D}^0 \to K^-\pi^+)}{\Gamma(D^0 \to K^+\pi^-) + \Gamma(\bar{D}^0 \to K^-\pi^+)}$$

$$A_K \equiv \frac{\Gamma(D^0 \to K^+K^-) - \Gamma(\bar{D}^0 \to K^-K^+)}{\Gamma(D^0 \to K^+K^-) + \Gamma(\bar{D}^0 \to K^-K^+)}$$

$$A_\pi \equiv \frac{\Gamma(D^0 \to \pi^+\pi^-) - \Gamma(\bar{D}^0 \to \pi^-\pi^+)}{\Gamma(D^0 \to \pi^+\pi^-) + \Gamma(\bar{D}^0 \to \pi^-\pi^+)},$$

where, as indicated, the decay rates are for the pure D^0 and $\bar{D}^0$ flavor eigenstates.

(iii) the ratio of doubly Cabibbo-suppressed (DCS) to Cabibbo-favored decay rates

$$R_D \equiv \frac{\Gamma(D^0 \to K^+\pi^-) + \Gamma(\bar{D}^0 \to K^-\pi^+)}{\Gamma(D^0 \to K^-\pi^+) + \Gamma(\bar{D}^0 \to K^+\pi^-)},$$

where the decay rates are for pure D^0 and $\bar{D}^0$ flavor eigenstates.

(iv) the strong phase difference δ between the amplitudes $\mathcal{A}(\bar{D}^0 \to K^-\pi^+)$ and $\mathcal{A}(D^0 \to K^-\pi^+)$; and

(v) the strong phase difference $\delta_{K\pi\pi}$ between the amplitudes $\mathcal{A}(\bar{D}^0 \to K^-\rho^+)$ and $\mathcal{A}(D^0 \to K^-\rho^+)$.

The 61 observables used in the fit are measured from the following decays:[34] $D^0 \to K^+\ell^-\bar{\nu}$, $D^0 \to K^+K^-$, $D^0 \to \pi^+\pi^-$, $D^0 \to K^+\pi^-$, $D^0 \to K^+\pi^-\pi^0$, $D^0 \to K^0_S\pi^+\pi^-$, $D^0 \to \pi^0\pi^+\pi^-$, $D^0 \to K^0_S K^+K^-$, and $D^0 \to K^+\pi^-\pi^+\pi^-$. The fit also uses measurements of mixing parameters and strong phases determined from double-tagged branching fractions measured at the $\psi(3770)$ resonance. The relationships between measured observables and fitted parameters are given in Table 267. Correlations among observables are accounted for by using covariance matrices provided by the experimental collaborations. Uncertainties are assumed to be Gaussian, and systematic uncertainties among different experiments are assumed to be uncorrelated unless specific correlations have been identified. We have compared this method with a second method that adds together three-dimensional log-likelihood functions for x, y, and δ obtained from several independent measurements; this combination accounts for non-Gaussian uncertainties. When both methods are applied to the same set of measurements, equivalent results are obtained. We have furthermore compared the results to those obtained from an independent fit based on the GAMMACOMBO framework [432] and found good agreement.

[34] Charge-conjugate modes are implicitly included.

TABLE 267. Left column: decay modes used to determine the fitted parameters x, y, δ, $\delta_{K\pi\pi}$, R_D, A_D, A_K, A_π, $|q/p|$, and ϕ. Middle column: measured observables for each decay mode. Right column: relationships between the measured observables and the fitted parameters. The symbol $\langle t \rangle$ denotes the mean reconstructed decay time for $D^0 \to K^+K^-$ or $D^0 \to \pi^+\pi^-$ decays.

Decay Mode	Observables	Relationship
$D^0 \to K^+K^-/\pi^+\pi^-$	y_{CP} A_Γ	$2y_{CP} = (\lvert q/p\rvert + \lvert p/q\rvert)y\cos\phi - (\lvert q/p\rvert - \lvert p/q\rvert)x\sin\phi$ $2A_\Gamma = (\lvert q/p\rvert - \lvert p/q\rvert)y\cos\phi - (\lvert q/p\rvert + \lvert p/q\rvert)x\sin\phi$
$D^0 \to K^0_S\pi^+\pi^-$	x y $\lvert q/p\rvert$ ϕ	
$D^0 \to K^+\ell^-\bar{\nu}$	R_M	$R_M = \frac{x^2+y^2}{2}$
$D^0 \to K^+\pi^-\pi^0$ (Dalitz plot analysis)	x'' y''	$x'' = x\cos\delta_{K\pi\pi} + y\sin\delta_{K\pi\pi}$ $y'' = y\cos\delta_{K\pi\pi} - x\sin\delta_{K\pi\pi}$
"Double-tagged" branching fractions measured in $\psi(3770) \to DD$ decays	R_M y R_D $\sqrt{R_D}\cos\delta$	$R_M = \frac{x^2+y^2}{2}$
$D^0 \to K^+\pi^-$	x'^2, y' x'^{2+}, x'^{2-} y'^+, y'^-	$x' = x\cos\delta + y\sin\delta$ $y' = y\cos\delta - x\sin\delta$ $x'^\pm = \lvert q/p\rvert^{\pm 1}(x'\cos\phi \pm y'\sin\phi)$ $y'^\pm = \lvert q/p\rvert^{\pm 1}(y'\cos\phi \mp x'\sin\phi)$
$D^0 \to K^+\pi^-/K^-\pi^+$ (time-integrated)	R_D A_D	
$D^0 \to K^+K^-/\pi^+\pi^-$ (time-integrated)	$\frac{\Gamma(D^0\to K^+K^-)-\Gamma(\bar{D}^0\to K^+K^-)}{\Gamma(D^0\to K^+K^-)+\Gamma(\bar{D}^0\to K^+K^-)} A_K + \frac{\langle t\rangle}{\tau_D}\mathcal{A}_{CP}^{\text{indirect}}$ $(\mathcal{A}_{CP}^{\text{indirect}} \approx -A_\Gamma)$ $\frac{\Gamma(D^0\to \pi^+\pi^-)-\Gamma(\bar{D}^0\to \pi^+\pi^-)}{\Gamma(D^0\to \pi^+\pi^-)+\Gamma(\bar{D}^0\to \pi^+\pi^-)} A_\pi + \frac{\langle t\rangle}{\tau_D}\mathcal{A}_{CP}^{\text{indirect}}$ $(\mathcal{A}_{CP}^{\text{indirect}} \approx -A_\Gamma)$	

Mixing in the heavy flavor B^0 and B^0_s systems is governed by a short-distance box diagram. In the D^0 system, this box diagram is both doubly Cabibbo-suppressed and GIM-suppressed [1195], and consequently the short-distance mixing rate is tiny. Thus, D^0-$\bar{D}^0$ mixing is dominated by long-distance processes. These are difficult to calculate, and theoretical estimates for x and y range over three orders of magnitude, up to the percent level [1196–1199].

Almost all experimental analyses besides that of the $\psi(3770) \to \bar{D}D$ measurements [1200] identify the flavor of the D^0 or $\bar{D}^0$ when produced by reconstructing the decay $D^{*+} \to D^0\pi^+$ or $D^{*-} \to \bar{D}^0\pi^-$. The charge of the pion, which has low momentum in the lab frame relative to that of the D^0 daughters and is often referred to as the "soft" pion, identifies the D^0 flavor. For $D^{*+} \to D^0\pi^+$, $M_{D^*} - M_{D^0} - M_{\pi^+} \equiv Q \approx 6$ MeV, which is close to the kinematic threshold; thus, analyses typically require that the reconstructed Q be less than some value (e.g., 20 MeV) to suppress backgrounds. In several analyses, LHCb identifies the flavor of the D^0 by partially reconstructing $\bar{B} \to D^{(*)}\mu^- X$ and $B \to \bar{D}^{(*)}\mu^+ X$ decays; in this case the charge of the $\mu^\mp$ identifies the flavor of the D^0 or $\bar{D}^0$.

For time-dependent measurements, the D^0 decay time is calculated as $t = M_{D^0}(\vec{d}\cdot\hat{p})/p$, where $\vec{d}$ is the displacement vector from the D^{*+} decay vertex to the D^0 decay vertex; $\hat{p}$ is the direction of the D^0 momentum; and p is its magnitude. The D^{*+} vertex position is taken as the intersection of the D^0 momentum vector with the beam spot profile for e^+e^- experiments, and at the primary interaction vertex for pp and $\bar{p}p$ experiments.

2. Input observables

The global fit determines central values and uncertainties for ten parameters by minimizing a χ^2 statistic. The fitted parameters are x, y, R_D, A_D, $|q/p|$, ϕ, δ, $\delta_{K\pi\pi}$, A_K, and A_π. In the $D \to K^+\pi^-\pi^0$ Dalitz plot analysis [1201], the phases of intermediate resonances in the $\bar{D}^0 \to K^+\pi^-\pi^0$ decay amplitude are fitted relative to the phase for $\mathcal{A}(\bar{D}^0 \to K^+\rho^-)$, and the phases of intermediate resonances for $D^0 \to K^+\pi^-\pi^0$ are fitted relative to the phase for $\mathcal{A}(D^0 \to K^+\rho^-)$. As the $\bar{D}^0$ and D^0 Dalitz plots are fitted separately, the phase difference $\delta_{K\pi\pi} = \text{Arg}[\mathcal{A}(\bar{D}^0 \to K^+\rho^-)/\mathcal{A}(D^0 \to K^+\rho^-)]$ between the reference amplitudes cannot be determined from these individual fits.

TABLE 268. Observables used in the global fit, except those from time-dependent $D^0 \to K^+\pi^-$ measurements and those from direct CPV measurements. The latter measurements are listed in Tables 269 and 270, respectively.

Mode	Observable	Values	Correlation coefficients
$D^0 \to K^+K^-/\pi^+\pi^-$, ϕK^0_S	y_{CP}	$(0.719 \pm 0.113)\%$	
	A_Γ	$(0.0089 \pm 0.0113)\%$	
$D^0 \to K^0_S\pi^+\pi^-$ [1211] (Belle: no CPV)	x	$(0.56 \pm 0.19^{+0.067}_{-0.127})\%$	$+0.012$
	y	$(0.30 \pm 0.15^{+0.050}_{-0.078})\%$	
$D^0 \to K^0_S\pi^+\pi^-$ [1211] (Belle: no direct CPV)	$\lvert q/p\rvert$	$0.90^{+0.16\ +0.078}_{-0.15\ -0.064}$	$\begin{pmatrix} 1 & 0.054 & -0.074 & -0.031 \\ & 1 & 0.034 & -0.019 \\ & & 1 & 0.044 \\ & & & 1 \end{pmatrix}$
	ϕ	$(-6 \pm 11^{+4.2}_{-5.0})$ degrees	
$D^0 \to K^0_S\pi^+\pi^-$ [1211] (Belle: direct CPV allowed)	x	$(0.58 \pm 0.19^{+0.0734}_{-0.1177})\%$	Same as above
	y	$(0.27 \pm 0.16^{+0.0546}_{-0.0854})\%$	
	$\lvert q/p\rvert$	$0.82^{+0.20\ +0.0807}_{-0.18\ -0.0645}$	
	ϕ	$(-13^{+12+4.15}_{-13\ -4.77})$ degrees	
$D^0 \to K^0_S\pi^+\pi^-$ [1213] (LHCb: 1 fb^{-1} no CPV)	x	$(-0.86 \pm 0.53 \pm 0.17)\%$	$+0.37$
	y	$(0.03 \pm 0.46 \pm 0.13)\%$	
$D^0 \to K^0_S\pi^+\pi^-$ [1214] (LHCb: 3 fb^{-1} CPV allowed)	x_{CP}	$(0.27 \pm 0.16 \pm 0.04)\%$	$\begin{pmatrix} 1 & (-0.17+0.15) & (0.04+0.01) & (-0.02-0.02) \\ & 1 & (-0.03-0.05) & (0.01-0.03) \\ & & 1 & (-0.13+0.14) \\ & & & 1 \end{pmatrix}$ Notation: above coefficients are (statistical + systematic). For $(x, y, \lvert q/p\rvert, \phi) \to (x_{CP}, y_{CP}, \Delta x, \Delta y)$ mapping, see [1217].
	y_{CP}	$(0.74 \pm 0.36 \pm 0.11)\%$	
	Δx	$(-0.053 \pm 0.070 \pm 0.022)\%$	
	Δy	$(0.06 \pm 0.16 \pm 0.03)\%$	
$D^0 \to K^0_S\pi^+\pi^-$ [1193] (LHCb: 5.4 fb^{-1} CPV allowed)	x_{CP}	$(0.397 \pm 0.046 \pm 0.029)\%$	$\begin{pmatrix} 1 & (0.11+0.13) & (-0.02+0.01) & (-0.01+0.01) \\ & 1 & (-0.01-0.02) & (-0.05+0.01) \\ & & 1 & (0.08+0.31) \\ & & & 1 \end{pmatrix}$
	y_{CP}	$(0.459 \pm 0.120 \pm 0.085)\%$	
	Δx	$(-0.027 \pm 0.018 \pm 0.001)\%$	
	Δy	$(0.020 \pm 0.036 \pm 0.013)\%$	
$D^0 \to K^0_S\pi^+\pi^-$ [1212] $K^0_SK^+K^-$ ($BABAR$: no CPV)	x	$(0.16 \pm 0.23 \pm 0.12 \pm 0.08)\%$	$+0.0615$
	y	$(0.57 \pm 0.20 \pm 0.13 \pm 0.07)\%$	
$D^0 \to \pi^0\pi^+\pi^-$ [1215] ($BABAR$: no CPV)	x	$(1.5 \pm 1.2 \pm 0.6)\%$	-0.006
	y	$(0.2 \pm 0.9 \pm 0.5)\%$	
$D^0 \to K^+\ell^-\bar{\nu}$	R_M	$(0.0130 \pm 0.0269)\%$	
$D^0 \to K^+\pi^-\pi^0$ [1201]	x''	$(2.61^{+0.57}_{-0.68} \pm 0.39)\%$	-0.75
	y''	$(-0.06^{+0.55}_{-0.64} \pm 0.34)\%$	
$D^0 \to K^+\pi^-\pi^+\pi^-$ [491]	$R_M/2$	$(4.8 \pm 1.8) \times 10^{-5}$	
$\psi(3770) \to \bar{D}D$ [1200] (CLEOc)	R_D	$(0.533 \pm 0.107 \pm 0.045)\%$	$\begin{pmatrix} 1 & 0 & 0 & -0.42 & 0.01 \\ & 1 & -0.73 & 0.39 & 0.02 \\ & & 1 & -0.53 & -0.03 \\ & & & 1 & 0.04 \\ & & & & 1 \end{pmatrix}$
	x^2	$(0.06 \pm 0.23 \pm 0.11)\%$	
	y	$(4.2 \pm 2.0 \pm 1.0)\%$	
	$\cos\delta$	$0.81^{+0.22\ +0.07}_{-0.18\ -0.05}$	
	$\sin\delta$	$-0.01 \pm 0.41 \pm 0.04$	

However, this phase difference can be constrained in the global fit and thus is included as a fitted parameter.

All input measurements are listed in Tables 268–270. There are three observables input to the fit that are world average values:

$$R_M = \frac{x^2 + y^2}{2} \tag{231}$$

$$y_{CP} = \frac{1}{2}\left(\left|\frac{q}{p}\right| + \left|\frac{p}{q}\right|\right) y\cos\phi - \frac{1}{2}\left(\left|\frac{q}{p}\right| - \left|\frac{p}{q}\right|\right) x\sin\phi \tag{232}$$

$$A_\Gamma = \frac{1}{2}\left(\left|\frac{q}{p}\right| - \left|\frac{p}{q}\right|\right) y\cos\phi - \frac{1}{2}\left(\left|\frac{q}{p}\right| + \left|\frac{p}{q}\right|\right) x\sin\phi. \tag{233}$$

TABLE 269. Time-dependent $D^0 \to K^+\pi^-$ observables used for the global fit. The observables R_D^+ and R_D^- are related to parameters R_D and A_D via $R_D^\pm = R_D(1 \pm A_D)$.

Mode	Observable	Values	Correlation coefficients
$D^0 \to K^+\pi^-$ [1189] (*BABAR* 384 fb^{-1})	R_D	$(0.303 \pm 0.0189)\%$	$\begin{Bmatrix} 1 & 0.77 & -0.87 \\ & 1 & -0.94 \\ & & 1 \end{Bmatrix}$
	x'^{2+}	$(-0.024 \pm 0.052)\%$	
	y'^{+}	$(0.98 \pm 0.78)\%$	
	A_D	$(-2.1 \pm 5.4)\%$	
$\bar{D}^0 \to K^-\pi^+$ [1189] (*BABAR* 384 fb^{-1})	x'^{2-}	$(-0.020 \pm 0.050)\%$	Same as above
	y'^{-}	$(0.96 \pm 0.75)\%$	
$D^0 \to K^+\pi^-$ [1207] (Belle 976 fb^{-1} No *CPV*)	R_D	$(0.353 \pm 0.013)\%$	$\begin{Bmatrix} 1 & 0.737 & -0.865 \\ & 1 & -0.948 \\ & & 1 \end{Bmatrix}$
	x'^{2}	$(0.009 \pm 0.022)\%$	
	y'	$(0.46 \pm 0.34)\%$	
$D^0 \to K^+\pi^-$ [1206] (Belle 400 fb^{-1} *CPV*-allowed)	R_D	$(0.364 \pm 0.018)\%$	$\begin{Bmatrix} 1 & 0.655 & -0.834 \\ & 1 & -0.909 \\ & & 1 \end{Bmatrix}$
	x'^{2+}	$(0.032 \pm 0.037)\%$	
	y'^{+}	$(-0.12 \pm 0.58)\%$	
	A_D	$(+2.3 \pm 4.7)\%$	
$\bar{D}^0 \to K^-\pi^+$ [1206] (Belle 400 fb^{-1} *CPV*-allowed)	x'^{2-}	$(0.006 \pm 0.034)\%$	Same as above
	y'^{-}	$(0.20 \pm 0.54)\%$	
$D^0 \to K^+\pi^-$ [1208] (CDF 9.6 fb^{-1} No *CPV*)	R_D	$(0.351 \pm 0.035)\%$	$\begin{Bmatrix} 1 & 0.90 & -0.97 \\ & 1 & -0.98 \\ & & 1 \end{Bmatrix}$
	x'^{2}	$(0.008 \pm 0.018)\%$	
	y'	$(0.43 \pm 0.43)\%$	
$D^0 \to K^+\pi^-$ [1209] (LHCb 3.0 fb^{-1} $B \to D^*\mu X$ tag *CPV*-allowed)	R_D^+	$(0.338 \pm 0.0161)\%$	$\begin{Bmatrix} 1 & 0.823 & -0.920 \\ & 1 & -0.962 \\ & & 1 \end{Bmatrix}$
	x'^{2+}	$(-0.0019 \pm 0.0447)\%$	
	y'^{+}	$(0.581 \pm 0.526)\%$	
$\bar{D}^0 \to K^-\pi^+$ [1209] (LHCb 3.0 fb^{-1} $B \to D^*\mu X$ tag *CPV*-allowed)	R_D^-	$(0.360 \pm 0.0166)\%$	$\begin{Bmatrix} 1 & 0.812 & -0.918 \\ & 1 & -0.956 \\ & & 1 \end{Bmatrix}$
	x'^{2-}	$(0.0079 \pm 0.0433)\%$	
	y'^{-}	$(0.332 \pm 0.523)\%$	
$D^0 \to K^+\pi^-$ [1210] (LHCb 5.0 fb^{-1} D^* tag *CPV*-allowed)	R_D^+	$(0.3454 \pm 0.0045)\%$	$\begin{Bmatrix} 1 & 0.843 & -0.935 \\ & 1 & -0.963 \\ & & 1 \end{Bmatrix}$
	x'^{2+}	$(0.0061 \pm 0.0037)\%$	
	y'^{+}	$(0.501 \pm 0.074)\%$	
$\bar{D}^0 \to K^-\pi^+$ [1210] (LHCb 5.0 fb^{-1} D^* tag *CPV*-allowed)	R_D^-	$(0.3454 \pm 0.0045)\%$	$\begin{Bmatrix} 1 & 0.846 & -0.935 \\ & 1 & -0.964 \\ & & 1 \end{Bmatrix}$
	x'^{2-}	$(0.0016 \pm 0.0039)\%$	
	y'^{-}	$(0.554 \pm 0.074)\%$	

TABLE 270. Measurements of time-integrated *CP* asymmetries. The observable $A_{CP}(f) = [\Gamma(D^0 \to f) - \Gamma(\bar{D}^0 \to f)]/[\Gamma(D^0 \to f) + \Gamma(\bar{D}^0 \to f)]$. The symbol $\Delta\langle t\rangle$ denotes the difference between the mean reconstructed decay times for $D^0 \to K^+K^-$ and $D^0 \to \pi^+\pi^-$ decays due to different trigger and reconstruction efficiencies.

Mode	Observable	Values	$\Delta\langle t\rangle/\tau_D$
$D^0 \to h^+h^-$ [1218] (*BABAR* 386 fb^{-1})	$A_{CP}(K^+K^-)$	$(+0.00 \pm 0.34 \pm 0.13)\%$	0
	$A_{CP}(\pi^+\pi^-)$	$(-0.24 \pm 0.52 \pm 0.22)\%$	
$D^0 \to h^+h^-$ [1219] (Belle 540 fb^{-1})	$A_{CP}(K^+K^-)$	$(-0.43 \pm 0.30 \pm 0.11)\%$	0
	$A_{CP}(\pi^+\pi^-)$	$(+0.43 \pm 0.52 \pm 0.12)\%$	
$D^0 \to h^+h^-$ [1220,1221] (CDF 9.7 fb^{-1})	$A_{CP}(K^+K^-) - A_{CP}(\pi^+\pi^-)$	$(-0.62 \pm 0.21 \pm 0.10)\%$	0.27 ± 0.01
	$A_{CP}(K^+K^-)$	$(-0.32 \pm 0.21)\%$	
	$A_{CP}(\pi^+\pi^-)$	$(+0.31 \pm 0.22)\%$	
$D^0 \to h^+h^-$ [1192] (LHCb 9.0 fb^{-1}, $D^{*+} \to D^0\pi^+ + \bar{B} \to D^0\mu^- X$ tags combined)	$A_{CP}(K^+K^-) - A_{CP}(\pi^+\pi^-)$	$(-0.154 \pm 0.029)\%$	0.115 ± 0.002

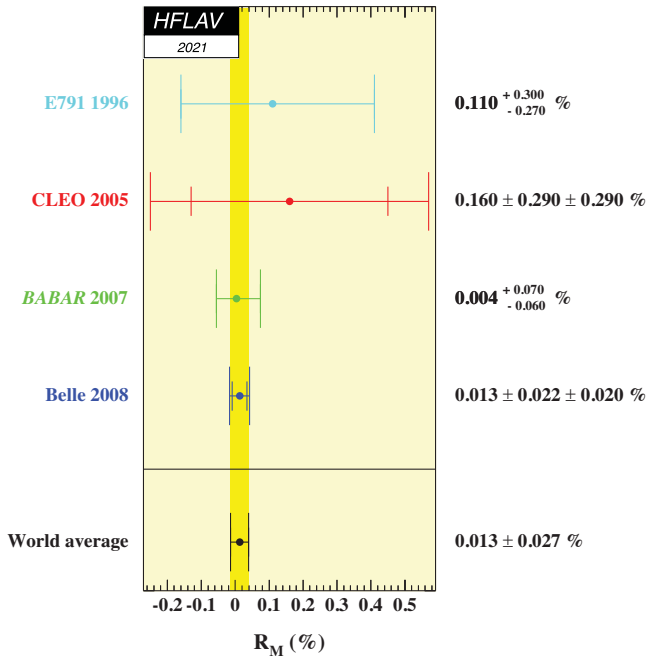

FIG. 84. World average value of $R_M = (x^2 + y^2)/2$ as calculated from $D^0 \to K^+\ell^-\bar{\nu}$ measurements [1202–1205]. The confidence level from the fit is 0.97.

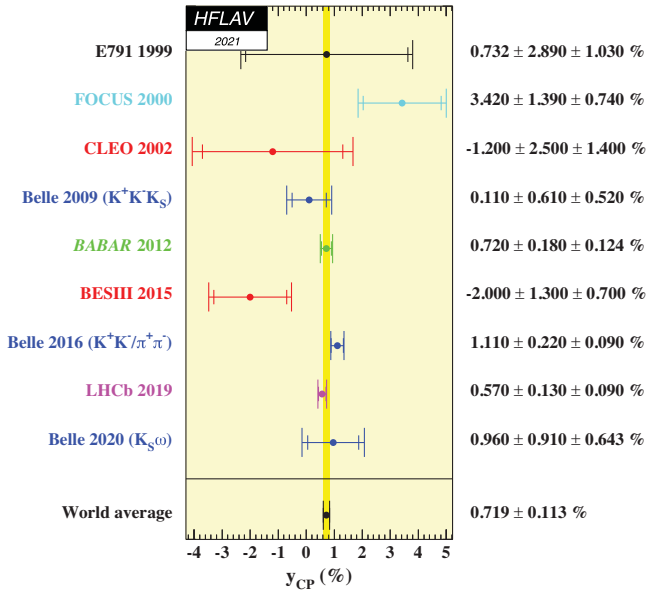

FIG. 85. World average value of y_{CP} as calculated from $D^0 \to K^+K^-, \pi^+\pi^-, K^+K^-K^0_S$, and $K^0_S\omega$ measurements [1222–1230]. The confidence level from the fit is 0.21.

These are calculated using the COMBOS program [6]. The world average for R_M is calculated from measurements of $D^0 \to K^+\ell^-\bar{\nu}$ decays [1202–1205]; see Fig. 84. A measurement of R_M using $D^0 \to K^+\pi^-\pi^+\pi^-$ decays [491] is separately input to the global fit. The inputs used for the world averages of y_{CP} and A_Γ are plotted in Figs. 85 and 86, respectively.

The $D^0 \to K^+\pi^-$ measurements used are from Belle [1206,1207], *BABAR* [1189], CDF [1208], and LHCb [1209,1210]; earlier measurements are either superseded or have much less precision and are not used. The observables from $D^0 \to K^0_S\pi^+\pi^-$ decays are measured in two ways: assuming CP conservation (D^0 and $\bar{D}^0$ decays combined), and allowing for CP violation (D^0 and $\bar{D}^0$ decays fitted separately). The no-CPV measurements are from Belle [1211], *BABAR* [1212], and LHCb [1213]; for the CPV-allowed case, Belle [1211] and LHCb [1193,1214] measurements are available. The $D^0 \to K^+\pi^-\pi^0$, $D^0 \to K^0_S K^+K^-$, and $D^0 \to \pi^0\pi^+\pi^-$ results are from *BABAR* [1201,1215]; the $D^0 \to K^+\pi^-\pi^+\pi^-$ results are from LHCb [491]; and the $\psi(3770) \to \bar{D}D$ results are from CLEOc [1200]. A measurement of the strong phase δ by BESIII [1216] using $\psi(3770) \to \bar{D}D$ events use HFLAV's world averages for R_D and y as external inputs; thus, we do not include this BESIII result in the global fit.

For each set of correlated observables, we construct a difference vector $\vec{V}$ between the measured values and those calculated from the fitted parameters using the relations of Table 267. For example, for $D^0 \to K^0_S\pi^+\pi^-$ decays, $\vec{V} = (\Delta x, \Delta y, \Delta|q/p|, \Delta\phi)$, where $\Delta x \equiv x_{\text{measured}} - x_{\text{fitted}}$ and similarly for Δy, $\Delta|q/p|$, and $\Delta\phi$. The contribution of a set of observables to the fit χ^2 is calculated as $\vec{V} \cdot (M^{-1}) \cdot \vec{V}^T$, where M^{-1} is the inverse of the covariance matrix for the measured observables. Covariance matrices are constructed from the correlation coefficients among the observables. These correlation coefficients are furnished by the experiments and listed in Tables 268–270.

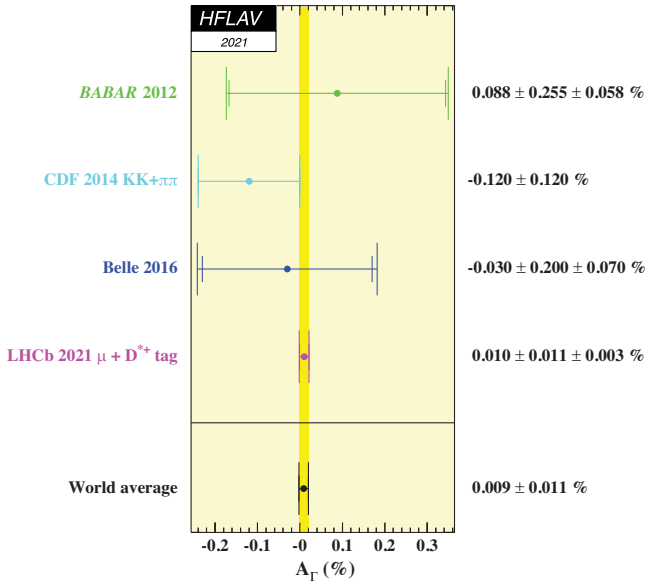

FIG. 86. World average value of A_Γ calculated from $D^0 \to K^+K^-, \pi^+\pi^-$ measurements [1226,1228,1231,1232]. The confidence level from the fit is 0.73.

3. Fit results

The global fitter uses MINUIT with the MIGRAD minimizer, and all uncertainties are obtained from MINOS [1233]. Three types of fits are performed, as described below.

(1) Assuming *CP* conservation, i.e., fixing $A_D = 0$, $A_K = 0$, $A_\pi = 0$, $\phi = 0$, and $|q/p| = 1$. All other parameters (x, y, δ, R_D, $\delta_{K\pi\pi}$) are floated.

(2) Assuming no subleading amplitudes in CF and DCS decays. In addition, subleading amplitudes in SCS decays are neglected in indirect *CPV* observables, as their contribution is suppressed by the mixing parameters x and y. These simplifictions have two consequences [1234]: *(a)* no direct *CPV* in CF or DCS decays ($A_D = 0$); and *(b)* only short-distance dispersive amplitudes contribute to indirect *CPV*. The latter implies that all indirect *CPV* is due to a phase difference between M_{12} and Γ_{12}, the off-diagonal elements of the mass and decay matrices. In this case the four parameters $\{x, y, |q/p|, \phi\}$ are related, and one fits for only three of them, in our case $\{x, y, \phi\}$ or $\{x, y, |q/p|\}$.

(2b) The same assumptions as for Fit 2a, but fitting for parameters $x_{12} \equiv 2|M_{12}|/\Gamma$, $y_{12} \equiv |\Gamma_{12}|/\Gamma$, and $\phi_{12} \equiv \mathrm{Arg}(M_{12}/\Gamma_{12})$ [1234,1235]. The parameter ϕ_{12} is the phase difference responsible for all indirect *CPV*. The conventional parameters $\{x, y, |q/p|, \phi\}$ can be derived from $\{x_{12}, y_{12}, \phi_{12}\}$; the result is [1234,1236]

$$x = \left[\frac{x_{12}^2 - y_{12}^2 + \sqrt{(x_{12}^2 + y_{12}^2)^2 - 4x_{12}^2 y_{12}^2 \sin^2\phi_{12}}}{2}\right]^{1/2}$$

$$y = \left[\frac{y_{12}^2 - x_{12}^2 + \sqrt{(x_{12}^2 + y_{12}^2)^2 - 4x_{12}^2 y_{12}^2 \sin^2\phi_{12}}}{2}\right]^{1/2}$$

$$\left|\frac{q}{p}\right| = \left(\frac{x_{12}^2 + y_{12}^2 + 2x_{12}y_{12}\sin\phi_{12}}{x_{12}^2 + y_{12}^2 - 2x_{12}y_{12}\sin\phi_{12}}\right)^{1/4}$$

$$\tan 2\phi = -\frac{\sin 2\phi_{12}}{\cos 2\phi_{12} + (y_{12}/x_{12})^2}.$$

(3) Allowing full *CPV* and fitting for all ten parameters: x, y, δ, R_D, A_D, $\delta_{K\pi\pi}$, $|q/p|$, ϕ, A_K, and A_π.

For fit (2a), we reduce four independent parameters to three using the relation [1234,1236,1237] $\tan\phi = (x/y) \times (1 - |q/p|^2)/(1 + |q/p|^2)$.[35] This constraint is imposed in two ways: first we float $\{x, y, \phi\}$ and from these derive $|q/p|$; second, we float $\{x, y, |q/p|\}$ and from these derive ϕ. The central values returned by the two fits are identical, but the first fit yields MINOS errors for ϕ, while the second fit yields MINOS errors for $|q/p|$. For fit (2b), the floated parameters are $\{x_{12}, y_{12}, \phi_{12}\}$: from these we derive $\{x, y, |q/p|, \phi\}$, and the latter are compared to measured observables to calculate the fit χ^2. All results are listed in Table 271. The χ^2 for the all-*CPV*-allowed Fit 3 is 63.6 for $61 - 10 = 51$ degrees of freedom. Table 272 lists the individual contributions to this χ^2.

Confidence contours in the two dimensions (x, y) or $(|q/p|, \phi)$ are obtained by finding the minimum χ^2 for each fixed point in the two-dimensional plane. The resulting 1σ–5σ contours are shown in Fig. 87 for Fit 2, and in Fig. 88 for Fit 3. The contours are determined from the increase of the χ^2 above the minimum value. For the all-*CPV*-allowed Fit 3, the χ^2 at the no-mixing point $(x, y) = (0, 0)$ is 2099 units above the minimum value; this corresponds to a statistical significance greater than 11.5σ (for two degrees of freedom). Thus, the no-mixing hypothesis is excluded at this high level. In the $(|q/p|, \phi)$ plot (Fig. 88, bottom), the χ^2 at the no-*CPV* point $(|q/p|, \phi) = (1, 0)$ is 5.63 units above the minimum value; this corresponds to a statistical significance of 1.6σ.

One-dimensional likelihood curves for individual parameters are obtained by finding the minimum χ^2 for fixed values of the parameter of interest. The resulting functions $\Delta\chi^2 = \chi^2 - \chi^2_{\mathrm{min}}$, where χ^2_{min} is the overall minimum value, are shown in Fig. 89. The points where $\Delta\chi^2 = 3.84$ determine 95% C.L. intervals for the parameters. These intervals are listed in Table 271. The value of $\Delta\chi^2$ at $x = 0$ is 68.3 (Fig. 89, upper left), and the value of $\Delta\chi^2$ at $y = 0$ is 477 (Fig. 89, upper right). These correspond to statistical significances of 8.2σ and $> 11.4\sigma$, respectively. These large values demonstrate that neutral D mesons undergo both dispersive mixing ($\Delta M \neq 0$) and absorptive mixing ($\Delta\Gamma \neq 0$).

4. Conclusions

From the results listed in Table 271 and shown in Figs. 88 and 89, we conclude the following:

(i) The experimental data consistently indicate D^0-$\bar{D}^0$ mixing. The no-mixing point $x = y = 0$ is excluded at $> 11.5\sigma$. The parameter x differs from zero with a significance of 8.2σ, and y differs from zero with a

[35] One can also use Eq. (16) of Ref. [1235] to reduce four parameters to three.

TABLE 271. Results of the global fit for different assumptions regarding *CPV*. The χ^2/d.o.f. for Fits no. 2 and no. 3 are considered satisfactory, although care should be taken when interpreting them in terms of probability due to unknown systematic uncertainties. The χ^2/d.o.f. for Fit no. 1 (no *CPV*) is large due to the LHCb measurement of $A_{CP}(K^+K^-) - A_{CP}(\pi^+\pi^-)$ [1192], which heavily disfavors both A_K and A_π being zero.

	No *CPV*	No subleading ampl. in indirect *CPV*	*CPV*-allowed	
Parameter	(Fit no. 1)	(Fit no. 2)	(Fit no. 3)	*CPV*-allowed 95% CL Interval
$x(\%)$	$0.44^{+0.13}_{-0.15}$	0.409 ± 0.048	$0.409^{+0.048}_{-0.049}$	$[0.313, 0.503]$
$y(\%)$	0.63 ± 0.07	$0.603^{+0.057}_{-0.056}$	$0.615^{+0.056}_{-0.055}$	$[0.509, 0.725]$
$\delta_{K\pi}(^\circ)$	$8.9^{+8.9}_{-9.8}$	$5.5^{+8.3}_{-9.9}$	$7.2^{+7.9}_{-9.2}$	$[-12.6, 21.8]$
$R_D(\%)$	0.344 ± 0.002	0.343 ± 0.002	0.343 ± 0.002	$[0.340, 0.347]$
$A_D(\%)$	…	…	-0.70 ± 0.36	$[-1.40, 0.00]$
$\lvert q/p\rvert$	…	1.005 ± 0.007	0.995 ± 0.016	$[0.96, 1.03]$
$\phi(^\circ)$	…	$-0.18^{+0.28}_{-0.29}$	-2.5 ± 1.2	$[-4.91, -0.19]$
$\delta_{K\pi\pi}(^\circ)$	…	$22.3^{+21.9}_{-23.0}$	$23.0^{+21.8}_{-22.9}$	$[-22.6, 64.9]$
$A_\pi(\%)$	$21.8^{+23.5}_{-23.9}$	0.027 ± 0.137	0.045 ± 0.137	$[-0.22, 0.31]$
$A_K(\%)$	…	-0.133 ± 0.136	-0.113 ± 0.137	$[-0.38, 0.15]$
$x_{12}(\%)$	…	0.409 ± 0.048	…	$[0.314, 0.503]$
$y_{12}(\%)$	…	$0.603^{+0.057}_{-0.056}$	…	$[0.495, 0.715]$
$\phi_{12}(^\circ)$	…	$0.58^{+0.91}_{-0.90}$	…	$[-1.20, 2.42]$
χ^2/d.o.f.	$98.68/52 = 1.90$	$66.27/53 = 1.25$	$63.64/51 = 1.25$	

TABLE 272. Individual contributions to the χ^2 for the all-*CPV*-allowed Fit 3.

Observable	Degrees of freedom	χ^2	$\sum\chi^2$
y_{CP} World Average (Fig. 85)	1	0.87	0.87
A_Γ World Average (Fig. 86)	1	0.24	1.12
$x_{K^0\pi^+\pi^-}$ Belle [1211]	1	0.59	1.70
$y_{K^0\pi^+\pi^-}$ Belle [1211]	1	3.61	5.32
$\lvert q/p\rvert_{K^0\pi^+\pi^-}$ Belle [1211]	1	0.65	5.97
$\phi_{K^0\pi^+\pi^-}$ Belle [1211]	1	0.63	6.60
$x_{CP}(K^0\pi^+\pi^-)$ LHCb 3 fb^{-1} [1214]	1	0.71	7.31
$y_{CP}(K^0\pi^+\pi^-)$ LHCb 3 fb^{-1} [1214]	1	0.11	7.42
$\Delta x(K^0\pi^+\pi^-)$ LHCb 3 fb^{-1} [1214]	1	0.11	7.53
$\Delta y(K^0\pi^+\pi^-)$ LHCb 3 fb^{-1} [1214]	1	0.02	7.54
$x_{CP}(K^0\pi^+\pi^-)$ LHCb 5.4 fb^{-1} [1193]	1	0.04	7.59
$y_{CP}(K^0\pi^+\pi^-)$ LHCb 5.4 fb^{-1} [1193]	1	1.11	8.70
$\Delta x(K^0\pi^+\pi^-)$ LHCb 5.4 fb^{-1} [1193]	1	0.01	8.71
$\Delta y(K^0\pi^+\pi^-)$ LHCb 5.4 fb^{-1} [1193]	1	−0.03	8.69
$x_{K^0h^+h^-}$ *BABAR* [1212]	1	0.84	9.52
$y_{K^0h^+h^-}$ *BABAR* [1212]	1	0.02	9.54
$x_{\pi^0\pi^+\pi^-}$ *BABAR* [1215]	1	0.66	10.20
$y_{\pi^0\pi^+\pi^-}$ *BABAR* [1215]	1	0.16	10.36
$(x^2+y^2)_{K^+\ell^-\nu}$ World Average (Fig. 84)	1	0.15	10.51
$x_{K^+\pi^-\pi^0}$ *BABAR* [1201]	1	7.24	17.75
$y_{K^+\pi^-\pi^0}$ *BABAR* [1201]	1	4.12	21.86
CLEOc [1200] $(x/y/R_D/\cos\delta/\sin\delta)$	5	10.32	32.19
$R_D^+/x'^{2+}/y'^+$ *BABAR* [1189]	3	8.45	40.63
$R_D^-/x'^{2-}/y'^-$ *BABAR* [1189]	3	4.17	44.80

(Table continued)

TABLE 272. *(Continued)*

Observable	Degrees of freedom	χ^2	$\sum\chi^2$
$R_D^+/x'^{2+}/y'^+$ Belle [1207]	3	1.93	46.73
$R_D^-/x'^{2-}/y'^-$ Belle [1207]	3	2.36	49.09
$R_D/x'^2/y'$ CDF [1208]	3	1.00	50.09
$R_D^+/x'^{2+}/y'^+$ LHCb D^* tag [1210]	3	1.40	51.49
$R_D^-/x'^{2-}/y'^-$ LHCb D^* tag [1210]	3	0.13	51.62
$R_D^+/x'^{2+}/y'^+$ LHCb $B \to D^*\mu X$ tag [1209]	3	0.62	52.24
$R_D^-/x'^{2-}/y'^-$ LHCb $B \to D^*\mu X$ tag [1209]	3	1.78	54.02
$A_{KK}/A_{\pi\pi}$ *BABAR* [1218]	2	0.35	54.38
$A_{KK}/A_{\pi\pi}$ Belle [1219]	2	1.45	55.83
$A_{KK}/A_{\pi\pi}$ CDF [1220]	2	4.08	59.91
$A_{KK} - A_{\pi\pi}$ LHCb [1192] (D^*, $B^0 \to D^0\mu X$ tags)	1	0.08	59.99
$(x^2+y^2)_{K^+\pi^-\pi^+\pi^-}$ LHCb [491]	1	3.65	63.64

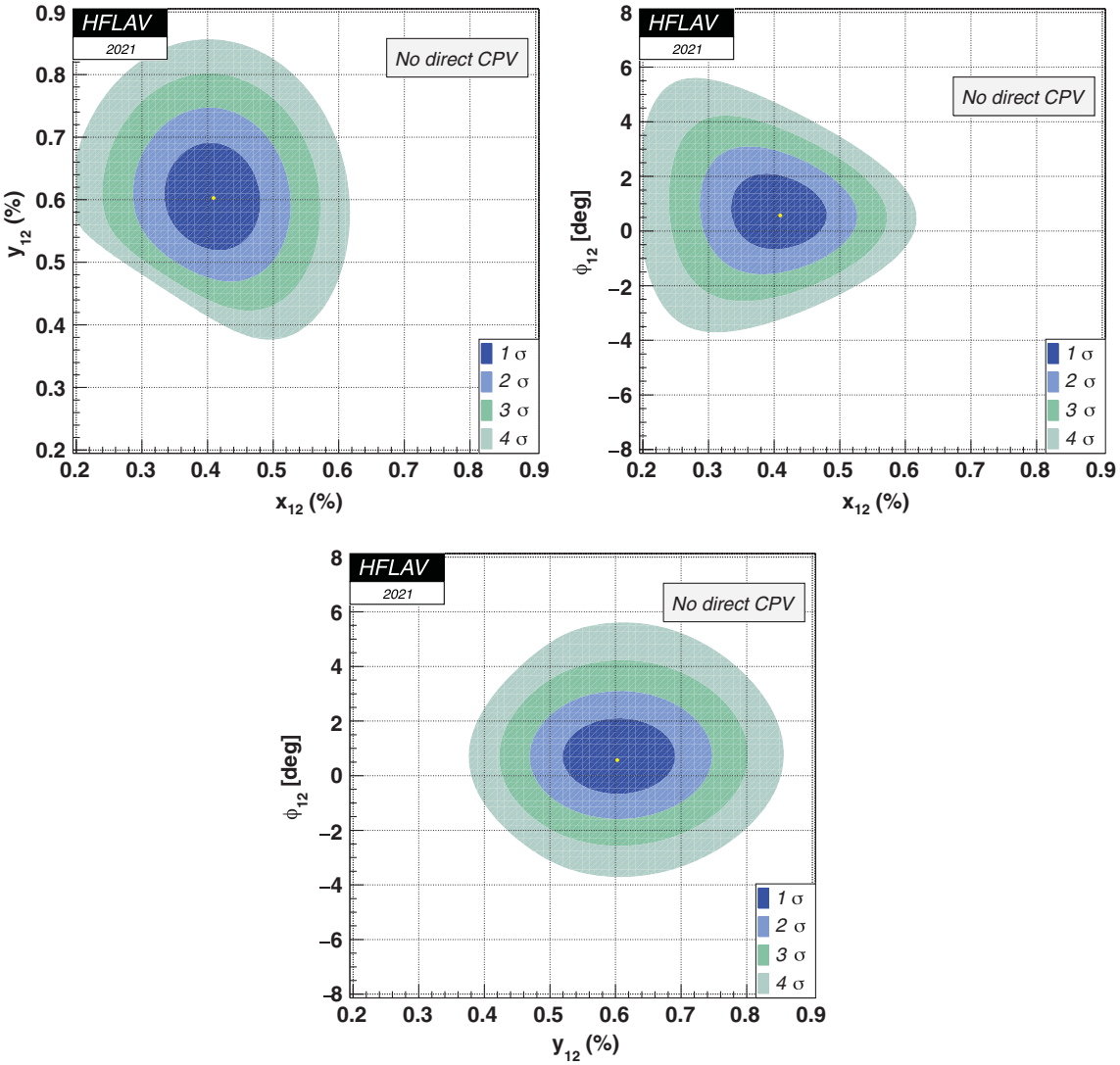

FIG. 87. Two-dimensional contours for theoretical parameters (x_{12}, y_{12}) (top left), (x_{12}, ϕ_{12}) (top right), and (y_{12}, ϕ_{12}) (bottom), under the assumption of no direct *CPV* in DCS decays (Fit 3).

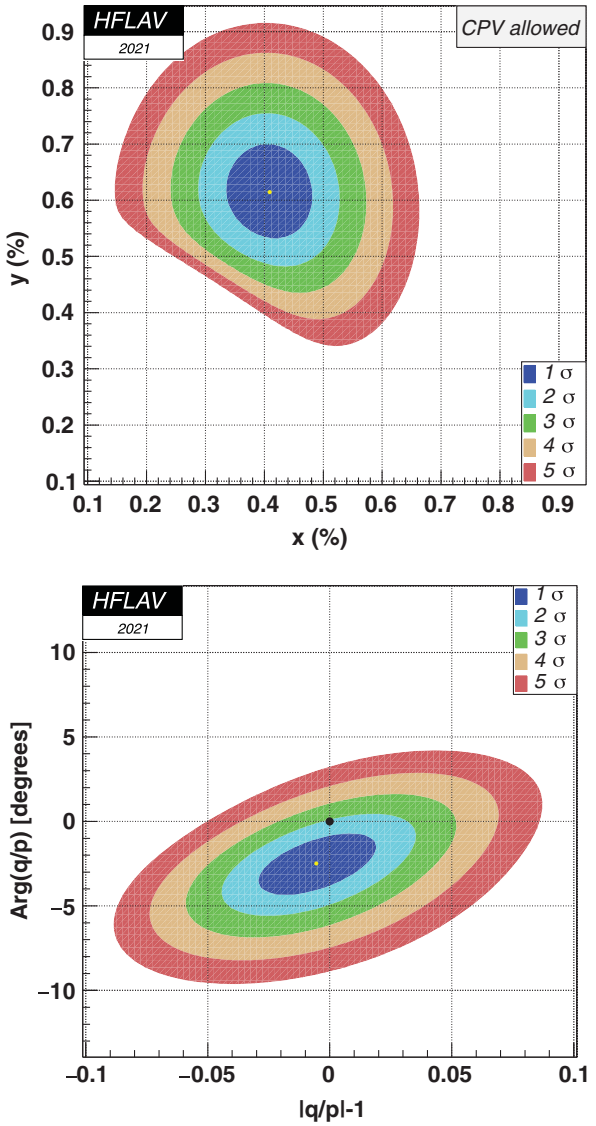

FIG. 88. Two-dimensional contours for parameters (x, y) (upper) and $(|q/p| - 1, \phi)$ (lower), allowing for CPV (fit 4).

significance $> 11.4\sigma$. Mixing at the observed level is dominated by long-distance processes, which are difficult to calculate.

(ii) Since y_{CP} is positive, the (mostly) CP-even state is shorter-lived, as in the K^0-$\bar{K}^0$ system. However, since x also appears to be positive, the (mostly) CP-even state is heavier, unlike in the K^0-$\bar{K}^0$ system.

(iii) There is no evidence for indirect CPV arising from D^0-$\bar{D}^0$ mixing ($|q/p| \neq 1$) or from a phase difference between the mixing amplitude and a direct decay amplitude ($\phi \neq 0$). The fitted values for these parameters differ from the no-CPV case with a statistical significance of 1.6σ, and more data is needed to indicate any indirect CPV. In contrast, small *direct* CPV (at the level of 0.15%) has been observed in time-integrated $D^0 \to K^+K^-, \pi^+\pi^-$ decays by LHCb [1192]. CP asymmetries are discussed in Sec. X B.

B. *CP* asymmetries

One manifestation of CP violation is a difference in decay rates between that of a particle and that of its CP-conjugate antiparticle [1238]. Such phenomena can be classified into two broad categories: *direct* CP violation and *indirect* CP violation [1239].

Direct CP violation refers to charm-changing $\Delta C = 1$ processes and can occur in both charged and neutral charm hadron decays. It results from interference between two different decay amplitudes, e.g., a penguin amplitude and a tree amplitude, that have different weak and strong phases. The weak phase difference between the interfering amplitudes ($\Delta\phi$) has opposite signs for $D \to f$ and $\bar{D} \to \bar{f}$ decays, while the strong phase difference ($\Delta\delta$) has the same sign. As a result, squaring the total amplitudes to obtain the decay rates gives an interference term proportional to $\cos(\Delta\phi + \Delta\delta)$ for $D \to f$ decays, and proportional to $\cos(-\Delta\phi + \Delta\delta)$ for $\bar{D} \to \bar{f}$ decays. Thus, the decay rates differ. This difference is time-independent and can be measured in time-integrated measurements.

In the Standard Model (SM), the strong-phase difference can arise due to differences in the final-state interactions (FSI) [1240], isospin amplitudes, intermediate-resonance contributions, or partial waves of the interfering decay amplitudes. A difference in weak phases arises from different CKM vertex factors, as is often the case for tree and penguin diagrams. Within the SM, direct CP violation is expected only in singly Cabibbo-suppressed (SCS) charm decays, as only these decays receive a non-negligible contribution from the penguin amplitude. This type of CP violation depends on the decay mode, and the CP asymmetries can reach the percent level.

Indirect CP violation refers to $\Delta C = 2$ processes and arises in D^0 decays due to D^0-$\bar{D}^0$ mixing. It can occur as an asymmetry in the mixing itself, or result from interference between a decay amplitude following mixing and a non-mixed amplitude. Within the SM, charm indirect CP violation is expected to be universal, i.e., independent of final state. Current experimental limits on indirect CP violation are discussed in Sec. X A.

The time-integrated CP asymmetry A_{CP} is defined as the difference between D and $\bar{D}$ partial widths divided by their sum:

$$A_{CP} = \frac{\Gamma(D) - \Gamma(\bar{D})}{\Gamma(D) + \Gamma(\bar{D})}. \tag{234}$$

In the case of D^+ and D_s^+ decays, A_{CP} measures direct CP violation; in the case of D^0 decays, A_{CP} measures direct and indirect CP violation combined (see also Sec. X D). Given experimental constraints on A_Γ, shown in Fig. 86, a contribution from indirect CP violation would be

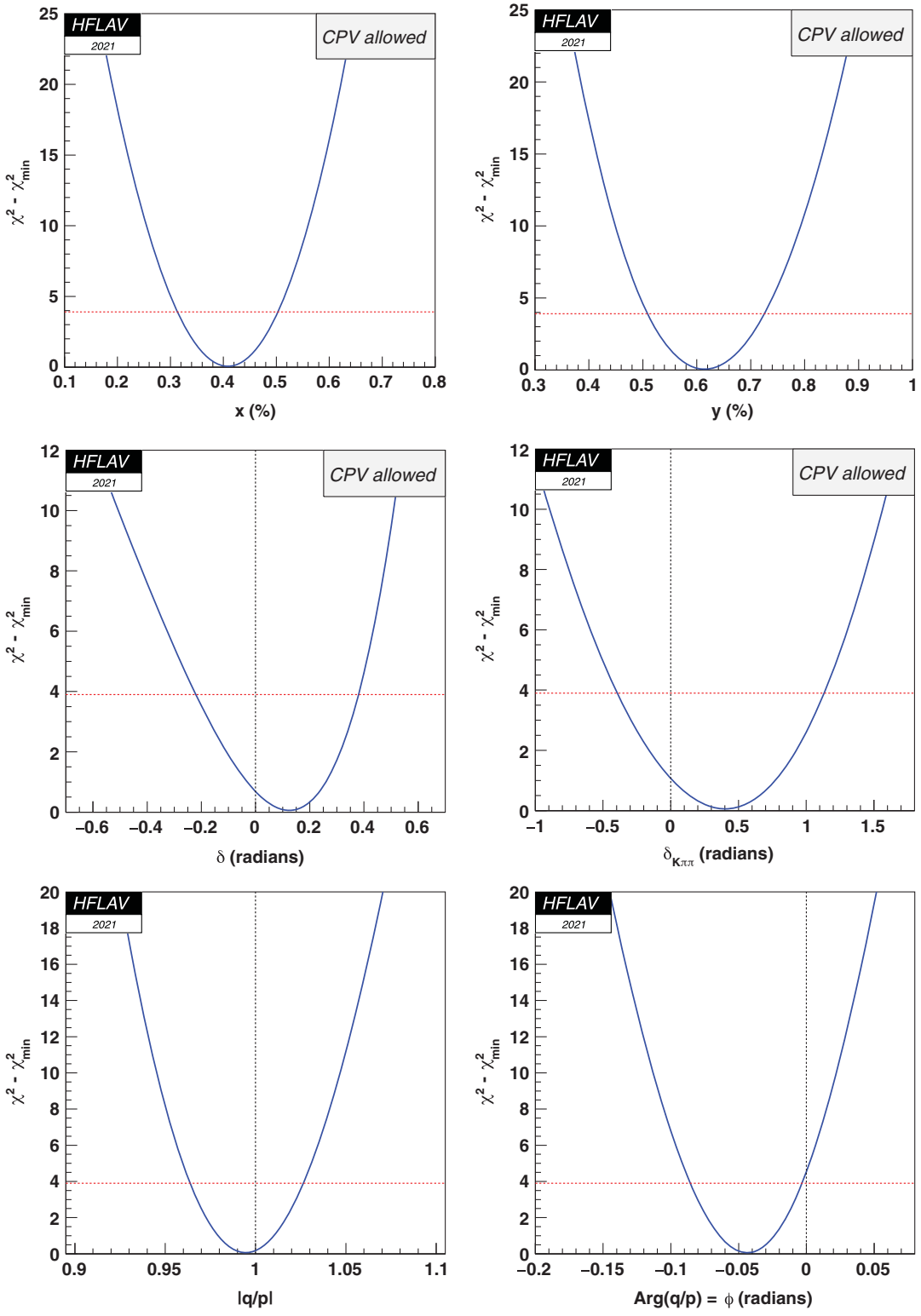

FIG. 89. The function $\Delta\chi^2 = \chi^2 - \chi^2_{\min}$ for fitted parameters $x, y, \delta, \delta_{K\pi\pi}, |q/p|$, and ϕ. The points where $\Delta\chi^2 = 3.84$ (denoted by dashed horizontal lines) determine 95% C.L. intervals.

TABLE 273. CP asymmetries $A_{CP} = [\Gamma(D^+) - \Gamma(D^-)]/[\Gamma(D^+) + \Gamma(D^-)]$ for two-body $D^\pm$ decays. For each entry, the first uncertainty is statistical, and the second is systematic. The third uncertainty in the $A_{CP}(D^+ \to \pi^+\eta')$ measurement from LHCb is due to $A_{CP}(D^+ \to \pi^+ K_S)$ used for calibration.

Mode	Year	Collaboration	A_{CP}
$D^+ \to \mu^+\nu$	2008	CLEO [1258]	$+0.08 \pm 0.08$
$D^+ \to \pi^+\pi^0$	2021	LHCb [1257]	$-0.013 \pm 0.009 \pm 0.006$
	2018	Belle [1256]	$+0.0231 \pm 0.0124 \pm 0.0023$
	2010	CLEO [1259]	$+0.029 \pm 0.029 \pm 0.003$
		HFLAV average	$+0.004 \pm 0.008$
$D^+ \to \pi^+\eta$	2021	LHCb [1257]	$-0.002 \pm 0.008 \pm 0.004$
	2011	Belle [1260]	$+0.0174 \pm 0.0113 \pm 0.0019$
	2010	CLEO [1259]	$-0.020 \pm 0.023 \pm 0.003$
		HFLAV average	$+0.003 \pm 0.007$
$D^+ \to \pi^+\eta'$	2017	LHCb [1261]	$-0.0061 \pm 0.0072 \pm 0.0053 \pm 0.0012$
	2011	Belle [1260]	$-0.0012 \pm 0.0112 \pm 0.0017$
	2010	CLEO [1259]	$-0.040 \pm 0.034 \pm 0.003$
		HFLAV average	-0.006 ± 0.007
$D^+ \to K^+\pi^0$	2021	LHCb [1257]	$-0.032 \pm 0.047 \pm 0.021$
	2010	CLEO [1259]	$-0.035 \pm 0.107 \pm 0.009$
		HFLAV average	-0.033 ± 0.046
$D^+ \to K^+\eta$	2021	LHCb [1257]	$-0.06 \pm 0.10 \pm 0.04$
$D^+ \to K_S\pi^+$	2014	CLEO [1262]	$-0.011 \pm 0.006 \pm 0.002$
	2012	Belle [1263]	$-0.00363 \pm 0.00094 \pm 0.00067$
	2011	*BABAR* [1264]	$-0.0044 \pm 0.0013 \pm 0.0010$
	2002	FOCUS [1265]	$-0.016 \pm 0.015 \pm 0.009$
		HFLAV average	-0.0041 ± 0.0009
$D^+ \to K_S K^+$	2018	BESIII [1243]	$-0.018 \pm 0.027 \pm 0.016$
	2013	*BABAR* [1266]	$+0.0013 \pm 0.0036 \pm 0.0025$
	2013	Belle [1267]	$-0.0025 \pm 0.0028 \pm 0.0014$
	2010	CLEO [1259]	$-0.002 \pm 0.015 \pm 0.009$
	2002	FOCUS [1265]	$+0.071 \pm 0.061 \pm 0.012$
		HFLAV average	-0.0011 ± 0.0025
$D^+ \to K_L K^+$	2018	BESIII [1243]	$-0.042 \pm 0.032 \pm 0.012$
$D^+ \to (\bar{K}^0/K^0)K^+$	2019	LHCb [1268]	$-0.00004 \pm 0.00061 \pm 0.00045$
	2013	*BABAR* [1266]	$+0.0046 \pm 0.0036 \pm 0.0025$
	2013	Belle [1267]	$-0.0008 \pm 0.0028 \pm 0.0014$
		HFLAV average	$+0.0001 \pm 0.0007$

negligible compared to current A_{CP} sensitivities. Values of A_{CP} for D^+, D^0 and D_s^+ decays are listed in Tables 273, 274, 275, 276, and 279 respectively. Modes with a single K_S meson in the final state can exhibit a CP asymmetry due to CP violation in K^0-$\bar{K}^0$ mixing [1241]; i.e., the rate for $\bar{K}^0 \to K_S$ differs slightly from that for $K^0 \to K_S$. This small effect is visible thus far only in $D^+ \to K_S\pi^+$ decays (see Table 273). For modes with a K^0 or $\bar{K}^0$ in the final state, the table entries are already corrected for this effect. The asymmetry for the DCS decay $D^0 \to K^+\pi^-$ is not included in these tables, as it is a by-product of charm-mixing measurements and thus is discussed in Sec. X A (where it is referred to as A_D).

In each experiment, care must be taken to correct for production and detection asymmetries, as they can reach the percent level. To take into account differences in production rates between D and $\bar{D}$, which would affect the number of respective decays observed, some experiments (such as E791 and FOCUS) normalize A_{CP} to that measured in a Cabibbo-favored mode. This method assumes there is negligible CP violation in the normalization mode. Explicitly, the CP asymmetry is calculated as

$$A_{CP} = \frac{\eta(D) - \eta(\bar{D})}{\eta(D) + \eta(\bar{D})}, \tag{235}$$

TABLE 274. *CP* asymmetries $A_{CP} = [\Gamma(D^+) - \Gamma(D^-)]/[\Gamma(D^+) + \Gamma(D^-)]$ for three- and four-body $D^{\pm}$ decays. For each entry, the first uncertainty is statistical, and the second (if quoted) is systematic.

Mode	Year	Collaboration	A_{CP}
$D^+ \to K_L e^+ \nu_e$	2015	BESIII [1269]	$-0.0059 \pm 0.0060 \pm 0.0148$
$D^+ \to \pi^+\pi^-\pi^+$	2014	LHCb [1270]	Model independent technique, no evidence for *CPV*
	1997	E791 [1271]	-0.017 ± 0.042 (stat.)
$D^+ \to K^-\pi^+\pi^+$	2014	D0 [1272]	$-0.0016 \pm 0.0015 \pm 0.0009$
	2014	CLEO [1262]	$-0.003 \pm 0.002 \pm 0.004$
		HFLAV average	-0.0018 ± 0.0016
$D^+ \to K_S\pi^+\pi^0$	2014	CLEO [1262]	$-0.001 \pm 0.007 \pm 0.002$
$D^+ \to K_S\pi^+\eta$	2020	BESIII [1273]	$-0.009 \pm 0.029 \pm 0.010$
$D^+ \to K_S K^+\pi^0$	2018	BESIII [1243]	$+0.014 \pm 0.037 \pm 0.024$
$D^+ \to K_L K^+\pi^0$	2018	BESIII [1243]	$-0.006 \pm 0.041 \pm 0.017$
$D^+ \to \phi[\to K^+K^-]\pi^+$	2019	LHCb [1268]	$+0.00003 \pm 0.00040 \pm 0.00029$
$D^+ \to K^+K^-\pi^+$	2014	CLEO [1262]	$-0.001 \pm 0.009 \pm 0.004$
	2013	*BABAR* [1274]	$+0.0037 \pm 0.0030 \pm 0.0015$
	2008	CLEO [1275]	Dalitz plot analysis, no evidence for *CPV*
	2000	FOCUS [1276]	$+0.006 \pm 0.011 \pm 0.005$
	1997	E791 [1271]	-0.014 ± 0.029 (stat.)
		HFLAV average	$+0.0032 \pm 0.0031$
$D^+ \to K^-\pi^+\pi^+\pi^0$	2014	CLEO [1262]	$-0.003 \pm 0.006 \pm 0.004$
$D^+ \to K_S\pi^+\pi^+\pi^-$	2014	CLEO [1262]	$+0.000 \pm 0.012 \pm 0.003$
$D^+ \to K_S K^+\pi^+\pi^-$	2005	FOCUS [1277]	$-0.042 \pm 0.064 \pm 0.022$
$D^+ \to \pi^+\pi^+\pi^-\eta$	2020	BESIII [1273]	$0.025 \pm 0.050 \pm 0.016$
$D^+ \to K^+\pi^+\pi^-\pi^0$	2020	BESIII [1278]	$-0.0004 \pm 0.0006 \pm 0.0001$

TABLE 275. *CP* asymmetries $A_{CP} = [\Gamma(D^0) - \Gamma(\bar{D}^0)]/[\Gamma(D^0) + \Gamma(\bar{D}^0)]$ for two-body $D^0, \bar{D}^0$ decays. In each entry, the first uncertainty is statistical, and the second (if quoted) is systematic, unless explicitly stated that they have been combined. The third uncertainty in the Belle and LHCb $A_{CP}(D^0 \to K_S K_S)$ measurements is due to A_{CP} of the normalization channels $D^0 \to K_S\pi^0$ (Belle) and $D^0 \to K^+K^-$ (LHCb).

Mode	Year	Collaboration	A_{CP}
$D^0 \to \pi^+\pi^-$	2017	LHCb [1279]	$+0.0007 \pm 0.0014 \pm 0.0011$
	2012	CDF [1280]	$+0.0022 \pm 0.0024 \pm 0.0011$
	2008	*BABAR* [1218]	$-0.0024 \pm 0.0052 \pm 0.0022$
	2012	Belle [1219]	$+0.0043 \pm 0.0052 \pm 0.0012$
	2002	CLEO [1224]	$+0.019 \pm 0.032 \pm 0.008$
	2000	FOCUS [1276]	$+0.048 \pm 0.039 \pm 0.025$
	1998	E791 [1281]	$-0.049 \pm 0.078 \pm 0.030$
		HFLAV average	$+0.0012 \pm 0.0014$
$D^0 \to \pi^0\pi^0$	2014	Belle [1282]	$-0.0003 \pm 0.0064 \pm 0.0010$
	2001	CLEO [1283]	$+0.001 \pm 0.048$ (stat and syst combined)
		HFLAV average	-0.0003 ± 0.0064
$D^0 \to K_S\pi^0$	2014	Belle [1282]	$-0.0021 \pm 0.0016 \pm 0.0007$
	2001	CLEO [1283]	$+0.001 \pm 0.013$ (stat and syst combined)
		HFLAV average	-0.0020 ± 0.0017
$D^0 \to K_S\eta$	2011	Belle [1284]	$+0.0054 \pm 0.0051 \pm 0.0016$

(Table continued)

TABLE 275. *(Continued)*

Mode	Year	Collaboration	A_{CP}
$D^0 \to K_S \eta'$	2011	Belle [1284]	$+0.0098 \pm 0.0067 \pm 0.0014$
$D^0 \to K_S K_S$	2021	LHCb [1285]	$-0.031 \pm 0.012 \pm 0.004 \pm 0.002$
	2017	Belle [1286]	$-0.0002 \pm 0.0153 \pm 0.0002 \pm 0.0017$
	2001	CLEO [1283]	-0.23 ± 0.19 (stat and syst combined)
		HFLAV average	-0.019 ± 0.010
$D^0 \to K^- \pi^+$	2014	CLEO [1262]	$+0.003 \pm 0.003 \pm 0.006$
$D^0 \to K^+ K^-$	2017	LHCb [1279]	$+0.0004 \pm 0.0012 \pm 0.0010$
	2012	CDF [1280]	$-0.0024 \pm 0.0022 \pm 0.0009$
	2008	*BABAR* [1218]	$+0.0000 \pm 0.0034 \pm 0.0013$
	2012	Belle [1219]	$-0.0043 \pm 0.0030 \pm 0.0011$
	2002	CLEO [1224]	$+0.000 \pm 0.022 \pm 0.008$
	2000	FOCUS [1276]	$-0.001 \pm 0.022 \pm 0.015$
	1998	E791 [1281]	$-0.010 \pm 0.049 \pm 0.012$
		HFLAV average	-0.0009 ± 0.0011

TABLE 276. *CP* asymmetries $A_{CP} = [\Gamma(D^0) - \Gamma(\bar{D}^0)]/[\Gamma(D^0) + \Gamma(\bar{D}^0)]$ for three- and four-body $D^0, \bar{D}^0$ decays. In each entry, the first uncertainty is statistical, and the second (if quoted) is systematic, unless explicitly stated that they have been combined. The Belle study of $D^0 \to K^+K^-\pi^+\pi^-$ [1287] employs a T-odd method for P-even variables, which corresponds to measuring a global A_{CP}.

Mode	Year	Collaboration	A_{CP}
$D^0 \to \pi^+\pi^-\pi^0$	2015	LHCb [1288]	Model-independent method, no evidence for *CPV*
	2008	*BABAR* [1247]	$+0.0031 \pm 0.0041 \pm 0.0017$
	2008	Belle [1289]	$+0.0043 \pm 0.0130$ (stat and syst combined)
	2005	CLEO [1290]	$+0.01^{+0.09}_{-0.07} \pm 0.05$
		HFLAV average	$+0.0032 \pm 0.0042$
$D^0 \to K^-\pi^+\pi^0$	2014	CLEO [1262]	$+0.001 \pm 0.003 \pm 0.004$
$D^0 \to K^-\pi^+\eta$	2020	BESIII [1273]	$-0.019 \pm 0.013 \pm 0.010$
$D^0 \to K^+\pi^-\pi^0$	2005	Belle [1291]	-0.006 ± 0.053 (stat)
	2001	CLEO [1292]	$+0.09^{+0.25}_{-0.22}$ (stat)
		HFLAV average	-0.0014 ± 0.0517
$D^0 \to K_S\pi^+\pi^-$	2012	CDF [1293]	$-0.0005 \pm 0.0057 \pm 0.0054$
	2004	CLEO [1294]	$-0.009 \pm 0.021^{+0.016}_{-0.057}$
		HFLAV average	-0.0008 ± 0.0077
$D^0 \to K_S\pi^0\eta$	2020	BESIII [1273]	$-0.039 \pm 0.032 \pm 0.008$
$D^0 \to K_S K^-\pi^+$	2016	LHCb [490]	Amplitude analysis, no evidence for *CPV*
$D^0 \to K_S K^+\pi^-$	2016	LHCb [490]	Amplitude analysis, no evidence for *CPV*
$D^0 \to K^+K^-\pi^0$	2008	*BABAR* [1247]	$-0.0100 \pm 0.0167 \pm 0.0025$
$D^0 \to \pi^+\pi^-\pi^+\pi^-$	2013	LHCb [1250]	Model-independent method, no evidence for *CPV*
$D^0 \to \pi^+\pi^-\pi^0\eta$	2020	BESIII [1273]	$-0.055 \pm 0.052 \pm 0.024$
$D^0 \to K^-\pi^+\pi^+\pi^-$	2014	CLEO [1262]	$+0.002 \pm 0.003 \pm 0.004$
$D^0 \to K^-\pi^+\pi^0\eta$	2020	BESIII [1273]	$-0.079 \pm 0.048 \pm 0.025$
$D^0 \to K^+\pi^-\pi^+\pi^-$	2005	Belle [1291]	-0.018 ± 0.044 (stat)

(Table continued)

TABLE 276. *(Continued)*

Mode	Year	Collaboration	A_{CP}
$D^0 \to K^+K^-\pi^+\pi^-$	2018	Belle [1287]	$+0.0034 \pm 0.0036 \pm 0.0006$
	2018	LHCb [1251]	Amplitude analysis, no evidence for *CPV*
	2013	LHCb [1250]	Model-independent method, no evidence for *CPV*
	2012	CLEO [1295]	Amplitude analysis, no evidence for *CPV*
	2005	FOCUS [1277]	$-0.082 \pm 0.056 \pm 0.047$
		HFLAV average	$+0.0032 \pm 0.0036$

where (considering, for example, $D^0 \to K^-K^+$)

$$\eta(D) = \frac{N(D^0 \to K^-K^+)}{N(D^0 \to K^-\pi^+)}, \tag{236}$$

$$\eta(\bar{D}) = \frac{N(\bar{D}^0 \to K^-K^+)}{N(\bar{D}^0 \to K^+\pi^-)}, \tag{237}$$

and $N(D \to f)$ is the number of $D \to f$ decays reconstructed. In this method there is the additional advantage that most corrections due to reconstruction inefficiencies cancel out, reducing systematic uncertainties.

Other experiments (such as Belle and LHCb) determine A_{CP} via the relation

$$A_{\text{meas}} = A_{CP} + A_{\text{prod}} + A_{\text{det}}, \tag{238}$$

where A_{meas} is the measured (raw) asymmetry, A_{prod} is the asymmetry in the charm hadron production, and A_{det} is due to a difference in detection efficiencies between positively and negatively charged hadrons. The production asymmetry at the LHC arises from a charge asymmetry of the colliding particles: in pp collisions more charm baryons are produced than antibaryons, and, as a result, charm mesons are less abundantly produced than anticharm mesons. Though not yet experimentally confirmed [1242], such a production asymmetry is expected to be dependent on the kinematics of the produced charm hadrons. The production asymmetry in e^+e^- collisions appears as a forward-backward (FB) asymmetry caused by an interference of the photon and off-shell Z^0 contributions. The detection asymmetries typically arise from differences in hadron interactions with detector material. In particular, the interaction cross sections for K^+ and K^- significantly differ, with the differences being dependent on the kaon momentum.

The B-factory strategy to separate the production and CP asymmetries relies on the former being odd, while the latter is even, with respect to the center-of-mass production polar angle (θ^*). The A_{meas} is measured in $|\cos\theta^*|$ bins and subsequently averaged; this removes the A_{prod} contribution. At LHCb, the production asymmetry is removed by measuring A_{CP} for D^*-tagged $D^0 \to K^-\pi^+$ decays; this also corrects for the soft π detection asymmetry. Subsequently, $D^+ \to K^-\pi^+\pi^+$ decays are used to correct for the detection asymmetry introduced by the $K^-\pi^+$ system itself, and $D^+ \to K_S\pi^+$ decays are then used to remove the asymmetries in D^+ production and π^+ detection. Finally, the asymmetry related to the neutral kaon, i.e., from regeneration and different interactions of K^0 and $\bar{K}^0$ with the detector, as well as from CP violation occurring in the K^0-$\bar{K}^0$ mixing, is calculated. Put together, this gives

$$\begin{aligned} A_{CP}(K^+K^-) = {} & A_{\text{meas}}(K^+K^-) - A_{\text{meas}}(K^-\pi^+) \\ & + A_{\text{meas}}(K^-\pi^+\pi^+) - A_{\text{meas}}(K_S\pi^+) \\ & + A(\bar{K}^0 - K^0). \end{aligned}$$

For some decays, typically the ones with lower statistics, one corrects for nuisance asymmetries by measuring A_{CP} relative to some well-measured reference channel, for instance

$$\begin{aligned} A_{CP}(D_s^+ \to \eta'\pi^+) = {} & A_{\text{meas}}(D_s^+ \to \eta'\pi^+) - A_{\text{meas}}(D_s^+ \to \phi\pi^+) \\ & + A_{CP}(D_s^+ \to \phi\pi^+). \end{aligned}$$

The uncertainty of the reference A_{CP} is treated as an external-input uncertainty.

There are also A_{CP} measurements performed recently for $D^+_{(s)}$ decays by BESIII using data collected at the $D_{(s)}\bar{D}_{(s)}$ threshold. Employing the double-tag technique, where both charm mesons produced are reconstructed, results in quite a limited statistical sensitivity. Therefore any impact of the production asymmetry, expected to be smaller than at the B-factories, would have a negligible impact and is not corrected for. Some of these BESIII measurements are for final states involving K_L [1243,1244], which makes them unique. Measurements of A_{CP} *differences*, denoted ΔA_{CP}, are often easier to interpret theoretically than individual A_{CP} measurements. The most important difference is that for $D^0 \to K^+K^-$ and $D^0 \to \pi^+\pi^-$ decays, which is discussed in Sec. X D. Notably, its measurement by LHCb, $\Delta A_{CP} = (-15.4 \pm 2.9) \times 10^{-4}$, constitutes the first observation of CP violation in the charm sector [1192]. The difference ΔA_{CP} of CP asymmetries for the baryon decays $\Lambda_c^+ \to pK^+K^-$ and $\Lambda_c^+ \to p\pi^+\pi^-$ was recently measured by LHCb [1245]. We note that, in the limit of U-spin symmetry, direct CP violation in $D^0 \to K^+K^-$ and $D^0 \to \pi^+\pi^-$ decays is

TABLE 277. CP asymmetries $A_{CP} = [\Gamma(D^0) - \Gamma(\bar{D}^0)]/[\Gamma(D^0) + \Gamma(\bar{D}^0)]$ for rare $D^0, \bar{D}^0$ decays. In each entry, the first uncertainty is statistical, and the second is systematic.

Mode	Year	Collaboration	A_{CP}
$D^0 \to K^{*0}[\to K^-\pi^+]\gamma$	2016	Belle [1296]	$-0.003 \pm 0.020 \pm 0.000$
$D^0 \to \phi[\to K^+K^-]\gamma$	2016	Belle [1296]	$-0.094 \pm 0.066 \pm 0.001$
$D^0 \to \rho^0[\to \pi^+\pi^-]\gamma$	2016	Belle [1296]	$+0.056 \pm 0.152 \pm 0.006$
$D^0 \to K^+K^-\mu^+\mu^-$	2018	LHCb [1297]	$+0.00 \pm 0.11 \pm 0.02$
$D^0 \to \pi^+\pi^-\mu^+\mu^-$	2018	LHCb [1297]	$+0.049 \pm 0.038 \pm 0.007$

expected to have equal magnitude but opposite sign [1246]; thus the measurement of ΔA_{CP} "doubles" the effect. However, no such U-spin argument exists for $\Lambda_c^+ \to pK^+K^-$ and $\Lambda_c^+ \to p\pi^+\pi^-$ decays.

Direct CP asymmetries require the presence of both weak and strong phase differences. The larger these phase differences are, the larger the CP asymmetry. Strong phase differences typically vary over the phase space of multibody decays, which usually proceed via intermediate states; thus, local CP asymmetries, i.e., those corresponding to a local region of phase space or those involving specific intermediate states, can offer better sensitivity to CP violation than a global asymmetry. Probing the multibody phase space is often done in a model-dependent way by employing a Dalitz-plot analysis or, more generally, an amplitude analysis, separately for D and $\bar{D}$ decays. A CP asymmetry is then determined for each contributing amplitude. The CP-violating observables are asymmetries in magnitudes and phases of CP-conjugate amplitudes, as well as asymmetries in the amplitude fit fractions.

For multibody decays, some experiments use model-independent techniques to search for local CP asymmetries. One technique (see Refs. [1247,1248]) uses a binned χ^2 approach to compare the relative density in a bin of phase space for $D \to f$ with that of the CP-conjugate decay. Another technique (the "energy test technique" [1249]) uses a test statistic variable (T) to determine the average distance between events in phase space. If the distribution of events in two CP-conjugate samples are identical (the CP-symmetric case), T will fluctuate around a value close to zero. This technique yields a p-value for the no-CP violation hypothesis and identifies any CP-asymmetric phase space regions.

CP asymmetries measured for charm-meson decays are listed in Tables 273, 274, 275, 276, 277, 279, and 280. The asymmetries for three- and four-body decays are reported for their observed final state, i.e., resonant substructure is implicitly included but not considered separately. Most asymmetries measured for three- and four-body channels are still only global asymmetries. The reported model-independent tests, which attempt to probe the decay phase space, yield p-values typically at the level of a few percent or higher and thus are consistent with no CP violation. The lowest p-value of 0.6%, corresponding to a significance for CP violation of 2.7σ, is obtained for the P-odd (parity-odd) test of $D^0 \to \pi^+\pi^-\pi^+\pi^-$ decays [1250]. This implies that the effect, if not a statistical fluctuation, originates in a P-odd amplitude such as $D^0 \to [\rho^0\rho^0]_{L=1}$. For $D^0 \to K^+K^-\pi^+\pi^-$ decays [1251], a model-dependent amplitude analysis was performed, and CP asymmetries were measured for 25 intermediate amplitudes. The uncertainties on these asymmetries ranged from 1% to 15% and were dominated by statistical errors. No significant CP violation was observed, and the most significant asymmetry of 2.8σ was observed for the phase of the P-odd amplitude $D^0 \to [\phi(1020)\rho(1450)^0]_{L=1}$. CP violation arising through P violation is discussed further in Sec. X C.

CP asymmetries have also been measured for decays classified as rare: radiative modes $D^0 \to V\gamma$, with $V = \bar{K}^{*0}, \phi(1020), \rho^0$, as well as dimuon decays $D^0 \to \pi^+\pi^-\mu^+\mu^-$ and $D^0 \to K^+K^-\mu^+\mu^-$ (see Table 277). For the dimuon modes, in addition to their global asymmetries listed in Table 276, CP asymmetries in bins of the dimuon invariant mass have been measured by LHCb for the ranges with significant signal yields. They are given in Table 278. Asymmetries for mass regions away from $\mu^+\mu^-$ production via η, $\rho - \omega$ or ϕ decays still have very limited sensitivities,

TABLE 278. CP asymmetries of $D^0, \bar{D}^0 \to h^+h^-\mu^+\mu^-$ decays in different dimuon invariant mass ranges, measured by LHCb. In each entry, the first uncertainty is statistical, and the second is systematic. Measurements are not performed for mass intervals with insignificant signal yields.

Mode	$m(\mu^+\mu^-)$ [MeV/c^2]	A_{CP}
$D^0 \to K^+K^-\mu^+\mu^-$ [1297]	<525	$+0.17 \pm 0.20 \pm 0.02$
	525–565	…
	565–780	$-0.129 \pm 0.071 \pm 0.007$
	780–950	$+0.17 \pm 0.10 \pm 0.01$
	950–1020	$+0.075 \pm 0.065 \pm 0.007$
	1020–1100	$+0.099 \pm 0.055 \pm 0.007$
$D^0 \to \pi^+\pi^-\mu^+\mu^-$ [1297]	<525	$-0.33 \pm 0.26 \pm 0.04$
	525–565	…
	>565	$+0.13 \pm 0.02 \pm 0.01$

TABLE 279. *CP* asymmetries $A_{CP} = [\Gamma(D_s^+) - \Gamma(D_s^-)]/[\Gamma(D_s^+) + \Gamma(D_s^-)]$ for two-body $D_s^\pm$ decays. In each entry, the first uncertainty is statistical and the second is systematic. The third uncertainty in $A_{CP}(D_s^+ \to \pi^+\eta')$ from LHCb is due to $A_{CP}(D^+ \to \pi^+\phi)$ used for calibration.

Mode	Year	Collaboration	A_{CP}
$D_s^+ \to \mu^+\nu$	2009	CLEO [1298]	$+0.048 \pm 0.061$
$D_s^+ \to \pi^+\eta$	2021	Belle [1299]	$+0.002 \pm 0.003 \pm 0.003$
	2021	LHCb [1257]	$+0.008 \pm 0.007 \pm 0.005$
	2013	CLEO [1300]	$+0.011 \pm 0.030 \pm 0.008$
		HFLAV average	$+0.003 \pm 0.004$
$D_s^+ \to \pi^+\eta'$	2017	LHCb [1261]	$-0.0082 \pm 0.0036 \pm 0.0022 \pm 0.002$
	2013	CLEO [1300]	$-0.022 \pm 0.022 \pm 0.006$
		HFLAV average	-0.0088 ± 0.0049
$D_s^+ \to K_S\pi^+$	2013	*BABAR* [1266]	$+0.006 \pm 0.020 \pm 0.003$
	2010	Belle [1301]	$+0.0545 \pm 0.0250 \pm 0.0033$
	2010	CLEO [1259]	$+0.163 \pm 0.073 \pm 0.003$
		HFLAV average	$+0.0311 \pm 0.0154$
$D_s^+ \to (K^0/\bar{K}^0)\pi^+$	2019	LHCb [1268]	$+0.0016 \pm 0.0017 \pm 0.0005$
	2013	*BABAR* [1266]	$+0.003 \pm 0.020 \pm 0.003$
		HFLAV average	$+0.0016 \pm 0.0018$
$D_s^+ \to K_S K^+$	2019	BESIII [1244]	$+0.006 \pm 0.028 \pm 0.006$
	2013	CLEO [1300]	$+0.026 \pm 0.015 \pm 0.006$
	2013	*BABAR* [1266]	$-0.0005 \pm 0.0023 \pm 0.0024$
	2010	Belle [1301]	$+0.0012 \pm 0.0036 \pm 0.0022$
		HFLAV average	$+0.0008 \pm 0.0026$
$D_s^+ \to K_L K^+$	2019	BESIII [1244]	$-0.011 \pm 0.026 \pm 0.006$
$D_s^+ \to K^+\pi^0$	2021	LHCb [1257]	$-0.008 \pm 0.039 \pm 0.012$
	2021	Belle [1299]	$+0.064 \pm 0.044 \pm 0.011$
	2010	CLEO [1259]	$+0.266 \pm 0.228 \pm 0.009$
		HFLAV average	$+0.020 \pm 0.030$
$D_s^+ \to K^+\eta$	2021	Belle [1299]	$+0.021 \pm 0.021 \pm 0.004$
	2021	LHCb [1257]	$+0.009 \pm 0.037 \pm 0.011$
	2010	CLEO [1259]	$+0.093 \pm 0.152 \pm 0.009$
		HFLAV average	$+0.019 \pm 0.019$
$D_s^+ \to K^+\eta'$	2010	CLEO [1259]	$+0.060 \pm 0.189 \pm 0.009$

TABLE 280. *CP* asymmetries $A_{CP} = [\Gamma(D_s^+) - \Gamma(D_s^-)]/[\Gamma(D_s^+) + \Gamma(D_s^-)]$ for multibody $D_s^\pm$ decays measured by CLEO in 2013 [1300]. In each entry, the first uncertainty is statistical, and the second is systematic.

Mode	A_{CP}
$D_s^+ \to \pi^+\pi^+\pi^-$	$-0.007 \pm 0.030 \pm 0.006$
$D_s^+ \to \pi^+\pi^0\eta$	$-0.005 \pm 0.039 \pm 0.020$
$D_s^+ \to \pi^+\pi^0\eta'$	$-0.004 \pm 0.074 \pm 0.019$
$D_s^+ \to K_S K^+\pi^0$	$-0.016 \pm 0.060 \pm 0.011$
$D_s^+ \to K_S K_S\pi^+$	$+0.031 \pm 0.052 \pm 0.006$
$D_s^+ \to K^+\pi^+\pi^-$	$+0.045 \pm 0.048 \pm 0.006$
$D_s^+ \to K^+K^-\pi^+$	$-0.005 \pm 0.008 \pm 0.004$
$D_s^+ \to K_S K^-\pi^+\pi^+$	$+0.041 \pm 0.027 \pm 0.009$
$D_s^+ \to K_S K^+\pi^+\pi^-$	$-0.057 \pm 0.053 \pm 0.009$
$D_s^+ \to K^+K^-\pi^+\pi^0$	$+0.000 \pm 0.027 \pm 0.012$

with uncertainties ranging from 12% to 26%. These nonresonance regions are particularly important for new physics searches (see Sec. XI F). Overall, *CP* asymmetries have been measured for more than 50 charm decay modes, and in several modes the uncertainty on A_{CP} is well below 5×10^{-3}. Only the modes $D^0 \to K^+K^-$ and $D^0 \to \pi^+\pi^-$ exhibit any *CP* violation. The *CP* asymmetry observed for the mode $D^+ \to K_S\pi^+$ is consistent with that expected from K^0-$\bar{K}^0$ mixing [1241]; thus, it is not attributed to direct *CP* violation in charm but to the K^0-$\bar{K}^0$ mixing.

In the charm baryon sector, there is no evidence of *CP* violation. Until recently, there were only two measurements for Λ_c^+; these were performed by CLEO [1252] and FOCUS [1253] and had limited sensitivity. The CLEO measurement used the semileptonic decay $\Lambda_c^+ \to \Lambda e^+\nu_e$, while the FOCUS measurement used the CF decay

$\Lambda_c^+ \to \Lambda\pi^+$. Both searched for CP violation through an angular analysis. Exploiting the Λ helicity angle, CP violation was probed by comparing the P (parity) asymmetry in decays of Λ_c^+ and Λ_c^-. This was done by measuring the weak-asymmetry parameters α_{Λ_c} and $\alpha_{\bar{\Lambda}_c}$, respectively. The α_{Λ_c} ($\alpha_{\bar{\Lambda}_c}$) parameter is defined as the difference between the rates of the Λ_c^+ (Λ_c^-) decays occurring through Λ ($\bar{\Lambda}$) with helicity $+\frac{1}{2}$ and $-\frac{1}{2}$; it thus describes a longitudinal polarization of the Λ ($\bar{\Lambda}$) baryon.

The α_{Λ_c} parameter is accessed through studying an angular distribution, which for $\Lambda_c^+ \to \Lambda\pi^+$ decays followed by $\Lambda \to p\pi^-$ is given by

$$\frac{d\Gamma}{d\cos\theta_p} \simeq 1 + \alpha_{\Lambda_c}\alpha_\Lambda \cos\theta_p, \tag{239}$$

where θ_p is the Λ helicity angle, defined as the angle between the momentum vector of the proton in the Λ rest frame and the Λ momentum in the Λ_c^+ rest frame. A weak-asymmetry parameter for $\Lambda \to p\pi^-$ decays, α_Λ, is defined similar to α_{Λ_c} but considering the proton helicities of $\pm\frac{1}{2}$. The corresponding angular distribution for charge conjugate process, $\Lambda_c^- \to \bar{\Lambda}\pi^-$ with $\bar{\Lambda} \to \bar{p}\pi^+$, involves $\alpha_{\bar{\Lambda}_c}$ and $\alpha_{\bar{\Lambda}}$. The weak-asymmetry parameters for the Λ and $\bar{\Lambda}$ decays are well measured [9] and used as external parameters. An angular distribution of the semileptonic decays $\Lambda_c^+ \to \Lambda e^+\nu_e$ is more complicated, owing to contribution from one more weakly decaying system, $W^+ \to e^+\nu_e$ (see Sec. XI A). Therefore, in addition to the Λ helicity angle, it also depends on the W^+ helicity angle, an angle between the decay planes of the W^+ and Λ, as well as $q^2 \equiv m^2(e^+\nu_e)$, making the CLEO measurement a four-dimensional analysis [1252].

As $\alpha_{\Lambda_c} = -\alpha_{\bar{\Lambda}_c}$ in the case of P-parity conservation, the CP-violating asymmetry is defined as

$$A_{CP}^{\alpha} = \frac{\alpha_{\Lambda_c} + \alpha_{\bar{\Lambda}_c}}{\alpha_{\Lambda_c} - \alpha_{\bar{\Lambda}_c}}. \tag{240}$$

The CLEO measurement [1252] gives

$$A_{CP}^{\alpha}(\Lambda_c^+ \to \Lambda e^+\nu_e) = 0.00 \pm 0.03 \pm 0.01 \pm 0.02,$$

where the third error is related to the uncertainty of the Λ weak-asymmetry parameter. The asymmetry measured by FOCUS [1253] is

$$A_{CP}^{\alpha}(\Lambda_c^+ \to \Lambda\pi^+) = -0.07 \pm 0.19 \pm 0.12.$$

This method of accessing CP violation occurring through P violation has also been applied by Belle [1254] to the channel $\Xi_c^0 \to \Xi^-\pi^+, \Xi^- \to \Lambda\pi^-$. Belle measures

$$A_{CP}^{\alpha}(\Xi_c^0 \to \Xi^-\pi^+) = 0.015 \pm 0.052 \pm 0.017.$$

The first high-statistics CPV measurement of charm baryons comes from LHCb in the form of ΔA_{CP} for the $\Lambda_c^+ \to pK^+K^-$ and $\Lambda_c^+ \to p\pi^+\pi^-$ SCS decays [1245], where the result is

$$\begin{aligned}\Delta A_{CP}(\Lambda_c^+ \to ph^+h^-) &\equiv A_{CP}(pK^+K^-) - A_{CP}(p\pi^+\pi^-) \\ &= 0.003 \pm 0.009 \pm 0.006.\end{aligned}$$

The measurement, performed in a phase-space-integrated manner, has limited sensitivity and does not facilitate an interpretation. However, the production asymmetry between Λ_c^+ and Λ_c^- baryons cancels in this difference. Given the potentially rich dynamics of these decays in their five-dimensional phase space,[36] ΔA_{CP} measured in phase-space regions or a model-dependent measurement of intermediate amplitude asymmetries would be very desirable.

For charm decays, one can construct various SU(3)-based sum rules which, in addition to testing SU(3) symmetry itself, are also useful for performing model-independent tests of the SM. Particularly useful are sum rules exploiting SU(3) subgroups such as U-spin or isospin (I), as they involve fewer decays and offer more precise tests. While U-spin symmetry in charm decays is broken by a non-negligible amount due to the s-quark mass, isospin symmetry holds at the $(m_u - m_d)$ level and thus is very precise. Important for our considerations are isospin sum rules that relate individual CP asymmetries of the isospin-related processes. Verifying such rules allows for tests to be performed with reduced uncertainty from strong interaction effects.

Such a sum rule has been proposed for $D \to \pi\pi$ decays in Ref. [1255]. Following the phase convention of [1255], the isospin decomposition of $D \to \pi\pi$ amplitudes gives

$$\begin{aligned}A_{\pi^+\pi^-} &= \sqrt{2}\mathcal{A}_3 + \sqrt{2}\mathcal{A}_1, \\ A_{\pi^0\pi^0} &= 2\mathcal{A}_3 - \mathcal{A}_1, \\ A_{\pi^+\pi^0} &= 3\mathcal{A}_3,\end{aligned}$$

where $\mathcal{A}_1$ and $\mathcal{A}_3$ are amplitudes corresponding to the $\Delta I = 1/2$ and $\Delta I = 3/2$ transitions, respectively (i.e., transitions to $\pi\pi$ final states with $I = 0$ and $I = 2$). From this, one can get an amplitude isospin sum rule

$$\frac{1}{\sqrt{2}}A_{\pi^+\pi^-} + A_{\pi^0\pi^0} - A_{\pi^+\pi^0} = 0. \tag{241}$$

[36]For unpolarized Λ_c, the decay phase space reduces to a two-dimensional Dalitz distribution.

Probing such a sum requires knowledge of strong phases, which are accessible only at charm-threshold experiments. However, without this knowledge the sum of differences of decay rates for D and $\bar{D}$ decays can be measured:

$$|A_{\pi^+\pi^-}|^2 - |\bar{A}_{\pi^+\pi^-}|^2 + |A_{\pi^0\pi^0}|^2 - |\bar{A}_{\pi^0\pi^0}|^2 - \frac{2}{3}(|A_{\pi^+\pi^0}|^2 - |\bar{A}_{\pi^-\pi^0}|^2) = 3(|\mathcal{A}_1|^2 - |\bar{\mathcal{A}}_1|^2). \quad (242)$$

This equation suggests several SM tests. As the penguin amplitude is, to excellent approximation within the SM, purely $\Delta I = 1/2$, any CP asymmetry observed in $D^+ \to \pi^+\pi^0$ would be a sign of new physics in the $\Delta I = 3/2$ amplitude. If the sum in Eq. (242), depending only on $\mathcal{A}_1$, is found to be nonzero, this would mean that CP violation arises from the $\Delta I = 1/2$ transitions. Moreover, a scenario in which the sum in Eq. (242) is zero and individual asymmetries are nonzero would suggest new physics contributing to the $\Delta I = 3/2$ amplitude.

To facilitate an experimental test, one can exploit also the sum of decay rates:

$$|A_{\pi^+\pi^-}|^2 + |\bar{A}_{\pi^+\pi^-}|^2 + |A_{\pi^0\pi^0}|^2 + |\bar{A}_{\pi^0\pi^0}|^2 - \frac{2}{3}(|A_{\pi^+\pi^0}|^2 + |\bar{A}_{\pi^-\pi^0}|^2) = 3(|\mathcal{A}_1|^2 + |\bar{\mathcal{A}}_1|^2). \quad (243)$$

Dividing Eq. (242) by Eq. (243) gives

$$R \equiv \frac{|A_{\pi^+\pi^-}|^2 - |\bar{A}_{\pi^+\pi^-}|^2 + |A_{\pi^0\pi^0}|^2 - |\bar{A}_{\pi^0\pi^0}|^2 - \frac{2}{3}(|A_{\pi^+\pi^0}|^2 - |\bar{A}_{\pi^-\pi^0}|^2)}{|A_{\pi^+\pi^-}|^2 + |\bar{A}_{\pi^+\pi^-}|^2 + |A_{\pi^0\pi^0}|^2 + |\bar{A}_{\pi^0\pi^0}|^2 - \frac{2}{3}(|A_{\pi^+\pi^0}|^2 + |\bar{A}_{\pi^-\pi^0}|^2)}. \quad (244)$$

Note that the last term of the denominator enters with the sign opposite compared to the one in the sum tested in Refs. [1256,1257]. An advantage of the ratio in Eq. (244) is that it corresponds to the CP asymmetry in the $\Delta I = 1/2$ process and has no dependence on the $\Delta I = 3/2$ amplitude, which facilitates an interpretation.

Relating the amplitude, the branching fraction, the lifetime, and the asymmetry with $|A|^2 \propto \mathcal{B}/\tau_D$ and $|A|^2 - |\bar{A}|^2 = A_{CP}(|A|^2 + |\bar{A}|^2)$, we rewrite Eq. (244) as

$$R = \frac{A_{CP}(D^0 \to \pi^+\pi^-)}{1 + \frac{\tau_{D^0}}{\mathcal{B}_{+-}}(\frac{\mathcal{B}_{00}}{\tau_{D^0}} - \frac{2}{3}\frac{\mathcal{B}_{+0}}{\tau_{D^+}})} + \frac{A_{CP}(D^0 \to \pi^0\pi^0)}{1 + \frac{\tau_{D^0}}{\mathcal{B}_{00}}(\frac{\mathcal{B}_{+-}}{\tau_{D^0}} - \frac{2}{3}\frac{\mathcal{B}_{+0}}{\tau_{D^+}})} + \frac{A_{CP}(D^+ \to \pi^+\pi^0)}{1 - \frac{3}{2}\frac{\tau_{D^+}}{\mathcal{B}_{+0}}(\frac{\mathcal{B}_{00}}{\tau_{D^0}} + \frac{\mathcal{B}_{+-}}{\tau_{D^0}})}, \quad (245)$$

where $\mathcal{B}_{+-}$, $\mathcal{B}_{00}$, and $\mathcal{B}_{+0}$ denote the branching fractions for $D^0 \to \pi^+\pi^-$, $D^0 \to \pi^0\pi^0$, and $D^+ \to \pi^+\pi^0$, respectively. The sum R is calculated using our averages for CP asymmetries (Tables 273 and 275) and PDG averages [9] for branching fractions and lifetimes. The result is

$$R = (+0.09 \pm 3.22) \times 10^{-3}, \quad (246)$$

which is consistent with zero. In addition, all the individual asymmetries contributing to R are consistent with zero. The uncertainty on R is dominated by the uncertainties on individual asymmetries.

The sum rule for $D \to \bar{K}K$ decays involves full SU(3) considerations and thus is imprecise. Reference [1255] proposes a set of isospin sum rules for $D \to \rho\pi$ or $D \to \bar{K}^{(*)}K^{(*)}\pi$, but to test these sum rules requires a number of experimental measurements that have not yet been performed.

C. *T*-odd asymmetries

Measuring T-odd asymmetries provides a complementary way to search for CP violation in the charm sector, exploiting CPT invariance. T-odd asymmetries are measured using triple-products of the form $\vec{a} \cdot (\vec{b} \times \vec{c})$, where a, b, and c are spins or momenta. This combination is odd under time reversal (T). If a triple product is formed using *both* spin and momenta, i.e.,

$$\overrightarrow{s_1} \cdot (\overrightarrow{p_2} \times \overrightarrow{p_3}),$$

it can be even under P-conjugation. However, if only momenta are used, i.e.,

$$\overrightarrow{p_1} \cdot (\overrightarrow{p_2} \times \overrightarrow{p_3}),$$

it is odd under P-conjugation. Thus, in this case the T-odd method becomes P-odd and allows one to probe CP violation occurring via P violation. This type of CPV, arising in P-odd amplitudes, can be studied in decays of mesons into final states with at least four spinless particles. Two- and three-body hadronic decays of charm mesons to spinless particles involve only P-even amplitudes,[37] for which CP violation can arise only through C-violation.

Taking as an example the decay mode $D^0 \to K^+K^-\pi^+\pi^-$, involving spinless particles only, one forms a triple-product correlation using momenta of the final-state particles in the D^0 center-of-mass frame.[38] Defining the T-odd (and P-odd) correlation for D^0

[37] P-even amplitudes are accessed with P-even variables, like invariant masses or helicity angles.

[38] For momentum-only triple products, at least four-daughter final states are required to give a nonzero correlation, as only three out of four momenta are independent. For three-body decays, the daughters are in a plane and the triple product is zero.

TABLE 281. Measurements of the T-odd CP asymmetry $\mathcal{A}_T = (A_T - \bar{A}_T)/2$.

Mode	Year	Collaboration	$\mathcal{A}_T$
$D^0 \to K^+K^-\pi^+\pi^-$	2018	Belle [1287]	$+0.0052 \pm 0.0037 \pm 0.0007$
	2014	LHCb [1309]	$+0.0018 \pm 0.0029 \pm 0.0004$
	2010	*BABAR* [1310]	$+0.0010 \pm 0.0051 \pm 0.0044$
	2005	FOCUS [1277]	$+0.010 \pm 0.057 \pm 0.037$
		HFLAV average	$+0.0035 \pm 0.0021$
$D^0 \to K_S\pi^+\pi^-\pi^0$	2017	Belle [1308]	$-0.00028 \pm 0.00138^{+0.00023}_{-0.00076}$
$D^+ \to K_SK^+\pi^+\pi^-$	2011	*BABAR* [1311]	$-0.0120 \pm 0.0100 \pm 0.0046$
	2005	FOCUS [1277]	$+0.023 \pm 0.062 \pm 0.022$
		HFLAV average	-0.0110 ± 0.0109
$D_s^+ \to K_SK^+\pi^+\pi^-$	2011	*BABAR* [1311]	$-0.0136 \pm 0.0077 \pm 0.0034$
	2005	FOCUS [1277]	$-0.036 \pm 0.067 \pm 0.023$
		HFLAV average	-0.0139 ± 0.0084

$$C_T \equiv \vec{p}_{K^+} \cdot (\vec{p}_{\pi^+} \times \vec{p}_{\pi^-}), \tag{247}$$

and the corresponding quantity for $\overline{D}^0$

$$\bar{C}_T \equiv \vec{p}_{K^-} \cdot (\vec{p}_{\pi^-} \times \vec{p}_{\pi^+}), \tag{248}$$

one can construct the asymmetry for the D^0 decays as

$$A_T = \frac{\Gamma(C_T > 0) - \Gamma(C_T < 0)}{\Gamma(C_T > 0) + \Gamma(C_T < 0)}, \tag{249}$$

and for their CP-conjugate decays as

$$\bar{A}_T = \frac{\Gamma(-\bar{C}_T > 0) - \Gamma(-\bar{C}_T < 0)}{\Gamma(-\bar{C}_T > 0) + \Gamma(-\bar{C}_T < 0)}. \tag{250}$$

In these expressions, Γ represents a partial width, and the following applies:

$$P(C_T) = -C_T, \quad C(C_T) = \overline{C_T}, \quad CP(A_T) = \overline{A}_T. \tag{251}$$

The asymmetries A_T and $\bar{A}_T$ depend on angular distributions of the daughter particles and may be nonzero due to final-state interactions or P violation in weak decays. Given Eq. (251), one can construct the CP-violating, i.e. CP-odd (and P-odd, T-odd) asymmetry

$$\mathcal{A}_T \equiv \frac{A_T - \bar{A}_T}{2}; \tag{252}$$

where a nonzero value indicates CP violation (see Refs. [1302–1307]). This asymmetry is referred to in the literature by several names: $A_{T\text{viol}}$, a_{CP}^P, and $a_{CP}^{T\text{-odd}}$.

Values of $\mathcal{A}_T$ for D^+, D_s^+, and D^0 decay modes are listed in Table 281. Despite relatively high precision (<1%), there is no evidence for CP violation. In order to increase sensitivity to CP violation (see Sec. X B), some of the measurements in Table 281 are also performed locally in phase-space regions. Decay phase space is divided according to two- or three-body invariant mass (for $D^0 \to K_S\pi^+\pi^-\pi^0$ decays in Ref. [1308]), helicity angles of the two-body systems ($D^0 \to K^+K^-\pi^+\pi^-$ in Ref. [1287]) or using both mass and angular observables ($D^0 \to K^+K^-\pi^+\pi^-$ in Ref. [1309]). None of the local $\mathcal{A}_T$ asymmetries is found to be significant.

All P-even contributions contributing to $\mathcal{A}_T$ cancel out in the difference. Thus, $\mathcal{A}_T$ is only sensitive to P-odd amplitudes or to interference between P-odd and P-even ones. The cancellation typically applies also to detection asymmetries and, at the hadron-collider experiments, the production asymmetry, making this is a significant advantage of the T-odd method.

Another way to probe P-odd amplitudes is through amplitude analysis using P-odd variables. One example is $\sin\Phi$, where Φ is the angle in the D^0 frame between the K^+K^- decay plane and the $\pi^+\pi^-$ decay plane for the decay $D^0 \to K^+K^-\pi^+\pi^-$ [1251]. It can be shown that $\sin\Phi$ is proportional to the triple product. However, P-odd amplitudes in four-body decays of charm mesons, for instance $D \to [VV]_{L=1}$, i.e. final states involving two vector mesons in a P-wave state, are typically quite suppressed (<10%) [1251,1312]. This makes searches for CP violation in these amplitudes challenging. As discussed in Sec. X B, no significant CP violation was observed for any of the amplitudes contributing into the $D^0 \to K^+K^-\pi^+\pi^-$ decays studied by LHCb [1251]. The most significant asymmetry of 2.8σ was observed for the phase of the P-odd amplitude $D^0 \to [\phi(1020)\rho(1450)^0]_{L=1}$. In another method, the model-independent technique used to search for CP asymmetries in $D^0 \to \pi^+\pi^-\pi^+\pi^-$ decays (see Sec. X B) has been carried out separately for P-odd and P-even contributions, separated out using a triple product [1250]. The p-value of 0.6%, corresponding to a significance for CP violation of

TABLE 282. Inputs to the fit for direct and indirect *CP* violation. The first uncertainty listed is statistical and the second is systematic. The uncertainties on $\Delta\langle t\rangle/\tau$ and $\langle t\rangle/\tau$ are ≤ 0.01 and are not quoted here.

Year	Experiment	Results	$\Delta\langle t\rangle/\tau$	$\langle t\rangle/\tau$	Reference
2012	*BABAR*	$A_\Gamma = (+0.09 \pm 0.26 \pm 0.06)\%$	···	···	[1226]
2021	LHCb	$\Delta Y(KK) = (-0.003 \pm 0.013 \pm 0.003)\%$	···	···	[1232]
		$\Delta Y(\pi\pi) = (-0.036 \pm 0.024 \pm 0.004)\%$	···	···	
2014	CDF	$A_\Gamma = (-0.12 \pm 0.12)\%$	···	···	[1231]
2015	Belle	$A_\Gamma = (-0.03 \pm 0.20 \pm 0.07)\%$	···	···	[1228]
2008	*BABAR*	$A_{CP}(KK) = (+0.00 \pm 0.34 \pm 0.13)\%$			
		$A_{CP}(\pi\pi) = (-0.24 \pm 0.52 \pm 0.22)\%$	0.00	1.00	[1218]
2012	CDF	$\Delta A_{CP} = (-0.62 \pm 0.21 \pm 0.10)\%$	0.25	2.58	[1221]
2014	LHCb SL	$\Delta A_{CP} = (+0.14 \pm 0.16 \pm 0.08)\%$	0.01	1.07	[1317]
2016	LHCb prompt	$\Delta A_{CP} = (-0.10 \pm 0.08 \pm 0.03)\%$	0.12	2.10	[1318]
2019	LHCb SL2	$\Delta A_{CP} = (-0.09 \pm 0.08 \pm 0.05)\%$	0.00	1.21	[1192]
2019	LHCb prompt2	$\Delta A_{CP} = (-0.18 \pm 0.03 \pm 0.09)\%$	0.13	1.74	[1192]

2.7σ, is obtained for the *P*-odd test of $D^0 \to \pi^+\pi^-\pi^+\pi^-$ decays.

Decays of charm baryons also offer access to *P*-odd amplitudes, e.g., Λ_c^+ decays with a weakly decaying baryon in the final state, such as $\Lambda_c^+ \to \Lambda\pi^+$. Moreover, for polarized charm baryons, e.g., Λ_c produced weakly in Λ_b decays, one can build a triple product using the Λ_c spin. Recently, the topic of symmetries has been revisited (see Refs. [1313,1314]), with the suggestion to exploit additional asymmetries constructed from triple products in multibody decays.

D. Interplay between direct and indirect *CP* violation

In decays of D^0 mesons, *CP* asymmetry measurements have contributions from both direct and indirect *CP* violation, as discussed in Sec. X A. The contribution from indirect *CP* violation depends on the decay-time distribution of the data sample [1234]. This section describes a combination of measurements that allows the determination of the individual contributions of the two types of *CP* violation. At the same time, the level of agreement for a no-*CP*-violation hypothesis is tested. The first observable is

$$A_\Gamma \equiv \frac{\tau(\bar{D}^0 \to h^+h^-) - \tau(D^0 \to h^+h^-)}{\tau(\bar{D}^0 \to h^+h^-) + \tau(D^0 \to h^+h^-)}, \quad (253)$$

where h^+h^- can be K^+K^- or $\pi^+\pi^-$ and $\tau(D^0 \to h^+h^-)$ indicates the effective D^0 lifetime as measured in the decay to h^+h^-. The second observable is

$$\Delta A_{CP} \equiv A_{CP}(K^+K^-) - A_{CP}(\pi^+\pi^-), \quad (254)$$

where A_{CP} are time-integrated *CP* asymmetries. The underlying theoretical parameters are

$$a_{CP}^{\rm dir} \equiv \frac{|\mathcal{A}_{D^0\to f}|^2 - |\mathcal{A}_{\bar{D}^0\to f}|^2}{|\mathcal{A}_{D^0\to f}|^2 + |\mathcal{A}_{\bar{D}^0\to f}|^2},$$
$$a_{CP}^{\rm ind} \equiv \frac{1}{2}\left[\left(\left|\frac{q}{p}\right| + \left|\frac{p}{q}\right|\right)x\sin\phi - \left(\left|\frac{q}{p}\right| - \left|\frac{p}{q}\right|\right)y\cos\phi\right], \quad (255)$$

where $\mathcal{A}_{D\to f}$ is the amplitude for $D \to f$ [1315]. We use the relations [1316]

$$A_\Gamma = -a_{CP}^{\rm ind} - a_{CP}^{\rm dir} y_{CP}, \quad (256)$$

$$\Delta A_{CP} = \Delta a_{CP}^{\rm dir}\left(1 + y_{CP}\frac{\overline{\langle t\rangle}}{\tau}\right) + a_{CP}^{\rm ind}\frac{\Delta\langle t\rangle}{\tau} + \overline{a_{CP}^{\rm dir}} y_{CP}\frac{\Delta\langle t\rangle}{\tau},$$
$$\approx \Delta a_{CP}^{\rm dir}\left(1 + y_{CP}\frac{\overline{\langle t\rangle}}{\tau}\right) + a_{CP}^{\rm ind}\frac{\Delta\langle t\rangle}{\tau} \quad (257)$$

between the observables and the underlying parameters. Equation (256) constrains mostly indirect *CP* violation, and the direct *CP* violation contribution can differ for different final states. In Eq. (257), $\langle t\rangle/\tau$ denotes the mean decay time in units of the D^0 lifetime; ΔX denotes the difference in quantity X between K^+K^- and $\pi^+\pi^-$ final states; and $\bar{X}$ denotes the average for quantity X. We neglect the last term in this relation, as all three factors are $\mathcal{O}(10^{-2})$ or smaller, and thus this term is negligible with respect to the other two terms. Note that $\Delta\langle t\rangle/\tau \ll \langle t\rangle/\tau$, and it is expected that $|a_{CP}^{\rm dir}| < |\Delta a_{CP}^{\rm dir}|$ because $a_{CP}^{\rm dir}(K^+K^-)$ and $a_{CP}^{\rm dir}(\pi^+\pi^-)$ are expected to have opposite signs in the Standard Model [1315].

We perform a χ^2 fit to extract $\Delta a_{CP}^{\rm dir}$ and $a_{CP}^{\rm ind}$ using the HFLAV average value $y_{CP} = (0.719 \pm 0.113)\%$ (see Sec. X A) and the measurements listed in Table 282. For the *BABAR* measurements of $A_{CP}(K^+K^-)$ and $A_{CP}(\pi^+\pi^-)$, we calculate ΔA_{CP} adding all uncertainties in quadrature.

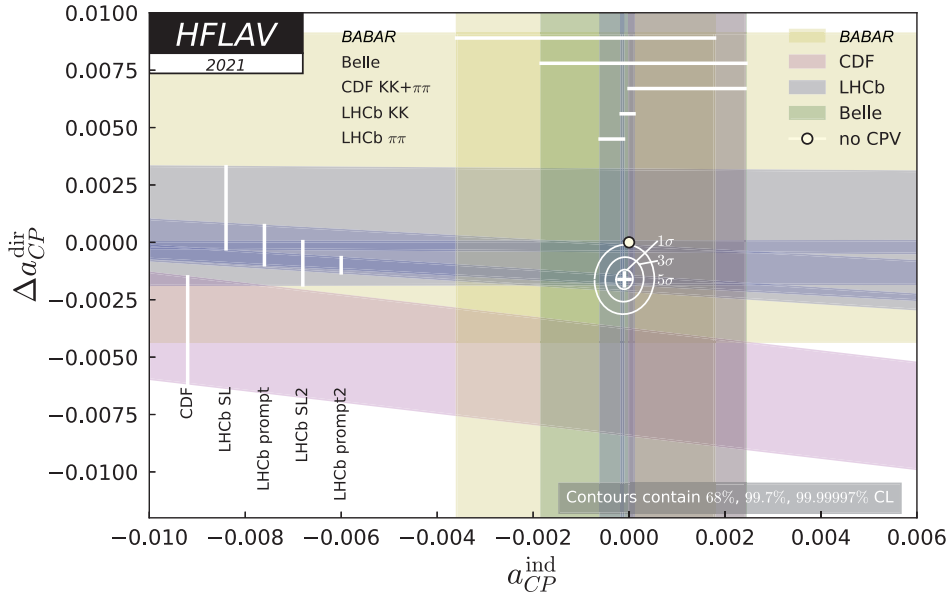

FIG. 90. Plot of all data and the fit result. Individual measurements are plotted as bands showing their $\pm 1\sigma$ range. The no-CPV point (0,0) is shown as a filled circle, and the best fit value is indicated by a cross showing the one-dimensional uncertainties. Two-dimensional 68% C.L., 99.7% C.L., and 99.99997% C.L. regions are plotted as ellipses.

This may overestimate the systematic uncertainty for the difference, as it neglects correlated uncertainties. However, the result is conservative, and the effect is small, as all measurements are statistically limited. For all measurements, statistical and systematic uncertainties are added in quadrature when calculating the χ^2. In this fit, $A_\Gamma(KK)$ and $A_\Gamma(\pi\pi)$ are assumed to be identical but are plotted separately in Fig. 90 to visualize their level of agreement. This approximation, which holds in the SM, is supported by all measurements to date. A significant relative shift of ΔA_{CP} due to final-state-dependent A_Γ values and different mean decay times, corresponding to a contribution from the last term in Eq. (257), is excluded by these measurements. The latest LHCb measurement measures ΔY, which is approximately equal to $-A_\Gamma$ with the relative difference being y_{CP}.

The fit results are shown in Fig. 90. From the fit, the change in χ^2 from the minimum value for the no-CPV point (0, 0) is 33.0, which corresponds to a C.L. of 6.9×10^{-8} for two degrees of freedom or 5.4 standard deviations. The central values and $\pm 1\sigma$ uncertainties for the individual parameters are

$$\begin{aligned} a_{CP}^{\rm ind} &= (-0.010 \pm 0.012)\% \\ \Delta a_{CP}^{\rm dir} &= (-0.161 \pm 0.028)\%. \end{aligned} \tag{258}$$

Relative to the average reported in our previous report [1], the level of rejection of the hypothesis of CP symmetry remains approximately unchanged, and the uncertainty on indirect CP violation has more than halved. The average clearly points at CP violation in the decays to two charged hadrons.

XI. CHARM DECAYS

A. Semileptonic decays

1. Introduction

Semileptonic decays of D mesons involve the interaction of a leptonic current with a hadronic current. The latter is nonperturbative and cannot be calculated from first principles; thus it is usually parametrized in terms of form factors. The transition matrix element is written

$$\mathcal{M} = -i \frac{G_F}{\sqrt{2}} V_{cq}\, L^\mu\, H_\mu, \tag{259}$$

where G_F is the Fermi constant and V_{cq} is a CKM matrix element. The leptonic current L^μ is evaluated directly from the lepton spinors and has a simple structure; this allows one to extract information about the form factors (in H_μ) from data on semileptonic decays [1319]. Conversely, because there are no strong final-state interactions between the leptonic and hadronic systems, semileptonic decays for which the form factors can be calculated allow one to determine $|V_{cq}|$ [3].

2. $D \to P\ell\nu_\ell$ decays

When the final state hadron is a pseudoscalar, the hadronic current is given by [1320]

TABLE 283. Results for $m_{\rm pole}$ and $\alpha_{\rm BK}$ from various experiments for $D^0 \to K^-\ell^+\nu$ and $D^+ \to \bar{K}^0\ell^+\nu$ decays. The last two rows list results for other $c \to se^+\nu_e$ decays, for comparison, because some theories [1344,1345] stated that the form factors of the semileptonic decays are possibly insensitive to the spectator quarks.

$D \to K\ell\nu_\ell$ experiment	Mode	References	$m_{\rm pole}$ (GeV/c^2)	$\alpha_{\rm BK}$
CLEO III	$(D^0;\ell = e,\mu)$	[1346]	$1.89 \pm 0.05^{+0.04}_{-0.03}$	$0.36 \pm 0.10^{+0.03}_{-0.07}$
FOCUS	$(D^0;\ell = \mu)$	[1347]	$1.93 \pm 0.05 \pm 0.03$	$0.28 \pm 0.08 \pm 0.07$
Belle	$(D^0;\ell = e,\mu)$	[1335]	$1.82 \pm 0.04 \pm 0.03$	$0.52 \pm 0.08 \pm 0.06$
BABAR	$(D^0;\ell = e)$	[1336]	$1.889 \pm 0.012 \pm 0.015$	$0.366 \pm 0.023 \pm 0.029$
CLEO-c (tagged)	$(D^0, D^+;\ell = e)$	[1337]	$1.93 \pm 0.02 \pm 0.01$	$0.30 \pm 0.03 \pm 0.01$
CLEO-c (untagged)	$(D^0;\ell = e)$	[1338]	$1.97 \pm 0.03 \pm 0.01$	$0.21 \pm 0.05 \pm 0.03$
CLEO-c (untagged)	$(D^+;\ell = e)$	[1338]	$1.96 \pm 0.04 \pm 0.02$	$0.22 \pm 0.08 \pm 0.03$
BESIII	$(D^0;\ell = e)$	[1334]	$1.921 \pm 0.010 \pm 0.007$	$0.309 \pm 0.020 \pm 0.013$
BESIII	$(D^+;\ell = e)$	[1269]	$1.953 \pm 0.044 \pm 0.036$	$0.239 \pm 0.077 \pm 0.065$
BESIII	$D^+ \to \bar{K}^0_{\pi^+\pi^-}e^+\nu_e$	[1339]	$1.935 \pm 0.017 \pm 0.006$	$0.294 \pm 0.031 \pm 0.010$
BESIII	$D_s^+ \to \eta e^+\nu_e$	[1348]	$3.759 \pm 0.084 \pm 0.045$	$0.304 \pm 0.044 \pm 0.22$
BESIII	$D_s^+ \to \eta' e^+\nu_e$	[1348]	$1.88 \pm 0.60 \pm 0.08$	$1.62 \pm 0.90 \pm 0.13$

$$\begin{aligned} H_\mu &= \langle P(p)|\bar{q}\gamma_\mu c|D(p')\rangle \\ &= f_+(q^2)\left[(p'+p)_\mu - \frac{m_D^2 - m_P^2}{q^2}q_\mu\right] \\ &\quad + f_0(q^2)\frac{m_D^2 - m_P^2}{q^2}q_\mu, \end{aligned} \tag{260}$$

where m_D and p' are the mass and four momentum of the parent D meson, m_P and p are those of the daughter meson, $f_+(q^2)$ and $f_0(q^2)$ are form factors, and $q = p' - p$. Kinematics require that $f_+(0) = f_0(0)$. The contraction $q_\mu L^\mu$ results in terms proportional to m_ℓ [1321], and thus for $\ell = e$ the terms proportional to q_μ in Eq. (260) are negligible and only the $f_+(q^2)$ vector form factor is relevant. The corresponding differential partial width is

$$\frac{d\Gamma(D \to Pe\nu_e)}{dq^2\, d\cos\theta_e} = \frac{G_F^2|V_{cq}|^2}{32\pi^3}p^{*3}|f_+(q^2)|^2 \sin\theta_e^2, \tag{261}$$

where $p^* = \frac{[(m_D^2-(m_P+q))^2(m_D^2-(m_P-q))]^{1/2}}{2m_D}$ is the magnitude of the momentum of the final state hadron in the D rest frame, and θ_e is the angle of the electron in the $e\nu$ rest frame with respect to the direction of the pseudoscalar meson in the D rest frame.

3. Form factor parametrizations

The form factor is traditionally parametrized with an explicit pole and a sum of effective poles:

$$f_+(q^2) = \frac{f_+(0)}{(1-\alpha)}\left[\left(\frac{1}{1 - q^2/m_{\rm pole}^2}\right) + \sum_{k=1}^{N}\frac{\rho_k}{1 - q^2/(\gamma_k m_{\rm pole}^2)}\right], \tag{262}$$

where ρ_k and γ_k are expansion parameters and α is a parameter that normalizes the form factor at $q^2 = 0$, $f_+(0)$. The parameter $m_{\rm pole}$ is the mass of the lowest-lying $c\bar{q}$ resonance with the vector quantum numbers; this is expected to provide the largest contribution to the form factor for the $c \to q$ transition. The sum over N gives the contribution of higher mass states. For example, for $D \to \pi$ transitions the dominant resonance is expected to be the $D^*(2010)$, and thus $m_{\rm pole} = m_{D^*(2010)}$. For $D \to K$ transitions, the dominant resonance is expected to be the $D_s^*(2112)$, and thus $m_{\rm pole} = m_{D_s^*(2112)}$.

4. Simple pole

Equation (262) can be simplified by neglecting the sum over effective poles, leaving only the explicit vector meson pole. This approximation is referred to as "nearest pole dominance" or "vector-meson dominance." The resulting parametrization is

$$f_+(q^2) = \frac{f_+(0)}{(1 - q^2/m_{\rm pole}^2)}. \tag{263}$$

However, values of $m_{\rm pole}$ that give a good fit to the data do not agree with the expected vector meson masses [1320]. To address this problem, the "modified pole" or Becirevic-Kaidalov (BK) parametrization [1322] was introduced. In this parametrization $m_{\rm pole}/\sqrt{\alpha_{\rm BK}}$ is interpreted as the mass of an effective pole higher than $m_{\rm pole}$, i.e., it is expected that $\alpha_{\rm BK} < 1$. The parametrization takes the form

$$f_+(q^2) = \frac{f_+(0)}{(1 - q^2/m_{\rm pole}^2)}\frac{1}{\left(1 - \alpha_{\rm BK}\frac{q^2}{m_{\rm pole}^2}\right)}, \tag{264}$$

where $\alpha_{\rm BK}$ is a free parameter that takes into account contributions from higher states in the form of

TABLE 284. Results for $m_{\rm pole}$ and $\alpha_{\rm BK}$ from various experiments for $D^0 \to \pi^- \ell^+ \nu$ and $D^+ \to \pi^0 \ell^+ \nu$ decays. The last two rows list results for other $c \to d e^+ \nu_e$ decays, for comparison, because some theories [1344,1345] stated that the form factors of the semileptonic decays are possibly insensitive to the spectator quarks.

$D \to \pi \ell \nu_\ell$ experiment	Mode	References	$m_{\rm pole}$ (GeV/c^2)	$\alpha_{\rm BK}$
CLEO III	$(D^0; \ell = e, \mu)$	[1346]	$1.86^{+0.10+0.07}_{-0.06-0.03}$	$0.37^{+0.20}_{-0.31} \pm 0.15$
FOCUS	$(D^0; \ell = \mu)$	[1347]	$1.91^{+0.30}_{-0.15} \pm 0.07$	⋯
Belle	$(D^0; \ell = e, \mu)$	[1335]	$1.97 \pm 0.08 \pm 0.04$	$0.10 \pm 0.21 \pm 0.10$
CLEO-c (tagged)	$(D^0, D^+; \ell = e)$	[1337]	$1.91 \pm 0.02 \pm 0.01$	$0.21 \pm 0.07 \pm 0.02$
CLEO-c (untagged)	$(D^0; \ell = e)$	[1338]	$1.87 \pm 0.03 \pm 0.01$	$0.37 \pm 0.08 \pm 0.03$
CLEO-c (untagged)	$(D^+; \ell = e)$	[1338]	$1.97 \pm 0.07 \pm 0.02$	$0.14 \pm 0.16 \pm 0.04$
BESIII	$(D^0; \ell = e)$	[1334]	$1.911 \pm 0.012 \pm 0.004$	$0.279 \pm 0.035 \pm 0.011$
BABAR	$(D^0; \ell = e)$	[1333]	$1.906 \pm 0.029 \pm 0.023$	$0.268 \pm 0.074 \pm 0.059$
BESIII	$D^+ \to \pi^0 e^+ \nu_e$	[1339]	$1.898 \pm 0.020 \pm 0.003$	$0.285 \pm 0.057 \pm 0.010$
CLEO-c	$D^+ \to \eta e^+ \nu_e$	[1349]	$1.87 \pm 0.24 \pm 0.00$	$0.21 \pm 0.44 \pm 0.05$
BESIII	$D^+ \to \eta e^+ \nu_e$	[1350]	$1.73 \pm 0.17 \pm 0.03$	$0.50 \pm 0.54 \pm 0.08$

an additional effective pole. This parametrization is used by several experiments to determine form factor parameters. Measured values of $m_{\rm pole}$ and $\alpha_{\rm BK}$ are listed in Tables 283 and 284 for $D \to K \ell \nu_\ell$ and $D \to \pi \ell \nu_\ell$ decays, respectively.

5. z expansion

Alternatively, a power series expansion around some value $q^2 = t_0$ can be used to parametrize $f_+(q^2)$ [1319,1323–1325]. This parametrization is model-independent and satisfies general QCD constraints. The expansion is given in terms of a complex parameter z, which is the analytic continuation of q^2 into the complex plane:

$$z(q^2, t_0) = \frac{\sqrt{t_+ - q^2} - \sqrt{t_+ - t_0}}{\sqrt{t_+ - q^2} + \sqrt{t_+ - t_0}}, \tag{265}$$

where $t_0 = t_+(1 - \sqrt{1 - t_-/t_+})$ and $t_\pm \equiv (m_D \pm m_P)^2$. In this parametrization, $q^2 = t_0$ corresponds to $z = 0$, and the physical region extends in either direction up to $\pm|z|_{\rm max} = \pm 0.051$ for $D \to K \ell \nu_\ell$ decays, and up to ± 0.17 for $D \to \pi \ell \nu_\ell$ decays.

The form factor is expressed as

$$f_+(q^2) = \frac{1}{P(q^2)\phi(q^2, t_0)} \sum_{k=0}^{\infty} a_k(t_0)[z(q^2, t_0)]^k, \tag{266}$$

where the Blaschke factor $P(q^2)$ is used to remove subthreshold poles, for instance, $P(q^2) = 1$ for $D \to \pi$ and $P(q^2) = z(q^2, M^2_{D_s^*})$. The "outer" function $\phi(t, t_0)$ can be any analytic function, but a preferred choice (see, e.g., Refs. [1323,1324,1326]), obtained from the operator product expansion (OPE), is

$$\phi(q^2, t_0) = \alpha(\sqrt{t_+ - q^2} + \sqrt{t_+ - t_0}) \times \frac{t_+ - q^2}{(t_+ - t_0)^{1/4}} \frac{(\sqrt{t_+ - q^2} + \sqrt{t_+ - t_-})^{3/2}}{(\sqrt{t_+ - q^2} + \sqrt{t_+})^5}, \tag{267}$$

with $\alpha = \sqrt{\pi m_c^2/3}$. The OPE analysis provides a constraint upon the expansion coefficients, $\sum_{k=0}^{N} a_k^2 \le 1$. These coefficients receive $1/M_D$ corrections, and thus the constraint is only approximate. However, the expansion is expected to converge rapidly since $|z| < 0.051(0.17)$ for $D \to K$ ($D \to \pi$) over the entire physical q^2 range, and Eq. (266) remains a useful parametrization. The main disadvantage as compared to phenomenological approaches is that there is no physical interpretation of the fitted coefficients a_K.

6. Three-pole formalism

An update of the vector pole dominance model has been developed for the $D \to \pi \ell \nu_\ell$ channel [1327]. It uses information of the residues of the semileptonic form factor at its first two poles, the $D^*(2010)$ and $D^{*'}(2600)$ resonances. The form factor is expressed as an infinite sum of residues from $J^P = 1^-$ states with masses $m_{D_n^*}$:

$$f_+(q^2) = \sum_{n=0}^{\infty} \frac{\underset{q^2 = m^2_{D_n^*}}{\rm Res} f_+(q^2)}{m^2_{D_n^*} - q^2}, \tag{268}$$

with the residues given by

$$\underset{q^2 = m^2_{D_n^*}}{\rm Res} f_+(q^2) = \frac{1}{2} m_{D_n^*} f_{D_n^*} g_{D_n^* D\pi}. \tag{269}$$

Values of the f_{D^*} and $f_{D^{*'}}$ decay constants have been calculated relative to f_D via lattice QCD, with 2% and 28% precision, respectively [1327]. The couplings to the $D\pi$

state, $g_{D^*D\pi}$ and $g_{D^{*\prime}D\pi}$, are extracted from measurements of the $D^*(2010)$ and $D^{*\prime}(2600)$ widths by the *BABAR* and LHCb experiments [1328–1330]. This results in the contribution from the first pole being determined with 3% accuracy. The contribution from the $D^{*\prime}(2600)$ pole is determined with poorer accuracy, ∼30%, mainly due to lattice uncertainties. A *superconvergence* condition [1331]

$$\sum_{n=0}^{\infty} \underset{q^2=m^2_{D^*_n}}{\text{Res}} f_+(q^2) = 0 \tag{270}$$

is applied, protecting the form factor behavior at large q^2. Within this model, the first two poles are not sufficient to describe the data, and a third effective pole needs to be included.

One of the advantages of this phenomenological model is that it can be extrapolated outside the charm physical region, providing a method to extract the magnitude of the CKM matrix element V_{ub} using the ratio of the form factors of the $D \to \pi\ell\nu$ and $B \to \pi\ell\nu$ decay channels. It will be used once lattice calculations provide the form factor ratio $f^+_{B\pi}(q^2)/f^+_{D\pi}(q^2)$ at the same pion energy.

This form factor description can be extended to the $D \to K\ell\nu$ decay channel, considering the contribution of several $c\bar{s}$ resonances with $J^P = 1^-$. The first two pole masses contributing to the form factor correspond to the $D^*_s(2112)$ and $D^*_{s1}(2700)$ resonant states [9]. A constraint on the first residue can be obtained using information of the f_K decay constant [9] and the g coupling extracted from the D^{*+} width [1328]. The contribution from the second pole can be evaluated using the decay constants from [1332], the measured total width, and the ratio of D^*K and DK decay branching fractions [9].

7. Experimental techniques and results

Various techniques have been used by several experiments to measure D semileptonic decays with a pseudoscalar particle in the final state. The most recent results are provided by the *BABAR* [1333] and BESIII [1269,1334] collaborations. Belle [1335], *BABAR* [1336], and CLEO-c [1337,1338] have all previously reported results. Belle fully reconstructs $e^+e^- \to D\bar{D}X$ events from the continuum under the $\Upsilon(4S)$ resonance, achieving very good q^2 resolution (15 MeV^2) and a low background level but with a low efficiency. Using 282 fb^{-1} of data, about 1300 $D \to K\ell^+\nu$ (Cabibbo-favored) and 115 $D \to \pi\ell^+\nu$ (Cabibbo-suppressed) decays are reconstructed, considering the electron and muon channels together. The *BABAR* experiment uses a partial reconstruction technique in which the semileptonic decays are tagged via $D^{*+} \to D^0\pi^+$ decays. The D direction and neutrino energy are obtained using information from the rest of the event. With 75 fb^{-1} of data, 74000 signal events in the $D^0 \to K^-e^+\nu$ mode are obtained. This technique provides a large signal yield but also a high background level and a poor q^2 resolution (ranging from 66 to 219 MeV^2). In this case, the measurement of the branching fraction is obtained by normalizing to the $D^0 \to K^-\pi^+$ decay channel; thus the measurement would benefit from future improvements in the determination of the branching fraction for this reference channel. The Cabibbo-suppressed mode has been recently measured using the same technique and 350 fb^{-1} data. For this measurement, 5000 $D^0 \to \pi^-e^+\nu$ signal events were reconstructed [1333].

The CLEO-c experiment uses two different methods to measure charm semileptonic decays. The *tagged* analyses [1337] rely on the full reconstruction of $\psi(3770) \to D\bar{D}$ events. One of the D mesons is reconstructed in a hadronic decay mode, and the other in the semileptonic channel. The only missing particle is the neutrino, and thus the q^2 resolution is very good and the background level very low. With the entire CLEO-c data sample of 818 pb^{-1}, 14123 and 1374 signal events are reconstructed for the $D^0 \to K^-e^+\nu$ and $D^0 \to \pi^-e^+\nu$ channels, respectively, and 8467 and 838 are reconstructed for the $D^+ \to \bar{K}^0e^+\nu$ and $D^+ \to \pi^0e^+\nu$ decays, respectively. An alternative method that does not tag the D decay in a hadronic mode (referred to as *untagged* analyses) has also been used by CLEO-c [1338]. In this method, the entire missing energy and momentum in an event are associated with the neutrino four momentum, with the penalty of larger backgrounds as compared to the tagged method.

Using the tagged method, the BESIII experiment measures the $D^0 \to K^-e^+\nu$ and $D^0 \to \pi^-e^+\nu$ decay channels. With 2.93 fb^{-1} of data, they fully reconstruct 70700 and 6300 signal events, respectively, for the two channels [1334]. In a separate analysis, BESIII measures the semileptonic decay $D^+ \to K^0_Le^+\nu$ [1269], with about 20100 semileptonic candidates. Since 2016, BESIII has reported additional measurements of $D \to \bar{K}\ell^+\nu_\ell$ and $\pi\ell^+\nu_\ell$. The signal yields are 26008, 5013, 47100, 20714, 3402, 2265, and 1335 events for $D^+ \to \bar{K}^0(\pi^+\pi^-)e^+\nu_e$, $D^+ \to \bar{K}^0(\pi^0\pi^0)e^+\nu_e$, $D^0 \to K^-\mu^+\nu_\mu$, $D^+ \to \bar{K}^0(\pi\pi)\mu^+\nu_\mu$, $D^+ \to \pi^0e^+\nu_e$, $D^0 \to \pi^-\mu^+\nu_\mu$, and $D^+ \to \pi^0\mu^+\nu_\mu$ [1339–1343], respectively. The corresponding branching fractions are determined with good precision. The most precise products of the $c \to s(d)$ CKM matrix element and the semileptonic form factor reported by BESIII are

$$|V_{cs}|f_+^{D\to K}(0) = 0.7053 \pm 0.0040 \pm 0.0112, \tag{271}$$

$$|V_{cs}|f_+^{D\to K}(0) = 0.7133 \pm 0.0038 \pm 0.0030, \tag{272}$$

$$|V_{cd}|f_+^{D\to \pi}(0) = 0.1400 \pm 0.0026 \pm 0.0007, \tag{273}$$

from $D^0 \to K^-e^+\nu_e$ [1334], $D^0 \to K^-\mu^+\nu_\mu$ [1340], $D^0 \to \pi^-e^+\nu_e$ [1334], respectively. These results are all based on a two-parameter series expansion, respectively.

TABLE 285. Results for r_1 and r_2 from various experiments for $D \to K\ell\nu_\ell$ decays. Some theories [1344,1345] stated that the form factors of the semileptonic decays are possibly insensitive to the spectator quarks. For comparison, the last four rows list results for $c \to se^+\nu_e$ decays in which only the first two terms of the z expansion were used.

Experiment $D \to K\ell\nu_\ell$	Mode	References	r_1	r_2
BABAR	$(D^0; \ell = e)$	[1336]	$-2.5 \pm 0.2 \pm 0.2$	$0.6 \pm 6.0 \pm 5.0$
CLEO-c (tagged)	$(D^0; \ell = e)$	[1337]	$-2.65 \pm 0.34 \pm 0.08$	$13 \pm 9 \pm 1$
CLEO-c (tagged)	$(D^+; \ell = e)$	[1337]	$-1.66 \pm 0.44 \pm 0.10$	$-14 \pm 11 \pm 1$
CLEO-c (untagged)	$(D^0; \ell = e)$	[1338]	$-2.4 \pm 0.4 \pm 0.1$	$21 \pm 11 \pm 2$
CLEO-c (untagged)	$(D^+; \ell = e)$	[1338]	$-2.8 \pm 6 \pm 2$	$32 \pm 18 \pm 4$
BESIII	$(D^0; \ell = e)$	[1334]	$-2.334 \pm 0.159 \pm 0.080$	$3.42 \pm 3.91 \pm 2.41$
BESIII	$(D^+; \ell = e)$	[1269]	$-2.23 \pm 0.42 \pm 0.53$	$11.3 \pm 8.5 \pm 8.7$
BESIII	$D^0 \to K^-\mu^+\nu_\mu$	[1340]	$-1.90 \pm 0.21 \pm 0.07$	…
BESIII	$D^+ \to \bar{K}^0_{\pi^+\pi^-}e^+\nu_e$	[1339]	$-1.76 \pm 0.25 \pm 0.06$	…
BESIII	$D_s^+ \to \eta e^+\nu_e$	[1348]	$-7.3 \pm 1.7 \pm 0.4$	…
BESIII	$D_s^+ \to \eta' e^+\nu_e$	[1348]	$-13.1 \pm 7.6 \pm 1.0$	…

Results of the hadronic form factor parameters, $m_{\rm pole}$ and $\alpha_{\rm BK}$, obtained from the measurements discussed above, are given in Tables 283 and 284. The z-expansion formalism has been used by *BABAR* [1333,1336], BESIII [1334] and CLEO-c [1337,1338]. Their fits use the first three terms of the expansion, and the results for the ratios $r_1 \equiv a_1/a_0$ and $r_2 \equiv a_2/a_0$ are listed in Tables 285 and 286.

8. Combined results for the $D \to P\ell\nu_\ell$ channels

Results and world averages for the products $f_+^K(0)|V_{cs}|$ and $f_+^\pi(0)|V_{cd}|$ as measured by CLEO-c, Belle, *BABAR*, and BESIII are summarized in Tables 288 and 289, and plotted in Fig. 91 (left) and Fig. 91 (middle), respectively. When calculating these world averages, the systematic uncertainties of the BESIII analyses are conservatively taken to be fully correlated.

The results and world averages of the products $f_+^{D\to\eta}(0)|V_{cd}|$, which have been measured by CLEO-c and BESIII, are summarized in Tables 290 and plotted in Fig. 91 (right). In averaging, the systematic uncertainties of the two BESIII analyses are conservatively taken to be fully correlated.

TABLE 286. Results for r_1 and r_2 from various experiments for $D \to \pi\ell\nu_\ell$ decays. Some theories [1344,1345] stated that the form factors of the semileptonic decays are possibly insensitive to the spectator quarks. For comparison, the last three rows list results for $c \to de^+\nu_e$ decays in which only the first two terms of the z expansion were used.

Experiment $D \to \pi\ell\nu_\ell$	Mode	References	r_1	r_2
CLEO-c (tagged)	$(D^0; \ell = e)$	[1337]	$-2.80 \pm 0.49 \pm 0.04$	$6 \pm 3 \pm 0$
CLEO-c (tagged)	$(D^+; \ell = e)$	[1337]	$-1.37 \pm 0.88 \pm 0.24$	$-4 \pm 5 \pm 1$
CLEO-c (untagged)	$(D^0; \ell = e)$	[1338]	$-2.1 \pm 0.7 \pm 0.3$	$-1.2 \pm 4.8 \pm 1.7$
CLEO-c (untagged)	$(D^+; \ell = e)$	[1338]	$-0.2 \pm 1.5 \pm 0.4$	$-9.8 \pm 9.1 \pm 2.1$
BESIII	$(D^0; \ell = e)$	[1334]	$-1.85 \pm 0.22 \pm 0.07$	$-1.4 \pm 1.5 \pm 0.5$
BABAR	$(D^0; \ell = e)$	[1333]	$-1.31 \pm 0.70 \pm 0.43$	$-4.2 \pm 4.0 \pm 1.9$
BESIII	$D^+ \to \pi^0 e^+\nu_e$	[1339]	$-2.23 \pm 0.42 \pm 0.06$	…
CLEO-c	$D^+ \to \eta e^+\nu_e$	[1349]	$1.83 \pm 2.23 \pm 0.28$	…
BESIII	$D^+ \to \eta e^+\nu_e$	[1350]	$1.88 \pm 0.60 \pm 0.08$	…
BESIII	$D^+ \to \eta\mu^+\nu_\mu$	[1351]	$-0.9 \pm 2.7 \pm 0.2$	…

TABLE 287. Comparison between theory and experiment for hadronic form factors of other $D_{(s)} \to P$ transitions. The BESIII result for $f_+^{D\to\eta}(0)$ with $D^+ \to \eta e^+ \nu_e$ is obtained by dividing the measured product $f_+^{D\to\eta}(0)|V_{cd}|$ by the world average value for $|V_{cd}|$. The uncertainties listed in the first and second parentheses are statistical and systematic uncertainties, respectively.

	$f_+^{D_s\to\eta}(0)$	$f_+^{D_s\to\eta'}(0)$	$f_+^{D\to\eta}(0)$	$f_+^{D\to\eta'}(0)$	$f_+^{D_s\to K}(0)$
CLEO-c(e)	...	...	0.38(03)(01) [1349]	...	...
BESIII(e)	0.458(05)(04) [1348]	0.49(05)(01) [1348]	0.35(03)(01) [1350]	...	0.72(08)(01) [1352]
BESIII(μ)	...	...	0.39(04)(01) [1349]	...	...
LQCD$_{m_\pi=470\text{ MeV}}$ [1353]	0.564 ± 0.011	0.437 ± 0.018	...	...	...
LQCD$_{m_\pi=370\text{ MeV}}$ [1353]	0.542 ± 0.013	0.404 ± 0.025	...	...	...
LCSR [1354]	$0.495^{+0.030}_{-0.029}$	$0.558^{+0.047}_{-0.045}$	$0.429^{+0.165}_{-0.141}$	$0.292^{+0.113}_{-0.104}$	
LCSR [1355]	0.432 ± 0.033	0.520 ± 0.080	0.552 ± 0.051	0.458 ± 0.105	...
LCSR [1356]	0.45 ± 0.14	0.55 ± 0.18	...	...	...
3PSR [1357]	0.50 ± 0.04	...	...	...	...
LFQM [1358]	0.76	...	0.71	...	0.66
LFQM(I) [1359]	0.50	0.62	...	...	...
LFQM(II) [1359]	0.48	0.60	...	...	...
CQM [1360]	0.78	0.78	...	...	0.72
CCQM [1361]	0.78 ± 0.12	0.73 ± 11	0.67 ± 0.11	0.76 ± 0.11	0.60 ± 0.09

TABLE 288. Results for $f_+^K(0)|V_{cs}|$ from various experiments. *BABAR* 2007 [1336] and Belle 2006 [1335] only reported $f_+^K(0)$ values. The listed $|V_{cs}|f_+^K(0)$ values of these two experiments are obtained by multiplying $f_+^K(0)$ with their quoted $|V_{cs}|$.

$D \to K\ell\nu_\ell$ measurement	Mode	$\lvert V_{cs}\rvert f_+^K(0)$	Comment
BESIII 2019 [1340]	$(D^0; \ell = \mu)$	0.7133(38)(30)	z expansion, 2 terms
BESIII 2017 [1339]	$(D^+; \ell = e)$	0.6983(56)(112)	z expansion, 3 terms
BESIII 2015B [1269]	$(D^+; \ell = e)$	0.7370(60)(90)	z expansion, 3 terms
BESIII 2015A [1334]	$(D^0; \ell = e)$	0.7195(35)(41)	z expansion, 3 terms
CLEO-c 2009 [1337]	$(D^0, D^+; \ell = e)$	0.7189(64)(48)	z expansion, 3 terms
BABAR 2007 [1336]	$(D^0; \ell = e)$	0.7211(69)(85)	Fitted pole mass + modified pole ansatze; $\lvert V_{cs}\rvert = 0.9729 \pm 0.0003$; corrected for $\mathcal{B}(D^0 \to K^-\pi^+)$
Belle 2006 [1335]	$(D^0; \ell = e, \mu)$	0.6762(68)(214)	$\lvert V_{cs}\rvert = 0.97296 \pm 0.00024$ (PDG 2006 w/unitarity)
World average		**0.7180(33)**	BESIII syst. fully correlated

TABLE 289. Results for $f_+^\pi(0)|V_{cd}|$ from various experiments.

$D \to \pi \ell \nu_\ell$ measurement	Mode	$\lvert V_{cd}\rvert f_+^\pi(0)$	Comment
BESIII 2017 [1339]	$(D^+; \ell = e)$	0.1413(35)(12)	z expansion, 3 terms
BESIII 2015A [1334]	$(D^0; \ell = e)$	0.1420(24)(10)	z expansion, 3 terms
CLEO-c 2009 [1337]	$(D^0, D^+; \ell = e)$	0.1500(40)(10)	z expansion, 3 terms
BABAR 2015 [1333]	$(D^0; \ell = e)$	0.1374(38)(24)	z expansion, 3 terms
Belle 2006 [1335]	$(D^0; \ell = e, \mu)$	0.1417(45)(68)	$\lvert V_{cd}\rvert = 0.2271 \pm 0.0010$ (PDG 2006 w/unitarity)
World average		**0.1426(18)**	BESIII syst. fully correlated

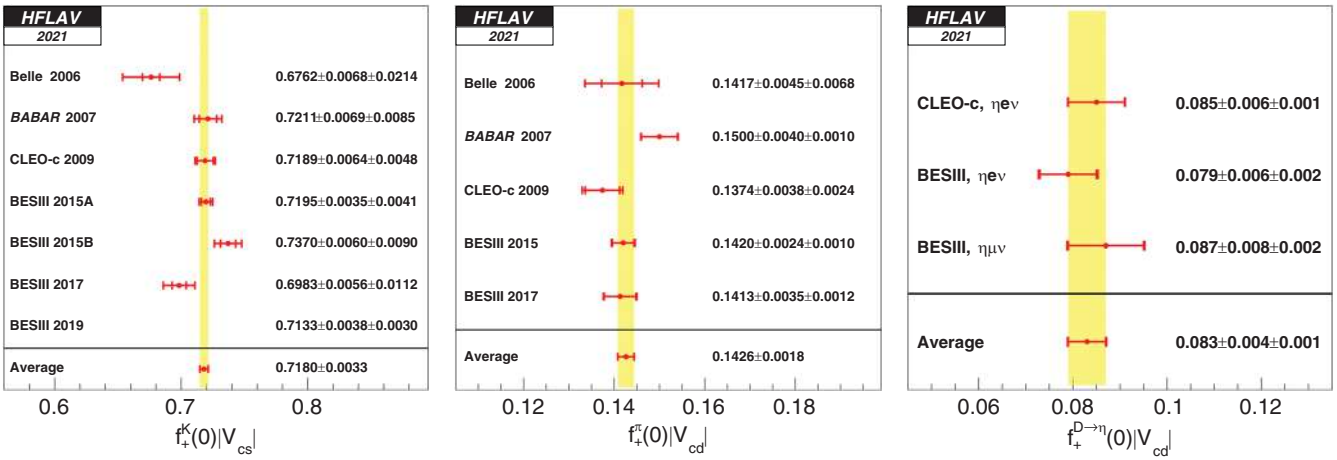

FIG. 91. Comparison of the results of $f_+^K(0)|V_{cs}|$ measured by the Belle [1335], *BABAR* [1336], CLEO-c [1337], and BESIII [1269,1334,1339,1340] experiments.

9. Form factors of other $D_{(s)} \to P\ell\nu_\ell$ decays

In the past two decades, rapid progress in lattice QCD calculations of $f_+^{D\to K(\pi)}(0)$ has been achieved, motivated by much improved experimental measurements of $D \to \bar{K}\ell\nu_\ell$ and $D \to \pi\ell\nu_\ell$. However, in contrast, progress in theoretical calculations of form factors in other $D_{(s)} \to P\ell^+\nu_\ell$ decays has been slow, and experimental measurements sparse. Before BESIII, only CLEO reported a measurement, that of $f_+^{D\to\eta}(0)$ [1349]. For this analysis both tagged and untagged methods were used. Recently, BESIII reported measurements of $f_+^{D\to\eta}(0)$, $f_+^{D_s\to\eta}(0)$, $f_+^{D_s\to\eta'}(0)$ and $f_+^{D_s\to K}(0)$ using a tagged method [1348,1350,1352]. These measurements greatly expand experimental knowledge of hadronic form factors in $D \to P\ell^+\nu_\ell$ decays. To date, there is still no measurement of $f_+^{D\to\eta'}(0)$ due to the small amount of data available.

On the theory side, lattice QCD calculations of $f_+^{D_s\to\eta^{(\prime)}}(0)$ for $D_s^+ \to \eta^{(\prime)}e^+\nu_e$ were presented in Ref. [1353], but with no systematic uncertainties included. Other calculations of $f_+^{D^+_{(s)}\to\eta^{(\prime)}}(0)$ and $f_+^{D_s\to K}(0)$ have been reported based on QCD light-cone sum rules (LCSR) [1354–1356], three-point QCD sum rules (3PSR) [1357], a light-front quark model

TABLE 290. Results for $f_+^{D\to\eta}(0)|V_{cd}|$ from various experiments.

$D^+ \to \eta\ell\nu_\ell$ measurement	Mode	$\lvert V_{cd}\rvert f_+^{D\to\eta}(0)$	Comment
BESIII 2017 [1351]	$(D^+; \ell = e)$	0.087(8)(2)	z expansion, 2 terms
BESIII 2015A [1350]	$(D^0; \ell = e)$	0.079(6)(2)	z expansion, 2 terms
CLEO-c 2009 [1349]	$(D^0, D^+; \ell = e)$	0.085(6)(1)	z expansion, 2 terms
World average		**0.083(4)**	BESIII syst fully correlated

TABLE 291. Summary of the latest LQCD calculations of $f_+^{D\to\pi}(0)$ and $f_+^{D\to K}(0)$ from the Fermilab/MILC, ETM, and HPQCD collaborations.

Collaboration	$f_+^{D\to\pi}(0)$	$f_+^{D\to K}(0)$
Fermilab Lattice and MILC [1365]	$0.625 \pm 0.017 \pm 0.013$	$0.768 \pm 0.012 \pm 0.011$
ETM$(2+1+1)$ [1362]	0.612 ± 0.035	0.765 ± 0.031
HPQCD$(2+1)$ [1363,1364]	0.666 ± 0.029	0.747 ± 0.019
Average	0.634 ± 0.015	0.760 ± 0.011

(LFQM) [1358,1359], a constituent quark model (CQM) [1360], and a covariant confined quark model (CCQM) [1361]. Table 287 summarizes both experimental measurements and theoretical calculations of these form factors. The $f_+^{D_s\to K}(0)$ value measured by BESIII is consistent with current theoretical calculations. The $f_+^{D_s\to\eta}(0)$ and $f_+^{D_s\to\eta'}(0)$ values measured by BESIII are consistent with the LCSR calculations of Refs. [1354,1355]; however, the calculation of Ref. [1355] is inconsistent with the measured value of $f_+^{D\to\eta}(0)$. More robust theoretical calculations of these form factors for both D^+ and D_s^+ semileptonic decays are desired.

10. Determinations of $|V_{cs}|$ and $|V_{cd}|$

Assuming unitarity of the CKM matrix, the values of the CKM matrix elements entering in charm semileptonic decays are evaluated as [9]

$$|V_{cs}| = 0.97320 \pm 0.00011,$$
$$|V_{cd}| = 0.22636 \pm 0.00048. \quad (274)$$

Using the world average values of $f_+^K(0)|V_{cs}|$ and $f_+^\pi(0)|V_{cd}|$ from Tables 288 and 289 leads to the form factor values

$$f_+^K(0) = 0.7361 \pm 0.0034,$$
$$f_+^\pi(0) = 0.6351 \pm 0.0081,$$

where the former one deviates with the present average of lattice QCD calculations by 2.1σ while good consistency is found for the latter one. Table 291 summarizes $f_+^{D\to\pi}(0)$ and $f_+^{D\to K}(0)$ results based on $N_f = 2+1+1$ flavor lattice QCD of the ETM collaboration [1362], and earlier results based on $N_f = 2+1$ flavor lattice QCD of the HPQCD collaboration [1363,1364]. Recently, the Fermilab Lattice and MILC collaborations released their preliminary results of $f_+^{D\to K}(0)$ and $f_+^{D\to\pi}(0)$ based on $N_f = 2+1+1$ flavor lattice QCD calculations [1365]. The weighted averages are $f_+^{D\to\pi}(0) = 0.634 \pm 0.015$ and $f_+^{D\to K}(0) = 0.760 \pm 0.011$, respectively. The experimental accuracy is at present better than that from lattice calculations.

Alternatively, if one assumes the lattice QCD form factor values, the averages in Tables 288 and 289 give

$$|V_{cs}| = 0.9447 \pm 0.0043(\text{exp}) \pm 0.0137(\text{LQCD}),$$
$$|V_{cd}| = 0.2249 \pm 0.0028(\text{exp}) \pm 0.0055(\text{LQCD}).$$

Here, the uncertainties are dominated by the lattice QCD calculations. These values are consistent within 1.9σ and 0.1σ, respectively, with those obtained from the PDG global fit assuming CKM unitarity [9].

11. Test of $e-\mu$ lepton flavor universality

In the Standard Model (SM), the couplings between the three families of leptons and gauge bosons are expected to be equal; this is known as lepton flavor universality (LFU). The semileptonic decays of pseudoscalar mesons are well understood in the SM and thus offer a robust way to test LFU and search for new physics. Various tests of LFU with B semileptonic decays have been reported by *BABAR*, Belle, and LHCb. The average of the ratio of the branching fractions $\mathcal{B}_{B\to\bar{D}^{(*)}\tau^+\nu_\tau}/\mathcal{B}_{B\to\bar{D}^{(*)}\ell^+\nu_\ell}$ ($\ell = \mu$, e) deviates from the SM prediction by 3.4σ (see Sec. VII F). Precision measurements of the semileptonic D decays also test LFU, and in a manner complimentary to that of B decays [1366]. Within the SM, the ratios $\mathcal{B}_{D\to\bar{K}\mu^+\nu_\mu}/\mathcal{B}_{D\to\bar{K}e^+\nu_e}$ and $\mathcal{B}_{D\to\pi\mu^+\nu_\mu}/\mathcal{B}_{D\to\pi e^+\nu_e}$ are predicted to be 0.975 ± 0.001 and 0.985 ± 0.002, respectively [1367]. The ratios are expected to be close to unity with negligible uncertainty mainly due to high correlation of the corresponding hadronic form factors [1367].

In the SM, the semimuonic D decays are expected to have lower branching fraction than their semielectronic counterparts. Before BESIII, however, the information related to the semimuonic D decays is relatively poor, mainly due to higher backgrounds caused due to difficulty of distinguishing muon and charged pions. In the charmed meson sector, only $D^0 \to K^-\mu^+\nu_\mu$, $D^0 \to K^{*-}\mu^+\nu_\mu$, $D^0 \to \pi^-\mu^+\nu_\mu$, $D^+ \to \bar{K}^0\mu^+\nu_\mu$, $D^+ \to \rho^0\mu^+\nu_\mu$, and $D^+ \to \bar{K}^{*0}\mu^+\nu_\mu$ have been investigated in experiments previously. Except for $D^+ \to \bar{K}^{*0}\mu^+\nu_\mu$, all measurements of the other decays are dominated by FOCUS and Belle experiments and the existing measurements suffer large uncertainties.

Since 2016, BESIII performed a series of studies of semimuonic D decays, including improved measurements of $D^+ \to \bar{K}^0\mu^+\nu_\mu$ [1341], $D^0 \to \pi^-\mu^+\nu_\mu$ [1343], and $D^0 \to K^-\mu^+\nu_\mu$ [1340], and the first observations of

$D^+ \to \pi^0\mu^+\nu_\mu$ [1343], $D^+ \to \omega\mu^+\nu_\mu$ [1368], $D^+ \to \eta\mu^+\nu_\mu$ [1351]. All these analyses used the tagged method and 2.93 fb^{-1} of data taken at 3.773 GeV. The reported branching fractions are

$$\mathcal{B}(D^+ \to \bar{K}^0\mu^+\nu_\mu) = (8.72 \pm 0.07 \pm 0.18)\%, \quad (275)$$

$$\mathcal{B}(D^0 \to \pi^-\mu^+\nu_\mu) = (0.272 \pm 0.008 \pm 0.006)\%, \quad (276)$$

$$\mathcal{B}(D^+ \to \pi^0\mu^+\nu_\mu) = (0.350 \pm 0.011 \pm 0.010)\%, \quad (277)$$

$$\mathcal{B}(D^0 \to K^-\mu^+\nu_\mu) = (3.413 \pm 0.019 \pm 0.035)\%, \quad (278)$$

$$\mathcal{B}(D^+ \to \omega\mu^+\nu_\mu) = (0.177 \pm 0.018 \pm 0.011)\%, \quad (279)$$

$$\mathcal{B}(D^+ \to \eta\mu^+\nu_\mu) = (0.104 \pm 0.010 \pm 0.005)\%. \quad (280)$$

Combining these results with previous BESIII measurements of their counterparts of the semielectronic decays using the same data sample, the ratios of branching fractions are

$$\frac{\mathcal{B}(D^0 \to \pi^-\mu^+\nu_\mu)}{\mathcal{B}(D^0 \to \pi^-e^+\nu_e)} = 0.922 \pm 0.030 \pm 0.022, \quad (281)$$

$$\frac{\mathcal{B}(D^+ \to \pi^0\mu^+\nu_\mu)}{\mathcal{B}(D^+ \to \pi^0e^+\nu_e)} = 0.964 \pm 0.037 \pm 0.026, \quad (282)$$

$$\frac{\mathcal{B}(D^0 \to K^-\mu^+\nu_\mu)}{\mathcal{B}(D^0 \to K^-e^+\nu_e)} = 0.974 \pm 0.007 \pm 0.012, \quad (283)$$

$$\frac{\mathcal{B}(D^+ \to \omega\mu^+\nu_\mu)}{\mathcal{B}(D^+ \to \omega e^+\nu_e)} = 1.05 \pm 0.14, \quad (284)$$

$$\frac{\mathcal{B}(D^+ \to \eta\mu^+\nu_\mu)}{\mathcal{B}(D^+ \to \eta e^+\nu_e)} = 0.91 \pm 0.13. \quad (285)$$

In addition, using the world average for $\mathcal{B}(D^+ \to \bar{K}^0e^+\nu_e)$ [9] gives

$$\frac{\mathcal{B}(D^+ \to \bar{K}^0\mu^+\nu_\mu)}{\mathcal{B}(D^+ \to \bar{K}^0e^+\nu_e)} = 1.00 \pm 0.03. \quad (286)$$

These results indicate that any $e-\mu$ LFU violation in D semileptonic decays has to be at the level of a few percent or less. BESIII also tested $e-\mu$ LFU in separate q^2 intervals using $D^{0(+)} \to \pi^{-(0)}\ell^+\nu_\ell$ [1343] and $D^0 \to K^-\ell^+\nu_\ell$ [1340] decays. No indication of LFU above the 2σ level was found.

In 2018, using 0.482 fb^{-1} of data taken at a center-of-mass energy of 4.009 GeV, BESIII reported measurements of the branching fractions for semileptonic decays $D_s^+ \to \phi\mu^+\nu_\mu$, $D_s^+ \to \eta\mu^+\nu_\mu$, and $D_s^+ \to \eta'\mu^+\nu_\mu$ [1369]. Combining these results with previous measurements of $D_s^+ \to \phi e^+\nu_e$ [1369], $D_s^+ \to \eta e^+\nu_e$, and $D_s^+ \to \eta' e^+\nu_e$ [1370] gives the ratios

$$\frac{\mathcal{B}(D_s^+ \to \phi\mu^+\nu_\mu)}{\mathcal{B}(D_s^+ \to \phi e^+\nu_e)} = 0.86 \pm 0.29, \quad (287)$$

$$\frac{\mathcal{B}(D_s^+ \to \eta\mu^+\nu_\mu)}{\mathcal{B}(D_s^+ \to \eta e^+\nu_e)} = 1.05 \pm 0.24, \quad (288)$$

$$\frac{\mathcal{B}(D_s^+ \to \eta'\mu^+\nu_\mu)}{\mathcal{B}(D_s^+ \to \eta' e^+\nu_e)} = 1.14 \pm 0.68. \quad (289)$$

These values are all consistent with unity. The uncertainties include both statistical and systematic uncertainties, the former of which dominates.

12. $D \to V\ell\nu_\ell$ decays

When the final state hadron is a vector meson, the decay can proceed through both vector and axial vector currents, and four form factors are needed. The hadronic current is $H_\mu = V_\mu + A_\mu$, where [1321]

$$V_\mu = \langle V(p,\varepsilon)|\bar{q}\gamma_\mu c|D(p')\rangle = \frac{2V(q^2)}{m_D + m_V}\varepsilon_{\mu\nu\rho\sigma}\varepsilon^{*\nu}p'^\rho p^\sigma, \quad (290)$$

$$\begin{aligned} A_\mu &= \langle V(p,\varepsilon)|-\bar{q}\gamma_\mu\gamma_5 c|D(p')\rangle \\ &= -i(m_D + m_V)A_1(q^2)\varepsilon_\mu^* \\ &\quad + i\frac{A_2(q^2)}{m_D + m_V}(\varepsilon^*\cdot q)(p' + p)_\mu \\ &\quad + i\frac{2m_V}{q^2}(A_3(q^2) - A_0(q^2))[\varepsilon^*\cdot(p' + p)]q_\mu. \end{aligned} \quad (291)$$

In this expression, m_V is the invariant mass of the daughter particles of the V meson and

$$A_3(q^2) = \frac{m_D + m_V}{2m_V}A_1(q^2) - \frac{m_D - m_V}{2m_V}A_2(q^2). \quad (292)$$

To avoid divergence of the $i\frac{2m_V}{q^2}(A_3(q^2) - A_0(q^2))$ item, kinematics require that $A_3(0) = A_0(0)$. Terms proportional to q_μ are negligible for $\ell = e$. Thus, only the three form factors $A_1(q^2)$, $A_2(q^2)$ and $V(q^2)$ are relevant for charm decays.

The differential decay rate is

$$\frac{d\Gamma(D\to V\bar{\ell}\nu_\ell)}{dq^2\,d\cos\theta_\ell}=\frac{G_F^2|V_{cq}|^2}{128\pi^3 m_D^2}p^*q^2\left[\frac{(1-\cos\theta_\ell)^2}{2}|H_-|^2+\frac{(1+\cos\theta_\ell)^2}{2}|H_+|^2+\sin^2\theta_\ell|H_0|^2\right], \tag{293}$$

where $H_\pm$ and H_0 are helicity amplitudes, corresponding to helicities of the vector (V) meson. The helicity amplitudes can be expressed in terms of the form factors as

$$H_\pm=\frac{1}{m_D+m_V}[(m_D+m_V)^2A_1(q^2)\mp 2m_Dp^*V(q^2)], \tag{294}$$

$$H_0=\frac{1}{|q|}\frac{m_D^2}{2m_V(m_D+m_V)}\left[\left(1-\frac{m_V^2-q^2}{m_D^2}\right)(m_D+m_V)^2A_1(q^2)-4p^{*2}A_2(q^2)\right]. \tag{295}$$

Here $p^*=\frac{[(m_D^2-(m_V+q))^2(m_D^2-(m_V-q))]^{1/2}}{2m_D}$ is the magnitude of the three-momentum of the V system as measured in the D rest frame, and θ_ℓ is the angle of the lepton momentum with respect to the direction opposite that of the D in the W rest frame (see Fig. 92 for the electron case, θ_e). The left-handed nature of the quark current manifests itself as $|H_-|>|H_+|$. The differential decay rate for $D\to V\ell\nu$ followed by the vector meson decaying into two pseudoscalars is

$$\begin{aligned}\frac{d\Gamma(D\to V\bar{\ell}\nu,V\to P_1P_2)}{dq^2d\cos\theta_V d\cos\theta_\ell d\chi}=&\frac{3G_F^2}{2048\pi^4}|V_{cq}|^2\frac{p^*(q^2)q^2}{m_D^2}\mathcal{B}(V\to P_1P_2)\\&\times\{(1+\cos\theta_\ell)^2\sin^2\theta_V|H_+(q^2)|^2+(1-\cos\theta_\ell)^2\sin^2\theta_V|H_-(q^2)|^2+4\sin^2\theta_\ell\cos^2\theta_V|H_0(q^2)|^2\\&-4\sin\theta_\ell(1+\cos\theta_\ell)\sin\theta_V\cos\theta_V\cos\chi H_+(q^2)H_0(q^2)\\&+4\sin\theta_\ell(1-\cos\theta_\ell)\sin\theta_V\cos\theta_V\cos\chi H_-(q^2)H_0(q^2)\\&-2\sin^2\theta_\ell\sin^2\theta_V\cos 2\chi H_+(q^2)H_-(q^2)\},\end{aligned} \tag{296}$$

where the helicity angles θ_ℓ, θ_V, and acoplanarity angle χ are defined as shown in Fig. 92. Usually, the ratios of the form factors at $q^2=0$ are defined as

$$r_V\equiv\frac{V(0)}{A_1(0)}, \tag{297}$$

$$r_2\equiv\frac{A_2(0)}{A_1(0)}. \tag{298}$$

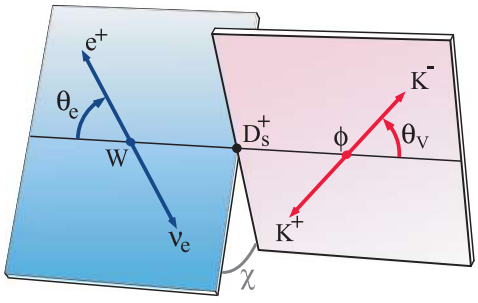

FIG. 92. Decay angles θ_V, θ_ℓ and χ. Note that the angle χ between the decay planes is defined in the D-meson reference frame, whereas the angles θ_V and θ_ℓ are defined in the V meson and W reference frames, respectively.

From the experimental point of view, these ratios can be obtained without any assumption about the total decay rates or the CKM matrix elements.

13. Vector form factor measurements

In 2002 FOCUS reported an asymmetry in the observed $\cos(\theta_V)$ distribution in $D^+\to K^-\pi^+\mu^+\nu$ decays [1371]. This was interpreted as evidence for an S-wave $K^-\pi^+$ component in the decay amplitude. It should be noted that $H_0(q^2)$ is equal to zero at for $q^2=q^2_{\mathrm{m\ max}}$ but dominated over a wide range of q^2, especially at $q^2=0$ [1372]. The distribution given by Eq. (296) is, after integration over χ, roughly proportional to $\cos^2\theta_V$. Inclusion of a constant S-wave amplitude of the form $Ae^{i\delta}$ leads to an interference term proportional to $|AH_0\sin\theta_\ell\cos\theta_V|$ which then causes an asymmetry in $\cos(\theta_V)$. When FOCUS fit their data including this S-wave amplitude, they obtained $A=0.330\pm0.022\pm0.015\,\mathrm{GeV}^{-1}$ and $\delta=0.68\pm0.07\pm0.05$ [1373]. Both *BABAR* [1374] and CLEO-c [1375] have also found evidence for an $f_0\to K^+K^-$ component in semileptonic D_s decays.

The CLEO-c collaboration extracted the form factors $H_+(q^2)$, $H_-(q^2)$, and $H_0(q^2)$ from 11000 $D^+\to K^-\pi^+\ell^+\nu_\ell$ events with purity greater than 96% in a model-independent

TABLE 292. Results for r_V and r_2 from various experiments. Experiments marked with * did not consider a separate S-wave contribution.

Experiment	References	r_V	r_2
$D^+ \to \bar{K}^{*0}\ell^+\nu_\ell$			
E691*	[1385]	$2.0 \pm 0.6 \pm 0.3$	$0.0 \pm 0.5 \pm 0.2$
E653*	[1386]	$2.00 \pm 0.33 \pm 0.16$	$0.82 \pm 0.22 \pm 0.11$
E687*	[1387]	$1.74 \pm 0.27 \pm 0.28$	$0.78 \pm 0.18 \pm 0.11$
E791 (e)*	[1388]	$1.90 \pm 0.11 \pm 0.09$	$0.71 \pm 0.08 \pm 0.09$
E791 (μ)*	[1389]	$1.84 \pm 0.11 \pm 0.09$	$0.75 \pm 0.08 \pm 0.09$
Beatrice*	[1390]	$1.45 \pm 0.23 \pm 0.07$	$1.00 \pm 0.15 \pm 0.03$
FOCUS	[1373]	$1.504 \pm 0.057 \pm 0.039$	$0.875 \pm 0.049 \pm 0.064$
BESIII (e)	[1381]	$1.406 \pm 0.058 \pm 0.022$	$0.784 \pm 0.041 \pm 0.024$
$D^0 \to \bar{K}^0\pi^-\ell^+\nu_\ell$			
FOCUS (μ)	[1391]	$1.706 \pm 0.677 \pm 0.342$	$0.912 \pm 0.370 \pm 0.104$
BABAR (μ)	[1377]	$1.493 \pm 0.014 \pm 0.021$	$0.775 \pm 0.011 \pm 0.011$
BESIII (e)	[1382]	$1.46 \pm 0.07 \pm 0.02$	$0.67 \pm 0.06 \pm 0.01$
$D^+ \to \omega e^+\nu_e$			
BESIII	[1383]	$1.24 \pm 0.09 \pm 0.06$	$1.06 \pm 0.15 \pm 0.05$
$D^{0,+} \to \rho e\nu_e$			
CLEO-c	[1380]	$1.48 \pm 0.15 \pm 0.05$	$0.83 \pm 0.11 \pm 0.04$
BESIII	[1384]	$1.695 \pm 0.083 \pm 0.051$	$0.845 \pm 0.056 \pm 0.039$
$D_s^+ \to \phi e^+\nu_e$			
BABAR	[1374]	$1.849 \pm 0.060 \pm 0.095$	$0.763 \pm 0.071 \pm 0.065$
$D_s^+ \to K^{*0}e^+\nu_e$			
BESIII*	[1352]	$1.67 \pm 0.34 \pm 0.16$	$0.77 \pm 0.28 \pm 0.07$

fashion directly as functions of q^2 [1376]. They also determined the S-wave form factor $h_0(q^2)$ via the interference term, despite the fact that the $K\pi$ mass distribution appears dominated by the vector $K^*(892)$ state. It is observed that $H_0(q^2)$ dominates over a wide range of q^2, especially at low q^2. The transverse form factor,

$$H_t(q^2) = \frac{M_D K}{m_{K\pi}\sqrt{q^2}}\left[(M_D + m_{K\pi})A_1(q^2) - \frac{(M_D^2 - m_{K\pi}^2 + q^2)}{M_D + m_{K\pi}}A_2(q^2) + \frac{2q^2}{M_D + m_{K\pi}}A_3(q^2)\right],$$

which can be related to $A_3(q^2)$, is small compared to LQCD calculations and suggests that the form factor ratio $r_3 \equiv A_3(0)/A_1(0)$ is large and negative.

The *BABAR* collaboration selected a large sample of 244×10^3 $D^+ \to K^-\pi^+e^+\nu_e$ candidates with a ratio $S/B \sim 2.3$ from an integrated luminosity of 347 fb^{-1} [1377]. With four particles emitted in the final state, the differential decay rate depends on five variables. In addition to the four variables defined in previous sections there is also m^2, the mass squared of the $K\pi$ system. To analyze the $D^+ \to K^-\pi^+e^+\nu_e$ decay channel, it was assumed that all form factors have a q^2 variation given by the simple pole model, and an effective pole mass of $m_A = (2.63 \pm 0.10 \pm 0.13)$ GeV/c^2 is fitted. This value is compatible with expectations when comparing to the mass of $J^P = 1^+$ charm mesons. For the mass dependence of the form factors, a Breit-Wigner with a mass-dependent width and a Blatt-Weisskopf damping factor is used. For the S-wave amplitude, a polynomial below the $\bar{K}_0^*(1430)$, and a Breit-Wigner distribution above, are used [1377]. These are consistent with measurements of $D^+ \to K^-\pi^+\pi^+$ decays. For the polynomial part, a linear term is sufficient to fit the data. It is verified that the variation of the S-wave phase is compatible with expectations from elastic $K\pi$ scattering [338,1378] (after correcting for $\delta^{3/2}$) according to Watson's theorem [1379]. As compared with elastic $K^-\pi^+$ scattering, there is an additional negative sign between the S and P waves. Contributions from other spin-1 and spin-2 resonances decaying into $K^-\pi^+$ are also considered.

In 2013, CLEO-c reported the first measurements of form factors in $D^{0,+} \to \rho e^+\nu_e$ [1380]. Since 2016, several new measurements of form factors in $D_{(s)} \to Ve^+\nu_e$ decays have been reported by BESIII. These measurements greatly increase the information available on $D \to V\ell^+\nu_e$ decays. The BESIII data was recorded at center-of-mass energies of 3.773 GeV (2.93 fb^{-1}) and 4.178 GeV (3.19 fb^{-1}). The $D \to Ve^+\nu_e$ samples are reconstructed using a tagged method, and 18262, 3112, 978, 491, and 155 signal events, respectively, are obtained for the $D^+ \to \bar{K}^{*0}e^+\nu_e$, $D^0 \to K^{*-}e^+\nu_e$, $D^{0,+} \to \rho e^+\nu_e$, $D^+ \to \omega e^+\nu_e$, and

$D_s^+ \to K^{*0} e^+ \nu_e$ decay modes [1352,1381–1384]. The form factor ratios $r_V = \frac{V(0)}{A_1(0)}$ and $r_2 = \frac{A_2(0)}{A_1(0)}$ are subsequently extracted.

Table 292 lists measurements of r_V and r_2 from several experiments. Most of the measurements assume that the q^2 dependence of the form factors is given by the simple pole ansatz. Some of these measurements do not consider a separate S-wave contribution; in this case such a contribution is implicitly included in the measured values.

14. $D \to S\ell\nu_\ell$ decays

In 2018, BESIII reported measurements of semileptonic D decays into a scalar meson, $D \to S\ell\nu$. The experiment measured $D^{0(+)} \to a_0(980) e^+ \nu_e$, with $a_0(980) \to \eta\pi$. Signal yields of $25.7^{+6.4}_{-5.7}$ events for $D^0 \to a_0(980)^- e^+ \nu_e$, and $10.2^{+5.0}_{-4.1}$ events for $D^+ \to a_0(980)^0 e^+ \nu_e$, were obtained, resulting in statistical significances of greater than 6.5σ and 3.0σ, respectively [1392]. As the branching fraction for $a_0(980) \to \eta\pi$ is not well measured, BESIII reports the product branching fractions

$$\mathcal{B}(D^0 \to a_0(980)^- e^+ \nu_e) \times \mathcal{B}(a_0(980)^- \to \eta\pi^-) = (1.33^{+0.33}_{-0.29} \pm 0.09) \times 10^{-4}, \quad (299)$$

$$\mathcal{B}(D^+ \to a_0(980)^0 e^+ \nu_e) \times \mathcal{B}(a_0(980)^0 \to \eta\pi^0) = (1.66^{+0.81}_{-0.66} \pm 0.11) \times 10^{-4}. \quad (300)$$

The ratio of these values can be compared to a prediction based on QCD light-cone sum rules [1393], after relating the $a_0(980) \to \eta\pi$ branching fractions via isospin. The result is a difference of more than 2σ. Taking the lifetimes of the D^0 and D^+ into account, and assuming $\mathcal{B}(a_0(980)^- \to \eta\pi^-) = \mathcal{B}(a_0(980)^0 \to \eta\pi^0)$, the ratio of the partial widths is

$$\frac{\Gamma(D^0 \to a_0(980)^- e^+ \nu_e)}{\Gamma(D^+ \to a_0(980)^0 e^+ \nu_e)} = 2.03 \pm 0.95 \pm 0.06. \quad (301)$$

This value is consistent with the prediction based on isospin symmetry.

Recently, BESIII searched for the semileptonic decay of $D_s^+ \to a_0(980) e^+ \nu_e$, with $a_0(980)^0 \to \eta\pi^0$. No significant signal is observed. The product branching fraction upper limit at the 90% confidence level is $\mathcal{B}(D_s^+ \to a_0(980) e^+ \nu_e) \times \mathcal{B}(a_0(980)^0 \to \eta\pi^0) < 1.2 \times 10^{-4}$ [1394].

15. $D \to A\ell\nu_\ell$ decays

Experimental studies of semileptonic D decays into an axial-vector meson $D \to A\ell\nu$ are challenging due to low statistics and high backgrounds. In 2007, CLEO-c reported first evidence for the Cabibbo-favored decay $D^0 \to K_1(1270)^- e^+ \nu_e$ with a statistical significance of 4σ [1395]. The branching fraction was measured to be $\mathcal{B}(D^0 \to K_1(1270)^- e^+ \nu_e) = (7.6^{+4.1}_{-3.0} \pm 0.6 \pm 0.7) \times 10^{-4}$. In 2019, BESIII reported the first observation of $D^+ \to \bar{K}_1(1270)^0 e^+ \nu_e$, with statistical significance greater than 10σ [1396]. The branching fraction was measured to be $\mathcal{B}(D^+ \to \bar{K}_1(1270)^0 e^+ \nu_e) = (23.0 \pm 2.6^{+1.8}_{-2.1} \pm 2.5) \times 10^{-4}$. In 2021, the $D^0 \to K_1(1270)^- e^+ \nu_e$ decay was observed for the first time by BESIII with a statistical significance greater than 10σ [1397]. The reported branching fraction is $\mathcal{B}(D^+ \to \bar{K}_1(1270)^0 e^+ \nu_e) = (10.9 \pm 1.3^{+0.9}_{-1.3} \pm 1.2) \times 10^{-4}$. Here, the third errors listed arise from the branching fraction for $K_1(1270) \to K\pi\pi$. The obtained branching fractions are consistent with the theoretical calculations with the K_1 mixing angle of 33° or 57°. Taking the lifetimes of D^0 and D^+ into account, the ratio of the partial widths is

$$\frac{\Gamma(D^+ \to \bar{K}_1(1270)^0 e^+ \nu_e)}{\Gamma(D^0 \to K_1(1270)^- e^+ \nu_e)} = 1.20 \pm 0.20 \pm 0.15. \quad (302)$$

This value agrees with unity as predicted by isospin symmetry.

In addition, BESIII has searched for the Cabibbo-suppressed semileptonic decays $D^+ \to b_1(1235)^0 e^+ \nu_e$ and $D^0 \to b_1(1235)^0 e^+ \nu_e$. No significant signal is observed. The product branching fraction upper limits at the 90% confidence level are $\mathcal{B}(D^+ \to b_1(1235)^0 e^+ \nu_e) \times \mathcal{B}(b_1(1235)^0 \to \omega\pi^0) < 1.12 \times 10^{-4}$ and $\mathcal{B}(D^0 \to b_1(1235)^- e^+ \nu_e) \times \mathcal{B}(b_1(1235)^0 \to \omega\pi^0) < 1.75 \times 10^{-4}$, respectively [1398].

B. Leptonic decays

Purely leptonic decays of D^+ and D_s^+ mesons are among the simplest and best understood probes of $c \to d$ and $c \to s$ quark flavor-changing transitions. The amplitude of purely leptonic decays consists of the annihilation of the initial quark-antiquark pair ($c\bar{d}$ or $c\bar{s}$) into a virtual W^+ that subsequently materializes as an antilepton-neutrino pair ($\ell^+ \nu_\ell$). The Standard Model branching fraction is given by

$$\mathcal{B}(D_q^+ \to \ell^+ \nu_\ell) = \frac{G_F^2}{8\pi} \tau_{D_q} f_{D_q}^2 |V_{cq}|^2 m_{D_q} m_\ell^2 \left(1 - \frac{m_\ell^2}{m_{D_q}^2}\right)^2, \quad (303)$$

where m_{D_q} is the D_q meson mass, τ_{D_q} is its lifetime, m_ℓ is the charged lepton mass, $|V_{cq}|$ is the magnitude of the relevant CKM matrix element, and G_F is the Fermi coupling constant. The parameter f_{D_q} is the D_q meson decay constant and parametrizes the overlap of the wave functions of the constituent quark and antiquark. The decay constants have been calculated using several theory methods, the most accurate and robust being that of lattice QCD (LQCD). Using the $N_f = 2 + 1 + 1$ flavor LQCD calculations of f_{D^+} and $f_{D_s^+}$ from the ETM [1399] and

TABLE 293. Experimental results and world averages for $\mathcal{B}(D^+ \to \ell^+\nu_\ell)$ and $f_D|V_{cd}|$. The first uncertainty is statistical and the second is experimental systematic. The third uncertainty in the case of $f_{D^+}|V_{cd}|$ is due to external inputs (dominated by the uncertainty on τ_D). Here, we take the unconstrained result from CLEO-c.

Mode	$\mathcal{B}$ (10^{-4})	$f_D\|V_{cd}\|$ (MeV)	References	
$\mu^+\nu_\mu$	$3.95 \pm 0.35 \pm 0.09$	$47.2 \pm 2.1 \pm 0.5 \pm 0.2$	CLEO-c	[1258]
	$3.71 \pm 0.19 \pm 0.06$	$45.7 \pm 1.2 \pm 0.4 \pm 0.2$	BESIII	[1408]
	$\mathbf{3.77 \pm 0.17 \pm 0.05}$	$\mathbf{46.1 \pm 1.0 \pm 0.3 \pm 0.2}$	*Average*	
$\tau^+\nu_\tau$	$12.0 \pm 2.4 \pm 1.2$	$50.4 \pm 5.0 \pm 2.5 \pm 0.2$	BESIII	[1407]
$\boldsymbol{\mu^+\nu_\mu + \tau^+\nu_\tau}$		$\mathbf{46.2 \pm 1.0 \pm 0.3 \pm 0.2}$	*Average*	
$e^+\nu_e$	<0.088 at 90% C.L.		CLEO-c	[1258]

FNAL/MILC [1400] Collaborations, the Flavour Lattice Averaging Group (FLAG) calculates world average values [1401]

$$f_{D^+}^{\text{FLAG}} = 212.0 \pm 0.7 \text{ MeV}, \tag{304}$$

$$f_{D_s^+}^{\text{FLAG}} = 249.9 \pm 0.5 \text{ MeV}, \tag{305}$$

and the ratio

$$\left(\frac{f_{D_s^+}}{f_{D^+}}\right)^{\text{FLAG}} = 1.1783 \pm 0.0016. \tag{306}$$

These values are used within this section to determine the magnitudes $|V_{cd}|$ and $|V_{cs}|$ from the measured branching fractions of $D^+ \to \ell^+\nu_\ell$ and $D_s^+ \to \ell^+\nu_\ell$.

The leptonic decays of pseudoscalar mesons are helicity-suppressed, meaning their decay rates are proportional to the square of the charged lepton mass. Thus, decays to $\tau^+\nu_\tau$ are favored over decays to $\mu^+\nu_\mu$, and decays to $e^+\nu_e$, with an expected $\mathcal{B} \lesssim 10^{-7}$, are not yet experimentally observable. The ratio of $\tau^+\nu_\tau$ to $\mu^+\nu_\tau$ decays is given by

$$R_{\tau/\mu}^{D_q} \equiv \frac{\mathcal{B}(D_q^+ \to \tau^+\nu_\tau)}{\mathcal{B}(D_q^+ \to \mu^+\nu_\mu)} = \left(\frac{m_\tau^2}{m_\mu^2}\right)\frac{(m_{D_q}^2 - m_\tau^2)^2}{(m_{D_q}^2 - m_\mu^2)^2}, \tag{307}$$

and equals 9.75 ± 0.01 for D_s^+ decays and 2.67 ± 0.01 for D^+ decays, based on the well-measured values of m_μ, m_τ, and $m_{D_{(s)}}$ [9]. A significant deviation from this expectation would be interpreted as LFU violation in charged currents [1402].

In this section we present world average values for the product $f_{D_q}|V_{cq}|$, where $q = d,\ s$. For these averages, correlations between measurements and dependencies on input parameters are taken into account. In 2019, BESIII reported a measurement of $D_s^+ \to \mu^+\nu_\mu$ [1403], by analyzing 3.19 fb^{-1} of e^+e^- collision data sample taken at a center-of-mass energy of 4.178 GeV. The muon counter is used to identify μ^+ lepton, thereby offering low background. In 2021, BESIII reported an updated measurement of $D_s^+ \to \mu^+\nu_\mu$ [1404], by analyzing 6.32 fb^{-1} of e^+e^- collision data sample taken at center-of-mass energies of 4.178–4.226 GeV without using the muon counter. The new measurement of $D_s^+ \to \mu^+\nu_\mu$ supersedes the 2019 result. Moreover, measurements of $D_s^+ \to \tau^+\nu_\tau$ were also reported with $\tau^+ \to \pi^+\bar{\nu}_\tau$ [1404], $\tau^+ \to \rho^+\bar{\nu}_\tau$ [1405] and $\tau^+ \to e^+\nu_e\bar{\nu}_\tau$ [1406] decays. In 2019, BESIII reported the first observation of $D_s^+ \to \tau^+\nu_\tau$ with a statistical significance of 5.1σ [1407].

1. $D^+ \to \ell^+\nu_\ell$ decays and $|V_{cd}|$

The branching fraction $\mathcal{B}(D^+ \to \mu^+\nu_\mu)$ has been determined by CLEO-c [1258] and BESIII [1408]. These lead to the world average (WA) value

$$\mathcal{B}^{\text{WA}}(D^+ \to \mu^+\nu_\mu) = (3.77 \pm 0.17) \times 10^{-4}. \tag{308}$$

For $D^+ \to \tau^+\nu_\tau$, the recent BESIII measurement [1407] gives

$$\mathcal{B}^{\text{WA}}(D^+ \to \tau^+\nu_\tau) = (1.20 \pm 0.27) \times 10^{-4}. \tag{309}$$

Based on these two branching fractions, we extract the weighted product of the decay constant and the CKM matrix element to be

$$f_D|V_{cd}| = (46.2 \pm 1.0) \text{ MeV}. \tag{310}$$

The uncertainty listed includes the uncertainty on $\mathcal{B}^{\text{WA}}(D^+ \to \mu^+\nu_\mu)$, and also uncertainties on the external parameters m_μ, m_D, and τ_D [9] needed to extract $f_D|V_{cd}|$ from the branching fraction via Eq. (303). Using the LQCD value for f_D from FLAG [Eq. (304)], we calculate the magnitude of the CKM matrix element V_{cd} to be

$$|V_{cd}| = 0.2181 \pm 0.0049(\text{exp}) \pm 0.0007(\text{LQCD}), \tag{311}$$

where the first and second uncertainties are from experiment and from LQCD, respectively. All input values and the resulting world average are summarized in Table 293 and plotted in Fig. 93 (left).

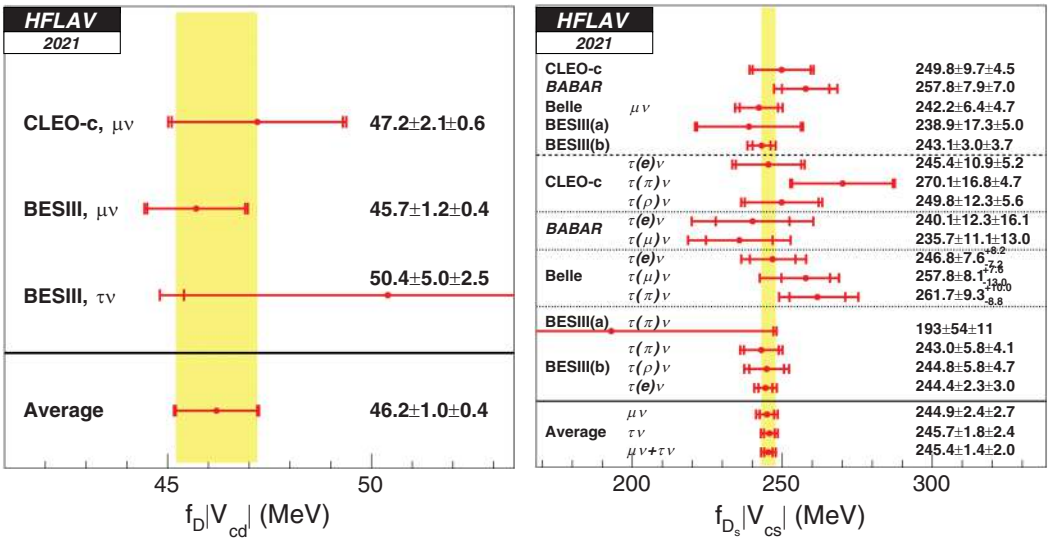

FIG. 93. WA values for $f_D|V_{cd}|$ (left) and $f_{D_s}|V_{cs}|$ (right). For each point, the first error is statistical and the second error is systematic. BESIII(a) represents results based on 0.48 fb^{-1} of data recorded at $\sqrt{s} = 4.009$ GeV [1412], and BESIII(b) represents results based on 6.32 fb^{-1} of data recorded at $\sqrt{s} = 4.178$–4.226 GeV [1405–1407].

Using the WA values of the branching fractions $\mathcal{B}(D^+ \to \mu^+\nu_\mu)$ and $\mathcal{B}(D^+ \to \tau^+\nu_\tau)$ [Eq. (308) and Eq. (314)], the ratio of these two branching fractions is determined to be

$$R^{D^+}_{\tau/\mu} = 3.18 \pm 0.73, \tag{312}$$

which is consistent with the ratio expected in the SM.

2. $D_s^+ \to \ell^+\nu_\ell$ decays and $|V_{cs}|$

We use measurements of the branching fraction $\mathcal{B}(D_s^+ \to \mu^+\nu_\mu)$ from CLEO-c [1298], *BABAR* [1409], Belle [1410], and BESIII [1404,1411] to obtain a WA value of

$$\mathcal{B}^{\text{WA}}(D_s^+ \to \mu^+\nu_\mu) = (5.43 \pm 0.16) \times 10^{-3}. \tag{313}$$

The WA value for $\mathcal{B}(D_s^+ \to \tau^+\nu_\tau)$ is also calculated from CLEO-c, *BABAR*, Belle, and BESIII measurements. CLEO-c made separate measurements using $\tau^+ \to e^+\nu_e\bar{\nu}_\tau$ [1412], $\tau^+ \to \pi^+\bar{\nu}_\tau$ [1298], and $\tau^+ \to \rho^+\bar{\nu}_\tau$ decays [1413]; *BABAR* made separate measurements using $\tau^+ \to e^+\nu_e\bar{\nu}_\tau$ and $\tau^+ \to \mu^+\nu_\mu\bar{\nu}_\tau$ decays [1409]; Belle made separate measurements using $\tau^+ \to e^+\nu_e\bar{\nu}_\tau$, $\tau^+ \to \mu^+\nu_\mu\bar{\nu}_\tau$, and $\tau^+ \to \pi^+\bar{\nu}_\tau$ decays [1410]; and BESIII made measurements using $\tau^+ \to \pi^+\bar{\nu}_\tau$ [1404,1411], $\tau^+ \to \rho^+\bar{\nu}_\tau$ [1405] and $\tau^+ \to e^+\nu_e\bar{\nu}_\tau$ [1406] decays. Combining all these results and accounting for correlations, we obtain a WA value of

$$\mathcal{B}^{\text{WA}}(D_s^+ \to \tau^+\nu_\tau) = (5.33 \pm 0.12) \times 10^{-2}. \tag{314}$$

The ratio of branching fractions is found to be

$$R^{D_s}_{\tau/\mu} = 9.82 \pm 0.36, \tag{315}$$

which is consistent with the ratio expected in the SM.

Taking the average of $\mathcal{B}^{\text{WA}}(D_s^+ \to \mu^+\nu)$ and $\mathcal{B}^{\text{WA}}(D_s^+ \to \tau^+\nu)$ [Eqs. (313) and (314)], and using the most recent values for m_τ, m_{D_s}, and τ_{D_s} [9], we calculate the product of the D_s decay constant and $|V_{cs}|$. The result is

$$f_{D_s}|V_{cs}| = (245.4 \pm 2.4)\ \text{MeV}, \tag{316}$$

where the uncertainty is due to the uncertainties on $\mathcal{B}^{\text{WA}}(D_s^+ \to \mu^+\nu_\mu)$, $\mathcal{B}^{\text{WA}}(D_s^+ \to \tau^+\nu_\tau)$, and the external inputs. All input values and the resulting world average are summarized in Table 294 and plotted in Fig. 93 (right). To calculate this average, we take into account correlations within each experiment[39] for uncertainties related to normalization, tracking, particle identification, signal and background parametrizations, and peaking background contributions.

Using the LQCD value for f_{D_s} from FLAG [Eq. (305)], we calculate the magnitude of the CKM matrix element V_{cs} to be

$$|V_{cs}| = 0.9820 \pm 0.0096(\text{exp}) \pm 0.0020(\text{LQCD}), \tag{317}$$

where the first and second uncertainties are from experiment and from lattice calculations, respectively.

[39]In the case of *BABAR*, we use the covariance matrix from the Errata of Ref. [1410].

TABLE 294. Experimental results and world averages for $\mathcal{B}(D_s^+ \to \ell^+\nu_\ell)$ and $f_{D_s}|V_{cs}|$. The first uncertainty is statistical and the second is experimental systematic. The third uncertainty in the case of $f_{D_s}|V_{cs}|$ is due to external inputs (dominated by the uncertainty on τ_{D_s}). We have adjusted the $\mathcal{B}(D_s^+ \to \tau^+\nu_\tau)$ values quoted by CLEO-c and *BABAR* to account for the most recent values of $\mathcal{B}(\tau^+ \to \pi^+\bar{\nu}_\tau)$, $\mathcal{B}(\tau^+ \to \mu^+\nu_\mu\bar{\nu}_\tau)$, and $\mathcal{B}(\tau^+ \to e^+\nu_e\bar{\nu}_\tau)$ [9]. CLEO-c and *BABAR* include the uncertainty in the number of D_s tags (denominator in the calculation of the branching fraction) in the statistical uncertainty of $\mathcal{B}$; however, we subtract this uncertainty from the statistical one and include it in the systematic uncertainty. When averaging the BESIII results of $\mathcal{B}(D_s^+ \to \tau^+\nu_\tau)$, small correlations among various measurements have been taken into account.

Mode	$\mathcal{B}$ (10^{-2})	$f_{D_s}\|V_{cs}\|$ (MeV)	References	
$\mu^+\nu_\mu$	$0.565 \pm 0.044 \pm 0.020$	$249.8 \pm 9.7 \pm 4.4 \pm 1.0$	CLEO-c	[1298]
	$0.602 \pm 0.037 \pm 0.032$	$257.8 \pm 7.9 \pm 6.9 \pm 1.0$	*BABAR*	[1409]
	$0.531 \pm 0.028 \pm 0.020$	$242.2 \pm 6.4 \pm 4.6 \pm 1.0$	Belle	[1410]
	$0.517 \pm 0.075 \pm 0.021$	$238.9 \pm 17.3 \pm 4.9 \pm 0.9$	BESIII	[1411]
	$0.535 \pm 0.013 \pm 0.016$	$243.1 \pm 3.0 \pm 3.6 \pm 1.0$	BESIII	[1404]
	$\mathbf{0.543 \pm 0.011 \pm 0.011}$	$\mathbf{244.9 \pm 2.4 \pm 2.5 \pm 1.0}$	*Average*	
$\tau^+(e^+)\nu_\tau$	$5.32 \pm 0.47 \pm 0.22$	$245.4 \pm 10.9 \pm 5.1 \pm 1.0$	CLEO-c	[1413]
$\tau^+(\pi^+)\nu_\tau$	$6.47 \pm 0.80 \pm 0.22$	$270.1 \pm 16.8 \pm 4.6 \pm 1.1$	CLEO-c	[1298]
$\tau^+(\rho^+)\nu_\tau$	$5.50 \pm 0.54 \pm 0.24$	$249.8 \pm 12.3 \pm 5.5 \pm 1.0$	CLEO-c	[1412]
$\tau^+\nu_\tau$	$5.59 \pm 0.32 \pm 0.14$	$251.7 \pm 7.2 \pm 3.2 \pm 1.0$	CLEO-c	
$\tau^+(e^+)\nu_\tau$	$5.09 \pm 0.52 \pm 0.68$	$240.1 \pm 12.3 \pm 16.1 \pm 1.0$	*BABAR*	[1409]
$\tau^+(\mu^+)\nu_\tau$	$4.90 \pm 0.46 \pm 0.54$	$235.7 \pm 11.1 \pm 13.0 \pm 1.0$		
$\tau^+\nu_\tau$	$4.96 \pm 0.37 \pm 0.57$	$237.1 \pm 8.8 \pm 13.6 \pm 1.0$	*BABAR*	
$\tau^+(e^+)\nu_\tau$	$5.38 \pm 0.33^{+0.35}_{-0.31}$	$246.8 \pm 7.6^{+8.1}_{-7.1} \pm 1.0$	Belle	[1410]
$\tau^+(\mu^+)\nu_\tau$	$5.86 \pm 0.37^{+0.34}_{-0.59}$	$257.8 \pm 8.1^{+7.5}_{-13.0} \pm 1.0$		
$\tau^+(\pi^+)\nu_\tau$	$6.05 \pm 0.43^{+0.46}_{-0.40}$	$261.7 \pm 9.3^{+10.0}_{-8.7} \pm 1.0$		
$\tau^+\nu_\tau$	$5.70 \pm 0.21 \pm 0.31$	$254.1 \pm 4.7 \pm 6.9 \pm 1.0$	Belle	
$\tau^+(\pi^+)\nu_\tau$	$3.28 \pm 1.83 \pm 0.37$	$193 \pm 54 \pm 11 \pm 1$	BESIII	[1411]
$\tau^+(\pi^+)\nu_\tau$	$5.21 \pm 0.25 \pm 0.17$	$243.0 \pm 5.8 \pm 4.0 \pm 1.0$	BESIII	[1404]
$\tau^+(\rho^+)\nu_\tau$	$5.29 \pm 0.25 \pm 0.20$	$244.8 \pm 5.8 \pm 4.6 \pm 1.0$	BESIII	[1405]
$\tau^+(e^+)\nu_\tau$	$5.27 \pm 0.10 \pm 0.12$	$244.4 \pm 2.3 \pm 2.8 \pm 1.0$	BESIII	[1406]
$\tau^+\nu_\tau$	$5.26 \pm 0.09 \pm 0.11$	$244.1 \pm 2.0 \pm 2.6 \pm 1.0$	BESIII	
	$\mathbf{5.33 \pm 0.08 \pm 0.09}$	$\mathbf{245.7 \pm 1.8 \pm 2.2 \pm 1.0}$	*Average*	
$\boldsymbol{\mu^+\nu_\mu + \tau^+\nu_\tau}$		$\mathbf{245.4 \pm 1.4 \pm 1.7 \pm 1.0}$	*Average*	
$e^+\nu_e$	<0.0083 at 90% C.L.		Belle	[1410]

3. *Comparison with other determinations of* $|V_{cd}|$ *and* $|V_{cs}|$

Table 295 summarizes, and Fig. 94 displays, all determinations of the magnitudes $|V_{cd}|$ and $|V_{cs}|$. The table and figure show that, currently, the most precise direct determinations are from leptonic D^+ and D_s^+ decays. The values obtained are in agreement within uncertainties with those obtained from a global fit assuming CKM unitarity [242]. However, there is a 2.1σ tension for the $|V_{cs}|$ values determined from leptonic and semileptonic $D_{(s)}$ decays.

TABLE 295. Averages of the magnitudes of CKM matrix elements $|V_{cd}|$ and $|V_{cs}|$, as determined from leptonic and semileptonic $D_{(s)}$ decays. In calculating these averages, we conservatively assume that uncertainties due to LQCD are fully correlated. For comparison, values determined from neutrino scattering, from W decays, and from a global fit to the CKM matrix assuming unitarity [242] are also listed.

Method	References	Value
		$\lvert V_{cd}\rvert$
$D \to \ell\nu_\ell$	This section	$0.2181 \pm 0.0049(\text{exp}) \pm 0.0007(\text{LQCD})$
$D \to \pi\ell\nu_\ell$	Sec. XI A	$0.2249 \pm 0.0028(\text{exp}) \pm 0.0055(\text{LQCD})$
$D \to \ell\nu_\ell$ $D \to \pi\ell\nu_\ell$	*Average*	$\mathbf{0.2208 \pm 0.0040}$
νN	PDG [9]	0.230 ± 0.011
Global CKM Fit	CKM Fitter [242]	0.22636 ± 0.00048
		$\lvert V_{cs}\rvert$
$D_s \to \ell\nu_\ell$	This section	$0.9820 \pm 0.0096(\text{exp}) \pm 0.0020(\text{LQCD})$
$D \to K\ell\nu_\ell$	Sec. XI A	$0.9447 \pm 0.0043(\text{exp}) \pm 0.0137(\text{LQCD})$
$D_s \to \ell\nu_\ell$ $D \to K\ell\nu_\ell$	*Average*	$\mathbf{0.9701 \pm 0.0081}$
$W \to c\bar{s}$	PDG [9]	$0.94^{+0.32}_{-0.26} \pm 0.13$
Global CKM Fit	CKMFitter [242]	0.97320 ± 0.00011

4. Extraction of $D_{(s)}$ meson decay constants

As listed in Table 295 (and plotted in Fig. 94), the values of $|V_{cs}|$ and $|V_{cd}|$ can be determined from a global fit of the CKM matrix assuming unitarity [242]. These values can be used to extract the D^+ and D_s^+ decay constants from the world average values of $f_D|V_{cd}|$ and $f_{D_s}|V_{cs}|$ given in Eqs. (310) and (316). The results are

$$f_D^{\text{exp}} = (205.1 \pm 4.4)\ \text{MeV}, \tag{318}$$

$$f_{D_s}^{\text{exp}} = (252.2 \pm 2.5)\ \text{MeV}, \tag{319}$$

and the ratio of the decay constants is

$$\frac{f_{D_s}^{\text{exp}}}{f_D^{\text{exp}}} = 1.230 \pm 0.030. \tag{320}$$

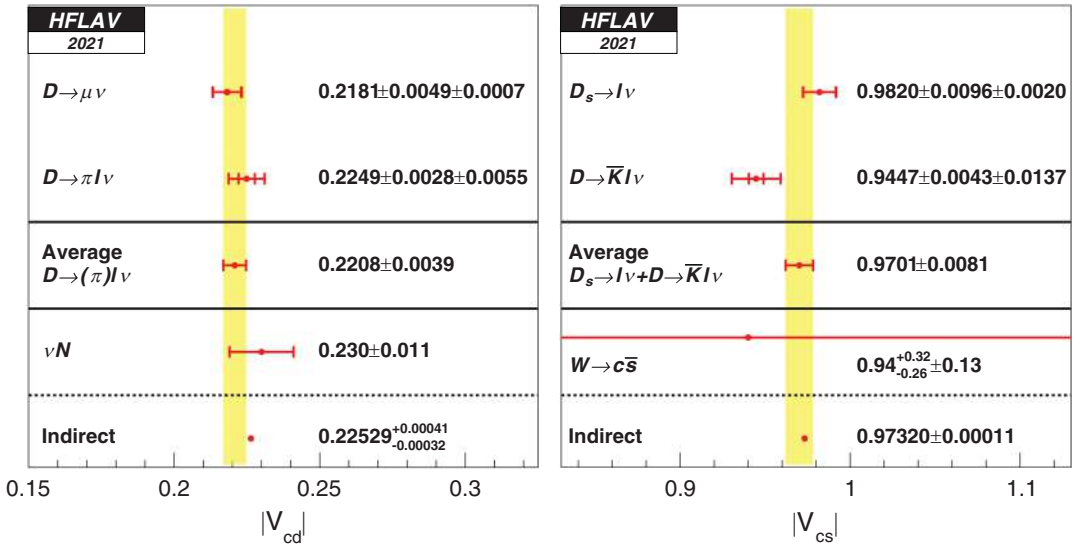

FIG. 94. Comparison of magnitudes of CKM matrix elements $|V_{cd}|$ (left) and $|V_{cs}|$ (right), as determined from leptonic and semileptonic $D_{(s)}$ decays. Also listed are results from neutrino scattering, from W decays, and from a global fit of the CKM matrix assuming unitarity [242].

These values are in agreement within their uncertainties with the LQCD values given by FLAG [Eqs. (304)–(306)]. The only discrepancy is in the ratio of decay constants; in this case the measurement is higher by 1.7σ than the LQCD prediction.

C. Hadronic D^0 decays and final state radiation

Measurements of the branching fractions for the decays $D^0 \to K^{\mp}\pi^{\pm}$, $D^0 \to \pi^+\pi^-$, and $D^0 \to K^+K^-$ have reached sufficient precision to allow averages with $\mathcal{O}(1\%)$ relative uncertainties. At this precision, final state radiation (FSR) must be treated correctly and consistently across the input measurements for the accuracy of the averages to match the precision. The sensitivity of measurements to FSR arises because of a tail in the distribution of radiated energy that extends to the kinematic limit. The tail beyond $\sum E_\gamma \approx 30$ MeV causes typical selection variables like the hadronic invariant mass to shift outside the selection range dictated by experimental resolution, as shown in Fig. 95. While the differential rate for the tail is small, the integrated rate amounts to several percent of the total $h^+h^-(n\gamma)$ rate because of the tail's extent. The tail therefore translates directly into a several percent loss in experimental efficiency.

All measurements that include a FSR correction have a correction based on the use of PHOTOS [1414–1418] within the experiment's Monte Carlo simulation. PHOTOS itself, however, has evolved, over the period spanning the set of measurements [1417]. In particular, the incorporation of interference between radiation from the two separate mesons has proceeded in stages: it was first available for particle-antiparticle pairs in version 2.00 (1993), extended to any two-body, all-charged, final states in version 2.02 (1999), and further extended to multibody final states in version 2.15 (2005). The effects of interference are clearly visible, as shown in Fig. 95, and cause a roughly 30% increase in the integrated rate into the high energy photon tail. To evaluate the FSR correction incorporated into a given measurement, we must therefore note whether any correction was made, the version of PHOTOS used in correction, and whether the interference terms in PHOTOS were turned on. Also worth noting, an exponentiated multiple-photon mode was introduced in PHOTOS version 2.09, which allows PHOTOS to also simulate photons with low energies; this mode can be switched on or off.

1. Updates to the branching fractions

Before averaging the measured branching fractions, the published results are updated, as necessary, to the FSR prediction of PHOTOS 2.15 with interference included and exponentiated multiple-photon mode turned on. The update will always shift a branching fraction to a higher value: with no FSR correction or a FSR correction suboptimally modeled, the experimental efficiency determination will be biased high, and therefore the branching fraction will be biased low.

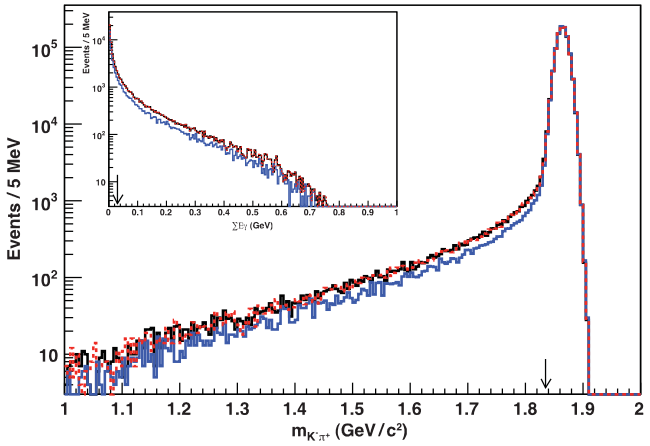

FIG. 95. The $K\pi$ invariant mass distribution for $D^0 \to K^-\pi^+(n\gamma)$ decays. The three curves correspond to three different configurations of PHOTOS for modeling FSR: version 2.02 without interference (blue/gray), version 2.02 with interference (red dashed) and version 2.15 with interference (black). The true invariant mass has been smeared with a typical experimental resolution of 10 MeV/c^2. Inset: The corresponding spectrum of total energy radiated per event. The arrow indicates the $\sum E_\gamma$ value that begins to shift kinematic quantities outside of the range typically accepted in a measurement.

Most of the branching fraction analyses used the kinematic quantity sensitive to FSR in the candidate selection criteria. For the analyses at the $\psi(3770)$, this variable was ΔE, the difference between the candidate D^0 energy and the beam energy (e.g., $E_K + E_\pi - E_{\text{beam}}$ for $D^0 \to K^-\pi^+$). In the remainder of the analyses, the relevant quantity was the reconstructed hadronic two-body mass $m_{h^+h^-}$. To make a FSR correction, we need to evaluate the fraction of decays that FSR moves outside of the range accepted for the analysis. The corrections were evaluated using an event generator (EVTGEN [1419,1420]) that incorporates PHOTOS to simulate the portions of the decay process most relevant to the correction.

We compared corrections determined both with and without smearing to account for experimental resolution; for the analyses using $m_{h^+h^-}$ as the kinematic quantity sensitive to FSR, the differences were negligible, typically of $\mathcal{O}(1\%)$ of the correction itself. The immunity of the correction to resolution effects comes about because most of the long FSR-induced tail in the $m_{h^+h^-}$ distribution resides well away from the selection boundaries. The smearing from resolution, on the other hand, mainly affects the distribution of events right at the boundary. For the analyses using ΔE however, events with low energy photons are found to substantially move events across the selection boundary; thus PHOTOS versions with exponentiated multiple-photon mode turned on and off, respectively, can give substantially different FSR corrections. In

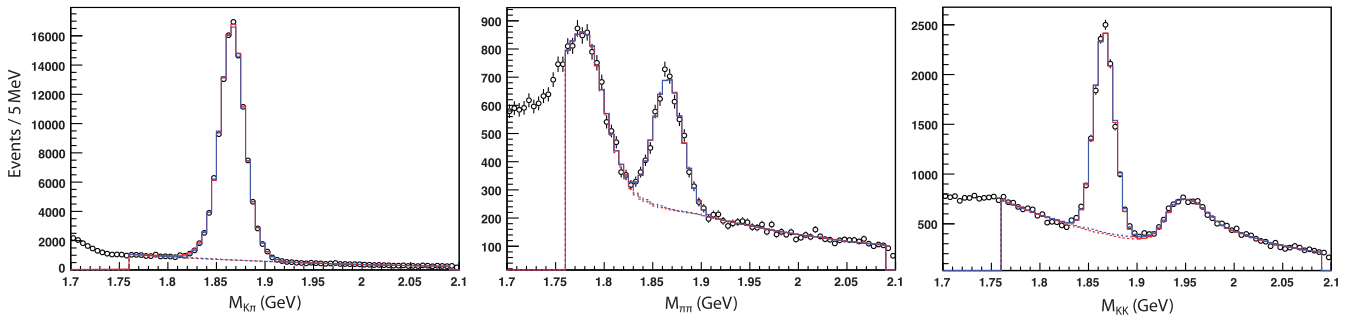

FIG. 96. FOCUS data (dots), original fits (blue) and toy MC parametrization (red) for $D^0 \to K^-\pi^+$ (left), $D^0 \to \pi^+\pi^-$ (center), and $D^0 \to \pi^+\pi^-$ (right).

the case that this mode is on, smearing of the events with low energy photons increases the amount of the FSR correction by about 10%. This is well within the uncertainty on the FSR correction, as discussed later in this section, and thus ignored.

For measurements incorporating a FSR correction that did not include interference and/or use exponentiated multiple-photon mode, we update by assessing the FSR-induced efficiency loss for both the PHOTOS version and configuration used in the analysis and our nominal version 2.15 (with interference included and exponentiated multiple-photon mode turned on). For measurements that published their sensitivity to FSR, our generator-level predictions for the original efficiency loss agreed to within a few percent of the correction. This agreement lends additional credence to the procedure.

Once the event loss from FSR in the most sensitive kinematic quantity is accounted for, the event loss in other quantities is typically very small. For example, analyses using D^{*+} tags show very little sensitivity to FSR in the reconstructed $D^{*+} - D^0$ mass difference, i.e., in $m_{h^+h^-\pi^+} - m_{h^+h^-}$. In this case, the effect of FSR tends to cancel in the difference of reconstructed masses. In the $\psi(3770)$ analyses, the beam-constrained mass distributions (e.g. $\sqrt{E^2_{\rm beam} - |\vec{p}_K + \vec{p}_\pi|^2}$) have some sensitivity, but provide negligible independent sensitivity after the ΔE selection.

The FOCUS [1421] analysis of the branching fraction ratios $\mathcal{B}(D^0 \to \pi^+\pi^-)/\mathcal{B}(D^0 \to K^-\pi^+)$ and $\mathcal{B}(D^0 \to K^+K^-)/\mathcal{B}(D^0 \to K^-\pi^+)$ obtained yields using fits to the two-body mass distributions. FSR will both distort the low end of the signal mass peak, and will contribute a signal component to the low side tail used to estimate the background. The fitting procedure is not sensitive to signal events out in the FSR tail, which would be counted as part of the background.

A more complex toy Monte Carlo procedure was required to analyze the effect of FSR on the fitted yields, which were published with no FSR corrections applied. Determining the update involved an iterative procedure in which samples of similar size to the FOCUS sample were generated and then fit using the FOCUS signal and background parametrizations. The MC parametrizations were tuned based on differences between the fits to the toy MC data and the FOCUS fits, and the procedure was repeated. These steps were iterated until the fit parameters matched the original FOCUS parameters.

The toy MC samples for the first iteration were based on the generator-level distributions of $m_{K^-\pi^+}$, $m_{\pi^+\pi^-}$, and $m_{K^+K^-}$, including the effects of FSR, smeared according to the original FOCUS resolution function, and on backgrounds generated using the parametrization from the final FOCUS fits. For each iteration, 400 to 1600 individual data-sized samples were generated and fit. The central values of the parameters from these fits determined the corrections to the generator parameters for the following iteration. The ratio between the number of signal events generated and the final signal yield provides the required FSR correction in the final iteration. Only a few iterations were required in each mode. Figure 96 shows the FOCUS data, the published FOCUS fits, and the final toy MC parametrizations. The toy MC provides an excellent description of the data.

The corrections obtained to the individual FOCUS yields were 1.0298 ± 0.0001 for $K^-\pi^+$, 1.062 ± 0.001 for $\pi^+\pi^-$, and 1.0183 ± 0.0003 for K^+K^-. These corrections tend to cancel in the branching ratios, leading to corrections (update shifts) of 1.031 ± 0.001 (3.10%) for $\mathcal{B}(D^0 \to \pi^+\pi^-)/\mathcal{B}(D^0 \to K^-\pi^+)$, and 0.9888 ± 0.0003 (-1.12%) for $\mathcal{B}(D^0 \to K^+K^-)/\mathcal{B}(D^0 \to K^-\pi^+)$.

Table 296 summarizes the updated branching fractions. The published FSR-related modeling uncertainties have been replaced with a new, common estimate; this estimate is based on the assumption that the dominant uncertainty in the FSR corrections comes from the fact that the mesons are treated as structureless particles. No contributions from structure-dependent terms in the decay process (e.g., radiation from individual quarks) are included in PHOTOS. Internal studies performed by various experiments have indicated that in $K\pi$ decays, the PHOTOS corrections agree with data at the 20%–30% level. We therefore attribute a 25% uncertainty to the (updated) FSR correction

TABLE 296. The experimental measurements relating to $\mathcal{B}(D^0 \to K^-\pi^+)$, $\mathcal{B}(D^0 \to \pi^+\pi^-)$, and $\mathcal{B}(D^0 \to K^+K^-)$ after updating them to the common version and configuration of PHOTOS. The uncertainties are statistical and total systematic, with the FSR-related systematic estimated in this procedure shown in parentheses. Also listed are the percent shifts in the results from those with the original correction (if any), in the case an update is applied here, as well as the original PHOTOS and interference configuration for each publication.

Experiment (acronym)	Result (rescaled)	Update shift [%]	PHOTOS
$D^0 \to K^-\pi^+$			
BES III 18 (BE18) [1422]	$3.931 \pm 0.006 \pm 0.067(44)\%$	1.25	2.03/Yes
CLEO-c 14 (CC14) [1262]	$3.934 \pm 0.021 \pm 0.061(31)\%$	–	2.15/Yes
BABAR 07 (BA07) [1423]	$4.035 \pm 0.037 \pm 0.074(24)\%$	0.69	2.02/No
CLEO II 98 (CL98) [1424]	$3.917 \pm 0.154 \pm 0.167(27)\%$	2.80	none
ALEPH 97 (AL97) [1425]	$3.931 \pm 0.091 \pm 0.124(27)\%$	0.79	2.0/No
ARGUS 94 (AR94) [1426]	$3.490 \pm 0.123 \pm 0.287(20)\%$	2.33	none
CLEO II 93 (CL93) [1427]	$3.965 \pm 0.080 \pm 0.171(13)\%$	0.38	2.0/No
ALEPH 91 (AL91) [1428]	$3.733 \pm 0.351 \pm 0.455(28)\%$	3.12	none
$D^0 \to \pi^+\pi^-$			
BES III 18 [1422]	$0.1529 \pm 0.0018 \pm 0.0032(23)\%$	1.39	2.03/Yes
$D^0 \to \pi^+\pi^-/D^0 \to K^-\pi^+$			
CLEO-c 10 (CC10) [1259]	$0.0370 \pm 0.0006 \pm 0.0009(02)$	–	2.15/Yes
CDF 05 (CD05) [1429]	$0.03594 \pm 0.00054 \pm 0.00043(15)$	–	2.15/Yes
FOCUS 02 (FO02) [1421]	$0.0364 \pm 0.0012 \pm 0.0006(02)$	3.10	none
$D^0 \to K^+K^-$			
BES III 18 [1422]	$0.4271 \pm 0.0021 \pm 0.0069(27)\%$	0.89	2.03/Yes
$D^0 \to K^+K^-/D^0 \to K^-\pi^+$			
CLEO-c 10 [1259]	$0.1041 \pm 0.0011 \pm 0.0012(03)$	–	2.15/Yes
CDF 05 [1429]	$0.0992 \pm 0.0011 \pm 0.0012(01)$	–	2.15/Yes
FOCUS 02 [1421]	$0.0982 \pm 0.0014 \pm 0.0014(01)$	−1.12	none

from potential structure-dependent contributions. For the other two modes, the only difference in structure is the final state valence quark content. While radiative corrections typically enter with a $1/M$ dependence, the additional contribution from the structure terms enters on a timescale shorter than the hadronization timescale. Thus, this contribution corresponds to $M \sim \Lambda_{\rm QCD}$ rather than that of the quark masses and would be the same for all three modes. We make this assumption when treating the correlations among measurements. We also assume that the PHOTOS amplitudes and any missing structure amplitudes interfere constructively. The uncertainties largely cancel in the branching fraction ratios. For the final average branching fractions, the FSR uncertainty on $K\pi$ is as large as the uncertainty due to other systematic effects. Note that because of the relative sizes of FSR in the different modes, the $\pi\pi/K\pi$ branching ratio uncertainty from FSR is positively correlated with that for the $K\pi$ branching fraction, while the $KK/K\pi$ branching ratio FSR uncertainty is negatively correlated.

The $\mathcal{B}(D^0 \to K^-\pi^+)$ measurement of Ref. [1430] (CLEO II), the $\mathcal{B}(D^0 \to \pi^+\pi^-)/\mathcal{B}(D^0 \to K^-\pi^+)$ measurements of Refs. [1281] (E791) and [1224] (CLEO II.V), and the $\mathcal{B}(D^0 \to K^+K^-)/\mathcal{B}(D^0 \to K^-\pi^+)$ measurement of Ref. [1224] are excluded from the branching fraction averages presented here. These measurements appear not to have incorporated any FSR corrections, and insufficient information is available to determine the 2%–3% update shifts that would be required.

2. Average branching fractions for $D^0 \to K^-\pi^+$, $D^0 \to \pi^+\pi^-$ and $D^0 \to K^+K^-$

The average branching fractions for $D^0 \to K^-\pi^+$, $D^0 \to \pi^+\pi^-$ and $D^0 \to K^+K^-$ decays are obtained from a single χ^2 minimization procedure, in which the three branching fractions are floating parameters. The central values are obtained from a fit in which the full covariance matrix, accounting for all statistical, systematic (excluding FSR), and FSR measurement uncertainties, is used. Table 297 presents the correlation matrix for this nominal fit. We then obtain the three reported uncertainties on those central values as follows: The statistical uncertainties are obtained from a fit using only the statistical covariance matrix. The systematic uncertainties are obtained by subtracting (in quadrature) the statistical uncertainties from the uncertainties determined via a fit using a covariance matrix that accounts for both statistical and systematic measurement uncertainties. The FSR uncertainties are obtained by subtracting (in quadrature) the uncertainties determined via a fit using a covariance matrix that accounts for both

TABLE 297. The correlation matrix corresponding to the full covariance matrix. Subscripts $h \in \{\pi, K\}$ denote which of the $D^0 \to h^+h^-$ decay results from a single experiment is represented in that row or column.

	BE18	CC14	BA07	CL98	AL97	AR94	CL93	AL91	$BE18_\pi$	$CC10_\pi$	$CD05_\pi$	$FO02_\pi$	$BE18_K$	$CC10_K$	$CD05_K$	$FO02_K$
BE18	1.0000	0 3143	0.1897	0.0777	0.1148	0.0419	0.0450	0.0319	0.6534	0.0930	0.1401	0.0948	0.5839	−0.1153	−0.0437	−0.0259
CC14	0. 3143	1.0000	0.1394	0.0571	0.0844	0.0308	0.0331	0.0234	0.3023	0.0683	0.1029	0.0697	0.1788	−0.0847	−0.0321	−0.0191
BA07	0.1897	0.1394	1.0000	0.0345	0.0509	0.0186	0.0200	0.0141	0.1825	0.0413	0.0621	0.0421	0.1079	−0.0511	−0.0194	−0.0115
CL98	0.0777	0.0571	0.0345	1.0000	0.0209	0.0076	0.0082	0.0058	0.0748	0.0169	0.0255	0.0172	0.0442	−0.0209	−0.0079	−0.0047
AL97	0.1148	0.0844	0.0509	0.0209	1.0000	0.0112	0.0121	0.1156	0.1104	0.0250	0.0376	0.0254	0.0653	−0.0309	−0.0117	−0.0070
AR94	0.0419	0.0308	0.0186	0.0076	0.0112	1.0000	0.0044	0.0031	0.0403	0.0091	0.0137	0.0093	0.0238	−0.0113	−0.0043	−0.0025
CL93	0.0450	0.0331	0.0200	0.0082	0.0121	0.0044	1.0000	0.0034	0.0433	0.0098	0.0147	0.0100	0.0256	−0.0121	−0.0046	−0.0027
AL91	0.0319	0.0234	0.0141	0.0058	0.1156	0.0031	0.0034	1.0000	0.0306	0.0069	0.0104	0.0071	0.0181	−0.0086	−0.0033	−0.0019
$BE18_\pi$	0.6534	0.3023	0.1825	0.0748	0.1104	0.0403	0.0433	0.0306	1.0000	0.0895	0.1347	0.0912	0.4334	−0.1109	−0.0421	−0.0249
$CC10_\pi$	0.0930	0.0683	0.0413	0.0169	0.0250	0.0091	0.0098	0.0069	0.0895	1.0000	0.0305	0.0206	0.0529	−0.0251	−0.0095	−0.0056
$CD05_\pi$	0.1401	0.1029	0.0621	0.0255	0.0376	0.0137	0.0147	0.0104	0.1347	0.0305	1.0000	0.0310	0.0797	−0.0378	−0.0143	−0.0085
$FO02_\pi$	0.0948	0.0697	0.0421	0.0172	0.0254	0.0093	0.0100	0.0071	0.0912	0.0206	0.0310	1.0000	0.0539	−0.0255	−0.0097	−0.0057
$BE18_K$	0.5839	0.1788	0.1079	0.0442	0.0653	0.0238	0.0256	0.0181	0.4334	0.0529	0.0797	0.0539	1.0000	−0.0656	−0.0249	−0.0148
$CC10_K$	−0.1153	−0.0847	−0.0511	−0.0209	−0.0309	−0.0113	−0.0121	−0.0086	−0.1109	−0.0251	−0.0378	−0.0255	−0.0656	1.0000	0.0118	0.0070
$CD05_K$	−0.0437	−0.0321	−0.0194	−0.0079	−0.0117	−0.0043	−0.0046	−0.0033	−0.0421	−0.0095	−0.0143	−0.0097	−0.0249	0.0118	1.0000	0.0027
$FO02_K$	−0.0259	−0.0191	−0.0115	−0.0047	−0.0070	−0.0025	−0.0027	−0.0019	−0.0249	−0.0056	−0.0085	−0.0057	−0.0148	0.0070	0.0027	1.0000

statistical and systematic measurement uncertainties from the uncertainties determined via the fit using the full covariance matrix.

In forming the full covariance matrix, the FSR uncertainties are treated as fully correlated (or anticorrelated) as described above. For the covariance matrices involving systematic measurement uncertainties, ALEPH's systematic uncertainties in the θ_{D^*} parameter are treated as fully correlated between the ALEPH 97 and ALEPH 91 measurements. Similarly, the tracking efficiency uncertainties in the CLEO II 98 and the CLEO II 93 measurements are treated as fully correlated. For the three BES III 18 results, both tracking and particle identification efficiencies for any particles shared between decay modes are treated as fully correlated. Finally, the BES III 18 results also have a fully correlated statistical dependence on the number of $D^0\bar{D}^0$ pairs produced.

The averaging procedure results in a final χ^2 of 36.0 for 13 $(16-3)$ degrees of freedom (p-value $= 5.9 \times 10^{-4}$). The branching fractions obtained are

$$\mathcal{B}(D^0 \to K^-\pi^+) = (3.999 \pm 0.006 \pm 0.031 \pm 0.032)\%, \tag{321}$$

$$\mathcal{B}(D^0 \to \pi^+\pi^-) = (0.1490 \pm 0.0012 \pm 0.0015 \pm 0.0019)\%, \tag{322}$$

$$\mathcal{B}(D^0 \to K^+K^-) = (0.4113 \pm 0.0017 \pm 0.0041 \pm 0.0025)\%. \tag{323}$$

The uncertainties, estimated as described above, are statistical, systematic (excluding FSR), and FSR modeling. The correlation coefficients from the fit using the total uncertainties are

	$K^-\pi^+$	$\pi^+\pi^-$	K^+K^-
$K^-\pi^+$	1.00	0.77	0.76
$\pi^+\pi^-$	0.77	1.00	0.58
K^+K^-	0.76	0.58	1.00

These results are explained in detail as follows. As Fig. 97 shows, the average value for $\mathcal{B}(D^0 \to K^-\pi^+)$ and the input branching fractions agree very well. For the $\mathcal{B}(D^0 \to K^-\pi^+)$ measurements only, the partial χ^2 is 4.9 in the final fit. With the estimated uncertainty in the FSR modeling used here, the FSR uncertainty dominates the statistical uncertainty in the average, suggesting that experimental work in the near future should focus on verification of FSR with $\sum E_\gamma \gtrsim 100$ MeV. Note that the systematic uncertainty excluding FSR has now approached the level of the FSR uncertainty; in the most precise

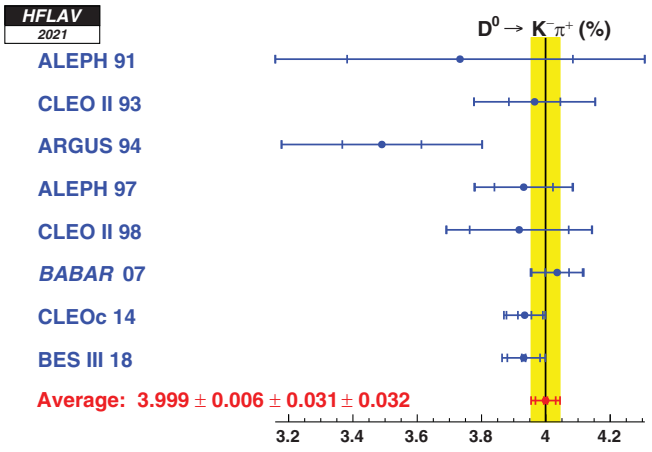

FIG. 97. Comparison of measurements of $\mathcal{B}(D^0 \to K^-\pi^+)$ (blue) with the average branching fraction obtained here (red, and yellow band). For these measurements only, the partial χ^2 is 4.9 in the final fit.

measurements of these branching fractions, the competing uncertainty is the uncertainty on the tracking efficiency.

The $\mathcal{B}(D^0 \to K^+K^-)$ and $\mathcal{B}(D^0 \to \pi^+\pi^-)$ measurements inferred from the branching ratio measurements do not agree as well (Fig. 98). There is some tension among the results when all measurements related to $\mathcal{B}(D^0 \to K^+K^-)$ and $\mathcal{B}(D^0 \to \pi^+\pi^-)$ are included in the average together. For the measurements related to $\mathcal{B}(D^0 \to K^+K^-)$ [$\mathcal{B}(D^0 \to \pi^+\pi^-)$] only, the partial χ^2 is 15.7 [6.0] in the final fit.

The $\mathcal{B}(D^0 \to K^-\pi^+)$ average obtained here is approximately two standard deviations higher than the PDG 2020 update average [9]. Table 298 shows the evolution from a fit similar to the PDG fit (no FSR updates or correlations, Ref. [1430] included) to the average presented here. There are three main contributions to the difference. The branching fraction in Ref. [1430] is low, and its exclusion shifts the result upwards. A subsequently larger shift (+0.035%) is due to the FSR updates, which as expected shift the result upwards. The largest shift (+0.050%) occurs as all of the measurements related to $\mathcal{B}(D^0 \to K^+K^-)$ and $\mathcal{B}(D^0 \to \pi^+\pi^-)$ are included in the average together with the $\mathcal{B}(D^0 \to K^-\pi^+)$ measurements.

3. Average branching fraction for $D^0 \to K^+\pi^-$

There is no reason to presume that the effects of FSR should be different in $D^0 \to K^+\pi^-$ and $D^0 \to K^-\pi^+$ decays, as both decay to one charged kaon and one charged pion; indeed, for the same version of PHOTOS the FSR simulations of these decays are identical. Measurements of the relative branching fraction ratio between the doubly Cabibbo-suppressed decay $D^0 \to K^+\pi^-$ and the Cabibbo-favored decay $D^0 \to K^-\pi^+$ (R_D, determined in Sec. X A) have now approached $\mathcal{O}(1\%)$ relative uncertainties. This makes it worthwhile to combine our R_D average with the $\mathcal{B}(D^0 \to K^-\pi^+)$ average obtained in Eq. (321), to provide a measurement of the branching fraction:

$$\mathcal{B}(D^0 \to K^+\pi^-) = (1.372 \pm 0.017) \times 10^{-4}. \quad (324)$$

Note that, by definition of R_D, these branching fractions do not include any contribution from Cabibbo-favored $\bar{D}^0 \to K^+\pi^-$ decays. Our result is more precise than the PDG 2020 value of $(1.364 \pm 0.026) \times 10^{-4}$ [9] due to our using a more precise value for the ratio R_D (obtained from a global fit to a range of mixing data, see Sec. X A).

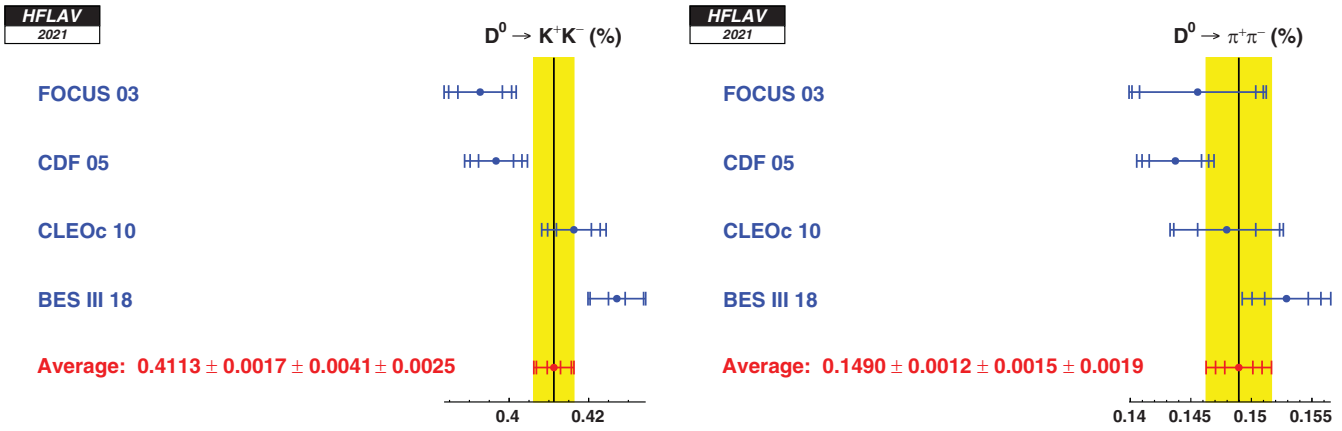

FIG. 98. The $\mathcal{B}(D^0 \to K^+K^-)$ (left) and $\mathcal{B}(D^0 \to \pi^+\pi^-)$ (right) values obtained either from absolute measurements or by scaling the measured branching ratios with the $\mathcal{B}(D^0 \to K^-\pi^+)$ branching fraction average obtained here. For the measurements (blue points), the error bars correspond to the statistical, systematic and either the $K\pi$ normalization uncertainties or, in case of an absolute measurement, the FSR modeling uncertainty. The average obtained here (red point, yellow band) lists the statistical, systematics excluding FSR, and the FSR systematic. For the measurements related to $\mathcal{B}(D^0 \to K^+K^-)$ [$\mathcal{B}(D^0 \to \pi^+\pi^-)$] only, the partial χ^2 is 15.7 [6.0] in the final fit.

TABLE 298. Evolution of the $D^0 \to K^-\pi^+$ branching fraction from a fit with no FSR updates or correlations (similar to the average in the PDG 2020 update [9]) to the nominal fit presented here.

Modes fit	Description	$\mathcal{B}(D^0 \to K^-\pi^+)$ (%)	χ^2/(degree of freedom)
$K^-\pi^+$	PDG 2020 [9] equivalent	$3.910 \pm 0.006 \pm 0.033$	$5.1/(9-1) = 0.64$
$K^-\pi^+$	Drop Ref. [1430]	$3.913 \pm 0.006 \pm 0.033$	$5.1/(8-1) = 0.73$
$K^-\pi^+$	Add FSR updates	$3.948 \pm 0.006 \pm 0.032 \pm 0.019$	$3.5/(8-1) = 0.50$
$K^-\pi^+$	Add FSR correlations	$3.949 \pm 0.006 \pm 0.032 \pm 0.033$	$3.7/(8-1) = 0.53$
All	Add CLEO-c, CDF, and FOCUS h^+h^-	$3.956 \pm 0.006 \pm 0.032 \pm 0.033$	$11.1/(14-3) = 1.01$
All	Add BES III h^+h^-	$3.999 \pm 0.006 \pm 0.031 \pm 0.032$	$36.0/(16-3) = 2.77$

4. Consideration of PHOTOS++

The versions of PHOTOS that existing measurements were performed with are now well over a decade out of date. The newest version, PHOTOS++ 3.61 [1431], is now fully based on C++ instead of the original FORTRAN. None of the measurements used in our branching fraction averages use PHOTOS++, so we have not yet undertaken an effort to update all results to this newest version. However, at this time it is worth continuing our procedure to evaluate whether there is any continued low bias in the branching fractions, due to suboptimal modeling of FSR.

We find that the FSR spectra for PHOTOS 2.15, with interference included and exponentiated multiple-photon mode turned on, and PHOTOS++ (in its default mode) are compatible. The distributions of $m_{K\pi}$ for simulated D mesons from $B \to D^*X$ decays produced at $\Upsilon(4S)$ threshold are nearly identical. As an example, the *BABAR* 07 selection criteria were applied to decays simulated with PHOTOS++ and our nominal version of PHOTOS 2.15; both produce identical FSR corrections to within 0.01%.

The distributions of ΔE for simulated D mesons produced at $\psi(3770)$ threshold also are nearly identical. As an example, for the BES III 18 $D^0 \to K^-\pi^+$, $D^0 \to \pi^+\pi^-$, and $D^0 \to K^+K^-$ branching fraction results, the additional update shifts required to correct from our nominal version of PHOTOS 2.15 to PHOTOS++ are less than or equal to 0.02%. However, if smearing is applied with the BES III 18 ΔE resolution, while the update for $D^0 \to K^-\pi^+$ remains negligible, the update shifts for $D^0 \to \pi^+\pi^-$ and $D^0 \to K^+K^-$ are modest at -0.25% and 0.19%, respectively; this level of shifts are well within the systematic uncertainty of our averages.

D. Excited $D_{(s)}$ mesons

Excited "open" charm mesons have received increased attention since the first observation of low mass, narrow D_{sJ} states that were inconsistent with QCD predictions [1432–1435]. Their properties can be measured in both prompt analyses as well as in amplitude analyses of multibody B decays. Tables 299, 300, and 301 summarize the measurements of masses and widths of excited D and D_s states. If a preferred assignment of spin and parity was measured, it is listed in the column J^P, where the label "natural" denotes $P = (-1)^J$ $(J^P = 0^+, 1^-, 2^+ \ldots)$ and "unnatural" denotes $P = (-1)^{J+1}$ $(J^P = 0^-, 1^+, 2^- \ldots)$. In some studies, it was possible to identify only whether the state has natural or unnatural spin-parity, but not the values of the quantum numbers.

For states in which multiple measurements are available, an average mass and width are calculated; these are listed in the gray shaded rows. For simplicity, when calculating averages we neglect possible correlations among individual measurements. All averaged masses and widths are summarized in Fig. 99. The resonances listed in the tables and figures are as they appear in the respective publications. In some cases, it is unclear whether separately listed states are in fact distinct or are the same resonance. An example is the $D_1^*(2680)^0$ state [1447], which has parameters close to those of the $D^*(2650)^0$. Further measurements are needed to resolve these ambiguities. Additionally, subsequent measurements can change the average value such as to change the relative masses of states, which may be in contradiction with the naming. An example is the $D_1(2430)^0$ state, whose average mass has been lowered by the latest LHCb measurement [1438] to become smaller than the average mass of the $D_1(2420)$ states.

The masses and widths of narrow ($\Gamma < 50$ MeV) orbitally excited D mesons (1P states), both neutral and charged, are well established. Measurements of broad states ($\Gamma \sim$ 200–400 MeV) are less abundant, as identifying the signal is more challenging. The measured masses and widths, as well as the J^P values, are in agreement with theoretical predictions based on potential models [527,1470–1472].

The spectroscopic assignment of heavier states remains less clear. Further theoretical studies suggest the identity of some 2S and 1D states [1473,1474] and tentatively discuss possible 1F, 3S and 2P states. Possible new states to be found in the future are suggested in Refs. [1474,1475]. Following precise measurements from LHCb, recent

TABLE 299. Measurements of masses and widths for excited D mesons. The column J^P lists the assignment of spin and parity. If possible, an average mass or width is calculated. Table 1 of 2.

Resonance	J^P	Decay mode	Mass [MeV/c^2]	Width [MeV]	Measured by	References
$D_0^*(2400)^0$	0^+	$D^+\pi^-$	$2297 \pm 8 \pm 20$	$273 \pm 12 \pm 48$	*BABAR*	[778]
		$D^+\pi^-$	$2308 \pm 17 \pm 32$	$276 \pm 21 \pm 63$	Belle	[779]
		$D^+\pi^-$	$2407 \pm 21 \pm 35$	$240 \pm 55 \pm 59$	FOCUS	[1436]
			2318.2 ± 16.9	267.4 ± 35.6	Our average	
$D_0^*(2400)^\pm$	0^+	$D^0\pi^+$	$2360 \pm 15 \pm 12 \pm 28$	$255 \pm 26 \pm 20 \pm 47$	LHCb	[1437]
		$D^0\pi^+$	$2349 \pm 6 \pm 1 \pm 4$	$217 \pm 13 \pm 5 \pm 12$	LHCb	[659]
		$D^0\pi^+$	$2403 \pm 14 \pm 35$	$283 \pm 24 \pm 34$	FOCUS (m & Γ) + Belle (J^P)	[650]
			2351.3 ± 7.0	229.9 ± 16.1	Our average	
$D_1(2420)^0$	1^+	$D^{*+}\pi^-$	$2424.8 \pm 0.1 \pm 0.7$	$33.6 \pm 0.3 \pm 2.7$	LHCb	[1438]
		$D^{*+}\pi^-$	$2419.6 \pm 0.1 \pm 0.7$	$35.2 \pm 0.4 \pm 0.9$	LHCb	[1330]
		$D^{*+}\pi^-$	$2423.1 \pm 1.5^{+0.4}_{-0.7}$	$38.8 \pm 5^{+1.9}_{-5.4}$	ZEUS	[1439]
		$D^{*+}\pi^-$	$2420.1 \pm 0.1 \pm 0.8$	$31.4 \pm 0.5 \pm 1.3$	*BABAR*	[1329]
		$D^{*+}\pi^-$		$20 \pm 1.7 \pm 1.3$	CDF	[1440]
		$D^{*+}\pi^-$	$2421.4 \pm 1.5 \pm 0.9$	$23.7 \pm 2.7 \pm 4$	Belle	[779]
		$D^0\pi^+\pi^-$	$2426 \pm 3 \pm 1$	$24 \pm 7 \pm 8$	Belle	[679]
		$D^{*+}\pi^-$	$2421^{+1}_{-2} \pm 2$	$20^{+6}_{-5} \pm 3$	CLEO	[1441]
		$D^{*+}\pi^-$	$2422 \pm 2 \pm 2$	$15 \pm 8 \pm 4$	E387	[1442]
		$D^{*+}\pi^-$	$2414 \pm 2 \pm 5$	$13 \pm 6^{+10}_{-5}$	ARGUS	[1443]
		$D^{*+}\pi^-$	$2428 \pm 3 \pm 2$	$23^{+8\ +10}_{-6\ -4}$	CLEO	[1444]
		$D^{*+}\pi^-$	$2428 \pm 8 \pm 5$	$58 \pm 14 \pm 20$	TPS	[1445]
			2421.8 ± 0.4	31.8 ± 0.7	Our average	
$D_1(2420)^\pm$	1^+	$D^{*0}\pi^+$	$2421.9 \pm 4.7^{+3.4}_{-1.2}$		ZEUS	[1439]
		$D^+\pi^-\pi^+$	$2421 \pm 2 \pm 1$	$21 \pm 5 \pm 8$	Belle	[679]
		$D^{*0}\pi^+$	$2425 \pm 2 \pm 2$	$26^{+8}_{-7} \pm 4$	CLEO	[1446]
		$D^{*0}\pi^+$	$2443 \pm 7 \pm 5$	$41 \pm 19 \pm 8$	TPS	[1445]
			2423.2 ± 1.6	25.0 ± 6.0	Our average	
$D_1(2430)^0$	1^+	$D^{*+}\pi^-$	$2411 \pm 3 \pm 9$	$309 \pm 9 \pm 28$	LHCb	[1438]
		$D^{*+}\pi^-$	$2427 \pm 26 \pm 25$	$384^{+107}_{-75} \pm 74$	Belle	[779]
			2412.0 ± 9.2	312.6 ± 28.6	Our average	
$D_2^*(2460)^0$	2^+	$D^+\pi^-$	$2463.7 \pm 0.4 \pm 0.4 \pm 0.6$	$47 \pm 0.8 \pm 0.9 \pm 0.3$	LHCb	[1447]
		$D^+\pi^-$	$2460.4 \pm 0.1 \pm 0.1$	$45.6 \pm 0.4 \pm 1.1$	LHCb	[1330]
		$D^{*+}\pi^-$	$2464 \pm 1.4 \pm 0.5 \pm 0.2$	$43.8 \pm 2.9 \pm 1.7 \pm 0.6$	LHCb	[784]
		$D^{*+}\pi^-$, $D^+\pi^-$	$2462.5 \pm 2.4^{+1.3}_{-1.1}$	$46.6 \pm 8.1^{+5.9}_{-3.8}$	ZEUS	[1439]
		$D^+\pi^-$	$2462.2 \pm 0.1 \pm 0.8$	$50.5 \pm 0.6 \pm 0.7$	*BABAR*	[1329]
		$D^+\pi^-$	$2460.4 \pm 1.2 \pm 2.2$	$41.8 \pm 2.5 \pm 2.9$	*BABAR*	[778]
		$D^+\pi^-$		$49.2 \pm 2.3 \pm 1.3$	CDF	[1440]
		$D^+\pi^-$	$2461.6 \pm 2.1 \pm 3.3$	$45.6 \pm 4.4 \pm 6.7$	Belle	[779]
		$D^+\pi^-$	$2464.5 \pm 1.1 \pm 1.9$	$38.7 \pm 5.3 \pm 2.9$	FOCUS	[1436]
		$D^+\pi^-$	$2465 \pm 3 \pm 3$	$28^{+8}_{-7} \pm 6$	CLEO	[1441]
		$D^+\pi^-$	$2455 \pm 3 \pm 5$	$15^{+13\ +5}_{-10\ -10}$	ARGUS	[1448]
		$D^+\pi^-$	$2459 \pm 3 \pm 2$	$20 \pm 10 \pm 5$	TPS	[1445]
		$D^{*+}\pi^-$	$2461 \pm 3 \pm 1$	$20^{+9\ +9}_{-12\ -10}$	CLEO	[1444]
			$2453 \pm 3 \pm 2$	$25 \pm 10 \pm 5$	E687	[1442]
			2460.6 ± 0.1	47.6 ± 0.6	Our average	

TABLE 300. Measurements of masses and widths for excited D mesons. The column J^P lists the assignment of spin and parity. If possible, an average mass or width is calculated. Table 2 of 2.

Resonance	J^P	Decay mode	Mass [MeV/c^2]	Width [MeV]	Measured by	References
		$D^0\pi^+$	$2463.1 \pm 0.2 \pm 0.6$	$48.6 \pm 1.3 \pm 1.9$	LHCb	[1330]
		$D^0\pi^+$	$2465.6 \pm 1.8 \pm 0.5 \pm 1.2$	$46 \pm 3.4 \pm 1.4 \pm 2.9$	LHCb	[1437]
		$D^0\pi^+$	$2468.6 \pm 0.6 \pm 0.0 \pm 0.3$	$47.3 \pm 1.5 \pm 0.3 \pm 0.6$	LHCb	[659]
		$D^{*0}\pi^+$, $D^0\pi^+$	$2460.6 \pm 4.4^{+3.6}_{-0.8}$		ZEUS	[1439]
		$D^0\pi^+$	$2465.4 \pm 0.2 \pm 1.1$		*BABAR*	[1329]
$D_2^*(2460)^\pm$	2^+	$D^0\pi^+$	$2465.7 \pm 1.8^{+1.4}_{-4.8}$	$49.7 \pm 3.8 \pm 6.4$	Belle	[650]
		$D^0\pi^+$	$2467.6 \pm 1.5 \pm 0.8$	$34.1 \pm 6.5 \pm 4.2$	FOCUS	[1436]
		$D^0\pi^+$	$2463 \pm 3 \pm 3$	$27^{+11}_{-8} \pm 5$	CLEO	[1446]
		$D^0\pi^+$	$2453 \pm 3 \pm 2$	$23 \pm 9 \pm 5$	E687	[1442]
		$D^0\pi^+$	$2469 \pm 4 \pm 6$		ARGUS	[1449]
			2465.6 ± 0.4	46.7 ± 1.2	Our average	
		$D^{*+}\pi^-$	$2518 \pm 2 \pm 7$	$199 \pm 5 \pm 17$	LHCb	[1438]
$D(2550)^0$	0^-	$D^{*+}\pi^-$	$2539.4 \pm 4.5 \pm 6.8$	$130 \pm 12 \pm 13$	*BABAR*	[1329]
			2527.5 ± 5.4	164.4 ± 12.5	Our average	
$D(2580)^0$	Unnatural	$D^{*+}\pi^-$	$2579.5 \pm 3.4 \pm 5.5$	$117.5 \pm 17.8 \pm 46$	LHCb	[1330]
		$D^{*+}\pi^-$	$2641.9 \pm 1.8 \pm 4.5$	$149 \pm 4 \pm 20$	LHCb	[1438]
$D(2600)^0$	1^-	$D^+\pi^-$	$2608.7 \pm 2.4 \pm 2.5$	$93 \pm 6 \pm 13$	*BABAR*	[1329]
			2619.9 ± 2.8	111.5 ± 11.7	Our average	
$D(2600)^\pm$	Natural	$D^0\pi^+$	$2621.3 \pm 3.7 \pm 4.2$		*BABAR*	[1329]
$D^*(2640)^\pm$	1^-	$D^{*+}\pi^+\pi^-$	$2637.0 \pm 2 \pm 6$		Delphi	[1450]
$D^*(2650)^0$	Natural	$D^{*+}\pi^-$	$2649.2 \pm 3.5 \pm 3.5$	$140.2 \pm 17.1 \pm 18.6$	LHCb	[1330]
$D^*(2680)^0$	1^-	$D^+\pi^-$	$2681.1 \pm 5.6 \pm 4.9 \pm 13.1$	$186.7 \pm 8.5 \pm 8.6 \pm 8.2$	LHCb	[1447]
		$D^{*+}\pi^-$	$2751 \pm 3 \pm 7$	$102 \pm 6 \pm 26$	LHCb	[1438]
$D(2740)^0$	2^-	$D^{*+}\pi^-$	$2737.0 \pm 3.5 \pm 11.2$	$73.2 \pm 13.4 \pm 25$	LHCb	[1330]
			2746.9 ± 6.4	88.5 ± 19.4	Our average	
		$D^{*+}\pi^-$	$2753 \pm 4 \pm 6$	$66 \pm 10 \pm 14$	LHCb	[1438]
$D(2750)^0$	3^-	$D^{*+}\pi^-$	$2752.4 \pm 1.7 \pm 2.7$	$71 \pm 6 \pm 11$	*BABAR*	[1329]
			2752.5 ± 2.9	69.3 ± 10.1	Our average	
		$D^+\pi^-$	$2781 \pm 18 \pm 11 \pm 6$	$177 \pm 32 \pm 20 \pm 7$	LHCb	[784]
		$D^{*+}\pi^-$	$2761.1 \pm 5.1 \pm 6.5$	$74.4 \pm 3.4 \pm 37$	LHCb	[1330]
$D_1^*(2760)^0$	1^+	$D^+\pi^-$	$2760.1 \pm 1.1 \pm 3.7$	$74.4 \pm 3.4 \pm 19.1$	LHCb	[1330]
		$D^+\pi^-$	$2763.3 \pm 2.3 \pm 2.3$	$60.9 \pm 5.1 \pm 3.6$	*BABAR*	[1329]
			2762.1 ± 2.4	65.1 ± 5.8	Our average	
$D_3^*(2760)^0$	3^-	$D^+\pi^-$	$2775.5 \pm 4.5 \pm 4.5 \pm 4.7$	$95.3 \pm 9.6 \pm 7.9 \pm 33.1$	LHCb	[1447]
		$D^0\pi^+$	$2771.7 \pm 1.7 \pm 3.8$	$66.7 \pm 6.6 \pm 10.5$	LHCb	[1330]
$D_3^*(2760)^\pm$	3^-	$D^0\pi^+$	$2798 \pm 7 \pm 1 \pm 7$	$105 \pm 18 \pm 6 \pm 23$	LHCb	[659]
		$D^0\pi^+$	$2769.7 \pm 3.8 \pm 1.5$		*BABAR*	[1329]
			2772.8 ± 2.8	72.3 ± 11.5	Our average	
$D_2^*(3000)^0$	2^+	$D^+\pi^-$	$3214 \pm 29 \pm 33 \pm 36$	$186 \pm 38 \pm 34 \pm 63$	LHCb	[1447]

studies based on unitarized chiral perturbation theory and lattice QCD propose a two-pole structure of the $D^*(2400)^0$ and predict the existence of a lighter state $D^*(2100)^0$ [1476,1477].

Tables 302, 303, and 304 summarize branching fractions of B meson decays to excited D and D_s states, respectively. The measurements listed are the products of the B meson branching fraction and the daughter D meson branching

TABLE 301. Measurements of masses and widths for excited D_s mesons. The column J^P lists the of spin and parity. If possible, an average mass or width is calculated.

Resonance	J^P	Decay mode	Mass [MeV/c^2]	Width [MeV]	Measured by	References
$D^*_{s0}(2317)^\pm$	0^+	$D^+_s\pi^0$	$2319.6 \pm 0.2 \pm 1.4$		*BABAR*	[1451]
		$D^+_s\pi^0$	$2317.3 \pm 0.4 \pm 0.8$		*BABAR*	[1435]
		$D^+_s\pi^0$	$2318.3 \pm 1.2 \pm 1.2$		BESIII	[1452]
			2318.0 ± 0.7		Our average	
$D_{s1}(2460)^\pm$	1^+	$D^{*+}_s\pi^0$, $D^+_s\pi^0\Gamma, D^+_s\Gamma, D^+_s\pi^+\pi^-$	$2460.1 \pm 0.2 \pm 0.8$		*BABAR*	[1451]
		$D^+_s\pi^0\Gamma$	$2458 \pm 1 \pm 1$		*BABAR*	[1435]
			2459.6 ± 0.7		Our average	
$D_{s1}(2536)^\pm$	1^+		$2537.7 \pm 0.5 \pm 3.1$	$1.7 \pm 1.2 \pm 0.6$	BESIII	[1453]
		$D^{*+}K^0_S$		$0.92 \pm 0.03 \pm 0.04$	*BABAR*	[1454]
		$D^{*+}K^0_S$	$2535.7 \pm 0.6 \pm 0.5$		DØ	[1455]
		$D^{*+}K^0_S, D^{*0}K^+$	$2534.78 \pm 0.31 \pm 0.4$		*BABAR*	[700]
		$D^+_s\pi^+\pi^-$	$2534.6 \pm 0.3 \pm 0.7$		*BABAR*	[1451]
		$D^{*+}K^0_S, D^{*0}K^+$	$2535.0 \pm 0.6 \pm 1.0$		E687	[1442]
		$D^{*0}K^+$	$2535.3 \pm 0.2 \pm 0.5$		CLEO	[1456]
		$D^{*+}K^0_S$	$2534.8 \pm 0.6 \pm 0.6$		CLEO	[1456]
		$D^{*0}K^+$	$2535.2 \pm 0.5 \pm 1.5$		ARGUS	[1457]
		$D^{*+}K^0_S$	$2535.6 \pm 0.7 \pm 0.4$		CLEO	[1444]
		$D^{*+}K^0_S$	$2535.9 \pm 0.6 \pm 2.0$		ARGUS	[1458]
			2535.1 ± 0.3	0.9 ± 0.0	Our average	
$D^*_{s2}(2573)^\pm$	2^+		$2570.7 \pm 2.0 \pm 1.7$	$17.2 \pm 3.6 \pm 1.1$	BESIII	[1453]
		$D^0K^+, D^{*+}K^0_S$	$2568.39 \pm 0.29 \pm 0.26$	$16.9 \pm 0.5 \pm 0.6$	LHCb	[1459]
		$D^+K^0_S, D^0K^+$	$2569.4 \pm 1.6 \pm 0.5$	$12.1 \pm 4.5 \pm 1.6$	LHCb	[1460]
		$D^+K^0_S, D^0K^+$	$2572.2 \pm 0.3 \pm 1.0$	$27.1 \pm 0.6 \pm 5.6$	*BABAR*	[1461]
		D^0K^+	$2574.25 \pm 3.3 \pm 1.6$	$10.4 \pm 8.3 \pm 3.0$	ARGUS	[1462]
		D^0K^+	$2573.2^{+1.7}_{-1.6} \pm 0.9$	$16^{+5}_{-4} \pm 3$	CLEO	[1463]
			2569.1 ± 0.3	16.9 ± 0.7	Our average	
$D_{s0}(2590)^\pm$	0^-	$D^+K^-\pi^-$	$2591 \pm 6.0 \pm 7$	$89 \pm 16 \pm 12$	LHCb	[1464]
$D^*_{s1}(2700)^\pm$	1^-	$D^{0+}K^0_S, D^{*0}K^+$	$2732.3 \pm 4.3 \pm 5.8$	$136 \pm 19 \pm 24$	LHCb	[1465]
		D^0K^+	2699^{+14}_{-7}	127^{+24}_{-19}	*BABAR*	[1466]
		$D^{*+}K^0_S, D^{*0}K^+$	$2709.2 \pm 1.9 \pm 4.5$	$115.8 \pm 7.3 \pm 12.1$	LHCb	[1467]
		DK, D^*K	$2710 \pm 2^{+12}_{-7}$	$149 \pm 7^{+39}_{-52}$	*BABAR*	[1468]
		D^0K^+	$2708 \pm 9^{+11}_{-10}$	$108 \pm 2^{+36}_{-31}$	Belle	[797]
			2713.0 ± 3.5	120.9 ± 10.3	Our average	
$D^*_{s1}(2860)^\pm$	1	D^0K^+	$2859 \pm 12 \pm 24$	$159 \pm 23 \pm 77$	LHCb	[1469]
$D^*_{s3}(2860)^\pm$	3^-	$D^{*+}K^0_S, D^{*0}K^+$	$2867.1 \pm 4.3 \pm 1.9$	$50 \pm 11 \pm 13$	LHCb	[1465]
		D^0K^+	$2860.5 \pm 2.6 \pm 6.5$	52.2 ± 8.6	LHCb	[1469]
			2865.0 ± 3.9	52.2 ± 8.6	Our average	
$D_{sJ}(3040)^\pm$	Unnatural	D^*K	$3044 \pm 8^{+30}_{-5}$	$239 \pm 35^{+46}_{-42}$	*BABAR* (m & Γ) + LHCb(J^P)	[1468]

fraction. It is notable that the branching fractions for B mesons decaying to a narrow D^* state and a pion are similar for charged and neutral B initial states, while the branching fractions to a broad D^* state and π^+ are much larger for B^+ than for B^0. This may be due to the fact that color-suppressed amplitudes contribute only to the B^+ decay and not to the B^0 decay (for a theoretical discussion, see Refs. [1478,1479]). Values for the branching fractions of the D mesons are difficult to extract due to the unknown (and difficult to calculate) $B \to D^*X$ branching fractions.

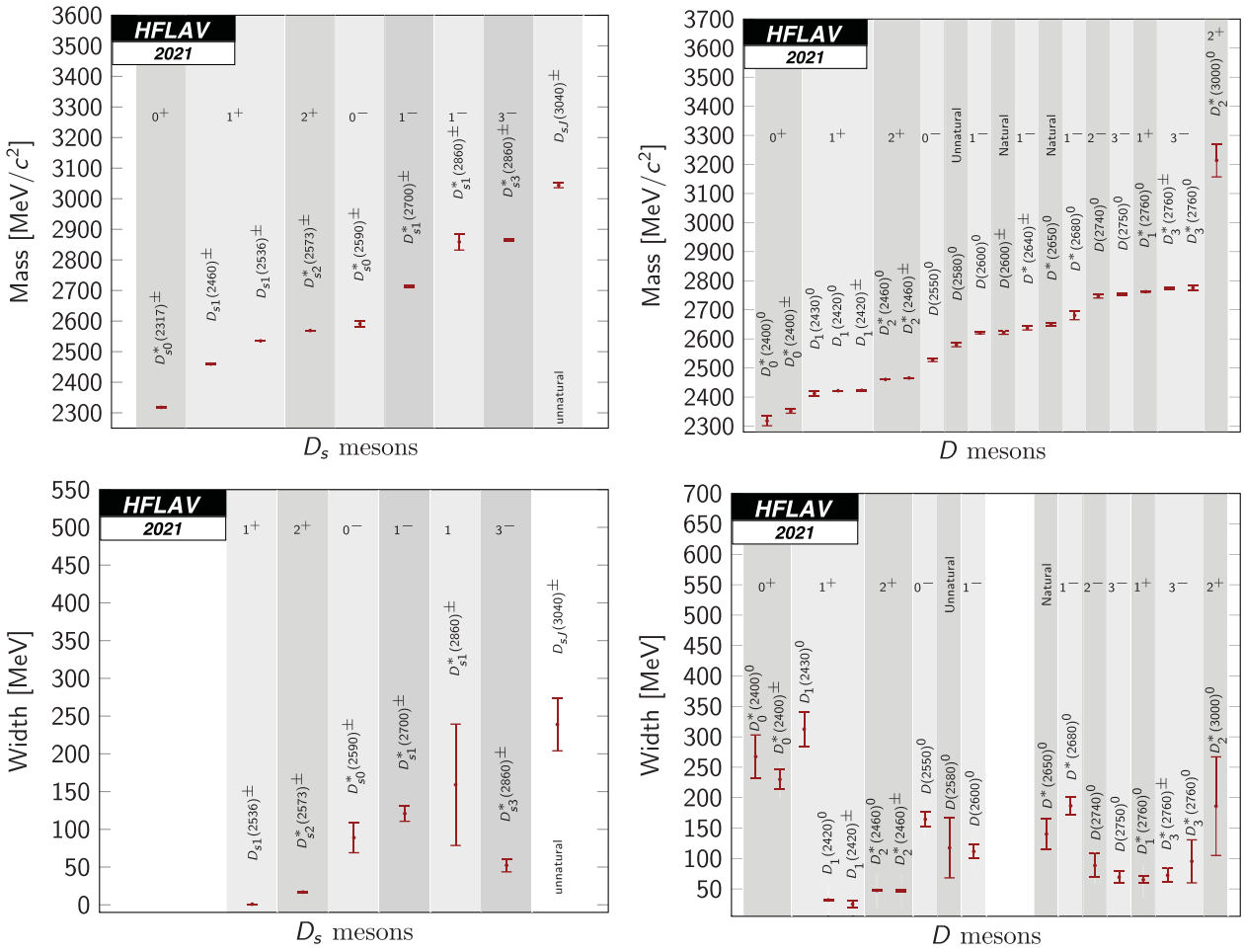

FIG. 99. (a) Average masses for excited D_s mesons; (b) average masses for excited D mesons; (c) average widths for excited D_s mesons; (d) average widths for excited D mesons. The vertical shaded regions distinguish between different spin-parity states.

TABLE 302. Product of the B meson branching fraction and the daughter (excited) D meson branching fraction. Table 1 of 2.

Resonance	Decay	$\mathcal{B}[10^{-4}]$	Measured by	References
$D_0^*(2400)^0$	$B^- \to D_0^*(2400)^0(\to D^+\pi^-)\pi^-$	$6.1 \pm 0.6 \pm 1.8$	Belle	[779]
		$6.8 \pm 0.3 \pm 2.0$	*BABAR*	[778]
		6.4 ± 1.4	Our average	
	$B^- \to D_0^*(2400)^0(\to D^+\pi^-)K^-$	$0.061 \pm 0.019 \pm 0.005 \pm 0.014 \pm 0.004$	LHCb	[784]
$D_0^*(2400)^\pm$	$\bar{B}^0 \to D_0^*(2400)^+(\to D^0\pi^+)\pi^-$	$0.77 \pm 0.05 \pm 0.03 \pm 0.03 \pm 0.04$	LHCb	[659]
		$0.60 \pm 0.13 \pm 0.27$	Belle	[650]
		0.76 ± 0.07	Our average	
	$\bar{B}^0 \to D_0^*(2400)^+(\to D^0\pi^+)K^-$	$0.177 \pm 0.026 \pm 0.019 \pm 0.067 \pm 0.20$	LHCb	[1437]
$D_1(2420)^0$	$B^- \to D_1(2420)^0(\to D^{*+}\pi^-)\pi^-$	$6.8 \pm 0.7 \pm 1.3$	Belle	[779]
		$8.42 \pm 0.08 \pm 0.40 \pm 1.40$	LHCb	[1438]
		7.6 ± 1.0	Our average	
	$B^- \to D_1(2420)^0(\to D^0\pi^+\pi^-)\pi^-$	$1.85 \pm 0.29 \pm 0.27 \pm 0.41$	Belle	[679]
	$\bar{B}^0 \to D_1(2420)^0(\to D^{*+}\pi^-)\omega$	$0.7 \pm 0.2^{+0.1}_{-0.0} \pm 0.1$	Belle	[655]

(Table continued)

TABLE 302. *(Continued)*

Resonance	Decay	$\mathcal{B}[10^{-4}]$	Measured by	References
$D_1(2420)^{\pm}$	$\bar{B}^0 \to D_1(2420)^+(\to D^+\pi^-\pi^+)\pi^-$	$0.89 \pm 0.15 \pm 0.22$	Belle	[679]
$D_1(2430)^0$	$B^- \to D_1(2430)^0(\to D^{*+}\pi^-)\pi^-$	$5.0 \pm 0.4 \pm 1.08$	Belle	[779]
		$3.51 \pm 0.06 \pm 0.23 \pm 0.57$	LHCb	[1438]
		4.5 ± 0.7	Our average	
	$\bar{B}^0 \to D_1(2430)^0(\to D^{*+}\pi^-)\omega$	$2.5 \pm 0.4^{+0.7\ +0.4}_{-0.2\ -0.1}$	Belle	[655]
$D_2^*(2460)^0$	$B^- \to D_2^*(2460)^0(\to D^+\pi^-)\pi^-$	$3.4 \pm 0.3 \pm 0.7$	Belle	[779]
		$3.5 \pm 0.2 \pm 0.5$	*BABAR*	[778]
		$3.62 \pm 0.06 \pm 0.14 \pm 0.09 \pm 0.25$	LHCb	[1447]
		3.58 ± 0.23	Our average	
	$B^- \to D_2^*(2460)^0(\to D^{*+}\pi^-)\pi^-$	$1.8 \pm 0.3 \pm 0.4$	Belle	[779]
		$2.08 \pm 0.03 \pm 0.14 \pm 0.34$	LHCb	[1438]
		1.8 ± 0.3	Our average	
	$B^- \to D_2^*(2460)^0(\to D^{*+}\pi^-)\omega$	$0.4 \pm 0.1^{+0.0}_{-0.1} \pm 0.1$	Belle	[655]
	$B^- \to D_2^*(2460)^0(\to D^+\pi^-)K^-$	$0.232 \pm 0.011 \pm 0.006 \pm 0.010 \pm 0.016$	LHCb	[784]
$D_2^*(2460)^{\pm}$	$\bar{B}^0 \to D_2^*(2460)^+(\to D^0\pi^+)\pi^-$	$2.44 \pm 0.07 \pm 0.10 \pm 0.04 \pm 0.12$	LHCb	[659]
		$2.15 \pm 0.17 \pm 0.31$	Belle	[650]
		2.38 ± 0.16	Our average	
	$\bar{B}^0 \to D_2^*(2460)^+(\to D^0\pi^+)K^-$	$0.212 \pm 0.010 \pm 0.011 \pm 0.011 \pm 0.25$	LHCb	[1437]

TABLE 303. Product of the B meson branching fraction and the daughter (excited) D meson branching fraction. Table 2 of 2.

Resonance	Decay	$\mathcal{B}[10^{-4}]$	Measured by	References
$D_0(2550)^0$	$B^- \to D_0(2550)^0(\to D^{*+}\pi^-)\pi^-$	$0.72 \pm 0.01 \pm 0.07 \pm 0.12$	LHCb	[1438]
$D_1^*(2600)^0$	$B^- \to D_1^*(2600)^0(\to D^{*+}\pi^-)\pi^-$	$0.68 \pm 0.01 \pm 0.07 \pm 0.11$	LHCb	[1438]
$D_1^*(2680)^0$	$B^- \to D_1^*(2680)^0(\to D^+\pi^-)\pi^-$	$0.84 \pm 0.06 \pm 0.07 \pm 0.18 \pm 0.06$	LHCb	[1447]
$D_2(2740)^0$	$B^- \to D_2(2740)^0(\to D^{*+}\pi^-)\pi^-$	$0.33 \pm 0.02 \pm 0.14 \pm 0.05$	LHCb	[1438]
$D_1^*(2760)^0$	$B^- \to D_1^*(2760)^0(\to D^+\pi^-)K^-$	$0.036 \pm 0.009 \pm 0.003 \pm 0.007 \pm 0.002$	LHCb	[784]
$D_3^*(2760)^0$	$\bar{B}^- \to D_3^*(2760)^0(\to D^+\pi^-)\pi^-$	$0.10 \pm 0.01 \pm 0.01 \pm 0.02 \pm 0.01$	LHCb	[1447]
$D_3^*(2760)^{\pm}$	$\bar{B}^- \to D_3^*(2760)^0(\to D^{*+}\pi^-)\pi^-$	$0.11 \pm 0.01 \pm 0.02 \pm 0.02$	LHCb	[1438]
	$\bar{B}^0 \to D_3^*(2760)^+(\to D^0\pi^+)\pi^-$	$0.103 \pm 0.016 \pm 0.007 \pm 0.008 \pm 0.005$	LHCb	[659]
$D_2^*(3000)^0$	$\bar{B}^0 \to D_2^*(3000)^0(\to D^+\pi^-)\pi^-$	$0.02 \pm 0.01 \pm 0.01 \pm 0.01 \pm 0.00$	LHCb	[1447]

The discoveries of the $D_{s0}^*(2317)^{\pm}$ and $D_{s1}(2460)^{\pm}$ have triggered increased interest in properties of, and searches for, excited D_s mesons. While the masses and widths of the $D_{s1}(2536)^{\pm}$ and $D_{s2}^*(2573)^{\pm}$ states are in relatively good agreement with potential model predictions, the masses of the $D_{s0}^*(2317)^{\pm}$ and $D_{s1}(2460)^{\pm}$ states are significantly lower than expected (see Ref. [1480] for a discussion of $c\bar{s}$ models). Moreover, the mass splitting between these two states greatly exceeds that between the $D_{s1}(2536)^{\pm}$ and $D_{s2}(2573)^{\pm}$. These unexpected properties have led to interpretations of the $D_{s0}^*(2317)^{\pm}$ and $D_{s1}(2460)^{\pm}$ as exotic four-quark states [1481,1482]. A molecule-like (DK) interpretation of the $D_{s0}^*(2317)^{\pm}$ and $D_{s1}(2460)^{\pm}$ [1481,1482] that can account for their low masses and isospin-breaking decay modes is tested by searching for charged and neutral isospin partners of these states; thus far such searches have yielded negative results. Therefore the models that predict equal production rates for different

TABLE 304. Product of the B meson branching fraction and the daughter (excited) D_s meson branching fraction.

Resonance	Decay	$\mathcal{B}[10^{-4}]$	Measured by	References
$D^*_{s0}(2317)^\pm$	$B^0 \to D^*_{s0}(2317)^+(\to D_s^+\pi^0)D^-$	$8.6^{+3.3}_{-2.6} \pm 2.6$	Belle	[699]
		$18.0 \pm 4.0^{+6.7}_{-5.0}$	*BABAR*	[698]
		$10.1^{+1.3}_{-1.2} \pm 1.0 \pm 0.4$	Belle	[697]
		10.2 ± 1.5	Our average	
	$B^+ \to D^*_{s0}(2317)^+(\to D_s^+\pi^0)\bar{D}^0$	$8.0^{+1.3}_{-1.2} \pm 1.0 \pm 0.4$	Belle	[697]
	$B^0 \to D^*_{s0}(2317)^+(\to D_s^+\pi^0)K^-$	$0.53^{+0.15}_{-0.13} \pm 0.16$	Belle	[680]
$D_{s1}(2460)^\pm$	$B^0 \to D_{s1}(2460)^+(\to D_s^{*+}\pi^0)D^-$	$22.7^{+7.3}_{-6.2} \pm 6.8$	Belle	[699]
		$28.0 \pm 8.0^{+11.2}_{-7.8}$	*BABAR*	[698]
		24.7 ± 7.6	Our average	
	$B^0 \to D_{s1}(2460)^+(\to D_s^{*+}\gamma)D^-$	$8.2^{+2.2}_{-1.9} \pm 2.5$	Belle	[699]
		$8.0 \pm 2.0^{+3.2}_{-2.3}$	*BABAR*	[698]
		8.1 ± 2.3	Our average	
	$D_{s1}(2460)^+ \to D_s^{*+}\pi^0$	$(56 \pm 13 \pm 9)\%$	*BABAR*	[693]
	$D_{s1}(2460)^+ \to D_s^{*+}\gamma$	$(16 \pm 4 \pm 3)\%$	*BABAR*	[693]
$D_{s1}(2536)^\pm$	$B^0 \to D_{s1}(2536)^+(\to D^{*0}K^+)D^-$	$1.71 \pm 0.48 \pm 0.32$	*BABAR*	[700]
	$B^0 \to D_{s1}(2536)^+(\to D^{*+}K^0)D^-$	$2.61 \pm 1.03 \pm 0.31$	*BABAR*	[700]
	$B^0 \to D_{s1}(2536)^+(\to D^{*0}K^+)D^{*-}$	$3.32 \pm 0.88 \pm 0.66$	*BABAR*	[700]
	$B^0 \to D_{s1}(2536)^+(\to D^{*+}K^0)D^{*-}$	$5.00 \pm 1.51 \pm 0.67$	*BABAR*	[700]
	$B^+ \to D_{s1}(2536)^+(\to D^{*0}K^+)\bar{D}^0$	$2.16 \pm 0.52 \pm 0.45$	*BABAR*	[700]
	$B^+ \to D_{s1}(2536)^+(\to D^{*+}K^0)\bar{D}^0$	$2.30 \pm 0.98 \pm 0.43$	*BABAR*	[700]
	$B^+ \to D_{s1}(2536)^+(\to D^{*0}K^+)\bar{D}^{*0}$	$5.46 \pm 1.17 \pm 1.04$	*BABAR*	[700]
	$B^+ \to D_{s1}(2536)^+(\to D^{*+}K^0)\bar{D}^{*0}$	$3.92 \pm 2.46 \pm 0.83$	*BABAR*	[700]
$D^*_{s2}(2573)^\pm$	$B^0 \to D^*_{s2}(2573)(\to D^0K^+)D^-$	$0.34 \pm 0.17 \pm 0.05$	*BABAR*	[1466]
	$B^+ \to D^*_{s2}(2573)(\to D^0K^+)\bar{D}^0$	$0.08 \pm 14 \pm 0.05$	*BABAR*	[1466]
${D_{s1}}^*(2700)^\pm$	$B^+ \to {D_{s1}}^*(2700)^+(\to D^0K^+)\bar{D}^0$	$11.3 \pm 2.2^{+1.4}_{-2.8}$	Belle	[797]
		$5.02 \pm 0.71 \pm 0.93$	*BABAR*	[1466]
		5.83 ± 1.09	Our average	
	$B^0 \to {D_{s1}}^*(2700)^+(\to D^0K^+)D^-$	$7.14 \pm 0.96 \pm 0.69$	*BABAR*	[1466]

charged states are excluded. The molecular picture can also be tested by measuring the rates for the radiative processes $D^*_{s0}(2317)^\pm/D_{s1}(2460)^\pm \to D_s^{(*)}\gamma$ and comparing to theoretical predictions. The predicted rates, however, are below the sensitivity of current experiments.

Another model successful in explaining the total widths and the $D^*_{s0}(2317)^\pm$–$D_{s1}(2460)^\pm$ mass splitting is based on the assumption that these states are chiral partners of the ground states D_s^+ and D_s^* [1483]. While some measured branching fraction ratios agree with predicted values, further experimental tests with better sensitivity are needed to confirm or refute this scenario. A summary of the mass difference measurements is given in Table 305.

Recently, a new study proposed modified properties when treating the $D^*_{s0}(2317)$ as a four-quark state in thermal medium using thermal QCD sum rules [1484].

Measurements by *BABAR* [1468] and LHCb [1467] first indicated the existence of the $D^*_{sJ}(2860)^\pm$ meson. An LHCb study of $B_s^0 \to \bar{D}^0\mathrm{K}^-\pi^+$ decays, in which they searched for excited D_s mesons [1469], showed with 10σ significance that this state comprises two different particles, one of spin 1 and one of spin 3. This represents the first measurement of a heavy flavored spin-3 particle, and the first observation of B meson decays to spin-3 particles. A subsequent study of $D_{sJ}^{(*)}$ mesons by the LHCb collaboration [1465] supports the natural parity

TABLE 305. Measurements of mass differences for excited D mesons.

Resonance	Relative to	Δm [MeV/c^2]	Measured by	References
$D_1^*(2420)^0$	D^{*+}	$410.2 \pm 2.1 \pm 0.9$	ZEUS	[1487]
		$411.7 \pm 0.7 \pm 0.4$	CDF	[1440]
		411.5 ± 0.8	Our average	
$D_1(2420)^\pm$	$D_1^*(2420)^0$	$4^{+2}_{-3} \pm 3$	CLEO	[1446]
$D_2^*(2460)^0$	D^+	$593.9 \pm 0.6 \pm 0.5$	CDF	[1440]
	D^{*+}	$458.8 \pm 3.7^{+1.2}_{-1.3}$	ZEUS	[1487]
$D_2^*(2460)^\pm$	$D_2^*(2460)^0$	$3.1 \pm 1.9 \pm 0.9$	FOCUS	[1436]
		$-2 \pm 4 \pm 4$	CLEO	[1446]
		$14 \pm 5 \pm 8$	ARGUS	[1449]
		3.0 ± 1.9	Our average	
$D_{s0}^*(2317)^\pm$	$D_s^\pm$	$348.7 \pm 0.5 \pm 0.7$	Belle	[1434]
		$350.0 \pm 1.2 \pm 1.0$	CLEO	[1433]
		$351.3 \pm 2.1 \pm 1.9$	Belle	[699]
		349.2 ± 0.7	Our average	
$D_{s1}(2460)^\pm$	$D_s^{*\pm}$	$344.1 \pm 1.3 \pm 1.1$	Belle	[1434]
		$351.2 \pm 1.7 \pm 1.0$	CLEO	[1433]
		$346.8 \pm 1.6 \pm 1.9$	Belle	[699]
		347.1 ± 1.1	Our average	
	$D_s^\pm$	$491.0 \pm 1.3 \pm 1.9$	Belle	[1434]
		$491.4 \pm 0.9 \pm 1.5$	Belle	[1434]
		491.3 ± 1.4	Our average	
$D_{s1}(2536)^\pm$	$D^*(2010)^\pm$	$524.83 \pm 0.01 \pm 0.04$	*BABAR*	[1454]
		$525.30^{+0.44}_{-0.41} \pm 0.10$	ZEUS	[1487]
		$525.3 \pm 0.6 \pm 0.1$	ALEPH	[1488]
		524.84 ± 0.04	Our average	
	$D^*(2007)^0$	$528.7 \pm 1.9 \pm 0.5$	ALEPH	[1488]
$D_{s2}^*(2573)^\pm$	D^0	$704 \pm 3 \pm 1$	ALEPH	[1488]

assignment for these states. This study also shows weak evidence for a further structure at a mass around 3040 MeV/c^2 with unnatural parity, which was first hinted at by a *BABAR* analysis [1468]. The second observation of a spin-3 charm meson was a subsequent LHCb analysis of $B^0 \to \bar{D}^0\pi^+\pi^-$ decays, which measured the spin-parity assignment of the state $D_3^*(2760)^\pm$ to be $J^P = 3^-$ [659]. This resonance was in fact observed previously by *BABAR* [1329] and LHCb [1330]. The measurement suggests a spectroscopic assignment of $^3D_3$. Recently, also the corresponding neutral state was observed by LHCb, the $D_3^*(2760)^0$ [1447].

Other observed excited D_s states include $D_{s1}^*(2700)^\pm$ and $D_{s2}^*(2573)^\pm$. The properties of both (mass, width, J^P) have been measured and determined in several analyses. A theoretical discussion [1485] investigates the possibility that the $D_{s1}(2700)^\pm$ could represent radial excitations of the $D_s^{*\pm}$. Similarly, the $D_{s1}^*(2860)^\pm$ and $D_{sJ}(3040)^\pm$ could be excitations of $D_{s0}^*(2317)^\pm$ and $D_{s1}(2460)^\pm$ or $D_{s1}(2536)^\pm$, respectively. The most recently discovered state is denoted as $D_{s0}(2590)^\pm$, and is a strong candidate to be the missing 2^1S_0 state, the radial excitation of the pseudoscalar ground-state D_s^+ meson [1464].

Table 306 summarizes measurements of the helicity parameter A_D (also referred to as the polarization parameter). In decays of orbitally excited charm mesons (D^{**}) to $D^*\pi$, $D^* \to D\pi$, the helicity distribution varies like $1 + A_D \cos^2\theta_H$, where θ_H is the angle in the D^* rest frame between the two pions emitted by decay $D^{**} \to D^*\pi$ and the $D^* \to D\pi$. The parameter is sensitive to possible S-wave contributions in the decay. In the case of a D meson decaying purely via D-wave, the helicity parameter is predicted to give $A_D = 3$. Studies of the $D_1(2420)^0$ meson by the ZEUS and *BABAR* collaborations suggest that there is an S-wave admixture in the decay, which is contrary to the expectation based on heavy quark effective theory [494,1486].

TABLE 306. Measurements of polarization amplitudes for excited D mesons.

Resonance	A_D	Measured by	References
$D_1(2420)^0$	$7.8^{+6.7\ +4.6}_{-2.7\ -1.8}$	ZEUS	[1439]
	5.72 ± 0.25	*BABAR*	[1329]
	$5.9^{+3.0\ +2.4}_{-1.7\ -1.0}$	ZEUS	[1487]
	$3.8 \pm 0.6 \pm 0.8$	*BABAR*	[535]
	5.61 ± 0.24	Our average	
$D_1(2420)^{\pm}$	$3.8 \pm 0.6 \pm 0.8$	*BABAR*	[535]
$D_2^*(2460)^0$	-1.16 ± 0.35 (stat.)	ZEUS	[1439]
$D(2750)^0$	0.33 ± 0.28 (stat.)	*BABAR*	[1329]

E. Excited charmed baryons

In this section we summarize the present status of excited charmed baryons decaying strongly or electromagnetically. We list their masses (or the mass difference between the excited baryon and the corresponding ground state), natural widths, decay modes, and assigned quantum numbers. The present ground-state measurements are: $M(\Lambda_c^+) = 2286.46 \pm 0.14$ MeV/c^2 measured by *BABAR* [1489], $M(\Xi_c^0) = (2470.90^{+0.22}_{-0.29})$ MeV/c^2 and $M(\Xi_c^+) = (2467.94^{+0.17}_{-0.20})$ MeV/c^2, both dominated by CDF [131], and $M(\Omega_c^0) = (2695.2 \pm 1.7)$ MeV/c^2, dominated by Belle [1490]. Should these values change, so will many of the values for the masses of the excited states.

Table 307 summarizes the excited Λ_c^+ baryons. The first two states listed, namely the $\Lambda_c(2595)^+$ and $\Lambda_c(2625)^+$, are well established. The measured masses and decay patterns suggest that they are orbitally excited Λ_c^+ baryons with total angular momentum of the light quarks $L = 1$. Thus their quantum numbers are assigned to be $J^P = \frac{1}{2}^-$ and $J^P = \frac{3}{2}^-$, respectively. Their mass measurements are dominated by CDF [1491]: $M(\Lambda_c(2595)^+) = (2592.25 \pm 0.28)$ MeV/c^2 and $M(\Lambda_c(2625)^+) = (2628.11 \pm 0.19)$ MeV/c^2. Earlier measurements did not fully take into account the restricted phase-space of the $\Lambda_c(2595)^+$ decays.

The next two states, $\Lambda_c(2765)^+$ and $\Lambda_c(2880)^+$, were discovered by CLEO [1492] in the $\Lambda_c^+\pi^+\pi^-$ final state. CLEO found that a significant fraction of the $\Lambda_c(2880)^+$ decays proceeds via an intermediate $\Sigma_c(2445)^{++,0}\pi^{-,+}$. Later, *BABAR* [1493] observed that this state has also a $D^0 p$ decay mode. This was the first example of an excited charmed baryon decaying into a charm meson plus a baryon; previously all excited charmed baryons were found via hadronic transitions into lower lying charmed baryons. In the same analysis, *BABAR* observed for the first time an additional state, $\Lambda_c(2940)^+$, decaying into $D^0 p$. Studying the $D^+ p$ final state, *BABAR* found no signal and this implies that the $\Lambda_c(2880)^+$ and $\Lambda_c(2940)^+$ are Λ_c^+ excited states rather than Σ_c excitations. Belle reported the result of an angular analysis that favors 5/2 for the $\Lambda_c(2880)^+$ spin hypothesis. Moreover, the measured ratio of branching fractions $\mathcal{B}(\Lambda_c(2880)^+ \to \Sigma_c(2520)\pi^{\pm})/\mathcal{B}(\Lambda_c(2880)^+ \to \Sigma_c(2455)\pi^{\pm}) = (0.225 \pm 0.062 \pm 0.025)$, combined with theoretical predictions based on HQS [527,1494], favor even parity. However this prediction is only valid if the P-wave portion of $\Sigma_c(2520)\pi$ is suppressed. LHCb [880]

TABLE 307. Summary of excited Λ_c^+ baryons. The uncertainties are the total of the statistical and systematic uncertainties.

Charmed baryon excited state	Mode	Mass (MeV/c^2)	Natural width (MeV)	J^P
$\Lambda_c(2595)^+$	$\Lambda_c^+\pi^+\pi^-$, $\Sigma_c(2455)\pi$	2592.25 ± 0.28	2.59 ± 0.57	$\frac{1}{2}^-$
$\Lambda_c(2625)^+$	$\Lambda_c^+\pi^+\pi^-$	2628.11 ± 0.19	<0.97	$\frac{3}{2}^-$
$\Lambda_c(2765)^+$	$\Lambda_c^+\pi^+\pi^-$, $\Sigma_c(2455)\pi$	2766.6 ± 2.4	50	?
$\Lambda_c(2860)^+$	$D^0 p$	$2856.1^{+2.3}_{-5.6}$	$67.6^{+11.8}_{-21.6}$	$\frac{3}{2}^+$
$\Lambda_c(2880)^+$	$\Lambda_c^+\pi^+\pi^-$, $\Sigma_c(2455)\pi$, $\Sigma_c(2520)\pi$, $D^0 p$	2881.63 ± 0.24	$5.6^{+11.3}_{-10.0}$	$\frac{5}{2}^+$
$\Lambda_c(2940)^+$	$D^0 p$, $\Sigma_c(2455)\pi$	$2939.6^{+1.3}_{-1.5}$	20^{+6}_{-5}	?

TABLE 308. Summary of the excited $\Sigma_c^{++,+,0}$ baryon family. The mass difference is given with respect to the Λ_c^+.

Charmed baryon excited state	Mode	Mass difference (MeV/c^2)	Natural width (MeV)	J^P
$\Sigma_c(2455)^{++}$	$\Lambda_c^+\pi^+$	167.510 ± 0.17	$1.89^{+0.09}_{-0.18}$	$\frac{1}{2}^+$
$\Sigma_c(2455)^{+}$	$\Lambda_c^+\pi^0$	166.4 ± 0.4	<4.6 @ 90% C.L.	$\frac{1}{2}^+$
$\Sigma_c(2455)^{0}$	$\Lambda_c^+\pi^-$	167.29 ± 0.17	$1.83^{+0.11}_{-0.19}$	$\frac{1}{2}^+$
$\Sigma_c(2520)^{++}$	$\Lambda_c^+\pi^+$	$231.95^{+0.17}_{-0.12}$	$14.78^{+0.30}_{-0.40}$	$\frac{3}{2}^+$
$\Sigma_c(2520)^{+}$	$\Lambda_c^+\pi^0$	231.0 ± 2.3	<17 @ 90% C.L.	$\frac{3}{2}^+$
$\Sigma_c(2520)^{0}$	$\Lambda_c^+\pi^-$	$232.02^{+0.15}_{-0.14}$	$15.3^{+0.4}_{-0.5}$	$\frac{3}{2}^+$
$\Sigma_c(2800)^{++}$	$\Lambda_c^+\pi^+$	514^{+4}_{-6}	75^{+22}_{-17}	$\frac{3}{2}^-$?
$\Sigma_c(2800)^{+}$	$\Lambda_c^+\pi^0$	505^{+15}_{-5}	62^{+64}_{-44}	
$\Sigma_c(2800)^{0}$	$\Lambda_c^+\pi^-$	519^{+5}_{-7}	72^{+22}_{-15}	
	$\Lambda_c^+\pi^-$	560 ± 13	86^{+33}_{-22}	

have analyzed the D^0p system in the resonant substructure of Λ_b decays. They confirm the $\frac{5}{2}^+$ identification of the $\Lambda_c(2880)^+$. In addition they find evidence for a further, wider, state they name the $\Lambda_c(2860)^+$, with $J^P = \frac{3}{2}^+$ (the parity is measured with respect to that of the $\Lambda_c(2880)^+$). The explanation for these states in the heavy quark-light diquark model is that they are a pair of orbital D-wave excitations. Furthermore, LHCb [880] find evidence for the spin-parity of the $\Lambda_c(2940)^+$ to be $\frac{3}{2}^-$, and improve the world average measurements of both the mass and width of this particle.

A current open question concerns the nature of the $\Lambda_c(2765)^+$ state. However, it has now been experimentally shown by Belle [1495] to be a Λ_c rather than a Σ_c, and implicit in this analysis is that the data can be explained by one resonance. The state has also been observed, but not measured, by LHCb [1496].

Table 308 summarizes the excited $\Sigma_c^{++,+,0}$ baryons. The ground state iso-triplets of $\Sigma_c(2455)^{++,+,0}$ and $\Sigma_c(2520)^{++,+,0}$ baryons are well established. Belle [1497] precisely measured the mass differences and widths of the doubly charged and neutral members of this triplet. The short list of excited Σ_c baryons is completed by the triplet of $\Sigma_c(2800)$ states observed by Belle [1498]. Based on the measured masses and theoretical predictions [1499,1500], these states are thought by some to be members of the predicted $\Sigma_{c2}\,\frac{3}{2}^-$ triplet, where the subscript 2 refers to the total spin of the light quark degrees of freedom. From a study of resonant substructure in $B^- \to \Lambda_c^+\bar{p}\pi^-$ decays, *BABAR* found a significant signal in the $\Lambda_c^+\pi^-$ final state with a mean value higher than measured for the $\Sigma_c(2800)$ by Belle by about 3σ (Table 308). The decay widths measured by Belle and *BABAR* are consistent, but it is an open question if the observed state is the same as the Belle state.It is possible that the present excesses will prove to be due to two or more overlapping states. Circumstantial evidence for this can be found by comparing with the Ξ_c and Ω_c states of similar excitation energies.

Table 309 summarizes the excited $\Xi_c^{+,0}$. The list of excited Ξ_c baryons has many states, of unknown quantum numbers, having masses above 2900 MeV/c^2 and decaying through three different types of modes: $\Lambda_c K n\pi$ or $\Sigma_c K n\pi$, $\Xi_c n\pi$, and ΛD. Some of these states ($\Xi_c(2970)^+$, $\Xi_c(3055)$ and $\Xi_c(3080)^{+,0}$) have been observed by both Belle [1501–1503] and *BABAR* [757], are produced in the charm continuum, and are considered well established. Recently LHCb [1504] reported three narrow states in $\Lambda_c^+K^-$. The masses of two of these states, named the $\Xi_c(2923)$ and $\Xi_c(2939)$ bookend the already discovered, wide $\Xi_c(2930)^0$. This state, also decaying into $\Lambda_c^+K^-$, was found in B decays by *BABAR* [1505]. It was also observed by Belle [824], who in addition observed a similar charged state. Table 309 shows the parameters measured by Belle, as they allow for the interference and other resonances in their analysis. However, given the low statistics of these observations in e^+e^- annihilation, it is possible that the LHCb data explains the peaks found by Belle and *BABAR* as the manifestation of these two states overlapping, and thus there is no distinct $\Xi_c(2930)$ state. LHCb [1504] note that there may well be a fourth resonance at a lower mass of ≈2880 MeV/c^2 and also that the pattern of masses of these states bears a remarkable similarity to that of the excited Ω_c masses, implying the same underlying spin-structure of the quarks. The highest mass of the LHCb Ω_c quintuplet does not appear to have an analogous state here. This state had the lowest signal of the five in the LHCb data and was not confirmed by Belle, so this may imply that it is of a completely different nature to the other four states. Alternatively there may exist an equivalent state in the excited $\Lambda_c^+K^-$ data but it cannot be seen because of its large width and alternative decay modes. The highest-mass of the three new states reported by LHCb is very close in mass to the $\Xi_c(2970)$; formerly

TABLE 309. Summary of excited $\Xi_c^{+,0}$ states. For the first four isodoublets, it is the mass difference with respect to the ground state to which they decay that is quoted as this avoids uncertainties in the ground state masses. For the remaining cases, the uncertainty on the measurement of the excited state itself dominates.

Charmed baryon excited state	Mode	Mass difference (MeV/c^2)	Natural width (MeV)	J^P
$\Xi_c'^+$	$\Xi_c^+\gamma$	110.5 ± 0.4		$\frac{1}{2}^+$
$\Xi_c'^0$	$\Xi_c^0\gamma$	108.3 ± 0.4		$\frac{1}{2}^+$
$\Xi_c(2645)^+$	$\Xi_c^0\pi^+$	174.7 ± 0.1	2.1 ± 0.2	$\frac{3}{2}^+$
$\Xi_c(2645)^0$	$\Xi_c^0\pi^-$	178.5 ± 0.1	2.4 ± 0.2	$\frac{3}{2}^+$
$\Xi_c(2790)^+$	$\Xi_c'^0\pi^+$	320.7 ± 0.5	9 ± 1	$\frac{1}{2}^-$
$\Xi_c(2790)^0$	$\Xi_c'^+\pi^-$	323.8 ± 0.5	10 ± 1	$\frac{1}{2}^-$
$\Xi_c(2815)^+$	$\Xi_c(2645)^0\pi^+$	348.8 ± 0.1	2.43 ± 0.23	$\frac{3}{2}^-$
$\Xi_c(2815)^0$	$\Xi_c(2645)^+\pi^-, \Xi_c^0\gamma$	349.4 ± 0.1	2.54 ± 0.23	$\frac{3}{2}^-$

Charmed baryon excited state	Mode	Mass difference (MeV/c^2)	Natural width (MeV)	J^P
$\Xi_c(2923)^0$	$\Lambda_c^+K^-$	2923.04 ± 0.35	7.1 ± 2.0	?
$\Xi_c(2930)^+$	$\Lambda_c^+K_S^0$	2942.3 ± 4.6	14.8 ± 9.1	?
$\Xi_c(2930)^0$	$\Lambda_c^+K^-$	$2928.6^{+3.1}_{-12.4}$	$19.5^{+10.2}_{-11.5}$	?
$\Xi_c(2939)^0$	$\Lambda_c^+K^-$	2938.55 ± 0.30	10.2 ± 1.4	?
$\Xi_c(2965)^0$	$\Lambda_c^+K^-$	2964.88 ± 0.33	14.1 ± 1.6	?
$\Xi_c(2970)^+$	$\Lambda_c^+K^-\pi^+, \Sigma_c^{++}K^-, \Xi_c(2645)^0\pi^+$	2967.2 ± 0.8	21 ± 3	?
$\Xi_c(2970)^0$	$\Xi_c(2645)^+\pi^-$	2970.4 ± 0.8	28 ± 3	?
$\Xi_c(3055)^+$	$\Sigma_c^{++}K^-, \Lambda D$	3055.7 ± 0.4	8.0 ± 1.9	?
$\Xi_c(3055)^0$	ΛD	3059.0 ± 0.8	6.2 ± 2.4	?
$\Xi_c(3080)^+$	$\Lambda_c^+K^-\pi^+, \Sigma_c^{++}K^-, \Sigma_c(2520)^{++}K^-, \Lambda D$	3077.8 ± 0.3	3.6 ± 0.7	?
$\Xi_c(3080)^0$	$\Lambda_c^+K_S^0\pi^-, \Sigma_c^0K_S^0, \Sigma_c(2520)^0K_S^0$	3079.9 ± 1.0	5.6 ± 2.2	?

named by the PDG as the $\Xi_c(2980)$. A recent analysis by Belle [1506] reveals that the favored spin-parity of this state is $J^P = \frac{1}{2}^+$, which corresponds to it being a (2S) radial excitation. The $\Xi_c(2765)$ and $\Xi_c(2970)$ properties seem to differ by enough to be able to say with reasonable confidence that they are completely different states, though the confusion due to their similar masses might help explain the poor consistency of the historical measurements of the $\Xi_c(2970)$. The properties of the $\Xi_c(2970)$ can be seen to have similarities to the $\Lambda_c(2765)$, not only in its mass difference with respect to the ground state, but also its decay pattern and large production in e^+e^- annihilation data. This strengthens the confidence in their identification as "Roper-like" resonances [1507], that is, as the charmed equivalents of the light quark $P_{11}(1440)$ which is often identified as a radial excitation.

In addition to the $\Xi_c(2970)$, Belle [1508] have analyzed large samples of Ξ_c', $\Xi_c(2645)$, $\Xi_c(2790)$, and $\Xi_c(2815)$ decays. From this analysis they obtain the most precise mass measurements of all five iso-doublets, and the first significant width measurements of the $\Xi_c(2645)$, $\Xi_c(2790)$ and $\Xi_c(2815)$. Though the spin-parity of these particles have not been directly measured, there seems little controversy that the simple quark-diquark model can explain the data. We note that the precision of the mass measurements allows for added information from the isospin mass-splitting to be used in identifying the underlying structure. In addition, the recent observation by Belle [1509] of photon transitions to the ground state from the neutral (but not charged) $\Xi_c(2815)$, and probably also the $\Xi_c(2790)$, can be interpreted as confirmation of the standard quark interpretation.

Several of the width and mass measurements for the $\Xi_c(3055)$ and $\Xi_c(3080)$ isodoublets are only in marginal agreement between experiments and decay modes. However, there seems little doubt that the differing measurements are of the same particle. The masses do indicate that their spin-parity might match those of the $\Lambda_c(2860)$ and $\Lambda_c(2880)$.

The $\Xi_c(3123)^+$ reported by *BABAR* [757] in the $\Sigma_c(2520)^{++}\pi^-$ final state has not been confirmed by Belle [1502] with twice the statistics; thus its existence is in doubt and it is omitted from Tab. 309 which summarizes the present situation in the excited Ξ_c sector.

TABLE 310. Summary of excited Ω_c^0 baryons. For the $\Omega_c(2770)^0$, the mass difference with respect to the ground state is given, as the uncertainty is dominated by the uncertainty in the ground state mass. In the remaining cases the total mass is shown, though the uncertainty in the Ξ_c^+ mass makes an important contribution to the total uncertainty.

Charmed baryon excited state	Mode	Mass difference (MeV/c^2)	Natural width (MeV)	J^P
$\Omega_c(2770)^0$	$\Omega_c^0\gamma$	$70.7^{+0.8}_{-0.9}$		$\frac{3}{2}^+$
Charmed baryon excited state	**Mode**	**Mass (MeV/c^2)**	**Natural width (MeV)**	J^P
$\Omega_c(3000)^0$	$\Xi_c^+K^-$	3000.4 ± 0.4	4.5 ± 0.7	?
$\Omega_c(3050)^0$	$\Xi_c^+K^-$	3050.2 ± 0.3	<1.2	?
$\Omega_c(3065)^0$	$\Xi_c^+K^-$	3065.5 ± 0.4	3.5 ± 0.5	?
$\Omega_c(3090)^0$	$\Xi_c^+K^-$	3090.0 ± 0.6	8.7 ± 1.4	?
$\Omega_c(3120)^0$	$\Xi_c^+K^-$	3119.1 ± 1.0	<2.6	?

The Ω_c^{*0} doubly strange charmed baryon has been seen by both *BABAR* [1510] and Belle [1490]. The mass differences $\Delta M = M(\Omega_c^{*0}) - M(\Omega_c^0)$ measured by the experiments are in good agreement and are also consistent with most theoretical predictions [1511–1514]. LHCb [1515] has found a family of five excited Ω_c^0 baryons decaying into $\Xi_c^+K^-$. A natural explanation is that they are the five states with $L = 1$ between the heavy quark and the light (ss) diquark; however, there is no consensus as to which state is which, and this overall interpretation is controversial. Four of the five states have been confirmed by Belle [1516] and, although the Belle dataset is much smaller than that of LHCb, these mass measurements do contribute to the world averages. There is evidence for a further, wider, state at higher mass in the LHCb data. Belle data shows a small excess in the same region, but it is of low significance. Table 310 summarizes the excited Ω_c baryons.

Figure 100 shows the levels of excited charm baryons along with corresponding transitions between them, and also transitions to the ground states. We note that Belle and *BABAR* discovered that transitions between "families" of baryons are possible, i.e., between the charmed-strange (Ξ_c) and charmed-nonstrange (Λ_c^+ and Σ_c) families of excited charmed baryons [757,1501], and that highly excited states are found to decay into a non-charmed baryon and a D meson [1493,1503]. Transitions of the ground state Ξ_c^0 to the Λ_c^+, corresponding to the weak decay of the stange quark, were observed first by Belle [1497], and then studied and measured by LHCb [1517].

F. Rare and forbidden decays

This section provides a summary of searches for rare and forbidden charm decays in tabular form. The decay modes

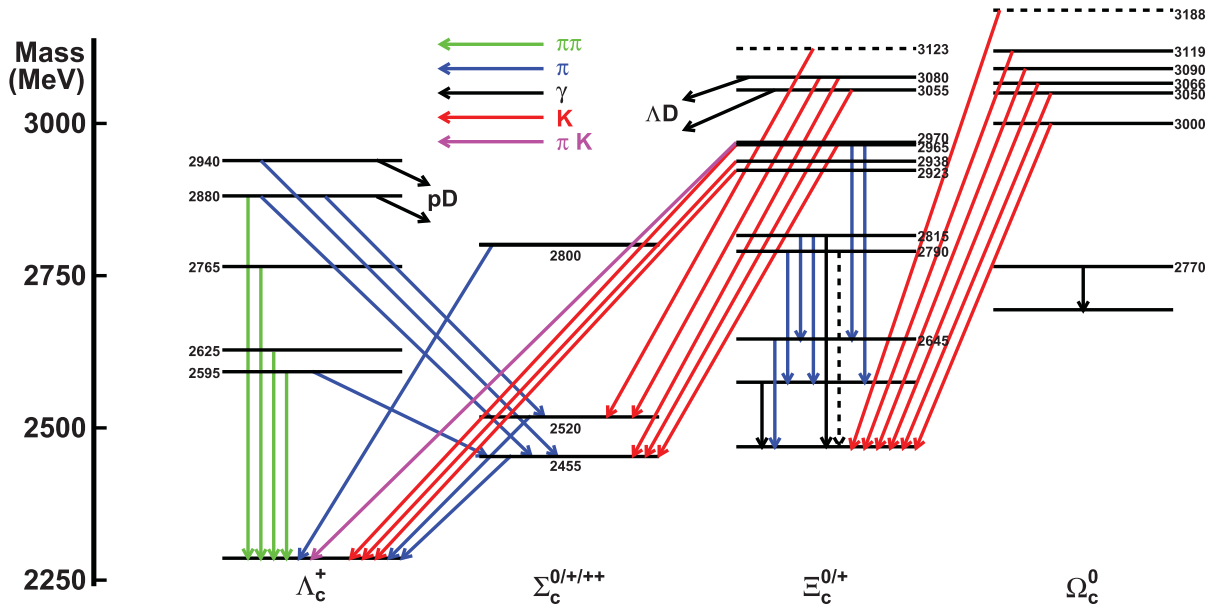

FIG. 100. Level diagram for multiplets and transitions for excited charm baryons.

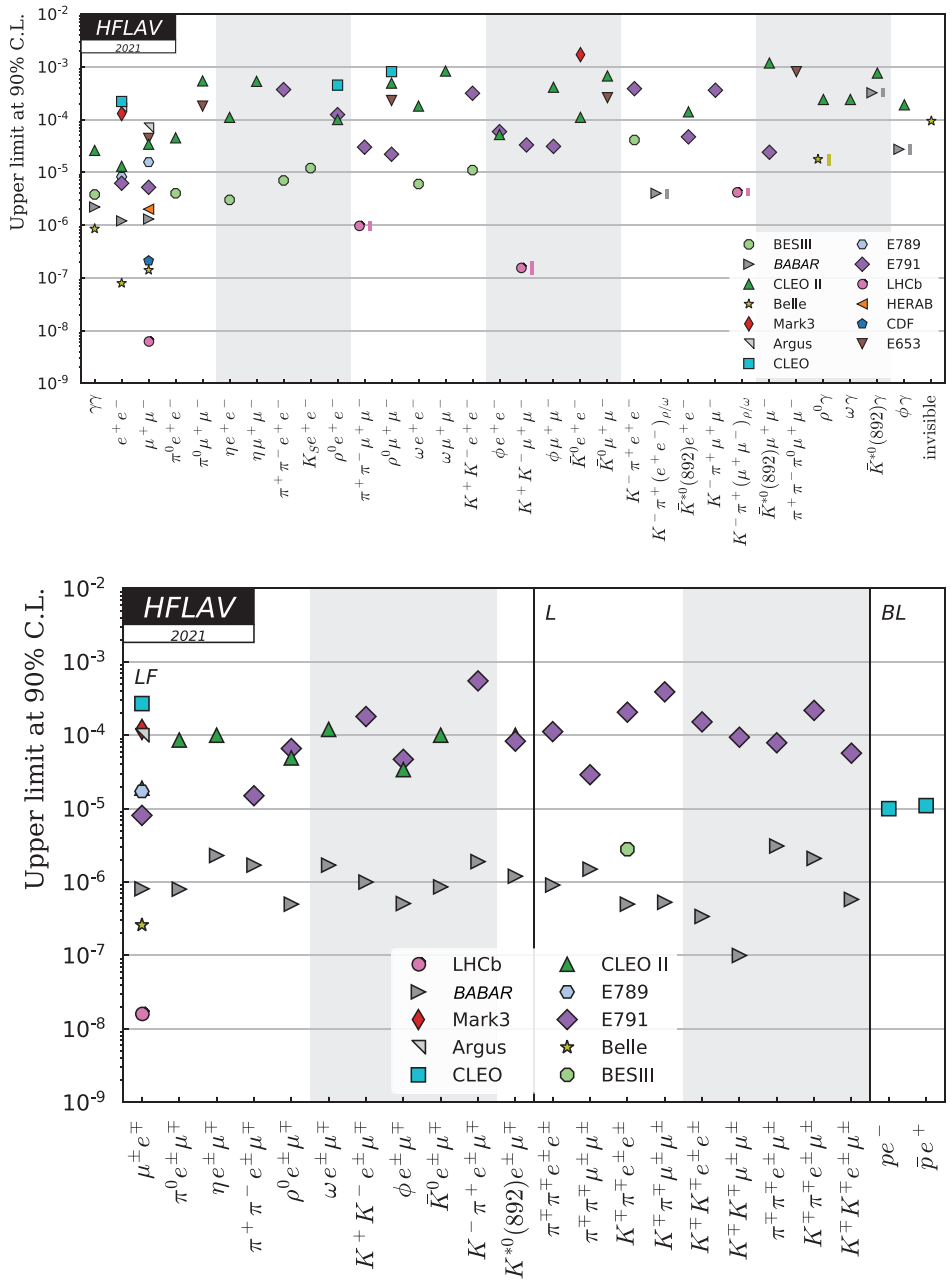

FIG. 101. Upper limits at 90% C.L. for D^0 decays. The top plot shows flavor-changing neutral current and radiative decays, and the bottom plot shows lepton-flavor-changing (LF), lepton-number-changing (L), and both baryon- and lepton-number-changing (BL) decays.

can be categorized as flavor-changing neutral currents, including decays with and without hadrons in the final state, and radiative, lepton-flavor-violating, lepton-number-violating, and both baryon- and lepton-number-violating decays. Figures 101–103 plot the upper limits for D^0, D^+, D_s^+, and Λ_c^+ decays. Tables 311–314 give the corresponding numerical results. Some theoretical predictions are given in Refs. [1518–1533].

Some D^0 decay modes have been observed and are quoted as branching fractions with uncertainties in the tables and shown as a symbol with a line representing the 68% C.L. interval in the plots.

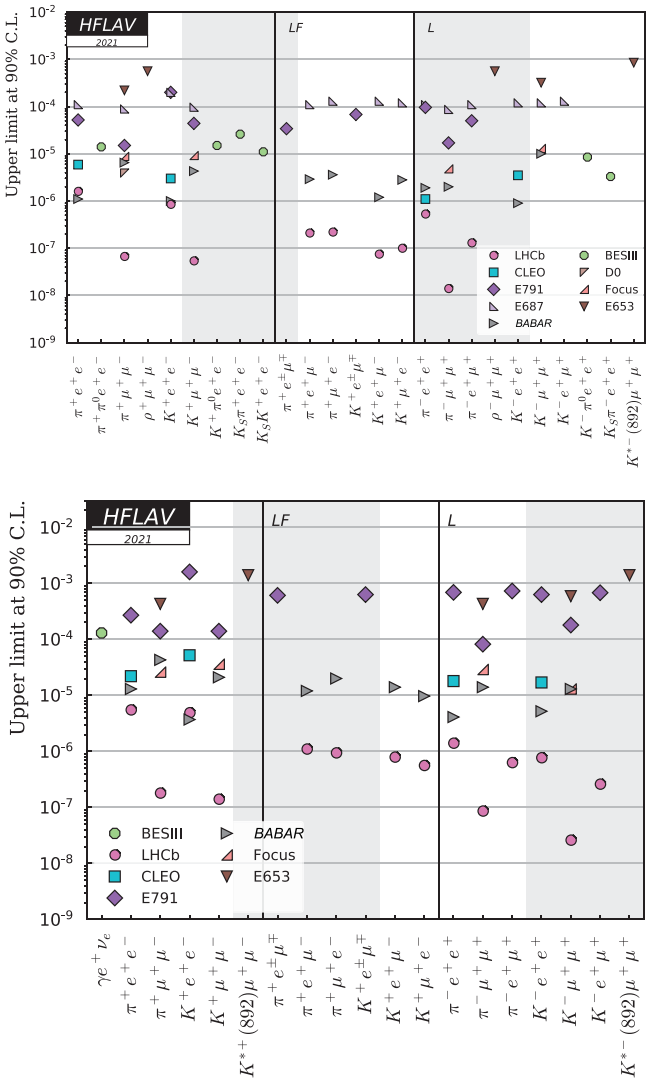

FIG. 102. Upper limits at 90% C.L. for D^+ (top) and D_s^+ (bottom) decays. Each plot shows flavor-changing neutral current and rare decays, lepton-flavor-changing decays (LF), and lepton-number-changing (L) decays.

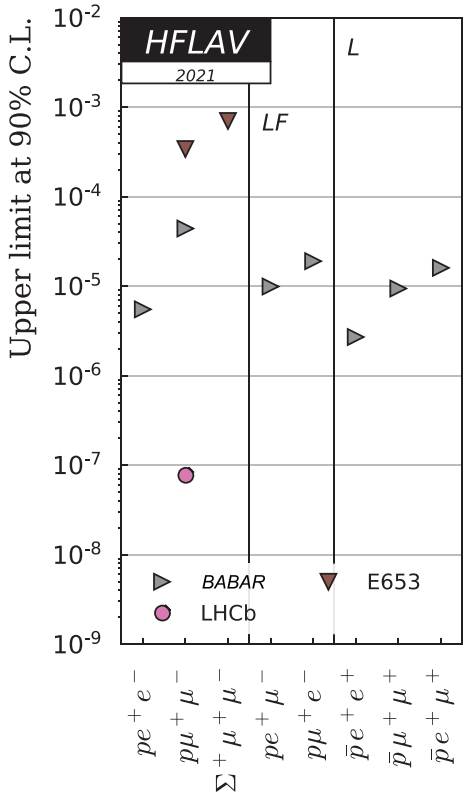

FIG. 103. Upper limits at 90% C.L. for Λ_c^+ decays. Shown are flavor-changing neutral current decays, lepton-flavor-changing (LF) decays, and lepton-number-changing (L) decays.

In several cases the rare-decay final states have been observed with the dilepton pair being the decay product of a vector meson. For these measurements the quoted limits are those expected for the nonresonant dilepton spectrum. For the extrapolation to the full spectrum a phase-space distribution of the nonresonant component has been assumed. This applies to the CLEO measurement of the decays $D_{(s)}^+ \to (K^+, \pi^+)e^+e^-$ [1534], to the D0 measurements of the decays $D_{(s)}^+ \to \pi^+\mu^+\mu^-$ [1535], and to the *BABAR* measurements of the decays $D_{(s)}^+ \to (K^+, \pi^+)e^+e^-$ and $D_{(s)}^+ \to (K^+, \pi^+)\mu^+\mu^-$, where the contribution from $\phi \to l^+l^-$ $(l = e,\ \mu)$ has been excluded. In the case of the LHCb measurements of the decays $D^0 \to \pi^+\pi^-\mu^+\mu^-$ [1536] as well as the decays $D_{(s)}^+ \to \pi^+\mu^+\mu^-$ [1537] the contributions from $\phi \to l^+l^-$ as well as from $\rho, \omega \to l^+l^-$ $(l = e,\ \mu)$ have been excluded.

TABLE 311. Upper limits for branching fractions at 90% C.L. for D^0 decays. Where values are quoted with uncertainties, these refer to observed branching fractions with the first uncertainty being statistical and all others systematic as detailed in the corresponding reference.

Mode	BF $\times 10^6$	Experiment	References
$\gamma\gamma$	26.0	CLEO II	[1538]
	3.8	BESIII	[1539]
	2.2	*BABAR*	[1540]
	0.85	Belle	[1541]
e^+e^-	220.0	CLEO	[1542]
	170.0	Argus	[1543]
	130.0	Mark3	[1544]
	13.0	CLEO II	[1545]
	8.19	E789	[1546]
	6.2	E791	[1547]
	1.2	*BABAR*	[1548]
	0.079	Belle	[1549]
$\mu^+\mu^-$	70.0	Argus	[1543]
	44.0	E653	[1550]
	34.0	CLEO II	[1545]
	15.6	E789	[1546]
	5.2	E791	[1547]
	2.0	HERAb	[1551]
	1.3	*BABAR*	[1548]
	0.21	CDF	[1552]
	0.14	Belle	[1549]
	0.0062	LHCb	[1553]
$\pi^0e^+e^-$	45.0	CLEO II	[1545]
	4.0	BESIII	[1554]
$\pi^0\mu^+\mu^-$	540.0	CLEO II	[1545]
	180.0	E653	[1550]
ηe^+e^-	110.0	CLEO II	[1545]
	3.0	BESIII	[1554]
$\eta\mu^+\mu^-$	530.0	CLEO II	[1545]
$\pi^+\pi^-e^+e^-$	370.0	E791	[1555]
	7.0	BESIII	[1554]
$K_Se^+e^-$	12.0	BESIII	[1554]
$\rho^0e^+e^-$	450.0	CLEO	[1542]
	124.0	E791	[1555]
	100.0	CLEO II	[1545]
$\pi^+\pi^-\mu^+\mu^-$	30.0	E791	[1555]
	$0.964 \pm 0.048 \pm 0.051 \pm 0.097$	LHCb	[1556]
$\rho^0\mu^+\mu^-$	810.0	CLEO	[1542]
	490.0	CLEO II	[1545]
	230.0	E653	[1550]
	22.0	E791	[1555]
ωe^+e^-	180.0	CLEO II	[1545]
	6.0	BESIII	[1554]
$\omega\mu^+\mu^-$	830.0	CLEO II	[1545]
$K^+K^-e^+e^-$	315.0	E791	[1555]
	11.0	BESIII	[1554]

(Table continued)

TABLE 311. *(Continued)*

Mode	BF $\times 10^6$	Experiment	References
ϕe^+e^-	59.0	E791	[1555]
	52.0	CLEO II	[1545]
$K^+K^-\mu^+\mu^-$	33.0	E791	[1555]
	$0.154 \pm 0.027 \pm 0.009 \pm 0.016$	LHCb	[1556]
$\phi\mu^+\mu^-$	410.0	CLEO II	[1545]
	31.0	E791	[1555]
$\bar{K}^0e^+e^-$	1700.0	Mark3	[1557]
	110.0	CLEO II	[1545]
$\bar{K}^0\mu^+\mu^-$	670.0	CLEO II	[1545]
	260.0	E653	[1550]
$K^-\pi^+e^+e^-$	385.0	E791	[1555]
	41.0	BESIII	[1554]
$K^-\pi^+(e^+e^-)_{\rho/\omega}$	$4.0 \pm 0.5 \pm 0.2 \pm 0.1$	*BABAR*	[1558]
$\bar{K}^{*0}(892)e^+e^-$	140.0	CLEO II	[1545]
	47.0	E791	[1555]
$K^-\pi^+\mu^+\mu^-$	360.0	E791	[1555]
$K^-\pi^+(\mu^+\mu^-)_{\rho/\omega}$	$4.17 \pm 0.12 \pm 0.40$	LHCb	[1559]
$\bar{K}^{*0}(892)\mu^+\mu^-$	1180.0	CLEO II	[1545]
	24.0	E791	[1555]
$\pi^+\pi^-\pi^0\mu^+\mu^-$	810.0	E653	[1550]
$\rho^0\gamma$	240.0	CLEO II	[1560]
	$17.7 \pm 3.0 \pm 0.7$	Belle	[1296]
$\omega\gamma$	240.0	CLEO II	[1560]
$\bar{K}^{*0}(892)\gamma$	760.0	CLEO II	[1560]
	$322.0 \pm 20.0 \pm 27.0$	*BABAR*	[1561]
$\phi\gamma$	190.0	CLEO II	[1560]
	$27.3 \pm 3.0 \pm 2.6$	*BABAR*	[1561]
invisible	94.0	Belle	[1562]
$\mu^\pm e^\mp$	270.0	CLEO	[1542]
	120.0	Mark3	[1563]
	100.0	Argus	[1543]
	19.0	CLEO II	[1545]
	17.2	E789	[1546]
	8.1	E791	[1547]
	0.81	*BABAR*	[1548]
	0.26	Belle	[1549]
	0.016	LHCb	[1564]
$\pi^0e^\pm\mu^\mp$	86.0	CLEO II	[1545]
	0.80	*BABAR*	[1565]
$\eta e^\pm\mu^\mp$	100.0	CLEO II	[1545]
	2.3	*BABAR*	[1565]
$\pi^+\pi^-e^\pm\mu^\mp$	15.0	E791	[1555]
	1.7	*BABAR*	[1566]
$\rho^0e^\pm\mu^\mp$	66.0	E791	[1555]
	49.0	CLEO II	[1545]
	0.5	*BABAR*	[1565]

(Table continued)

TABLE 311. *(Continued)*

Mode	BF × 10^6	Experiment	References
$\omega e^{\pm}\mu^{\mp}$	120.0	CLEO II	[1545]
	1.7	*BABAR*	[1565]
$K^+K^-e^{\pm}\mu^{\mp}$	180.0	E791	[1555]
	1.0	*BABAR*	[1566]
$\phi e^{\pm}\mu^{\mp}$	47.0	E791	[1555]
	34.0	CLEO II	[1545]
	0.51	*BABAR*	[1565]
$\bar{K}^0 e^{\pm}\mu^{\mp}$	100.0	CLEO II	[1545]
	0.86	*BABAR*	[1565]
$K^-\pi^+ e^{\pm}\mu^{\mp}$	550.0	E791	[1555]
	1.9	*BABAR*	[1566]
$K^{*0}(892)e^{\pm}\mu^{\mp}$	100.0	CLEO II	[1545]
	83.0	E791	[1555]
	1.2	*BABAR*	[1565]
$\pi^{\mp}\pi^{\mp}e^{\pm}e^{\pm}$	112.0	E791	[1555]
	0.91	*BABAR*	[1566]
$\pi^{\mp}\pi^{\mp}\mu^{\pm}\mu^{\pm}$	29.0	E791	[1555]
	1.5	*BABAR*	[1566]
$K^{\mp}\pi^{\mp}e^{\pm}e^{\pm}$	206.0	E791	[1555]
	2.8	BESIII	[1567]
	0.5	*BABAR*	[1566]
$K^{\mp}\pi^{\mp}\mu^{\pm}\mu^{\pm}$	390.0	E791	[1555]
	0.53	*BABAR*	[1566]
$K^{\mp}K^{\mp}e^{\pm}e^{\pm}$	152.0	E791	[1555]
	0.34	*BABAR*	[1566]
$K^{\mp}K^{\mp}\mu^{\pm}\mu^{\pm}$	94.0	E791	[1555]
	0.10	*BABAR*	[1566]
$\pi^{\mp}\pi^{\mp}e^{\pm}\mu^{\pm}$	79.0	E791	[1555]
	3.1	*BABAR*	[1566]
$K^{\mp}\pi^{\mp}e^{\pm}\mu^{\pm}$	218.0	E791	[1555]
	2.1	*BABAR*	[1566]
$K^{\mp}K^{\mp}e^{\pm}\mu^{\pm}$	57.0	E791	[1555]
	0.58	*BABAR*	[1566]
pe^-	10.0	CLEO	[1568]
$\bar{p}e^+$	11.0	CLEO	[1568]

TABLE 312. Upper limits at 90% C.L. for D^+ decays.

Mode	Limit ×10^6	Experiment	Reference
$\pi^+e^+e^-$	110.0	E687	[1569]
	52.0	E791	[1547]
	5.9	CLEO	[1534]
	1.6	LHCb	[1570]
	1.1	*BABAR*	[1571]

(Table continued)

TABLE 312. *(Continued)*

Mode	Limit $\times 10^6$	Experiment	Reference
$\pi^+\pi^0 e^+ e^-$	14.0	BESIII	[1554]
$\pi^+\mu^+\mu^-$	220.0	E653	[1550]
	89.0	E687	[1569]
	15.0	E791	[1547]
	8.8	Focus	[1572]
	6.5	*BABAR*	[1571]
	3.9	D0	[1535]
	0.067	LHCb	[1570]
$\rho^+\mu^+\mu^-$	560.0	E653	[1550]
$K^+ e^+ e^-$	200.0	E687	[1569]
	3.0	CLEO	[1534]
	1.0	*BABAR*	[1571]
	0.85	LHCb	[1570]
$K^+\mu^+\mu^-$	97.0	E687	[1569]
	44.0	E791	[1547]
	9.2	Focus	[1572]
	4.3	*BABAR*	[1571]
	0.054	LHCb	[1570]
$K^+\pi^0 e^+ e^-$	15.0	BESIII	[1554]
$K_S\pi^+ e^+ e^-$	26.0	BESIII	[1554]
$K_S K^+ e^+ e^-$	11.0	BESIII	[1554]
$\pi^+ e^\pm \mu^\mp$	34.0	E791	[1547]
$\pi^+ e^+ \mu^-$	110.0	E687	[1569]
	2.9	*BABAR*	[1571]
	0.21	LHCb	[1570]
$\pi^+\mu^+ e^-$	130.0	E687	[1569]
	3.6	*BABAR*	[1571]
	0.22	LHCb	[1570]
$K^+ e^\pm \mu^\mp$	68.0	E791	[1547]
$K^+ e^+ \mu^-$	130.0	E687	[1569]
	1.2	*BABAR*	[1571]
	0.075	LHCb	[1570]
$K^+\mu^+ e^-$	120.0	E687	[1569]
	2.8	*BABAR*	[1571]
	0.10	LHCb	[1570]
$\pi^- e^+ e^+$	110.0	E687	[1569]
	96.0	E791	[1547]
	1.9	*BABAR*	[1571]
	1.1	CLEO	[1534]
	0.53	LHCb	[1570]
$\pi^-\mu^+\mu^+$	87.0	E687	[1569]
	17.0	E791	[1547]
	4.8	Focus	[1572]
	2.0	*BABAR*	[1571]
	0.014	LHCb	[1570]
$\pi^- e^+\mu^+$	110.0	E687	[1569]
	50.0	E791	[1547]
	0.13	LHCb	[1570]

(Table continued)

TABLE 312. *(Continued)*

Mode	Limit $\times 10^6$	Experiment	Reference
$\rho^- \mu^+ \mu^+$	560.0	E653	[1550]
$K^- e^+ e^+$	120.0	E687	[1569]
	3.5	CLEO	[1534]
	0.9	*BABAR*	[1571]
$K^- \mu^+ \mu^+$	320.0	E653	[1550]
	120.0	E687	[1569]
	13.0	Focus	[1572]
	10.0	*BABAR*	[1571]
$K^- e^+ \mu^+$	130.0	E687	[1569]
$K^- \pi^0 e^+ e^+$	8.5	BESIII	[1567]
$K_S \pi^- e^+ e^+$	3.3	BESIII	[1567]
$K^{*-}(892) \mu^+ \mu^+$	850.0	E653	[1550]

TABLE 313. Upper limits at 90% C.L. for D_s^+ decays.

Mode	Limit $\times 10^6$	Experiment	Reference
$\gamma e^+ \nu_e$	130.0	BESIII	[1573]
$\pi^+ e^+ e^-$	270.0	E791	[1547]
	22.0	CLEO	[1534]
	13.0	*BABAR*	[1571]
	5.5	LHCb	[1570]
$\pi^+ \mu^+ \mu^-$	430.0	E653	[1550]
	140.0	E791	[1547]
	43.0	*BABAR*	[1571]
	26.0	Focus	[1572]
	0.18	LHCb	[1570]
$K^+ e^+ e^-$	1600.0	E791	[1547]
	52.0	CLEO	[1534]
	4.9	LHCb	[1570]
	3.7	*BABAR*	[1571]
$K^+ \mu^+ \mu^-$	140.0	E791	[1547]
	36.0	Focus	[1572]
	21.0	*BABAR*	[1571]
	0.14	LHCb	[1570]
$K^{*+}(892) \mu^+ \mu^-$	1400.0	E653	[1550]
$\pi^+ e^\pm \mu^\mp$	610.0	E791	[1547]
$\pi^+ e^+ \mu^-$	12.0	*BABAR*	[1571]
	1.1	LHCb	[1570]
$\pi^+ \mu^+ e^-$	20.0	*BABAR*	[1571]
	0.94	LHCb	[1570]
$K^+ e^\pm \mu^\mp$	630.0	E791	[1547]
$K^+ e^+ \mu^-$	14.0	*BABAR*	[1571]
	0.79	LHCb	[1570]
$K^+ \mu^+ e^-$	9.7	*BABAR*	[1571]
	0.56	LHCb	[1570]

(Table continued)

TABLE 313. *(Continued)*

Mode	Limit × 10^6	Experiment	Reference
$\pi^- e^+ e^+$	690.0	E791	[1547]
	18.0	CLEO	[1534]
	4.1	*BABAR*	[1571]
	1.4	LHCb	[1570]
$\pi^- \mu^+ \mu^+$	430.0	E653	[1550]
	82.0	E791	[1547]
	29.0	Focus	[1572]
	14.0	*BABAR*	[1571]
	0.086	LHCb	[1570]
$\pi^- e^+ \mu^+$	730.0	E791	[1547]
	0.63	LHCb	[1570]
$K^- e^+ e^+$	630.0	E791	[1547]
	17.0	CLEO	[1534]
	5.2	*BABAR*	[1571]
	0.77	LHCb	[1570]
$K^- \mu^+ \mu^+$	590.0	E653	[1550]
	180.0	E791	[1547]
	13.0	*BABAR*	[1571]
	0.026	LHCb	[1570]
$K^- e^+ \mu^+$	680.0	E791	[1547]
	0.26	LHCb	[1570]
$K^{*-}(892)\mu^+ \mu^+$	1400.0	E653	[1550]

TABLE 314. Upper limits at 90% C.L. for Λ_c^+ decays.

Mode	Limit × 10^6	Experiment	Reference
$p e^+ e^-$	5.5	*BABAR*	[1571]
$p \mu^+ \mu^-$	340.0	E653	[1550]
	44.0	*BABAR*	[1571]
	0.077	LHCb	[1574]
$\Sigma^+ \mu^+ \mu^-$	700.0	E653	[1550]
$p e^+ \mu^-$	9.9	*BABAR*	[1571]
$p \mu^+ e^-$	19.0	*BABAR*	[1571]
$\bar{p} e^+ e^+$	2.7	*BABAR*	[1571]
$\bar{p} \mu^+ \mu^+$	9.4	*BABAR*	[1571]
$\bar{p} e^+ \mu^+$	16.0	*BABAR*	[1571]

XII. TAU LEPTON PROPERTIES

This section reports a global fit of the available measurements of τ branching fractions and some elaborations of the fit results. In this edition, we do not include the combinations of upper limits on τ lepton-flavor-violating branching fractions, which were published in previous editions, since it was not possible to update this contribution in due time.

Branching fractions averages are obtained with a fit of branching fractions measurements so as to optimally exploit the available experimental information. The fit is described in Sec. XII. A. The fit results are used in Sec. XII. B to test the lepton-flavor universality of the charged-current weak interaction. A "universality-improved" [1575] branching fraction $\mathcal{B}_e = \mathcal{B}(\tau \to e\nu\bar{\nu})$ and the ratio between the hadronic branching fraction

and $\mathcal{B}_e$ are obtained in Sec. XII. C. The value of the Cabibbo-Kobayashi-Maskawa (CKM) matrix element $|V_{us}|$ obtained from τ decays is given in Sec. XII. D.

A. Branching fraction fit

A fit of the available experimental measurements is used to determine the τ branching fractions, together with their uncertainties and correlations.

All relevant published statistical and systematic correlations among the measurements are used. In addition, for a selection of measurements, particularly the most precise and the most recent ones, the documented systematic uncertainty contributions are examined to consider systematic dependence on external parameters. We follow the procedures detailed in Sec. III A to account for the updated values and uncertainties of the external parameters and for the correlations induced on different measurements that have a systematic dependence on the same external parameter.

Both the measurements and the fitted quantities consist of either τ decay branching fractions, labeled $\mathcal{B}_i$, or ratios of two τ decay branching fractions, labeled $\mathcal{B}_i/\mathcal{B}_j$. Some branching fractions are sums of other branching fractions, for instance, $\mathcal{B}_8 = \mathcal{B}(\tau^- \to h^-\nu_\tau)$, which is the sum of $\mathcal{B}_9 = \mathcal{B}(\tau^- \to \pi^-\nu_\tau)$ and $\mathcal{B}_{10} = \mathcal{B}(\tau^- \to K^-\nu_\tau)$, with the symbol h referring to a π or a K. The fit χ^2 is constructed following Eq. (1) and minimized subject to a list of constraints on the fitted quantities:

(i) the fitted quantity corresponding to the ratio $\mathcal{B}_i/\mathcal{B}_j$ must be equal to the ratio of the respective quantities $\mathcal{B}_i$ and $\mathcal{B}_j$;

(ii) the fitted quantity corresponding to a branching-fraction sum must be equal to the sum of the quantities corresponding to the summed branching fractions.

The constraints are implemented with Lagrange multipliers (see Sec. III. In some cases, constraints arise from approximate relations that nevertheless hold within the present experimental precision and are treated as exact. For instance, the constraint $\mathcal{B}(\tau^- \to K^-K^-K^+\nu_\tau) = \mathcal{B}(\tau^- \to K^-\phi\nu_\tau) \times \mathcal{B}(\phi \to K^+K^-)$ is justified given the current experimental evidence. Section XII. A. 6 lists all constraint equations relating the fitted quantities.

Following a convention established in the Review of Particle Physics, τ branching fractions are often labeled with the final state content of $\pi^\pm$, π^0, $K^\pm$, γ, implicitly including decay chains that involve intermediate particles, e.g., $K^0_S \to \pi^+\pi^-$, and η, ω, ϕ decays. When measurements exclude the contribution of some or all the known intermediate particles, the branching fraction notation flags this information by adding, e.g., "ex. K^0".

1. Fit results

We use a total of 171 measurements to fit 135 quantities subject to 88 constraints. The fit has $\chi^2/\text{d.o.f.} = 134/124$, corresponding to a confidence level CL = 24.56%. The fitted quantity values and uncertainties are listed in Table 315. Although the fit treats all quantities in the same way, for the purpose of presenting correlations we select a set of 47 "basis quantities" from which all remaining quantities can be calculated using the definitions listed in Sec. XII. A. 6. The off-diagonal correlation coefficients between the basis quantities are listed in Sec. XII. A. 5.

Table 315 also reports $\mathcal{B}_{110} = \mathcal{B}(\tau^- \to X_s^-\nu_\tau)$ (see Sec. XII. A. 6), the total measured branching fraction for τ

TABLE 315. HFLAV 2021 branching fractions fit results.

τ lepton branching fraction	Experiment	References
$\mathcal{B}_1 =$ particle$^- \geq 0$ neutrals $> 0\, K^0\nu_\tau$		
0.8518 ± 0.0011	Average	
$\mathcal{B}_2 =$ particle$^- \geq 0$ neutrals $> 0\, K^0_L\nu_\tau$		
0.8452 ± 0.0010	Average	
$\mathcal{B}_3 = \mu^-\bar{\nu}_\mu\nu_\tau$		
0.17387 ± 0.00040	Average	
$0.17319 \pm 0.00070 \pm 0.00032$	ALEPH	[1577]
$0.17325 \pm 0.00095 \pm 0.00077$	DELPHI	[1585]
$0.17342 \pm 0.00110 \pm 0.00067$	L3	[1586]
$0.17340 + 0.00090 + 0.00060$	OPAL	[1587]
$\frac{\mathcal{B}_3}{\mathcal{B}_5} = \frac{\mu^-\bar{\nu}_\mu\nu_\tau}{e^-\bar{\nu}_e\nu_\tau}$		
0.9762 ± 0.0028	Average	
$0.9970 \pm 0.0350 \pm 0.0400$	ARGUS	[1588]
$0.9796 \pm 0.0016 \pm 0.0036$	*BABAR*	[1589]
$0.9777 \pm 0.0063 \pm 0.0087$	CLEO	[1590]

(Table continued)

TABLE 315. *(Continued)*

τ lepton branching fraction	Experiment	References
$\mathcal{B}_5 = e^-\bar{\nu}_e\nu_\tau$		
0.17811 ± 0.00041	Average	
$0.17837 \pm 0.00072 \pm 0.00036$	ALEPH	[1577]
$0.17760 \pm 0.00060 \pm 0.00170$	CLEO	[1590]
$0.17877 \pm 0.00109 \pm 0.00110$	DELPHI	[1585]
$0.17806 \pm 0.00104 \pm 0.00076$	L3	[1586]
$0.17810 \pm 0.00090 \pm 0.00060$	OPAL	[1591]
$\mathcal{B}_7 = h^- \geq 0\, K_L^0\nu_\tau$		
0.12020 ± 0.00055	Average	
$0.12400 \pm 0.00700 \pm 0.00700$	DELPHI	[1592]
$0.12470 \pm 0.00260 \pm 0.00430$	L3	[1593]
$0.12100 \pm 0.00700 \pm 0.00500$	OPAL	[1594]
$\mathcal{B}_8 = h^-\nu_\tau$		
0.11504 ± 0.00054	Average	
$0.11520 \pm 0.00050 \pm 0.00120$	CLEO	[1590]
$0.11571 \pm 0.00120 \pm 0.00114$	DELPHI	[1595]
$0.11980 \pm 0.00130 \pm 0.00160$	OPAL	[1596]
$\frac{\mathcal{B}_8}{\mathcal{B}_5} = \frac{h^-\nu_\tau}{e^-\bar{\nu}_e\nu_\tau}$		
0.6459 ± 0.0033	Average	
$\mathcal{B}_9 = \pi^-\nu_\tau$		
0.10808 ± 0.00053	Average	
$0.10828 \pm 0.00070 \pm 0.00078$	ALEPH	[1577]
$\frac{\mathcal{B}_9}{\mathcal{B}_5} = \frac{\pi^-\nu_\tau}{e^-\bar{\nu}_e\nu_\tau}$		
0.6068 ± 0.0032	Average	
$0.5945 \pm 0.0014 \pm 0.0061$	*BABAR*	[1589]
$\mathcal{B}_{10} = K^-\nu_\tau$		
$(0.6957 \pm 0.0096) \times 10^{-2}$	Average	
$(0.6960 \pm 0.0250 \pm 0.0140) \times 10^{-2}$	ALEPH	[1597]
$(0.6600 \pm 0.0700 \pm 0.0900) \times 10^{-2}$	CLEO	[1598]
$(0.8500 \pm 0.1800 \pm 0.0000) \times 10^{-2}$	DELPHI	[1599]
$(0.6580 \pm 0.0270 \pm 0.0290) \times 10^{-2}$	OPAL	[1600]
$\frac{\mathcal{B}_{10}}{\mathcal{B}_5} = \frac{K^-\nu_\tau}{e^-\bar{\nu}_e\nu_\tau}$		
$(3.906 \pm 0.054) \times 10^{-2}$	Average	
$(3.882 \pm 0.032 \pm 0.057) \times 10^{-2}$	*BABAR*	[1589]
$\frac{\mathcal{B}_{10}}{\mathcal{B}_9} = \frac{K^-\nu_\tau}{\pi^-\nu_\tau}$		
$(6.437 \pm 0.092) \times 10^{-2}$	Average	
$\mathcal{B}_{11} = h^- \geq 1\,\text{neutrals}\,\nu_\tau$		
0.36977 ± 0.00098	Average	
$\mathcal{B}_{12} = h^- \geq 1\,\pi^0\nu_\tau\,(\text{ex.}K^0)$		
0.36477 ± 0.00098	Average	
$\mathcal{B}_{13} = h^-\pi^0\nu_\tau$		
0.25918 ± 0.00090	Average	
$0.25670 \pm 0.00010 \pm 0.00390$	Belle	[1601]
$0.25870 \pm 0.00120 \pm 0.00420$	CLEO	[1602]
$0.25740 \pm 0.00201 \pm 0.00138$	DELPHI	[1595]
$0.25050 \pm 0.00350 \pm 0.00500$	L3	[1593]
$0.25890 \pm 0.00170 \pm 0.00290$	OPAL	[1596]

(Table continued)

TABLE 315. *(Continued)*

τ lepton branching fraction	Experiment	References
$\mathcal{B}_{14} = \pi^-\pi^0\nu_\tau$		
0.25486 ± 0.00090	Average	
$0.25471 \pm 0.00097 \pm 0.00085$	ALEPH	[1577]
$\mathcal{B}_{16} = K^-\pi^0\nu_\tau$		
$(0.4322 \pm 0.0148) \times 10^{-2}$	Average	
$(0.4440 \pm 0.0260 \pm 0.0240) \times 10^{-2}$	ALEPH	[1597]
$(0.4160 \pm 0.0030 \pm 0.0180) \times 10^{-2}$	*BABAR*	[1579]
$(0.5100 \pm 0.1000 \pm 0.0700) \times 10^{-2}$	CLEO	[1598]
$(0.4710 \pm 0.0590 \pm 0.0230) \times 10^{-2}$	OPAL	[1603]
$\mathcal{B}_{17} = h^- \geq 2\pi^0\nu_\tau$		
0.10794 ± 0.00097	Average	
$0.09910 \pm 0.00310 \pm 0.00270$	OPAL	[1596]
$\mathcal{B}_{18} = h^-2\pi^0\nu_\tau$		
$(9.460 \pm 0.100) \times 10^{-2}$	Average	
$\mathcal{B}_{19} = h^-2\pi^0\nu_\tau\,(\mathrm{ex.}K^0)$		
$(9.309 \pm 0.100) \times 10^{-2}$	Average	
$(9.498 \pm 0.320 \pm 0.275) \times 10^{-2}$	DELPHI	[1595]
$(8.880 \pm 0.370 \pm 0.420) \times 10^{-2}$	L3	[1593]
$\frac{\mathcal{B}_{19}}{\mathcal{B}_{13}} = \frac{h^-2\pi^0\nu_\tau(\mathrm{ex.}K^0)}{h^-\pi^0\nu_\tau}$		
0.3592 ± 0.0045	Average	
$0.3420 \pm 0.0060 \pm 0.0160$	CLEO	[1604]
$\mathcal{B}_{20} = \pi^-2\pi^0\nu_\tau(\mathrm{ex.}K^0)$		
$(9.245 \pm 0.099) \times 10^{-2}$	Average	
$(9.239 \pm 0.086 \pm 0.090) \times 10^{-2}$	ALEPH	[1577]
$\mathcal{B}_{23} = K^-2\pi^0\nu_\tau(\mathrm{ex.}K^0)$		
$(0.0634 \pm 0.0219) \times 10^{-2}$	Average	
$(0.0560 \pm 0.0200 \pm 0.0150) \times 10^{-2}$	ALEPH	[1597]
$(0.0900 \pm 0.1000 \pm 0.0300) \times 10^{-2}$	CLEO	[1598]
$\mathcal{B}_{24} = h^- \geq 3\pi^0\nu_\tau$		
$(1.335 \pm 0.066) \times 10^{-2}$	Average	
$\mathcal{B}_{25} = h^- \geq 3\pi^0\nu_\tau(\mathrm{ex.}K^0)$		
$(1.250 \pm 0.066) \times 10^{-2}$	Average	
$(1.403 \pm 0.214 \pm 0.224) \times 10^{-2}$	DELPHI	[1595]
$\mathcal{B}_{26} = h^-3\pi^0\nu_\tau$		
$(1.173 \pm 0.072) \times 10^{-2}$	Average	
$(1.700 \pm 0.240 \pm 0.380) \times 10^{-2}$	L3	[1593]
$\frac{\mathcal{B}_{26}}{\mathcal{B}_{13}} = \frac{h^-3\pi^0\nu_\tau}{h^-\pi^0\nu_\tau}$		
$(4.526 \pm 0.278) \times 10^{-2}$	Average	
$(4.400 \pm 0.300 \pm 0.500) \times 10^{-2}$	CLEO	[1604]
$\mathcal{B}_{27} = \pi^-3\pi^0\nu_\tau(\mathrm{ex.}K^0)$		
$(1.040 \pm 0.071) \times 10^{-2}$	Average	
$(0.977 \pm 0.069 \pm 0.058) \times 10^{-2}$	ALEPH	[1577]
$\mathcal{B}_{28} = K^-3\pi^0\nu_\tau(\mathrm{ex.}K^0, \eta)$		
$(4.648 \pm 2.131) \times 10^{-4}$	Average	
$(3.700 \pm 2.100 \pm 1.100) \times 10^{-4}$	ALEPH	[1597]

(Table continued)

TABLE 315. *(Continued)*

τ lepton branching fraction	Experiment	References
$\mathcal{B}_{29} = h^- 4\pi^0 \nu_\tau \,(\text{ex.}K^0)$		
$(0.1587 \pm 0.0391) \times 10^{-2}$	Average	
$(0.1600 \pm 0.0500 \pm 0.0500) \times 10^{-2}$	CLEO	[1604]
$\mathcal{B}_{30} = h^- 4\pi^0 \nu_\tau \,(\text{ex.}K^0, \eta)$		
$(0.1118 \pm 0.0391) \times 10^{-2}$	Average	
$(0.1120 \pm 0.0370 \pm 0.0350) \times 10^{-2}$	ALEPH	[1577]
$\mathcal{B}_{31} = K^- \geq 0\,\pi^0 \geq 0\,K^0 \geq 0\,\gamma \nu_\tau$		
$(1.548 \pm 0.029) \times 10^{-2}$	Average	
$(1.700 \pm 0.120 \pm 0.190) \times 10^{-2}$	CLEO	[1598]
$(1.540 \pm 0.240 \pm 0.000) \times 10^{-2}$	DELPHI	[1599]
$(1.528 \pm 0.039 \pm 0.040) \times 10^{-2}$	OPAL	[1600]
$\mathcal{B}_{32} = K^- \geq 1\,(\pi^0 \text{ or } K^0 \text{ or } \gamma)\nu_\tau$		
$(0.8556 \pm 0.0282) \times 10^{-2}$	Average	
$\mathcal{B}_{33} = K^0_S(\text{particles})^- \nu_\tau$		
$(0.9370 \pm 0.0292) \times 10^{-2}$	Average	
$(0.9700 \pm 0.0580 \pm 0.0620) \times 10^{-2}$	ALEPH	[1605]
$(0.9700 \pm 0.0900 \pm 0.0600) \times 10^{-2}$	OPAL	[1606]
$\mathcal{B}_{34} = h^- \bar{K}^0 \nu_\tau$		
$(0.9861 \pm 0.0138) \times 10^{-2}$	Average	
$(0.8550 \pm 0.0360 \pm 0.0730) \times 10^{-2}$	CLEO	[1607]
$\mathcal{B}_{35} = \pi^- \bar{K}^0 \nu_\tau$		
$(0.8375 \pm 0.0139) \times 10^{-2}$	Average	
$(0.9280 \pm 0.0450 \pm 0.0340) \times 10^{-2}$	ALEPH	[1597]
$(0.8320 \pm 0.0025 \pm 0.0150) \times 10^{-2}$	Belle	[1608]
$(0.9500 \pm 0.1500 \pm 0.0600) \times 10^{-2}$	L3	[1609]
$(0.9330 \pm 0.0680 \pm 0.0490) \times 10^{-2}$	OPAL	[1610]
$\mathcal{B}_{37} = K^- K^0 \nu_\tau$		
$(0.1486 \pm 0.0034) \times 10^{-2}$	Average	
$(0.1580 \pm 0.0420 \pm 0.0170) \times 10^{-2}$	ALEPH	[1605]
$(0.1620 \pm 0.0210 \pm 0.0110) \times 10^{-2}$	ALEPH	[1597]
$(0.1478 \pm 0.0022 \pm 0.0040) \times 10^{-2}$	*BABAR*	[1611]
$(0.1480 \pm 0.0013 \pm 0.0055) \times 10^{-2}$	Belle	[1608]
$(0.1510 \pm 0.0210 \pm 0.0220) \times 10^{-2}$	CLEO	[1607]
$\mathcal{B}_{38} = K^- K^0 \geq 0\pi^0 \nu_\tau$		
$(0.2985 \pm 0.0073) \times 10^{-2}$	Average	
$(0.3300 \pm 0.0550 \pm 0.0390) \times 10^{-2}$	OPAL	[1610]
$\mathcal{B}_{39} = h^- \bar{K}^0 \pi^0 \nu_\tau$		
$(0.5310 \pm 0.0134) \times 10^{-2}$	Average	
$(0.5620 \pm 0.0500 \pm 0.0480) \times 10^{-2}$	CLEO	[1607]
$\mathcal{B}_{40} = \pi^- \bar{K}^0 \pi^0 \nu_\tau$		
$(0.3810 \pm 0.0129) \times 10^{-2}$	Average	
$(0.2940 \pm 0.0730 \pm 0.0370) \times 10^{-2}$	ALEPH	[1605]
$(0.3470 \pm 0.0530 \pm 0.0370) \times 10^{-2}$	ALEPH	[1597]
$(0.3860 \pm 0.0031 \pm 0.0135) \times 10^{-2}$	Belle	[1608]
$(0.4100 \pm 0.1200 \pm 0.0300) \times 10^{-2}$	L3	[1609]

(Table continued)

TABLE 315. *(Continued)*

τ lepton branching fraction	Experiment	References
$\mathcal{B}_{42} = K^- K^0 \pi^0 \nu_\tau$		
$(0.1499 \pm 0.0070) \times 10^{-2}$	Average	
$(0.1520 \pm 0.0760 \pm 0.0210) \times 10^{-2}$	ALEPH	[1605]
$(0.1430 \pm 0.0250 \pm 0.0150) \times 10^{-2}$	ALEPH	[1597]
$(0.1496 \pm 0.0019 \pm 0.0073) \times 10^{-2}$	Belle	[1608]
$(0.1450 \pm 0.0360 \pm 0.0200) \times 10^{-2}$	CLEO	[1607]
$\mathcal{B}_{43} = \pi^- \bar{K}^0 \geq 1\, \pi^0 \nu_\tau$		
$(0.4045 \pm 0.0260) \times 10^{-2}$	Average	
$(0.3240 \pm 0.0740 \pm 0.0660) \times 10^{-2}$	OPAL	[1610]
$\mathcal{B}_{44} = \pi^- \bar{K}^0 2\pi^0 \nu_\tau\, (\text{ex.} K^0)$		
$(2.342 \pm 2.306) \times 10^{-4}$	Average	
$(2.600 \pm 2.400 \pm 0.000) \times 10^{-4}$	ALEPH	[1612]
$\mathcal{B}_{46} = \pi^- K^0 \bar{K}^0 \nu_\tau$		
$(0.1517 \pm 0.0247) \times 10^{-2}$	Average	
$\mathcal{B}_{47} = \pi^- K_S^0 K_S^0 \nu_\tau$		
$(2.349 \pm 0.065) \times 10^{-4}$	Average	
$(2.600 \pm 1.000 \pm 0.500) \times 10^{-4}$	ALEPH	[1605]
$(2.310 \pm 0.040 \pm 0.080) \times 10^{-4}$	*BABAR*	[1613]
$(2.330 \pm 0.033 \pm 0.093) \times 10^{-4}$	Belle	[1608]
$(2.300 \pm 0.500 \pm 0.300) \times 10^{-4}$	CLEO	[1607]
$\mathcal{B}_{48} = \pi^- K_S^0 K_L^0 \nu_\tau$		
$(0.1048 \pm 0.0247) \times 10^{-2}$	Average	
$(0.1010 \pm 0.0230 \pm 0.0130) \times 10^{-2}$	ALEPH	[1605]
$\mathcal{B}_{49} = \pi^- \pi^0 K^0 \bar{K}^0 \nu_\tau$		
$(3.543 \pm 1.193) \times 10^{-4}$	Average	
$\mathcal{B}_{50} = \pi^- K_S^0 K_S^0 \pi^0 \nu_\tau$		
$(1.820 \pm 0.207) \times 10^{-5}$	Average	
$(1.600 \pm 0.200 \pm 0.220) \times 10^{-5}$	*BABAR*	[1613]
$(2.000 \pm 0.216 \pm 0.202) \times 10^{-5}$	Belle	[1608]
$\mathcal{B}_{51} = \pi^- K_S^0 K_L^0 \pi^0 \nu_\tau$		
$(3.179 \pm 1.192) \times 10^{-4}$	Average	
$(3.100 \pm 1.100 \pm 0.500) \times 10^{-4}$	ALEPH	[1605]
$\mathcal{B}_{53} = \bar{K}^0 h^- h^- h^+ \nu_\tau$		
$(2.223 \pm 2.024) \times 10^{-4}$	Average	
$(2.300 \pm 1.900 \pm 0.700) \times 10^{-4}$	ALEPH	[1605]
$\mathcal{B}_{54} = h^- h^- h^+ \geq 0\,\text{neutrals} \geq 0\, K_L^0 \nu_\tau$		
0.15193 ± 0.00063	Average	
$0.15000 \pm 0.00400 \pm 0.00300$	CELLO	[1614]
$0.14400 \pm 0.00600 \pm 0.00300$	L3	[1615]
$0.15100 \pm 0.00800 \pm 0.00600$	TPC	[1616]
$\mathcal{B}_{55} = h^- h^- h^+ \geq 0\,\text{neutrals}\, \nu_\tau\, (\text{ex.} K^0)$		
0.14545 ± 0.00058	Average	
$0.14556 \pm 0.00105 \pm 0.00076$	L3	[1617]
$0.14960 \pm 0.00090 \pm 0.00220$	OPAL	[1618]
$\mathcal{B}_{56} = h^- h^- h^+ \nu_\tau$		
$(9.790 \pm 0.055) \times 10^{-2}$	Average	

(Table continued)

TABLE 315. *(Continued)*

τ lepton branching fraction	Experiment	References
$\mathcal{B}_{57} = h^-h^-h^+\nu_\tau\,(\mathrm{ex.}K^0)$		
$(9.449 \pm 0.054) \times 10^{-2}$	Average	
$(9.510 \pm 0.070 \pm 0.200) \times 10^{-2}$	CLEO	[1619]
$(9.317 \pm 0.090 \pm 0.082) \times 10^{-2}$	DELPHI	[1595]
$\frac{\mathcal{B}_{57}}{\mathcal{B}_{55}} = \frac{h^-h^-h^+\nu_\tau(\mathrm{ex.}K^0)}{h^-h^-h^+\geq 0\,\mathrm{neutrals}\,\nu_\tau\,(\mathrm{ex.}K^0)}$		
0.6496 ± 0.0031	Average	
$0.6600 \pm 0.0040 \pm 0.0140$	OPAL	[1618]
$\mathcal{B}_{58} = h^-h^-h^+\nu_\tau\,(\mathrm{ex.}K^0, \omega)$		
$(9.419 \pm 0.054) \times 10^{-2}$	Average	
$\mathcal{B}_{59} = \pi^-\pi^+\pi^-\nu_\tau$		
$(9.300 \pm 0.052) \times 10^{-2}$	Average	
$\mathcal{B}_{60} = \pi^-\pi^+\pi^-\nu_\tau\,(\mathrm{ex.}K^0)$		
$(9.010 \pm 0.052) \times 10^{-2}$	Average	
$(8.830 \pm 0.010 \pm 0.130) \times 10^{-2}$	*BABAR*	[1620]
$(8.420 \pm 0.000^{+0.260}_{-0.250}) \times 10^{-2}$	Belle	[1621]
$(9.130 \pm 0.050 \pm 0.460) \times 10^{-2}$	CLEO3	[1622]
$\mathcal{B}_{62} = \pi^-\pi^+\pi^+\nu_\tau\,(\mathrm{ex.}K^0, \omega)$		
$(8.981 \pm 0.052) \times 10^{-2}$	Average	
$(9.041 \pm 0.060 \pm 0.076) \times 10^{-2}$	ALEPH	[1577]
$\mathcal{B}_{63} = h^-h^-h^+ \geq 1\,\mathrm{neutrals}\,\nu_\tau$		
$(5.293 \pm 0.052) \times 10^{-2}$	Average	
$\mathcal{B}_{64} = h^-h^-h^+ \geq 1\,\pi^0\nu_\tau\,(\mathrm{ex.}K^0)$		
$(5.088 \pm 0.052) \times 10^{-2}$	Average	
$\mathcal{B}_{65} = h^-h^-h^+\pi^0\nu_\tau$		
$(4.757 \pm 0.054) \times 10^{-2}$	Average	
$\mathcal{B}_{66} = h^-h^-h^+\pi^0\nu_\tau\,(\mathrm{ex.}K^0)$		
$(4.573 \pm 0.054) \times 10^{-2}$	Average	
$(4.230 \pm 0.060 \pm 0.220) \times 10^{-2}$	CLEO	[1619]
$(4.545 \pm 0.106 \pm 0.103) \times 10^{-2}$	DELPHI	[1595]
$\mathcal{B}_{67} = h^-h^-h^+\pi^0\nu_\tau\,(\mathrm{ex.}K^0, \omega)$		
$(2.791 \pm 0.071) \times 10^{-2}$	Average	
$\mathcal{B}_{68} = \pi^-\pi^+\pi^-\pi^0\nu_\tau$		
$(4.620 \pm 0.054) \times 10^{-2}$	Average	
$\mathcal{B}_{69} = \pi^-\pi^+\pi^-\pi^0\nu_\tau\,(\mathrm{ex.}K^0)$		
$(4.488 \pm 0.054) \times 10^{-2}$	Average	
$(4.598 \pm 0.057 \pm 0.064) \times 10^{-2}$	ALEPH	[1577]
$(4.190 \pm 0.100 \pm 0.210) \times 10^{-2}$	CLEO	[1623]
$\mathcal{B}_{70} = \pi^-\pi^+\pi^-\pi^0\nu_\tau\,(\mathrm{ex.}K^0, \omega)$		
$(2.743 \pm 0.071) \times 10^{-2}$	Average	
$\mathcal{B}_{74} = h^-h^-h^+ \geq 2\pi^0\nu_\tau\,(\mathrm{ex.}K^0)$		
$(0.5154 \pm 0.0312) \times 10^{-2}$	Average	
$(0.5610 \pm 0.0680 \pm 0.0950) \times 10^{-2}$	DELPHI	[1595]
$\mathcal{B}_{75} = h^-h^-h^+2\pi^0\nu_\tau$		
$(0.5041 \pm 0.0311) \times 10^{-2}$	Average	

(Table continued)

TABLE 315. *(Continued)*

τ lepton branching fraction	Experiment	References
$\mathcal{B}_{76} = h^-h^-h^+2\pi^0\nu_\tau\,(\mathrm{ex}.K^0)$		
$(0.4942 \pm 0.0311) \times 10^{-2}$	Average	
$(0.4350 \pm 0.0300 \pm 0.0350) \times 10^{-2}$	ALEPH	[1577]
$\frac{\mathcal{B}_{76}}{\mathcal{B}_{54}} = \frac{h^-h^-h^+2\pi^0\nu_\tau\,(\mathrm{ex}.K^0)}{h^-h^-h^+\geq 0\,\mathrm{neutrals} \geq 0\,K^0_L\nu_\tau}$		
$(3.252 \pm 0.203) \times 10^{-2}$	Average	
$(3.400 \pm 0.200 \pm 0.300) \times 10^{-2}$	CLEO	[1624]
$\mathcal{B}_{77} = h^-h^-h^+2\pi^0\nu_\tau\,(\mathrm{ex}.K^0, \omega, \eta)$		
$(9.790 \pm 3.562) \times 10^{-4}$	Average	
$\mathcal{B}_{78} = h^-h^-h^+3\pi^0\nu_\tau$		
$(2.124 \pm 0.299) \times 10^{-4}$	Average	
$(2.200 \pm 0.300 \pm 0.400) \times 10^{-4}$	CLEO	[1625]
$\mathcal{B}_{79} = K^-h^-h^+ \geq 0\,\mathrm{neutrals}\,\nu_\tau$		
$(0.6276 \pm 0.0140) \times 10^{-2}$	Average	
$\mathcal{B}_{80} = K^-\pi^-h^+\nu_\tau\,(\mathrm{ex}.K^0)$		
$(0.4364 \pm 0.0073) \times 10^{-2}$	Average	
$\frac{\mathcal{B}_{80}}{\mathcal{B}_{60}} = \frac{K^-\pi^-h^+\nu_\tau\,(\mathrm{ex}.K^0)}{\pi^-\pi^+\pi^-\nu_\tau\,(\mathrm{ex}.K^0)}$		
$(4.843 \pm 0.079) \times 10^{-2}$	Average	
$(5.440 \pm 0.210 \pm 0.530) \times 10^{-2}$	CLEO	[1626]
$\mathcal{B}_{81} = K^-\pi^-h^+\pi^0\nu_\tau\,(\mathrm{ex}.K^0)$		
$(8.498 \pm 1.169) \times 10^{-4}$	Average	
$\frac{\mathcal{B}_{81}}{\mathcal{B}_{69}} = \frac{K^-\pi^-h^+\pi^0\nu_\tau\,(\mathrm{ex}.K^0)}{\pi^-\pi^+\pi^-\pi^0\nu_\tau\,(\mathrm{ex}.K^0)}$		
$(1.893 \pm 0.264) \times 10^{-2}$	Average	
$(2.610 \pm 0.450 \pm 0.420) \times 10^{-2}$	CLEO	[1626]
$\mathcal{B}_{82} = K^-\pi^-\pi^+ \geq 0\,\mathrm{neutrals}\,\nu_\tau$		
$(0.4759 \pm 0.0136) \times 10^{-2}$	Average	
$(0.5800^{+0.1500}_{-0.1300} \pm 0.1200) \times 10^{-2}$	TPC	[1627]
$\mathcal{B}_{83} = K^-\pi^-\pi^+ \geq 0\,\pi^0\nu_\tau\,(\mathrm{ex}.K^0)$		
$(0.3719 \pm 0.0134) \times 10^{-2}$	Average	
$\mathcal{B}_{84} = K^-\pi^-\pi^+\nu_\tau$		
$(0.3444 \pm 0.0069) \times 10^{-2}$	Average	
$\mathcal{B}_{85} = K^-\pi^+\pi^-\nu_\tau\,(\mathrm{ex}.K^0)$		
$(0.2930 \pm 0.0068) \times 10^{-2}$		
$(0.2140 \pm 0.0370 \pm 0.0290) \times 10^{-2}$	ALEPH	[1628]
$(0.2730 \pm 0.0020 \pm 0.0090) \times 10^{-2}$	*BABAR*	[1620]
$(0.3300 \pm 0.0010^{+0.0160}_{-0.0170}) \times 10^{-2}$	Belle	[1621]
$(0.3840 \pm 0.0140 \pm 0.0380) \times 10^{-2}$	CLEO3	[1622]
$(0.4150 \pm 0.0530 \pm 0.0400) \times 10^{-2}$	OPAL	[1603]
$\frac{\mathcal{B}_{85}}{\mathcal{B}_{60}} = \frac{K^-\pi^+\pi^-\nu_\tau(\mathrm{ex}.K^0)}{\pi^-\pi^+\pi^-\nu_\tau\,(\mathrm{ex}.K^0)}$		
$(3.252 \pm 0.074) \times 10^{-2}$	Average	
$\mathcal{B}_{87} = k^-\pi^-\pi^+\pi^0\nu_\tau$		
$(0.1308 \pm 0.0119) \times 10^{-2}$	Average	
$\mathcal{B}_{88} = K^-\pi^-\pi^+\pi^0\nu_\tau\,(\mathrm{ex}.K^0)$	Average	
$(6.100 \pm 3.900 \pm 1.800) \times 10^{-4}$	ALEPH	[1628]
$(7.400 \pm 0.800 \pm 1.100) \times 10^{-4}$	CLEO3	[1629]

(Table continued)

TABLE 315. *(Continued)*

τ lepton branching fraction	Experiment	References
$\mathcal{B}_{89} = K^-\pi^-\pi^+\pi^0\nu_\tau\,(\text{ex.}K^0,\eta)$		
$(7.536 \pm 1.161) \times 10^{-4}$	Average	
$(7.536 \pm 1.161) \times 10^{-4}$	Average	
$\mathcal{B}_{92} = \pi^-K^-K^+ \geq 0\,\text{neutrals}\,\nu_\tau$		
$(0.1495 \pm 0.0033) \times 10^{-2}$	Average	
$(0.1590 \pm 0.0530 \pm 0.0200) \times 10^{-2}$	OPAL	[1630]
$(0.1500^{+0.0900}_{-0.0700} \pm 0.0300) \times 10^{-2}$	TPC	[1627]
$\mathcal{B}_{93} = \pi^-K^-K^+\nu_\tau$		
$(0.1434 \pm 0.0027) \times 10^{-2}$	Average	
$(0.1630 \pm 0.0210 \pm 0.0170) \times 10^{-2}$	ALEPH	[1628]
$(0.1346 \pm 0.0010 \pm 0.0036) \times 10^{-2}$	*BABAR*	[1620]
$(0.1550 \pm 0.0010^{+0.0060}_{-0.0050}) \times 10^{-2}$	Belle	[1621]
$(0.1550 \pm 0.0060 \pm 0.0090) \times 10^{-2}$	CLEO3	[1622]
$\frac{\mathcal{B}_{93}}{\mathcal{B}_{60}} = \frac{\pi^-K^-K^+\nu_\tau}{\pi^-\pi^+\pi^-\nu_\tau\,(\text{ex.}K^0)}$		
$(1.592 \pm 0.030) \times 10^{-2}$	Average	
$(1.600 \pm 0.150 \pm 0.300) \times 10^{-2}$	CLEO	[1626]
$\mathcal{B}_{94} = \pi^-K^-K^+\pi^0\nu_\tau$		
$(0.607 \pm 0.183) \times 10^{-4}$	Average	
$(7.500 \pm 2.900 \pm 1.500) \times 10^{-4}$	ALEPH	[1628]
$(0.550 \pm 0.140 \pm 0.120) \times 10^{-4}$	CLEO3	[1629]
$\frac{\mathcal{B}_{94}}{\mathcal{B}_{69}} = \frac{\pi^-K^-K^+\pi^0\nu_\tau}{\pi^-\pi^+\pi^-\pi^0\nu_\tau(\text{ex.}K^0)}$		
$(0.1352 \pm 0.0408) \times 10^{-2}$	Average	
$(0.7900 \pm 0.4400 \pm 0.1600) \times 10^{-2}$	CLEO	[1626]
$\mathcal{B}_{96} = K^-K^-K^+\nu_\tau$		
$(2.169 \pm 0.800) \times 10^{-5}$		
$(1.578 \pm 0.130 \pm 0.123) \times 10^{-5}$	*BABAR*	[1620]
$(3.290 \pm 0.170^{+0.190}_{-0.200}) \times 10^{-5}$	Belle	[1621]
$\mathcal{B}_{102} = 3h^-2h^+ \geq 0\,\text{neutrals}\,\nu_\tau\,(\text{ex.}K^0)$		
$(0.0993 \pm 0.0037) \times 10^{-2}$	Average	
$(0.0970 \pm 0.0050 \pm 0.0110) \times 10^{-2}$	CLEO	[1631]
$(0.1020 \pm 0.0290 \pm 0.0000) \times 10^{-2}$	HRS	[1632]
$(0.1700 \pm 0.0220 \pm 0.0260) \times 10^{-2}$	L3	[1617]
$\mathcal{B}_{103} = 3h^-2h^+\nu_\tau\,(\text{ex.}K^0)$		
$(8.281 \pm 0.314) \times 10^{-4}$	Average	
$(7.200 \pm 0.900 \pm 1.200) \times 10^{-4}$	ALEPH	[1577]
$(6.400 \pm 2.300 \pm 1.000) \times 10^{-4}$	ARGUS	[1633]
$(7.700 \pm 0.500 \pm 0.900) \times 10^{-4}$	CLEO	[1631]
$(9.700 \pm 1.500 \pm 0.500) \times 10^{-4}$	DELPHI	[1595]
$(5.100 \pm 2.000 \pm 0.000) \times 10^{-4}$	HRS	[1632]
$(9.100 \pm 1.400 \pm 0.600) \times 10^{-4}$	OPAL	[1634]
$\mathcal{B}_{104} = 3h^-2h^+\pi^0\nu_\tau\,(\text{ex.}K^0)$		
$(1.645 \pm 0.114) \times 10^{-4}$	Average	
$(2.100 \pm 0.700 \pm 0.900) \cdot 10^{-4}$	ALEPH	[1577]
$(1.700 \pm 0.200 \pm 0.200) \times 10^{-4}$	CLEO	[1625]
$(1.600 \pm 1.200 \pm 0.600) \times 10^{-4}$	DELPHI	[1595]
$(2.700 \pm 1.800 \pm 0.900) \times 10^{-4}$	OPAL	[1634]
$\mathcal{B}_{106} = (5\pi)^-\nu_\tau$		
$(0.7793 \pm 0.0534) \times 10^{-2}$	Average	

(Table continued)

TABLE 315. *(Continued)*

τ lepton branching fraction	Experiment	References
$\mathcal{B}_{110} = X_s^- \nu_\tau$		
$(2.908 \pm 0.048) \times 10^{-2}$	Average	
$\mathcal{B}_{126} = \pi^- \pi^0 \eta \nu_\tau$		
$(0.1386 \pm 0.0072) \times 10^{-2}$	Average	
$(0.1800 \pm 0.0400 \pm 0.0200) \times 10^{-2}$	ALEPH	[1635]
$(0.1350 \pm 0.0030 \pm 0.0070) \times 10^{-2}$	Belle	[1636]
$(0.1700 \pm 0.0200 \pm 0.0200) \times 10^{-2}$	CLEO	[1637]
$\mathcal{B}_{128} = K^- \eta \nu_\tau$		
$(1.547 \pm 0.080) \times 10^{-4}$	Average	
$(2.900^{+1.300}_{-1.200} \pm 0.700) \times 10^{-4}$	ALEPH	[1635]
$(1.420 \pm 0.110 \pm 0.070) \times 10^{-4}$	*BABAR*	[1638]
$(1.580 \pm 0.050 \pm 0.090) \times 10^{-4}$	Belle	[1636]
$(2.600 \pm 0.500 \pm 0.500) \times 10^{-4}$	CLEO	[1639]
$\mathcal{B}_{130} = K^- \pi^0 \eta \nu_\tau$		
$(0.483 \pm 0.116) \times 10^{-4}$	Average	
$(0.460 \pm 0.110 \pm 0.040) \times 10^{-4}$	Belle	[1636]
$(1.770 \pm 0.560 \pm 0.710) \times 10^{-4}$	CLEO	[1640]
$\mathcal{B}_{132} = \pi^- \bar{K}^0 \eta \nu_\tau$		
$(0.937 \pm 0.149) \times 10^{-4}$	Average	
$(0.880 \pm 0.140 \pm 0.060) \times 10^{-4}$	Belle	[1636]
$(2.200 \pm 0.700 \pm 0.220) \times 10^{-4}$	CLEO	[1640]
$\mathcal{B}_{136} = \pi^- \pi^+ \pi^- \eta \nu_\tau \, (\text{ex.} K^0)$		
$(2.202 \pm 0.129) \times 10^{-4}$	Average	
$\mathcal{B}_{149} = h^- \omega \geq 0 \, \text{neutrals} \, \nu_\tau$		
$(2.395 \pm 0.075) \times 10^{-2}$	Average	
$\mathcal{B}_{150} = h^- \omega \nu_\tau$		
$(1.988 \pm 0.064) \times 10^{-2}$	Average	
$(1.910 \pm 0.070 \pm 0.060) \times 10^{-2}$	ALEPH	[1635]
$(1.600 \pm 0.270 \pm 0.410) \times 10^{-2}$	CLEO	[1641]
$\frac{\mathcal{B}_{150}}{\mathcal{B}_{66}} = \frac{h^- \omega \nu_\tau}{h^- h^- h^+ \pi^0 \nu_\tau (\text{ex.} K^0)}$		
0.4348 ± 0.0140	Average	
$0.4310 \pm 0.0330 \pm 0.0000$	ALEPH	[1642]
$0.4640 \pm 0.0160 \pm 0.0170$	CLEO	[1619]
$\mathcal{B}_{151} = K^- \omega \nu_\tau$		
$(4.101 \pm 0.922) \times 10^{-4}$	Average	
$(4.100 \pm 0.600 \pm 0.700) \times 10^{-4}$	CLEO3	[1629]
$\mathcal{B}_{152} = h^- \pi^0 \omega \nu_\tau$		
$(0.4069 \pm 0.0419) \times 10^{-2}$	Average	
$(0.4300 \pm 0.0600 \pm 0.0500) \times 10^{-2}$	ALEPH	[1635]
$\frac{\mathcal{B}_{152}}{\mathcal{B}_{54}} = \frac{h^- \omega \pi^0 \nu_\tau}{h^- h^- h^+ \geq 0 \, \text{neutrals} \geq 0 \, K_L^0 \nu_\tau}$		
$(2.678 \pm 0.275) \times 10^{-2}$	Average	
$\frac{\mathcal{B}_{152}}{\mathcal{B}_{76}} = \frac{h^- \omega \pi^0 \nu_\tau}{h^- h^- h^+ 2\pi^0 \nu_\tau (\text{ex.} K^0)}$		
0.8235 ± 0.0757	Average	
$0.8100 \pm 0.0600 \pm 0.0600$	CLEO	[1624]
$\mathcal{B}_{167} = K^- \phi \nu_\tau$		
$(4.408 \pm 1.626) \times 10^{-5}$	Average	

(Table continued)

TABLE 315. *(Continued)*

τ lepton branching fraction	Experiment	References
$\mathcal{B}_{168} = K^-\phi(K^+K^-)\nu_\tau$		
$(2.169 \pm 0.800) \times 10^{-5}$	Average	
$\mathcal{B}_{169} = K^-\phi(K^0_S K^0_L)\nu_\tau$		
$(1.499 \pm 0.553) \times 10^{-5}$	Average	
$\mathcal{B}_{800} = \pi^-\omega\nu_\tau$		
$(1.947 \pm 0.065) \times 10^{-2}$	Average	
$\mathcal{B}_{802} = K^-\pi^-\pi^+\nu_\tau\,(\mathrm{ex.}K^0, \omega)$		
$(0.2924 \pm 0.0068) \times 10^{-2}$	Average	
$\mathcal{B}_{803} = K^-\pi^-\pi^+\pi^0\nu_\tau\,(\mathrm{ex.}K^0, \omega, \eta)$		
$(3.874 \pm 1.423) \times 10^{-4}$	Average	
$\mathcal{B}_{804} = \pi^- K^0_L K^0_L \nu_\tau$		
$(2.349 \pm 0.065) \times 10^{-4}$	Average	
$\mathcal{B}_{805} = a_1^-(\pi^-\gamma)\nu_\tau$		
$(4.000 \pm 2.000) \times 10^{-4}$	Average	
$(4.000 \pm 2.000 \pm 0.000) \times 10^{-4}$	ALEPH	[1577]
$\mathcal{B}_{806} = \pi^- K^0_L K^0_L \pi^0 \nu_\tau$		
$(1.820 \pm 0.207) \times 10^{-5}$	Average	
$\mathcal{B}_{806} = \pi^- K^0_L K^0_L \pi^0 \nu_\tau$		
$(1.820 \pm 0.207) \times 10^{-5}$	Average	
$\mathcal{B}_{810} = 2\pi^-\pi^+ 3\pi^0 \nu_\tau\,(\mathrm{ex.}K^0)$		
$(1.940 \pm 0.298) \times 10^{-4}$	Average	
$\mathcal{B}_{811} = \pi^- 2\pi^0 \omega \nu_\tau$		
$(7.164 \pm 1.586) \times 10^{-5}$	Average	
$(7.300 \pm 1.200 \pm 1.200) \times 10^{-5}$	*BABAR*	[1643]
$\mathcal{B}_{812} = 2\pi^-\pi^+ 3\pi^0 \nu_\tau\,(\mathrm{ex.}K^0, \eta, \omega, f_1)$		
$(1.353 \pm 2.683) \times 10^{-5}$	Average	
$(1.000 \pm 0.800 \pm 3.000) \times 10^{-5}$	*BABAR*	[1643]
$\mathcal{B}_{820} = 3\pi^- 2\pi^+ \nu_\tau\,(\mathrm{ex.}K^0, \omega)$		
$(8.262 \pm 0.313) \times 10^{-4}$	Average	
$\mathcal{B}_{821} = 3\pi^- 2\pi^+ \nu_\tau\,(\mathrm{ex.}K^0, \omega, f_1)$		
$(7.738 \pm 0.295) \times 10^{-4}$	Average	
$(7.680 \pm 0.040 \pm 0.400) \times 10^{-4}$	*BABAR*	[1643]
$\mathcal{B}_{822} = K^- 2\pi^- 2\pi^+ \nu_\tau\,(\mathrm{ex.}K^0)$		
$(0.593 \pm 1.208) \times 10^{-6}$	Average	
$(0.600 \pm 0.500 \pm 1.100) \times 10^{-6}$	*BABAR*	[1643]
$\mathcal{B}_{830} = 3\pi^- 2\pi^+ \pi^0 \nu_\tau\,(\mathrm{ex.}K^0)$		
$(1.633 \pm 0.113) \times 10^{-4}$	Average	
$\mathcal{B}_{831} = 2\pi^-\pi^+\omega\nu_\tau\,(\mathrm{ex.}K^0)$		
$(8.417 \pm 0.624) \times 10^{-5}$	Average	
$(8.400 \pm 0.400 \pm 0.600) \times 10^{-5}$	*BABAR*	[1643]
$\mathcal{B}_{832} = 3\pi^- 2\pi^+ \pi^0 \nu_\tau\,(\mathrm{ex.}K^0, \eta, \omega, f_1)$		
$(3.772 \pm 0.874) \times 10^{-5}$	Average	
$(3.600 \pm 0.300 \pm 0.900) \times 10^{-5}$	*BABAR*	[1643]

(Table continued)

TABLE 315. *(Continued)*

τ lepton branching fraction	Experiment	References
$\mathcal{B}_{833} = K^-2\pi^-2\pi^+\pi^0\nu_\tau\,(\mathrm{ex.}K^0)$		
$(1.107 \pm 0.566) \times 10^{-6}$	Average	
$(1.100 \pm 0.400 \pm 0.400) \times 10^{-6}$	*BABAR*	[1643]
$\mathcal{B}_{910} = 2\pi^-\pi^+\eta(3\pi^0)\nu_\tau\,(\mathrm{ex.}K^0)$		
$(7.195 \pm 0.422) \times 10^{-5}$	Average	
$(8.270 \pm 0.880 \pm 0.810) \times 10^{-5}$	*BABAR*	[1643]
$\mathcal{B}_{911} = \pi^-2\pi^0\eta(\pi^+\pi^-\pi^0)\nu_\tau(\mathrm{ex.}K^0)$		
$(4.457 \pm 0.867) \times 10^{-5}$	Average	
$(4.570 \pm 0.770 \pm 0.500) \times 10^{-5}$	*BABAR*	[1643]
$\mathcal{B}_{920} = \pi^- f_1(2\pi^-2\pi^+)\nu_\tau$		
$(5.237 \pm 0.444) \times 10^{-5}$	Average	
$(5.200 \pm 0.310 \pm 0.370) \times 10^{-5}$	*BABAR*	[1643]
$\mathcal{B}_{930} = 2\pi^-\pi^+\eta(\pi^+\pi^-\pi^0)\nu_\tau\,(\mathrm{ex.}K^0)$		
$(5.046 \pm 0.296) \times 10^{-5}$	Average	
$(5.390 \pm 0.270 \pm 0.410) \times 10^{-5}$	*BABAR*	[1643]
$\mathcal{B}_{944} = 2\pi^-\pi^+\eta(\gamma\gamma)\nu_\tau\,(\mathrm{ex.}K^0)$		
$(8.676 \pm 0.509) \times 10^{-5}$	Average	
$(8.260 \pm 0.350 \pm 0.510) \times 10^{-5}$	*BABAR*	[1643]
$\mathcal{B}_{945} = \pi^-2\pi^0\eta\nu_\tau\,(\mathrm{ex.}K^0)$		
$(1.945 \pm 0.378) \times 10^{-4}$	Average	
$\mathcal{B}_{998} = 1 - \mathcal{B}_{\mathrm{All}}$		
$(0.0684 \pm 0.1068) \times 10^{-2}$	Average	

decays to final states with strangeness 1. Also reported is the unitarity residual $\mathcal{B}_{998} = 1 - \mathcal{B}_{\mathrm{All}} = (0.0684 \pm 0.1068) \times 10^{-2}$, where $1 - \mathcal{B}_{\mathrm{All}}$ is the sum of the τ branching fractions into all measured final states. We find that $\mathcal{B}_{998}$ is consistent with 0 to within the experimental uncertainty. A unitarity constraint forcing $\mathcal{B}_{998}$ to be 0 is not applied.

In performing the fit, a scale factor of 5.44 was applied to the published uncertainties of the two severely inconsistent measurements of $\mathcal{B}_{96} = \tau \to KKK\nu$ by *BABAR* and Belle. The scale-factor value was chosen using the PDG procedure, i.e., it is such that $\chi^2/\mathrm{d.o.f.} = 1$ when fitting just the two $\mathcal{B}_{96}$ measurements.

2. Changes with respect to the previous report

In the previous HFLAV reports [1,221,441,1576], information from the ALEPH Collaboration [1577] was used to compute inclusive τ branching fractions for final states with one or more hadron, where each hadron can be either a pion or a kaon. In the current report, we use Ref. [1577] for the branching fractions for exclusive final states containing one or more charged pions. The past choice granted some minor advantages, which are now dropped in the interest of simplicity. As a consequence, the τ branching fraction global fit reported here matches more closely the fit that we supply to the PDG, reported in Ref. [9].

A set of preliminary *BABAR* results presented in 2018 [1578], used in the τ branching fraction fit in the previous HFLAV report [1], are not used here since they have not yet been published. Therefore, we now use the older *BABAR* measurement of $\mathcal{B}_{16} = \mathcal{B}(\tau^- \to K^-\pi^0\nu_\tau)$ in Ref. [1579]. This revision of input measurements causes a significant shift of the value of $\mathcal{B}(\tau^- \to K^{-3}\pi^0\nu_\tau(\mathrm{ex.}K^0, \eta))$, which is however consistent with the large uncertainty on the sole direct measurement of this mode by ALEPH.

Since this edition, we use new improved calculations of the radiative corrections for the theory predictions of the τ decays to pseudoscalar mesons [1580]. The estimated uncertainties are increased but more reliable in comparison to the previous estimations [1581–1584]. There is a minor increase of the uncertainties on the lepton universality tests based on hadronic τ decays (Sec. XII. B) and on $|V_{us}|$ (Sec. XII. D).

The parameters used to update the measurements' systematic biases and the parameters appearing in the constraint equations in Sec. XII. A. 6 have been updated to the PDG 2020 update [9].

3. Differences between the HFLAV 2021 fit and the PDG 2021 fit

Our branching-fraction fit is different from that of the PDG [9] in several ways.

The PDG fit enforces the unitarity constraint $\mathcal{B}_{998} = 0$, while the HFLAV 2021 fit does not.

As in our previous report [1], we use the ALEPH [9] estimate for $\mathcal{B}_{805} = \mathcal{B}(\tau^- \to a_1^-(\pi^-\gamma)\nu_\tau)$, which is not a direct measurement. By contrast, the PDG fit defines $\mathcal{B}_{805} = \mathcal{B}(a_1 \to \pi\gamma) \times \mathcal{B}(\tau \to 3\pi\nu)$, using the PDG average of $\mathcal{B}(a_1 \to \pi\gamma)$ as a parameter in the fit. As a consequence, the PDG fit procedure does not take into account the large uncertainty on $\mathcal{B}(a_1 \to \pi\gamma)$. This results in an underestimated uncertainty on $\mathcal{B}_{805}$, which is then properly adjusted with respect to the fit result in the PDG listings.

4. Branching fraction fit results and experimental inputs

Table 315 reports the experimental inputs to the τ branching-fraction fit and the fit results.

5. Correlation coefficients between basis branching fractions uncertainties

The following tables 316–325 report the correlation coefficients between basis quantities that were obtained from the τ branching fractions fit, in percent.

TABLE 316. Basis quantities correlation coefficients in percent, subtable 1.

$\mathcal{B}_5$	23													
$\mathcal{B}_9$	8	5												
$\mathcal{B}_{10}$	5	7	7											
$\mathcal{B}_{14}$	−14	−15	−13	−3										
$\mathcal{B}_{16}$	1	1	2	−1	−8									
$\mathcal{B}_{20}$	−5	−5	−8	−1	−41	1								
$\mathcal{B}_{23}$	2	2	0	−2	0	−13	−7							
$\mathcal{B}_{27}$	−5	−4	−8	−1	1	1	−36	1						
$\mathcal{B}_{28}$	2	2	1	−1	1	−13	−1	−22	−10					
$\mathcal{B}_{30}$	−4	−3	−10	−1	−8	0	6	−2	−44	2				
$\mathcal{B}_{35}$	0	0	0	0	0	0	0	0	0	0	0			
$\mathcal{B}_{37}$	0	−1	1	0	0	0	0	−2	0	−2	0	−15		
$\mathcal{B}_{40}$	0	0	0	0	0	1	0	1	−1	1	0	−12	2	
	$\mathcal{B}_3$	$\mathcal{B}_5$	$\mathcal{B}_9$	$\mathcal{B}_{10}$	$\mathcal{B}_{14}$	$\mathcal{B}_{16}$	$\mathcal{B}_{20}$	$\mathcal{B}_{23}$	$\mathcal{B}_{27}$	$\mathcal{B}_{28}$	$\mathcal{B}_{30}$	$\mathcal{B}_{35}$	$\mathcal{B}_{37}$	$\mathcal{B}_{40}$

TABLE 317. Basis quantities correlation coefficients in percent, subtable 2.

$\mathcal{B}_{42}$	0	0	0	0	0	−3	1	−5	0	−5	0	−1	−14	−20
$\mathcal{B}_{44}$	0	0	0	0	0	0	0	0	0	0	0	−1	0	−4
$\mathcal{B}_{47}$	0	−1	2	0	0	2	0	0	0	0	0	−1	3	−4
$\mathcal{B}_{48}$	0	0	0	0	0	0	0	0	0	0	0	−3	0	−2
$\mathcal{B}_{50}$	0	0	0	0	0	0	0	0	0	0	0	1	5	0
$\mathcal{B}_{51}$	0	0	0	0	0	0	0	0	0	0	0	−1	0	−1
$\mathcal{B}_{53}$	0	0	0	0	0	0	0	0	0	0	0	0	0	0
$\mathcal{B}_{62}$	−2	−4	8	0	−3	4	−7	0	−6	0	−5	−1	3	0
$\mathcal{B}_{70}$	−6	−6	−7	−1	−10	0	−1	0	−1	0	3	0	−1	0
$\mathcal{B}_{77}$	−1	0	−3	0	−2	0	0	0	2	0	2	0	0	0
$\mathcal{B}_{93}$	0	−1	3	0	−1	2	−1	0	−1	0	−1	0	2	0
$\mathcal{B}_{94}$	0	0	0	0	0	0	0	0	0	0	0	0	0	0
$\mathcal{B}_{126}$	0	0	0	0	0	0	−1	0	0	0	−2	0	0	0
$\mathcal{B}_{128}$	0	0	1	0	0	1	0	−1	0	−1	0	0	1	0
	$\mathcal{B}_3$	$\mathcal{B}_5$	$\mathcal{B}_9$	$\mathcal{B}_{10}$	$\mathcal{B}_{14}$	$\mathcal{B}_{16}$	$\mathcal{B}_{20}$	$\mathcal{B}_{23}$	$\mathcal{B}_{27}$	$\mathcal{B}_{28}$	$\mathcal{B}_{30}$	$\mathcal{B}_{35}$	$\mathcal{B}_{37}$	$\mathcal{B}_{40}$

TABLE 318. Basis quantities correlation coefficients in percent, subtable 3.

$\mathcal{B}_{130}$	0	0	0	0	0	0	0	0	0	0	0	0	0	0
$\mathcal{B}_{132}$	0	0	0	0	0	0	0	0	0	0	0	0	0	0
$\mathcal{B}_{136}$	0	0	1	0	0	1	0	0	0	0	−1	0	1	0
$\mathcal{B}_{151}$	0	0	0	0	0	0	0	0	0	0	0	0	0	0
$\mathcal{B}_{152}$	−1	−1	−3	0	−2	0	−1	0	2	0	2	0	0	0
$\mathcal{B}_{167}$	0	0	0	0	0	0	0	0	0	0	0	0	0	0

(Table continued)

TABLE 318. *(Continued)*

$\mathcal{B}_{800}$	−1	−1	−2	0	−3	0	0	0	0	0	1	0	0	0
$\mathcal{B}_{802}$	1	0	1	0	0	0	−2	0	−1	0	−1	0	0	0
$\mathcal{B}_{803}$	2	2	1	0	2	0	0	0	0	0	−1	0	0	0
$\mathcal{B}_{805}$	0	0	0	0	0	0	0	0	0	0	0	0	0	0
$\mathcal{B}_{811}$	0	0	0	0	0	0	0	0	0	0	0	0	0	0
$\mathcal{B}_{812}$	0	1	0	0	0	0	0	0	0	0	0	0	0	0
$\mathcal{B}_{821}$	0	0	2	0	0	1	−1	0	−1	0	−1	0	1	0
$\mathcal{B}_{822}$	0	0	0	0	0	0	0	0	0	0	0	0	0	0
	$\mathcal{B}_3$	$\mathcal{B}_5$	$\mathcal{B}_9$	$\mathcal{B}_{10}$	$\mathcal{B}_{14}$	$\mathcal{B}_{16}$	$\mathcal{B}_{20}$	$\mathcal{B}_{23}$	$\mathcal{B}_{27}$	$\mathcal{B}_{28}$	$\mathcal{B}_{30}$	$\mathcal{B}_{35}$	$\mathcal{B}_{37}$	$\mathcal{B}_{40}$

TABLE 319. Basis quantities correlation coefficients in percent, subtable 4.

$\mathcal{B}_{831}$	0	0	1	0	0	1	0	0	0	0	−1	0	1	0
$\mathcal{B}_{832}$	0	0	0	0	0	0	0	0	0	0	0	0	0	0
$\mathcal{B}_{833}$	0	0	0	0	0	0	0	0	0	0	0	0	0	0
$\mathcal{B}_{920}$	0	0	1	0	0	1	0	0	0	0	−1	0	1	0
$\mathcal{B}_{945}$	0	0	0	0	0	0	0	0	0	0	0	0	0	0
	$\mathcal{B}_3$	$\mathcal{B}_5$	$\mathcal{B}_9$	$\mathcal{B}_{10}$	$\mathcal{B}_{14}$	$\mathcal{B}_{16}$	$\mathcal{B}_{20}$	$\mathcal{B}_{23}$	$\mathcal{B}_{27}$	$\mathcal{B}_{28}$	$\mathcal{B}_{30}$	$\mathcal{B}_{35}$	$\mathcal{B}_{37}$	$\mathcal{B}_{40}$

TABLE 320. Basis quantities correlation coefficients in percent, subtable 5.

$\mathcal{B}_{44}$	0													
$\mathcal{B}_{47}$	1	0												
$\mathcal{B}_{48}$	−1	−6	0											
$\mathcal{B}_{50}$	6	0	−7	0										
$\mathcal{B}_{51}$	0	−3	0	−6	0									
$\mathcal{B}_{53}$	0	0	0	0	0	0								
$\mathcal{B}_{62}$	−1	0	5	0	1	0	0							
$\mathcal{B}_{70}$	0	0	−1	0	0	0	0	−20						
$\mathcal{B}_{77}$	0	0	0	0	0	0	0	−1	−7					
$\mathcal{B}_{93}$	0	0	2	0	0	0	0	16	−4	0				
$\mathcal{B}_{94}$	0	0	0	0	0	0	0	0	−1	0	0			
$\mathcal{B}_{126}$	0	0	0	0	0	0	0	1	0	−5	0	0		
$\mathcal{B}_{128}$	0	0	1	0	0	0	0	2	0	0	1	0	4	
	$\mathcal{B}_{42}$	$\mathcal{B}_{44}$	$\mathcal{B}_{47}$	$\mathcal{B}_{48}$	$\mathcal{B}_{50}$	$\mathcal{B}_{51}$	$\mathcal{B}_{53}$	$\mathcal{B}_{62}$	$\mathcal{B}_{70}$	$\mathcal{B}_{77}$	$\mathcal{B}_{93}$	$\mathcal{B}_{94}$	$\mathcal{B}_{126}$	$\mathcal{B}_{128}$

TABLE 321. Basis quantities correlation coefficients in percent, subtable 6.

$\mathcal{B}_{130}$	0	0	0	0	0	0	0	0	0	−1	0	0	1	1
$\mathcal{B}_{132}$	0	0	0	0	0	0	0	0	0	0	0	0	2	1
$\mathcal{B}_{136}$	0	0	1	0	0	0	0	2	−1	0	1	0	0	0
$\mathcal{B}_{151}$	0	0	0	0	0	0	0	0	12	0	0	0	0	0
$\mathcal{B}_{152}$	0	0	0	0	0	0	0	−1	−11	−64	0	0	0	0
$\mathcal{B}_{167}$	0	0	0	0	0	0	0	−1	0	0	1	0	0	0
$\mathcal{B}_{800}$	0	0	0	0	0	0	0	−8	−67	−3	−1	0	0	0
$\mathcal{B}_{802}$	0	0	0	0	0	0	0	20	−7	0	1	0	0	0
$\mathcal{B}_{803}$	0	0	0	0	0	0	0	−3	−14	−1	−1	−3	0	−1
$\mathcal{B}_{805}$	0	0	0	0	0	0	0	0	0	0	0	0	0	0
$\mathcal{B}_{811}$	0	0	0	0	0	0	0	0	−1	0	0	0	0	0
$\mathcal{B}_{812}$	0	0	0	0	−1	0	0	−1	−1	0	0	0	0	0
$\mathcal{B}_{821}$	0	0	2	0	0	0	0	3	−1	0	1	0	0	1
$\mathcal{B}_{822}$	0	0	0	0	0	0	0	0	0	0	0	0	0	0
	$\mathcal{B}_{42}$	$\mathcal{B}_{44}$	$\mathcal{B}_{47}$	$\mathcal{B}_{48}$	$\mathcal{B}_{50}$	$\mathcal{B}_{51}$	$\mathcal{B}_{53}$	$\mathcal{B}_{62}$	$\mathcal{B}_{70}$	$\mathcal{B}_{77}$	$\mathcal{B}_{93}$	$\mathcal{B}_{94}$	$\mathcal{B}_{126}$	$\mathcal{B}_{128}$

TABLE 322. Basis quantities correlation coefficients in percent, subtable 7.

$\mathcal{B}_{831}$	0	0	1	0	0	0	0	1	−1	0	1	0	0	0
$\mathcal{B}_{832}$	0	0	0	0	0	0	0	0	0	0	0	0	0	0
$\mathcal{B}_{833}$	0	0	0	0	0	0	0	0	0	0	0	0	0	0
$\mathcal{B}_{920}$	0	0	1	0	0	0	0	1	−1	0	1	0	0	0
$\mathcal{B}_{945}$	0	0	0	0	0	0	0	0	−1	0	0	0	0	0
	$\mathcal{B}_{42}$	$\mathcal{B}_{44}$	$\mathcal{B}_{47}$	$\mathcal{B}_{48}$	$\mathcal{B}_{50}$	$\mathcal{B}_{51}$	$\mathcal{B}_{53}$	$\mathcal{B}_{62}$	$\mathcal{B}_{70}$	$\mathcal{B}_{77}$	$\mathcal{B}_{93}$	$\mathcal{B}_{94}$	$\mathcal{B}_{126}$	$\mathcal{B}_{128}$

TABLE 323. Basis quantities correlation coefficients in percent, subtable 8.

$\mathcal{B}_{132}$	0													
$\mathcal{B}_{136}$	0	0												
$\mathcal{B}_{151}$	0	0	0											
$\mathcal{B}_{152}$	0	0	0	0										
$\mathcal{B}_{167}$	0	0	0	0	0									
$\mathcal{B}_{800}$	0	0	0	−14	−3	0								
$\mathcal{B}_{802}$	0	0	0	−2	0	1	−2							
$\mathcal{B}_{803}$	0	0	0	−58	−1	0	10	0						
$\mathcal{B}_{805}$	0	0	0	0	0	0	0	0	0					
$\mathcal{B}_{811}$	0	−1	20	0	0	0	0	0	0	0				
$\mathcal{B}_{812}$	0	−2	−8	0	0	0	0	0	0	0	−16			
$\mathcal{B}_{821}$	0	0	46	0	0	0	0	0	0	0	8	−4		
$\mathcal{B}_{822}$	0	0	−1	0	0	0	0	0	0	0	0	0	−1	
	$\mathcal{B}_{130}$	$\mathcal{B}_{132}$	$\mathcal{B}_{136}$	$\mathcal{B}_{151}$	$\mathcal{B}_{152}$	$\mathcal{B}_{167}$	$\mathcal{B}_{800}$	$\mathcal{B}_{802}$	$\mathcal{B}_{803}$	$\mathcal{B}_{805}$	$\mathcal{B}_{811}$	$\mathcal{B}_{812}$	$\mathcal{B}_{821}$	$\mathcal{B}_{822}$

TABLE 324. Basis quantities correlation coefficients in percent, subtable 9.

$\mathcal{B}_{831}$	0	0	39	0	0	0	0	0	0	0	14	−4	39	−1
$\mathcal{B}_{832}$	0	0	3	0	0	0	0	0	0	0	2	0	3	0
$\mathcal{B}_{833}$	0	0	−1	0	0	0	0	0	0	0	0	0	−1	0
$\mathcal{B}_{920}$	0	0	20	0	0	0	0	0	0	0	3	−2	34	−1
$\mathcal{B}_{945}$	0	−1	25	0	0	0	0	0	0	0	10	−11	10	0
	$\mathcal{B}_{130}$	$\mathcal{B}_{132}$	$\mathcal{B}_{136}$	$\mathcal{B}_{151}$	$\mathcal{B}_{152}$	$\mathcal{B}_{167}$	$\mathcal{B}_{800}$	$\mathcal{B}_{802}$	$\mathcal{B}_{803}$	$\mathcal{B}_{805}$	$\mathcal{B}_{811}$	$\mathcal{B}_{812}$	$\mathcal{B}_{821}$	$\mathcal{B}_{822}$

TABLE 325. Basis quantities correlation coefficients in percent, subtable 10.

$\mathcal{B}_{832}$	−2				
$\mathcal{B}_{833}$	−1	−1			
$\mathcal{B}_{920}$	17	1	0		
$\mathcal{B}_{945}$	17	2	0	4	
	$\mathcal{B}_{831}$	$\mathcal{B}_{832}$	$\mathcal{B}_{833}$	$\mathcal{B}_{920}$	$\mathcal{B}_{945}$

6. Equality constraints

The constraints on the τ branching-fractions fit quantities are listed in the following equations. When a quantity such as $\mathcal{B}_3/\mathcal{B}_5$ appears on the left side of the equation it represents a fitted quantity, while when it appears on the right side it represents the ratio of two separate fitted quantities.

The equations include coefficients that arise from non-τ branching fractions, denoted, e.g., with the self-describing notation $\mathcal{B}_{K_S\to\pi^0\pi^0}$. Some coefficients are probabilities corresponding to the squared moduli of amplitudes describing quantum state mixtures, such as K^0, $\bar{K}^0$, K_S, K_L. These are denoted with, e.g., $\mathcal{B}_{\langle K^0|K_S\rangle} = |\langle K^0|K_S\rangle|^2$. The values of all non-$\tau$ quantities are taken from the PDG 2021 [9] averages. The fit procedure does not account for their uncertainties, which are generally small with respect to the uncertainties on the τ branching fractions.

$$\mathcal{B}_1 = \mathcal{B}_3 + \mathcal{B}_5 + \mathcal{B}_9 + \mathcal{B}_{10} + \mathcal{B}_{14} + \mathcal{B}_{16} + \mathcal{B}_{20} + \mathcal{B}_{23} + \mathcal{B}_{27} + \mathcal{B}_{28} + \mathcal{B}_{30} + \mathcal{B}_{35} + \mathcal{B}_{40} + \mathcal{B}_{44} + \mathcal{B}_{37}$$
$$+ \mathcal{B}_{42} + \mathcal{B}_{47} + \mathcal{B}_{48} + \mathcal{B}_{804} + \mathcal{B}_{50} + \mathcal{B}_{51} + \mathcal{B}_{806} + \mathcal{B}_{126} \cdot \mathcal{B}_{\eta\to\text{neutral}} + \mathcal{B}_{128} \cdot \mathcal{B}_{\eta\to\text{neutral}} + \mathcal{B}_{130} \cdot \mathcal{B}_{\eta\to\text{neutral}}$$
$$+ \mathcal{B}_{132} \cdot \mathcal{B}_{\eta\to\text{neutral}} + \mathcal{B}_{800} \cdot \mathcal{B}_{\omega\to\pi^0\gamma} + \mathcal{B}_{151} \cdot \mathcal{B}_{\omega\to\pi^0\gamma} + \mathcal{B}_{152} \cdot \mathcal{B}_{\omega\to\pi^0\gamma} + \mathcal{B}_{167} \cdot \mathcal{B}_{\phi\to K_S K_L}$$

$$\mathcal{B}_2 = \mathcal{B}_3 + \mathcal{B}_5 + \mathcal{B}_9 + \mathcal{B}_{10} + \mathcal{B}_{14} + \mathcal{B}_{16} + \mathcal{B}_{20} + \mathcal{B}_{23} + \mathcal{B}_{27} + \mathcal{B}_{28} + \mathcal{B}_{30} + \mathcal{B}_{35} \cdot (\mathcal{B}_{\langle\bar{K}^0|K_S\rangle} \cdot \mathcal{B}_{K_S\to\pi^0\pi^0} + \mathcal{B}_{\langle\bar{K}^0|K_L\rangle})$$
$$+ \mathcal{B}_{40} \cdot (\mathcal{B}_{\langle\bar{K}^0|K_S\rangle} \cdot \mathcal{B}_{K_S\to\pi^0\pi^0} + \mathcal{B}_{\langle\bar{K}^0|K_L\rangle}) + \mathcal{B}_{44} \cdot (\mathcal{B}_{\langle\bar{K}^0|K_S\rangle} \cdot \mathcal{B}_{K_S\to\pi^0\pi^0} + \mathcal{B}_{\langle\bar{K}^0|K_L\rangle})$$
$$+ \mathcal{B}_{37} \cdot (\mathcal{B}_{\langle\bar{K}^0|K_S\rangle} \cdot \mathcal{B}_{K_S\to\pi^0\pi^0} + \mathcal{B}_{\langle\bar{K}^0|K_L\rangle}) + \mathcal{B}_{42} \cdot (\mathcal{B}_{\langle\bar{K}^0|K_S\rangle} \cdot \mathcal{B}_{K_S\to\pi^0\pi^0} + \mathcal{B}_{\langle\bar{K}^0|K_L\rangle})$$
$$+ \mathcal{B}_{47} \cdot (\mathcal{B}_{K_S\to\pi^0\pi^0} \cdot \mathcal{B}_{K_S\to\pi^0\pi^0}) + \mathcal{B}_{48} \cdot \mathcal{B}_{K_S\to\pi^0\pi^0} + \mathcal{B}_{804} + \mathcal{B}_{50} \cdot (\mathcal{B}_{K_S\to\pi^0\pi^0} \cdot \mathcal{B}_{K_S\to\pi^0\pi^0})$$
$$+ \mathcal{B}_{51} \cdot \mathcal{B}_{K_S\to\pi^0\pi^0} + \mathcal{B}_{806} + \mathcal{B}_{126} \cdot \mathcal{B}_{\eta\to\text{neutral}} + \mathcal{B}_{128} \cdot \mathcal{B}_{\eta\to\text{neutral}} + \mathcal{B}_{130} \cdot \mathcal{B}_{\eta\to\text{neutral}}$$
$$+ \mathcal{B}_{132} \cdot (\mathcal{B}_{\eta\to\text{neutral}} \cdot (\mathcal{B}_{\langle\bar{K}^0|K_S\rangle} \cdot \mathcal{B}_{K_S\to\pi^0\pi^0} + \mathcal{B}_{\langle\bar{K}^0|K_L\rangle})) + \mathcal{B}_{800} \cdot \mathcal{B}_{\omega\to\pi^0\gamma} + \mathcal{B}_{151} \cdot \mathcal{B}_{\omega\to\pi^0\gamma}$$
$$+ \mathcal{B}_{152} \cdot \mathcal{B}_{\omega\to\pi^0\gamma} + \mathcal{B}_{167} \cdot (\mathcal{B}_{\phi\to K_S K_L} \cdot \mathcal{B}_{K_S\to\pi^0\pi^0})$$

$$\frac{\mathcal{B}_3}{\mathcal{B}_5} = \frac{\mathcal{B}_3}{\mathcal{B}_5}$$

$$\mathcal{B}_7 = \mathcal{B}_{35} \cdot \mathcal{B}_{\langle\bar{K}^0|K_L\rangle} + \mathcal{B}_9 + \mathcal{B}_{804} + \mathcal{B}_{37} \cdot \mathcal{B}_{\langle K^0|K_L\rangle} + \mathcal{B}_{10}$$

$$\mathcal{B}_8 = \mathcal{B}_9 + \mathcal{B}_{10}$$

$$\frac{\mathcal{B}_8}{\mathcal{B}_5} = \frac{\mathcal{B}_8}{\mathcal{B}_5}$$

$$\frac{\mathcal{B}_9}{\mathcal{B}_5} = \frac{\mathcal{B}_9}{\mathcal{B}_5}$$

$$\frac{\mathcal{B}_{10}}{\mathcal{B}_5} = \frac{\mathcal{B}_{10}}{\mathcal{B}_5}$$

$$\frac{\mathcal{B}_{10}}{\mathcal{B}_9} = \frac{\mathcal{B}_{10}}{\mathcal{B}_9}$$

$$\mathcal{B}_{11} = \mathcal{B}_{14} + \mathcal{B}_{16} + \mathcal{B}_{20} + \mathcal{B}_{23} + \mathcal{B}_{27} + \mathcal{B}_{28} + \mathcal{B}_{30} + \mathcal{B}_{35} \cdot (\mathcal{B}_{\langle K^0|K_S\rangle} \cdot \mathcal{B}_{K_S\to\pi^0\pi^0}) + \mathcal{B}_{37} \cdot (\mathcal{B}_{\langle K^0|K_S\rangle} \cdot \mathcal{B}_{K_S\to\pi^0\pi^0})$$
$$+ \mathcal{B}_{40} \cdot (\mathcal{B}_{\langle K^0|K_S\rangle} \cdot \mathcal{B}_{K_S\to\pi^0\pi^0}) + \mathcal{B}_{42} \cdot (\mathcal{B}_{\langle K^0|K_S\rangle} \cdot \mathcal{B}_{K_S\to\pi^0\pi^0}) + \mathcal{B}_{47} \cdot (\mathcal{B}_{K_S\to\pi^0\pi^0} \cdot \mathcal{B}_{K_S\to\pi^0\pi^0})$$
$$+ \mathcal{B}_{50} \cdot (\mathcal{B}_{K_S\to\pi^0\pi^0} \cdot \mathcal{B}_{K_S\to\pi^0\pi^0}) + \mathcal{B}_{126} \cdot \mathcal{B}_{\eta\to\text{neutral}} + \mathcal{B}_{128} \cdot \mathcal{B}_{\eta\to\text{neutral}} + \mathcal{B}_{130} \cdot \mathcal{B}_{\eta\to\text{neutral}}$$
$$+ \mathcal{B}_{132} \cdot (\mathcal{B}_{\langle K^0|K_S\rangle} \cdot \mathcal{B}_{K_S\to\pi^0\pi^0} \cdot \mathcal{B}_{\eta\to\text{neutral}}) + \mathcal{B}_{151} \cdot \mathcal{B}_{\omega\to\pi^0\gamma} + \mathcal{B}_{152} \cdot \mathcal{B}_{\omega\to\pi^0\gamma} + \mathcal{B}_{800} \cdot \mathcal{B}_{\omega\to\pi^0\gamma}$$

$$\mathcal{B}_{12} = \mathcal{B}_{128} \cdot \mathcal{B}_{\eta\to 3\pi^0} + \mathcal{B}_{30} + \mathcal{B}_{23} + \mathcal{B}_{28} + \mathcal{B}_{14} + \mathcal{B}_{16} + \mathcal{B}_{20} + \mathcal{B}_{27} + \mathcal{B}_{126} \cdot \mathcal{B}_{\eta\to 3\pi^0} + \mathcal{B}_{130} \cdot \mathcal{B}_{\eta\to 3\pi^0}$$

$$\mathcal{B}_{13} = \mathcal{B}_{14} + \mathcal{B}_{16}$$

$$\mathcal{B}_{17} = \mathcal{B}_{128} \cdot \mathcal{B}_{\eta\to 3\pi^0} + \mathcal{B}_{30} + \mathcal{B}_{23} + \mathcal{B}_{28} + \mathcal{B}_{35} \cdot (\mathcal{B}_{\langle K^0|K_S\rangle} \cdot \mathcal{B}_{K_S\to\pi^0\pi^0}) + \mathcal{B}_{40} \cdot (\mathcal{B}_{\langle K^0|K_S\rangle} \cdot \mathcal{B}_{K_S\to\pi^0\pi^0})$$
$$+ \mathcal{B}_{42} \cdot (\mathcal{B}_{\langle K^0|K_S\rangle} \cdot \mathcal{B}_{K_S\to\pi^0\pi^0}) + \mathcal{B}_{20} + \mathcal{B}_{27} + \mathcal{B}_{47} \cdot (\mathcal{B}_{K_S\to\pi^0\pi^0} \cdot \mathcal{B}_{K_S\to\pi^0\pi^0})$$
$$+ \mathcal{B}_{50} \cdot (\mathcal{B}_{K_S\to\pi^0\pi^0} \cdot \mathcal{B}_{K_S\to\pi^0\pi^0}) + \mathcal{B}_{126} \cdot \mathcal{B}_{\eta\to 3\pi^0} + \mathcal{B}_{37} \cdot (\mathcal{B}_{\langle K^0|K_S\rangle} \cdot \mathcal{B}_{K_S\to\pi^0\pi^0}) + \mathcal{B}_{130} \cdot \mathcal{B}_{\eta\to 3\pi^0}$$

$$\mathcal{B}_{18} = \mathcal{B}_{23} + \mathcal{B}_{35} \cdot (\mathcal{B}_{\langle K^0|K_S\rangle} \cdot \mathcal{B}_{K_S\to\pi^0\pi^0}) + \mathcal{B}_{20} + \mathcal{B}_{37} \cdot (\mathcal{B}_{\langle K^0|K_S\rangle} \cdot \mathcal{B}_{K_S\to\pi^0\pi^0})$$

$$\mathcal{B}_{19} = \mathcal{B}_{23} + \mathcal{B}_{20}$$

$$\frac{\mathcal{B}_{19}}{\mathcal{B}_{13}} = \frac{\mathcal{B}_{19}}{\mathcal{B}_{13}}$$

$$\mathcal{B}_{24} = \mathcal{B}_{27} + \mathcal{B}_{28} + \mathcal{B}_{30} + \mathcal{B}_{40} \cdot (\mathcal{B}_{\langle K^0|K_S\rangle} \cdot \mathcal{B}_{K_S\to\pi^0\pi^0}) + \mathcal{B}_{42} \cdot (\mathcal{B}_{\langle K^0|K_S\rangle} \cdot \mathcal{B}_{K_S\to\pi^0\pi^0}) + \mathcal{B}_{47} \cdot (\mathcal{B}_{K_S\to\pi^0\pi^0} \cdot \mathcal{B}_{K_S\to\pi^0\pi^0})$$
$$+ \mathcal{B}_{50} \cdot (\mathcal{B}_{K_S\to\pi^0\pi^0} \cdot \mathcal{B}_{K_S\to\pi^0\pi^0}) + \mathcal{B}_{126} \cdot \mathcal{B}_{\eta\to 3\pi^0} + \mathcal{B}_{128} \cdot \mathcal{B}_{\eta\to 3\pi^0} + \mathcal{B}_{130} \cdot \mathcal{B}_{\eta\to 3\pi^0}$$
$$+ \mathcal{B}_{132} \cdot (\mathcal{B}_{\langle K^0|K_S\rangle} \cdot \mathcal{B}_{K_S\to\pi^0\pi^0} \cdot \mathcal{B}_{\eta\to 3\pi^0})$$

$$\mathcal{B}_{25} = \mathcal{B}_{128}\cdot\mathcal{B}_{\eta\to 3\pi^0} + \mathcal{B}_{30} + \mathcal{B}_{28} + \mathcal{B}_{27} + \mathcal{B}_{126}\cdot\mathcal{B}_{\eta\to 3\pi^0} + \mathcal{B}_{130}\cdot\mathcal{B}_{\eta\to 3\pi^0}$$

$$\mathcal{B}_{26} = \mathcal{B}_{128}\cdot\mathcal{B}_{\eta\to 3\pi^0} + \mathcal{B}_{28} + \mathcal{B}_{40}\cdot(\mathcal{B}_{\langle K^0|K_S\rangle}\cdot\mathcal{B}_{K_S\to\pi^0\pi^0}) + \mathcal{B}_{42}\cdot(\mathcal{B}_{\langle K^0|K_S\rangle}\cdot\mathcal{B}_{K_S\to\pi^0\pi^0}) + \mathcal{B}_{27}$$

$$\frac{\mathcal{B}_{26}}{\mathcal{B}_{13}} = \frac{\mathcal{B}_{26}}{\mathcal{B}_{13}}$$

$$\mathcal{B}_{29} = \mathcal{B}_{30} + \mathcal{B}_{126}\cdot\mathcal{B}_{\eta\to 3\pi^0} + \mathcal{B}_{130}\cdot\mathcal{B}_{\eta\to 3\pi^0}$$

$$\mathcal{B}_{31} = \mathcal{B}_{128}\cdot\mathcal{B}_{\eta\to\text{neutral}} + \mathcal{B}_{23} + \mathcal{B}_{28} + \mathcal{B}_{42} + \mathcal{B}_{16} + \mathcal{B}_{37} + \mathcal{B}_{10} + \mathcal{B}_{167}\cdot(\mathcal{B}_{\phi\to K_SK_L}\cdot\mathcal{B}_{K_S\to\pi^0\pi^0})$$

$$\mathcal{B}_{32} = \mathcal{B}_{16} + \mathcal{B}_{23} + \mathcal{B}_{28} + \mathcal{B}_{37} + \mathcal{B}_{42} + \mathcal{B}_{128}\cdot\mathcal{B}_{\eta\to\text{neutral}} + \mathcal{B}_{130}\cdot\mathcal{B}_{\eta\to\text{neutral}} + \mathcal{B}_{167}\cdot(\mathcal{B}_{\phi\to K_SK_L}\cdot\mathcal{B}_{K_S\to\pi^0\pi^0})$$

$$\begin{aligned}\mathcal{B}_{33} = {}& \mathcal{B}_{35}\cdot\mathcal{B}_{\langle\bar{K}^0|K_S\rangle} + \mathcal{B}_{40}\cdot\mathcal{B}_{\langle\bar{K}^0|K_S\rangle} + \mathcal{B}_{42}\cdot\mathcal{B}_{\langle K^0|K_S\rangle} + \mathcal{B}_{47} + \mathcal{B}_{48} + \mathcal{B}_{50} + \mathcal{B}_{51} + \mathcal{B}_{37}\cdot\mathcal{B}_{\langle K^0|K_S\rangle}\\ & + \mathcal{B}_{132}\cdot(\mathcal{B}_{\langle\bar{K}^0|K_S\rangle}\cdot\mathcal{B}_{\eta\to\text{neutral}}) + \mathcal{B}_{44}\cdot\mathcal{B}_{\langle\bar{K}^0|K_S\rangle} + \mathcal{B}_{167}\cdot\mathcal{B}_{\phi\to K_SK_L}\end{aligned}$$

$$\mathcal{B}_{34} = \mathcal{B}_{35} + \mathcal{B}_{37}$$

$$\mathcal{B}_{38} = \mathcal{B}_{42} + \mathcal{B}_{37}$$

$$\mathcal{B}_{39} = \mathcal{B}_{40} + \mathcal{B}_{42}$$

$$\mathcal{B}_{43} = \mathcal{B}_{40} + \mathcal{B}_{44}$$

$$\mathcal{B}_{46} = \mathcal{B}_{48} + \mathcal{B}_{47} + \mathcal{B}_{804}$$

$$\mathcal{B}_{49} = \mathcal{B}_{50} + \mathcal{B}_{51} + \mathcal{B}_{806}$$

$$\begin{aligned}\mathcal{B}_{54} = {}& \mathcal{B}_{35}\cdot(\mathcal{B}_{\langle K^0|K_S\rangle}\cdot\mathcal{B}_{K_S\to\pi^+\pi^-}) + \mathcal{B}_{37}\cdot(\mathcal{B}_{\langle K^0|K_S\rangle}\cdot\mathcal{B}_{K_S\to\pi^+\pi^-}) + \mathcal{B}_{40}\cdot(\mathcal{B}_{\langle K^0|K_S\rangle}\cdot\mathcal{B}_{K_S\to\pi^+\pi^-})\\ & + \mathcal{B}_{42}\cdot(\mathcal{B}_{\langle K^0|K_S\rangle}\cdot\mathcal{B}_{K_S\to\pi^+\pi^-}) + \mathcal{B}_{47}\cdot(2\cdot\mathcal{B}_{K_S\to\pi^+\pi^-}\cdot\mathcal{B}_{K_S\to\pi^0\pi^0}) + \mathcal{B}_{48}\cdot\mathcal{B}_{K_S\to\pi^+\pi^-}\\ & + \mathcal{B}_{50}\cdot(2\cdot\mathcal{B}_{K_S\to\pi^+\pi^-}\cdot\mathcal{B}_{K_S\to\pi^0\pi^0}) + \mathcal{B}_{51}\cdot\mathcal{B}_{K_S\to\pi^+\pi^-} + \mathcal{B}_{53}\cdot(\mathcal{B}_{\langle\bar{K}^0|K_S\rangle}\cdot\mathcal{B}_{K_S\to\pi^0\pi^0} + \mathcal{B}_{\langle\bar{K}^0|K_L\rangle})\\ & + \mathcal{B}_{62} + \mathcal{B}_{70} + \mathcal{B}_{77} + \mathcal{B}_{78} + \mathcal{B}_{93} + \mathcal{B}_{94} + \mathcal{B}_{126}\cdot\mathcal{B}_{\eta\to\text{charged}} + \mathcal{B}_{128}\cdot\mathcal{B}_{\eta\to\text{charged}} + \mathcal{B}_{130}\cdot\mathcal{B}_{\eta\to\text{charged}}\\ & + \mathcal{B}_{132}\cdot(\mathcal{B}_{\langle\bar{K}^0|K_L\rangle}\cdot\mathcal{B}_{\eta\to\pi^+\pi^-\pi^0} + \mathcal{B}_{\langle\bar{K}^0|K_S\rangle}\cdot\mathcal{B}_{K_S\to\pi^0\pi^0}\cdot\mathcal{B}_{\eta\to\pi^+\pi^-\pi^0} + \mathcal{B}_{\langle\bar{K}^0|K_S\rangle}\cdot\mathcal{B}_{K_S\to\pi^+\pi^-}\cdot\mathcal{B}_{\eta\to 3\pi^0})\\ & + \mathcal{B}_{151}\cdot(\mathcal{B}_{\omega\to\pi^+\pi^-\pi^0} + \mathcal{B}_{\omega\to\pi^+\pi^-}) + \mathcal{B}_{152}\cdot(\mathcal{B}_{\omega\to\pi^+\pi^-\pi^0} + \mathcal{B}_{\omega\to\pi^+\pi^-}) + \mathcal{B}_{167}\cdot(\mathcal{B}_{\phi\to K^+K^-} + \mathcal{B}_{\phi\to K_SK_L}\cdot\mathcal{B}_{K_S\to\pi^+\pi^-})\\ & + \mathcal{B}_{802} + \mathcal{B}_{803} + \mathcal{B}_{800}\cdot(\mathcal{B}_{\omega\to\pi^+\pi^-\pi^0} + \mathcal{B}_{\omega\to\pi^+\pi^-})\end{aligned}$$

$$\begin{aligned}\mathcal{B}_{55} = {}& \mathcal{B}_{128}\cdot\mathcal{B}_{\eta\to\text{charged}} + \mathcal{B}_{152}\cdot(\mathcal{B}_{\omega\to\pi^+\pi^-\pi^0} + \mathcal{B}_{\omega\to\pi^+\pi^-}) + \mathcal{B}_{78} + \mathcal{B}_{77} + \mathcal{B}_{94} + \mathcal{B}_{62} + \mathcal{B}_{70} + \mathcal{B}_{93}\\ & + \mathcal{B}_{126}\cdot\mathcal{B}_{\eta\to\text{charged}} + \mathcal{B}_{802} + \mathcal{B}_{803} + \mathcal{B}_{800}\cdot(\mathcal{B}_{\omega\to\pi^+\pi^-\pi^0} + \mathcal{B}_{\omega\to\pi^+\pi^-}) + \mathcal{B}_{151}\cdot(\mathcal{B}_{\omega\to\pi^+\pi^-\pi^0} + \mathcal{B}_{\omega\to\pi^+\pi^-})\\ & + \mathcal{B}_{130}\cdot\mathcal{B}_{\eta\to\text{charged}} + \mathcal{B}_{168}\end{aligned}$$

$$\begin{aligned}\mathcal{B}_{56} = {}& \mathcal{B}_{35}\cdot(\mathcal{B}_{\langle K^0|K_S\rangle}\cdot\mathcal{B}_{K_S\to\pi^+\pi^-}) + \mathcal{B}_{62} + \mathcal{B}_{93} + \mathcal{B}_{37}\cdot(\mathcal{B}_{\langle K^0|K_S\rangle}\cdot\mathcal{B}_{K_S\to\pi^+\pi^-}) + \mathcal{B}_{802} + \mathcal{B}_{800}\cdot\mathcal{B}_{\omega\to\pi^+\pi^-}\\ & + \mathcal{B}_{151}\cdot\mathcal{B}_{\omega\to\pi^+\pi^-} + \mathcal{B}_{168}\end{aligned}$$

$$\mathcal{B}_{57} = \mathcal{B}_{62} + \mathcal{B}_{93} + \mathcal{B}_{802} + \mathcal{B}_{800}\cdot\mathcal{B}_{\omega\to\pi^+\pi^-} + \mathcal{B}_{151}\cdot\mathcal{B}_{\omega\to\pi^+\pi^-} + \mathcal{B}_{167}\cdot\mathcal{B}_{\phi\to K^+K^-}$$

$$\frac{\mathcal{B}_{57}}{\mathcal{B}_{55}} = \frac{\mathcal{B}_{57}}{\mathcal{B}_{55}}$$

$$\mathcal{B}_{58} = \mathcal{B}_{62} + \mathcal{B}_{93} + \mathcal{B}_{802} + \mathcal{B}_{167}\cdot\mathcal{B}_{\phi\to K^+K^-}$$

$$\mathcal{B}_{59} = \mathcal{B}_{35}\cdot(\mathcal{B}_{\langle K^0|K_S\rangle}\cdot\mathcal{B}_{K_S\to\pi^+\pi^-}) + \mathcal{B}_{62} + \mathcal{B}_{800}\cdot\mathcal{B}_{\omega\to\pi^+\pi^-}$$

$$\mathcal{B}_{60} = \mathcal{B}_{62} + \mathcal{B}_{800}\cdot\mathcal{B}_{\omega\to\pi^+\pi^-}$$

$$\begin{aligned}\mathcal{B}_{63} = {}& \mathcal{B}_{40}\cdot(\mathcal{B}_{\langle K^0|K_S\rangle}\cdot\mathcal{B}_{K_S\to\pi^+\pi^-}) + \mathcal{B}_{42}\cdot(\mathcal{B}_{\langle K^0|K_S\rangle}\cdot\mathcal{B}_{K_S\to\pi^+\pi^-}) + \mathcal{B}_{47}\cdot(2\cdot\mathcal{B}_{K_S\to\pi^+\pi^-}\cdot\mathcal{B}_{K_S\to\pi^0\pi^0})\\ & + \mathcal{B}_{50}\cdot(2\cdot\mathcal{B}_{K_S\to\pi^+\pi^-}\cdot\mathcal{B}_{K_S\to\pi^0\pi^0}) + \mathcal{B}_{70} + \mathcal{B}_{77} + \mathcal{B}_{78} + \mathcal{B}_{94} + \mathcal{B}_{126}\cdot\mathcal{B}_{\eta\to\text{charged}} + \mathcal{B}_{128}\cdot\mathcal{B}_{\eta\to\text{charged}}\\ & + \mathcal{B}_{130}\cdot\mathcal{B}_{\eta\to\text{charged}} + \mathcal{B}_{132}\cdot(\mathcal{B}_{\langle\bar{K}^0|K_S\rangle}\cdot\mathcal{B}_{K_S\to\pi^+\pi^-}\cdot\mathcal{B}_{\eta\to\text{neutral}} + \mathcal{B}_{\langle\bar{K}^0|K_S\rangle}\cdot\mathcal{B}_{K_S\to\pi^0\pi^0}\cdot\mathcal{B}_{\eta\to\text{charged}})\\ & + \mathcal{B}_{151}\cdot\mathcal{B}_{\omega\to\pi^+\pi^-\pi^0} + \mathcal{B}_{152}\cdot(\mathcal{B}_{\omega\to\pi^+\pi^-\pi^0} + \mathcal{B}_{\omega\to\pi^+\pi^-}) + \mathcal{B}_{800}\cdot\mathcal{B}_{\omega\to\pi^+\pi^-\pi^0} + \mathcal{B}_{803}\end{aligned}$$

$$\mathcal{B}_{64} = \mathcal{B}_{78} + \mathcal{B}_{77} + \mathcal{B}_{94} + \mathcal{B}_{70} + \mathcal{B}_{126} \cdot \mathcal{B}_{\eta\to\pi^+\pi^-\pi^0} + \mathcal{B}_{128} \cdot \mathcal{B}_{\eta\to\pi^+\pi^-\pi^0} + \mathcal{B}_{130} \cdot \mathcal{B}_{\eta\to\pi^+\pi^-\pi^0} + \mathcal{B}_{800} \cdot \mathcal{B}_{\omega\to\pi^+\pi^-\pi^0} + \mathcal{B}_{151} \cdot \mathcal{B}_{\omega\to\pi^+\pi^-\pi^0} + \mathcal{B}_{152} \cdot (\mathcal{B}_{\omega\to\pi^+\pi^-\pi^0} + \mathcal{B}_{\omega\to\pi^+\pi^-}) + \mathcal{B}_{803}$$

$$\mathcal{B}_{65} = \mathcal{B}_{40} \cdot (\mathcal{B}_{\langle K^0|K_S\rangle} \cdot \mathcal{B}_{K_S\to\pi^+\pi^-}) + \mathcal{B}_{42} \cdot (\mathcal{B}_{\langle K^0|K_S\rangle} \cdot \mathcal{B}_{K_S\to\pi^+\pi^-}) + \mathcal{B}_{70} + \mathcal{B}_{94} + \mathcal{B}_{128} \cdot \mathcal{B}_{\eta\to\pi^+\pi^-\pi^0} + \mathcal{B}_{151} \cdot \mathcal{B}_{\omega\to\pi^+\pi^-\pi^0} + \mathcal{B}_{152} \cdot \mathcal{B}_{\omega\to\pi^+\pi^-} + \mathcal{B}_{800} \cdot \mathcal{B}_{\omega\to\pi^+\pi^-\pi^0} + \mathcal{B}_{803}$$

$$\mathcal{B}_{66} = \mathcal{B}_{70} + \mathcal{B}_{94} + \mathcal{B}_{128} \cdot \mathcal{B}_{\eta\to\pi^+\pi^-\pi^0} + \mathcal{B}_{151} \cdot \mathcal{B}_{\omega\to\pi^+\pi^-\pi^0} + \mathcal{B}_{152} \cdot \mathcal{B}_{\omega\to\pi^+\pi^-} + \mathcal{B}_{800} \cdot \mathcal{B}_{\omega\to\pi^+\pi^-\pi^0} + \mathcal{B}_{803}$$

$$\mathcal{B}_{67} = \mathcal{B}_{70} + \mathcal{B}_{94} + \mathcal{B}_{128} \cdot \mathcal{B}_{\eta\to\pi^+\pi^-\pi^0} + \mathcal{B}_{803}$$

$$\mathcal{B}_{68} = \mathcal{B}_{40} \cdot (\mathcal{B}_{\langle K^0|K_S\rangle} \cdot \mathcal{B}_{K_S\to\pi^+\pi^-}) + \mathcal{B}_{70} + \mathcal{B}_{152} \cdot \mathcal{B}_{\omega\to\pi^+\pi^-} + \mathcal{B}_{800} \cdot \mathcal{B}_{\omega\to\pi^+\pi^-\pi^0}$$

$$\mathcal{B}_{69} = \mathcal{B}_{152} \cdot \mathcal{B}_{\omega\to\pi^+\pi^-} + \mathcal{B}_{70} + \mathcal{B}_{800} \cdot \mathcal{B}_{\omega\to\pi^+\pi^-\pi^0}$$

$$\mathcal{B}_{74} = \mathcal{B}_{152} \cdot \mathcal{B}_{\omega\to\pi^+\pi^-\pi^0} + \mathcal{B}_{78} + \mathcal{B}_{77} + \mathcal{B}_{126} \cdot \mathcal{B}_{\eta\to\pi^+\pi^-\pi^0} + \mathcal{B}_{130} \cdot \mathcal{B}_{\eta\to\pi^+\pi^-\pi^0}$$

$$\mathcal{B}_{75} = \mathcal{B}_{152} \cdot \mathcal{B}_{\omega\to\pi^+\pi^-\pi^0} + \mathcal{B}_{47} \cdot (2 \cdot \mathcal{B}_{K_S\to\pi^+\pi^-} \cdot \mathcal{B}_{K_S\to\pi^0\pi^0}) + \mathcal{B}_{77} + \mathcal{B}_{126} \cdot \mathcal{B}_{\eta\to\pi^+\pi^-\pi^0} + \mathcal{B}_{130} \cdot \mathcal{B}_{\eta\to\pi^+\pi^-\pi^0}$$

$$\mathcal{B}_{76} = \mathcal{B}_{152} \cdot \mathcal{B}_{\omega\to\pi^+\pi^-\pi^0} + \mathcal{B}_{77} + \mathcal{B}_{126} \cdot \mathcal{B}_{\eta\to\pi^+\pi^-\pi^0} + \mathcal{B}_{130} \cdot \mathcal{B}_{\eta\to\pi^+\pi^-\pi^0}$$

$$\frac{\mathcal{B}_{76}}{\mathcal{B}_{54}} = \frac{\mathcal{B}_{76}}{\mathcal{B}_{54}}$$

$$\mathcal{B}_{78} = \mathcal{B}_{810} + \mathcal{B}_{50} \cdot (2 \cdot \mathcal{B}_{K_S\to\pi^+\pi^-} \cdot \mathcal{B}_{K_S\to\pi^0\pi^0}) + \mathcal{B}_{132} \cdot (\mathcal{B}_{\langle \bar{K}^0|K_S\rangle} \cdot \mathcal{B}_{K_S\to\pi^+\pi^-} \cdot \mathcal{B}_{\eta\to 3\pi^0})$$

$$\mathcal{B}_{79} = \mathcal{B}_{37} \cdot (\mathcal{B}_{\langle K^0|K_S\rangle} \cdot \mathcal{B}_{K_S\to\pi^+\pi^-}) + \mathcal{B}_{42} \cdot (\mathcal{B}_{\langle K^0|K_S\rangle} \cdot \mathcal{B}_{K_S\to\pi^+\pi^-}) + \mathcal{B}_{93} + \mathcal{B}_{94} + \mathcal{B}_{128} \cdot \mathcal{B}_{\eta\to\text{charged}} + \mathcal{B}_{151} \cdot (\mathcal{B}_{\omega\to\pi^+\pi^-\pi^0} + \mathcal{B}_{\omega\to\pi^+\pi^-}) + \mathcal{B}_{168} + \mathcal{B}_{802} + \mathcal{B}_{803}$$

$$\mathcal{B}_{80} = \mathcal{B}_{93} + \mathcal{B}_{802} + \mathcal{B}_{151} \cdot \mathcal{B}_{\omega\to\pi^+\pi^-}$$

$$\frac{\mathcal{B}_{80}}{\mathcal{B}_{60}} = \frac{\mathcal{B}_{80}}{\mathcal{B}_{60}}$$

$$\mathcal{B}_{81} = \mathcal{B}_{128} \cdot \mathcal{B}_{\eta\to\pi^+\pi^-\pi^0} + \mathcal{B}_{94} + \mathcal{B}_{803} + \mathcal{B}_{151} \cdot \mathcal{B}_{\omega\to\pi^+\pi^-\pi^0}$$

$$\frac{\mathcal{B}_{81}}{\mathcal{B}_{69}} = \frac{\mathcal{B}_{81}}{\mathcal{B}_{69}}$$

$$\mathcal{B}_{82} = \mathcal{B}_{128} \cdot \mathcal{B}_{\eta\to\text{charged}} + \mathcal{B}_{42} \cdot (\mathcal{B}_{\langle K^0|K_S\rangle} \cdot \mathcal{B}_{K_S\to\pi^+\pi^-}) + \mathcal{B}_{802} + \mathcal{B}_{803} + \mathcal{B}_{151} \cdot (\mathcal{B}_{\omega\to\pi^+\pi^-\pi^0} + \mathcal{B}_{\omega\to\pi^+\pi^-}) + \mathcal{B}_{37} \cdot (\mathcal{B}_{\langle K^0|K_S\rangle} \cdot \mathcal{B}_{K_S\to\pi^+\pi^-})$$

$$\mathcal{B}_{83} = \mathcal{B}_{128} \cdot \mathcal{B}_{\eta\to\pi^+\pi^-\pi^0} + \mathcal{B}_{802} + \mathcal{B}_{803} + \mathcal{B}_{151} \cdot (\mathcal{B}_{\omega\to\pi^+\pi^-\pi^0} + \mathcal{B}_{\omega\to\pi^+\pi^-})$$

$$\mathcal{B}_{84} = \mathcal{B}_{802} + \mathcal{B}_{151} \cdot \mathcal{B}_{\omega\to\pi^+\pi^-} + \mathcal{B}_{37} \cdot (\mathcal{B}_{\langle K^0|K_S\rangle} \cdot \mathcal{B}_{K_S\to\pi^+\pi^-})$$

$$\mathcal{B}_{85} = \mathcal{B}_{802} + \mathcal{B}_{151} \cdot \mathcal{B}_{\omega\to\pi^+\pi^-}$$

$$\frac{\mathcal{B}_{85}}{\mathcal{B}_{60}} = \frac{\mathcal{B}_{85}}{\mathcal{B}_{60}}$$

$$\mathcal{B}_{87} = \mathcal{B}_{42} \cdot (\mathcal{B}_{\langle K^0|K_S\rangle} \cdot \mathcal{B}_{K_S\to\pi^+\pi^-}) + \mathcal{B}_{128} \cdot \mathcal{B}_{\eta\to\pi^+\pi^-\pi^0} + \mathcal{B}_{151} \cdot \mathcal{B}_{\omega\to\pi^+\pi^-\pi^0} + \mathcal{B}_{803}$$

$$\mathcal{B}_{88} = \mathcal{B}_{128} \cdot \mathcal{B}_{\eta\to\pi^+\pi^-\pi^0} + \mathcal{B}_{803} + \mathcal{B}_{151} \cdot \mathcal{B}_{\omega\to\pi^+\pi^-\pi^0}$$

$$\mathcal{B}_{89} = \mathcal{B}_{803} + \mathcal{B}_{151} \cdot \mathcal{B}_{\omega\to\pi^+\pi^-\pi^0}$$

$$\mathcal{B}_{92} = \mathcal{B}_{94} + \mathcal{B}_{93}$$

$$\frac{\mathcal{B}_{93}}{\mathcal{B}_{60}} = \frac{\mathcal{B}_{93}}{\mathcal{B}_{60}}$$

$$\frac{\mathcal{B}_{94}}{\mathcal{B}_{69}} = \frac{\mathcal{B}_{94}}{\mathcal{B}_{69}}$$

$$
\begin{aligned}
\mathcal{B}_{96} &= \mathcal{B}_{167}\cdot\mathcal{B}_{\phi\to K^+K^-}\\
\mathcal{B}_{102} &= \mathcal{B}_{103}+\mathcal{B}_{104}\\
\mathcal{B}_{103} &= \mathcal{B}_{820}+\mathcal{B}_{822}+\mathcal{B}_{831}\cdot\mathcal{B}_{\omega\to\pi^+\pi^-}\\
\mathcal{B}_{104} &= \mathcal{B}_{830}+\mathcal{B}_{833}\\
\mathcal{B}_{106} &= \mathcal{B}_{30}+\mathcal{B}_{44}\cdot\mathcal{B}_{\langle\bar{K}^0|K_S\rangle}+\mathcal{B}_{47}+\mathcal{B}_{53}\cdot\mathcal{B}_{\langle K^0|K_S\rangle}+\mathcal{B}_{77}+\mathcal{B}_{103}\\
&\quad+\mathcal{B}_{126}\cdot(\mathcal{B}_{\eta\to 3\pi^0}+\mathcal{B}_{\eta\to\pi^+\pi^-\pi^0})+\mathcal{B}_{152}\cdot\mathcal{B}_{\omega\to\pi^+\pi^-\pi^0}\\
\mathcal{B}_{110} &= \mathcal{B}_{10}+\mathcal{B}_{16}+\mathcal{B}_{23}+\mathcal{B}_{28}+\mathcal{B}_{35}+\mathcal{B}_{40}+\mathcal{B}_{128}+\mathcal{B}_{802}+\mathcal{B}_{803}+\mathcal{B}_{151}+\mathcal{B}_{130}\\
&\quad+\mathcal{B}_{132}+\mathcal{B}_{44}+\mathcal{B}_{53}+\mathcal{B}_{168}+\mathcal{B}_{169}+\mathcal{B}_{822}+\mathcal{B}_{833}\\
\mathcal{B}_{149} &= \mathcal{B}_{152}+\mathcal{B}_{800}+\mathcal{B}_{151}\\
\mathcal{B}_{150} &= \mathcal{B}_{800}+\mathcal{B}_{151}\\
\frac{\mathcal{B}_{150}}{\mathcal{B}_{66}} &= \frac{\mathcal{B}_{150}}{\mathcal{B}_{66}}\\
\frac{\mathcal{B}_{152}}{\mathcal{B}_{54}} &= \frac{\mathcal{B}_{152}}{\mathcal{B}_{54}}\\
\frac{\mathcal{B}_{152}}{\mathcal{B}_{76}} &= \frac{\mathcal{B}_{152}}{\mathcal{B}_{76}}
\end{aligned}
$$

$$
\begin{aligned}
\mathcal{B}_{168} &= \mathcal{B}_{167}\cdot\mathcal{B}_{\phi\to K^+K^-}\\
\mathcal{B}_{169} &= \mathcal{B}_{167}\cdot\mathcal{B}_{\phi\to K_SK_L}\\
\mathcal{B}_{804} &= \mathcal{B}_{47}\cdot((\mathcal{B}_{\langle K^0|K_L\rangle}\cdot\mathcal{B}_{\langle\bar{K}^0|K_L\rangle})/(\mathcal{B}_{\langle K^0|K_S\rangle}\cdot\mathcal{B}_{\langle\bar{K}^0|K_S\rangle}))\\
\mathcal{B}_{806} &= \mathcal{B}_{50}\cdot((\mathcal{B}_{\langle K^0|K_L\rangle}\cdot\mathcal{B}_{\langle\bar{K}^0|K_L\rangle})/(\mathcal{B}_{\langle K^0|K_S\rangle}\cdot\mathcal{B}_{\langle\bar{K}^0|K_S\rangle}))\\
\mathcal{B}_{810} &= \mathcal{B}_{910}+\mathcal{B}_{911}+\mathcal{B}_{811}\cdot\mathcal{B}_{\omega\to\pi^+\pi^-\pi^0}+\mathcal{B}_{812}\\
\mathcal{B}_{820} &= \mathcal{B}_{920}+\mathcal{B}_{821}\\
\mathcal{B}_{830} &= \mathcal{B}_{930}+\mathcal{B}_{831}\cdot\mathcal{B}_{\omega\to\pi^+\pi^-\pi^0}+\mathcal{B}_{832}\\
\mathcal{B}_{910} &= \mathcal{B}_{136}\cdot\mathcal{B}_{\eta\to 3\pi^0}\\
\mathcal{B}_{911} &= \mathcal{B}_{945}\cdot\mathcal{B}_{\eta\to\pi^+\pi^-\pi^0}\\
\mathcal{B}_{930} &= \mathcal{B}_{136}\cdot\mathcal{B}_{\eta\to\pi^+\pi^-\pi^0}\\
\mathcal{B}_{944} &= \mathcal{B}_{136}\cdot\mathcal{B}_{\eta\to\gamma\gamma}\\
\mathcal{B}_{\mathrm{All}} &= \mathcal{B}_{3}+\mathcal{B}_{5}+\mathcal{B}_{9}+\mathcal{B}_{10}+\mathcal{B}_{14}+\mathcal{B}_{16}+\mathcal{B}_{20}+\mathcal{B}_{23}+\mathcal{B}_{27}+\mathcal{B}_{28}+\mathcal{B}_{30}+\mathcal{B}_{35}+\mathcal{B}_{37}+\mathcal{B}_{40}\\
&\quad+\mathcal{B}_{42}+\mathcal{B}_{47}\cdot(1+((\mathcal{B}_{\langle K^0|K_L\rangle}\cdot\mathcal{B}_{\langle\bar{K}^0|K_L\rangle})/(\mathcal{B}_{\langle K^0|K_S\rangle}\cdot\mathcal{B}_{\langle\bar{K}^0|K_S\rangle})))+\mathcal{B}_{48}+\mathcal{B}_{62}\\
&\quad+\mathcal{B}_{70}+\mathcal{B}_{77}+\mathcal{B}_{811}+\mathcal{B}_{812}+\mathcal{B}_{93}+\mathcal{B}_{94}+\mathcal{B}_{832}+\mathcal{B}_{833}+\mathcal{B}_{126}+\mathcal{B}_{128}\\
&\quad+\mathcal{B}_{802}+\mathcal{B}_{803}+\mathcal{B}_{800}+\mathcal{B}_{151}+\mathcal{B}_{130}+\mathcal{B}_{132}+\mathcal{B}_{44}+\mathcal{B}_{53}\\
&\quad+\mathcal{B}_{50}\cdot(1+((\mathcal{B}_{\langle K^0|K_L\rangle}\cdot\mathcal{B}_{\langle\bar{K}^0|K_L\rangle})/(\mathcal{B}_{\langle K^0|K_S\rangle}\cdot\mathcal{B}_{\langle\bar{K}^0|K_S\rangle})))\\
&\quad+\mathcal{B}_{51}+\mathcal{B}_{167}\cdot(\mathcal{B}_{\phi\to K^+K^-}+\mathcal{B}_{\phi\to K_SK_L})+\mathcal{B}_{152}+\mathcal{B}_{920}+\mathcal{B}_{821}+\mathcal{B}_{822}+\mathcal{B}_{831}+\mathcal{B}_{136}+\mathcal{B}_{945}+\mathcal{B}_{805}
\end{aligned}
$$

B. Tests of lepton universality

Lepton universality tests probe the Standard-Model prediction that the weak charged-current interaction has the same coupling for all lepton generations. Starting with our 2014 report [1576], the precision of such tests was significantly improved due to use of the Belle τ lifetime measurement [1644], while improvements from the τ branching fraction fit are

negligible. We perform the universality tests by using ratios of the partial widths of a heavier lepton α decaying to a lighter lepton β [1645],

$$\Gamma(\alpha \to \nu_\alpha \beta \bar{\nu}_\beta(\gamma)) = \frac{\mathcal{B}(\alpha \to \nu_\alpha \beta \bar{\nu}_\beta)}{\tau_\alpha} = \frac{G_\alpha G_\beta m_\alpha^5}{192\pi^3} f\left(\frac{m_\beta^2}{m_\alpha^2}\right) R_W^{\alpha\beta} R_\gamma^\alpha, \quad (325)$$

where (Refs. [1646–1648])

$$G_\beta = \frac{g_\beta^2}{4\sqrt{2}M_W^2}, \qquad f(x) = 1 - 8x + 8x^3 - x^4 - 12x^2 \ln x, \quad (326)$$

$$R_W^{\alpha\beta} = 1 + \frac{3}{5}\frac{m_\alpha^2}{M_W^2} + \frac{9}{5}\frac{m_\beta^2}{M_W^2}, \qquad R_\gamma^\alpha = 1 + \frac{\alpha(m_\alpha)}{2\pi}\left(\frac{25}{4} - \pi^2\right). \quad (327)$$

The equation holds at leading perturbative order (with some corrections being computed at next-to-leading order) for branching fractions to final states that include a soft photon, as detailed in the notation. The inclusion of soft photons is not explicitly mentioned in the branching fractions notation used in this section, but ought to be implicitly assumed, since experimental measurements do include soft photons. For most measurements of τ branching fractions, soft photons are not experimentally reconstructed but accounted for in the simulations used to estimate the experimental efficiency. We use $R_\gamma^\tau = 1\text{–}43.2 \times 10^{-4}$ and $R_\gamma^\mu = 1\text{–}42.4 \times 10^{-4}$ [1645] and M_W from PDG 2021 [9]. We use HFLAV 2021 averages and PDG 2021 for the other quantities. Using pure leptonic processes we obtain the coupling ratios

$$\left(\frac{g_\tau}{g_\mu}\right)_\tau = 1.0009 \pm 0.0014, \quad (328)$$

$$\left(\frac{g_\tau}{g_e}\right)_\tau = 1.0027 \pm 0.0014, \quad (329)$$

$$\left(\frac{g_\mu}{g_e}\right)_\tau = 1.0019 \pm 0.0014. \quad (330)$$

Using the expressions for the τ hadronic partial widths, we obtain

$$\left(\frac{g_\tau}{g_\mu}\right)_h^2 = \frac{\mathcal{B}(\tau \to h\nu_\tau)}{\mathcal{B}(h \to \mu\bar{\nu}_\mu)} \frac{2m_h m_\mu^2 \tau_h}{(1 + \delta R_{\tau/h}) m_\tau^3 \tau_\tau} \left(\frac{1 - m_\mu^2/m_h^2}{1 - m_h^2/m_\tau^2}\right)^2, \quad (331)$$

TABLE 326. Universality coupling ratios correlation coefficients (%).

$\left(\frac{g_\tau}{g_e}\right)_\tau$	51			
$\left(\frac{g_\mu}{g_e}\right)_\tau$	−50	49		
$\left(\frac{g_\tau}{g_\mu}\right)_\pi$	16	18	1	
$\left(\frac{g_\tau}{g_\mu}\right)_K$	12	11	−1	7
	$\left(\frac{g_\tau}{g_\mu}\right)_\tau$	$\left(\frac{g_\tau}{g_e}\right)_\tau$	$\left(\frac{g_\mu}{g_e}\right)_\tau$	$\left(\frac{g_\tau}{g_\mu}\right)_\pi$

where $h = \pi$ or K. The radiative corrections $\delta R_{\tau/\pi}$ and $\delta R_{\tau/K}$ have been recently updated with an improved estimation of their uncertainties and their values are $(0.18 \pm 0.57)\%$ and $(0.97 \pm 0.58)\%$ [1580], respectively. We obtain:

$$\left(\frac{g_\tau}{g_\mu}\right)_\pi = 0.9959 \pm 0.0038, \quad \left(\frac{g_\tau}{g_\mu}\right)_K = 0.9855 \pm 0.0075. \quad (332)$$

The largest contributions to the uncertainties of the tests are the uncertainty on $\delta R_{\tau/\pi}$ for $(g_\tau/g_\mu)_\pi$ and the uncertainty on the τ branching fraction for $(g_\tau/g_\mu)_K$. Similar tests can be performed using measurements of decay modes with electrons, but are less precise because the meson decays to electrons are helicity suppressed and have less precise experimental measurements. Averaging the three (g_τ/g_μ) ratios we obtain

$$\left(\frac{g_\tau}{g_\mu}\right)_{\tau+\pi+K} = 1.0003 \pm 0.0014, \quad (333)$$

accounting for correlations and assuming that the $\delta R_{\tau/\pi}$ and $\delta R_{\tau/K}$ uncertainties are uncorrelated as they are estimated to be with good approximation [1580]. Table 326 reports the correlation coefficients for the fitted coupling ratios.

Since $(g_\tau/g_\mu)_\tau = (g_\tau/g_e)_\tau/(g_\mu/g_e)_\tau$, the correlation matrix is expected to be positive semi-definite, with one eigenvalue equal to zero. Indeed, in the reported correlation matrix there is one eigenvalue that is consistent with zero within the numerical accuracy of the reported figures.

C. Universality-improved $\mathcal{B}(\tau \to e\nu\bar{\nu})$ and R_{had}

We compute two quantities that are used for further tests involving the τ branching fractions:

(i) the "universality-improved" value $\mathcal{B}_e^{\text{uni}}$ of $\mathcal{B}_e = \mathcal{B}(\tau \to e\nu\bar{\nu})$, determined with the assumption that the Standard Model and lepton universality hold;

(ii) the ratio R_{had} between the total branching fraction of the τ to hadrons, $\mathcal{B}_{\text{had}}$ and the universality-improved $\mathcal{B}_e^{\text{uni}}$, which is a measure of the ratio $\Gamma(\tau \to \text{had})/\Gamma(\tau \to e\nu\bar{\nu})$ of the respective partial widths.

Following Ref. [1575], we obtain the improved value $\mathcal{B}_e^{\rm uni}$ using the τ branching fraction to $\mu\nu\bar{\nu}$, $\mathcal{B}_\mu$, and the τ lifetime. We average:

(i) the $\mathcal{B}_e$ fit value $\mathcal{B}_5$

(ii) the $\mathcal{B}_e$ determination from the $\mathcal{B}_\mu = \mathcal{B}(\tau \to \mu\nu\bar{\nu})$ fit value $\mathcal{B}_3$ assuming that $g_\mu/g_e = 1$, hence (see also Sec. XII. B)

$$\mathcal{B}_e = \mathcal{B}_\mu \cdot f(m_e^2/m_\tau^2)/f(m_\mu^2/m_\tau^2), \quad (334)$$

(iii) the $\mathcal{B}_e$ determination from the τ lifetime assuming that $g_\tau/g_\mu = 1$, hence

$$\mathcal{B}_e = \mathcal{B}(\mu \to e\bar{\nu}_e\nu_\mu) \cdot \frac{\tau_\tau}{\tau_\mu} \cdot \frac{m_\tau^5}{m_\mu^5} \cdot f\left(\frac{m_e^2}{m_\tau^2}\right) \Big/ f\left(\frac{m_e^2}{m_\mu^2}\right) \cdot (R_\gamma^\tau R_W^\tau)/(R_\gamma^\mu R_W^\mu), \quad (335)$$

where $\mathcal{B}(\mu \to e\bar{\nu}_e\nu_\mu) = 1$.

Accounting for correlations, we obtain

$$\mathcal{B}_e^{\rm uni} = (17.812 \pm 0.022)\%. \quad (336)$$

We use $\mathcal{B}_e^{\rm uni}$ to obtain the ratio

$$R_{\rm had} = \frac{\Gamma(\tau \to \text{hadrons})}{\Gamma(\tau \to e\nu\bar{\nu})} = \frac{\mathcal{B}_{\rm had}}{\mathcal{B}_e^{\rm uni}} = 3.6343 \pm 0.0082, \quad (337)$$

where $\mathcal{B}_{\rm had}$ is the sum of all *measured* branching fractions to hadrons. An alternative definition of $\mathcal{B}_{\rm had}$ uses the unitarity of the sum of all branching fractions, $\mathcal{B}_{\rm had}^{\rm uni} = 1 - \mathcal{B}_e - \mathcal{B}_\mu = (64.80 \pm 0.06)\%$, and results in:

$$R_{\rm had}^{\rm uni} = \frac{1 - \mathcal{B}_e - \mathcal{B}_\mu}{\mathcal{B}_e^{\rm uni}} = 3.6381 \pm 0.0075. \quad (338)$$

A third definition of $\mathcal{B}_{\rm had}$ uses the unitarity of the sum of all branching fractions, the Standard Model prediction $\mathcal{B}_\mu = \mathcal{B}_e \cdot f(m_\mu^2/m_\tau^2)/f(m_e^2/m_\tau^2)$ and $\mathcal{B}_e^{\rm uni}$ to define $\mathcal{B}_{\rm had}^{\rm uni,SM} = 1 - \mathcal{B}_e^{\rm uni} - \mathcal{B}_e^{\rm uni} \cdot f(m_\mu^2/m_\tau^2)/f(m_e^2/m_\tau^2) = (64.87 \pm 0.04)\%$, yielding

$$R_{\rm had}^{\rm uni,SM} = \frac{1 - \mathcal{B}_e^{\rm uni} - \mathcal{B}_e^{\rm uni} \cdot f(m_\mu^2/m_\tau^2)/f(m_e^2/m_\tau^2)}{\mathcal{B}_e^{\rm uni}} = 3.6417 \pm 0.0070. \quad (339)$$

Although $\mathcal{B}_{\rm had}^{\rm uni}$ and $\mathcal{B}_{\rm had}^{\rm uni,SM}$ are more precise than $\mathcal{B}_{\rm had}$, the precision of $R_{\rm had}^{\rm uni}$ and $R_{\rm had}^{\rm uni,SM}$ is just slightly better than the one of $R_{\rm had}$ because there are larger correlations between $\mathcal{B}_{\rm had}^{\rm uni}$, $\mathcal{B}_{\rm had}^{\rm uni,SM}$ and $\mathcal{B}_e^{\rm uni}$ than between $\mathcal{B}_{\rm had}$ and $\mathcal{B}_e^{\rm uni}$.

D. Measurements of $|V_{us}|$

The CKM matrix element magnitude $|V_{us}|$ is most precisely determined from kaon decays [1649] (see Figure 104), and its precision is limited by the uncertainties of the lattice QCD estimates of the meson form factor $f_+^{K\pi}(0)$ and decay constant in $f_{K\pm}/f_{\pi\pm}$. Using the τ branching fractions, it is possible to determine $|V_{us}|$ in an alternative way [1650,1651] that does not depend on lattice QCD and has small theory uncertainties (as discussed in Sec. XII. D. 1). Moreover, $|V_{us}|$ can be determined using the τ branching fractions similarly to the kaon case, using the lattice QCD predictions for the meson decay constants.

1. $|V_{us}|$ from $\mathcal{B}(\tau \to X_s\nu)$

The τ hadronic partial width is the sum of the τ partial widths to strange and to nonstrange hadronic final states, $\Gamma_{\rm had} = \Gamma_s + \Gamma_{\rm VA}$. The suffix "VA" traditionally denotes the sum of the τ partial widths to nonstrange final states, which proceed through either vector or axial-vector currents.

Dividing any partial width Γ_x by the electronic partial width, Γ_e, we obtain partial-width ratios R_x, which satisfy $R_{\rm had} = R_s + R_{\rm VA}$. In terms of such ratios, $|V_{us}|$ can be measured as [1650,1651]

$$|V_{us}|_{\tau s} = \sqrt{R_s \Big/ \left[\frac{R_{\rm VA}}{|V_{ud}|^2} - \delta R_{\rm theory}\right]}, \quad (340)$$

where $\delta R_{\rm theory}$ can be determined using perturbative QCD and partly relying on experimental low energy scattering data [1652–1654]. The calculations in the first two references have been criticized for falling short in dealing with the biases and uncertainties in the low-energy regime of QCD [1655], but are still supported by the authors. In order to obtain smaller and more reliable QCD uncertainties, alternative procedures for computing $|V_{us}|$ using τ decays have been proposed, which involve the τ spectral functions [1655] and lattice QCD methods [1656].

In the following, we compute $|V_{us}|$ using the τ branching fraction fit results according to Eq. (340), since the complexity of the other proposed procedures and the effort that is required to reproduce them exceed the scope of this report. We use Ref. [1652] and the s-quark mass $m_s = 93.00 \pm 8.54$ MeV [9] to calculate $\delta R_{\rm theory} = 0.238 \pm 0.033$, since that reference quotes uncertainties that are intermediate with respect to the other two assessments in the above mentioned existing literature.

We proceed following the same procedure of the 2012 HFLAV report [221]. We sum the strange and nonstrange hadronic τ branching fractions $\mathcal{B}_s$ and $\mathcal{B}_{\rm VA}$, and use the universality-improved $\mathcal{B}_e^{\rm uni}$ (see Sec. XII. C) to compute the R_s and $R_{\rm VA}$ ratios. In past determinations of $|V_{us}|$, such as the 2009 HFLAV report [424], the total hadronic branching fraction was computed using unitarity

TABLE 327. HFLAV 2021 τ branching fractions to strange final states.

Branching fraction	HFLAV 2021 fit (%)
$K^-\nu_\tau$	0.6957 ± 0.0096
$K^-\pi^0\nu_\tau$	0.4322 ± 0.0148
$K^-2\pi^0\nu_\tau(\text{ex.}K^0)$	0.0634 ± 0.0219
$K^-3\pi^0\nu_\tau(\text{ex.}K^0,\eta)$	0.0465 ± 0.0213
$\pi^-\bar{K}^0\nu_\tau$	0.8375 ± 0.0139
$\pi^-\bar{K}^0\pi^0\nu_\tau$	0.3810 ± 0.0129
$\pi^-\bar{K}^0 2\pi^0\nu_\tau(\text{ex.}K^0)$	0.0234 ± 0.0231
$\bar{K}^0 h^- h^- h^+\nu_\tau$	0.0222 ± 0.0202
$K^-\eta\nu_\tau$	0.0155 ± 0.0008
$K^-\pi^0\eta\nu_\tau$	0.0048 ± 0.0012
$\pi^-\bar{K}^0\eta\nu_\tau$	0.0094 ± 0.0015
$K^-\omega\nu_\tau$	0.0410 ± 0.0092
$K^-\phi(K^+K^-)\nu_\tau$	0.0022 ± 0.0008
$K^-\phi(K^0_S K^0_L)\nu_\tau$	0.0015 ± 0.0006
$K^-\pi^-\pi^+\nu_\tau(\text{ex.}K^0,\omega)$	0.2924 ± 0.0068
$K^-\pi^-\pi^+\pi^0\nu_\tau(\text{ex.}K^0,\omega,\eta)$	0.0387 ± 0.0142
$K^-2\pi^-2\pi^+\nu_\tau(\text{ex.}K^0)$	0.0001 ± 0.0001
$K^-2\pi^-2\pi^+\pi^0\nu_\tau(\text{ex.}K^0)$	0.0001 ± 0.0001
$X_s^-\nu_\tau$	2.9076 ± 0.0478

as $\mathcal{B}^{\text{uni}}_{\text{had}} = 1 - \mathcal{B}_e - \mathcal{B}_\mu$, and $\mathcal{B}_{\text{VA}}$ was obtained from $\mathcal{B}^{\text{uni}}_{\text{had}} - \mathcal{B}_s$. Here we use the direct experimental determination of $\mathcal{B}_{\text{VA}}$ for two reasons. First, both methods result in comparable uncertainties on $|V_{us}|$, since the better precision on $\mathcal{B}^{\text{uni}}_{\text{had}} = 1 - \mathcal{B}_e - \mathcal{B}_\mu$ is offset by increased correlations in the expressions $(1 - \mathcal{B}_e - \mathcal{B}_\mu)/\mathcal{B}^{\text{uni}}_e$ and $\mathcal{B}_s/(\mathcal{B}_{\text{had}} - \mathcal{B}_s)$ used in the $|V_{us}|$ calculation. Second, if there are unobserved τ hadronic decay modes, they will affect $\mathcal{B}_{\text{VA}}$ and $\mathcal{B}_s$ in a more asymmetric way when using unitarity.

Using the τ branching fraction fit results with their uncertainties and correlations (Sec. XII. A), we compute $\mathcal{B}_s = (2.908 \pm 0.048)\%$ (see Table 327) and $\mathcal{B}_{\text{VA}} = \mathcal{B}_{\text{had}} - \mathcal{B}_s = (61.83 \pm 0.10)\%$. PDG 2021 averages [9] are used for quantities other than the results of the HFLAV τ branching fractions fit; $|V_{ud}| = 0.97373 \pm 0.00031$ is taken from a 2020 updated determination [1657]. We obtain $|V_{us}|_{\tau s} = 0.2184 \pm 0.0021$, where the uncertainty includes a systematic error contribution of 0.0011 from the theory uncertainty on δR_{theory}. This value is 3.7σ lower than the value $|V_{us}|_{\text{uni}} = 0.2277 \pm 0.0013$ predicted from the CKM unitarity relation $(|V_{us}|_{\text{uni}})^2 = 1 - |V_{ud}|^2 - |V_{ub}|^2$. We also compute $(|V_{us}|/|V_{ud}|)_{\tau s} = 0.2243 \pm 0.0022$.

2. $|V_{us}|$ from $\mathcal{B}(\tau \to K\nu)/\mathcal{B}(\tau \to \pi\nu)$

We compute $|V_{us}|/|V_{ud}|$ from the ratio of branching fractions $\mathcal{B}(\tau \to K^-\nu_\tau)/\mathcal{B}(\tau \to \pi^-\nu_\tau) = (6.437 \pm 0.092) \times 10^{-2}$ using the equation [1658]:

$$\frac{\mathcal{B}(\tau^- \to K^-\nu_\tau)}{\mathcal{B}(\tau^- \to \pi^-\nu_\tau)} = \frac{f^2_{K\pm}|V_{us}|^2}{f^2_{\pi\pm}|V_{ud}|^2}\frac{(m_\tau^2 - m_K^2)^2}{(m_\tau^2 - m_\pi^2)^2}(1 + \delta R_{\tau K/\tau\pi}), \tag{341}$$

and we get $|V_{us}|/|V_{ud}| = 0.2289 \pm 0.0019$, using the ratio of decay constants $f_{K\pm}/f_{\pi\pm} = 1.1932 \pm 0.0021$ from the FLAG 2019 lattice QCD averages with $N_f = 2 + 1 + 1$ [209,1399,1400,1659,1660] and $\delta R_{\tau K/\tau\pi} = (0.10 \pm 0.80)\%$ [1580].

By using $|V_{ud}|$ [1657] we compute $|V_{us}|_{\tau K/\pi} = 0.2229 \pm 0.0019$, 2.1σ below the CKM unitarity prediction.

3. $|V_{us}|$ from $\mathcal{B}(\tau \to K\nu)$

We determine $|V_{us}|$ from the branching fraction $\mathcal{B}(\tau^- \to K^-\nu_\tau)$ using

$$\mathcal{B}(\tau^- \to K^-\nu_\tau) = \frac{G_F^2}{16\pi\hbar} f^2_{K\pm}|V_{us}|^2\tau_\tau m_\tau^3 \times \left(1 - \frac{m_K^2}{m_\tau^2}\right)^2 S_{\text{EW}}(1 + \delta R_{\tau K}). \tag{342}$$

We use $f_{K\pm} = 155.7 \pm 0.3$ MeV from the FLAG 2019 lattice QCD averages with $N_f = 2 + 1 + 1$ [209,1399,1660,1661], $S_{\text{EW}} = 1.02320 \pm 0.00030$ [1662] and $\delta R_{\tau K} = (-0.15 \pm 0.57)\%$ [1580]. We obtain $|V_{us}|_{\tau K} = 0.2219 \pm 0.0017$, which is 2.6σ below the CKM unitarity prediction. The physical constants G_F and $\hbar$ are taken from CODATA 2018 [1663]. This edition fixes a transcription error on the physical constants taken from PDG 2018 that caused an incorrect shift of the $|V_{us}|_{\tau K}$ determination by about $+0.5\sigma$ in the previous HFLAV report [1].

4. Summary of $|V_{us}|$ from τ decays

We summarize the $|V_{us}|$ results reporting the values, the discrepancy with respect to the $|V_{us}|$ determination from CKM unitarity, and an illustration of the measurement method:

$$|V_{us}|_{\text{uni}} = 0.2277 \pm 0.0013 \quad 0.0\sigma \quad \left[\sqrt{1 - |V_{ud}|^2 - |V_{ub}|^2}(\text{CKM unitarity})\right], \tag{343}$$

$$|V_{us}|_{\tau s} = 0.2184 \pm 0.0021 \quad -3.7\sigma \quad [\mathcal{B}(\tau^- \to X_s^-\nu_\tau)], \tag{344}$$

$$|V_{us}|_{\tau K/\pi} = 0.2229 \pm 0.0019 \quad -2.1\sigma \quad [\mathcal{B}(\tau^- \to K^-\nu_\tau)/\mathcal{B}(\tau^- \to \pi^-\nu_\tau)], \tag{345}$$

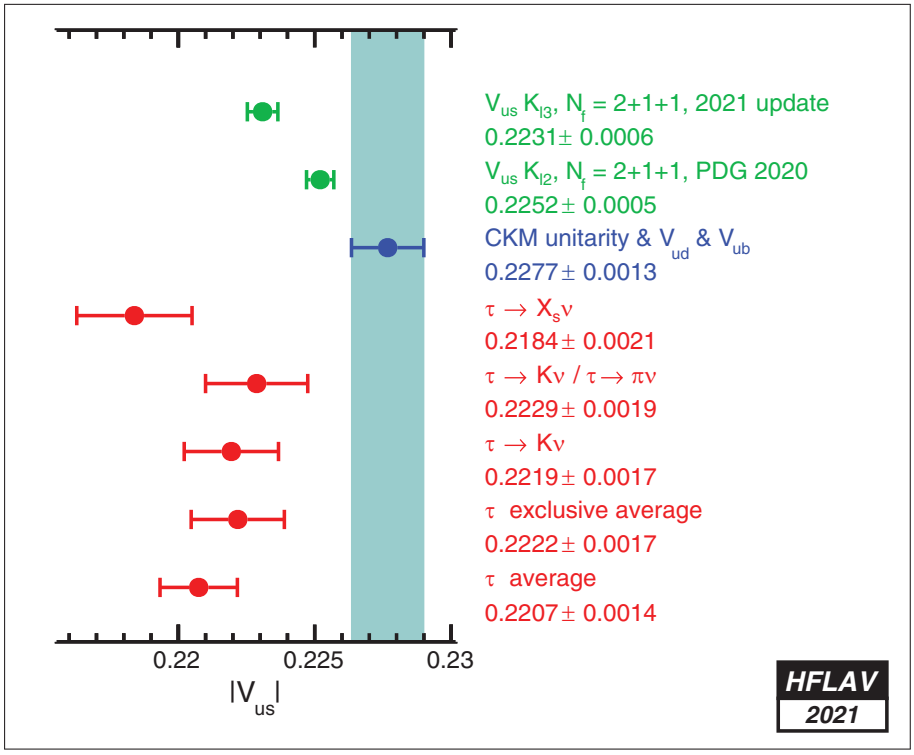

FIG. 104. $|V_{us}|$ determinations. In the CKM-unitarity evaluation, $|V_{ud}|$ is taken from a 2020 experimental update [1658]. The value $|V_{us}|_{K\ell 3}$ from $K^- \to \pi^0 \mu^- \bar{\nu}_\mu$ decays is taken from a 2021 update [1665]. The value $|V_{us}|_{K\ell 2}$ from $K^- \to \mu^- \bar{\nu}_\mu$ decays is taken from Ref. [9].

$$|V_{us}|_{\tau K} = 0.2219 \pm 0.0017 \quad -2.6\sigma \quad [\mathcal{B}(\tau^- \to K^- \nu_\tau)]. \tag{346}$$

Averaging the two $|V_{us}|$ determinations that rely on exclusive τ branching fractions, we obtain:

$$|V_{us}|_{\tau\,\mathrm{excl}} = 0.2222 + 0.0017 \quad -2.5\sigma \quad [\text{average of } \tau \text{ exclusive measurements}]. \tag{347}$$

Averaging the τ inclusive and exclusive $|V_{us}|$ determinations, we obtain:

$$|V_{us}|_{\tau} = 0.2207 \pm 0.0014 \quad -3.5\sigma \quad [\text{average of 3 } |V_{us}|\, \tau \text{ measurements}]. \tag{348}$$

In calculating the averages, the correlation between $f_{K\pm}$ and $f_{K\pm}/f_{\pi\pm}$ is taken to be zero, in absence of public information. Taking it to be $\pm 100\%$ varies the $|V_{us}|$ central value by about 8% of its uncertainty and the $|V_{us}|$ uncertainty by about 1% relative. From the purpose of estimating the correlations between $\delta R_{\tau K}$, $\delta R_{\tau\pi}$ and $\delta R_{\tau K/\tau\pi}$ we use the information [1580] that the uncertainties on $\delta R_{\tau K}$ and $\delta R_{\tau\pi}$ are uncorrelated to a good approximation and that $\delta R_{\tau K/\tau\pi} = \delta R_{\tau K} - \delta R_{\tau\pi}$.

All $|V_{us}|$ determinations based on measured τ branching fractions are lower than both the kaon and the CKM-unitarity determinations. This is correlated with the fact that the direct measurements of the three largest τ branching fractions to kaons [$\mathcal{B}(\tau^- \to K^- \nu_\tau)$, $\mathcal{B}(\tau^- \to K^- \pi^0 \nu_\tau)$ and $\mathcal{B}(\tau^- \to \pi^- \bar{K}^0 \nu_\tau)$] yield lower values than their SM predictions based on the branching fractions of leptonic kaon decays [1646,1665,1666].

Alternative determinations of $|V_{us}|$ from $\mathcal{B}(\tau \to X_s \nu)$ [1655,1656], based on partially different sets of experimental inputs, report $|V_{us}|$ values consistent with the unitarity determination.

Figure 104 reports our $|V_{us}|$ determinations using the τ branching fractions, compared to two determinations based on kaon data [9] and to the value obtained from $|V_{ud}|$ with CKM-matrix unitarity [9].

ACKNOWLEDGMENTS

We are grateful for the strong support of the ATLAS, *BABAR*, Belle, Belle II, BES III, CLEO(c), CDF, CMS, D0

and LHCb collaborations, without whom this compilation of results and world averages would not have been possible. The success of these experiments in turn would not have been possible without the excellent operations of the BEPC-II, CESR, KEKB, SuperKEKB, LHC, PEP-II, and Tevatron accelerators. We also recognize the interplay between theoretical and experimental communities that has provided a stimulus for many of the measurements in this document. We thank the CERN for providing computing resources and support to HFLAV in past years. Our averages and this compilation have benefitted greatly from contributions to the Heavy Flavor Averaging Group from numerous individuals. In particular, we would like to thank D. Martínez Santos and S. Esen for their valuable input to the averaging procedure of B_s^0 meson properties in decays through $b \to c\bar{c}s$ transitions. We also thank all past members of the HFLAV. We thank the following for their careful review of the text in preparing this paper for publication: H. Dembinski, M. Kirk, L. Grillo, S. Malde, E. Kou, F. De Fazio, S. Hashimoto, M. Smith, R. Fleischer, K. Trabelsi, A. Bharucha, J. Dalseno, J. Libby, S. Fajfer, R. Briere, G. Hiller, A. Rostomyan and P. Roig Garcés. Members of HFLAV are supported by the following funding agencies: Australian Research Council (Australia); Ministry of Science and Technology, National Natural Science Foundation, Key Research Program of Frontier Sciences of the Chinese Academy of Sciences (China); CNRS/IN2P3 (France); Deutsche Forschungsgemeinschaft (Germany); German-Israeli Foundation for Scientific research and Development, Israel Science Foundation, Ministry of Science and Technology, US-Israel Binational Science Fund (Israel); Istituto Nazionale di Fisica Nucleare (Italy); Ministry of Education, Culture, Sports, Science and Technology, Japan Society for the Promotion of Science (Japan); National Agency for Academic Exchange, Ministry of Science and Higher Education, National Science Centre (Poland); Swiss National Science Foundation (Switzerland); Science and Technology Facilities Council (UK); Department of Energy (USA); National Science Foundation (USA).

[1] Y. S. Amhis *et al.* (HFLAV Collaboration), Averages of b-hadron, c-hadron, and τ-lepton properties as of 2018, Eur. Phys. J. C **81**, 226 (2021).
[2] N. Cabibbo, Unitary Symmetry and Leptonic Decays, Phys. Rev. Lett. **10**, 531 (1963).
[3] M. Kobayashi and T. Maskawa, *CP* violation in the renormalizable theory of weak interaction, Prog. Theor. Phys. **49**, 652 (1973).
[4] D. Abbaneo *et al.*, Combined results on b-hadron production rates, lifetimes, oscillations and semileptonic decays, Report No. CERN-EP-2000-096; Report No. CERN-EP-2001-050.
[5] HFLAV web page, https://hflav.web.cern.ch.
[6] O. Schneider and H. Seywerd, COMBOS: A program to combine results from B oscillations analyses, https://gitlab.cern.ch/hflav/shared-material/-/blob/main/combos.pdf (1999).
[7] E. Bertholet and T. Kuhr, HFLAV averaging, https://gitlab.cern.ch/hflav/averaging (2022); 10.5281/zenodo.6632075.
[8] A. C. Aitken, On least squares and linear combination of observations, Proc. R. Soc. Edinburgh, Sect. A **55**, 42 (1936).
[9] P. A. Zyla *et al.* (Particle Data Group), Review of particle physics, Prog. Theor. Exp. Phys. **2020**, 083C01 (2020).
[10] R. Barlow, Asymmetric statistical errors, arXiv:physics/0406120.
[11] J. P. Alexander *et al.* (CLEO Collaboration), Measurement of the Relative Branching Fraction of $\Upsilon(4S)$ to Charged and Neutral B Meson Pairs, Phys. Rev. Lett. **86**, 2737 (2001).
[12] S. B. Athar *et al.* (CLEO Collaboration), Measurement of the ratio of branching fractions of the $\Upsilon(4S)$ to charged and neutral B mesons, Phys. Rev. D **66**, 052003 (2002).
[13] N. C. Hastings *et al.* (Belle Collaboration), Studies of $B^0 - \bar{B}^0$ mixing properties with inclusive dilepton events, Phys. Rev. D **67**, 052004 (2003).
[14] B. Aubert *et al.* (*BABAR* Collaboration), Measurement of Branching Fractions and Charge Asymmetries for Exclusive B Decays to Charmonium, Phys. Rev. Lett. **94**, 141801 (2005).
[15] B. Barish *et al.* (CLEO Collaboration), Measurement of the $\bar{B} \to D^* \ell \bar{\nu}$ branching fractions and $|V_{cb}|$, Phys. Rev. D **51**, 1014 (1995).
[16] B. Aubert *et al.* (*BABAR* Collaboration), Measurement of the Branching Fraction of $\Upsilon(4S) \to B^0\bar{B}^0$, Phys. Rev. Lett. **95**, 042001 (2005).
[17] B. Aubert *et al.* (*BABAR* Collaboration), Study of hadronic transitions between Upsilon states and observation of $\Upsilon(4S) \to \eta\Upsilon(1S)$ decay, Phys. Rev. D **78**, 112002 (2008).
[18] E. Guido *et al.* (Belle Collaboration), Study of η and dipion transitions in $\Upsilon(4S)$ decays to lower bottomonia, Phys. Rev. D **96**, 052005 (2017).
[19] E. Guido *et al.* (Belle Collaboration), Observation of $\Upsilon(4S) \to \eta'\Upsilon(1S)$, Phys. Rev. Lett. **121**, 062001 (2018).
[20] U. Tamponi *et al.* (Belle Collaboration), First Observation of the Hadronic Transition $\Upsilon(4S) \to \eta h_b(1P)$ and New Measurement of the $h_b(1P)$ and $\eta_b(1S)$ Parameters, Phys. Rev. Lett. **115**, 142001 (2015).
[21] A. E. Bondar, R. V. Mizuk, and M. B. Voloshin, Bottomonium-like states: Physics case for energy scan above the $B\bar{B}$ threshold at Belle-II, Mod. Phys. Lett. A **32**, 1750025 (2017).
[22] A. Drutskoy *et al.* (Belle Collaboration), Measurement of $\Upsilon(5S)$ decays to B^0 and B^+ mesons, Phys. Rev. D **81**, 112003 (2010).

[23] G. S. Huang *et al.* (CLEO Collaboration), Measurement of $\mathcal{B}(\Upsilon(5S) \to B_s^{(*)}\bar{B}_s^{(*)})$ using ϕ mesons, Phys. Rev. D **75**, 012002 (2007).

[24] A. Drutskoy *et al.* (Belle Collaboration), Measurement of Inclusive D_s, D^0 and J/ψ Rates and Determination of the $B_s^{(*)}\bar{B}_s^{(*)}$ Production Fraction in $b\bar{b}$ Events at the $\Upsilon(5S)$ Resonance, Phys. Rev. Lett. **98**, 052001 (2007).

[25] M. Artuso *et al.* (CLEO Collaboration), Evidence for $B_s^{(*)}\bar{B}_s^{(*)}$ Production at the $\Upsilon(5S)$ Resonance, Phys. Rev. Lett. **95**, 261801 (2005).

[26] A. Garmash *et al.* (Belle Collaboration), Amplitude analysis of $e^+e^- \to \Upsilon(nS)\pi^+\pi^-$ at $\sqrt{s} = 10.865$ GeV, Phys. Rev. D **91**, 072003 (2015).

[27] P. Krokovny *et al.* (Belle Collaboration), First observation of the $Z_b^0(10610)$ in a Dalitz analysis of $\Upsilon(10860) \to \Upsilon(\mathrm{nS})\pi^0\pi^0$, Phys. Rev. D **88**, 052016 (2013).

[28] I. Adachi *et al.* (Belle Collaboration), First Observation of the P-Wave Spin-Singlet Bottomonium States $h_b(1P)$ and $h_b(2P)$, Phys. Rev. Lett. **108**, 032001 (2012).

[29] X. H. He *et al.* (Belle Collaboration), Observation of $e^+e^- \to \pi^+\pi^-\pi^0\chi_{bJ}$ and Search for $X_b \to \omega\Upsilon(1S)$ at $\sqrt{s} = 10.867$ GeV, Phys. Rev. Lett. **113**, 142001 (2014).

[30] U. Tamponi *et al.* (Belle Collaboration), Inclusive study of bottomonium production in association with an η meson in e^+e^- annihilations near $\Upsilon(5S)$, Eur. Phys. J. C **78**, 633 (2018).

[31] S. Esen *et al.* (Belle Collaboration), Precise measurement of the branching fractions for $B_s \to D_s^{(*)+}D_s^{(*)-}$ and first measurement of the $D_s^{*+}D_s^{*-}$ polarization using e^+e^- collisions, Phys. Rev. D **87**, 031101 (2013).

[32] R. Louvot, Study of B_s meson production and measurement of B_s decays into a $D_s^{(*)-}$ and a light meson in e^+e^- collisions at $\sqrt{s} = 10.87$ GeV, Ph.D. thesis, École Polytechnique Fédérale De Lausanne, Lausanne, 2012, 10.5075/epfl-thesis-5213.

[33] J. P. Lees *et al.* (*BABAR* Collaboration), A measurement of the semileptonic branching fraction of the B_s^0 meson, Phys. Rev. D **85**, 011101 (2012).

[34] J. Li *et al.* (Belle Collaboration), Observation of $B_s^0 \to J/\psi f_0(980)$ and Evidence for $B_s^0 \to J/\psi f_0(1370)$, Phys. Rev. Lett. **106**, 121802 (2011).

[35] R. Louvot *et al.* (Belle Collaboration), Measurement of the Decay $B_s^0 \to D_s^-\pi^+$ and Evidence for $B_s^0 \to D_s^\mp K^\pm$ in e^+e^- Annihilation at $\sqrt{s} \simeq 10.87$ GeV, Phys. Rev. Lett. **102**, 021801 (2009).

[36] M. A. Shifman and M. B. Voloshin, Hierarchy of lifetimes of charmed and beautiful hadrons, Sov. Phys. JETP **64**, 698 (1986).

[37] J. Chay, H. Georgi, and B. Grinstein, Lepton energy distributions in heavy meson decays from QCD, Phys. Lett. B **247**, 399 (1990).

[38] I. I. Bigi, N. G. Uraltsev, and A. I. Vainshtein, Nonperturbative corrections to inclusive beauty and charm decays: QCD versus phenomenological models, Phys. Lett. B **293**, 430 (1992); **297**, 477(E) (1992).

[39] K. G. Wilson, Nonlagrangian models of current algebra, Phys. Rev. **179**, 1499 (1969).

[40] M. A. Shifman, Quark-hadron duality, in At The Frontier of Particle Physics (2001), pp. 1447–1494, 10.1142/9789812810458_0032.

[41] I. I. Y. Bigi and N. Uraltsev, A vademecum on quark hadron duality, Int. J. Mod. Phys. A **16**, 5201 (2001).

[42] T. Jubb, M. Kirk, A. Lenz, and G. Tetlalmatzi-Xolocotzi, On the ultimate precision of meson mixing observables, Nucl. Phys. **B915**, 431 (2017).

[43] M. B. Voloshin, Relations between inclusive decay rates of heavy baryons, Phys. Rep. **320**, 275 (1999); B. Guberina, B. Melic, and H. Stefancic, Enhancement of preasymptotic effects in inclusive beauty decays, Phys. Lett. B **469**, 253 (1999); M. Neubert and C. T. Sachrajda, Spectator effects in inclusive decays of beauty hadrons, Nucl. Phys. **B483**, 339 (1997); I. I. Y. Bigi, M. A. Shifman, and N. Uraltsev, Aspects of heavy quark theory, Annu. Rev. Nucl. Part. Sci. **47**, 591 (1997).

[44] M. Beneke, G. Buchalla, and I. Dunietz, Width difference in the $B_s - \bar{B}_s$ system, Phys. Rev. D **54**, 4419 (1996); **83**, 119902(E) (2011).

[45] A. Lenz and U. Nierste, Numerical updates of lifetimes and mixing parameters of B mesons, arXiv:1102.4274; Theoretical update of $B_s - \bar{B}_s$ mixing, J. High Energy Phys. 06 (2007) 072.

[46] M. Beneke, G. Buchalla, C. Greub, A. Lenz, and U. Nierste, Next-to-leading order QCD corrections to the lifetime difference of B_s mesons, Phys. Lett. B **459**, 631 (1999).

[47] M. Beneke, G. Buchalla, C. Greub, A. Lenz, and U. Nierste, The $B^+ - B_d^0$ lifetime difference beyond leading logarithms, Nucl. Phys. **B639**, 389 (2002).

[48] E. Franco, V. Lubicz, F. Mescia, and C. Tarantino, Lifetime ratios of beauty hadrons at the next-to-leading order in QCD, Nucl. Phys. **B633**, 212 (2002).

[49] M. Ciuchini, V. Lubicz, C. Tarantino, E. Franco, and F. Mescia, Lifetime differences and CP violation parameters of neutral B mesons at the next-to-leading order in QCD, J. High Energy Phys. 08 (2003) 031.

[50] M. Beneke, G. Buchalla, A. Lenz, and U. Nierste, CP asymmetry in flavor specific B decays beyond leading logarithms, Phys. Lett. B **576**, 173 (2003).

[51] M. Ciuchini, E. Franco, V. Lubicz, and F. Mescia, Next-to-leading order QCD corrections to spectator effects in lifetimes of beauty hadrons, Nucl. Phys. **B625**, 211 (2002).

[52] C. Tarantino, Beauty hadron lifetimes and B-meson CP-violation parameters from lattice QCD, Eur. Phys. J. C **33**, S895 (2004).

[53] F. Gabbiani, A. I. Onishchenko, and A. A. Petrov, Λ_b lifetime puzzle in heavy-quark expansion, Phys. Rev. D **68**, 114006 (2003).

[54] F. Gabbiani, A. I. Onishchenko, and A. A. Petrov, Spectator effects and lifetimes of heavy hadrons, Phys. Rev. D **70**, 094031 (2004).

[55] A. Lenz, Lifetimes and heavy quark expansion, Int. J. Mod. Phys. A **30**, 1543005 (2015).

[56] M. Kirk, A. Lenz, and T. Rauh, Dimension-six matrix elements for meson mixing and lifetimes from sum rules, J. High Energy Phys. 12 (2017) 068; 06 (2020) 162(E).

[57] J. Abdallah *et al.* (DELPHI Collaboration), A precise measurement of the B^+, B^0 and mean b-hadron lifetime with the DELPHI detector at LEP1, Eur. Phys. J. C **33**, 307 (2004).

[58] R. Barate *et al.* (ALEPH Collaboration), Measurement of the $\bar{B}^0$ and B^- meson lifetimes, Phys. Lett. B **492**, 275 (2000).

[59] D. Buskulic *et al.* (ALEPH Collaboration), Improved measurement of the $\bar{B}^0$ and B^- meson lifetimes, Z. Phys. C **71**, 31 (1996).

[60] P. Abreu *et al.* (DELPHI Collaboration), A measurement of B^+ and B^0 lifetimes using $\bar{D}\ell^+$ events, Z. Phys. C **68**, 13 (1995).

[61] W. Adam *et al.* (DELPHI Collaboration), Lifetimes of charged and neutral B hadrons using event topology, Z. Phys. C **68**, 363 (1995).

[62] P. Abreu *et al.* (DELPHI Collaboration), A precise measurement of the B_d^0 meson lifetime using a new technique, Z. Phys. C **74**, 19 (1997); **75**, 579(E) (1997).

[63] M. Acciarri *et al.* (L3 Collaboration), Upper limit on the lifetime difference of shortlived and longlived B_s^0 mesons, Phys. Lett. B **438**, 417 (1998).

[64] R. Akers *et al.* (OPAL Collaboration), Improved measurements of the B^0 and B^+ meson lifetimes, Z. Phys. C **67**, 379 (1995).

[65] G. Abbiendi *et al.* (OPAL Collaboration), Measurement of the B^+ and B^0 lifetimes and search for $CP(T)$ violation using reconstructed secondary vertices, Eur. Phys. J. C **12**, 609 (2000).

[66] G. Abbiendi *et al.* (OPAL Collaboration), Measurement of the B^0 lifetime and oscillation frequency using $\bar{B}^0 \to D^{*+}\ell^-\bar{\nu}$ decays, Phys. Lett. B **493**, 266 (2000).

[67] K. Abe *et al.* (SLD Collaboration), Measurement of the B^+ and B^0 Lifetimes Using Topological Reconstruction of Inclusive and Semileptonic Decays, Phys. Rev. Lett. **79**, 590 (1997).

[68] F. Abe *et al.* (CDF Collaboration), Improved measurement of the B^- and $\bar{B}^0$ meson lifetimes using semileptonic decays, Phys. Rev. D **58**, 092002 (1998).

[69] D. Acosta *et al.* (CDF Collaboration), Measurement of B meson lifetimes using fully reconstructed B decays produced in $p\bar{p}$ collisions at $\sqrt{s} = 1.8$ TeV, Phys. Rev. D **65**, 092009 (2002).

[70] T. Aaltonen *et al.* (CDF Collaboration), Measurement of b Hadron Lifetimes in Exclusive Decays Containing a J/ψ in $p\bar{p}$ Collisions at $\sqrt{s} = 1.96$ TeV, Phys. Rev. Lett. **106**, 121804 (2011).

[71] V. M. Abazov *et al.* (D0 Collaboration), Measurement of the Angular And Lifetime Parameters of the Decays $B_d^0 \to J/\psi K^{*0}$ and $B_s^0 \to J/\psi\phi$, Phys. Rev. Lett. **102**, 032001 (2009).

[72] V. M. Abazov *et al.* (D0 Collaboration), Measurement of the Λ_b^0 lifetime in the exclusive decay $\Lambda_b^0 \to J/\psi\Lambda^0$ in $p\bar{p}$ collisions at $\sqrt{s} = 1.96$ TeV, Phys. Rev. D **85**, 112003 (2012).

[73] V. M. Abazov *et al.* (D0 Collaboration), Measurement of the B_s^0 Lifetime in the Flavor-Specific Decay Channel $B_s^0 \to D_s^-\mu^+\nu X$, Phys. Rev. Lett. **114**, 062001 (2015).

[74] B. Aubert *et al.* (*BABAR* Collaboration), Measurement of the B^0 and B^+ Meson Lifetimes with Fully Reconstructed Hadronic Final States, Phys. Rev. Lett. **87**, 201803 (2001).

[75] B. Aubert *et al.* (*BABAR* Collaboration), Measurement of the B^0 Lifetime with Partially Reconstructed $B^0 \to D^{*-}\ell + \nu_\ell$ Decays, Phys. Rev. Lett. **89**, 011802 (2002); **89**, 169903(E) (2002).

[76] B. Aubert *et al.* (*BABAR* Collaboration), Simultaneous measurement of the B^0 meson lifetime and mixing frequency with $B^0 \to D^{*-}\ell^+\nu_\ell$ decays, Phys. Rev. D **67**, 072002 (2003).

[77] B. Aubert *et al.* (*BABAR* Collaboration), Measurement of the B^0 meson lifetime with partial reconstruction of $B^0 \to D^{*-}\pi^+$ and $B^0 \to D^{*-}\rho^+$ decays, Phys. Rev. D **67**, 091101 (2003).

[78] B. Aubert *et al.* (*BABAR* Collaboration), Measurement of the $\bar{B}^0$ lifetime and the $B^0\bar{B}^0$ oscillation frequency using partially reconstructed $\bar{B}^0 \to D^{*+}\ell^-\bar{\nu}_\ell$ decays, Phys. Rev. D **73**, 012004 (2006).

[79] K. Abe *et al.* (Belle Collaboration), Improved measurement of CP-violation parameters $\sin(2\phi_1)$ and $|\lambda|$, B meson lifetimes, and $B^0 - \bar{B}^0$ mixing parameter Δm_d, Phys. Rev. D **71**, 072003 (2005); **71**, 079903(E) (2005).

[80] G. Aad *et al.* (ATLAS Collaboration), Measurement of the Λ_b lifetime and mass in the ATLAS experiment, Phys. Rev. D **87**, 032002 (2013).

[81] A. M. Sirunyan *et al.* (CMS Collaboration), Measurement of b hadron lifetimes in pp collisions at $\sqrt{s} = 8$ TeV, Eur. Phys. J. C **78**, 457 (2018); **78**, 561(E) (2018).

[82] R. Aaij *et al.* (LHCb Collaboration), Measurements of the B^+, B^0, B_s^0 meson and Λ_b^0 baryon lifetimes, J. High Energy Phys. 04 (2014) 114.

[83] R. Aaij *et al.* (LHCb Collaboration), Effective lifetime measurements in the $B_s^0 \to K^+K^-$, $B^0 \to K^+\pi^-$ and $B_s^0 \to \pi^+K^-$ decays, Phys. Lett. B **736**, 446 (2014).

[84] T. Aaltonen *et al.* (CDF Collaboration), Measurement of the B^- lifetime using a simulation free approach for trigger bias correction, Phys. Rev. D **83**, 032008 (2011).

[85] V. M. Abazov *et al.* (D0 Collaboration), Measurement of the Ratio of B^+ and B^0 Meson Lifetimes, Phys. Rev. Lett. **94**, 182001 (2005).

[86] R. Aaij *et al.* (LHCb Collaboration), Determination of the Sign of the Decay Width Difference in the B_s^0 System, Phys. Rev. Lett. **108**, 241801 (2012).

[87] A. Lenz and G. Tetlalmatzi-Xolocotzi, Model-independent bounds on new physics effects in non-leptonic tree-level decays of B-mesons, J. High Energy Phys. 07 (2020) 177.

[88] M. Artuso, G. Borissov, and A. Lenz, CP violation in the B_s^0 system, Rev. Mod. Phys. **88**, 045002 (2016).

[89] S. Laplace, Z. Ligeti, Y. Nir, and G. Perez, Implications of the CP asymmetry in semileptonic B decay, Phys. Rev. D **65**, 094040 (2002).

[90] K. Hartkorn and H. G. Moser, A new method of measuring $\Delta\Gamma/\Gamma$ in the $B_s^0 - \bar{B}_s^0$ system, Eur. Phys. J. C **8**, 381 (1999).

[91] I. Dunietz, R. Fleischer, and U. Nierste, In pursuit of new physics with B_s decays, Phys. Rev. D **63**, 114015 (2001).

[92] R. Fleischer and R. Knegjens, Effective lifetimes of B_s decays and their constraints on the $B_s^0 - \bar{B}_s^0$ mixing parameters, Eur. Phys. J. C **71**, 1789 (2011).

[93] R. Aaij *et al.* (LHCb Collaboration), Measurement of the CP-violating phase ϕ_s from $B_s^0 \to J/\psi\pi^+\pi^-$ decays in 13 TeV pp collisions, Phys. Lett. B **797**, 134789 (2019).

[94] R. Barate *et al.* (ALEPH Collaboration), Study of B_s^0 oscillations and lifetime using fully reconstructed D_s^- decays, Eur. Phys. J. C **4**, 367 (1998).

[95] P. Abreu *et al.* (DELPHI Collaboration), Study of $B_s^0 - \bar{B}_s^0$ oscillations and B_s^0 lifetimes using hadronic decays of B_s^0 mesons, Eur. Phys. J. C **18**, 229 (2000).

[96] K. Ackerstaff *et al.* (OPAL Collaboration), A measurement of the B_s^0 lifetime using reconstructed D_s^- mesons, Eur. Phys. J. C **2**, 407 (1998).

[97] D. Buskulic *et al.* (ALEPH Collaboration), Study of the $B_s^0 - \bar{B}_s^0$ oscillation frequency using $D_s^-\ell^+$ combinations in Z decays, Phys. Lett. B **377**, 205 (1996).

[98] F. Abe *et al.* (CDF Collaboration), Measurement of the B_s^0 meson lifetime using semileptonic decays, Phys. Rev. D **59**, 032004 (1999).

[99] P. Abreu *et al.* (DELPHI Collaboration), Measurement of the B_s^0 lifetime and study of $B_s^0 - \bar{B}_s^0$ oscillations using $D_s\ell$ events, Eur. Phys. J. C **16**, 555 (2000).

[100] K. Ackerstaff *et al.* (OPAL Collaboration), Measurements of the B_s^0 and Λ_b^0 lifetimes, Phys. Lett. B **426**, 161 (1998).

[101] T. Aaltonen *et al.* (CDF Collaboration), Measurement of the B_s^0 Lifetime in Fully and Partially Reconstructed $B_s^0 \to D_s^-(\phi\pi^-)X$ Decays in $\bar{p}p$ Collisions at $\sqrt{s} = 1.96$ TeV, Phys. Rev. Lett. **107**, 272001 (2011).

[102] R. Aaij *et al.* (LHCb Collaboration), Measurement of the $\bar{B}_s^0 \to D_s^- D_s^+$ and $\bar{B}_s^0 \to D^- D_s^+$ Effective Lifetimes, Phys. Rev. Lett. **112**, 111802 (2014).

[103] R. Aaij *et al.* (LHCb Collaboration), Measurement of the $\bar{B}_s^0$ Meson Lifetime in $D_s^+\pi^-$ Decays, Phys. Rev. Lett. **113**, 172001 (2014).

[104] R. Aaij *et al.* (LHCb Collaboration), Measurement of B_s^0 and D_s^- Meson Lifetimes, Phys. Rev. Lett. **119**, 101801 (2017).

[105] F. Abe *et al.* (CDF Collaboration), Measurement of B hadron lifetimes using J/ψ final states at CDF, Phys. Rev. D **57**, 5382 (1998).

[106] V. M. Abazov *et al.* (D0 Collaboration), Measurement of the B_s^0 lifetime in the Exclusive Decay Channel $B_s^0 \to J/\psi\phi$, Phys. Rev. Lett. **94**, 042001 (2005).

[107] R. Aaij *et al.* (LHCb Collaboration), Analysis of Neutral B-Meson Decays into Two Muons, Phys. Rev. Lett. **128**, 041801 (2022); R. Aaij *et al.* (LHCb Collaboration), Measurement of the $B_s^0 \to \mu^+\mu^-$ decay properties and search for the $B^0 \to \mu^+\mu^-$ and $B_s^0 \to \mu^+\mu^-\gamma$ decays, Phys. Rev. D **105**, 012010 (2022).

[108] A. M. Sirunyan *et al.* (CMS Collaboration), Measurement of properties of $B_s^0 \to \mu^+\mu^-$ decays and search for $B^0 \to \mu^+\mu^-$ with the CMS experiment, J. High Energy Phys. 04 (2020) 188.

[109] R. Barate *et al.* (ALEPH Collaboration), A study of the decay width difference in the $B_s^0 - \bar{B}_s^0$ system using $\phi\phi$ correlations, Phys. Lett. B **486**, 286 (2000).

[110] R. Aaij *et al.* (LHCb Collaboration), Measurement of the effective $B_s^0 \to K^+K^-$ lifetime, Phys. Lett. B **707**, 349 (2012).

[111] R. Aaij *et al.* (LHCb Collaboration), Measurement of the $B_s^0 \to J/\psi\eta$ lifetime, Phys. Lett. B **762**, 484 (2016).

[112] R. Aaij *et al.* (LHCb Collaboration), Measurement of the effective $B_s^0 \to J/\psi K_S^0$ lifetime, Nucl. Phys. **B873**, 275 (2013).

[113] T. Aaltonen *et al.* (CDF Collaboration), Measurement of branching ratio and B_s^0 lifetime in the decay $B_s^0 \to J/\psi f_0(980)$ at CDF, Phys. Rev. D **84**, 052012 (2011).

[114] V. M. Abazov *et al.* (D0 Collaboration), B_s^0 lifetime measurement in the CP-odd decay channel $B_s^0 \to J/\psi f_0(980)$, Phys. Rev. D **94**, 012001 (2016).

[115] R. Aaij *et al.* (LHCb Collaboration), Measurement of CP violation and the B_s^0 meson decay width difference with $B_s^0 \to J/\psi K^+K^-$ and $B_s^0 \to J/\psi\pi^+\pi^-$ decays, Phys. Rev. D **87**, 112010 (2013).

[116] R. Aaij *et al.* (LHCb Collaboration), Measurement of the $\bar{B}^0 - B^0$ and $\bar{B}_s^0 - B_s^0$ production asymmetries in pp collisions at $\sqrt{s} = 7$ TeV, Phys. Lett. B **739**, 218 (2014).

[117] F. Abe *et al.* (CDF Collaboration), Observation of the B_c Meson in $p\bar{p}$ Collisions at $\sqrt{s} = 1.8$ TeV, Phys. Rev. Lett. **81**, 2432 (1998).

[118] A. Abulencia *et al.* (CDF Collaboration), Measurement of the B_c^+ Meson Lifetime Using $B_c^+ \to J/\psi e^+\nu_e$, Phys. Rev. Lett. **97**, 012002 (2006).

[119] V. M. Abazov *et al.* (D0 Collaboration), Measurement of the Lifetime of the $B_c^\pm$ Meson in the Semileptonic Decay Channel, Phys. Rev. Lett. **102**, 092001 (2009).

[120] T. Aaltonen *et al.* (CDF Collaboration), Measurement of the B_c^- meson lifetime in the decay $B_c^- \to J/\psi\pi^-$, Phys. Rev. D **87**, 011101 (2013).

[121] R. Aaij *et al.* (LHCb Collaboration), Measurement of the B_c^+ meson lifetime using $B_c^+ \to J/\psi\mu^+\nu_\mu X$ decays, Eur. Phys. J. C **74**, 2839 (2014).

[122] R. Aaij *et al.* (LHCb Collaboration), Measurement of the lifetime of the B_c^+ meson using the $B_c^+ \to J/\psi\pi^+$ decay mode, Phys. Lett. B **742**, 29 (2015).

[123] S. Schael *et al.* (ALEPH, CDF, DELPHI, L3, OPAL, and SLD Collaborations, LEP Electroweak Working Group, SLD Electroweak and Heavy Flavour Working Groups), Precision electroweak measurements on the Z resonance, Phys. Rep. **427**, 257 (2006).

[124] R. Barate *et al.* (ALEPH Collaboration), Measurement of the b baryon lifetime and branching fractions in Z decays, Eur. Phys. J. C **2**, 197 (1998).

[125] P. Abreu *et al.* (DELPHI Collaboration), Measurement of the lifetime of b baryons, Eur. Phys. J. C **10**, 185 (1999).

[126] P. Abreu *et al.* (DELPHI Collaboration), Determination of the average lifetime of b baryons, Z. Phys. C **71**, 199 (1996).

[127] R. Akers *et al.* (OPAL Collaboration), Measurement of the average b baryon lifetime and the product branching ratio $f(b \to \Lambda_b) \times \mathrm{BR}(\Lambda_b \to \Lambda\ell^-\bar{\nu}X)$, Z. Phys. C **69**, 195 (1996).

[128] F. Abe *et al.* (CDF Collaboration), Measurement of Λ_b^0 Lifetime Using $\Lambda_b^0 \to \Lambda_c^+\ell^-\bar{\nu}$, Phys. Rev. Lett. **77**, 1439 (1996).

[129] V. M. Abazov *et al.* (D0 Collaboration), Measurement of the Λ_b^0 Lifetime Using Semileptonic Decays, Phys. Rev. Lett. **99**, 182001 (2007).

[130] T. Aaltonen *et al.* (CDF Collaboration), Measurement of the Λ_b Lifetime in $\Lambda_b \to \Lambda_c^+ \pi^-$ Decays in $p\bar{p}$ Collisions at $\sqrt{s} = 1.96$ TeV, Phys. Rev. Lett. **104**, 102002 (2010).

[131] T. A. Aaltonen *et al.* (CDF Collaboration), Mass and lifetime measurements of bottom and charm baryons in $p\bar{p}$ collisions at $\sqrt{s} = 1.96$ TeV, Phys. Rev. D **89**, 072014 (2014).

[132] S. Chatrchyan *et al.* (CMS Collaboration), Measurement of the Λ_b^0 lifetime in pp collisions at $\sqrt{s} = 7$ TeV, J. High Energy Phys. 07 (2013) 163.

[133] R. Aaij *et al.* (LHCb Collaboration), Precision measurement of the ratio of the Λ_b^0 to $\bar{B}^0$ lifetimes, Phys. Lett. B **734**, 122 (2014).

[134] D. Buskulic *et al.* (ALEPH Collaboration), Strange b baryon production and lifetime in Z decays, Phys. Lett. B **384**, 449 (1996).

[135] P. Abreu *et al.* (DELPHI Collaboration), Production of strange B-baryons decaying into $\Xi^\mp - \ell^\mp$ pairs at LEP, Z. Phys. C **68**, 541 (1995).

[136] J. Abdallah *et al.* (DELPHI Collaboration), Production of Ξ_c^0 and Ξ_b in Z decays and lifetime measurement of Ξ_b, Eur. Phys. J. C **44**, 299 (2005).

[137] R. Aaij *et al.* (LHCb Collaboration), Measurement of the Ξ_b^- and Ω_b^- baryon lifetimes, Phys. Lett. B **736**, 154 (2014).

[138] R. Aaij *et al.* (LHCb Collaboration), Precision Measurement of the Mass and Lifetime of the Ξ_b^- Baryon, Phys. Rev. Lett. **113**, 242002 (2014).

[139] R. Aaij *et al.* (LHCb Collaboration), Precision Measurement of the Mass and Lifetime of the Ξ_b^0 Baryon, Phys. Rev. Lett. **113**, 032001 (2014).

[140] R. Aaij *et al.* (LHCb Collaboration), Measurement of the mass and lifetime of the Ω_b^- baryon, Phys. Rev. D **93**, 092007 (2016).

[141] Y.-Y. Keum and U. Nierste, Probing penguin coefficients with the lifetime ratio $\tau(B_s)/\tau(B_d)$, Phys. Rev. D **57**, 4282 (1998).

[142] N. G. Uraltsev, On the problem of boosting nonleptonic b baryon decays, Phys. Lett. B **376**, 303 (1996); D. Pirjol and N. Uraltsev, Four fermion heavy quark operators and light current amplitudes in heavy flavor hadrons, Phys. Rev. D **59**, 034012 (1999); P. Colangelo and F. De Fazio, Role of four-quark operators in the inclusive Λ_b decays, Phys. Lett. B **387**, 371 (1996); M. Di Pierro, C. T. Sachrajda, and C. Michael (UKQCD Collaboration), An exploratory lattice study of spectator effects in inclusive decays of the Λ_b baryon, Phys. Lett. B **468**, 143 (1999); **525**, 360(E) (2002).

[143] D. Buskulic *et al.* (ALEPH Collaboration), Improved measurement of the $B_d^0 - \bar{B}_d^0$ oscillation frequency, Z. Phys. C **75**, 397 (1997).

[144] P. Abreu *et al.* (DELPHI Collaboration), Measurement of $B_d^0 - \bar{B}_d^0$ oscillations, Z. Phys. C **76**, 579 (1997).

[145] J. Abdallah *et al.* (DELPHI Collaboration), Search for $B_s^0 - \bar{B}_s^0$ oscillations and a measurement of $B_d^0 - \bar{B}_d^0$ oscillations using events with an inclusively reconstructed vertex, Eur. Phys. J. C **28**, 155 (2003).

[146] M. Acciarri *et al.* (L3 Collaboration), Measurement of the $B_d^0 - \bar{B}_d^0$ oscillation frequency, Eur. Phys. J. C **5**, 195 (1998).

[147] K. Ackerstaff *et al.* (OPAL Collaboration), An updated study of B meson oscillations using dilepton events, Z. Phys. C **76**, 417 (1997).

[148] K. Ackerstaff *et al.* (OPAL Collaboration), A study of B meson oscillations using hadronic Z^0 decays containing leptons, Z. Phys. C **76**, 401 (1997).

[149] G. Alexander *et al.* (OPAL Collaboration), A measurement of the B_d^0 oscillation frequency using leptons and $D^{*\pm}$ mesons, Z. Phys. C **72**, 377 (1996).

[150] F. Abe *et al.* (CDF Collaboration), Measurement of the $B^0 - \bar{B}^0$ Oscillation Frequency Using πB Meson Charge-Flavor Correlations in $p\bar{p}$ Collisions at $\sqrt{s} = 1.8$ TeV, Phys. Rev. Lett. **80**, 2057 (1998); Measurement of the $B_d^0 - \bar{B}_d^0$ Flavor Oscillation Frequency and Study of Same Side Flavor Tagging of B Mesons in $p\bar{p}$ Collisions, Phys. Rev. D **59**, 032001 (1998).

[151] F. Abe *et al.* (CDF Collaboration), Measurement of the $B_d^0 - \bar{B}_d^0$ oscillation frequency using dimuon data in $p\bar{p}$ collisions at $\sqrt{s} = 1.8$ TeV, Phys. Rev. D **60**, 051101 (1999).

[152] F. Abe *et al.* (CDF Collaboration), Measurement of $B^0 - \bar{B}^0$ flavor oscillations using jet-charge and lepton flavor tagging in $p\bar{p}$ collisions at $\sqrt{s} = 1.8$ TeV, Phys. Rev. D **60**, 072003 (1999).

[153] T. Affolder *et al.* (CDF Collaboration), Measurement of the $B^0 - \bar{B}^0$ oscillation frequency using $\ell^- D^{*+}$ pairs and lepton flavor tags, Phys. Rev. D **60**, 112004 (1999).

[154] V. M. Abazov *et al.* (D0 Collaboration), Measurement of B_d mixing using opposite-side flavor tagging, Phys. Rev. D **74**, 112002 (2006).

[155] B. Aubert *et al.* (*BABAR* Collaboration), Measurement of $B^0 - \bar{B}^0$ Flavor Oscillations in Hadronic B^0 Decays, Phys. Rev. Lett. **88**, 221802 (2002); A study of time dependent CP-violating asymmetries and flavor oscillations in neutral B decays at the $\Upsilon(4S)$, Phys. Rev. D **66**, 032003 (2002).

[156] B. Aubert *et al.* (*BABAR* Collaboration), Measurement of the $B^0 - \bar{B}^0$ Oscillation Frequency with Inclusive Dilepton Events, Phys. Rev. Lett. **88**, 221803 (2002).

[157] Y. Zheng *et al.* (Belle Collaboration), Measurement of the $B^0 - \bar{B}^0$ mixing rate with $B^0(\bar{B}^0) \to D^{*\mp}\pi^\pm$ partial reconstruction, Phys. Rev. D **67**, 092004 (2003).

[158] LHCb Collaboration, Measurement of Δm_d in $B^0 \to D^-(K^+\pi^-\pi^-)\pi^+$, Report No. LHCb-CONF-2011-010, 2011, https://cdsweb.cern.ch/record/1331124, this result has been published in Ref. [198].

[159] R. Aaij *et al.* (LHCb Collaboration), Measurement of the $B^0 - \bar{B}^0$ oscillation frequency Δm_d with the decays $B^0 \to D^-\pi^+$ and $B^0 \to J/\psi K^{*0}$, Phys. Lett. B **719**, 318 (2013).

[160] R. Aaij *et al.* (LHCb Collaboration), Observation of $B_s^0 - \bar{B}_s^0$ mixing and measurement of mixing frequencies using semileptonic B decays, Eur. Phys. J. C **73**, 2655 (2013).

[161] R. Aaij *et al.* (LHCb Collaboration), A precise measurement of the B^0 meson oscillation frequency, Eur. Phys. J. C **76**, 412 (2016).

[162] H. Albrecht *et al.* (ARGUS Collaboration), A new determination of the $B^0 - \bar{B}^0$ oscillation strength, Z. Phys. C **55**, 357 (1992); H. Albrecht *et al.* (ARGUS Collaboration), A

study of $\bar{B}^0 \to D^{*+}\ell^-\bar{\nu}$ and $B^0\bar{B}^0$ mixing using partial D^{*+} reconstruction, Phys. Lett. B **324**, 249 (1994).
[163] J. E. Bartelt *et al.* (CLEO Collaboration), Two Measurements of $B^0 - \bar{B}^0$ Mixing, Phys. Rev. Lett. **71**, 1680 (1993).
[164] B. H. Behrens *et al.* (CLEO Collaboration), Precise measurement of $B^0\bar{B}^0$ mixing parameters at the $\Upsilon(4S)$, Phys. Lett. B **490**, 36 (2000).
[165] B. Aubert *et al.* (*BABAR* Collaboration), Limits on the Decay-Rate Difference of Neutral B Mesons and on CP, T, and CPT Violation in $B^0 - \bar{B}^0$ Oscillations, Phys. Rev. Lett. **92**, 181801 (2004); Limits on the decay-rate difference of neutral B mesons and on CP, T, and CPT violation in $B^0 - \bar{B}^0$ oscillations, Phys. Rev. D **70**, 012007 (2004).
[166] T. Higuchi *et al.* (Belle Collaboration), Search for time-dependent CPT violation in hadronic and semileptonic B decays, Phys. Rev. D **85**, 071105 (2012).
[167] T. Gershon, $\Delta\Gamma_d$: A forgotten null test of the standard model, J. Phys. G **38**, 015007 (2011); **42**, 119501(E) (2015).
[168] M. Aaboud *et al.* (ATLAS Collaboration), Measurement of the relative width difference of the $B^0 - \bar{B}^0$ system with the ATLAS detector, J. High Energy Phys. 06 (2016) 081.
[169] J. Charles *et al.*, Current status of the Standard Model CKM fit and constraints on $\Delta F = 2$ New Physics, Phys. Rev. D **91**, 073007 (2015); with updated results and plots available at http://ckmfitter.in2p3.fr; M. Bona *et al.* (UTfit Collaboration), The unitarity triangle fit in the standard model and hadronic parameters from lattice QCD: A reappraisal after the measurements of Δm_s and $\mathrm{BR}(B \to \tau\nu_\tau)$, J. High Energy Phys. 10 (2006) 081; with similar updated results and plots available at http://www.utfit.org.
[170] V. M. Abazov *et al.* (D0 Collaboration), Study of CP-violating charge asymmetries of single muons and like-sign dimuons in $p\bar{p}$ collisions, Phys. Rev. D **89**, 012002 (2014).
[171] U. Nierste, Effect of $\Delta\Gamma$ on the dimuon asymmetry in B decays, in *Proceedings of the 8th International Workshop on the CKM unitarity triangle (CKM 2014)* (2014), http://indico.cern.ch/event/253826/contributions/567426/.
[172] T. Aaltonen *et al.* (CDF Collaboration), Measurement of the Bottom-Strange Meson Mixing Phase in the Full CDF Data Set, Phys. Rev. Lett. **109**, 171802 (2012).
[173] V. M. Abazov *et al.* (D0 Collaboration), Measurement of the CP-violating phase $\phi_s^{J/\psi\phi}$ using the flavor-tagged decay $B_s^0 \to J/\psi\phi$ in 8 fb^{-1} of $p\bar{p}$ collisions, Phys. Rev. D **85**, 032006 (2012).
[174] G. Aad *et al.* (ATLAS Collaboration), Flavour tagged time dependent angular analysis of the $B_s \to J/\psi\phi$ decay and extraction of $\Delta\Gamma$ and the weak phase ϕ_s in ATLAS, Phys. Rev. D **90**, 052007 (2014).
[175] G. Aad *et al.* (ATLAS Collaboration), Measurement of the CP-violating phase ϕ_s and the B_s^0 meson decay width difference with $B_s^0 \to J/\psi\phi$ decays in ATLAS, J. High Energy Phys. 08 (2016) 147.
[176] G. Aad *et al.* (ATLAS Collaboration), Measurement of the CP-violating phase ϕ_s in $B_s^0 \to J/\psi\phi$ decays in ATLAS at 13 TeV, Eur. Phys. J. C **81**, 342 (2021).
[177] V. Khachatryan *et al.* (CMS Collaboration), Measurement of the CP-violating weak phase ϕ_s and the decay width difference $\Delta\Gamma_s$ using the $B_s^0 \to J/\psi\phi(1020)$ decay channel in pp collisions at $\sqrt{s} = 8$ TeV, Phys. Lett. B **757**, 97 (2016).
[178] A. M. Sirunyan *et al.* (CMS Collaboration), Measurement of the CP-violating phase ϕ_s in the $B_s^0 \to J/\psi\phi(1020) \to \mu^+\mu^-K^+K^-$ channel in proton-proton collisions at $\sqrt{s} = 13$ TeV, Phys. Lett. B **816**, 136188 (2021).
[179] R. Aaij *et al.* (LHCb Collaboration), Precision Measurement of CP Violation in $B_s^0 \to J/\psi K^+K^-$ Decays, Phys. Rev. Lett. **114**, 041801 (2015).
[180] R. Aaij *et al.* (LHCb Collaboration), Resonances and CP violation in B_s^0 and $\bar{B}_s^0 \to J/\psi K^+K^-$ decays in the mass region above the $\phi(1020)$, J. High Energy Phys. 08 (2017) 037.
[181] R. Aaij *et al.* (LHCb Collaboration), First study of the CP-violating phase and decay-width difference in $B_s^0 \to \psi(2S)\phi$ decays, Phys. Lett. B **762**, 253 (2016).
[182] R. Aaij *et al.* (LHCb Collaboration), First measurement of the CP-violating phase in $B_s^0 \to J/\psi(\to e^+e^-)\phi$ decays, Eur. Phys. J. C **81**, 1026 (2021).
[183] R. Aaij *et al.* (LHCb Collaboration), Updated measurement of time-dependent CP-violating observables in $B_s^0 \to J/\psi K^+K^-$ decays, Eur. Phys. J. C **79**, 706 (2019); **80**, 601 (E) (2020).
[184] A. Lenz, Theoretical update of B-mixing and lifetimes, arXiv:1205.1444.
[185] S. Esen *et al.* (Belle Collaboration), Observation of $B_s^0 \to D_s^{(*)+}D_s^{(*)-}$ Using e^+e^- Collisions and a Determination of the $B_s - \bar{B}_s$ Width Difference $\Delta\Gamma_s$, Phys. Rev. Lett. **105**, 201802 (2010).
[186] V. M. Abazov *et al.* (D0 Collaboration), Evidence for Decay $B_s^0 \to D_s^{(*)}D_s^{(*)}$ and a Measurement of $\Delta\Gamma_s^{CP}/\Gamma_s$, Phys. Rev. Lett. **102**, 091801 (2009).
[187] T. Aaltonen *et al.* (CDF Collaboration), First Observation of the Decay $B_s^0 \to D_s^-D_s^+$ and Measurement of its Branching Ratio, Phys. Rev. Lett. **100**, 021803 (2008).
[188] T. Aaltonen *et al.* (CDF Collaboration), Measurement of $B_s^0 \to D_s^{(*)+}D_s^{(*)-}$ Branching Ratios, Phys. Rev. Lett. **108**, 201801 (2012).
[189] A. Heister *et al.* (ALEPH Collaboration), Improved search for $B_s^0 - \bar{B}_s^0$ oscillations, Eur. Phys. J. C **29**, 143 (2003).
[190] J. Abdallah *et al.* (DELPHI Collaboration), Search for $B_s^0 - \bar{B}_s^0$ oscillations in DELPHI using high-p_t leptons, Eur. Phys. J. C **35**, 35 (2004).
[191] G. Abbiendi *et al.* (OPAL Collaboration), A study of B_s^0 meson oscillation using hadronic Z^0 decays containing leptons, Eur. Phys. J. C **11**, 587 (1999).
[192] G. Abbiendi *et al.* (OPAL Collaboration), A study of B_s meson oscillation using D_s-lepton correlations, Eur. Phys. J. C **19**, 241 (2001).
[193] K. Abe *et al.* (SLD Collaboration), Search for time-dependent $B_s^0 - \bar{B}_s^0$ oscillations using a vertex charge dipole technique, Phys. Rev. D **67**, 012006 (2003).
[194] K. Abe *et al.* (SLD Collaboration), A search for time-dependent $B_s^0 - \bar{B}_s^0$ oscillations using exclusively reconstructed $D_s^\pm$ mesons, Phys. Rev. D **66**, 032009 (2002).

[195] F. Abe *et al.* (CDF Collaboration), A Search for $B_s^0 - \bar{B}_s^0$ Oscillations Using the Semileptonic Decay $B_s^0 \to \phi \ell^+ X \nu$, Phys. Rev. Lett. **82**, 3576 (1999).

[196] V. M. Abazov *et al.* (D0 Collaboration), First Direct Two-Sided Bound on the B_s^0 Oscillation Frequency, Phys. Rev. Lett. **97**, 021802 (2006).

[197] A. Abulencia *et al.* (CDF Collaboration), Observation of $B_s^0 - \bar{B}_s^0$ Oscillations, Phys. Rev. Lett. **97**, 242003 (2006).

[198] R. Aaij *et al.* (LHCb Collaboration), Measurement of the $B_s^0 - \bar{B}_s^0$ oscillation frequency Δm_s in $B_s^0 \to D_s^-(3)\pi$ decays, Phys. Lett. B **709**, 177 (2012).

[199] R. Aaij *et al.* (LHCb Collaboration), Precision measurement of the $B_s^0 - \bar{B}_s^0$ oscillation frequency with the decay $B_s^0 \to D_s^- \pi^+$, New J. Phys. **15**, 053021 (2013).

[200] R. Aaij *et al.* (LHCb Collaboration), Measurement of the CKM angle γ and $B_s^0 - \bar{B}_s^0$ mixing frequency with $B_s^0 \to D_s^\mp h^\pm \pi^\pm \pi^\mp$ decays, J. High Energy Phys. 03 (2021) 137.

[201] R. Aaij *et al.* (LHCb Collaboration), Precise determination of the $B_s^0 - \bar{B}_s^0$ oscillation frequency, Nat. Phys. **18**, 1 (2022).

[202] L. Di Luzio, M. Kirk, A. Lenz, and T. Rauh, ΔM_s theory precision confronts flavour anomalies, J. High Energy Phys. 12 (2019) 009.

[203] A. Bazavov *et al.* (Fermilab Lattice and MILC Collaborations), $B_{(s)}^0$-mixing matrix elements from lattice QCD for the Standard Model and beyond, Phys. Rev. D **93**, 113016 (2016).

[204] A. G. Grozin, R. Klein, T. Mannel, and A. A. Pivovarov, $B^0 - \bar{B}^0$ mixing at next-to-leading order, Phys. Rev. D **94**, 034024 (2016).

[205] P. A. Boyle *et al.* (RBC/UKQCD Collaboration), SU(3)-breaking ratios for $D_{(s)}$ and $B_{(s)}$ mesons, arXiv:1812.08791.

[206] D. King, A. Lenz, and T. Rauh, B_s mixing observables and $|V_{td}/V_{ts}|$ from sum rules, J. High Energy Phys. 05 (2019) 034.

[207] R. J. Dowdall, C. T. H. Davies, R. R. Horgan, G. P. Lepage, C. J. Monahan, J. Shigemitsu, and M. Wingate, Neutral B-meson mixing from full lattice QCD at the physical point, Phys. Rev. D **100**, 094508 (2019).

[208] C. T. H. Davies, J. Harrison, G. Peter Lepage, C. J. Monahan, J. Shigemitsu, and M. Wingate (HPQCD Collaboration), Lattice QCD Matrix Elements for the $B_s^0 - \bar{B}_s^0$ Width Difference Beyond Leading Order, Phys. Rev. Lett. **124**, 082001 (2020).

[209] S. Aoki *et al.* (FLAG Collaboration), FLAG review 2019, arXiv:1902.08191.

[210] D. E. Jaffe *et al.* (CLEO Collaboration), Bounds on the CP Asymmetry in Like Sign Dileptons from $B^0\bar{B}^0$ Meson Decays, Phys. Rev. Lett. **86**, 5000 (2001).

[211] J. P. Lees *et al.* (*BABAR* Collaboration), Study of CP Asymmetry in $B^0 - \bar{B}^0$ Mixing with Inclusive Dilepton Events, Phys. Rev. Lett. **114**, 081801 (2015).

[212] F. Abe *et al.* (CDF Collaboration), Measurement of $b\bar{b}$ production correlations, $B^0\bar{B}^0$ mixing, and a limit on $\epsilon(B)$ in $p\bar{p}$ collisions at $\sqrt{s} = 1.8$ TeV, Phys. Rev. D **55**, 2546 (1997).

[213] R. Barate *et al.* (ALEPH Collaboration), Investigation of inclusive CP asymmetries in B^0 decays, Eur. Phys. J. C **20**, 431 (2001).

[214] J. P. Lees *et al.* (*BABAR* Collaboration), Search for CP Violation in $B^0 - \bar{B}^0$ Mixing Using Partial Reconstruction of $B^0 \to D^{*-} X \ell^+ \nu_\ell$ and a Kaon Tag, Phys. Rev. Lett. **111**, 101802 (2013); **111**, 159901(E) (2013).

[215] B. Aubert *et al.* (*BABAR* Collaboration), Search for T, CP and CPT Violation in $B^0 - \bar{B}^0$ Mixing with Inclusive Dilepton Events, Phys. Rev. Lett. **96**, 251802 (2006).

[216] E. Nakano *et al.* (Belle Collaboration), Charge asymmetry of same-sign dileptons in $B^0 - \bar{B}^0$ mixing, Phys. Rev. D **73**, 112002 (2006).

[217] M. Beneke, G. Buchalla, and I. Dunietz, Mixing induced CP asymmetries in inclusive B decays, Phys. Lett. B **393**, 132 (1997); I. Dunietz, CP asymmetries in semiinclusive B^0 decays, Eur. Phys. J. C **7**, 197 (1999).

[218] V. M. Abazov *et al.* (D0 Collaboration), Measurement of the semileptonic charge asymmetry in B^0 meson mixing with the D0 detector, Phys. Rev. D **86**, 072009 (2012).

[219] R. Aaij *et al.* (LHCb Collaboration), Measurement of the Semileptonic CP Asymmetry in $B^0 - \bar{B}^0$ Mixing, Phys. Rev. Lett. **114**, 041601 (2015).

[220] V. M. Abazov *et al.* (D0 Collaboration), Measurement of the CP-violation parameter of B^0 mixing and decay with $p\bar{p} \to \mu\mu X$ data, Phys. Rev. D **74**, 092001 (2006).

[221] Y. Amhis *et al.*, Averages of b-hadron, c-hadron, and τ-lepton properties as of early 2012, arXiv:1207.1158.

[222] V. M. Abazov *et al.* (D0 Collaboration), Measurement of the Semileptonic Charge Asymmetry Using $B_s^0 \to D_s \mu X$ Decays, Phys. Rev. Lett. **110**, 011801 (2013).

[223] R. Aaij *et al.* (LHCb Collaboration), Measurement of the CP Asymmetry in $B_s^0 - \bar{B}_s^0$ Mixing, Phys. Rev. Lett. **117**, 061803 (2016).

[224] A. Lenz (private communication).

[225] S. Descotes-Genon and J. F. Kamenik, A possible explanation of the D0 like-sign dimuon charge asymmetry, Phys. Rev. D **87**, 074036 (2013); **92**, 079903(E) (2015).

[226] M. Aaboud *et al.* (ATLAS Collaboration), Measurements of charge and CP asymmetries in b-hadron decays using top-quark events collected by the ATLAS detector in pp collisions at $\sqrt{s} = 8$ TeV, J. High Energy Phys. 02 (2017) 071.

[227] R. Aaij *et al.* (LHCb Collaboration), Measurement of the CP-violating phase ϕ_s in $\bar{B}_s^0 \to J/\psi\pi^+\pi^-$ decays, Phys. Lett. B **736**, 186 (2014).

[228] R. Aaij *et al.* (LHCb Collaboration), Analysis of the resonant components in $B_s \to J/\psi\pi^+\pi^-$, Phys. Rev. D **86**, 052006 (2012).

[229] R. Aaij *et al.* (LHCb Collaboration), Measurement of the CP-Violating Phase ϕ_s in $\bar{B}_s^0 \to D_s^+ D_s^-$ Decays, Phys. Rev. Lett. **113**, 211801 (2014).

[230] P. Frings, U. Nierste, and M. Wiebusch, Penguin Contributions to CP Phases in $B_{d,s}$ Decays to Charmonium, Phys. Rev. Lett. **115**, 061802 (2015).

[231] R. Aaij *et al.* (LHCb Collaboration), Measurement of the CP-violating phase β in $B^0 \to J/\psi\pi^+\pi^-$ decays and limits on penguin effects, Phys. Lett. B **742**, 38 (2015).

[232] R. Aaij *et al.* (LHCb Collaboration), Measurement of CP violation parameters and polarisation fractions in $B_s^0 \to J/\psi \bar{K}^{*0}$ decays, J. High Energy Phys. 11 (2015) 082.

[233] R. Aaij *et al.* (LHCb Collaboration), Determination of γ and $-2\beta_s$ from charmless two-body decays of beauty mesons, Phys. Lett. B **741**, 1 (2015).

[234] L.-L. Chau and W.-Y. Keung, Comments on the Parametrization of the Kobayashi-Maskawa Matrix, Phys. Rev. Lett. **53**, 1802 (1984).

[235] L. Wolfenstein, Parametrization of the Kobayashi-Maskawa Matrix, Phys. Rev. Lett. **51**, 1945 (1983).

[236] A. J. Buras, M. E. Lautenbacher, and G. Ostermaier, Waiting for the top quark mass, $K^+ \to \pi^+ \nu\bar{\nu}$, $B_s^0 - \bar{B}_s^0$ mixing and CP asymmetries in B decays, Phys. Rev. D **50**, 3433 (1994).

[237] C. Jarlskog, Commutator of the Quark Mass Matrices in the Standard Electroweak Model and a Measure of Maximal CP Violation, Phys. Rev. Lett. **55**, 1039 (1985).

[238] C. Jarlskog, The quark mixing matrix with manifest Cabibbo substructure and an angle of the unitarity triangle as one of its parameters, Phys. Lett. B **615**, 207 (2005).

[239] P. F. Harrison, S. Dallison, and W. G. Scott, The matrix of unitarity triangle angles for quarks, Phys. Lett. B **680**, 328 (2009).

[240] P. H. Frampton and X.-G. He, Unitarity boomerang, Phys. Lett. B **688**, 67 (2010).

[241] P. H. Frampton and X.-G. He, Hunting for new physics with unitarity boomerangs, Phys. Rev. D **82**, 017301 (2010).

[242] J. Charles, A. Höcker, H. Lacker, S. Laplace, F. R. Le Diberder, J. Malclés, J. Ocariz, M. Pivk, and L. Roos, CP violation and the CKM matrix: Assessing the impact of the asymmetric B factories, Eur. Phys. J. C **41**, 1 (2005); updated results and plots available at: http://ckmfitter.in2p3.fr.

[243] B. Aubert *et al.* (*BABAR* Collaboration), Measurement of CP Violating Asymmetries in B^0 Decays to CP Eigenstates, Phys. Rev. Lett. **86**, 2515 (2001).

[244] R. Aaij *et al.* (LHCb Collaboration), Measurement of the time-dependent CP asymmetry in $B^0 \to J/\psi K_S^0$ decays, Phys. Lett. B **721**, 24 (2013).

[245] K. Abe *et al.* (Belle Collaboration), Observation of Large CP Violation in the Neutral B Meson System, Phys. Rev. Lett. **87**, 091802 (2001).

[246] A. B. Carter and A. I. Sanda, CP violation in B meson decays, Phys. Rev. D **23**, 1567 (1981).

[247] I. I. Y. Bigi and A. I. Sanda, Notes on the observability of CP violations in B decays, Nucl. Phys. **B193**, 85 (1981).

[248] B. Aubert *et al.* (*BABAR* Collaboration), Measurements of time-dependent CP asymmetries in $B^0 \to D^{*+}D^{*-}$ decays, Phys. Rev. D **79**, 032002 (2009).

[249] P. Krokovny *et al.* (Belle Collaboration), Measurement of the Quark Mixing Parameter $\cos 2\phi_1$ Using Time-Dependent Dalitz Analysis of $\bar{B}^0 \to D(K_S^0\pi^+\pi^-)h^0$, Phys. Rev. Lett. **97**, 081801 (2006).

[250] B. Aubert *et al.* (*BABAR* Collaboration), Measurement of $\cos 2\beta$ in $B^0 \to D^{(*)}h^0$ Decays with a Time-Dependent Dalitz Plot Analysis of $D \to K_s^0\pi^+\pi^-$, Phys. Rev. Lett. **99**, 231802 (2007).

[251] I. Adachi *et al.*, First Evidence for $\cos 2\beta > 0$ and Resolution of the Cabibbo-Kobayashi-Maskawa Quark-Mixing Unitarity Triangle Ambiguity, Phys. Rev. Lett. **121**, 261801 (2018).

[252] I. Adachi *et al.*, Measurement of $\cos 2\beta$ in $B^0 \to D^{(*)}h^0$ with $D \to K_S^0\pi^+\pi^-$ decays by a combined time-dependent Dalitz plot analysis of *BABAR* and Belle data, Phys. Rev. D **98**, 112012 (2018).

[253] V. Vorobyev *et al.* (Belle Collaboration), Measurement of the CKM angle φ_1 in $B^0 \to \bar{D}^{(*)0}h^0$, $\bar{D}^0 \to K_S^0\pi^+\pi^-$ decays with time-dependent binned Dalitz plot analysis, Phys. Rev. D **94**, 052004 (2016).

[254] J. Libby *et al.* (CLEO Collaboration), Model-independent determination of the strong-phase difference between D^0 and $\bar{D}^0 \to K_{S,L}^0 h^+h^-$ ($h = \pi$, K) and its impact on the measurement of the CKM angle γ/ϕ_3, Phys. Rev. D **82**, 112006 (2010).

[255] T. E. Browder, A. Datta, P. J. O'Donnell, and S. Pakvasa, Measuring $\sin(2\beta)$ in $B \to D^{*+}D^{*-}K_s$ decays, Phys. Rev. D **61**, 054009 (2000).

[256] B. Aubert *et al.* (*BABAR* Collaboration), Measurement of the branching fraction and time-dependent CP asymmetry in the decay $B^0 \to D^{*+}D^{*-}K_S^0$, Phys. Rev. D **74**, 091101 (2006).

[257] J. Dalseno *et al.* (Belle Collaboration), Measurement of branching fraction and time-dependent CP asymmetry parameters in $B^0 \to D^{*+}D^{*-}K_s^0$ decays, Phys. Rev. D **76**, 072004 (2007).

[258] R. Aaij *et al.* (LHCb Collaboration), Measurement of the resonant and CP components in $\bar{B}^0 \to J/\psi\pi^+\pi^-$ decays, Phys. Rev. D **90**, 012003 (2014).

[259] J. R. Pelaez, From controversy to precision on the sigma meson: A review on the status of the non-ordinary $f_0(500)$ resonance, Phys. Rep. **658**, 1 (2016).

[260] B. Aubert *et al.* (*BABAR* Collaboration), Measurements of CP-Violating Asymmetries in the Decay $B^0 \to K^+K^-K^0$, Phys. Rev. Lett. **99**, 161802 (2007).

[261] Y. Nakahama *et al.* (Belle Collaboration), Measurement of CP violating asymmetries in $B^0 \to K^+K^-K_S^0$ decays with a time-dependent Dalitz approach, Phys. Rev. D **82**, 073011 (2010).

[262] J. P. Lees *et al.* (*BABAR* Collaboration), Study of CP violation in Dalitz-plot analyses of $B^0 \to K^+K^-K_S^0$, $B^+ \to K^+K^-K^+$, and $B^+ \to K_S^0K_S^0K^+$, Phys. Rev. D **85**, 112010 (2012).

[263] A. Garmash *et al.* (Belle Collaboration), Dalitz analysis of the three-body charmless decays $B^+ \to K^+\pi^+\pi^-$ and $B^+ \to K^+K^+K^-$, Phys. Rev. D **71**, 092003 (2005).

[264] B. Aubert *et al.* (*BABAR* Collaboration), Dalitz plot analysis of the decay $B^\pm \to K^\pm K^\pm K^\mp$, Phys. Rev. D **74**, 032003 (2006).

[265] B. Aubert *et al.* (*BABAR* Collaboration), Time-dependent amplitude analysis of $B^0 \to K_S^0\pi^+\pi^-$, Phys. Rev. D **80**, 112001 (2009).

[266] J. Dalseno *et al.* (Belle Collaboration), Time-dependent Dalitz plot measurement of CP parameters in $B^0 \to K_S^0\pi^+\pi^-$ decays, Phys. Rev. D **79**, 072004 (2009).

[267] A. Garmash *et al.* (Belle Collaboration), Evidence for Large Direct CP Violation in $B^\pm \to \rho(770)^0K^\pm$ from Analysis of the Three-Body Charmless $B^\pm \to K^\pm\pi^\pm\pi^\mp$ Decay, Phys. Rev. Lett. **96**, 251803 (2006).

[268] B. Aubert *et al.* (*BABAR* Collaboration), Dalitz-plot analysis of the decays $B^{\pm} \to K^{\pm}\pi^{\mp}\pi^{\pm}$, Phys. Rev. D **72**, 072003 (2005); **74**, 099903(E) (2006).

[269] B. Aubert *et al.* (*BABAR* Collaboration), Evidence for direct *CP* violation from Dalitz-plot analysis of $B^{\pm} \to K^{\pm}\pi^{\mp}\pi^{\pm}$, Phys. Rev. D **78**, 012004 (2008).

[270] A. E. Snyder and H. R. Quinn, Measuring *CP* asymmetry in $B \to \rho\pi$ decays without ambiguities, Phys. Rev. D **48**, 2139 (1993).

[271] H. R. Quinn and J. P. Silva, The use of early data on $B \to \rho\pi$ decays, Phys. Rev. D **62**, 054002 (2000).

[272] B. Aubert *et al.* (*BABAR* Collaboration), Measurement of *CP*-violating asymmetries in $B^0 \to (\rho\pi)^0$ using a time-dependent Dalitz plot analysis, Phys. Rev. D **76**, 012004 (2007).

[273] J. P. Lees *et al.* (*BABAR* Collaboration), Measurement of *CP*-violating asymmetries in $B^0 \to (\rho\pi)^0$ decays using a time-dependent Dalitz plot analysis, Phys. Rev. D **88**, 012003 (2013).

[274] A. Kusaka *et al.* (Belle Collaboration), Measurement of *CP* Asymmetry in a Time-Dependent Dalitz Analysis of $B0 \to (\rho\pi)^0$ and a Constraint on the Quark Mixing Matrix Angle ϕ_2, Phys. Rev. Lett. **98**, 221602 (2007).

[275] A. Kusaka *et al.* (Belle Collaboration), Measurement of *CP* asymmetries and branching fractions in a time-dependent Dalitz analysis of $B^0 \to (\rho\pi)^0$ and a constraint on the quark mixing angle ϕ_2, Phys. Rev. D **77**, 072001 (2008).

[276] B. Aubert *et al.* (*BABAR* Collaboration), Measurement of *CP*-Violating Asymmetries in $B^0 \to D^{(*)\pm}D^{\mp}$, Phys. Rev. Lett. **99**, 071801 (2007).

[277] T. Aushev *et al.* (Belle Collaboration), Search for *CP* Violation in the Decay $B^0 \to D^{*\pm}D^{\mp}$, Phys. Rev. Lett. **93**, 201802 (2004).

[278] M. Rohrken *et al.* (Belle Collaboration), Measurements of branching fractions and time-dependent *CP* violating asymmetries in $B^0 \to D^{(*)\pm}D^{\mp}$ decays, Phys. Rev. D **85**, 091106 (2012).

[279] B. Aubert *et al.* (*BABAR* Collaboration), Measurements of Branching Fractions and *CP*-Violating Asymmetries in $B^0 \to \rho^{\pm}h^{\mp}$ Decays, Phys. Rev. Lett. **91**, 201802 (2003).

[280] C. C. Wang *et al.* (Belle Collaboration), Study of $B^0 \to \rho^{\pm}\pi^{\mp}$ Time-Dependent *CP* Violation at Belle, Phys. Rev. Lett. **94**, 121801 (2005).

[281] B. Aubert *et al.* (*BABAR* Collaboration), Measurement of time-dependent *CP* asymmetries in $B^0 \to D^{(*)\pm}\pi^{\mp}$ and $B^0 \to D^{\pm}\rho^{\mp}$ decays, Phys. Rev. D **73**, 111101 (2006).

[282] B. Aubert *et al.* (*BABAR* Collaboration), Measurement of time-dependent *CP*-violating asymmetries and constraints on $\sin(2\beta + \gamma)$ with partial reconstruction of $B \to D^{*\mp}\pi^{\pm}$ decays, Phys. Rev. D **71**, 112003 (2005).

[283] O. Long, M. Baak, R. N. Cahn, and D. Kirkby, Impact of tag-side interference on time dependent *CP* asymmetry measurements using coherent $B^0\bar{B}^0$ pairs, Phys. Rev. D **68**, 034010 (2003).

[284] S. Bahinipati *et al.* (Belle Collaboration), Measurements of time-dependent *CP* asymmetries in $B \to D^{*\mp}\pi^{\pm}$ decays using a partial reconstruction technique, Phys. Rev. D **84**, 021101 (2011).

[285] F. J. Ronga *et al.* (Belle Collaboration), Measurements of *CP* violation in $B^0 \to D^{*-}\pi^{+}$ and $B^0 \to D^{-}\pi^{+}$ decays, Phys. Rev. D **73**, 092003 (2006).

[286] R. Fleischer, New strategies to obtain insights into *CP* violation through $B_s \to D_s^{\pm}K^{\mp}, D_s^{*\pm}K^{\mp}, \ldots$ and $B_d \to D^{\pm}\pi^{\mp}, D^{*\pm}\pi^{\mp}, \ldots$ decays, Nucl. Phys. **B671**, 459 (2003).

[287] R. Aaij *et al.* (LHCb Collaboration), Measurement of *CP* violation in $B^0 \to D^{\mp}\pi^{\pm}$ decays, J. High Energy Phys. 06 (2018) 084.

[288] R. Aaij *et al.* (LHCb Collaboration), Measurement of *CP* asymmetry in $B_s^0 \to D_s^{\mp}K^{\pm}$ decays, J. High Energy Phys. 11 (2014) 060.

[289] R. Aaij *et al.* (LHCb Collaboration), Measurement of *CP* asymmetry in $B_s^0 \to D_s^{\mp}K^{\pm}$ decays, J. High Energy Phys. 03 (2018) 059.

[290] D. Atwood, M. Gronau, and A. Soni, Mixing-Induced *CP* Asymmetries in Radiative *B* Decays in and Beyond the Standard Model, Phys. Rev. Lett. **79**, 185 (1997).

[291] D. Atwood, T. Gershon, M. Hazumi, and A. Soni, Mixing-induced *CP* violation in $B \to P(1)P(2)\gamma$ in search of clean new physics signals, Phys. Rev. D **71**, 076003 (2005).

[292] B. Grinstein, Y. Grossman, Z. Ligeti, and D. Pirjol, The photon polarization in $B \to X\gamma$ in the Standard Model, Phys. Rev. D **71**, 011504 (2005).

[293] B. Grinstein and D. Pirjol, The *CP* asymmetry in $B^0(t) \to K_S\pi^0\gamma$ in the Standard Model, Phys. Rev. D **73**, 014013 (2006).

[294] M. Matsumori and A. I. Sanda, The mixing-induced *CP* asymmetry in $B \to K^*\gamma$ decays with perturbative QCD approach, Phys. Rev. D **73**, 114022 (2006).

[295] P. Ball and R. Zwicky, Time-dependent *CP* asymmetry in $B \to K^*\gamma$ as a (quasi) null test of the Standard Model, Phys. Lett. B **642**, 478 (2006).

[296] F. Muheim, Y. Xie, and R. Zwicky, Exploiting the width difference in $B_s \to \phi\gamma$, Phys. Lett. B **664**, 174 (2008).

[297] I. I. Y. Bigi and A. I. Sanda, On direct *CP* violation in $B \to D^0/\bar{D}^0 K\pi$'s versus $\bar{B} \to D^0/\bar{D}^0 \bar{K}\pi$'s decays, Phys. Lett. B **211**, 213 (1988).

[298] M. Gronau and D. London, How to determine all the angles of the unitarity triangle from $B_d^0 \to DK_s$ and $B_s^0 \to D_\varphi$, Phys. Lett. B **253**, 483 (1991).

[299] M. Gronau and D. Wyler, On determining a weak phase from *CP* asymmetries in charged *B* decays, Phys. Lett. B **265**, 172 (1991).

[300] D. Atwood, I. Dunietz, and A. Soni, Enhanced *CP* Violation with $B \to KD^0(\bar{D}^0)$ Modes and Extraction of the CKM Angle γ, Phys. Rev. Lett. **78**, 3257 (1997).

[301] D. Atwood, I. Dunietz, and A. Soni, Improved methods for observing *CP* violation in $B^{\pm} \to KD$ and measuring the CKM phase γ, Phys. Rev. D **63**, 036005 (2001).

[302] A. Giri, Y. Grossman, A. Soffer, and J. Zupan, Determining γ using $B^{\pm} \to DK^{\pm}$ with multibody *D* decays, Phys. Rev. D **68**, 054018 (2003).

[303] A. Poluektov *et al.* (Belle Collaboration), Measurement of φ_3 with Dalitz plot analysis of $B^p m \to D^{(*)}K^{\pm}$ decay, Phys. Rev. D **70**, 072003 (2004).

[304] J. Brod and J. Zupan, The ultimate theoretical error on γ from $B \to DK$ decays, J. High Energy Phys. 01 (2014) 051.

[305] M. Gronau, Improving bounds on γ in $B^{\pm} \to DK^{\pm}$ and $B^{\pm,0} \to DX_s^{\pm,0}$, Phys. Lett. B **557**, 198 (2003).

[306] R. Aleksan, T. C. Petersen, and A. Soffer, Measuring the weak phase γ in color allowed $B \to DK\pi$ decays, Phys. Rev. D **67**, 096002 (2003).

[307] T. Gershon, On the measurement of the unitarity triangle angle γ from $B^0 \to DK^{*0}$ decays, Phys. Rev. D **79**, 051301 (2009).

[308] T. Gershon and M. Williams, Prospects for the measurement of the unitarity triangle angle γ from $B^0 \to DK^+\pi^-$ decays, Phys. Rev. D **80**, 092002 (2009).

[309] D. Craik, T. Gershon, and A. Poluektov, Optimising sensitivity to γ with $B^0 \to DK^+\pi^-$, $D \to K^0_S\pi^+\pi^-$ double Dalitz plot analysis, Phys. Rev. D **97**, 056002 (2018).

[310] A. Bondar and T. Gershon, On φ_3 measurements using $B^- \to D^*K^-$ decays, Phys. Rev. D **70**, 091503 (2004).

[311] D. Atwood and A. Soni, Role of charm factory in extracting CKM-phase information via $B \to DK$, Phys. Rev. D **68**, 033003 (2003).

[312] Y. Grossman, Z. Ligeti, and A. Soffer, Measuring γ in $B^{\pm} \to K^{\pm}(KK^*)(D)$ decays, Phys. Rev. D **67**, 071301 (2003).

[313] M. Nayak, J. Libby, S. Malde, C. Thomas, G. Wilkinson, R. A. Briere, P. Naik, T. Gershon, and G. Bonvicini, First determination of the CP content of $D \to \pi^+\pi^-\pi^0$ and $D \to K^+K^-\pi^0$, Phys. Lett. B **740**, 1 (2015).

[314] A. Bondar and A. Poluektov, Feasibility study of model-independent approach to φ_3 measurement using Dalitz plot analysis, Eur. Phys. J. C **47**, 347 (2006).

[315] A. Bondar and A. Poluektov, The use of quantum-correlated D^0 decays for φ_3 measurement, Eur. Phys. J. C **55**, 51 (2008).

[316] T. Gershon, J. Libby, and G. Wilkinson, Contributions to the width difference in the neutral D system from hadronic decays, Phys. Lett. B **750**, 338 (2015).

[317] B. Aubert *et al.* (*BABAR* Collaboration), Measurement of CP Violation Parameters with a Dalitz Plot Analysis of $B^{\pm} \to \mathrm{D(pi}+\pi^-0)\ K^{\pm}$, Phys. Rev. Lett. **99**, 251801 (2007).

[318] B. Aubert *et al.* (*BABAR* Collaboration), Measurement of decay amplitudes of $B \to J/\psi K^*$, $\psi(2S)K^*$, and $\chi_{c1}K^*$ with an angular analysis, Phys. Rev. D **76**, 031102 (2007).

[319] R. Itoh *et al.* (Belle Collaboration), Studies of CP Violation in $B \to J/\psi K^*$ Decays, Phys. Rev. Lett. **95**, 091601 (2005).

[320] D. Acosta *et al.* (CDF Collaboration), Measurement of the Lifetime Difference Between B_s^0 Mass Eigenstates, Phys. Rev. Lett. **94**, 101803 (2005).

[321] R. Aaij *et al.* (LHCb Collaboration), Measurement of the polarization amplitudes in $B^0 \to J/\psi K^*(892)^0$ decays, Phys. Rev. D **88**, 052002 (2013).

[322] M. Jung, Determining weak phases from $B \to J/\psi P$ decays, Phys. Rev. D **86**, 053008 (2012).

[323] K. De Bruyn and R. Fleischer, A roadmap to control penguin effects in $B_d^0 \to J/\psi K_S^0$ and $B_s^0 \to J/\psi\phi$, J. High Energy Phys. 03 (2015) 145.

[324] B. Aubert *et al.* (*BABAR* Collaboration), Measurement of time-dependent CP asymmetry in $B^0 \to c\bar{c}K^{(*)0}$ decays, Phys. Rev. D **79**, 072009 (2009).

[325] I. Adachi *et al.* (Belle Collaboration), Precise Measurement of the CP Violation Parameter $\sin 2\phi_1$ in $B^0 \to (c\bar{c})K^0$ Decays, Phys. Rev. Lett. **108**, 171802 (2012).

[326] R. Aaij *et al.* (LHCb Collaboration), Measurement of CP Violation in $B^0 \to J/\psi K_S^0$ Decays, Phys. Rev. Lett. **115**, 031601 (2015).

[327] R. Aaij *et al.* (LHCb Collaboration), Measurement of CP violation in $B^0 \to J/\psi K_S^0$ and $B^0 \to \psi(2S)K_S^0$ decays, J. High Energy Phys. 11 (2017) 170.

[328] B. Aubert *et al.* (*BABAR* Collaboration), Measurement of $\sin(2\beta)$ using hadronic J/ψ decays, Phys. Rev. D **69**, 052001 (2004).

[329] R. Barate *et al.* (ALEPH Collaboration), Study of the CP asymmetry of $B0 \to J/\psi K_S^0$ decays in ALEPH, Phys. Lett. B **492**, 259 (2000).

[330] K. Ackerstaff *et al.* (OPAL Collaboration), Investigation of CP violation in $B^0 \to J/\psi K_S^0$ decays at LEP, Eur. Phys. J. C **5**, 379 (1998).

[331] A. A. Affolder *et al.* (CDF Collaboration), A measurement of $\sin(2\beta)$ from $B \to J/\psi K_S^0$ with the CDF detector, Phys. Rev. D **61**, 072005 (2000).

[332] Y. Sato *et al.* (Belle Collaboration), Measurement of the CP-Violation Parameter $\sin 2\phi_1$ with a New Tagging Method at the $\Upsilon(5S)$ Resonance, Phys. Rev. Lett. **108**, 171801 (2012).

[333] Belle II Collaboration, Prompt measurements of time-dependent CP-violation and mixing, KEK Report No. BELLE2-NOTE-PL-2020-011, 2020, http://docs.belle2.org/record/2024/files/BELLE2-NOTE-PL-2020-11.pdf.

[334] M. Bona *et al.* (UTfit Collaboration), The 2004 UTfit Collaboration report on the status of the unitarity triangle in the standard model, J. High Energy Phys. 07 (2005) 028.

[335] E. Lunghi and A. Soni, Possible indications of new physics in B_d-mixing and in $\sin(2\beta)$ determinations, Phys. Lett. B **666**, 162 (2008).

[336] G. Eigen, G. Dubois-Felsmann, D. G. Hitlin, and F. C. Porter, Global CKM fits with the scan method, Phys. Rev. D **89**, 033004 (2014).

[337] I. Dunietz, H. Quinn, A. Snyder, W. Toki, and H. J. Lipkin, How to extract CP violating asymmetries from angular correlations, Phys. Rev. D **43**, 2193 (1991).

[338] D. Aston *et al.*, A study of $K^-\pi^+$ scattering in the reaction $K^-p \to K^-\pi + n$ at 11 GeV/c, Nucl. Phys. **B296**, 493 (1988).

[339] M. Suzuki, Final-state interactions and s^- quark helicity conservation in $B \to J/\psi K^*$, Phys. Rev. D **64**, 117503 (2001).

[340] B. Aubert *et al.* (*BABAR* Collaboration), Ambiguity-free measurement of $\cos(2\beta)$: Time- integrated and time-dependent angular analyses of $B \to J/\psi K\pi$, Phys. Rev. D **71**, 032005 (2005).

[341] Y. Grossman and M. P. Worah, CP asymmetries in B decays with new physics in decay amplitudes, Phys. Lett. B **395**, 241 (1997).

[342] R. Fleischer, New, efficient and clean strategies to explore CP violation through neutral B decays, Phys. Lett. B **562**, 234 (2003).

[343] R. Fleischer, A closer look at $B_{d,s} \to Df(r)$ decays and novel avenues to determine γ, Nucl. Phys. **B659**, 321 (2003).

[344] A. Abdesselam *et al.*, First Observation of *CP* Violation in $\bar{B}^0 \to D_{CP}^{(*)}h^0$ Decays by a Combined Time-Dependent Analysis of *BABAR* and Belle Data, Phys. Rev. Lett. **115**, 121604 (2015).

[345] A. Bondar, T. Gershon, and P. Krokovny, A method to measure φ_1 using $\bar{B}^0 \to Dh^0$ with multibody D decay, Phys. Lett. B **624**, 1 (2005).

[346] F. J. Botella and J. P. Silva, Reparametrization invariance of B decay amplitudes and implications for new physics searches in B decays, Phys. Rev. D **71**, 094008 (2005).

[347] B. Aubert *et al.* (*BABAR* Collaboration), Evidence for *CP* Violation in $B^0 \to J/\psi\pi^0$ Decays, Phys. Rev. Lett. **101**, 021801 (2008).

[348] B. Pal *et al.* (Belle Collaboration), Measurement of the branching fraction and time-dependent *CP* asymmetry for $B^0 \to J/\psi\pi^0$ decays, Phys. Rev. D **98**, 112008 (2018).

[349] R. Aaij *et al.* (LHCb Collaboration), Measurement of *CP* Violation in $B^0 \to D^+D^-$ Decays, Phys. Rev. Lett. **117**, 261801 (2016).

[350] J. P. Lees *et al.* (*BABAR* Collaboration), Measurement of the time-dependent *CP* asymmetry of partially reconstructed $B^0 \to D^{*+}D^{*-}$ decays, Phys. Rev. D **86**, 112006 (2012).

[351] B. Kronenbitter *et al.* (Belle Collaboration), First observation of *CP* violation and improved measurement of the branching fraction and polarization of $B^0 \to D^{*+}D^{*-}$ decays, Phys. Rev. D **86**, 071103 (2012).

[352] R. Aaij *et al.* (LHCb Collaboration), Measurement of *CP* violation in $B^0 \to D^{*\pm}D^{\mp}$ decays, J. High Energy Phys. 03 (2020) 147.

[353] S. Fratina *et al.* (Belle Collaboration), Evidence for *CP* Violation in $B^0 \to D^+D^-$ Decays, Phys. Rev. Lett. **98**, 221802 (2007).

[354] R. Fleischer, Extracting γ from $B(s/d) \to J/\psi K_S$ and $B(d/s) \to D^+(d/s)D^-(d/s)$, Eur. Phys. J. C **10**, 299 (1999).

[355] K. De Bruyn, R. Fleischer, and P. Koppenburg, Extracting γ and penguin topologies through *CP* violation in $B_s^0 \to J/\psi K_S$, Eur. Phys. J. C **70**, 1025 (2010).

[356] R. Aaij *et al.* (LHCb Collaboration), Measurement of the time-dependent *CP* asymmetries in $B_s^0 \to J/\psi K_S^0$, J. High Energy Phys. 06 (2015) 131.

[357] R. Fleischer, *CP* violation and the role of electroweak penguins in nonleptonic B decays, Int. J. Mod. Phys. A **12**, 2459 (1997).

[358] D. London and A. Soni, Measuring the *CP* angle beta in hadronic $b \to s$ penguin decays, Phys. Lett. B **407**, 61 (1997).

[359] M. Ciuchini, E. Franco, G. Martinelli, A. Masiero, and L. Silvestrini, *CP* Violating B Decays in the Standard Model and Supersymmetry, Phys. Rev. Lett. **79**, 978 (1997).

[360] S. Okubo, Phi meson and unitary symmetry model, Phys. Lett. **5**, 165 (1963).

[361] G. Zweig, An SU(3) model for strong interaction symmetry and its breaking. Version 2, CERN Report No. CERN-TH-412, 1964.

[362] J. Iizuka, Systematics and phenomenology of meson family, Prog. Theor. Phys. Suppl. **37**, 21 (1966).

[363] T. Gershon and M. Hazumi, Time-dependent *CP* violation in $B^0 \to P^0P^0X^0$ decays, Phys. Lett. B **596**, 163 (2004).

[364] Y. Grossman, Z. Ligeti, Y. Nir, and H. Quinn, SU(3) relations and the *CP* asymmetries in B decays to $\eta' K_S^0$, ϕK_S^0 and $K^+K^-K_S^0$, Phys. Rev. D **68**, 015004 (2003).

[365] M. Gronau and J. L. Rosner, I-spin and U-spin in $B \to KK\bar{K}$, Phys. Lett. B **564**, 90 (2003).

[366] M. Gronau, Y. Grossman, and J. L. Rosner, Interpreting the time-dependent *CP* asymmetry in $B^0 \to \pi^0 K_S$, Phys. Lett. B **579**, 331 (2004).

[367] M. Gronau, J. L. Rosner, and J. Zupan, Correlated bounds on *CP* asymmetries in $B^0 \to \eta' K_S$, Phys. Lett. B **596**, 107 (2004).

[368] H.-Y. Cheng, C.-K. Chua, and A. Soni, Effects of final-state interactions on mixing-induced *CP* violation in Penguin-dominated B decays, Phys. Rev. D **72**, 014006 (2005).

[369] M. Gronau and J. L. Rosner, The $b \to s$ penguin amplitude in charmless $B \to PP$ decays, Phys. Rev. D **71**, 074019 (2005).

[370] G. Buchalla, G. Hiller, Y. Nir, and G. Raz, The pattern of *CP* asymmetries in $b \to s$ transitions, J. High Energy Phys. 09 (2005) 074.

[371] M. Beneke, Corrections to $sin(2\beta)$ from *CP* asymmetries in $B^0 \to (\pi^0, \rho^0, \eta, \eta', \omega, \varphi)K_S$ decays, Phys. Lett. B **620**, 143 (2005).

[372] G. Engelhard, Y. Nir, and G. Raz, SU(3) relations and the *CP* asymmetry in $B \to K_S K_S K_S$, Phys. Rev. D **72**, 075013 (2005).

[373] H.-Y. Cheng, C.-K. Chua, and A. Soni, *CP*-violating asymmetries in B^0 decays to $K^+K^-K^0_{S_{(L)}}$ and $K_S^0K_S^0K^0_{S_{(L)}}$, Phys. Rev. D **72**, 094003 (2005).

[374] G. Engelhard and G. Raz, Using SU(3) relations to bound the *CP* asymmetries in $B \to KKK$ decays, Phys. Rev. D **72**, 114017 (2005).

[375] M. Gronau, J. L. Rosner, and J. Zupan, Updated bounds on *CP* asymmetries in $B^0 \to \eta' K_S$ and $B^0 \to \pi^0 K_S$, Phys. Rev. D **74**, 093003 (2006).

[376] L. Silvestrini, Searching for new physics in $b \to s$ hadronic penguin decays, Annu. Rev. Nucl. Part. Sci. **57**, 405 (2007).

[377] R. Dutta and S. Gardner, *CP* Asymmetries in $B \to f_0 K_S$ decays, Phys. Rev. D **78**, 034021 (2008).

[378] M. Fujikawa *et al.* (Belle Collaboration), Measurement of *CP* asymmetries in $B^0 \to K^0\pi^0$ decays, Phys. Rev. D **81**, 011101 (2010).

[379] K. Abe *et al.* (Belle Collaboration), Measurements of time-dependent *CP* violation in $B^0 \to \omega K_S^0$, $f^0(980)K_S^0$, $K_S^0\pi^0$ and $K^+K^-K_S^0$ decays, Phys. Rev. D **76**, 091103 (2007).

[380] B. Aubert *et al.* (*BABAR* Collaboration), Measurement of *CP* asymmetries in $B^0 \to \phi K^0$ and $B^0 \to K^+K^-K_S^0$ decays, Phys. Rev. D **71**, 091102 (2005).

[381] B. Aubert *et al.* (*BABAR* Collaboration), Measurement of time dependent *CP* asymmetry parameters in B^0 meson decays to ωK_S^0, $\eta' K^0$, and $\pi^0 K_S^0$, Phys. Rev. D **79**, 052003 (2009).

[382] L. Šantelj *et al.* (Belle Collaboration), Measurement of time-dependent CP violation in $B^0 \to \eta' K^0$ decays, J. High Energy Phys. 10 (2014) 165.

[383] J. P. Lees *et al.* (*BABAR* Collaboration), Amplitude analysis and measurement of the time-dependent CP asymmetry of $B^0 \to K^0_S K^0_S K^0_S$ decays, Phys. Rev. D **85**, 054023 (2012).

[384] K. H. Kang *et al.* (Belle Collaboration), Measurement of time-dependent CP violation parameters in $B^0 \to K^S_0 K^S_0 K^S_0$ decays at Belle, Phys. Rev. D **103**, 032003 (2021).

[385] V. Chobanova *et al.* (Belle Collaboration), Measurement of branching fractions and CP violation parameters in $B \to \omega K$ decays with first evidence of CP violation in $B^0 \to \omega K^0_S$, Phys. Rev. D **90**, 012002 (2014).

[386] B. Aubert *et al.* (*BABAR* Collaboration), Measurement of CP asymmetry in $B^0 \to K_s \pi^0 \pi^0$ decays, Phys. Rev. D **76**, 071101 (2007).

[387] Y. Yusa *et al.* (Belle Collaboration), Measurement of time-dependent CP violation in $B^0 \to K^0_S \pi^0 \pi^0$ decays, Phys. Rev. D **99**, 011102 (2019).

[388] B. Aubert *et al.* (*BABAR* Collaboration), Time-dependent and time-integrated angular analysis of $B \to \phi K_S \pi^0$ and $B \to \phi K^+ \pi^-$, Phys. Rev. D **78**, 092008 (2008).

[389] I. Dunietz, Extracting CKM parameters from B decays, Fermilab Report No. FERMILAB-CONF-93-090-T, 1993.

[390] R. Fleischer, New strategies to extract β and γ from $B_d \to \pi^+ \pi^-$ and $B_s \to K^+ K^-$, Phys. Lett. B **459**, 306 (1999).

[391] R. Aaij *et al.* (LHCb Collaboration), Measurement of CP asymmetries in two-body $B^0_{(s)}$-meson decays to charged pions and kaons, Phys. Rev. D **98**, 032004 (2018).

[392] R. Aaij *et al.* (LHCb Collaboration), Observation of CP violation in two-body $B^0_{(s)}$-meson decays to charged pions and kaons, J. High Energy Phys. 03 (2021) 075.

[393] R. Aaij *et al.* (LHCb Collaboration), First measurement of time-dependent CP violation in $B^0_s \to K^+ K^-$ decays, J. High Energy Phys. 10 (2013) 183.

[394] M. Raidal, CP Asymmetry in $B \to \varphi K_S$ Decays in Left-Right Models and its Implications on B_s Decays, Phys. Rev. Lett. **89**, 231803 (2002).

[395] R. Aaij *et al.* (LHCb Collaboration), Measurement of CP violation in the $B^0_s \to \phi\phi$ decay and search for the $B^0 \to \phi\phi$ decay, J. High Energy Phys. 12 (2019) 155.

[396] M. Ciuchini, M. Pierini, and L. Silvestrini, $B^0_s \to K^{*0} \bar{K}^{*0}$ Decays: The Golden Channels for New Physics Searches, Phys. Rev. Lett. **100**, 031802 (2008).

[397] S. Descotes-Genon, J. Matias, and J. Virto, Penguin-mediated $B_{d,s} \to VV$ decays and the $B_s - \bar{B}_s$ mixing angle, Phys. Rev. D **76**, 074005 (2007); **84**, 039901(E) (2011).

[398] S. Descotes-Genon, J. Matias, and J. Virto, An analysis of $B_{d,s}$ mixing angles in presence of new physics and an update of $B_s \to \bar{K}^{0*} K^{0*}$, Phys. Rev. D **85**, 034010 (2012).

[399] R. Aaij *et al.* (LHCb Collaboration), First measurement of the CP-violating phase $\phi_s^{d\bar{d}}$ in $B^0_s \to (K^+\pi^-)(K^-\pi^+)$ decays, J. High Energy Phys. 03 (2018) 140.

[400] B. Aubert *et al.* (*BABAR* Collaboration), Observation of $B^+ \to \bar{K}^0 K^+$ and $B^0 \to K^0 \bar{K}^0$, Phys. Rev. Lett. **97**, 171805 (2006).

[401] Y. Nakahama *et al.* (Belle Collaboration), Measurement of Time-Dependent CP-Violating Parameters in $B^0 \to K^0_S K^0_S$ Decays, Phys. Rev. Lett. **100**, 121601 (2008).

[402] S. Akar, E. Ben-Haim, J. Hebinger, E. Kou, and F.-S. Yu, The time-dependent CP asymmetry in $B^0 \to K_{\rm res}\gamma \to \pi^+\pi^- K^0_S \gamma$ decays, J. High Energy Phys. 09 (2019) 034.

[403] S. Akar, Study of $B \to K\pi\pi\gamma$ decays with the *BABAR* Experiment: the photon helicity and the resonant structure of the $K\pi\pi$ system, Ph.D. thesis, LPNHE, Université Pierre et Marie Curie—Paris VI, 2013.

[404] P. del Amo Sanchez *et al.* (*BABAR* Collaboration), Time-dependent analysis of $B^0 \to K^0_S \pi^- \pi^+ \gamma$ decays and studies of the $K^+\pi^-\pi^+$ system in $B^+ \to K^+\pi^-\pi^+\gamma$ decays, Phys. Rev. D **93**, 052013 (2016).

[405] J. Li *et al.* (Belle Collaboration), Time-dependent CP Asymmetries in $B^0 \to K^0_S \rho^0 \gamma$ Decays, Phys. Rev. Lett. **101**, 251601 (2008).

[406] B. Aubert *et al.* (*BABAR* Collaboration), Measurement of time-dependent CP asymmetry in $B^0 \to K^0_S \pi^0 \gamma$ decays, Phys. Rev. D **78**, 071102 (2008).

[407] Y. Ushiroda *et al.* (Belle Collaboration), Time-dependent CP asymmetries in $B^0 \to K^0_S \pi^0 \gamma$ transitions, Phys. Rev. D **74**, 111104 (2006).

[408] B. Aubert *et al.* (*BABAR* Collaboration), Branching fractions and CP-violating asymmetries in radiative B decays to $\eta K \gamma$, Phys. Rev. D **79**, 011102 (2009).

[409] H. Nakano *et al.* (Belle Collaboration), Measurement of time-dependent CP asymmetries in $B^0 \to K^0_S \eta\eta$ decays, Phys. Rev. D **97**, 092003 (2018).

[410] H. Sahoo *et al.* (Belle Collaboration), First observation of radiative $B^0 \to \phi K^0 \gamma$ decays and measurements of their time-dependent CP violation, Phys. Rev. D **84**, 071101 (2011).

[411] R. Aaij *et al.* (LHCb Collaboration), Measurement of CP-Violating and Mixing-Induced Observables in $B^0_s \to \phi\gamma$ Decays, Phys. Rev. Lett. **123**, 081802 (2019).

[412] Y. Ushiroda *et al.* (Belle Collaboration), Time-Dependent CP-Violating Asymmetry in $B^0 \to \rho^0 \gamma$ Decays, Phys. Rev. Lett. **100**, 021602 (2008).

[413] B. Aubert *et al.* (*BABAR* Collaboration), A study of $B^0 \to \rho^+\rho^-$ decays and constraints on the CKM angle α, Phys. Rev. D **76**, 052007 (2007).

[414] P. Vanhoefer *et al.* (Belle Collaboration), Study of $B^0 \to \rho^+\rho^-$ decays and implications for the CKM angle ϕ_2, Phys. Rev. D**93**, 032010 (2016); **94**, 099903(A) (2016).

[415] B. Aubert *et al.* (*BABAR* Collaboration), Measurement of the branching fraction, polarization, and CP asymmetries in $B^0 \to \rho^0\rho^0$ decay, and implications for the CKM angle α, Phys. Rev. D **78**, 071104 (2008).

[416] I. Adachi *et al.* (Belle Collaboration), Study of $B^0 \to \rho^0\rho^0$ decays, implications for the CKM angle ϕ_2 and search for other B^0 decay modes with a four-pion final state, Phys. Rev. D **89**, 072008 (2014); **89**, 119903 (2014).

[417] R. Aaij *et al.* (LHCb Collaboration), Observation of the $B^0 \to \rho^0\rho^0$ decay from an amplitude analysis of $B^0 \to (\pi^+\pi^-)(\pi^+\pi^-)$ decays, Phys. Lett. B **747**, 468 (2015).

[418] B. Aubert *et al.* (*BABAR* Collaboration), Measurements of *CP*-Violating Asymmetries in $B^0 \to a_1^{\pm}(1260)\pi^{\mp}$ Decays, Phys. Rev. Lett. **98**, 181803 (2007).

[419] J. Dalseno *et al.* (Belle Collaboration), Measurement of branching fraction and first evidence of *CP* violation in $B^0 \to a_1^{\pm}(1260)\pi^{\mp}$ decays, Phys. Rev. D **86**, 092012 (2012).

[420] B. Aubert *et al.* (*BABAR* Collaboration), Measurement of branching fractions of B decays to $K(1)(1270)\pi$ and $K(1)(1400)\pi$ and determination of the CKM angle alpha from $B^0 \to a(1)(1260)^{\pm}\pi^{\mp}$, Phys. Rev. D **81**, 052009 (2010).

[421] J. P. Lees *et al.* (*BABAR* Collaboration), Measurement of *CP* asymmetries and branching fractions in charmless two-body B-meson decays to pions and kaons, Phys. Rev. D **87**, 052009 (2013).

[422] I. Adachi *et al.* (Belle Collaboration), Measurement of the *CP* violation parameters in $B^0 \to \pi^+\pi^-$ decays, Phys. Rev. D **88**, 092003 (2013).

[423] M. Gronau and D. London, Isospin Analysis of *CP* Asymmetries in B Decays, Phys. Rev. Lett. **65**, 3381 (1990).

[424] D. Asner *et al.*, Averages of b-hadron, c-hadron, and τ-lepton properties, arXiv:1010.1589.

[425] B. Aubert *et al.* (*BABAR* Collaboration), Improved Measurement of $B^+ \to \rho^+\rho^0$ and Determination of the Quark-Mixing Phase Angle Alpha, Phys. Rev. Lett. **102**, 141802 (2009).

[426] H. J. Lipkin, Y. Nir, H. R. Quinn, and A. Snyder, Penguin trapping with isospin analysis and *CP* asymmetries in B decays, Phys. Rev. D **44**, 1454 (1991).

[427] M. Gronau and J. Zupan, Weak phase α from $B^0 \to a_1(1260)^{\pm}\pi^{\mp}$, Phys. Rev. D **73**, 057502 (2006).

[428] A. J. Bevan *et al.*, The physics of the B factories, Eur. Phys. J. C **74**, 3026 (2014).

[429] M. Gronau and J. Zupan, Isospin-breaking effects on α extracted in $B \to \pi\pi, \rho\rho, \rho\pi$, Phys. Rev. D **71**, 074017 (2005).

[430] S. Gardner, Towards a precision determination of α in $B \to \pi\pi$ decays, Phys. Rev. D **72**, 034015 (2005).

[431] J. Charles, O. Deschamps, S. Descotes-Genon, and V. Niess, Isospin analysis of charmless B-meson decays, Eur. Phys. J. C **77**, 574 (2017).

[432] `GammaCombo` framework for combinations of measurements and computation of confidence intervals, CERN.

[433] T. Julius *et al.* (Belle Collaboration), Measurement of the branching fraction and *CP* asymmetry in $B^0 \to \pi^0\pi^0$ decays, and an improved constraint on ϕ_2, Phys. Rev. D **96**, 032007 (2017).

[434] I. Dunietz, Clean CKM information from $B_d(t) \to D^{*\mp}\pi^{\pm}$, Phys. Lett. B **427**, 179 (1998).

[435] M. A. Baak, Measurement of CKM angle γ with charmed B^0 meson decays, Ph.D. thesis, Vrije University, Amsterdam, 2007.

[436] K. De Bruyn, R. Fleischer, R. Knegjens, M. Merk, M. Schiller, and N. Tuning, Exploring $B_s \to D_s^{(*)\pm}K^{\mp}$ decays in the presence of a sizable width difference $\Delta\Gamma_s$, Nucl. Phys. **B868**, 351 (2013).

[437] M. Kenzie, M. Martinelli, and N. Tuning, Estimating $r_B^{D\pi}$ as an input to the determination of the CKM angle γ, Phys. Rev. D **94**, 054021 (2016).

[438] B. Aubert *et al.* (*BABAR* Collaboration), Time-dependent Dalitz plot analysis of $B^0 \to D^{\mp}K^0\pi^{\pm}$ decays, Phys. Rev. D **77**, 071102 (2008).

[439] I. Dunietz and R. G. Sachs, Asymmetry Between Inclusive Charmed and Anticharmed Modes in B^0, B^{-0} Decay as a Measure of *CP* Violation, Phys. Rev. D **37**, 3186 (1988); **39**, 3515(E) (1989).

[440] R. Aleksan, I. Dunietz, and B. Kayser, Determining the *CP* violating phase γ, Z. Phys. C **54**, 653 (1992).

[441] Y. Amhis *et al.*, Averages of b-hadron, c-hadron, and τ-lepton properties as of summer 2016, Eur. Phys. J. C **77**, 895 (2017).

[442] M. Rama, Effect of $D - \bar{D}$ mixing in the extraction of γ with $B^- \to D^0K^-$ and $B^- \to D^0\pi^-$ decays, Phys. Rev. D **89**, 014021 (2014).

[443] P. del Amo Sanchez *et al.* (*BABAR* Collaboration), Measurement of *CP* observables in $B^{\pm} \to D_{CP}K^{\pm}$ decays and constraints on the CKM angle γ, Phys. Rev. D **82**, 072004 (2010).

[444] K. Abe *et al.* (Belle Collaboration), Study of $B^{\pm} \to D_{CP}K^{\pm}$ and $D_{CP}^*K^{\pm}$ decays, Phys. Rev. D **73**, 051106 (2006).

[445] T. Aaltonen *et al.* (CDF Collaboration), Measurements of branching fraction ratios and *CP* asymmetries in $B^{\pm} \to D_{CP}K^{\pm}$ decays in hadron collisions, Phys. Rev. D **81**, 031105 (2010).

[446] R. Aaij *et al.* (LHCb Collaboration), Measurement of *CP* observables in $B^{\pm} \to D^{(*)}K^{\pm}$ and $B^{\pm} \to D^{(*)}\pi^{\pm}$ decays using two-body D final states, J. High Energy Phys. 04 (2021) 081.

[447] B. Aubert *et al.* (*BABAR* Collaboration), Measurement of ratios of branching fractions and *CP*-violating asymmetries of $B^{\pm} \to D^*K^{\pm}$ decays, Phys. Rev. D **78**, 092002 (2008).

[448] B. Aubert *et al.* (*BABAR* Collaboration), Measurement of *CP* violation observables and parameters for the decays $B^{\pm} \to DK^{*\pm}$, Phys. Rev. D **80**, 092001 (2009).

[449] R. Aaij *et al.* (LHCb Collaboration), Measurement of *CP* observables in $B^{\pm} \to DK^{*\pm}$ decays using two- and four-body D final states, J. High Energy Phys. 11 (2017) 156; 05 (2018) 067(E).

[450] R. Aaij *et al.* (LHCb Collaboration), Study of $B^- \to DK^-\pi^+\pi^-$ and $B^- \to D\pi^-\pi^+\pi^-$ decays and determination of the CKM angle γ, Phys. Rev. D **92**, 112005 (2015).

[451] R. Aaij *et al.* (LHCb Collaboration), Measurement of *CP* observables in the process $B^0 \to DK^{*0}$ with two- and four-body D decays, J. High Energy Phys. 08 (2019) 041.

[452] R. Aaij *et al.* (LHCb Collaboration), Constraints on the unitarity triangle angle γ from Dalitz plot analysis of $B^0 \to DK^+\pi^-$ decays, Phys. Rev. D **93**, 112018 (2016).

[453] S. Malde, C. Thomas, G. Wilkinson, P. Naik, C. Prouve, J. Rademacker, J. Libby, M. Nayak, T. Gershon, and R. A. Briere, First determination of the *CP* content of $D \to \pi^+\pi^-\pi^+\pi^-$ and updated determination of the *CP* contents of $D \to \pi^+\pi^-\pi^0$ and $D \to K^+K^-\pi^0$, Phys. Lett. B **747**, 9 (2015).

[454] R. Aaij *et al.* (LHCb Collaboration), A study of *CP* violation in $B^{\mp} \to Dh^{\mp}$ ($h = K$, π) with the modes $D \to K^{\mp}\pi^{\pm}\pi^0$, $D \to \pi^+\pi^-\pi^0$ and $D \to K^+K^-\pi^0$, Phys. Rev. D **91**, 112014 (2015).

[455] R. Aaij *et al.* (LHCb Collaboration), Measurement of *CP* observables in $B^{\pm} \to DK^{\pm}$ and $B^{\pm} \to D\pi^{\pm}$ with two- and four-body D decays, Phys. Lett. B **760**, 117 (2016).

[456] P. del Amo Sanchez *et al.* (*BABAR* Collaboration), Search for $b \to u$ transitions in $B^- \to DK^-$ and $B^- \to D^*K^-$ decays, Phys. Rev. D **82**, 072006 (2010).

[457] Y. Horii *et al.* (Belle Collaboration), Evidence for the Suppressed Decay $B^- \to DK^-$, $D \to K^+\pi^-$, Phys. Rev. Lett. **106**, 231803 (2011).

[458] T. Aaltonen *et al.* (CDF Collaboration), Measurements of branching fraction ratios and *CP*-asymmetries in suppressed $B^- \to D(\to K^+\pi^-)K^-$ and $B^- \to D(\to K^+\pi^-)\pi^-$ decays, Phys. Rev. D **84**, 091504 (2011).

[459] J. P. Lees *et al.* (*BABAR* Collaboration), Search for $b \to u$ transitions in $B^{\pm} \to [K^{\mp}\pi^{\pm}\pi^0]_D K^{\pm}$ decays, Phys. Rev. D **84**, 012002 (2011).

[460] M. Nayak *et al.* (Belle Collaboration), Evidence for the suppressed decay $B^- \to DK^-$, $D \to K^+\pi^-\pi^0$, Phys. Rev. D **88**, 091104 (2013).

[461] B. Aubert *et al.* (*BABAR* Collaboration), Search for $b \to u$ transitions in $B^0 \to D^0K^{*0}$ decays, Phys. Rev. D **80**, 031102 (2009).

[462] K. Negishi *et al.* (Belle Collaboration), Search for the decay $B^0 \to DK^{*0}$ followed by $D \to K^-\pi^+$, Phys. Rev. D **86**, 011101 (2012).

[463] D. M. Asner *et al.* (CLEO Collaboration), Determination of the $D^0 \to K^+\pi^-$ relative strong phase using quantum-correlated measurements in $e^+e^- \to D^0\bar{D}^0$ at CLEO, Phys. Rev. D **78**, 012001 (2008).

[464] N. Lowrey *et al.* (CLEO Collaboration), Determination of the $D^0 \to K^-\pi^+\pi^0$ and $D^0 \to K^-\pi^+\pi^+\pi^-$ coherence factors and average strong-phase differences using quantum-correlated measurements, Phys. Rev. D **80**, 031105 (2009).

[465] A. Poluektov *et al.* (Belle Collaboration), Evidence for direct *CP* violation in the decay $B \to D^{(*)}K$, $D \to K_s\pi^+\pi^-$ and measurement of the CKM phase φ_3, Phys. Rev. D **81**, 112002 (2010).

[466] P. del Amo Sanchez *et al.* (*BABAR* Collaboration), Evidence for Direct *CP* Violation in the Measurement of the Cabibbo-Kobayashi-Maskawa Angle γ with $B^{\mp} \to D^{(*)}K^{(*)\mp}$ Decays, Phys. Rev. Lett. **105**, 121801 (2010).

[467] R. Aaij *et al.* (LHCb Collaboration), Measurement of *CP* violation and constraints on the CKM angle γ in $B^{\pm} \to DK^{\pm}$ with $D \to K^0_S\pi^+\pi^-$ decays, Nucl. Phys. **B888**, 169 (2014).

[468] A. Poluektov *et al.* (Belle Collaboration), Measurement of φ_3 with Dalitz plot analysis of $B^+ \to D^{(*)}K^{(*)+}$ decay, Phys. Rev. D **73**, 112009 (2006).

[469] R. Aaij *et al.* (LHCb Collaboration), Measurement of the CKM angle γ using $B^0 \to DK^{*0}$ with $D \to K^0_S\pi^+\pi^-$ decays, J. High Energy Phys. 08 (2016) 137.

[470] B. Aubert *et al.* (*BABAR* Collaboration), Constraints on the CKM angle γ in $B^0 \to \bar{D}^0(D^0)K^{*0}$ with a Dalitz analysis of $D^0 \to K_S\pi^+\pi^-$, Phys. Rev. D **79**, 072003 (2009).

[471] R. A. Briere *et al.* (CLEO Collaboration), First model-independent determination of the relative strong phase between D^0 and $\bar{D}^0 \to K^0_S\pi^+\pi^-$ and its impact on the CKM Angle γ/φ_3 measurement, Phys. Rev. D **80**, 032002 (2009).

[472] M. Ablikim *et al.* (BESIII Collaboration), Determination of Strong-Phase Parameters in $D \to K^0_{S,L}\pi^+\pi^-$, Phys. Rev. Lett. **124**, 241802 (2020).

[473] M. Ablikim *et al.* (BESIII Collaboration), Model-independent determination of the relative strong-phase difference between D^0 and $\bar{D}^0 \to K^0_{S,L}\pi^+\pi^-$ and its impact on the measurement of the CKM angle γ/ϕ_3, Phys. Rev. D **101**, 112002 (2020).

[474] M. Ablikim *et al.* (BESIII Collaboration), Improved model-independent determination of the strong-phase difference between D^0 and $\bar{D}^0 \to K^0_{S,L}K^+K^-$ decays, Phys. Rev. D **102**, 052008 (2020).

[475] H. Aihara *et al.* (Belle Collaboration), First measurement of ϕ_3 with a model-independent Dalitz plot analysis of $B \to DK$, $D \to K_S\pi\pi$ decay, Phys. Rev. D **85**, 112014 (2012).

[476] R. Aaij *et al.* (LHCb Collaboration), Measurement of the CKM angle γ in $B^{\pm} \to DK^{\pm}$ and $B^{\pm} \to D\pi^{\pm}$ decays with $D \to K^0_S h^+h^-$, J. High Energy Phys. 02 (2021) 169.

[477] J. Garra Ticó, V. Gibson, S. C. Haines, C. R. Jones, M. Kenzie, and G. Lovell, Study of the sensitivity to CKM angle γ under simultaneous determination from multiple B meson decay modes, Phys. Rev. D **102**, 053003 (2020).

[478] K. Negishi *et al.* (Belle Collaboration), First model-independent Dalitz analysis of $B^0 \to DK^{*0}$, $D \to K^0_S\pi^+\pi^-$ decay, Prog. Theor. Exp. Phys. **2016**, 043C01 (2016).

[479] R. Aaij *et al.* (LHCb Collaboration), Model-independent measurement of the CKM angle γ using $B^0 \to DK^{*0}$ decays with $D \to K^0_S\pi^+\pi^-$ and $K^0_SK^+K^-$, J. High Energy Phys. 06 (2016) 131.

[480] P. K. Resmi *et al.* (Belle Collaboration), First measurement of the CKM angle ϕ_3 with $B^{\pm} \to D(K^0_S\pi^+\pi^-\pi^0)K^{\pm}$ decays, J. High Energy Phys. 10 (2019) 178.

[481] R. Aaij *et al.* (LHCb Collaboration), Measurement of *CP* observables in $B^{\pm} \to DK^{\pm}$ and $B^{\pm} \to D\pi^{\pm}$ with $D \to K^0_SK^{\pm}\pi^{\mp}$ decays, J. High Energy Phys. 06 (2020) 058.

[482] J. Insler *et al.* (CLEO Collaboration), Studies of the decays $D^0 \to K^0_SK^-\pi^+$ and $D^0 \to K^0_SK^+\pi^-$, Phys. Rev. D **85**, 092016 (2012); **94**, 099905(E) (2016).

[483] J. P. Lees *et al.* (*BABAR* Collaboration), Observation of direct *CP* violation in the measurement of the Cabibbo-Kobayashi-Maskawa angle γ with $B^{\pm} \to D^{(*)}K^{(*)\pm}$ decays, Phys. Rev. D **87**, 052015 (2013).

[484] LHCb Collaboration, Updated LHCb combination of the CKM angle γ, Report No. LHCb-CONF-2020-003, 2020.

[485] R. Aaij *et al.* (LHCb Collaboration), Simultaneous determination of CKM angle γ and charm mixing parameters, J. High Energy Phys. 12 (2021) 141.

[486] R. Aaij *et al.* (LHCb Collaboration), Measurement of the CKM angle γ from a combination of $B^{\pm} \to Dh^{\pm}$ analyses, Phys. Lett. B **726**, 151 (2013).

[487] R. Aaij *et al.* (LHCb Collaboration), Measurement of the CKM angle γ from a combination of LHCb results, J. High Energy Phys. 12 (2016) 087.

[488] T. Evans, S. T. Harnew, J. Libby, S. Malde, J. Rademacker, and G. Wilkinson, Improved determination of the $D \to K^-\pi^+\pi^+\pi^-$ coherence factor and associated hadronic parameters from a combination of $e^+e^- \to \psi(3770) \to c\bar{c}$ and

$pp \to c\bar{c}X$ data, Phys. Lett. B **757**, 520 (2016); **765**, 402(C) (2017).

[489] M. Ablikim *et al.* (BESIII Collaboration), Measurement of the $D \to K^-\pi^+\pi^+\pi^-$ and $D \to K^-\pi^+\pi^0$ coherence factors and average strong-phase differences in quantum-correlated $D\bar{D}$ decays, J. High Energy Phys. 05 (2021) 164.

[490] R. Aaij *et al.* (LHCb Collaboration), Studies of the resonance structure in $D^0 \to K^0_S K^\pm \pi^\mp$ decays, Phys. Rev. D **93**, 052018 (2016).

[491] R. Aaij *et al.* (LHCb Collaboration), First Observation of $D^0 - \bar{D}^0$ Oscillations in $D^0 \to K^+\pi^-\pi^+\pi^-$ Decays and Measurement of the Associated Coherence Parameters, Phys. Rev. Lett. **116**, 241801 (2016).

[492] J. P. Silva and A. Soffer, Impact of D^0–$\bar{D}^0$ mixing on the experimental determination of γ, Phys. Rev. D **61**, 112001 (2000).

[493] Y. Grossman, A. Soffer, and J. Zupan, The effect of D–$\bar{D}$ mixing on the measurement of γ in $B \to DK$ decays, Phys. Rev. D **72**, 031501 (2005).

[494] M. Neubert, Heavy quark symmetry, Phys. Rep. **245**, 259 (1994).

[495] A. Sirlin, Large m_W, m_Z behavior of the $O(\alpha)$ corrections to semileptonic processes mediated by W, Nucl. Phys. **B196**, 83 (1982).

[496] D. Buskulic *et al.* (ALEPH Collaboration), Measurements of $|V_{cb}|$, form factors and branching fractions in the decays $\bar{B}^0 \to D^{*+}\ell^-\bar{\nu}_l$ and $\bar{B}^0 \to D + \ell^-\bar{\nu}_l$, Phys. Lett. B **395**, 373 (1997).

[497] G. Abbiendi *et al.* (OPAL Collaboration), Measurement of $|V_{cb}|$ using $\bar{B}^0 \to D^{*+}\ell^-\bar{\nu}$ decays, Phys. Lett. B **482**, 15 (2000).

[498] P. Abreu *et al.* (DELPHI Collaboration), Measurement of V_{cb} from the decay process $\bar{B}^0 \to D^{*+}\ell^-\bar{\nu}$, Phys. Lett. B **510**, 55 (2001).

[499] J. Abdallah *et al.* (DELPHI Collaboration), Measurement of $|V_{cb}|$ using the semileptonic decay $\bar{B}^0_d \to D^{*+}\ell^-\overline{\nu_\ell}$, Eur. Phys. J. C **33**, 213 (2004).

[500] N. E. Adam *et al.* (CLEO Collaboration), Determination of the $\bar{B} \to D^*\ell\bar{\nu}$ decay width and $|V_{cb}|$, Phys. Rev. D **67**, 032001 (2003).

[501] E. Waheed *et al.* (Belle Collaboration), Measurement of the CKM matrix element $|V_{cb}|$ from $B^0 \to D^{*-}\ell^+\nu_\ell$ at Belle, Phys. Rev. D **100**, 052007 (2019); **103**, 079901(E) (2021).

[502] B. Aubert *et al.* (*BABAR* Collaboration), Determination of the form-factors for the decay $B^0 \to D^{*-}\ell^+\nu_l$ and of the CKM matrix element $|V_{cb}|$, Phys. Rev. D **77**, 032002 (2008).

[503] B. Aubert *et al.* (*BABAR* Collaboration), A Measurement of the Branching Fractions of Exclusive $\bar{B} \to D^{(*)}$ (π) $\ell^-\bar{\nu}_\ell$ Decays in Events with a Fully Reconstructed B Meson, Phys. Rev. Lett. **100**, 151802 (2008).

[504] F. Abudinén *et al.* (Belle-II Collaboration), Studies of the semileptonic $\overline{B}^0 \to D^{*+}\ell^-\bar{\nu}_\ell$ and $B^- \to D^0\ell^-\bar{\nu}_\ell$ decay processes with 34.6 fb^{-1} of Belle II data, arXiv:2008.07198.

[505] F. Abudinén *et al.* (Belle-II Collaboration), Measurement of the semileptonic $\bar{B}^0 \to D^{*+}\ell^-\nu_\ell$ branching fraction with fully reconstructed B meson decays and 34.6 fb^{-1} of Belle II data, arXiv:2008.10299.

[506] B. Aubert *et al.* (*BABAR* Collaboration), Measurement of the Decay $B^- \to D^{*0}\, e^-\bar{\nu}(e)$, Phys. Rev. Lett. **100**, 231803 (2008).

[507] I. Caprini, L. Lellouch, and M. Neubert, Dispersive bounds on the shape of $\bar{B} \to D^{(*)}\ell\bar{\nu}$ form factors, Nucl. Phys. **B530**, 153 (1998).

[508] B. Aubert *et al.* (*BABAR* Collaboration), Measurements of the semileptonic decays $\bar{B} \to D\ell\bar{\nu}$ and $\bar{B} \to D^*\ell\bar{\nu}$ using a global fit to $DX\ell\bar{\nu}$ final states, Phys. Rev. D **79**, 012002 (2009).

[509] Y. Aoki *et al.*, FLAG review 2021, arXiv:2111.09849.

[510] J. A. Bailey *et al.*, Update of $|V_{cb}|$ from the $\bar{B} \to D^*\ell\bar{\nu}$ form factor at zero recoil with three-flavor lattice QCD, Phys. Rev. D **89**, 114504 (2014).

[511] J. Harrison, C. Davies, and M. Wingate (HPQCD Collboration), Lattice QCD calculation of the $B_{(s)} \to D^*_{(s)}\ell\nu$ form factors at zero recoil and implications for $|V_{cb}|$, Phys. Rev. D **97**, 054502 (2018).

[512] J. A. Bailey *et al.* (MILC Collaboration), $B \to D\ell\nu$ form factors at nonzero recoil and $|V_{cb}|$ from $2+1$-flavor lattice QCD, Phys. Rev. D **92**, 034506 (2015).

[513] C. G. Boyd, B. Grinstein, and R. F. Lebed, Precision corrections to dispersive bounds on form-factors, Phys. Rev. D **56**, 6895 (1997).

[514] B. Grinstein and A. Kobach, Model-independent extraction of $|V_{cb}|$ from $\bar{B} \to D^*\ell\bar{\nu}$, Phys. Lett. B **771**, 359 (2017).

[515] D. Bigi, P. Gambino, and S. Schacht, A fresh look at the determination of $|V_{cb}|$ from $B \to D^*\ell\nu$, Phys. Lett. B **769**, 441 (2017).

[516] J. P. Lees *et al.* (*BABAR* Collaboration), A test of heavy quark effective theory using a four-dimensional angular analysis of $\bar{B} \to D^*\ell^-\bar{\nu}_\ell$, arXiv:1903.10002.

[517] J. P. Lees *et al.* (*BABAR* Collaboration), Extraction of form Factors from a Four-Dimensional Angular Analysis of $\bar{B} \to D^*\ell^-\bar{\nu}_\ell$, Phys. Rev. Lett. **123**, 091801 (2019).

[518] J. E. Bartelt *et al.* (CLEO Collaboration), Measurement of the $B \to D\ell\nu$ Branching Fractions and Form Factor, Phys. Rev. Lett. **82**, 3746 (1999).

[519] B. Aubert *et al.* (*BABAR* Collaboration), Measurement of $|V_{cb}|$ and the Form-Factor Slope in $\bar{B} \to D\ell^-\bar{\nu}$ Decays in Events Tagged by a Fully Reconstructed B Meson, Phys. Rev. Lett. **104**, 011802 (2010).

[520] R. Glattauer *et al.* (Belle Collaboration), Measurement of the decay $B \to D\ell\nu_\ell$ in fully reconstructed events and determination of the Cabibbo-Kobayashi-Maskawa matrix element $|V_{cb}|$, Phys. Rev. D **93**, 032006 (2016).

[521] H. Na, C. M. Bouchard, G. Peter Lepage, C. Monahan, and J. Shigemitsu (HPQCD Collaboration), $B \to Dl\nu$ form factors at nonzero recoil and extraction of $|V_{cb}|$, Phys. Rev. D **92**, 054510 (2015); **93**, 119906(E) (2016).

[522] R. Aaij *et al.* (LHCb Collaboration), Measurement of $|V_{cb}|$ with $B^0_s \to D^{(*)-}_s \mu^+\nu_\mu$ decays, Phys. Rev. D **101**, 072004 (2020).

[523] E. McLean, C. T. H. Davies, A. T. Lytle, and J. Koponen, Lattice QCD form factor for $B_s \to D^*_s l\nu$ at zero recoil with non-perturbative current renormalisation, Phys. Rev. D **99**, 114512 (2019).

[524] E. McLean, C. T. H. Davies, J. Koponen, and A. T. Lytle, $B_s \to D_s\ell\nu$ Form Factors for the full q^2 range from Lattice

QCD with nonperturbatively normalized currents, Phys. Rev. D **101**, 074513 (2020).
[525] R. Aaij *et al.* (LHCb Collaboration), Precise measurement of the f_s/f_d ratio of fragmentation fractions and of B_s^0 decay branching fractions, Phys. Rev. D **104**, 032005 (2021).
[526] A. Vossen *et al.* (Belle Collaboration), Measurement of the branching fraction of $B \to D^{(*)}\pi\ell\nu$ at Belle using hadronic tagging in fully reconstructed events, Phys. Rev. D **98**, 012005 (2018).
[527] N. Isgur and M. B. Wise, Spectroscopy with Heavy Quark Symmetry, Phys. Rev. Lett. **66**, 1130 (1991).
[528] B. Aubert *et al.* (*BABAR* Collaboration), Measurement of the Branching Fractions of $\bar{B} \to D^{**}l^-\bar{\nu}_l$ Decays in Events Tagged by a Fully Reconstructed B Meson, Phys. Rev. Lett. **101**, 261802 (2008).
[529] D. Liventsev *et al.* (Belle Collaboration), Study of $B \to D^{**}\ell\nu$ with full reconstruction tagging, Phys. Rev. D **77**, 091503 (2008).
[530] J. Abdallah *et al.* (DELPHI Collaboration), Determination of heavy quark non-perturbative parameters from spectral moments in semileptonic B decays, Eur. Phys. J. C **45**, 35 (2006).
[531] D. Buskulic *et al.* (ALEPH Collaboration), Production of orbitally excited charm mesons in semileptonic B decays, Z. Phys. C **73**, 601 (1997).
[532] G. Abbiendi *et al.* (OPAL Collaboration), A measurement of semileptonic B decays to narrow orbitally-excited charm mesons, Eur. Phys. J. C **30**, 467 (2003).
[533] A. Anastassov *et al.* (CLEO Collaboration), Investigation of Semileptonic B Meson Decay to P-Wave Charm Mesons, Phys. Rev. Lett. **80**, 4127 (1998).
[534] V. M. Abazov *et al.* (D0 Collaboration), Measurement of Semileptonic Branching Fractions of B Mesons to Narrow D^{**} States, Phys. Rev. Lett. **95**, 171803 (2005).
[535] B. Aubert *et al.* (*BABAR* Collaboration), Measurement of Semileptonic B Decays into Orbitally-Excited Charmed Mesons, Phys. Rev. Lett. **103**, 051803 (2009).
[536] D. Benson, I. I. Bigi, T. Mannel, and N. Uraltsev, Imprecated, yet impeccable: On the theoretical evaluation of $\Gamma(B \to X_c\ell\nu)$, Nucl. Phys. **B665**, 367 (2003).
[537] P. Gambino and N. Uraltsev, Moments of semileptonic B decay distributions in the $1/m_b$ expansion, Eur. Phys. J. C **34**, 181 (2004).
[538] P. Gambino, B semileptonic moments at NNLO, J. High Energy Phys. 09 (2011) 055.
[539] A. Alberti, P. Gambino, K. J. Healey, and S. Nandi, Precision Determination of the Cabibbo-Kobayashi-Maskawa Element V_{cb}, Phys. Rev. Lett. **114**, 061802 (2015).
[540] C. W. Bauer, Z. Ligeti, M. Luke, A. V. Manohar, and M. Trott, Global analysis of inclusive B decays, Phys. Rev. D **70**, 094017 (2004).
[541] B. Aubert *et al.* (*BABAR* Collaboration), Measurement and interpretation of moments in inclusive semileptonic decays $\bar{B} \to X_c\ell^-\bar{\nu}$, Phys. Rev. D **81**, 032003 (2010).
[542] B. Aubert *et al.* (*BABAR* Collaboration), Measurement of the electron energy spectrum and its moments in inclusive $B \to Xe\nu$ decays, Phys. Rev. D **69**, 111104 (2004).
[543] C. Schwanda *et al.* (Belle Collaboration), Moments of the hadronic invariant mass spectrum in $B \to X_c\ell\nu$ decays at Belle, Phys. Rev. D **75**, 032005 (2007).
[544] P. Urquijo *et al.* (Belle Collaboration), Moments of the electron energy spectrum and partial branching fraction of $B \to X_c e\nu$ decays at Belle, Phys. Rev. D **75**, 032001 (2007).
[545] D. E. Acosta *et al.* (CDF Collaboration), Measurement of the moments of the hadronic invariant mass distribution in semileptonic B decays, Phys. Rev. D **71**, 051103 (2005).
[546] S. E. Csorna *et al.* (CLEO Collaboration), Moments of the B meson inclusive semileptonic decay rate using neutrino reconstruction, Phys. Rev. D **70**, 032002 (2004).
[547] K. G. Chetyrkin, J. H. Kühn, A. Maier, P. Maierhöfer, P. Marquard, M. Steinhauser, and C. Sturm, Charm and bottom quark masses: An update, Phys. Rev. D **80**, 074010 (2009).
[548] B. Aubert *et al.* (*BABAR* Collaboration), Measurements of the $B \to X_s\gamma$ branching fraction and photon spectrum from a sum of exclusive final states, Phys. Rev. D **72**, 052004 (2005).
[549] B. Aubert *et al.* (*BABAR* Collaboration), Measurement of the Branching Fraction and Photon Energy Moments of $B \to X_s\gamma$ and $A_{CP}(B \to X_{s+d}\gamma)$, Phys. Rev. Lett. **97**, 171803 (2006).
[550] A. Limosani *et al.* (Belle Collaboration), Measurement of Inclusive Radiative B-Meson Decays with a Photon Energy Threshold of 1.7-GeV, Phys. Rev. Lett. **103**, 241801 (2009).
[551] S. Chen *et al.* (CLEO Collaboration), Branching Fraction and Photon Energy Spectrum for $b \to s\gamma$, Phys. Rev. Lett. **87**, 251807 (2001).
[552] P. Gambino and C. Schwanda, Inclusive semileptonic fits, heavy quark masses, and V_{cb}, Phys. Rev. D **89**, 014022 (2014).
[553] C. Schwanda *et al.* (Belle Collaboration), Measurement of the moments of the photon energy spectrum in $B \to X_s\gamma$ decays and determination of $|V_{cb}|$ and m_b at Belle, Phys. Rev. D **78**, 032016 (2008).
[554] R. Aaij *et al.* (LHCb Collaboration), Determination of the quark coupling strength $|V_{ub}|$ using baryonic decays, Nat. Phys. **11**, 743 (2015).
[555] R. Aaij *et al.* (LHCb Collaboration), First Observation of the Decay $B_s^0 \to K^-\mu^+\nu_\mu$ and Measurement of $|V_{ub}|/|V_{cb}|$, Phys. Rev. Lett. **126**, 081804 (2021).
[556] H. Ha *et al.* (Belle Collaboration), Measurement of the decay $B^0 \to \pi^-\ell^+\nu$ and determination of $|V_{ub}|$, Phys. Rev. D **83**, 071101 (2011).
[557] A. Sibidanov *et al.* (Belle Collaboration), Study of exclusive $B \to X_u\ell\nu$ decays and extraction of $\|V_{ub}\|$ using full reconstruction tagging at the Belle experiment, Phys. Rev. D **88**, 032005 (2013).
[558] P. del Amo Sanchez *et al.* (*BABAR* Collaboration), Study of $B \to \pi\ell\nu$ and $B \to \rho\ell\nu$ decays and determination of $|V_{ub}|$, Phys. Rev. D **83**, 032007 (2011).
[559] J. P. Lees *et al.* (*BABAR* Collaboration), Branching fraction and form-factor shape measurements of exclusive charmless semileptonic B decays, and determination of $|V_{ub}|$, Phys. Rev. D **86**, 092004 (2012).

[560] C. Bourrely, I. Caprini, and L. Lellouch, Model-independent description of $B \to \pi \ell \nu$ decays and a determination of $|V_{ub}|$, Phys. Rev. D **79**, 013008 (2009); **82**, 099902(E) (2010).

[561] J. A. Bailey *et al.*, $|V_{ub}|$ from $B \to \pi \ell \nu$ decays and $(2+1)$-flavor lattice QCD, Phys. Rev. D **92**, 014024 (2015).

[562] J. M. Flynn, T. Izubuchi, T. Kawanai, C. Lehner, A. Soni, R. S. Van de Water, and O. Witzel, $B \to \pi \ell \nu$ and $B_s \to K \ell \nu$ form factors and $|V_{ub}|$ from $2+1$-flavor lattice QCD with domain-wall light quarks and relativistic heavy quarks, Phys. Rev. D **91**, 074510 (2015).

[563] A. Bharucha, Two-loop corrections to the $B \to \pi$ form factor from QCD sum rules on the light-cone and $|V_{ub}|$, J. High Energy Phys. 05 (2012) 092.

[564] B. H. Behrens *et al.* (CLEO Collaboration), Measurement of $B \to \rho \ell \nu$ decay and $|V_{ub}|$, Phys. Rev. D **61**, 052001 (2000).

[565] N. E. Adam *et al.* (CLEO Collaboration), A Study of Exclusive Charmless Semileptonic B Decay and $|V_{ub}|$, Phys. Rev. Lett. **99**, 041802 (2007).

[566] T. Hokuue *et al.* (Belle Collaboration), Measurements of branching fractions and q^2 distributions for $B \to \pi \ell \nu$ and $B \to \rho \ell \nu$ Decays with $B \to D^{(*)} \ell \nu$ Decay Tagging, Phys. Lett. B **648**, 139 (2007).

[567] C. Schwanda *et al.* (Belle Collaboration), Evidence for $B^+ \to \omega \ell^+ \nu$, Phys. Rev. Lett. **93**, 131803 (2004).

[568] J. P. Lees *et al.* (*BABAR* Collaboration), Branching fraction measurement of $B^+ \to \omega \ell^+ \nu$ decays, Phys. Rev. D **87**, 032004 (2013).

[569] J. P. Lees *et al.* (*BABAR* Collaboration), Measurement of the $B^+ \to \omega \ell^+ \nu$ branching fraction with semileptonically tagged B mesons, Phys. Rev. D **88**, 072006 (2013).

[570] A. Bharucha, D. M. Straub, and R. Zwicky, $B \to V \ell^+ \ell^-$ in the standard model from light-cone sum rules, J. High Energy Phys. 08 (2016) 098.

[571] R. Gray *et al.* (CLEO Collaboration), A study of exclusive charmless semileptonic B decays and extraction of $|V_{ub}|$ at CLEO, Phys. Rev. D **76**, 012007 (2007).

[572] B. Aubert *et al.* (*BABAR* Collaboration), Measurement of the $B^+ \to \omega \ell^+ \nu$ and $B^+ \to \eta \ell^+ \nu$ branching fractions, Phys. Rev. D **79**, 052011 (2009).

[573] B. Aubert *et al.* (*BABAR* Collaboration), Measurements of $B \to \{\pi, \eta, \eta'\} \ell \nu_\ell$ Branching Fractions and Determination of $|V_{ub}|$ with Semileptonically Tagged B Mesons, Phys. Rev. Lett. **101**, 081801 (2008).

[574] C. Beleño *et al.* (Belle Collaboration), Measurement of the decays $B \to \eta \ell \nu_\ell$ and $B \to \eta' \ell \nu_\ell$ in fully reconstructed events at Belle, Phys. Rev. D **96**, 091102 (2017).

[575] U. Gebauer *et al.* (Belle Collaboration), Measurement of the branching fractions of the $B^+ \to \eta \ell^+ \nu_\ell$ and $B^+ \to \eta' \ell^+ \nu_\ell$ decays with signal-side only reconstruction in the full q^2 range, Phys. Rev. D **106**, 032013 (2022).

[576] W. Detmold, C. Lehner, and S. Meinel, $\Lambda_b \to p \ell^- \bar{\nu}_\ell$ and $\Lambda_b \to \Lambda_c \ell^- \bar{\nu}_\ell$ form factors from lattice QCD with relativistic heavy quarks, Phys. Rev. D **92**, 034503 (2015).

[577] A. Khodjamirian and A. V. Rusov, $B_s \to K \ell \nu_\ell$ and $B_{(s)} \to \pi(K) \ell^+ \ell^-$ decays at large recoil and CKM matrix elements, J. High Energy Phys. 08 (2017) 112.

[578] A. Bazavov *et al.* (Fermilab Lattice and MILC Collaborations), $B_s \to K \ell \nu$ decay from lattice QCD, Phys. Rev. D **100**, 034501 (2019).

[579] P. Urquijo *et al.* (Belle Collaboration), Measurement Of $|V_{ub}|$ From Inclusive Charmless Semileptonic B Decays, Phys. Rev. Lett. **104**, 021801 (2010).

[580] J. P. Lees *et al.* (*BABAR* Collaboration), Study of $\bar{B} \to X_u \ell \bar{\nu}$ decays in $B\bar{B}$ events tagged by a fully reconstructed B-meson decay and determination of $\|V_{ub}\|$, Phys. Rev. D **86**, 032004 (2012).

[581] C. W. Bauer, Z. Ligeti, and M. E. Luke, Precision determination of $|V_{ub}|$ from inclusive decays, Phys. Rev. D **64**, 113004 (2001).

[582] M. Neubert, Analysis of the photon spectrum in inclusive $B \to X_s \gamma$ decays, Phys. Rev. D **49**, 4623 (1994).

[583] A. K. Leibovich, I. Low, and I. Z. Rothstein, Extracting V_{ub} without recourse to structure functions, Phys. Rev. D **61**, 053006 (2000).

[584] B. O. Lange, M. Neubert, and G. Paz, A two-loop relation between inclusive radiative and semileptonic B decay spectra, J. High Energy Phys. 10 (2005) 084.

[585] J. P. Lees *et al.* (*BABAR* Collaboration), Measurement of the inclusive electron spectrum from B meson decays and determination of $|V_{ub}|$, Phys. Rev. D **95**, 072001 (2017).

[586] B. Aubert *et al.* (*BABAR* Collaboration), Measurement of the inclusive electron spectrum in charmless semileptonic B decays near the kinematic endpoint and determination of $|V_{ub}|$, Phys. Rev. D **73**, 012006 (2006).

[587] R. V. Kowalewski and S. Menke, Complementary observables for the determination of $|V_{ub}|$ in inclusive semileptonic B decays, Phys. Lett. B **541**, 29 (2002).

[588] B. Aubert *et al.* (*BABAR* Collaboration), Determination of $|V_{ub}|$ from Measurements of the Electron and Neutrino Momenta in Inclusive Semileptonic B Decays, Phys. Rev. Lett. **95**, 111801 (2005).

[589] A. Bornheim *et al.* (CLEO Collaboration), Improved Measurement of $|V_{ub}|$ with Inclusive Semileptonic B Decays, Phys. Rev. Lett. **88**, 231803 (2002).

[590] A. Limosani *et al.* (Belle Collaboration), Measurement of inclusive charmless semileptonic B-meson decays at the endpoint of the electron momentum spectrum, Phys. Lett. B **621**, 28 (2005).

[591] H. Kakuno *et al.* (Belle Collaboration), Measurement of $|V_{ub}|$ Using Inclusive $B \to X_u \ell \nu$ Decays with a Novel X_u Reconstruction Method, Phys. Rev. Lett. **92**, 101801 (2004).

[592] I. Bizjak *et al.* (Belle Collaboration), Measurement of the Inclusive Charmless Semileptonic Partial Branching Fraction of B Mesons and Determination of $|V_{ub}|$ Using the Full Reconstruction Tag, Phys. Rev. Lett. **95**, 241801 (2005).

[593] L. Cao *et al.* (Belle Collaboration), Measurements of partial branching fractions of inclusive $B \to X_u \ell^+ \nu_\ell$ decays with hadronic tagging, Phys. Rev. D **104**, 012008 (2021).

[594] B. O. Lange, M. Neubert, and G. Paz, Theory of charmless inclusive B decays and the extraction of V_{ub}, Phys. Rev. D **72**, 073006 (2005).

[595] S. W. Bosch, B. O. Lange, M. Neubert, and G. Paz, Factorization and shape-function effects in inclusive B-meson decays, Nucl. Phys. **B699**, 335 (2004).

[596] S. W. Bosch, M. Neubert, and G. Paz, Subleading shape functions in inclusive B decays, J. High Energy Phys. 11 (2004) 073.

[597] M. Neubert, Impact of four-quark shape functions on inclusive B decay spectra, Eur. Phys. J. C **44**, 205 (2005).

[598] M. Neubert, Two-loop relations for heavy-quark parameters in the shape-function scheme, Phys. Lett. B **612**, 13 (2005).

[599] M. Neubert, Advanced predictions for moments of the $\bar{B} \to X_s\gamma$ photon spectrum, Phys. Rev. D **72**, 074025 (2005).

[600] J. R. Andersen and E. Gardi, Inclusive spectra in charmless semileptonic B decays by dressed gluon exponentiation, J. High Energy Phys. 01 (2006) 097.

[601] U. Aglietti, G. Ferrera, and G. Ricciardi, Semi-inclusive B decays and a model for soft-gluon effects, Nucl. Phys. **B768**, 85 (2007).

[602] I. R. Blokland, A. Czarnecki, M. Misiak, M. Ślusarczyk, and F. Tkachov, The electromagnetic dipole operator effect on $\bar{B} \to X_s\gamma$ at $O(\alpha^2 - s)$, Phys. Rev. D **72**, 033014 (2005).

[603] P. Gambino and P. Giordano, Normalizing inclusive rare B decays, Phys. Lett. B **669**, 69 (2008).

[604] P. Gambino, P. Giordano, G. Ossola, and N. Uraltsev, Inclusive semileptonic B decays and the determination of $|V_{ub}|$, J. High Energy Phys. 10 (2007) 058.

[605] U. Aglietti, F. Di Lodovico, G. Ferrera, and G. Ricciardi, Inclusive measure of $|V_{ub}|$ with the analytic coupling model, Eur. Phys. J. C **59**, 831 (2009).

[606] U. Aglietti, G. Ricciardi, and G. Ferrera, Threshold resummed spectra in $B \to X_u\ell\nu$ decays in NLO. I, Phys. Rev. D **74**, 034004 (2006).

[607] U. Aglietti, G. Ricciardi, and G. Ferrera, Threshold resummed spectra in $B \to X_u\ell\nu$ decays in NLO (II), Phys. Rev. D **74**, 034005 (2006).

[608] U. Aglietti, G. Ricciardi, and G. Ferrera, Threshold resummed spectra in $B \to X_u\ell\nu$ decays in NLO (III), Phys. Rev. D **74**, 034006 (2006).

[609] M. Duraisamy, P. Sharma, and A. Datta, The azimuthal $B \to D^*\tau^-\overline{\nu_\tau}$ angular distribution with tensor operators, Phys. Rev. D **90**, 074013 (2014).

[610] D. Bigi and P. Gambino, Revisiting $B \to D\ell\nu$, Phys. Rev. D **94**, 094008 (2016).

[611] F. U. Bernlochner, Z. Ligeti, M. Papucci, and D. J. Robinson, Combined analysis of semileptonic B decays to D and D^*: $R(D^{(*)})$, $|V_{cb}|$, and new physics, Phys. Rev. D **95**, 115008 (2017); **97**, 059902(E) (2018).

[612] S. Jaiswal, S. Nandi, and S. K. Patra, Extraction of $|V_{cb}|$ from $B \to D^{(*)}\ell\nu_\ell$ and the standard model predictions of $R(D^{(*)})$, J. High Energy Phys. 12 (2017) 060.

[613] M. Bordone, M. Jung, and D. van Dyk, Theory determination of $\overline{B} \to D^{(*)}\ell^-\bar{\nu}$ form factors at $\mathcal{O}(1/m_c^2)$, Eur. Phys. J. C **80**, 74 (2020).

[614] G. Martinelli, S. Simula, and L. Vittorio, $|V_{cb}|$ and $R(D)^{(*)}$ using lattice QCD and unitarity, Phys. Rev. D **105**, 034503 (2022).

[615] P. Gambino, M. Jung, and S. Schacht, The V_{cb} puzzle: An update, Phys. Lett. B **795**, 386 (2019).

[616] MILC, A. Bazavov *et al.* (Fermilab Lattice Collaboration), Semileptonic form factors for $B \to D^*\ell\nu$ at nonzero recoil from 2 + 1-flavor lattice QCD, arXiv:2105.14019.

[617] A. Matyja *et al.* (Belle Collaboration), Observation of $B^0 \to D^{*-}\tau^+\nu_\tau$ Decay at Belle, Phys. Rev. Lett. **99**, 191807 (2007).

[618] B. Aubert *et al.* (*BABAR* Collaboration), Observation of the Semileptonic Decays $B \to D^*\tau^-\bar{\nu}_\tau$ and Evidence for $B \to D\tau^-\bar{\nu}_\tau$, Phys. Rev. Lett. **100**, 021801 (2008).

[619] A. Bozek *et al.* (Belle Collaboration), Observation of $B^+ \to \bar{D}^{*0}\tau^+\nu_\tau$ and evidence for $B^+ \to \bar{D}^0\tau^+\nu_\tau$ at Belle, Phys. Rev. D **82**, 072005 (2010).

[620] J. P. Lees *et al.* (*BABAR* Collaboration), Evidence for an Excess of $\bar{B} \to D^{(*)}\tau^-\bar{\nu}_\tau$ Decays, Phys. Rev. Lett. **109**, 101802 (2012).

[621] M. Huschle *et al.* (Belle Collaboration), Measurement of the branching ratio of $\bar{B} \to D^{(*)}\tau^-\bar{\nu}_\tau$ relative to $\bar{B} \to D^{(*)}\ell^-\bar{\nu}_\ell$ decays with hadronic tagging at Belle, Phys. Rev. D **92**, 072014 (2015).

[622] G. Caria *et al.* (Belle Collaboration), Measurement of $\mathcal{R}(D)$ and $\mathcal{R}(D^*)$ with a Semileptonic Tagging Method, Phys. Rev. Lett. **124**, 161803 (2020).

[623] S. Hirose *et al.* (Belle Collaboration), Measurement of the τ Lepton Polarization and $R(D^*)$ in the Decay $\bar{B} \to D^*\tau^-\bar{\nu}_\tau$, Phys. Rev. Lett. **118**, 211801 (2017).

[624] R. Aaij *et al.* (LHCb Collaboration), Measurement of the Ratio of Branching Fractions $\mathcal{B}(\bar{B}^0 \to D^{*+}\tau^-\bar{\nu}_\tau)/\mathcal{B}(\bar{B}^0 \to D^{*+}\mu^-\bar{\nu}_\mu)$, Phys. Rev. Lett. **115**, 111803 (2015); **115**, 159901(A) (2015).

[625] R. Aaij *et al.* (LHCb Collaboration), Measurement of the Ratio of the $B^0 \to D^{*-}\tau^+\nu_\tau$ and $B^0 \to D^{*-}\mu^+\nu_\mu$ Branching Fractions Using Three-Prong τ-Lepton Decays, Phys. Rev. Lett. **120**, 171802 (2018).

[626] R. Aaij *et al.* (LHCb Collaboration), Measurement of the Ratio of Branching Fractions $\mathcal{B}(B_c^+ \to J/\psi\tau^+\nu_\tau)/\mathcal{B}(B_c^+ \to J/\psi\mu^+\nu_\mu)$, Phys. Rev. Lett. **120**, 121801 (2018).

[627] J. Harrison, C. T. H. Davies, and A. Lytle (LATTICE-HPQCD Collaboration), $R(J/\psi)$ and $B_c^- \to J/\psi\ell^-\bar{\nu}_\ell$ Lepton Flavor Universality Violating Observables from Lattice QCD, Phys. Rev. Lett. **125**, 222003 (2020).

[628] R. Aaij *et al.* (LHCb Collaboration), Observation of the decay $\Lambda_b^0 \to \Lambda_c^+\tau^-\bar{\nu}_\tau$, Phys. Rev. Lett. **128**, 191803 (2022).

[629] F. U. Bernlochner, Z. Ligeti, D. J. Robinson, and W. L. Sutcliffe, Precise predictions for $\Lambda_b \to \Lambda_c$ semileptonic decays, Phys. Rev. D **99**, 055008 (2019).

[630] J. P. Lees *et al.* (*BABAR* Collaboration), Measurement of an excess of $\bar{B} \to D^{(*)}\tau^-\bar{\nu}_\tau$ decays and implications for charged Higgs bosons, Phys. Rev. D **88**, 072012 (2013).

[631] R. Aaij *et al.* (LHCb Collaboration), Test of lepton flavor universality by the measurement of the $B^0 \to D^{*-}\tau^+\nu_\tau$ branching fraction using three-prong τ decays, Phys. Rev. D **97**, 072013 (2018).

[632] A. J. Lenz, Selected topics in heavy flavour physics, J. Phys. G **41**, 103001 (2014).

[633] S. K. Choi *et al.* (Belle Collaboration), Observation of a Narrow Charmoniumlike State in Exclusive $B^\pm \to K^\pm\pi^+ pi^- J/\psi$ Decays, Phys. Rev. Lett. **91**, 262001 (2003).

[634] R. Aaij *et al.* (LHCb Collaboration), Quantum numbers of the $X(3872)$ state and orbital angular momentum in its $\rho^0 J/\psi$ decay, Phys. Rev. D **92**, 011102 (2015).

[635] S. K. Choi *et al.* (Belle Collaboration), Observation of a Resonancelike Structure in the $\pi^{\pm}\psi'$ Mass Distribution in Exclusive $B \to K\pi^{\pm}\psi'$ Decays, Phys. Rev. Lett. **100**, 142001 (2008).

[636] R. Aaij *et al.* (LHCb Collaboration), Observation of the Resonant Character of the $Z(4430)^-$ State, Phys. Rev. Lett. **112**, 222002 (2014).

[637] R. Aaij *et al.* (LHCb Collaboration), Observation of $J/\psi p$ Resonances Consistent with Pentaquark States in $\Lambda_b^0 \to J/\psi K^- p$ Decays, Phys. Rev. Lett. **115**, 072001 (2015).

[638] Hflav web page on hadronic b decays into open or hidden charm, https://hflav.web.cern.ch/content/b-hadron-decays-open-or-hidden-charm-hadrons.

[639] K. De Bruyn, R. Fleischer, R. Knegjens, P. Koppenburg, M. Merk, and N. Tuning, Branching ratio measurements of B_s decays, Phys. Rev. D **86**, 014027 (2012).

[640] M. Jung, Branching ratio measurements and isospin violation in B-meson decays, Phys. Lett. B **753**, 187 (2016).

[641] B. Aubert *et al.* (*BABAR* Collaboration), Branching fraction measurement of $B^0 \to D^{(*)} + \pi^-$, $B^- \to D^{(*)}0\pi^-$ and isospin analysis of $\bar{B} \to D^{(*)}\pi$ decays, Phys. Rev. D **75**, 031101 (2007).

[642] B. Aubert *et al.* (*BABAR* Collaboration), Measurement of the absolute branching fractions B to $D\pi$, $D^*\pi$, $D^{**}\pi$ with a missing mass method, Phys. Rev. D **74**, 111102 (2006).

[643] K. Abe *et al.* (Belle Collaboration), Observation of Cabibbo Suppressed $B \to D^{(*)}K^-$ Decays at BELLE, Phys. Rev. Lett. **87**, 111801 (2001).

[644] A. Abulencia *et al.* (CDF Collaboration), Measurement of the Ratios of Branching Fractions $B(B_s^0 \to D_s^-\pi^+)/B(B^0 \to D^-\pi^+)$ and $B(B^+ \to \bar{D}^0\pi^+)/B(B^0 \to D^-\pi^+)$, Phys. Rev. Lett. **96**, 191801 (2006).

[645] A. Abulencia *et al.* (CDF Collaboration), Measurement of the Ratios of Branching Fractions $B(B_s^0 \to D_s^-\pi^+\pi^+ pi^-)/B(B^0 \to D^-\pi^+\pi^+ pi^-)$ and $B(B_s^0 \to D_s^-\pi^+)/B(B^0 \to D^-\pi^+)$, Phys. Rev. Lett. **98**, 061802 (2007).

[646] A. Abulencia *et al.* (CDF Collaboration), Measurement of $\sigma(\Lambda_b^0)/\sigma(\bar{B}^0) \times \mathrm{BR}(\Lambda_b^0 \to \Lambda_c^+\pi^-)/\mathrm{BR}(\bar{B}^0 \to D^+\pi^-)$ in $p\bar{p}$ Collisions at $\sqrt{s} = 1.96$-TeV, Phys. Rev. Lett. **98**, 122002 (2007).

[647] R. Aaij *et al.* (LHCb Collaboration), Measurements of the branching fractions for $B_{(s)} \to D_{(s)}\pi\pi\pi$ and $\Lambda_b^0 \to \Lambda_c^+\pi\pi\pi$, Phys. Rev. D **84**, 092001 (2011).

[648] R. Aaij *et al.* (LHCb Collaboration), Measurement of the fragmentation fraction ratio f_s/f_d and its dependence on B meson kinematics, J. High Energy Phys. 04 (2013) 001, with numerical results and full covariance matrix available at http://cdsweb.cern.ch/record/1507868.

[649] R. Aaij *et al.* (LHCb Collaboration), First Observation of the Decays $\bar{B}^0 \to D^+K^-\pi^+\pi^-$ and $B^- \to D^0K^-\pi^+\pi^-$, Phys. Rev. Lett. **108**, 161801 (2012).

[650] A. Kuzmin *et al.* (Belle Collaboration), Study of $\bar{B}^0 \to D^0\pi^+\pi^-$ decays, Phys. Rev. D **76**, 012006 (2007).

[651] B. Aubert *et al.* (*BABAR* Collaboration), Measurement of Branching Fractions and Resonance Contributions for $B^0 \to \bar{D}^0K^+\pi^-$ and Search for $B^0 \to D^0K^+\pi^-$ Decays, Phys. Rev. Lett. **96**, 011803 (2006).

[652] R. Aaij *et al.* (LHCb Collaboration), Study of $B^0 \to D^{*-}\pi^+\pi^-\pi^+$ and $B^0 \to D^{*-}K^+\pi^-\pi^+$ decays, Phys. Rev. D **87**, 092001 (2013).

[653] J. P. Lees *et al.* (*BABAR* Collaboration), Measurement of the $B^0 \to D^* - \pi^+\pi^-\pi^+$ branching fraction, Phys. Rev. D **94**, 091101 (2016).

[654] G. Majumder *et al.* (Belle Collaboration), Observation of $B^0 \to D^{*-}(5\pi)^+$, $B^+ \to D^{*-}(4\pi)^{++}$ and $B^+ \to \bar{D}^{*0}(5\pi)^+$, Phys. Rev. D **70**, 111103 (2004).

[655] D. Matvienko *et al.* (Belle Collaboration), Study of D^{**} production and light hadronic states in the $\bar{B}^0 \to D^{*+}\omega\pi^-$ decay, Phys. Rev. D **92**, 012013 (2015).

[656] B. Aubert *et al.* (*BABAR* Collaboration), Study of the decay $\bar{B}^0 \to D^{*+}\omega\pi^-$, Phys. Rev. D **74**, 012001 (2006).

[657] J. P. Lees *et al.* (*BABAR* Collaboration), Branching fraction measurements of the color-suppressed decays $\bar{B}^0 \to D^{(*)0}\pi^0$, $D^{(*)0}\eta$, $D^{(*)0}\omega$, and $D^{(*)0}\eta'$ and measurement of the polarization in the decay $\bar{B}^0 \to D^*0\omega$, Phys. Rev. D **84**, 112007 (2011).

[658] S. Blyth *et al.* (Belle Collaboration), Improved measurements of color-suppressed decays $\bar{B}^0 \to D^0\pi^0$, $D^0\eta$, $D^0\omega$, $D^{*0}\pi^0$, $D^{*0}\eta$ and $D^{*0}\omega$, Phys. Rev. D **74**, 092002 (2006).

[659] R. Aaij *et al.* (LHCb Collaboration), Dalitz plot analysis of $B^0 \to \bar{D}^0\pi^+\pi^-$ decays, Phys. Rev. D **92**, 032002 (2015).

[660] R. Aaij *et al.* (LHCb Collaboration), Measurement of the branching fractions of the decays $B_s^0 \to \bar{D}^0K^-\pi^+$ and $B^0 \to \bar{D}^0K^+\pi^-$, Phys. Rev. D **87**, 112009 (2013).

[661] R. Aaij *et al.* (LHCb Collaboration), Observation of $B_s^0 \to \bar{D}^{*0}\phi$ and search for $B^0 \to \bar{D}^0\phi$ decays, Phys. Rev. D **98**, 071103 (2018).

[662] R. Aaij *et al.* (LHCb Collaboration), Observation of the decay $B_s^0 \to \bar{D}^0K^+K^-$, Phys. Rev. D **98**, 072006 (2018).

[663] A. Satpathy *et al.* (Belle Collaboration), Study of $\bar{B}^0 \to D^{0(*)}\pi^+\pi^-$ decays, Phys. Lett. B **553**, 159 (2003).

[664] R. Aaij *et al.* (LHCb Collaboration), First observation of the decay $\bar{B}_s^0 \to D^0K^{*0}$ and a measurement of the ratio of branching fractions $\frac{\mathcal{B}(\bar{B}_s^0 \to D^0K^{*0})}{\mathcal{B}(\bar{B}^0 \to D^0\rho^0)}$, Phys. Lett. B **706**, 32 (2011).

[665] J. Schumann *et al.* (Belle Collaboration), Observation of $\bar{B}^0 \to D^0\eta'$ and $\bar{B}^0 \to D^{*0}\eta'$, Phys. Rev. D **72**, 011103 (2005).

[666] B. Aubert *et al.* (*BABAR* Collaboration), Measurement of Branching Fraction and Dalitz Distribution for $B^0 \to D^{(*)\pm}K^0\pi^{\mp}$ Decays, Phys. Rev. Lett. **95**, 171802 (2005).

[667] A. Drutskoy *et al.* (Belle Collaboration), Observation of $B \to D^{(*)}K^-K^{0(*)}$ decays, Phys. Lett. B **542**, 171 (2002).

[668] B. Aubert *et al.* (*BABAR* Collaboration), Measurement of $\bar{B}^0 \to D^{(*)0}\bar{K}^{(*)0}$ branching fractions, Phys. Rev. D **74**, 031101 (2006).

[669] P. Krokovny *et al.* (Belle Collaboration), Observation of $\bar{B}^0 \to D^0\bar{K}^0$ and $\bar{B}^0 t0D^0\bar{K}^{*0}$ Decays, Phys. Rev. Lett. **90**, 141802 (2003).

[670] R. Aaij *et al.* (LHCb Collaboration), Observation of the decay $B_s^0 \to \bar{D}^0\phi$, Phys. Lett. B **727**, 403 (2013).

[671] A. Das *et al.* (Belle Collaboration), Measurements of branching fractions for $B^0 \to D_s^+\pi^-$ and $\bar{B}^0 \to D_s^+K^-$, Phys. Rev. D **82**, 051103 (2010).

[672] B. Aubert *et al.* (*BABAR* Collaboration), Measurement of the branching fractions of the rare decays $B^0 \to D_s^{(*)+}\pi^-$, $B^0 \to D_s^{(*)+}\rho^-$, and $B^0 \to D_s^{(*)-}K^{(*)+}$, Phys. Rev. D **78**, 032005 (2008).

[673] N. J. Joshi *et al.* (Belle Collaboration), Measurement of the branching fractions for $B^0 \to D_s^{*+}\pi^-$ and $B^0 \to D_s^{*-}K^+$ decays, Phys. Rev. D **81**, 031101 (2010).

[674] B. Aubert *et al.* (*BABAR* Collaboration), Search for the rare decays $B^0 \to D^{(*)+}a_{0(2)}^-$, Phys. Rev. D **73**, 071103 (2006).

[675] R. Aaij *et al.* (LHCb Collaboration), Determination of the branching fractions of $B_s^0 \to D_s^{\mp}K^{\pm}$ and $B^0 \to D_s^-K^+$, J. High Energy Phys. 05 (2015) 019.

[676] B. Aubert *et al.* (*BABAR* Collaboration), Observation of Tree-Level B Decays with $s\bar{s}$ Production from Gluon Radiation., Phys. Rev. Lett. **100**, 171803 (2008).

[677] R. Aaij *et al.* (LHCb Collaboration), First observation of the decays $\bar{B}_{(s)}^0 \to D_s^+K^-\pi^+\pi^-$ and $\bar{B}_s^0 \to D_{s1}(2536)^+\pi^-$, Phys. Rev. D **86**, 112005 (2012).

[678] B. Aubert *et al.* (*BABAR* Collaboration), Measurement of the $B^0 \to D^{*-}D_s^{*+}$ and $D_s^+ \to \phi\pi^+$ branching fractions, Phys. Rev. D **71**, 091104 (2005).

[679] K. Abe *et al.* (Belle Collaboration), Observation of the $D_1(2420) \to D\pi^+\pi^-$ Decays, Phys. Rev. Lett. **94**, 221805 (2005).

[680] A. Drutskoy *et al.* (Belle Collaboration), Observation of $\bar{B}^0 \to D_{sJ}^*(2317)^+K^-$ Decay, Phys. Rev. Lett. **94**, 061802 (2005).

[681] P. del Amo Sanchez *et al.* (*BABAR* Collaboration), Observation and study of the baryonic B-meson decays $B \to D^{(*)}p\bar{p}(\pi)(\pi)$, Phys. Rev. D **85**, 092017 (2012).

[682] K. Abe *et al.* (Belle Collaboration), Observation of $\bar{B}^0 \to D^0(*)p\bar{p}$, Phys. Rev. Lett. **89**, 151802 (2002).

[683] T. Medvedeva *et al.* (Belle Collaboration), Observation of the decay $\overline{B}^0 \to D_S^+\Lambda\bar{p}$, Phys. Rev. D **76**, 051102 (2007).

[684] J. P. Lees *et al.* (*BABAR* Collaboration), Evidence for the baryonic decay $\bar{B}^0 \to D^0\Lambda\bar{\Lambda}$, Phys. Rev. D **89**, 112002 (2014).

[685] Y.-W. Chang *et al.* (Belle Collaboration), Observation of $B^0 \to \Lambda\bar{\Lambda}K^0$ and B^0 to $\Lambda\bar{\Lambda}K^{*0}$ at Belle, Phys. Rev. D **79**, 052006 (2009).

[686] Y.-Y. Chang *et al.*, Observation of $B^0 \to p\bar{\Lambda}D^{(*)-}$, Phys. Rev. Lett. **115**, 221803 (2015).

[687] B. Aubert *et al.* (*BABAR* Collaboration), Measurement of branching fractions and CP-violating charge asymmetries for B meson decays to $D^{(*)}\bar{D}^{(*)}$, and implications for the CKM angle γ, Phys. Rev. D **73**, 112004 (2006).

[688] R. Aaij *et al.* (LHCb Collaboration), First observations of $\bar{B}_s^0 \to D^+D^-$, $D_s^+D^-$ and $D^0\bar{D}^0$ decays, Phys. Rev. D **87**, 092007 (2013).

[689] I. Adachi *et al.* (Belle Collaboration), Measurement of the branching fraction and charge asymmetry of the decay $B^+ \to D^+\bar{D}^0$ and search for $B^0 \to D^0\bar{D}^0$, Phys. Rev. D **77**, 091101 (2008).

[690] P. del Amo Sanchez *et al.* (*BABAR* Collaboration), Measurement of the $B \to \overline{D}^{(*)}D^{(*)}K$ branching fractions, Phys. Rev. D **83**, 032004 (2011).

[691] G. Gokhroo *et al.* (Belle Collaboration), Observation of a Near-Threshold $D^0\bar{D}^0\pi^0$ Enhancement in $B \to D^0\bar{D}^0\pi^0K$ Decay, Phys. Rev. Lett. **97**, 162002 (2006).

[692] A. Zupanc *et al.*, Improved measurement of $\bar{B}^0 \to D_s^-D^+$ and search for $\bar{B}^0 \to D_s^+D_s^-$ at Belle, Phys. Rev. D **75**, 091102 (2007).

[693] B. Aubert *et al.* (*BABAR* Collaboration), Study of $B \to D^{(*)}D^{(*)}$ (s(J)) decays and measurement of D_s^- and D_{sJ} (2460)—branching fractions, Phys. Rev. D **74**, 031103 (2006).

[694] R. Aaij *et al.* (LHCb Collaboration), Study of Beauty Hadron Decays into Pairs of Charm Hadrons, Phys. Rev. Lett. **112**, 202001 (2014).

[695] B. Aubert *et al.* (*BABAR* Collaboration), Measurement of $B^0 \to D_s^{(*)+}D^{*-}$ branching fractions and $B^0 \to D_s^{(*)+}D^{*-}$ polarization with a partial reconstruction technique, Phys. Rev. D **67**, 092003 (2003).

[696] B. Aubert *et al.* (*BABAR* Collaboration), Search for the W^- exchange decays $B^0 \to D_s^{(*)-}D_s^{(*)+}$, Phys. Rev. D **72**, 111101 (2005).

[697] S.-K. Choi *et al.* (Belle Collaboration), Measurements of $B \to \bar{D}D_{s0}^{*+}(2317)$ decay rates and a search for isospin partners of the $D_{s0}^{*+}(2317)$, Phys. Rev. D **91**, 092011 (2015); **92**, 039905(A) (2015).

[698] B. Aubert *et al.* (*BABAR* Collaboration), Study of $B \to D_{sJ}^{(*)+}\bar{D}^{(*)}$ Decays, Phys. Rev. Lett. **93**, 181801 (2004).

[699] P. Krokovny *et al.* (Belle Collaboration), Observation of the $D_{sJ}(2317)$ and $D_{sJ}(2457)$ in B Decays, Phys. Rev. Lett. **91**, 262002 (2003).

[700] B. Aubert *et al.* (*BABAR* Collaboration), Study of resonances in exclusive B decays to $\bar{D}^{(*)}D^{(*)}K$, Phys. Rev. D **77**, 011102 (2008).

[701] T. Aushev *et al.* (Belle Collaboration), Study of the decays $B \to D_{s1}(2536)^+\bar{D}^{(*)}$, Phys. Rev. D **83**, 051102 (2011).

[702] K. Abe *et al.* (Belle Collaboration), Measurement of branching fractions and charge asymmetries for two-body B meson decays with charmonium, Phys. Rev. D **67**, 032003 (2003).

[703] F. Abe *et al.* (CDF Collaboration), Reconstruction of $B^0 \to J/\psi K_S^0$ and Measurement of Ratios of Branching Ratios Involving $B \to J/\psi K^*$, Phys. Rev. Lett. **76**, 2015 (1996).

[704] B. Aubert *et al.* (*BABAR* Collaboration), Branching fraction measurements of $B \to \eta_c K$ decays, Phys. Rev. D **70**, 011101 (2004).

[705] F. Abe *et al.* (CDF Collaboration), Ratios of bottom meson branching fractions involving J/ψ mesons and determination of b quark fragmentation fractions, Phys. Rev. D **54**, 6596 (1996).

[706] R. Aaij *et al.* (LHCb Collaboration), Measurement of the $B_s^0 \to J/\psi K_S^0$ branching fraction, Phys. Lett. B **713**, 172 (2012).

[707] R. Aaij *et al.* (LHCb Collaboration), Observation of the $B_s^0 \to J/\psi K_s^0 K^{\pm}\pi^{\mp}$ decay, J. High Energy Phys. 07 (2014) 140.

[708] K. Chilikin *et al.* (Belle Collaboration), Observation of a new charged charmonium-like state in $B \to J/\psi K\pi$ decays, Phys. Rev. D **90**, 112009 (2014).

[709] R. Aaij *et al.* (LHCb Collaboration), Evidence for an $\eta_c(1S)\pi^-$ resonance in $B^0 \to \eta_c(1S)K^+\pi^-$ decays, Eur. Phys. J. C **78**, 1019 (2018).

[710] F. Abe *et al.* (CDF Collaboration), Observation of $B^+ \to \psi(2S)K^+$ and $B^0 \to \psi(2S)K*(892)^0$ decays and measurements of B meson branching fractions into J/ψ and $\psi(2S)$ final states, Phys. Rev. D **58**, 072001 (1998).

[711] R. Aaij *et al.* (LHCb Collaboration), Measurement of relative branching fractions of B decays to $\psi(2S)$ and J/ψ mesons, Eur. Phys. J. C **72**, 2118 (2012).

[712] T. Affolder *et al.* (CDF Collaboration), A Study of $B^0 \to J/\psi K^{(*)0}\pi^+\pi^-$ Decays with the Collider Detector at Fermilab, Phys. Rev. Lett. **88**, 071801 (2002).

[713] P. del Amo Sanchez *et al.* (*BABAR* Collaboration), Evidence for the decay $X(3872) \to J/\psi\omega$, Phys. Rev. D **82**, 011101 (2010).

[714] B. Aubert *et al.* (*BABAR* Collaboration), Rare B Decays into States Containing a J/ψ Meson and a Meson with $s\bar{s}$ Quark Content, Phys. Rev. Lett. **91**, 071801 (2003).

[715] K. Abe *et al.* (Belle Collaboration), Observation of $B \to J/\psi K_1(1270)$, Phys. Rev. Lett. **87**, 161601 (2001).

[716] T. Iwashita *et al.* (Belle Collaboration), Measurement of branching fractions for $B \to J/\psi\eta K$ decays and search for a narrow resonance in the $J/\psi\eta$ final state, Prog. Theor. Exp. Phys. **2014**, 043C01 (2014).

[717] B. Aubert *et al.* (*BABAR* Collaboration), Observation of the Decay $B \to J/\psi\eta K$ and Search for $X(3872) \to J/\psi\eta$, Phys. Rev. Lett. **93**, 041801 (2004).

[718] V. Bhardwaj *et al.* (Belle Collaboration), Evidence of a New Narrow Resonance Decaying to $\chi_{c1}\gamma$ in $B \to \chi_{c1}\gamma K$, Phys. Rev. Lett. **111**, 032001 (2013).

[719] R. Mizuk *et al.* (Belle Collaboration), Dalitz analysis of $B \to K\pi^+\psi'$ decays and the $Z(4430)^+$, Phys. Rev. D **80**, 031104 (2009).

[720] R. Aaij *et al.* (LHCb Collaboration), Observation of the decay $\bar{B}_s^0 \to \psi(2S)K^+\pi^-$, Phys. Lett. B **747**, 484 (2015).

[721] B. Aubert *et al.* (*BABAR* Collaboration), Evidence for the $B^0 \to p\bar{p}K^{*0}$ and $B^+ \to \eta_c K^{*+}$ decays and study of the decay dynamics of B meson decays into $p\bar{p}h$ final states, Phys. Rev. D **76**, 092004 (2007).

[722] F. Fang *et al.* (Belle Collaboration), Measurement of Branching Fractions for $B \to \eta_c K^{(*)}$ Decays, Phys. Rev. Lett. **90**, 071801 (2003).

[723] B. Aubert *et al.* (*BABAR* Collaboration), Study of B-meson decays to $\eta_c K^{(*)}$, $\eta_c(2S)K^{(*)}$ and $\eta_c\gamma K^{(*)}$, Phys. Rev. D **78**, 012006 (2008).

[724] B. Aubert *et al.* (*BABAR* Collaboration), Search for Factorization-Suppressed $B \to \chi_c K^{(*)}$ Decays, Phys. Rev. Lett. **94**, 171801 (2005).

[725] B. Aubert *et al.* (*BABAR* Collaboration), Observation of $B^0 \to \chi_{c0}K^{*0}$ and evidence for $B^+ \to \chi_{c0}K^{*+}$, Phys. Rev. D **78**, 091101 (2008).

[726] V. Bhardwaj *et al.* (Belle Collaboration), Observation of $X(3872) \to J/\psi\gamma$ and Search for $X(3872) \to \psi'\gamma$ in B Decays, Phys. Rev. Lett. **107**, 091803 (2011).

[727] B. Aubert *et al.* (*BABAR* Collaboration), Evidence for $X(3872) \to \psi_{2S}\gamma$ in $B^\pm \to X_{3872}K^\pm$ Decays, and a Study of $B \to c\bar{c}\gamma K$, Phys. Rev. Lett. **102**, 132001 (2009).

[728] V. Bhardwaj *et al.* (Belle Collaboration), Inclusive and exclusive measurements of B decays to χ_{c1} and χ_{c2} at Belle, Phys. Rev. D **93**, 052016 (2016).

[729] J. P. Lees *et al.* (*BABAR* Collaboration), Search for the $Z_1(4050)^+$ and $Z_2(4250)^+$ states in $\bar{B}^0 \to \chi_{c1}K^-\pi^+$ and $B^+ \to \chi_{c1}K_S^0\pi^+$, Phys. Rev. D **85**, 052003 (2012).

[730] N. Soni *et al.* (Belle Collaboration), Measurement of branching fractions for $B \to \chi_{c1(2)}K(K^*)$ at BELLE, Phys. Lett. B **634**, 155 (2006).

[731] B. Aubert *et al.* (*BABAR* Collaboration), A Measurement of the $B^0 \to J/\psi\pi^+\pi^-$ Branching Fraction, Phys. Rev. Lett. **90**, 091801 (2003).

[732] R. Aaij *et al.* (LHCb Collaboration), Observations of $B_s^0 \to \psi(2S)\eta$ and $B_{(s)}^0 \to \psi(2S)\pi^+\pi^-$ decays, Nucl. Phys. **B871**, 403 (2013).

[733] B. Aubert *et al.* (*BABAR* Collaboration), Branching fraction and charge asymmetry measurements in $B \to J/\psi\pi\pi$ decays, Phys. Rev. D **76**, 031101 (2007).

[734] R. Aaij *et al.* (LHCb Collaboration), Evidence for the decay $B^0 \to J/\psi\omega$ and measurement of the relative branching fractions of B_s^0 meson decays to $J/\psi\eta$ and $J/\psi\eta'$, Nucl. Phys. **B867**, 547 (2013).

[735] M. C. Chang *et al.*, Measurement of $B^0 \to J/\psi\eta^{(\prime)}$ and constraint on the $\eta - \eta'$ mixing angle, Phys. Rev. D **85**, 091102 (2012).

[736] R. Aaij *et al.* (LHCb Collaboration), Study of $\eta - \eta'$ mixing from measurement of $B_{(s)}^0 \to J/\psi\eta^{(\prime)}$ decay rates, J. High Energy Phys. 01 (2015) 024.

[737] R. Aaij *et al.* (LHCb Collaboration), Analysis of the resonant components in $B^0 \to J/\psi\pi^+\pi^-$, Phys. Rev. D **87**, 052001 (2013).

[738] R. Aaij *et al.* (LHCb Collaboration), Observation of $B_(s)^0 \to J/\psi f_1(1285)$ Decays and Measurement of the $f_1(1285)$ Mixing Angle, Phys. Rev. Lett. **112**, 091802 (2014).

[739] R. Aaij *et al.* (LHCb Collaboration), First observation of $\bar{B}^0 \to J/\psi K^+K^-$ and search for $\bar{B}^0 \to J/\psi\phi$ decays, Phys. Rev. D **88**, 072005 (2013).

[740] Y. Liu *et al.* (Belle Collaboration), Search for $B^0 \to J/\psi\phi$ decays, Phys. Rev. D **78**, 011106 (2008).

[741] R. Kumar *et al.* (Belle Collaboration), Evidence for $B^0 \to \chi_{c1}\pi^0$ at Belle, Phys. Rev. D **78**, 091104 (2008).

[742] R. Aaij *et al.* (LHCb Collaboration), Search for the rare decays $B^0 \to J/\psi\gamma$ and $B_s^0 \to J/\psi\gamma$, Phys. Rev. D **92**, 112002 (2015).

[743] B. Aubert *et al.* (*BABAR* Collaboration), Search for the decay $B^0 \to J/\psi\gamma$, Phys. Rev. D **70**, 091104 (2004).

[744] R. Aaij *et al.* (LHCb Collaboration), Observation of $B_{(s)}^0 \to J/\psi p\bar{p}$ Decays and Precision Measurements of the $B_{(s)}^0$ Masses, Phys. Rev. Lett. **122**, 191804 (2019).

[745] R. Aaij *et al.* (LHCb Collaboration), Searches for $B_{(s)}^0 \to J/\psi p\bar{p}$ and $B^+ \to J/\psi p\bar{p}\pi^+$ decays, J. High Energy Phys. 09 (2013) 006.

[746] Q. L. Xie *et al.* (Belle Collaboration), Observation of $B^- \to J/\psi\Lambda\bar{p}$ and searches for $B^- \to J/\psi\Sigma^0\bar{p}$ and $B^0 \to J/\psi p\bar{p}$ decays, Phys. Rev. D **72**, 051105 (2005).

[747] B. Aubert *et al.* (*BABAR* Collaboration), Evidence for $B^+ \to J/\psi p\bar{\Lambda}$ and Search for $B^0 \to J/\psi p\bar{p}$, Phys. Rev. Lett. **90**, 231801 (2003).

[748] B. Aubert *et al.* (*BABAR* Collaboration), Search for $B \to J/\psi D$ decays, Phys. Rev. D **71**, 091103 (2005).

[749] L. M. Zhang *et al.* (Belle Collaboration), Search for $B^0 \to J/\psi \overline{D}^0$ and $B^+ \to J/\psi \bar{D}^0 \pi^+$ decays, Phys. Rev. D **71**, 091107 (2005).

[750] B. Aubert *et al.* (*BABAR* Collaboration), Measurement of the Ratio of Decay Amplitudes for $\bar{B}^0 \to J/\psi K^{*0}$ and $B^0 \to J/\psi K^{*0}$, Phys. Rev. Lett. **93**, 081801 (2004).

[751] B. Aubert *et al.* (*BABAR* Collaboration), Observation of the decay $\bar{B}^0 \to \Lambda_c^+ \bar{p}\pi^0$, Phys. Rev. D **82**, 031102 (2010).

[752] J. P. Lees *et al.* (*BABAR* Collaboration), Study of the decay $\bar{B}^0 \to \Lambda_c^+ \bar{p}\pi^+\pi^-$ and its intermediate states, Phys. Rev. D **87**, 092004 (2013).

[753] N. Gabyshev *et al.* (Belle Collaboration), Study of exclusive B decays to charmed baryons at BELLE, Phys. Rev. D **66**, 091102 (2002).

[754] K. S. Park *et al.* (Belle Collaboration), Study of the charmed baryonic decays $\bar{B}^0 \to \Sigma_c^{++} \bar{p}\pi^-$ and $\bar{B}^0 \to \Sigma_c^0 \bar{p}\pi^+$, Phys. Rev. D **75**, 011101 (2007).

[755] Y. Uchida *et al.* (Belle Collaboration), Search for $\bar{B}^0 \Lambda_c^+ \bar{\Lambda}_c^-$ decay at Belle, Phys. Rev. D **77**, 051101(R) (2008).

[756] N. Gabyshev *et al.* (Belle Collaboration), Observation of $B^+ \to \Lambda_c^+ \Lambda_c^- K^+$ and $B^0 \to \Lambda_c^+ \Lambda_c^- K^0$ Decays, Phys. Rev. Lett. **97**, 202003 (2006).

[757] B. Aubert *et al.* (*BABAR* Collaboration), A study of excited charm-strange baryons with evidence for new baryons $\Xi_c(3055)^+$ and $\Xi_c(3123)^+$, Phys. Rev. D **77**, 012002 (2008).

[758] R. Chistov *et al.* (Belle Collaboration), Observation of $B^+ \to \bar{\xi}_c 0 \Lambda_c^+$ and evidence for $B^0 \to \bar{\xi}_c^- \Lambda_c^+$, Phys. Rev. D **74**, 111105 (2006).

[759] J. P. Lees *et al.* (*BABAR* Collaboration), Observation of the baryonic decay $\bar{B}^0 \to \Lambda_c^+ \bar{p} K^- K^+$, Phys. Rev. D **91**, 031102 (2015).

[760] B. Aubert *et al.* (*BABAR* Collaboration), Measurements of $\mathrm{B}(\bar{B}^0 \to \Lambda_c^+ \bar{p})$ and $\mathrm{B}(B^- \to \Lambda_c^+ \bar{p}\pi^-)$ and studies of $\Lambda_c^+ \pi^-$ resonances, Phys. Rev. D **78**, 112003 (2008).

[761] N. Gabyshev *et al.* (Belle Collaboration), Observation of $\bar{B}^0 \to \Lambda_c^+ \bar{p}$ Decay, Phys. Rev. Lett. **90**, 121802 (2003).

[762] B. Aubert *et al.* (*BABAR* Collaboration), Observation of the baryonic B-decay $\bar{B}^0 \to \Lambda_c^+ \bar{p} K^- \pi^+$, Phys. Rev. D **80**, 051105 (2009).

[763] J. P. Lees *et al.* (*BABAR* Collaboration), Observation of the baryonic B decay $\bar{B}^0 \to \Lambda_c^+ \bar{\Lambda} K^-$, Phys. Rev. D **84**, 071102 (2011).

[764] J. P. Lees *et al.* (*BABAR* Collaboration), Search for the decay $\bar{B}^0 \to \Lambda_c^+ \bar{p} p \bar{p}$, Phys. Rev. D **89**, 071102 (2014).

[765] S.-K. Choi *et al.* (Belle Collaboration), Bounds on the width, mass difference and other properties of $X(3872) \to \pi^+\pi^- J/\psi$ decays, Phys. Rev. D **84**, 052004 (2011).

[766] B. Aubert *et al.* (*BABAR* Collaboration), A study of $B \to X(3872) K$, with $X_{3872} \to J/\Psi \pi^+\pi^-$, Phys. Rev. D **77**, 111101 (2008).

[767] A. Bala *et al.* (Belle Collaboration), Observation of X (3872) in $B \to X(3872) K\pi$ decays, Phys. Rev. D **91**, 051101 (2015).

[768] R. Mizuk *et al.* (Belle Collaboration), Observation of two resonance-like structures in the $\pi^+ \chi_{c1}$ mass distribution in exclusive $\bar{B}^0 \to K^- \pi^+ \chi_{c1}$ decays, Phys. Rev. D **78**, 072004 (2008).

[769] B. Aubert *et al.* (*BABAR* Collaboration), Measurements of the Absolute Branching Fractions of $B^\pm \to K^\pm$ X($c\bar{c}$), Phys. Rev. Lett. **96**, 052002 (2006).

[770] B. Aubert *et al.* (*BABAR* Collaboration), Search for a charged partner of the X(3872) in the B meson decay $B \to X^- K$, $X^- \to J/\psi \pi^- \pi^0$, Phys. Rev. D **71**, 031501 (2005).

[771] B. Aubert *et al.* (*BABAR* Collaboration), Search for the $Z(4430)^-$ at *BABAR*, Phys. Rev. D **79**, 112001 (2009).

[772] Y. Kato *et al.* (Belle Collaboration), Measurements of the absolute branching fractions of $B^+ \to X_{c\bar{c}} K^+$ and $B^+ \to \bar{D}^{(*)0} \pi^+$ at Belle, Phys. Rev. D **97**, 012005 (2018).

[773] B. Aubert *et al.* (*BABAR* Collaboration), Measurement of the Branching Fractions and CP-Asymmetry of $B^- \to D^0(CP) K^-$ Decays with the *BABAR* Detector, Phys. Rev. Lett. **92**, 202002 (2004).

[774] Y. Horii *et al.* (Belle Collaboration), Study of the suppressed B meson decay $B^- \to DK^-$, $D \to K^+\pi^-$, Phys. Rev. D **78**, 071901 (2008).

[775] S. K. Swain *et al.* (Belle Collaboration), Measurement of branching fraction ratios and CP asymmetries in $B^\pm \to D(CP) K^\pm$, Phys. Rev. D **68**, 051101 (2003).

[776] R. Aaij *et al.* (LHCb Collaboration), Measurement of CP observables in $B^\pm \to D^{(*)} K^\pm$ and $B^\pm \to D^{(*)} \pi^\pm$ decays, Phys. Lett. B **777**, 16 (2018).

[777] B. Aubert *et al.* (*BABAR* Collaboration), Measurement of the ratio $\mathcal{B}(B^- \to D^{*0} K^-)/\mathcal{B}(B^- \to D^{*0} \pi^-)$ and of the CP asymmetry of $B^- \to D^{*0}_{CP+} K^-$ decays, Phys. Rev. D **71**, 031102 (2005).

[778] B. Aubert *et al.* (*BABAR* Collaboration), Dalitz plot analysis of $B^- \to D^+ \pi^- \pi^-$, Phys. Rev. D **79**, 112004 (2009).

[779] K. Abe *et al.* (Belle Collaboration), Study of $B^- \to D^{**0} \pi^- (D^{**0} \to D^{(*)+} \pi^-)$ decays, Phys. Rev. D **69**, 112002 (2004).

[780] B. Aubert *et al.* (*BABAR* Collaboration), Study of the decays $B^- \to D^{(*)} + \pi^- \pi^-$, arXiv:hep-ex/0308026.

[781] R. Aaij *et al.* (LHCb Collaboration), Observation of the $B^+ \to D^{*-} K^+ \pi^+$ decay, Phys. Rev. D **96**, 011101 (2017).

[782] B. Aubert *et al.* (*BABAR* Collaboration), Measurement of the $B^- \to D^0 K^{*-}$ branching fraction, Phys. Rev. D **73**, 111104 (2006).

[783] B. Aubert *et al.* (*BABAR* Collaboration), Measurement of the Branching Fraction and Polarization for the Decay $B^- \to D^{0*} K^{*-}$, Phys. Rev. Lett. **92**, 141801 (2004).

[784] R. Aaij *et al.* (LHCb Collaboration), First observation and amplitude analysis of the $B^- \to D^+ K^- \pi^-$ decay, Phys. Rev. D **91**, 092002 (2015); **93**, 119901(E) (2016).

[785] P. del Amo Sanchez *et al.* (*BABAR* Collaboration), Search for $B^+ \to D^+ K^0$ and $B^+ \to D^+ K^{*0}$ decays, Phys. Rev. D **82**, 092006 (2010).

[786] R. Aaij *et al.* (LHCb Collaboration), First observation of the rare $B^+ \to D^+ K^+ \pi^-$ decay, Phys. Rev. D **93**, 051101 (2016); **93**, 119902(E) (2016).

[787] B. Aubert *et al.* (*BABAR* Collaboration), Search for the rare decays $B^+ \to D^{(*)+}K^0_S$, Phys. Rev. D **72**, 011102 (2005).

[788] M. Iwabuchi *et al.* (Belle Collaboration), Search for $B^+ \to D^{*+}\pi^0$ Decay, Phys. Rev. Lett. **101**, 041601 (2008).

[789] J. Wiechczynski *et al.* (Belle Collaboration), Measurement of $B \to D_s^{(*)}K\pi$ branching fractions, Phys. Rev. D **80**, 052005 (2009).

[790] B. Aubert *et al.* (*BABAR* Collaboration), Evidence for the Rare Decay $B^+ \to D_s^+\pi^0$, Phys. Rev. Lett. **98**, 171801 (2007).

[791] R. Aaij *et al.* (LHCb Collaboration), First observation of $B^+ \to D_s^+K^+K^-$ decays and a search for $B^+ \to D_s^+\phi$ decays, J. High Energy Phys. 01 (2018) 131.

[792] B. Aubert *et al.* (*BABAR* Collaboration), Search for rare quark-annihilation decays, $B^- \to D_s(*) - \phi$, Phys. Rev. D **73**, 011103 (2006).

[793] P. Chen *et al.* (Belle Collaboration), Observation of $B^- \to \bar{p}\Lambda D^0$ at Belle, Phys. Rev. D **84**, 071501 (2011).

[794] O. Seon *et al.* (BELLE Collaboration), Search for lepton-number-violating $B^+ \to D^-l^+l'^+$ decays, Phys. Rev. D **84**, 071106 (2011).

[795] R. Aaij *et al.* (LHCb Collaboration), Search for B_c^+ decays to two charm mesons, Nucl. Phys. **B930**, 563 (2018).

[796] G. Majumder *et al.* (Belle Collaboration), Evidence for $B^0 \to D^+D^-$ and Observation of $B^- \to D^0D^-$ and $B^- \to D^0D^{*-}$ Decays, Phys. Rev. Lett. **95**, 041803 (2005).

[797] J. Brodzicka *et al.* (Belle Collaboration), Observation of a New D_{sJ} Meson in $B^+ \to \bar{D}^0D^0K^+$ Decays, Phys. Rev. Lett. **100**, 092001 (2008).

[798] K. Abe *et al.* (Belle Collaboration), Observation of $B^+ \to \psi(3770)K^+$, Phys. Rev. Lett. **93**, 051803 (2004).

[799] C.-H. Wu *et al.* (Belle Collaboration), Study of $J/\psi \to p\bar{p},\Lambda\bar{\Lambda}$ and Observation of $\eta_c \to \Lambda\bar{\Lambda}$ at Belle, Phys. Rev. Lett. **97**, 162003 (2006).

[800] B. Aubert *et al.* (*BABAR* Collaboration), Measurement of the $B^+ \to p\bar{p}K^+$ branching fraction and study of the decay dynamics, Phys. Rev. D **72**, 051101 (2005).

[801] B. Aubert *et al.* (*BABAR* Collaboration), Study of $B^\pm \to J/\psi\pi^\pm$ and $B^\pm \to J/\psi K^\pm$ decays: Measurement of the Ratio of Branching Fractions and Search for Direct *CP* Violation, Phys. Rev. Lett. **92**, 241802 (2004).

[802] K. Abe *et al.* (Belle Collaboration), Observation of $B^+ \to \chi_{c0}K^+$, Phys. Rev. Lett. **88**, 031802 (2002).

[803] F. Abe *et al.* (CDF Collaboration), Measurement of the Branching Fraction $B(B_u^+ \to J/\psi\pi^+)$ and Search for $B_c^+ \to J/\psi\pi^+$, Phys. Rev. Lett. **77**, 5176 (1996).

[804] A. Abulencia *et al.* (CDF Collaboration), Measurement of the ratio of branching fractions $\mathcal{B}(B^\pm \to J/\psi\pi^\pm)/\mathcal{B}(B^\pm \to J/\psi K^\pm)$, Phys. Rev. D **79**, 112003 (2009).

[805] V. Khachatryan *et al.* (CMS Collaboration), Measurement of the ratio of the production cross sections times branching fractions of $B_c^\pm \to J/\psi\pi^\pm$ and $B^\pm \to J/\psi K^\pm$ and $\mathcal{B}(B_c^\pm \to J/\psi\pi^\pm\pi^\pm\pi^\mp)/\mathcal{B}(B_c^\pm \to J/\psi\pi^\pm)$ in pp collisions at $\sqrt{s} = 7$ TeV, J. High Energy Phys. 01 (2015) 063.

[806] V. M. Abazov *et al.* (D0 Collaboration), Relative rates of B meson decays into ψ_{2S} and J/ψ mesons, Phys. Rev. D **79**, 111102 (2009).

[807] R. Aaij *et al.* (LHCb Collaboration), Measurements of B_c^+ Production and Mass with the $B_c^+ \to J/\psi\pi^+$ Decay, Phys. Rev. Lett. **109**, 232001 (2012).

[808] R. Aaij *et al.* (LHCb Collaboration), Measurements of the branching fractions of $B^+ \to p\bar{p}K^+$ decays, Eur. Phys. J. C **73**, 2462 (2013).

[809] R. Aaij *et al.* (LHCb Collaboration), Measurement of B_c^+ Production in Proton-Proton Collisions at $\sqrt{s} = 8$ TeV, Phys. Rev. Lett. **114**, 132001 (2015).

[810] K. Abe *et al.* (Belle Collaboration), Measurements of branching fractions and decay amplitudes in $B \to J/\psi K^*$ decays, Phys. Lett. B **538**, 11 (2002).

[811] H. Guler *et al.* (Belle Collaboration), Study of the $K^+\pi^+\pi^-$ final state in $B^+ \to J/\psi K^+\pi^+\pi^-$ and $B^+ \to \psi' K^+\pi^+\pi^-$, Phys. Rev. D **83**, 032005 (2011).

[812] B. Aubert *et al.* (*BABAR* Collaboration), Study of the $B \to J/\psi K^-\pi^+\pi^-$ decay and measurement of the $B \to X(3872)K^-$ branching fraction, Phys. Rev. D **71**, 071103 (2005).

[813] D. Acosta *et al.* (CDF Collaboration), Branching ratio measurements of exclusive B^+ decays to charmonium with the collider detector at Fermilab, Phys. Rev. D **66**, 052005 (2002).

[814] V. M. Abazov *et al.* (D0 Collaboration), Search for the $X(4140)$ state in $B^+ \to J/\psi\phi K^+$ decays with the D0 detector, Phys. Rev. D **89**, 012004 (2014).

[815] R. Aaij *et al.* (LHCb Collaboration), Observation of $J/\psi\phi$ Structures Consistent with Exotic States from Amplitude Analysis of $B^+ \to J/\psi\phi K^+$ Decays, Phys. Rev. Lett. **118**, 022003 (2017).

[816] V. Khachatryan *et al.* (CMS Collaboration), Observation of the decay $B^+ \to \psi(2S)\phi(1020)K^+$ in pp collisions at $\sqrt{s} = 8$ TeV, Phys. Lett. B **764**, 66 (2017).

[817] A. Vinokurova *et al.* (Belle Collaboration), Study of $B^\pm \to K^\pm(K_S K\pi)^0$ decay and determination of η_c and $\eta_c(2S)$ parameters, Phys. Lett. B **706**, 139 (2011).

[818] F. Fang *et al.* (Belle Collaboration), Search for the h_c meson in $B^\pm \to h_c K^\pm$, Phys. Rev. D **74**, 012007 (2006).

[819] R. Kumar *et al.* (Belle Collaboration), Observation of $B^\pm \to \chi_{c1}\pi^\pm$ and search for direct *CP* violation, Phys. Rev. D **74**, 051103 (2006).

[820] R. Aaij *et al.* (LHCb Collaboration), Measurements of the branching fractions and *CP* asymmetries of $B^+ \to J/\psi\pi^+$ and $B^+ \to \psi(2S)\pi^+$ decays, Phys. Rev. D **85**, 091105 (2012).

[821] R. Aaij *et al.* (LHCb Collaboration), Measurement of the branching fraction and *CP* asymmetry in $B^+ \to J/\psi\rho^+$ decays, Eur. Phys. J. C **79**, 537 (2019).

[822] B. Aubert *et al.* (*BABAR* Collaboration), An amplitude analysis of the decay $B^\pm \to \pi^\pm\pi^\pm\pi^\mp$, Phys. Rev. D **72**, 052002 (2005).

[823] V. M. Abazov *et al.* (D0 Collaboration), Measurement of Direct *CP* Violation Parameters in $B^\pm \to J/\psi K^\pm$ and $B^\pm \to J/\psi\pi^\pm$ Decays with 10.4 fb^{-1} of Tevatron Data, Phys. Rev. Lett. **110**, 241801 (2013).

[824] Y. B. Li *et al.* (Belle Collaboration), Observation of $\Xi_c(2930)^0$ and updated measurement of $B^- \to K^-\Lambda_c^+\bar{\Lambda}_c^-$ at Belle, Eur. Phys. J. C **78**, 252 (2018).

[825] J. P. Lees *et al.* (*BABAR* Collaboration), Study of the baryonic B decay $B^- \to \Sigma_c^{++}\bar{p}\pi^-\pi^-$, Phys. Rev. D **86**, 091102 (2012).

[826] B. Aubert *et al.* (*BABAR* Collaboration), Search for $B^+ \to X(3872)K^+$, $X_{3872} \to J/\psi\gamma$, Phys. Rev. D **74**, 071101 (2006).

[827] B. Aubert *et al.* (*BABAR* Collaboration), Study of $J/\psi\pi^+\pi^-$ states produced in $B^0 \to J/\psi\pi^+\pi^-K^0$ and $B^- \to J/\psi\pi^+\pi^-K^-$, Phys. Rev. D **73**, 011101 (2006).

[828] T. Aushev *et al.* (Belle Collaboration), Study of the $B \to X(3872)(D^{*0}\bar{D}^0)K$ decay, Phys. Rev. D **81**, 031103 (2010).

[829] K. Abe *et al.* (Belle Collaboration), Observation of a Near-Threshold $\omega J/\psi$ Mass Enhancement in Exclusive $B \to K\omega J/\psi$ Decays, Phys. Rev. Lett. **94**, 182002 (2005).

[830] R. Aaij *et al.* (LHCb Collaboration), Measurements of the branching fractions of the decays $B_s^0 \to D_s^{\mp}K^{\pm}$ and $B_s^0 \to D_s^-\pi^+$, J. High Energy Phys. 06 (2012) 115.

[831] T. Aaltonen *et al.* (CDF Collaboration), First Observation of $\bar{B}_s^0 \to D_s^{\pm}K^{\mp}$ and Measurement of the Ratio of Branching Fractions B $\mathcal{B}(\bar{B}_s^0 \to D_s^{\pm}K^{\mp})/\mathcal{B}(\bar{B}_s^0 \to D_s^+\pi^-)$, Phys. Rev. Lett. **103**, 191802 (2009).

[832] R. Louvot *et al.* (Belle Collaboration), Observation of $B_s^0 \to D_s^{*-}\pi^+$, $B_s^0 \to D_s^{(*)-}\rho^+$ Decays and Measurement of $B_s^0 \to D_s^{*-}\rho^+$ Polarization, Phys. Rev. Lett. **104**, 231801 (2010).

[833] R. Aaij *et al.* (LHCb Collaboration), First observation and measurement of the branching fraction for the decay $B_s^0 \to D_s^{*\mp}K^{\pm}$, J. High Energy Phys. 06 (2015) 130.

[834] R. Aaij *et al.* (LHCb Collaboration), Observation of $B_s^0 \to \bar{D}^0K_S^0$ and Evidence for $B_s^0 \to \bar{D}^{*0}K_S^0$ Decays, Phys. Rev. Lett. **116**, 161802 (2016).

[835] R. Aaij *et al.* (LHCb Collaboration), Search for the decay $B_s^0 \to D^{*\mp}\pi^{\pm}$, Phys. Rev. D **87**, 071101 (2013).

[836] R. Aaij *et al.* (LHCb Collaboration), Search for the decay $B_s^0 \to \bar{D}^0 f_0(980)$, J. High Energy Phys. 08 (2015) 005.

[837] R. Aaij *et al.* (LHCb Collaboration), Measurement of the $B_s^0 \to D_s^{(*)+}D_s^{(*)-}$ branching fractions, Phys. Rev. D **93**, 092008 (2016).

[838] R. Aaij *et al.* (LHCb Collaboration), Amplitude analysis and the branching fraction measurement of $\bar{B}_s^0 \to J/\psi K^+K^-$, Phys. Rev. D **87**, 072004 (2013).

[839] F. Thorne *et al.* (Belle Collaboration), Measurement of the decays $B_s^0 \to J/\psi\phi(1020)$, $B_s^0 \to J/\psi f_2'(1525)$ and $B_s^0 \to J/\psi K^+K^-$ at Belle, Phys. Rev. D **88**, 114006 (2013).

[840] A. Abulencia *et al.* (CDF Collaboration), Observation of $B_s^0 \to \psi(2S)\phi$ and Measurement of Ratio of Branching Fractions $\mathcal{B}(B_s^0 \to \psi(2S)\phi)/\mathcal{B}(B_s^0 \to J/\psi\phi)$, Phys. Rev. Lett. **96**, 231801 (2006).

[841] V. Khachatryan *et al.* (CMS Collaboration), Measurement of the ratio $\mathcal{B}(\mathrm{B}_s^0 \to \mathrm{J}/\psi \mathrm{f}_0(980))/\mathcal{B}(\mathrm{B}_s^0 \to \mathrm{J}/\psi\phi(1020))$ in pp collisions at $\sqrt{s} = 7$ TeV, Phys. Lett. B **756**, 84 (2016).

[842] V. M. Abazov *et al.* (D0 Collaboration), Measurement of the relative branching ratio of $B_s^0 \to J/\psi f_0(980) \to B_s^0 \to J/\psi\phi$, Phys. Rev. D **85**, 011103 (2012).

[843] V. M. Abazov *et al.* (D0 Collaboration), Study of the decay $B_s^0 \to J/\psi f_2'(1525)$ in $\mu^+\mu^-K^+K^-$ final states, Phys. Rev. D **86**, 092011 (2012).

[844] R. Aaij *et al.* (LHCb Collaboration), Observation of $B_s \to J/\psi f_2'(1525)$ in $J/\psi K^+K^-$ Final States, Phys. Rev. Lett. **108**, 151801 (2012).

[845] R. Aaij *et al.* (LHCb Collaboration), First observation of $B_s^0 \to J/\psi f_0(980)$ decays, Phys. Lett. B **698**, 115 (2011).

[846] R. Aaij *et al.* (LHCb Collaboration), Observation of the $B_s^0 \to J/\psi\phi\phi$ decay, J. High Energy Phys. 03 (2016) 040.

[847] J. Li *et al.* (Belle Collaboration), First Observation of $B_s^0 \to J/\psi\eta$ and $B_s^0 \to J/\psi\eta'$, Phys. Rev. Lett. **108**, 181808 (2012).

[848] T. Aaltonen *et al.* (CDF Collaboration), Observation of $B_s^0 \to J/\psi K^{*0}(892)$ and $B_s^0 \to J/\psi K_S^0$ decays, Phys. Rev. D **83**, 052012 (2011).

[849] R. Aaij *et al.* (LHCb Collaboration), Measurement of resonant and CP components in $\bar{B}_s^0 \to J/\psi\pi^+\pi^-$ decays, Phys. Rev. D **89**, 092006 (2014).

[850] R. Aaij *et al.* (LHCb Collaboration), Observation of the decay $\Lambda_b^0 \to \psi(2S)p\pi^-$, J. High Energy Phys. 08 (2018) 131.

[851] E. Solovieva *et al.* (Belle Collaboration), Evidence for $\bar{B}_s^0 \to \Lambda_c^+\bar{\Lambda}\pi^-$, Phys. Lett. B **726**, 206 (2013).

[852] R. Aaij *et al.* (LHCb Collaboration), Observation of $B_c^+ \to D^0K^+$ Decays, Phys. Rev. Lett. **118**, 111803 (2017).

[853] R. Aaij *et al.* (LHCb Collaboration), Study of B_c^+ decays to the $K^+K^-\pi^+$ final state and evidence for the decay $B_c^+ \to \chi_{c0}\pi^+$, Phys. Rev. D **94**, 091102 (2016).

[854] R. Aaij *et al.* (LHCb Collaboration), Observation of $B_c^+ \to J/\psi D_s^+$ and $B_c^+ \to J/\psi D_s^{*+}$ decays, Phys. Rev. D **87**, 112012 (2013).

[855] G. Aad *et al.* (ATLAS Collaboration), Study of the $B_c^+ \to J/\psi D_s^+$ and $B_c^+ \to J/\psi D_s^{*+}$ decays with the ATLAS detector, Eur. Phys. J. C **76**, 4 (2016).

[856] R. Aaij *et al.* (LHCb Collaboration), First Observation of the Decay $B_c^+ \to J/\psi\pi^+\pi^-\pi^+$, Phys. Rev. Lett. **108**, 251802 (2012).

[857] R. Aaij *et al.* (LHCb Collaboration), Observation of $B_c^+ \to J/\psi D^{(*)}K^{(*)}$ Decays, Phys. Rev. D **95**, 032005 (2017).

[858] R. Aaij *et al.* (LHCb Collaboration), First observation of the decay $B_c^+ \to J/\psi K^+$, J. High Energy Phys. 09 (2013) 075.

[859] R. Aaij *et al.* (LHCb Collaboration), Observation of the decay $B_c \to J/\psi K^+K^-\pi^+$, J. High Energy Phys. 11 (2013) 094.

[860] R. Aaij *et al.* (LHCb Collaboration), Measurement of the branching fraction ratio $\mathcal{B}(B_c^+ \to \psi(2S)\pi^+)/\mathcal{B}(B_c^+ \to J/\psi\pi^+)$, Phys. Rev. D **92**, 072007 (2015).

[861] R. Aaij *et al.* (LHCb Collaboration), Observation of the Decay $B_c^+ \to B_s^0\pi^+$, Phys. Rev. Lett. **111**, 181801 (2013).

[862] R. Aaij *et al.* (LHCb Collaboration), Studies of beauty baryon decays to D^0ph^- and $\Lambda_c^+h^-$ final states, Phys. Rev. D **89**, 032001 (2014).

[863] R. Aaij *et al.* (LHCb Collaboration), Study of the production of Λ_b^0 and $\bar{B}^0$ hadrons in pp collisions and first measurement of the $\Lambda_b^0 \to J/\psi pK^-$ branching fraction, Chin. Phys. C **40**, 011001 (2016).

[864] R. Aaij *et al.* (LHCb Collaboration), Observation of the $\Lambda_b^0 \to J/\psi p\pi^-$ decay, J. High Energy Phys. 07 (2014) 103.

[865] R. Aaij *et al.* (LHCb Collaboration), Observation of $\Lambda_b^0 \to \psi(2S)pK^-$ and $\Lambda_b^0 \to J/\psi\pi^+\pi^- pK^-$ decays and a measurement of the Λ_b^0 baryon mass, J. High Energy Phys. 05 (2016) 132.

[866] R. Aaij *et al.* (LHCb Collaboration), Evidence for Exotic Hadron Contributions to $\Lambda_b^0 \to J/\psi p\pi^-$ Decays, Phys. Rev. Lett. **117**, 082003 (2016); **117**, 109902(A) (2016); **118**, 119901(A) (2017).

[867] R. Aaij *et al.* (LHCb Collaboration), Observation of the Decays $\Lambda_b^0 \to \chi_{c1} pK^-$ and $\Lambda_b^0 \to \chi_{c2} pK^-$, Phys. Rev. Lett. **119**, 062001 (2017).

[868] F. Abe *et al.* (CDF Collaboration), Observation of $\Lambda_b^0 \to J/\psi\Lambda$ at the Fermilab proton antiproton collider, Phys. Rev. D **55**, 1142 (1997).

[869] G. Aad *et al.* (ATLAS Collaboration), Measurement of the branching ratio $\Gamma(\Lambda_b^0 \to \psi(2S)\Lambda^0)/\Gamma(\Lambda_b^0 \to J/\psi\Lambda^0)$ with the ATLAS detector, Phys. Lett. B **751**, 63 (2015).

[870] T. Aaltonen *et al.* (CDF Collaboration), Observation of the Ω_b^- baryon and measurement of the properties of the Ξ_b^- and Ω_b^- baryons, Phys. Rev. D **80**, 072003 (2009).

[871] R. Aaij *et al.* (LHCb Collaboration), Measurement of the ratio of branching fractions of the decays $\Lambda_b^0 \to \psi(2S)\Lambda$ and $\Lambda_b^0 \to J/\psi\Lambda$, J. High Energy Phys. 03 (2019) 126.

[872] V. M. Abazov *et al.* (D0 Collaboration), Measurement of the production fraction times branching fraction $f(b \to \Lambda_b) \cdot \mathcal{B}(\Lambda_b \to J/\psi\Lambda)$, Phys. Rev. D **84**, 031102 (2011).

[873] A. M. Sirunyan *et al.* (CMS Collaboration), Measurement of the Λ_b polarization and angular parameters in $\Lambda_b \to J/\psi\Lambda$ decays from pp collisions at $\sqrt{s} = 7$ and 8 TeV, Phys. Rev. D **97**, 072010 (2018).

[874] G. Aad *et al.* (ATLAS Collaboration), Measurement of the parity-violating asymmetry parameter α_b and the helicity amplitudes for the decay $\Lambda_b^0 \to J/\psi + \Lambda^0$ with the ATLAS detector, Phys. Rev. D **89**, 092009 (2014).

[875] R. Aaij *et al.* (LHCb Collaboration), Measurements of the $\Lambda_b^0 \to J/\psi\Lambda$ decay amplitudes and the Λ_b^0 polarisation in pp collisions at $\sqrt{s} = 7$ TeV, Phys. Lett. B **724**, 27 (2013).

[876] R. Aaij *et al.* (LHCb Collaboration), Study of the kinematic dependences of Λ_b^0 production in pp collisions and a measurement of the $\Lambda_b^0 \to \Lambda_c^+ \pi^-$ branching fraction, J. High Energy Phys. 08 (2014) 143.

[877] T. Aaltonen *et al.* (CDF Collaboration), Measurement of the branching fraction $\mathcal{B}(\Lambda_b^0 \to \Lambda_c^+\pi^-\pi^+\pi^-)$ at CDF, Phys. Rev. D **85**, 032003 (2012).

[878] R. Aaij *et al.* (LHCb Collaboration), Observation of the decay $\Lambda_b^0 \to \Lambda_c^+ p\bar{p}\pi^-$, Phys. Lett. B **784**, 101 (2018).

[879] R. Aaij *et al.* (LHCb Collaboration), Evidence for the Strangeness-Changing Weak Decay $\Xi_b^- \to \Lambda_b^0\pi^-$, Phys. Rev. Lett. **115**, 241801 (2015).

[880] R. Aaij *et al.* (LHCb Collaboration), Study of the $D^0 p$ amplitude in $\Lambda_b^0 \to D^0 p\pi^-$ decays, J. High Energy Phys. 05 (2017) 030.

[881] HFLAV rare B decays web page, https://hflav.web.cern.ch/content/rare-b-decays.

[882] Y.-T. Duh *et al.* (Belle Collaboration), Measurements of branching fractions and direct CP asymmetries for $B \to K\pi, B \to \pi\pi$ and $B \to KK$ decays, Phys. Rev. D **87**, 031103 (2013).

[883] F. Abudinén *et al.* (Belle-II Collaboration), Measurements of branching fractions and direct CP asymmetries in $B^0 \to K^+\pi^-$, $B^+ \to K_S^0\pi^+$ and $B^0 \to \pi^+\pi^-$ using 2019 and 2020 data, arXiv:2106.03766.

[884] A. Bornheim *et al.* (CLEO Collaboration), Measurements of charmless hadronic two body B meson decays and the ratio $B(B \to DK)/B(B \to D\pi)$, Phys. Rev. D **68**, 052002 (2003); **75**, 119907(E) (2007).

[885] R. Aaij *et al.* (LHCb Collaboration), Branching fraction and CP asymmetry of the decays $B^+ \to K_S^0\pi^+$ and $B^+ \to K_S^0 K^+$, Phys. Lett. B **726**, 646 (2013).

[886] B. Aubert *et al.* (*BABAR* Collaboration), Study of $B^0 \to \pi^0\pi^0$, $B^\pm \to \pi^\pm\pi^0$, and $B^\pm \to K^\pm\pi^0$ decays, and isospin analysis of $B \to \pi\pi$ decays, Phys. Rev. D **76**, 091102 (2007).

[887] F. Abudinén *et al.* (Belle-II Collaboration), Measurements of branching fractions and direct CP-violating asymmetries in $B^+ \to K^+\pi^0$ and $\pi^+\pi^0$ decays using 2019 and 2020 Belle II data, arXiv:2105.04111.

[888] B. Aubert *et al.* (*BABAR* Collaboration), B meson decays to charmless meson pairs containing η or η' mesons, Phys. Rev. D **80**, 112002 (2009).

[889] J. Schumann *et al.* (Belle Collaboration), Evidence for $B \to \eta'\pi$ and Improved Measurements for $B \to \eta' K$, Phys. Rev. Lett. **97**, 061802 (2006).

[890] F. Abudinén *et al.* (Belle-II Collaboration), Measurement of the branching fractions of $B \to \eta' K$ decays using 2019/2020 Belle II data, arXiv:2104.06224.

[891] I. Adachi *et al.* (Belle Collaboration), Search for resonant $B^\pm \to K^\pm h \to K^\pm\gamma\gamma$ Decays at Belle, Phys. Lett. B **662**, 323 (2008).

[892] S. J. Richichi *et al.* (CLEO Collaboration), Two-Body B Meson Decays to η and η': Observation of $B \to \eta K^*$, Phys. Rev. Lett. **85**, 520 (2000).

[893] R. Aaij *et al.* (LHCb Collaboration), Observation of the $B_s^0 \to \eta'\eta'$ Decay, Phys. Rev. Lett. **115**, 051801 (2015).

[894] P. del Amo Sanchez *et al.* (*BABAR* Collaboration), B-meson decays to $\eta'\rho$, $\eta' f_0$, and $\eta' K^*$, Phys. Rev. D **82**, 011502 (2010).

[895] J. Schumann *et al.* (Belle Collaboration), Search for B decays into $\eta'\rho$, $\eta' K^*$, $\eta'\varphi$, $\eta'\omega$ and $\eta'\eta'^-$ at Belle, Phys. Rev. D **75**, 092002 (2007).

[896] C. T. Hoi *et al.* (Belle Collaboration), Evidence for Direct CP Violation in $B^\pm \to \eta h^\pm$ and Observation of $B^0 \to \eta K^0$, Phys. Rev. Lett. **108**, 031801 (2012).

[897] B. Aubert *et al.* (*BABAR* Collaboration), Measurement of Branching Fractions and Charge Asymmetries in B Decays to an η Meson and a K^* Meson, Phys. Rev. Lett. **97**, 201802 (2006).

[898] C. H. Wang *et al.* (Belle Collaboration), Measurement of charmless B Decays to ηK^* and $\eta\rho$, Phys. Rev. D **75**, 092005 (2007).

[899] B. Aubert *et al.* (*BABAR* Collaboration), Study of B Meson Decays with Excited η and η' Mesons, Phys. Rev. Lett. **101**, 091801 (2008).

[900] B. Aubert *et al.* (*BABAR* Collaboration), Branching fraction and *CP*-violation charge asymmetry measurements for B-meson decays to $\eta K^{\pm}$, $\eta\pi^{\pm}$, $\eta' K$, $\eta'\pi^{\pm}$, ωK, and $\omega\pi^{\pm}$, Phys. Rev. D **76**, 031103 (2007).

[901] C. P. Jessop *et al.* (CLEO Collaboration), Study of Charmless Hadronic B Meson Decays to Pseudoscalar Vector Final States, Phys. Rev. Lett. **85**, 2881 (2000).

[902] B. Aubert *et al.* (*BABAR* Collaboration), Observation of B meson decays to ωK^* and improved measurements for $\omega\rho$ and ωf_0, Phys. Rev. D **79**, 052005 (2009).

[903] B. Aubert *et al.* (*BABAR* Collaboration), Search for B-meson decays to two-body final states with $a_0(980)$ mesons, Phys. Rev. D **70**, 111102 (2004).

[904] J. P. Lees *et al.* (*BABAR* Collaboration), Evidence for *CP* violation in $B^+ \to K^*(892)^+\pi^0$ from a Dalitz plot analysis of $B^+ \to K^0_S\pi^+\pi^0$ decays, Phys. Rev. D **96**, 072001 (2017).

[905] J. P. Lees *et al.* (*BABAR* Collaboration), Observation of the rare decay $B^+ \to K^+\pi^0\pi^0$ and measurement of the quasi-two body contributions $B^+ \to K^*(892)^+\pi^0$, $B^+ \to f_0(980)K^+$ and $B^+ \to \chi_{c0}K^+$, Phys. Rev. D **84**, 092007 (2011).

[906] R. Aaij *et al.* (LHCb Collaboration), Measurement of the relative branching fractions of $B^+ \to h^+h'^+h'^-$ decays, Phys. Rev. D **102**, 112010 (2020).

[907] R. Aaij *et al.* (LHCb Collaboration), Search for the suppressed decays $B^+ \to K^+K^+\pi^-$ and $B^+ \to \pi^+\pi^+K^-$, Phys. Lett. B **765**, 307 (2017).

[908] B. Aubert *et al.* (*BABAR* Collaboration), Search for the highly suppressed decays $B^- \to K^+\pi^-\pi^-$ and $B^- \to K^-K^-\pi^+$, Phys. Rev. D **78**, 091102 (2008).

[909] A. Garmash *et al.* (Belle Collaboration), Study of B meson decays to three body charmless hadronic final states, Phys. Rev. D **69**, 012001 (2004).

[910] T. Bergfeld *et al.* (CLEO Collaboration), A Search for Nonresonant $B^+ \to h^+h^-h^+$ Decays, Phys. Rev. Lett. **77**, 4503 (1996).

[911] E. Eckhart *et al.* (CLEO Collaboration), Observation of $B \to K^0_S\pi^+\pi^-$ and Evidence for $B \to K^{*\pm}\pi^{\mp}$, Phys. Rev. Lett. **89**, 251801 (2002).

[912] B. Aubert *et al.* (*BABAR* Collaboration), Branching fraction measurements of charged B decays to $K^{*+}K^+K^-$, $K^{*+}\pi^+K^-$, $K^{*+}K^+\pi^-$ and $K^{*+}\pi^+\pi^-$ final states, Phys. Rev. D **74**, 051104 (2006).

[913] P. del Amo Sanchez *et al.* (*BABAR* Collaboration), Measurements of branching fractions, polarizations, and direct *CP*-violation asymmetries in $B^+ \to \rho^0K^{*+}$ and $B^+ \to f^0(980)K^{*+}$ decays, Phys. Rev. D **83**, 051101 (2011).

[914] B. Aubert *et al.* (*BABAR* Collaboration), Observation of $B^+ \to a_1^+(1260)K^0$ and $B^0 \to a_1^-(1260)K^+$, Phys. Rev. Lett. **100**, 051803 (2008).

[915] B. Aubert *et al.* (*BABAR* Collaboration), Measurements of Branching Fractions, Polarizations, and Direct *CP*-Violation Asymmetries in $B \to \rho K^*$ and $B \to f_0(980)K^*$ Decays, Phys. Rev. Lett. **97**, 201801 (2006).

[916] J. Zhang *et al.* (Belle Collaboration), Measurements of Branching Fractions and Polarization in $B \to K^*\rho$ Decays, Phys. Rev. Lett. **95**, 141801 (2005).

[917] H. Albrecht *et al.* (ARGUS Collaboration), Search for $b \to s$ gluon in B meson decays, Phys. Lett. B **254**, 288 (1991).

[918] B. Aubert *et al.* (*BABAR* Collaboration), Observation of $B^+ \to b_1^+K^0$ and search for B-meson decays to $b_1^0K^0$ and $b_1\pi^0$, Phys. Rev. D **78**, 011104 (2008).

[919] B. Aubert *et al.* (*BABAR* Collaboration), Observation of B-Meson Decays to $b(1)\pi$ and $b(1)K$, Phys. Rev. Lett. **99**, 241803 (2007).

[920] B. Aubert *et al.* (*BABAR* Collaboration), Search for B-meson decays to $b(1)\rho$ and $b(1)K^*$, Phys. Rev. D **80**, 051101 (2009).

[921] J. Zhang *et al.* (Belle Collaboration), Measurements of branching fraction and polarization in $B^+ \to \rho^+K^{*0}$ decay, arXiv:hep-ex/0505039.

[922] A. B. Kaliyar *et al.* (Belle Collaboration), Measurements of branching fraction and direct *CP* asymmetry in $B^{\pm} \to K^0_SK^0_SK^{\pm}$ and a search for $B^{\pm} \to K^0_SK^0_S\pi^{\pm}$, Phys. Rev. D **99**, 031102 (2019).

[923] B. Aubert *et al.* (*BABAR* Collaboration), Search for the decay $B^+ \to K^0_SK^0_S\pi^+$, Phys. Rev. D **79**, 051101 (2009).

[924] C.-L. Hsu *et al.* (Belle Collaboration), Measurement of branching fraction and direct *CP* asymmetry in charmless $B^+ \to K^+K^-\pi^+$ decays at Belle, Phys. Rev. D **96**, 031101 (2017).

[925] B. Aubert *et al.* (*BABAR* Collaboration), Observation of the Decay $B^+ \to K^+K^-\pi^+$, Phys. Rev. Lett. **99**, 221801 (2007).

[926] R. Aaij *et al.* (LHCb Collaboration), Amplitude Analysis of $B^{\pm} \to \pi^{\pm}K^+K^-$ Decays, Phys. Rev. Lett. **123**, 231802 (2019).

[927] B. Aubert *et al.* (*BABAR* Collaboration), Search for the decay $B^+ \to \bar{K}^*$ 0(892) K^+, Phys. Rev. D **76**, 071103 (2007).

[928] M.-Z. Wang *et al.* (Belle Collaboration), Study of the baryon-antibaryon low-mass enhancements in charmless three-body baryonic B decays, Phys. Lett. B **617**, 141 (2005).

[929] Y. M. Goh *et al.* (Belle Collaboration), Search for the decay $B^+ \to \bar{K}^{*0}K^{*+}$ at Belle, Phys. Rev. D **91**, 071101 (2015).

[930] B. Aubert *et al.* (*BABAR* Collaboration), Evidence for $B^+ \to \bar{K}^{*0}K^{*+}$, Phys. Rev. D **79**, 051102 (2009).

[931] F. Abudinén *et al.* (Belle-II Collaboration), Measurements of branching fractions and *CP*-violating charge asymmetries in charmless B decays reconstructed in 2019–2020 Belle II data, arXiv:2009.09452.

[932] F. Abudinén *et al.* (Belle-II Collaboration), Rediscovery of $B \to \phi K^{(*)}$ decays and measurement of the longitudinal polarization fraction f_L in $B \to \phi K^*$ decays using the Summer 2020 Belle II dataset, arXiv:2008.03873.

[933] D. Acosta *et al.* (CDF Collaboration), First Evidence for $B_s^0 \to \phi\phi$ Decay and Measurements of Branching Ratio and A_{CP} for $B^+ \to \phi K^+$, Phys. Rev. Lett. **95**, 031801 (2005).

[934] R. A. Briere *et al.* (CLEO Collaboration), Observation of $B \to \varphi K$ and $B \to \varphi K^*$, Phys. Rev. Lett. **86**, 3718 (2001).

[935] B. Aubert *et al.* (*BABAR* Collaboration), Amplitude Analysis of the $B^{\pm} \to \phi K*(892)^{\pm}$ Decay, Phys. Rev. Lett. **99**, 201802 (2007).

[936] K. F. Chen *et al.* (Belle Collaboration), Measurement of Branching Fractions and Polarization in $B \to \phi K^{(*)}$ Decays, Phys. Rev. Lett. **91**, 201801 (2003).

[937] B. Aubert *et al.* (*BABAR* Collaboration), Observation and Polarization Measurements of $B^{\pm} \to \phi K_1^{\pm}$ and $B^{\pm} \to \phi K_2^{*\pm}$, Phys. Rev. Lett. **101**, 161801 (2008).

[938] P. del Amo Sanchez *et al.* (*BABAR* Collaboration), Search for B^+ meson decay to $a_1^+(1260)K^{*0}(892)$, Phys. Rev. D **82**, 091101 (2010).

[939] J. P. Lees *et al.* (*BABAR* Collaboration), Measurements of branching fractions and *CP* asymmetries and studies of angular distributions for $B \to \phi\phi K$ decays, Phys. Rev. D **84**, 012001 (2011).

[940] H.-C. Huang *et al.* (Belle Collaboration), Evidence for $B \to \phi\phi K$, Phys. Rev. Lett. **91**, 241802 (2003).

[941] B. Aubert *et al.* (*BABAR* Collaboration), Search for B meson decays to $\eta'\eta' K$, Phys. Rev. D **74**, 031105 (2006).

[942] C. Liu *et al.* (Belle Collaboration), Search for the $X(1812)$ in $B^{\pm} \to K^{\pm}\omega\phi$, Phys. Rev. D **79**, 071102 (2009).

[943] R. Ammar *et al.* (CLEO Collaboration), Search for the Familon via $B^{\pm} \to \pi^{\pm} X_0$, $B^{\pm} \to K^{\pm} X_0$, and $B^0 \to K_S^0 X_0$ Decays, Phys. Rev. Lett. **87**, 271801 (2001).

[944] B. Aubert *et al.* (*BABAR* Collaboration), Dalitz plot analysis of $B^{\pm} \to \pi^{\pm}\pi^{\pm}\pi^{\mp}$ decays, Phys. Rev. D **79**, 072006 (2009).

[945] R. Aaij *et al.* (LHCb Collaboration), Observation of Several Sources of *CP* Violation in $B^+ \to \pi^+\pi^+\pi^-$ Decays, Phys. Rev. Lett. **124**, 031801 (2020).

[946] A. Gordon *et al.* (Belle Collaboration), Study of $B \to \rho\pi$ decays at Belle, Phys. Lett. B **542**, 183 (2002).

[947] R. Aaij *et al.* (LHCb Collaboration), Amplitude analysis of the $B^+ \to \pi^+\pi^+\pi^-$ decay, Phys. Rev. D **101**, 012006 (2020).

[948] H. Albrecht *et al.* (ARGUS Collaboration), Search for hadronic $b \to u$ decays, Phys. Lett. B **241**, 278 (1990).

[949] B. Aubert *et al.* (*BABAR* Collaboration), Measurement of the $B^{\pm} \to \rho^{\pm}\pi^0$ branching fraction and direct *CP* asymmetry, Phys. Rev. D **75**, 091103 (2007).

[950] J. Zhang *et al.* (Belle Collaboration), Measurement of Branching Fraction and *CP* Asymmetry in $B^+ \to \rho^+\pi^0$, Phys. Rev. Lett. **94**, 031801 (2005).

[951] J. Zhang *et al.* (Belle Collaboration), Observation of $B^+ \to \rho^+\rho^0$, Phys. Rev. Lett. **91**, 221801 (2003).

[952] B. Aubert *et al.* (*BABAR* Collaboration), Evidence for Charged B Meson Decays to $a^{\pm}(1)(1260)\pi^0$ and $a_1^0(1260)\pi^{\pm}$, Phys. Rev. Lett. **99**, 261801 (2007).

[953] C.-M. Jen *et al.* (Belle Collaboration), Improved measurements of branching fractions and *CP* partial rate asymmetries for $B \to \omega K$ and $B \to \omega\pi$, Phys. Rev. D **74**, 111101 (2006).

[954] B. Aubert *et al.* (*BABAR* Collaboration), Observation of $B^+ \to \eta\rho^+$ and search for B^0 decays to $\eta'\eta$, $\eta\pi^0$, η, π^0, and $\omega\pi^0$, Phys. Rev. D **78**, 011107 (2008).

[955] B. Aubert *et al.* (*BABAR* Collaboration), Search for $B^+ \to \phi\pi^+$ and $B^0 \to \phi\pi^0$ decays, Phys. Rev. D **74**, 011102 (2006).

[956] J. H. Kim *et al.* (Belle Collaboration), Search for $B \to \phi\pi$ decays, Phys. Rev. D **86**, 031101 (2012).

[957] B. Aubert *et al.* (*BABAR* Collaboration), Searches for B Meson Decays to $\phi\phi$, $\phi\rho$, $\phi f_0(980)$, and $f_0(980)f_0(980)$ Final States, Phys. Rev. Lett. **101**, 201801 (2008).

[958] D. Bortoletto *et al.* (CLEO Collaboration), A Search for $b \to u$ Transitions in Exclusive Hadronic B Meson Decays, Phys. Rev. Lett. **62**, 2436 (1989).

[959] B. Aubert *et al.* (*BABAR* Collaboration), Improved measurements of the branching fractions for $B^0 \to \pi^+\pi^-$ and $B^0 \to K^+\pi^-$, and a search for $B^0 \to K^+K^-$, Phys. Rev. D **75**, 012008 (2007).

[960] T. Aaltonen *et al.* (CDF Collaboration), Observation of New Charmless Decays of Bottom Hadrons, Phys. Rev. Lett. **103**, 031801 (2009).

[961] T. Aaltonen *et al.* (CDF Collaboration), Evidence for the Charmless Annihilation Decay Mode $B_s^0 \to \pi^+\pi^-$, Phys. Rev. Lett. **108**, 211803 (2012).

[962] T. Aaltonen *et al.* (CDF Collaboration), Measurements of Direct *CP* Violating Asymmetries in Charmless Decays of Strange Bottom Mesons and Bottom Baryons, Phys. Rev. Lett. **106**, 181802 (2011).

[963] R. Aaij *et al.* (LHCb Collaboration), Measurement of b-hadron branching fractions for two-body decays into charmless charged hadrons, J. High Energy Phys. 10 (2012) 037.

[964] R. Aaij *et al.* (LHCb Collaboration), Observation of the Annihilation Decay Mode $B^0 \to K^+K^-$, Phys. Rev. Lett. **118**, 081801 (2017).

[965] R. Aaij *et al.* (LHCb Collaboration), Search for the $\Lambda_b^0 \to \Lambda\eta'$ and $\Lambda_b^0 \to \Lambda\eta$ decays with the LHCb detector, J. High Energy Phys. 09 (2015) 006.

[966] S. Sato *et al.* (Belle Collaboration), Observation of the decay $B^0 \to \eta' K^*(892)^0$, Phys. Rev. D **90**, 072009 (2014).

[967] P. Goldenzweig *et al.* (Belle Collaboration), Evidence for Neutral B Meson Decays to ωK^{*0}, Phys. Rev. Lett. **101**, 231801 (2008).

[968] B. Aubert *et al.* (*BABAR* Collaboration), Search for neutral B-meson decays to $a_0\pi$, $a_0 K$, $\eta\rho^0$, and ηf_0, Phys. Rev. D **75**, 111102 (2007).

[969] J. P. Lees *et al.* (*BABAR* Collaboration), Amplitude analysis of $B^0 \to K^+\pi^-\pi^0$ and evidence of direct *CP* violation in $B \to K^*\pi$ decays, Phys. Rev. D **83**, 112010 (2011).

[970] P. Chang *et al.* (Belle Collaboration), Observation of the decays $B^0 \to K^+\pi^-\pi^0$ and $B^0 \to \rho^- K^+$, Phys. Lett. B **599**, 148 (2004).

[971] B. Aubert *et al.* (*BABAR* Collaboration), Dalitz plot analysis of the decay $B^0(\bar{B}^0) \to K^{\pm}\pi^{\mp}\pi^0$, Phys. Rev. D **78**, 052005 (2008).

[972] A. Garmash *et al.* (Belle Collaboration), Dalitz analysis of three-body charmless $B^0 \to K^0\pi^+\pi^-$ decay, Phys. Rev. D **75**, 012006 (2007).

[973] R. Aaij *et al.* (LHCb Collaboration), Searches for Λ_b^0 and Ξ_b^0 decays to $K_S^0 p\pi^-$ and $K_S^0 pK^-$ final states with first observation of the $\Lambda_b^0 \to K_S^0 p\pi^-$ decay, J. High Energy Phys. 04 (2014) 087.

[974] R. Aaij *et al.* (LHCb Collaboration), First observation of the decay $B_s^0 \to K_S^0 K^{*0}(892)$ at LHCb, J. High Energy Phys. 01 (2016) 012.

[975] R. Aaij *et al.* (LHCb Collaboration), Updated branching fraction measurements of $B_{(s)}^0 \to K_S^0 h^+ h'^-$ decays, J. High Energy Phys. 11 (2017) 027.

[976] R. Aaij *et al.* (LHCb Collaboration), Amplitude Analysis of the Decay $\bar{B}^0 \to K_S^0\pi^+\pi^-$ and First Observation of the

CP Asymmetry in $\bar{B}^0 \to K^*(892)^-\pi^+$, Phys. Rev. Lett. **120**, 261801 (2018).
[977] R. Aaij *et al.* (LHCb Collaboration), Observation of $B_s^0 \to K^{*\pm}K^{\mp}$ and evidence for $B_s^0 \to K^{*-}\pi^+$ decays, New J. Phys. **16**, 123001 (2014).
[978] W. Adam *et al.* (DELPHI Collaboration), Study of rare b decays with the DELPHI detector at LEP, Z. Phys. C **72**, 207 (1996).
[979] S.-H. Kyeong *et al.* (Belle Collaboration), Measurements of charmless hadronic $b \to s$ penguin decays in the $\pi^+\pi^-K^+\pi^-$ final state and observation of $B^0 \to \rho^0 K^+\pi^-$, Phys. Rev. D **80**, 051103 (2009).
[980] B. Aubert *et al.* (*BABAR* Collaboration), Measurements of the branching fractions of $B^0 \to K^{*0}K^+K^-$, $B^0 \to K^{*0}\pi^+K^-$, $B^0 \to K^{*0}K^+\pi^-$, and $B^0 \to K^{*0}\pi^+\pi^-$, Phys. Rev. D **76**, 071104 (2007).
[981] J. P. Lees *et al.* (*BABAR* Collaboration), B^0 meson decays to $\rho^0 K^{*0}$, $f_0 K^{*0}$, and $\rho^- K^{*+}$, including higher K^* resonances, Phys. Rev. D **85**, 072005 (2012).
[982] Y. T. Lai *et al.* (Belle Collaboration), Measurement of branching fraction and final-state asymmetry for the $\bar{B}^0 \to K_S^0 K^{\mp}\pi^{\pm}$ decay, Phys. Rev. D **100**, 011101 (2019).
[983] P. del Amo Sanchez *et al.* (*BABAR* Collaboration), Observation of the rare decay $B^0 \to K_S^0 K^{\pm}\pi^{\mp}$, Phys. Rev. D **82**, 031101 (2010).
[984] B. Aubert *et al.* (*BABAR* Collaboration), Search for the decay of a B^0 or $\bar{B}^0$ meson to $\bar{K}^{*0}K^0$ or $K^{*0}\bar{K}^0$, Phys. Rev. D **74**, 072008 (2006).
[985] V. Gaur *et al.* (Belle Collaboration), Evidence for the decay $B^0 \to K^+K^-\pi^0$, Phys. Rev. D **87**, 091101 (2013).
[986] B. Aubert *et al.* (*BABAR* Collaboration), Search for B^0 meson decays to $\pi^0 K_S^0 K_S^0$, $\eta K_S^0 K_S^0$, and $\eta' K_S^0 K_S^0$, Phys. Rev. D **80**, 011101 (2009).
[987] R. Aaij *et al.* (LHCb Collaboration), Observation of the $\Lambda_b^0 \to \Lambda\phi$ decay, Phys. Lett. B **759**, 282 (2016).
[988] R. Aaij *et al.* (LHCb Collaboration), Measurement of the branching fraction of the decay $B_s^0 \to K_S^0 K_S^0$, Phys. Rev. D **102**, 012011 (2020).
[989] B. Aubert *et al.* (*BABAR* Collaboration), Search for the decay $B^0 \to K_s^0 K_s^0 K_L^0$, Phys. Rev. D **74**, 032005 (2006).
[990] M. Prim *et al.* (Belle Collaboration), Angular analysis of $B^0 \to \phi K^*$ decays and search for CP violation at Belle, Phys. Rev. D **88**, 072004 (2013).
[991] R. Aaij *et al.* (LHCb Collaboration), First observation of the decay $B_s^0 \to \phi\bar{K}^{*0}$, J. High Energy Phys. 11 (2013) 092.
[992] R. Aaij *et al.* (LHCb Collaboration), Measurement of the $B_s^0 \to \phi\phi$ branching fraction and search for the decay $B^0 \to \phi\phi$, J. High Energy Phys. 10 (2015) 053.
[993] R. Aaij *et al.* (LHCb Collaboration), Measurement of CP asymmetries and polarisation fractions in $B_s^0 \to K^{*0}\bar{K}^{*0}$ decays, J. High Energy Phys. 07 (2015) 166.
[994] C.-C. Chiang *et al.* (Belle Collaboration), Search for $B^0 \to K^{*0}\bar{K}^{*0}$, $B^0 \to K^{*0}K^{*0}$ and $B^0 \to K^+\pi^-K^{\mp}\pi^{\pm}$ decays, Phys. Rev. D **81**, 071101 (2010).
[995] R. Aaij *et al.* (LHCb Collaboration), Amplitude analysis of the $B_{(s)}^0 \to K^{*0}\bar{K}^{*0}$ decays and measurement of the branching fraction of the $B^0 \to K^{*0}\bar{K}^{*0}$ decay, J. High Energy Phys. 07 (2019) 032.
[996] B. Aubert *et al.* (*BABAR* Collaboration), Observation of $B^0 \to K^{*0}\bar{K}^{*0}$ and Search for $B^0 \to K^{*0}K^{*0}$, Phys. Rev. Lett. **100**, 081801 (2008).
[997] B. Aubert *et al.* (*BABAR* Collaboration), Search for $B^0 \to K^{*+}K^{*-}$, Phys. Rev. D **78**, 051103 (2008).
[998] B. Aubert *et al.* (*BABAR* Collaboration), Search for $B^0 \to \phi(K+\pi^-)$ decays with large $K^+\pi^-$ invariant mass, Phys. Rev. D **76**, 051103 (2007).
[999] B. Pal *et al.* (Belle Collaboration), Evidence for the decay $B^0 \to \eta\pi^0$, Phys. Rev. D **92**, 011101 (2015).
[1000] J. P. Lees *et al.* (*BABAR* Collaboration), Evidence for the decay $B^0 \to \omega\omega$ and search for $B^0 \to \omega\phi$, Phys. Rev. D **89**, 051101 (2014).
[1001] R. Aaij *et al.* (LHCb Collaboration), Observation of the decay $B_s^0 \to \phi\pi^+\pi^-$ and evidence for $B^0 \to \phi\pi^+\pi^-$, Phys. Rev. D **95**, 012006 (2017).
[1002] R. Aaij *et al.* (LHCb Collaboration), Measurement of CP violation in the $B_s^0 \to \phi\phi$ decay and search for the $B^0 \to \phi\phi$ decay, arXiv:1907.10003.
[1003] B. Aubert *et al.* (*BABAR* Collaboration), Measurement of Branching Fractions and Charge Asymmetries in $B^{\pm} \to \rho^{\pm}\pi^0$ and $B^{\pm} \to \rho^0\pi^{\pm}$ Decays, and Search for $B^0 \to \rho^0\pi^0$, Phys. Rev. Lett. **93**, 051802 (2004).
[1004] B. Aubert *et al.* (*BABAR* Collaboration), Observation of B^0 Meson Decay to $a_1^{\pm}(1260)\pi^{\mp}$, Phys. Rev. Lett. **97**, 051802 (2006).
[1005] B. Aubert *et al.* (*BABAR* Collaboration), Search for the decay $B^0 \to a_1^{\pm}\rho^{\pm}$, Phys. Rev. D **74**, 031104 (2006).
[1006] B. Aubert *et al.* (*BABAR* Collaboration), Observation and polarization measurement of $B^0 \to a_1(1260)^+ a_1(1260)^-$ decay, Phys. Rev. D **80**, 092007 (2009).
[1007] R. Aaij *et al.* (LHCb Collaboration), Study of the rare B_s^0 and B^0 decays into the $\pi^+\pi^-\mu^+\mu^-$ final state, Phys. Lett. B **743**, 46 (2015).
[1008] J. T. Wei *et al.* (Belle Collaboration), Study of $B^+ \to p\bar{p}K^+$ and $B^+ \to p\bar{p}\pi^+$, Phys. Lett. B **659**, 80 (2008).
[1009] R. Aaij *et al.* (LHCb Collaboration), Evidence for CP Violation in $B^+ \to p\bar{p}K^+$ Decays, Phys. Rev. Lett. **113**, 141801 (2014).
[1010] K. Chu *et al.* (Belle Collaboration), Study of $B \to p\bar{p}\pi\pi$, Phys. Rev. D **101**, 052012 (2020).
[1011] H. Albrecht *et al.* (ARGUS Collaboration), Observation of the charmless B meson decays, Phys. Lett. B **209**, 119 (1988).
[1012] J. H. Chen *et al.* (Belle Collaboration), Observation of $B^0 \to p\bar{p}K^{*0}$ with a Large K^{*0} Polarization, Phys. Rev. Lett. **100**, 251801 (2008).
[1013] R. Aaij *et al.* (LHCb Collaboration), Evidence for the two-body charmless baryonic decay $B^+ \to p\bar{\Lambda}$, J. High Energy Phys. 04 (2017) 162.
[1014] Y.-T. Tsai *et al.* (Belle Collaboration), Search for $B^0 \to p\bar{p}$, $\Lambda\bar{\Lambda}$ and $B^+ \to p\bar{\Lambda}$ at Belle, Phys. Rev. D **75**, 111101 (2007).
[1015] M.-Z. Wang *et al.* (Belle Collaboration), Study of $B^+ \to p\bar{\Lambda}\gamma$, $p\bar{\Lambda}\pi^0$ and $B^0 \to p\bar{\Lambda}\pi^-$, Phys. Rev. D **76**, 052004 (2007).
[1016] P. Chen *et al.* (Belle Collaboration), Observation of $B^+ \to p\bar{\Lambda}\pi^+\pi^-$ at Belle, Phys. Rev. D **80**, 111103 (2009).

[1017] P.-C. Lu *et al.* (Belle Collaboration), Observation of $B^+ \to p\bar{\Lambda}K^+K^-$ and $B^+ \to \bar{p}\Lambda K^+K^+$, Phys. Rev. D **99**, 032003 (2019).

[1018] R. Aaij *et al.* (LHCb Collaboration), First Observation of the Rare Purely Baryonic Decay $B^0 \to p\bar{p}$, Phys. Rev. Lett. **119**, 232001 (2017).

[1019] B. Aubert *et al.* (*BABAR* Collaboration), Search for the decay $B^0 \to p\bar{p}$, Phys. Rev. D **69**, 091503 (2004).

[1020] R. Aaij *et al.* (LHCb Collaboration), Observation of charmless baryonic decays $B^0_{(s)} \to p\bar{p}h^+h'^-$, Phys. Rev. D **96**, 051103 (2017).

[1021] B. Pal *et al.* (Belle Collaboration), Evidence for the decay $B^0 \to p\bar{p}\pi^0$, Phys. Rev. D **99**, 091104 (2019).

[1022] J. P. Lees *et al.* (*BABAR* Collaboration), Search for the decay mode $B^0 \to pp\bar{p}\,\bar{p}$, Phys. Rev. D **98**, 071102 (2018).

[1023] B. Aubert *et al.* (*BABAR* Collaboration), Measurement of the branching fraction and $\bar{\Lambda}$ polarization in $B^0 \to \bar{\Lambda}p\pi^-$, Phys. Rev. D **79**, 112009 (2009).

[1024] M. Z. Wang *et al.* (Belle Collaboration), Observation of $B^0 \to p\bar{\Lambda}\pi^-$, Phys. Rev. Lett. **90**, 201802 (2003).

[1025] R. Aaij *et al.* (LHCb Collaboration), Measurement of the differential branching fraction of the decay $\Lambda_b^0 \to \Lambda\mu^+\mu^-$, Phys. Lett. B **725**, 25 (2013).

[1026] T. Aaltonen *et al.* (CDF Collaboration), Observation of the Baryonic Flavor-Changing Neutral Current Decay $\Lambda_b \to \Lambda\mu^+\mu^-$, Phys. Rev. Lett. **107**, 201802 (2011).

[1027] R. Aaij *et al.* (LHCb Collaboration), Observation of the suppressed decay $\Lambda_b^0 \to p\pi^-\mu^+\mu^-$, J. High Energy Phys. 04 (2017) 029.

[1028] R. Aaij *et al.* (LHCb Collaboration), Test of lepton universality with $\Lambda_b^0 \to pK^-\ell^+\ell^-$ decays, J. High Energy Phys. 05 (2020) 040.

[1029] R. Aaij *et al.* (LHCb Collaboration), First Observation of the Radiative Decay $\Lambda_b^0 \to \Lambda\gamma$, Phys. Rev. Lett. **123**, 031801 (2019).

[1030] R. Aaij *et al.* (LHCb Collaboration), Observations of $\Lambda_b^0 \to \Lambda K^+\pi^-$ and $\Lambda_b^0 \to \Lambda K^+K^-$ decays and searches for other Λ_b^0 and Ξ_b^0 decays to $\Lambda h^+h'^-$ final states, J. High Energy Phys. 05 (2016) 081.

[1031] R. Aaij *et al.* (LHCb Collaboration), Measurement of branching fractions of charmless four-body Λ_b^0 and Ξ_b^0 decays, J. High Energy Phys. 02 (2018) 098.

[1032] R. Aaij *et al.* (LHCb Collaboration), Differential branching fraction and angular analysis of $\Lambda_b^0 \to \Lambda\mu^+\mu^-$ decays, J. High Energy Phys. 06 (2015) 115; J. High Energy Phys. 09 (2018) 145(E).

[1033] R. Aaij *et al.* (LHCb Collaboration), Observation of the Decay $\Xi_b^- \to pK^-K^-$, Phys. Rev. Lett. **118**, 071801 (2017).

[1034] R. Aaij *et al.* (LHCb Collaboration), Angular moments of the decay $\Lambda_b^0 \to \Lambda\mu^+\mu^-$ at low hadronic recoil, J. High Energy Phys. 09 (2018) 146.

[1035] R. Aaij *et al.* (LHCb Collaboration), Search for Baryon-Number-Violating Ξ_b^0 Oscillations, Phys. Rev. Lett. **119**, 181807 (2017).

[1036] M. Acciarri *et al.* (L3 Collaboration), Search for neutral charmless B decays at LEP, Phys. Lett. B **363**, 127 (1995).

[1037] K. Abe *et al.* (SLD Collaboration), Search for charmless hadronic decays of B mesons with the SLD detector, Phys. Rev. D **62**, 071101 (2000).

[1038] R. Aaij *et al.* (LHCb Collaboration), Search for the $B_s^0 \to \eta'\phi$ decay, J. High Energy Phys. 05 (2017) 158.

[1039] T. Aaltonen *et al.* (CDF Collaboration), Measurement of Polarization and Search for CP-Violation in $B_s^0 \to \phi\phi$ Decays, Phys. Rev. Lett. **107**, 261802 (2011).

[1040] C.-C. Peng *et al.* (Belle Collaboration), Search for $B_s^0 \to hh$ decays at the $\Upsilon(5S)$ resonance, Phys. Rev. D **82**, 072007 (2010).

[1041] B. Pal *et al.* (Belle Collaboration), Observation of the Decay $B_s^0 \to K^0\bar{K}^0$, Phys. Rev. Lett. **116**, 161801 (2016).

[1042] R. Aaij *et al.* (LHCb Collaboration), Amplitude analysis of $B_s^0 \to K_S^0K^\pm\pi^\mp$ decays, J. High Energy Phys. 06 (2019) 114.

[1043] R. Aaij *et al.* (LHCb Collaboration), First Observation of a Baryonic B_s^0 Decay, Phys. Rev. Lett. **119**, 041802 (2017).

[1044] D. Dutta *et al.* (Belle Collaboration), Search for $B_s^0 \to \gamma\gamma$ and a measurement of the branching fraction for $B_s^0 \to \phi\gamma$, Phys. Rev. D **91**, 011101 (2015).

[1045] R. Aaij *et al.* (LHCb Collaboration), Measurement of the ratio of branching fractions $\mathrm{BR}(B_0 \to K^{\star 0}\gamma)/\mathrm{BR}(B_{s0} \to \phi\gamma)$ and the direct CP asymmetry in $B_0 \to K^{\star 0}\gamma$, Nucl. Phys. **B867**, 1 (2013).

[1046] M. Aaboud *et al.* (ATLAS Collaboration), Study of the rare decays of B_s^0 and B^0 mesons into muon pairs using data collected during 2015 and 2016 with the ATLAS detector, J. High Energy Phys. 04 (2019) 098.

[1047] R. Aaij *et al.* (LHCb Collaboration), Measurement of the $B_s^0 \to \mu^+\mu^-$ Branching Fraction and Effective Lifetime and Search for $B^0 \to \mu^+\mu^-$ Decays, Phys. Rev. Lett. **118**, 191801 (2017).

[1048] T. Aaltonen *et al.* (CDF Collaboration), Search for $B_s^0 \to \mu^+\mu^-$ and $B^0 \to \mu^+\mu^-$ decays with the full CDF Run II dataset, Phys. Rev. D **87**, 072003 (2013); Phys. Rev. D **97**, 099901(E) (2018).

[1049] R. Aaij *et al.* (LHCb Collaboration), Search for the Rare Decays $B_s^0 \to e^+e^-$ and $B^0 \to e^+e^-$, Phys. Rev. Lett. **124**, 211802 (2020).

[1050] T. Aaltonen *et al.* (CDF Collaboration), Search for the Decays $B_s^0 \to e^+\mu^-$ and $B_s^0 \to e^+e^-$ in CDF Run II, Phys. Rev. Lett. **102**, 201801 (2009).

[1051] R. Aaij *et al.* (LHCb Collaboration), Search for the Decays $B_s^0 \to \tau^+\tau^-$ and $B^0 \to \tau^+\tau^-$, Phys. Rev. Lett. **118**, 251802 (2017).

[1052] R. Aaij *et al.* (LHCb Collaboration), Search for decays of neutral beauty mesons into four muons, J. High Energy Phys. 03 (2017) 001.

[1053] R. Aaij *et al.* (LHCb Collaboration), Branching Fraction Measurements of the Rare $B_s^0 \to \phi\mu^+\mu^-$ and $B_s^0 \to f_2'(1525)\mu^+\mu^-$-Decays, Phys. Rev. Lett. **127**, 151801 (2021).

[1054] R. Aaij *et al.* (LHCb Collaboration), Evidence for the decay $B_S^0 \to \bar{K}^{*0}\mu^+\mu^-$, J. High Energy Phys. 07 (2018) 020.

[1055] R. Aaij *et al.* (LHCb Collaboration), Search for the lepton-flavour violating decays $B^0_{(s)} \to e^\pm\mu^\mp$, J. High Energy Phys. 03 (2018) 078.

[1056] R. Aaij *et al.* (LHCb Collaboration), Search for the Lepton-Flavour-Violating Decays $B_s^0 \to \tau^{\pm}\mu^{\mp}$ and $B^0 \to \tau^{\pm}\mu^{\mp}$, Phys. Rev. Lett. **123**, 211801 (2019).

[1057] N. K. Nisar *et al.* (Belle Collaboration), Search for the decay $B_s^0 \to \eta'\eta$, Phys. Rev. D **104**, L031101 (2021).

[1058] CMS, LHCb, and ATLAS Collaborations, Combination of the ATLAS, CMS and LHCb results on the $B_{(s)}^0 \to \mu^+\mu^-$ decays, Technical Report No. LHCb-CONF-2020-002, CERN, Geneva, 2020.

[1059] R. Aaij *et al.* (LHCb Collaboration), Study of charmonium production in b-hadron decays and first evidence for the decay $B_s^0 \to \phi\phi\phi$, Eur. Phys. J. C **77**, 609 (2017).

[1060] R. Aaij *et al.* (LHCb Collaboration), Angular analysis and differential branching fraction of the decay $B_s^0 \to \phi\mu^+\mu^-$, J. High Energy Phys. 09 (2015) 179.

[1061] R. Aaij *et al.* (LHCb Collaboration), First Experimental Study of Photon Polarization in Radiative B_s^0 Decays, Phys. Rev. Lett. **118**, 021801 (2017).

[1062] R. Aaij *et al.* (LHCb Collaboration), Search for B_c^+ decays to the $p\bar{p}\pi^+$ final state, Phys. Lett. B **759**, 313 (2016).

[1063] T. Horiguchi *et al.* (Belle Collaboration), Evidence for Isospin Violation and Measurement of CP Asymmetries in $B \to K^*(892)\gamma$, Phys. Rev. Lett. **119**, 191802 (2017).

[1064] B. Aubert *et al.* (*BABAR* Collaboration), Measurement of Branching Fractions and CP and Isospin Asymmetries in $B \to K^*(892)\gamma$ Decays, Phys. Rev. Lett. **103**, 211802 (2009).

[1065] T. E. Coan *et al.* (CLEO Collaboration), Study of Exclusive Radiative B Meson Decays, Phys. Rev. Lett. **84**, 5283 (2000).

[1066] H. Yang *et al.* (Belle Collaboration), Observation of $B^+ \to K_1(1270)^+\gamma$, Phys. Rev. Lett. **94**, 111802 (2005).

[1067] S. Nishida *et al.* (Belle Collaboration), Observation of $B^+ \to K^+\eta\gamma$, Phys. Lett. B **610**, 23 (2005).

[1068] R. Wedd *et al.* (Belle Collaboration), Evidence for $B \to K\eta'\gamma$ decays at Belle, Phys. Rev. D **81**, 111104 (2010).

[1069] B. Aubert *et al.* (*BABAR* Collaboration), Measurement of branching fractions in radiative B decays to $\eta K\gamma$ and search for B decays to $\eta' K\gamma$, Phys. Rev. D **74**, 031102 (2006).

[1070] B. Aubert *et al.* (*BABAR* Collaboration), Measurement of B decays to $\phi K\gamma$, Phys. Rev. D **75**, 051102 (2007).

[1071] S. Nishida *et al.* (Belle Collaboration), Radiative B Meson Decays into $K\pi\gamma$ and $K\pi\pi\gamma$ Final States, Phys. Rev. Lett. **89**, 231801 (2002).

[1072] B. Aubert *et al.* (*BABAR* Collaboration), Measurement of Branching Fractions and Mass Spectra of $B \to K\pi\pi\gamma$, Phys. Rev. Lett. **98**, 211804 (2007); Phys. Rev. Lett. **100**, 189903(E) (2008); **100**, 199905(E) (2008).

[1073] B. Aubert *et al.* (*BABAR* Collaboration), Measurement of the $B^0 \to K_2^*(1430)^0\gamma$ and $B^+ \to K_2^*(1430)^+\gamma$ branching fractions, Phys. Rev. D **70**, 091105 (2004).

[1074] H. Albrecht *et al.* (ARGUS Collaboration), Search for $b \to s\gamma$ in exclusive decays of B mesons, Phys. Lett. B **229**, 304 (1989).

[1075] N. Taniguchi *et al.* (Belle Collaboration), Measurement of Branching Fractions, Isospin and CP-Violating Asymmetries for Exclusive $b \to d\gamma$ Modes, Phys. Rev. Lett. **101**, 111801 (2008); Phys. Rev. Lett. **101**, 129904(E) (2008).

[1076] B. Aubert *et al.* (*BABAR* Collaboration), Measurements of branching fractions for $B^+ \to \rho^+\gamma$, $B^0 \to \rho^0\gamma$, and $B^0 \to \omega\gamma$, Phys. Rev. D **78**, 112001 (2008).

[1077] Y.-J. Lee *et al.* (Belle Collaboration), Observation of $B^+ \to p\bar{\Lambda}\gamma$, Phys. Rev. Lett. **95**, 061802 (2005).

[1078] J.-T. Wei *et al.* (Belle Collaboration), Search for $B \to \pi\ell^+\ell^-$ decays at Belle, Phys. Rev. D **78**, 011101 (2008).

[1079] J. P. Lees *et al.* (*BABAR* Collaboration), Search for the rare decays $B \to \pi\ell^+\ell^-$ and $B^0 \to \eta\ell^+\ell^-$, Phys. Rev. D **88**, 032012 (2013).

[1080] R. Aaij *et al.* (LHCb Collaboration), First measurement of the differential branching fraction and CP asymmetry of the $B^{\pm} \to \pi^{\pm}\mu^+\mu^-$ decay, J. High Energy Phys. 10 (2015) 034.

[1081] J. Grygier *et al.* (Belle Collaboration), Search for $B \to h\nu\bar{\nu}$ decays with semileptonic tagging at Belle, Phys. Rev. D **96**, 091101 (2017).Phys. Rev. D **97**, 099902(A) (2018).

[1082] B. Aubert *et al.* (*BABAR* Collaboration), A Search for the Decay $B^+ \to K^+\nu\bar{\nu}$, Phys. Rev. Lett. **94**, 101801 (2005).

[1083] R. Aaij *et al.* (LHCb Collaboration), Differential branching fractions and isospin asymmetries of $B \to K^{(*)}\mu^+\mu^-$ decays, J. High Energy Phys. 06 (2014) 133.

[1084] S. Choudhury *et al.* (BELLE Collaboration), Test of lepton flavor universality and search for lepton flavor violation in $B \to K\ell\ell$ decays, J. High Energy Phys. 03 (2021) 105.

[1085] B. Aubert *et al.* (*BABAR* Collaboration), Direct CP, Lepton Flavor and Isospin Asymmetries in the Decays $B \to K^{(*)}\ell^+\ell^-$, Phys. Rev. Lett. **102**, 091803 (2009).

[1086] J. P. Lees *et al.* (*BABAR* Collaboration), Search for $B^+ \to K^+\tau^+\tau^-$ at the *BABAR* Experiment, Phys. Rev. Lett. **118**, 031802 (2017).

[1087] J. P. Lees *et al.* (*BABAR* Collaboration), Search for $B \to K^{(*)}\nu\bar{\nu}$ and invisible quarkonium decays, Phys. Rev. D **87**, 112005 (2013).

[1088] F. Abudinén *et al.* (Belle-II Collaboration), Search for $B^+ \to K^+\nu\bar{\nu}$ Decays Using an Inclusive Tagging Method at Belle II, Phys. Rev. Lett. **127**, 181802 (2021).

[1089] J.-T. Wei *et al.* (Belle Collaboration), Measurement of the Differential Branching Fraction and Forward-Backward Asymmetry for $B \to K^{(*)}\ell^+\ell^-$, Phys. Rev. Lett. **103**, 171801 (2009).

[1090] O. Lutz *et al.* (Belle Collaboration), Search for $B \to h^{(*)}\nu\bar{\nu}$ with the full Belle $\Upsilon(4S)$ data sample, Phys. Rev. D **87**, 111103 (2013).

[1091] R. Aaij *et al.* (LHCb Collaboration), First observations of the rare decays $B^+ \to K^+\pi^+\pi^-\mu^+\mu^-$ and $B^+ \to \phi K^+\mu^+\mu^-$, J. High Energy Phys. 10 (2014) 064.

[1092] J. P. Lees *et al.* (*BABAR* Collaboration), Search for $B^- \to \Lambda\overline{p}\nu\bar{\nu}$ with the *BABAR* experiment, Phys. Rev. D **100**, 111101 (2019).

[1093] H. J. Hyun *et al.* (Belle Collaboration), Search for a Low Mass Particle Decaying into $\mu^+\mu^-$ in $B^0 \to K^{*0}X$ and $B^0 \to \rho^0 X$ at Belle, Phys. Rev. Lett. **105**, 091801 (2010).

[1094] Z. King *et al.* (Belle Collaboration), Search for the decay $B^0 \to \phi\gamma$, Phys. Rev. D **93**, 111101 (2016).

[1095] B. Aubert *et al.* (*BABAR* Collaboration), Search for the radiative decay $B \to \phi\gamma$, Phys. Rev. D **72**, 091103 (2005).

[1096] Y. T. Lai *et al.* (Belle Collaboration), Search for $B^0 \to p\bar{\Lambda}\pi^-\gamma$ at Belle, Phys. Rev. D **89**, 051103 (2014).

[1097] R. Aaij *et al.* (LHCb Collaboration), Measurements of the S-wave fraction in $B^0 \to K^+\pi^-\mu^+\mu^-$ decays and the $B^0 \to K^*(892)^0\mu^+\mu^-$ differential branching fraction, J. High Energy Phys. 11 (2016) 047; J. High Energy Phys. 04 (2017) 142(E).

[1098] B. Aubert *et al.* (*BABAR* Collaboration), Search for the Rare Decay $B \to \pi\ell^+\ell^-$, Phys. Rev. Lett. **99**, 051801 (2007).

[1099] B. Aubert *et al.* (*BABAR* Collaboration), Measurements of branching fractions, rate asymmetries, and angular distributions in the rare decays $B \to K\ell^+\ell^-$ and $B \to K^*\ell^+\ell^-$, Phys. Rev. D **73**, 092001 (2006).

[1100] S. Sandilya *et al.* (Belle Collaboration), Search for the lepton-flavor-violating decay $B^0 \to K^{*0}\mu^\pm e^\mp$, Phys. Rev. D **98**, 071101 (2018).

[1101] P. del Amo Sanchez *et al.* (*BABAR* Collaboration), Searches for the baryon- and lepton-number violating decays $B^0 \to \Lambda_c^+\ell^-$, $B^- \to \Lambda\ell^-$, and $B^- \to \bar{\Lambda}\ell^-$, Phys. Rev. D **83**, 091101 (2011).

[1102] J. P. Lees *et al.* (*BABAR* Collaboration), Precision Measurement of the $B \to X_s\gamma$ Photon Energy Spectrum, Branching Fraction, and Direct *CP* Asymmetry $A_{CP}(B \to X_{s+d}\gamma)$, Phys. Rev. Lett. **109**, 191801 (2012).

[1103] T. Saito *et al.* (Belle Collaboration), Measurement of the $\bar{B} \to X_s\gamma$ branching fraction with a sum of exclusive decays, Phys. Rev. D **91**, 052004 (2015).

[1104] J. P. Lees *et al.* (*BABAR* Collaboration), Exclusive measurements of $b \to s\gamma$ transition rate and photon energy spectrum, Phys. Rev. D **86**, 052012 (2012).

[1105] B. Aubert *et al.* (*BABAR* Collaboration), Measurement of the $B \to X_s\gamma$ branching fraction and photon energy spectrum using the recoil method, Phys. Rev. D **77**, 051103 (2008).

[1106] P. del Amo Sanchez *et al.* (*BABAR* Collaboration), Study of $B \to X\gamma$ decays and determination of $|V_{td}/V_{ts}|$, Phys. Rev. D **82**, 051101 (2010).

[1107] J. P. Lees *et al.* (*BABAR* Collaboration), Measurement of the $B \to X_s l^+ l^-$ Branching Fraction and Search for Direct *CP* Violation from a Sum of Exclusive Final States, Phys. Rev. Lett. **112**, 211802 (2014).

[1108] M. Iwasaki *et al.* (Belle Collaboration), Improved measurement of the electroweak penguin process $B \to X_s l^+ l^-$, Phys. Rev. D **72**, 092005 (2005).

[1109] O. Buchmuller and H. Flacher, Fit to moment from $B \to X_c\ell\bar{\nu}$ and $B \to X_s\gamma$ decays using heavy quark expansions in the kinetic scheme, Phys. Rev. D **73**, 073008 (2006).

[1110] J. P. Lees *et al.* (*BABAR* Collaboration), Measurement of branching fractions and rate asymmetries in the rare decays $B \to K^{(*)} l^+ l^-$, Phys. Rev. D **86**, 032012 (2012).

[1111] K. W. Edwards *et al.* (CLEO Collaboration), Search for lepton flavor violating decays of B mesons, Phys. Rev. D **65**, 111102 (2002).

[1112] N. Satoyama *et al.* (Belle Collaboration), A search for the rare leptonic decays $B^+ \to \mu^+\nu_\mu$ and $B^+ \to e^+\nu_e$, Phys. Lett. B **647**, 67 (2007).

[1113] B. Aubert *et al.* (*BABAR* Collaboration), Search for the rare leptonic decays $B^+ \to \ell^+\nu_l$ ($l = e, \mu$), Phys. Rev. D **79**, 091101 (2009).

[1114] M. T. Prim *et al.* (Belle Collaboration), Search for $B^+ \to \mu^+\nu_\mu$ and $B^+ \to \mu^+ N$ with inclusive tagging, Phys. Rev. D **101**, 032007 (2020).

[1115] A. Sibidanov *et al.* (Belle Collaboration), Search for $B^- \to \mu^-\bar{\nu}_\mu$ Decays at the Belle Experiment, Phys. Rev. Lett. **121**, 031801 (2018).

[1116] I. Adachi *et al.* (Belle Collaboration), Evidence for $B^- \to \tau^-\bar{\nu}_\tau$ with a Hadronic Tagging Method Using the Full Data Sample of Belle, Phys. Rev. Lett. **110**, 131801 (2013).

[1117] B. Kronenbitter *et al.* (Belle Collaboration), Measurement of the branching fraction of $B^+ \to \tau^+\nu_\tau$ decays with the semileptonic tagging method, Phys. Rev. D **92**, 051102 (2015).

[1118] J. P. Lees *et al.* (*BABAR* Collaboration), Evidence of $B^+ \to \tau^+\nu$ decays with hadronic B tags, Phys. Rev. D **88**, 031102 (2013).

[1119] B. Aubert *et al.* (*BABAR* Collaboration), A search for $B^+ \to \ell^+\nu_\ell$ recoiling against $B^- \to D^0\ell^-\bar{\nu}X$, Phys. Rev. D **81**, 051101 (2010).

[1120] M. Gelb *et al.* (Belle Collaboration), Search for the rare decay of $B^+ \to \ell^+\nu_\ell\gamma$ with improved hadronic tagging, Phys. Rev. D **98**, 112016 (2018).

[1121] B. Aubert *et al.* (*BABAR* Collaboration), A model-independent search for the decay $B^+ \to \ell^+\nu_l\gamma$, Phys. Rev. D **80**, 111105 (2009).

[1122] P. del Amo Sanchez *et al.* (*BABAR* Collaboration), Search for the decay $B^0 \to \gamma\gamma$, Phys. Rev. D **83**, 032006 (2011).

[1123] S. Villa *et al.* (Belle Collaboration), Search for the decay $B^0 \to \gamma\gamma$, Phys. Rev. D **73**, 051107 (2006).

[1124] B. Aubert *et al.* (*BABAR* Collaboration), Search for decays of B^0 into mesons into e^+e^-, $\mu^+\mu^-$, and $e^\pm\mu^\mp$ final states, Phys. Rev. D **77**, 032007 (2008).

[1125] M. C. Chang *et al.* (Belle Collaboration), Search for $B^0 \to \ell^+\ell^-$ at BELLE, Phys. Rev. D **68**, 111101 (2003).

[1126] B. Aubert *et al.* (*BABAR* Collaboration), Search for the decays $B^0 \to e^+e^-\gamma$ and $B^0 \to \mu^+\mu^-\gamma$, Phys. Rev. D **77**, 011104 (2008).

[1127] B. Aubert *et al.* (*BABAR* Collaboration), A Search for the Rare Decay $B^0 \to \tau^+\tau^-$ at *BABAR*, Phys. Rev. Lett. **96**, 241802 (2006).

[1128] J. P. Lees *et al.* (*BABAR* Collaboration), Improved limits on B^0 decays to invisible final states and to $\nu\bar{\nu}\gamma$, Phys. Rev. D **86**, 051105 (2012).

[1129] Y. Ku *et al.* (Belle Collaboration), Search for B^0 decays to invisible final states ($+\gamma$) at Belle, Phys. Rev. D **102**, 012003 (2020).

[1130] R. Aaij *et al.* (LHCb Collaboration), Search for the rare decay $B^+ \to \mu^+\mu^-\mu^+\nu_\mu$, Eur. Phys. J. C **79**, 675 (2019).

[1131] R. Aaij *et al.* (LHCb Collaboration), Test of lepton universality in beauty-quark decays, Nat. Phys. **18**, 277 (2022).

[1132] A. Abdesselam *et al.* (Belle Collaboration), Test of Lepton-Flavor Universality in $B \to K^* \ell^+ \ell^-$ Decays at Belle, Phys. Rev. Lett. **126**, 161801 (2021).

[1133] R. Aaij *et al.* (LHCb Collaboration), Test of lepton universality with $B^0 \to K^{*0} \ell^+ \ell^-$ decays, J. High Energy Phys. 08 (2017) 055.

[1134] K. Nishimura *et al.* (Belle Collaboration), First Measurement of Inclusive $B \to X_s \eta$ Decays, Phys. Rev. Lett. **105**, 191803 (2010).

[1135] T. E. Browder *et al.* (CLEO Collaboration), Observation of High Momentum η' Production in B Decay, Phys. Rev. Lett. **81**, 1786 (1998).

[1136] B. Aubert *et al.* (*BABAR* Collaboration), Study of High Momentum η' Production in $B \to \eta' X_s$, Phys. Rev. Lett. **93**, 061801 (2004).

[1137] G. Bonvicini *et al.* (CLEO Collaboration), Study of the charmless inclusive $B \to \eta' X$ decay, Phys. Rev. D **68**, 011101 (2003).

[1138] P. del Amo Sanchez *et al.* (*BABAR* Collaboration), Measurement of partial branching fractions of inclusive charmless B meson decays to K^+, K^0, and π^+, Phys. Rev. D **83**, 031103 (2011).

[1139] S. Watanuki *et al.* (Belle Collaboration), Measurements of isospin asymmetry and difference of direct CP asymmetries in inclusive $B \to X_s \gamma$ decays, Phys. Rev. D **99**, 032012 (2019).

[1140] J. P. Lees *et al.* (*BABAR* Collaboration), A search for the decay modes $B^{\pm} \to h^{\pm} \tau^{\pm} l$, Phys. Rev. D **86**, 012004 (2012).

[1141] R. Aaij *et al.* (LHCb Collaboration), Search for Lepton-Flavor Violating Decays $B^+ \to K^+ \mu^{\pm} e^{\mp}$, Phys. Rev. Lett. **123**, 241802 (2019).

[1142] R. Aaij *et al.* (LHCb Collaboration), Search for the lepton flavour violating decay $B^+ \to K^+ \mu^- \tau^+$ using B^{*0}_{s2} decays, J. High Energy Phys. 06 (2020) 129.

[1143] J. P. Lees *et al.* (*BABAR* Collaboration), Search for lepton-number violating processes in $B^+ \to h^- l^+ l^+$ decays, Phys. Rev. D **85**, 071103 (2012).

[1144] R. Aaij *et al.* (LHCb Collaboration), Search for Majorana Neutrinos in $B^- \to \pi^+ \mu^- \mu^-$ Decays, Phys. Rev. Lett. **112**, 131802 (2014).

[1145] J. P. Lees *et al.* (*BABAR* Collaboration), Search for lepton-number violating $B^+ \to X^- \ell^+ \ell'^+$ decays, Phys. Rev. D **89**, 011102 (2014).

[1146] R. Aaij *et al.* (LHCb Collaboration), Search for the Lepton Number Violating Decays $B^+ \to \pi^- \mu^+ \mu^+$ and $B^+ \to K^- \mu^+ \mu^+$, Phys. Rev. Lett. **108**, 101601 (2012).

[1147] R. Aaij *et al.* (LHCb Collaboration), Searches for Majorana neutrinos in B^- decays, Phys. Rev. D **85**, 112004 (2012).

[1148] B. Aubert *et al.* (*BABAR* Collaboration), Searches for the decays $B^0 \to \ell^{\pm} \tau^{\mp}$ and $B^+ \to \ell^+ \nu$ $(l = e,\ \mu)$ using hadronic tag reconstruction, Phys. Rev. D **77**, 091104 (2008).

[1149] R. Aaij *et al.* (LHCb Collaboration), Observation of Photon Polarization in the $b \to s\gamma$ Transition, Phys. Rev. Lett. **112**, 161801 (2014).

[1150] R. Aaij *et al.* (LHCb Collaboration), Angular analysis of charged and neutral $B \to K \mu^+ \mu^-$ decays, J. High Energy Phys. 05 (2014) 082.

[1151] R. Aaij *et al.* (LHCb Collaboration), Strong constraints on the $b \to s\gamma$ photon polarisation from $B^0 \to K^{*0} e^+ e^-$ decays, J. High Energy Phys. 12 (2020) 081.

[1152] R. Aaij *et al.* (LHCb Collaboration), Measurement of the $B^0 \to K^{*0} e^+ e^-$ branching fraction at low dilepton mass, J. High Energy Phys. 05 (2013) 159.

[1153] A. Abdesselam *et al.* (Belle Collaboration), Angular analysis of $B^0 \to K^*(892)^0 \ell^+ \ell^-$, arXiv:1604.04042.

[1154] S. Wehle *et al.* (Belle Collaboration), Lepton-Flavor-Dependent Angular Analysis of $B \to K^* \ell^+ \ell^-$, Phys. Rev. Lett. **118**, 111801 (2017).

[1155] J. P. Lees *et al.* (*BABAR* Collaboration), Measurement of angular asymmetries in the decays $B \to K^* \ell^+ \ell^-$, Phys. Rev. D **93**, 052015 (2016).

[1156] R. Aaij *et al.* (LHCb Collaboration), Angular analysis of the $B^0 \to K^{*0} \mu^+ \mu^-$ decay using 3 fb^{-1} of integrated luminosity, J. High Energy Phys. 02 (2016) 104.

[1157] R. Aaij *et al.* (LHCb Collaboration), Measurement of CP-Averaged Observables in the $B^0 \to K^{*0} \mu^+ \mu^-$ Decay, Phys. Rev. Lett. **125**, 011802 (2020).

[1158] V. Khachatryan *et al.* (CMS Collaboration), Angular analysis of the decay $B^0 \to K^{*0} \mu^+ \mu^-$ from pp collisions at $\sqrt{s} = 8$ TeV, Phys. Lett. B **753**, 424 (2016).

[1159] A. M. Sirunyan *et al.* (CMS Collaboration), Measurement of angular parameters from the decay $B^0 \to K^{*0} \mu^+ \mu^-$ in proton-proton collisions at $\sqrt{s} = 8$ TeV, Phys. Lett. B **781**, 517 (2018).

[1160] M. Aaboud *et al.* (ATLAS Collaboration), Angular analysis of $B^0_d \to K^* \mu^+ \mu^-$ decays in pp collisions at $\sqrt{s} = 8$ TeV with the ATLAS detector, J. High Energy Phys. 10 (2018) 047.

[1161] R. Aaij *et al.* (LHCb Collaboration), Angular Analysis of the $B^+ \to K^{*+} \mu^+ \mu^-$ Decay, Phys. Rev. Lett. **126**, 161802 (2021).

[1162] A. M. Sirunyan *et al.* (CMS Collaboration), Angular analysis of the decay $B^+ \to K^{*+}(892) \mu^+ \mu^-$ in proton-proton collisions at $\sqrt{s} = 8$ TeV, J. High Energy Phys. 04 (2021) 124.

[1163] Y. Sato *et al.* (Belle Collaboration), Measurement of the lepton forward-backward asymmetry in $B \to X_s \ell^+ \ell^-$ decays with a sum of exclusive modes, Phys. Rev. D **93**, 032008 (2016); **93**, 059901(A) (2016).

[1164] R. Aaij *et al.* (LHCb Collaboration), Differential branching fraction and angular moments analysis of the decay $B^0 \to K^+ \pi^- \mu^+ \mu^-$ in the $K^*_{0,2}(1430)^0$ region, J. High Energy Phys. 12 (2016) 065.

[1165] R. Aaij *et al.* (LHCb Collaboration), Measurement of the phase difference between short- and long-distance amplitudes in the $B^+ \to K^+ \mu^+ \mu^-$ decay, Eur. Phys. J. C **77**, 161 (2017).

[1166] A. M. Sirunyan *et al.* (CMS Collaboration), Angular analysis of the decay $B^+ \to K^+ \mu^+ \mu^-$ in proton-proton collisions at $\sqrt{s} = 8$ TeV, Phys. Rev. D **98**, 112011 (2018).

[1167] R. Aaij *et al.* (LHCb Collaboration), Search for Hidden-Sector Bosons in $B^0 \to K^{*0} \mu^+ \mu^-$ Decays, Phys. Rev. Lett. **115**, 161802 (2015).

[1168] R. Aaij *et al.* (LHCb Collaboration), Search for long-lived scalar particles in $B^+ \to K^+ \chi(\mu^+ \mu^-)$ decays, Phys. Rev. D **95**, 071101 (2017).

[1169] S. Chen *et al.* (CLEO Collaboration), Measurement of Charge Asymmetries in Charmless Hadronic in b Meson Decays, Phys. Rev. Lett. **85**, 525 (2000).

[1170] R. Aaij *et al.* (LHCb Collaboration), Measurement of CP Violation in the Decay $B^+ \to K^+\pi^0$, Phys. Rev. Lett. **126**, 091802 (2021).

[1171] R. Aaij *et al.* (LHCb Collaboration), Measurements of CP violation in the three-body phase space of charmless $B^\pm$ decays, Phys. Rev. D **90**, 112004 (2014).

[1172] K.-F. Chen *et al.* (Belle Collaboration), Measurement of Polarization and Triple-Product Correlations in $B \to \phi K^*$ Decays, Phys. Rev. Lett. **94**, 221804 (2005).

[1173] R. Aaij *et al.* (LHCb Collaboration), Measurement of CP asymmetries in the decays $B^0 \to K^{*0}\mu^+\mu^-$ and $B^+ \to K^+\mu^+\mu^-$, J. High Energy Phys. 09 (2014) 177.

[1174] R. Aaij *et al.* (LHCb Collaboration), Observation of CP violation in two-body $B^0_{(s)}$-meson decays to charged pions and kaons, J. High Energy Phys. 03 (2021) 075.

[1175] T. A. Aaltonen *et al.* (CDF Collaboration), Measurements of Direct CP-Violating Asymmetries in Charmless Decays of Bottom Baryons, Phys. Rev. Lett. **113**, 242001 (2014).

[1176] R. Aaij *et al.* (LHCb Collaboration), Measurement of CP asymmetries in two-body $B^0_{(s)}$-meson decays to charged pions and kaons, Phys. Rev. D **98**, 032004 (2018).

[1177] K. Abe *et al.* (Belle Collaboration), Observation of B Decays to Two Kaons, Phys. Rev. Lett. **98**, 181804 (2007).

[1178] J. P. Lees *et al.* (*BABAR* Collaboration), Measurements of direct CP asymmetries in $B \to X_s\gamma$ decays using sum of exclusive decays, Phys. Rev. D **90**, 092001 (2014).

[1179] L. Pesántez *et al.* (Belle Collaboration), Measurement of the Direct CP Asymmetry in $\bar{B} \to X_{s+d}\gamma$ Decays with a Lepton Tag, Phys. Rev. Lett. **114**, 151601 (2015).

[1180] R. Aaij *et al.* (LHCb Collaboration), Search for CP violation in $\Lambda_b^0 \to pK^-$ and $\Lambda_b^0 \to p\pi^-$ decays, Phys. Lett. B **787**, 124 (2018).

[1181] R. Aaij *et al.* (LHCb Collaboration), Measurement of matter-antimatter differences in beauty baryon decays, Nat. Phys. **13**, 391 (2017).

[1182] R. Aaij *et al.* (LHCb Collaboration), Observation of the decay $\Lambda_b^0 \to pK^-\mu^+\mu^-$ and a search for CP violation, J. High Energy Phys. 06 (2017) 108.

[1183] R. Aaij *et al.* (LHCb Collaboration), Search for CP violation using triple product asymmetries in $\Lambda_b^0 \to pK^-\pi^+\pi^-$, $\Lambda_b^0 \to pK^-K^+K^-$ and $\Xi_b^0 \to pK^-K^-\pi^+$ decays, J. High Energy Phys. 08 (2018) 039.

[1184] R. Aaij *et al.* (LHCb Collaboration), Measurements of CP asymmetries in charmless four-body Λ_b^0 and Ξ_b^0 decays, Eur. Phys. J. C **79**, 745 (2019).

[1185] R. Aaij *et al.* (LHCb Collaboration), Study of the $B^0 \to \rho(770)^0 K^*(892)^0$ decay with an amplitude analysis of $B^0 \to (\pi^+\pi^-)(K^+\pi^-)$ decays, J. High Energy Phys. 05 (2019) 026.

[1186] R. Aaij *et al.* (LHCb Collaboration), Measurement of polarization amplitudes and CP asymmetries in $B^0 \to \phi K^*(892)^0$, J. High Energy Phys. 05 (2014) 069.

[1187] R. Aaij *et al.* (LHCb Collaboration), Angular analysis of the $B^0 \to K^{*0}e^+e^-$ decay in the low-q^2 region, J. High Energy Phys. 04 (2015) 064.

[1188] M. Staric *et al.* (Belle Collaboration), Evidence for D^0-$\bar{D}^0$ Mixing, Phys. Rev. Lett. **98**, 211803 (2007).

[1189] B. Aubert *et al.* (*BABAR* Collaboration), Evidence for $D^0 - \bar{D}^0$ Mixing, Phys. Rev. Lett. **98**, 211802 (2007).

[1190] T. Aaltonen *et al.* (CDF Collaboration), Evidence for $D^0 - \bar{D}^0$ Mixing Using the CDF II Detector, Phys. Rev. Lett. **100**, 121802 (2008).

[1191] R. Aaij *et al.* (LHCb Collaboration), Observation of $D^0 - \bar{D}^0$ Oscillations, Phys. Rev. Lett. **110**, 101802 (2013).

[1192] R. Aaij *et al.* (LHCb Collaboration), Observation of CP Violation in Charm Decays, Phys. Rev. Lett. **122**, 211803 (2019).

[1193] R. Aaij *et al.* (LHCb Collaboration), Observation of the Mass Difference between Neutral Charm-Meson Eigenstates, Phys. Rev. Lett. **127**, 111801 (2021).

[1194] S. Bergmann, Y. Grossman, Z. Ligeti, Y. Nir, and A. A. Petrov, Lessons from CLEO and FOCUS measurements of $D^0 - \bar{D}^0$ mixing parameters, Phys. Lett. B **486**, 418 (2000).

[1195] S. L. Glashow, J. Iliopoulos, and L. Maiani, Weak interactions with lepton-hadron symmetry, Phys. Rev. D **2**, 1285 (1970).

[1196] I. I. Y. Bigi and N. G. Uraltsev, $D^0\bar{D}^0$ oscillations as a probe of quark-hadron duality, Nucl. Phys. **B592**, 92 (2001).

[1197] A. A. Petrov, Charm physics: Theoretical review, arXiv: hep-ph/0311371.

[1198] A. A. Petrov, Mixing and CP-violation in charm, Nucl. Phys. B, Proc. Suppl. **142**, 333 (2005).

[1199] A. F. Falk, Y. Grossman, Z. Ligeti, Y. Nir, and A. A. Petrov, The $D^0 - \bar{D}^0$ mass difference from a dispersion relation, Phys. Rev. D **69**, 114021 (2004).

[1200] D. M. Asner *et al.* (CLEO Collaboration), Updated measurement of the strong phase in $D^0 \to K^+\pi^-$ decay using quantum correlations in $e^+e^- \to D^0\bar{D}^0$ at CLEO, Phys. Rev. D **86**, 112001 (2012).

[1201] B. Aubert *et al.* (*BABAR* Collaboration), Measurement of $D^0 - \bar{D}^0$ Mixing from a Time-Dependent Amplitude Analysis of $D^0 \to K^+\pi^-\pi^0$ Decays, Phys. Rev. Lett. **103**, 211801 (2009).

[1202] E. M. Aitala *et al.* (Fermilab E791 Collaboration), Search for $D^0 - \bar{D}^0$ Mixing in Semileptonic Decay Modes, Phys. Rev. Lett. **77**, 2384 (1996).

[1203] C. Cawlfield *et al.* (CLEO Collaboration), Limits on neutral D mixing in semileptonic decays, Phys. Rev. D **71**, 077101 (2005).

[1204] B. Aubert *et al.* (*BABAR* Collaboration), Search for $D^0 - \bar{D}^0$ mixing using doubly flavor tagged semileptonic decay modes, Phys. Rev. D **76**, 014018 (2007).

[1205] U. Bitenc *et al.* (Belle Collaboration), Improved search for D^0 mixing using semileptonic decays at Belle, Phys. Rev. D **77**, 112003 (2008).

[1206] L. M. Zhang *et al.* (Belle Collaboration), Improved Constraints on $D^0 - \bar{D}^0$ Mixing in $D^0 \to K^+\pi^-$ Decays at Belle, Phys. Rev. Lett. **96**, 151801 (2006).

[1207] B. R. Ko *et al.* (Belle Collaboration), Observation of $D^0 - \bar{D}^0$ Mixing in e^+e^- Collisions, Phys. Rev. Lett. **112**, 111801 (2014).

[1208] T. A. Aaltonen *et al.* (CDF Collaboration), Observation of $D^0 - \bar{D}^0$ Mixing Using the CDF II Detector, Phys. Rev. Lett. **111**, 231802 (2013).

[1209] R. Aaij *et al.* (LHCb Collaboration), Measurements of charm mixing and CP violation using $D^0 \to K^{\pm}\pi^{\mp}$ decays, Phys. Rev. D **95**, 052004 (2017); Phys. Rev. D **96**, 099907(E) (2017).

[1210] R. Aaij *et al.* (LHCb Collaboration), Updated determination of D^0-$\bar{D}^0$ mixing and CP violation parameters with $D^0 \to K^+\pi^-$ decays, Phys. Rev. D **97**, 031101 (2018).

[1211] T. Peng *et al.* (Belle Collaboration), Measurement of D^0-$\bar{D}^0$ mixing and search for indirect CP violation using $D^0 \to K^0_S\pi^+\pi^-$ decays, Phys. Rev. D **89**, 091103 (2014).

[1212] P. del Amo Sanchez *et al.* (*BABAR* Collaboration), Measurement of D^0-$\bar{D}^0$ Mixing Parameters Using $D^0 \to K^0_S\pi^+\pi^-$ and $D^0 \to K^0_S K^+ K^-$ Decays, Phys. Rev. Lett. **105**, 081803 (2010).

[1213] R. Aaij *et al.* (LHCb Collaboration), Model-independent measurement of mixing parameters in $D^0 \to K^0_S\pi^+\pi^-$ decays, J. High Energy Phys. 04 (2016) 033.

[1214] R. Aaij *et al.* (LHCb Collaboration), Measurement of the Mass Difference Between Neutral Charm-Meson Eigenstates, Phys. Rev. Lett. **122**, 231802 (2019).

[1215] J. P. Lees *et al.* (*BABAR* Collaboration), Measurement of the neutral D meson mixing parameters in a time-dependent amplitude analysis of the $D^0 \to \pi^+\pi^-\pi^0$ decay, Phys. Rev. D **93**, 112014 (2016).

[1216] M. Ablikim *et al.* (BESIII Collaboration), Measurement of the $D \to K^-\pi^+$ strong phase difference in $\psi(3770) \to D^0\bar{D}^0$, Phys. Lett. B **734**, 227 (2014).

[1217] A. Di Canto, J. Garra Ticó, T. Gershon, N. Jurik, M. Martinelli, T. Pilař, S. Stahl, and D. Tonelli, Novel method for measuring charm-mixing parameters using multibody decays, Phys. Rev. D **99**, 012007 (2019).

[1218] B. Aubert *et al.* (*BABAR* Collaboration), Search for CP Violation in the Decays $D^0 \to K^-K^+$ and $D^0 \to \pi^-\pi^+$, Phys. Rev. Lett. **100**, 061803 (2008).

[1219] M. Staric *et al.* (Belle Collaboration), Measurement of CP asymmetry in Cabibbo suppressed D^0 decays, Phys. Lett. B **670**, 190 (2008).

[1220] CDF Collaboration, Improved measurement of the difference between time-integrated CP asymmetries in $D^0 \to K^+K^-$ and $D^0 \to \pi^+\pi^-$ decays at CDF, CDF Report No. 10784, 2012.

[1221] T. Aaltonen *et al.* (CDF Collaboration), Measurement of the Difference of CP–Violating Asymmetries in $D^0 \to K^+K^-$ and $D^0 \to \pi^+\pi^-$ Decays at CDF, Phys. Rev. Lett. **109**, 111801 (2012).

[1222] E. M. Aitala *et al.* (Fermilab E791 Collaboration), Measurements of Lifetimes and a Limit on the Lifetime Difference in the Neutral D Meson System, Phys. Rev. Lett. **83**, 32 (1999).

[1223] J. M. Link *et al.* (FOCUS Collaboration), A measurement of lifetime differences in the neutral D meson system, Phys. Lett. B **485**, 62 (2000).

[1224] S. E. Csorna *et al.* (CLEO Collaboration), Lifetime differences, direct CP violation and partial widths in D^0 meson decays to K^+K^- and $\pi^+\pi^-$, Phys. Rev. D **65**, 092001 (2002).

[1225] A. Zupanc *et al.* (Belle Collaboration), Measurement of y_{CP} in D^0 meson decays to the $K^0_S K^+ K^-$ final state, Phys. Rev. D **80**, 052006 (2009).

[1226] J. P. Lees *et al.* (*BABAR* Collaboration), Measurement of $D^0 - \bar{D}^0$ mixing and CP violation in two-body D^0 decays, Phys. Rev. D **87**, 012004 (2013).

[1227] M. Ablikim *et al.* (BESIII Collaboration), Measurement of y_{CP} in $D^0 - \bar{D}^0$ oscillation using quantum correlations in $e^+e^- \to D^0\bar{D}^0$ at $\sqrt{s} = 3.773$ GeV, Phys. Lett. B **744**, 339 (2015).

[1228] M. Staric *et al.* (Belle Collaboration), Measurement of $D^0 - \bar{D}$ mixing and search for CP violation in $D^0 \to K^+K^-, \pi^+\pi^-$ decays with the full Belle dataset, Phys. Lett. B **753**, 412 (2016).

[1229] R. Aaij *et al.* (LHCb Collaboration), Measurement of the Charm-Mixing Parameter y_{CP}, Phys. Rev. Lett. **122**, 011802 (2019).

[1230] M. Nayak *et al.* (Belle Collaboration), Measurement of the charm-mixing parameter y_{CP} in $D^0 \to K^0_S\omega$ decays at Belle, Phys. Rev. D **102**, 071102 (2020).

[1231] T. A. Aaltonen *et al.* (CDF Collaboration), Measurement of indirect CP-violating asymmetries in $D^0 \to K^+K^-$ and $D^0 \to \pi^+\pi^-$ decays at CDF, Phys. Rev. D **90**, 111103 (2014).

[1232] R. Aaij *et al.* (LHCb Collaboration), Search for time-dependent CP violation in $D^0 \to K^+K^-$ and $D^0 \to \pi^+\pi^-$ decays, Phys. Rev. D **104**, 072010 (2021).

[1233] F. James, MINUIT—Function minimization and error analysis, reference manual version 94.1, CERN Program Library Long Writeup D506, 1994.

[1234] A. L. Kagan and M. D. Sokoloff, On indirect CP violation and implications for $D^0 - \bar{D}^0$ and $B_s - \bar{B}_s$ mixing, Phys. Rev. D **80**, 076008 (2009).

[1235] Y. Grossman, Y. Nir, and G. Perez, Testing New Indirect CP Violation, Phys. Rev. Lett. **103**, 071602 (2009).

[1236] A. L. Kagan and L. Silvestrini, Dispersive and absorptive CP violation in $D^0 - \overline{D^0}$ mixing, Phys. Rev. D **103**, 053008 (2021).

[1237] M. Ciuchini, E. Franco, D. Guadagnoli, V. Lubicz, M. Pierini, V. Porretti, and L. Silvestrini, $D - \bar{D}$ mixing and new physics: General considerations and constraints on the MSSM, Phys. Lett. B **655**, 162 (2007).

[1238] I. I. Y. Bigi and A. I. Sanda, CP violation, Cambridge Monogr. Part. Phys., Nucl. Phys., Cosmol. **9**, 1 (2000).

[1239] Y. Nir, CP violation in and beyond the standard model, arXiv:hep-ph/9911321.

[1240] F. Buccella, M. Lusignoli, G. Miele, A. Pugliese, and P. Santorelli, Nonleptonic weak decays of charmed mesons, Phys. Rev. D **51**, 3478 (1995).

[1241] Y. Grossman and Y. Nir, CP violation in $\tau \to \nu\pi K_S$ and $D \to \pi K_S$: The importance of $K_S - K_L$ interference, J. High Energy Phys. 04 (2012) 002.

[1242] R. Aaij *et al.* (LHCb Collaboration), Measurement of the $D^{\pm}$ production asymmetry in 7 TeV pp collisions, Phys. Lett. B **718**, 902 (2013).

[1243] M. Ablikim *et al.* (BESIII Collaboration), Measurements of the absolute branching fractions and CP asymmetries for $D^+ \to K^0_{S,L}K^+(\pi^0)$, Phys. Rev. D **99**, 032002 (2019).

[1244] M. Ablikim *et al.* (BESIII Collaboration), Study of the decays $D_s^+ \to K_S^0 K^+$ and $K_L^0 K^+$, Phys. Rev. D **99**, 112005 (2019).

[1245] R. Aaij *et al.* (LHCb Collaboration), A measurement of the *CP* asymmetry difference in $\Lambda_c^+ \to pK^-K^+$ and $p\pi^-\pi^+$ decays, J. High Energy Phys. 03 (2018) 182.

[1246] J. Brod, Y. Grossman, A. L. Kagan, and J. Zupan, A consistent picture for large penguins in $D \to \pi^+\pi^-$, K^+K^-, J. High Energy Phys. 10 (2012) 161.

[1247] B. Aubert *et al.* (*BABAR* Collaboration), Search for *CP* violation in neutral D meson Cabibbo-suppressed three-body decays, Phys. Rev. D **78**, 051102 (2008).

[1248] I. Bediaga, I. I. Bigi, A. Gomes, G. Guerrer, J. Miranda, and A. C. dos Reis, On a *CP* anisotropy measurement in the Dalitz plot, Phys. Rev. D **80**, 096006 (2009).

[1249] B. Aslan and G. Zech, New test for the multivariate two-sample problem based on the concept of minimum energy, J. Stat. Comput. Simul. **75**, 109 (2005).

[1250] R. Aaij *et al.* (LHCb Collaboration), Model-independent search for *CP* violation in $D^0 \to K^-K^+\pi^-\pi^+$ and $D^0 \to \pi^-\pi^+\pi^+\pi^-$ decay, Phys. Lett. B **726**, 623 (2013).

[1251] R. Aaij *et al.* (LHCb Collaboration), Search for *CP* violation through an amplitude analysis of $D^0 \to K^+K^-\pi^+\pi^-$ decays, J. High Energy Phys. 02 (2019) 126.

[1252] J. W. Hinson *et al.* (CLEO Collaboration), Improved Measurement of the Form-Factors in the Decay $\Lambda_c^+ \to \Lambda e^+\nu_e$, Phys. Rev. Lett. **94**, 191801 (2005).

[1253] J. M. Link *et al.* (FOCUS Collaboration), Study of the decay asymmetry parameter and *CP* violation parameter in the $\Lambda_c^+ \to \Lambda\pi^+$ decay, Phys. Lett. B **634**, 165 (2006).

[1254] Y. B. Li *et al.* (Belle Collaboration), Measurements of the branching fractions of the semileptonic decays $\Xi_c^0 \to \Xi^-\ell^+\nu_\ell$ and the asymmetry parameter of $\Xi_c^0 \to \Xi^-\pi^+$, Phys. Rev. Lett. **127**, 121803 (2021).

[1255] Y. Grossman, A. L. Kagan, and J. Zupan, Testing for new physics in singly Cabibbo suppressed D decays, Phys. Rev. D **85**, 114036 (2012).

[1256] V. Babu *et al.* (Belle Collaboration), Search for *CP* violation in the $D^+ \to \pi^+\pi^0$ decay at Belle, Phys. Rev. D **97**, 011101 (2018).

[1257] R. Aaij *et al.* (LHCb Collaboration), Search for *CP* violation in $D_{(s)}^+ \to h^+\pi^0$ and $D_{(s)}^+ \to h^+\eta$ decays, J. High Energy Phys. 06 (2021) 019.

[1258] B. I. Eisenstein *et al.* (CLEO Collaboration), Precision measurement of $B(D^+ \to \mu^+\nu)$ and the pseudoscalar decay constant f_+^D, Phys. Rev. D **78**, 052003 (2008).

[1259] H. Mendez *et al.* (CLEO Collaboration), Measurements of D meson decays to two pseudoscalar mesons, Phys. Rev. D **81**, 052013 (2010).

[1260] E. Won *et al.* (Belle Collaboration), Observation of $D^+ \to K^+\eta^{(\prime)}$ and Search for *CP* Violation in $D^+ \to \pi^+\eta^{(\prime)}$ Decays, Phys. Rev. Lett. **107**, 221801 (2011).

[1261] R. Aaij *et al.* (LHCb Collaboration), Measurement of *CP* asymmetries in $D^\pm \to \eta'\pi^\pm$ and $D_s^\pm \to \eta'\pi^\pm$ decays, Phys. Lett. B **771**, 21 (2017).

[1262] G. Bonvicini *et al.* (CLEO Collaboration), Updated measurements of absolute D^+ and D^0 hadronic branching fractions and $\sigma(e^+e^- \to D\bar{D})$ at $E_{cm} = 3774$ MeV, Phys. Rev. D **89**, 072002 (2014).

[1263] B. R. Ko *et al.* (Belle Collaboration), Evidence for *CP* Violation in the Decay $D^+ \to K_S^0\pi^+$, Phys. Rev. Lett. **109**, 021601 (2012).

[1264] P. del Amo Sanchez *et al.* (*BABAR* Collaboration), Search for *CP* violation in the Decay $D^\pm \to K_S\pi^\pm$, Phys. Rev. D **83**, 071103 (2011).

[1265] J. M. Link *et al.* (FOCUS Collaboration), Search for *CP* Violation in the Decays $D^+ \to K_S\pi^+$ and $D^+ \to K_S K^+$, Phys. Rev. Lett. **88**, 041602 (2002); Phys. Rev. Lett. **88**, 159903(E) (2002).

[1266] J. P. Lees *et al.* (*BABAR* Collaboration), Search for *CP* violation in the decays $D^\pm \to K_s^0 K^\pm$, $D_s^\pm \to K_s^0 K^\pm$, and $D_s^\pm \to K_s^0\pi^\pm$, Phys. Rev. D **87**, 052012 (2013).

[1267] B. R. Ko *et al.* (Belle Collaboration), Search for *CP* violation in the decay $D_s^+ \to K_S^0\pi^+$, J. High Energy Phys. 02 (2013) 098.

[1268] R. Aaij *et al.* (LHCb Collaboration), Search for *CP* Violation in $D_s^+ \to K_S^0\pi^+$, $D^+ \to K_S^0 K^+$ and $D^+ \to \phi\pi^+$ Decays, Phys. Rev. Lett. **122**, 191803 (2019).

[1269] M. Ablikim *et al.* (BESIII Collaboration), Study of decay dynamics and *CP* asymmetry in $D^+ \to K_L^0 e^+\nu_e$ decay, Phys. Rev. D **92**, 112008 (2015).

[1270] R. Aaij *et al.* (LHCb Collaboration), Search for *CP* violation in the decay $D^+ \to \pi^-\pi^+\pi^+$, Phys. Lett. B **728**, 585 (2014).

[1271] E. M. Aitala *et al.* (Fermilab E791 Collaboration), Search for *CP* violation in charged D meson decays, Phys. Lett. B **403**, 377 (1997).

[1272] V. M. Abazov *et al.* (D0 Collaboration), Measurement of the direct *CP*-violating parameter A_{CP} in the decay $D^+ \to K^-\pi^+\pi^+$, Phys. Rev. D **90**, 111102 (2014).

[1273] M. Ablikim *et al.* (BESIII Collaboration), Measurements of Absolute Branching Fractions of Fourteen Exclusive Hadronic D Decays to η, Phys. Rev. Lett. **124**, 241803 (2020).

[1274] J. P. Lees *et al.* (*BABAR* Collaboration), Search for direct *CP* violation in singly Cabibbo-suppressed $D^\pm \to K^+K^-\pi^\pm$ decays, Phys. Rev. D **87**, 052010 (2013).

[1275] P. Rubin *et al.* (CLEO Collaboration), Search for *CP* violation in the Dalitz-plot analysis of $D^\pm \to K^+K^-\pi^\pm$, Phys. Rev. D **78**, 072003 (2008).

[1276] J. M. Link *et al.* (FOCUS Collaboration), Search for *CP* violation in D^0 and D^+ decays, Phys. Lett. B **491**, 232 (2000).

[1277] J. M. Link *et al.* (FOCUS Collaboration), Search for T violation in charm meson decays, Phys. Lett. B **622**, 239 (2005).

[1278] M. Ablikim *et al.* (BESIII Collaboration), Observation of the Doubly Cabibbo-Suppressed Decay $D^+ \to K^+\pi^+\pi^-\pi^0$ and Evidence for $D^+ \to K^+\omega$, Phys. Rev. Lett. **125**, 141802 (2020).

[1279] R. Aaij *et al.* (LHCb Collaboration), Measurement of *CP* asymmetry in $D^0 \to K^-K^+$ decays, Phys. Lett. B **767**, 177 (2017).

[1280] T. Aaltonen *et al.* (CDF Collaboration), Measurement of *CP*–violating asymmetries in $D^0 \to \pi^+\pi^-$ and $D^0 \to K^+K^-$ decays at CDF, Phys. Rev. D **85**, 012009 (2012).

[1281] E. M. Aitala *et al.* (Fermilab E791 Collaboration), Branching fractions for $D^0 \to K^+K^-$ and $D^0 \to \pi^+\pi^-$,

and a search for CP violation in D^0 decays, Phys. Lett. B **421**, 405 (1998).
[1282] N. K. Nisar *et al.* (Belle Collaboration), Search for CP Violation in $D^0 \to \pi^0\pi^0$ Decays, Phys. Rev. Lett. **112**, 211601 (2014).
[1283] G. Bonvicini *et al.* (CLEO Collaboration), Search for CP violation in $D^0 \to K^0_S\pi^0$ and $D^0 \to \pi^0\pi^0$ and $D^0 \to K^0_S K^0_S$ decays, Phys. Rev. D **63**, 071101 (2001).
[1284] B. R. Ko *et al.* (Belle Collaboration), Search for CP Violation in the Decays $D^0 \to K^0_S\pi^0$, Phys. Rev. Lett. **106**, 211801 (2011).
[1285] R. Aaij *et al.* (LHCb Collaboration), Measurement of CP asymmetry in $D^0 \to K^0_S K^0_S$ decays, Phys. Rev. D **104**, L031102 (2021).
[1286] N. Dash *et al.*, Search for CP Violation and Measurement of the Branching Fraction in the Decay $D^0 \to K^0_S K^0_S$, Phys. Rev. Lett. **119**, 171801 (2017).
[1287] J. B. Kim *et al.* (Belle Collaboration), Search for CP violation with kinematic asymmetries in the $D^0 \to K^+K^-\pi^+\pi^-$ decay, Phys. Rev. D **99**, 011104 (2019).
[1288] R. Aaij *et al.* (LHCb Collaboration), Search for CP violation in $D^0 \to \pi^-\pi^+\pi^0$ decays with the energy test, Phys. Lett. B **740**, 158 (2015).
[1289] Belle and K. Arinstein, Measurement of the ratio $B(D^0 \to \pi^+\pi^-\pi^0)/B(D^0 \to K^-\pi^+\pi^0)$ and the time- integrated CP asymmetry in $D^0 \to \pi^+\pi^-\pi^0$, Phys. Lett. B **662**, 102 (2008).
[1290] D. Cronin-Hennessy *et al.* (CLEO Collaboration), Searches for CP violation and $\pi\pi S$-wave in the Dalitz-plot of $D^0 \to \pi^+\pi^-\pi^0$, Phys. Rev. D **72**, 031102 (2005).
[1291] X. C. Tian *et al.* (Belle Collaboration), Measurement of the Wrong-Sign Decays $D^0 \to K^+\pi^-(\pi^0, \pi^+\pi^-)$ and Search for CP Violation, Phys. Rev. Lett. **95**, 231801 (2005).
[1292] G. Brandenburg *et al.* (CLEO Collaboration), Rate Measurement of $D^0 \to K^+\pi^-\pi^0$ and Constraints on $D^0\bar{D}^0$ Mixing, Phys. Rev. Lett. **87**, 071802 (2001).
[1293] T. Aaltonen *et al.* (CDF Collaboration), Measurement of CP-violation asymmetries in $D^0 \to K_S\pi^+\pi^-$, Phys. Rev. D **86**, 032007 (2012).
[1294] D. M. Asner *et al.* (CLEO Collaboration), Search for CP violation in $D^0 \to K^0_S\pi^+\pi^-$, Phys. Rev. D **70**, 091101 (2004).
[1295] M. Artuso *et al.* (CLEO Collaboration), Amplitude analysis of $D^0 \to K^-K^+\pi^-\pi^+$, Phys. Rev. D **85**, 122002 (2012).
[1296] A. Abdesselam *et al.* (Belle Collaboration), Observation of $D^0 \to \rho^0\gamma$ and Search for CP Violation in Radiative Charm Decays, Phys. Rev. Lett. **118**, 051801 (2017).
[1297] R. Aaij *et al.* (LHCb Collaboration), Measurement of Angular and CP Asymmetries in $D^0 \to \pi^+\pi^-\mu^+\mu^-$ and $D^0 \to K^+K^-\mu^+\mu^-$ decays, Phys. Rev. Lett. **121**, 091801 (2018).
[1298] J. P. Alexander *et al.* (CLEO Collaboration), Measurement of $BD_s^+ \to \ell^+\nu$ and the decay constant fD_s^+ From 600/pb^{-1} of $e^\pm$ annihilation data near 4170 MeV, Phys. Rev. D **79**, 052001 (2009).
[1299] Y. Guan *et al.* (Belle Collaboration), Measurement of branching fractions and CP asymmetries for $D_s^+ \to K^+(\eta, \pi^0)$ and $D_s^+ \to \pi^+(\eta, \pi^0)$ decays at Belle, Phys. Rev. D **103**, 112005 (2021).
[1300] P. U. E. Onyisi *et al.* (CLEO Collaboration), Improved measurement of absolute hadronic branching fractions of the D_s^+ meson, Phys. Rev. D **88**, 032009 (2013).
[1301] B. R. Ko *et al.* (Belle Collaboration), Search for CP Violation in the Decays $D^+_{(s)} \to K^0_S\pi^+$ and $D^+_{(s)} \to K^0_S K^+$, Phys. Rev. Lett. **104**, 181602 (2010).
[1302] E. Golowich and G. Valencia, Triple product correlations in semileptonic $B^\pm$ decays, Phys. Rev. D **40**, 112 (1989).
[1303] I. I. Y. Bigi, Charm physics—like Botticelli in the Sistine chapel, arXiv:hep-ph/0107102.
[1304] W. Bensalem, A. Datta, and D. London, New-physics effects on triple-product correlations in Λ_b decays, Phys. Rev. D **66**, 094004 (2002).
[1305] W. Bensalem and D. London, T odd triple product correlations in hadronic b decays, Phys. Rev. D **64**, 116003 (2001).
[1306] W. Bensalem, A. Datta, and D. London, T-violating triple-product correlations in charmless Λ_b decays, Phys. Lett. B **538**, 309 (2002).
[1307] M. Gronau and J. L. Rosner, Triple product asymmetries in K, $D_{(s)}$ and $B_{(s)}$ decays, Phys. Rev. D **84**, 096013 (2011).
[1308] K. Prasanth *et al.* (Belle Collaboration), First measurement of T-odd moments in $D^0 \to K^0_S\pi^+\pi^-\pi^0$ decays, Phys. Rev. D **95**, 091101 (2017).
[1309] R. Aaij *et al.* (LHCb Collaboration), Search for CP violation using T-odd correlations in $D^0 \to K^+K^-\pi^+\pi^-$ decays, J. High Energy Phys. 10 (2014) 005.
[1310] P. del Amo Sanchez *et al.* (*BABAR* Collaboration), Search for CP violation using T-odd correlations in $D^0 \to K^+K^-\pi^+\pi^-$ decays, Phys. Rev. D **81**, 111103 (2010).
[1311] J. P. Lees *et al.* (*BABAR* Collaboration), Search for CP violation using T-odd correlations in $D^+ \to K^+K^0_S\pi^+\pi^-$ and $D_s^+ \to K^+K^0_S\pi^+\pi^-$ decays, Phys. Rev. D **84**, 031103 (2011).
[1312] R. Aaij *et al.* (LHCb Collaboration), Studies of the resonance structure in $D^0 \to K^\mp\pi^\pm\pi^\pm\pi^\mp$ decays, Eur. Phys. J. C **78**, 443 (2018).
[1313] A. J. Bevan, C, P, and CP asymmetry observables based on triple product asymmetries, arXiv:1506.04246.
[1314] G. Durieux and Y. Grossman, Probing CP violation systematically in differential distributions, Phys. Rev. D **92**, 076013 (2015).
[1315] Y. Grossman, A. L. Kagan, and Y. Nir, New physics and CP violation in singly Cabibbo suppressed D decays, Phys. Rev. D **75**, 036008 (2007).
[1316] M. Gersabeck, M. Alexander, S. Borghi, V. V. Gligorov, and C. Parkes, On the interplay of direct and indirect CP violation in the charm sector, J. Phys. G **39**, 045005 (2012).
[1317] R. Aaij *et al.* (LHCb Collaboration), Measurement of CP asymmetry in $D^0 \to K^-K^+$ and $D^0 \to \pi^-\pi^+$ decays, J. High Energy Phys. 07 (2014) 041.
[1318] R. Aaij *et al.* (LHCb Collaboration), Measurement of the Difference of Time-Integrated CP Asymmetries in $D^0 \to K^-K^+$ and $D^0 \to \pi^-\pi^+$ Decays, Phys. Rev. Lett. **116**, 191601 (2016).

[1319] T. Becher and R. J. Hill, Comment on form-factor shape and extraction of $|V_{ub}|$ from $B \to \pi \ell \nu$, Phys. Lett. B **633**, 61 (2006).

[1320] R. J. Hill, The modern description of semileptonic meson form factors, eConf **C060409**, 027 (2006); arXiv:hep-ph/0606023.

[1321] F. J. Gilman and R. L. Singleton, Analysis of semileptonic decays of mesons containing heavy quarks, Phys. Rev. D **41**, 142 (1990).

[1322] D. Becirevic and A. B. Kaidalov, Comment on the heavy to light form-factors, Phys. Lett. B **478**, 417 (2000).

[1323] C. G. Boyd, B. Grinstein, and R. F. Lebed, Constraints on Form-Factors for Exclusive Semileptonic Heavy to Light Meson Decays, Phys. Rev. Lett. **74**, 4603 (1995).

[1324] C. G. Boyd and M. J. Savage, Analyticity, shapes of semileptonic form-factors, and $\bar{B} \to \pi \ell \bar{\nu}$, Phys. Rev. D **56**, 303 (1997).

[1325] M. C. Arnesen, B. Grinstein, I. Z. Rothstein, and I. W. Stewart, Precision Model Independent Determination of $|V_{ub}|$ from $B \to \pi l \nu$, Phys. Rev. Lett. **95**, 071802 (2005).

[1326] C. Bourrely, B. Machet, and E. de Rafael, Semileptonic decays of pseudoscalar particles ($M \to M' + \ell + \nu \ell$) and short-distance behaviour of quantum chromodynamics, Nucl. Phys. **B189**, 157 (1981).

[1327] D. Becirevic *et al.*, Insight into $D/B \to \pi \ell \nu_\ell$ decay using the pole models, arXiv:1407.1019.

[1328] J. P. Lees *et al.* (*BABAR* Collaboration), Measurement of the $D^*(2010)^+$ natural line width and the $D^*(2010)^+ - D^0$ mass difference, Phys. Rev. D **88**, 052003 (2013); Phys. Rev. D **88**, 079902(E) (2013).

[1329] P. del Amo Sanchez *et al.* (*BABAR* Collaboration), Observation of new resonances decaying to $D\pi$ and $D^*\pi$ in inclusive e^+e^- collisions near $\sqrt{s} = 10.58\,\mathrm{GeV}$, Phys. Rev. D **82**, 111101 (2010).

[1330] R. Aaij *et al.* (LHCb Collaboration), Study of D_J meson decays to $D^+\pi^-$, $D^0\pi^+$ and $D^{*+}\pi^-$ final states in pp collision, J. High Energy Phys. 09 (2013) 145.

[1331] G. Burdman and J. Kambor, Dispersive approach to semileptonic form-factors in heavy to light meson decays, Phys. Rev. D **55**, 2817 (1997).

[1332] D. Bečirević, A. Le Yaouanc, L. Oliver, J.-C. Raynal, P. Roudeau, and J. Serrano, Proposal to study $B_s \to D_{sJ}^-$ transitions, Phys. Rev. D **87**, 054007 (2013).

[1333] J. P. Lees *et al.* (*BABAR* Collaboration), Measurement of the $D^0 \to \pi^- e^+ \nu_e$ differential decay branching fraction as a function of q^2 and study of form factor parametrizations, Phys. Rev. D **91**, 052022 (2015).

[1334] M. Ablikim *et al.* (BESIII Collaboration), Study of dynamics of $D^0 \to K^- e^+ \nu_e$ and $D^0 \to \pi^- e^+ \nu_e$ decays, Phys. Rev. D **92**, 072012 (2015).

[1335] L. Widhalm *et al.* (Belle Collaboration), Measurement of $D^0 \to \pi l \nu\,(K l \nu)$ Form Factors and Absolute Branching Fractions, Phys. Rev. Lett. **97**, 061804 (2006).

[1336] B. Aubert *et al.* (*BABAR* Collaboration), Measurement of the hadronic form-factor in $D^0 \to K^- e^+ \nu_e$ decays, Phys. Rev. D **76**, 052005 (2007).

[1337] D. Besson *et al.* (CLEO Collaboration), Improved measurements of D meson semileptonic decays to π and K mesons, Phys. Rev. D **80**, 032005 (2009).

[1338] S. Dobbs *et al.* (CLEO Collaboration), A study of the semileptonic charm decays $D^0 \to \pi^- e^+ \nu_e$, $D^+ \to \pi^0 e^+ \nu_e$, $D^0 \to K^- e^+ \nu_e$, and $D^+ \to \bar{K}^0 e^+ \nu_e$, Phys. Rev. D **77**, 112005 (2008).

[1339] M. Ablikim *et al.* (BESIII Collaboration), Analysis of $D^+ \to \bar{K}^0 e^+ \nu_e$ and $D^+ \to \pi^0 e^+ \nu_e$ semileptonic decays, Phys. Rev. D **96**, 012002 (2017).

[1340] M. Ablikim *et al.* (BESIII Collaboration), Study of the $D^0 \to K^- \mu^+ \nu_\mu$ Dynamics and Test of Lepton Flavor Universality with $D^0 \to K^- \ell^+ \nu_\ell$ Decays, Phys. Rev. Lett. **122**, 011804 (2019).

[1341] M. Ablikim *et al.* (BESIII Collaboration), Improved measurement of the absolute branching fraction of $D^+ \to \bar{K}^0 \mu^+ \nu_\mu$, Eur. Phys. J. C **76**, 369 (2016).

[1342] M. Ablikim *et al.* (BESIII Collaboration), Measurement of the absolute branching fraction of $D^+ \to \bar{K}^0 e^+ \nu_e$ via $\bar{K}^0 \to \pi^0 \pi^0$, Chin. Phys. C **40**, 113001 (2016).

[1343] M. Ablikim *et al.* (BESIII Collaboration), Measurement of the Branching Fraction for the Semi-Leptonic Decay $D^{0(+)} \to \pi^{-(0)} \mu^+ \nu_\mu$ and Test of Lepton Universality, Phys. Rev. Lett. **121**, 171803 (2018).

[1344] J. Koponen *et al.* (HPQCD Collaboration), $D \to K$ and $D \to \pi$ semileptonic form factors from Lattice QCD, arXiv:1208.6242.

[1345] J. Koponen *et al.* (HPQCD Collaboration), The shape of the $D \to K$ semileptonic form factor from full lattice QCD and V_{cs}, arXiv:1305.1462.

[1346] G. S. Huang *et al.* (CLEO Collaboration), Study of Semileptonic Charm Decays $D^0 \to \pi^- \ell^+ \nu$ and $D^0 \to K^- \ell^+ \nu$, Phys. Rev. Lett. **94**, 011802 (2005).

[1347] J. M. Link *et al.* (FOCUS Collaboration), Measurements of the q^2 dependence of the $D^0 \to K^- \mu^+ \nu$ and $D^0 \to \pi^- \mu^+ \nu$ form factors, Phys. Lett. B **607**, 233 (2005).

[1348] M. Ablikim *et al.* (BESIII Collaboration), Measurement of the Dynamics of the Decays $D_s^+ \to \eta^{(\prime)} e^+ \nu_e$, Phys. Rev. Lett. **122**, 121801 (2019).

[1349] J. Yelton *et al.* (CLEO Collaboration), Studies of $D^+ \to \{\eta, \eta', \phi\} e^+ \nu_e$, Phys. Rev. D **84**, 032001 (2011).

[1350] M. Ablikim *et al.* (BESIII Collaboration), Study of the decays $D^+ \to \eta^{(\prime)} e^+ \nu_e$, Phys. Rev. D **97**, 092009 (2018).

[1351] M. Ablikim *et al.* (BESIII Collaboration), First Observation of $D^+ \to \eta \mu^+ \nu_\mu$ and Measurement of Its Decay Dynamics, Phys. Rev. Lett. **124**, 231801 (2020).

[1352] M. Ablikim *et al.* (BESIII Collaboration), First Measurement of the Form Factors in $D_s^+ \to K^0 e^+ \nu_e$ and $D_s^+ \to K^{*0} e^+ \nu_e$ Decays, Phys. Rev. Lett. **122**, 061801 (2019).

[1353] G. S. Bali, S. Collins, S. Dürr, and I. Kanamori, $D_s \to \eta, \eta'$ semileptonic decay form factors with disconnected quark loop contributions, Phys. Rev. D **91**, 014503 (2015).

[1354] G. Duplančić, and B. Melić, Form factors of B, $B_s \to \eta^{(\prime)}$ and D, $D_s \to \eta^{(\prime)}$ transitions from QCD light-cone sum rules, J. High Energy Phys. 11 (2015) 138.

[1355] N. Offen, F. A. Porkert, and A. Schäfer, Light-cone sum rules for the $D_{(s)}^+ \to \eta^{(\prime)} \ell^+ \nu_\ell$ form factor, Phys. Rev. D **88**, 034023 (2013).

[1356] K. Azizi, R. Khosravi, and F. Falahati, Exclusive $D_s^+ \to (\eta, \eta') \ell^+ \nu_\ell$ decays in light cone QCD, J. Phys. G **38**, 095001 (2011).

[1357] P. Colangelo and F. De Fazio, D_s decays to η and η' final states: A phenomenological analysis, Phys. Lett. B **520**, 78 (2001).

[1358] R. C. Verma, Decay constants and form factors of s-wave and p-wave mesons in the covariant light-front quark model, J. Phys. G **39**, 025005 (2012).

[1359] Z. T. Wei, H.-W. Ke, and X.-F. Yang, Interpretation of the $f_{D_{(s)}}$ puzzle' in SM and beyond, Phys. Rev. D **80**, 015022 (2009).

[1360] D. Melikhov and B. Stech, Weak form-factors for heavy meson decays: An update, Phys. Rev. D **62**, 014006 (2000).

[1361] N. R. Soni, M. A. Ivanov, J. G. Körner, J. N. Pandya, P. Santorelli, and C. T. Tran, Decay constants and form factors of s-wave and p-wave mesons in the covariant light-front quark model, Phys. Rev. D **98**, 114031 (2018).

[1362] V. Lubicz, L. Riggio, G. Salerno, S. Simula, and C. Tarantino (ETM Collaboration), Scalar and vector form factors of $D \to \pi(K)\ell\nu$ decays with $N_f = 2 + 1 + 1$ twisted fermions, Phys. Rev. D **96**, 054514 (2017).

[1363] H. Na, C. T. H. Davies, E. Follana, G. Peter Lepage, and J. Shigemitsu (HPQCD Collaboration), $D \to K, l\nu$ semileptonic decay scalar form factor and V_{cd} from lattice QCD, Phys. Rev. D **82**, 114506 (2010).

[1364] H. Na, C. T. H. Davies, E. Follana, J. Koponen, G. Peter Lepage, and J. Shigemitsu (HPQCD Collaboration), $D \to \pi l\nu$ semileptonic decays, V_{cd} and second row unitarity from lattice QCD, Phys. Rev. D **84**, 114505 (2011).

[1365] R. Li *et al.* (Fermilab Lattice and MILC Collaborations), D meson semileptonic decay form factors at $q^2 = 0$, Proc. Sci., LATTICE2018 (**2019**) 269 [arXiv:1901.08989].

[1366] S. Fajfer, I. Nišandžić, and U. Rojec, Discerning new physics in charm meson leptonic and semileptonic decays, Phys. Rev. D **91**, 094009 (2015).

[1367] L. Riggio, G. Salerno, and S. Simula, Scalar and vector form factors of $D \to \pi(K)\ell\nu$ decays with $N_f = 2 + 1 + 1$ twisted fermions, Eur. Phys. J. C **78**, 501 (2018).

[1368] M. Ablikim *et al.* (BESIII Collaboration), Observation of the semimuonic decay $D^+ \to \omega\mu^+\nu_\mu$, Phys. Rev. D **101**, 072005 (2020).

[1369] M. Ablikim *et al.* (BESIII Collaboration), Measurements of the branching fractions for the semi-leptonic decays $D_s^+ \to \phi e^+\nu_e$, $\phi\mu^+\nu_\mu$, $\eta\mu^+\nu_\mu$, and $\eta'\mu^+\nu_\mu$, Phys. Rev. D **97**, 012006 (2018).

[1370] M. Ablikim *et al.* (BESIII Collaboration), Measurements of the absolute branching fractions for $D_s^+ \to \eta e^+\nu_e$ and $D_s^+ \to \eta' e^+\nu_e$, Phys. Rev. D **94**, 112003 (2016).

[1371] J. M. Link *et al.* (FOCUS Collaboration), Evidence for new interference phenomena in the decay $D^+ \to K^-\pi^+\mu^+\nu$, Phys. Lett. B **535**, 43 (2002).

[1372] M. A. Ivanov, J. G. Körner, J. N. Pandya, P. Santorelli, N. R. Soni, and C. T. Tran, Exclusive semileptonic decays of D and D_s mesons in the covariant confining quark model, Front. Phys. **14**, 64401 (2019).

[1373] J. M. Link *et al.* (FOCUS Collaboration), New measurements of the $D^+ \to \bar{K}^{*0}\mu^+\nu$ form-factor ratios, Phys. Lett. B **544**, 89 (2002).

[1374] B. Aubert *et al.* (*BABAR* Collaboration), Study of the decay $D_s^+ \to K^+K^-e^+\nu_e$, Phys. Rev. D **78**, 051101 (2008).

[1375] K. M. Ecklund *et al.* (CLEO Collaboration), Study of the semileptonic decay $D_s^+ \to f_0(980)e^+\nu$ and implications for $B_s \to J/\psi f_0$, Phys. Rev. D **80**, 052009 (2009).

[1376] R. A. Briere *et al.* (CLEO Collaboration), Analysis of $D^+ \to K^-\pi^+e^+\nu_e$ and $D^+ \to K^-\pi^+\mu^+\nu_\mu$ semileptonic decays, Phys. Rev. D **81**, 112001 (2010).

[1377] P. del Amo Sanchez *et al.* (*BABAR* Collaboration), Analysis of the $D^+ \to K^-\pi^+e^+\nu_e$ decay channel, Phys. Rev. D **83**, 072001 (2011).

[1378] P. Estabrooks, R. K. Carnegie, A. D. Martin, W. M. Dunwoodie, T. A. Lasinski, and D. W. G. S. Leith, Study of $K\pi$ scattering using the reactions $K^\pm p \to K^\pm\pi^+n$ and $K^\pm p \to K^\pm\pi^-\Delta^{++}$ at 13-GeV/c, Nucl. Phys. **B133**, 490 (1978).

[1379] K. M. Watson, Some general relations between the photoproduction and scattering of π mesons, Phys. Rev. **95**, 228 (1954).

[1380] S. Dobbs *et al.* (CLEO Collaboration), First Measurement of the Form Factors in the Decays $D^0 \to \rho^-e^+\nu_e$ and $D^+ \to \rho^0e^+\nu_e$, Phys. Rev. Lett. **110**, 131802 (2013).

[1381] M. Ablikim *et al.* (BESIII Collaboration), Study of $D^+ \to K^-\pi^+e^+\nu_e$, Phys. Rev. D **94**, 032001 (2016).

[1382] M. Ablikim *et al.* (BESIII Collaboration), Study of the decay $D^0 \to \overline{K}^0\pi^-e^+\nu_e$, Phys. Rev. D **99**, 011103 (2019).

[1383] M. Ablikim *et al.* (BESIII Collaboration), Measurement of the form factors in the decay $D^+ \to \omega e^+\nu_e$ and search for the decay $D^+ \to \phi e^+\nu_e$, Phys. Rev. D **92**, 071101(R) (2015).

[1384] M. Ablikim *et al.* (BESIII Collaboration), First Observation of $D^+ \to f_0(500)e^+\nu_e$ and Improved Measurements of $D \to \rho e^+\nu_e$, Phys. Rev. Lett. **122**, 062001 (2019).

[1385] J. C. Anjos *et al.* (Fermilab E691 Collaboration), Measurement of the Form-Factors in the Decay $D^+ \to \bar{K}^{*0}e^+\nu_e$, Phys. Rev. Lett. **65**, 2630 (1990).

[1386] K. Kodama *et al.* (Fermilab E653 Collaboration), Measurement of the form-factor ratios in the decay $D^+ \to \bar{K}^{*0}(892)\mu^+\nu$, Phys. Lett. B **274**, 246 (1992).

[1387] P. L. Frabetti *et al.* (Fermilab E687 Collaboration), Analysis of the decay mode $D^+ \to \bar{K} * 0\mu^+\nu$, Phys. Lett. B **307**, 262 (1993).

[1388] E. M. Aitala *et al.* (Fermilab E791 Collaboration), Measurement of the Form-Factor Ratios for $D^+ \to \bar{K}^{*0}e^+\nu_e$, Phys. Rev. Lett. **80**, 1393 (1998).

[1389] E. M. Aitala *et al.* (Fermilab E791 Collaboration), Measurement of the form-factor ratios for $D^+ \to \bar{K}^{*0}\ell^+\nu_\ell$, Phys. Lett. B **440**, 435 (1998).

[1390] M. Adamovich *et al.* (BEATRICE Collaboration), A measurement of the form-factor ratios in the decay $D^+ \to \bar{K}^{*0}\mu^+\nu_\mu$, Eur. Phys. J. C **6**, 35 (1999).

[1391] J. M. Link *et al.* (FOCUS Collaboration), Analysis of the semileptonic decay $D^0 \to \bar{K}^0\pi^-\mu^+\nu$, Phys. Lett. B **607**, 67 (2005).

[1392] M. Ablikim *et al.* (BESIII Collaboration), Observation of the Semileptonic Decay $D^0 \to a_0(980)^-e^+\nu_e$ and Evidence for $D^+ \to a_0(980)^0e^+\nu_e$, Phys. Rev. Lett. **121**, 081802 (2018).

[1393] X.-D. Cheng, H.-B. Li, B. Wei, Y.-G. Xu, and M.-Z. Yang, Study of $D \to a_0(980)e^+\nu_e$ decay in the light-cone sum rules approach, Phys. Rev. D **96**, 033002 (2017).

[1394] M. Ablikim *et al.* (BESIII Collaboration), Search for the decay $D_s^+ \to a_0(1270)^0 e^+ \nu_e$, Phys. Rev. D **103**, 092004 (2021).

[1395] M. Artuso *et al.* (CLEO Collaboration), Evidence for the Decay $D^0 \to K^- \pi^+ \pi^- e^+ \nu_e$, Phys. Rev. Lett. **99**, 191801 (2007).

[1396] M. Ablikim *et al.* (BESIII Collaboration), Observation of the Semileptonic D^+ Transition into an Axial-Vector Meson $\bar{K}_1(1270)^0$, Phys. Rev. Lett. **123**, 231801 (2019).

[1397] M. Ablikim *et al.* (BESIII Collaboration), Observation of $D^0 \to K_1(1270)^- e^+ \nu_e$, Phys. Rev. Lett. **127**, 131801 (2021).

[1398] M. Ablikim *et al.* (BESIII Collaboration), Search for the semileptonic decays $D^+ \to b_1(1235)^0 e^+ \nu_e$ and $D^0 \to b_1(1235)^- e^+ \nu_e$, Phys. Rev. D **102**, 112005 (2020).

[1399] N. Carrasco *et al.* (ETM Collaboration), Leptonic decay constants f_K, f_D, and f_{D_s} with $N_f = 2 + 1 + 1$ twisted-mass lattice QCD, Phys. Rev. D **91**, 054507 (2015).

[1400] A. Bazavov *et al.*, B- and D-meson leptonic decay constants from four-flavor lattice QCD, Phys. Rev. D **98**, 074512 (2018).

[1401] S. Aoki *et al.* (FLAG Collaboration), FLAG review 2019, Eur. Phys. J. C **80**, 113 (2020).

[1402] A. Filipuzzi, J. Portoles, and M. Gonzalez-Alonso, $U(2)^5$ flavor symmetry and lepton universality violation in $W \to \tau \nu_\tau$, Phys. Rev. D **85**, 116010 (2012).

[1403] M. Ablikim *et al.* (BESIII Collaboration), Determination of the Pseudoscalar Decay Constant $f_{D_s^+}$ via $D_s^+ \to \mu^+ \nu_\mu$, Phys. Rev. Lett. **122**, 071802 (2019).

[1404] M. Ablikim *et al.* (BESIII Collaboration), Measurement of the absolute branching fractions for purely leptonic D_s^+ decays, Phys. Rev. D **104**, 052009 (2021).

[1405] M. Ablikim *et al.* (BESIII Collaboration), Measurement of the branching fraction of leptonic decay $D_s^+ \to \tau^+ \nu_\tau$ via $\tau^+ \to \pi^+ \pi^0 \bar{\nu}_\tau$, Phys. Rev. D **104**, 032001 (2021).

[1406] M. Ablikim *et al.* (BESIII Collaboration), Measurement of the Absolute Branching Fraction of $D_s^+ \to \tau^+ \nu_\tau$ via $\tau^+ \to e^+ \nu_e \bar{\nu}_\tau$, Phys. Rev. Lett. **127**, 171801 (2021).

[1407] M. Ablikim *et al.* (BESIII Collaboration), Observation of the Leptonic Decay $D^+ \to \tau^+ \nu_\tau$, Phys. Rev. Lett. **123**, 211802 (2019).

[1408] M. Ablikim *et al.* (BESIII Collaboration), Precision measurements of $B(D^+ \to \mu^+ \nu_\mu)$, the pseudoscalar decay constant f_{D^+}, and the quark mixing matrix element $|V_{cd}|$, Phys. Rev. D **89**, 051104 (2014).

[1409] P. del Amo Sanchez *et al.* (*BABAR* Collaboration), Measurement of the absolute branching fractions for $D_s^- \to \ell^- \bar{\nu}_\ell$ and extraction of the decay constant f_{D_s}, Phys. Rev. D **82**, 091103(R) (2010); Phys. Rev. D **91**, 019901(E) (2015).

[1410] A. Zupanc *et al.* (Belle Collaboration), Measurements of branching fractions of leptonic and hadronic D_s^+ meson decays and extraction of the D_s^+ meson decay constant, J. High Energy Phys. 09 (2013) 139.

[1411] M. Ablikim *et al.* (BESIII Collaboration), Measurement of the $D_s^+ \to \ell^+ \nu_\ell$ branching fractions and the decay constant $f_{D_s^+}$, Phys. Rev. D **94**, 072004 (2016).

[1412] P. Naik *et al.* (CLEO Collaboration), Measurement of the pseudoscalar decay constant f_{D_s} using $D_s^+ \to \tau^+ \nu$, $\tau^+ \to \rho^+ \bar{\nu}$ decays, Phys. Rev. D **80**, 112004 (2009).

[1413] P. U. E. Onyisi *et al.* (CLEO Collaboration), Improved measurement of absolute branching fraction of $D_s^+ \to \tau^+ \nu_\tau$, Phys. Rev. D **79**, 052002 (2009).

[1414] E. Barberio, B. van Eijk, and Z. Was, PHOTOS: A universal Monte Carlo for QED radiative corrections in decays, Comput. Phys. Commun. **66**, 115 (1991).

[1415] E. Barberio and Z. Was, PHOTOS: A universal Monte Carlo for QED radiative corrections. Version 2.0, Comput. Phys. Commun. **79**, 291 (1994).

[1416] P. Golonka and Z. Was, PHOTOS Monte Carlo: A precision tool for QED corrections in Z and W decays, Eur. Phys. J. C **45**, 97 (2006).

[1417] P. Golonka, B. Kersevan, T. Pierzchała, E. Richter-Wąs, Z. Wąs, and M. Worek, The Tauola photos F environment for the TAUOLA and PHOTOS packages: Release. 2., Comput. Phys. Commun. **174**, 818 (2006).

[1418] P. Golonka and Z. Was, Next to leading logarithms and the PHOTOS Monte Carlo, Eur. Phys. J. C **50**, 53 (2007).

[1419] A. Ryd *et al.*, EvtGen: A Monte Carlo generator for B-physics, Report No. EVTGEN-V00-11-07, 2005.

[1420] D. J. Lange, The EvtGen particle decay simulation package, Nucl. Instrum. Methods Phys. Res., Sect. A **462**, 152 (2001).

[1421] J. M. Link *et al.* (FOCUS Collaboration), Study of the Cabibbo-suppressed decay modes $D^0 \to \pi^- \pi^+$ and $D^0 \to K^- K^+$, Phys. Lett. B **555**, 167 (2003).

[1422] M. Ablikim *et al.* (BESIII Collaboration), Measurements of absolute branching fractions for D mesons decays into two pseudoscalar mesons, Phys. Rev. D **97**, 072004 (2018).

[1423] B. Aubert *et al.* (*BABAR* Collaboration), Measurement of the Absolute Branching Fraction of $D^0 \to K^- \pi^+$, Phys. Rev. Lett. **100**, 051802 (2008).

[1424] M. Artuso *et al.* (CLEO Collaboration), Measurement of $\mathrm{Br}(D^0 \to K^- \pi^+)$ Using Partial Reconstruction of $\bar{B} \to D^{*+} X \ell^- \bar{\nu} u$, Phys. Rev. Lett. **80**, 3193 (1998).

[1425] R. Barate *et al.* (ALEPH Collaboration), Measurement of the branching fraction for $D^0 \to K^- \pi^+$, Phys. Lett. B **403**, 367 (1997).

[1426] H. Albrecht *et al.* (ARGUS Collaboration), Measurement of the absolute branching fractions for D^0 decays into $K^- \pi^+$, $K^- \pi^+ \pi^+ \pi^-$, $\bar{K}^0 \pi^+ \pi^-$, Phys. Lett. B **340**, 125 (1994).

[1427] D. S. Akerib *et al.* (CLEO Collaboration), Measurement of the Absolute Branching Fraction for $D^0 \to K^- \pi^+$, Phys. Rev. Lett. **71**, 3070 (1993).

[1428] D. Decamp *et al.* (ALEPH Collaboration), Production and decay of charmed mesons at the Z resonance, Phys. Lett. B **266**, 218 (1991).

[1429] D. E. Acosta *et al.* (CDF Collaboration), Measurement of Partial Widths and Search for Direct CP Violation in D^0 Meson Decays to $K^- K^+$ and $\pi^- \pi^+$, Phys. Rev. Lett. **94**, 122001 (2005).

[1430] T. E. Coan *et al.* (CLEO Collaboration), Flavor-Specific Inclusive B Decays to Charm, Phys. Rev. Lett. **80**, 1150 (1998).

[1431] N. Davidson, T. Przedzinski, and Z. Was, PHOTOS interface in C + +: Technical and physics documentation, Comput. Phys. Commun. **199**, 86 (2016).

[1432] B. Aubert *et al.* (*BABAR* Collaboration), Observation of a Narrow Meson Decaying to $D_s^+\pi^0$ at a Mass of 2.32-GeV/c^2, Phys. Rev. Lett. **90**, 242001 (2003).

[1433] D. Besson *et al.* (CLEO Collaboration), Observation of a narrow resonance of mass 2.46-GeV/c^2 decaying to $D_s^{*+}\pi^0$ and confirmation of the $D_{sJ}^*(2317)$ state, Phys. Rev. D **68**, 032002 (2003); Phys. Rev. D **75**, 119908(E) (2007).

[1434] K. Abe *et al.* (Belle Collaboration), Measurements of the D_{sJ} Resonance Properties, Phys. Rev. Lett. **92**, 012002 (2004).

[1435] B. Aubert *et al.* (*BABAR* Collaboration), Observation of a narrow meson decaying to $D_s^+\pi^0\gamma$ at a mass of 2.458 GeV/c^2, Phys. Rev. D **69**, 031101 (2004).

[1436] J. M. Link *et al.* (FOCUS Collaboration), Measurement of masses and widths of excited charm mesons D_2^* and evidence for broad states, Phys. Lett. B **586**, 11 (2004).

[1437] R. Aaij *et al.* (LHCb Collaboration), Amplitude analysis of $B^0 \to \bar{D}^0 K^+\pi^-$ decays, Phys. Rev. D **92**, 012012 (2015).

[1438] R. Aaij *et al.* (LHCb Collaboration), Determination of quantum numbers for several excited charmed mesons observed in $B^- \to D^{*+}\pi^-\pi^-$ decays, Phys. Rev. D **101**, 032005 (2020).

[1439] H. Abramowicz *et al.* (ZEUS Collaboration), Production of the excited charm mesons D_1 and D_2^* at HERA, Nucl. Phys. **B866**, 229 (2013).

[1440] A. Abulencia *et al.* (CDF Collaboration), Measurement of mass and width of the excited charmed meson states D_1^0 and D_2^{*0} at CDF, Phys. Rev. D **73**, 051104 (2006).

[1441] P. Avery *et al.* (CLEO Collaboration), Production and decay of $D_1^0(2420)$ and $D_2^{*0}(2460)$, Phys. Lett. B **331**, 236 (1994).

[1442] P. L. Frabetti *et al.* (Fermilab E687 Collaboration), Measurement of the Masses and Widths of $L = 1$ Charm Mesons, Phys. Rev. Lett. **72**, 324 (1994).

[1443] H. Albrecht *et al.* (ARGUS Collaboration), Resonance decomposition of the $D^{*0}(2420)$ through a decay angular analysis, Phys. Lett. B **232**, 398 (1989).

[1444] P. Avery *et al.* (CLEO Collaboration), P wave charmed mesons in e^+e^- annihilation, Phys. Rev. D **41**, 774 (1990).

[1445] J. C. Anjos *et al.* (Tagged Photon Spectrometer Collaboration), Observation of Excited Charmed Mesons, Phys. Rev. Lett. **62**, 1717 (1989).

[1446] T. Bergfeld *et al.* (CLEO Collaboration), Observation of $D_1^+(2420)$ and $D_2^{*+}(2460)$, Phys. Lett. B **340**, 194 (1994).

[1447] R. Aaij *et al.* (LHCb Collaboration), Amplitude analysis of $B^- \to D^+\pi^-\pi^-$ decays, Phys. Rev. D **94**, 072001 (2016).

[1448] H. Albrecht *et al.* (ARGUS Collaboration), Observation of the $D^{*0}(2459)$ in e^+e^- annihilation, Phys. Lett. B **221**, 422 (1989).

[1449] H. Albrecht *et al.* (ARGUS Collaboration), Observation of the charged isospin partner of the D^*0 (2459), Phys. Lett. B **231**, 208 (1989).

[1450] P. Abreu *et al.* (DELPHI Collaboration), First evidence for a charm radial excitation, $D^{*\prime}$, Phys. Lett. B **426**, 231 (1998).

[1451] B. Aubert *et al.* (*BABAR* Collaboration), A study of the $D_{sJ}^*(2317)$ and $D_{sJ}(2460)$ mesons in inclusive $c\bar{c}$ production near $\sqrt{s} = 10.6$ GeV, Phys. Rev. D **74**, 032007 (2006).

[1452] M. Ablikim *et al.* (BESIII Collaboration), Measurement of the absolute branching fraction of $D_{s0}^{*\pm}(2317) \to \pi^0 D_s^{\pm}$, Phys. Rev. D **97**, 051103 (2018).

[1453] M. Ablikim *et al.* (BESIII Collaboration), Observation of $e^+e^- \to D_s^+\bar{D}^{(*)0}K^-$ and study of the P-wave D_s mesons, Chin. Phys. C **43**, 031001 (2019).

[1454] J. P. Lees *et al.* (*BABAR* Collaboration), Measurement of the mass and width of the $D_{s1}(2536)^+$ meson, Phys. Rev. D **83**, 072003 (2011).

[1455] V. M. Abazov *et al.* (D0 Collaboration), Measurement of the B_s^0 Semileptonic Branching Ratio to an Orbitally Excited D_s State, $\mathrm{Br}(B_s^0 \to D_{s1}^-(2536)\mu^+\nu X)$, Phys. Rev. Lett. **102**, 051801 (2009).

[1456] J. P. Alexander *et al.* (CLEO Collaboration), Production and decay of the $D_{s1}^+(2536)$, Phys. Lett. B **303**, 377 (1993).

[1457] H. Albrecht *et al.* (ARGUS Collaboration), Observation of the decay $D_{s1}(2536) \to D^{*0}K^+$, Phys. Lett. B **297**, 425 (1992).

[1458] H. Albrecht *et al.* (ARGUS Collaboration), Observation of a new charmed—strange meson, Phys. Lett. B **230**, 162 (1989).

[1459] R. Aaij *et al.* (LHCb Collaboration), Dalitz plot analysis of $B_s^0 \to \bar{D}^0 K^-\pi^+$ decays, Phys. Rev. D **90**, 072003 (2014).

[1460] R. Aaij *et al.* (LHCb Collaboration), First observation of $\bar{B}_s^0 \to D_{s2}^{*+}X\mu^-\bar{\nu}$ decays, Phys. Lett. B **698**, 14 (2011).

[1461] B. Aubert *et al.* (*BABAR* Collaboration), Observation of a New D_s Meson Decaying to DK at a Mass of 2.86 GeV/c^2, Phys. Rev. Lett. **97**, 222001 (2006).

[1462] H. Albrecht *et al.* (ARGUS Collaboration), Measurement of the decay $D_{s2}^{*+} \to D^0K^+$, Z. Phys. C **69**, 405 (1996).

[1463] Y. Kubota *et al.* (CLEO Collaboration), Observation of a New Charmed Strange Meson, Phys. Rev. Lett. **72**, 1972 (1994).

[1464] R. Aaij *et al.* (LHCb Collaboration), Observation of a New Excited D_s^+ Meson in $B^0 \to D^-D^+K^+\pi^-$ Decays, Phys. Rev. Lett. **126**, 122002 (2021).

[1465] R. Aaij *et al.* (LHCb Collaboration), Study of $D_{sJ}^{(*)+}$ mesons decaying to $D^{*+}K_S^0$ and $D^{*0}K^+$ final states, J. High Energy Phys. 02 (2016) 133.

[1466] J. P. Lees *et al.* (*BABAR* Collaboration), Dalitz plot analyses of $B^0 \to D^-D^0K^+$ and $B^+ \to \bar{D}^0D^0K^+$ decays, Phys. Rev. D **91**, 052002 (2015).

[1467] R. Aaij *et al.* (LHCb Collaboration), Study of D_{sJ} decays to $D^+K_S^0$ and D^0K^+ final states in pp collisions, J. High Energy Phys. 10 (2012) 151.

[1468] B. Aubert *et al.* (*BABAR* Collaboration), Study of D_{sJ} decays to D^*K in inclusive e^+e^- interactions, Phys. Rev. D **80**, 092003 (2009).

[1469] R. Aaij *et al.* (LHCb Collaboration), Observation of Overlapping Spin-1 and Spin-3 $\bar{D}^0K^-$ Resonances at Mass 2.86 GeV/c^2, Phys. Rev. Lett. **113**, 162001 (2014).

[1470] S. Godfrey and N. Isgur, Mesons in a relativized quark model with chromodynamics, Phys. Rev. D **32**, 189 (1985).

[1471] S. Godfrey and R. Kokoski, The properties of p wave mesons with one heavy quark, Phys. Rev. D **43**, 1679 (1991).

[1472] P. Schweitzer, S. Boffi, and M. Radici, Polynomiality of unpolarized off forward distribution functions and the D term in the chiral quark soliton model, Phys. Rev. D **66**, 114004 (2002).

[1473] B. Chen, X. Liu, and A. Zhang, Combined study of $2S$ and $1D$ open-charm mesons with natural spin-parity, Phys. Rev. D **92**, 034005 (2015).

[1474] S. Godfrey and K. Moats, Properties of excited charm and charm-strange mesons, Phys. Rev. D **93**, 034035 (2016).

[1475] A. M. Badalian and B. L. G. Bakker, The charmed mesons in the region above 3.0 GeV, Phys. At. Nucl. **84**, 354 (2021).

[1476] M. Albaladejo, P. Fernandez-Soler, F.-K. Guo, and J. Nieves, Two-pole structure of the $D_0^*(2400)$, Phys. Lett. B **767**, 465 (2017).

[1477] M.-L. Du, F.-K. Guo, C. Hanhart, B. Kubis, and U.-G. Meißner, Where is the Lightest Charmed Scalar Meson?, Phys. Rev. Lett. **126**, 192001 (2021).

[1478] F. Jugeau, A. Le Yaouanc, L. Oliver, and J.-C. Raynal, The decays $\bar{B} \to D^{**}\pi$ and the Isgur-Wise functions $\tau_{1/2}(w)$, $\tau_{3/2}(w)$, Phys. Rev. D **72**, 094010 (2005).

[1479] P. Colangelo, F. De Fazio, and R. Ferrandes, Excited charmed mesons: Observations, analyses and puzzles, Mod. Phys. Lett. A **19**, 2083 (2004).

[1480] R. N. Cahn and J. D. Jackson, Spin orbit and tensor forces in heavy quark light quark mesons: Implications of the new D_s state at 2.32-GeV, Phys. Rev. D **68**, 037502 (2003).

[1481] T. Barnes, F. E. Close, and H. J. Lipkin, Implications of a DK molecule at 2.32-GeV, Phys. Rev. D **68**, 054006 (2003).

[1482] H. J. Lipkin, New predictions for multiquark hadron masses, Phys. Lett. B **580**, 50 (2004).

[1483] W. A. Bardeen, E. J. Eichten, and C. T. Hill, Chiral multiplets of heavy—light mesons, Phys. Rev. D **68**, 054024 (2003).

[1484] A. Türkan, J. Y. Süngü, and E. V. Veliev, Modifications on the properties of $D_{s0}^*(2317)$ as four-quark state in thermal medium, Acta Phys. Pol. B **53**, 1 (2022).

[1485] T. Matsuki, T. Morii, and K. Sudoh, Radial excitations of heavy mesons, Eur. Phys. J. A **31**, 701 (2007).

[1486] N. Isgur and M. B. Wise, Weak decays of heavy mesons in the static quark approximation, Phys. Lett. B **232**, 113 (1989).

[1487] S. Chekanov *et al.* (ZEUS Collaboration), Production of excited charm and charm-strange mesons at HERA, Eur. Phys. J. C **60**, 25 (2009).

[1488] A. Heister *et al.* (ALEPH Collaboration), Production of D_s^{**} mesons in hadronic Z decays, Phys. Lett. B **526**, 34 (2002).

[1489] B. Aubert *et al.* (*BABAR* Collaboration), A precision measurement of the Λ_c^+ baryon mass, Phys. Rev. D **72**, 052006 (2005).

[1490] E. Solovieva *et al.* (Belle Collaboration), Study of Ω_c^0 and Ω_c^{*0} baryons at Belle, Phys. Lett. B **672**, 1 (2009).

[1491] T. Aaltonen *et al.* (CDF Collaboration), Measurements of the properties of $\Lambda_c(2595)$, $\Lambda_c(2625)$, $\Sigma_c(2455)$, and $\Sigma_c(2520)$ baryons, Phys. Rev. D **84**, 012003 (2011).

[1492] M. Artuso *et al.* (CLEO Collaboration), Observation of New States Decaying into $\Lambda_c^+\pi^-\pi^+$, Phys. Rev. Lett. **86**, 4479 (2001).

[1493] B. Aubert *et al.* (*BABAR* Collaboration), Observation of a Charmed Baryon Decaying to D^0p at a Mass Near 2.94-GeV/c^2, Phys. Rev. Lett. **98**, 012001 (2007).

[1494] H.-Y. Cheng and C.-K. Chua, Strong decays of charmed baryons in heavy hadron chiral perturbation theory, Phys. Rev. D **75**, 014006 (2007).

[1495] K. Tanida *et al.* (Belle Collaboration), Experimental determination of the isospin of $\Lambda_c(2765)^+/\Sigma_c(2765)^+$, in *Proceedings of the 18th International Conference on Hadron Spectroscopy and Structure* (2019), 10.1142/9789811219313_0028.

[1496] R. Aaij *et al.* (LHCb Collaboration), Measurement of the shape of the $\Lambda_b^0 \to \Lambda_c^+\mu^-\bar{\nu}_\mu$ differential decay rate, Phys. Rev. D **96**, 112005 (2017).

[1497] S. H. Lee *et al.* (Belle Collaboration), Measurements of the masses and widths of the $\Sigma_c(2455)^{0/++}$ and $\Sigma_c(2520)^{0/++}$ baryons, Phys. Rev. D **89**, 091102 (2014).

[1498] R. Mizuk *et al.* (Belle Collaboration), Observation of an Isotriplet of Excited Charmed Baryons Decaying to $\Lambda_c^+\pi$, Phys. Rev. Lett. **94**, 122002 (2005).

[1499] L. A. Copley, N. Isgur, and G. Karl, Charmed baryons in a quark model with hyperfine interactions, Phys. Rev. D **20**, 768 (1979); Phys. Rev. D **23**, 817(E) (1981).

[1500] D. Pirjol and T.-M. Yan, Predictions for s wave and p wave heavy baryons from sum rules and constituent quark model. 1. Strong interactions, Phys. Rev. D **56**, 5483 (1997).

[1501] R. Chistov *et al.* (Belle Collaboration), Observation of New States Decaying into $\Lambda_c^+K^-\pi^+$ and $\Lambda_c^+K_S^0\pi^-$, Phys. Rev. Lett. **97**, 162001 (2006).

[1502] Y. Kato *et al.* (Belle Collaboration), Search for doubly charmed baryons and study of charmed strange baryons at Belle, Phys. Rev. D **89**, 052003 (2014).

[1503] Y. Kato *et al.* (Belle Collaboration), Studies of charmed baryons in the $\Lambda - D$ final state at Belle, Phys. Rev. D **94**, 032002 (2016).

[1504] R. Aaij *et al.* (LHCb Collaboration), Observation of New Ξ_c^0 Baryons Decaying to $\Lambda_c^+K^-$, Phys. Rev. Lett. **124**, 222001 (2020).

[1505] B. Aubert *et al.* (*BABAR* Collaboration), A Study of $\bar{B} \to \Xi_c\bar{\Lambda}_c^-$ and $\bar{B} \to \Lambda_c^+\bar{\Lambda}_c^-\bar{K}$ decays at *BABAR*, Phys. Rev. D **77**, 031101 (2008).

[1506] T. J. Moon *et al.* (Belle Collaboration), First determination of the spin and parity of a charmed-strange baryon, $\Xi_c(2970)^+$, Phys. Rev. D **103**, L111101 (2021).

[1507] L. D. Roper, Evidence for a P-11 Pion-Nucleon Resonance at 556 MeV, Phys. Rev. Lett. **12**, 340 (1964).

[1508] J. Yelton *et al.* (Belle Collaboration), Study of excited Ξ_c states decaying into Ξ_c^0 and Ξ_c^+ baryons, Phys. Rev. D **94**, 052011 (2016).

[1509] J. Yelton *et al.* (Belle Collaboration), Study of electromagnetic decays of orbitally excited Ξ_c baryons, Phys. Rev. D **102**, 071103 (2020).

[1510] B. Aubert *et al.* (*BABAR* Collaboration), Observation of an Excited Charm Baryon Ω_c^* Decaying to $\Omega_c^0\gamma$, Phys. Rev. Lett. **97**, 232001 (2006).

[1511] J. L. Rosner, Charmed baryons with $J = 3/2$, Phys. Rev. D **52**, 6461 (1995).

[1512] L. Y. Glozman and D. O. Riska, The charm and bottom hyperons and chiral dynamics, Nucl. Phys. **A603**, 326 (1996); Nucl. Phys. **A620**, 510(E) (1997).

[1513] E. E. Jenkins, Heavy baryon masses in the $1/m_Q$ and $1/N_c$ expansions, Phys. Rev. D **54**, 4515 (1996).

[1514] L. Burakovsky, J. T. Goldman, and L. P. Horwitz, New quadratic baryon mass relations, Phys. Rev. D **56**, 7124 (1997).

[1515] R. Aaij *et al.* (LHCb Collaboration), Observation of Five New Narrow Ω_c^0 States Decaying to $\Xi_c^+K^-$, Phys. Rev. Lett. **118**, 182001 (2017).

[1516] J. Yelton *et al.* (Belle Collaboration), Observation of excited Ω_c charmed baryons in e^+e^- collisions, Phys. Rev. D **97**, 051102 (2018).

[1517] R. Aaij *et al.* (LHCb Collaboration), First branching fraction measurement of the suppressed decay $\Xi_c^0 \to \pi^-\Lambda_c^+$, Phys. Rev. D **102**, 071101 (2020).

[1518] G. Burdman, E. Golowich, J. L. Hewett, and S. Pakvasa, Rare charm decays in the standard model and beyond, Phys. Rev. D **66**, 014009 (2002).

[1519] S. Fajfer, A. Prapotnik, S. Prelovšek, P. Singer, and J. Zupan, The rare decays of D mesons, Nucl. Phys. B, Proc. Suppl. **115**, 93 (2003).

[1520] S. Fajfer, N. Kosnik, and S. Prelovsek, Updated constraints on new physics in rare charm decays, Phys. Rev. D **76**, 074010 (2007).

[1521] E. Golowich, J. Hewett, S. Pakvasa, and A. A. Petrov, Relating $D^0 - \bar{D}^0$ mixing and $D^0 \to \ell^+\ell^-$ with new physics, Phys. Rev. D **79**, 114030 (2009).

[1522] A. Paul, I. I. Bigi, and S. Recksiegel, $D^0 \to \gamma\gamma$ and $D^0 \to \mu^+\mu^-$ rates on an unlikely impact of the littlest Higgs model with T-parity, Phys. Rev. D **82**, 094006 (2010); Phys. Rev. D **83**, 019901(E) (2011).

[1523] A. V. Borisov, Lepton-number violating meson decays in theories beyond the standard model, arXiv:1112.3269.

[1524] R.-M. Wang, J.-H. Sheng, J. Zhu, Y.-Y. Fan, and Y. Gao, Studying the lepton number and lepton flavor violating $D^0 \to e^\pm\mu^\mp$ and $D_{d/s}^+ \to \pi(K)^+e^\pm\mu^\mp$ decays, Int. J. Mod. Phys. A **29**, 1450169 (2014).

[1525] S. de Boer and G. Hiller, Flavor and new physics opportunities with rare charm decays into leptons, Phys. Rev. D **93**, 074001 (2016).

[1526] S. Fajfer and N. Košnik, Prospects of discovering new physics in rare charm decays, Eur. Phys. J. C **75**, 567 (2015).

[1527] S. Sahoo and R. Mohanta, New physics effects in charm meson decays involving $c \to ul^+l^-(l_i^\mp l_j^\pm)$ transitions, Eur. Phys. J. C **77**, 344 (2017).

[1528] S. de Boer and G. Hiller, Rare radiative charm decays within the standard model and beyond, J. High Energy Phys. 08 (2017) 091.

[1529] S. De Boer and G. Hiller, Null tests from angular distributions in $D \to P_1P_2l^+l^-$, $l = e, \mu$ decays on and off peak, Phys. Rev. D **98**, 035041 (2018).

[1530] R. Bause, M. Golz, G. Hiller, and A. Tayduganov, The new physics reach of null tests with $D \to \pi\ell\ell$ and $D_s \to K\ell\ell$ decays, Eur. Phys. J. C **80**, 65 (2020); Eur. Phys. J. C **81**, 219(E) (2021).

[1531] R. Bause, H. Gisbert, M. Golz, and G. Hiller, Rare charm $c \to u\nu\bar{\nu}$ dineutrino null tests for e^+e^- machines, Phys. Rev. D **103**, 015033 (2021).

[1532] B. Bhattacharya, C. M. Grant, and A. A. Petrov, Invisible widths of heavy mesons, Phys. Rev. D **99**, 093010 (2019).

[1533] S. Fajfer and A. Novosel, Coloured scalars mediated rare charm meson decays to invisible fermions, Phys. Rev. D **104**, 015014 (2021).

[1534] P. Rubin *et al.* (CLEO Collaboration), Search for rare and forbidden decays of charm and charmed-strange mesons to final states $h^+ - e^- + e^+$, Phys. Rev. D **82**, 092007 (2010).

[1535] V. M. Abazov *et al.* (D0 Collaboration), Search for Flavor-Changing-Neutral-Current D Meson Decays, Phys. Rev. Lett. **100**, 101801 (2008).

[1536] R. Aaij *et al.* (LHCb Collaboration), Search for the decay $D^0 \to \pi^+\pi^-\mu^+\mu^-$, Phys. Lett. B **728**, 234 (2014).

[1537] R. Aaij *et al.* (LHCb Collaboration), Search for $D_{(s)}^+ \to \pi^+\mu^+\mu^-$ and $D_{(s)}^+ \to \pi^-\mu^+\mu^+$ decays, Phys. Lett. B **724**, 203 (2013).

[1538] T. E. Coan *et al.* (CLEO Collaboration), First Search for the Flavor Changing Neutral Current Decay $D^0 \to \gamma\gamma$, Phys. Rev. Lett. **90**, 101801 (2003).

[1539] M. Ablikim *et al.* (BESIII Collaboration), Search for $D^0 \to \gamma\gamma$ and improved measurement of the branching fraction for $D^0 \to \pi^0\pi^0$, Phys. Rev. D **91**, 112015 (2015).

[1540] J. P. Lees *et al.* (*BABAR* Collaboration), Search for the decay $D^0 \to \gamma\gamma$ and measurement of the branching fraction for $D^0 \to \pi^0\pi^0$, Phys. Rev. D **85**, 091107 (2012).

[1541] N. K. Nisar *et al.* (Belle Collaboration), Search for the rare decay $D^0 \to \gamma\gamma$ at Belle, Phys. Rev. D **93**, 051102 (2016).

[1542] P. Haas *et al.* (CLEO Collaboration), Upper Limits on Charm Changing Neutral Current Interactions, Phys. Rev. Lett. **60**, 1614 (1988).

[1543] H. Albrecht *et al.* (ARGUS Collaboration), Search for D^0 decays into lepton pairs, Phys. Lett. B **209**, 380 (1988).

[1544] J. Adler *et al.* (MARK-III Collaboration), A search for the decay $D^0 \to e^+e^-$, Phys. Rev. D **37**, 2023 (1988); Phys. Rev. D **40**, 3788(E) (1989).

[1545] A. Freyberger *et al.* (CLEO Collaboration), Limits on Flavor Changing Neutral Currents in D^0 Meson Decays, Phys. Rev. Lett. **76**, 3065 (1996).

[1546] D. Pripstein *et al.* (Fermilab E789 Collaboration), Search for flavor changing neutral currents and lepton family number violation in two-body D^0 decays, Phys. Rev. D **61**, 032005 (2000).

[1547] E. M. Aitala *et al.* (Fermilab E791 Collaboration), Search for rare and forbidden dilepton decays of the D^+, D_s^+, and D^0 charmed mesons, Phys. Lett. B **462**, 401 (1999).

[1548] B. Aubert *et al.* (*BABAR* Collaboration), Search for Flavor-Changing Neutral Current and Lepton Flavor Violating Decays of $D^0 \to \ell^+\ell^-$, Phys. Rev. Lett. **93**, 191801 (2004).

[1549] M. Petric *et al.* (Belle Collaboration), Search for leptonic decays of D^0 mesons, Phys. Rev. D **81**, 091102 (2010).

[1550] K. Kodama *et al.* (Fermilab E653 Collaboration), Upper limits of charm hadron decays to two muons plus hadrons, Phys. Lett. B **345**, 85 (1995).

[1551] I. Abt *et al.* (HERA-B Collaboration), Search for the flavor changing neutral current decay $D^0 \to \mu^+\mu^-$ with the HERA-B detector, Phys. Lett. B **596**, 173 (2004).

[1552] T. Aaltonen *et al.* (CDF Collaboration), Updated search for the flavor-changing neutral-current decay $D^0 \to \mu^+\mu^-$, Phys. Rev. D **82**, 091105 (2010).

[1553] R. Aaij *et al.* (LHCb Collaboration), Search for the rare decay $D^0 \to \mu^+\mu^-$, Phys. Lett. B **725**, 15 (2013).

[1554] M. Ablikim *et al.* (BESIII Collaboration), Search for the rare decays $D \to h(h')e^+e^-$, Phys. Rev. D **97**, 072015 (2018).

[1555] E. M. Aitala *et al.* (Fermilab E791 Collaboration), Search for Rare and Forbidden Charm Meson Decays $D^0 \to V\ell^+\ell^-$ and $hh\ell\ell$, Phys. Rev. Lett. **86**, 3969 (2001).

[1556] R. Aaij *et al.* (LHCb Collaboration), Observation of D^0 Meson Decays to $\pi^+\pi^-\mu^+\mu^-$ and $K^+K^-\mu^+\mu^-$ Final States, Phys. Rev. Lett. **119**, 181805 (2017).

[1557] J. Adler *et al.* (MARK-III Collaboration), A search for the decay $D^0 \to \bar{K}^0e^+e^-$, Phys. Rev. D **40**, 906 (1989).

[1558] J. P. Lees *et al.* (*BABAR* Collaboration), Observation of the Decay $D^0 \to K^-\pi^+e^+e^-$, Phys. Rev. Lett. **122**, 081802 (2019).

[1559] R. Aaij *et al.* (LHCb Collaboration), First observation of the decay $D^0 \to K^-\pi^+\mu^+\mu^-$ in the ρ^0-ω region of the dimuon mass spectrum, Phys. Lett. B **757**, 558 (2016).

[1560] D. M. Asner *et al.* (CLEO Collaboration), Radiative decay modes of the D^0 meson, Phys. Rev. D **58**, 092001 (1998).

[1561] B. Aubert *et al.* (*BABAR* Collaboration), Measurement of the branching fractions of the radiative charm decays $D^0 \to \bar{K}^{*0}\gamma$ and $D^0 \to \phi\gamma$, Phys. Rev. D **78**, 071101 (2008).

[1562] Y.-T. Lai *et al.* (Belle Collaboration), Search for D^0 decays to invisible final states at Belle, Phys. Rev. D **95**, 011102 (2017).

[1563] J. Becker *et al.* (MARK-III Collaboration), A search for the lepton family number violating decay $D^0 \to \mu e$, Phys. Lett. B **193**, 147 (1987).

[1564] R. Aaij *et al.* (LHCb Collaboration), Search for the lepton-flavour violating decay $D^0 \to e^\pm\mu^\mp$, Phys. Lett. B **754**, 167 (2016).

[1565] J. P. Lees *et al.* (*BABAR* Collaboration), Search for lepton-flavor-violating decays $D^0 \to X^0e^\pm\mu^\mp$, Phys. Rev. D **101**, 112003 (2020).

[1566] J. P. Lees *et al.* (*BABAR* Collaboration), Search for Rare or Forbidden Decays of the D^0 Meson, Phys. Rev. Lett. **124**, 071802 (2020).

[1567] M. Ablikim *et al.* (BESIII Collaboration), Search for heavy Majorana neutrino in lepton number violating decays of $D \to K\pi e^+e^+$, Phys. Rev. D **99**, 112002 (2019).

[1568] P. Rubin *et al.* (CLEO Collaboration), Search for $D^0 \to \bar{p}e^+$ and $D^0 \to pe^-$, Phys. Rev. D **79**, 097101 (2009).

[1569] P. L. Frabetti *et al.* (Fermilab E687 Collaboration), Search for rare and forbidden decays of the charmed meson D^+, Phys. Lett. B **398**, 239 (1997).

[1570] R. Aaij *et al.* (LHCb Collaboration), Searches for 25 rare and forbidden decays of D^+ and D_s^+ mesons, J. High Energy Phys. 06 (2021) 44.

[1571] J. P. Lees *et al.* (*BABAR* Collaboration), Searches for rare or forbidden semileptonic charm decays, Phys. Rev. D **84**, 072006 (2011).

[1572] J. M. Link *et al.* (FOCUS Collaboration), Search for rare and forbidden three body dimuon decays of the charmed mesons D^+ and $D_s s^+$, Phys. Lett. B **572**, 21 (2003).

[1573] M. Ablikim *et al.* (BESIII Collaboration), Search for the decay $D_s^+ \to \gamma e^+\nu_e$, Phys. Rev. D **99**, 072002 (2019).

[1574] R. Aaij *et al.* (LHCb Collaboration), Search for the rare decay $\Lambda_c^+ \to p\mu^+\mu^-$, Phys. Rev. D **97**, 091101 (2018).

[1575] M. Davier, A. Hocker, and Z. Zhang, The physics of hadronic τ decays, Rev. Mod. Phys. **78**, 1043 (2006).

[1576] Y. Amhis *et al.*, Averages of b-hadron, c-hadron, and τ-lepton properties as of summer 2014, arXiv:1412.7515.

[1577] S. Schael *et al.* (ALEPH Collaboration), Branching ratios and spectral functions of τ decays: Final ALEPH measurements and physics implications, Phys. Rep. **421**, 191 (2005), HFLAV-tau uses measurements of $\tau \to hX$ and $\tau \to KX$ and obtains $\tau \to \pi X$ by difference; the measurement of $\mathcal{B}(\tau^- \to 3h^-2h^+\pi^0\nu_\tau(\text{ex.}K^0))$ has been read as $(2.1 \pm 0.7 \pm 0.6) \times 10^{-4}$ whereas PDG11 uses $(2.1 \pm 0.7 \pm 0.9) \times 10^{-4}$.

[1578] A. Lusiani, Measurement of the branching fractions of the decays $\tau^- \to K^-n\pi^0\nu_\tau$ ($n = 0, 1, 2, 3$) and $\tau^- \to \pi^-n\pi^0\nu_\tau$ ($n = 3, 4$) by *BABAR*, EPJ Web Conf. **212**, 08001 (2019).

[1579] B. Aubert *et al.* (*BABAR* Collaboration), Measurement of the $\tau^- \to K^-\pi^0\nu_\tau$ branching fraction, Phys. Rev. D **76**, 051104 (2007).

[1580] M. A. Arroyo-Ureña, G. Hernández-Tomé, G. López-Castro, P. Roig, and I. Rosell, Radiative corrections to $\tau \to \pi(K)\nu\tau[\gamma]$: A reliable new physics test, Phys. Rev. D **104**, L091502 (2021).

[1581] W. J. Marciano and A. Sirlin, Radiative Corrections to $\pi_{\ell 2}$ Decays, Phys. Rev. Lett. **71**, 3629 (1993).

[1582] R. Decker and M. Finkemeier, Radiative corrections to the decay $\tau \to \pi(K)\nu_\tau$, Phys. Lett. B **334**, 199 (1994).

[1583] R. Decker and M. Finkemeier, Short and long distance effects in the decay $\tau \to \pi\nu_\tau(\gamma)$, Nucl. Phys. **B438**, 17 (1995).

[1584] R. Decker and M. Finkemeier, Radiative corrections to the decay $\tau \to \pi\nu_\tau$, Nucl. Phys. B, Proc. Suppl. **40**, 453 (1995).

[1585] P. Abreu *et al.* (DELPHI Collaboration), Measurements of the leptonic branching fractions of the τ, Eur. Phys. J. C **10**, 201 (1999).

[1586] M. Acciarri *et al.* (L3 Collaboration), Measurement of the τ branching fractions into leptons, Phys. Lett. B **507**, 47 (2001).

[1587] G. Abbiendi *et al.* (OPAL Collaboration), A measurement of the $\tau^- \to \mu^-\bar{\nu}_\mu\nu_\tau$ branching ratios, Phys. Lett. B **551**, 35 (2003).

[1588] H. Albrecht *et al.* (ARGUS Collaboration), Measurement of exclusive one prong and inclusive three prong

branching ratios of the τ lepton, Z. Phys. C **53**, 367 (1992).
[1589] B. Aubert *et al.* (*BABAR* Collaboration), Measurements of Charged Current Lepton Universality and $|V_{us}|$ using Tau Lepton Decays to $e^-\bar{\nu}_e\nu_\tau$, $\mu^-\bar{\nu}_\mu\nu_\tau$, $\pi^-\nu_\tau$, and $K^-\nu_\tau$, Phys. Rev. Lett. **105**, 051602 (2010).
[1590] A. Anastassov *et al.* (CLEO Collaboration), Experimental test of lepton universality in τ decay, Phys. Rev. D **55**, 2559 (1997); Phys. Rev. D **58**, 119903(E) (1998).
[1591] G. Abbiendi *et al.* (OPAL Collaboration), A measurement of the $\tau^- \to e^-\bar{\nu}\nu_\tau$ branching ratio, Phys. Lett. B **447**, 134 (1999).
[1592] P. Abreu *et al.* (DELPHI Collaboration), A study of the decays of τ leptons produced on the Z resonance at LEP, Z. Phys. C **55**, 555 (1992).
[1593] M. Acciarri *et al.* (L3 Collaboration), Measurement of exclusive branching fractions of hadronic one space prong τ decays, Phys. Lett. B **345**, 93 (1995).
[1594] G. Alexander *et al.* (OPAL Collaboration), Measurement of branching ratios and τ polarization from $\tau \to e\nu\bar{\nu}$, $\tau \to \mu\nu\bar{\nu}$, and $\tau\pi(K)\nu$ decays at LEP, Phys. Lett. B **266**, 201 (1991).
[1595] J. Abdallah *et al.* (DELPHI Collaboration), A measurement of the τ hadronic branching ratios, Eur. Phys. J. C **46**, 1 (2006).
[1596] K. Ackerstaff *et al.* (OPAL Collaboration), Measurement of the one prong hadronic τ branching ratios at LEP, Eur. Phys. J. C **4**, 193 (1998).
[1597] R. Barate *et al.* (ALEPH Collaboration), One prong τ decays with kaons, Eur. Phys. J. C **10**, 1 (1999).
[1598] M. Battle *et al.* (CLEO Collaboration), Measurement of Cabibbo-Suppressed Decays of the τ Lepton, Phys. Rev. Lett. **73**, 1079 (1994).
[1599] P. Abreu *et al.* (DELPHI Collaboration), Charged kaon production in τ decays at LEP, Phys. Lett. B **334**, 435 (1994).
[1600] G. Abbiendi *et al.* (OPAL Collaboration), A study of one prong τ decays with a charged kaon, Eur. Phys. J. C **19**, 653 (2001).
[1601] M. Fujikawa *et al.* (Belle Collaboration), High-statistics study of the $\tau^- \to \pi^-\pi^0\nu_\tau$ decay, Phys. Rev. D **78**, 072006 (2008).
[1602] M. Artuso *et al.* (CLEO Collaboration), A Measurement of the Branching Fraction $B(\tau^- \to h^-\pi^0\nu_\tau)$, Phys. Rev. Lett. **72**, 3762 (1994).
[1603] G. Abbiendi *et al.* (OPAL Collaboration), Measurement of the strange spectral function in hadronic τ decays, Eur. Phys. J. C **35**, 437 (2004).
[1604] M. Procario *et al.* (CLEO Collaboration), Tau Decays with One Charged Particle Plus Multiple π^0s, Phys. Rev. Lett. **70**, 1207 (1993).
[1605] R. Barate *et al.* (ALEPH Collaboration), K^0_S production in τ decays, Eur. Phys. J. C **4**, 29 (1998).
[1606] R. Akers *et al.* (OPAL Collaboration), Measurements of the inclusive branching ratios of τ leptons to K^0_s and charged K*(892), Phys. Lett. B **339**, 278 (1994).
[1607] T. E. Coan *et al.* (CLEO Collaboration), Decays of τ leptons to final states containing K^0_S mesons, Phys. Rev. D **53**, 6037 (1996).
[1608] S. Ryu *et al.* (Belle Collaboration), Measurements of branching fractions of τ lepton decays with one or more K^0_S, Phys. Rev. D **89**, 072009 (2014).
[1609] M. Acciarri *et al.* (L3 Collaboration), One prong τ decays with neutral kaons, Phys. Lett. B **352**, 487 (1995).
[1610] G. Abbiendi *et al.* (OPAL Collaboration), Tau decays with neutral kaons, Eur. Phys. J. C **13**, 213 (2000).
[1611] J. P. Lees *et al.* (*BABAR* Collaboration), Measurement of the spectral function for the $\tau^- \to K^-K_S\nu_\tau$ decay, Phys. Rev. D **98**, 032010 (2018).
[1612] R. Barate *et al.* (ALEPH Collaboration), Study of τ decays involving kaons, spectral functions and determination of the strange quark mass, Eur. Phys. J. C **11**, 599 (1999).
[1613] J. P. Lees *et al.* (*BABAR* Collaboration), The branching fraction of $\tau^- \to \pi^-K^0_SK^0_S(\pi^0)\nu_\tau$ decays, Phys. Rev. D **86**, 092013 (2012).
[1614] H. J. Behrend *et al.* (CELLO Collaboration), Tau production and decay with the CELLO detector at PETRA, Phys. Lett. B **222**, 163 (1989).
[1615] B. Adeva, O. Adriani, M. Aguilar-Benitez, H. Akbari, J. Alcaraz, A. Aloisio, G. Alverson, M. G. Alviggi, and G. Ambrosi (L3 Collaboration), Decay properties of τ leptons measured at the Z^0 resonance, Phys. Lett. B **265**, 451 (1991).
[1616] H. Aihara *et al.* (TPC/Two Gamma Collaboration), Measurement of τ branching ratios, Phys. Rev. D **35**, 1553 (1987).
[1617] P. Achard *et al.* (L3 Collaboration), Measurement of the topological branching fractions of the τ lepton at LEP, Phys. Lett. B **519**, 189 (2001).
[1618] R. Akers *et al.* (OPAL Collaboration), Measurement of the $\tau^- \to h^-h^+h^-\nu_\tau$ and $\tau^- \to h^-h^+h^- >= 1\pi^0\nu_\tau$ branching ratios, Z. Phys. C **68**, 555 (1995).
[1619] R. Balest *et al.* (CLEO Collaboration), Measurements of the Decays $\tau^- \to h^-h^+h^-\nu_\tau$ and $\tau^- \to h^-h^+h^-\pi^0\nu_\tau$, Phys. Rev. Lett. **75**, 3809 (1995).
[1620] B. Aubert *et al.* (*BABAR* Collaboration), Exclusive Branching Fraction Measurements of Semileptonic Tau Decays into Three Charged Hadrons, $\tau^- \to \phi\pi^-\nu_\tau$ and $\tau^- \to \phi K^-\nu_\tau$, Phys. Rev. Lett. **100**, 011801 (2008).
[1621] M. J. Lee *et al.* (Belle Collaboration), Measurement of the branching fractions and the invariant mass distributions for $\tau^- \to h^-h^+h^-\nu_\tau$ decays, Phys. Rev. D **81**, 113007 (2010).
[1622] R. A. Briere *et al.* (CLEO Collaboration), Branching Fractions of τ Leptons Decays to Three Charged Hadrons, Phys. Rev. Lett. **90**, 181802 (2003).
[1623] K. W. Edwards *et al.* (CLEO Collaboration), Resonant structure of $\tau \to 3\pi\pi^0\nu_\tau$ and $\tau \to \omega\pi\nu_\tau$ decays, Phys. Rev. D **61**, 072003 (2000).
[1624] D. Bortoletto *et al.* (CLEO Collaboration), Measurement of the Decay $\tau^- \to \pi^-\pi^+\pi^-2\pi^0\nu_\tau$, Phys. Rev. Lett. **71**, 1791 (1993).
[1625] A. Anastassov *et al.* (CLEO Collaboration), Study of τ Decays to Six Pions and Neutrino, Phys. Rev. Lett. **86**, 4467 (2001).
[1626] S. J. Richichi *et al.* (CLEO Collaboration), Study of three prong hadronic τ decays with charged kaons, Phys. Rev. D **60**, 112002 (1999).

[1627] D. A. Bauer *et al.* (TPC/Two Gamma Collaboration), Measurement of the kaon content of three prong τ decays, Phys. Rev. D **50**, R13 (1994).

[1628] R. Barate *et al.* (ALEPH Collaboration), Three prong τ decays with charged kaons, Eur. Phys. J. C **1**, 65 (1998).

[1629] K. E. Arms *et al.* (CLEO Collaboration), Study of τ Decays to Four-Hadron Final States with Kaons, Phys. Rev. Lett. **94**, 241802 (2005).

[1630] G. Abbiendi *et al.* (OPAL Collaboration), A study of three prong τ decays with charged kaons, Eur. Phys. J. C **13**, 197 (2000).

[1631] D. Gibaut *et al.* (CLEO Collaboration), Study of the Five Charged Pion Decay of the T Lepton, Phys. Rev. Lett. **73**, 934 (1994).

[1632] B. G. Bylsma *et al.*, Limit on τ decay to seven charged particles, Phys. Rev. D **35**, 2269 (1987).

[1633] H. Albrecht *et al.* (ARGUS Collaboration), An improved upper limit on the τ-neutrino mass from the decay $\tau^- \to \pi^-\pi^-\pi^-\pi^+\pi^+\nu_\tau$, Phys. Lett. B **202**, 149 (1988).

[1634] K. Ackerstaff *et al.* (OPAL Collaboration), Measurement of τ branching ratios to five charged hadrons, Eur. Phys. J. C **8**, 183 (1999).

[1635] D. Buskulic *et al.* (ALEPH Collaboration), A study of τ decays involving η and ω mesons, Z. Phys. C **74**, 263 (1997).

[1636] K. Inami *et al.* (Belle Collaboration), Precise measurement of hadronic τ-decays with an η meson, Phys. Lett. B **672**, 209 (2009).

[1637] M. Artuso *et al.* (CLEO Collaboration), Measurement of T Decays Involving η Mesons, Phys. Rev. Lett. **69**, 3278 (1992).

[1638] P. del Amo Sanchez *et al.* (*BABAR* Collaboration), Studies of $\tau^- \to \eta K^-\nu_\tau$ and $\tau^- \to \eta\pi^-\nu_\tau$ at *BABAR* and a search for a second-class current, Phys. Rev. D **83**, 032002 (2011).

[1639] J. E. Bartelt *et al.* (CLEO Collaboration), First Observation of the Decay $\tau^- \to K^-\eta\nu_\tau$, Phys. Rev. Lett. **76**, 4119 (1996).

[1640] M. Bishai *et al.* (CLEO Collaboration), First Observation of the Decay $\tau^- \to K^{*-}\eta\nu_\tau$, Phys. Rev. Lett. **82**, 281 (1999).

[1641] P. S. Baringer *et al.* (CLEO Collaboration), Production of η and ω Mesons in τ Decay and a Search for Second Class Currents, Phys. Rev. Lett. **59**, 1993 (1987).

[1642] D. Buskulic *et al.* (ALEPH Collaboration), Tau hadronic branching ratios, Z. Phys. C **70**, 579 (1996).

[1643] J. P. Lees *et al.* (*BABAR* Collaboration), Study of high-multiplicity 3-prong and 5-prong τ decays at *BABAR*, Phys. Rev. D **86**, 092010 (2012).

[1644] K. Belous *et al.* (Belle Collaboration), Measurement of the τ-Lepton Lifetime at Belle, Phys. Rev. Lett. **112**, 031801 (2014).

[1645] W. J. Marciano and A. Sirlin, Electroweak Radiative Corrections to τ Decay, Phys. Rev. Lett. **61**, 1815 (1988).

[1646] A. Pich, Precision τ physics, Prog. Part. Nucl. Phys. **75**, 41 (2014).

[1647] A. Ferroglia, C. Greub, A. Sirlin, and Z. Zhang, Contributions of the W-boson propagator to μ and τ leptonic decay rates, Phys. Rev. D **88**, 033012 (2013).

[1648] M. Fael, L. Mercolli, and M. Passera, W-propagator corrections to μ and τ leptonic decays, Phys. Rev. D **88**, 093011 (2013).

[1649] M. Antonelli *et al.*, An Evaluation of $|V_{us}|$ and precise tests of the Standard Model from world data on leptonic and semileptonic kaon decays, Eur. Phys. J. C **69**, 399 (2010).

[1650] E. Gamiz, J. Prades, M. Jamin, F. Schwab, and A. Pich, Determination of m_s and $|V_{us}|$ from hadronic τ decays, J. High Energy Phys. 01 (2003) 060.

[1651] E. Gamiz, M. Jamin, A. Pich, J. Prades, and F. Schwab, V_{us} and m_s from Hadronic τ Decays, Phys. Rev. Lett. **94**, 011803 (2005).

[1652] E. Gamiz, M. Jamin, A. Pich, J. Prades, and F. Schwab, $|V_{us}|$ and m_s from hadronic τ decays, Nucl. Phys. B, Proc. Suppl. **169**, 85 (2007).

[1653] E. Gamiz *et al.*, Theoretical progress on the V_{us} determination from τ decays, *Proc. Sci.*, KAON2008 (2008) 008 [arXiv:0709.0282].

[1654] K. Maltman, A critical look at V_{us} determinations from hadronic τ decay data, Nucl. Phys. B, Proc. Suppl. **218**, 146 (2011).

[1655] R. J. Hudspith, R. Lewis, K. Maltman, and J. Zanotti, A resolution of the inclusive flavor-breaking $\tau|V_{us}|$ puzzle, Phys. Lett. B **781**, 206 (2018).

[1656] P. Boyle, R. James Hudspith, T. Izubuchi, A. Jüttner, C. Lehner, R. Lewis, K. Maltman, H. Ohki, A. Portelli, and M. Spraggs (RBC and UKQCD Collaborations), Novel $|V_{us}|$ Determination Using Inclusive Strange τ Decay and Lattice Hadronic Vacuum Polarization Functions, Phys. Rev. Lett. **121**, 202003 (2018).

[1657] J. C. Hardy and I. S. Towner, Superallowed $0^+ \to 0^+$ nuclear β decays: 2020 critical survey, with implications for V_{ud} and CKM unitarity, Phys. Rev. C **102**, 045501 (2020).

[1658] S. Banerjee (*BABAR* Collaboration), Lepton universality, $|V_{us}|$ and search for second class current in τ decays, in *Proceedings of the 34th International Conference on High Energy Physics* (2008), arXiv:0811.1429.

[1659] N. Miller *et al.*, F_K/F_π from Möbius domain-wall fermions solved on gradient-flowed HISQ ensembles, Phys. Rev. D **102**, 034507 (2020).

[1660] R. J. Dowdall, C. T. H. Davies, G. P. Lepage, and C. McNeile, V_{us} from π and K decay constants in full lattice QCD with physical u, d, s and c quarks, Phys. Rev. D **88**, 074504 (2013).

[1661] A. Bazavov *et al.* (Fermilab Lattice and MILC Collaborations), Charmed and light pseudoscalar meson decay constants from four-flavor lattice QCD with physical light quarks, Phys. Rev. D **90**, 074509 (2014).

[1662] J. Erler, Electroweak radiative corrections to semileptonic τ decays, Rev. Mex. Fis. **50**, 200 (2004).

[1663] E. Tiesinga, P. J. Mohr, D. B. Newell, and B. N. Taylor, CODATA recommended values of the fundamental physical constants: 2018, Rev. Mod. Phys. **93**, 025010 (2021); Database developed by J. Baker, M. Douma, and

S. Kotochigova. Available at http://physics.nist.gov/constants, National Institute of Standards and Technology, Gaithersburg, MD 20899.

[1664] C.-Y. Seng, D. Galviz, W. J. Marciano, and U.-G. Meißner, Update on $|V_{us}|$ and $|V_{us}/V_{ud}|$ from semileptonic kaon and pion decays, Phys. Rev. D **105**, 013005 (2022).

[1665] M. Jamin, A. Pich, and J. Portoles, What can be learned from the Belle spectrum for the decay $\tau^- \to \nu_\tau K_S \pi^-$, Phys. Lett. B **664**, 78 (2008).

[1666] M. Antonelli, V. Cirigliano, A. Lusiani, and E. Passemar, Predicting the τ strange branching ratios and implications for V_{us}, J. High Energy Phys. 10 (2013) 070.